Volume 4

HANDBOOK OF

Immunohistochemistry and *in situ* Hybridization of Human Carcinomas

MOLECULAR GENETICS, GASTROINTESTINAL CARCINOMA, and OVARIAN CARCINOMA

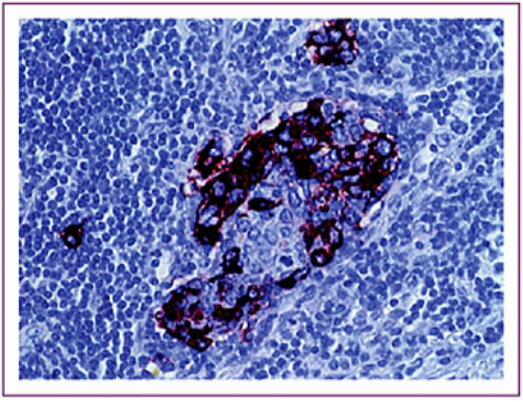

Edited by M.A. HAYAT

Handbook of Immunohistochemistry and *in situ* Hybridization of Human Carcinomas, Volume 4

Handbook of Immunohistochemistry and *in situ* Hybridization of Human Carcinomas

Edited by M.A. Hayat

Volume 1
Molecular Genetics; Lung and Breast Carcinomas

Volume 2
Molecular Pathology, Colorectal Carcinoma, and Prostate Carcinoma

Volume 3
Molecular Genetics, Liver Carcinoma, and Pancreatic Carcinoma

Volume 4
Molecular Genetics, Gastrointestinal Carcinoma, and Ovarian Carcinoma

Handbook of Immunohistochemistry and *in situ* Hybridization of Human Carcinomas, Volume 4

Molecular Genetics, Gastrointestinal Carcinoma, and Ovarian Carcinoma

Edited by

M.A. Hayat
Distinguished Professor
Department of Biological Sciences
Kean University
Union, New Jersey

ELSEVIER

Amsterdam • Boston • Heidelberg • London • New York
Oxford • Paris • San Diego • San Francisco • Singapore
Sydney • Tokyo

Academic Press is an imprint of Elsevier

Elsevier Academic Press
30 Corporate Drive, Suite 400, Burlington, MA 01803, USA
525 B Street, Suite 1900, San Diego, California 92101-4495, USA
84 Theobald's Road, London WC1X 8RR, UK

This book is printed on acid-free paper.

Library of Congress Cataloging-in-Publication Data
Application submitted

British Library Cataloguing in Publication Data
A catalogue record for this book is available from the British Library

ISBN-13: 978-0-12-369402-7
ISBN-10: 0-12-369402-7

For all information on all Elsevier Academic Press publications
visit our Web site at www.books.elsevier.com

Printed in China
06 07 08 09 10 9 8 7 6 5 4 3 2 1

To

Molecular Geneticists/Clinical Pathologists

This Page Intentionally Left Blank

Contents

Authors and Coauthors of Volume 4

Nuzhat Ahmed
Gynaecological Cancer Research Centre, Royal Women's Hospital, Translational Proteomics, Baker Medical Research Institute and The Department of Obstetrics and Gynaecology, University of Melbourne, 132 Grattan Street, Carlton VIC 3053, Melbourne, Australia

Syed Mahfuzul Alam
Department of Obstetrics and Gynecology, Gifu University, School of Medicine, 1-1 Yanagido, Gifu City 501-1194, Japan

Rouba Ali-Fehmi
Wayne State University School of Medicine, Department of Pathology, 3990 John R., Detroit, MI 48201

Yoichi Aoki
Niigata University, Graduate School of Medical and Dental Sciences, Department of Obstetrics and Gynecology, 1-757 Asahimachi dori, Niigata 951-8510, Japan

Eri Arai
Pathology Division, National Cancer Center Research Institute, 5-1-1 Tsukiji, Chuo-ku, Tokyo 104-0045, Japan

Hideo Baba
Graduate School of Medical Sciences, Department of Gastroenterological Surgery, Kumamoto University, 1-1-1, Honsho, Kumamoto 860–8556, Japan

Karl-Friedrich Becker
Technische Universität München, Klinikum rechts der Isar, Institut für Allgemeine Pathologie und Pathologische Anatomie, Trogerstr. 18, 81675 München, Germany

Richard V. Benya
University of Illinois at Chicago, Department of Medicine, GI Cancers Program, Chicago, IL 60612

Max M. Burger
Friedrich Miescher Institute, Novartis Science Board, Maulbeerstrasse 66, CH-4058, Chm Novartis Science Board, Novartis International A6, WKL 125.13.02, Klybeckstrasse 141, CH-4057, Basel, Switzerland

Ralf Bützow
Haartman Institute, Department of Pathology, University of Helsinki, P.O. Box 21, FIN-00014, Finland

Helen P. Cathro
Department of Pathology, University of Virginia, Health Sciences Center, P.O. Box 800214, Charlottesville, VA 22908

Gaoping Chen
Royal Victoria Hospital, RM H4-72, McGill University Health Center, 687 Pine W., Montreal, QC, Canada, H3A 1A1

Zong-Ming E. Chen
Washington University School of Medicine, Department of Pathology, 660 South Euclid Avenue, Box 8118, St. Louis, MO 63110

Liang Cheng
Department of Pathology and Laboratory Medicine, University Hospital 3465, Indiana University Medical Center, 550 North University Boulevard, Indianapolis, IN 46202

David C. Chhieng
Department of Pathology, University of Alabama at Birmingham, KB 605, 619 19th Street South, Birmingham, AL 35249-6823

Brenda L. Coomber
Department of Biomedical Sciences, Ontario Veterinary College, University of Guelph, Guelph, ON, Canada, NIG 2WI

Randal Cox
University of Illinois at Chicago, Department of Biochemistry and Molecular Genetics, Bio-Informatics Group, Chicago, IL 60612

Leonor David
Medical Faculty of the University of Porto, IPATIMUP, Rua Dr. Roberto Frias s/n, 4200-465 Porto, Portugal

Gaetano De Rosa
Department of Biomorphological and Functional Sciences, Pathology Section, University Federico II Faculty of Medicine and Surgery, Via S. Pansini 5, 80131 Naples, Italy

Dipok Kumar Dhar
Department of Digestive and General Surgery, Faculty of Medicine, Shimane University, Izumo, Japan

Joachim Diebold
Pathological Institute, Ludwig-Maximilians University Munich, Thalkirchner Strasse, 80337 Munich, Germany

K. Diedrich
Klinik fur Frauenheilkunde und Geburtshilfe des Universitatsklinikums Schleswig-Holstein, Campus Lubeck Ratzeburger Allee 160, D-23538 Lubeck, Germany

Thomas Dittmar
University of Witten/Herdecke, Institute of Immunology, Stockumer Strasse 10, Witten 58448, Germany

Piotr Dziegiel
Department of Histology and Embryology, Wroclaw Medical University, Chalubinskiego 6a, 50-368 Wroclaw, Poland

Luis Alberto Espinoza
Georgetown University School of Medicine, Department of Biochemistry and Molecular Biology, Basic Science Bldg., R348, 3900 Reservoir Road NW, Washington, DC 20057

Tsuyoshi Etoh
Department of Surgery I, Oita University Faculty of Medicine, 1-1 Hasama-machi, Yufu-city, Oita 879-5593, Japan

Cristina Faleiro-Rodrigues
Anatomy and Pathology Department, Portuguese Institute of Oncology Francisco Gentil Centro Regional do Norte, Rua Dr. António Bernardino de Almeida, 4200-072 Porto, Portugal

R. Felberbaum
Klinik fur Frauenheilkunde und Geburtshilfe des Universitatsklinikums Schleswig-Holstein, Campus Lubeck Ratzeburger Allee 160, D-23538 Lubeck, Germany

Falko Fend
Technische Universität München, Klinikum rechts der Isar, Institut für Allgemeine Pathologie und Pathologische Anatomie, Trogerstr. 18, 81675 München, Germany

N. Fersis
Klinik fur Frauenheilkunde und Geburtshilfe des Universitatsklinikums Schleswig-Holstein, Campus Lubeck Ratzeburger Allee 160, D-23538 Lubeck, Germany

Hans-Peter Fischer
Department of Pathology, University of Bonn, Sigmund-Freud-Str. 25, D-53127 Bonn, Germany

Constantino Fondevila
Servicio de Cirugia General y Digestiva, Hospital Clinic, Villarroel 170, 08036 Barcelona, Spain

M. Friedrich
Klinik fur Frauenheilkunde und Geburtshilfe des Universitatsklinikums Schleswig-Holstein, Campus Lubeck Ratzeburger Allee 160, D-23538 Lubeck, Germany

Jiro Fujimoto
Department of Obstetrics and Gynecology, Gifu University, School of Medicine, 1-1 Yanagido, Gifu City 501-1194, Japan

Armando Gamboa-Dominguez
Department of Pathology, Instituto Nacional de Ciencias Medicas y Nutricion Salvador Zubiran, Tlalpan 14000, Mexico City, Mexico

Jens Peter Goetze
Department of Clinical Biochemistry Rigshospitalet, University of Copenhagen, Blegdamsveg 9, 2100 Copenhagen, Denmark

Heike Grabsch
St. James's University Hospital, Leeds Institute for Molecular Medicine, Academic Unit of Pathology, Level 4, JIF Building, Beckett Street, Leeds LS9 7TF, United Kingdom

William E. Grizzle
Department of Pathology, University of Alabama at Birmingham, ZRB 408, 619 18th Street South, Birmingham, AL 35249

Christian Gulmann
Department of Pathology, Beaumont Hospital, Dublin 9, Ireland

Mala Gupta
Department of Pathology, Winthrop University Hospital, 222 Station Plaza North, Suite 606, Mineola, NY 11501

Aaron Han
Department of Pathology and Laboratory Medicine, American Hospital Dubai, P.O. Box 5566, Dubai, United Arab Emirates

Tadashi Hasegawa
Department of Surgical Pathology, Sapporo Medical University School of Medicine, Sapporo, Japan

Christian Haslinger
Boehringer Ingelheim Austria, Lead Discovery, Dr. Boehringer-Gasse 5-11, A-1121 Vienna, Austria

Kohkichi Hata
Department of Nursing, Faculty of Health Science Kagawa Prefectural College of Health Sciences, Kagawa 761-0123, Japan

Takanori Hattori
Division of Diagnostic Pathology, Shiga University of Medical Science Hospital, Seta, Otsu 520-2192, Japan

Wolfgang Hatzmann
Department of Gynecology, Marien-Hospital, Witten, Herdecke University, Marienplatz 2, 58453 Witten, Germany

M.A. Hayat
Kean University, Department of Biological Sciences, 1000 Morris Avenue, Union, NJ 07083

Qing-Yu He
Department of Chemistry, University of Hong Kong, Pokfulam, Hong Kong

Christoph Heyder
Laboratory for Immunology and Molecular Cancer Research, Federal Hospital Salzburg, Salzburg, Austria

Toshio Hirakawa
Department of Anatomic Pathology, Graduate School of Medical Sciences, Kyushu University, 3-1-1 Maidashi, Higashi-ku, Fukuoka 812-8582, Japan

Heinz Höfler
Technische Universität München, Klinikum rechts der Isar, Institut für Allgemeine Pathologie und Pathologische Anatomie, Trogerstr. 18, 81675 München, Germany

Ngan F. Huang
Center for Tissue Bioengineering, University of California Berkeley, 471 Evans, #1762, Berkeley, CA 94720

Kazuhiko Ino
Nagoya University Graduate School of Medicine, Department of Obstetrics and Gynecology, Tsurumai-cho 65, Showa-ku, Nagoya 466-8550, Japan

Irmgard Irminger-Finger
Biology of Aging Laboratory, Department of Geriatrics, Geneva University Hospitals, Chemin de petit Bel Air 2, CH-1225 Chêne-Bourg, Geneva, Switzerland

Naoki Isobe
Department of Surgery, Hakuaikai Hospital, 1928-3 Fuchu, Tarui-cho, Fuwa-gun, Gifu 503-2114, Japan

Israt Jahan
Department of Obstetrics and Gynecology, Gifu University, School of Medicine, 1-1 Yanagido, Gifu City 501-1194, Japan

Charles Edward Jefford
Biology of Aging Laboratory, Department of Geriatrics, Geneva University Hospitals, Chemin de petit Bel Air 2, CH-1225 Chêne-Bourg, Geneva, Switzerland

Tomáš Jirásek
Department of Pathology, 3rd Faculty of Medicine, Charles University, Srobárova 50, 100 34 Prague, Czech Republic

Hiroaki Kajiyama
Nagoya University Graduate School of Medicine, Department of Obstetrics and Gynecology, Tsurumai-cho 65, Showa-ku, Nagoya 466-8550, Japan

Yoshihiro Kakeji
Department of Surgery and Science, Graduate School of Medical Sciences, Kyushu University, 3-1-1 Higashi-ku, Fukuoka 812-8582, Japan

Tsunehisa Kaku
Division of Maternal Health, Department of Health Sciences, School of Medicine, Kyushu University, Fukuoka, Japan

Toshiharu Kamura
Department of Obstetrics and Gynecology, Kurume University School of Medicine, Research Center of Innovative Cancer Therapy of the 21st Century COE Program for Medical Science, Kurume, Japan

Yae Kanai
Pathology Division, National Cancer Center Research Institute, 5-1-1 Tsukiji, Chuo-ku, Tokyo 104-0045, Japan

Eisuke Kaneki
Department of Obstetrics and Gynecology, Kyushu University, Fukuoka, Japan

Hirotaka Kato
Division of Surgical Pathology, Department of Biomedical Informatics, Kobe University, Graduate School of Medicine, 7-5-1 Kusunoki-cho, Kobe 650-0017, Japan

Elaine Kay
Department of Pathology, Beaumont Hospital, Dublin 9, Ireland

Fumitaka Kikkawa
Nagoya University Graduate School of Medicine, Department of Obstetrics and Gynecology, Tsurumai-cho 65, Showa-ku, Nagoya 466-8550, Japan

Masamichi Kojiro
Department of Pathology, Kurume University School of Medicine, Research Center of Innovative Cancer Therapy of the 21st Century COE Program for Medical Science, Kurume, Japan

Kan Komai
Department of Obstetrics and Gynecology, Kurume University School of Medicine, Research Center of Innovative Cancer Therapy of the 21st Century COE Program for Medical Science, Kurume, Japan

S. Krämer
Universitats-Frauenklinik mit Poliklinik der Eberhard-Karls-Universitat, Calwersstrasse 7, D-72076 Tübingen, Germany

Ryoji Kushima
Division of Diagnostic Pathology, Shiga University of Medical Science Hospital, Seta, Otsu 520-2192, Japan

Heini Lassus
Department of Obstetrics and Gynecology, Helsinki University Central Hospital and Jorvi Hospital, Turuntie 150, 02740 Espoo, Finland

Wai K. Leung
Institute of Digestive Disease and Department of Medicine and Therapeutics, The Chinese University of Hong Kong, Prince of Wales Hospital, 9/F, Clinical Sciences Building, Shatin, Hong Kong

Anne-Marie Levin-Jakobsen
Sahlgrenska University Hospital, Department of Pathology, S-413 45 Göteborg, Sweden

Birgit Luber
Technische Universität München, Klinikum rechts der Isar, Institut für Allgemeine Pathologie und Pathologische Anatomie, Trogerstr. 18, 81675 München, Germany

Sunny Luke
Tissue Engineering Research and Development, Ortec International Inc., 3960 Broadway, New York, NY 10032

Isabel Macedo-Pinto
Anatomy and Pathology Department, Portuguese Institute of Oncology Francisco Gentil Centro Regional do Norte, Rua Dr. António Bernardino de Almeida, 4200-072 Porto, Portugal

Yoshihiko Maehara
Graduate School of Kyushu University, Department of Surgery and Science, 3-1-1 Higashi-ku, Fukuoka 812-8582, Japan

Eva Gloria-Maercker
Institute of Immunology, Witten/Herdecke University, Stockumerstrasse 10, 58448 Witten, Germany

Václav Mandys
Department of Pathology, 3rd Faculty of Medicine, Charles University, Šrobárova 50, 100 34 Prague, Czech Republic

Kristina A. Matkowskyj
University of Illinois at Chicago, Research Associate, Chicago, IL 60612

Yasuko Matsukawa
Division of Surgical Pathology, Department of Biomedical Informatics, Kobe University, Graduate School of Medicine, 7-5-1 Kusunoki-cho, Kobe 650-0017, Japan

Jean Philippe Metges
Institut de Cancerologie et d'Hematologie, Chu Morvan, 5 Avenne Foch, 29200 Brest, France

Upik Anderiani Miskad
Division of Surgical Pathology, Department of Biomedical Informatics, Kobe University, Graduate School of Medicine, 7-5-1 Kusunoki-cho, Kobe 650-0017, Japan

Isao Miyakawa
Department of Obstetrics and Gynecology, Oita University Faculty of Medicine, 1-1 Idaigaoka, Hasama-machi, Yufu-shi, Oita 879-5593, Japan

Shingo Miyamoto
Department of Obstetrics and Gynecology, Kyushu University, Fukuoka, Japan

Takashi Miyatake
Department of Pathology, Mail Stop 8104, University of Colorado at Denver and Health Sciences Center, 12800 East 19th Avenue, P.O. Box 6511, Aurora, CO 80045

Hideki Mizunuma
Department of Obstetrics and Gynecology, Hirosaki University School of Medicine, 5-Zaifu-cho, Hirosaki, Aomori, 036-8562, Japan

Shigehiko Mizutani
Nagoya University Graduate School of Medicine, Department of Obstetrics and Gynecology, Tsurumai-cho 65, Showa-ku, Nagoya 466-8550, Japan

Wolfram Mueller
Gemeinschaftspraxis Pathologie Starnberg, Am Fuchsengraben 3, 82319 Starnberg, Germany

Adnan R. Munkarah
Wayne State University School of Medicine, Department of Obstetrics and Gynecology, Division of Gynecologic Oncology, 4160 John R., Suite 2135, Detroit, MI 48201

Naofumi Nagasue
Department of Digestive and General Surgery, Faculty of Medicine, Shimane University, Izumo, Japan

Hitoo Nakano
Department of Obstetrics and Gynecology, Kyushu University, Fukuoka, Japan

Gerardo Nardone
Department of Clinical and Experimental Medicine, Gastroenterology Unit, University of Naples Federico II, Via Pansini 5, 80131 Napoli, Italy

Ola Nilsson
Sahlgrenska University Hospital, Department of Pathology, S-413 45 Göteborg, Sweden

Naoyo Nishida
Department of Pathology, Kurume University School of Medicine, Research Center of Innovative Cancer Therapy of the 21st Century COE Program for Medical Science, Kurume, Japan

Takashi Nishida
Hita Saiseikai Hospital, Hita, Japan

Seiji Nomura
Nagoya University Graduate School of Medicine, Department of Obstetrics and Gynecology, Tsurumai-cho 65, Showa-ku, Nagoya 466-8550, Japan

Yoshinao Oda
Department of Anatomic Pathology, Graduate School of Medical Sciences, Kyushu University, Fukuoka, Japan

Anthony O´Grady
Department of Pathology, Royal College of Surgeons in Ireland, Smurfit Building, Beaumont Hospital, Dublin 9, Ireland

Yoshihiro Ohishi
Department of Anatomic Pathology, Graduate School of Medical Sciences, Kyushu University, Fukuoka, Japan; Department of Central Medical Examination, Surgical Pathology, Iizuka Hospital, Fukuoka, Japan

Eiji Oki
Department of Surgery and Science, Graduate School of Medical Sciences, Kyushu University 3-1-1, Maidashi, Higashi-ku, Fukuoka 812-8582, Japan

R. I. Olivier
Department of Gynaecology, The Netherlands Cancer Institute/Antoni van Leeuwenhoek Hospital, Plesmanlaan 121, 1066 CX Amsterdam, The Netherlands

Hisashi Onodera
Director of Surgery, St. Luke International Hospital, 9-1 Akashi-cho, Chuo-ku, Tokyo 104-8560, Japan

Antonio Palacín
Service of Pathology, Hospital Clinic, Villaroel 170, 08036 Barcelona, Spain

Manuel Pera
Section of Gastrointestinal Surgery, Hospital Universitaro del Mar, Passeig Maritim 25-29, 08003 Barcelona, Spain

Deolinda Pereira
Medical Oncology Department, Portuguese Institute of Oncology Francisco Gentil Centro Regional do Norte, Rua Dr. António Bernardino de Almeida, 4200-072 Porto, Portugal

João Pinto de Sousa
Surgery B, Hospital S. João, Medical Faculty of the University of Porto, Institute of Molecular Pathology and Immunology of the University of Porto, (IPATIMUP), Alameda Prof. Hernañi Monteiro, 4202-451 Porto, Portugal

Claire L. Plumb
Department of Biomedical Sciences, Ontario Veterinary College, University of Guelph, Guelph, ON, Canada, NIG 2WI

Jens F. Rehfeld
Department of Clinical Biochemistry Rigshospitalet, University of Copenhagen, Blegdamsveg 9, 2100 Copenhagen, Denmark

Bernice Robinson-Bennett
The University of Texas Medical Branch, Department of Obstetrics and Gynecology, Division of Gynecologic Oncology, 301 University Boulevard, Galveston, TX 77555-0587

Cristina Rodriguez-Burford
Department of Pathology, University of Alabama at Birmingham, ZRB 408, 619 18th Street South, Birmingham, AL 35249-6823

Hideki Sakaguchi
Department of Obstetrics and Gynecology, Gifu University, School of Medicine, 1-1 Yanagido, Gifu City 501-1194, Japan

Akiko Sakamoto
Department of Obstetrics and Gynecology, Hirosaki University School of Medicine, 5-Zaifu-cho, Hirosaki, Aomori 036-8562, Japan

Alessandro D. Santin
Department of Obstetrics and Gynecology, Slot 51B, Division of Gynecologic Oncology, University of Arkansas for Medical Sciences Medical Center, 4301 W. Markham, Little Rock, AR 72205

Eriko Sato
Department of Obstetrics and Gynecology, Gifu University, School of Medicine, 1-1 Yanagido, Gifu City 501-1194, Japan

Martin Schreiber
Medical University of Vienna, Department of Obstetrics and Gynecology, Waehringer Guertel 18-20, A-1090 Vienna, Austria

Shuho Semba
Division of Surgical Pathology, Department of Biomedical Informatics, Kobe University, Graduate School of Medicine, 7-5-1 Kusunoki-cho, Kobe 650-0017, Japan

Kiyosumi Shibata
Nagoya University Graduate School of Medicine, Department of Obstetrics and Gynecology, Tsurumai-cho 65, Showa-ku, Nagoya 466-8550, Japan

Kazushi Shigemasa
Department of Obstetrics and Gynecology, Shigemasa Women's Center, 5-6-23, Okinogami, Fukuyama 720-0825, Japan

Shouji Shimoyama
Department of Gastrointestinal Surgery, University of Tokyo, 7-3-1 Hongo, Bunkyo-ku, Tokyo 113-8655, Japan

Kenneth R. Shroyer
Department of Pathology, Mail Stop 8104, University of Colorado at Denver and Health Sciences Center, Room 5127, 12800 East 19th Avenue, P.O. Box 6511, Aurora, CO 80045

Gad Singer
Institute of Pathology, University Hospital of Basel, Schöenbeinstrasse 40, 4031 Basel, Switzerland

Susan F. Slovin
Genitourinary Oncology Service, Department of Medicine, Memorial Sloan-Kettering Cancer Center, New York, NY 10021

Wolfgang Sommergruber
Boehringer Ingelheim Austria, Lead Discovery, Dr. Boehringer-Gasse 5-11, A-1121 Vienna, Austria

Stefania Staibano
Department of Biomorphological and Functional Sciences, Pathology Section, University Federico II Faculty of Medicine and Surgery, Via S. Pansini 5, 80131 Naples, Italy

Mark H. Stoler
Department of Pathology, University of Virginia, Health Sciences Center, P.O. Box 800214, Charlottesville, VA 22908

Stephen L. Strobel
St. Vincent Mercy Medical Center, Department of Pathology, 2222 Cherry Street, Toledo, OH 43608

Wenshu Sun
Department of Obstetrics and Gynecology, Gifu University, School of Medicine, 1-1 Yanagido, Gifu City 501-1194, Japan

Hideki Tabara
Department of Digestive and General Surgery, Faculty of Medicine, Shimane University, Izumo, Japan

Noriyuki Takai
Department of Obstetrics and Gynecology, Oita University Faculty of Medicine, 1-1 Idaigaoka, Hasama-machi, Yufu-shi, Oita 879-5593, Japan

Teruhiko Tamaya
Department of Obstetrics and Gynecology, Gifu University, School of Medicine, 1-1 Yanagido, Gifu City 501-1194, Japan

Sadafumi Tamiya
Department of Anatomic Pathology, Graduate School of Medical Sciences, Kyushu University, Fukuoka, Japan

Kong-Bing Tan
Department of Pathology, Yong Loo Lin School of Medicine, National University of Singapore, National University Hospital, Lower Kent Ridge Road, Singapore 119074

Kenichi Tanaka
Niigata University, Graduate School of Medical and Dental Sciences, Department of Obstetrics and Gynecology, 1-757 Asahimachi dori, Niigata 951-8510, Japan

Ming Teh
Department of Pathology, Yong Loo Lin School of Medicine, National University of Singapore, National University Hospital, Lower Kent Ridge Road, Singapore 119074

Antoinette Thomas
Department of Pathology and Laboratory Medicine, Indiana University School of Medicine, University Hospital 3465, 550 North University Boulevard, Indianapolis, IN 46202

Andrew J. Tiltman
University of Cape Town, South Africa

Eriko Tokunaga
Graduate School of Kyushu University, Department of Surgery and Science, 3-1-1 Higashi-ku, Fukuoka 812-8582, Japan

Luigi Tornillo
Institute of Pathology, University Hospital of Basel, Schöenbeinstrasse 40, 4031 Basel, Switzerland

Hiroshi Toyoki
Department of Obstetrics and Gynecology, Gifu University, School of Medicine, 1-1 Yanagido, Gifu City 501-1194, Japan

Shizuki Tsukashita
Division of Diagnostic Pathology, Shiga University of Medical Science Hospital, Seta, Otsu 520-2192, Japan

Masazumi Tsuneyoshi
Department of Anatomic Pathology, Graduate School of Medical Sciences, Kyushu University, Fukuoka, Japan

M. van Beurden
Department of Gynaecology, The Netherlands Cancer Institute, Antoni van Leeuwenhoek Hospital, Plesmanlaan 121, 1066 CX Amsterdam, The Netherlands

Caroline Van Haaften
Carocell, Pty, Ltd, Veerstraat 31, 2311 NA Leiden, The Netherlands

Oscar Vidal
Service of General and Digestive Surgery, Hospital Clinic, Villarroel 170, 08036 Barcelona, Spain

Alain Volant
Service d'Anatomie Pathologique, Chu de la Cavale Blançhe, Boulevard Tanguy Prigent, 29200 Brest, France

Tilman Voss
Boehringer Ingelheim Austria, Lead Discovery, Dr. Boehringer-Gasse 5-11, A-1121 Vienna, Austria

Hanlin L. Wang
Department of Pathology and Immunology, Washington University School of Medicine, 660 South Euclid Avenue, Box 8118, St. Louis, MO 63110-1093

Timothy C. Wang
Division of Digestive and Liver Diseases, Columbia University Medical Center, New York, NY 10032

A. Woll-Herrmann
Klinik fur Frauenheilkunde und Geburtshilfe des Universitatsklinikums Schleswig-Holstein, Campus Lubeck Ratzeburger Allee 160, D-23538 Lubeck, Germany

Jian Yu Wu
Biology of Aging Laboratory, Department of Geriatrics, Geneva University Hospitals, Chemin de petit Bel Air 2, CH-1225 Chêne-Bourg, Geneva, Switzerland

Hirohisa Yano
Department of Pathology, Kurume University School of Medicine, Research Center of Innovative Cancer Therapy of the 21st Century COE Program for Medical Science, Kurume University, Kurume, Japan

Yoshihito Yokoyama
Department of Obstetrics and Gynecology, Hirosaki University School of Medicine, 5-Zaifu-cho, Hirosaki, Aomori 036-8562, Japan

Hiroshi Yokozaki
Division of Surgical Pathology, Department of Biomedical Informatics, Kobe University, Graduate School of Medicine, 7-5-1 Kusunoki-cho, Kobe 650-0017, Japan

Jun Yu
Institute of Digestive Disease and the Department of Medicine and Therapeutics, The Chinese University of Hong Kong, Prince of Wales Hospital 9/F, Clinical Sciences Building, Shatin, Hong Kong

Maciej Zabel
Department of Histology and Embryology, Wroclaw Medical University, Chalubinskiego 6a, 50-368 Wroclaw, Poland

Kurt S. Zänker
Institute of Immunology, University of Witten/Herdecke, Stockumerstrasse 10, 58448 Witten, Germany

Hui Zhou
Department of Pathology, University of Bonn, Sigmund-Freud-Str. 25, D-53127 Bonn, Germany

This Page Intentionally Left Blank

Foreword

According to mortality data from the National Center for Health Statistics, approximately 1,334,100 new cases of cancer will have been diagnosed and 556,500 people will have died from cancer in the United States by the end of 2003. Although the number of cancer-related deaths has been on the decline since 1992, the incidence has increased over the same period. This increase is largely the result of implementation of improved screening techniques that have been made possible by advances in immunochemical diagnostic testing. As immunochemical techniques, such as *in situ* hybridization (ISH) and immunohistochemisty (IHC), continue to be refined, their use in improving patient care through research and improved methods of diagnosis is becoming ever more valuable.

The ISH technique is a well-established approach for identifying the organization and physical position of a specific nucleic acid within the cellular environment, by means of hybridizing a complementary nucleotide probe to the sequence of interest. The use of deoxyribonucleic acid (DNA) and ribonucleic acid (RNA) as probes to assay biological material has been the custom for approximately 30 years. However, advances in ISH have led to the replacement of radioactive detection by more adaptable colorimetric and fluorescence *in situ* hybridization methods for the interrogation of nuclei; metaphase chromosomes; DNA fibers; patient tissue; and, most recently, deriving information from patient samples using DNA microarrays. Technologic advances, including array comparative genomic hybridization, spectral karyotyping, and multicolor banding, have provided a refinement in the study of genome organization and chromosomal rearrangements. In addition, ISH using RNA has allowed for a determination of the expression pattern and the abundance of specific transcripts on a cell-to-cell basis. Advances in DNA and RNA ISH have migrated from the research setting and are becoming routine tests in the clinical setting, permitting examination of the steps involved in tumorigenesis, which would not have been possible by the use of classical cytogenetic analysis.

Since the introduction of monoclonal antibodies, IHC has developed into a vital tool that is now extensively used in many research laboratories, as well as for clinical diagnosis. IHC is a collective term for a variety of methods, which can be used to identify cellular or tissue components by means of antigen–antibody interactions. Immunostaining techniques date to the pioneering work by Albert Coons in the early 1940s, using fluorescein-labeled antibodies. Since then, developments in the techniques have permitted visualization of antigen–antibody interactions by conjugation of the antibody to additional fluorophores, enzymes, or radioactive elements. Because there is wide variation in tissue types, antigen availability, antigen–antibody affinity, antibody types, and detection methods, it is essential to select antibodies almost on a case-to-case basis. The consideration of these factors has led to the identification of several key antibodies that have great utility in the study and diagnosis of tumors.

The scientific advances in the field of IHC have necessitated rapid developments in microscopy, image capture, and analytical software to objectively quantify results. These cutting-edge experimental systems have already produced many significant differences between cancers that might not have been distinguished by conventional means.

The focus of these volumes is the use of ISH and IHC to study the molecular events occurring at the DNA, RNA, and protein levels during development and progression of human carcinomas. Continued investment of time and expertise by researchers worldwide has contributed significantly to a greater understanding of the disease processes. Because the technical requirements for many immunohistochemical techniques are quite demanding and the methodology itself poses many pitfalls, the step-by-step methods provided in these volumes will serve as an excellent guide for both clinical and basic researchers studying human malignancies.

Simon Hughes
Ontario Cancer Institute
Princess Margaret Hospital
Toronto, Canada

This Page Intentionally Left Blank

Preface

Mutations cause ~10% of all human diseases (other than infections) ranging from single-gene disorders to complex diseases and cancer. Approximately 5% of all people reaching 25 years of age are affected by mutations, and 60% of all humans are affected in some way by mutations. The World Cancer Report states that in the year 2000 there were 10 million new cases of cancer worldwide. This figure is predicted to increase to 15 million new cases by the year 2020 as a result of steadily aging populations, smoking prevalence, and unhealthy lifestyles. Cancer accounts for 12% of 56 million annual deaths globally from all causes. By 2020, it is estimated that >16% of the U.S. population will be ~65 years of age, increasing to >20% by the year 2050, and reaching nearly 20 million individuals >85 years of age by mid-century. These data clearly indicate the enormity of the health problem we are facing and the need for early diagnosis of cancer. In this volume and the other three volumes of the series, an attempt has been made to translate molecular genetics into clinical practice. In this regard it is important to understand the role of biomarkers in cancer initiation, progression, and metastasis, which are discussed in these volumes.

For commonly occurring cancers, including gastrointestinal cancer and ovarian cancer, it is likely that interaction of multiple proteins in pathways, as well as interactions between genetic variants, and exposures are involved in the causal etiology of the phenotype. In understanding cancer development, priority should be given both to studies that consider molecularly plausible interactions of multiple genes in a pathway and to interactions of environmental exposures with genetic variants that are involved in the metabolism of these exposures. Comparatively, single-gene studies are becoming less important. It is likely that in most cases genes do not act alone; instead they interact with other genes or biomarkers in identifiable pathways. This approach will provide more meaningful information about disease etiology or outcome and thus allow it to be further translated into the elucidation of disease mechanisms and cancer prevention.

One of the primary objectives of this volume is the same as that of Volumes 1, 2, and 3—that is, discussion of procedures of immunohistochemistry (IHC) and *in situ* hybridization (ISH), including fluorescence *in situ* hybridization (FISH), as they are used in the field of pathology, especially in cancer diagnosis. The practical importance of the antigen-retrieval protocol in IHC was realized in 1991, and since then it has been used routinely in pathology laboratories. Many chapters in this volume contain the details of this protocol, although not all antigens require antigen retrieval for their detection. In this volume, IHC, ISH, and FISH of two major carcinomas (gastrointestinal and ovarian) are presented. Lung and breast carcinomas were discussed in Volume 1, colorectal and prostate carcinomas were detailed in Volume 2, and hepatocellular and pancreatic carcinomas were presented in Volume 3.

Another objective of this volume is the discussion of the role of molecular genetics (molecular pathology, molecular medicine, and molecular morphology) in understanding and achieving correct diagnosis and therapy in neoplastic diseases. Cancer is ultimately a genetic disease, and as such, the focus of much cancer research has been directed toward understanding which, and how many, oncogenes are activated and which tumor-suppressor genes become dysfunctional in human malignancies.

The elucidation of the genetic events underlying the initiation and progression of malignancy has been hampered by limitations inherent in both *in vitro* and *in vivo* methods of study. The limitation of an *in vitro*–based system is that genetic information obtained from cell lines may not accurately represent the molecular events occurring in the actual tissue milieu from which they were derived. *In vivo* genetic analysis is limited because of the inability to procure pure populations of cells from complex, heterogeneous tumor tissue. The development and use of molecular-based therapy for human malignancies will require a detailed molecular genetic analysis of patient tissue, including resolving the two previously mentioned limitations.

Molecular genetics/pathology has the advantage of assessing genes directly. Knowledge of the genetic basis of disease will, in turn, allow more specific targeting of the cause, rather than only the symptoms of the disease. The time is overdue to apply our knowledge of molecular genetics, in conjunction with IHC, FISH, and histology, to diagnostic, therapeutic, and prognostic decisions.

Genetic information will improve the prognosis used to monitor both the efficacy of treatment and disease recurrence. Molecular markers, largely from tumors but also from the germline, have great potential for diagnosis, for directing treatment, and as indicators of the outcome. The role of mutations in cancer is emphasized because the characteristics of the tumor depend on the mutations that led to their emergence. Widespread molecular testing is the future for clinical practice. Indeed, methods of molecular testing of tumors are well established and are discussed in this and other volumes of this series of handbooks.

Unfortunately, clinical practice has lagged behind the current knowledge of research in molecular genetics. Both technicians and pathologists need to be aware of the importance of molecular pathology testing. Somatic mutations are rarely performed, although some histopathology and cytogenetics laboratories have done limited testing, such as chromosomal rearrangements in lymphoma. Molecular testing should be regarded as a means of complementing, rather than replacing, established methods such as IHC and FISH.

It was challenging to bring some semblance of order to the vast body of information in the field of molecular genetics (molecular pathology), which has become available primarily in scientific journals during the past decade. The contributions in this volume by expert molecular geneticists and clinical pathologists in each of their disciplines have made it possible to accept this challenge.

The range of methods to examine genetic abnormalities has widened enormously, and many new and powerful molecular, IHC, and ISH techniques have become available. These include the detection of mutations using the polymerase chain reaction (PCR), reverse transcription-PCR, differential display of gene expression, DNA sequencing, and comparative genomic hybridization on genomic microarrays to detect gene amplifications and detentions on a genome-wide basis. Other relevant techniques include serial analysis of gene expression, suppression substractive hybridization, rolling circle amplification, Southern blot hybridization, specific-cloned probes, and flow cytometry.

Various signal amplification approaches have also been introduced to increase the sensitivity, accompanied by reduced nonspecific background staining of IHC. Similarly, the conventional PCR method has been improved through quantitative real-time PCR. Standard ISH has been improved by modifications such as FISH and chromogenic ISH. Most of the aforementioned methods are discussed in Volumes 1–3, and the remaining are presented in this volume.

Pathologists are well advised to adapt to modern therapeutic shifts (i.e., morphologic interpretation needs to be combined with molecular diagnostic modalities). The latter protocols can provide a second level of testing that is particularly useful for the analysis of neoplasms for which histologic and immunophenotypic data are inconclusive. We are already on a path that has the potential to alter oncology clinical practice. Therapies are beginning to move toward specific molecular targets. My hope, through these volumes, is to expedite the translation of molecular genetics into clinical practice.

Each chapter is comprehensive and stands alone in terms of determination of cancer diagnosis, so the reader does not have to scour multiple places in the book or outside sources. A literature review of the subject matter from the early 1990s to the present is also included in most chapters. The results of most methods are shown by including a color photomicrograph that contains useful immunohistochemical or FISH diagnostic information: these illustrations facilitate the interpretation of the results obtained. Each chapter is organized logically, providing an introduction, materials required (including reagents, antibodies, apparatuses, and commercial sources), methods, results, and discussion. The procedures are explained in a detailed, step-by-step fashion so that the reader can use them without additional references. Advantages and limitations of the methods used for cancer diagnosis are also presented.

There are several reasons for the limited use of molecular genetics in clinical practice. One reason is the high cost of establishing facilities for molecular techniques; another is our comparatively meager understanding of the nature of many diseases, including cancer. Although equipment for molecular testing is available, some investment is needed. Another reason is the dearth of clinician/scientist training programs, resulting in limited clinician/scientists. Also, an inequity in pay exists between those working in clinical practice and research faculty. Accordingly, the difference in pay may be a disincentive for choosing a full-time career in medical research. The length of time (8 years as an average) necessary to receive the MD/PhD is probably also a barrier in the development of new clinician/scientists. Also, many clinician/scientist trainees are married or in stable relationships, and personal time for family life and children is increasingly important to them. Narrowing the gap in income between clinical

practitioners and full-time medical researchers would provide a positive incentive for this profession.

I am indebted to the authors of the chapters for their promptness, and I appreciate their dedication and hard work in sharing their expertise with the readers. In most cases the protocols presented were either introduced or refined by the authors and are routinely used in their clinical pathology laboratories. The methods presented offer much more detailed information than is available in scientific journals. Because of its relatively recent emergence from the research laboratory, many molecular pathology protocols are still found in scientific journals and have not appeared in a book. Each chapter provides unique, individual, practical knowledge based on the expertise of the author. As with all clinical laboratory testing, the results obtained should be interpreted in conjunction with other established and proven laboratory data and clinical findings.

This volume has been developed through the efforts of 159 authors and co-authors representing 24 countries. The high quality of each manuscript made my work as the editor an easy one. The authors were gracious and prompt. Considering the increasing volume of original research being published rapidly in a variety of journals and formats, there is a need to provide busy physicians with authoritative, timely overviews of key developments in a compact form and, most importantly, practical information on how these advancements can be applied in the diagnosis and treatment of patients. These volumes attempt to provide this assistance. This volume also is intended for use in research and clinical laboratories by medical technicians and pathologists, especially in the field of oncology. This volume and other volumes of the series will also be of interest and help to teachers and medical students.

I am thankful to Dr. Dawood Farahi and the Board of Trustees of Kean University for recognizing the importance of scholarship. I appreciate the cooperation extended to me by Philip Carpenter, and I am grateful to Elizabeth McGovern for her expert help in preparing this volume.

M.A. Hayat
June 2005

This Page Intentionally Left Blank

Selected Definitions

Ablation: Ablation consists of removal of a body part or the destruction of its function.

Adenocarcinoma: Adenocarcinoma is a malignant neoplasm of epithelial cells in a glandular or glandlike pattern.

Adenoma: Adenoma is a benign epithelial neoplasm in which the tumor cells form glands or glandlike structures. It does not infiltrate or invade adjacent tissues.

Adjuvent: Adjuvent is a substance that nonspecifically enhances or potentiates an immune response to an antigen; something that enhances the effectiveness of a medical treatment.

Affinity: Affinity is a measure of the bonding strength (association constant) between a receptor (one binding site on an antibody) and a ligand (antigenic determinant).

Algorithm: An algorithm is a step-by-step procedure for management of a health care problem.

Allele: An allele is one of two or more alternative forms of a single gene locus. Different alleles of a gene have unique nucleotide sequences, and their activities are all concerned with the same biochemical and developmental process, although their individual phenotypes may differ. An allele is one of several alternate forms of a gene at a single locus that controls a particular characteristic.

Alternative Splicing: Genes with new functions often evolve by gene duplication. Alternative splicing is another means of evolutionary innovation in eukaryotes, which allows a single gene to encode functionally diverse proteins (Kondrashov and Koonin, 2001). In other words, alternative splicing refers to splicing the same pre-mRNA in two or more ways to yield two or more different protein products. Alternative splicing can produce variant proteins and expression patterns as different as the products of different genes. Alternative splicing either substitutes one protein sequence segment for another (substitution alternative splicing) or involves insertion or deletion of a part of the protein sequence (length-difference alternative splicing). Thus, alternative splicing is a major source of functional diversity in animal proteins. Many types and large numbers of proteins are required to perform immensely diverse functions in a eukaryote.

Lack of correlation between the complexity of an organism and the number of genes can be partially explained if a gene often codes for more than one protein. Individual genes with mutually alternative exons are capable of producing many more protein isoforms than there are genes in the entire genome. A substantial amount of exon duplication events lead to alternative splicing, which is a common phenomenon. Indeed, alternative splicing is widespread in multicellular eukaryotes, with as many as one (or more) in every three human genes producing multiple isoforms (Mironov *et al.,* 1999). Alternative splicing is an ubiquitous mechanism for the generation of multiple protein isoforms from single genes, resulting in the increased diversity in the proteomic world.

Amplification: Amplification refers to the production of additional copies of a chromosomal sequence, found as intrachromosomal or extrachromosomal DNA. Amplification is selective replication of a gene to produce more than the normal single copy in a haploid genome.

Anaplasia: Anaplasia results in the regression of cells and tissues to an undifferentiated state (dedifferentiation) in most malignant neoplasms.

Aneuploidy: Aneuploidy is the abnormal condition in which one or more whole chromosomes of a normal set of chromosomes either are missing or are present in more than the usual number of copies. Aneuploidy refers to not having the normal diploid number of chromosomes.

Annealing of DNA: Annealing of DNA is the process of bringing back together two separate strands of denatured DNA to re-form a double helix.

Antibody: Antibody (immunoglobulin) is a protein produced by B lymphocytes that recognizes a particular foreign antigenic determinant and facilitates clearance of that antigen; antigens can also be carbohydrates and even DNA.

Antigen: An antigen is a foreign substance that binds specifically to antibody or T-cell receptors and elicits an immune response.

Antigenic Determinant: Antigenic determinant is the site on an antigenic molecule that is recognized and bound by antibody.

Apoptosis: Apoptosis is the capacity of a cell to undergo programmed cell death. In response to a stimulus, a pathway is triggered that leads to destruction of the cell by a characteristic set of reactions. Failure to apoptose allows tumorigenic cells to survive and thus contribute to cancer.

Avidity: Avidity is referred to as the functional binding strength between two molecules such as an antibody and an antigen. Avidity differs from affinity because it reflects the valency of the antigen–antibody interaction.

Carcinoma: Carcinoma is one of various types of malignant neoplasms arising from epithelial cells, mainly glandular (adenocarcinoma) or squamous cells. Carcinoma is the most common cancer and displays uncontrolled cellular proliferation, anaplasia, and invasion of other tissues, spreading to distant sites by metastasis. The origin of carcinoma in both sexes is skin (in men it originates in the prostate, and in women it originates in the breast). The most frequent carcinoma in both sexes is bronchogenic carcinoma.

Cardia: The part of the stomach close to the esophageal opening, which contains the cardiac glands.

cDNA (Complementary Deoxyribonucleic Acid): mRNA molecules are isolated from cells, and DNA copies of these RNAs are made and inserted into a cloning vector. The analysis of that cloned cDNA molecule can then provide information about the gene that encoded the mRNA. The end result is a cDNA library.

Chromosomal Aberration: Chromosomal aberration is a change in the structure or number of chromosomes. The variation from the wild-type condition is either chromosome number or chromosome structure. Four major types of aberrations are deletions, duplications, inversions, and translocations. Variations in the chromosome number of a cell give rise to aneuploidy, monoploidy, or polyploidy.

Chromosomal Instability: Chromosomal instability is defined as an increased rate of chromosome aberrations, in contrast to microsatellite instability, which induces alterations of DNA repeat sequences but no changes in chromosome number or structure. Chromosomal instability is associated with aggressive tumor behavior and poor prognosis.

Clinical Guidelines: Clinical guidelines are statements aimed to assist clinicians in making decisions regarding treatment for specific conditions. They are systematically developed, evidence-based, and clinically workable statements that aim to provide consistent and high-quality care for patients. From the perspective of litigation, the key question has been whether guidelines can be admitted as evidence of the standard of expected practice or whether this would be regarded as hearsay. Guidelines may be admissible as evidence in the United States if qualified as authoritative material or a learned treatise, although judges may objectively scrutinize the motivation and rationale behind guidelines before accepting their evidential value (Samanta *et al.,* 2003). The reason for this scrutiny is the inability of guidelines to address all the uncertainties inherent in clinical practice. However, clinical guidelines should form a vital part of clinical governance.

Clone: A clone is a group of cells that are genetically identical to the original individual cell.

Codon: A codon is a three-base sequence in mRNA that causes the insertion of a specific amino acid into polypeptide or causes termination of translation.

Cohort: A designated group followed or traced over a period of time.

Concatemers: Concatemers are DNAs of multiple genome length.

Constitutive Gene: A constitutive gene is a gene whose products are essential to normal cell functioning, no matter what the life-supporting environmental conditions are. These genes are always active in growing cells.

Constitutive Mutation: Constitutive mutation is a mutation that causes a gene to be expressed at all times, regardless of normal controls.

Cytokines: Cytokines are a group of secreted low-molecular-weight proteins that regulate the intensity and duration of an immune response by stimulating or inhibiting the proliferation of various immune cells or their secretion of antibodies or other cytokines.

Deletion: Deletion is a mutation involving a loss of one or more base pairs; a chromosomal segment or gene is missing.

Dendritic Cell: A dendritic cell is a type of antigen-presenting cell that has long membrane processes (resembling dendrites of nerve cells) and is found in the lymph nodes, spleen, thymus, skin, and other tissues.

Determinant: The determinant is the portion of an antigen molecule that is recognized by a complementary section of an antibody or T-cell receptor.

Diagnosis: Diagnosis means the differentiation of malignant from benign disease or of a particular malignant disease from others. A tumor marker that helps in diagnosis may be helpful in identifying the most effective treatment plan.

DNA Methylation: Genetic mutations or deletions often inactivate tumor-suppressor genes. Another mechanism for silencing genes involves DNA methylation.

In other words, in addition to genetic alterations, epigenetics controls gene expression, which does not involve changes of genomic sequences. DNA methylation is an enzymatic reaction that brings a methyl group to the 5th carbon position of cystine located 5′ to guanosine in a cytosine guanine (CpG) dinucleotide within the gene promoter region. This results in the prevention of transcription. Usually multiple genes are silenced by DNA methylation in a tumor; DNA methylation of genes, however, is not common in normal tissues. Gene methylation profiles, almost unique for each tumor type, can be detected in cytologic specimens by methylation-specific polymerase chain reaction (Pu and Clark, 2003).

In the human genome, ~80% of CpG dinucleotides are heavily methylated, but some areas remain unmethylated in GC-rich CpG island (Bird, 2002). In cancer cells, aberrant DNA methylation is frequently observed in normally unmethylated CpG islands, resulting in the silencing of the function of normally expressed genes. If the silencing occurs in genes critical to growth inhibition, the epigenetic alteration could promote tumor progression resulting from uncontrolled cell growth. However, pharmacologic demethylation can restore gene function and promote death of tumor cells (Shi *et al.,* 2003).

ELISA: Enzyme-linked immunosorbent assay in which antibody or antigen can be quantitated by using an enzyme-linked antibody and a colored substance to measure the activity of the bound enzyme.

Encode: Encode refers to containing the information for making an RNA or polyeptide; a gene can encode an RNA or a polypeptide.

Epidemiology: The study of the occurrence of disease in specified populations to control health problems.

Epigenetics: Epigenetics can be defined as the study of mitotically or meiotically heritable changes in gene function that cannot be explained by changes in DNA sequence. Epigenetic change means an alteration in the expression of a gene but not in the structure of the gene itself. Processes less irrevocable than mutation fall under the umbrella term "epigenetic." Known molecular mechanisms involved in epigenetic phenomenon include DNA methylation, chromatin remodeling, histone modification, and RNA interference. Patterns of gene expression regulated by chromatin factors can be inherited through the germline (Cavalli and Paro, l999). The evidence that heritable epigentic variation is common raises questions about the contribution of epigenetic variation to quantitative traits in general (Rutherford and Henikoff, 2003).

Epitope: An epitope is the antigenic determinant or antigen site that interacts with an antibody or T-cell receptor.

Exon/Intron: An exon is the region of a gene that is ultimately represented in the gene's mature transcript, in both the DNA and its RNA product. Eukaryotic genes contain noncoding sequences (introns) embedded into coding sequences (exons). The introns are removed (splicing) following transcription of DNA into RNA.

Familial Trait: A familial trait is a trait shared by members of a family.

FISH: Fluorescent *in situ* hybridization is a technique of hybridizing a fluorescence probe to whole chromosome to determine the location of a gene or other DNA sequence within a chromosome.

Gastritis: Gastritis refers to the inflammation, especially mucosal, of the stomach.

Gene: A gene is the basic unit of heredity and contains the information for making one RNA and, in most cases, one polypeptide.

Gene Cloning: Gene cloning means generating many copies of a gene by inserting it into an organism (e.g., bacterium) where it can replicate along with the host.

Gene Expression: Gene expression is the process by which gene products are made.

Gene Family: A gene family consists of a set of genes whose exons are related; the members were derived by duplication and variation from some ancestral genes.

Gene Mutation: A gene mutation is a heritable alteration of the genetic material, usually from one allele form to another. A gene mutation is confined to a single gene.

Gene Therapy: Gene therapy is defined as a therapy in which a gene(s) or gene-transducer cells are introduced to the patient's body for a therapeutic or gene-marking purpose. Gene therapy by definition is not necessarily a molecular targeting therapy, but the reason for the high expectations is that new mechanisms of cancer cell targeting can be integrated into the therapy.

Genetic Code: Genetic code is the set of 64 codons and the amino acids (or terminations) they stand for. It is the correspondence between triplets in DNA (or RNA) and amino acids in protein.

Genetic Mapping: Genetic mapping determines the linear order of genes and the distances between them.

Genome: The genome is the total amount of genetic material in a cell. In eukaryotes it is the haploid set of chromosomes of an organism.

Genomic Instability: It takes many years to get a cancer. Approximately 20 years may elapse from the time of exposure to a carcinogen to the development of a clinically detectable tumor. During this time, tumors are characterized by genomic instability, resulting in the progressive accumulation of mutations and phenotypic changes. Some of the mutations bypass the host regulatory processes that control cell location, division,

expression, adaptation, and death. Genetic instability is manifested by extensive heterogeneity of cancer cells within each tumor.

Destabilized DNA repair mechanisms can play an important role in genomic instability. Human cells may use at least seven different repair mechanisms to deal with DNA lesions that represent clear danger to survival and genomic stability. For example, homologous recombination repair, nonhomologous end-joining, and mismatch repair mechanisms normally act to maintain genetic stability, but, if they are deregulated, genomic instability and malignant transformation might occur (Pierce *et al.,* 2001). Also, because the human genome contains ~500,000 members of the *Alu* family, increased levels of homologous/homologous recombination events between such repeats might lead to increased genomic instability and contribute to malignant progression (Rinehart *et al.,* 1981).

In addition, BCR/ABL oncogenic tyrosine kinase allows cells to proliferate in the absence of growth factors, protects them from apoptosis in the absence of growth factors or external survival factors, and promotes invasion and metastasis. The unrepaired and/or aberrantly repaired DNA lesions resulting from spontaneous or drug-induced damage can accumulate in BCR/ABL-transformed cells, which may lead to genomic instability and malignant progression of the disease (Skorski, 2002).

Genomic Imprinting: Genomic imprinting is a phenomenon by which the two alleles of certain genes are differentially expressed according to their parental origin.

Genomic Library: The genomic library is a set of clones containing DNA fragments derived directly from a genome, rather than from RNA; the collection of molecular clones that contain at least one copy of every DNA sequence in the genome.

Genotype: The genotype is the combined genetic material inherited from both parents; also the alleles present at one or more specific loci. In other words, the genotype is the allelic constitution of a given individual.

Germline: The germline is the unmodified genetic material that is transmitted from one generation to the next through the gametes.

Germline Mutations: Mutations in the germline of sexually reproducing organisms may be transmitted by the gametes to the next generation, giving rise to an individual with the mutant state in both its somatic and germline cells.

G1 Phase: G1 phase is the period of the eukaryotic cell cycle between the last mitosis and the start of DNA replication.

G2 Phase: G2 phase is the period of the eukaryotic cell cycle between the end of DNA replication and the start of the next mitosis.

Haploinsufficiency: Although classically tumor-suppressor genes are thought to require mutation or loss of both alleles to facilitate tumor progression, for some genes, haploinsufficiency, which is loss of only one allele, may contribute to carcinogenesis.

Hepatitis: Hepatitis consists of inflammation of the liver caused by viral infection or toxic agents.

Heterozygous: Heterozygous refers to a diploid organism having different alleles of one or more genes. As a result, the organism produces gametes of different genotypes.

Humoral Immunity: Humoral immunity is the immunity that can be transferred by antibodies present in the plasma, lymph, and tissue fluids.

Hybridization: Hybridization is the pairing of complementary RNA and DNA strands to give an RNA/DNA hybrid. In other words, pairing of two complementary single-stranded nucleotides according to the base pairing rules: cytosine with guanine and adenine with thymine.

Immunotherapy: Immunotherapy involves delivering therapeutic agents conjugated to monoclonal antibodies that bind to the antigens at the surface of cancer cells. Ideal antigens for immunotherapy should be strongly and uniformally expressed on the external surface of the plasma membrane of all cancer cells. Many solid neoplasms often demonstrate regional variation in the phenotypic expression of antigens. These regional differences in the immunophenotypic profile within the same tumor are referred to as intratumoral heterogeneity. Therapeutic agents that have been used include radioisotopes, toxins, cytokines, chemotherapeutic agents, and immunologic cells.

Kaposi's Sarcoma: Kaposi's sarcoma is a multifocal malignant neoplasm that occurs in the skin and lymph nodes. It consists of cutaneous lesions that are reddish to dark blue in color, found commonly in men older than 60 years of age or in patients with AIDS.

Laser-Capture Microdissection: Tissue heterogeneity and the consequent need for precision before specimen analysis present a major problem in the study of disease. Even a tissue biopsy consists of a heterogenous population of cells and extracellular material, and analysis of such material may yield misleading or confusing results. Cell cultures can be homogenous but not necessarily reflect the *in vivo* condition. Therefore, a strategy is required to facilitate selective purification of relevant homogenous cell types.

The technology of laser-capture microdissection allows extraction of single cells or defined groups of cells from a tissue section. This technique is important for characterizing molecular profiles of cell populations within a heterogeneous tissue. In combination with various downstream applications, this method provides the possibility of cell-type of even cell-specific investigation

of DNA, RNA, and proteins (Mikulowska-Mennis *et al.,* 2002).

Library: A library is a set of cloned fragments together representing the entire genome.

Ligand: A ligand is a molecule recognized by a receptor structure.

Linkage: Linkage is the tendency of genes or other DNA sequences at specific loci to be inherited together as a consequence of their physical proximity on a single chromosome.

Loss of Heterozygosity: Loss of one copy of a chromosomal region is termed loss of heterozygosity (LOH). In the majority of cases where the gene mutation is recessive, tumor cells often retain only the mutated allele and lose the wild-type one. This loss is known as LOH.

Lymph: Lymph is the intercellular tissue fluid that circulates through the lymphatic vessels.

Lymphadenopathy: Lymphadenopathy is the enlargement of the lymph nodes.

Lymph Nodes: Lymph nodes are small secondary lymphoid organs containing populations of lymphocytes, macrophages, and dendric cells, which serve as sites of filtration of foreign antigens and activation of lymphocytes.

Lymphokines: Lymphokines is a generic term for cytokines produced by activated lymphocytes, especially T cells, that act as intercellular mediators of the immune response.

Lymphoma: Lymphoma is a cancer of lymphoid cells that tends to proliferate as solid tumors.

Malignant: Malignant tumors have the capacity to invade and alter normal tissue.

Marker (Biomarker): A marker is a mutated gene or its product that serves as a signpost at a known location in the genome.

Metastasis: Initially tumor growth is confined to the original tissue of origin, but eventually the mass grows sufficiently large to push through the basement membrane and invade other tissues. When some cells lose adhesiveness, they are free to be picked up by lymph and carried to lymph nodes, or they may invade capillaries and enter blood circulation. If the migrant cells can escape host defenses and continue to grow in the new location, a metastasis is established. More than half of cancers have metastasized by the time of diagnosis. Usually it is the metastasis that kills the person rather than the primary (original) tumor.

Metastasis itself is a multistep process. The cancer must break through any surrounding covering (capsule) and invade the neighboring (surrounding) tissue. Cancer cells must separate from the main mass and must be picked up by the lymphatic or vascular circulation. The circulating cancer cells must lodge in another tissue. Cancer cells traveling through the lymphatic system must lodge in a lymph node. Cancer cells in vascular circulation must adhere to the endothelial cells and pass through the blood vessel wall into the tissue. For cancer cells to grow, they must establish a blood supply to bring oxygen and nutrients; this usually involves angiogenesis factors. All of these events must occur before host defenses can kill the migrating cancer cells.

If host defenses are to be able to attack and kill malignant cells, they must be able to distinguish between cancer and normal cells. In other words, there must be immunogens on cancer cells not found on normal cells. In the case of virally induced cancer circulating cells, viral antigens are often expressed, and such cancer cells can be killed by mechanisms similar to those for virally infected tissues. Some cancers do express antigens specific for those cancers (tumor-specific antigens), and such antigens are not expressed by normal cells.

As already stated, metastasis is the principal cause of death in individuals with cancer; yet, its molecular basis is poorly understood. To explore the molecular difference between human primary tumors and metastases, Ramaswamy and Golub (2003) compared the gene-expression profiles of adenocarcinoma metastases of multiple tumor types with unmatched primary adenocarcinomas. They found a gene-expression signature that distinguished primary from metastatic adenocarcinomas. More importantly, they found that a subset of primary tumors resembled metastatic tumors with respect to this gene-expression signature. The results of this study differ from most earlier studies in that the metastatic potential of human tumors is encoded in the bulk of a primary tumor. In contrast, some earlier studies suggest that most primary tumor cells have low metastatic potential, and cells within large primary tumors rarely acquire metastatic capacity through somatic mutation (Poste and Fidler, 1980). The emerging notion is that the clinical outcome of individuals with cancer can be predicted using the gene profiles of primary tumors at diagnosis.

Methylation: DNA methylation (an epigenetic change) in mammals occurs at the cytosine residues of cytosine guanine (CpG) dinucleotides by an enzymatic reaction that produces 5-methylcytosine (5-mc). In other words, methylation of normal unmethylated CpG islands in gene-promoter regions is an important method for silencing tumor-suppressor genes. Methylation results in transcriptional inactivation of several tumor-suppressor genes in human cancer and serves as an alternative for the genetic loss of gene function by deletion or mutation.

One of the first alterations of DNA methylation to be recognized in neoplastic cells was a decrease in overall 5-mc content, referred to as genomewide or

global DNA hypomethylation. Despite the frequently observed cancer-associated increases of regional hypermethylation, the prevalence of global DNA hypomethylation in many types of human cancers suggests that such hypomethylation plays a significant and fundamental role in tumorigenesis.

Microsatellite: A microsatellite is a short DNA sequence (usually 2–4 pb) repeated many times in tandem. A given microsatellite is found in varying lengths, scattered around a eukaryotic genome.

Mitogen: Mitogen is a substance (e.g., hormone or growth factor) that stimulates cell division.

Molecular Genetics: Molecular genetics is a subdivision of the science of genetics, involving how genetic information is encoded within the DNA and how the cell's biochemical processes translate the genetic information into the phenotype.

Monitoring: Monitoring means repeated assessment if there are early relapses or other signs of disease activity or progression. If early relapse of the disease is identified, a change in patient management will be considered, which may lead to a favorable outcome for the patient.

Monoclonal Antibody: Monoclonal antibodies are homogeneous antibodies produced by a clone of hybridoma cells.

mRNA Splicing: Messenger ribonucleic acid (mRNA) splicing is a process whereby an intervening sequence between two coding sequences in an RNA molecule is excised and the coding sequences are ligated (spliced) together.

Multifactorial Trait: A multifactorial trait is a trait influenced by multiple genes and environmental factors. When multiple genes and environmental factors influence a trait, it is difficult to find a simple relationship between genotype and phenotype that exists in discontinuous traits.

Mutagens: A mutagen is any physical or chemical agent that significantly increases the frequency of mutational events above the rate of spontaneous mutation.

Mutant: A mutant is an organism (or genetic system) that has suffered at least one mutation.

Mutation: Mutation is the original source of genetic variation caused, for example, by a change in a DNA base or a chromosome. Mutation is a permanent change in the sequence of DNA.

Neoplasia: Neoplasia refers to the pathologic process that causes the formation and growth of an abnormal tissue.

Neoplasm: A neoplasm is an abnormal tissue that grows by cellular proliferation faster than normal and continues to grow.

Oligonucleotide: An olignucleotide is a short piece of RNA or DNA.

Oncogene: An oncogene is a gene that transforms a normal cell to a tumorous (cancerous) state. Products of oncogenes are capable of causing cellular transformations. Oncogenes derived from viruses are denoted v-onc, whereas their cellular counterparts, or protooncogenes, are denoted c-onc.

Palliative: A palliative reduces the severity of the disease without curing it.

Pancreatitis: Pancreatitis refers to the inflammation of the pancreas. It can be caused by alcoholism, endocrine diseases, heredity, a virus, parasites, allergies, immunology, pregnancy, drug effects, and abdominal injury.

PCNA: PCNA is a proliferating cell nuclear antigen.

Penetrance: Penetrance is the frequency (expressed as a percentage) of individuals who are phenotypically affected among persons of an appropriate genotype. A trait may show incomplete penetrance or complete (full) penetrance.

Phenotype: A phenotype is the observed biochemical, physical, or morphologic characteristics of an individual. The phenotype is the physical manifestation of a genetic trait, resulting from a specific genotype and its interaction with the environment. Genes give only the potential for the development of a particular phenotypic characteristic; the extent to which that potential is realized depends on interactions with the other genes and their products and also on environmental influences.

Polymerase Chain Reaction: The polymerase chain reaction (PCR) method is used to selectively and repeatedly replicate defined DNA sequences from a DNA mixture. The starting point for PCR is the DNA mixture containing the DNA sequence to be amplified and a pair of oligonucleotide primers that flank that DNA sequence.

Polymorphism: Polymorphism refers to the simultaneous occurrence in the population of genomes showing allelic variations, which are seen either in alleles producing different phenotypes or, for example, in changes in DNA affecting the restriction pattern. A polymorphic locus is any locus that has more than one allele present within a population. It is the occurrence of two or more alternative genotypes in a population at a higher frequency than what could be maintained by recurrent mutations. Single nucleotide polymorphism (SNP) is the variation in the DNA sequence limited to a single base pair.

Prognosis: Prognosis is defined as the prediction of how well or how poorly a patient is likely to fare in terms of response to therapy, relapse, survival time, or other outcome measures.

Prophylactic-Prophylaxis: Prophylactic-prophylaxis is prevention of disease or of a process that can lead

Transduction: Transduction refers to the use of a phage (or virus) to carry host genes from one cell to another cell of a different genotype.

Transgenic Animals: Transgenic animals are created by introducing new DNA sequences into the germline via addition to the egg.

Tumor Markers: Tumor markers are molecular entities that distinguish tumor cells from normal cells. They may be unique genes or their products that are found only in tumor cells, or they may be genes or gene products that are found in normal cells but are aberrantly expressed in unique locations in the tumor cells, or are present in abnormal amounts, or function abnormally in response to cellular stress or to environmental signals (Schilsky and Taube, 2002). Tumor markers may be located intracellularly (within the nucleus, in the cytoplasm, or on the membrane) or on the cell surface, or they may be secreted into the extracellular space, including into the circulation. Tumor markers usually are used for monitoring and detection of early response in asymptomatic patients. For example, tissue-based estrogen receptor and HER-2/*neu* amplification/overexpression markers in breast cancer have been validated to predict response to therapy in breast cancer. Other examples are prostate-specific antigen (PSA), which is a marker for early detection of prostate cancer, and carcinoembryonic antigen, which is used for detecting colon cancer.

Viral Oncogene: A viral oncogene transforms a cell it infects to a cancerous state.

Wild-Type: Wild-type is a term used to indicate the normal allele or the normal genotype. It is a strain, organism, or gene of the type that is designated as the standard for the organism with respect to genotype and phenotype.

Xenograft: Xenograft refers to transferring a graft or tissue from one species to another.

References

Birch, J.M., Alson, R.D., Kelsey, A.M., Quinn, M.J., Babb, P., and McNally, R.J.Q. 2002. Classification and incidence of cancers in adolescents and young adults in England 1979–1997. *Br. J. Cancer 87*:1267–1274.

Bird, A. 2002. DNA methylation patterns and epigenetic memory. *Genes Dev. 16*:6–21.

Cavalli, G., and Paro, R. 1999. Epigenetic inheritance of active chromatin after removal of the main transactivator. *Science 286*:955–958.

Kondrashov, F.A., and Koonin, E.V. 2001. Origin of alternative splicing by tandem exon duplication. *Hum. Mol. Genet. 10*:2661–2669.

Mikulowska-Mennis, A., Taylor, T.B., Vishnu, P., Michie, S.A., Raja, R., Horner, N., and Kunitake, S.T. 2002. High quality RNA from cells isolated by laser capture microdissection. *Biotechniques 33*:1–4.

Mironov, A.A., Fickett, J.W., and Gelfand, M.S. 1999. Frequent alternative splicing of human genes. *Genome Res. 9*:1288–1293.

Pierce, AJ., Stark, J.M., Araujo, F.D., Moynahan, M.E., Berwick, M., and Jasin, M. 2001. Double-strand breaks and tumorgenesis. *Trends Cell. Biol. 11*:S52–S59.

Porter, D.A., Krop, I.E., Nasser, S., Sgroi, D., Kaelin, C.M., Marks, J.R., Riggins, G., and Polyak, K. 2001. A SAGE (serial analysis of gene expression) view of breast tumor progression. *Cancer Res. 611*:5697–5702.

Poste, G., and Filder, I.J. 1980. The pathogenesis of cancer metastatis. *Nature 283:*139–146.

Pu, R.T., and Clark, D.P. 2003. Detection of DNA methylation: potential applications to diagnostic cytopathology. *Acta. Cytol. 47*:247–252.

Ramaswamy, S., and Golub, T.R. 2002. DNA microarrays in clinical oncology. *J. Clin. Oncol. 20*:1932–1941.

Rinehart, F.P., Ritch, T.G., Deininger, P., and Schmid, C.W. 1981. Renaturation rate studies of a single family of interspersed repeated sequences in human deoxyribonucleic acid. *Biochemistry 20*:3003–3010.

Rutherford, S.L., and Henikoff, S. 2003. Quantitative epigenetics. *Nat. Genet. 33*:6–8.

Saha, S., Bardelli, A., Buckhaults, P., Velculescu, V.E., Rago, C., St. Croix, B., Romans, K.E., Choti, A., Lengauer, C., Kinzler, K.W., and Vogelstein, B. 2001. A phosphate associated with metastasis of colorectal cancer. *Science 294*:1343–1345.

Saha, S., Sparks, A.B., Rago, C., Akmaev, V., Wang, C.J., Vogelstein, B., Kinzler, K.W., and Velculescu, V.E. 2002. Using the transcriptome to annotate the genome. *Nat. Biotechnol. 19*:508–512.

Samanta, A., Samanta, J., and Gunn, M. 2003. Legal considerations of clinical guidelines: will NICE make a difference? *J.R. Soc. Med. 9*:133–138.

Schilsky, R.L., and Taube, S.E. 2002. Introduction: tumor markers as clinical cancer tests—are we there yet? *Sem. Oncol. 29*:211–212.

Shi, H., Maier, S., Nimmrich, I., Yan, P.S., Caldwell, C.W., Olek, A., and Huang, T.H.-M. 2003. Oligonucleotide-based microarray for DNA methylation analysis: principles and applications. *J. Cellular Biochem. 88*:138–143.

Skorski, T. 2002. BCR/ABL regulates response to DNA damage: the role in resistance to genotoxic treatment and in genomic instability. *Oncogene 21*:8591–8604.

Velculescu, V.E., Zhang, L., Vogelstein, B., and Kinzler, K.W. 1995. Serial analysis of gene expression. *Science 270*:484–487.

Zhang, L., Zhou, W., Velculstein, V.E., Kern, S.E., Hruban, R.H., Hamilton, S.R., Vogelstein, B., and Kinzler, K.W. 1997. Gene expression profiles in normal and cancer cells. *Science 276*:1268–1272.

Classification Scheme of Human Cancers

- Leukemias
  - Acute lymphoid leukemia (ALL)
  - Acute myeloid leukemia (AML)
  - Chronic myeloid leukemia (CML)
  - Other and unspecified leukemia (Other Leuk)
    - Other and unspecified lymphoid leukemias
    - Other and unspecified myeloid leukemias
    - Other specified leukemias (not elsewhere classified [NEC])
- Lymphomas
  - Non-Hodgkin's lymphoma (NHL)
    - Non-Hodgkin's lymphoma, specified subtype
    - Non-Hodgkin's lymphoma, subtype not specified
  - Hodgkin's disease (HD)
    - Hodgkin's disease, specified subtype
    - Hodgin's disease, subtype not specified
- Central nervous system and other intracranial and intraspinal neoplasms (central nervous system [CNS] tumors)
  - Astrocytoma
    - Specified low-grade astrocytoma
    - Glioblastoma and anaplastic astrocytoma
    - Astrocytoma not otherwise specified
  - Other gliomas
  - Ependymoma
  - Medulloblastoma and other primitive neuroectodermal tumors (Medulloblastoma)
  - Other and unspecified malignant intracranial and entraspinal neoplasms (Other CNS)
    - Other specified malignant intracranial and intraspinal neoplasms
    - Unspecified malignant intracranial and intraspinal neoplasms
  - Nonmalignant intracranial and intraspinal neoplasms
    - Specified nonmalignant intracranial or intraspinal neoplasms
    - Unspecified intracranial or intraspinal neoplasms
- Osseous and chondromatous neoplasms, Ewing's tumor, and other neoplasms of bone (bone tumors)
  - Osteosarcoma
  - Chondrosarcoma
  - Ewing's tumor
  - Other specified and unspecified bone tumors (Other bone tumors)
    - Other specified bone tumors
    - Unspecified bone tumors
- Soft-tissue sarcomas (STS)
  - Fibromatous neoplasms (Fibrosarcoma)
  - Rhabdomyosarcoma
  - Other soft-tissue sarcomas
    - Other soft-tissue sarcomas
    - Unspecified soft-tissue sarcomas
- Germ-cell and trophoblastic neoplasms (germ-cell tumors)
  - Gonadal germ-cell and trophoblastic neoplasms
  - Germ-cell and trophoblastic neoplasms of nongonadal sites
    - Intracranial germ-cell and trophoblastic tumors
    - Other nongonadal germ-cell and trophoblastic tumors
- Melanoma and skin carcinoma
  - Melanoma
  - Skin carcinoma

- Carcinomas (except of skin)
  - Carcinoma of thyroid
  - Other carcinoma of head and neck
    - Nasopharyngeal carcinoma
    - Carcinoma of other sites in lip, oral cavity, and pharynx
    - Carcinoma of nasal cavity, middle ear, sinuses, larynx, and other ill-defined sites in head and neck
  - Carcinoma of trachea, bronchus, lung, and pleura
  - Carcinoma of breast
  - Carcinoma of genitourinary (GU) tract
    - Carcinoma of kidney
    - Carcinoma of bladder
    - Carcinoma of ovary and testis
    - Carcinoma of cervix and uterus
    - Carcinoma of other and ill-defined sites in GU tract
  - Carcinoma of gastrointestinal (GI) tract
    - Carcinoma of colon and rectum
    - Carcinoma of stomach
    - Carcinoma of liver and ill-defined sites in GI tract
  - Carcinomas of other and ill-defined sites NEC
    - Adrenocortical carcinoma
    - Other carcinomas NEC
- Miscellaneous specified neoplasms NEC
  - Embryonal tumors NEC
    - Wilms' tumor
    - Neuroblastoma
    - Other embryonal tumors NEC
  - Other rare miscellaneous specified neoplasms
    - Paraganglioma and glomus tumors
    - Other specified gonadal tumors NEC
    - Myeloma, mast cell tumors, and miscellaneous reticuloendothelial neoplasms NEC
  - Other specified neoplasms NEC
- Unspecified malignant neoplasms NEC

Birch *et al.*, 2002.

to disease. It is the use of an antigenic (immunogenic) agent to actively stimulate the immunologic mechanism or the administration of chemicals or drugs to members of a community to reduce the number of carriers of a disease and to prevent others from contracting the disease. Alternatively, use of an anti-serum from another person or animal to provide temporary protection against a specific infection or toxic agent can be tried.

Proteomics (Proteome): Proteomics facilitates making inventory of all proteins encoded in the genome of an organism and analysis of interaction of these proteins. One of the primary goals of this technology is to describe the composition, dynamics, and connections of the multiprotein modules that catalyze a wide range of biological functions in cells. This technique provides exhaustive information on biochemical properties in living systems such as level of protein expression, post-translational modifications, and protein-protein interactions.

Protooncogene: A protooncogene is the normal counterpart in the eukaryotic genome to the oncogene carried by some viruses. In other words, a protooncogene is a gene that, in normal cells, functions to control the normal proliferation of cells and that, when mutated or changed in any other way, becomes an oncogene.

PSA (Prostate-Specific Antigen): PSA is a marker for early detection of prostate cancer.

***PTEN*:** The *PTEN* gene is phosphorylase and tensin homologue detected on chromosome 10. It is a tumor-suppressor gene that can be inactivated by mutation or genetic deletion or by epigenetic changes, including methylation. *PTEN* is involved in several types of human cancers and cancer cell lines, including brain, endometrium, prostate, breast, skin, colorectal, ovarian, and oral squamous cell carcinomas and leukemia, melanoma, and lymphoma.

Repressor Gene: A repressor gene is a regulatory gene whose product is a protein that controls the transcriptional activity of a particular operon.

Sarcoma: Sarcoma is a connective tissue neoplasm that is usually highly malignant. It is formed by proliferation of mesodermal cells.

Sarcomatoid: Sarcomatoid is a neoplasm that resembles a sarcoma.

Screening: Screening is defined as the application of a test to detect disease in a population of individuals who do not show any symptoms of their disease. The objective of screening is to detect disease at an early stage, when curative treatment is more effective.

Serial Analysis of Gene Expression (SAGE): SAGE is an approach that allows rapid and detailed analysis of thousands of transcripts. The LongSAGE method (Saha *et al.,* 2002) is similar to the original SAGE protocol (Velculescu *et al.,* 1995), but it produces longer transcript tags. The resulting 21 bp consists of a constant 4-bp sequence representing the restriction site at which the transcript has been cleaved, followed by a unique 17-bp sequence derived from an adjacent sequence in each transcript. This improved method was used for characterizing ~28,000 transcript tags from the colorectal cancer cell line DLD-1. The SAGE method was also used for identifying and quantifying a total of 303,706 transcripts derived from colorectal and pancreatic cancers (Zhang *et al.,* 1997).

Metastatic colorectal cancer showed multiple copies of the *PRL-3* gene that was located at chromosome 8q24.3 (Saha *et al.,* 2001). Several genes and pathways have been identified in breast cancer using the SAGE method (Porter *et al.,* 2001). The SAGE method is particularly useful for organisms whose genome is not completely sequenced because it does not require a hybridization probe for each transcript and allows new genes to be discovered. Because SAGE tag numbers directly reflect the abundance of the mRNAs, these data are highly accurate and quantitative. For further details, see Part II, Chapter 6 (by Dr. Ye), page 85 in Volume I of this series.

Signal Transduction: Signal transduction describes the process by which a receptor interacts with a ligand at the surface of the cell and then transmits a signal to trigger a pathway within the cell. The basic principle of this interaction is that ligand binding on the extracellular side influences the activity of the receptor domain on the cytoplasmic side. The signal is transduced across the membrane. Signal transduction provides a means for amplification of the original signal.

Somatic Mutation: A somatic mutation is a mutation occurring in a somatic cell and therefore affecting only its daughter cells; it is not inherited by descendents of the organism.

Specificity: Specificity is the capacity for discrimination between antigenic determinants by antibody or lymphocyte receptor.

Splicing: Splicing is the process of linking together two RNA exons while removing the intron that lies between them.

Suppressor Gene: A suppressor gene is a gene that suppresses mutations in other genes. The effects of a mutation may be diminished or abolished by a mutation at another site. The latter may totally or partially restore a function lost because of a primary mutation at another site. A suppressor mutation does not result in a reversal of the original mutation; instead, it masks or compensates for the effects of the primary mutation.

Transcription: Transcription is the process by which an RNA copy of a gene is made.

I

Molecular Genetics

This Page Intentionally Left Blank

1

Identification of Tumor-Specific Genes

Christian Haslinger, Wolfgang Sommergruber, Tilman Voss, and Martin Schreiber

Tumor-Specific and Tumor-Associated Genes

Tumors result from the perturbation of processes that control the normal growth, localization, and mortality of cells. The loss of normal control mechanisms arises from the acquisition of mutation in three broad categories of genes: (1) protooncogenes, the physiologic (normal) products of which are components of signaling pathways that regulate proliferation, whereas the mutated forms represent dominant oncogenes; (2) tumor-suppressor genes, which generally exhibit recessive behavior and loss of function of which in cancers leads to deregulated control of the cell cycle, migration, cellular adhesion, etc.; and (3) deoxyribonucleic acid (DNA) enzymes, mutations in which promote genetic instability. In general, there is a clear causal relationship between susceptibility to cancer and an impaired ability of cells to repair damaged DNA. Mutations in genes in all these categories lead to changes in cell-surface protein expression, protein secretion, motility, etc. The idea that uncontrolled proliferation (including loss of ability to induce apoptosis) is sufficient for tumor development is also supported by mathematic modeling. However, tumorigenesis in humans is a multistep process. Clinical, epidemiologic, and experimental evidence (Hahn *et al.,* 1999) suggest that a minimum of four or five independent genetic changes are required for the development of a malignant human tumor. Others claim that many more genetic alterations are necessary for tumor formation (Boland and Ricciardiello, 1999). Regardless of the number of genetic changes, tumorigenesis resembles Darwinian evolution. Every genetic change increases the growth advantage of the cell, finally progressing into a tumor cell.

The combined results of several decades of research lead to the identification of a rather small number of features shared by most, if not all, types of human cancers. Hanahan and Weinberg (2000) list the following six essential alterations: self-sufficiency in growth signals (e.g., constitutive autocrine growth signaling via epidermal growth factor/epidermal growth factor receptor [EGF/EGFR] in breast cancer), insensitivity to growth-inhibitory signals (e.g., mutational inactivation of retinoblastoma [*Rb*] gene), evasion of apoptosis (e.g., mutational inactivation of the tumor suppressor *p53* or loss of tumor suppressor PTEN [phosphatase and tensin homolog deleted on chromosome ten]), limitless replicative life span (e.g., constitutive expression of telomerase), sustained angiogenesis (e.g., expression of vascular endothelial growth factor [VEGF], hypoxia-inducible factor-1α [HIF-1α]), and tissue invasion and metastasis (e.g., inactivating mutations of E-cadherin/β-catenin). In addition, aberrant DNA methylation of genes that suppress tumorigenesis also contributes to a malignant phenotype. In tumors, mainly loss of

Handbook of Immunohistochemistry and *in situ* Hybridization of Human Carcinomas, Volume 4: Molecular Genetics, Gastrointestinal Carcinoma, and Ovarian Carcinoma

heterozygosity (LOH) is observed, whereas the second allele is inactivated by aberrant DNA methylation. So far, a large number of cancer-related genes that are silenced by this mechanism have been identified (Jones and Laird, 1999; Tsou *et al.,* 2002).

The situation with tumor-associated antigens (TAAs) is somewhat different because this heterogeneous group is represented by genes either definitely known to be involved in tumorigenesis, such as the tumor suppressor *p53, BRAF,* or *bcr-abl* (to name but a few); by genes the function of which is not yet clear (especially regarding their contribution to tumorigenesis) but that exhibit a distinct expression profile in tumors and immune-privileged tissues (e.g., members of the cancer/testis antigens, such as members of the MAGE family); or by tumor-associated genes that are also expressed—although at a low level—in certain normal tissues. Except for the tissue-specific expression pattern, it is of lesser importance to know the function of these genes unless they contain putative CTL (cytotoxic T cell lymphocytes), Th (helper T cells), and B cell epitopes that might be used in active and passive cancer vaccine programs. The presence of potential T cell epitopes is most important for the establishment of a tumor vaccine because T cell epitopes are peptides presented by MHC-I and MHC-II (major histocompatibility complex class I and class II) molecules and can be defined as synthetic peptides (for literature and details see later). The application of TAAs is limited by the frequency of their presence in primary tumors and corresponding metastases and by the ability of tumors to immunologically escape from induced T or B cell responses simply via rapid down-regulation of the respective TAA or by its immunologic "disappearance." Therefore, the identification of several TAAs for a given tumor type or even for an individual patient seems to be a prerequisite for the development of an efficient tumor vaccine.

Identification of Tumor-Associated Antigens

Introduction

From "Mice and Men" we have learned that there is solid scientific basis for the immunotherapy of cancer. In mice it has been shown that tumors induced by radiation, chemicals, and viruses are immunogenic, meaning that they can induce protective immunity, but that nonimmunogenic murine tumors nevertheless can be antigenic because they can be rejected by a vaccine-primed immune response. From humans it is known that immunosuppressed patients are at an increased risk of neoplasia (e.g., renal allograft recipients treated with cyclosporine have a > sixfold higher chance to develop a tumor within 20 years than do normal individuals). Spontaneous remissions in at least a small proportion of patients with melanoma and renal cell carcinoma (RCC) seem to be mediated by the immune system. Last but not least, tumor antigens recognized by tumor-destroying T cells were identified in both laboratory mice and human patients. The design of a tailored vaccine based on defined antigens has evolved into defined concepts, and clinical trials with both partial success and drawbacks have been conducted (Finn, 2004; Rammensee *et al.,* 2002). A TAA that serves as an immunogen for a clinically efficient cancer vaccine must fulfill at least the following selection criteria: 1) the gene (protein) of interest renders tumors, but not critical normal tissues, vulnerable to CTLs; thus, TAAs should become tumor-rejection antigens; 2) the TAAs are preferentially expressed on multiple tumor types or on at least one major tumor type with a high proportion of primary tumors or metastases and no or low expression on critical normal tissues; 3) the presence of potential T cell epitopes allowing the design of high-affinity immunogenic peptides; and 4) proof of a T cell response in *in vitro* and *in vivo* models. However, there are clear restrictions to the use of defined immunogens, such as differences in the extent of antigen expression (e.g., patients with melanoma express *MAGE*-1 on their primary tumors with a frequency of 15% and with a frequency of 45% on corresponding metastases; for MAGE-3 the ratio is 30–70%) and varying MHC frequency in patients (26% are human leukocyte antigen [HLA] A1-, 49% are HLA-A2.1, and 7% are HLA-Cw16.1-positive). The "epitope frequency," which is represented as the product of [%antigen] × [%HLA], is a measure of the feasibility of a given vaccine setting. Thus, only 12% of white patients with melanoma will respond to a MAGE-1-based tumor vaccine; a MAGE-3-based immune therapy has a theoretical 18% response rate. This clearly indicates that more than one TAA is necessary for the development of an efficient cancer vaccine program. The cellular key players in generating immunity to tumors are T lymphocytes, Th cells ($CD4^+$) interacting with MHC class II molecules (HLA-DR, -DQ, -DP), and CTLs ($CD8^+$) recognizing MHC class I molecules (HLA-A, -B, -C). Because peptides derived from degraded proteins (antigens) are presented on MHC molecules, which are the most polymorphic genes, the need for the development of a tailored and individual cancer vaccine becomes obvious (Rosenberg, 2001).

The "ingredients" for a cancer vaccine comprise 1) the delivery vehicle, which might be the entire tumor cell *per se,* liposomes/microparticles, recombinant bacteria/viruses or plasmids ("naked DNA"); 2) the modulator of immune response ("adjuvant") such as the immunogenic microorganisms *Bacille Calmette-Guérin* (BCG; standard therapy for bladder carcinoma)

and *Corynebacterium parvum (C. parvum),* vaccine adjuvants derived from plants such as QS21, as well as immune-modulating cytokines such as interleukin-2 [IL-2] (unspecific proliferation factor for T cells and activated B cells), interferon-gamma [IFN-γ] etc.; and 3) the most important part of the tumor vaccine, the antigen (immunogen) which can be the tumor itself; autologous/allogenic tumor cells or cell lines; tumor cell lysates; or tumor-specific proteins, genes, and peptides (Finn, 2004). Although it will not be possible to cover all relevant antigens expressed in a tumor, the antigens that can be identified with the present technical possibilities might already be sufficient for improved immunotherapy. It will be of great importance to explore the feasibility of a tailored individual therapeutic immunization. However, tumors are able to escape from immune response via genetic and antigenic variation of tumor cells (Loeb, 2001) and by selection of antigen-negative cells in response to the action of tumor-destroying T cells. It is clearly the aim of a tumor vaccine program to immunize with not only one or two, but with a number of different antigens simultaneously to reduce the chance of tumor escape.

It would be desirable to immunize the patient with all tumor antigens relevant for the particular tumor. In principle, this can be achieved if the entire tumor, complex extracts thereof, unseparated tumor nucleic acid, or heat shock proteins associated with complex tumor antigens are used for immunization (Rammensee *et al.,* 2002). However, trials of this sort carry the potential danger of inducing autoimmunity because such complex mixtures of TAAs usually contain normal self structures as well (Ludewig *et al.,* 2000). Based on these considerations, it is clearly necessary to determine more exactly the spectrum of TAAs in a given individual tumor, mainly by focusing on T cell epitopes to identify the TAA profiles of individual cancer patients. The use of T cell epitopes is advantageous because they can be represented by synthetic peptides for immunizations. Peptides are relatively easy to produce, in contrast to recombinant proteins or viral vectors. A strategy for individual patient antigen-defined tumor immunotherapy is discussed by Rammensee *et al.* (2002).

The categorization of TAAs is based either on their biological function or on the mechanisms responsible for the generation of T cell epitopes in these genes (for details see Kawakami *et al.,* 2004; Old, 2003; Rammensee *et al.,* 2002). The first group of TAAs comprises the following: 1) developmental self-antigens (cancer/germ cell-, cancer/testis-antigens) normally occurring only during embryonic development or in immune-privileged tissues, such as testis or retina (mainly epigenetically regulated). These tissues escape the immunosurveillance by various strategies, such as expressing truncated MHC molecules or secreting immunosuppressive cytokines. The best characterized antigens belonging to this family are the MAGE, BAGE, and GAGE antigens (Van den Eynde and Boon, 1997). They are expressed in a significant portion of melanomas, whereas their expression in other tumors is heterogeneous in regard to the frequency of cells within the tumor and to patients in general; 2) differentiation self-antigens expressed by tumors and the corresponding normal tissue, but not by tumors and normal cells of different histologic origin. Examples are the tyrosinase gene, which is part of the melanin biosynthesis pathway, and *Melan-A/MART-1;* both are expressed by melanomas, melanocytes, and retina; 3) oncogenic virus proteins. These are the ultimate antigens because they are recognized by the immune system as "foreign." For instance, the human papillomaviruses HPV16 and HPV18 play a pivotal role in the development of cervical cancer because their proteins E6 and E7 are required to maintain the transformed state of the malignant cell by blocking tumor-suppressor genes such as *Rb* and *p53.* They are constitutively expressed in >90% of cervical cancer and are *per se* highly immunogenic.

The second group of TAAs comprises genes that are categorized according to the mechanism by which novel epitopes have been generated: 1) point mutations in genes such as *p53, RAS, CDK4,* and *β-catenin.* It is interesting that none of these common cancer genes have turned out to be promising cancer vaccine targets as yet (Old, 2003); 2) rare or unusual splice variants (e.g., *restin* in Hodgkin lymphoma or *CD44v6* in head and neck cancer); 3) overexpression (e.g., *HER2/neu* in breast cancer or *galectin* in Hodgkin lymphoma); 4) translated intron regions (e.g., NAc-glucosaminyl transferase); 5) amplification such as the translation initiation factor 4G *(eIF-4G)* in squamous cell carcinoma (SCC) of the lung (Brass *et al.,* 1997); 6) usage of different initiation codons or alternative reading frames (e.g., *LAGE-1* and *CAMEL*); 7) translation of fusion proteins after chromosomal translocation (e.g., bcr-abl); and 8) incomplete/aberrant glycosylation as in the case of mucin where a novel antigenic determinant becomes available, or the generation of novel epitopes in melanomas and tumors of the central nervous system, where gangliosides are expressed in high density on the cell surface, whereby the antigenic determinant resides in their sugar moiety.

Strategies for the Identification of Tumor-Associated Antigens

In principle, there are two approaches to the identification of TAAs: 1) use of the already existing immunologic response of a tumor patient to identify TAAs; and 2) the combination of molecular biology and biochemistry with immunologic characterization techniques.

The first approach is based on the humoral (B cell) response or the cellular response and has the advantage that, from the beginning, it is known that an immune response against a TAA is possible. In contrast, the second approach initially uses a more statistical setting that requires proof that the selected putative target proteins can indeed be used for the generation of an immune response in patients ("reverse immunology"). Reverse immunology comprises technologies such as T cell expression cloning; "peptide stripping" from MHC-I; reverse tumor cytogenetics in combination with data mining; biochemical and molecular biology approaches, including transcription profiling (cDNA [Complementary DNA] Chip); and proteomics. All these methods and combinations thereof have already been successfully used for the identification of TAAs (Rosenberg, 2000). Many of the TAAs identified, particularly molecules involved in the proliferation and survival of the tumor cells, may function as targets for immunotherapy and for molecular targeted therapy. Examples are p53, HER2/neu, β-catenin, BRAF, and bcr-abl (Kawakami *et al.,* 2004; Rammensee *et al.,* 2002).

Approaches Based on Patient Immune Response

1. SEREX: Serologic Analysis of Autologous Tumor-Associated Antigen by Recombinant cDNA Expression Cloning

The SEREX approach is based on antibodies specifically present in the serum of patients with cancer directed against TAAs in the growing tumor (Tureci *et al.,* 1997). For the identification of TAAs, prokaryotic expression libraries based, for example, on λ-phage expression vectors are established using cDNAs derived from human tumor tissue. Single clones or plaques are transferred to nitrocellulose filters and immunoscreened with patient sera for detection of those TAAs that elicit a high-titer immunoglobulin G (IgG) response. According to Tureci *et al*. (1997) the presence of high-titer antibodies (IgG and IgA) implies the coexistence of T cells; long-lasting production or secretion of IgG and IgA antibodies is dependent on cognate help by antigen-specific $CD4^+$ T cel1s. These TAAs are appropriate targets for the immune system to be recognized by antibodies and $CD4^+$ T cells. Although there is no direct link, at least some of the TAAs identified via detection of antibodies in the sera of a patient with cancer were shown to be also recognized by $CD8^+$ T cells (Jager *et al.,* 1998). Furthermore, antigens identified by SEREX are, in general, immunogenic (www.licr.org/SEREX.html). The restrictions of this method are 1) the patient serum must be extensively preadsorbed against mock-transfected *Escherichia coli* to remove all naturally occurring antibodies, 2) the nitrocellulose membrane must be preincubated with anti-human IgG to exclude false-positive results (all insert cDNAs derived from IgGs), 3) only high-titer (high-affinity) IgG antibodies will lead to an efficient and specific signal on membranes, and 4) this approach cannot detect glycosylated epitopes or epitopes that undergo conformational changes when expressed in bacteria.

T cell and cDNA Expression Cloning

An impressive example of how the immune response can be used to identify TAAs or even the peptide epitope is the method pioneered by the group of Thierry Boon. They identified the first tumor-specific T cell epitope by use of expression libraries prepared from the recognized tumor cell. The TAA used in this study was MAGE-1 and the restricting MHC molecule was HLA-A∗0101 (Traversari *et al.,* 1992). Because of this MHC restriction, COS CV1 origin SV40 cells were co-transfected with both the *HLA-A∗0101* gene and a fragment of the tumor cell's cDNA comprising the *MAGE-1* sequence. The immunogenic peptide region (EADPTGHSY) was then identified by truncation of the *MAGE-1* coding region and the application of autologous melanoma-reactive $CD8^+$ CTLs generated from patient peripheral blood mononuclear cells (PBMCs). These CTLs also recognized this peptide when presented by mouse cells transfected with an *HLA-A1* gene, confirming the association of antigen MAGE-1 with the HLA-A1 molecule. cDNA expression cloning then became the basic technique for the isolation of TAAs recognized by $CD8^+$ T cells but with various modifications, including transient expression in COS and 293 cells or the transduction of retroviral cDNA libraries on autologous fibroblasts. The retroviral system made it possible to isolate unique TAAs expressed only on autologous tumor cells without the need to identify MHC restriction (Wang *et al.,* 1998). In general, the determination of MHC restriction for a given TAA is difficult unless MHC-blocking monoclonal antibodies (mAbs) or tumor variants with autologous MHC loss are available. Melanocyte-specific antigens such as tyrosinase, TRPI and TRP2, and the mutated antigens β-catenin and MART-2/Ski (skinny hedgehog acyltransferase) were identified via transient expression cloning (Kawakami *et al.,* 2004). Tumor-infiltrating T cells (TILs) were also used for the identification of TAAs relevant to *in vivo* tumor rejection (Kawakami *et al.,* 2004 and references therein). In addition, MHC class II restricted TAAs for $CD4^+$ T cells also have been identified by cDNA expression cloning, using cDNA libraries in which the endosome-targeting

invariant chain sequence was attached to insert cDNAs, leading to efficient antigen loading to MHC class II pathways (Wang *et al.,* 1999).

Approaches Based on "Reverse Immunology"

Peptides of 8 to 11 amino acids in length are found to be associated with MHC-I molecules. The specificity for this interaction is guided according to a specific pattern of amino acids within a sequence (Rammensee *et al.,* 1995). Proteasomes are involved in antigen processing and the generation of such peptides. In recent years, advanced methodologies in peptide elution together with sequence determination have led to the characterization of MHC-I binding motifs. Screening of random peptide phage display libraries or synthetic peptide libraries have also been used to identify potential MHC-I peptide ligands (Djaballah, 1997).

Peptide Elution from Major Histocompatability Complex-I Molecules ("Peptide Stripping")

Epitope peptides bound to tumor HLA have been directly identified by using high-performance liquid chromatography (HPLC) fractionation and mass spectrometry. Peptides are eluted via a pH-dependent (mostly acidic) release from MHC-I of tumor cells. Parallel to their separation on HPLC gradients, peptide pools are used to probe for CTL activation *in vitro.* Peptide sequences of the active HPLC fractions are determined by mass spectrometry. As holds true for all approaches of reverse immunology, synthetic peptides must be transloaded on various cell lines lacking expression of the respective antigen to demonstrate lysis by specifically activated CTLs. Following this approach, some of the first epitopes characterized were a gpl00 peptide from HLA-A2 affinity-purified complexes, as well as two murine Kb-restricted TAA peptides from the spontaneous C57BL/6 Lewis lung carcinoma antigen (3LL) (Mandelboim *et al.,* 1997). In contrast to predicted T cell epitopes (see later), the advantage of this approach is that only naturally occurring epitope peptides are identified. However, isolation of low MHC-binding tumor epitopes is rather difficult. This approach is especially useful for the isolation of epitope peptides with posttranslational modifications.

Reverse Tumor Cytogenetics

The amplification of genes contributes to the transformed phenotype in a variety of different human neoplasias. Amplified regions of chromosomes derived from malignant tumors contain genes important for tumorigenesis; the majority of these are co-amplified with the "target gene(s)." By combining techniques, such as fluorescence *in situ* hybridization (FISH) for the identification of amplified regions, chromosomal microdissection for subcloning the cDNA of the respective region, and SEREX for identification of genes, the gene products of which led to a specific immune response in patients, it was possible to identify genes relevant for tumorigenesis. Consequently, *eIF-4G* was shown to be amplified (3q26.1-q26.3) and overexpressed in human squamous cell carcinoma of the lung (L-SCC), leading to an antibody response in patients. In parallel, serum antibodies from patients suffering from L-SCC were used for the isolation of amplified target genes in this tumor type (Brass *et al.,* 1997).

Enzyme-Linked Immunospot Assay

The enzyme-linked immunospot (ELISPOT) assay is a sensitive immunologic method measuring cytokine release on a single-cell basis to detect epitope-specific $CD8^+$ T cells. $CD8^+$ T cells are incubated with a putative antigenic peptide presented by MHC-I on antigen presenting cells (APCs). On specific recognition of the MHC-I-bound peptide, cytokines (e.g., interferon) are released from T cells and subsequently captured by an antibody in a precoated dish. Similar to an enzyme-linked immunosorbent assay (ELISA) the bound cytokine can then be detected by a second antibody coupled to a detection system (Scheibenbogen *et al.,* 1997). We and others have used this method to identify and test a large number of tumor antigen–derived and other immunologic epitope peptides (Andersen *et al.,* 2001; Konopitzky *et al.,* 2002).

Transcription Profiling

In recent years, transcription profiling based on DNA Chips has become state of the art (see later discussion). In most cases, transcriptional portraits are compared—for example, tumor with the corresponding normal tissue or tumor with its corresponding metastases (Amatschek *et al.,* 2004; Ramaswamy *et al.,* 2003). A great advantage of transcriptional profiling studies is the possibility to obtain expression levels for all known TAAs in an individual patient at once, allowing the design of tailored tumor vaccine programs (Rammensee *et al.,* 2002). A disadvantage of transcription profiling is the fact that some TAAs are not products of frameshift mutations, nor fusion proteins such as bcr-abl, nor partially translated proteins from the intron regions such as NAc-glucosaminyl transferase and therefore do not lead to the presentation of a novel putative epitope peptide on tumors. However, the availability of single nucleotide polymorphism (SNP) Chips and Resequencing Chips from Affymetrix soon will facilitate greatly the identification of TAAs (www.affymetrix.com). The SNP Chips can be used for genomewide analysis of changes in the DNA copy number, thereby identifying

amplified chromosomal regions and subsequently genes that might contribute to the transformed phenotype (as previously mentioned). A microarray for detection of mutations in the tumor-suppressor gene *p53* is already commercially available (Okamoto *et al.,* 2000); however, generation of custom-made Resequencing Chips could lead to the detection of point mutations and frameshifts within hundreds of potential TAAs in parallel. The identified mutations might be responsible for the generation of novel immunogenic epitopes. Subsequently, prediction algorithms can be used and selected peptides can be tested for their immunogenic behavior (see earlier). In general, data mining will become more and more important for the prediction of putative TAAs suitable for a tumor vaccine. Certain epitopes can be generated only on tumor cells expressing the immunoproteasome such as the tumor-specific T cell epitope of MAGE-3 (Schultz *et al.,* 2002). Because expression data for each gene in almost all normal human tissues and many different tumor types are available from many existing databases or currently being generated. Rammensee *et al.,* 2002 suggested a differential "MHC-ligandome" analysis of the tumor and the corresponding normal cells to detect differences in antigen processing (www.syfpeithi.de).

Computer-Aided Prediction of T Cell Epitopes

Predictive algorithms have been developed and applied to screen antigens for potential CTL epitopes. A number of programs are available that offer free epitope predictions for a wide range of MHC-I–and MHC-II–restricted epitopes (Schirle *et al.,* 2001). For instance, the algorithm HLA_BIND (bimas.dcrt.nih.gov/molbio/hla_bind) ranks potential 8- to 10-mer peptides based on the predicted half-time of dissociation to HLA class I molecules. Another program for predicting which peptides bind to MHC molecules is SYFPEITHI (www.syfpeithi.de). However, because not all predicted epitopes will be generated *in vivo* and will function as efficient immunodominant peptides, they must be verified experimentally. For example, they can be used to restimulate precursor T cells of healthy blood donors or tumor patients *in vitro.* Subsequently, these "primed" T cells must be tested for tumor cell recognition.

Identification of Tumor-Specific Genes via Differential Ribonucleic Acid Expression

Introduction

Most disease processes are accompanied not only by characteristic macroscopic or histological changes but also by systematic changes in gene expression patterns. In particular cancer is, in essence, a genetic disease, and inappropriate gene expression is fundamental to its pathogenesis (Hanahan and Weinberg, 2000; Vogelstein and Kinzler, 2004). Accordingly, genomic approaches have tremendously deepened our understanding of the molecular mechanisms of tumor development and progression, highlighted novel diagnostic and therapeutic target genes, and refined the classification of tumors to levels that classical methods have been unable to reach. The most successful applications of DNA microarrays to cancer research include the comparison of tumor and corresponding normal tissues to identify tumor-specific genes, the identification of potential diagnostic marker genes and therapeutic target genes, and the identification of new genes and pathways involved in cancer biology. Furthermore, new and refined tumor subclasses based on underlying molecular, potentially causal differences were discovered. In particular, several studies have identified sets of prognostic marker genes that could predict the clinical outcome of patients with cancer with high accuracy based on the expression of these genes in the primary tumor. The predictive power of these microarray-based classification schemes was far superior to that of standard prognostic systems based on clinical and histologic criteria (Sotiriou *et al.,* 2003; van de Vijver *et al.,* 2002; van't Veer *et al.,* 2002). To date, several general conclusions could be drawn: 1) reasonably small (<100), well-defined sets of prognostic genes usually can be identified, which are as informative with respect to overall survival and development of distant metastasis as are DNA microarrays containing thousands of genes, permitting the development of inexpensive and simple diagnostic tools; 2) similar classes of prognostic genes were identified in many of these studies, many of them being cell-cycle regulators, factors involved in invasion and metastasis such as extracellular matrix (ECM) proteases, angiogenic factors, and signal transduction molecules; and 3) the ability to metastasize to distant sites, which eventually determines the overall survival, is acquired relatively early during multistep tumorigenesis and thus can be diagnosed based on expression profiling of the primary tumor at the time of diagnosis, several years before these metastases become manifest.

Identification of Metastasis-Specific Expression Profiles

Because an estimated 90% of all cancer deaths arise from metastasis formation, metastasis is clinically the most relevant event in cancer progression. To gain insight into the genes and pathways involved in metastasis, Ramaswamy *et al.* (2003) have compared the gene expression profiles of 12 adenocarcinoma metastases of

multiple tumor types (lung, breast, prostate, colorectal, uterus, and ovary) to those of 64 unmatched primary adenocarcinomas of the same tumor types. A set of 128 genes that best distinguished primary adenocarcinomas from metastatic nodules was identified; this was then refined to a smaller set of 17 genes, of which 8 were up- and 9 were down-regulated in metastases. Of the 8 up-regulated genes, 4 were components of the protein translation apparatus (eIF4EL3, SNRPF, HNRPAB, and DHPS): the other 4 were securin, lamin B1, and collagens 1Al and 1A2. It is interesting that many of these 17 metastasis-associated genes appeared to be specific for tumor-derived stromal cells rather than the epithelial tumor cells themselves, such as genes usually expressed in fibroblasts (collagens 1A1 and 1A2), smooth muscle cells (myosin heavy chain, myosin light chain kinase, and calponin), or hematopoietic cells (MHC class II DP-β1 and RUNX). Most importantly, this "metastatic gene expression signature" was also found in a subset of primary tumors. The presence of this signature in primary tumors was significantly associated with progression to metastatic disease and poor prognosis. These findings support a model in which some primary tumors are predetermined to metastasize and indicate that this property is detectable in the primary tumor at the time of diagnosis, often years before such metastases become clinically manifest. Thus, the metastatic potential must be present in the bulk of a primary tumor, challenging current theories of cancer biology in which the metastatic process originates from rare cells within the primary tumor. The metastatic signature was subsequently applied to the expression profiles of primary tumors determined by others: 78 primary breast tumors, 21 prostate carcinomas, and 60 medulloblastomas. In all cases, tumors bearing the metastatic gene expression signature were significantly more likely to progress to distant metastasis than those tumors lacking this signature, suggesting that a general, tissue-independent signature associated with metastasis exists (Ramaswamy *et al.,* 2003).

Body-wide Expression Profiling to Identify Tumor-Specific Genes

We have combined two powerful technologies, polymerase chain reaction (PCR) based cDNA subtraction and cDNA microarrays, to determine the transcriptional profiles of 20 breast tumors, 11 lung squamous cell cancers, 11 lung adenocarcinomas, and 8 renal cell cancer samples (Amatschek *et al.,* 2004). Seven subtractive libraries consisting of ~9250 clones were established, enriched for tumor-specific transcripts. These clones, together with ~1750 additional genes with a known or suspected role in tumorigenesis, were used for cDNA microarray preparation. We searched for genes that were highly expressed in the majority of samples of each of these tumor types and that also exhibited no or a very low expression in 16 different normal tissues. This "body wide expression profiling" allowed us to discriminate truly tumor-specific genes from genes that also exhibit high expression in one or more normal tissues. Similarly, expression signatures of genes that are derived from infiltrating cells of the immune system could be eliminated. Also 527 expressed sequence tags (ESTs) were identified, which exhibited a twofold or higher up-regulation in at least 20% of samples of any of these 4 tumor types, compared to the highest expression value in any of the 16 critical normal tissues, which makes them promising putative targets for an anti-cancer therapy. Hierarchic clustering based on these 527 ESTs clearly separated the different tumor types, with RCC exhibiting the most homogenous and lung-adenocarcinoma (AC) the most diverse expression profile. Some of the 527 genes/ESTs identified have been described previously as tumor markers (e.g., pronapsin A, a gene specifically up-regulated in lung-AC but absent in lung-SCC, or NAT-1, which is used as a potential breast cancer marker). However, the majority of identified genes have not yet been examined in the context of tumorigenesis, such as genes involved in bone matrix mineralization *(OSN, OPN, OSF-2)* found to be up-regulated in lung, breast, and kidney cancer or genes controlling Ca^{2+} homeostasis (*RCN1, CALCA, S100* protein family). Some identified genes were overexpressed in almost 100% of a specific cancer type such as *VEGF* or *IGF-BP3* in renal cell cancer, whereas others were up-regulated only in a subset of a given tumor type, such as *stromelysin 3* or *thrombospondin 2* in breast cancer (Amatschek *et al.,* 2004).

Transcriptional Profiling of Human Breast Cancer

In a key microarray study of human cancer, van't Veer *et al*. (2002) analyzed the messenger ribonucleic acid (mRNA) expression pattern of 25,000 genes in a series of 117 primary human breast tumors. Via supervised classification, these authors identified a set of 70 genes, the expression pattern of which allowed the categorization of 78 of these patients with breast cancer into those with a short interval to distant metastases (poor prognosis signature) and those with a good prognosis with 83% accuracy (i.e., 65 of these 78 tumors were assigned to the correct prognosis group). It is interesting that none of the prognostic marker proteins for breast cancer used in current clinical practice, such as estrogen receptor or HER2, were contained in this set of 70 marker genes. Many of the prognostic marker

genes identified are involved in cell cycle regulation, invasion and metastasis, angiogenesis, and signal transduction, such as the metalloproteinases *MMP9* and *MP1;* the cell cycle regulators *cyclin B2, cyclin E2, PCTAIRE* and *CDC25B;* and angiogenic factors such as *FLT1* and *VEGF.* Subsequently, this prognostic set was also applied successfully to tumors distinct from those on which it had been based initially (van de Vijver *et al.,* 2002). Later studies have largely supported the major conclusions of the hallmark studies of van't Veer *et al*. (2002) and van de Vijver *et al*. (2002), despite considerable differences in patient selection, study design, and the type of microarray used, even if the overlap between the prognostic gene sets derived from different studies was almost zero (Amatschek *et al.,* 2004; Sotiriou *et al.,* 2003). These findings justify the hopes that an accurate prediction of a tumor's behavior based on gene expression profiling can be applied to all patients with (breast) cancer. An important clinical question is whether the considerable predictive power achieved in this study (83% accuracy) could be further improved to approach an ideal 100% accuracy. Obvious sources of improvement are the analysis of even more genes and/or the analysis of pure populations of tumor cells isolated (e.g., by laser microdissection).

In a different, unselected group of 99 patients with breast cancer (Sotiriou *et al.,* 2003), unsupervised hierarchic clustering separated the tumors into two main groups (i.e., estrogen receptor–positive and estrogen receptor–negative tumors) in agreement with previous reports (e.g., van't Veer *et al.,* 2002). Moreover, 16 genes with a significant association with relapse-free survival were identified by Cox proportional hazards regression analysis (Sotiriou *et al.,* 2003). Although there was no overlap with the "survival genes" previously reported by van't Veer *et al*. (2002), their prognostic gene set also predicted the relapse-free survival in the patients with breast cancer analyzed by Sotiriou *et al*. (2003): 93 of 231 prognostic genes reported by van't Veer *et al*. were contained on their microarray, which segregated the population of 99 patients into two distinct subgroups with different relapse-free survival.

We have used tumors and lymph-node metastases of seven patients with lymph-node positive breast cancer with known clinical outcome (Amatschek *et al.,* 2004). Three patients succumbed to their disease within 3 years after diagnosis, and four patients were still alive at least 9 years after diagnosis. This allowed us to classify the patients into two groups and apply a statistical filter criterion to select the genes that are most significantly correlated with overall survival. Starting with the expression values of a set of 11,040 tumor-specific clones isolated by suppression subtractive hybridization, a PCR-based differential cloning approach, we identified a set of 42 genes that strongly correlated with the overall survival rate (Amatschek *et al.,* 2004). We next subjected the expression profile of these 42 genes to two distinct unsupervised cluster methods: hierarchic clustering and principal component analysis (PCA). Both methods clearly separated the samples into two distinct groups. Several genes found to be overexpressed in patients with short survival time have already been discussed in the context of breast cancer, such as *TGFβ3, VCAM-1, CD44, thyroid hormone receptor,* and *cyclin B1*. Other genes have not yet been directly linked with breast cancer progression such as *ERG2, B-Myb MTH1,* and *NET-1*. Among the genes down-regulated in patients with short survival are, for example, *MIG-6, Eps15, CAK,* and *APLP2. MIG-6* and *Eps15* are negative regulators of signaling via the EGF receptor, a positive key regulator of breast tumorigenesis. *In vitro,* EGFR-induced transformation can be suppressed by MIG-6.

It is important that several microarray studies of breast cancer reported to date independently arrived at the same general conclusions despite considerable differences with respect to microarray technologies used, gene content of these microarrays, patient populations analyzed, methods of statistical analyses, or criteria for selecting prognostic genes (e.g., Amatschek *et al.,* 2004; Sotiriou *et al.,* 2003; van't Veer *et al.,* 2002). Apparently, the ability to metastasize to distant sites, which eventually determines the overall survival, is acquired relatively early during multistep tumorigenesis and thus can be diagnosed in the primary tumor, several years before these metastases become manifest. Unexpectedly, this ability to form hematogenous (distant) metastases appears to be largely independent of the presence or absence of lymph-node metastases. For example, all patients analyzed in our study (Amatschek *et al.,* 2004) had lymph-node metastases at the time of diagnosis; nevertheless, four of them remained free of distant metastases and disease relapse for at least 9 years of follow-up. This "good prognosis" group could be readily distinguished from the patients with survival times of 3 years or less based on expression profiling of the primary tumor at the time of diagnosis. Many of the prognostic marker genes identified by various studies are involved in cell cycle regulation, invasion and metastasis (such as ECM proteases), angiogenesis, and signal transduction.

Lack of Overlap between Different Sets of Prognostic Marker Genes

Several microarray studies have yielded gene lists whose expression profiles successfully predicted survival of patients with cancer, often with a predictive power superior to that of standard prognostic systems

based on clinical and histologic criteria (Sotiriou *et al.,* 2003; van de Vijver *et al.,* 2002). However, in many cases the overlap between the prognostic gene sets derived from different studies was almost zero, even when the same type of cancer was analyzed. Thus, the important question of whether these differences can be attributed to trivial reasons such as different microarray technologies, different patients, different types of statistical analyses, or different criteria for selecting prognostic genes remains open. To address this question, Ein-Dor *et al*. (2005) have analyzed a single breast cancer data set (van't Veer *et al.,* 2002) by a single statistical method and found that the resulting list of prognostic genes is not unique but is strongly influenced by the subset of patients used for gene selection. Accordingly, many equally predictive, non-overlapping sets of prognostic genes could have been produced from the same dataset and same type of analysis. These findings are explained by the fact that many (e.g., 1234 out of 5852) differentially regulated genes correlated with survival and that the differences between these correlations among different genes are small. Accordingly, the precise composition of a small set of <100 prognostic marker genes fluctuates strongly when determined under even slightly different conditions—for instance, different subsets of patients. Thus, although the top 70 prognostic genes selected in a specific setting usually provide good prediction, other groups of 70 genes may do the same (i.e., the identities of the top 70 genes are not robust). Nevertheless, it is generally possible to produce one or in fact several sets of genes that outperform all clinical and histopathologic criteria currently used for prognosis. Apparently, many genes correlate with survival, and using a large enough subset of them will compensate for the fluctuations in the predictive power of individual genes for individual patients (Ein-Dor *et al.,* 2005).

Serial Analysis of Gene Expression

Serial analysis of gene expression (SAGE) is a technically unique approach used to quantitatively interrogate the expression of thousands of genes simultaneously (Velculescu *et al.,* 1995). It is based on analyzing short (10–11 bp) sequence tags derived from a defined position within a transcript, which contains sufficient information to unequivocally identify this transcript (Tuteja and Tuteja, 2004). These tags are isolated, ligated together (concatemerized), cloned, and sequenced in a high-throughput manner. In a typical SAGE experiment, tens of thousands of these short sequence tags are sequenced per sample, and the frequency of each tag in the sequenced concatemers directly reflects the transcript abundance. Different samples are each analyzed individually, and the relative abundance of transcripts in each sample is then compared to identify up- or down-regulated genes. The major advantage of SAGE is that it does not require a preexisting clone or hybridization probe and hence can be used to identify and quantify known as well as novel genes. It is thus particularly well-suited for organisms with no or incomplete genome sequence information. In cancer research, SAGE has been applied primarily to the discovery of genes differentially expressed between cancerous and normal tissues or cell lines. Usually the sets of differentially expressed genes determined by SAGE tend to be smaller and to contain fewer false-positive hits than those determined by DNA microarray approaches. Extensive online SAGE databases have been established in recent years, such as the National Center for Biotechnology Information (NCBI) SAGE database (www.ncbi.nlm.nih.gov/SAGE/). This freely accessible database contains SAGE results of hundreds of tissue samples and cell lines of human and other species of origin. Via online comparison of two or more analyzed samples contained in the database, differentially regulated genes can be readily identified, providing a very useful starting point for the identification and characterization of tumor-specific or tissue-specific marker genes. To identify genes specific for tumor endothelial cells, St. Croix *et al.,* 2000) have immunopurified endothelial cells from a colorectal tumor and from normal mucosa of the same patient. SAGE libraries of ~100,000 tags of each sample were generated and compared with ~1.8 million tags from a variety of cell lines derived from tumors of non-endothelial origin. In this way, genes that were specific for endothelial cells *in vivo* could be identified. Furthermore, transcripts that were considerably more abundant in tumor endothelium than in normal endothelium, and *vice versa,* were found, including many uncharacterized genes, which should provide a valuable resource for future investigations of tumor angiogenesis.

SAGE was also applied to assess the relevance of a specific genetically engineered mouse model of breast cancer for the study of the human disease (Hu *et al.,* 2004). This mouse model relies on the transplant of p53 null mouse mammary epithelial cells into the cleared fat pad of syngeneic hosts. SAGE was used to obtain gene expression profiles of normal and tumor samples from this mouse model of breast cancer. In a cross-species comparison, these results were compared to 25 human breast cancer SAGE libraries. Significant similarities between mouse and human breast tumors were observed, and a number of transcripts were identified as commonly deregulated in both species (Hu *et al.,* 2004). These findings demonstrate that this particular mouse model of breast cancer indeed closely mimics

the human cancer it attempts to model. This elegant study highlights a distinct advantage of SAGE analysis when compared to DNA microarrays (i.e., that cross-species comparisons of comprehensive gene expression profiles are much more reliable and much easier to accomplish with SAGE data). Normalization of microarray data is a nontrivial task and, in the widely used two-color hybridization method, relies on a common reference probe hybridized to each of the samples to be compared. Such a common reference probe obviously does not exist if the samples to be compared are derived from different species. In SAGE, the frequency of each tag representing a particular transcript (i.e., the number of such tags divided by the number of all tags sequenced) directly reflects the abundance of that transcript. To determine if and to what extent a gene is differentially expressed in two or more different samples, the frequencies of the corresponding tags in these samples are simply compared; whether these different samples are all from the same or from different species is irrelevant for such comparisons. Moreover, DNA microarrays can interrogate only the expression of those genes that are represented on the array; when different species are compared, different arrays for each of the species must be used, and the overlap between the genes contained on these different arrays is usually incomplete. Because SAGE is not limited to preexisting clones or hybridization probes, this limitation of cross-species comparisons with DNA microarrays is readily avoided with SAGE.

Representational Difference Analysis

Representational difference analysis (RDA) is based on a combination of subtractive hybridization and suppression PCR (Diatchenko *et al.,* 1996). In the first step, cDNA of the tumor tissue (tester) and cDNA of normal tissue (driver) are synthesized and fragmented by a restriction enzyme with a four base-pair recognition site such as *Rsa I* generating blunt ends. The tester cDNA is separately ligated to two different adapters and both samples are hybridized with an excess of the unmodified driver. Subsequently, the samples are heat denatured and allowed to anneal, generating homodimers and heterodimers between tester and driver molecules and a class of single-stranded (ss) tester cDNA, which represents a set of low abundant tester-specific genes. During the second hybridization, the two primary hybridization samples are mixed together without denaturing and fresh denatured driver is added (normalization). During a PCR with adapter primers, only tester–tester homohybrids are amplified exponentially, leading to a selective enrichment of cDNAs that are significantly more abundant (up-regulated) in the tester sample. Other members of the cDNA population can be amplified only linearly or not at all (suppressive PCR). Applying this method, several tumor-specific and tumor-associated genes have been identified especially in combination with cDNA arrays (Frohme *et al.,* 2000).

The advantage of this method is the capability of isolating rare mRNAs differentially expressed in two cell populations. RDA can detect sequences represented at 0.0001% in the starting mRNA. However, the standard protocol depends on the presence of specific restriction sites in each cDNA (preferentially with four base recognition sequences) to reduce the cDNA size and provide primer sites for subsequent PCR amplification. Because not all transcripts contain these recognition sites in an appropriate number and distance, alternatives have been developed such as the utilization of random hexamer-primed cDNA for the generation of subtractive cDNA libraries (O'Hara *et al.,* 2005). Furthermore, alpha-thio-deoxynucleotides have been used to fill in 5´ends of homoduplexes of interest (tester–tester) and protect them from being degraded by Exonuclease III and Mung Bean Nuclease prior to PCR subtraction. In contrast, unprotected duplexes as well as the ss DNA fragments are degraded, reducing the complexity of the post-hybridization mix and facilitating the amplification of differentially expressed products (Kuvbachieva and Goffinet, 2002). We have developed a protocol for the generation of cDNA fragments with increased size (Amatschek *et al.,* 2004). Instead of one 4-base cutter, we have used a set of 6-base cutters, 3 with A/T-rich (primarily found at the 3´ends of eukaryotic cDNAs) and 3 with G/C-rich recognition sequences (characteristic for 5´ends of eukaryotic genes). Our approach resulted in an increase in average length to about 800 bp. Such longer cDNA fragments are more favorable for cDNA microarrays because they warrant efficient hybridization, minimize cross-hybridization, and facilitate annotation after sequencing.

Identification of Tumor-Specific Genes by Proteomic Approaches

Introduction

Although research over the last 10 years has widely expanded our knowledge of cancer biology, a gap remains between our understanding of cancer and the development of novel and effective strategies for early diagnostics and therapy. Both the identification of useful therapeutic targets and validated biomarkers is lagging behind. Studies on the genome and transcriptome level have provided a wealth of information, but studies on this level have not allowed us to understand the

cancer-relevant changes in signaling networks that are based on altered patterns of splice variants, on numerous post-translational modification, or on changes in subcellular localization. Furthermore, expression levels as determined by DNA microarray experiments do not necessarily reflect the actual protein levels that can be regulated by translation and protein stability. An extensive study on lung adenocarcinoma revealed that only 21% of the analyzed 98 gene products showed a statistically significant correlation between protein and mRNA levels (Chen *et al.,* 2002). Thus, there is considerable rationale for also studying cancer biology on the level of the proteome.

Methodology

The proteome profiling relies primarily on the use of two-dimensional polyacrylamide gel electrophoresis (2D-PAGE), coupled to the identification of proteins by mass spectroscopy. Matrix-assisted laser desorption ionization (MALDI) and electro-spray ionization (ESI) and combinations thereof are used for the actual mass analysis. 2D-PAGE is based on the separation of complex protein mixtures by 1) their differences in charge (i.e., their different isoelectric points) and 2) their different molecular mass. The method allows an exceptional parallel as well as quantitative display of many proteins. However, only abundant proteins are detectable as a result of intrinsic sensitivity limitations of all detection techniques. Current technologies based on silver or fluorescence stains allows detection of a maximum of about 2000 spots per gel. The highly sensitive [^{35}S] methionine labeling technique pushes the limits up to 4000 to 5000 protein spots on a gel (Celis and Gromov, 2003). This is obviously only a fraction of the number of proteins and isoforms (i.e., differentially modified forms and splice variants) that may be present in a given cell type or tissue. Large proteins, very acidic and very basic proteins, as well as hydrophobic proteins such as membrane proteins are likely to escape detection under standard conditions and thus require special methodologies and efforts.

Another critical issue is the standardization of gel running conditions. Slight variations will, in the end, require more manual intervention in the alignment of the spots, which is the crucial step in the identification of qualitative and quantitative differences (Voss and Haberl, 2000). Two-dimensional difference gel electrophoresis technology circumvents some of these variability problems because it allows the direct comparison of protein abundance across multiple samples simultaneously without interferences resulting from gel-to-gel variations. Protein samples are first differentially labeled with fluorescent dyes (Cy2, Cy3, Cy4) and mixed together to be run on the same gel. Quantification of abundance changes are obtained in a highly sensitive manner over a linear dynamic range of about 4 orders of magnitude, thus surpassing the conventional silver stain. Despite all these improvements, ranging from gel electrophoresis through sensitive differential stains and sophisticated spot alignment and detection algorithms, this technology is still rather labor-intensive and does not really allow high-throughput procedures.

Sample Preparation

Differential proteomics analysis aims at the detection and characterization of proteins characteristic for diseased versus normal tissue. Comparative analysis of tissue biopsies is generally accepted as an appropriate method to reach this goal. The quality of the starting biopsies is of general importance. Here a stringent standardization of carefully optimized procedures from the operating table to the lab must be established. Ideally, fresh material should be used for protein extraction to allow maximal yield and minimal loss from degradation. The use of frozen tissue is always hampered by poorer solubility and extractability of the proteins. These issues become even more important if different clinical centers are involved in the sample accrual process. Tumor biopsies may contain only small amounts of the actual tumor tissue. Thus, laser capture microdissection (LCM) was introduced to generate samples of a few thousand cells out of a tissue that are enriched in tumor or control cells (Jain, 2002). This works well for DNA and RNA analysis because nucleic acid can be amplified easily. This is definitely not possible for proteins. Therefore, rather large amounts of cells (at least 10^5 cells) are required, which makes this step very labor-intensive. Furthermore, the constant problem of which cells to choose must be solved. Cell morphology may not always be the optimal parameter to discriminate normal cells from tumor cells. The subjectivity involved may seriously impair the quality of cell preparations.

The biochemical quality of the dissected samples is also of relevance. Here, fixatives must be avoided because these chemically modify the proteins in an unwanted manner. Working with unfixed tissue samples will, however, result in degradation or loss of important modifications such as phosphorylation. Nevertheless, this rather simple approach of comparing normal and diseased tissue can be seriously questioned. Solid tumors are dynamic and heterogeneous tissue structures. A global differential analysis of their proteomes will finally result in a comparative study of mixed cell populations with different proportions of tumor, epithelial, endothelial, and other cell types from the tumor stroma.

Over the years, many differences between normal tissue and tumor tissue have been described (Hondermarck, 2003). However, the sets of differentially expressed proteins identified by the various studies differ greatly, indicative of either a lack of experimental standardization or, more likely, of problems with the heterogeneity of the materials used in each study. The comparison of normal and tumor tissue leads to the fundamental physiologic question of what is normal tissue. A tumor cell may be derived from a rare stem cell–like precursor cell. Thus, the normal tissue chosen as control would contain only very few of these precursors but many other cells at various stages of differentiation in addition to other cell types. Moreover, the normal cells may be exposed to changing levels of various hormones (e.g., during the menstrual cycle in breast tissue). Thus, the definition of a reference state is rather difficult because every biopsy may reflect a different hormonal environment.

Sample Fractionation

Analysis of total cell or tissue lysates is limited to the most abundant proteins. Several studies have successfully analyzed well-defined groups of proteins (e.g., proteins of purified organelles, membrane microdomain, or isolated protein complex). Not all of these methods can be applied to tissue samples, in particular if one has to work with frozen or fixed samples. Different prefractionation strategies exist, such as subcellular fractionation, affinity purification, and fractionation of proteins and peptides according to their physicochemical properties. Coupling of these advanced separation methodologies to the highly sensitive mass spectrometry finally provides a powerful tool to detect and analyze dynamic changes of low-abundance proteins (Stasyk and Huber, 2004). Phosphorylation is a ubiquitous post-translational modification that affects a significant subset of the proteome and plays an important role in signal transduction and cell cycle control. Immobilized metal affinity chromatography (IMAC) has been established as a means to specifically enrich phosphoproteins for the subsequent separation by 2D-PAGE and mass spectroscopy (Metodiev *et al.,* 2004). Another study focused specifically on the analysis of membrane proteins from breast tumor cell lines (Adam *et al.,* 2003). More than 500 were identified, 27% of which have unknown function. Several of these unknown proteins were demonstrated by immunohistochemistry (IHC) of breast tumors to be localized at the membranes of the tumor cells only.

Recent Developments

Several nonseparation–based strategies have been developed to overcome the labor-intensive 2D-PAGE or multi-dimensional chromatography. The potential of mass spectroscopy to directly yield comprehensive profiles of peptides and proteins from serum without prefractionation has attracted great interest. Surface enhanced laser desorption ionization mass spectroscopy (SELDI-TOF) is the most widely used method (Yip and Lomas, 2002). Small amounts of serum proteins are applied to protein-binding surfaces of different affinities. The bound proteins are then analyzed by MALDI. Proteins and peptides are detected in a mass range of 1,000–20,000 m/z. SELDI merely generates peak patterns and does not identify the nature of the underlying proteins or peptides, so that additional efforts are required to obtain this information. This technology has been criticized as still suffering from a lack of reproducibility, poor resolution, and mass accuracy (Veenstra *et al.,* 2004). Nevertheless, this technique has the clear advantage to being capable of analyzing hundreds of samples per day. It may thus turn out to be a potentially sensitive diagnostic tool for the early detection of malignancy or as a predictor of response to therapy (Petricoin and Liotta, 2004). *In situ* proteomics of tissue slices has been developed (Stoeckli *et al.,* 2001). Frozen tissue sections are blotted on a conductive polyethylene membrane, which is then dried, coated with matrix, and directly analyzed at regular intervals in the mass spectrometer. Generally more than 100 peptides and proteins in the 2–30 kD range can be detected, with 30–50 having relatively high signal intensities (Chaurand *et al.,* 1999). Mass profiles from tissue sections obtained from normal and tumor tissue may be compared to detect tumor-specific differences. However, this method is limited with respect to its sensitivity because only a few low-molecular-weight proteins seem to be detectable.

Identification of Tumor-Specific Differences

Early studies focused on the elucidation of disease mechanisms by proteomics approaches. It was assumed that an industrial-scale discovery approach would generate validated and robust targets for therapeutic intervention in addition to useful biomarkers (Ryan and Patterson, 2002). Since then, the focus has clearly shifted to identification of tumor antigens, markers for the detection of early stages of cancer or tumor classification, and markers correlating with clinical observations or response to treatment. Two basic concepts have been followed. One aims at the identification of unambiguously identified biomarkers. The other focuses on the identification of nonannotated descriptor patterns characteristic for a sample population.

Proteomics Studies of Different Cancer Types

Different tumor types such as breast, colon, melanoma, pancreas, and stomach cancer have been

analyzed with proteomics tools to identify tumor-specific expression differences. These studies intended to elucidate tumor-specific alternations in signaling pathways or to describe biomarkers for tumor typing or as indicators of patient performance. Most studies were performed with sample numbers in the range of 4–30 which might reflect the labor-intensive nature of this type of study. A large study with more than 1000 samples was performed on lung adenocarcinoma. The results were compiled in a database containing integrated expression data at the protein and the mRNA level (Oh *et al.,* 2001). Similar databases were also established for bladder cancer (Celis *et al.,* 1999). Such database should, in principle, allow the identification of protein spots from samples based on their co-migration with the corresponding spots on the reference gel. However, because the resolution of 2D-PAGE is rather low, a given spot may contain several molecularly different protein species, making the use of a database as the only way of identifying a protein rather unreliable.

Analysis of Serum for Autoantibodies against Tumor-Specific Proteins

There is ample evidence for an immune response against tumor-associated proteins. 2D-PAGE in combination with Western blot analysis using patient sera has allowed the identification of proteins that induce a tumor-specific autoimmune response (Naour *et al.,* 2002; Seliger and Kellner, 2002). To identify TAAs in RCC, we introduced a novel approach by combining serology with proteomics technologies dubbed SERPA (*Ser*ological *P*roteome *A*nalysis; Klade *et al.,* 2001). RCC is an immunogenic tumor; however, cancer/testis antigens such as the MAGE, BAGE, or GAGE protein families that are shared between several tumor types are not expressed in RCC (Van den Eynde and van der Bruggen, 1997). TAAs were identified by comparing the reactivity of protein resolved by 2D-PAGE with sera from patients and healthy donors. 2D-PAGE immunoblotting revealed five RCC-specific spots, reproducibly reactive with RCC-patient but not healthy-donor control sera. Two of these antigens were isolated by preparative 2D-PAGE and identified by Edman sequencing of tryptic peptides. One identified TAA is the smooth muscle protein 22-alpha (SM-22-α), which is an actin-binding protein of unknown function predominantly expressed in smooth muscle cells. *In situ* hybridization showed that SM-22-α is not expressed in the malignant cells but is expressed in mesenchymal stromal cells. The second gene identified was *carbonic anhydrase I (CAI),* an isoform usually not expressed in normal kidney. It is interesting that a different isoform (CAXII) has been identified by SEREX as a TAA overexpressed in some RCCs.

Antibodies to recombinant CAI or SM-22-α were detected in sera from 3/11 or 5/11 patients with RCC with respectively, whereas sera from 13 healthy individuals did not react. The SERPA method is clearly limited by the resolution of the immunostaining and silver-staining process. A study on hepatocellular carcinoma (HCC) identified auto-antibodies against calreticulin in about 27% of the patients. This study concluded that a distinct repertoire of autoantibodies seems to be associated with HCC that may have utility in early diagnosis of HCC among high-risk subjects with chronic hepatitis (Le Naour *et al.,* 2002). Autoantibodies against calreticulin isoforms were also identified in sera from 21 of 36 patients with pancreatic cancer. The control groups demonstrated only a limited response to calreticulin isoform 1 (chronic pancreatitis: 1 in 18; healthy controls: 1 in 15). None of the noncancer controls but 60% of patients with lung adenocarcinoma and 33% of patients with squamous cell lung carcinoma were shown to exhibit IgG-based reactivity against proteins identified as glycosylated annexins I and/or II (Le Naour *et al.,* 2002).

An important goal in cancer control is the detection of the disease in an early stage to allow rapid intervention and an efficient treatment. One of the most extensive proteomics studies with tissue specimens was performed on bladder cancer. More than 1000 samples from tumors, biopsies, and cystectomies have been analyzed (Celis *et al.,* 2000). These studies identified several protein markers for transitional cell carcinoma (Brichory *et al.,* 2001). Adipocyte fatty-acid binding protein was shown to be significantly reduced in high-grade tumors. Psoriasin was shown to be a specific marker of squamous cell carcinoma, which is secreted into the urine (Celis *et al.,* 2000). One interesting study combined the enrichment of glycoproteins of tissue-extracted proteins with SELDI to identify markers for prostate cancer. The SELDI profiles demonstrated similar features for samples from similar tumor stages. TIMP-1 could be shown to be down-regulated in cancer samples (Liu *et al.,* 2005).

Identifying Markers in Serum

Serum proteomic pattern diagnostics represents a novel proteomics concepts in which either specific biomarkers are identified or entire patterns are derived from the mass spectroscopy data to be used as discriminators. The latter approach does not rely absolutely on the actual identification of the proteins generating the pattern. The complexity of proteomics data requires extensive data mining to uncover the differences in these patterns and convert them into reliable discriminators. A comparative study based on sets of serum SELDI data for ovarian cancer concludes that genetic algorithm-based methods outperform statistical tests

(Li *et al.,* 2004). Several preliminary studies (Conrads *et al.,* 2004; Yu *et al.,* 2003) had suggested that such an approach has the potential to be a highly sensitive diagnostic tool for the early detection of cancer. One larger study applied data mining strategies to the SELDI pattern from serum protein from patients with ovarian cancer and respective control (Conrads *et al.,* 2004; Petricoin *et al.,* 2002). In a first step, the data for 50 controls and 50 patients were used as a training set to generate a pattern that discriminates these two sample sets. This discriminatory pattern was then shown to correctly identify all 50 tumors and 63 of 66 control samples in a masked test set. This particular approach of using serum-derived patterns was criticized after the data were reanalyzed by other investigators, revealing reliability problems (Check, 2004).

Another general problem in the context of serum markers is the lack of any evidence for the source of the diagnostic information in the serum samples. Tumors are likely to contribute differently to the final composition of serum (e.g., by tumor-specific proteins or fragments generated by tumor-associated metalloproteases). Alternatively, the observed differences may stem from other tissues in response to the tumor burdon. Thus, several issues, such as the bioinformatics tools used, patient's selection, reproducibility, or sample handling, remain to be solved before final judgment on the value of this approach can be made.

Another large five-center case control study pinpointed three biomarkers for ovarian cancer (Zhang *et al.,* 2004). Chromatographically prefractionated serum samples from 153 patients and more than 300 controls were analyzed by SELDI. Samples from two centers were analyzed independently and cross-validated. The samples from two other centers were used for validation. The three biomarkers, apolipoprotein A1, a fragment of transthyretin, and a fragment of inter-alpha-trypsin inhibitor heavy chain H4 were analyzed by immunoassays in the samples from the fifth center. The first two markers are down-regulated in tumors, and the third is up-regulated. The predictive sensitivity of these three markers in combination with the existing serum marker CA125 could be shown to be higher than CA125 alone.

Correlation with Clinical Features

Several studies explored the potential of proteomics for identifying markers that correlate with tumor staging and with clinical parameters such as drug resistance or patient performance. Direct MALDI analysis of 79 frozen non-small-cell lung cancer samples identified a pattern of 15 distinct mass peaks out of more than 1600 (Yanagisawa *et al.,* 2003), which distinguished between patients who had poor prognosis (median survival 6 months) and patients with a good prognosis (median survival 33 months). The actual proteins in this pattern were not identified. The proteomics pattern of high- and low-grade glioma generated by 2D gels and MALDI allowed the identification of a biologically distinct subset of aggressive astrocytoma. A set of 37 proteins differentially expressed based on histologic grading and correlating with patient survival was identified. Among those increased in glioma were signal transduction proteins such as small G proteins. These data were confirmed by IHC. B cell chronic lymphocytic leukemia (B-CLL) is a disease characterized by broad clinical variability. Statistical methods were devised to analyze the spot pattern from 24 patient samples (Voss *et al.,* 2001). This analysis allowed the identification of proteins that clearly discriminated between the patient groups with defined chromosomal characteristics or that correlated with clinical parameters such as patient survival. B-CLL patient populations with shorter survival times exhibited changed levels of redox enzymes, heat shock protein 27, and protein disulfide isomerase. These molecules potentially may be involved in drug resistance.

CONCLUSION

Common to all proteomics studies of cancer is the observation that expression change correlate with features such as tumor specificity, therapy resistance, or adverse outcome. In general, only very few differences are described between tumor and control samples. One might argue that only limited numbers of changes are required to make a tumor cell (Hanahan and Weinberg, 2000). Alternatively, sensitivity limits of current proteomics technologies allow a view of only the most abundant proteins. Most relevant changes in tumorigenesis occur within low abundant signaling proteins, cell cycle regulators, or transcription factors, and they are not detectable (Gygi *et al.,* 1999). The differentially expressed proteins observed by proteomics belong, among others, to the group of heat shock proteins, cytokeratins, proteins involved in the cytoskeletal organization, metabolism, and the anti-oxidation system. The evidence for a possible functional role of all these proteins in carcinogenesis, metastasis, and tumor aggressivity and the development of chemoresistance is, at the moment, circumstantial, and detailed functional tests are required to establish mechanistic links. Up to now, all the studies aiming at the identification of unannotated discriminative patterns have been based on rather small training and test sets. Larger studies are necessary to demonstrate the value of this approach.

Role of Bioinformatics in Identification of Tumor-Specific Genes

Multiple different microarray platforms for gene expression profiling exist, all of which call for strong bioinformatics support during experiment design and data analysis. In addition to a consistent data management, the conversion of chip images to numbers and finally to a biological meaning is both a great opportunity and a challenge for bioinformatics scientists. All steps require close collaboration with the scientists at the workbench, particularly the experimental design. After the hybridizations are completed, the quality check already benefits from advanced bioinformatics methods. Different parameters are used for the quality check of chip hybridizations. For affymetrix chips, a very helpful tool produces pseudochip images that facilitate the exclusion of erroneous chips (www.stat.berkeley.edu/~bolstad/AffyExtensions/AffyExtensions.html). Data preprocessing converts the scanned images into single values for each spot/probe set. Preprocessing includes the so-called normalization step, which makes the chips comparable. If possible, model-based methods like dChip (www.dchip.org), RMA and GCRMA (www.bioconductor.org) should be applied.

The subsequent statistical analysis can be divided into two main classes: unsupervised and supervised methods. Unsupervised methods do not make use of any known sample attributes such as tumor type, tissue of origin, gender, and so forth. Instead they try to reveal patterns and structures in the data set. Clustering methods such as hierarchic or k-means clustering as well as dimension reduction methods (PCA, MDS) are frequently used to that end. It is not advisable to apply these algorithms to all the genes on the chip; therefore, a gene filter should be applied prior to all unsupervised methods. A frequently used method includes only those genes that are expressed in a given percentage of hybridizations. The co-efficient of variation (standard deviation divided by the mean) is another example. The combination of k-means and hierarchic clustering is a more sophisticated procedure in which k-means is used to cluster all genes into a predefined number of groups. One representative gene is selected from each cluster to form a basis for the subsequent hierarchic clustering. Of course, all three methods could be combined. On the one hand, an unsupervised data inspection has the potential to deliver spectacular results, such as new tumor subtypes; on the other hand, it might reveal an experimental bias or confounding factors.

Various supervised approaches, which use sample annotation to guide the statistical analysis, have been developed or adapted, ranging from the classical t-test to machine learning methods (e.g., neuronal networks and support vector machine [SVM]). All of them face the problem that the number of variables (genes) exceeds the number of observation (hybridizations) by far. Therefore, it is mandatory to use multiple comparison procedures to account for that fact. In tumor biology, probably the most frequent task is the search for genes that are differentially expressed in normal and tumor tissues. The bioconductor (www.bioconductor.org) project offers an up-to-date collection of several methods for statistical group comparisons including multiple comparisons. Algorithms that result in predictors for sample classification, particularly the correlation of expression data with patient survival and the subsequent predictor design, is another focus of many studies. However, the correlation of high-dimensional hybridization results with censored data poses a problem that has not yet been completely solved.

A much more infrequently addressed question is the change of co-expression between two groups of samples (e.g., tumor versus normal). Beside the computational challenge, it can be quite difficult to derive and test biological hypotheses from co-expression changes. After all, gene lists must be put into the context of the current biological and medical knowledge. An indispensable prerequisite is an accurate gene annotation, whereby unknown genes especially can cause some work along that road. A plethora of different alignment algorithms form the core of the classical bioinformatics task of sequence annotation. They range from the simple BLAST search (www.ncbi.nlm.nih.gov/BLAST/) to sophisticated hidden markov models (HMM) for protein domain prediction. Pfam (www.sanger.ac.uk/Software/Pfam/) and SMART (smart.embl-heidelberg.de/) are two of the most frequently used databases of protein domain models, whose associated Internet sites allow sequence scanning. Prosite (www.expasy.org/prosite/) allows the scanning of sequences for smaller entities such as sequence patterns and motifs. InterPro (www.ebi.ac.uk/interpro/) provides an integrated access to an even bigger set of methods including Uniprot, Prodom, TIGRFams, Pfam, SMART, Prosite, and many more. A frequently overlooked possibility of annotating an unknown gene is by gene expression similarity. This requires an extensive database of gene expression data, possibly from a diversity of different tissues but hybridized against a common platform. The most prominent access points for public hybridization data are the Array Express at the EBI (www.ebi.ac.uk/arrayexpress/); the Gene Expression Omnibus (www.ncbi.nlm.nih.gov/geo/); the Stanford Microarray Database (genome-www5.Stanford.edu/); and the Whitefield Institute Center, which provides data sets from cancer

genomics programs (www.broad.mit.edu/cgi-bin/cancer/datasets.cgi).

The accurate annotation of differentially expressed genes is just the beginning. An extremely valuable initiative that gives insight into gene lists is Gene Ontology (GO) (www.geneontology.org/). The GO collaborators are developing three structured, controlled vocabularies (ontologies) that describe gene products in terms of their associated biological processes, cellular components, and molecular functions in a species-independent manner. There are many tools that use GO in the context of gene expression data analysis (e.g., FatiGO: fatigo.bioinfo.cnio.es/). Each gene on a list can be assigned to its GO terms. Statistical tests indicate whether certain processes or functions are over-represented or under-represented. Some tools can also be used to compare two lists of genes and find GO terms differentially represented between them. Pathway mapping software is an additional resource to elucidate gene correlations. Public domain database such as KEGG (www.genome.jp/kegg) and BioCarta (www.biocarta.com/genes/index.asp) are good starting points. A much more convenient way to investigate pathway is GenMAPP (www.genmapp.org/). GenMAPP is a free computer application designed to visualize gene expression and other genomic data on maps representing biological pathways and grouping of genes. Integrated with GenMAPP are programs to perform a global analysis of gene expression or genomic data in the context of hundreds of pathway MAPPs and thousands of Gene Onotology Terms (MAPPFinder), import lists of genes and proteins to build new MAPPs (MAPPBuilders) and export archives of MAPPs and expression and genomic data to the Web. Despite all these valuable approaches, the interpretation of gene expression data on the level of proteins or protein activities is misleading. In fact, microarrays measure mRNA expression levels, and tightly co-expressed genes should share common transcription regulation features. Unfortunately, the co-regulation of transcripts is known only for very limited examples. A set of tools can be found at the TRANSFAC site (www.generegulation.com/pub/databases.html#transfac), a database on eukaryotic cis-acting regulatory DNA elements and trans-acting factors. A worthwhile extension to TRANSFAC is offered by the commercial vendor Genomatix (www.genomatix.de).

The Molecular Signature of a Tumor

Cancer is one of the prime causes of human morbidity and mortality. Worldwide, one in three people are diagnosed with cancer, and one out of five will die from it. Cancer is expected to become the leading cause of death in the United States by 2005. Outcomes studies for the United States for all types of cancer show a 10-year survival rate of 57% (www.seer.cancer.gov). The revolution in cancer research in the last decade has revealed that cancer is, in essence, a genetic disease. Accordingly, genomic approaches to human cancer have tremendously deepened our understanding of the molecular mechanisms of tumorigenesis and have highlighted novel diagnostic and therapeutic target genes. In addition, the immune response that is induced in patients with a tumor can also be used for the identification of novel TAAs. As few as 5–15% of patients benefit from current anti-cancer agents, and even then only months, not years, are added to their lives. Pharmacogenomic research has the great potential of improving the targeting of available and novel cancer therapies to those patients most likely to respond, based on their genetic makeup ("oncogenomic signature"). For example, clinical responses to the anti-HER2 antibody trastuzumab (Herceptin) appear to be limited to breast tumors with HER2 gene amplification. Likewise, only those gastrointestinal stromal tumors (GISTs) with mutations in c-Kit respond to the small molecule kinase inhibitors imatinib (Gleevec), although all GISTs aberrantly express c-Kit. The ~8% of lung tumors with *EGFR* gene mutations exhibit robust clinical responses to the EGFR tyrosine kinase inhibitor gefitinib (Iressa), whereas EGFR inhibitors have shown limited to no clinical activity in unselected patients (Vogelstein and Kinzler, 2004). It is important to note that these findings underscore the existence of molecular signatures that can predict drug efficacy and indicate that mutations are more reliable targets/predictors of responsiveness to targeted therapies than is abnormal expression. Activating mutations in other key tumorigenic signalling molecules are being discovered continuously, such as in *HER2, K-RAS, B-RAF, PI3KCA,* and SMOH; whereas in tumor suppressor genes loss of heterozygosity (LOH) (e.g., *PTEN,* or inactivating mutations, e.g., in *PTCH)* patched homolog of Drosophilia are observed.

In summary, the understanding of what makes a gene "tumor specific" has changed somewhat in the last several years. It has become clear that in many cases, not only the presence or overexpression of those genes but also their "molecular appearance" (mutational status) within the context of a complex network of signaling cascades contribute effectively to tumorigenesis. Therefore, the identification of those patient-specific "oncogenomic signatures," including the definition of individual patient-selective antigens ("immunologic appearance"), should enlarge our understanding of tumorigenesis and enable the development of individualized therapies.

Acknowledgment

We thank Diane Thompson for helpful discussion and for critically reading the manuscript.

References

Adam, P.J., Boyd, R., Tyson, K.L., Fletcher, G.C., Stamps, A., Hudson, L., Poyser, H.R., Redpath, N., Griffiths, M., Steers, G., Harris, A.L., Patel, S., Berry, J., Loader, J.A., Townsend, R.R., Daviet, L., Legrain, P., Parekh, R., and Terrett, J.A. 2003. Comprehensive proteomic analysis of breast cancer cell membranes reveals unique proteins with potential roles in clinical cancer. *J. Biol. Chem. 278*:6482–6489.

Amatschek, S., Koenig, U., Auer, H., Steinlein, P., Pacher, M., Gruenfelder, A., Dekan, G., Vogl, S., Kubista, E., Heider, K.H., Stratowa, C., Schreiber, M., and Sommergruber, W. 2004. Tissue-wide expression profiling using cDNA subtraction and microarrays to identify tumor-specific genes. *Cancer Res. 64*: 844–856.

Andersen, M.H., Pedersen, L.O., Becker, J.C., and Straten, P.T. 2001. Identification of a cytotoxic T lymphocyte response to the apoptosis inhibitor protein surviving in cancer patients. *Cancer Res. 61*:869–872.

Boland, C.R. and Ricciardiello, L. 1999. How many mutations does it take to make a tumor? *Proc. Natl. Acad. Sci. USA 96*: 14675–14677.

Brass, N., Heckel, D., Sahin, U., Pfreundschuh, M., Sybrecht, G.W., and Meese, E. 1997. Translation initiation factor eLF-4gamma is encoded by an amplified gene and induces an immune response in squamous cell lung carcinoma. *Hum. Mol. Genet. 6*:33–39.

Brichory, F.M., Misek, D.E., Yim, A.M., Krause, M.C., Giordano, T.J., Beer, D.G., and Hanash, S.M. 2001. An immune response manifested by the common occurrence of annexins I and II autoantibodies and high circulating levels of IL-6 in lung cancer. *Proc. Natl. Acad. Sci. USA 98*:9824–9829.

Celis, J.E. and Gromov, P. 2003. Proteomics in translational cancer research: toward an integrated approach. *Cancer Cell 3*:9–15.

Celis, J.E., Ostergaard, M., Rasmussen, H.H., Gromov, P., Gromova, I., Varmark, H., Paladottir, H., Magnusson, N., Andersen, I., Basse, B., Lauridsen, J.B., Ratz, G., Wolf, H., Orntoft, T.F., Celis, P., and Celis, A. 1999. A comprehensive protein resource for the study of bladder cancer: http://biobase.dk/cgi-bin/celis. *Electrophoresis 20*:300–309.

Celis, J.E., Wolf, H., and Ostergaard, M. 2000. Bladder squamous cell carcinoma biomarkers derived from proteomics. *Electrophoresis 21*:2115–2121.

Chaurand, P., Stoeckli, M., and Caprioil, R.M. 1999. Direct profiling of proteins in biological tissue sections by MALDI mass spectrometry. *Anal. Chem. 71*:5263–5270.

Check, E. 2004. Proteomics and cancer: running before we can walk? *Nature 429*:496–497.

Chen, G., Gharib, T.G., Huang, C.C., Taylor, J.M., Misek, D.E., Kardia, S.L., Giordano, T.J., Iannettoni, M.D., Orringer, M.B., Hanash, S.M., and Beer, D.G. 2002. Discordant protein and mRNA expression in lung adenocarcinomas. *Mos. Cell Proteomics 1*:304–313.

Conrads, T.P., Hood, B.L., Issaq, H.J., and Veenstra, T.D. 2004. Proteomic patterns as a diagnostic tool for early-stage cancer: a review of its progress to a clinically relevant tool. *Mol. Diagn. 8*:77–85.

Diatchenko, L., Lau, Y.F., Campbell, A.P., Chenchik, A., Moqadam, F., Huang, B., Lukyanov, S., Lukyanov, K., Gurskaya, N., Sverdlov, E.D., and Siebert, P.D. 1996. Suppression subtractive hybridization: a method for generating differentially regulated or tissue-specific cDNA probes and libraries. *Proc. Natl. Acad. Sci. USA 93*:6025–6030.

Djaballah, H. 1997. Antigen processing by proteasomes: insights into the molecular basis of crypticity. *Mol. Biol. Rep. 24*:63–67.

Ein-Dor, L., Kela, I., Getz, G., Givol, D., and Domany, E. 2005. Outcome signature genes in breast cancer: is there a unique set? *Bioinformatics 21*:171–178.

Finn, O. 2004. History of tumour vaccines and novel approaches for preventive cancer vaccines. *Dev. Biol. (Basel) 116*:3–12.

Frohme, M., Scharm, B., Delius, H., Knecht, R., and Hoheisel, J.D. 2000. Use of representational difference analysis and cDNA arrays for transcriptional profiling of tumor tissue. *Ann. NY Acad. Sci. 910*:85–104.

Gygi, S.P., Rochon, Y., Franza, B.R., and Aebersold, R. 1999. Correlation between protein and mRNA abundance in yeast. *Mol. Cell Biol. 19*:1720–1730.

Hahn, W.C., Counter, C.M., Lundberg, A.S., Beijersbergen, R.L., Brooks, M.W., and Weinberg, R.A. 1999. Creation of human tumour cells with defined genetic elements. *Nature 400*: 464–468.

Hanahan, D. and Weinberg, R.A. 2000. The hallmarks of cancer. *Cell 100*:57–70.

Hondermarck, H. 2003. Breast cancer: when proteomics challenges biological complexity. *Mol. Cell Proteomics 2*:281–29l.

Hu, Y., Sun, H., Drake, J., Kittrell, F., Abba, M.C., Deng, L., Gaddis, S., Sahin, A., Baggerly, K., Medina, D., and Aldaz, C.M. 2004. From mice to humans: identification of commonly deregulated genes in mammary cancer via comparative SAGE studies. *Cancer Res. 64*:7748–7755.

Jager, E., Chen, Y.T., Drijfhout, J.W., Karbach, J., Ringhoffer, M., Jager, D., Arand, M., Wada, H., Noguchi, Y., Stockert, F., Old, L.J., and Knuth, A. 1998. Simultaneous humoral and cellular immune response against cancer-testis antigen NY-ESO-1: definition of human histocompatibility leukocyte antigen (HLA)-A2-binding peptide epitopes. *J. Exp. Med. 187*: 265–270.

Jain, K.K. 2002. Application of laser capture microdissection to proteomics. *Methods Enzymol. 356*:157–167.

Jones, P.A. and Laird, P.W. 1999. Cancer epigenetics comes of age. *Nat. Genet. 21*:163–167.

Kawakami, Y., Fujita, T., Matsuzaki, Y., Sakurai, T., Tsukamoto, M., Toda, M., and Sumimoto, H. 2004. Identification of human tumor antigens and its implications for diagnosis and treatment of cancer. *Cancer Sci. 95*:784–791.

Klade, C.S., Voss, T., Krystek, E., Ahorn, H., Zatloukal, K., Pummer, K., and Adolf, G.R. 2001. Identification of tumor antigens in renal cell carcinoma by serological proteome analysis. *Proteomics 1*:890–898.

Konopitzky, R., Konig, U., Meyer, R.G., Sommergruber, W., Wolfel, T., and Schweighoffer, T. 2002. Identification of HLA-A*0201-restricted T cell epitopes derived from the novel overexpressed tumor antigen calcium-activated chloride channel 2. *J. Immunol. 169*:540–547.

Kuvbachieva, A.A. and Goffinet, A.M. 2002. A modification of Representational Difference Analysis, with application to the cloning of a candidate in the Reelin signalling pathway. *BMC Mol. Biol. 3*:6.

Le Naour, F., Brichory, F., Misek, D.E., Brechot, C., Hanash, S.M., and Beretta, L. 2002. A distinct repertoire of autoantibodies in hepatocellular carcinoma identified by proteomic analysis. *Mol. Cell Proteomics 1*:197–203.

Li, L., Tang, H., Wu, Z., Gong, J., Gruidl, M., Zou, J., Tockman, M., and Clark, R.A. 2004. Data mining techniques for cancer detection using serum proteomic profiling. *Artif. Intell. Med. 32*:71–83.

Liu, A.Y., Zhang, H., Sorensen, C.M., and Diamond, D.L. 2005. Analysis of prostate cancer by proteomics using tissue specimens. *J. Urol. 173*:73–78.

Loeb, L.A. 2001. A mutator phenotype in cancer. *Cancer Res. 61*: 3230–3239.

Ludewig, B., Ochsenbein, A.F., Odermatt, B., Paulin, D., Hengartner, H., and Zinkernagel, R.M. 2000. Immunotherapy with dendritic cells directed against tumor antigens shared with normal host cells results in severe autoimmune disease. *J. Exp. Med. 191*:795–804.

Mandelboim, O., Bar-Haim, E., Vadai, E., Fridkin, M., and Eisenbach, L. 1997. Identification of shared tumor-associated antigen peptides between two spontaneous lung carcinomas. *J. Immunol. 159*:6030–6036.

Metodiev, M.V., Timanova, A., and Stone, D.E. 2004. Differential phosphoproteome profiling by affinity capture and tandem matrix-assisted laser desorption/ionization mass spectrometry. *Proteomics 4*:1433–1438.

Naour, F.L., Brichory, F., Beretta, L., and Hanash, S.M. 2002. Identification of tumor-associated antigens using proteomics. *Technol. Cancer Res. Treat. 1*:257–262.

Oh, J.M., Brichory, F., Puravs, E., Kuick, R., Wood, C., Rouillard, J.M., Tra, J., Kardia, S., Beer, D., and Hanash, S. 2001. A database of protein expression in lung cancer. *Proteomics 1*:1303–13l9.

O'Hara, E.F., Williams, M.B., Rott, L., Abola, P., Hansen, N., Jones, T., Gurjal, M.R., Federspiel, N., and Butcher, E.C. 2005. Modified representational difference analysis: isolation of differentially expressed mRNAs from rare cell populations. *Anal. Biochem. 336*:221–230.

Okamoto, T., Suzuki, T., and Yamamoto, N. 2000. Microarray fabrication with covalent attachment of DNA using bubble jet technology. *Nat. Biotechnol. 18*:438–441.

Old, L.J. 2003. Cancer vaccines 2003: opening address. *Cancer Immun. 3 Suppl 2*:1.

Petricoin, E.F., Ardekani, A.M., Hitt, B.A., Levine, P.J., Fusaro, V.A., Steinberg, S.M., Mills, G.B., Simone, C., Fishman, D.A., Kohn, E.C., and Liotta, L.A. 2002. Use of proteomic patterns in serum to identify ovarian cancer. *Lancet 359*:572–577.

Petricoin, E.F. and Liotta, L.A. 2004. SELDI-TOF-based serum proteomic pattern diagnostics for early detection of cancer. *Curr. Opin. Biotechnol. 15*:24–30.

Ramaswamy, S., Ross, K.N., Lander, E.S., and Golub, T.R. 2003. A molecular signature of metastasis in primary solid tumors. *Nat. Genet. 33*:49–54.

Rammensee, H.G., Friede, T., and Stevanoviic, S. 1995. MHC ligands and peptide motifs: first listing. *Immunogenetics 41*: 178–228.

Rammensee, H.G., Weinschenk, T., Gouttefangeas, C., and Stevanovic, S. 2002. Towards patient-specific tumor antigen selection for vaccination. *Immunol. Rev. 188*:164–176.

Rosenberg, S.A. 2000. Identification of cancer antigens: impact on development of cancer immunotherapies. *Cancer J. 6 Suppl 3*: S200–S207.

Rosenberg, S.A. 2001. Progress in human tumour immunology and immunotherapy. *Nature 411*:380–384.

Ryan, T.E. and Patterson, S.D. 2002. Proteomics: drug target discovery on an industrial scale. *Trends Biotechnol. 20*:S45–S51.

Scheibenbogen, C., Lee, K.H., Stevanovic, S., Witzens, M., Willhauck, M., Waldmann, V., Naeher, H., Rammensee, H.G., and Keilholz, U. 1997. Analysis of the T cell response to tumor and viral peptide antigens by an IFNγ-ELISPOT assay. *Int. J. Cancer 71*:932–936.

Schirle, M., Weinschenk, T., and Stevanovic, S. 2001. Combining computer algorithms with experimental approaches permits the rapid and accurate identification of T cell epitopes from defined antigens. *J. Immunol. Methods 257*:1–16.

Schultz, E.S., Chapiro, J., Lurquin, C., Claverol, S., Burlet-Schiltz, O., Warnier, G., Russo, V., Morel, S., Levy, F., Boon, T., Van den Eynde, B.J., and van der Bruggen, P. 2002. The production of a new MAGE-3 peptide presented to cytolytic T lymphocytes by HLA-B40 requires the immunoproteasome. *J. Exp. Med. 195*: 391–399.

Seliger, B. and Kellner, R. 2002. Design of proteome-based studies in combination with serology for the identification of biomarkers and novel targets. *Proteomics 2*:1641–1651.

Sotiriou, C., Neo, S.Y., MeShane, L.M., Korn, E.L., Long, P.M., Jazaeri, A., Martiat, P., Fox, S.B., Harris, A.L., and Liu, E.T. 2003. Breast cancer classification and prognosis based on gene expression profiles from a population-based study. *Proc. Natl. Acad. Sci. USA 100*:10393–10398.

St. Croix, B., Rago, C., Velculescu, V., Traverso, G., Romans, K.E., Montgomery, E., Lal, A., Riggins, G.J., Lengauer, C., Vogelstein, B., and Kinzler, K.W. 2000. Genes expressed in human tumor endothelium. *Science 289*:1197–1202.

Stasyk, T. and Huber, L.A. 2004. Zooming in: fractionation strategies in proteomics. *Proteomics 4*:3704–3716.

Stoeckli, M., Chaurand, P., Hallahan, D.E., and Caprioli, R.M. 2001. Imaging mass spectrometry: a new technology for the analysis of protein expression in mammalian tissues. *Nat. Med. 7*: 493–496.

Traversari, C., van der Bruggen, B.P., Luescher, I.F., Lurquin, C., Chomez, P., Van Pel, A., De Plaen, E., Amar-Costesec, A., and Boon, T. 1992. A nonapeptide encoded by human gene MAGE-1 is recognized on HLA-A1 by cytolytic T lymphocytes directed against tumor antigen MZ2-E. *J. Exp. Med. 176*:1453–1457.

Tsou, J.A., Hagen, J.A., Carpenter, C.L., and Laird-Offringa, l.A. 2002. DNA methylation analysis: a powerful new tool for lung cancer diagnosis. *Oncogene 21*:5450–5461.

Tureci, O., Sahin, U., and Pfreundschuh, M. 1997. Serological analysis of human tumor antigens: molecular definition and implications. *Mol. Med. Today 3*:342–349.

Tuteja, R. and Tuteja, N. 2004. Serial Analysis of Gene Expression: applications in Human Studies. *J. Biomed. Biotechnol. 2004*:113–120.

van de Vijver, M.J., He, Y.D., van't Veer, L.J., Dai, H., Hart, A.A., Voskuil, D.W., Schreiber, G.J., Peterse, J.L., Roberts, C., Marton, M.J., Parrish, M., Atsma, D., Witteveen, A., Glas, A., Delahaye, L., van der Velde, T., Bartelink, H., Rodenhuis, S., Rutgers, E.T., Friend, S.H., and Bernards, R. 2002. A gene-expression signature as a predictor of survival in breast cancer. *N. Engl. J. Med. 347*:1999–2009.

Van den Eynde, B.J. and Boon, T. 1997. Tumor antigens recognized by T lymphocytes. *Int. J. Clin. Lab. Res. 27*:81–86.

Van den Eynde, B.J. and van der Bruggen, P. 1997. T cell defined tumor antigens. *Curr. Opin. Immunol. 9*:684–693.

van't Veer, L.J., Dai, H., van de Vijver, M.J., He, Y.D., Hart, A.A., Mao, M., Peterse, H.L., van der Kooy, K., Marton, M.J., Witteveen, A.T., Schreiber, G.J., Kerkhoven, R.M., Roberts, C., Linsley, P.S., Bernards, R., and Friend, S.H. 2002. Gene expression profiling predicts clinical outcome of breast cancer. *Nature 451*:530–536.

Veenstra, T.D., Prieto, D.A., and Conrads, T.P. 2004. Proteomic patterns for early cancer detection. *Drug. Discov. Today 9*: 889–897.

Velculescu, V.E., Zhang, L., Vogelstein, B., and Kinzler, K.W. 1995. Serial analysis of gene expression. *Science 270*:484–487.

Vogelstein, B. and Kinzler, K.W. 2004. Cancer genes and the pathways they control. *Nat. Med. 10*:789–799.

Voss, T., Ahorn, H., Haberl, P., Dohner, H., and Wilgenbus, K. 2001. Correlation of clinical data with proteomics profiles in 24 patients with B-cell chronic lymphocytic leukemia. *Int. J. Cancer 91*:180–186.

Voss, T. and Haberl, P. 2000. Observations on the reproducibility and matching efficiency of two-dimensional electrophoresis gels: consequences for comprehensive data analysis. *Electrophoresis 21*:3345–3350.

Wang, R.F., Wang, X., Johnston, S.L., Zeng, G., Robbins, P.F., and Rosenberg, S.A. 1998. Development of a retrovirus-based complementary DNA expression system for the cloning of tumor antigens. *Cancer Res. 58*:3519–3525.

Wang, R.F., Wang, X., and Rosenberg, S.A. 1999. Identification of a novel major histocompatibility complex class II-restricted tumor antigen resulting from a chromosomal rearrangement recognized by CD4(+) T cells. *J. Exp. Med. 189*:1659–1668.

Yanagisawa, K., Shyr, Y., Xu, B.J., Massion, P.P., H.Larsen, P., White, B.C., Roberts, J.R., Edgerton, M., Gonzalez, A., Nadaf, S., Moore, J.H., Caprioli, R.M., and Carbone, D.P. 2003. Proteomic patterns of tumour subsets in non-small-cell lung cancer. *Lancet. 362*:433–439.

Yip, T.T. and Lomas, L. 2002. SELDI ProteinChip array in oncoproteomic research. Technol. *Cancer Res. Treat. 1*:273–280.

Yu, L.R., Zhou, M., Conrads, T.P., and Veenstra, T.D. 2003. Diagnostic proteomics: serum proteomic patterns for the detection of early stage cancers. *Dis. Markers 19*:209–218.

Zhang, Z., Bast, Jr., R.C., Yu, Y., Li, J., Sokoll, L.J., Rai, A.J., Rosenzweig, J.M., Cameron, B., Wang, Y.Y., Meng, X.Y., Berchuck, A., Haaften-Day, C., Hacker, N.F., de Bruijn, H.W., van der Zee, A.G., Jacobs, I.J., Fung, E.T., and Chan, D.W. 2004. Three biomarkers identified from serum proteomic analysis for the detection of early stage ovarian cancer. *Cancer Res. 64*: 5882–5890.

This Page Intentionally Left Blank

2

The Post-Translational Phase of Gene Expression in Tumor Diagnosis

Jens F. Rehfeld and Jens Peter Goetze

Introduction

The progress in molecular biology with the mapping and identification of the human genome has resulted in a shift of paradigms in diagnosis, therapy and prevention of malignant diseases. The understanding of the pathogenesis at an exact molecular and cellular level and the implementation of molecular biology with its vast toolbox of technology in diagnosis, therapy and screening has led to the now generally accepted concept of molecular medicine, and more specifically of molecular oncology.

In the last decade, mainly deoxyribonucleic acid (DNA) techniques have attracted attention with an exponential increase in the number of recognized disease genes. More recently, DNA-array technologies have shown disease-specific patterns of gene expression that are bound to influence research, drug development and molecular diagnosis. In the wake of gene diagnostics, new and improved molecular diagnosis at the protein level is also appearing under headings such as post- or functional genomics and proteomics. Advanced mass spectrometry of proteins and peptides has already shown great diagnostic promise (Petricoin *et al.,* 2002; Srinivas *et al.,* 2001). Also the development in protein-array technology is now followed with great expectations (Gavin *et al.,* 2002; Ho *et al.,* 2002).

The functional or bioactive structure of a protein is defined not only by the gene and messenger ribonucleic acid (mRNA) encoding the protein. Proteins, and among them secretory proteins and polypeptides, often undergo multiple covalent modifications before they reach the structure required to exert their function. The post-translational modifications of proteins are often affected in cancer cells in a way that determines not only the amount of the functional protein or peptide synthetized in the cell but also changes the concentration pattern of precursor, processing intermediates and degradation products.

Recognition of the pathologic significance of post-translational processing and measurement of processing changes in specific tissues opens new possibilities for diagnosis of tumors and other cellular disturbances (for review, see Rehfeld and Goetze, 2003).

In the following, the diagnostic possibilities inherent in the post-translational maturation process are illustrated for secretory proteins and peptides belonging to the neuroendocrine system. First, however, general

Handbook of Immunohistochemistry and *in situ* Hybridization of Human Carcinomas, Volume 4: Molecular Genetics, Gastrointestinal Carcinoma, and Ovarian Carcinoma

biochemical aspects of processing mechanisms are reviewed. Insight into such mechanisms are important for appreciation of the diagnostic possibilities.

General Aspects of Proprotein Processing

Standard textbooks in molecular biology and medical biochemistry generally pay little attention to the occasional complex and elaborate maturation of the product of ribosomal translation, the proprotein (Figure 1). The co-translational removal of the N-terminal signal sequence from preproproteins is often acknowledged, but without emphasis of the fact that removal occurs in the endoplasmatic reticulum before the translation of the C-terminal sequence of the protein is terminated (see Figure 1). Accordingly, complementary DNA (cDNA)-deduced preproproteins are theoretic structures that never occur in living cells. They exist only in theory or *in vitro* in cell-free translational extracts. It is, however, important to know the exact cleavage site of the signal sequence in order to define the N-terminus of the proprotein. In turn, precise knowledge of the proprotein structure is necessary for understanding of post-translational processing mechanisms, of which there are three main categories: endoproteolytic cleavages, exoproteolytic trimmings, and amino acid derivatizations.

Endoproteolytic Cleavages

The primary sites for endoproteolytic maturation are located at the peptide bond of the C-terminus of the basic amino acid residues, Arg and Lys. As pointed out by Steiner after his discovery of proinsulin, cleavage often occurs at dibasic sites. Of these, Lys–Arg sites are most commonly cleaved, and Arg–Arg constitutes

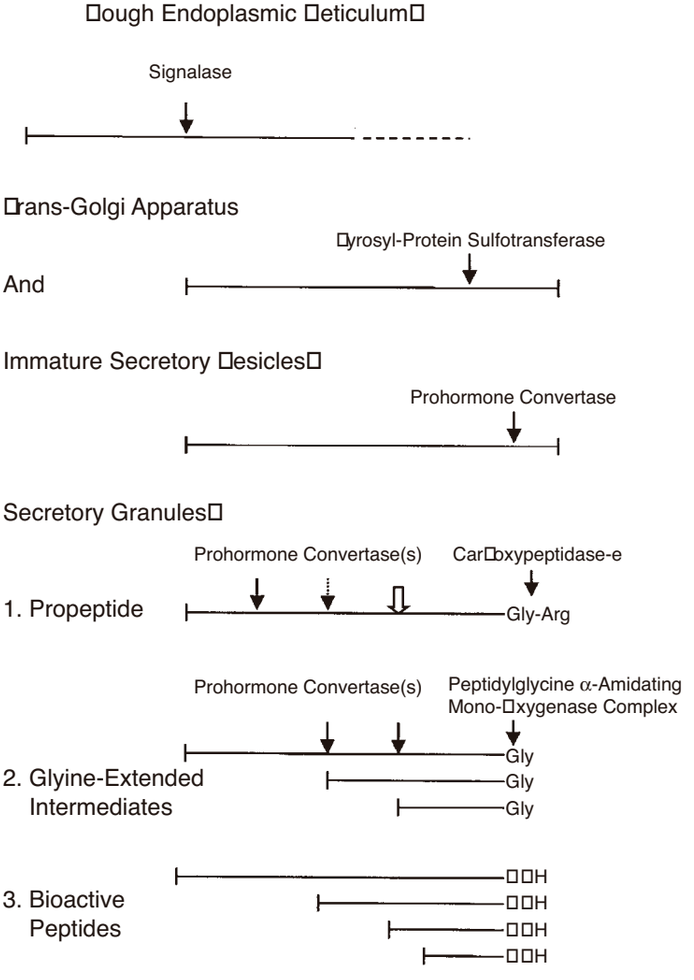

Figure 1. Example of cellular steps in the post-translational processing of secretory proteins and peptides.

the second most common dibasic cleavage site. In contrast, Arg–Lys and especially Lys–Lys sites are rarely cleaved. Cleavages at monobasic and tri- or tetrabasic sites are also common (Bresnahan *et al.,* 1999; Devi, 1991). However, many peptide bonds after Arg and Lys residues are never processed. Although several attempts have been made, it is not possible to predict cleavage at a given site.

The endoproteolytic cleavage at mono- and dibasic sites is achieved by subtilisin-like proprotein convertases of which nine are currently known (for reviews, see Müller and Lindberg, 2000; Rouillé *et al.,* 1995). The cleavage of most neuroendocrine protein precursors can be explained by prohormone convertases 1 and 2 (PC1 and PC2) (Smeekens *et al.,* 1991). After cleavage at the C-terminus of Arg or Lys, the basic residue is removed by a carboxypeptidase. So far, carboxypeptidase E appears responsible for most C-terminal trimming of basic residues (Fricker *et al.,* 1989; see also Figure 1). In accordance with the assumed significance of these processing enzymes, spontaneous endocrine syndromes in humans and mice (Müller and Lindberg, 2000; O'Rahilly *et al.,* 1995) as well as phenotypes of knock-out animals are seen by deficiency or elimination of the enzymes. The neuroendocrine disturbances most often comprise obesity, mild diabetes mellitus, and severe Cushing's disease (Furuta *et al.,* 1997; Naggert *et al.,* 1995; O'Rahilly *et al.,* 1995; Westphal *et al.,* 1999) and, in PC4 deficiency, impaired fertility (Mbikay *et al.,* 1997).

In addition to the processing at basic sites by the subtilisin-like proprotein convertases, some protein precursors also undergo secondary endoproteolytic cleavage at other residues. Hence, systematic cleavage has been reported after Phe-residues (Jensen *et al.,* 2001), after polyacidic (Glu, Asp) sequences (Rehfeld *et al.,* 1995; Schmutzler *et al.,* 1992) and others. Also N-terminal trimming by dipeptidyl peptidases has been reported for a number of protein precursors. The processing enzymes responsible for endoproteolysis at secondary sites, have not yet been identified. Some of these sites resemble those cleaved by lysosomal degradation enzymes, because the processings observed occur along the secretory pathway in the cells, it has been suggested that minute amounts of less specific lysosomal enzymes, such as cathepsins, occasionally are present along the secretory pathway and thereby contribute to the post-translational maturation.

Exoproteolytic Trimming

A characteristic feature of many peptide hormones and neuropeptides is covalent modification of their N- and C-termini. The modifications protect against extracellular degradation by amino peptidases and carboxypeptidases. Some peptides are modified in both ends, others only in one. In half of all regulatory peptides (hormones, peptide transmitters, growth factors, and cytokines in their active form), the C-terminal amino acid residue is α-amidated (for review, see Eipper *et al.,* 1992). The α-amidation is a prerequisite for binding to specific receptors and hence for biological activity for most of these peptides. The carboxyamidation process is accomplished by a now well-characterized enzyme, PAM (peptidylglycine, α-amidating monooxygenase), which has turned out to be a complex of two enzymes derived from the same proenzyme present in secretory granules (Eipper *et al.,* 1992). In the presence of copper and ascorbic acid and at a pH of 5 in the mature secretory granules, the PAM complex hydrolyses the C-terminal glycyl residue in the immediate precursor of α-amidated peptides and proteins. Hence, glycine is the obligatory amide donor. Accordingly, the sequence –X–Gly–Arg/Lys– in a proprotein constitutes a phylogenetically highly preserved "amidation site" to be cleaved and trimmed sequentially by a prohormone convertase (often PC1), carboxypeptidase E, and the PAM complex (see Figure 1).

The N-terminal trimmings are more variable. N-terminal glutaminyl residues are often cyclized to pyroglutamic acid by the specific enzyme, glutaminyl cyclase (Fischer and Spiess, 1987). Also N-terminal or near N-terminal acetylation or other acylations and O-sulfations seem to protect against aminopeptidase degradation (Bundgaard *et al.,* 2002; Kojima *et al.,* 1999). As already mentioned, some N-termini are trimmed by dipeptidyl peptidases.

Amino Acid Derivatizations

The list of post-translational amino acid derivatizations is still growing. Primary and secondary protein structures are now deduced from cDNA sequences. Amino acid derivatizations, however, cannot be deduced. Therefore, mass spectrometry of proteins and peptides is necessary to determine the degree and nature of derivatizations. Moreover, it is likely that mass spectrometry in the coming years will reveal new amino acid modifications along with identification of the entire human proteome. The genes encoding the processing enzymes responsible for the amino acid derivatizations are being cloned, and the enzyme structure and function are being identified. Just as several proprotein convertases may participate in the endoproteolytic processing of monobasic and dibasic cleavage sites, a certain redundancy is seen for enzymatic amino acid derivatizations. For instance, mammals express two different

tyrosyl-sulfotransferases (for review, see Bundgaard *et al.,* 2002).

The exact role of each derivatization has not yet been fully elucidated. As mentioned, however, some seem to protect the protein or peptide from enzymatic degradation both before and after cellular release. Other derivatizations increase or determine the interaction with binding proteins such as chaperones, processing enzymes, and receptors. Derivatizations may also serve as intracellular signals in the molecular trafficking. Irrespective of the functional significance of a given derivatization, it influences measurement of the protein or peptide. The methods used for measurement are most often immunochemical, and, if a given epitope on the protein or peptide contains one or more derivatizations, they may determine whether the epitope is bound to antibodies.

Examples of Proprotein Processing

Progastrin

Progastrin is the precursor of the gastrointestinal hormone, gastrin, which regulates gastric mucosal growth and gastric acid secretion. As indicated in Figures 1 and 2, the maturation of progastrin in the antroduodenal G-cells is complex and requires multiple enzymatic processes. The first is initiated in the transGolgi network, where progastrin becomes tyrosyl-sulfated and seryl-phosphorylated. Simultaneously, or even earlier, cleavage at two double Arg sites begins (Arg_{36}–Arg_{37} and Arg_{73}–Arg_{74}). The cleavages, however, are not complete (see Figure 2). They are followed by partial endoproteolytic cleavages at the double Lys site (Lys_{53}–Lys_{54}) and the monobasic Arg_{19} site (see Figure 2). Minor cleavages also occur after Trp_{58} and the poly-$Glu_{60\text{-}64}$ sequence (Bundgaard *et al.,* 2002; Rehfeld *et al.,* 1995). To ensure carboxyamidation, carboxypeptidase E removes the C-terminal Arg-residues so that PAM can use the glycyl residue as amide donor. Along the secretory pathway, the free N-terminal glutaminyl residues (Gln_{38} and Gln_{55}) are also cyclized to pyroglutamic acid.

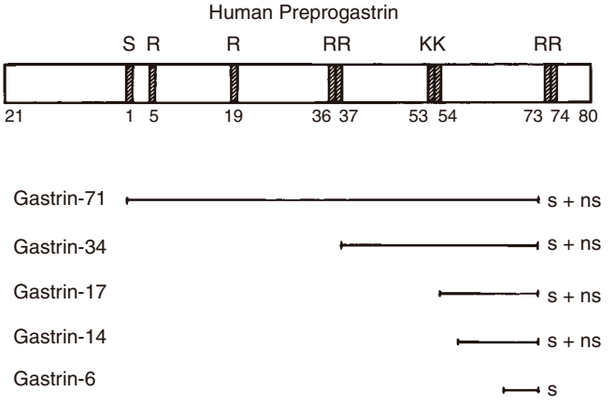

Figure 2. Bioactive processing products of human preprogastrin in antroduodenal G-cells. The monobasic and dibasic cleavage sites on progastrin products is indicated in amino acid monoletter code (R, RR, and KK). The signal peptide is removed co-translationally at the N-terminus of serine (S) in position 1 of progastrin. The small s and ns indicates whether the peptides are O-sulfated (right).

The multiple modifications result in that the G-cells release a mixture of α-carboxyamidated gastrins into the circulation (see Figure 2). The dominating molecular forms in normal human plasma are gastrin-34 and gastrin-17, which both circulate in tyrosyl-sulfated and unsulfated variants. In addition, longer (gastrin-52 and gastrin-71) and shorter (gastrin-14 and gastrin-6) forms are also released to plasma. In addition to the bioactive gastrins, however, the G-cells also secrete processing intermediates and N- and C-terminal progastrin fragments without known bioactivity. The pattern of amidated gastrins and other progastrin products in circulation is influenced by age, gender, meals, and pH in the stomach. The ratio between acid stimulatory gastrins and inactive precursors and precursor fragments therefore vary considerably and individually. As a general rule, the fraction of unprocessed and incompletely processed progastrin fragments increases exponentially with increased cellular synthesis as seen in tumors (gastrinomas) and in hypochlorhydria and achlorhydria associated with gastritis or treatment with acid-reducing drugs (Bardram, 1990; Goetze and Rehfeld, 2003). Consequently, methods that measure only the concentration of carboxyamidated gastrins can provide a false low impression of the cellular synthesis. In contrast, methods that measure the total progastrin product provide a more accurate measure. This distinction has diagnostic impact (Bardram, 1990).

ProBNP

ProBNP is the precursor of brain natriuretic peptide (BNP), a natriuretic and vasodilatory hormone originally discovered in the brain (hence the name) (Sudoh *et al.,* 1988). Today we know that BNP is synthetized primarily in the heart. In the normal heart, BNP is expressed together with ANP (atrial natriuretic peptide) in atrial myocytes (Christoffersen *et al.,* 2002). In heart failure, however, most BNP is synthetized in left-ventricular myocytes, from which proBNP and its products are released into the circulation (Goetze, 2004).

ProBNP-derived peptides in plasma have now attracted massive clinical interest as sensitive markers of heart failure (for review, see de Lemos *et al.,* 2003). BNP was identified in porcine brain extracts, and the primary structure of human proBNP was deduced shortly thereafter. In comparison with other hormones, the knowledge and number of studies of the post-translational processing of proBNP are therefore limited. At present, however, the cellular processing looks simple (Goetze, 2004). Human proBNP is a small protein of 108 amino acid residues. It is cleaved at a monobasic site (Arg_{76}) to yield the biologically inactive N-terminal fragment 1-76 and the natriuretic C-terminal BNP hormone of 32 amino acids, which is cyclized by a disulfide bridge. Chromatographic studies of plasma have accordingly shown that intact proBNP, the N-terminal fragment 1-76, and BNP itself are released to circulation (Hunt *et al.,* 1995). In contrast with progastrin, proBNP illustrates a simple precursor processing scheme as is known also for proinsulin and some other polypeptide hormones (for review, see Rehfeld, 1998b). In view of its diagnostic potential, proBNP and its products seem at present one of the clinically most interesting peptide systems to study.

Chromogranin A

Chromogranin A (CgA) is a large and highly acidic secretory protein of 439 amino acids expressed in most neuroendocrine cells, where it is packed closely together with hormonal or neurotransmitter peptides as well as monoamines in secretory granules or synaptic vesicles. The definitive function of CgA is not yet known, but different roles have been suggested (for reviews, see Helle, 2004; and Huttner *et al.,* 1991). They include cellular chaperone function, modulation of prohormone processing, or a precursor role for new bioactive peptides. Irrespective of possible functions, circulating CgA has turned out to be a promising marker for neuroendocrine tumors, including "silent" endocrine tumors and the fairly frequent intestinal carcinoid tumors that otherwise have been difficult to diagnose in an early stage.

As suggested by the many monobasic and dibasic sites in the sequence, CgA is subject to extensive and tissue-specific post-translational processing. Accordingly, many endoproteolytic fragments have been identified in tissue and plasma, with some fragments claimed to exert independent functions (for reviews, see Helle, 2004; Huttner *et al.,* 1991; Natori and Huttner, 1994). However, solid evidence for such functions still remains to be demonstrated. The cellular cleavages of CgA vary considerably and individually. Moreover, the cleavage pattern is tissue and tumor specific. Consequently, measurements of CgA in human plasma are troublesome, not only because the processing of CgA varies between tumors but also because the epitopes targeted by CgA immunoassays differ markedly (Taupenot *et al.,* 2003). To avoid false-negative results and to compare measurements from different laboratories, it is therefore essential to reach consensus on a method for measurement that uniformly quantitates as much CgA in plasma as possible, irrespective of the degree and individuality of the post-translational processing.

Processing-Independent Analysis

As illustrated with the previous descriptions of progastrin, proBNP, and CgA, the processing of proproteins varies in several respects. Not only are there major variations from protein to protein, but the processing of the same protein can also vary in the same person in a cell- and tissue-specific manner. In addition, the processing may change in a given cell both during the ontogenetic development and during oncogenetic transformation. Finally, the processing of a proprotein varies individually in the same type of tumor in different patients. With the clarification of the sequence of the human genome, and with knowledge about the encoded primary structure of all proproteins, it is foreseeable that new patterns and types of post-translational processing will appear. This will increase the demand for the diagnostic use of protein and peptide measurements.

To overcome the excessive variability, we have designed an analytic principle according to which methods can be developed to measure any protein or peptide in tissue or plasma irrespective of the nature and degree of post-translational processing (Bardam and Rehfeld, 1988). The principle of such processing-independent analysis (PIA) is illustrated in Figure 3. PIA measurements are based on three premises:

- Known proprotein structure, which requires knowledge of the cDNA sequence.
- Known or deductible cellular, and post-cellular processing in the circulation.
- Recognition of the shortcomings of conventional diagnostic methods.

The immunochemical version of PIA is then developed in the following way: A sequence of approximately 10 to 12 amino acid residues of the proprotein is synthetized. The selected sequence is one that is neither modified nor cleaved during cellular processing, but, that neighbors *in vitro* cleavage sites, usually a trypsin-sensitive basic residue. The synthetic fragment is then directionally coupled through either its N- or C-terminal

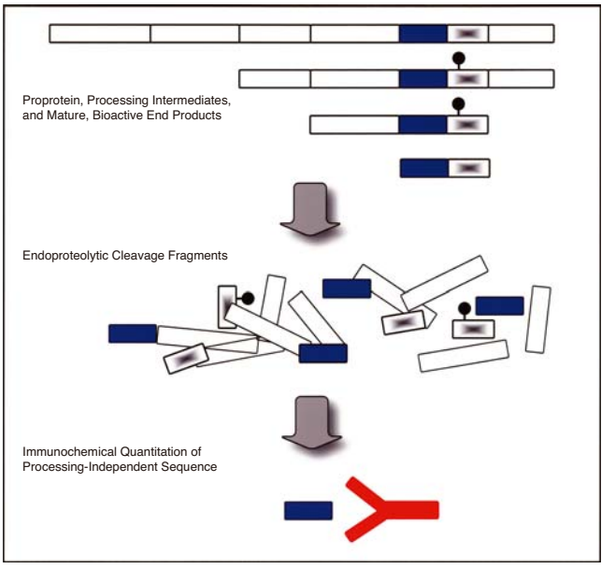

Figure 3. General scheme of post-translational maturation of secretory proteins showing the principle of processing-independent analysis (PIA). The blue bars represent a sequence that does not undergo post-translational modification and is present in precursors, processing-intermediates, and mature end-products. The black dots indicate variable amino acid derivatization (i.e., sulfated and nonsulfated gastrin). The processing-independent sequence must be located between suitable cleavage sites that allow release of one processing-independent fragment per molecule translated proprotein by a suitable endoprotease (i.e., trypsin). After inactivation of the endoprotease, *in vitro* quantitation of the released processing-independent peptide fragment can be performed by a specific assay. The quantity is an accurate measure of the total translation product, irrespective of its degree of processing.

residue to a suitable carrier protein. We generally use bovine serum albumin. To facilitate coupling, a cystein residue is added during synthesis at the terminus of the peptide through which coupling is going to take place.

The peptide carrier complex is mixed in a suitable vehicle and then injected conventionally for production of antibodies specific for the peptide. We use subcutaneous injection over the groins of rabbits. For development of a suitable radioimmunoassay (RIA), a variant hapten peptide is also synthetized with a tyrosyl residue inserted in the end opposite to the epitope. The tyrosylated peptide is then ^{125}I-iodinated to be used as tracer. In this way, a monospecific RIA directed against either the N- or C-terminus of the processing-independent sequence is produced. The sample to be assayed (plasma or tissue extract) is preincubated with a suitable endoprotease (we generally use trypsin). The endoprotease treatment ensures that the selected epitope is fully exposed for antibody binding, and, moreover, that fragments of equal size are released from unprocessed proproteins or partly modified processing intermediates. After inactivation of the protease by addition of inhibitors or by boiling of the sample, the total translation product is then quantitated by the PIA-designed RIA. Such assay measures per definition proprotein, processing intermediates and endproducts with equimolar potency. Hence, each translated molecule of protein is measured irrespective of the degree of processing. Details of assay design is described elsewhere (Bardam and Rehfeld, 1988; Paloheimo and Rehfeld, 1995).

Problems and Pitfalls of Processing-Independent Analysis Measurements

The first problem is simple and technical. Because the initial protease preincubation and inactivation add two analytic steps, it increases the variance and labor intensiveness of the measurements. This is particularly obvious in comparison with assays that do not require extraction of other pretreatments of the sample, for instance, direct RIA measurements on serum or plasma samples. However many peptide hormones cannot be measured in plasma without initial extraction or denaturation of plasma proteins and enzymes. Fortunately, treatment with trypsin also degrades common plasma proteins, and hence eliminates the necessity of extraction before measurement (Goetze *et al.,* 2002). In this way PIA measurements may make other pretreatment extractions superfluous and can be performed without extra work. It is also possible that the protease treatment can be simplified by coupling of the protease to plastic beads or tubes, so that the pretreatment requires only an extra centrifugation and decantation.

The second problem is of a more general and theoretical nature. Whereas PIA measurement on *tissue extracts* affords an accurate measure of protein translation, molecule for molecule (provided that the tissue extraction is complete), measurements of *plasma samples* are affected by the large variability in clearance of the different precursors, processing intermediates, and bioactive end products. As a rule, the longer the peptide chain, the slower the clearance. Proproteins and longer processing intermediates consequently accumulate in plasma in comparison with the shorter and more extensively processed bioactive peptides. In diagnostic terms, this phenomenon is nevertheless an advantage because tumor cells with disturbed and deteriorated processing mechanisms release more unprocessed and partly processed precursors and relatively less of the shorter end products. Thus, the incomplete processing contributes to increase the plasma concentration as

measured with a PIA method, whereas conventional methods that are directed against the bioactive end product of the cellular processing will measure peptide concentrations that represent a false low estimate of the underlying disturbances of the cell. Consequently PIA measurements improve both the diagnostic and analytical sensitivity considerably (see Figure 3).

A third question to consider is the analytical specificity. Proteins display various degrees of homology and similarity, which often reflect the phylogenetic evolution from common ancestors. Therefore, when a certain epitope (i.e., a sequence of 5 to 8 amino acid residues) is selected—irrespective of whether it is for RIA, PIA, enzyme-linked immunoassay (ELISA), immunoradiometric assay (IRMA), or other antibody-based measurements—it is important to ensure from protein sequence banks that the selected epitope is specific for the proprotein to be measured. This is not only a theoretical consideration. The history of diagnostic immunoassays and immunocytochemistry abounds with examples of false-positive results caused by unforeseen similarity or homology between unknown or known proteins.

Processing-Independent Analysis in Tumor Diagnosis

Progastrin

Increased secretion of progastrin products has been encountered by most diseases of the stomach and by cancers in the gastrointestinal tract, pancreas, lungs and ovaries (for review, see Rehfeld and van Solinge, 1994). So far, however, the diagnostic use of measurement of gastrin peptides by conventional assays or by PIA measurements have not been shown for the individual disease, except for gastrinomas. Gastrinomas occur mostly in the pancreas and the duodenum; ovarian gastrinomas are less frequent, and occasionally gastrinomas have been found in the antrum, lungs, and heart (Ginbril *et al.,* 1997). When gastrin assays became generally available in the 1970s, large and metastatic gastrinomas were frequently discovered. They are easy to diagnose, but today they are rarely found in countries with an organized gastrin assay service. Most gastrinomas detected today are pinhead sized and contribute only moderately to the circulating concentrations of amidated gastrin. Patients with small gastrinomas may even periodically have normal gastrin concentrations in plasma (Zimmer *et al.,* 1995). Consequently, today's gastrinomas show borderline concentrations—not least in the increasing population of people with occasional dyspepsia who take proton pump inhibitors and other inhibitors of gastric acid that also increase the gastrin concentrations in plasma. In that situation, PIA measurements of the total progastrin concentration in plasma may help to ensure correct diagnosis in patients with recurrent dyspepsia (Jørgensen *et al.,* 1998). In metastatic gastrinomas, PIA measurements show larger abnormalities than conventional measurement of amidated gastrins (Bardram, 1990). A gastrinoma case is shown in Table 1, which illustrates the significance of early PIA measurements.

Procholecystokinin

Cholecystokinin (CCK) is a peptide hormone and a neurotransmitter. Like progastrin, proCCK undergoes multiple posttranslational modifications in both endocrine cells and neurons. Accordingly, the bioactive end products are extensively processed (i.e., carboxyamidated, tyrosyl-sulfated and cleaved at several monobasic and dibasic sites). Modest proCCK expression has been observed in several neuroendocrine tumors without effect on plasma CCK concentrations, but so far neither carcinomas nor specific endocrine tumors that produce CCK in analogy with gastrinomas, insulinomas, and glucagonomas have been found (for review, see Rehfeld and van Solinge, 1994). Recently, however, certain childhood sarcomas have been shown to express the CCK gene (Friedman *et al.,* 1992), and correspondingly the proCCK protein (Schaer and Reubi, 1999). The sarcoma cells, however, neither amidate nor O-sulfate the proCCK fragments. Therefore, the plasma concentrations of bioactive α-amidated and O-sulfated CCK peptides are completely normal (Rehfeld, 1998a),

Table 1. Concentrations of α-Amidated Gastrins and the Total Progastrin Product in Serum from a Gastrinoma Patient at Different Clinical Stages

Patient	α-Amidated Gastrins (pmol/l)	Total Progastrin Product (pmol/l)
Zollinger-Ellison syndrome suspected	27	276
3 yr later, no tumor found	60	642
4 yr later, after resection of pancreatic tumor	10	75
6 yr later, recurrence with hepatic metastases	1500	7200

From ref. 1 with kind permission from Dr. L. Bardram.

but the total proCCK product is significantly increased in sarcoma patients (Reubi *et al.,* 2004). Moreover, the proCCK concentration is associated with tumor size, and therefore PIA measurements of proCCK (Paloheimo and Rehfeld, 1995) show promise as a marker of development and therapy of certain sarcomas (Reubi *et al.,* 2004). Figure 4 shows the difference in plasma concentrations between RIA measurements of amidated and O-sulfated CCK peptides and proCCK PIA measurements in children with Ewing sarcomas.

Chromogranin A

Because of the extensive but variable post-translational cleavage, quantitation of the total CgA product in plasma provides a more accurate measure of CgA secretion than conventional measurement where the epitope most often is unknown. For endocrine tumors without known hormone products such as mid-intestinal carcinoids, "silent" tumors of the pancreas and the pituitary, and small-cell bronchial cancer, CgA measurements have attracted interest as a possible tumor marker. In a study of CgA measurements using RIA against six different epitopes in human CgA—with and without preanalytical tryptic cleavage (PIA)—the best diagnostic specificity was obtained using RIA measurement directed against sequence 340-348 after tryptic cleavage of Arg-339 (Jensen *et al.,* 1999). Preliminary results suggest that PIA measurements based on this assay provided the best discrimination in the mentioned categories of tumor patients (Jensen, Rehfeld, and Hilsted, unpublished data).

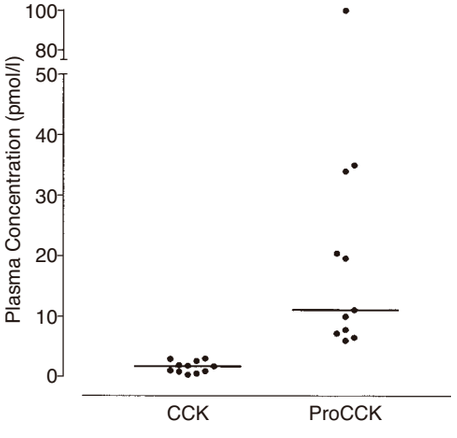

Figure 4. The concentrations of cholecystokinin (CCK) and proCCK in plasma from patients with Ewing sarcoma. The CCK concentrations were measured using a conventional radioimmunoassay (RIA) specific for the O-sulfated and α-amidated C-terminus of bioactive CCKs (Rehfeld, 1998), while the concentrations of the total proCCK product were measured by processing-independent analysis (PIA) of proCCK and its products (Paloheimo and Rehfeld, 1995).

Perspective

The concept of molecular biology was founded 50 years ago in the wake of the discovery of the DNA double helix. From the very beginning, it was never doubted that molecular biology was going to have a major impact on medical diagnosis and therapy. Over the last decades, development has rendered this prophecy more than true in all areas of medicine, particularly so in cancer biology and clinical oncology. Hence, even the term molecular medicine may in the future get a flavor of tautology, because most clinical oncological practice *per se* will require insight in and use of molecular biology.

In molecular biology, understanding of the gene expression cascade is of central significance. Knowledge of the cascade is also of decisive importance for insight in the pathogenesis of a rapidly growing list of common diseases—not least including tumor diseases. Studies of expression cascades have so far, however, given only modest attention to the last phase of expression, the post-translational phase. The purpose of this chapter has been to facilitate to a better balance by indicating that there are promising possibilities for improved molecular diagnosis by also exploring our knowledge about the post-translational processing.

Post-translational processing of proproteins may in many cases be simple and without obvious possibilities for new diagnostic procedures, but the post-genomic era of biology we now are entering will display a host of new protein structures. Among these are secretory proteins, which, like many known protein and peptide hormones, have undergone multiple maturation steps along the secretory pathway. In the study of the biosynthesis of these proteins, new possibilities are likely to appear and contribute to improved diagnosis in cardiology, endocrinology, gastroenterology, oncology, and other areas of clinical medicine.

Summary

Many proteins undergo post-translational maturation before they reach the structure in which they can fulfill their function. The maturation includes a variety of endoproteolytic cleavages, N- and C-terminal trimmings and amino acid derivatizations. Occasionally the protein precursor is differently processed in different cell types and, in addition, tumor cells may process a given precursor abnormally. For instance, the translational

process is often either increased or decreased in malignant cells. As a result, a variable mixture of precursors and processing intermediates accumulates, and measurement of a single protein or peptide component of the processing cascade may not facilitate the diagnosis, because the pattern of precursors and processing products vary individually among patients.

In order to exploit disturbed post-translational processing for diagnostic use, and, at the same time, provide an accurate measure of the translational products, a simple analytical principle named *processing-independent analysis* (PIA) has been designed. The PIA methods quantitate the total mRNA product, irrespective of the degree of precursor processing. Methods of PIA have recently been developed for a number of prohormones and neuroendocrine proteins, and their diagnostic potential appears promising in early diagnosis of tumors.

This chapter described processing patterns for some neuroendocrine proteins and PIA measurements with indications of problems and pitfalls for this analysis.

Acknowledgments

The skillful secretarial assistance of Christina Bak Fleischer is gratefully acknowledged. The studies from the authors laboratory on which parts of the review are based, were supported by grants from the Danish Medical Research Council, the Danish Cancer Union, and the Danish Biotechnology Center for Cellular Communication.

References

Bardram, L. 1990. Progastrin in serum from Zollinger-Ellison patients. An indicator of malignancy. *Gastroenterology 98*: 1420–1425.

Bardram, L., and Rehfeld, J.F. 1988. Processing-independent radioimmunoanalysis: a general analytical principle applied to progastrin and its products. *Anal. Biochem. 175*:537–543.

Bresnahan, P.A., Leduc, R., Thomas, L., Thorner, J., Gibson, H.L., Brake, A.J., Barr, P.J., and Thomas, G. 1999. Human fur gene encodes a yeast KEX2-like endoprotease that cleaves pro-beta-NGF *in vivo*. *J. Cell Biol. 111*:2851–2860.

Bundgaard, J.R., Johnsen, A.H., and Rehfeld, J.F. 2002. Analysis of tyrosine-O-sulfation. *Meth. Mol. Biol. 194*:223–239.

Christoffersen, C., Goetze, J.P., Bartels, E.D., Larsen, M.O., Ribel, U., Rehfeld, J.F., Rolin, B., and Nielsen, L.B. 2002. Chamber-dependent expression of brain natriuretic peptide and its mRNA in normal and diabetic pig heart. *Hypertension 40*: 54–60.

de Lemos, J.A., McGuire, D.K., and Drazner, M.H. 2003. B-type natriuretic peptide in cardiovascular disease. *Lancet 362*:316–22.

Devi, L. 1991. Consensus sequence for processing of peptide precursors at monobasic sites. *FEBS Lett. 280*:189–194.

Eipper, B.A., Stoffers, D.A., and Mains, R.E. 1992. The biosynthesis of neuropeptides: peptide α-amidation. *Annu. Rev. Neurosci. 15*:57–85.

Fischer, W.H., and Spiess, J. 1987. Identification of a mammalian glutaminyl cyclase converting glutaminyl into pyroglutamyl peptides. *Proc. Natl. Acad. Sci. USA 84*:3628–3632.

Fricker, L.D., Adelman, J.P., Douglass, J., Thompson, R.C., von Strandmann, R.P., and Hutton, J. 1989. Isolation and sequence analysis of cDNA for rat carboxypeptidase E (EC 3.4.17.10), a neuropeptide processing enzyme. *Mol. Endocrinol. 3*:666–673.

Friedman, J.M., Vitale, M., Maimon, J., Israel, M.A., Horowitz, M.E., and Schneider, B.S. 1992. Expression of the cholecystokinin gene in pediatric tumors. *Proc. Natl. Acad. Sci. USA 89*: 5819–5823.

Furuta, M., Yano, H., Zhou, A., Rouillé, Y., Holst, J.J., Carroll, R., Ravazzola, M., Orci, L., Furuta, H., and Steiner, D.F. 1997. Defective prohormone processing and altered pancreatic islet morphology in mice lacking active SPC2. *Proc. Natl. Acad. Sci. USA 94*:6646–6649.

Gavin, A.C., Bösche, M., Krause, R., Grandi, P., Marzioch, M., Bauer, A., Schultz, J., Rick, J.M., Michon, A.M., Cruciat, C.M., Remor, M., Hofert , C., Schelder, M., Brajenovic, M., Ruffner, H., Merino, A., Klein, K., Hudak, M., Dickson, D., Rudi, T., Gnau, V., Bauch, A., Bastuck, S., Huhse, B., Leutwein, C., Heurtier, M.A., Copley, R.R., Edelmann, A., Querfurth, E., Rybin, V., Drewes, G., Raida, M., Bouwmeester, T., Bork, P., Seraphin, B., Kuster, B., Neubauer, G., and Superti-Furga, G. 2002. Functional organization of the yeast proteome by systematic analysis of protein complexes. *Nature 415*:141–147.

Ginbril, F., Curtis, L.T., Termanini, B., Fritsch, M.K., Lubensky, I.R., Doppman, J.L., and Jensen, R.T. 1997. Primary cardiac gastrinoma causing Zollinger-Ellison syndrome. *Gastroenterology 112*:567–574.

Goetze, J.P. 2004. Biochemistry of pro-B-type natriuretic peptide-derived peptides: the endocrine heart revisited. *Clin. Chem. 50*: 1503–1510.

Goetze, J.P., Kastrup, J., Pedersen, F., and Rehfeld, J.F. 2002. Quantification of pro-B-type natriuretic peptide and its products in human plasma by use of an analysis independent of precursor processing. *Clin. Chem. 48*:1035–1042.

Goetze, J.P., and Rehfeld, J.F. 2003. Impact of assay epitope specificity in gastrinoma diagnosis. *Clin. Chem. 49*:333–334.

Helle, K.B. 2004. The granin family of uniquely acidic proteins of the diffuse neuroendocrine system: comparative and functional aspects. *Biol. Rev. 79*:769–764.

Ho, Y., Gruhler, A., Heilbut, A., Bader, G.D., Moore, L., Adams, S.L., Millar, A., Taylor, P., Bennett, K., Boutilier, K., Yang, L., Woiting, C., Donaldson, I., Schandorff, S., Shewnarane, J., Vo, M., Taggart, J., Goudreault, M., Muskat, B., Alfarano, C., Dewar, D., Lin Z., Michalickova, K., Willems, A.R., Sassi, H., Nielsen, P.A., Rasmussen, K.J., Andersen, J.R., Johansen, L.E., Hansen, L.H., Jespersen, H., Podtelejnikov, A., Nielsen, E., Crawford, J., Poulsen, V., Sorensen, B.D., Matthiesen, J., Hendrickson, R.C., Gleeson, F., Pawson, T., Moran, M.F., Durocher, D., Mann, M., Hogue, C.W., Figeys, D., and Tyers, M. 2002. Systematic identification of protein complexes in Saccharomyces cerevisiae by mass spectrometry. *Nature 415*:180–182.

Hunt, P.J., Yandle, T.G., Nicholis, M.G., Richards, A.M., and Espiner, E.A. 1995. The amino-terminal portion of pro-brain natriuretic peptide (Pro-BNP) circulates in human plasma. *Biochem. Biophys. Res. Commun. 214*:1175–1183.

Huttner, W.B., Gerdes, H.H., and Rosa, P. 1991. The granin (chromogranin/secretogranin) family. *Trends Biochem. Sci. 16*: 27–30.

Jensen, H., Ørskov, C., Rehfeld, J.F., and Johnsen, A.H. 2001. A processing enzyme cleaving avian progastrin at post-Phe bonds. *Biochim. Biophys. Acta. 1547*:64–71.

Jensen, T.B., Hilsted, L., and Rehfeld, J.F. 1999. Library of sequence-specific radioimmunoassays for human chromogranin A. *Clin. Chem. 45*:549–560.

Jørgensen, N.R., Rehfeld, J.F., Bardram, L., and Hilsted, L. 1998. Processing-independent analysis in the diagnosis of gastrinomas. *Scand. J. Gastroenterol. 33*:379–385.

Kojima, M., Hasoda, H., Date, Y., Nakazato, M., Matsuo, H., and Kongawa, K. 1999. Ghrelin is a growth-hormone-releasing acylated peptide from stomach. *Nature 402*:656–660.

Mbikay, M., Tadros, H., Ishida, N., Lemer, C.P., De Lamirande, B., Chen, A., El-Alfy, M., Clermont, Y., Seidah, N.G., and Chretien, M. 1997. Impaired fertility in mice deficient for the testicular germ-cell protease PC4. *Proc. Natl. Acad. Sci. USA 94*:6842–6846.

Müller, L., and Lindberg, I. 2000. The cell biology of the prohormone convertases PC1 and PC2. *Prog. Nucl. Acid Res. Mol. Biol. 63*:69–108.

Naggert, J.K., Fricker, L.D., Rouillé, Y., Steiner, D.F., Carroll, R.J., Paigen, B.J., and Leiter, E.H. 1995. Hyperproinsulinaemia in obese fat/fat mice associated with a carboxypeptidase E mutation which reduces enzyme activity. *Nature Genet. 10*:135–142.

Natori, S., and Huttner, W.B. 1994. Peptides derived from the granins (chromogranins/secretogranins). *Biochimie 76*: 277–282.

O'Rahilly, S., Gray, H., Humphreys, P.J., Krook, A., Polonsky, K.S., White, A., Gibson, S., Taylor, K., and Carr, C. 1995. Impaired processing of prohormones associated with abnormalities of glucose homeostasis and adrenal function. *N. Engl. J. Med. 333*:1386–1390.

Paloheimo, L.I., and Rehfeld, J.F. 1995. Quantitation of procholecystokinin and its products in plasma by processing-independent analysis. *Clin. Chim. Acta. 238*:21–33.

Petricoin, E.F., Ardekani, A.M., Hitt, B.A., Levine, P.J., Fusaro, V.A., Steinberg, S.M., Mills, G.B., Simone, C., Fishman, D.A., Kohn, E.C., and Liotta, L.A. 2002. Use of proteomic patterns in serum to identify ovarian cancer. *Lancet 359*:572–577.

Rehfeld, J.F. 1998a. Accurate measurement of cholecystokinin in plasma. *Clin. Chem. 44*:991–1001.

Rehfeld, J.F. 1998b. Processing of precursors of gastroenteropancreatic hormones: diagnostic significance. *J. Mol. Med. 76*: 338–345.

Rehfeld, J.F., and Goetze, J.P. 2003. The posttranslational phase of gene expression: new possibilities in molecular diagnosis. *Curr. Mol. Med. 3*:25–38.

Rehfeld, J.F., Hansen, C.P., and Johnsen, A.H. 1995. Post-poly(Glu) cleavage and degradation modified by O-sulfated tyrosine: a novel post-translational processing mechanism. *EMBO J. 14*: 389–396.

Rehfeld, J.F., and van Solinge, W.W. 1994. The tumor biology of gastrin and cholecystokinin. *Adv. Cancer Res. 63*:295–346.

Reubi, J.C., Koefoed, P., Hansen, T.O., Stauffer, E., Rausch, D., Nielsen, F.C., and Rehfeld, J.F. 2004. Procholecystokinin as marker of human Ewing sarcomas. *Clin. Cancer Res. 10*: 5523–5530.

Rouillé, Y., Duguay, S.J., Lund, K., Furuta, M., Gong, Q., Lipkind, G., Oliva, A.A., Chan, S.J., and Steiner, D.F. 1995. Proteolytic processing mechanisms in the biosynthesis of neuroendocrine peptides: the subtilisin-like proprotein convertases. *Front. Neuroendocrinol. 16*:322–361.

Schaer, J.C., and Reubi, J.C. 1999. High gastrin and cholecystokinin (CCK) gene expression in human neuronal, renal, and myogenic stem cell tumors: comparison with CCK-A and CCK-B receptor contents. *J. Clin. Endocr. Metab. 84*:233–239.

Schmutzler, C., Darmer, D., Diekhoff, D., and Grimmelikhuijzen, C.J.P. 1992. Identification of a novel type of processing sites in the precursor for the sea anemone neuropeptide Antho-RFamide (<Glu-Gly-Arg-Phe-NH2) from Anthopleura elegantissima. *J. Biol. Chem. 267*:22534–22541.

Smeekens, S.P., Avruch, A.S., La Mendola, J., Chan, S.J., and Steiner, D.F. 1991. Identification of a cDNA encoding a second putative prohormone convertase related to PC2 in AtT2O cells and islets of Langerhans. *Proc. Natl. Acad. Sci. USA 88*: 340–344.

Srinivas, P.R., Srivastava, S., Hanash, S., and Wright, G.L. 2001. Proteomics in early detection of cancer. *Clin. Chem. 47*: 1901–1911.

Sudoh, T., Kangawa, K., Minamino, N., and Matsuo, H. 1988. A new natriuretic peptide in porcine brain. *Nature 332*: 78–81.

Taupenot, L., Harper, K.L., and O'Connor, D.T. 2003. The chromogranin-secretogranin family. *N. Engl. J. Med. 348*: 1134–1149.

Westphal, C.H., Muller, L., Zhou, A., Zhu, X., Bonner-Fraser, M., Schambelan, M., Steiner, D.F., Lindberg, I., and Leder, P. 1999. The neuroendocrine protein 7B2 is required for peptide hormone processing *in vivo* and provides a novel mechanism for pituitary Cushing's disease. *Cell 96*:689–701.

Zimmer, T., Stölzel, U., Bader, M., Fett, U., Foss, K.H., Riecken, E.O., Rehfeld, J.F., and Wiedermann, B. 1995. A duodenal gastrinoma in a patient with diarrhea and normal serum gastrin concentrations. *N. Engl. J. Med. 333*:634–636.

3

Role of Tumor Suppressor BARD1 in Apoptosis and Cancer

Charles Edward Jefford, Jian Yu Wu, and Irmgard Irminger-Finger

Epidemiology and Prognostic Factors of Cancer

Cancer is the second leading cause of death, after heart disease, in Western countries. A total of 1,368,030 new cancer cases and 563,700 deaths were expected in the United States in 2002. Lung cancer, with high incidence, is still the leading cause of cancer death in both sexes (32% for men and 25% for women), but breast cancer and ovarian cancer are two of the major cancers in women. In 2004 the estimated new cancer cases in the United States were 699,560 for men and 668,470 for women, among which lung cancer accounted for 12–13% for men and women, and breast cancer and ovarian cancer accounted for approximately 32% and 4%, respectively, in women (Jemal *et al.,* 2004).

Many factors have been reported to influence the prognosis for breast cancer, such as primary tumor size; lymph-node involvement; pathologic type and grade; and status of estrogen and progesterone receptors and biomarkers such as HER-2, p53, bcl-2, Bfl-1, Ki-67, VEGF-C (Menard *et al.,* 2001; Sirvent *et al.,* 2004; Tsutsui *et al.,* 2003). The p53 tumor suppressor is often inactivated and overexpressed in breast cancers. Although there are some reports that p53 mutations have a negative correlation with DFS or RFS (relapse-free survival), especially in older patients (Bartley and Ross, 2002; Maciel Mdo *et al.,* 2002; Tsutsui *et al.,* 2001), the prognostic value of p53 is still controversial.

The majority of ovarian cancers are of epithelial origin. Epithelial ovarian cancers (EOC) include serous tumors, mucinous tumors, endometrioid tumors, clear cell tumors, Brenner tumors, undifferentiated tumors, and mixed epithelial tumors (Young and Clement, 1996), among which clear cell carcinoma is reported to have specific biologic features and worst prognosis (Bjorge *et al.,* 1998; Makar *et al.,* 1995; McGuire *et al.,* 2002; Tammela *et al.,* 1998). A small number of potential prognostic factors has been identified in ovarian cancer so far, such as cyclin D, p53 and p21, and CA125, but their prognostic value is still controversial (Bali *et al.,* 2004; Barbieri *et al.,* 2004; Camilleri-Broet *et al.,* 2004; Concin *et al.,* 2004; Hashiguchi *et al.,* 2004; Mano *et al.,* 2004). The frequency of overexpression of a mutant p53 is significantly higher in advanced stage III/IV ovarian cancer than in stage I cases (10–20%). This may indicate that p53 inactivation is a late event in ovarian carcinogenesis (Feki and Irminger-Finger, 2004). However, in lung cancer p53 is the most frequently mutated gene and has been linked to lung cancer development (Roth *et al.,* 1999)

Handbook of Immunohistochemistry and *in situ* Hybridization of Human Carcinomas, Volume 4: Molecular Genetics, Gastrointestinal Carcinoma, and Ovarian Carcinoma

and to unfavorable prognosis in any stage of NSCLC (Steels *et al.,* 2001; Tan *et al.,* 2003).

Despite the recent progress in the treatment of cancers, cancer incidence and mortality have changed very little and the 5-year survival rate for cancer has not improved. From 1974 to 1999, the 5-year survival rate, for breast cancer and lung cancer were 78–87% and 12–15%, respectively. It seems as if the focus was more on the subjects, on early diagnosis, and on prevention, and progress was made in the development of genetic studies.

Breast Cancer and the *BRCA* Genes

Breast and ovarian cancers are highly prevalent in Western societies. For instance, the cumulative risk of developing breast cancer by the age of 80 years amounts to 11% for a woman in the United States (Casey, 1997). Most cases of breast cancer are sporadic, and only 5–l0% of all breast cancers are of inherited origin. About half of the familial breast and ovarian cancers are linked to germline mutations in the breast cancer susceptibility genes 1 and 2 (*BRCA1* and *BRCA2*) (Miki *et al.,* 1994; Wooster *et al.,* 1994). Furthermore, in hereditary breast and ovarian tumors with *BRCA1* and *BRCA2* mutations, the wild-type allele usually is lost or inactive. This loss of heterozygosity (LOH) underscores that these two genes act as potent tumor suppressors. Women harboring mutations in either BRCA1 or *BRCA2* have a lifetime risk of 80–90% of developing tumors in the breast or in the ovaries, and they account for about 40–50% of early-onset breast and ovarian cancers (Hall *et al.,* 2001). Furthermore, sporadic breast and ovarian tumors show also defects in *BRCA1* and *BRCA2* genes, albeit in rare occurrences. These observations infer that *BRCA1* and *BRCA2* host crucial and vital cellular functions. BRCA1 and BRCA2 are highly ubiquitous proteins expressed in almost all tissues, but tumors arise only in breast and ovaries with defects in *BRCA* genes. Despite this conundrum, a large fraction of familial breast and ovarian cancers do not show mutations in BRCA1 or BRCA2 and could be caused by mutations in associated proteins.

Multiple Functions of BRCA1 and BRCA2

To assess the function of *BRCA1* and *BRCA2* genes in breast cancer, reverse genetic experiments were performed. The knockout mouse models for BRCA1 have shown that this gene is absolutely essential for cellular growth and homeostasis. Both BRCA1 and BRCA2 knockout mice display embryonic lethality at days E8–E13, with viable cells showing a fair degree of aneuploidy, suggestive of chromosomal instability (Hakem *et al.,* 1998). Mice that were heterozygous for either *Brca1* or *Brca2* developed normally and were not more susceptible to breast cancer than the normal wild-type littermates. However, mice carrying conditional deletion knockout mutants for *Brca1* and driven under a mammary tissue-specific promoter displayed mammary gland tumors by 10–13 months of age (Xu *et al.,* 1999).

BRCA1 and BRCA2 interact with a large number of proteins. They have a wide spectrum of activities ranging from deoxyribonucleic acid (DNA) repair and replication to centrosome duplication and mitotic checkpoint functions. Their role in tumorigenesis has been discussed in multiple reviews (Scully and Livingston, 2000; Venkitaraman, 2004). BRCA1 is a ubiquitously expressed protein of 1863 amino acids harboring two highly conserved domains: RING finger domain and two BRCT domains. BRCA1 functions in diverse pathways: DNA damage repair of double-stranded breaks (DSB), transcription-coupled repair, transcriptional regulation, chromatin remodeling, ubiquitination, centrosome duplication, and cell cycle checkpoints (Deng and Brodie, 2000; Hsu *et al.,* 2001; Khanna and Jackson, 2001; Narod and Foulkes, 2004; Starita and Parvin, 2003; Venkitaraman, 2004). Several studies converge on the hypothesis stipulating that BRCA1 serves as a scaffolding protein for the assembly of a multiprotein heterocomplex, thus integrating the aforementioned mechanisms as proposed (Irminger-Finger *et al.,* 1999).

The functions of BRCA2 are less diverse. The *BRCA2* gene codes for a large polypeptide of 3418 amino acids, conserved through evolution and widely expressed in adult and embryonic tissues (Rajan *et al.,* 1997). It is structurally and phylogenetically unrelated to BRCA1 and bears no homology conservation with BRCA1 whatsoever. Like BRCA1, BRCA2 is specifically crucial in homologous-directed repair (HDR) and in nonhomologous end joining (NHEJ) because BRCA2 may bind directly to DNA and interacts with Rad51 at sites of DSB. The functions of BRCA1 and BRCA2 converge in one goal: maintaining genome integrity. The common phenotypic feature of BRCA1- and BRCA2-deficient cells is spontaneous chromosomal instability and a hypersensitivity to DNA damage–inducing agents such as ionizing radiation and interstrand cross-linking drugs. The result is increased genomic instability, manifested by chromosomal aberrations and aneuploid karyotypes (Jasin, 2002). Chromosomal aberrations are common to all cancers and could be the pathogenic basis of breast and ovarian cancers caused by mutations in BRCA1 or BRCA2.

BARD1 Discovery and Structure Overview

In the search for novel partners of BRCA1, BARD1 (BRCA1-Associated RING finger Domain protein 1) was discovered in a yeast two hybrid screen using the N-terminal BRCA1 RING domain as bait (Wu *et al.,* 1996). The human BARD1 gene is localized on chromosome 2 (2q34–q35), and its complementary DNA (cDNA) encodes a protein of 777 amino acids (Wu *et al.,* 1996), corresponding to 765 amino acids in the mouse (Irminger-Finger *et al.,* 1998) and 768 in the rat (Gautier *et al.,* 2000). *BARD1* homologs have been cloned from *Xenopus leavis, Arabidopsis thaliana* (Irminger-Finger and Leung, 2002; Joukov *et al.,* 2001), and *Caenorhabditis elegans* (Boulton *et al.,* 2004). A doubt remains on the initiation site of translation, which could be situated either at amino acid position 1 or 26. BARD1 resembles BRCA1 in structural organization and shares sequence homologies with BRCA1's conserved domains. Like BRCA1, BARD1 contains a RING finger domain at its N-terminus (residues 46–90) and two BRCT domains at the C-terminus (residues 616–653 and 743–777) (Figure 5), but BARD1, albeit less than half the size of the BRCA1 protein (1863 residues), contains an additional conserved domain, of three ankyrin repeats (ANK), for which BRCA1 is void. Apart from the conserved domains, the rest of the BARD1 protein sequence bears

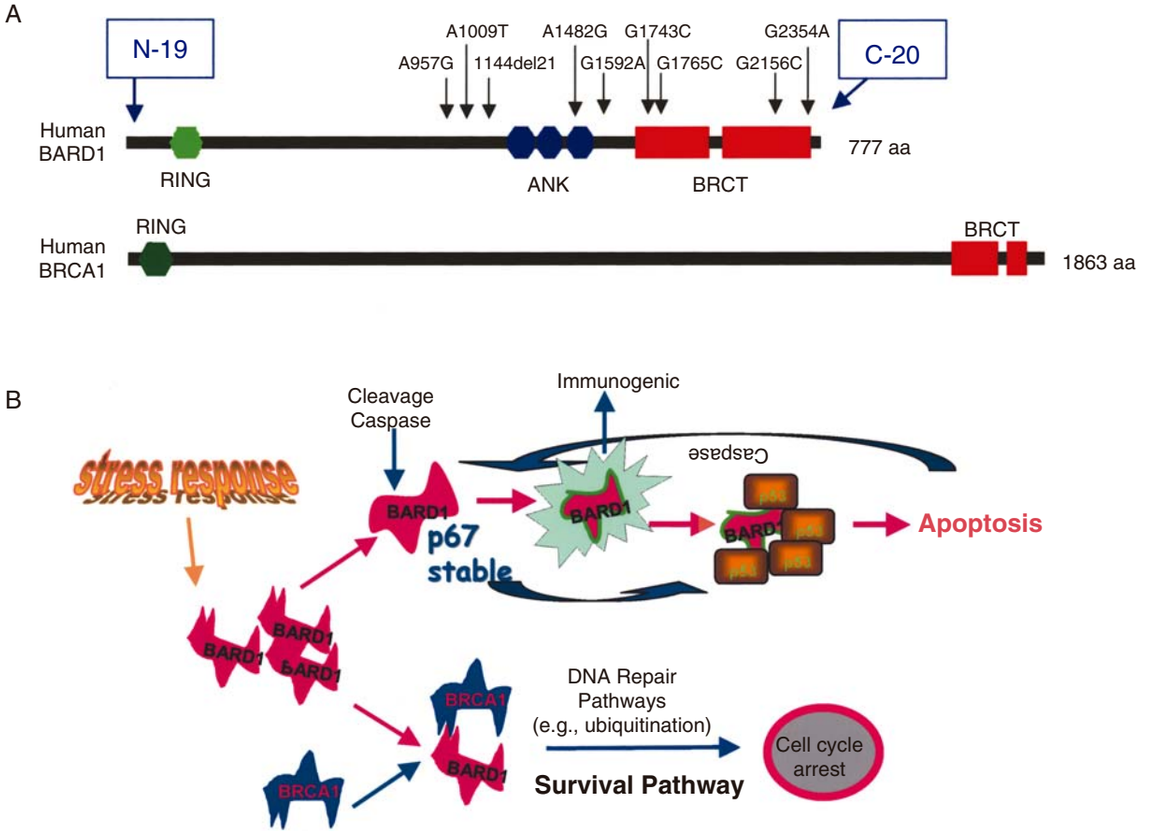

***Figure 5.* Schematic presentation of BARD1 and BRCA1 structure and functions.** **A:** Functional domains are presented: RING finger, ANKyrin repeats, and BRCT domains. Positions of cancer-associated mutations are indicated as arrows for BARD1. N-19 and C-20 indicate positions of epitopes recognized by respective antibodies. **B:** Proposed model of BARD1 function in normal tissues and in tumorigenesis. BARD1 is associated with three pathways: 1) as heterodimer with BRCA1 in repair and survival mode; 2) excess of BARD1 over BRCA1 in apoptosis function (Irminger-Finger *et al.,* 2001); and 3) deficiency of p53 stabilization permits overriding of gatekeeper function of p53, either through deficiency of BARD1 or p53. During apoptosis BARD1 is cleaved by the caspase-dependent kinase calpaine. The resulting p67 protein is more stable than full-length BARD1 (97 kDa) and is immunogenic (Gautier *et al.,* 2000).

no homology with other proteins. Alignment of human and mouse BARD1 orthologues show low levels of amino-acid sequence homology (i.e., 70.4% over the total protein), whereas the RING, ANK repeats, and BRCT motifs have 86.7%, 90.1%, and 79.8% identity, respectively (Ayi *et al.,* 1998; Irminger-Finger *et al.,* 1998; Irminger-Finger and Leung, 2002), which suggests that the three conserved domains mediate essential functions. It is interesting that, no proteins with significant sequence homology to regions other than RING, ANK, and BRCT domains were found in databases. BRCA1 is the only vertebrate protein that shares homology with BARD1 in both the RING and BRCT domains. Homology in gene structure and protein sequence of BARD1 and BRCA1 indicate that both proteins are phylogenetically related. In a similar fashion, the mouse Brca1 and Brca2 proteins share less than 60% homology with their human counterparts, in contrast with other known tumor suppressors, such as p53 with 78% identity. Comparison of amino-acid homology between BARD1 and BRCA1 shows that they have co-evolved at the same rate, providing further evidence that these proteins function in the same complex.

Human BARD1 contains six putative nuclear localization signal (NLS) sequences, located closely or embedded in each of the three functional domains, incurring a predicted nuclear localization of BARD1 (Jefford *et al.,* 2004). In comparison, mouse BARD1 has only three putative NLS sequences and a marginally lower prediction score for nuclear localization (psort.nibb.ac.jp/). Although the RING domains of BARD1 and BRCA1 can form homodimers *in vitro*, these structures are unstable (Meza *et al.,* 1999), and only BARD1-BRCA1 heterodimeric complexes have been found *in vivo.* The paired RING domains of BARD1 and BRCA1 form a stable four-helix bundle (Morris *et al.,* 2002). This structure is more resistant to proteolysis than homodimers, supporting the notion that the BRCA1–BARD1 heterodimer acts as a functional unit.

BARD1 Expression Pattern and Subcellular Localization

The BARD1 gene spans over a 10 kb region close to the telomere on chromosome 2q34–q35 (Wu *et al.,* 1996), but the regulation of transcription of *BARD1* has not been elucidated. Its most abundant transcript is composed of 11 exons stretched over 2530 base pairs. *BARD1* has several putative transcripts issued by alternative splicing (Feki *et al.,* 2004, 2005). Nevertheless, *BARD1* and *BRCA1* messenger ribonucleic acid (mRNA) expression patterns, as observed from Northern blots, are coordinated in several tissues. Northern blot and ribonuclease (RNase) protection data showed that mRNAs were abundantly expressed in spleen and testis but not in heart, brain, liver, lung, skeletal muscle, or kidney tissues (Ayi *et al.,* 1998; Irminger-Finger *et al.,* 1998). Hormonally regulated organs were also assayed and showed that *BARD1* expression in uterus is increased from diestrus through post-estrus phase, whereas *BRCA1* expression increases from diestrus to early estrus and decreases during estrus and post-estrus (Irminger-Finger *et al.,* 1998). This in-coordinate expression of *BARD1* with *BRCA1* was the first indication of a putative BRCA1-independent role of BARD1. More recently, *BARD1* expression in testis was explored, showing that *BARD1* is expressed at all stages of spermatocyte maturation, whereas *BRCA1* expression is only seen in meiotic and early round spermatocytes (Feki *et al.,* 2004a).

At the cellular level, BARD1 protein expression was first reported to be constant throughout the cell cycle, in contrast to the elevated levels of BRCA1 in S-phase (Jin *et al.,* 1997). However, a more recent study reports that BARD1 expression levels fluctuate in a cell cycle–dependent manner, with an increase during mitosis (Choudhury *et al.,* 2004).

BARD1 was first described as a nuclear protein. It was found in nuclear extracts and localized to BRCA1 "nuclear dots" in the nucleus during S phase (Scully *et al.,* 1997). BARD1 regulates the subcellular location of BRCA1 by masking the nuclear export signal (NES) of BRCA1 (Fabbro *et al.,* 2002). However, data in 2004 show that BARD1 is a protein shuttling between nucleus and cytoplasm, and an NES identified near the RING domain of BARD1 may be masked by co-expression of BRCA1 and results in nuclear retention (Rodriguez *et al.,* 2004a). The cytoplasmic location of BARD1 is associated with its apoptotic function, which is markedly reduced by BRCA1 (Jefford *et al.,* 2004).

BARD1 degradation was also reported, and a 67 kDa proteolytic cleavage product was found to be associated with apoptosis in cancer cells (Gautier *et al.,* 2000). Autoubiquitination on RING domain may be one of the mechanisms of protein degradation (Jefford *et al.,* 2004).

Biological Functions of BARD1

BARD1 plays an important role in maintaining genomic stability and phenotype. After BARD1 repression in cultured mammary epithelial cells, marked phenotypic changes were observed, including altered cell shape, increased cell size, high frequency of multinucleated cells, and aberrant cell cycle progression (Irminger-Finger *et al.,* 1998). Loss of BARD1 resulted in chromosomal instability and early embryonic

lethality, which caused severe impairment of cell cycle proliferation but was not accompanied by increased apoptosis (McCarthy *et al.,* 2003).

For most biological functions the BARD1–BRCA1 complex is essential. BARD1 and BRCA1 stabilize each other, and a mutation in BRCA1 C61G that abolishes binding to BARD1 is associated with breast and ovarian cancer, suggesting a role of BARD1 in BRCA1-mediated tumor suppression. A fragment of BARD1, comprising half of ANK through BRCT domain (residues 464–777), binds *in vitro* to the ANK domains of Bcl-3 and modulates the transcriptional activity of NF-κB and NF-κB–driven gene expression (Dechend *et al.,* 1999). BARD1 also interacts with CstF-50 (cleavage stimulating factor), inhibits polyadenylation *in vitro,* and prevents inappropriate RNA processing (Kleiman and Manley, 1999). These functions are abrogated by a tumor-associated germline mutation in BARD1 (Q564H) (Kleiman and Manley, 2001).

Ubiquitination is recognized as a multifunctional signaling mechanism with regulatory significance comparable to that of phosphorylation. The functional consequence of ubiquitination varies, including protein degradation, repair activation, transcriptional regulation, and cell cycle control. BARD1 and BRCA1 have very low ubiquitin ligase activity (E3), but the BARD1–BRCA1 complex shows dramatically higher ubiquitin ligase activity than individual preparations of BARD1 or BRCA1 (Hashizume *et al.,* 2001). Although the exact target protein of BARD1–BRCA1 ubiquitination is not clear, RNA polymerase II holoenzyme (Pol II), reported to be one of the BRCA1-associated proteins (Chiba and Parvin, 2002), might be suspected. On DNA damage, BARD1–BRCA1 ubiquitination activity increases, and degradation of RNA polymerase II and transcription arrest is observed. The BARD1 RING domain or BARD1–BRCA1 complexes also have autoubiquitination function (Chen *et al.,* 2002), which may serve as a signaling event, such as in DNA repair or in regulating the BARD1-mediated inhibition of mRNA polyadenylation after DNA damage (Kleiman and Manley, 2001), instead of serving as target for proteasomal degradation. Alternatively, the BARD1 RING domain might be the target of ubiquitination and degradation by the ubiquititin pathway, as speculated for BRCA1 (Fabbro and Henderson, 2003).

BRCA1-Independent Function of BARD1 in Apoptosis

Because BARD1 has a vital role in normal cell survival, BARD1 expression was measured during apoptosis. It was found that *BARD1* expression, through transcription, may be up-regulated in response to genotoxic stress or hypoxia after induction of an ischemic stroke in a mouse (Irminger-Finger *et al.,* 2001). Additionally, overexpression of exogenous BARD1 leads to apoptosis as measured by DNA fragmentation assays. It is dependent of p53, but independent of BRCA1, because BARD1 may trigger apoptosis in a BRCA1-negative stem cell line and not in p53 deficient cell lines (Irminger-Finger *et al.,* 2001). These experiments identified BARD1 as a possible mediator between proapoptotic stress and p53-dependent apoptosis. It is interesting that the Q564H missense mutation of BARD1 led to less efficient induction of apoptosis. This implies that this region could harbor a role necessary for tumor suppression and for BARD1's proapoptotic function. Furthermore, it was also shown that BARD1 co-immunoprecipitates p53, suggesting a physical interaction between p53 and BARD1 to induce apoptosis. Nevertheless, BRCA1–BARD1 heterodimers are required for phosphorylation of p53 on serine 15, which in turn is necessary for a G1–S cell cycle arrest following DNA damage induced by a source of ionizing radiation (Fabbro *et al.,* 2004a). These results were confirmed by a study showing that BARD1-induced apoptosis catalyzes the phosphorylation of p53 by a DNA-damage response kinase (Feki *et al.,* 2005). The p53 protein must be phosphorylated on serine residues for a function in apoptosis, and it appears that BARD1 stabilizes p53 for repair and for apoptosis.

On genotoxic stress, BARD1 expression increases and induces BRCA1-independent apoptosis (see Figure 5). BARD1 transfection or overexpression induces cell death, which displays features of apoptosis, whereas BARD1-repressed cells are defective for apoptotic response to genotoxic stress (Irminger-Finger *et al.,* 2001). A proteolytic product, 67 kDa protein, found in apoptotic bodies of rat colon cancer cells was identified as an apoptotic cleavage product of BARD1, and antibodies against this product were detected in rats immunized with apoptotic bodies against experimentally induced colon cancer (Gautier *et al.,* 2000). In prostate cancer, treatment with camptothecin caused BARD1 and NF-κB up-regulation and induced apoptosis (Zuco *et al.,* 2003). These examples suggest that BARD1 mediates apoptotic response to cellular stress. The mechanism of BARD1-induced apoptosis is presumed to act through a p53 pathway by catalyzing p53 phosphorylation by the DNA damage response kinase DNA-PK, by binding to the kinase and its substrate (Feki *et al.,* 2005; Irminger-Finger *et al.,* 2001). In contrast to the nuclear retention of BARD1–BRCA1 complex in DNA repair, BARD1-induced apoptosis is reported to be associated with cytoplasmic location of BARD1 (Figure 6) (Jefford *et al.,* 2004; Rodriguez *et al.,* 2004b).

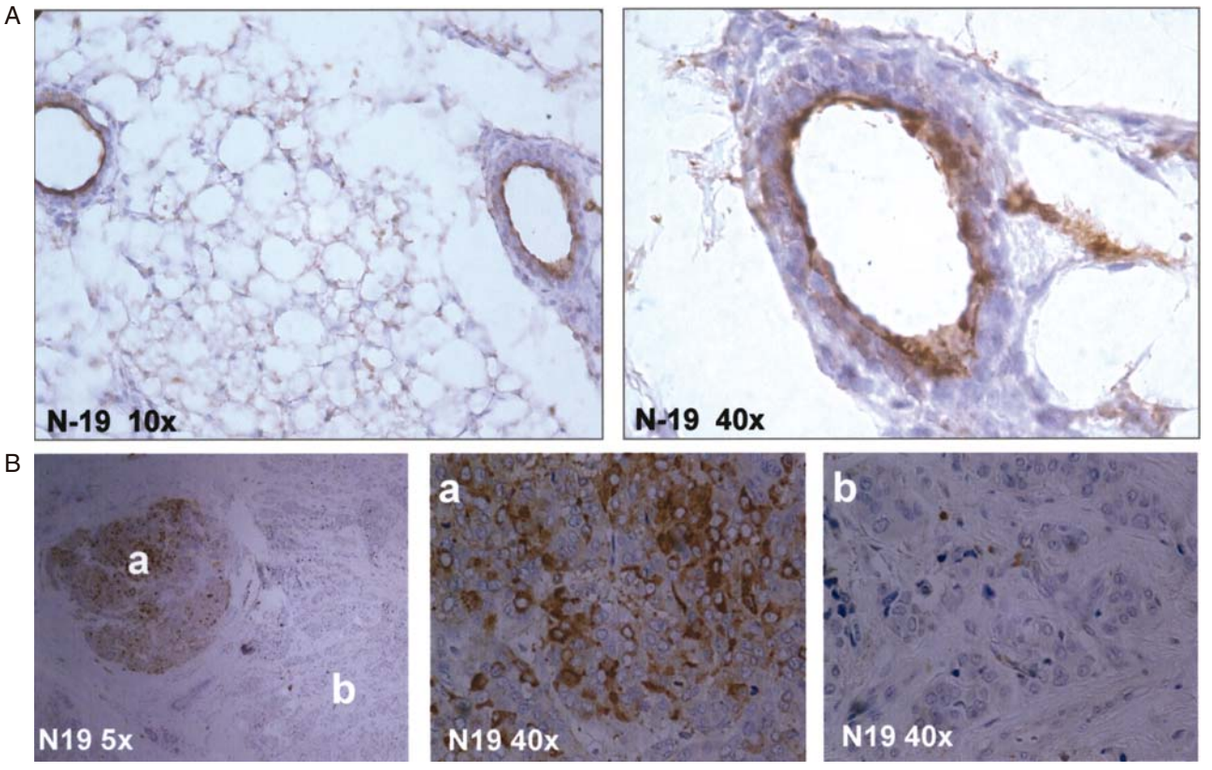

Figure 6. BARD1 expression in breast tissue and breast tumors. Mouse mammary gland tissue stained with anti-BARD1 N-19 antibody **(A).** Staining of breast cancer sample with anti-BARD1 N-19 **(B),** as described (Wu *et al.,* 2005). Cytoplasmic staining is observed in tumor region *(a)* but not in surrounding tissue *(b)*.

One report shows that BARD1 may also localize in the cytoplasm, albeit in discreet levels, and it was observed that increased cytoplasmic localization was accompanied by apoptosis (Jefford *et al.,* 2004). Moreover, BARD1 shuttling out of the nucleus into the cytoplasm is stimulating its apoptotic activity (Rodriguez *et al.,* 2004b). Using deletion constructs, the apoptotic domain of BARD1 was defined to residues 510–604 between the ANK repeats and BRCT domains (Jefford *et al.,* 2004), coinciding with two known cancer predisposing mutations, supporting the notion that this region is important for the tumor-suppressor functions of BARD1.

Expression of BARD1 in Cancer

There is accumulating evidence that BARD1 is a tumor suppressor in its own right. Repression of BARD1 in murine mammary epithelial cells resulted in the phenotypic changes reminiscent of premalignancy (Irminger-Finger *et al.,* 1998). BARD1 expression is reported to be reduced in breast cancer cell lines (Yoshikawa *et al.,* 2000). Thai *et al*. have described the BARD1 somatic and germline mutations in a subset of primary breast, ovarian, and uterine cancers (Thai *et al.,* 1998). Ishitobi reported a germline mutation in Japanese familial breast cancers (Ishitobi *et al.,* 2003). Mutation of BARD1 was also found with elevated frequency in Finnish families with breast cancer (Karppinen *et al.,* 2004). BARD1 germline mutations were particularly identified in families with breast or breast and ovarian cancer without BRCA1 or BRCA2 alterations (Ghimenti *et al.,* 2002).

So far these observations show that BARD1 germline mutations account for a very small fraction of familial breast cancers, thus questioning the implication of *BARD1* in predisposition to gynecologic cancers. However, correct *BARD1* expression is necessary because homozygous *BARD1* knockout mice are not viable (McCarthy *et al.,* 2003), and the conditional mice knockouts of *BARD1*, an allele, through inducible recombinase cre/loxp system, produce tumors in mammary glands of mice several months after induction (personal communication, Thomas Ludwig).

BRCA1 mRNA expression is often reduced in breast carcinomas (Thompson *et al.,* 1995; Yoshikawa *et al.,*

2000). In contrast, BARD1 and the two mismatch repair enzymes, hMSH2 and hMLH1, are not reduced as frequently (Yoshikawa *et al.,* 2000). However, p53 mRNA expression in sporadic breast cancers is diminished, although the detection of a mutated p53 is frequent (Feki and Irminger-Finger, 2004).

A 2004 report examined the expression pattern of several genes, including *BARD1, Smad7,* and *Smad2,* that are implicated in the transforming growth factor β (TGFβ) signaling pathways of normal and breast cancers. As measured by real-time, reverse transcriptase-polymerase chain reaction (RT-PCR), a decrease was observed in breast cancer, which supports the notion that these genes are tumor suppressors and are repressed in tumors (Reinholz *et al.,* 2004). Another study also showed a diminution of *BARD1* expression at the mRNA level in breast carcinomas (Qiu *et al.,* 2004). Although these studies provide evidence that BARD1 is a tumor suppressor, the specific function of BARD1 in cancer and in carcinogenesis remains unclear.

BARD1 Protein Expression in Cancer

It was shown previously that BARD1 is expressed in many tissues, including those in the breast and ovary, on the mRNA level. The cell-type specificity has not been determined. Analysis of BARD1 protein expression in epithelial breast and ovarian cancers adds to the discussion of biological functions of BARD1 in tumorigenesis. Using antibodies against BARD1 N-terminal (N-19) and C-terminal (C-20) regions, BARD1 expression was determined in the mouse mammary gland. Tissues were from mice of 3, 5, and 9 months of age. BARD1 staining was found in the cells lining the lumen of mammary glands (Figure 6A) at all stages of development. Staining was mostly nuclear. Interestingly, in tumor cells BARD1 was highly expressed in the cytoplasm. In healthy tissue surrounding the tumor, however, little staining and nuclear localization was observed (Figure 6B). This result contrasts with the expression of BRCA1, which is generally downregulated in ovarian and breast carcinoma. Analysis of BARD1 expression in a series of sporadic breast cancers showed that BARD1 was localized in the cytoplasm. The expression levels of BARD1, detected with N-19 and C-20, were variable. The extent and pattern of BARD1 expression varied in the different pathologic types of tumors (Wu *et al.,* 2005).

Also, comparing expression of p53 in the same samples could not establish any correlation between p53 and BARD1 expression. Unlike BARD1, p53 levels did not increase with tumor size or undifferentiated state. BARD1 expression was correlated with tumor differentiation and tumor size, and considerably more staining was observed in G3 grade tumors than in G1 and more in T4 staged tumors than in T1. Because tumor differentiation, size, and stage are prognostic factors for breast cancer, it seems likely that BARD1, rather than p53, staining is associated with a poor prognosis for breast cancer, and it may be a prognostic marker of breast cancer (Wu *et al.,* 2005). Several mutations of BARD1 have been reported associated with breast and ovarian cancer, and analysis of BARD1 protein expression in tumors with mutation sites A957G, A1009T, G1743C, 1144del21, respectively (Ghimenti *et al.,* 2002), showed, similar to sporadic breast cancers, intensive cytoplasmic staining (Wu *et al.,* 2005). The staining intensity and the percentage of positive cells were not correlated with a specific mutation site. It was unclear at this point whether all BARD1 mutations investigated result in a cytoplasmic localization of the protein or whether the cytoplasmic localization of BARD1 is dictated by other tumor factors and not influenced by specific mutations. It can be concluded that aberrant location of BARD1 is a negative prognostic factor but not necessarily associated with a specific mutation.

In the normal ovary BARD1 is expressed in the germ cells, as demonstrated by staining of mouse ovarian tissue (Irminger-Finger *et al.,* 2001). In developing and mature follicles BARD1 is expressed in the germ cells. After ovulation no staining is observed in granulosa or theca cells.

BARD1 protein expression in four types of ovarian cancers—clear cell, serous, endometrioid, and mucinous carcinoma—showed elevated BARD1 staining in the cytoplasm of cancer cells but very faint staining in the nucleus of cells in surrounding tissue. The extent of BARD1 expression varied considerably between the different histologic types of ovarian cancer. In clear cell carcinoma, all cells were stained homogeneously and all cases had high positivity of BARD1 staining (90% of the cells were stained in average), whereas in the other types of ovarian carcinomas, BARD1 expression varied from 0 to 95% of positive cells and showed a mosaic expression pattern, which was most prominent in serous carcinoma.

In the majority of the cases, N-19 and C-20 antibodies stained the same regions when tested on adjacent tissue sections, but differences in N-19 and C-20 staining were observed in endometrioid, mucinous, and serous carcinoma. In most of these cases N-19 staining was lost and C-20 staining was retained. This loss of N-terminal epitopes could be explained by changes on the gene, the transcript, or the post-translational level.

Because BARD1 can act as apoptosis inducer by stabilizing the tumor suppressor p53 (Irminger-Finger

et al., 2001), p53 expression levels were also determined in the same cases. Consistent with many previous reports (reviewed in Feki *et al.,* 2005), p53 showed nuclear localization, whereas BARD1 was localized to the cytoplasm, which excluded a BARD1–p53 interaction. In some cases, BARD1 and p53 co-localized in the same region, in others BARD1 and p53 expression showed completely different distributions in the same region.

Clear cell carcinoma showed the highest percentage of BARD1-positive cells. Whereas the variation within the other types of ovarian tumors was from 0–90%, 80–100% of positive cells were found in clear cell carcinoma (Wu *et al.,* 2005).

BARD1 expression was not limited to tumors of hormonally regulated tissues. BARD1 was also found in the cytoplasm in lung cancer cells. Comparing the expression of BARD1 and p53 expression in NSCLC tumors of various histologic type, pathologic grade, and clinical stage, no correlation of BARD1 with p53 expression levels was found. However, the expression of p53 was clearly increasing with the stage of tumors and was elevated in poorly differentiated cancers as compared to well-differentiated NSCLC (Wu *et al.,* 2005). This finding is consistent with the observation that more than 50% of lung cancers exhibit p53 mutations and that p53 is the major target for mutations during malignant transformation (Roth *et al.,* 1999).

Aberrant Form(s) of BARD1 Expressed in Tumors?

Several reported functions of BARD1 suggest a role in tumor suppression. Its up-regulation in tumors therefore led to speculation that the form of BARD1 expressed in tumors might be an aberrant form deficient of its tumor-suppressor function. RT-PCR cloning of BARD1 cDNAs from frozen tissue sections of ovarian tumor samples showed that in 70% of the cases, the 5′ half of the transcript (nucleotides 74 to 1481) was very weakly expressed or the segment including nucleotides 74 to 1441 was not expressed (Wu *et al.,* 2005), consistent with the observed loss of N-terminal but not C-terminal epitopes detected by immunohistochemistry.

This lead to the conclusion that the form of BARD1, overexpressed in cancer cells and localized to the cytoplasm, presumably presents an aberrant form of BARD1. It is interesting that BARD1 expression is highly elevated in clear cell ovarian carcinoma and in poorly differentiated, large sized breast cancers that have the worst prognosis for 5-year survival. This expression pattern of BARD1 is similar to p53 expression in lung cancer, with elevated expression in tumors, correlated with poor prognosis, and when expressed in tumors, mostly presenting a mutated form.

Tumor-associated mutations of BARD1 were found for both somatic and germline mutations in a subset of primary breast, ovarian, and uterine cancers (Ghimenti *et al.,* 2002; Ishitobi *et al.,* 2003; Karppinen *et al.,* 2004; Thai *et al.,* 1998). It is generally assumed that genetic mutations could induce structural changes of the protein product, leading to a loss of function as a result of a presumed decrease of protein stability. Therefore, the striking up-regulation of BARD1 protein expression in cancer tissue as compared to normal tissue adds to the complexity of mechanisms of tumorigenesis (see Figure 6). BARD1 up-regulation is even observed in tumors with BRCA1 mutations (Wu *et al.,* 2005), whereas BARD1 destabilization would be expected in the absence of the stabilizing binding partner BRCA1 (Joukov *et al.,* 2001).

BARD1 was described as a nuclear protein (Scully *et al.,* 1997; Wu *et al.,* 1996) and in association with apoptosis its translocation to the cytoplasm is observed (Fabbro *et al.,* 2004b; Jefford *et al.,* 2004). However, *BARD1* localizes to the cytoplasm in cancer cells that are not apoptotic. This suggests that BARD1, when expressed in cancers, represents an aberrant form, a form that lacks tumor-suppressor functions as a result of post-translational modifications, or both. It even is possible that BARD1 acquires novel (dominant-negative) functions in favor of tumor cell growth. Alternatively, factors influencing the intracellular localization of BARD1 and/or its stability could be modified in tumor cells.

The observed loss of the 5′ half of *BARD1* transcript in 70% of ovarian tumors is suggestive of a mechanism that is not the result of random genomic instability. Indeed, a finding of a splice variant of BARD1 in a rat ovarian cancer cell line, missing exons 2–7 (Feki *et al.,* 2005), is in support of the argument that aberrant transcripts, missing the coding region that comprises regions upstream of the ANK repeat, might be associated with ovarian and breast cancer.

According to our previously proposed model (Irminger-Finger *et al.,* 2001) (see Figure 5) an excess of BARD1 over BRCA1 in BRCA1-mutated cells should lead to BARD1-induced p53-dependent apoptosis. Therefore, tumor cells would inactivate either BARD1 or p53 to escape from apoptosis; however, the propensity for mutations or epigenetic alterations of one or the other could depend on the specific tissue. The prevalence of BARD1 mutations in hormonal tissues could be the result of the reported hormonal regulation of BARD1 in such tissues (Feki *et al.,* 2004b; Irminger-Finger *et al.,* 1998).

In conclusion, abundantly expressed BARD1 in cancer cells is likely to be an aberrant form deficient of

its tumor-suppressor functions because BARD1 up-regulation is observed independently of p53, excluding a function in p53 stabilization. BARD1 expression is elevated in breast and ovarian cancers with reported poor outcome, which suggests that BARD1 staining in the cytoplasm of tumor cells might be a negative prognostic factor.

SUMMARY

Mutations in the tumor-suppressor gene *BARD1* have been found in cases of inherited and spontaneous breast, ovarian, and uterine cancers. The BARD1 protein plays a role in DNA repair and ubiquitination as binding partner of BRCA1 with which it co-localizes to nuclear dots. Independently of BRCA1, BARD1 can induce p53-dependent apoptosis in response to genotoxic stress. DNA repair and apoptosis are tumor-suppressor functions that are often defective in cancer cells. In cancer cells that escaped from apoptosis, one would expect that either BARD1 or p53 might be defective. Investigation of BARD1 and p53 expression levels in breast, ovarian, and non–small-cell lung cancers (NSCLC) showed that BARD1 was highly up-regulated and located to the cytoplasm in most cancer cells, whereas a weak nuclear staining was observed in the surrounding normal tissue. A maximum of BARD1 expression was associated with the most malignant form of ovarian cancer, clear cell carcinoma. Similarly, in breast cancer, BARD1 expression was correlated with poor differentiation, large tumor size, and short disease-free-surviva1 (DFS) time. Tumors with either BARD1 or BRCA1 mutations showed similar BARD1 protein levels. In contrast to breast and ovarian cancers, no correlation of BARD1 expression with either grade or stage could be determined for NSCLC. This suggests that an aberrant form of BARD1, deficient of its tumor-suppressor function, might be expressed in cancer cells and that elevated cytoplasmic expression of BARD1 might be a poor prognostic factor for breast and ovarian cancers.

Acknowledgments

This works was supported by Swiss National Science Foundation grant to IIF.

References

Ayi, T.C., Tsan, J.T., Hwang, L.Y., Bowcock, A.M., and Baer, R. 1998. Conservation of function and primary structure in the BRCA1-associated RING domain (BARD1) protein. *Oncogene 17*:2143–2148.

Bali, A., O'Brien P.M., Edwards, L.S., Sutherland, R.L., Hacker, N.F., and Henshall, S.M. 2004. Cyclin D1, p53, and p21 Waf1/Cip1 expression is predictive of poor clinical outcome in serous epithelial ovarian cancer. *Clin. Cancer Res. 10*:5168–5177.

Barbieri, F., Lorenzi, P., Ragni, N., Schettini, G., Bruzzo, C., Pedulla, F., and Alam, A. 2004. Overexpression of cyclin D1 is associated with poor survival in epithelial ovarian cancer. *Oncology 66*:310–315.

Bartley, A.N., and Ross, D.W. 2002. Validation of p53 immunohistochemistry as a prognostic factor in breast cancer in clinical practice. *Arch. Pathol. Lab. Med. 126*:456–458.

Bjorge, T., Engeland, A., Hansen, S., and Trope, C.G. 1998. Prognosis of patients with ovarian cancer and borderline tumours diagnosed in Norway between 1954 and 1993. *Int. J. Cancer 75*:663–670.

Boulton, S.J., Martin, J.S., Polanowska, J., Hill, D.E., Gartner, A., and Vidal, M. 2004. BRCA1/BARD1 orthologs required for DNA repair in Caenorhabditis elegans. *Curr. Biol. 14*:33–39.

Camilleri-Broet, S., Hardy-Bessard, A.C., Le Tourneau, A., Paraiso, D., Levrel, O., Leduc, B., Bain, S., Orfeuvre, H., Audouin, J., and Pujade-Lauraine, E. 2004. HER-2 overexpression is an independent marker of poor prognosis of advanced primary ovarian carcinoma: a multicenter study of the GINECO group. *Ann. Oncol. 15*:104–112.

Casey, G. 1997. The BRCA1 and BRCA2 breast cancer genes. *Curr. Opin. Oncol. 19*:88–93.

Chen, A., Kleiman, F.E., Manley, J.L., Ouchi, T., and Pan, Z.Q. 2002. Autoubiquitination of the BRCA1 *BARD1 RING ubiquitin ligase. *J. Biol. Chem. 227*:22085–22092.

Chiba, N., and Parvin, J.D. (2002). The BRCA1 and BARD1 association with the RNA polymerase II holoenzyme. *Cancer Res. 62*:4222–4228.

Choudhury, A.D., Xu, H., and Baer, R. 2004. Ubiquitination and proteasomal degradation of the BRCA1 tumor suppressor is regulated during cell cycle progression. *J. Biol. Chem. 279*: 33909–33918.

Concin, N., Becker, K., Slade, N., Erster, S., Mueller-Holzner, E., Ulmer, H., Daxenbichler, G., Zeimet, A., Zeillinger, R., Marth, C., and Moll, U.M. 2004. Transdominant DeltaTAp73 isoforms are frequently up-regulated in ovarian cancer. Evidence for their role as epigenetic p53 inhibitors in vivo. *Cancer Res. 64*: 2449–2460.

Dechend, R., Hirano, F., Lehmann, K., Heissmeyer, V., Ansieau, S., Wulczyn, F.G., Scheidereit, C., and Leutz, A. 1999. The Bcl-3 oncoprotein acts as a bridging factor between NF-kappaB/Rel and nuclear co-regulators. *Oncogene 18*:3316–3323.

Deng, C.X., and Brodie, S.G. 2000. Roles of BRCA1 and its interacting proteins. *Bioessays 22*:728–737.

Fabbro, M., and Henderson, B.R. 2003. Regulation of tumor suppressors by nuclear-cytoplasmic shuttling. *Exp. Cell. Res. 285*:59–69.

Fabbro, M., Rodriguez, J.A., Baer, R., and Henderson, B.R. 2002. BARD1 induces BRCA1 intranuclear foci formation by increasing RING-dependent BRCA1 nuclear import and inhibiting BRCA1 nuclear export. *J. Biol. Chem. 277*:21315–21324.

Fabbro, M., Savage, K., Hobson, K., Deans, A.J., Powell, S.N., McArthur, G.A., and Khanna, K.K. 2004a. BRCA1-BARD1 complexes are required for p53Ser-15 phosphorylation and a G1/S arrest following ionizing radiation-induced DNA damage. *J. Biol. Chem. 279*:31251–31258.

Fabbro, M., Schuechner, S., Au, W.W., and Henderson, B.R. 2004b. BARD1 regulates BRCA1 apoptotic function by a mechanism involving nuclear retention. *Exp. Cell. Res. 298*:661–673.

Feki, A., and Irminger-Finger, I. 2004. Mutational spectrum of p53 mutations in primary breast and ovarian tumors. *Crit. Rev. Oncol. Hematol. 52*:103–116.

Feki, A., Jefford, C.E., Berardi, P., Wu, J.Y., Cartier, L., Krause, K.H., and Irminger-Finger, I. 2005. BARD1 induces apoptosis

by catalysing phosphorylation of p53 by DNA-damage response kinase. *Oncogene 24*:3726–3736.

Feki, A., Jefford, C.E., Durand, P., Harb, J., Lucas, H., Krause, K.H., and Irminger-Finger, I. 2004a. BARD1 expression during spermatogenesis is associated with apoptosis and hormonally regulated. *Biol. Report. 71*:1614–1624.

Gautier, F., Irminger-Finger, I., Gregoire, M., Meflah, K., and Harb, J. 2000. Identification of an apoptotic cleavage product of BARD1 as an autoantigen: a potential factor in the antitumoral response mediated by apoptotic bodies. *Cancer Res. 60*: 6895–6900.

Ghimenti, C., Sensi, E., Presciuttini, S., Brunetti, I.M., Conte, P., Bevilacqua, G., and Caligo, M.A. 2002. Germline mutations of the BRCA1-associated ring domain (BARD1) gene in breast and breast/ovarian families negative for BRCA1 and BRCA2 alterations. *Genes Chromosomes Cancer 33*:235–242.

Hakem, R., de la Pompa, J.L., and Mak, T.W. 1998. Developmental studies of Brca1 and Brca2 knock-out mice. *J. Mammary Gland Biol. Neoplasia 3*:431–445.

Hall, I.J., Burke, W., Coughlin, S., and Lee, N.C. 2001. Population-based estimates of the prevalence of family history of cancer among women. *Community Genet. 4*:134–142.

Hashiguchi, Y., Tsuda, H., Inoue, T., Nishimura, S., Suzuki, T., and Kawamura, N. 2004. Alteration of cell cycle regulators correlates with survival in epithelial ovarian cancer patients. *Hum. Pathol. 35*:165–175.

Hashizume, R., Fukuda, M., Maeda, I., Nishikawa, H., Oyake, D., Yabuki, Y., Ogata, H., and Ohta, T. 2001. The RING heterodimer BRCA1-BARD1 is a ubiquitin ligase inactivated by a breast cancer-derived mutation. *J. Biol. Chem. 276*: 14537–14540.

Hsu, L.C., Doan, T.P., and White, R.L. 2001. Identification of a gamma-tubulin-binding domain in BRCA1. *Cancer Res. 61*: 7713–7718.

Irminger-Finger, I., and Leung, W.C. (2002). BRCA1-dependent and independent functions of BARD1. *Int. J. Biochem. Cell. Biol. 34*:582–587.

Irminger-Finger, I., Leung, W.C., Li, J., Dubois-Dauphin, M., Harb, J., Feki, A., Jefford, C.E., Soriano, J.V., Jaconi, M., Montesano, R., and Krause, K.H. 2001. Identification of BARD1 as mediator between proapoptotic stress and p53-dependent apoptosis. *Mol. Cell. 8*:1255–1266.

Irminger-Finger, I., Siegel, B.D., and Leung, W.C. 1999. The functions of breast cancer susceptibility gene 1 (BRCA1) product and its associated proteins. *Biol. Chem. 380*:117–128.

Irminger-Finger, I., Soriano, J.V., Vaudan, G., Montesano, R., and Sappino, A.P. 1998. *In vitro* repression of Brcal-associated RING domain gene, Bard1, induces phenotypic changes in mammary epithelial cells. *J. Cell. Biol. 143*:1329–1339.

Ishitobi, M., Miyoshi, Y., Hasegawa, S., Egawa, C., Tamaki, Y., Monden, M., and Noguchi, S. 2003. Mutational analysis of BARD1 in familial breast cancer patients in Japan. *Cancer Lett. 200*:1–7.

Jasin, M. 2002. Homologous repair of DNA damage and tumorigenesis: the BRCA connection. *Oncogene 21*:8981–8993.

Jefford, C.E., Feki, A., Harb, J., Krause, K.H., and Irminger-Finger, I. 2004. Nuclear-cytoplasmic translocation of BARD1 is linked to its apoptotic activity. *Oncogene 23*:3509–3520.

Jemal, A., Clegg, L.X., Ward, E., Ries, L.A., Wu, X., Jamison, P.M., Wingo, P.A., Howe, H.L., Anderson, R.N., and Edwards, B.K. 2004. Annual report to the nation on the status of cancer, 1975–2001, with a special feature regarding survival. *Cancer 101*:3–27.

Jin, Y., Xu, X.L., Yang, M.C., Wei, F., Ayi, T.C., Bowcock, A.M., and Baer, R. 1997. Cell cycle-dependent colocalization of BARD1 and BRCA1 proteins in discrete nuclear domains. *Proc. Natl. Acad. Sci. U.S.A. 94*:12075–12080.

Joukov, V., Chen, J., Fox, E.A., Green, J.B., and Livingston, D.M. 2001. Functional communication between endogenous BRCA1 and its partner, BARD1, during *Xenopus laevis* development. *Proc. Natl. Acad. Sci. U.S.A. 98*:12078–12083.

Karppinen, S.M., Heikkinen, K., Rapakko, K., and Winqvist, 2004. Mutation screening of the BARD1 gene: evidence for involvement of the Cys557Ser allele in hereditary susceptibility to breast cancer. *J. Med. Genet. 41*:e114.

Khanna, K.K., and Jackson, S.P. 2001. DNA double-strand breaks: Signaling, repair and the cancer connection. *Nat. Genet. 27*:247–254.

Kleiman, F.E., and Manley, J.L. 1999. Functional interaction of BRCA1-associated BARD1 with polyadenylation factor CstF-50. *Science 285*:1576–1579.

Kleiman, F.E., and Manley, J.L. 2001. The BARD1-CstF-50 interaction links mRNA 3′ end formation to DNA damage and tumor suppression. *Cell 104*:743–753.

Maciel Mdo, S., Viegas, L.C., Nonogaki, S., Nishimoto, I.N., Abrao, F.S., Mourao Neto, M., and Brentani, M.M. 2002. p53 expression is a factor for prognostic assessment in breast sarcoma. *Breast Cancer Res. Treat 71*:193–202.

Makar, A.P., Baekelandt, M., Trope, C.G., and Kristensen, G.B. 1995. The prognostic significance of residual disease, FIGO substage, tumor histology, and grade in patients with FIGO stage III ovarian cancer. *Gynecol. Oncol. 56*:175–180.

Mano, M.S., Awada, A., Di Leo, A., Durbecq, V., Paesmans, M., Cardoso, F., Larsimont, D., and Piccart, M. 2004. Rates of topoisomerase II-alpha and HER-2 gene amplification and expression in epithelial ovarian carcinoma. *Gynecol. Oncol. 92*:887–895.

McCarthy, E.E., Celebi, J.T., Baer, R., and Ludwig, T. 2003. Loss of Bard1, the heterodimeric partner of the Brca1 tumor suppressor, results in early embryonic lethality and chromosomal instability. *Mol. Cell. Biol. 23*:5056–5063.

McGuire, V., Jesser, C.A., and Whittemore, A.S. 2002. Survival among U.S. Women with invasive epithelial ovarian cancer. *Gynecol. Oncol. 84*:399–403.

Menard, S., Fortis, S., Castiglioni, F., Agresti, R., and Balsari, A. 2001. HER-2 as a prognostic factor in breast cancer. *Oncology 61 suppl 2*:67–72.

Meza, J.E., Brzovic, P.S., King, M.C., and Kievit, R.E. 1999. Mapping the functional domains of BRCA1. Interaction of the ring finger domains of BRCA1 and BARD1. *J. Biol. Chem. 274*:5659–5665.

Miki, Y., Swensen, J., Shattuck-Eidens, D., Futreal, P.A., Harshman, K., Tavtigian, S., Liu, Q., Cochran, C., Bennett, L.M., Ding, W., and *et al*. 1994. A strong candidate for the breast ovarian cancer susceptibility gene BRCA1. *Science 266*:66–71.

Morris, J.R., Keep, N.H., and Solomon, E. 2002. Identification of residues required for the interaction of BARD1 with BRCA1. *J. Biol. Chem. 277*:9382–9386.

Narod, S.A., and Foulkes, W.D. 2004. BRCA1 and BRCA2: 1994 and beyond. *Nat. Rev. Cancer 4*:665–676.

Qiu, Y., Langnian, M.J., and Eggo, M.C. 2004. Targets of l7beta-oestradiol-induced apoptosis in colon cancer cells: a mechanism for the protective effects of hormone replacement therapy? *J. Endocrinol. 181*:327–337.

Rajan, J.V., Marquis, S.T., Gardner, H.P., and Chodosh, L.A. 1997. Developmental expression of Brca2 colocalizes with Brca1 and is associated with proliferation and differentiation in multiple tissues. *Dev. Biol. 184*:385–401.

Reinholz, M.M., An, M.W., Johnsen, S.A., Subramaniam, M., Suman, V.J., Ingle, J.N., Roche, P.C., and Spelsberg, T.C. 2004.

Differential gene expression of TGF beta inducible early gene (TIEG), Smad7, Smad2 and Bard1 in normal and malignant breast tissue. *Breast Cancer Res. Treat. 86*:75–88.

Rodriguez, J.A., Au, W.W., and Henderson, B.R. 2004a. Cytoplasmic mislocalization of BRCA1 caused by cancer-associated mutations in the BRCT domain. *Exp. Cell. Res. 293*:14–21.

Rodriguez, J.A., Schuchner, S., Au, W.W., Fabbro, M., and Henderson, B.R. 2004b. Nuclear-cytoplasmic shuttling of BARD1 contributes to its proapoptotic activity and is regulated by dimerization with BRCA1. *Oncogene 23*:1809–1820.

Roth, J.A., Swisher, S.G., and Meyn, R.E. 1999. p53 tumor suppressor gene therapy for cancer. *Oncology (Huntingt) 13*:148–154.

Scully, R., Chen, J., Ochs, R.L., Keegan, K., Hoekstra, M., Feunteun, J., and Livingston, D.M. 1997. Dynamic changes of BRCA1 subnuclear location and phosphorylation state are initiated by DNA damage. *Cell 90*:425–435.

Scully, R., and Livingston, D.M. 2000. In search of the tumour-suppressor functions of BRCA1 and BRCA2. *Nature 408*: 429–432.

Sirvent, J.J., Aguilar, M.C., Olona, M., Pelegri, A., Blazquez, S., and Gutierrez, C. 2004. Prognostic value of apoptosis in breast cancer (pT1-pT2). A TUNEL, p53, bcl-2, bag-1 and Bax immunohistochemical study. *Histol. Histopathol. 19*:759–770.

Starita, L.M., and Parvin, J.D. 2003. The multiple nuclear functions of BRCA1: transcription, ubiquitination and DNA repair. *Curr. Opin. Cell. Biol. 15*:345–350.

Steels, E., Paesmans, M., Berghmans, T., Branle, F., Lemaitre, F., Mascaux, C., Meert, A.P.,Vallot, F., Lafitte, J.J., and Sculier, J.P. 2001. Role of p53 as a prognostic factor for survival in lung cancer: a systematic review of the literature with a meta-analysis. *Eur. Respir. J. 18*:705–719.

Tammela, J., Geisler, J.P., Eskew, P.N., Jr., and Geisler, H.E. 1998. Clear cell carcinoma of the ovary: poor prognosis compared to serous carcinoma. *Eur. J. Gynaecol. Oncol. 19*:438–440.

Tan, D.F., Li, Q., Rammath, N., Beck, A., Wiseman, S., Anderson, T., al-Salameh, A., Brooks, J., and Bepler, G. 2003. Prognostic significance of expression of p53 oncoprotein in primary (stage I-IIIa) non-small cell lung cancer. *Anticancer Res. 23*:1665–1672.

Thai, T.H., Du, F., Tsan, J.T., Jin, Y., Phung, A., Spillman, M.A., Massa, H.F., Muller, C.Y., Ashfaq, R., Mathis, J.M., Miller, D.S., Trask, B.J., Baer, R., and Bowcock, A.M. 1998. Mutations in the BRCA1-associated RING domain (BARD1) gene in primary breast, ovarian and uterine cancers. *Hum. Mol. Genet. 7*:195–202.

Thompson, M.E., Jensen, R.A., Obermiller, P.S., Page, D.L., and Holt, J.T. 1995. Decreased expression of BRCA1 accelerates growth and is often present during sporadic breast cancer progression. *Nat. Genet 9*:444–450.

Tsutsui, S., Ohno, S., Murakami, S., Hachitanda, Y., and Oda, S. 2001. Prognostic value of p53 protein expression in breast cancer; an immunohistochemical analysis of frozen sections in 514 Japanese women. *Breast Cancer 8*:194–201

Tsutsui, S., Ohno, S., Murakami, S., Kataoka, A., Kinoshita, J., and Hachitanda, Y. 2003. Prognostic significance of the coexpression of p53 protein and c-erbB2 in breast cancer. *Am. J. Surg. 185*:165–167.

Venkitaraman, A.R. 2004. Tracing the network connecting BRCA and Fanconi anaemia proteins. *Nat. Rev. Cancer 4*:266–276.

Wooster, R., Neuhausen, S.L., Mangion, J., Quirk, Y., Ford, D., Collins, N., Nguyen, K., Seal, S., Tran, T., Averill, D., *et al.* 1994. Localization of a breast cancer susceptibility gene, BRCA2, to chromosome 13q12-13. *Science 265*:2088–2090.

Wu, J., Vlastos, A.-T., Pelte, M.-F., Caligo, M.-A., Bianco, A., Krause, K.-H., Laurent, G.J., and Irminger-Finger, I. 2005. Aberrant expression of BARD1 in breast and ovarian cancers with poor prognosis. *Int. J. Cancer.*

Wu, L.C., Wang, Z.W., Tsan, J.T., Spillman, M.A., Phung, A., Xu, X.L., Yang, M.C., Hwang, L.Y., Bowcock, A.M., and Baer, R. 1996. Identification of a RING protein that can interact *in vivo* with the BRCA1 gene product. *Nat. Genet. 14*: 430–440.

Xu, X., Wagner, K.U., Larson, D., Weaver, Z., Li, C., Ried, T., Hennighausen, L., Wynshaw-Boris, A., and Deng, C.X. 1999. Conditional mutation of Brca1 in mammary epithelial cells results in blunted ductal morphogenesis and tumour formation. *Nat. Genet. 22*:37–43.

Yoshikawa, K., Ogawa, T., Baer, R., Hemmi, H., Honda, K., Yamauchi, A., Inamoto, T., Ko, K., Yazumi, S., Motoda, H., Kodama, H., Noguchi, S., Gazdar, A.F., Yamaoka, Y., and Takanashi, R. 2000. Abnormal expression of BRCA1 and BRCA1-interactive DNA-repair proteins in breast carcinomas. *Int. J. Cancer 88*:28–36

Young, R.H., and Clement, P.R. (eds.). 1996. *Atlas of Tumor Pathology,* 3rd series. Washington, DC: Armed Forces Institute of Pathology, p. 27.

Zuco, V., Supino, R., De Cesare, M., Carenini, N., Perego, P., Gatti, L., Pratesi, G., Pisano, C., Martinelli, R., Bucci, F., Zanier, R., Carminati, P., and Zunino, F. 2003. Cellular bases of the antitumor activity of a 7-substituted camptothecin in hormone-refractory human prostate carcinoma models. *Biochem. Pharmacol*, *65*:1281–1294.

This Page Intentionally Left Blank

4

Angiogenesis, Metastasis, and Epigenetics in Cancer

Claire L. Plumb and Brenda L. Coomber

Introduction

In this chapter we review the implications epigenetic mechanisms may have in the progression of cancer, and in particular where epigenetics may be important for angiogenesis and metastasis, and introduce assays useful for evaluating angiogenesis and metastasis in experimental settings.

Epigenetic Influence on Gene Expression

Epigenetic control of gene expression, and its importance in cancer and disease, has been reviewed extensively in several articles (cited later in this chapter). In the following sections we provide an introduction to the processes as a background for the discussion that follows.

Methylation and Demethylation

Methylation of cystine residues in the promoter region of mammalian genes is an important cause of gene silencing. Methylation of deoxyribonucleic acid (DNA) occurs almost exclusively on the sequence CpG. As much as 80% of all CpG dinucleotides in the mammalian genome are methylated; the remaining unmethylated CpG residues are located in promoter regions of constitutively active genes—these are the CpG islands of DNA (Cheung and Lau, 2005). When CpG islands are methylated, the gene remains inactive and is heritably silenced through successive cellular generations. DNA methyltransferases (DNMTs) catalyze the transfer of methyl groups onto DNA, resulting in maintenance of silenced transposable elements and repression of gene transcription (Szyf *et al.,* 2004). Epigenetic silencing and reactivation via methylation and demethylation is emerging as an important method of transcriptional control (Cheung and Lau, 2005). In cancer, there are three patterns of methylation changes: global hypomethylation; hypomethylation of individual genes; and local and discrete regions of hypermethylation at CpG islands (Feinberg, 2004).

Global hypomethylation occurs as a result of loss of methyl groups in the coding region and introns, leading to chromosomal instability, reactivation of transposable elements, loss of imprinting, loss of heterozygosity, chromosome rearrangements, and centromeric instability leading to aneuploidy (Esteller and Herman, 2002). The converse, hypermethylation, also occurs at specific areas of the genome in cancer. The enzymes that bring about changes in methylation status, DMNTs, are also linked to the generation of C to G transitions. Methylation of CpG islands has been associated with

Handbook of Immunohistochemistry and *in situ* Hybridization of Human Carcinomas, Volume 4: Molecular Genetics, Gastrointestinal Carcinoma, and Ovarian Carcinoma

gene silencing in tumors, affecting such genes as *TGF-type I receptor* (Kang *et al.,* 2003), *BRCA1* (Esteller *et al.,* 2000b), and *O^6-methylguanine-DNA methyltransferase* (Esteller *et al.,* 2000a). Depending on the cell type, form of cancer, and its staging, the methylation status of diverse genes changes—leading to the possibility of a molecular signature of methylated genes that could be of diagnostic, prognostic, and therapeutic importance.

Histone Alterations

Chromatin structure is determined by the packaging of genomic DNA with histone proteins. The basic repeating unit of chromatin is termed the nucleosome and consists of 146 base pairs of DNA wrapped around a core of eight histone proteins consisting of two copies each of histones H2A, H2B, H3, and H4 (Kornberg and Lorch, 1999). Histones exhibit post-translational modifications such as acetylation of lysines, methylation of lysines and arginines, phosphorylation of serines and threonines, ADP-ribosylation of glutamic acids, and ubiquitination and sumolyation of lysine residues (Lund and van Lohuizen, 2004). Histone acetylation and phosphorylation are reversible and dynamic and result in inducible expression of individual genes; histone methylation is more stable and thus maintains long-term expression status (Cheung and Lau, 2005). Epigenetic silencing by promoter methylation is almost always associated with histone deacetylation (Egger *et al.,* 2004). Transcriptionally active euchromatin has acetylated histones, whereas inactive DNA such as euchromatin or heterochromatin exhibits hypoacetylated histones. Histone modification is now understood to both precede DNA methylation and follow it (Szyf *et al.,* 2004), making histone modification an even more important consideration in epigenetic disease. Post-translational modifications of the histones therefore allow the cell machinery to interpret how the DNA should be treated—the sum of these modifications is known as the "histone code" (Egger *et al.,* 2004). Methylation events on DNA are more stable modifications than histone tail acetylations; the histone code can therefore be rapidly reset to allow transcription and therefore rapid response to environmental changes (Drummond *et al.,* 2005).

Tumor Angiogenesis

Angiogenesis

Angiogenesis is the formation of blood vessels from the preexisting vascular architecture (Papetti and Herman, 2002). Essential during embryonic development, this process establishes the blood vascular system allowing perfusion of the tissues of the body. Angiogenesis is more restricted in the adult—it occurs physiologically during wound healing and in the female reproductive tract where remodeling of the vasculature ensures proper organ perfusion to growing tissues (Davis *et al.,* 2003). Angiogenesis is normally controlled by an orderly set of instructions defined by the nature of the perfusion requirements of the tissue. The result of this carefully orchestrated signaling system is an orderly vascular architecture. Soluble factors, such as vascular endothelial growth factor (VEGF), are secreted by tissues and result in vascular recruitment and stabilization (Xie *et al.,* 2004). Other factors affecting angiogenesis include angiopoietins and tie receptors, acidic and basic fibroblast growth factor (aFGF and bFGF), platelet-derived growth factor (PDGF), transforming growth factor-β (TGF-β), interleukin-8 (IL-8), and tumor necrosis factor-α (TNF-α) (Papetti and Herman, 2002). Endogenous inhibitors of angiogenesis are naturally occurring proteins that have an anti-angiogenic effect. Included in this group of soluble factors are interferon-γ, cortisone, thrombospondin, platelet factor IV, and the more recently discovered angiostatin and endostatin (Eliceiri and Cheresh, 2001). Several membrane bound proteins such as integrins (specifically $\alpha_v\beta_3$-integrin), cadherins such as VE-cadherin, and Eph receptors and ephrin ligands (Papetti and Herman, 2002) also play prominent roles in angiogenesis. These molecules require close cell–cell or cell–matrix contact for their effects to be transduced.

Angiogenesis in Cancer

Angiogenesis allows growing tumors to recruit their own blood supply. Cancer cells cannot expand as a tumor past the minuscule size of 1 mm^3 because diffusion of oxygen and nutrients is insufficient in masses larger than that size (Kerbel and Folkman, 2002). Thus, being able to recruit the vasculature necessary for the maintenance of a supportive growth environment is an important determinant of cancer cell survival and the ensuing tumor growth and metastasis. Angiogenesis is also important in hematologic malignancies where new blood vessel growth is present in the bone marrow and lymph nodes of patients with acute lymphoblastic leukemia and B-cell non-Hodgkin's lymphoma (Kerbel and Folkman, 2002). In contrast to the physiologic angiogenic signaling system, the tumor generates signals that are a result of the stresses of low oxygen and nutrient supply, or a result of oncogenic alterations, leading to aberrant gene expression of angiogenesis controlling substances (Rak *et al.,* 2002), often in the absence of normal levels of endogenous inhibitors. This results in development of a disorganized and chaotic

angiogenic response. Tumor blood vasculature exhibits numerous abnormalities, including dilations, incomplete or absent vascular endothelial linings and basement membranes, leakiness, irregular and tortuous architecture, arteriovenous shunts, blind ends, and lack of contractile wall components and cellular receptors (Jain, 2005).

Vascular Targeting Therapies in Cancer

The dependence of tumors on the vasculature provided by normal endothelial cells led to the proposition of anti-angiogenic therapies. First proposed by Dr. Judah Folkman in the 1970s (Folkman, 1971), anti-angiogenic therapies rely on the fact that the endothelial cells in the tumor do not exhibit the genetic instability of cancer cells. Therapies designed to target these cells should therefore result in destruction of the tumor vasculature and degradation of vascular perfusion within the tumor without the drug resistance encountered in traditional chemotherapies (Kerbel and Folkman, 2002). Pharmacologic inhibitors of angiogenesis may be classified as exerting their actions via indirect or direct means. Indirect inhibitors target cancer cells and prevent expression of proangiogenic molecules (e.g., thalidomide) or target their receptors on endothelial cells (e.g., DC101; the monoclonal neutralizing antibody of the FLK-1/KDR receptor for VEGF) (Kerbel and Folkman, 2002). Direct angiogenesis inhibitors affect endothelial cells (e.g., vitaxin, angiostatin) and prevent vascular endothelial cells from proliferating or migrating or induce apoptosis by targeting proangiogenic signaling cascades of molecules such as VEGF, bFGF, IL-8, PDGF, and platelet-derived-endothelial growth factor (PD-EGF) (Kerbel and Folkman, 2002). When used in animal models, inhibitors of angiogenesis cause regression or stabilization of a tumor's volume resulting from targeting of the blood vasculature. In addition, they may initially normalize the blood vasculature and increase the efficacy of other chemotherapeutics by decreasing plasma leakage and thus decreasing intratumoral pressure and its adverse affect on drug infiltration (Kerbel and Folkman, 2002). Whereas chemotherapeutic agents are generally used at a maximum tolerated dose followed by a period of rest to allow recovery of the bone marrow and intestinal lining, anti-angiogenic therapeutics can be administered at lower doses for an extended period to target the endothelial lining of blood vessels (Browder *et al.,* 2000). Now termed *metronomic therapy* this treatment regimen was proposed and proved effective using cyclophosphamide (Browder *et al.,* 2000). In February 2004, the first therapeutic agent designed specifically to target angiogenesis was approved by the U.S. Food and Drug Administration (FDA) Bevacizumab (Avastin) is an antibody against VEGF, thereby acting as a VEGF sink and blocking its ability to stimulate proliferation, migration, and survival of endothelial cells (Muhsin *et al.,* 2004). Although its clinical efficacy in combination with fluorouracil is the subject of current debate, the drug's availability to patients should allow greater treatment options in clinical trials (Sobrero and Bruzzi, 2005).

The clinical effectiveness of anti-angiogenic therapies is currently somewhat hampered by the lack of appropriate surrogate markers of angiogenesis for monitoring of their effectiveness (Kerbel and Folkman, 2002). Without an independent method of determining therapeutic efficacy, it remains difficult to tailor drug administration to the individual needs of the patient. Endothelial cells in the vicinity of a local tumor replicate, migrate, and invade, thereby participating in a sprouting angiogenesis, but there is another source of endothelial cells contributing to the newly formed blood vessels of a tumor. The bone marrow contains endothelial progenitor cells (EPCs) that can be mobilized to release their progency, circulating endothelial progenitors (CEPs), into the peripheral circulation (Asahara *et al.,* 1999). New results assessing the levels of circulating peripheral blood endothelial cells in mice demonstrate that blood levels of these cells reflect levels of VEGF, Tie-2, and TSP-1 (thrombospondin-1), known regulators of angiogenesis (Shaked *et al.,* 2005).

Angiogenic Assays

Studying angiogenic responses in the context of cancer biology and response to therapy requires an understanding of relevant models and assays. Many useful approaches have been described in considerable methodologic detail in a 2004 monograph (Augustin, 2004); here we will discuss the general principles and useful features of several. At their simplest, angiogenic assays determine the ability of endothelial cells to respond to an angiogenic factor. At their most complex, angiogenic assays attempt to understand the interplay between the vasculature, the tissue microenvironment, and the cancer cell. A critical issue in setting up an *in vitro* assay is the ***choice of endothelial cells.*** Although immortalized endothelial cells are easy to use, they have often lost some of the characteristics of endothelial cells, including specific molecular markers, they may exhibit changes in function (Taraboletti and Giavazzi, 2004), and they may be unable to respond to angiogenic stimuli because they are spontaneously activated. Primary cultures of human endothelial cells are often obtained from the human umbilical cord vein endothelial cell (HUVEC), and murine and bovine cells from the aorta. Because the source of these cells is large blood vessels, they have different phenotypic and behavioral

characteristics than the microvessels that are responsible for tumor angiogenesis. Microvascular cells can therefore be obtained from tissues such as skin, brain, adipose tissue, and adrenal gland (Taraboletti and Giavazzi, 2004). Here again, the site from which the cells are obtained is important because the microvascular of different tissues and organs are often heterogeneous (St. Croix *et al.,* 2000). Thus, the most ideal source of endothelial cells is often the tumor of interest: unfortunately, isolation and culture of such cells is challenging (Nanda and St. Croix, 2004). Once in culture, endothelial cells must be handled carefully because they can easily be stimulated to proliferate rapidly by media rich in growth factors and can lose phenotypic, antigenic, and functional characteristics important for their site of origin (Taraboletti and Giavazzi, 2004).

The effects of compounds of interest on ***cell proliferation and apoptosis*** can be measured by standard mitogenic assays (incorporation of thymidine, 5-bromodeoxyuridine) or by counting the increase in cell number (direct counts or indirect colorimetric evaluation such as crystal Violet or MMT). Apoptosis can be measured by TUNEL (terminal deoxynucleotidyl transferase biotin-dUTP Nick End Labeling) or by analyzing the expression of apoptosis markers such as caspases and annexin V (Taraboletti and Giavazzi, 2004). When assessing anti-angiogenic activity, inhibition of endothelial cell proliferation may not be the most appropriate endpoint—this may simply indicate low toxicity for an anti-angiogenic agent that targets another endothelial process (Taraboletti and Giavazzi, 2004). Further studies, of cell motility, morphogenesis, etc., are therefore required to understand the nuances of an anti-angiogenic agent.

The standard ***motility*** assay is the Boyden motility assay. The substance of interest is placed in a tissue culture well, and a chamber with a cell-permeable filter containing endothelial cells is placed above. After a specified amount of time, the number of cells crossing the membrane to meet the test agent is counted (Auerbach *et al.,* 2003). The system is useful for testing concentration gradients and thus may reflect the conditions that are operative *in vivo* (Auerbach *et al.,* 2003). Endothelial cells degrade the matrix and invade tissue structures during angiogenesis. Therefore, *in vitro* ***matrix degradation and invasion*** assays have been developed to evaluate these activities. The wound-healing assay analyzes the plannar motility of cells by measuring the ability of a confluent nonolayer of cells to close a wound created through it (Taraboletti and Giavazzi, 2004). Matrix invasion assays can be performed using a modified version of the Boyden chamber assay described earlier, except a thick layer of matrix separates the endothelial cells from chemotactic or growth factors. Cells must be capable of both matrix degradation and invasion to reach the underside of the support matrix to be counted (Taraboletti and Giavazzi, 2004).

To test the effect of substances on endothelial tube formation, endothelial cells are layered above collagen or fibrin clots coating plastic culture dishes. Tube formation in the presence of the test agents in combination with the clot substrate is reasonably indicative of microvascular stimulation *in vivo* (Auerbach *et al.,* 2003). In the aortic ring assay and chick aortic arch assay, isolated murine or chick aorta is cut into pieces and placed in culture over a support matrix such as Matrigel. The agent of interest is placed in the growth medium, and the sprouting of endothelial cell processes is monitored over time (Auerbach *et al.,* 2003). This technique can be used with human surgical specimens as a source of primary human tissue for research into anti-angiogenic compounds (Woltering *et al.,* 2003). Digital technology has aided the quantification of vessel outgrowth—in 2004 it was used to demonstrate that the antiangiogenic compounds suramin and endostain are most effective if administered early in angiogenesis (Berger *et al.,* 2004), suggesting that anti-angiogenics would be able to inhibit angiogenesis in newly forming metastases.

The ability to assess angiogenic activity *in vivo* in transgenic mice allows monitoring of both vascular growth and tumor–vascular interactions. ***Microcirculatory preparations*** have the great advantage of allowing direct visualization of angiogenesis across time, thereby evaluating phenomena associated with both onset and regression. The intravital microscopic techniques developed in these models have proved a powerful tool for the noninvasive, continuous monitoring of cellular and molecular events (Taraboletti and Giavazzi, 2004). ***Chorio-allantoic membrance (CAM) assays*** are suitable for large-scale screening of new compounds. The egg contents of a 72-hour-old chicken embryo are maintained as a whole embryo culture. Angiogenesis is stimulated by placing a coated glass or plastic matrix on the CAM or by allografting or xenografting tumors (Auerbach *et al.,* 2003). Because the tests are run on chicken cells, and because the CAM is rapidly changing with development, CAM assays must be used with some care (Auerbach *et al.,* 2003). They are, however, still useful in drug effect studies; use of the CAM assay demonstrated the anti-angiogenic effects of FK288 (Depsipeptide), a histone deacetylase inhibitor (Kwon *et al.,* 2002). The ***rabbit ear chamber*** provides a method to quantify the structural and functional chances in newly formed vessels in an optically clear way (Hasan *et al.,* 2004). In this technique, the ear is stablilized and an area is surgically cleared of vasculature, creating a

growth chamber. After a 4–6-week period of recovery, therapeutic agents can be introduced into the chamber and effects on neovascularization are observed. Because the procedure relies on wounding, this can compound the results of the test agent. The rabbit ear chamber is used extensively in analysis of angiogenesis in wound healing research (Komori *et al.,* 2005).

The ***dorsal skin chamber*** preparation is a long-standing assay that allows quantification of angiogenesis by intravital microscopy or analysis of excised tissues. The preparation involves removing one skin layer from the back of a murine host to expose the cutaneous muscle. After implantation of tumor cells or the agent of interest, the area is enclosed using a sterile coverslip. Newly formed blood vessels are visible on day 10, and peak vascular density is obtained by day 25 (Hasan *et al.,* 2004). The dorsal-skin chamber is used to study vascularization for wound healing angiogenesis into tumor implants (Gelaw and Levin, 2001); this model also allows evaluation of *in vivo* effectiveness of anti-angiogenic agents including VEGF and PDGF signaling inhibitors (Erber *et al.,* 2004). Although this technique allows visualization of newly forming blood vessels, it does not display the optical resolution of techniques such as the rabbit ear chamber or the CAM assay. Similarly, ***subcutaneous air-sac preparations*** allow monitoring of vascularization when cells or tissue fragments are placed in an air pocket created on the dorsum of a rat temporarily, creating a thin, isolated vascularized membrane for the introduced substance to establish a new blood supply (Hasan *et al.,* 2004). Unlike the dorsal skin chamber, it is not possible to monitor vascularization in real-time.

The ***corneal angiogenesis assay*** is still considered one of the best *in vivo* assays because the cornea itself is avascular, and therefore any vessels arising after the commencement of the experiment are truly a result of the intervention (Auerbach *et al.,* 2002). A pocket is made in the cornea, and test tumors or tissues are introduced; over time, angiogenic factors elicit the ingrowth of new vessels from the peripheral limbal vasculature. Anti-angiogenic factors can be tested simultaneously, by both topical application via the implant and systematic exposure via the circulatory system. This method is currently used in cancer research to test the effectiveness of anti-angiogenic compounds (Morbidelli *et al.,* 2003).

Matrix-implant systems are relatively easier to perform than the surgical preparations outlined earlier (Hasan *et al.,* 2004). Compounds of interest are mixed directly with matrix, and the preparation is surgically implanted (Hasan *et al.,* 2004). The ***sponge implant assay*** and the ***disc angiogenesis assay*** use inert matrices as carriers for the agent of interest. Once implanted in the animal, they are encapsulated by granulation tissue and invaded by new vessels. The matrices are harvested after 1–3 weeks and then fixed and processed for histology and immunohistochemistry to assess vessel infiltration and microvessel density (Hasan *et al.,* 2004). These assays allow studies that evaluate tumor angiogenesis, as well as proangiogenic and anti-angiogenic compounds in an easily reproducible manner (Hasan *et al.,* 2004). The sponge implant assay has been effective in demonstrating effective gene transfer (Wang *et al.,* 2004). Although these matrices stimulate new vasculature, subcutaneous tumors are not typical sites for pathologic angiogenesis *in vivo.* This limits the usefulness of results for studies of tumor–vascular interactions.

Injection of noninert carrier materials can also be used to assay angiogenic activity. In the ***Matrigel-plug assay,*** the gelling properties of Matrigel are used to assay the angiogenic capacity of different compounds. Matrigel is a laminin rich reconstituted matrix extracted from the growth medium of the Engelbreth–Holm–Swarm tumor; it is a liquid at 4°C and forms a gel at 37°C. Subcutaneous plugs containing Matrigel alone (Matrigel is itself angiogenic), or Matrigel plus test cells or agents, are recovered after 7–21 days in the animal and examined histologically to determine the extent of vascular infiltration (Hasan *et al.,* 2004). Quantification of the vessels in histologic sections is tedious but accurate (Hasan *et al.,* 2004). Alternately, a modified method called the sponge/Matrigel assay allows quantification of angiogenesis using photometric methods (Auerbach *et al.,* 2002). By combining Matrigel and a sponge or tissue fragment, new vessels can be measured by injection of Fluorescein isothiocyanate (FITC) dextran; inhibition by endostatin contained in Alzet osmotic pumps is readily seen by this method (Akhtar *et al.,* 2002). Although more time consuming than the standard Matrigel assay, the ease of imaging makes this method attractive.

As previously mentioned, tissues grown using *in vivo* techniques can be harvested for further analysis. Tissues obtained from the CAM assay, anterior chamber assays, and xenografted human cells in immune-deficient animals are often used (Hasan *et al.,* 2004). Both routine histology and immunohistochemistry for specific markers of endothelial cell activation can be performed. In addition, specific methods can be used to identify tumor and endothelial cell response to chemotherapy. Syngeneic murine models allow implantation of cancer cells into an animal of the same species where the host response, including the vasculature, is intact (Taraboletti and Giavazzi, 2004). The classical syngeneic model is of the Lewis lung carcinoma, which is rapid, reproducible, and metastatic; this model has been used extensively to test anti-angiogenic compounds (Browder *et al.,* 2000). Xenograft models,

where cells from one species are transplanted into an immunocompromised recipient (e.g., athymic nude, severe combined immunodeficient mice [SCID] or Rag1 null), reflect the growth factor expression of human tumors (Taraboletti and Giavazzi, 2004). Unfortunately, xenografts do not contend with host immune response, so they cannot model the entire tumor–host environment.

Quantification of the Angiogenic Response

Quantification of effects of experiments is relatively straightforward in excised tissues. Techniques used include measurement of morphometric parameters by light or electron microscopy of vascular casts and immunohistologic examination of tissue sections stained with endothelial antibodies or perfused with intravascular markers (e.g., colloidal carbon, India ink, radioactively labeled red blood cells, high molecular weight tracers). The "gold standard" for quantitative evaluation of angiogenesis is the measurement of microvessel density (MVD), which gives an estimate of intercapillary distance in the tumor (reviewed in Hasan *et al.,* 2004). Weidner *et al.* (1991) first suggested that counting of immunohistochemically stained tumor blood vessels could allow malignant neoplasms to be grouped into highly and poorly angiogenic tumors. To count capillaries, antibodies against pan-endothelial cell markers, which stain small and large vessels with equal intensity, are usually used (Hasan *et al.,* 2004). Generally, anti-CD31 (PECAM) antibodies are used, but von Willebrand factor (vWF), anti-CD34, and thrombomodulin are also effective, although the fact that CD34 is also present on lympthatic vessels highlights the importance of carefully choosing vascular endothelial-specific markers (Hasan *et al.,* 2004). Using markers for activated endothelium such as CD105, integrin $\alpha_v\beta_3$ and VEGF receptors, it is now possible to distinguish between tumor neovascularization and preexisting vessels.

Although calculation of MVD is the currently used method of scoring tumors for vasculogenic activity, the *"edvin"* (*ed*ge *v*ersus *in*ner) method of tumor scoring has been developed to more accurately score tumors with varying vascular density throughout (Giatromanolaki *et al.,* 2004). This method uses a scoring system that evaluates both the vascular density at the edge of the tumor where tumor angiogenesis occurs (tumor angiogenic activity, or TAA) and the vasculature density in the center of the tumor where blood vessels are turning to anti-apoptotic pathways (vascular survival) ability, or VSA (Giatromanolaki *et al.,* 2004). The *"edvin"* method of assessing vasculogenic ability of human tumor specimens is prognostic of metastasis and survival (Giatromanolaki *et al.,* 2004). This type of scoring system may prove useful in classifying patients into anti-angiogenic or chemotherapy groups and with experimental models to assess the overall effect of therapeutic agents on the vasculature of a tumor.

Tissue Invasion and the Metastatic Process

Metastasis

The metastatic process can be divided into several steps, each of which is thought to be rate-limiting. The steps can be described as follows: 1) primary malignant neoplasm; 2) neovascularization; 3) invasion (lymphatics, venules, capillaries); 4) embolism (aggregates of cells survive in circulation); 5) arrest in distant organ capillary bed; 6) adherence; 7) extravasation (response to organ microenvironment and proliferation); 8) establishment of new tumor (metastases); and 9) metastasis of metastasis (Fidler, 2002). Failure to overcome the challenge of any one step presumably results in abortion of the process, and metastasis cannot be accomplished.

In 1889, Paget published his "seed and soil" hypothesis to explain why cancer of the breast metastasizes in a predictable manner. He suggested that just as certain seeds require a soil type to germinate, so too does a cancer cell require its own fertile metastatic environment. Although Paget's initial hypothesis explains why a cancer cell will metastasize to a given area, it is a simplistic interpretation of metastasis because the process is far more complicated, both in principle and process (Fidler, 2002). Neoplasms are heterogeneous; cells making up the tumor exist in subpopulations of differing growth and survival abilities. As well, metastasis selects cells that are capable of one more of the processes involved in the metastatic cascade (see earlier). Finally, the establishment of the metastatic lesion is dependent on the multiple interactions between metastatic cells and homeostatic mechanisms.

Although cancer cells circulate through and extravasate into many tissues, the tissue site in which cells exit the circulation can be controlled by the interaction of receptors for chemokines and their ligands (Moore, 2001), or the interaction of selectins and their binding partners in organs (Kim *et al.,* 1999). The number of cells that survive injection into the bloodstream, arrest in the microcirculation, extravasate, and grow into metastatic tumors is very small (approximately 0.01%) (Chambers *et al.,* 2000). This inability of cancer cells to produce growth in tissues after extravasation is termed metastatic insufficiency. High proportions (70–80%) of single cells that extravasate, do not divide; instead, they enter into a dormant state (Chambers

et al., 2000). Cells that avoid dormancy by initiation of growth in the metastatic site may still remain as "dormant" tumors as long as their rate of apoptosis remains equal to their rate of cellular proliferation (Holmgren *et al.,* 1995). If the tumor is capable of growing and inducing angiogenesis, tumor dormancy is reversed and rapid growth can ensue (Chambers *et al.,* 2000; Holmgren *et al.,* 1995).

Factors Influencing Cell Invasion and Survival

Once capable of detachment from the primary tumor, the invading cancer cells migrate through the stroma of the tissue, resulting in remodeling of the extracellular matrix (ECM). Matrix metalloproteinases (MMPs) and their inhibitors, tissue inhibitors of metalloproteinases (TIMPS), are hence important effectors of the metastatic process (Stamenkovic, 2000). Cancer cells that enter the circulation must evade the immune system; one mechanism used is the decreased expression of immune marker molecules such as major histocompatibility complex class (MHC), resulting in resistance to cytotoxic T-cells (Bubenik, 2003). Normal somatic epithelial cells are incapable of surviving estrangement from their lateral neighbors or their basal ECM. If this occurs, they undergo a form of apoptosis termed "anoikis" (Frisch and Ruoslahti, 1997). The ability to become anoikis-resistant is the process that allows cancer cells to survive in the circulation long enough to become lodged in another location and extravasate. Adhesion through integrins allows cells to avoid anoikis and activates signaling pathways associated with actin cytoskeleton organization, cell motility, and survival. Integrins are therefore fundamental in transducing inside-out and outside-in signals, leading to focal adhesion kinase (FAK) activation and stimulation of the Akt/PKB (Protein Kinase B) and mitogen-activated Protein Kinase (MAPK) pathways (Nicholson and Anderson, 2002).

Cell–cell contacts are mediated by integrins and other adhesion proteins such as members of the immunoglobulin superfamily, selectins, and cadherins. Colon carcinoma cells express cell-surface and secreted tumor mucins that contain selectin binding sites (Kim *et al.,* 1999), providing an example of the cancer cell using the body's normal adhesion molecule expression to promote metastasis. Cadherins are transmembrane glycoproteins that mediate calcium-dependent homophilic cell–cell adhesion. Cadherin junctions are the major cell–cell adhesion receptors in epithelia; they attach to actin filaments and are the principal proteins of desmosomes, which link intermediate filament cytoskeletal proteins to adhesion complexes (Goodwin and Yap, 2004). Signaling by N-cadherin prevents apoptosis in ovarian cells by maintaining calcium homeostasis (Pelluso, 1997). E-cadherin promotes aggregation-induced cell survival in prostate and mammary cells (Day *et al.,* 1999). Together, these results suggest that cadherin-mediated cell–cell adhesion can generate compensatory signals that are able to suppress cell death. Whereas cancer cells continue to survive and grow even when detached from the substratum, cell–cell contact is often fundamental for cell survival even when cells grow in an anchorage-independent manner (Santini *et al.,* 2000).

Metastasis Assays

Assays for angiogenesis and metastasis have numerous similarities as they test some of the same cellular properties. In culture, all cells are subjected to the same conditions, and the effects of individual environmental factors or genetic alterations can be examined (MacDonald *et al.,* 2002). Migration and invasion studies are essentially the same; the modified Boyden chamber assay is used for both in order to model degradation of the ECM and in particular the basement membrance by MMPs and the inhibitory action of TIMP proteins (Kleiner and Stetler-Stevenson, 1999). The standard method for zymography uses sodium dodecyl sulfate (SDS) polyacrylamide gels co-polymerized with a protein substrate, in particular, gelatin, casein, or fibrin to resolve MMP activity (Frederiks and Mook, 2004). Proteases such as MMP-2 and MMP-9 have the ability to exert proteolytic activity, which can be analyzed using this method. By adding a crude gelatinase mixture to SDS-polyacrylamide gelatinase gels, it is possible to assess expression of TIMPs in a protein sample (Snoek-van Beurden and Von den Hoff, 2005). *In situ* zymography allows visualization of gelatanolytic activity *in situ,* based on the principle of gel substrate zymography (Frederiks and Mook, 2004). This method has been made more precise by the addition of dye-quenched (DQ)-gelatin that is reactivated by lytic cleavage (Frederiks and Mook, 2004).

Cultures that inhibit the ability of cells to contact substrate, such as shaking cultures, can be used to modify anoikis survival characteristics and make metastatic variants of cell lines (Zhu *et al.,* 2001). To assess the ability of cells to survive and form colonies in contact-withdrawn conditions, cells are sometimes suspended in soft agarose and left to incubate for long periods of time. The soft agarose colony formation assay is still used as a test of tumorigenic potential (Santini *et al.,* 2000).

Assays allowing analysis of functional ability to metastasize have also been developed. Common *in vivo* models include the following: transplantable cancer cell systems commonly characterized in rodents

(experimental metastasis models); genetically engineered mice that develop metastatic cancer; and cancers that naturally develop in outbred large animals, primarily companion animals such as dogs (often referred to as comparative models). By using immune-compromised mice, it is possible to evaluate the ability of human cancer cells to form tumors in a metastatic site. Cells are injected into the peripheral circulation in an area that is appropriate for the tumor type of interest. This assay tests the ability of cells to lodge in the microvasculature, extravasate, and form tumors in that location. Injecting cells into the splenic or hepatic portal veins allows cells to travel into the hepatic portal system and infiltrate the liver. Intracardiac injection of cells may result in metastases to several sites, including bone. Injection via the tail vein of a given number of tumor cells, and counting of macroscopic lung tumors, tells us whether the experimental conditions have an effect on the metastatic outcome (Khanna and Hunter, 2005). Intravital videomicroscopy (IVVM) can be used to follow cancer cells through the early stages of adhesion, extravasation, and therefore the metastatic process in the living animal. This process, although technically challenging, allows quantification of specific criteria such as the survival of cancer cells, formation of micrometastatics, and the fate of cells that fail to establish (MacDonald *et al.,* 2002).

Orthotopic transplantation refers to the delivery of cancer cells to the anatomic location or tissue from which a tumor was derived (Khanna and Hunter, 2005). Cancer cells may be directly injected, or a piece of intact tumor may be surgically placed in the orthotopic location (Khanna and Hunter, 2005). Metastatic orthotopic models produce metastatic foci originating from the primary tumor; however, the primary tumor may require removal because it can grow to an overwhelming size. Xenografts grown subcutaneously in mice can be used to test the effectiveness of treatments on metastatic disease by first growing a tumor under the skin and allowing metastases to form and then removing the primary tumor—treatments can then be administered that will affect the metastatic foci (Kerbel, 2003). Using the Lewis lung carcinoma model allows understanding of how metastasis and other processes such as angiogenesis function together *in vivo* (Camphausen *et al.,* 2001). Transgenic mice, which display spontaneous development of primary lesions and subsequent metastasis, have also been developed. For instance, the H19-Igf2 transgenic mouse overexpresses the IGF-2 (insulin-like growth factor 2) protein and after a 9-month latency period produces mammary tumors, which spontaneously metastasize to liver, lung, and spleen in ~40% of the mice (Pravtcheva and Wise, 1998). Such systems most accurately model the progression of human clinical disease.

Epigenetic Influence on Angiogenesis and Metastasis

Gene products involved in angiogenesis, cell migration, attachment, and survival are all potential targets for epigenetic regulation via CpG methylation and histone modifications. This area of cancer biology is relatively understudied, but evidence is accumulating for both direct and indirect epigenetic influences on angiogenic and metastatic processes in cancer.

Methylation of the *TSP-1* promoter leads to its silencing (Li *et al.,* 1999), allowing neovascularization of the tumor mass. Aberrant promoter methylation leads to the silencing of the tumor-suppressor protein and ubiquitin ligase component Von Hippet-Lindan (VHL) (Herman *et al.,* 1994), which normally targets hypoxia-inducible factors (HIFs) for proteolysis. Cyclooxygensae-2 (Cox-2) favors tumorigenesis and metastasis in epithelial cells by inhibiting apoptosis and increasing invasiveness. In gastric carcinoma cell lines, Cox-2 is overexpressed; methylation of the promoter led to repression of the excess gene expression, showing in principle that *Cox-2* can be silenced by epigenetic means (Song *et al.,* 2001). This is important because overexpression of Cox-2 in intestinal epithelial cells stimulates the production of metastatic factors such a MMP-2 and MT-MMP (Tsujii *et al.,* 1997) and is also implicated in VEGF up-regulation and thus angiogenesis (Li *et al.,* 2002).

E-cadherin gene expression or regulation is modified by promoter methylation (Graff *et al.,* 2000), *E-cadherin* promoter methylation status is associated with adverse prognostic indicators in cancer (i.e., decreased survival rates) (Graziano *et al.,* 2004). Metastasized oral cancer cells show decreased *E-cadherin* expression as a result of promoter methylation (Kudo *et al.,* 2004). This event may be spontaneously reversible because some cells at the metastatic site have lost methylation of this gene, leading to a situation where a fraction of tumor cells can be in a favorable state for invasion and yet be capable of reestablishing appropriate intercellular associations at a metastatic site (Graff *et al.,* 2000).

Molecules involved in tissue destruction and invasion are also targets of epigenetic changes. For instance, *TIMP3* methylation leads to a decrease in MMP inactivation and hence an increase in MMP activity (Bachman *et al.,* 1999). The net effect is to cause a loosening of the control of matrix remodeling by MMPs and allow increased movement and thus metastatic potential in the tumor. When the *urokinase (uPA)* promoter is hypomethylated, it is expressed in highly invasive cancer cells; uPA catayzes the coversion of

the inactive zymogen plasminogen to the active protein plasmin, which degrades the surrounding extracellular matix (Pakneshan *et al.,* 2004). When a hypermethylating agent was used, *uPA* expression was decreased, whereas the estrogen receptor promoter whose expression is decreased by hypermethylation was not affected by this treatment (Pakneshan *et al.,* 2004). The cumulative effect was a decrease in cell invasion *in vitro* and a decrease in tumor growth rate and metastatic rate in nude mice carrying human cancer cells in their mammary fat pads.

Therapeutic Implications

Therapeutic agents are designed to target epigenetic effects either by altering methylation patterns on DNA or modifying histones. Inhibitors of DNA methylation are currently in phase II/III of clinical trials. These molecules (e.g., 5-azacytidine and 5-aza-2′-deoxycytidine; 2′-deoxy-5-azacytidine) reactivate gene expression by inhibiting DNA methylation. They work as nucleoside analogs after metabolic conversion into deoxynucleotide triphosphates. Incorporation of these nucleoside analogs traps DNMTs and depletes these enzymes in the cell, thus decreasing methylation on other cytidine residues (Egger *et al.,* 2004). DNA methylation inhibitors therefore require DNA replication to be effective and hence target actively dividing cells. These agents show promise, especially in hematogenous cancers such as leukemia, because these forms of cancer can exhibit methylation-mediated silencing of genes such as the p53 homologue *p73* (Corn *et al.,* 1999). Defects in the mismatch repair (MMR) pathway lead to mutation in key proteins such as oncogenes and tumor suppressors. Tumors with promoter methylation–induced silencing of the MMR gene *hMLH-1* display impaired DNA repair and demethylation treatment–induced reexpression of *MLH-1* and reestablished sensitivity to the chemotherapeutics cisplatin, carboplatin, temozolomide, and epirubicin (Plumb *et al.,* 2000).

Aberrant methylation of the *integrin* α_4 gene leads to loss of gene expression in human gastric cancer cell lines and increased invasiveness compared to their integrin α_4-expressing counterparts (Park *et al.,* 2004). DNMT-inhibitor treatment led to reestablishment of integrin expression, implying that clinical treatment of these cell lines with such agents could be effective therapy. *TIMP-3* is silenced by methylation in its promoter region in cell lines derived from human kidney and brain cancers but not in normal cells (Bachman *et al.,* 1999). This methylation is removed on treatment with the demethylating agent 5-aza-2′deoxycytidine and coincides with reexpression of TIMP-3. The picture is, however, complicated by the fact that normal tissues have different levels of TIMP-3 expression—a finding that shows that demethylating agents may have variable efficacy depending on the tumor's type, location, and thus specific microenvironment.

Whereas methylation inhibitors do cause demethylation of imprinted genes in cell culture, patients with cancer who undergo treatment with azanucleosides seem to be able to correct altered methylation status in normal tissue within a few weeks of the end of treatment (Egger *et al.,* 2004). However, the effectiveness of methylation inhibitors must be carefully weighed against possible side effects. Hypomethylation can lead directly to promoter demethylation and gene reexpression, as occurs in the transcripational reactivation of the protease uPA, which may lead to induced angiogenesis or metastasis (Szyf *et al.,* 2004). By using DNMT-specific antagonists (such as procainamide and procaine), versus cytidine analogues (such as 5-azacytidine), it may be possible to induce cell cycle arrest rather than hypomethylation of DNA and the resulting increase in expression of prometastatic molecules (Szyf *et al.,* 2004). This being said, it is still important to realize that these nucleoside analogs can have effects—their therapeutic use must be carefully considered.

Histone acetyl transferase (HAT) and histone deacetylase (HDAC) are enzymes that act on histones as well as many nonhistone targets. Transcription factors and signal transduction mediators are among the additional proteins that may be affected by treatments that target the acetylation status of histones (Drummond *et al.,* 2005). Histone deacetylation inhibitors are small molecules designed to inhibit global or specific HDACs. They cause acetylation of histone and other proteins and therefore induce or up-regulate genes that had been silenced (e.g., *p21, p53*). These agents are currently in phase III clinical trials. Representatives from three of the five structural classes of HDAC inhibitors exert some clinical effect by inhibition of angiogenesis and metastasis. Trichostatin A (TSA), a member of the hydroxamic acid group of HDAC inhibitors, causes up-regulation of the MMP inhibitor protein RECK and therefore inhibits activation of MMP-2 and tumor cell invasion (Liu *et al.,* 2003). Depsipeptide (FK228) suppresses VEGF and bFGF expression (Saskawa *et al.,* 2003) and thus represents a direct inhibitor of angiogenesis working through an epigenetic mechanism.

The anti-angiogenic and anti-metastatic effects of these agents have only recently been demonstrated, but TSA in particular has been administered in what can be defined as a metronomic low-dose schedule, and it has been shown to have antitumoral activity with little systemic toxicity (Vigushin *et al.,* 2001). Metronomic therapy in general may work best for HDAC inhibitors

because to inhibit HDAC-regulated processes in the cell, intracellular concentrations of the drug must be kept high (Drummond *et al.,* 2005). Depsipeptide is more effective against leukemia and lymphoma when combined with another agent, the cell differentiation–inducing retinoid ARTA (Kosugi *et al.,* 2001), providing an example of how HDACs with anti-angiogenic activity can be combined successfully with other agents to bring about stronger therapeutic effects. Combination therapy of HDAC inhibitors and demethylation agents such as 5-aza-2′-deoxycytidine are interesting because of the interaction between DNA methylation and histone deacetylation. For example, 5-aza-2′-deoxycytidine + TSA or depsipeptide can be used to reactivate silenced tumor-suppressor genes including *MLH-1* and *TIMP-3* (Drummond *et al.,* 2005). Alternatively, it may be possible to "sensitize" tumors with epigenetic therapy, followed by conventional chemotherapy (Egger *et al.,* 2004).

Methylation of specific genes can be identified in peripheral blood of patients with primary undifferentiated nasopharyngeal carcinoma (Wong *et al.,* 2003). This opens the possibility of using methylation-specific polymerase chainreaction (PCR) as a cancer detection method. Additionaly, CpG island microarrays containing short GC (guanine cytosine)-rich tags tethered to glass slide surfaces can be used for methylation profiling of tumors (Yan *et al.,* 2001). However, interpreting the methylation profile of a given patient may prove to be the most challenging part of using methylation-specific screening test in the clinic (Ushijima, 2005). Similar to the case with anti-angiogenic therapies, there currently exist no suitable surrogate markers for HAT or HDAC inhibitor effectiveness, making it difficult to assess these agents in the clinic (Drummond *et al.,* 2005). However, using CpG island hypermethylation as a marker of cancer cells may be an informative way to detect aberrant DNA methylation in serum samples or biopsy specimens, as a marker for tumor behavior, and as a predictor of response to treatment.

Beyond the Epigenome

As with traditional chemotherapeutic agents, the new compounds that target epigenetic processes require integration into the cell high enough concentration to be effective. This can be a problem in areas of the tumor that are not sufficiently perfused. In addition, regions of the tumor that are not well oxygenated and supplied with nutrients become areas of increased selective pressure within the tumor—leading to mutation of the cells (Rak *et al.,* 2002). Collars of viable cells are located around perfused blood vessels, with gradients of oxygen, nutrients, and metabolites finally leading to necrotic areas. This creates microenvironments within solid tumors that cause altered cellular reactions and behaviors to a given therapeutic agent. For instance, low tissue oxygen causes activation of the HIF system and results in expression of angiogenic factors. Likewise, genes involved in cellular survival become important under stressful conditions and thus may be selected for. Analysis of the role of the microenvironment in cellular selection has identified factors such as hypoxia (Yu *et al.,* 2002) which can affect cells with altered methylation status (Okami *et al.,* 2004) and contribute to dynamic changes in the cells making up the tumor mass (Graff *et al.,* 2000).

HIF-1α protein is subject to a variety of post-transcriptional modifications, including acetylation. Levels of acetyltransferases are not known to be affected by oxygen concentration; however as a result of hypoxic conditions, less HIF-1α is acetylated than expected due to the down-regulation of another factor, arrest-defective protein-1 (ARD-1) (Brahimi-Horn *et al.,* 2005). HIF1-α acetylation leads to its destabilization and subsequent destruction and inability to signal. This opens the possibility that HDAC inhibitors may interact with the microenvironment and affect HIF-1α stability; when HIF-1α is exposed to global inhibitors of deacetylation in oxygenated tissues, its acetylation state was maintained, leading to an anti-angiogenic effect (Brahimi-Horn *et al.,* 2005). HIF transcription factor complex acts on metabolism by first inducing a shift in cells from ATP (adenosine triphosphate) production via oxidative phosphorylation to anaerobic glycolysis. Occuring at the same time is an overexpression of glucose transporters (GLUT-1) and catabolic enzymes (hexokinase). Glucose is essential for hypoxia to stimulate phosphorylation of the AP-1 transcription factor c-Jun (Laderoute *et al.,* 2004) and subsequent expression of numerous proliferation and survival factors. Thus, cellular proliferation resulting from HIF activiation may only occur at the interface of hypoxia and hypoglycemia.

Genetic instability is also enhanced by harsh tumor microenvironments. Hypoxia interacts with other aspects of the extracellular environment to produce mutations within the tumor (Bindra and Glazer, 2005). Hypoxia can lead to point mutations, gene amplification, and chromosomal rearrangements, thus increasing genetic instability. In addition, hypoxia reoxygenation results in point mutations and DNA strand breakage leading to deletions, amplifications, and genomic instability—a potent mutagenic force—and a harsh tumor microenvironment is able to interface with DNA repair mechanism (Bindra *et al.,* 2004; Shahrzad *et al.,* 2005).

How do all these factors interact to influence angiogenesis and metastasis? Does the microenvironment affect methylation status of genes important for mutation, angiogenesis, and metastasis? Reports indicate that hyperoxygenation leads to both increased DNA damage and decreased DNA methylation (Panayiotidis *et al.,* 2004), suggesting the possibility that physicochemical aspects of the tumor microenvironment may, theoretically at least, influence epigenetic cancer progression. Although there are many unanswered questions, a better understanding of mechanisms that control epigenetic modifications in cancer is essential for the effective treatment of the disease.

References

Akhtar, N., Dickerson, E.B., and Auerbach, R. 2002. The sponge/Martrigel angiogenesis assay. *Angiogensis 5*:75–80.

Asahara, T., Takahashi, T., Masuda, H., Kalka, C., Chen, D., Iwaguro, H., Inai, Y., Silver, M., and Isner, J.M. 1999. VEGF contributes to postnatal neovascularization by mobilizing bone marrow-derived endothelial progenitor cells. *EMBO J. 18*: 3964–3972.

Auerbach, R., Lewis, R., Shinners, B., Kubai, L., and Akhtar, N. 2003. Angiogenesis assays: a critical overview. *Clin. Chem. 49*:132–140.

Augustin, H.G. (Ed.). 2004. *Methods in Endothelial Cell Biology*. New York. Springer Lab Manuals, p 383.

Bachman, K.E., Herman, J.G., Corn, P.G., Merlo, A., Costello, J.F., Cavenee, W.K., Baylin, S.B., and Graff, J.R. 1999. Methylation-associated silencing of the tissue inhibitor of metalloproteinase-3 gene suggest a suppressor role in kidney, brain, and other human cancers. *Cancer Res. 59*:798–802.

Berger, A.C., Wang, X.Q., Zalatoris, A., Cenna, J., and Watson, J.C. 2004. A murine model of *ex vivo* angiogenesis using aortic disks grown in fibrin clot. *Microvasc. Res. 68*:179–187.

Bindra, R.S. and Glazer, P.M. 2005. Genetic instability and the tumor microenvironment: towards the concept of microenvironment-induced mutagenesis. *Mutat. Res. 569*:75–85.

Bindra, R.S., Schaffer, P.J., Meng, A., Woo, J., Maseide, K., Roth, M.E., Lizardi, P., Hedley, D.W., Bristow, R.G., and Glazer, P.M. 2004. Down-regulation of Rad51 and decreased homologous recombination in hypoxic cancer cells. *Mol. Cell Biol. 24*:8504–8518.

Brahimi-Horn, C., Mazure, N., and Pouhssegur, J. 2005. Signalling via the hypoxia-inducible factor-1α requires multiple posttranslational modifications. *Cell Signal. 17*:1–9.

Browder, T., Butterfield, C.E., Kraling, B.M., Shi, B., Marshall, B., O'Reilly, M.S., and Folkman, J. 2000. Anti-angiogenic scheduling of chemotherapy improves efficacy against experimental drug-resistant cancer. *Cancer Res. 60*:1878–1886.

Bubenik, J. 2003. Tumour MHC class I downregulation and immunotherapy. *Oncol. Rep. 10*:2005–2008.

Camphausen, K., Moses, M.A., Beecken, W.D., Khan, M.D., Folkman, J., and O'Reilly, M.S. 2001. Radiation therapy to primary tumor accelerates metastatic growth in mice. *Cancer Res. 61*:2207–2211.

Chambers, A.F., MacDonald, I.C., Schmidt, E.E., Morris, V.L., and Groom, A.C. 2000. Clinical targets for anti-metastasis therapy. *Adv. Cancer Res. 79*:91–121.

Cheung, P. and Lau, P. 2005. Epigenetic regulation by histone methylation and histone variants. *Mol. Endocrinol. 19*:563–573.

Corn, P.G., Kuerbitz, S.J., van Noesel, M.M., Esteller, M., Compitello, N., Baylin, S.B., and Herman, J.G. 1999. Transcriptional silencing of the p73 gene in acute lymphoblastic leukemia and Burkitt's lymphoma is associated with 5′ CpG island methylation. *Cancer Res. 59*:3352–3356.

Davis, J.S., Ruea, B.R., and Spanel-Borowski, K. 2003. Mirovascular endothelial cells of the corpus luteum. *Reprod. Biol. Endocrinol. 1*:89.

Day, M.L., Zhao, X., Vallorosi, C.J., Putzi, M., Powell, T., Lin, C., and Day, K.X. 1999. E-cadhein mediates aggregation-dependent cell survival of prostate and mammary epithelial cells through the retinoblastoma cell cycle control pathway. *J. Biol. Chem. 274*:9656–9664.

Drummond, D.C., Noble, C.O., Kirpotin, D.B., Guo, Z., Scott, G.K., and Benz, C.C. 2005. Clinical development of histone deacetylase inhibitors as anticancer agents. *Annu. Rev. Pharmacol. Toxicol. 45*:495–528.

Egger, G., Liang, G., Aparicio, A., and Jones, P.A. 2004. Epigenetics in human disease and prospects for epigenetic therapy. *Nature 429*:457–463.

Eliceiri, B.P. and Cheresh, D.A. 2001. Adhesion events in angiogenesis. *Curr. Opin. Cell. Biol. 13*:563–568.

Erber, R., Thurnher, A., Katsen, A.D., Groth, G., Kerger, H., Hammes, H.P., Menger, M.D., Ullrich, A., and Vajkoczy, P. 2004. Combined inhibition of VEGF and PDGF signaling enforces tumor vessel regression by interfering with pericyte-mediated endothelial cell survival mechanisms. *FASEB J. 18*:338–340.

Esteller, M. and Herman, J.G. 2002. Cancer as an *epigenetic disease*: *DNA methylation* and chromatin alterations in human tumours. *J. Pathol. 196*:1–7.

Esteller, M., Silva, J.M., Dominguez, G., Bonilla, F., Matias-Guiu, X., Lerma, E., Bussaglia, E., Prat, J., Harkes, I.C., Repasky, E.A., Gabrielson, E., Schutte, M., Baylin, S.B., and Herman, J.G. 2000b. Promoter hypermethylation and BRCA1 inactivation in sporadia breast and ovarian tumors. *J. Natl. Cancer Inst. 92*: 564–569.

Esteller, M., Toyota, M., Sanchez-Cespedes, M., Capella, G., Peinado, M.A., Watkins, D.N., Issa, J.P., Sidransky, D., Baylin, S.B., and Herman, J.G. 2000a. Inactivation of the DNA repair gene O6-methylguanine-DNA methyltranserase by promoter hypermethylation is associated with G to A mutations in K-ras in colorectal tumorigenesis. *Cancer Res. 60*:2368–2371.

Feinberg, A.P. 2004. The epigenetics of cancer etiology. *Sem. Cancer Biol. 14*:427–432.

Fidler, I.J. 2002. Critical determinants of metastasis. *Cancer Biol. 12*:89–96.

Folkman, J. 1971. Tumor angiogenesis: therapeutic implications. *N. Engl. J. Med. 285*:1182–1186.

Frederiks, W.M. and Mook, O.R. 2004. Metabolic mapping of proteinase activity with emphasis on *in situ* zymography of gelatinases: review and protocols. *J. Histochem. Cytochem. 52*: 711–722.

Frisch, S.M. and Ruoslahti, E. 1997. Integrins and anoikis. *Curr. Opin. Cell Biol. 9*:701–706.

Gelaw, B. and Levin, S. 2001. Wound-induced angiogenesis and its pharmacologic inhibition in a murine model. *Surgery 130*: 497–501.

Giatromanolaki, A., Sivridis, E., and Koukourakis, M.I. 2004. Tumour angiogenesis: vascular growth and survival. *APMIS. 112*:431–440.

Goodwin, M. and Yap, A.S. 2004. Classical cadherin adhesion molecules: coordinating cell adhesion, signaling and the cytoskeleton. *J. Mol. Histol. 35*:839–844.

Graff, J.R., Gabrielson, E., Fujii, H., Baylin, S.B., and Herman, J.G. 2000. Methylation patterns of the E-cadherin 5′ CpG island are unstable and reflect the dynamic, heterogeneous loss of E-cadherin expression during metastatic progression. *J. Biol. Chem. 275*:2727–2732.

Graziano, F., Arduini, F., Ruzzo, A., Bearzi, I., Humar, B., More, H., Silva, R., Muretto, P., Guilford, P., Testa, E., Mari, D., Magnani, M., and Cascinu, S. 2004. Prognostic analysis of E-cadherin gene promoter hypermethylation in patients with surgically resected, node-positive, diffuse gastric cancer. *Clin. Cancer Res. 10*:2784–2789.

Hasan, J., Shnyder, S.D., Bibby, M., Double, J.A., Bicknell, R., and Jayson, G.C. 2004. Quantitative angiogenesis assays *in vivo*: a review. *Angiogenesis 7*:1–16.

Herman, J.G., Latif, F., Weng, Y., Lerman, M.I., Zbar, B., Liu, S., Samid, D., Duan, D.R., Gnarra, J.J., Linethan, W.M., and Baylin, S.B. 1994. Silencing of the *VHL* tumor-suppressor gene by DNA methylation in renal carcinoma. *Proc. Natl. Acad. Sci. USA 91*:9700–9704.

Holmgren, L., O'Reily, M.S., and Folkman, J. 1995. Dormancy of micrometastases: balanced proliferation and apoptosis in the presence of angiogenesis suppression. *Nat. Med. 1*:149–153.

Jain, R.K. 2005. Normalization of tumor vasculature: an emerging concept in antiangiogenic therapy. *Science 307*:58–62.

Kang, G.H., Lee, S., Kim, J.S., and Jund, H.Y. 2003. Profile of aberrant CpG island methylation along the multistep pathway of gastric carcinogenesis. *Lab Invest 83*:635–641.

Kerbel, R. and Folkman, J. 2002. Clinical translation of angiogenesis inhibitors. *Nat. Rev. Cancer 2*:727–739.

Kerbel, R.S. 2003. Human tumor xenografts as preclinical models for anticancer drug activity in humans: better than commonly perceived—but they can be improved. *Cancer Biol. Ther. 2*: S134–139.

Khanna, C. and Hunter, K. 2005. Modeling metastasis *in vivo*. *Carcinogenesis 26*:513–523.

Kim, H.R., Lin, H.M., Biliran, H., Raz, A. 1999. Cell cycle arrest and inhibition of anoikis by galectin-3 in human breast epithelial cells. *Cancer Res. 59*:4148–4154.

Kleiner, D.E. and Stetler-Stevenson, W.G. 1999. Matrix metalloproteinases and metastasis. *Cancer Chemother. Pharmacol. 43*: S42–S51.

Komori, M., Tomizawa, Y., Takada, K., and Ozaki, M. 2005. A single local application of recombinant human basic fibroblast growth factor accelerates initial angiogenesis during wound healing in rabbit ear chamber. *Anesth. Analog. 100*:830-834.

Kornberg, R.D. and Lorch, Y. 1999. Twenty-five years of the nucleosome, fundamental particle of the eukaryote chromosome. *Cell 98*:457–463.

Kosugi, H., Ito, M., Yamaoto, Y., Towatari, M., Ueda, R., Saito, H., and Naoe, T. 2001. *In vivo* effects of a histone deacetylase inhibitor, FK228, on human acute promyelocytic leukemia in NOD/Shi-scid/scid mice. *Jpn. J. Cancer Res. 92*:529–536.

Kudo, Y., Kitajima, S., Ogawa, I., Hiraoka, M., Sargolzaei, S., Keikhaee, M.R., Sato, S., Miyauchi, M., and Takata, T. 2004. Invasion and metastasis of oral cancer cells require methylation of E-cadherin and/or degradation of membranous Beta-catenin. *Clin. Cancer Res. 10*:5444–5463.

Kwon, H.J., Kim, M.S., Kim, M.J., Nakajima, H., and Kim, K.W. 2002. Histone deacetylase inhibitor FK228 inhibits tumor angiogenesis. *Int. J. Cancer 97*:290–296.

Laderoute, K.R., Calaoagan, J.M., Knapp, M., and Johnson, R.S. 2004. Glucose utilization is essential for hypoxia-inducible factor 1α-dependent phosphorylation of c-Jun. *Mol. Cell. Biol. 24*:4128–4137.

Li, G., Yang, T., and Yan, J. 2002. Cyclooxygenase-2 increased the angiogenic and metastatic potential of tumor cells. *Biochem. Biophys. Res. Commun. 299*:886–890.

Li, Q., Ahuja, N., Burger, P.C., and Issa, J-P.J. 1999. Methylation and silencing of the Thrombospondin-1 promoter in human cancer. *Oncogene 18*:3284–3289.

Liu, L.T., Chang, H.C., Chiang, L.C., and Hung, W.C. 2003. Histone deacetylase inhibitor upregulates RECK to inhibit MMP-2 activation and cancer cell invasion. *Cancer Res. 63*:3069–3072.

Lund, A.H. and van Lohuizen, M. 2004. Epigenetics and cancer. *Genes Dev. 18*:2315–2335.

MacDonald, I.C., Groom, A.C., and Chambers, A.F. 2002. Cancer spread and micrometastasis development: quantitative approaches for *in vivo* models. *Bioessays 24*:885–893.

Moore, M.A. 2001. The role of chemoattraction in cancer metastases. *Bioessays 23*:674–676.

Morbidelli, L., Donnini, S., Chillemi, F., Giachetti, A., and Ziche, M. 2003. Angiosuppressive and angiostimulatory effects exerted by synthetic partial sequences of endostatin. *Clin. Cancer Res. 9*:5358–5369.

Muhsin, M., Graham, J., Kirkpatrick, P. 2004. Bevacizumab. *Nat. Rev. Drug Discov. 3*:995–996.

Nanda, A. and St. Croix, B. 2004. Tumor endothelial markers: new targets for cancer therapy. *Curr. Opin. Oncol. 16*:44–49.

Nicholson, K.M. and Anderson, N.G. 2002. The protein kinase B/Akt signaling pathway in human malignancy. *Cell Signal. 14*:381–395.

Okami, J., Simeone, D.M., and Logsdon, C.D. 2004. Silencing of the hypoxia-inducible cell death protein BNIP3 in pancreatic cancer. *Cancer Res. 64*:5338–5346.

Pakneshan, P., Szyf, M., Farias-Eisner, R., and Rabbini, S.A. 2004. Reversal of hypomethylation status of urokinase (uPA) promoter blocks breast cancer growth and metastasis. *J. Biol. Chem. 279*:31735–31744.

Panayiotidis, M.I., Rancourts, R.C., Allen, C.B., Riddle, S.R., Schneider, B.K., Ahmad, S., and White, C.W. 2004. Hyperoxia-induced DNA damage causes decreased DNA methylation in human lung epithelial-like A549 cells. *Antioxid. Redox Signal 6*:129–136.

Papetti, M. and Herman, R.M. 2002. Mechanisms of normal and tumor-derived angiogenesis. *Am. J. Physiol. Cell Physiol. 282*:C947–C970.

Park, J., Song, S-H., Kim, T.Y., Choi, M-C., Jong, H-S., Kim, T-Y., Lee, J.W., Kim, N.K., Kim, W-H., and Band, Y-J. 2004. Aberrant methylation of integin α4 gene in human gastric cancer cells. *Oncogene 23*:3474–3480.

Pelluso, J.J. 1997. Putative mechanism through which N-cadherin-mediated cell contact maintains calcium homeostasis and thereby prevents ovarian cells from undergoing apoptosis. *Biochem. Pharmacol. 54*:847–853.

Plumb, J.A., Strathdee, G., Sludden, J., Kaye, S.B., and Brown, R. 2000. Reversal of drug resistance in human exnografts by 2′deoxy-5-azacytidine-induced demethylation of the *hMLHI* gene promoter. *Cancer Res. 60*:6039–6044.

Pravtcheva, D.D. and Wise, T.L. 1998. Metastasizing mammary carcinomas in H19 enhancers-Igf2 transgenic mice. *J. Exp. Zool. 281*:43–57.

Rak, J., Yu, J.L., Kerbel, R.S., and Coomber, B.L. 2002. What do oncogenic mutations have to do with angiogenesis/vascular dependence of tumors? *Cancer Res. 62*:1931–1934.

Santini, M.T., Rainaldin, G., and Indovina, P.L. 2000. Apoptosis, cell adhesion and the extracellular matrix in the three-dimensional growth of multicellular tumor spheroids. *Crit. Rev. Oncol. Hematol. 36*:75–87.

Saskawa, Y., Naoe, Y., Noto, T., Inoue, T., Saskawa, T., Matsuo, M., Manda, T., and Mutoh, S. 2003. Antitumor efficacy of FK288, a novel histone deacetylase inhibitor, depends on the effect on expression of angiogenesis factors. *Biochem. Pharmacol. 66*:897–906.

Shahrzad, S., Qualye, L., Stone, C., Plumb, C., Shirasawa, S., Rak, J.W., and Coomber, B.L. 2005. Ischemia-induced K-ras mutations in human colorectal cancer cells: role of microenvironmental regulation of MSH2 expression. *Cancer Res. 65*:8134–8141.

Shaked, Y., Bertolini, F., Man, S., Rogers, M.S., Cervi, D., Foutz, T., Rawn, K., Voskas, D., Dumont, D.J., Ben-David, Y., Lawler, J., Henkin, J., Huber, J., Hicklin, D.J., D'Amato, R.J., and Kerbel, R.S. 2005. Genetic heterogeneity of the vasculogenic phenotype parallels angiogenesis: implications for cellular surrogate marker analysis of antiangiogenesis. *Cancer Cell 7*:101–111.

Snoek-van Beurden, P.A., and Von den Hoff, J.W. 2005. Zymographic techniques for the analysis of matrix metalloproteinases and their inhibitors. *Biotechniques 38*:73–83.

Sobrero, A. and Bruzzi, P. 2005. Bevacizumab plus fluorouracil: the value of being part of a developing story. *J. Clin. Oncol. 23*:1–3.

Song, S-H., Jong, H-S., Choi, H.H., Inoue, H., Tanabe, T., Kim, N.K., and Bang, Y-J. 2001. Transcriptional silencing of *Cyclooxygenase-2* by hyper-methylation of the 5′CpG island in human gastric carcinoma cells. *Cancer Res. 61*:4628–4635.

St. Croix, B., Rago, C., Velculescu, V., Traverso, G., Romans, K.E., Montgomery, E., Lal, A., Riggins, G.J., Lengauer, C., Vogelstein, B., and Kinzler, K.W. 2000. Genes expressed in human tumor endothelium. *Science 289*:1197–1202.

Stamenkovic, I. 2000. Matrix metalloproteinases in tumor invasion and metastasis. *Semin. Cancer Biol. 10*:415–433.

Szyf, M., Pakneshan, P., and Rabbani, S.A. 2004. DNA demethylation and cancer: therapeutic implications. *Cancer Lett. 211*:133–143.

Taraboletti, G. and Giavazzi, R. 2004. Modelling approaches for angiogenesis. *Eur. J. Cancer 40*:881–889.

Tsujii, M., Kawano, S., and Dubois, R.N. 1997. Cyclooxygenase-2 expression in human colon cancer cells increases metastatic potential. *Proc. Natl. Acad. Sci. USA 94*:3336–3340.

Ushijima, T. 2005. Innovation: detection and interpretation of altered methylation patterns in cancer cells. *Nat. Rev. Cancer 5*:223–231.

Vigushin, D.M., Ali, S., Pace, P.E., Mirsaidi, R., Ito, K., Adcock, I., and Coombes, R.C. 2001. Trichostatin A is a histone deacetylase inhibitor with potent antitumor activity against breast cancer. *Clin. Cancer Res. 7*:971–976.

Wang, H., Keiser, J.A., Olszewski, B., Rosebury, W., Robertson, A., Kovesdi, I., and Gordon, D. 2004. Delayed angiogenesis in aging rats and therapeutic effect of adenoviral gene transfer of VEGF. *Int. J. Mol. Med. 13*:581–587.

Weidner, N., Semple, J.P., Welch, W.R., and Folkman, J. 1991. Tumor angiogenesis and metastasis: correlation in invasive breast carcinoma. *N. Engl. J. Med. 324*:1–18.

Woltering, E.A., Lewis, J.M. Maxwell, P.J. 4th, Frey, D.J., Wang, Y.Z., Rothermel, J., Anthony, C.T., Balster, D.A., O'Leary, J.P., and Harrison, L.H. 2003. Development of a novel *in vitro* human tissue-based angiogenesis assay to evaluate the effect of antiangiogenic drugs. *Ann. Surg. 237*:790–798.

Wong, T.S., Tang, K.C., Kwong, D.L-W., Sham, J.S-T., Wei, W.I., Kwong, Y.L., and Yuen, A.P-W. 2003. Differential gene methylation in undifferentiated nasopharyngeal carcinoma. *Int. J. Oncol. 22*:869–874.

Xie, K., Wei, D., Shi, Q., and Huang, S. 2004. Constitutive and inducible expression and regulation of vascular endothelial growth factor. *Cytokine Growth Factor Rev. 15*:297–324.

Yan, P.S., Chen, C-M., Shi, H., Rahmatpanah, F., Wei, S.H., Caldwell, C.W., and Huang, T.H-M. 2001. Dissecting complex epigenetic alterations in breast cancer using CpG island microarrays. *Cancer Res. 61*:8375–8380.

Yu, J.L., Coomber, B.L., and Kerbel, R.S. 2002. A paradigm for therapy-induced microenvironmental changes in solid tumors leading to drug resistance. *Differentiation 70*:599–609.

Zhu, Z., Sanchez-Sweatmena, O., Huang, X., Wiltrout, R., Khokha, R., Zhao, Q., and Gorelik, E. 2001. Anoikis and metastatic potential of cloudman S91 melanoma cells. *Cancer Res. 61*:1707–1716.

This Page Intentionally Left Blank

5

Can Effector Cells Really "Effect" an Anti-Tumor Response as Cancer Therapy?

Susan F. Slovin

How Do We See the Immune System?

The immune system has often been likened to that of a divine orchestra, a milieu of different cell populations that are intimately caressed by a multitude of different soluble factors or cytokines that interplay in subtle ways to generate a uniform response to foreign substances within the body. The "conductor" was the "generator of diversity," or "GOD," in whose power was the direction of this complex interplay of events, but whose more intimate nature was still elusive. Twenty years since the dawn of this analogy by Dr. Richard Gershon (Cantor, 2004), who originally coined the term "generator of diversity," we have now come to realize that although Dr. Gershon was correct in suggesting that the immune response was indeed a complicated interaction of different effector cell populations and subtypes of these populations, he did not have any idea as to the diversity of such populations, nor the relative importance of each population in controlling the progression of cancer cells. These observations were particularly important in considering how to best develop immunotherapeutic approaches for treatment of cancer.

Diversity: Is It a True Reflection of Function?

Dr. Gershon (Gershon, 1975) postulated that specialized white cells or T lymphocytes were capable of dual functionality. This included the ability to both enhance and inhibit immunity by behaving as a suppressor/cytotoxic ($CD8^+$) cell or a helper cell ($CD4^+$) (von Herrath *et al.,* 2003). With this area newly developed, more creative immunotherapeutic strategies, which were custom tailored to induce these specific cell populations, have been designed. These "effector" cells can be any cell population or subset of cells that have the ability to carry out or "effect" a specific function, such as killing, helping, antigen processing, or any combination of these. They include B and T lymphocytes as well as an unusual cell type known as a dendritic cell (DC).

The DCs are present within the skin, where they are called Langerhans cells. They also circulate within the bloodstream. Their function is to attack foreign proteins or antigens, which are present on tumor cells within the circulation, and to break them down into smaller peptides. Once this "antigen processing" is done, these

Handbook of Immunohistochemistry and *in situ* Hybridization of Human Carcinomas, Volume 4: Molecular Genetics, Gastrointestinal Carcinoma, and Ovarian Carcinoma

peptides are displayed on the DC surface so that they can be recognized by specialized T lymphocytes, which will then be "primed" into recognizing this similar molecule on tumor cells. This educational effect serves to teach the T lymphocyte to seek, identify, and kill tumor cells that display such unique molecules on their surface. These interactions also cause the secretion of cytokines and chemical signals such as B7 and CD28, which allow cells to be targeted for killing.

Induction of Immunity

Immunotherapeutic approaches for the treatment of either solid tumors or hematologic malignancies have been based on a refined understanding of the mechanism of action of these populations and how they can cause an "anti-tumor" response. This is referred to as "active" rather than "passive" immunization. In the former, a treatment (i.e., a vaccine containing an immunogenic antigen or other immune preparation) is given to the patient so that the patient's own immune system will react to the immunologic stimulus. The body will generate a response to the immunogen by eliciting a series of humoral and cellular responses. These responses can be measured by specific assays. To assess the presence of specific T cells that react to a specific immunogen, one can measure the ability of the T cells to proliferate in the presence of the immunogen. Using the *in vitro* EliSpot assay, T cells, which have been stimulated by immunogen, can be shown to secrete a cytokine, interferon-γ. The ability to secrete interferon-γ confirms that the T cell population is of $CD8^+$ or cytotoxic T cell origin.

Passive Immunity

The "passive" approach to immunity usually infers that in lieu of the individual making antibodies or generating specific effector cells, antibodies can be made *ex vivo*. The success of this approach was demonstrated by the "passive" administration of sera from patients who had been infected with hepatitis viruses to those who wished to be prophylaxed against the disease. Use of monoclonal antibodies (MAbs) has largely replaced use of passively administered human sera. The MAb represents a highly specific antibody produced usually in a murine hybridoma. This reagent has been "humanized" so that only a small portion of the antibody structure has any feature of the mouse antibody component. This prevents any reaction to the murine component if antibodies can be passive, administered and specifically sensitized DCs can be returned to a patient after *ex vivo* exposure to antigen.

The B cell network induces humoral or antibody responses. We make diverse antibodies to any molecule that does not belong within the body. This includes viruses and bacteria. However, whereas bacterial antigens are still the most robust immunogens in inducing high titers of antibodies, the same is not true for the immune response to cancer.

Keep in mind that most tumor antigens are really altered "self" antigens. There are a variety of such molecules that are expressed on normal cells, which make up organs, throughout the body. It is unclear as to the role of these many carbohydrate and protein antigens. However, what is clear is that these molecules change in very subtle ways when the normal organ becomes malignantly transformed. This includes their overexpression or their under glycosylation. This is particularly true in molecules known as "mucins." An example of this would be a patient who has received a vaccine against prostate cancer that focuses on the prostate specific antigen (PSA) or prostate specific membrane antigen (PSMA). The patient has no native immunity against these glycoprotein antigens. Following a vaccine produced against purified PSA or PSMA proteins alone, no immune response is generated. What is needed is an "adjuvant," a drug that nonspecifically stimulates the immune system and acts together with the antigen in question to try to break the immune status quo.

The immune status quo is termed "immunologic tolerance." Once a vaccine causes an antibody or T cell response, we have "broken" immunologic tolerance and caused an immune response. If one were to remove T lymphocytes from the patient and stimulate them against a similar or related antigens *in vitro,* the ability of the cells to react to this molecule can be measured by its ability to secrete a cytokine such as interferon-γ or interleukin 12, soluble factors that indicate that a certain population of lymphocytes have been stimulated (i.e., T_H1 or helper T cell response). Similarly, if interleukins 4, 6, 13, or 10 are secreted by the T cell, a T_H2 response has been elicited. However, in many cases, it is still not understood how a T_H1 or T_H2 response is preferentially induced (Luther and Cyster, 2001).

Chemokines as Regulators of T Cell Differentiation

Cellular responses do not occur without a fierce interplay of co-stimulatory molecules, receptors on the T cell, major histocompatibility complex (MHC) into which the tumor antigen sits and is ultimately presented, and chemokines. The chemokines have a well-defined role in directing the cell trafficking necessary for induction of a cellular immune response. They are needed to attract monocytes and immature DCs to sites of

local inflammation. They also direct maturing antigen presenting cells (APCs) to lymphatic structures and bring T cells and APCs together within the various lymphoid pockets, which channel these cells to sites of action. These chemokines must in some way know which effector cell populations will be needed for recruitment including the differential recruitment of T_H1 and T_H2 cells. Luther and Cyster (2001) have suggested that the chemokine ligand 2 (CCL2), also known as monocyte chemoattractant protein 1, or MCP-1, and CCL3 (macrophage inflammatory protein 1 alpha, or MIP-1α) as well as several other chemoattractants influence the direction of T cell differentiation. Of note, DCs express a variety of chemokines in addition to CCL2–CC15. The receptor CCR4 may have some selectivity for T_H2 cell, and CCL22 expression by DCs might be a mechanism to preferentially expand the T_H2 arm of the response. Similarly, DC expression of CCL3, CCL4, or CCL5 may favor expansion of T_H1 cells.

To add to the complexity of the pool of stimulatory factors, which assist in the engagement of tumor cell and lymphocyte, is another co-stimulatory molecule, cytotoxic T lymphocyte antigen 4 (CTLA-4) (Egen *et al.,* 2002). It is clear that CD28 and CTLA-4 are the critical co-stimulatory receptors that determine the early outcome of stimulation through the T cell antigen receptor, the business end of the T cell–tumor cell interaction. Research during the last decade has established that engagement of CD28 on the T cell by B7-1 and B7-2 (two co-stimulatory molecules on the APC) provides the second signal for T cell activation with the first signal being the actual stimulation of the T cell antigen receptor. The messenger ribonucleic acid from the CTLA-4 gene, a close homolog of CD28, was detected in both activated $CD4^+$ and $CD8^+$ T cells. Soluble recombinant CTLA-4 could bind to the same ligands as CD28 but with higher avidity. However, the development of a MAb specific for CTLA-4 allowed further delineation of its function and suggested an inhibitory role.

In animal models, anti-CTLA-4 can exacerbate autoimmune disease. A fully humanized MAb to CTLA-4 has been generated and found to be safe when injected into primates. Phase I clinical trials have been performed on patients with prostate cancer (Davis *et al.,* 2002) and in patients with melanoma (Tchekmedyian *et al.,* 2002). The former were those patients who did not respond to androgen ablation in the face of progressive metastatic disease. No significant increase in peripheral activated T cells and no signs of overt autoimmunity were observed. An impact on the serum biomarker, PSA, was noted, suggesting a change or diminution in tumor burden. These patients responded as well to re-treatment with changes again seen serologically in the biomarker, PSA. Similarly, a trial was also performed in patients with malignant melanoma with tumor biopsies showing necrosis with inflammatory infiltrates within the tumor mass. These results, although not definitive or conclusive, suggest that this drug may be a useful strategy for the manipulation of T cell responses in treating human cancer. This would be particularly useful in strategies that focus on vaccination via peptides or proteins, deoxyribonucleic acid (DNA) vaccines, antigen-loaded DCs, or even genetically engineered tumor cells given with or without the addition of systemic cytokines such as granulocyte-macrophage colony-stimulating-factor (Gm-CSF).

Effector Populations and Breaking Immunologic Tolerance

The concept of immunologic tolerance is pivotal to understanding how the immune system works. With the exception of bacterial antigens, most of the antigens associated with cancer are "self-antigens." The immune system has evolved to avert reacting against self-antigens as a means to prevent autoimmune disease, largely through a variety of complex mechanisms of immunologic tolerance and ignorance. Overcoming these last two mechanisms is of major importance and has been an obstacle in the development of immunologic approaches, especially vaccines (Wolchok *et al.,* 2003). However, although true cancer antigens are quite rare, more often than not the immune system is reacting to by-products of the tumor cells in the circulation (i.e., shedding of tumor cell membrane or degradation products, which are then picked up and processed by DCs for efficient presentation to the immune effector cells). The self-molecules can often result from subtle changes in glycosylation patterns or overexpression of specific sugars or proteins, which may change as the cell goes from a normal to a transformed state.

Immunity can also be induced passively. This occurs when patients do not generate their own immune response but receive a treatment by which immunity can be conveyed to them. This is particularly true of patients receiving a MAb against a particular tumor-associated antigen. Binding of the MAb to the antigen in question on the tumor cell can often lead to internalization of the antigen–MAb complex and then set forth a cascade of events leading to the generation of antibody-dependent cell-mediated cytotoxicity or complement lysis.

Tumor Cell Escape from Effector Cells

Despite evoking cellular or humoral responses, tumor cells may avoid recognition by the immune system by several distinct mechanisms. One possibility is that

the tumor cell may "shed" or lose the immunogenic antigen as it circulates through the body. Second, the cell may lose an important molecule on its surface that is necessary for T cell recognition and killing. The loss of expression of the MHC in mice or histocompatibility locus A class I molecules in humans may end up not allowing the presentation of tumor peptides to $CD8^+$ T cells. The production of immunosuppressive cytokines such as interleukin 10 or transforming growth factor-β (TGF-β) is another means by which tumor cells may avoid recognition and lysis by immune effector cells (Alpan *et al.,* 2004). Tumors may also kill attacking lymphocytes by virtue of expression of apoptosis-inducing cell-surface molecules such as FasL, although this is still under controversy. In fact, a larger tumor burden may affect the innate immune system compared with minimal disease burden.

One should keep in mind that we do not completely understand why the immune system allows the primary tumor to emerge, yet may actively be involved in a vaccine approach once micrometastatic disease returns after eradication of the primary target. A model postulated by Dr. Matzinger (Fuchs and Matzinger, 1996) argued that many cancers do not appear dangerous at first because they can initially grow as healthy cells and do not send out distress signals to activate APCs or DCs. However, these danger signals may be suppressed by other factors at the site, which may include even the treatment for the disease itself.

Dendritic Cells as a Unique Immune Interloper

DCs are professional APCs that have the unique capacity to stimulate naive T cells and initiate a primary immune response (Ridgway, 2003; Slovin, 2003). DCs produce the T helper subset 1 (T_H1) cytokine interleukin (IL)-12. However, if all DCs produce IL-12, how can a T_H2 response ever be induced? This may be explained by the fact that DCs are heterogeneous and that, depending on the precursor cell, only certain types of DCs may secrete IL-12 (Sallusto *et al.,* 1999). This was borne out by the fact that there are two distinct types of DC precursors: myeloid monocytes (pre-DC1s) and plasmacytoid DC precursors (pre-DC2s). Although humans and mice vary in their functional classification of DC subsets, several studies showed the existence of a high IL-12–producing DC subset that induces T_H1 responses and a low IL-12–producing subset that induces T_H2 responses (Rissoan *et al.,* 1999). Despite the controversy regarding DC classification, the findings suggest that a given DC subset has a remarkable "plasticity" in channeling different types of T cell responses (Kalinski *et al.,* 1999).

The DCs are bone marrow–derived monocytic cells, which are potent APCs that are able to migrate to primary and secondary lymphoid organs and stimulate T cell responses to antigens associated with MHC molecules on the DC surface. A specific population of DCs are found in the skin and are known as Langerhans cells. They, too, can process antigens, particularly in the setting of an intradermal vaccine. Techniques have been developed to generate large quantities of DCs *in vitro* using cytokine mixtures to selectively stimulate the DCs from the peripheral mononuclear cell population (Figure 7). DCs produced in this fashion can be "loaded" or co-incubated with peptides of interest and reinfused into patients for use as an immunotherapy (Ridgway, 2003; Slovin, 2003). In many clinical trials, autologous leukocyte preparations obtained through peripheral blood leukopheresis were enriched for DCs by density gradients, selective adherence, monoclonal depletion steps, or cytokine stimulation culture or any combination of methods. The *ex vivo* exposure of DCs with known soluble tumor antigens, and their subsequent expansion using cytokines such as IL-4 and GM-CSF, has been a straightforward preparation strategy. This has been particularly true in the face of several malignancies where well-characterized tumor-differentiation antigens have been identified, such as PSA and acid phosphatase (ACP) in prostate cancer, Mart 1, Mage 3, gpl00 in malignant melanoma and colorectal carcinoma using Mart peptides, or peptides derived from carcinoembryonic antigen (CEA) (Smyth *et al.,* 2001).

In some studies, DCs have been exposed *ex vivo* to mRNA for CEA or PSA resulting in cytoplasmic gene expression and appropriate appearance of the tumor antigen on the cell surface. In a review, Ridgway (2003) cites more than 1000 clinical trials in the literature that have used DCs as an immunologic therapy not only in malignancies but also in autoimmune diseases. In 21 trials, DCs were exposed to total tumor RNA, apoptotic tumor cells, transfection with tumor protein DNA, the protein component of lysed tumor cells, and the formation of a hybrid or fusion product composed of DCs and tumor cells.

It needs to be noted that, although approach of DC immunotherapy is very attractive in that there is minimal toxicity to the patients, who are receiving back their own primed DCs, the technology has been further enhanced such that pharmaceutical company-sponsored trials are now underway in different malignancies. However, *ex vivo* expansion is labor-intensive and expensive, requiring that the patient not only be present for the initial removal of the cells but return within 48 hours to receive back the primed cells. To improve recruitment

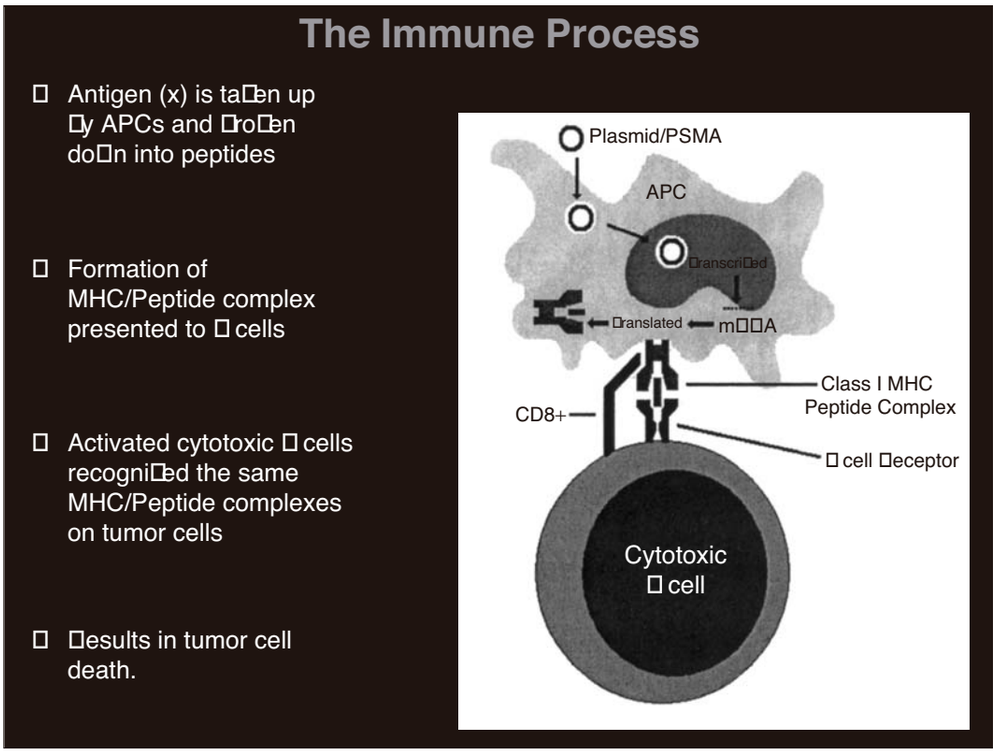

Figure 7. Cartoon demonstrating the complex interplay between cytokines, T cell, APC (antigen presenting cell), and antigen. MHC, Major histocompatability complex; PSMA, prostate specific membrane antigen; mRNA, messenger ribonucleic acid.

of DCs to sites of vaccination, GM-CSF has been used in both the protein and DNA formulation. Intradermal or subcutaneous delivery of GM-CSF results in infiltration of DCs at the site of application. After several days, the same site is used to administer the vaccine (peptide, DNA, protein, etc.), and the hypothesis is that the locally concentrated DCs will present antigen efficiently and induce an immune response to the vaccine. This approach has been used previously in a variety of vaccine trials. The use of the GM-CSF gene may obviate the need for using exogenous GM-CSF (Wolchok *et al.,* 2003).

Vaccines for Cancer

One of the biggest problems facing any vaccine strategy is determining what is the appropriate end point for the trial in question. There is no question that breaking immunologic tolerance to "self" antigens implies that an immune response has occurred and can be easily measured for its cellular or humoral response by a series of validated assays. It remains unclear as to what the optimal patient population should be (i.e., heavy tumor burden versus those patients who have minimal measurable disease). However, although scientists can monitor immune induction, there still remains the problem of how to judge clinical response, especially in patients who have micrometastatic disease without frank evidence of radiographic metastases. Therefore, scientists and clinicians must join forces at the outset of clinical trial investigations and decide how "response" will be evaluated in such trials.

A theoretic concern related to the use of DC vaccines prepared from host tumor cells is that indiscriminate adoption and presentation of host proteins by DC cells might result in T cell–mediated autoimmunity. To date, no reports of patients who have developed autoimmune disease have been reported. This includes the approaches of DCs primed with tumor lysate, total tumor RNA, or tumor DNA following synthetic peptide-pulsed DCs.

Although the DC vaccination approach has been shown to be feasible and safe, many of the studies to date were not designed with an immunologic end point in mind. This may well be because many of the populations studied were patients with heavy tumor burden who failed conventional therapy compared with those patients who may have had minimal disease in the setting of failing first-line therapy (Fong and Small 2003; Lodge *et al.,* 2000). None of the clinical trials that

claimed a "response" had large numbers of patients enrolled, so the statistical significance was severely lacking. However, complete responses were reported in 1 of 4 patients with bladder cancer (Nishiyama *et al.,* 2001), 2 of 12 patients with lung or colorectal cancer (Fong *et al.,* 2001), 3 of 26 with lymphoma (Hsu *et al.,* 1996), 15 of 168 with malignant melanoma (Cajal *et al.,* 2000; Fay *et al.,* 2000), 8 of 46 with multiple myeloma (Lacy *et al.,* 2000, 2002), and 4 of 17 with renal cell carcinoma (Kugler *et al.,* 2000). Although the observed responses in multiple trials have been variable and insufficient and unconvincing data have not encouraged phase III investigations in some diseases, there are reasons to pursue a treatment that is labor-intensive and mandates significant patient cooperation.

By exploring DC immunizations, we have been obliged to further investigate the nuances associated with the ability of the DC to do its job more efficiently and to entertain questions that would not have been addressed through other venues. These include whether DCs can be manipulated *in vivo,* rather than *ex vivo;* the use of FLt-3L or other cytokines to induce DC maturation; the relationship of DCs with other effector cell populations such as natural killer (NK) cells; the stimulatory effect of DCs on NKT cells, and further characterization of sensitized T cells after induction by DCs. The DCs should not be glorified as the only successful means by which a targeted approach to a particular antigen can be attained. It is, however, tantalizing to think of the many consequences of this approach that could lead to enhanced understanding of the immune response to cancer. Thus, a negative trial may still contribute information of interest.

Enhancing Cellular Immune Responses—The Prime-Boost Strategy

Immnunologic strategies involving effector cells have their limitations, particularly in the face of the need for repetitive immunizations to maintain immunologic memory. This is true whether it is for reinduction of humoral or cellular responses and leaves open the concern about how to reestablish robust antigen presentation and the generation of appropriate inflammatory signals over a longer period of time. To date, there has not been any one means by which to maintain an anti-tumor response with any length of durability.

No one vaccination schedule has succeeded in maintaining immunity unless used in what is known as a "prime-boost" strategy (Woodland, 2004). The basic prime-boost strategy involves priming the immune system to a target antigen, which can be delivered by one vector, and then selectively "boosting" this immunity by readministration of the antigen in the context of a second and distinct vector. Greater levels of immunity can then be established by a heterologous prime boost than can be attained by a single vaccine administration or homologous boost strategy (Wolchok *et al.,* 2003). As a means to overcome the limitations caused by immunodominant responses to viral vectors, for example, investigators studying vaccines for infectious diseases have used plasmid DNA for prime immune responses and recombinant viruses as a boost. This capitalizes on the limited immunogenicity of the plasmid backbone of DNA vaccines and the potency of single administration of recombinant viral vaccines.

It should be noted that early approaches of the prime-boost strategy were merely "additive," whereas with newer vaccine strategies, which use poxvirus or adenovirus boosting, significant "synergistic" effects can be attained. Any vaccine that is designed to promote cellular immunity must depend on long-lived memory T cells. As mentioned earlier, central memory T cells express CCR7 and CD26L and can persist in secondary lymphoid organs. Other effector memory T cells express no, or low, levels of CCR7 and CD62L and persist in various peripheral sites as well as the secondary lymphoid sites.

Both populations are able to mediate recall responses, but effector memory cells are located at key entry points where pathogens may enter, as an example. Central memory T cells exist to deal with systemic infections. It is essential that vaccines be developed that can promote the specific cellular immunity that is required (i.e., T_H1 versus T_H2, or CD4 versus CD8). Clearly, different prime-boost strategies will be needed to generate distinct types of immunity, and it is fundamental that an inappropriate immune response (autoimmunity) not be generated.

In conclusion, as can be appreciated from the discussion, the immunologic orchestra remains a complex chorus that still needs refinement to achieve maximum immunity in humans. The nature of the immune system, although varied, is nevertheless somewhat predictable in how it will behave if certain components do not interact maximally, as long as the inherent systems of checks and balances are maintained. Clearly, we have made enormous strides in understanding the complex nature of the immune system and have developed strategies that allow us to try to assist it in maximizing *in vivo* reactions. This review has been merely an introduction to a diverse and complex system, which we hope can be used in novel capacities to "effect" anti-tumor responses.

Acknowledgments

Supported by the Prostate Cancer Foundation, The Byrne Foundation, The Carol Ann Mazzella Fund, and The John B. Reed and Sharon Hels Fund.

References

Alpan, O., Bachelder, E., Isil, E., Arnheiter, H., and Matzinger, P. 2004. "Educated" dendritic cells act as messengers from memory to naïve T helper cells. *Nat. Immunol. 5*:615–622.

Cajal, R., Mayordomo, J.I., Yubero, A., Lasierra, P., Isla, D., Blasco, C., Fuertes, M.A., Palomera, R., Sousa, R., Guemes, A., Escudero, P., Saenz, A., Garcia, M., Larrad, L., and Tres, A. 2000. Immunological and clinical effects of immunotherapy with dendritic cells pulsed with tumor lysates in patients with advanced cancer. A pilot trial. *Proc. Am. Soc. Clin. Oncol. 19*:454a (Abstr).

Cantor, H. 2004. Reviving suppression? *Nat. Immunol. 5*:347–349.

Davis, T.A., Tchekmedyian S., Korman, A., Keler, T., Deo., Y., and Small, E.J. 2002. MDZ-010 (human anti-CTLA4): a phase I trial in hormone refractory prostate carcinoma (CaP). *Proc. Am. Soc. Oncol. 24*:19a (Abstr#74).

Egen, J.G., Kuhns, M.S., and Allison, JP. 2002. CTLA-4: new insights into its biological function and use in tumor immunotherapy. *Nat. Immunol. 3*:611–618.

Fay, J., Palucka, K., Dhodapkar, M., Burkeholder, S., Taque, N., Rolland, A., Bhardwaj, N., Piniero, L., Stone, M., Steinman, R., and Banchereau, J. 2000. Dendritic cell immunotherapy of metastatic melanoma using CD34+ hematopoietic progenitor-derived cells (CD34-DC) induced immune responses to melanoma antigen and results in clinical regression of metastatic disease. *Blood 96*:807a (Abstr).

Fong, L., Hou, Y., Benike, C., Wu, L., and Engleman, E.G. 2001. Altered peptide ligand vaccination with Flt3 ligand expanded dendritic cells for tumor immunotherapy. *Proc. Natl. Assoc. Sci. 98*:8809–8814.

Fong, L. and Small, E.J. 2003. Immunotherapy for prostate cancer. *Semin. Oncol. 30*:649–658.

Fuchs, E.I. and Matzinger, P. 1996. Is cancer dangerous to the immune system? *Sem. Immunol. 8*:271–280.

Gershon, R.K. 1975. A disquisition on suppressor T cells. *Transplant. Rev. 26*:170–185.

Hsu, F.J., Benike, C., Fagnoni, F., Liles, T.M., Czerwinski, D., Taidi, B., Engleman, E.G., and Levy, R. 1996. Vaccinations of patients with B-cell lymphoma using autologous antigen-puled dendritic cells. *Nat. Med. 2*:52–58.

Kalinski, P., Hilkens, C.M., Wierenga, E.A., and Kapsenberg, M.L. 1999. T-cell priming by type-1 and type-2 polarized dendritic cells: the concept of a third signal. *Immunol. Today 20*:561–567.

Kugler, A., Stuhler, G., Walden, P., Zoller, G., Zobywaslci, A., Brossart, P, et al. 2000. Regression of human metastatic renal cell carcinoma after vaccination with tumor cell-dendritic cell hybrids. *Nat. Med. 6*:332–336.

Lacy, M., Wettstein, P., Gertz, M.A., Gastineau, D.A. Greipp, P.R., Folneca, R., et al. 2002. Postautologous transplantation consolidation of multiple myeloma with idiotype-pulsed antigen presenting (dendritic) cells (APC8020). *Proc. Am. Soc. Clin. Oncol. 21*:31a (Abstr).

Lacy, M.Q., Wettstein, P., Gertz, M.A., Gastineau, D.A., Greipp, P.R., Fonseca, R., Lust, J., Witzig, T., Rajkuman, S.V., Valone, F., and Kyle, R.A. 2000. Dendritic cell-based idiotype vaccination in post transplant multiple myeloma. *Blood 96*:374a (Abstr).

Lodge, P.A., Jones, L.A., Bader, R.A., Murphy, G.P., and Salgaller, M.L. 2000. Dendritic cell-based immunotherapy of prostate: immune monitoring of a phase II clinical trial. *Cancer Res. 60*:829–833.

Luther, S.A. and Cyster, J. 2001. Chemokines as regulators of T cell differentiation. *Nat. Immunol. 2*:102–107.

Nishiyama, T., Tafchibana, M., Horiguchi, Y., Nakamura, K., Ikeda, Y., Takesako, K., and Murai, M. 2001. Immunotherapy of bladder cancer using autologous dendritic cells pulsed with human lymphocyte antigen-A24-specific MAGE-3 peptide. *Clin. Cancer Res. 7*:23–31.

Ridgway, D. 2003. The first 1000 dendritic cell vaccines. *Cancer Invest. 21*:873–886.

Rissoan, M.-C., Soumelis, V., Kadowaki, N., Grouard, G., Briere, F., Maleft, R., and Liu, Y-J. 1999. Reciprocal control of T helper cell and dendritic cell differentiation. *Science 283*:1183–1186.

Sallusto, F., Palermo, B., Lenig, D., Miettinen, M., Matikainen, S., Julkunen, I., Forster, R., Burgstahler, R., Lipp, M., and Lanzavecchia, A. 1999. Distinct patterns and kinetics of chemokine production regulate dendritic cell function. *Eur. J. Immunol. 29*:1617–1625.

Slovin, S.F. 2003. Dendritic cell vaccines—Hopeful or hopeless? *Cancer Invest. 21*:969–970.

Smyth, M.J., Godfrey, D.I., and Trampani, J.A. 2001. A fresh look at tumor immunosurveillance and immunotherapy. *Nat. Immunol. 2*:293–299.

Tchekmedyian, S., Glasby, J., Korman, A., Keler, T., Deo, Y., and Davis, T.A. 2002. MDX-010 (human anti-CTLA4); a phase I trial in malignant melanoma. *Proc. Amer. Soc. Clin. Oncol. 24*: 15a (Abstr#56).

Von Herrath, M. and Homann, D. 2003. Introducing baselines for therapeutic use of regulatory T cells and cytokines in autoimmunity. *Trends Immunol. 24*:540–545.

Wolchok, J.D., Gregor, P.D., Nordquist, L.T., Slovin, S.F., and Scher, H.I. 2003. DNA vaccines: an active immunization strategy for prostate cancer. *Semin. Oncol. 30:*659–666.

Woodland, D.L. 2004. Jump-starting the immune system: prime-boosting comes of age. *Trends Immunol. 25*:98-104.

This Page Intentionally Left Blank

6

Circulating Cancer Cells

Eiji Oki, Eriko Tokunaga, Yoshihiro Kakeji, Hideo Baba, and Yoshihiko Maehara

Introduction

When only a very small amount of cancer cells is found in the bloodstream, it is defined as circulating cancer cell (CCC). In a broad sense, all small amounts of cancer cells discovered anywhere except in a primary or metastatic lesion can be called CCC. A similar phrase that can be used to describe CCC in a TNM (tumor, node, metastasis) classification is "isolated tumor cells" (ITC). A paragraph concerning the ITC was added into the TNM classification in 2002. This phrase is explained as a single cancer cell or a small cancer cell cluster less than 0.2 mm in diameter that can be detected by the molecular method, immunostaining, or conventional staining. Recently, ITC has been treated separately from conventional pathologic findings. The detection of CCC and micrometastases has an important prognostic and therapeutic implication. Because there are so few of these cancer cells, they cannot be easily detected with conventional methods. In 1995, Engell used a cell block technique and reported the detection of CCC in patients with various types of carcinomas. Several researchers followed this method between 1955 and 1965 (Christopherson, 1965; Engell, 1955). These initial studies reported a very high positive rate among patients with cancer. However, these observations were soon shown to be false-positive results, and so these assays were abandoned for many years. After immunostaining became popular, the CCC and micrometastases issue began to attract attention again. In the last decade, numerous groups have attempted to detect CCCs in solid malignancies using the highly sensitive reverse transcription-polymerase chain reaction (RT-PCR). However, not all of the methodologic problems have been solved, and many groups are now developing new approaches toward the detection of CCC. Approaches, such as flow cytometry, video microscopy, and confocal laser scanning microscopy, are being used for studying CCCs.

METHODOLOGY

Target Organ and Sample Collection

There are three patterns for cancer metastasis: the blood circulation pattern, the lymph-node pattern, and the abdominal-dissemination pattern. These sites have been targeted to find recurrence or metastasis for the post-operative imaging investigation. The investigation for ITC or CCC is mainly focused on peripheral blood (PB), lymph nodes, ascites, and bone marrow (BM).

Peripheral Blood

The shedding of cancer cells from either primary tumors or lymphatic organs into the circulating blood can be a result of primary dissemination. However, secondary events during certain procedures, such as biopsies and operations, can sometimes be the cause. On entering circulation, many of these cells are killed by immune cells. However, a certain percentage of these cells will eventually survive and successfully extravagate. The detection of the presence or quantity of these

Handbook of Immunohistochemistry and *in situ* Hybridization of Human Carcinomas, Volume 4: Molecular Genetics, Gastrointestinal Carcinoma, and Ovarian Carcinoma

cells could be valuable in monitoring treatments and predicting prognoses, as well as in understanding underlying metastatic biology.

Lymph Nodes

Despite the abundant knowledge of the biology of cancer, the single most important prognostic factor for most solid tumors is the presence of histologically detectable regional lymph-node metastases. Patients without metastasized regional lymph nodes tend to do far better than patients with lymph-node metastasis. However, a significant amount of patients who are node negative will develop distant metastasis. In reality, the routine histopathologic examination of lymph nodes is only a sampling. In all cases, it is evident that routine processing and histologic examination of regional lymph nodes are inadequate when attempting to detect the presence of tumors. There have been several reports concerning the detection of occult lymph-node metastases in the breast, colon, lung, and prostate. As a target organ in finding ITC, the lymph node is a solid organ and is easy to study with immunohistochemistry (IHC) or PCR.

Bone Marrow

Bone marrow is a specific organ. Even in cancers such as carcinoma of the stomach and colon, where overt skeletal metastasis is rare, bone marrow is still a prognostically relevant indicator for micrometastasis. (Thorban *et al.,* 1996a, 1996b). One explanation is that BM might function as an important reservoir for disseminated epithelial cancer cells, which may be destined for other organs. Isolated tumor cells in BM can be used to establish cancer cell lines and can also be used for the preparation of tumor cell vaccines because cancer cells in BM can disseminate and grow *in vitro* (Pantel *et al.,* 1995; Putz *et al.,* 1999). Based on this evidence, the investigation of cancer cells in BM may prove to be a pertinent diagnostic technique when identifying metastasis. Preoperatively, in the case of BM, 1 ml to 2 ml aliquots of BM aspirates were taken from the sternum into syringes containing 100 units of heparin/ml marrow. The BM cells were then prepared. After density centrifugation through Ficoll-Hypaque (Pharmacia Biotech AB, Uppsala Sweden, 400 g, 30 min), interphase mononuclear cells were collected and RNA extraction was carried out.

Ascites

The routine cytologic method for finding metastasis in ascites is microscopic examination. Metastasis in ascites provided important information that can change the operative procedure. Japanese groups have mainly been using the PCR to find ITC in the ascites of patients with gastric cancer (Kodera *et al.,* 2002). The sample collection of ascites is sometimes controversial. Usually, 50 ml of ascites is aspirated after being washed with 100 ml of normal saline. The obtained lavage is then placed into a centrifuge, and the cell component is collected.

Immunohistochemistry

A number of groups have used the immunohistochemical method to identify ITC or CCC in the bone marrow and lymph nodes of patients with cancer. Immunohistochemical methods are based on the ability of monoclonal or polyclonal antibodies to distinguish specific histogenesis cells among others. The antibodies most widely used to detect ITC are the antibodies of epithelial specific antigens because there are normally no epithelial cells in the BM or lymph nodes. Since 1992, we have been using IHC for investigating cancer cells in the BM of patients with gastric cancer (Maehara *et al.,* 1996b). Preoperatively, 1 ml of BM aspirates were taken from the sternum in syringes containing 100 units of heparin. The BM cells were then diluted with 10 ml of Hanks' balanced salt solution, and the marrow fat was separated by centrifugation (180 g, 10 min). After density centrifugation through Ficoll-Hypaque (400 g, 30 min), the mononuclear cells were collected from interphase. After being wasted twice in phosphate buffer saline (PBS) and centrifuged (200 g, 5 min), the cells were suspended in 0.5 ml of RPMI 1640 medium containing 10% fetal calf serum yielding a concentration of 2×10^6/ml on glass slides. They were then fixed with acetone (30 min, 4°C). Ten to 20 slides containing 6×10^5-nucleated cells were routinely examined for each patient. One additional slide served as an immunoglobulin G (IgG) isotype control. For immunostaining, a monoclonal antibody such as cytokeratin was used. The antibody reaction was developed using the labeled avidin–biotin technique. Figure 8 shows the photomicrograph obtained from the BM samples.

Polymerase Chain Reaction–Based Method

The PCR technique is a molecular biological procedure that was developed in the 1980s to amplify deoxyribonucleic acid (DNA) with thermostable DNA polymerase. The procedure consists of a repetitive series of cycles, each consisting of template denaturation, primer annealing, and extension of the annealed primers to create the exponential accumulation of a specific DNA fragment whose ends are determined by the 5′ ends of the primers. The PCR amplification can be accomplished using ribonucleic acid (RNA) as

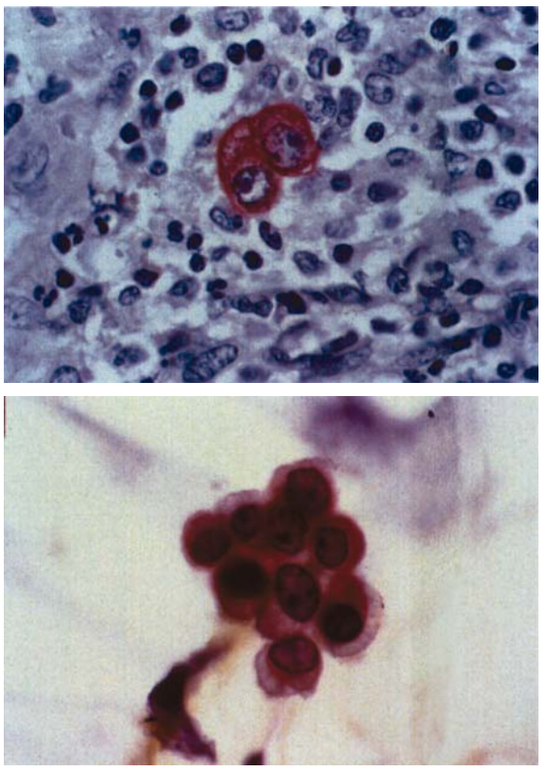

Figure 8. Photomicrophotograph of isolated cancer cells in the lymph node and bone marrow. High-power photomicrograph of lymph node for those with a single cytokeratin-positive cell **(A)** or a small cluster of cells in bone marrow **(B)**. (Reproduced with permission of Maehara *et al.,* 1996a, 1996b.)

Table 2. Markers for RT-PCR Methods for Detecting Circulating Cancer Cells in Solid Tumors

Tumor Type	Molecular Target
Breast carcinoma	CEA
	MUC1
	Cytokeratin 19
Prostate	PSA
	PSMA
	PTI-1
	hK2-1
Gastrointestinal carcinomas	CEA
	Cytokeratin 19
	Cytokeratin 20
	MUC2, MUC6
	k-ras
Hepatocellular carcinoma	AFP
	Albumin
Lung carcinoma	CEA
	Cytokeratin-19
	Surfactant protein
Melanoma	MAGE-3
	MART-1
	p97
Ovarian cancer	MUC1

AFP, Alpha fetoprotein; CEA, carcinoembryonic antigen; hK2-1, human kallikrein 2-1; MAGE-3, melanoma antigens-3; MART-1, melanoma antigen recognized by T cell 1; MUC1, mucin 1; PSA prostate specific antigen; PSMA, prostate specific membrane antigen; PTI-1, prostate tumor-inducing gene; RT-PCR, reverse transcription-polymerase chain reaction.

starting material. This procedure is known as RT-PCR. It is used for the modification of genomic PCR so that amplification is preceded by reverse transcription of RNA into complementary DNA (cDNA). The main PCR strategy for the detection of CCC involves the amplification of cancer-tissue–specific messenger RNA (mRNA) by RT-PCR. Table 2 shows the specific mRNA that has been most often used for the detection of CCC and ITC is solid tumors. This approach was used because malignant cells continue to characteristically or specifically express markers or the normal tissue from which the tumor originated or shares a histotype. It is necessary to find the specific mRNA in an organ where these transcripts are not normally present, implying that a tumor has spread.

The detection of CCC using RT-PCR has attracted much interest. However, although many investigators have published encouraging results (Fields *et al.,* 1996; Moscinski *et al.,* 1996; Slade *et al.,* 1999; Soeth, *et al.,* 1996), other studies have raised some serious problems (Champelovier *et al.,* 1999; Lambrechts *et al.,* 1998). At present, these problems are as follows: First, in the usual RT-PCR, the amplified PCR products are quantified only after all cycles of amplification, even though the amplification products increase. This shows a sigmoidal curve at the same time as the increase in the PCR cycle. It was not considered whether each sample reaches a plateau phase. Thus, the positive rate might change if the PCR cycle number decreases or increases. For a quantitative RT-PCR, an internal control co-amplified with the target sequence is needed (Slade *et al.,* 1999). Absolute quantitation requires an accurate determination of the internal control concentration. Thus, well-trained staff capable of performing this kind of complicated procedure should carry out a quantitative RT-PCR. However, the quantity of the amplified targeted and the co-amplified internal control is usually determined by the assessment of the ethidium bromide staining intensity of the PCR products on the agarose gel, and approach not without contradictions.

Another problem is the target gene. For epithelial tumors, genes that are thought to be tissue specific for epithelium-derived cells are the logical choices for RT-PCR investigations. Thus, target genes such as CEA, CK18, CK19, and CK20 have been independently tested (Schoenfeld, *et al.,* 1997; Wulf, *et al.,* 1997; Wyld

et al., 1998). Defining the best marker has remained contestable. It is also possible that low transcription levels of the epithelial-specific genes in nonepithelial cells could be detected in RT-PCR (Champelovier *et al.,* 1999; Lambrechts *et al.,* 1998).

We used real-time quantitative RT-PCR to develop a highly sensitive diagnostic device that could detect ITC and CCC in BM and PB. Real-time quantitative RT-PCR requires a hybridization probe labeled with two different fluorescent dyes (Heid *et al.,* 1996). When the probe is intact, fluorescent energy transfer occurs, and the fluorescent emission is absorbed by one dye. During PCR reactions, exonuclease activity of the Taq polymerase will cleave an oligonucleotide probe that is hybridized to the target DNA (Holland *et al.,* 1991). The fluorescent reporter FAM (6-carboxyfluorescein), which is located on the 5′ end of the probe, is released from the quencher dye (TAMRA, 6-carboxytetramethylrhodamine) on the 3′ end, resulting in an increase of the reported dye's fluorescent emission spectra. Fluorescent emission is measured in real time, and the calculated threshold (Ct) value reflects the quantity of the starting target (Figure 8). Lower Ct values reflect a greater amount of starting target molecules. First, we generated three control plasmids containing human cDNAs of CEA, CK18, and CK20, which were obtained from healthy human volunteers. To verify the detection characteristics of this system, we first examined the Ct value in cases of various amounts of PCR template. Figure 9A shows the amplification plots of serial 10-fold dilutions of control plasmids containing cDNA of CEA. Figure 9B represents the Ct value versus the sample dilution value. The Ct value decreased linearly with the increasing target quantity from 10 copies per tube to 100 million copies per tube. Thus, this system has a 10 million-fold range of input target molecules. We investigated CEA, CK18, and CK20 mRNA expression in several human cancer cell lines and the nonepithelial normal tissue cell lines. Each sample was amplified in triplicate, and Figure 10 shows the mean value with the standard deviation. Although CK20 expression was lower than that of CK18, all of the cancer cell lines showed a similarly high expression level. However, we found 50- to 100-fold differences between the carcinoma cell lines and the normal tissue cell lines. Concerning CEA, we found a huge difference in expression among four carcinoma cell lines. For a 2–cancer cell line, the expression was 50,000-fold higher than it was for the other 2–cell lines. The 2–cancer cell line showed the same low CEA mRNA expression that is seen in normal cell lines. Thus, real-time quantitative RT-PCR is sensitive and quantitative for detection of ITC and CCC. To evaluate the clinical significance of this method, development of other dependable markers and further long-term clinical follow-up studies are needed.

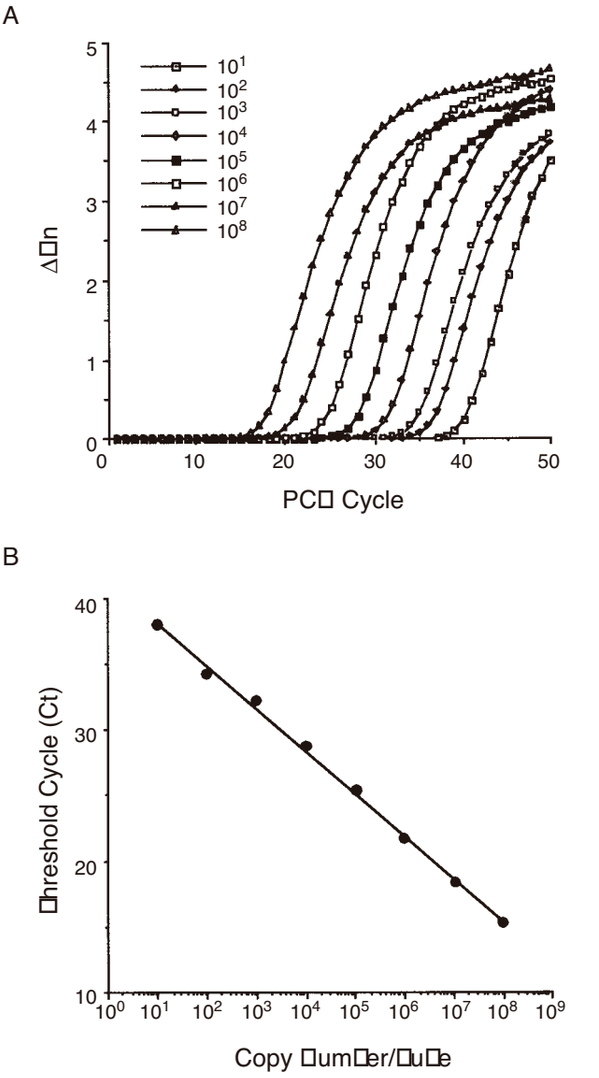

Figure 9. A: Amplification of carcinoembryonic antigen (CEA) messenger ribonucleic acid (mRNA). Serial dilutions of pT7Blue T-vectors, including human carcinoembryonic complementary deoxyribonucleic acid (cDNA), were amplified using real-time "Taqman™" technology and analyzed using Model 7700 Sequence Detector (Perkin-Elmer Corp.). **B:** Input cDNA concentration (serial dilutions of pT7Blue T-vector) of samples plotted versus Ct (threshold cycle). (Reproduced with permission of Oki *et al.,* 2002.)

Investigation of Various Cancers

Breast Cancer

Many patients with breast cancer can be diagnosed at an early stage. Usually, after primary surgery most of the patients are free of any detectable disease using usual imaging procedures (Seiden and Sklar, 1996).

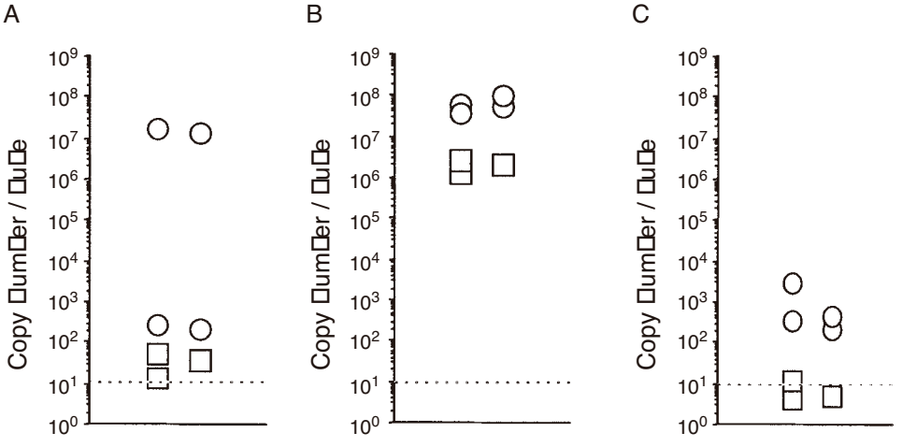

Figure 10. Quantitated copy number of messenger ribonucleic acid (mRNA). Copy numbers are calculated based on the Ct (Calculated threshold cycle) value and are plotted on histograms. **A:** CEA (Carcinoembryonic antigen); **B:** CK18; **C:** CK20. Solid circles represent mRNA expression of each gastric cancer cell line (KATO-III, MKN45, MKN74, NUGC4), and solid squares represent the mRNA expression of normal tissue cell lines (MRC5, WI38, HASMC). Broken line shows the assessible lower limit of this assay (1×10^1 copy/tube).

Despite highly efficient locoregional therapy, 30–40% of these patients will develop clinically detectable metastases within 10 years if no further treatment is performed (Seiden and Sklar, 1996). The main reason for these relapses is that breast carcinoma cells disseminate throughout the body early during tumor development (Schlimock and Riethmuller, 1990). As a result, several groups have recommended adjuvant treatment for patients with no metastasis, and so approximately two-thirds of the patients diagnosed with breast cancer in stages I to III are candidates for adjuvant or neoadjuvant chemotherapy. In these groups, the patients who have occult metastasis should be the most successful with adjuvant therapy. The detection of occult cancer cells in these patients could be extremely beneficial in the determination prognosis and in making treatment decisions. A number of methods have been used for detecting micrometastasis and circulating breast cancer cells.

One of the sites most often visited by metastatic breast cancer cells is BM. To find the patients who will most benefit from adjuvant chemotherapy, several groups have attempted to detect BM micrometastases using IHC or RT-PCR (Yu *et al.,* 2004). Some authors have reported encouraging information about the prognostic significance of immunocytochemical assays (Cote *et al.,* 1991; Diel *et al.,* 1992), but others have failed to demonstrate such relevance (Salvadori *et al.,* 1990; Singletary *et al.,* 1991). Some patients whose BM results were positive by IHC have remained free of recurrent and metastatic diseases after long intervals (Seiden *et al.,* 1996). These findings could be the result of several factors, one being that some micrometastases may be incapable of developing into clinically significant lesions (Seiden *et al.,* 1996). Alternatively, the antibodies may have cross-reacted with normal marrow cells, leading to false-positive results. The CEA and CK19 assays showed good specificity as markers that could be used to detect BM micrometastasis using RT-PCR. The study of 42 patients showed that CK19- and CEA-positive RT-PCR assays in BM positively correlated with a positive axillary lymph-node status. We have tried to use RT-PCR to reduce the amount of false-positive results (Tokunaga *et al.,* 2003).

Several authors were able to use highly sensitive RT-PCR assays to detect tissue-specific transcripts in the PB of patients with breast carcinomas (Brown *et al.,* 1995; Mori *et al.,* 1996a, 1996b). When Taqman was performed for RT-PCR analysis of CEA, it was revealed that as little as one breast cancer cell could be reliably detected in 5 ml of blood. Some investigators found abnormally high levels of CK19 mRNA in the PB of patients with metastatic breast cancer and in patients with primary tumors. The clinical impact of their findings is unknown because of the lack of a follow-up. Clearly, there is a need for more specific PCR markers in breast carcinoma.

A few of the earliest destinations during the metastatic spread of breast cancer cells are the local lymph, axillary, and costal nodes. As one would expect, most of the studies have used axillary lymph nodes, which were dissected from mastectomies. Using keratin 19 as a marker, Schoenfeld *et al.* (1994) has demonstrated that 18 of the 57 axillary nodes examined were positive for K19 staining, compared to the 32 positive nodes that were revealed when RT-PCR and Southern

blotting of K19 molecules were used. Mucins and MUC1 are also useful in finding micrometastases in breast cancer PB.

Mammaglobin is a recently described marker that was found to be present only in adult mammary tissue (Zehentner and Carter, 2004). This is frequently overexpressed in 80–95% of primary breast carcinomas (Watson and Fleming, 1996). According to Min *et al*. (1998), this marker is present in the breast carcinoma cell lines and absent in the 20 normal lymph nodes when using RT-PCR. Zach *et al*. (1999) were able to detect mammaglobin mRNA in the PB of 28% of the patients with breast carcinoma in various stages, in 5% of the patients with non-breast carcinoma malignancies, and in none of 27 healthy volunteers. In a small group of patients with breast carcinoma, Aihara *et al*. (1999) found mammaglobin transcripts by using RT-PCR in all of the histologically proven metastatic lymph nodes and in 31% of histologically negative lymph nodes. Some groups have recently used immunomagnetic-based assays for the detection of CCC in breast cancer (Choesmel *et al.,* 2004; Hu *et al.,* 2003). In one instance, the immunomagnetic procedure was followed by the assessment of telomerase activity using PCR (Soria *et al.,* 1999). This latter technique revealed telomerase activity in 21 out of 25 (84%) patients with metastatic breast carcinoma, whereas all of the healthy volunteers were telomerase negative. Engel *et al*. (1999) used immunobead isolation, which was followed by fluorescence *in situ* hybridization (FISH) and immunocytochemistry.

Prostate Cancer

Many patients with prostate cancer who undergo radical prostatectomies will suffer recurrence, even in the absence of clinically or pathologically detectable regional or systemic metastasis. The thought of developing a method to reliably determine the risks of developing advanced disease using a simple PB test is alluring. Because prostate specific antigen (PSA) has been thought to be specific for prostate cancer, the longstanding clinical use of serum PSA levels in patient follow-ups has been shown to be valuable. Methods have been developed to increase the sensitivity of PSA detection in the blood. The most promising methods have been the use of RT-PCR on peripheral blood samples to determine the presence of PSA. Some investigators have used RT-PCR to detect circulating cancer cells in the PB and BM of patients with prostate cancers (Ghossein *et al.,* 1995).

The frequency of RT-PCR positivity in PB increases with the tumor stage and high serum PSA levels (Ghossein *et al.,* 1995). One article reported the detection of CCC in 20% of the patients who were previously RT-PCR negative after needle biopsies (Price *et al.,* 1998). Most patients showed CCC after their biopsy reverted to a RT-PCR negative PCR assay with 4 weeks (Price *et al.,* 1998). Two groups showed the presence of CCC by RT-PCR correlated with both capsular penetration and positive surgical margins (Grassa *et al.,* 1998; Katz *et al.,* 1994). They found that RT-PCR was better than other staging modalities in predicting the pathologic stage, and they proposed the use of this test as a staging modality for radical prostatectomy candidates. No other groups found a statistically significant correlation between blood RT-PCR positivity and the pathologic stage (Gao *et al.,* 1999; Sokoloff *et al.,* 1996). Some groups have found a statistically significant correlation between the preoperative RT-PCR positivity of PSA mRNA in the PB and its outcome (de la Taille *et al.,* 1999). However, there are indications from some groups that the RT-PCR methods used to detect PSA may be too sensitive.

RT-PCR for PSA mRNA has also been used to detect ITC in lymph nodes and in the BM of patients with prostate cancers, as stated earlier (Corey *et al.,* 1997). This technique was shown to be more sensitive than IHC and standard histopathology in detecting lymph-node micrometastases in localized diseases. All of the controlled lymph nodes and BM tested negative for PSA RT-PCR (Olsson *et al.,* 1997). Wood and Banerjee (1997) investigated 86 patients with clinically localized diseases in which preoperative BM PSA RT-PCR was performed. They found that 4% of the patients who were RT-PCR negative had recurrences after their prostatectomies, Whereas 26% of the patients who were RT-PCR positive failed post-operatively. In the last few years, RT-PCR assays for two additional prostatic markers, the prostate tumor-inducing gene *(PTI-1)* and prostate specific membrane antigen (PSMA), have been reported (Gao *et al.,* 1999; Schmidt *et al.,* 2003). *PTI-1* is a novel oncogene that was cloned from an LNCaP cDNA library (Shen *et al.,* 1995). Sun *et al*. (1997) reported that they were able to detect *PTI-1* mRNA in the PB of patients with metastatic prostate cancer using RT-PCR. A cell-surface protein with sequence homology, PSMA is used in transferring. Transcripts were detected in the PB of patients with localized and metastatic prostate cancer using RT-PCR (Sokoloff *et al.,* 1996). However, some investigators reported a high PCR positive rate for PSMA mRNA in the blood of healthy individuals (Hisatomi *et al.,* 2002).

Gastrointestinal Cancer

Gastrointestinal (GI) cancer is one of the most common malignancies in the Western and Asian countries. The detection of early metastatic spread of GI

malignancies may help stratify patients for radical surgery and guide adjuvant therapies. Several authors have reported the detection of CEA mRNA in the PB, BM, ascites, and lymph nodes of patients with gastric, colorectal, and pancreatic carcinomas but in none of the control subjects (Mori *et al.,* 1996a).

Several investigators have demonstrated the immunohistochemical detection of ITCs in patients with localized diseases (Dukes'B). Although most of the studies showed that a substantial portion of patients with localized colorectal cancer demonstrated ITC in the regional lymph node, not all of the studies showed the prognostic significance of finding these ITCs. We reported that micrometastases in lymph nodes were found in patients with pathologically negative nodes (Maehara *et al.,* 1996a, 1996b). In patients with tumor node metastasis gastric carcinomas (there are no histologic lymph-node metastases), the detection of micrometastasis in regional lymph nodes was shown to correlate with a poorer 5-year survival rate. Cytokeratin 20 mRNA has also been used as a marker for colorectal carcinoma cells in the lymph nodes, BM, and blood (Weitz *et al.,* 1999). We reported that the micrometastasis of gastric cancer in bone marrow was detectable by the real-time quantitative RT-PCR using cytokeratin 2 as a marker (Oki *et al.,* 2002; Tokunaga *et al.,* 2000). However, clinical importance of BM metastasis is not yet identified.

Some investigators have reported the clinical importance of CCC in PB of colorectal cancers for monitoring the early marker for recurrence and relapse and for monitoring the response of chemotherapy (Molnar *et al.,* 2003). We have investigated the CCC in the PB of patients with gastric cancer and have demonstrated that the detection of CCC or ITC in PB could be feasible by real-time quantitative RT-PCR. The patients with gastric cancer of the CK19- or CK20-positive cases were more advanced in their cancer and had shorter survivals (unpublished data).

Future Prospects

Over the years, many investigators have attempted to improve techniques for the detection of CCC and occult metastatic cells and to attribute clinical significance to the detection of such micrometastases. Because of the methodologic problem of PCR, it is now clear that other approaches are needed to detect CCC. In recent years, some investigators have used an immunomagnetic separation technology as a means to improve such detection (Nozawa *et al.,* 2003; Ulmer *et al.,* 2004). In this technique, the specimen is incubated with magnetic beads coated with antibodies and directed against a specific tissue type to select only the tumor cells. Frequent hypermethylation of DNA is also a prominent feature in malignant cells. It has been shown that methylation-specific PCR can be used to detect hypermethylated cyclin D2, retinoic acid receptor RAR, and p16 (Evron *et al.,* 2001; Wong *et al.,* 2003). This approach should be useful in detecting cancer cells, specifically those that are in circulation. Immunocytochemical analysis of the specimen also promises better quantification of the tumor cells and their assessment for various markers of tumor proliferation and progression. This will help to monitor the effect of molecular targeted therapy. Many investigators have been improving their methods to detect CCC. Although larger prospective randomized control studies are required to confirm the prognostic significance of detecting ITC and CCC, the molecular biological methods for finding CCC will be the main factor that will indicate the tumor stage and patient prognosis in the near future.

References

Aihara, T., Fujiwara, Y., Ooka, M., Sakita, I., Tamaki, Y., and Monden, M. 1999. Mammaglobin B as a novel marker for detection of breast cancer micrometastases in axillary lymph nodes by reverse transcription-polymerase chain reaction. *Breast Cancer Res. Treat. 58*:137–140.

Brown, D.C., Purushotam, A.D., Birnie, G.D., and George, W.D. 1995. Detection of intraoperative tumor cell dissemination in patients with breast cancer by use of the reverse transcription and polymerase chain reaction. *Surgery 117*:96–111.

Champelovier, P., Mongelard, F., Seigneurin, D. 1999. CK20 gene expression: technical limits for the detection of circulating tumor cells. *Anticancer Res. 19*:2073–2078.

Choesmel, V., Anract, P., Hoifodt, H., Thiery, J.P., and Blin, N. 2004. A relevant immunomagnetic assay to detect and characterize epithelial cell adhesion molecule-positive cells in bone marrow from patients with breast carcinoma: immunomagnetic purification of micrometastases. *Cancer 15*:693–703.

Christopherson, W. 1965. Cancer cells in the peripheral blood: a second look. *Acta. Cytol. 9*:169–174.

Corey, E., Arfman, E.W., Oswin, MM., Melchior, S.W., Tindall, D.J., Young, C.Y., Ellis, W.J., and Vessella, R.L. 1997. Detection of circulating prostatic cells by reverse transcriptase-polymerase chain reaction of human glandular kallikrein (HK2) and prostatic-specific antigen (PSA) messages. *Urology 50*:184–188.

Cote, R.J., Rosen, P.P., Lesser, M.L., Old, L.J., and Osborne, M.P. 1991. Prediction of early relapse in patients with operable breast cancer by detection of occult bone marrow micrometastases. *J. Clin. Oncol. 9*:1749–1756.

de la Taille, A., Olssan, C.A., Buttyan, R., Benson, M.C., Bagiella, E., Cao, Y., Burchardt, M., Chopin, D.K., and Katz, A.E. 1999. Blood based reverse transcriptase polymerase chain reaction assays for prostatic specific antigen: long term follow-up confirms the potential utility of this assay in identifying patients more likely to have biochemical recurrence (rising PSA) following radical prostatectomy. *Int. J. Cancer 84*: 360–364.

Diel, I.J., Kaufmann, M., Goerner, R., Costa, S.D., Kaul, S., and Bastert, G. 1992. Detection of tumor cells in bone marrow of

patients with primary breast cancer: a prognostic factor for distant metastasis. *J. Clin. Oncol. 10*:1534–1539.

Engel, H., Kleespies, C., Friedrich, J., Breidenbach, M., Kallenborn, A., Schondorf, T., Kolhagen, H., and Mallmann, P. 1999. Detection of circulating tumor cells in patients with breast or ovarian cancer by molecular cytogenetics. *Br. J. Cancer 81*:1165–1173.

Engell, H.C. 1955. Cancer cells in the circulating blood. *Acta. Chir. Scand. Suppl. 201*:1–70.

Evron, E., Dooley, W.C., Umbricht, C.B., Rosenthal, D., Sacchi, N., Gabrielson, E., Soito, A.B., Hung. D.T., Ljung, B., Davidson, N.E., and Sukumar, S. 2001. Detection of breast cancer cells in ductal lavage fluid by methylation specific PCR. *Lancet 357*:1335–1336.

Fields, K.K., Elfenbein, G.J., Trudeau, W.L., Perkins, J.B., Janssen, W.E., and Moscinski, L.C. 1996. Clinical significance of bone marrow metastases as detected using the polymerase chain reaction in patients with breast cancer undergoing high-dose chemotherapy and autologous bone marrow transplantation. *J. Clin. Oncol. 14*:1868–1876.

Gao, C-L., Maheshwari, S., Dean, R.C., Tatum, L., Mooneyhan, R., Connely, R.R., McLeod, D.G., Srivastava, S., and Moul, J.W. 1999. Blinded evaluation of reverse transcriptase-polymerase chain reaction prostate-specific antigen peripheral blood assay for molecular staging of prostate cancer. *Urology 53*:714–721.

Ghossein, R.A., Scher, H.I., Gerald, W.L., Kelly, W.K., Curley, T., Amsterdam, A., Zhang, Z.F., and Rosai, J. 1995. Detection of circulating tumor cells in patients with localized and metastatic prostatic carcinoma: clinical implications. *J. Clin. Oncol. 13*: 1195–1200.

Grassa, Y.Z., Gupta, M.K., Levin, H.S., Zippe, C.D., and Klein, E.A. 1998. Combined nested RT-PCR assay for prostate-specific antigen and prostate-specific membrane antigen in prostate cancer patients: correlation with pathological stage. *Cancer Res. 58*:1456–1459.

Heid, C.A., Stevens, J., Livak, K.J., and Williams, P.M. 1996. Real time quantitative PCR. *Genome Res. 6*:986–994.

Hisatomi, H., Nagao, K., Kawakita, M., Matsuda, T., Hirata, H., Yamamoto, S., Nakamoto, T., Harasawa, H., Kaneko, N., Hikiji, K., and Tsukada, Y. 2002. Detection of circulating prostate tumor cells: alternative spliced variant of PSM induced false-positive result. *Int. J. Mol. Med. 10*:619–622.

Holland, P.M., Abramson, R.D., Watson, R., and Gelfand, D.H. 1991. Detection of specific polymerase chain reaction product by utilizing the 5′-3′ exonuclease activity of Thermus aquaticus DNA polymerase. *Proc. Natl. Acad. Sci. USA 88*: 7276–7280.

Hu, X.C., Wang, Y., Shi, D.R., Loo, T.Y., and Chow, L.W. 2003. Immunomagnetic tumor cell enrichment is promising in detecting circulating breast cancer cells. *Oncology. 64*:160–165.

Katz, A.E., Olsson, C.A., Raffo, A.J., Katz, A.E., Olsson, C.A., Raffo, A.J., Cama, C., Perlman, H., Seaman, E., O'Toole, K.M., McMahon, D., Benson, M.C., and Buttyan, R. 1994. Molecular staging of prostate cancer with the use of an enhanced reverse transcriptase-PCR assay. *Urology 43*:765–775.

Kodera, Y., Nakanishi, H., Ito, S., Yamamura, Y., Kanemitsu, Y., Shimizu, Y., Hirai, T., Yasui, K., Kato, T., and Tatematsu, M. 2002. Quantitative detection of disseminated free cancer cells in peritoneal washes with real-time reverse transcriptase-polymerase chain reaction: a sensitive predictor of outcome for patients with gastric carcinoma. *Ann. Surg. 235*:499–506.

Lambrechts, A.C., van't Veer, L.J., and Rodenhuis, S. 1998. The detection of minimal numbers of contaminating epithelial tumor cells in blood or bone marrow: use limitations and future of RNA-based methods. *Ann. Oncol. 9*:1269–1276.

Maehara, Y., Oshiro, T., Endo, K., Baba, H., Oda, S., Ichiyoshi, Y., Kohnoe, S., and Sugimachi, K. 1996a. Clinical significance of occult micrometastasis in lymph nodes from patients with early gastric cancer who died of reccurence. *Surgery 119*:397–402.

Maehara, Y., Yamamoto, Y., Oda, S., Baba, H., Kusumoto, T., Ohno, S., Ichiyoshi, Y., and Sugimachi, K. 1996b. Cytokeratin-positive cells in bone marrow for identifying distant micrometastasis of gastric cancer. *Br. J. Cancer 73*:83–87.

Min, C.J., Tafra, L., and Verbanac, K.M. 1998. Identification of superior markers for polymerase chain reaction detection of breast cancer metastases in sentinel lymph nodes. *Cancer Res. 58*:4581–4584.

Molnar, B., Sipos, F., Galamb, O., and Tulassay, Z. 2003. Molecular detection of circulating cancer cells. Role in diagnosis, prognosis and follow-up of colon cancer patients. *Dig. Dis. 21*:320–325.

Mori, M., Mimori, K., Ueo, H., Karimine, N., Barnard, G.F., Sugimachi, K., and Akiyoshi, T. 1996a. Molecular detection of circulating solid carcinoma cells in the peripheral blood: the concepts of early systemic disease. *Int. J. Cancer 68*:739–743.

Mori, M., Mimori, K., Ueo, H., Tsuji, K., Shiraishi, T., Barnard, G.F., Sugimachi, K., and Akiyoshi, T. 1996b. Clinical sigificance of molecular detection of carcinoma cells in lymph nodes and peripheral blood by reverse transcription-polymerase chain reaction in the patients with gastrointestinal or breast carcinomas. *J. Clin. Oncol. 16*:128–132.

Moscinski, L.C, Trudeau, W.L., Fields, K.K., and Elfenbein, G.J. 1996. High-sensitivity detection of minimal residual breast carcinoma using the polymerase chain reaction and primers for cytokeratin 19. *Diag. Mol. Pathol. 5*:173–180.

Nozawa, H., Watanabe, T., Ohnishi, T., Tada, T., Tsurita, G., Sasaki, S., Kitayama, J., and Nagawa, H. 2003. Detection of cancer cells in mesenteric vein and peripheral vessels by measuring telomerase activity in patients with colorectal cancer. *Surgery 134*: 791–798.

Oki, E., Maehara, Y., Tokunaga, E., Shibahara, K., Hasuda, S., Kakeji, Y., and Sugimachi, K. 2002. Detection of disseminated cancer cells in bone marrow of gastric cancer using real time quantitative reverse transcriptase polymerase chain reaction. *Cancer Lett. 188*:191–198.

Olsson, C.A., de Vries, G.M., Buttyan, R., and Katz, A.E. 1997. Reverse transcriptase-polymerase chain reaction for prostate cancer. *Urol. Clin. North. Am. 24*:367–378.

Pantel, K., Dickmanns, A., Zippelius, A., Klein, C., Shi, J., Hoechtlen-Vollmar, W., Schlimok, G., Weckermann, D., Oberneder, R., Fanning, E., and Riethmuller, G. 1995. Establishment of micrometastatic carcinoma cell lines: a novel source of tumor cell vaccines. *J. Natl. Cancer Inst. 87*: 1162–1168.

Price, D.K., Clontz, D.R., Woodard, W.L. 3rd., Kaufman, J.S., Daniels, J.M., Stolzenberg, S.J., and Teigland, C.M. 1998. Detection and clearance of prostate cells subsequent to ultrasound-guided needle biopsy as determined by multiplex nested reverse transcription chain reaction assay. *Urology 52*:261–266.

Putz, E., Witter, K., Offner, S., Stosiek, P., Zippelius, A., Johnson, R., Zahn, R., Riethmuller, G., and Pantel, K. 1999. Phenotypic characteristics of cell lines derived from disseminated cancer cells in bone marrow of patients with solid epithelial tumors: establishment of working models for human micrometastasis. *Cancer Res. 59*:241–248.

Salvadori, B., Squicciarni, P., and Rovini, D. 1990. Use of monoclonal antibody Mbr1 to detect micrometastases in bone marrow specimens of breast cancer patients. *Eur. J. Cancer 26*: 865–867.

Schlimock, G. and Riethmuller, G. 1990. Detection, characterization and tumorigenecity of disseminated tumor cells in human bone marrow. *Semin. Cancer Biol. 1*:207.

Schmidt, B., Anastasiadis, A.G., Seifert, H.H., Franke, K.H., Oya, M., and Ackermann, R. 2003. Detection of circulating prostate cells during radical prostatectomy by standardized PSMA RT-PCR: association with positive lymph nodes and high malignant grade. *Anticancer Res. 23*:3991–3999.

Schoenfeld, A., Kruger, K.H., Gomm, J., Sinnett, H.D., Gazet, J.C., Sacks, N., Bender, H.G., Luqmani, Y., and Coombes, R.C. 1997. The detection of micrometastases in the peripheral blood and bone marrow of patients with breast cancer using immunohistochemistry and reverse transcriptase polymerase chain reaction for keratin 19. *Eur. J. Cancer 33*:854–861.

Schoenfeld, A., Luqmani, E., Smit, D., Oreilly, S., Shousha, S., and Sinnett, H.D. 1994. Coombes Rc detection of breast cancer micrometastases in axillary lymph-nodes by using polymerase chain-reaction. *Cancer Res. 54*:2986–2990.

Seiden, M. and Sklar, J.L. 1996. PCR and RT-PCR-based methods of tumor detection: potential applications and clinical implications. *Important Adv. Oncol.* 191–204.

Shen, R., Su, Z., Olsson, C.A., and Fisher, P.B. 1995. Identification of the human prostatic carcinoma oncogene PTI-1 by rapid expression cloning and differential RNA display. *Proc. Natl. Acad. Sci. USA 92*:6778–6782.

Singletary, S.E., Larry, L., Tucker, S.L., and Spitzer, G. 1991. Detection of micrometastatic tumor cells in bone marrow of breast carcinoma patients. *J. Surg. Oncol. 47*:32–36.

Slade, M.J., Smith, B.M., Sinnett, H.D., Cross, N.C., and Coombes, R.C. 1999. Quantitative polymerase chain reaction for the detection of micrometastases in patients with breast cancer. *J. Clin. Oncol. 17*:870–879.

Soeth, E., Roder, C., Juhl, H., Kruger, U., Kremer, B., and Kalthoff, H. 1996. The detection of disseminated tumor cells in bone marrow from colorectal-cancer patients by a cytokeratin-20-specific nested reverse-transcriptase-polymerase-chain reaction is related to the stage of disease. *Int. J. Cancer 69*: 278–282.

Sokoloff, M.H., Tso, C.L., Koboo, R., Nelson, S., Ko, J., Dorey, F., Figlin, R.A., Pang, S., deKernion, J., and Belldegrun, A. 1996. Quantitative polymerase chain reaction does not improve preoperative prostate cancer staging: a clinicopathological molecular analysis of 121 patients. *J. Urol. 56*:1560–1566.

Soria, J.C., Gauthier, L.R., Raymond, E., Granotier, C., Morat, L., Armand, J.P., Boussin, F.D., and Sabatier, L. 1999. Molecular detection of telomerase-positive circulating epithelial cells in metastatic breast cancer patients. *Clin. Cancer Res. 5*:971–975.

Sun, Y., Lin, J., Katz, A.E., and Fisher, P.B. 1997. Human prostatic carcinoma PTI-1 is expressed in human tumor cell lines and prostate carcinoma patient blood samples. *Cancer Res. 57*:18–23.

Thorban, S., Roder, J.D., Nekarda, H., Funk, A., Siewert, J.R., and Pantel, K. 1996a. Immunocytochemical detection of disseminated tumor cells in the bone marrow of patients with esophageal carcinoma. *J. Natl. Cancer Inst. 88*:1222–1227.

Thorban, S., Roder, J.D., Pantel, K., and Siewert, J.R. 1996b. Immunocytochemical detection of isoloted epithelial tumor cells in bone marrow of patients with pancreatic carcinoma. *Am. J. Surg. 172*:297–298.

Tokunaga, E., Ishida, M., Kimura, Y., and Maehara, Y. 2003. Correlation with bone metastasis and high expression of CK 19 mRNA measured by quantitative RT-PCR in the bone marrow of breast cancer patients. *Breast J. 9*:440–442.

Tokunaga, E., Maehara, Y., Oki, E., Koga, T., Kakeji, Y., and Sugimachi, K. 2000. Application of quantitative RT-PCR using "TaqMan" technology to evaluate the expression of CK 18 mRNA in various cell lines. *J. Exp. Clin. Cancer Res. 19*:375–381.

Ulmer, A., Schmidt-Kittler, O., Fischer, J., Elwanger, U., Rassner, G., Riethmuller, G., Fierlbeck, G., and Klein, C.A. 2004. Immunomagnetic enrichment, genomic characterization, and prognostic impact of circulating melanoma cells. *Clin. Cancer Res. 15*:531–537.

Watson, M.A. and Fleming, T.P. 1996. Mammaglobin, a mammary-specific member of the uteroglobin gene family, is overexpressed in human breast cancer. *Cancer Res. 56*:860–865.

Weitz, J., Kienle, P., Magener, A., Koch, M., Schrodel, A., Willeke, F., Autschbach, F., Lacroix, J., Lehnert, T., Herfarth, C., and von Knebel Doeberitz, M. 1999. Detection of disseminated colorectal cancer cells in lymph nodes, blood and bone marrow. *Clin. Cancer Res. 5*:1830–1836.

Wong, I.H., Zhang, J., Lai, P.B., Lau, W.Y., and Lo, Y.M. 2003. Quantitative analysis of tumor-derived methylated p16INK4a sequences in plasma, serum, and blood cells and hepatocellular carcinoma patients. *Clin. Cancer Res. 9*:1047–1052.

Wood, D.P. and Banerjee, M. 1997. Presence of circulating prostate cells in the bone marrow of patients undergoing radical prostatectomy is predictive of disease free survival. *J. Clin. Oncol. 15*:3451–3457.

Wulf, G.G., Jurgens, B., Liersch, T., Gatzemeier, W., Rauschecker, H., Buske, C., Hufner, M., Hiddemann, W., Wormann, B. 1997. Reverse transcriptase/polymerase chain reaction analysis of parathyroid hormone-related protein for the detection of tumor cell dissemination in the peripheral blood and bone marrow of patients with breast cancer. *J. Cancer Res. Clin. Oncol. 123*:514–521.

Wyld, D.K., Selby, P., Perren, T.J., Jonas, S.K., Allen-Mersh, T.G., Wheeldon, J., and Burchill, S.A. 1998. Detection of colorectal cancer cell in peripheral blood by reverse-transcriptae polymerase chain reaction for cytokeratin 20. *Int. J. Cancer 79*:288–293.

Yu, JJ., Brennan, M., Christos, P., Osborne, M.P., Hoda, S., and Simmons, R.M. 2004. Bone marrow micrometastases and adjuvant treatment of breast cancer. *Breast J. 10*:181–185.

Zach, O., Kasparu, H., Krieger, O., Hehenwarter, W., Girschikofsky, M., and Lutz, D. 1999. Detection of circulating mammary carcinoma cells in the peripheral blood of breast cancer patients via a nested reverse transcriptase polymerase chain reaction assay for mammaglobin mRNA. *J. Clin. Oncol. 17*:2015–2019.

Zehentner, B.K. and Carter, D. 2004. Mammaglobin: a candidate diagnostic marker for breast cancer. *Clin. Biochem. 37*:249–257.

This Page Intentionally Left Blank

7

Circulating Cancer Cells: Flow Cytometry, Video Microscopy, and Confocal Laser Scanning Microscopy

Christoph Heyder, Eva Gloria-Maercker, Wolfgang Hatzmann, Kurt S. Zänker, and Thomas Dittmar

Introduction

Cancer as a disease is described in the earliest medical records found in the history of mankind, dating back to ancient Egypt. The term "cancer" is attributed to the Greek physician Hippocrates and is derived from bizarre "crablike" growth forms of tumors (*karkinoma* is the Greek word for *crab*). Today, cancer is the second most prevalent cause of death, after heart disease, in the industrialized world, and the formation of metastasis is the primary cause of death in cancer. Metastasizing tumor cells must traverse natural barriers, such as connective tissue components and organ epithelia at multiple stages of the metastatic process. The events leading to metastasis can be summarized as follows: 1) detachment from the primary tumor, 2) accession of the lymphatic or blood circulatory system, 3) survival in the circulation, 4) arrest at distant sites, 5) transfer of cancer cells across the vessel wall into the parenchymal tissue, and 6) tumor growth at the secondary site (Figure 11).

The process of extravasation, the active migration of tumor cells across the endothelial barrier, has been described as a rate-regulating event in metastasis (Haier *et al.,* 2003; Orr *et al.,* 2000). Thereby, it can be subdivided into the following steps: 1) adhesion of tumor cells to the vascular endothelium, 2) transmigration across the endothelial lining and the underlying basement membrane, and 3) invasion of the surrounding tissue. Our understanding of the sequential steps of tumor cell extravasation is mainly based on *in vitro* models using fixed sample preparations and electron microscopy (Akedo *et al.,* 1989). However, it is inherent in this approach that the time dimension of the dynamic cellular and molecular interactions cannot be resolved. Recent investigations overcome this restriction by using fluorescent-labeled tumor cells, which allows for the time series recording of metastatic processes using intravital microscopy (Al-Mehdi *et al.,* 2000). Here, we will describe an *in vitro* model to study the extravasation of tumor cell clusters. The advantage of this *in vitro* model is that the transmigration process is viewed perpendicular to the endothelial monolayer, which allows visualization of endothelial cell–tumor cell interactions with the aid of fluorescence staining and live microscopy. By using this *in vitro* extravasation assay we were able to see the transendothelial migration of tumor spheroids in real-time and, more importantly, we could see that

Handbook of Immunohistochemistry and *in situ* Hybridization of Human Carcinomas, Volume 4: Molecular Genetics, Gastrointestinal Carcinoma, and Ovarian Carcinoma

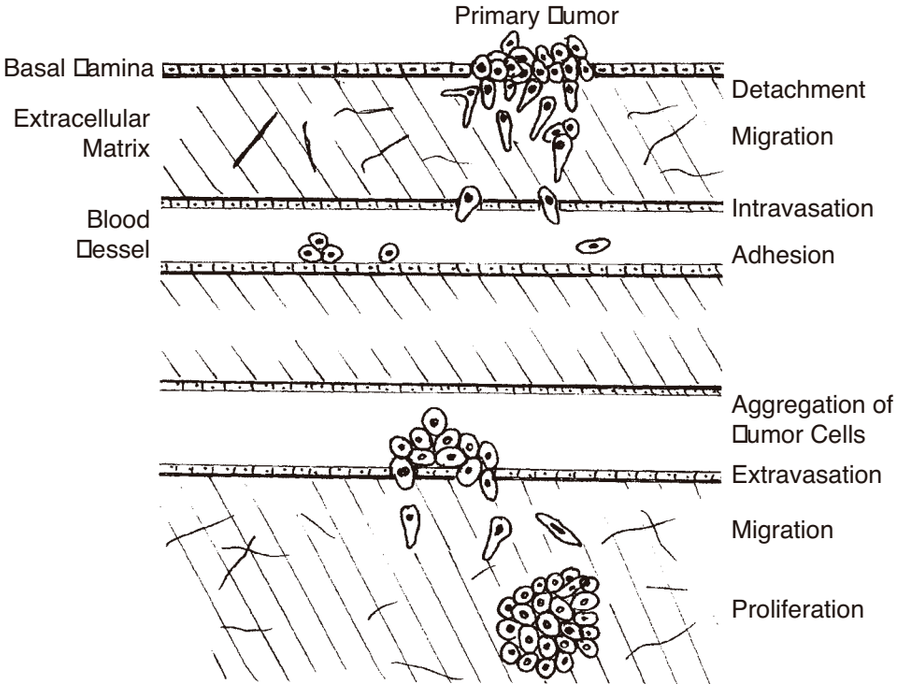

Figure 11. Metastasis cascade. The schematic overview summarizes the single steps leading to metastasis formation. The metastasis cascade is initiated by detachment of single tumor cells or cell clusters from the primary tumor and subsequent migration through the extracellular matrix. To spread to distant organ metastazing tumor cells or cell clusters must gain access to the circulatory blood vessel system. Finally, tumor cells or cell clusters adhere to the endothelium at distant sites and subsequently extravasate into the underlying tissue to form a secondary tumor.

extravasation of tumor spheroids leads to irreversible damage of endothelial cells located at the infiltration site.

Also, see Chapter 6, in Part I discussing immunohistochemistry and polymerase chain reaction of circulating cancer cells in cancers of breast, prostate, and gastrointestine.

MATERIALS AND METHODS

Protocol 1. Isolation of human umbilical cord endothelial cells (Jaffe *et al.,* 1973).

1. Dissolve 100 mg collagenase IV (Sigma-Aldrich) in 50 ml Hank's Balanced Salt Solution (HBSS; PAA) and prewarm the solution to 37°C.
2. Wash the vein of an umbilical cord 2× with 10 ml phosphate buffer saline (PBS). Use a syringe for this step. Note: Only umbilical cords from cesarean delivery should be used because they are sterile. Umbilical cords can be stored in PBS at 4°C prior to isolation of endothelial cells for 24–48 hr.
3. Close one end of the umbilical cord with a clamp and inject 20 ml of prewarmed collagenase intravenous (IV) solution into the vein. Use a syringe for this step. Close the other end with a clamp and incubate for 15 min at room temperature.
4. Remove one clamp and transfer the collagenase IV solution (now containing endothelial cells) into a 50 ml Falcon tube prefilled with 5 ml fetal calf serum (FCS) to stop collagenase activity. Wash the vein 1× with 10 ml PBS. Use a syringe for this step.
5. Centrifuge the cells (310 × g, 10 min, room temperature) and wash 2× with PBS.
6. Seed human umbilical vein endothelial cells (HUVEC) in either three T25- or one T75-cell culture flask(s) HUVECs are maintained in endothelial cell growth media (ECGM; PAA) containing 2% FCS, 0.4% ECG supplement/heparin, 0.1 ng/ml epidermal growth factor (EGF), 1 ng/ml basic fibroblast growth factor (FGF), and 1 µg/ml hydrocortisone in a humidified atmosphere at 37°C and 5% CO_2.
7. The following day, unattached cells are discarded by removal of supernatant. Wash cells 3× with PBS and add fresh culture media.
8. Replace culture media every second day until HUVECs reach a confluency of 80%. HUVEC can

be passaged in 1:3 ratio using 0.25%/0.02% Trypsin ETDA (ethylene diamine tetracetic acid) (Sigma). HUVECs up to passage 2 were used for experiments.

Protocol 2. Quantification of transendothelial tumor cell migration through a HUVEC monolayer by flow cytometry.

1. Coat transwell inserts (pore size: 8.0 µm; Becton-Dickenson Falcon) with 0.1% gelatine solution (Sigma) or Vitrogen 100 (Nutagon) and place them in 12-well plate. Air-dry transwell inserts under sterile conditions and rinse 3× with PBS/HBSS.
2. Seed 1×10^5 HUVEC per transwell insert and cultivate cells in ECGM until they form a confluent monolayer.
3. Seed tumor cells ($2.5–5 \times 10^5$) in a 6-well plate and incubate overnight.
4. Stain tumor cells with CellTracker Green. Prepare staining solution by dissolving 0.8 µM CellTracker Green (Molecular Probes) in 1.5 ml of serumfree media and prewarm to 37°C. Replace old media with staining solution and incubate for 30 min at 37°C. Replace staining solution with fresh media (containing supplements) and incubate again for 30 min at 37°C.
5. Add 2.5×10^4 CellTracker Green–stained tumor cells to HUVEC in the upper compartment and incubate cells in a humidified atmosphere at 37°C and 5% CO_2 for 16 hr.
6. Aspirate the media in the upper compartment and clean the upper side of the membrane containing the HUVEC monolayer with a cotton swab.
7. Aspirate the media in the lower compartment and store on ice. Remove the transmigrated cells that adhered to the underside of the porous membrane in the lower compartment by trypsinization for 10–12 min. Stop trypsinization by addition of 20% FCS (final concentration) and combine with the media from the lower compartment.
8. Wash samples 2× with PBS, resuspend in 350 µl of PBS, and store on ice prior to flow cytometry.
9. Determine number of CellTracker Green–stained tumor cells by flow cytometry for a predefined time (1–2 min) at a constant flow rate or, alternatively, by determining the fluorescence intensity using a fluorimeter using a standard curve.

Protocol 3. Generation of tumor cell spheroids.

1. Add 1.5 g agar (Agar Noble, DIFCO Laboratories) to 20 ml of deionized water, autoclave, and add 80 ml of prewarmed (56°C) RPMI 1640 media.
2. Use 9 ml of the agar solution per one T75-cell culture flask.

Note: Use only cell culture flasks without filter caps.

3. Air-dry cell culture flasks under sterile conditions for approximately 2 hr.
4. Store agar-coated cell culture flasks at 4°C. Seal the cap with parafilm.
5. Resuspend harvested tumor cells (2×10^6) in 25 ml of the appropriate media and add to an agar-coated cell culture flask. Incubate the cells in a humidified atmosphere at 37°C and 5% CO_2 and cultivate until spheroids have formed. Change media every second or third day.
6. Tumor spheroids of 5–200 cells were used for experiments.

Protocol 4. Analysis of transendothelial migration of tumor cell spheroids by timelapse video microscopy.

1. Build transmigration chambers by mounting a coverslip on a glass slide by use of separating U-shaped paraffin/petroleum jelly barrier of 1–1.5 min thickness (Figure 12). Prepare a minimum number of 10 transmigration chambers per experiment.
2. Prepare collagen solution by dissolving liquid collagen type I (Vitrogen 100, Nutagon) in ECGM (pH 7.2–7.4) to a final collagen concentration of 1.67 mg/ml.
3. Fill transmigration chambers with 100–150 µl of collagen solution, store chambers in an upright position, and incubate in a humidified atmosphere at 37°C and 5% CO_2 until the collagen is polymerized. Avoid the generation of air bubbles in the collagen lattice.
4. Seed 1×10^4 HUVEC on the collagen lattice. Fill transmigration chambers with ECGM and incubate them overnight in an upright position under the culturing conditions stated earlier, allowing the cells to settle down, to spread, and to build a confluent monolayer.
5. Harvest tumor cell spheroids (see Protocol 3), wash 2× with PBS at low speed (80 rcf), and resuspend carefully in ECGM.

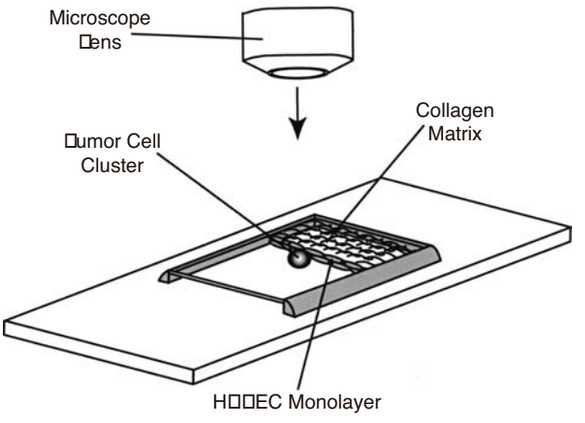

***Figure 12.* Transmigration chamber.** Experimental setup for monitoring extravasation events by confocal laser scanning microscopy.

6. Add 50 µl of collagen solution (see **Step 2**) to the HUVEC monolayer and apply single spheroids with a GelLoader tip to the collagen solution. Store the transmigration in an upright position and incubate in a humidified atmosphere at 37°C and 5% CO_2 until the collagen is polymerized.

Note: It is important that the collagen solution is still liquid when the spheroids are applied. Otherwise they will not sink into the collagen solution close to the HUVEC monolayer.

7. Fill up transmigration chambers with ECGM and seal the fourth side with wax.

8. Place transmigration chambers under a light microscope, under constant temperature conditions (37°C), and record transendothelial migration by time lapse using a factor of 1800 (1 hr real-time is compressed to 2 seconds).

Protocol 5. Analysis of transendothelial migration of tumor cell spheroids by confocal laser scanning microscopy.

1. Prepare transmigration chambers as described in Protocol 4 **Steps 1–4.**

2. Prepare a 0.8 µM Calcein AM (Molecular Probes) staining solution.

3. Remove old media carefully using a GelLoader tip, add Calcein AM staining solution, and incubate for 90 min at 37°C. Carefully wash Calcein AM–stained HUVEC 3× with ECGM.

4. Harvest tumor cell spheroids (see Protocol 3), wash 1× with PBS at low speed (80 rcf), and resuspend spheroids carefully in 500 µl Diluent C (Sigma).

5. Prepare 500 µl of a 2 µM PKH-26 (dissolved in Diluent C; Sigma) staining solution, add the staining solution to the tumor spheroid suspension, and incubate for 4 seconds.

6. Stop staining reaction by applying 500 µl of heat-inactivated FCS. Wash tumor spheroids carefully 3× with culture media supplemented with 10% FCS.

7. Apply single PKH-26–stained tumor spheroids to the Calcein AM–stained HUVEC monolayer. Incubate the transmigration chambers in an upright position at 37°C and 5% CO_2 for 30 min to allow the tumor spheroids to settle on the HUVEC monolayer.

8. Seal the fourth site with wax, place transmigration under a confocal laser scanning microscope, and keep them at a temperature of 37°C. Record images at specified time intervals.

Protocol 6. Visualization of apoptotic events during transendothelial migration of tumor cell spheroids by confocal laser scanning microscopy.

1. Prepare transmigration chambers as described in Protocol 4 **Steps 1–4.**

2. Prepare tumor cell spheroids as described in Protocol 3 and apply a single tumor spheroid to the endothelial monolayer.

3. Add Annexin V-Cy3 conjugate (final concentration: 0.8 ng/ml; Sigma) and Calcein AM (final concentration: 2 µM; Molecular Probes) to the sample to distinguish apoptotic cells from necrotic cells.

Note: The plasma membrane integrity of early apoptotic cells is in an uncompromised stage. Therefore, apoptotic cells are labeled by Annexin V-Cy3 (plasma membrane) as well as by the vital-dye Calcein AM (cytosol).

4. Incubate the transmigration chambers in an upright position at 37°C and 5% CO_2 for 30 min to allow the tumor spheroids to settle on the HUVEC monolayer.

5. Seal the fourth site with wax, place transmigration under a confocal laser scanning microscope, and keep them at a temperature of 37°C. Record images at specified time intervals.

Protocol 7. Visualizing tumor metastasis by *in vivo* imaging.

1. Generate tumor cell lines stably transfected with either enhanced green fluorescent protein (EGFP) or firefly luciferase by using commercially available vectors.

2. Screen EGFP-transfected cells by flow cytometry and luciferase-transfected cells by using a luminometer or a cooled charge-coupled device (CCD) camera (C4742-98-24LWG; Hamamatsu Photonics, Herrsching, Germany).

3. Anesthetize immunodeficient mice with Ketamin and inject EGFP or luciferase stable expressing cells.

Note: The number of cells that are injected into mice depends on the following: 1) the relative EGFP or luciferase expression of the stable transfected tumor cells, and 2) the tumorigenecity of the tumor cells. Therefore, different amounts of tumor cells should be tested first. In addition to this, luciferase activity could be viewed in both nude and nonnude mice, whereas EGFP fluorescence could only be viewed in nude mice as a result of the autofluorescence of hairs and the hair follicles.

4. Breed mice for a specified time interval. Check tumor status once a week by *in vivo* imaging. Before imaging, anesthetize mice with Ketamin (20 mg/kg) and place them in a light-tight chamber. If luciferase-expressing tumors are used, inject an aqueous solution of the substrate luciferin (50 mM; Molecular Probes) into the peritoneal cavity 5 min before imaging. Take a grayscale body-surface reference image either by slightly opening the door or by switching on the internal light source.

5. Close the door and shut down the light in the room. Collect the EGFP fluorescence or the photons emitted from luciferase using a cooled camera

(Hamamatsu Photonics). Generate a pseudocolor image (blue least intense and red most intense) using the WASABI Imaging Software (Hamamatsu Photonics).

RESULTS AND DISCUSSION

Flow Cytometry Based on Quantification of Transendothelial Migration of Various Tumor Cell Lines

Transmigration of malignant cells across the endothelial barrier at the site of secondary tumor formation comprises strong interactions of transmigrating tumor cells with vascular endothelium. Many studies concerning the transendothelial migration of tumor cells are performed using modified Boyden chamber, or transwell, assays (Boyden, 1962). The advantage of these systems is their relative simplicity, which reduces the number of involved variables to a minimum, thereby allowing the isolated investigation of selected aspects of adhesive or migratory processes. Cells of interest are seeded into the upper compartment, the system is incubated for a specified time interval (mostly overnight), and on the following day transmigrated cells are stained with hematoxilin and subsequently counted. However, it has to be considered that the analysis of transendothelial migration is necessarily carried out in a two-cell system consisting of endothelial cells and the appropriate cell type, for which transmigration capacity is of interest. Because endothelial cells can migrate, which in turn is a prerequisite in angiogenesis, the to-be-counted fraction of transmigrated cells may be contaminated by an unknown number of endothelial cells. For instance, we observed in control experiments of transendothelial migration studies that an average amount of 3.6% of HUVEC migrated into the lower compartment (Figure 13).

Thus, it is recommended that one or both cell type(s) are stained for subsequent analysis to exclude HUVEC contamination. We recommend that the cells (both cell types or solely one cell type) be stained with fluorescent dyes because the usage of such markers allows for the subsequent quantification by flow cytometry or by fluorimetry. However, it is also possible to quantify the number of transmigrated cells by using a fluorescence microplate reader. The advantage of both systems is that all transmigrated cells are quantified automatically, which has less risk of error than if transmigrated cells are counted manually. Several fluorescent dyes that are suitable for live imaging can be used.

Lipophilic tracers such as DiD or PKH-26 label cells by lateral diffusion in the plasma membrane.

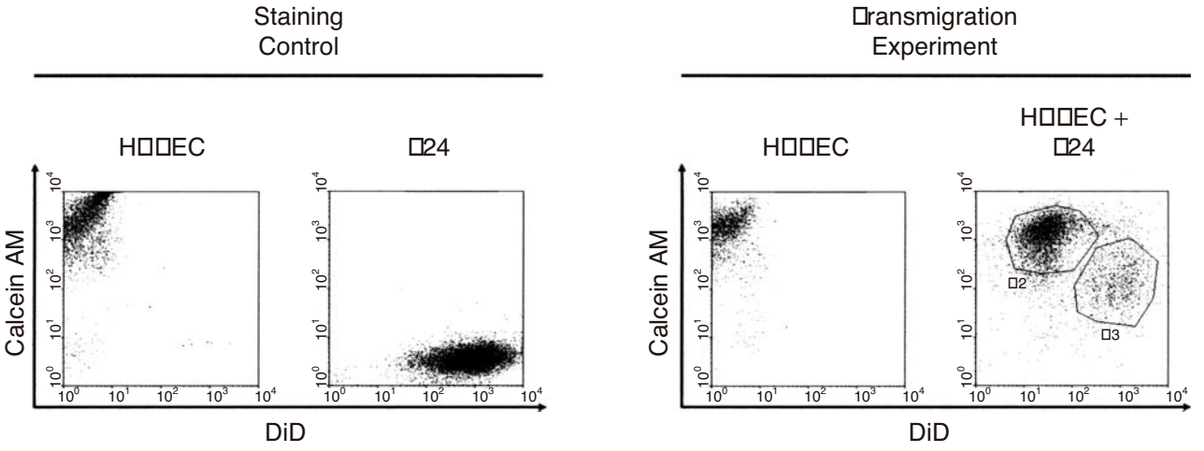

Figure 13. Intercellular dye transfer during extravasation of DiD-labeled T24 tumor cells across the HUVEC (human umbilical cord vein endothelial cell) monolayer stained with Calcein AM. Extravasation of tumor cells can be quantified by flow cytometry. However, because the analysis of transendothelial migration is necessarily carried out in a two-cell system and HUVECs are also migratory active, one or both cell types have to be stained with vital dyes for subsequent analysis to exclude HUVEC contamination. Depending on the used dyes it is possible that an intercellular dye transfer can occur, which might result in false-positive findings. Here, HUVEC and T24 tumor cells were stained with Calcein AM and DiD, respectively. Both cell types display a bright fluorescence (staining control). During the transmigration process an intercellular dye transfer occurred in both cell types indicated by originally Calcein AM–labeled HUVECs, which now display a faint DiD fluorescence and vice versa.

Although the plasma membrane–bound dyes should not transfer from labeled to unlabeled cells, some transfer could occur when the membrane is disrupted or if clumps of nonbound dyes remain on the cell surface. Acetoxymethyl (AM) ester derivates of fluorescent indicators, such as Calcein Green AM, are uncharged molecules that can permeate cell membranes. Once inside the cell, the lipophilic AM blocking groups are cleaved by nonspecific esterases, resulting in a charged form that leaks out of cells far more slowly than its parent compound does. As a consequence of this, unlabeled cells are stained with both uncleaved and cleaved Calcein Green AM. An example of this intercellular dye transfer in a transendothelial migration assay is shown in Figure 13. Here, HUVEC were stained with Calcein Green AM, and T24 cells were labeled with DiD. After the specified time interval, cells that moved into the lower compartment were collected and analyzed by flow cytometry. From flow cytometry data it can be clearly deduced that originally Calcein Green AM–labeled HUVEC now display a faint DiD fluorescence and vice versa. However, because the sensitivity of a flow cytometer is very high, it is possible to titrate different concentrations of these fluorescent dyes to minimize the intercellular dye transfer.

We obtained better results and observed no intercellular dye transfer when cells were stained with a fluorescent dye that is covalently linked to intracellular structures. An example for such fluorescent dye is the CellTracker probe (Molecular Probes). Once a CellTracker probe has entered a cell, its chloromethyl group reacts with free thiol residues of amino acids. As a result of this covalent linkage to cytoplasmatic proteins, the CellTracker probe stays in the cell and is not transferred to adjacent cells in a population as would be the case for AM ester derivates of fluorescent indicators or lipophilic tracers.

Here, we used this method to determine the transmigration rates of different tumor cell lines. As mentioned earlier, the extravasation of tumor cells is a rate-limiting step in metastasis, and a broad variation concerning the ability to transmigrate through the endothelial barrier is observed between cell lines and even among single cells. As a consequence, it is recommended that the respective cell line or cell lines are tested in regard to their transendothelial migration capacity first. Five different tumor cell lines were tested for their ability to transmigrate across an endothelial monolayer in a transwell assay setup (Figure 14). The urinary bladder carcinoma cell line T24 was the most effective in traversing the HUVEC monolayer, followed by the fibrosarcoma cell line HT-1080. The breast adenocarcinoma cell lines MDA-MB-468 and MCF-7 were also capable of transmigrating across the endothelial layer, although to a lesser extent. The colon carcinoma cell line SW480 showed the least transmigratory activity in this assay. These data clearly show the differences between tumor cell lines and their capacity for transmigration. Furthermore, the results demonstrate the feasibility of quantifying transendothelial migrating tumor cells using fluorescent dye–labeled cells combined with flow cytometry.

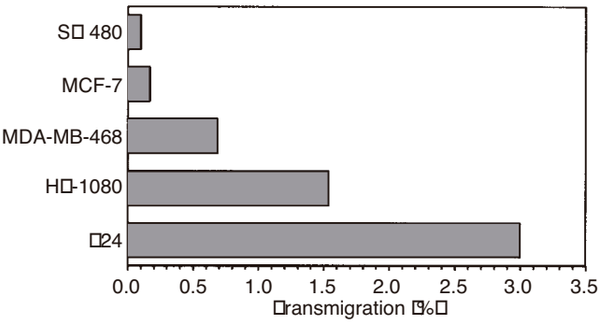

Figure 14. Endothelial transmigration of different tumor cell lines. Transmigration rates were determined using a transwell assay combined with subsequent flow cytometry–based quantification as described in Protocol 2. The urinary bladder carcinoma cell line T24 was the most active cell line (approximately 3%) in traversing a HUVEC (human umbilical cord vein endothelial cell) monolayer.

Investigating Transendothelial Migration of Tumor Cell Spheroids by Time-Lapse Video Microscopy

Transendothelial migration studies are mostly performed using modified Boyden chambers. However, regarding the dynamic, cross-wise influencing changes of regulatory events taking place during the extravasation process, a transmigration assay is necessary that allows continuous monitoring of transendothelial migration of tumor cells.

The three-dimensional collagen matrix migration assay allows for a continuous observation of an appropriate cell population. In this assay, cells are embedded within a three-dimensional collagen environment, and real-time cell migration is recorded by timelapse video microscopy and subsequently analyzed by computer-assisted cell tracking. A broad range of cell types can be analyzed using this system, including tumor cells (Dittmar *et al.,* 2002; Katterle *et al.,* 2004), immunocompetent cells (Dittmar *et al.,* 2000a), and stem cells (Weidt *et al.,* 2004). Furthermore, the advantage of this system is that it allows for the visualization of the dynamics of cell migration in real-time and changes

in the migration pattern on a single cell level (Weidt *et al.,* 2004).

Here, we used the three-dimensional collagen matrix migration assay for analyzing the dynamics of the transendothelial migration of a single MV3 tumor cell spheroid. MV3 tumor spheroids were embedded within a three-dimensional collagen lattice close to the endothelial monolayer as described in Protocol 4. To visualize the dynamics of transendothelial migrating tumor cells or cell clusters, the transmigration process is viewed perpendicular to the endothelial monolayer. The image sequence, which was recorded for 39 hr, is shown in Figure 15. After 3 hr in culture the MV3 tumor spheroid changed its morphology from a round shape toward a more oval shape. Furthermore, single MV3 cells (see Figure 15, 3 hr, *black arrowheads*) already started to migrate out of the spheroid body. An initial contact between the MV3 tumor spheroid and the endothelial monolayer is formed after 6 hr. We observed that the embedded MV3 tumor spheroid divided itself into two parts, which takes about 9 hr (see Figure 15, 9–18 hr, *black and white arrows*). The larger MV3 tumor mass moved away from the endothelial monolayer deeper into the collagen lattice. The minor MV3 tumor mass resides close to the HUVEC monolayer. Approximately 12 hr after starting the experiment, the first single MV3 tumor cells successfully transmigrated through the HUVEC monolayer (see Figure 15, 12 hr; *white arrowheads*). In the following, an increased number of MV3 tumor cells passed the endothelial monolayer and moved into the underlying collagen lattice. Because of the mass of transendothelial migrating MV3 cells it can be assumed that transendothelial migration of tumor cells goes along with an irreversible damage of the endothelial monolayer. In summary, these results clearly demonstrate the dynamics of the transendothelial migration of tumor spheroids and the advantages of the three-dimensional collagen matrix assay combined with timelapse video microscopy, which cannot be resolved using a simple modified Boyden chamber assay.

Investigating Transendothelial Migration of Tumor Cell Spheroids by Confocal Laser Scanning Microscopy

The study of transendothelial migration of tumor spheroids by light microscopy combined with timelapse video microscopy reveals the dynamics of this rate-limiting process of the metastasis cascade. To date, there are contradicting reports regarding the fate of endothelial cells in the extravasation sequence. It is a matter of controversy whether the retraction of endothelium is a reversible phenomenon as described for melanoma cells (Nicolson, 1988) or if endothelial cells are permanently impaired during the process of tumor cell extravasation (Kebers *et al.,* 1998; Voura *et al.,* 1998).

Therefore, we analyzed the infiltration of the endothelial monolayer by tumor spheroids in real-time by confocal laser scanning microscopy. Endothelial cells and tumor spheroids were stained with fluorescent dyes (endothelial cells: calcein AM; T24 tumor spheroids: PKH-26) prior to analysis. Calcein Green AM remains in the cytosol after esterase-mediated cleavage of the AM group, and PKH-26 is a lipophilic tracer, which labels cells by lateral diffusion in the plasma membrane. As mentioned earlier, both fluorescent dyes are capable of intercellular dye transfer. However, because both cell types can be discriminated by their morphology, the intercellular dye transfer could be neglected in this assay.

The image sequences in Figure 16 show the transmigration process of a single T24 tumor spheroid through the endothelial monolayer. In Figure 16A only the endothelial cells were stained with Calcein Green AM, whereas in Figure 16B both endothelial cells and tumor spheroids were stained with Calcein Green AM and PKH-26, respectively. Overlay images were created using the appropriate channels. Both image sequences clearly indicate that the complete T24 tumor spheroid transmigrates across the endothelial monolayer within a time period of 4 hr. Approximately 90 min after addition of the T24 spheroid, tumor cells established a close contact to the apical surface of the endothelial cells. In Figure 16A and B the same T24 spheroid is shown but in different focal planes (step size 4 μm). One hour later, the endothelial cells showed a contracted morphology (see Figure 16A, B; *white arrows*) at the site of contact to the T24 tumor cell cluster, finally assuming an almost rounded shape after 3.5 hr (see Figure 16A, B; *yellow arrows*). During this time period, the T24 tumor spheroid completely invaded the collagen matrix beneath the endothelium, concomitant with a complete destruction of the endothelial layer at the site of infiltration. Single endothelial cells showed a rounded morphology with structures resembling membrane blebbing (see Figure 16B; *red arrows*). The cell-to-cell contacts between the endothelial cells were completely destroyed at the site of transmigration. The image sequences indicate that the T24 tumor spheroid established a close contact to the endothelium before this barrier was ruptured. The destruction of the endothelial monolayer was restricted locally to the site of transmigration and did not occur in more distant parts of the endothelium. This was verified at a lower magnification view (see Figure 16A).

For a better definition of the processes involved in the destruction of the endothelial monolayer, an

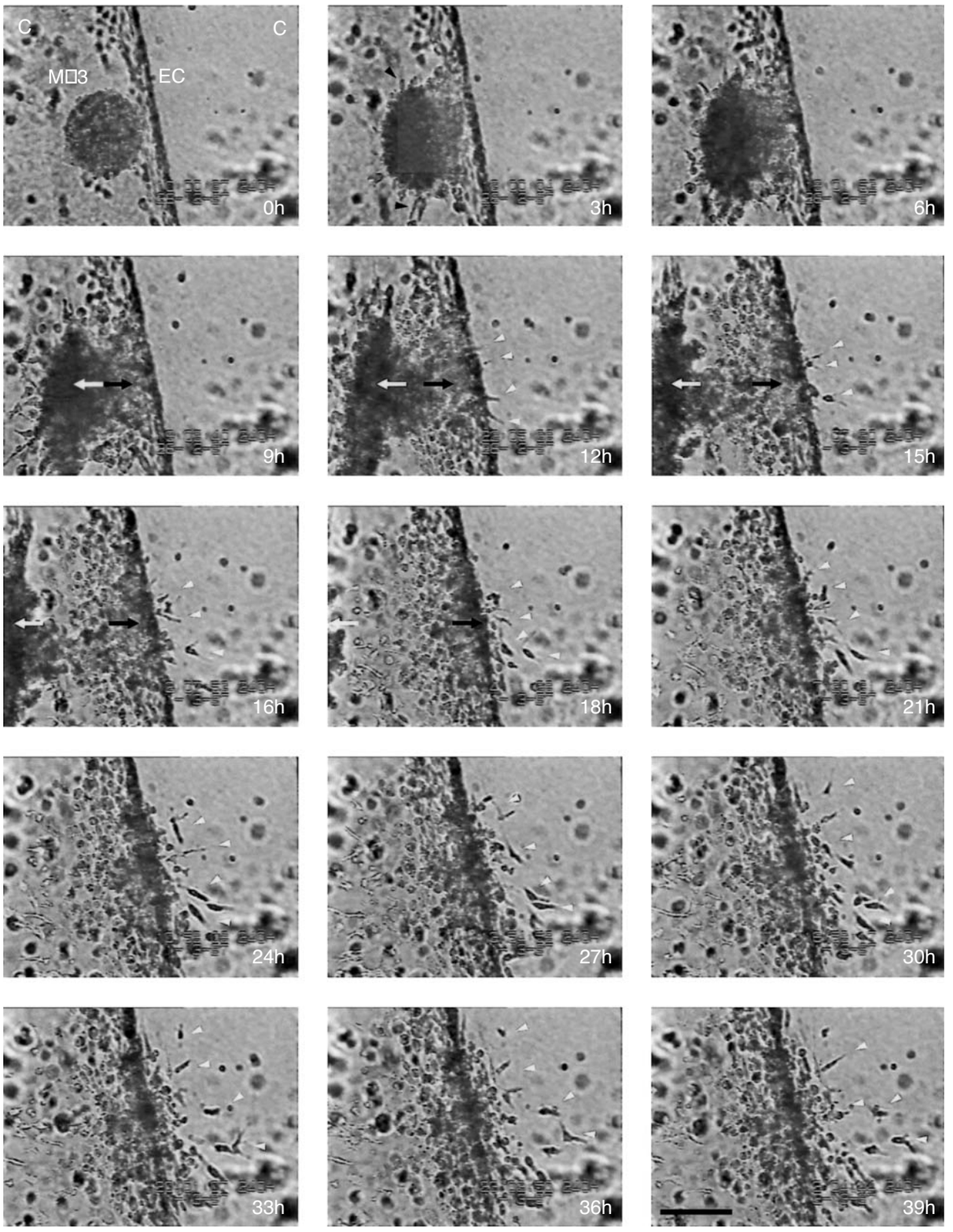
C
C
M□3
EC
0h
3h
6h
9h
12h
15h
16h
18h
21h
24h
27h
30h
33h
36h
39h

Figure 15. Time-lapse video microscopy image sequence reveals the dynamics of the extravasation process of a MV3 tumor spheroid. The three-dimensional collagen matrix migration assay allows for a continuous observation of an appropriate cell population. Because of the combination with time-lapse video microscopy and computer-assisted cell tracking this system allows for resolution and quantification of the dynamics cell migration and extravasation. Here, a MV3 melanoma spheroid was embedded within the three-dimensional collagen matrix close to a HUVEC (human umbilical cord vein endothelial cell) monolayer. To visualize the dynamics of extravasation, the transendothelial process is viewed perpendicular to the endothelial monolayer. The complete extravasation sequence was recorded for 39 hr. It is interesting, that the applied MV3 tumor spheroid divided itself into two parts (3–9 hr), whereby the larger spheroid mass moved away from the HUVEC monolayer deeper into the collagen lattice *(black arrows)*. The smaller MV3 tumor mass resides close to the HUVEC monolayer *(white arrows)*. Approximately 12 hr after starting the experiment, the first single MV3 tumor cells successfully transmigrated through the HUVEC monolayer (12 hr, *white arrowheads*). In the following, more MV3 tumor cells passed the endothelial monolayer. Because of the mass of transendothelial migrating MV3 cells it can be assumed that endothelial monolayer is irreversibly damaged at the extravasation site. The bar represents 150 μm. A movie file (Quicktime) of the complete image sequence can be viewed at www.uni-wh.de/immunology.

Annexin-V–based assay was conducted to test if endothelial cells undergo apoptosis or necrosis at the site of transmigration (see Figure 16C). During early stages of apoptosis, the phospholipid phosphatidylserine (PS) changes its position from the inner to the outer leaflet of the plasma membrane, where it can be detected by the PS-binding protein Annexin-V. Here, a red fluorescent Annexin-V-Cy3 conjugate was used in conjunction with Calcein Green AM staining. In early apoptosis, the plasma membrane integrity is still uncompromised, and cells are thus stained by Annexin-V-Cy3 (plasma membrane) and by Calcein Green AM (cytosol) simultaneously. Tumor cells (see Figure 16C; *blue arrow*) and endothelial cells (see Figure 16C; *white arrow*) were distinguished by their different morphology. After 3.5 hr, the tumor cell cluster was in the process of transmigrating across the endothelium into the underlying collagen matrix. The endothelium at the site of invasion was disintegrated and showed strong Annexin-V staining (red fluorescence). The retention of Calcein Green AM within the cytosol indicates that the plasma membrane of endothelial cells was still intact. In combination with Annexin-V staining, this is a typical indication for early apoptotic events (see Figure 16C; *yellow arrows*). Moreover, the formation of membrane blebs is visible, which is a characteristic morphologic, feature in apoptotic cell death. At a later stage, only the Annexin-V staining remains (red fluorescence), clearly indicating that the endothelial plasma membrane was damaged (see Figure 16C; *red arrows*). Thereby, the intracellular dye Calcein Green AM was released, leading to a solely red fluorescent signal from the endothelial cells at the site of tumor cell transmigration.

However, in our experiments, tumor-cell or cell-cluster transmigration through the endothelial barrier is a relatively rare event and, therefore, only a small number of tumor spheroids transmigrated successfully through the endothelial monolayer. For instance, most tumor spheroids established a close contact to the endothelial monolayer but did not transmigrate in the observed time period.

As a consequence, the investigation of tumor spheroid transmigration is a time-intensive procedure. However, the probability of observing a transmigration event can be raised 1) by using cells with a high transmigration efficiency, 2) if several tumor spheroids are applied to the endothelial monolayer, and 3) if several transmigration chambers are prepared. However, despite these limitations, the real-time visualization of tumor spheroid transendothelial migration by using the described *in vitro* model may provide new insights into the process of tumor cell extravasation and will help to develop new strategies to block this rate-limiting step in a cancer disease.

Visualizing Tumor Metastasis by *in vivo* Imaging

The initial site of tumor cell arrest during metastasis is effectively determined by size constraints, depending on the relative size of tumor cells and the capillaries. Thus, the observation that some tumors preferentially metastasize to certain organs may be explained by 1) anatomic criteria, such as the location of the next capillary bed, and by 2) the "seed and soil" hypothesis, which was originally postulated by Paget (Paget, 1989), where both "seed" (cancer cells) and "soil" (organ environment) contribute to an organ-specific pattern of secondary tumor formation (Chambers *et al.,* 2002).

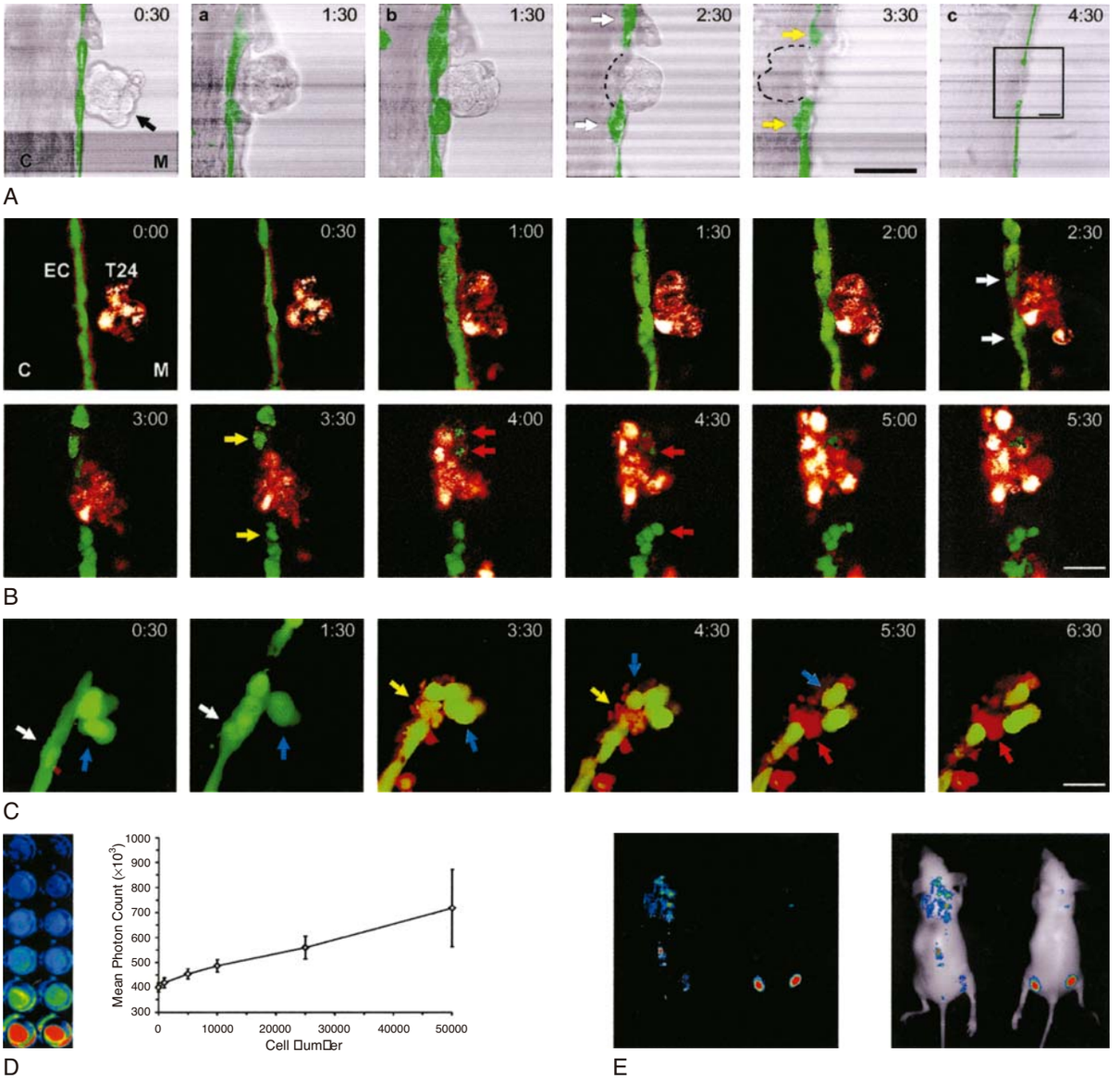

Figure 16. **Confocal laser scanning microscopy analysis of T24 tumor cell extravasation. A:** The endothelial monolayer was stained by Calcein AM *(green fluorescence)* and dissociates irreversibly in the course of tumor spheroid *(black arrow)* transmigration. The dotted line indicates the cell body mass of the invaded spheroid. The images (**a** and **b**) show a different focal plane (step size 4 µm) at 1:30 hr. The T24 spheroid established a close contact to the apical surface of the endothelial cell layer. **(c)** Lower magnification view at 4:30 hr showing that disruption of the HUVEC monolayer integrity is restricted to the extravasation site. **B:** T24 cell spheroids were stained with the lipophilic dye PKH-26 *(red fluorescence)*, whereas HUVEC were labeled by using Calcein AM *(green fluorescence)*. The image sequences clearly indicate that within a time period of 4 hr a complete tumor spheroid transmigrates across the endothelium. White arrows indicate the retraction process of endothelial cells at the invasion front of the tumor spheroid. Yellow and red arrows indicate rounded morphologies on endothelial cells with structures resembling membrane blebbing. **C:** HUVEC *(white arrows)* and T24 tumor spheroid *(blue arrow)* were stained by Calcein AM. Annexin-V-Cy3 labeling *(red fluorescence)* in conjunction with a strong green fluorescent signal from Calcein AM after 3.30 hr indicates that endothelial cells are triggered to undergo apoptosis *(yellow and red arrows)* at the site of tumor spheroid infiltration. **A, B, C:** Time is shown in hours; the bar represents 50 µm. Movie files (Quicktime) of the complete image sequences can be viewed at

www.uni-wh.de/immunology. **D:** Dilution series of HS578T-EGFP-MCS cells embedded within a three-dimensional collagen lattice. Cells were seeded in 96-well culture plates over a range of 0–50,000 cells. EGFP (enhanced green fluorescent protein) fluorescence was measured over a l second integration time. Red indicates the highest and blue indicates the lowest EGFP fluorescence intensity. The graph represents the mean photon count in relation to the cell number. **E:** Fluorescence of HS578T-EGFP-MCS cells in nude mice. Cells (*left mouse*: 5×10^5, *right mouse*: $l \times 10^6$) were injected into nude mice, and EGFP fluorescence was measured over a 5 second integration time. The left image shows the detected EGFP fluorescence in false colors, whereby red indicates the highest and blue indicates the lowest EGFP fluorescence intensity. The right image is an overlay image of the false color image and the appropriate background image.

Findings indicate that the guidance of metastasizing tumor cells or cell clusters is also controlled by chemokines. In general, chemokines play a pivotal role in regulating the immune response by attracting and guiding immune competent cells toward the inflammatory tissue. However, it was shown by Muller *et al.* (2001) that the metastatic pattern of breast tumors depended on the interaction between the chemokine SDF-lα, which is expressed by several tissues such as bone marrow, lung, liver, and brain, and its receptor CXCR4, which was expressed by breast cancer cells (Muller *et al.,*2001).

The investigation of the metastatic pattern of certain tumors can only be analyzed in a living organism. However, detection of neoplastic cells in current animal models of human disease requires a large number of target cells, and such models usually use the therapeutic end points of gross tumor growth or death of the animal. A general disadvantage of this common procedure is that the pattern of tumor growth and distribution in minimal residual states cannot be studied over time (Sweeney *et al.,* 1999). The use of bioluminescent or biofluorescent reporter genes such as the firefly luciferase or the EGFP, combined with highly sensitive camera systems overcomes these limitations. Both proteins can be expressed in a broad range of various cell types without altering the cellular phenotype. Once EGFP or firefly luciferase–expressing tumor cells are injected into mice, their localization can be seen by either applying ultraviolet light (for EGFP excitation) or by injecting the substrate luciferin into the peritoneal cavity of the mice. Luciferin is then catabolized by the firefly luciferase. In both cases light is emitted, which can be collected by a sensitive CCD camera. Because the whole animal is investigated, the transmitted light through the anesthetized animal's tissues monitors the distribution and growth of tumor cells (Edinger *et al.,* 1999). Furthermore, because animals are only anesthetized, this system allowed sensitive, real-time analyses of the dynamics and quantification of neoplasia in time and space (Sweeney *et al.,* 1999).

However, it needs to be kept in mind that a two-dimensional image is taken from a three-dimensional animal. Therefore, it is not possible to quantify the size of the tumors and to determine the absolute localization of the tumor inside the animal. For that purpose, the animal must be imaged from different views. Furthermore, the emitted light is scattered and absorbed by the surrounding tissue, so the level of scattering and absorption is dependent on the tumor localization. Consequently, a liver tumor, for example, may appear larger than a subcutaneous tumor as a result of the higher degree of light scattering and absorption. The scattering and absorption of light has to be kept in mind if EGFP-positive tumors are investigated because animals have to be exposed with ultraviolet (UV) light. Because of scattering and absorption of the UV light, only a certain amount of the originally exposed UV will reach the tumor and will excite EGFP molecules. Again, because of the scattering and absorption only a certain amount of the EGFP fluorescence will be transmitted through the tissue. Therefore, the detection of small EGFP-positive tumors may be difficult. In addition to that, it has to be kept in mind that detection of EGFP-expressing tumors can only be investigated in nude mice because UV light is absorbed by hairs and, more importantly, by the hair follicles.

The intensity of EGFP fluorescence and activity of firefly luciferase in stable transfected tumor cells is dependent on the relative expression levels of the appropriate proteins. EGFP-expressing tumors could be easily sorted by flow cytometry, whereas detection of firefly luciferase expression can be performed by analyzing the light emission. Nonetheless, the relative EGFP or firefly luciferase expression and activity should be tested in a cell culture approach prior to injection of those cells into animals. In Figure 16D we analyzed the relative EGFP fluorescence of the breast cancer cell line HS578T stably transfected with the pEGFP-MCS vector (Dittmar *et al.,* 2000b). HS578T-EGFP-MCS cells were embedded within a three-dimensional collagen lattice

over a range of 0–5 × 10^4 cells. Cells were seeded in duplicates, and EGFP fluorescence was determined with a 1 second integration time. In Figure 16E the EGFP fluorescence of HS578T-EGFP-MCS cells is shown, which were injected into nude mice. In the mouse shown on the left, EGFP-expressing cells (5 × 10^5) are located in the ventral area of the mouse. In the mouse shown on the right, EGFP-expressing cells (1 × 10^6) were injected subcutaneously in the dorsal region. The relative EGFP fluorescence was determined with a 5 second integration time and is shown in false colors (red indicates the highest, and blue indicates the lowest EGFP intensity).

Acknowledgments

The authors are grateful for the technical assistance of Silvia Keil and Gabi Troost and would like to thank Dr. Frank Entschladen and Daniel Palm for providing nude mice for the *in vivo* imaging analysis. This work was supported by the Fritz Bender-Foundation, Munich, Germany.

References

Akedo, H., Shinkai, K., Mukai, M., and Komatsu, K. 1989. Potentiation and inhibition of tumor cell invasion by host cells and mediators. *Invasion Metastasis 9*:134–l48.

Al-Mehdi, A.B., Tozawa, K., Fisher, A.B., Shientag, L., Lee, A., and Muschel, R.J. 2000. Intravascular origin of metastasis from the proliferation of endothelium-attached tumor cells: a new model for metastasis. *Nat. Med. 6*:100–l02.

Boyden, S. 1962. The chemotactic effect of mixtures of antibody and antigen on polymorphonuclear leucocytes. *J. Exp. Med. 115*: 453–466.

Chambers, A.F., Groom, A.C., and MacDonald, I.C. 2002. Dissemination and growth of cancer cells in metastatic sites. *Nat. Rev. Cancer 2*:563–572.

Dittmar, T., Husemann, A., Schewe, Y., Nofer, J.R., Niggemann, B., Zänker, K.S., and Brandt, B.H. 2002. Induction of cancer cell migration by epidermal growth factor is initiated by specific phosphorylation of tyrosine 1248 of c-erbB-2 receptor via EGFR. *FASEB J. 16*:1823–1825.

Dittmar, T., Brandt, B.H., Lang, K., Zänker, K.S., and Entschladen, F. 2000a. Lessons from tumor and immunocompetent cells. The quantitative engagement of ligand-receptor interactions modulates stop-and-go behavior as well as proliferation. *Medicina (B. Aires) 60 Suppl. 2*:27–33.

Dittmar, T., Schafer, F., Brandt, B.H., and Zänker, K.S. 2000b. Accelerated assessing of antisense RNA efficacy using a chimeric enhanced green fluorescent protein-antisense RNA-producing vector. *Antisense Nucleic Acid Drug Dev. 10*:401–408.

Edinger, M., Sweeney, T.J., Tucker, A.A., Olomu, A.B., Negrin, R.S., and Contag, C.H. 1999. Noninvasive assessment of tumor cell proliferation in animal models. *Neoplasia 1*:303–310.

Haier, J., Korb, T., Hotz, B., Spiegel, H.U., and Senninger, N. 2003. An intravital model to monitor steps of metastatic tumor cell adhesion within the hepatic microcirculation. *J. Gastrointest. Surg. 7*:507–514; discussion 514–515.

Jaffe, E.A., Nachman, R.L., Becker, C.G., and Minick, C.R. 1973. Culture of human endothelial cells derived from umbilical veins. Identification by morphologic and immunologic criteria. *J. Clin. Invest. 52*:2745–2756.

Katterle, Y., Brandt, B.H., Dowdy, S.F., Niggemann, B., Zanker, K.S., and Dittmar, T. 2004. Antitumour effects of PLC-gamma l-(SH2)(2)-TAT fusion proteins on EGFR/c-erbB-2-positive breast cancer cells. *Br. J. Cancer 90*:230–235.

Kebers, F., Lewalle, J.M., Desreux, J., Munaut, C., Devy, L., Foidart, J.M., and Noel, A. 1998. Induction of endothelial cell apoptosis by solid tumor cells. *Exp. Cell. Res. 240*:197–205.

Muller, A., Homey, B., Soto, H., Ge, N., Catron, D., Buchanan, M.E., McClanahan, T., Murphy, E., Yuan, W., Wagner, S.N., Barrera, J.L., Mohar, A., Verastegui, E., and Zlotnik, A. 2001. Involvement of chemokine receptors in breast cancer metastasis. *Nature 410*:50–56.

Nicolson, G.L. 1988. Cancer metastasis: tumor cell and host organ properties important in metastasis to specific secondary sites. *Biochim. Biophys. Acta 948*:175–224.

Orr, F.W., Wang, H.H., Lafrenie, R.M., Scherbarth, S., and Nance, D.M. 2000. Interactions between cancer cells and the endothelium in metastasis. *J. Pathol. 190*:310–329.

Paget, S. 1989. The distribution of secondary growths in cancer of the breast. *Cancer Metastasis Rev. 8*:98–101.

Sweeney, T.J., Mailander, V., Tucker, A.A., Olomu, A.B., Zhang, W., Cao, Y., Negrin, R.S., and Contag, C.H. 1999. Visualizing the kinetics of tumor-cell clearance in living animals. *Proc. Natl. Acad. Sci. U.S.A. 96*:12044–12049.

Voura, E.B., Sandig, M., and Siu, C.H. 1998. Cell-cell interactions during transendothelial migration of tumor cells. *Microsc. Res. Tech. 43*:265–275.

Weidt, C., Niggemann, B., Hatzmann, W., Zänker, K.S., and Dittmar, T. 2004. Differential effects of culture conditions on the migration pattern of SDF stimulated hematopoietic stem cells. *Stem Cells 22*:890–896.

II

Gastrointestinal Carcinoma

This Page Intentionally Left Blank

1

Gastrointestinal Carcinoma: An Introduction

M.A. Hayat

Gastric glands are highly organized tubular structures consisting of a complex mixture of diverse types of cells that are properly differentiated and located. The upper region of the glands close to the gastric lumen is mainly composed of the surface mucus cells that secrete neutral mucins to protect the mucosa from gastric acid (Miyaoka *et al.,* 2004). The lower region distal to the lumen is composed of chief cells that secrete pepsinogens, parietal cells that produce gastric acid, and enteroendocrine cells that secrete signaling factors. Between these two regions is located the neck region, where the proliferating progenitor cells are located. Daughters from the progenitor cells follow a specific program of differentiation as they migrate either upward toward the lumen, forming the surface mucus cells, or downward toward the base, forming chief cells, parietal cells, and enteroendocrine cells (Karam and Leblond, 1993).

Although less prominent in North America, neoplasia of the stomach is the second most common cancer worldwide and is associated with a 5-year survival rate of less than 20%. Gastric adenocarcinoma accounts for >95% of these cases. Gastric cancer is also the second most frequent malignancy worldwide, accounting for 9.9% of all cancer incidences and 12.1% of all cancer deaths. The disease kills 600,000 individuals annually worldwide. In the United States, the estimated mortality rate in Caucasian males was 33/100,000 in the early 20th century, and this rate declined to 5/100,000 in the late 20th century. The declining trend is worldwide, and it began earlier in developed countries. The age-adjusted incidence reaches as high as 70/100,000 in Japanese and Korean males (Ushijima and Sasako, 2004). Global geographic variability in the rate of gastric cancer as well as patient survival has been established. The male-to-female ratio is 2:1 in many geographic regions. This cancer is more prevalent in East Asia and South America. It is presently unclear whether the molecular pathology of gastric cancer is similar in Western, Asian, and Eastern European countries.

All existing gastric cancer classification systems are based on histology (e.g., World Health Organization [WHO] and Lauren classification). The Lauren system uses cell morphology to distinguish three broad subtypes: 1) intestinal-type gastric cancer (distal stomach), 2) diffuse-type gastric cancer (proximal stomach), and 3) mixed-type gastric cancer representing a combination of the other two types. Diffuse-type gastric cancer shows infiltrating, noncohesive tumor cells, whereas intestinal-type contains cohesive, glandularlike cell groups.

These designations of different histologic subtypes have value in understanding the epidemiology, demography, progression, and survival of the patients. The most common histologic variant present in high-risk populations is intestinal type. It results from exposure

Handbook of Immunohistochemistry and *in situ* Hybridization of Human Carcinomas, Volume 4: Molecular Genetics, Gastrointestinal Carcinoma, and Ovarian Carcinoma

to various environmental factors including *Helicobacter pylori* infection, and it evolves via a series of sequential events such as chronic gastritis atrophy, intestinal metaplasia, dysplasia, early carcinoma, invasion, and metastases. In low-risk populations, the diffuse type is more common. Diffuse tumors associate with the same superficial gastritis as intestinal tumors. The former also demonstrate high *H. pylori* antibody levels. Intestinal and diffuse types may result from the transformation of different epithelial cells or distinct molecular changes in a common cell type. The molecular understanding of these gastric cancer subtypes is limited, and, unlike some other solid tumors, molecular features of gastric cancer are not used to individualize treatment. Based on the information available it can be stated that the molecular genetics involved in intestinal gastric cancer differ from those responsible for diffuse-type gastric cancer; these differences are summarized next.

Beta-catenin mutation is more common in the intestinal gastric cancer, whereas mutation in CDH1 (E-cadherin) is more often found in the diffuse type, including familial gastric cancer (Grady *et al.,* 2000); however, neither mutation is exclusive to either type. Somatic mutations were found within the *E-cadherin* gene in 50% of the investigated diffuse-type gastric cancers and lymph-node metastasis derived thereof but not in the intestinal-type gastric cancer (Becker *et al.,* 1994a). Chronic infection by *H. pylori* is commonly associated with all subtypes of gastric cancer but specifically to intestinal gastric cancer.

Intestinal-type gastric cancer is characterized by proliferation markers such as topoisomerase (TOP2A) and CDC25B, whereas diffuse-type gastric cancer is characterized by genes (e.g., *SPARC* and *Wnt5a*) encoding components of the extracellular matrix (Boussioutas *et al.,* 2003). This information suggests that patients with intestinal gastric cancer may particularly benefit from antiproliferative chemotherapeutic agents.

Gastric carcinogenesis is a multistep process with morphologic progression involving multiple genetic and epigenetic events, and an intestinal metaplasia–dysplasia–invasive carcinoma sequence exists. This carcinogenesis involves a slow but continuous stepwise evolution from superficial gastritis, glandular atrophy to metaplasia, and eventually to adenocarcinoma. In general, this cancer initially spreads locally within the gastric wall serosa and then metastasizes to lymph nodes via the peritoneal cavity. This slow process of carcinogenesis, which may extend over decades, provides an excellent opportunity for early detection and intervention to prevent further progress or regression of the carcinogenic process. Complete surgical resection at early stages offers the best chance for a cure and thus emphasizes the need for early diagnosis and treatment.

Despite the large proportion of patients who relapse and undergo longer-term treatment, the question of optimal treatment duration has not been fully addressed to date. Patients who do not show progress on a certain therapy are switched to a different active agent, presumably one with a different mechanism of action from previous therapy, with the hope of limited overlapping toxicities. As a result, the question of optimal treatment duration remains unanswered and may remain unanswered in the absence of individualized targeted therapy. Therefore, these agents should be used with the critical goal of balancing the efficacy and toxicity and their effect on symptoms and quality of life. For further details of this subject, the reader is referred to Herzog (2004).

Many oncologists have embraced six cycles of chemotherapy as a standard treatment duration and believe that treatment beyond this duration does not provide any additional benefit to patients. However, this limit is not rigorously supported in the recurrent disease setting. It is possible that patients with recurrent disease might benefit from extended treatment, if the disease is stable or in partial response. Agents that are potentially suited for extended treatment intervals should possess properties such as absence of cumulative toxicity, non–cross-resistance, positive benefit with regard to quality of life, and convenient schedule.

Early Gastric Cancer

Early gastric cancer (EGC) is defined as a gastric carcinoma confined to the mucosa or submucosa regardless of the presence of lymph-node status. The detection rate of EGC has been steadily increasing because of technical advances and increasing awareness of early diagnostic benefit, especially in high-incidence areas. Patients who undergo resection for EGC have an encouraging prognosis, with a 5-year survival rate of ~90% (Yokota *et al.,* 1998). Lymph-node metastasis is the most important factor in determining the prognosis of patients with EGC, which is associated with submucosal invasion of neoplastic cells.

Role of *Helicobacter pylori* in Gastric Cancer

H. pylori (a Gram-negative bacillus) infection is an important etiologic risk factor in gastric cancer and has been classified as a group I or definite carcinogen by WHO's International Agency for Research on Cancer. This pathogen infects a high proportion of the population in third-world countries and up to 50% in Western countries. The incidence of infection increases

with age, reaching ~50% in people aged 60 years. Transmission is from person to person by the fecal–oral route. Multiple factors play a role in gastric carcinogenesis, including diet, lifestyle, infectious agents such as *H. pylori,* genetic factors, as well as gene-environment interactions. The clinical outcome of *H. pylori* infection depends on multiple variables including the environment, host factors, and bacterial virulence factors. In some patients, the infection is associated with duodenal ulcers, and in others, with gastric cancer (Uemura *et al.,* 2001).

Although approximately two-thirds of gastric cancer can be prevented by changing lifestyle and diet habits, the fact that some individuals develop this cancer but others under similar exposure do not suggests that genetic predisposition also plays an important role in the etiology of gastric cancer. In addition to dietary and socioeconomic factors, *H. pylori* infection has emerged from epidemiologic studies as the environmental etiologic factor causing this cancer (Moayyedi and Ford, 2002). In fact, *H pylori* is the main etiologic agent of initiating gastric cancer. Other etiologic factors alone are not sufficient to induce this cancer.

H. pylori is associated with an increase in the circulating concentration of the gastric hormone gastrin. Gastrin stimulates acid secretion and activates mechanisms that facilitate mucosal protection, including stimulation of epithelial cell migration, cell renewal, and release of growth factors of the epidermal growth factor (EGF) family. Gastrin is increased in *H. pylori* infection, which stimulates gastric expression of plasminogen activator inhibitor-2 (PAI-2) (serpin B2) (Varro *et al.,* 2004). In other words, oncogenic *H. pylori* induces PAI-2 in gastric epithelial cells. Gastrin increases the expression of the gene encoding PAI-2. It is also known that PAI-2 is an inhibitor of the urokinase plasminogen activator and has been known to be increased in gastric adenocarcinoma.

H. pylori causes chronic active gastritis and peptic ulcer disease and is linked with gastric adenocarcinomas, including gastric mucosa–associated lymphoid tissue lymphoma. Generally, gastric adenocarcinoma develops through a multistep process from normal gastric mucosa to chronic active gastritis, to gastric atrophy and intestinal metaplasia, and finally to dysplasia and neoplasia. It is thought that infection with *H. pylori* plays a causative role in the early phases of this malignant progression (Wang *et al.,* 2002). However, consensus is lacking on whether *H. pylori* is a carcinogen or a cancer promoter. It is also not clear if eradication of this bacterium is beneficial to persons free of gastric tumors.

A possible explanation for the link between *H. pylori* infection and gastric carcinogenesis is that infection with this pathogen increases cyclooxygenase-2 (COX-2) messenger ribonucleic acid (mRNA) protein levels. It is known that COX-2 is involved in gastrointestinal (GI) cancer. Infection with *H. pylori* also stimulates release of prostaglandin E_2 in *H. pylori*–associated premalignant and malignant lesions. It has been shown that *H. pylori* increases release of prostaglandin E_2 and COX-2 in most metaplastic and adenomatous tissues as well as in gastric adenocarcinoma (Lim *et al.,* 2000). Gastric tumorigenesis was significantly attenuated by long-term administration of the COX-2 inhibitor, nimesulide, in an *H. pylori*–associated gastric cancer mouse model (Nam *et al.,* 2004). Nimesulide is a nonsteroidal anti-inflammatory drug that may be used as a selective COX-2 inhibitor and thus may be useful in protecting against gastric cancer development.

Because two main histologic gastric carcinoma types, intestinal and diffuse, may be associated with different genetic pathways Jiao *et al.* (2004) have carried out a study analyzing loss of heterozygosity (LOH) and, microsatellite instability (MSI) status in different types of gastric carcinomas. This study indicates that LOH and MSI are more common in intestinal tumors (and solid-type tumors) than in diffuse-type tumors. In this study the crypt isolation technique was used, isolating tumor tissue from stromal tissue. Because primary tumor tissues always contain stromal tissues, the preparation of tumor deoxyribonucleic acid (DNA) is contaminated with normal DNA, making it difficult to assess LOH status accurately as a result of false-negative results with respect to allelic loss. This problem can be solved by using the crypt isolation method, which can separate tumor tissue from stromal tissue.

Some information is available regarding the genotoxic insult resulting from *H. pylori* infection. It is well established that oxidative stress is induced by *H. pylori,* which is involved in carcinogenesis including GI cancers (Seril *et al.,* 2003).

Oxidative stress is linked to carcinogenesis because of its ability to damage DNA. *H. pylori* infection leads to the increased expression of an important polyamine catabolic enzyme, the spermine oxidase (SMO [PAOh1]) (Xu *et al.,* 2004). This enzyme oxidizes spermine, producing the DNA-damaging reactive oxygen species (ROS), hydrogen peroxide. One link between *H. pylori* infection and gastric cancer is thought to be SMO (PAOh1)–produced hydrogen peroxide. Thus, the reactive species responsible for the inflammation and carcinogenesis is bacterial infection–induced hydrogen peroxide production.

Another study also indicates that *H. pylori* infection causes inflammation, accumulation of ROS, and oxidative DNA damage in the gastric mucosa (Ding *et al.,* 2003). *H. pylori* or ROS enhances APE-1/Ref-1 protein synthesis and nuclear accumulation in human gastric epithelial

cells, implicating this protein in the modulation of pathogenesis of *H. pylori* infection. Future studies should focus on determining the role that APE-1/Ref-1 may play in coordinating gastric epithelial cellular responses to *H. pylori* infection or oxidative stress.

A pathway that may be relevant to malignant transformation induced by *H. pylori* involves the down-regulation of p27 (a cell cycle inhibitor) a tumor suppressor and apoptosis regulator. Immunohistochemical studies have demonstrated that chronic *H. pylori* infection is associated with reduced expression of p27 protein in gastric epithelial cells in biopsy specimens (Shirin *et al.,* 2000). It has also been demonstrated that the reduction in levels of p27 protein expression can be reproduced by the co-culture of *H. pylori* with gastric epithelial cells and that it is dose and time dependent (Eguchi *et al.,* 2003). The decrease in p27 protein is mediated through increased breakdown of this protein rather than its decreased transcription.

H. pylori decreases p27 protein by up-regulating proteasome-dependent degradation. This degradation is not associated with increased phosphorylation of p27 at T187, enhanced SKP2 expression, or increased p27 ubiquitination (Eguchi *et al.,* 2003). Increased activation of T187-dependent ubiquitin proteasome pathway associated with increased SKP2 expression has been reported in several human cancers including gastric cancer (Mori *et al.,* 1997). Low p27 expression is generally associated with a poor prognosis in cancer. Thus, *H. pylori* increases p27 protein degradation by a mechanism different from that responsible for its degradation during normal cell cycling. It is worth noting that reduction in p27 occurs independent of *H. pylori* effects on cell cycle.

Granulomatous Gastritis

Granulomatous gastritis (GG) is inflammation of the stomach, representing a nonspecific reaction to a variety of agents, and its incidence is uncommon. This condition results from a sustained tissue irritation by poorly degradable substances. Ectors *et al.* (1993) have classified GG cases based on the cause: Crohn's disease (52%), idiopathic GG (25%), foreign bodies (10%), underlying malignancies (7%), sarcoidosis (1%), Whipple's disease (1%), and unclassified (3%). They also reported that 89% of the 72 cases were accompanied by chronic atrophic gastritis, 95% showed adjacent chronic gastritis, and 92% were positive for *H. pylori* infection.

The clinicopathologic diagnosis of the 18 patients with GG were as follows: chronic gastritis with *H. pylori* infection (n = 14) and without (n = 1), gastric adenocarcinomas (n = 2), and Crohn's disease (n = 1) (Maeng *et al.,* 2004). These and other studies indicate that a variety of factors are involved in causing GG. In the absence of other aforementioned causative factors, GG can appear as isolated/idiopathic. In other words, *H. pylori* is causal in the pathogenesis of GG after excluding all other causes. The granulomas are found more frequently in the antrum, are superficially located, and are related to damage within a pit in which the *H. pylori* are commonly observed (Maeng *et al.,* 2004). Almost all cases of GG show small erosions or ulcers by the endoscopic examination.

Genetics of Gastric Cancer

Carcinogenesis, including the development of gastric cancer, is a multistep process involving a number of factors such as the accumulation of genetic alterations in cellular oncogenes, tumor-suppressor genes, regulators of the cell cycle, and DNA-repair genes. Indeed, a multifactorial model of human gastric carcinogenesis is currently accepted, according to which different dietary and nondietary factors, including genetic susceptibility, are involved at different stages in this cancer.

Various techniques have been used for detecting a large number of genes involved in various stages of gastric carcinogenesis. Recently available genomic technologies have enabled us to accumulate genetic information at a rapid pace. The chromosomal localization of many thousands of genes in the human genome have already been mapped accurately. Differential gene-expression profiling and suppression substractive hybridization, analysis have been performed for identifying genes in gastric adenoma and gastric adenocarcinoma, and on these bases distinct gene expression patterns have been found (Takenawa *et al.,* 2004). These approaches add new insight into understanding the molecular pathogenesis involved in the early stages of gastric carcinogenesis. Such information helps in determining specific markers for clinical practice and in designing potentially novel therapeutic targets.

An increasing interest is being shown in correlating clinical outcomes with gene expression signatures. Indeed, increasing information is being obtained through systematic comparison of molecular features of individual cancer with key clinical parameters. The expression profiling of a large set of gastric cancer and nonneoplastic specimens enables distinction between premalignant and malignant subtypes of gastric cancer. In this respect, differences in gene expression between tumor tissue and adjacent mucosa are also important. The identification of molecular signatures that are characteristic of subtypes of this cancer and associated

premalignant changes should enable further analysis of the steps involved in the initiation and progression of this disease.

With respect to molecular etiology, abnormalities in a number of genes at different stages and in different types of gastric cancers have been identified. Such studies help to understand the molecular basis of these cancers. As stated earlier, both oncogenes and tumor-suppressor genes are altered in gastric cancer. Activation of oncogenes involved in this cancer include *β-catenin, K-ras, HER-2/neu, K-sam, and c-met.* Inactivation of *p53, APC* (adenomatous polyposis coli) *E-cadherin* and *p16* tumor-suppressor genes is also common in gastric cancer. Another tumor-suppressor gene, $RUNX_3$, was reported in gastric cancer, but its mutations were rare (Li *et al.,* 2002). *p53* mutations are more common in the intestinal type of gastric adenocarcinomas than in the diffuse type. Mutations of the *APC* gene are found frequently in gastric adenomas but infrequently in adenocarcinomas (Lee *et al.,* 2002). It is important to note that many of these genes are also involved in other cancers. It is also emphasized that epigenetic silencing of gene expression by promoter CpG hypermethylation is an important alternative mechanism in inactivating tumor-suppressor genes. Chromosomal alteration at the 17q region is also known to be a frequent finding in gastric cancer. Three genes (*HER-2/neu, TOP2A,* and *DARPP32*) have been characterized at the 17q21 locus in human gastric cancer primary tumors (Varis *et al.,* 2004).

Cell-adhesion molecules mentioned earlier, cell cycle mediators (e.g., cyclin D1), and CD44 are also involved in gastric cancer (El-Rifai and Powell, 2002; Yasui *et al.,* 2001). A novel factor, DEGA/AMIGO-2, has been identified, which may function not only as a signaling cell-adhesion molecule but also is required for the tumorigenesis of a subset of human gastric adenocarcinomas (Rabenau *et al.,* 2004). The inhibition of the expression of this gene negatively affects tumor growth and alters chromosomal ploidy and stability. Further molecular genetic characterization is required to determine its precise function or mechanism in gastric adenocarcinoma. The role of some of these genes in this cancer is discussed in detail in this chapter and other chapters in this volume. MSI and LOH also play a role in gastric cancer. Losses and gains of chromosomal regions in gastric cancer are summarized in the section on MSI in this chapter.

Because of the genetic instability (characteristic of almost all cancer types), patients suffering from superficially identical tumors show an enormous variability in their gene expression profiles termed patient-specific transcription profile. To aim at a more efficient and individual therapy, it will be necessary to distinguish between patient-specific transcription profiles and the altered expression pattern underlying all tumors of the same type.

Role of Microsatellite Instability and Loss of Heterozygosity

It is known that alterations in DNA mismatch repair (MMR) proteins result in MSI, increased mutation accumulations at target genes, and cancer development. Gastric carcinomas are among the tumors that most frequently display MSI. MSI analysis, Western blot analysis, immunohistochemistry (IHC), and promoter methylation assays confirm that approximately one-third of gastric cancers display high-level MSI and low-level MSI (Yao *et al.,* 2004). In this study a panel of five microsatellite markers were used for characterizing the MMR system and MSI of 14 established gastric cancer cell lines. More specifically, MSI is observed in 5–10% of the diffuse type of gastric cancers and in 15–40% of the intestinal type of these cancers (Ushijima and Sasako, 2004).

The major mechanism for the MSI in gastric cancer, as stated earlier, is inactivation of the MMR gene, resulting from hypermethylation of its promoter (Fang *et al.,* 2003). The MMR system is essential for replication fidelity, correcting DNA base mismatches left uncorrected by DNA polymerase. It has been demonstrated that MSI phenotype occurring in tumors is caused by deficiency of one of the main DNA MMR proteins (hMLH1 and hMLH2) and in a small number of cases it results from deficiency of hMSH6, hMSH3, and hMSH2 (Bae *et al.,* 2000). These studies represent a useful tool for future experimental investigations addressing the role of DNA MMR in the molecular behavior of gastric cancer.

Efficient MMR requires combining function of MutL (e.g., hMLH1) and Muts (e.g., hMSH2) heterodimers. In MMR-deficient cells, insertion or deletion of nucleotide bases at microsatellite sequences causing MSI-type mutations occurs at high frequency.

Inactivation of genes by base insertion or deletion in small mononucleotide repeats in the coding region contributes to cancer development and progression. In a fraction of sporadic tumors, including gastric adenocarcinoma (Duval and Hamelin, 2002), MSI occurs at multiple microsatellite loci. Although hMLH1 (also p16) is inactivated in gastric cancers by mutation or promoter hypermethylation, inactivation by the latter is much more frequent than mutation in sporadic gastric cancers.

As in many types of human cancers, LOH contributes to gastric cancer because it inactivates tumor-suppressor genes. (The LOH study is a comparison of polymorphilic

loci in DNA and the finding of contiguous regions of tumor DNA where one allele is absent.) Such inactivation is caused by mutation or allelic loss. Regions that demonstrate high rates of LOH represent loci that potentially harbor tumor-suppressor genes. Chromosomal gains have been found on 1p, 6p, 7q, 8q, 11q, 16q, 17q, 20q, and 22q, and losses have been found on 3p, 4q, 5q, 9p, 16p, 17p, 18p, and 19p in gastric cancer. Gains at 20q, 17q, and 8q and losses at 14p and 18q are especially crucial in the development and progression of gastric cancer. Gains at 20q are most frequent, and losses at 18q are associated with clinicopathologic factors, which may be considered markers for this cancer. LOH at the DCC locus (18q21) is frequently found in gastric cancer (Sato *et al.,* 2001). Chromosomal losses are higher in gastric cancer with lymph-node metastasis, and the mean number of gains and total alterations are higher in gastric carcinomas with venous invasion.

Comparative genomic hybridization (CGH) has also been used for studying chromosomal alterations in gastric cancer. This procedure facilitates detection of genetic amplification and deletions in each chromosome. CGH studies also indicate gains at 20q, 17q, and 8q and losses at 19p and 18q in the development and progression of gastric cancer (Kimura *et al.,* 2004). These data and those discussed earlier suggest a relationship between gastric carcinogenesis and potential tumor-suppressor genes. However, such relevant genes within these chromosomal regions remain to be identified, and whether such genes behave as oncogenes has not been discerned.

The extent of chromosomal losses and the presence of an MSI determined on a biopsy specimen can provide valuable information for making a preoperative genetic diagnosis of a gastric cancer (Hong *et al.,* 2005). Such a diagnosis aimed at predicting the tumor stage and the survival based on the biopsy genotype and the tumor size measurable during a surgical resection is likely to be clinically relevant.

Biomarkers for Gastric Carcinoma

The development of cancer is a relatively slow multistep process, so often it takes several years to become clinically manifested. During tumor progression, cancer cells acquire multiple alterations that render them increasingly able to establish metastatic lesions in specific organs. However, primary tumors may already contain a gene(s) expression profile that is strongly predictive of metastasis and poor survival thus challenging the notion that metastatic ability is acquired only late during tumor progression.

Presently, techniques that may possess the sensitivity and specificity to detect a tumor at its earliest stage are lacking. Because reduction of cancer mortality is dependent partly on early detection, the importance of such detection of neoplasia is obvious. Early detection of tumor development also facilitates accurate clinical decisions such as risk assessment, monitoring the course of disease, and positive or negative response to therapy. Thus, through early detection, longer disease-free survival, longer overall survival, and improved quality of life for the patient can be achieved. Early detection of certain tumor types can be ascertained by detecting specific biomarkers.

Biomarkers are molecular signatures of a cellular phenotype, which facilitate early cancer detection, pathologic grading and staging, and risk assessment to help in the development and use of molecularly targeted therapies tailored to the patient and to increase the rate of survival as a result of early detection or improved therapies. In other words, tumor markers can help in at least six areas: 1) screening (finding cancer early), 2) diagnosis (is it really a cancer?), 3) prognosis (how will the cancer behave?), 4) monitoring (how is the treatment working?), 5) predicting a response (will a drug be effective?), and 6) surveillance (will the patient need more treatment?). Because early detection and effective prevention represent the most promising clinical approaches, the identification of biomarkers to stratify patients into different risk groups would be a potential strategy for clinical trials.

The ideal biomarker should be sensitive and specific for the given cellular entity, not detected anywhere else, and sufficiently sensitive, enabling optimal detection, especially at an early stage of the disease. An early detection increases the chances of curative treatment. In addition, the marker should be relatively easily measurable and the test should be reproducible (reliable) and minimally invasive. Many new markers are being discovered based on several methods, including gene microarray, proteomics, and IHC. Most of the known markers have not yet been tested clinically, although some of them in this respect appear to be promising (Table 3).

The main reasons for lack of more than a few specific markers to achieve exact intervention and exact prognosis of gastric cancer is that it is a very heterogeneous tumor entity and multiple changes at the cellular, subcellular, and molecular levels occur during its development and progression. The complex nature of this cancer becomes clear when one considers that although gastric adenomas are precancerous lesions, some of these adenomas persist unchanged for a long time. However, in recent years the number of gastric tumor markers that are clinically useful for predicting therapeutic responses or patient outcome has been slowly increasing.

To guide the process of biomarker development, evaluation, and application, a five-phase program is recommended by the Early Detection Research Network

Table 3. Biomarkers for Gastric Cancer

*APC (adenomatous polyposis coli)	This volume
ARP2/3	Kaneda *et al*. (2004)
BAK gene	Sakamoto *et al*. (2004)
**Bcl-2*	Fricke *et al*. (2003)
*Beta-catenin	This volume
BNIP3	Murai *et al*. (2005)
*BUB1 protein	This volume
CA 72-4	Louhimo *et al*. (2004a)
*Caspase-3	This volume
*CD-34	Yamaguchi *et al*. (2004)
CDHI3	Hibi *et al*. (2004)
*Chromogranin A	This volume
*Cyclin D2	This volume
*Cyclin E	Bani-Hani *et al*. (2005)
Cyclooxygenase-2	Okano *et al*. (2004)
*Cytokeratin	Kim *et al*. (2004a)
DEGA/AMIGO-2	Rabenau *et al*. (2004)
*Desmin	Yamaguchi *et al*. (2004)
Dihydropyrimidine dehydrogenase	Ichikawa *et al*. (2004)
*DNAmethyltransferase 1 protein	This volume
*E-cadherin	This volume
*Epidermal growth factor receptor	This volume
*FAS-associated factor 1	Bjørling-Poulsen *et al*. (2003)
hCGB	Louhimo *et al*. (2004b)
**hMSH2*	Yao *et al*. (2004)
**HER-2*	Okano *et al*. (2004)
*Ki-67	Fricke *et al*. (2003)
*KiSS-1	This volume
*KIT	This volume
*MUC5B	This volume
*MUC 5AC	Sun *et al*. (2005)
MYH gene	Kim *et al*. (2004b)
*$p16^{INK4A}$	This volume
*$p21^{WAF/CIPI}$	Sun *et al*. (2005)
**p53*	This volume
p73	Tomkova *et al*. (2004)
*p150	Chen *et al*. (2004a)
*PCNA (proliferating cell nuclear antigen)	This volume
*Placenta growth factor	Chen *et al*. (2004b)
*Plasminogen activator inhibitor-2	Varro *et al*. (2004)
*Platelet-derived growth factor receptor	Rossi *et al*. (2005)
*Reg protein	Miyaoka *et al*. (2004)
*S-100	Yamaguchi *et al*. (2004)
Siah-1 gene	Kim *et al*. (2004c)
SLC5A8	Ueno *et al*. (2004)
*Smad-4	Okano *et al*. (2004)
*Thymidylate synthase protein	Grau *et al*. (2004)
*Transforming growth factor α	Espinoza *et al*. (2004)
*Trefoil factor	Dhar *et al*. (2003)
*Vascular endothelial growth factor receptor	Gong *et al*. (2005)
*Vascular epidermal growth factor	This volume
*Vesicle proteins	This volume

*These markers have been identified with immunohistochemistry, *in situ* hybridization, or both.

(EDRN) of the National Cancer Institute (Table 4) (Pepe *et al.,* 2001). This program assists in defining the criteria to determine the current status of biomarkers in the published literature and assess how close these markers are to clinical application, and it serves as a guide for future marker development (Marrero and Lok, 2004). The program essentially is biomarker validation protocol: 1) preclinical exploratory studies, 2) clinical assay development for disease, 3) retrospective longitudinal study to detect preclinical disease, 4) prospective screening study, and 5) cancer control studies. There is an urgent need for clinical biomarkers for early detection of gastric carcinoma. A number of markers, including those studied with IHC and fluorescence *in situ* hybridization (FISH), for gastric cancer are discussed next and given in Table 3.

BAK

The invasion of apoptosis is linked to the development of cancer. *Bax* and *Bak* genes produce proapoptotic proteins, the activation of which is essential for triggering apoptosis in response to diverse stimuli. Whether these genes undergo somatic mutations in gastric cancer is controversial. According to Sakamoto *et al.* (2004), somatic mutations in the *Bak* gene are rare in gastric cancers, whereas according to Kondo *et al.* (2000); a significant frequency of such mutations are found in this gene in advanced gastric cancer. Immunohistochemical studies demonstrate that *Bak* expression is reduced in gastric cancer cells as compared with corresponding normal epithelial cells (Krajewska *et al.,* 1996). These contradictating results may be explained by assuming that the *Bak* gene is inactivated by other molecular mechanisms such as aberrant hypermethylation or haploinsufficiency (Largaespada, 2001).

β-Catenin

β-Catenin is a multifunctional protein that plays an important role in the transduction of Wnt signals and in the intercellular adhesion by linking the cytoplasmic domain of cadherin. β-Catenin exists in three different subcellular forms: membrane bound, cytosolic, and nuclear. However, cytosolic β-catenin is kept at a low level, eliminated by degradation, or translocated to the nucleus. The low-level concentration of β-catenin is accomplished through interaction with a protein complex composed of APC, Axin, protein phosphatase 2A, or glycogen synthase kinase 3β (GSK3β). This complex phosphorylates the β-catenin, resulting in the ubiquitination-dependent proteolysis of β-catenin (Kim *et al.,* 2004a, b). Alterations of these genes cause accumulation of cytosolic β-catenin and its nuclear translocation. After the translocation into the nucleus,

Table 4. Phases of Biomarker Validation in Cancer Surveillance

Phases	Type of Study	Aims
1	Preclinical exploratory	Promising markers identified
2	Clinical assay and validation	Assay detects established disease
3	Retrospective longitudinal	Biomarker detects preclinical disease
4	Prospective screening	Confirm ability of marker to detect early-stage disease
5	Cancer control	Impact of screening on reducing tumor burden in at-risk population

From Marrero and Lok (2004).

β-catenin binds to members of the T-cell factor/Lef family, activating target genes such as *cyclin D1* and *myc.* Only one of these genes is mutated in a given tumor type, reflecting their role in a common pathway.

Most of the β-catenin mutations are activating mutations, mainly occurring at one of the four phosphorylation sites in exon 3 (Polakis, 2001). These genetic alterations, especially in GSK3β, are mentioned, earlier. These and other findings suggest that genes for β-catenin degradation are associated with the development of gastric cancer.

As mentioned earlier, cytosolic β-catenin is eliminated by APC-dependent proteosomal degradation pathways regulated by GSK3β or *p53*-inducible *Siah-1*. Similar to *p53,* overexpression of *Siah-1* inhibits cell proliferation, promotes apoptosis, and suppresses tumor formation. These observations suggest that *Siah-1* is one of the tumor-suppressor genes that participates in the APC-mediated down-regulation of cytosolic β-catenin (Kim *et al.,* 2004a, b). Thus mutations of the *Siah-1* gene play an important role in the development or progression in a subset of gastric cancer through β-catenin stabilization and blockage of apoptosis. Immunohistochemical studies demonstrate the presence of β-catenin at the plasma membrane in the normal gastric mucosa, whereas this protein is nuclear and cytosolic in gastric cancer cells (Kim *et al.,* 2004a, b).

E-Cadherin

E-cadherin is a transmembrane glycoprotein expressed on epithelial cells. This cell-cell adhesion molecule executes important functions in embryogenesis and tissue architecture by forming intercellular junction complexes and establishing cell polarization. The extracellular domain of E-cadherin is involved in a molecular zipper mediating cell-cell adhesion, whereas the cytoplasmic tail is linked to the actin cytoskeleton via cytosolic catenin proteins; catenins serve as bridging molecules. In the presence of E-cadherin mutations, β-catenin is found in an abnormal perinuclear location.

E-cadherin is not only involved in cell-cell contact, but multiple signaling pathways are also activated or repressed by the functions of this protein. One of the best-known pathways is the β-catenin/LEF/T-cell factor signaling cascade (Nollet *et al.,* 1999). It has been reported that loss of E-cadherin and cytosolic β-catenin induces *p38*-mediated NF*k*B activation (Kuphal *et al.,* 2004). NF*k*B activation is connected with multiple aspects of oncogenesis, including the control of apoptosis, the cell cycle, differentiation, and cell migration. Mitogen-activated protein (MAP) kinases are also regulated via E-cadherin (Pece and Gutkind, 2000).

Cell–cell and cell–matrix interactions are crucially involved in neoplastic transformation and metastasis. Defective cell adhesion contributes to loss of contact inhibition of growth, which is an important early step in the neoplastic process. Furthermore, loss of cell adhesion accounts for the ability of cancer cells to cross normal tissue boundaries and metastasize. The importance of E-cadherin in maintaining cell adhesion implies that its dysfunction plays an important role in tumorigenesis. Tumor-associated E-cadherin mutations influence regulatory cellular networks. Owing to its critical function in intercellular adhesion, E-cadherin acts as a tumor suppressor, negatively regulating several critical steps of invasion and metastasis. Loss of E-cadherin expression during tumor development has been observed in a variety of different tumors including gastric tumors. Abnormalities of cell-adhesion molecules lead to dysfunction of intercellular adhesion, which is accompanied by higher mobility of tumor cells and aggressive tumor behavior.

Several mechanisms impair E-cadherin function, including E-cadherin inactivation caused by mutations and promoter inactivation attributed to hypermethylation. The latter is the predominant mechanism, whereas the former is fairly common in specific gastric cancer subtypes. The transcription factor Snail (a member of the Snail family of zinc-finger) is also a repressor of E-cadherin gene expression by binding to its proximal promoter in epithelial tumor cells. Endogenous Snail proteins are present in human carcinoma cell lines and

in tumors in which E-cadherin has been lost with associated acquisition of a fibroblastic phenotype (Batlle *et al.,* 2000). This family occupies a central role in morphogenesis because it is essential for mesoderm formation. The importance of Snail proteins becomes apparent considering that down-regulation of E-cadherin occurs during epithelial–mesenchymal transitions, the process of cellular morphologic changes in epithelial cells from epithelial features to a more fibroblastic and flattened phenotype (Rosivatz *et al.,* 2002).

E-cadherin is involved in tumor invasion and metastasis. Silencing of *E-cadherin* by promoter CpG methylation has been shown in both familial and sporadic gastric cancers. The second hit in *E-cadherin* germline mutation carriers is also generally the result of methylation. Somatic mutations of *E-cadherin* are found specifically in sporadic diffuse type of gastric cancers (Becker *et al.,* 1999). It should be noted that aberrant methylations are widely distributed and can be present even in noncancerous gastric mucosae.

E-cadherin methylation is an early event in gastric carcinogenesis and is initiated by *H. pylori* infection. Disruption of the E-cadherin complex is expected to induce loss of cell adhesion with a concomitant increased cell motility. Direct evidence of *E-cadherin* mutations triggering tumorigenesis has come from the finding of inactivating germline mutations of the *CDH1* gene in hereditary diffuse gastric cancer.

Among the genetic alterations associated with diffuse-type gastric carcinoma are mutations in the tumor-suppressor genes *E-cadherin* and *p53*. Tumor cell proliferation and loss of tumor cells by apoptosis determine tumor growth. Evading apoptosis is critical for the expansion of tumors. *E-cadherin* mutations and *p53* mutations are critical for the regulation of apoptosis program and thus for tumor growth because both proliferation and apoptosis determine the number of tumor cells. *E-cadherin* mutations alter the function of wild-type molecules such as *p53* and provide tumor cells with the properties that promote tumor cell dissemination. Immunohistochemical analysis of E-cadherin expression and localization shows that E-cadherin is detectable in tumor cells (Fricke *et al.,* 2003). The role of E-cadherin as a prognostic marker in gastric cancer has been shown not only by immunohistochemical studies but also by methylation-specific polymerase chain reaction (Chan *et al.,* 2003). Membrane localization of E-cadherin protein is common in diffuse-type gastric cancer, which is consistent with the role of this protein as an adhesion molecule. *E-cadherin* mutations and the development and progression of diffuse-type gastric cancer has been demonstrated (Becker *et al.,* 1999). Such analyses also indicate that E-cadherin is not common in the intestinal-type gastric cancer.

Epidermal Growth Factor Receptor

Alterations in several genes coding for proteins that play a role in cell multiplication, cellular adhesion, or DNA repair contribute to the development and progression of gastric adenocarcinomas.

Abnormal expression of epidermal growth factor receptor (EGFR) or mutated EGFR protein, or both, are associated with poor prognosis in many types of human cancers, including gastric tumors. Co-expression of transforming growth factor (TGFα) (an EGFR ligand) with EGFR in cancer cells is thought to constitute an autocrine loop influencing various processes that determine tumor progression such as continuous cell proliferation, cell migration, cell adhesion, cell survival, and angiogenesis. Furthermore, it has been shown that co-expression of EGFR and TGFα associated with the accumulation of mutated *p53* occurs frequently in advanced primary gastric adenocarcinomas (Espinoza *et al.,* 2004). It is known that *p53* mutations can occur in up to 50% of human malignancies, including gastric carcinoma.

MUC5B

Mucins, the main protectors of most epithelial interfaces, are high molecular weight glycoproteins containing many serine and threonine residues that are potentially glycosylated. They are synthesized by secretory epithelial cells as membrane or secreted proteins. Thus far, at least 14 mucin genes have been identified that code for mucin proteins. Mucin genes are expressed in a regulated cell- and tissue-specific manner. These genes play important roles during cell differentiation and carcinogenesis, and their expression is altered during pathogenesis of neoplastic diseases. In a normal stomach, MUC1 is detected in mucus cells of the surface epithelium and neck regions of the gastric antrum as well as in pyloric glands and oxynthic glands of the body region (Ho *et al.,* 1995).

Distinct patterns of mucin expression are found with intestinal metaplasia. Complete intestinal metaplasia shows little or no expression of MUC1, MUC5AC, or MUC6, although goblet cells strongly express MUC2. MUC5B is expressed in trachea, bronchus, and submaxillary glands and endocervix, gall bladder, and pancreas (Desseyn *et al.,* 1998). Under normal conditions, MUC5B is absent in the adult stomach (it is present only during a brief period of fetal life). MUC5B is expressed *de novo* in gastric mucosa only in cases of gastric carcinoma (Perrais *et al.,* 2001).

Pinto-de-Sousa *et al.* (2004) have evaluated the role of MUC5B expression in gastric carcinoma using monoclonal antibody EU-MUC5Ba; this antibody is

specific for nonglycosylated domains of the secreted MUC5B and MUC7. This study showed that MUC5B expression was associated with gastric carcinoma differentiation with an absence of venous invasion. MUC5B expression was associated with the co-expression of MUC5AC but not with MUC1, MUC2, and MUC6. The former association suggests that both genes share more than their close location on the chromosome 11p15.

Thymidylate Synthase

Thymidylate synthase (TS) provides the sole *de novo* source of thymidylate for DNA synthesis. Expression of TS has been widely investigated in the setting of fluoropyrimidine resistance. Specifically, TS overexpression as a result of gene amplification in cancer cell lines has been closely associated with 5-FU (5-fluoroacil) drug resistance (Berger *et al.,* 1987). Studies in patients with gastric cancer with locally advanced or metastatic disease treated with fluoropyrimidines have demonstrated that TS expression is inversely related to treatment response and survival (Johnston *et al.,* 1995). Patients with a low TS expression have higher tumor responses to these drugs and longer survival than patients with high TS expression. TS has a role in the selection of candidates for fluoropyrimidine treatment among patients with gastric cancer. Expression of TS protein has been studied in the histologically confirmed adenocarcinomas of the stomach using the immunohistochemical method (Grau *et al.,* 2004).

References

Bae, S.I., Park, J.G., Kim, Y.I., and Kim, W.H. 2000. Genetic alterations in gastric cancer cell lines and their original tissues. *Int. J. Cancer 87*:512–516.

Bani-Hani, K.E., Almasri, N.M., Khader, Y.S., Sheyab, F.M., and Karam, H.N. 2005. Combined evaluation of expressions of cyclin E and p53 proteins as prognostic factors for patients with gastric cancer. *Clin. Cancer Res. 11*:1447–1453.

Batlle, E., Sancho, E., Franci, C., Dominguez, D., Monfar, M., Baulida, J., and Garcia De Herreros, A. 2000. The transcription factor snail is a repressor of E-cadherin gene expression in epithelial tumour cells. *Nat. Cell Biol. 2*:84–89.

Becker, K.F., Atkinson, M.J., Reich, U., Becker, I., Nekarda, H., Siewert, J.R., and Höfler, H. 1994a. E-cadherin gene mutations provide clues to diffuse-type gastric carcinomas. *Cancer Res. 54*:3845–3852.

Becker, K.F., Kremmer, E., Eulitz, M., Becker, I., Handschuh, G., Schuhmacher, C., Muller, W., Gabbert, H.E., Ochiai, A., Hirohashi, S., and Höfler, H. 1999. Analysis of E-cadherin in diffuse-type gastric cancer using a mutation-specific monoclonal antibody. *Am. J. Pathol. 155*:1803–l809.

Berger, S.H., Jenh, C.H., Johnson, L.F., and Berger, F.G. 1987. Thymidylate synthase overproduction and gene amplification in fluorodeoxyuridine-resistant human cells. *Mol. Pharmacol. 28*: 461–467.

Bjørling-Poulsen, M., Seitz, G., Guerra, B., and Issinger, O.G. 2003. The pro-apoptotic FAS-associated factor 1 is specifically reduced in human gastric carcinomas. *Int. J. Oncol. 23*: 1015–l023.

Boussioutas, A., Li, H., Liu , J., Waring, P., Lade, S., Holloway, A.J., Taupin, D., Gorringe, K., Haviv, I., Desmond, P.V., and Bowtell, D.D. 2003. Distinctive patterns of gene expression in premalignant gastric mucosa and gastric cancer. *Cancer Res. 63*:2569–2577.

Chan, A.O., Lam, S.K., Wong, B.C., Wong, W.M., Yuen, M.F., Yeung, Y.H., Hui, W.M., Rashid, A., and Kwong, Y.L. 2003. Promoter methylation of E-cadherin gene in gastric mucosa associated with *Helicobacter pylori* infection and in gastric cancer. *Gut 52*:502–506.

Chen, C.N., Hsieh, F.J., Cheng, Y.M., Cheng, W.F., Su, Y.N., Chang, K.J., and Lee, P.H. 2004b. The significance of placenta growth factor in angiogenesis and clinical outcome of human gastric cancer. *Cancer Lett. 213*:73–82.

Chen, G., and Burger, M.M. 2004a. p150 overexpression in gastric carcinoma: the association with p53, apoptosis and cell proliferation. *Int. J. Cancer 112*:393–398.

Desseyn, J.L., Buisine, M.P., Porchet, N., Aubert, J.P., Degand, P., and Laine, A. 1998. Evolutionary history of the 11p15 human mucin gene family. *J. Mol. Evol. 46*:102–106.

Dhar, D.K., Wang, T.C., Maruyama, R., Udagawa, J., Kubota, H., Fuji, T., Tachibana, M., Ono, T., Otani, H., and Nagasue, N. 2003. Expression of cytoplasmic TFF2 is a marker of tumor metastasis and negative prognostic factor in gastric cancer. *Lab. Invest. 83*:1343–1352.

Ding, Y., Le, X.P., Zhang, Q.X., and Du, P. 2003. Methylation and mutation analysis of P16 gene in gastric cancer. *World J. Gastroenterol. 9*:423–426.

Duval, A., and Hamelin, R. 2002. Genetic instability in human mismatch repair deficient cancers. *Ann. Genet. 45*:71–75.

Ectors, N.L., Dixon, M.F., Geboes, K.J., Rutgeerts, P.J., Desmet, V.J., and Vantrappen, G.R. 1993. Granulomatous gastritis: a morphological and diagnostic approach. *Histopathology 23*: 55–61

Eguchi, H., Herschenhenhous, N., Kuzushita, N., and Moss, S.F. 2003. *Helicobacter pylori* increases proteosome-mediated degredation of p27 (kip1) in gastric epithelial cells. *Cancer Res. 63*:4739–4746.

El-Rifai, W., and Powell, S.M. 2002. Molecular biology of gastric cancer. *Semin. Radiat. Oncol. 12*:128–l40.

Espinoza, L.A., Tone, L.G., Neto, J.B., Costa, R.S., Wang, Q.J., and Ballejo, G. 2004. Enhanced TGFalpha-EGFR expression and P53 gene alterations contributes to gastric tumors aggressiveness. *Cancer Lett. 212*:33–41.

Fang, D.C., Wang, R.Q., Yang, J.M., Liu, H.F., Peng, G.Y., Xiao, T.L., and Luo, Y.H. 2003. Mutation and methylation of hMLH1 in gastric carcinomas with microsatellite instability. *J. Gastroenterol. 9*:655–659.

Fricke, E., Keller, G., Becker, I., Rosivatz, E., Schott, C., Plaschke, S., Rudelius, M., Hermannstadter, C., Busch, R., Hofler, H., Becker, K-F., and Luber, B. 2003. Relationship between E-cadherin gene mutation and p53 gene mutation, p53 accumulation, Bcl-2 expression and Ki-67 staining in diffuse-type gastric carcinoma. *Int J. Cancer 104*:60–65.

Gong, W., Wang, L., Yao, J.C., Ajani, J.A., Wei, D., Aldape, K.D., Xie, K., Sawaya, R., and Huang, S. 2005. Expression of activated signal transducer and activator of transcription 3 predicts expression of vascular endothelial growth factor in an angiogenic phenotype of human gastric cancer. *Clin. Cancer Res 11*: 1386–1393.

Grady, W.M., Willis, J., Guilford, P.J., Dunbier, A.K., Toro, T.T., Lynch, H., Wiesner, G., Ferguson, K., Eng, C., Park, J.G., Kim, S.J., and Markowitz, S. 2000. Methylation of the CDH1 promoter as the second genetic hit in hereditary diffuse gastric cancer. *Nat. Genet. 26*:16–17.

Grau, J.J., Domingo-Domenech, J., Morente, V., Pera, M., Garcia-Valdecasas, J.C., Fuster, J., Bombi, A., Mellado, B., Albanell, J., Gascon, P.R. 2004. Low thymidylate synthase expression in the primary tumor predicts favorable clinical outcome in resected gastric cancer patients treated with adjuvant Tegafur. *Oncology 6*:226–233.

Herzog, T.J. 2004. Recurrent ovarian cancer: how important is it to treat to disease progression? *Clin. Cancer Res. 10*: 7439–7449.

Hibi, K., Kodera, Y., Ito, K., Akiyama, S., and Nakao, A. 2004. Methylation pattern of CDH13 gene in digestive tract cancers. *Br. J. Cancer 91*:1139–1142.

Ho, S.B., Shekels, L.L., Toribara, N.W., Kim, Y.S., Lyftogt, C., Cherwitz, D.L., and Niehans, G.A. 1995. Mucin gene expression in normal, preneoplastic, and neoplastic human gastric epithelium. *Cancer Res. 55*:2681–2690.

Hong, S.J., Choi, S.W., Lee, K.H., Lee, S., Min, K-O., and Rhyu, M.G. 2005. Preoperative genetic diagnosis of gastric carcinoma based on chromosomal loss and microsatellite instability. *Int. J. Cancer 113*:249–258.

Ichikawa, W., Takahashi, T., Suto, K., Nihei, Z., Shirota, Y., Shimizu, M., Sasaki, Y., and Hirayama, R. 2004. Thymidylate synthase and dihydropyrimidine dehydrogenase gene expression in relation to differentiation of gastric cancer. *Int. J. Cancer 112*: 967–973.

Jiao, Y.-F., Sugai, T., Habano, W., Suzuki, M., Takagane, A., and Nakamura, S.-I. 2004. Analysis of microsatellite alterations in gastric carcinoma using the crypt isolation technique. *J. Pathol. 204*:200–207.

Johnston, P.G., Lenz, H.J., Leichman, C.G., Danenberg, K.D., Allegra, C.J., Danenberg, P.V., and Leichman, L. 1995. Thymidylate synthase gene and protein expression correlate and are associated with response to 5-fluorouracil in human colorectal and gastric tumors. *Cancer Res. 55*:1407–1412.

Kaneda, A., Kaminishi, M., Sugimura, T., and Ushijima, T. 2004. Decreased expression of the seven ARP2/3 complex genes in human gastric cancers. *Cancer Lett. 212*:203–210.

Karam, S.M., and Leblond, C.P. 1993. Dynamics of epithelial cells in the corpus of the mouse stomach. V. Behavior of entero-endocrine and caveolated cells: general conclusions on cell kinetics in the oxyntic epithelium. *Anat. Rec. 623*:333–340.

Kim, C.J., Cho, Y.G., Park, C.H., Jeong, S.W., Nam, S.W., Kim, S.Y., Lee, S.H., Yoo, N.J., Lee, J.Y., and Park, W.S. 2004c. Inactivating mutations of the Siah-1 gene in gastric cancer. *Oncogene 23*:8591–8596.

Kim, C.J., Cho, Y.G., Park, C.H., Kim, S.Y., Nam, S.W., Lee, S.H., Yoo, N.J., Lee, J.Y., and Park, W.S. 2004a. Genetic alterations of the MYH gene in gastric cancer. *Oncogene 23*: 6820–6822.

Kim, M.A., Lee, H.S., Yang, H.K., and Kim, W.H. 2004b. Cytokeratin expression profile in gastric carcinomas. *Hum. Pathol. 35*:576–581.

Kimura, Y., Noguchi, T., Kawahara, K., Kashima, K., Dan, T., and Yokoyama, S. 2004. Genetic alterations in 102 primary gastric cancers by comparative genomic hybridization: gain of 20q and loss of 18q are associated with tumor progression. *Mod. Pathol. 17*:1328–1337.

Kondo, S., Shinomura, Y., Miyazaki, Y., Kiyohara, T., Tsutsui, S., Kitamura, S., Nagasawa, Y., Nakahara, M., Kanayama, S., and Matsuzawa, Y. 2000. Mutations of the bak gene in human gastric and colorectal cancers. *Cancer Res. 60*:4328–4330.

Krajewska, M., Fenoglio-Preiser, C.M., Krajewski, S., Song, K., Macdonald, J.S., Stemmerman, G., and Reed, J.C. 1996. Immunohistochemical analysis of Bcl-2 family proteins in adenocarcinomas of the stomach. *Am. J. Pathol. 149*:1449–1457.

Kuphal, S., Poser, I., Jobin, C., Hellerbrand, C., and Bosserhoff, A.K. 2004. Loss of E-cadherin leads to upregulation of NFkappaB activity in malignant melanoma. *Oncogene 23*:8509–8519.

Largaespada, D.A. 2001. Haploinsufficiency for tumor suppression: the hazards of being single and living a long time. *J. Exp. Med. 193*:F15–F18.

Lee, J.H., Abraham, S.C., Kim, H.S., Nam, C., Choi, C., and Lee, M.C. 2002. Inverse relationship between APC gene mutation in gastric adenomas and development of adenocarcinoma. *Am. J. Pathol. 161*:611–618.

Li, Q.L., Ito, K., Sakakura, C., Fukamachi, H., Inoue, K., Chi, X.Z., Lee, K.Y., Nomura, S., Lee, C.W., Han, S.B., Kim, H.M., Kim, W.J., Yamamoto, H., Yamashita, N., Yano, T., Ikeda, T., Itohara, S., Inazawa, J., Abe, T., Hagiwara, A., Yamagishi, H., Ooe, A., Kaneda, A., Sugimura, T., Ushijima, T., Bae, S.C., and Ito, Y. 2002. Casual relationship between the loss of RUNX3 expression and gastric cancer. *Cell 109*:113–124.

Lim, H.Y., Joo, H.J., Choi, J.H., Yi, J.W., Yang, M.S., Cho, D.Y., Kim, H.S., Nam, D.K., Lee, K.B., and Kim, H.C. 2000. Increased expression of cyclooxygenase-2 protein in human gastric carcinoma. *Clin. Cancer Res. 6*:519–525.

Louhimo, J., Kokkola, A., Alfthan, H., Stenman, U.H., and Haglund, C. 2004a. Preoperative hCGbeta and CA 72-4 are prognostic factors in gastric cancer. *Int. J. Cancer 111*:929–933.

Louhimo, J., Alfthan, H., Stenman, U.H., and Haglund, C. 2004b. Serum HCG beta and CA 72-4 are stronger prognostic factors than CEA, CA 19-9 and CA 242 in pancreatic cancer. *Oncology 66*:126–131.

Maeng, L., Lee, A., Choi, K.Y., Kang, C.S., and Kim, K.M. 2004. Granulomatous gastritis. *Am. J. Surg. Pathol. 28:*941–945.

Marrero, J.A., and Lok, A.S. 2004. Newer markers for hepatocellular carcinoma. *Gastroenterology 127*:S113–S119.

Miyaoka, Y., Kadowaki, Y., Ishihara, S., Ose, T., Fukuhara, H., Kazumori, H., Takasawa, S., Okamoto, H., Chiba, T., and Kinoshita, Y. 2004. Transgenic overexpression of Reg protein caused gastric cell proliferation and differentiation along parietal cell and chief cell lineages. *Oncogene 23*:3572–3579.

Moayyedi, P., and Ford, A. 2002. Recent developments in gastroenterology. *BMJ 325*:1399–1402.

Mori, M., Mimori, K., Shiraishi, T., Tanaka, S., Ueo, H., Sugimachi, K., and Akiyoshi, T. 1997. p27 expression and gastric carcinoma. *Nat. Med. 3*:593.

Murai, M., Toyota, M., Suzuki, H., Satoh, A., Sasaki, Y., Akino, K., Ueno, M., Takahashi, F., Kusano, M., Mita, H., Yanagihara, K., Endo, T., Hinoda, Y., Tokino, T., and Imai, K. 2005. Abberent methylation and silencing of the BNIP3 gene in colorectal and gastric cancer. *Clin. Cancer Res. 11*:1021–1027.

Nam, K.T., Hahm, K-B., Oh, S-Y., Yeo, M., Han, S-U., Ahn, B., Kim, Y-B., Kang, J.S., Jang, D.D., Yang, K-H., and Kim, D-Y. 2004. The selective cyclooxygenase-2 inhibitor nimesulide prevents *Helicobacter pylori*-associated gastric cancer development in a mouse model. *Clin. Cancer Res. 10*:8105–8113.

Nollet, F., Berx, G., and Roy, F. 1999. The role of the E-cadherin/catenin adhesion complex in the development and progression of cancer. *Mol. Cell Biol. Res. Commun. 2*:77–85.

Okano, H., Shinohara, H., Hiyamoyo, A., Takaori, K., and Tanigawa, N. 2004. Concomitant overexpression of cyclooxygenase-2 in HER-2-positive on Smad 4-reduced

human gastric carcinomas is associated with a poor patient outcome. *Clin. Cancer Res. 10*:6938–6945.

Pece, S., and Gutkind, J.S. 2000. Signaling from E-caderins to the MAPK pathway by the recruitment and activation of epidermal growth factor receptors upon cell-cell contact formation. *J. Biol. Chem. 275*:41227–41233.

Pepe, M., Etzioni, R., Feng, Z., Potter, J.D., Thompson, M.L., Thornquist, M., Winget, M, and Yasui, Y. 2001. Phases of biomarker development for early detection of cancer. *J. Natl. Cancer Inst. 93*:1054–1061.

Perrais, M., Pigny, P., Buisine, M.P., Porchet, N., Aubert, J.P., and Van Seuningeir-Lempire, I. 2001. Aberrant expression of human mucin gene MUC5B in gastric carcinoma and cancer cells. Identification and regulation of a distal promoter. *J. Biol. Chem. 276*:15386–15396.

Pinto-de-Sousa, J., Reis, C.A., David, L., Pimenta, A., and Cardoso-de-Oliveira, M. 2004. MUC5B expression in gastric carcinoma: relationship with clinicopathological parameters and with expression of mucins MUC1, MUC2, MUC5AC and MUC6. *Virchows Arch. 444*:224–230.

Polakis, P. 2001. More than one way to skin a catenin. *Cell 105*: 563–566.

Rabenau, K.E., O′Toole, J.M., Bassi, R., Kotanides, H., Witte, L., Ludwig, D.L., and Pereira, D.S. 2004. DEGA/AMIGO-2, a leucine-rich repeat family member, differentially expressed in human gastric adenocarcinoma: effects on ploidy, chromosomal stability, cell adhesion/migration and tumorigenicity. *Oncogene 23*:5056–5067.

Rosivatz, E., Becker, I., Specht, K., Fricke, E., Luber, B., Busch, R., Hofler, H., and Becker, K.F. 2002. Differential expression of the epithelial-mesenchymal transition regulators snail, SIP1, and twist in gastric cancer. *Am. J. Pathol. 161*:1881–1891.

Rossi, G., Valli, R., Bertolini, F., Marchioni, A., Cavazza, A., Mucciarini, C., Migaldi, M., Federico, M., Trentini, G.P., and Sgambato, A. 2005. PDGFR expression in differential diagnosis between KIT-negative gastrointestinal stromel tumors and other primary soft tissue tumors of the gastrointestinal tract. *Histopathology 46*:522–531.

Sakamoto, I., Yamada, T., Ohwada, S., Koyama, T., Nakano, T., Okabe, T., Hamada, K., Kawate, S., Takeyoshi, I., Iino, Y., and Morishita, Y. 2004. Mutational analysis of the BAK gene in 192 advanced gastric and colorectal cancers. *Int. J. Mol. Med. 13*: 53–55.

Sato, K., Tamura, G., Tsuchiya, T., Endoh, Y., Usuba, O., Kimura, W., and Motoyama, T. 2001. Frequent loss of expression without sequence mutations of the DCC gene in primary gastric cancer. *Br. J. Cancer 85*:199–203.

Seril, D.N., Liao, J., Yang, G.Y., and Yang, C.S. 2003. Oxidative stress and ulcerative colitis-associated carcinogenesis: studies in humans and animal models. *Carcinogenesis 24*:353–362.

Shirin, H., Sordillo, E.M., Kolevska, T.K., Hibshoosh, H., Kawabata, Y., Oh, S.H., Kuebler, J.F., Delohery, T., Weghorst, C.M., Weinstein, I.B., and Moss, S.F. 2000. Chronic *Helicobacter pylori* infection induces an apoptosis-resistant phenotype associated with decreased expression of p27(kipl). *Infect. Immun. 68*:5321–5328.

Sun, Y., Li, J-Y., He, J.S., Zhou, L-X., and Chen, K. 2005. Tissue microarray analysis of multiple gene expression in intestinal metaplasia, dysplasia, and carcinoma of the stomach. *Histopathology 46*:505–514.

Takenawa, H., Kurosaki, M., Enomoto, N., Miyasaka, Y., Kanazawa, N., Sakamoto, N., Ikeda, T., Izumi, N., Sato, C., and Watanabe, M. 2004. Differential gene-expression profiles associated with gastric adenoma. *Br. J. Cancer 90*:216–223.

Tomkova, K., Belkhiri, A., El-Rifai, W., and Zaika, A.I. 2004. p73 isoforms can induce T-cell factor-dependent transcription in gastrointestinal cells. *Cancer Res. 64*:6390–6393.

Uemura, N., Okamoto, S., Yamamoto, S., Matsumura, N., Yamaguchi, S., Yamakido, M., Taniyama, K., Sasaki, N., and Schlemper, R.J. 2001. *Helicobacter pylori* infection and the development of gastric cancer. *N. Engl. J. Med. 345*:784–789.

Ueno, M., Toyota, M., Akino, K., Suzuki, H., Kusano, M., Satoh, A., Mita, H., Sasaki, Y., Nojima, M., Yanagihara, K., Hinoda, Y., Tokino, T., and Imai, K. 2004. Aberrant methylation and histone deacetylation associated with silencing of SLC5A8 in gastric cancer. *Tumour Biol. 25*:134–140.

Ushijima, T., and Sasako, M. 2004. Focus on gastric cancer. *Cancer Cell 5*:121–125.

Varis, A., Zaika, A., Puolakkainen, P., Nagy, B., Madrigal, I., Kokkola, A., Vayrynen, A., Karkkainen P, Moskaluk C, El-Rifai W, and Knuutila, S. 2004. Coamplified and overexpressed genes at ERBB2 locus in gastric cancer. *Int. J. Cancer 109*:548–553.

Varro, A., Noble, P.J., Pritchard, D.M., Kennedy, S., Hart, C.A., Dimaline, R., and Dockray, G.J. 2004. *Helicobacter pylori* induces plasminogen activator inhibitor 2 in gastric epithelial cells through nuclear factor-kappaB and RhoA: implications for invasion and apoptosis. *Cancer Res. 64*:1695–1702.

Wang, J., Chi, D.S., Kalin, G.B., Sosinski, C., Miller, M.E., Burja, I., and Thomas E. 2002. *Helicobacter pylori* infection and oncogene expression in gastric carcinoma and its precursor lesions. *Dig. Dis. Sci. 47*:107–113.

Xu, H., Chaturvedi, R., Cheng, Y., Bussiere, F.I., Asim, M., Yao, M.D., Potosky, D., Meltzer, S.J., Rhee, J.G., Kim, S.S., Moss, S.F., Hacker, A., Wang, Y., Casero, R.A., and Wilson, K.T. 2004. Spermine oxidation-induced by *Helicobacter pylori* results in apoptosis and DNA damage: implications for gastric carcinogenesis. *Cancer Res.* 64:8521–8525.

Yamaguchi, U., Hasegawa, T., Masuda, T., Sekine, S., Kawai, A., Chuman, H., and Shimoda, T. 2004. Differential diagnosis of gastrointestinal stromal tumor and other spindle cell tumors in the gastrointestinal tract based on immunohistochemical analysis. *Virchows Arch. 445*:142–150.

Yao, Y., Tao, H., Kim, J.J., Burkhead, B., Carloni, E., Gasbarrini, A., and Sepulveda, A.R. 2004. Alterations of DNA mismatch repair proteins and microsatellite instability levels in gastric cancer cell lines. *Lab. Invest. 84*:915–922.

Yasui, W., Oue, N., Kuniyasu, H., Ito, R., Tahara, E., and Yokozaki, H. 2001. Molecular diagnosis of gastric cancer: present and future. *Gastric Cancer 4*:113–121.

Yokota, T., Saito, T., Teshima, S., Kikuchi, S., Kunii, Y., and Yamauchi, H. 1998. Lymph node metastasis in early gastric cancer: how can surgeons perform limited surgery? *Int. Surg. 83*:287–290.

2

Role of Immunohistochemical Expression of p53 in Gastric Carcinoma

Ming Teh and Kong-Bing Tan

Introduction

Gastric carcinoma is an important gastrointestinal (GI) malignancy that carries with it high morbidity and mortality when detected late. Although its incidence is on a worldwide decline, it remains one of the most common cancers worldwide, particularly in Asia. In Singapore, it ranks as the fourth most common cancer: the age-standardized incidence rate among Chinese males was 29.3 per 100,000 per year (1988–1992), a figure between those of Western populations and populations with a high incidence of the disease, such as the Japanese (Parkin *et al.,* 1997).

Gastric intestinal metaplasia and gastric dysplasia are well-recognized precursor lesions of gastric carcinoma. They often arise in the setting *of Helicobacter pylori*–associated chronic atrophic gastritis, a condition that is itself a risk factor for the development of gastric carcinoma. All of these lesions are well-characterized histologically. Patients with low-grade gastric dysplasia undergo surveillance gastric endoscopy with biopsy, whereas those with high-grade dysplasia are often advised to undergo resection of the lesion. Where the technique is available, endoscopic mucosal resections may offer a nonsurgical cure.

Whereas gastric carcinogenesis is a multistep process associated with multiple causes, p53 mutations play an important role in this transformation. They are thought to be early events in the stepwise progression to gastric carcinoma (Teh and Lee, 1994), especially the intestinal type (Ranzani *et al.,* 1995). Studies of p53 mutagenesis have mainly been by the use of polymerase chain reaction (PCR)–single-strand conformation polymorphism (SSCP) assays, and gene-sequencing studies (Fenoglio-Preiser *et al.,* 2003; Murakami *et al.,* 1999).

Immunohistochemical overexpression of p53 has been used as a convenient surrogate marker of p53 mutations. This is based on the concept that wild-type p53 is normally present in amounts that are undetectable by the usual immunohistochemical methods. The mutated protein, however, has a much longer half-life, leading to intranuclear accumulation and, hence, detectability using specific monoclonal antibodies (Finlay *et al.,* 1989). Problems with this assumption exist. On the one hand, wild-type p53 accumulation may occur as a repair-type response during inflammatory conditions and may be immunohistochemically positive, especially with the use of efficient antigen-retrieval methods (McKee *et al.,* 1993). On the other hand, some p53 mutations may not produce immunodetectable p53 (Fenoglio-Preiser *et al.,* 2003). Nevertheless, there has been a large number of studies on p53 immunoexpression in gastric carcinoma and its precursor lesions (Fenoglio-Preiser *et al.,* 2003; Teh and Lee, 1994; Teh *et al.,* 2002).

Handbook of Immunohistochemistry and *in situ* Hybridization of Human Carcinomas, Volume 4: Molecular Genetics, Gastrointestinal Carcinoma, and Ovarian Carcinoma

Although there are variations in the findings, which are probably contributed by differences in the methodology used, these studies have advanced our understanding of the role of p53 abnormalities in gastric carcinogenesis. This chapter summarizes the relevant findings to date, discusses the implications, and suggests future directions in this area.

MATERIALS

1. Dako EnVision+ System Kit
2. MICROMED T/T Microwave
3. Citrate buffer (0.01M)
4. Iris-buffer saline (TBS) (pH 7.6)
5. Gill's Hematoxylin (MERCK, modified solution, 0B315401)
6. p53 antibody (Dako, clone DO-7)

METHODS

1. Dewax sections in xylene, and hydrate to water in descending grade of alcohol.
2. Treat section in 0.01M citrate buffer (pH 6) by Micromed T/T oven for 20 min.
3. Wash in water.
4. Quench any endogenous peroxidase activity by incubating the section with 3% H_2O_2 for 10 min.
5. Wash in TBS for 5 min.
6. Apply p53 (diluted 1/500) on section and incubate for 1 hr.
7. Rinse gently with buffer, and place in a fresh buffer bath for 10 min.
8. Incubate the sections with the labeled polymer for 30 min.
9. Wash in TBS for l0 min.
10. Incubate with DAB (diaminobenzidine) + substrate for 5–10 min.
11. Rinse gently with distilled water. Collect substrate-chromogen waste in a hazardous materials container for proper disposal.
12. Counterstain the nuclei with Gill's haematoxylin for 30 sec to 1 min.
13. Wash in water, dehydrate in alcohol, clear in xylene, and mount with DPX.

RESULTS AND DISCUSSION

The p53 oncoprotein is detected in many cases of gastric carcinomas—60% in our experience (Teh and Lee, 1994) (Figure 17A). Muitiple studies have been done in this area and have shown that p53 is immunohistochemically detectable in 4–90% of gastric carcinomas (Martin *et al.,* 1990; Setala *et al.,* 1998). As with any series of studies involving differing methodologies, this variability is not unexpected. This range of p53 immunoexpression is fairly comparable to that of p53 mutations, which are found in 0–77% of carcinomas (Correa and Shiao, 1994; Yamada *et al.,* 1991). In a 2003 review, Fenoglio-Preiser *et al.,* stated that there was poor correlation between p53 immunoexpression and the presence of p53 mutations; however, p53 immunonegative cases tended to be negative for mutations. In a series by Ranzani *et al*. (1995), 88% of cases with p53 mutations had immunoexpression of the protein as well. Taken together, these observations indicate that p53 immunoexpression in gastric carcinoma can detect the presence of p53 mutations with fairly high

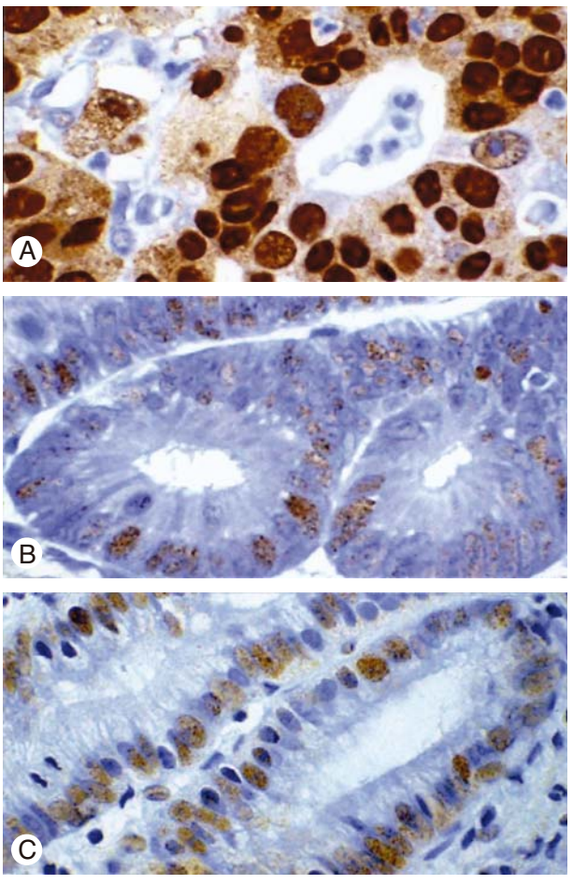

Figure 17. A: Strong nuclear p53 immunoexpression in a case of gastric adenocarcinoma (original magnification, 600X). **B:** Moderate nuclear p53 immunoexpression in a case of gastric dysplasia (original magnification, 600X). **C:** Moderate p53 immunoexpression, similar to that of Figure 17B, in nonneoplastic, nondysplastic gastric epithelium, from a case of *Helicobacter pylori* chronic gastritis (original magnification, 500X).

sensitivity. The presence of cases with false positivity, however, implies an unreliable positive predictive value.

The protein p53 is commonly detected in both the intestinal and diffuse subtypes of gastric carcinomas. It remains controversial which of these two subtypes has higher p53 immunoexpression. A few studies have shown that the intestinal subtype is associated with a higher incidence of p53 immunoexpression (Victorzon *et al.,* 1996). A 2002 study has also revealed that p53 immunoexpression is present more commonly in the mixed type of carcinoma than in the pure poorly differentiated diffuse carcinoma *(*56% versus 19%) (Kozuki *et al.,* 2002). Our experience, however, has been that there is a higher incidence of p53 immunoexpression in the diffuse subtype as compared to the intestinal subtype (69% versus 55%), although this difference was just short of statistical significance ($p < 0.075$) (Teh and Lee, 1994). Regardless of the previously mentioned controversy, it has become widely accepted that p53 is one of the genes involved in the stepwise process of gastric malignant transformation. It is established that this mutation occurs early in the progression to gastric carcinoma, in particular the intestinal subtype (Teh and Lee, 1994; Ranzani *et al.,* 1995). Immunoexpression of p53 has also been described in 24% of minute type of gastric carcinomas (<5 mm in size), as compared with 35% of surrounding nonminute carcinomas. It has been theorized that p53 aberration was needed more for the progression of these small lesions rather than for its formation (Sasaki *et al.,* 1999).

The potential uses of p53 immunoexpression in gastric carcinoma workup have been intensively studied. Although the diagnosis of frank gastric carcinoma is not usually a problem, the recognition of very well-differentiated carcinomas in superficial biopsies may occasionally be challenging. Niimi *et al*. (2002) have found that a high p53 and Ki-67 labeling index highlights the carcinomatous areas from the surrounding nonneoplastic areas and may prove helpful in this context.

The correlation between p53 immunoexpression and disease stage as well as survival in gastric carcinoma is controversial. A survey of a number of studies has revealed conflicting results (Fenoglio-Preiser *et al.,* 2003). In a series by Victorzon *et al*. (1996), p53 immunoexpression was significantly associated with survival only on univariate analysis but not on multivariate analysis. Only the stage of the disease, including the presence of metastases, emerged as independent prognostic factors. In an interesting study by Shiao *et al*. (2000), p53 mutations combined with the lowest or highest level of p53 accumulation independently predicted regional metastases. A tissue microarray study showed that the immunoprofile of a panel of tumor-suppressor genes, including p53 expression, was associated with stage of disease and patient survival (Lee *et al.,* 2003). As in other malignancies, tissue microarray–based multimarker prognostication for gastric carcinoma appears promising. However, p53 immunoexpression in gastric carcinomas has been reported to be fairly heterogeneous (Jiang *et al.,* 1997). Therefore, whether a restricted sample, as in a microarray tissue core, can adequately evaluate for p53 immunoexpression would have to be addressed.

The value of p53 immunoexpression in gastric carcinoma for predicting response to chemotherapy has also been evaluated in several studies. More studies have tended to show p53 immunoexpression to be associated with a reduced likelihood of response to chemotherapy than the contrary (Diez *et al.,* 2000; Fenoglio-Preiser *et al.,* 2003; Kikuyama *et al.,* 2001).

p53 is also commonly immunoexpressed in gastric dysplasias, particularly high-grade lesions (see Figure 17B). Varying studies have shown p53 immunoexpression in 15–67% of high-grade lesions (Brito *et al.,* 1994; Miracco *et al.,* 1995). Studies on p53 mutations in gastric dysplasia also showed a range of incidence up to 42% (Hao *et al*., 1997). Gastric epithelium with regenerative atypia may resemble gastric dysplasia microscopically. Some authors have suggested that p53 immunoexpression may help differentiate high-grade gastric dysplasia from less significant lesions (Brito *et al.,* 1994). However, p53 immunoexpression has been demonstrated in the gastric epithelium of intestinal metaplasia and *H. pylori* gastritis *(vide infra),* implying that caution should be exercised with regard to the use of p53 immunoexpression to aid in the diagnosis of gastric dysplasia.

In our experience of *H. pylori* gastritis, 23% of the cases exhibited definite staining for p53 (Teh *et al.,* 2002). Besides staining in the epithelium of intestinal metaplasia, p53 was also demonstrable in adjacent nonmetaplastic, nonneoplastic gastric epithelium (see Figure 17C). The literature has shown variable p53 immunoexpression in gastric mucosa with intestinal metaplasia; variable absent-to-low expression has also been reported in chronic gastritis (Fenoglio-Preiser *et al.,* 2003). Controversy exists with regards to the nature of the immunoexpressed p53 in such nonneoplastic and nonmetaplastic gastric epithelium. Jones *et al*. (1997) attributed this to overexpression of wild-type p53 as well as the sensitivity of the antigen-retrieval methods. This was supported by Marinone *et al*. (2001) who were unable to find p53 mutations in a study of 130 cases of dysplasia, which included cases of *H. pylori* gastritis. However, Murakami *et al*. (1999) have sequenced the p53 gene in *H. pylori* gastritis mucosa without dysplasia and metaplasia and found non–hot spot codon mutations of the gene, indicating that *H. pylori* infection may be associated with point mutations of p53 and thus involved

in the process leading to dysplasia and malignancy. Nardone *et al.* (1999) also found expression of p53 in *H. pylori* gastritis and further demonstrated diminished p53 after eradication of the organism. They concluded that chronic *H. pylori* infection may be responsible for the *genomic instability* observed in at least some cases of *H. pylori* gastritis. More work has to be done, in particular, deoxyribonucleic acid (DNA) sequencing of clean samples of p53 positive cells with laser capture, before a firm conclusion can be drawn on the nature of p53 immunoexpression in this context.

If the immunodetectable p53 in nonneoplastic and nondysplastic gastric epithelium is indeed the result of p53 mutations, it would mean that p53 mutations occur much earlier in the stepwise progression to malignant transformation. Further studies are needed to see if patients with such *at-risk* epithelium would benefit from closer attention during gastric endoscopic surveillance. If, however, the immunodetectable p53 is the result of increased wild-type p53, it would still indicate that the gastric epithelial cells in question were sustaining chronic cellular injury. This could provide the milieu for *genomic instability* to occur, giving rise to possible gene mutations. Thus, p53 immunoexpression in the context of chronically inflamed gastric mucosa, whether the result of actual gene mutation or increased expression of wild-type protein, may just represent parts of the same spectrum of *p53 abnormalities.* Such epithelium could conceivably have the potential of acquiring further genomic alterations, leading to neoplastic progression, at least in some cases.

Our experience with the cagA-positive strain of *H. pylori* infection suggests that this strain results in higher p53 immunoexpression in nonneoplastic gastric mucosa, as compared with infection by the cagA-negative strain (Teh *et al.,* 2002). This finding is in keeping with studies in gastric carcinoma, where cagA-positive *H. pylori* infection also appeared to result in a higher rate of p53 mutations (Shibata *et al.,* 2002). The cagA-positive strain of *H. pylori* is more virulent than its cagA-negative counterpart. It is also associated with increased cell proliferation and, more controversially, with decreased apoptotic activity (Moss *et al.,* 2001; Peek *et al.,* 1997). If the p53 overexpression in *H. pylori* gastritis is a consequence of mutation to a more stable protein, our findings may help to explain the decreased apoptosis associated with infection by the cagA-positive strain.

As compared with p53 mutational studies, immunohistochemical detection of p53 is more convenient and can readily be used in the routine diagnostic laboratory. The alternative of DNA studies does not appear to be an advantage because the wide variation of p53 immunoexpression in gastric carcinoma and gastric dysplasia is paralleled by the similar degree of variation of incidence of p53 mutations in these lesions. The variability of p53 immunoexpression in gastric carcinoma needs to be addressed by closer interlaboratory collaboration, the institution of standardized immunohistochemical protocols, and participation in external quality assurance programs. Only then can we address whether there are actual geographically determined differences in gastric p53 abnormalities.

In conclusion, research on p53 expression has indicated its importance in the pathogenesis of gastric carcinoma. Notably, it is present in the nonneoplastic mucosa of some cases of *H. pylori* gastritis. Its expression tends to be increased as gastric epithelium progresses to intestinal metaplasia, the various grades of dysplasia, and finally carcinoma. Either alone or in combination with other markers, p53 deserves further investigation as a prognostic marker in gastric carcinoma. Its expression in gastric intestinal metaplasia and *H. pylori* gastritis may signify genomic instability and further exploration into its potential use in risk stratifying such patients for appropriate follow-up is needed.

Acknowledgments

We thank Mr. C.K. Ow and Mr. S.N. Choo for the immunohistochemical work, Mr. T.C. Tan and Mr. C. Chia for the photomicrographs, and Mr. H. Matsuni for the artwork.

References

Brito, M.J., Williams, G.T., Thompson, H., and Filipe, M.U. 1994. Expression of p53 in early (Tl) gastric carcinoma and precancerous adjacent mucosa. *Gut 35*:1697–1700.

Correa, P., and Shiao, Y. 1994. Phenotypic and genotypic events in gastric carcinogenesis. *Cancer Res. 54*:1914s–1943s.

Diez, M., Medrano, M.J., Guitierrez, A., Lopez, A., Muguerza, J.M., Hemandez, P., Lozano, O., Noguerales, F., Ruiz, A., and Granell, J. 2000. p53 protein expression in gastric adenocarcinoma. Negative predictor of survival after postoperative adjuvant chemotherapy. *Anticancer. Res. 20*:3929–3933.

Fenoglio-Preiser, C.M., Wang, J., Stemmermann, G.N., and Noffsinger, A. 2003. TP53 and gastric carcinoma: a review. *Hum. Mutat. 21*:258–270.

Finlay, C.A., Hinds, P.W., and Levine, A.J. 1989. The p53 proto-oncogene can act as a suppressor of transformation. *Cell 57*:1083–1093.

Hao, Y., Zhang, J., Yi, C., and Qian, W. 1997. Abnormal change of p53 gene in gastric and precancerous lesions and APC gene deletion in gastric carcinoma and near tissues. *J. Tongji Med. Univ. 17*:75–78.

Jiang, H., Han, P., Jiang, Y., Liang, X., Hu, C., and Yang, D. 1997. The clinical significance of the immunohistochemical detection of p53 protein in endoscopic biopsy specimens. *Chin. Med. J. 110*:202–205.

Jones, N.L., Shannon, P.T., Cutz, E., Yeger, H., and Sherman, P.M. 1997. Increase in proliferation and apoptosis of gastric epithelial cells early in the natural history of *Helicobacter pylori* infection. *Am. J. Pathol. 151*:1695–1703.

Kikuyama, S., Inada, T., Shimizu, K., Miyakita, M., and Ogata, Y. 2001. p53, bcl-2 and thymidine phosphorylase as predictive markers of chemotherapy in patients with advanced and recurrent gastric cancer. *Anticancer Res. 21*:2149–2154.

Kozuki, T., Yao, T., Nakamura, S., Matsumoto, T., and Tsuneyoshi, M. 2002. Differences in p53 and cadherin–catenin complex expression between histological subtypes in diffusely infiltrating gastric carcinoma. *Histopathology 41*:56–64.

Lee, H.S., Lee, H.K., Kim, H.S., Yang, H.K., and Kim, W.H. 2003. Tumour suppressor gene expression correlates with gastric cancer prognosis. *J. Pathol. 200*:39–46.

Marinone, C., Martinetti, A., Mestriner, M., Seregni, E., Geuna, M., Ferrari, L., Strola, G., Bonardi, L., Fea, E., and Bombardieri, E. 2001. p53 evaluation in gastric mucosa of patients with chronic *Helicobacter pylori* infection. *Anticancer Res. 21*:1115–1118.

Martin, I.G., Scott, N.S., Bell, S., Pickles, A., Murday, V., Dixon, M.F., Johnston, and Quirke. 1990. Gastric cancer is not associated with K-ras mutations or with abnormal p53 expression. *Gut 31*: A1178.

McKee, P.H., Hobbs, *C.,* and Hall, P.A. 1993. Antigen retrieval by microwave irradiation lowers immunohistochemical detection thresholds. *Histopathology 23*:377–379.

Miracco, C., Spina, D., Vindigni, C., Filipe, M.I., and Tosi, P. 1995. Cell proliferation patterns and p53 expression in gastric dysplasia. *Int. J. Cancer 62*:149–154.

Moss, S.F., Sordillo, E.M., Abdalla, A.M., Makarov, V., Hanzely, Z., Perez-Perez, G.I., Blaser, M.J., and Holt, P.R. 2001. Increased gastric epithelial cell apoptosis associated with colonization with cagA+ *Helicobacter pylori* strains. *Cancer Res. 61*: 1406–1411.

Murakami, K., Fujioka, T., Okimoto, T., Mitsuisbi, Y., Oda, T., Nishizono, A., and Nasu, M. 1999. Analysis of p53 gene mutations in *Helicobacter pylori*-associated gastritis mucosa in endoscopic biopsy specimens. *Scand. J. Gastroenterol. 5*: 474–477

Nardone, G., Staibano, S., Rocco, A., Mezza, E., D'armiento, F.P., Insabato, L., Coppola, A., Salvatore, G., Lucariello, A., Figura, N., De Rosa, G., and Budillon, G. 1999. Effect of *Helicobacter pylori* infection and its eradication on cell proliferation, DNA status, and oncogene expression in patients with chronic gastritis. *Gut 44*:788–799.

Niimi, C., Goto, H., Ohmiya, N., Niwa, Y., Hayakawa, T., Nagasaka, T., and Nakashima, N. 2002. Usefulness of p53 and Ki-67 immunohistochemical analysis for preoperative diagnosis of extremely well-differentiated gastric adenocarcinoma. *Am. J. Clin. Pathol. 118*:683–692.

Parkin, D.M., Whelan, S.L., Ferlay, J., Raymond, L., and Young, J. (eds). 1997. *Cancer Incidence in Five Continents, Volume VII*. No. 143. Lyon: IARC Scientific Publications.

Peek, R.M. Jr., Moss, S.F., Tham, K.T., Perez-Perez, G.I., Wang, S., Miller, G.G., Atherton, J.C., Holt, P.R., and Blaser, M.J. 1997. *Helicobacter Pylori* cagA+ strains and dissociation of gastric epithelial cell proliferation from apoptosis. *J. Natl. Cancer Inst. 89*:863–868.

Ranzani, G.N., Luinetti, O., Padovan, L.S., Calistri, D., Renault, B., Burrel, M., Amadori, D., Fiocca, R., and Solcia, E. 1995. p53 gene mutations and protein nuclear accumulation are early events in intestinal type gastric cancer but late events in diffuse type. *Cancer Epidemiol. Biomarkers Prev. 4*:223–231.

Sasaki, I., Yao, T., Nawata, H., and Tsuneyoshi, M. 1999. Minute gastric carcinoma of differentiated type with special reference to the significance of intestinal metaplasia, proliferative zone, and p53 protein during tumor development. *Cancer 85*:1719–1729.

Setala, L., Kosma, V.-M., Lipponen, P., Naukkarinen, A., Nordling, S., Hollmen, S., Eskelinen, M., Syrjanen, K., and Alhava, E. 1998. Clinical relevance of p53 index and expression of proliferating cell nuclear antigen and Ki-67 in gastric cancer. *J. Cancer Res. Clin. Oncol. 124*:497–502.

Shiao, Y.-H., Palli, D., Caporaso, N.E., Alvord, W.G., Amorosi, A., Nesi, G., Saieva, C., Masala, G., Fraumeni, J.F. Jr., and Rice, J.M. 2000. Genetic and immunohistochemical analyses of p53 independently predict regional metastasis of gastric cancers. *Cancer Epidemiol. Biomarkers Prev. 9*:631–633.

Shibata, A., Parsonnet, J., Longacre, T.A., Garcia, M.I., Puligandla, B., Davis, R.E., Vogelman, J.H., Orentreich, N., and Habel, L.A. 2002. CagA status of *Helicobacter pylori* infection and p53 mutations in gastric adenocarcinoma. *Carcinogenesis 23*:419–424.

Teh, M., and Lee, Y.S. 1994. An immunohistochemical study of p53 protein in the different histological subtypes of gastric carcinoma. *Pathology 26*:432–434.

Teh, M., Tan, K.B., Seet, B.L., and Yeoh, K.G. 2002. Study of p53 immunostaining in the gastric epithelium of cagA positive and cagA negative *Helicobacter pylori* gastritis. *Cancer 95*:499–505.

Victorzon, M., Nordling, S., Haglund, C., Lundin, J., and Roberts, P.J. 1996. Expression of p53 protein as a prognostic factor in patients with gastric cancer. *Eur. J. Cancer 32A*:215–220.

Yamada, Y., Yoshida, T., Hayashi, K., Sekiya, T., Yokata, J., Hirohashi, S., Nakatani, K., Nakano, H., Sugimura, T., and Terada, M. 1991. p53 gene mutations in gastric cancer metastases and in gastric cancer cell lines derived from metastases. *Cancer Res. 51*:5800–5805.

This Page Intentionally Left Blank

3

Role of Immunohistochemical Expression of p53 and Vascular Endothelial Growth Factor in Gastric Carcinoma

Manuel Pera, Alain Volant, Constantino Fondevila, Jean Philippe Metges, Oscar Vidal, and Antonio Palacín

Introduction

Until the 1980s, gastric cancer was one of the most frequent tumors in the world and the leading cause of cancer death (Parkin *et al.,* 1999). In recent decades the incidence has declined, but the prognosis of gastric cancer in the Western countries has not improved, the 5-year survival being 20–30% (Greenlee *et al.,* 2001; Hundahl *et al.,* 2000). Surgical resection is the most powerful tool to improve prognosis, whereas the major problem is delayed diagnosis resulting in advanced disease. In most American and European series, almost 60% of operated patients have pathologic tumor (pT) stages III and IV.

In curatively resected patients, the biologic nature of the tumor determines survival because almost half will die from recurrent cancer (Averbach and Jacquet, 1996). The poor prognosis of patients with recurrent disease results from the lack of an effective rescue treatment. In fact, the number of patients with recurrent gastric cancer for which it is feasible to perform curative surgery is less than 4% (Yoo *et al.,* 2000). During the last few years many attempts have been made to better define the biological profile of gastric tumors with the aim to improve early diagnosis and prognostic stratification and eventually cure. Newer tumor markers include tumor-suppressor gene *p53 (TP53),* vascular endothelial growth factors (VEGF), and microvessel density (MVD) as a measure of new blood-vessel growth or angiogenesis. Without blood vessels, tumors cannot grow beyond a critical mass or create metastases (Castells and Rustgi, 2003). A hypoxic environment and genetic instability in the center of the tumor allow the evolution of cellular clones with loss of p53 function. These cells have lower apoptotic rate and produce angiogenic factors such as VEGF, inducing new vasculature (Harris, 1997). The study of these factors could provide valuable information in predicting the prognosis of patients with gastric cancer. In this chapter we describe our technique for immunohistochemical detection of p53 and VEGF in gastric carcinomas and the possible role of their expression as prognostic factors of survival, recurrence, and response to treatments.

Handbook of Immunohistochemistry and *in situ* Hybridization of Human Carcinomas, Volume 4: Molecular Genetics, Gastrointestinal Carcinoma, and Ovarian Carcinoma

The Role of p53 and Vascular Endothelial Growth Factor in Human Cancers

TP53 is the most commonly mutated gene in human tumors (Hollstein *et al.,* 1991). *TP53* encodes for a nuclear protein, which plays a key role in tumor progression by regulating deoxyribonucleic acid (DNA) repair, cell division, and apoptosis. The gene spans 20 Kb of genomic DNA located at 17p13, contains 11 exons, and encodes a 53-kd phosphoprotein that is a transcription factor for genes that induce cell cycle arrest or apoptosis (Levine, 1997). p53 is also a genomic stabilizer and an inhibitor of angiogenesis. p53 function in cancer can be lost by various mechanisms, including lesions that prevent activation of p53, mutations within the *TP53* gene (which encodes p53) itself, or mutations of downstream mediators of p53 function (Vousden and Lu, 2002). It is important to note that more than 50% of human cancers contain mutations in p53 and that these mutations can affect the angiogenic balance. Tumor-associated mutations in *TP53* are predominantly point mutations (93.6%) that result is single amino-acid substitutions—a mutational spectrum that is quite different from that seem in other tumor-suppressor genes, in which large deletions or frameshift mutations tend to result in complete loss of protein expression (Vousden and Lu, 2002).

The result of the mutational inactivation of *TP53* by single-amino-acid substitutions is that many tumor cells retain the ability to express the mutant p53 protein. These proteins are often more stable than the wild-type p53 and are present at very high levels in the tumor cell. One explanation for the selection of such mutations is that the mutant p53 proteins can act as dominant-negative inhibitors of the wild-type p53, which functions as a tetramer. The observation that many tumors that harbour *TP53* point mutations also show loss of heterozygosity—effectively eliminating the wild-type allele—indicates that the efficiency of dominant-negative inhibition might not be complete and almost certainly depends on the nature of the initial point mutation. However, partial inactivation of wild-type p53 function by mutant p53 might allow for some selective advantage during tumor progression. Nuclear accumulations of the p53 protein can also result from up-regulated expression of the wild-type p53 protein or decreased protein degradation in response to various cellular stresses, including DNA damage. Overexpression of the wild-type protein is a normal physiologic response to slow down the cell cycle at the G1 phase to allow repair of damaged DNA. In addition, during DNA damage, Mdm-2-dependent p53 degradation is inhibited (Ashcroft *et al.,* 1999). Therefore, low levels of wild-type p53 can be detected in the nucleus, especially if sensitive immunohistochemical detection techniques, such as antigen retrieval, are used (Fenoglio-Preiser *et al.,* 2003).

In addition to the genetic and epigenetic changes that occur during malignant transformation, another discrete step is required to allow tumor propagation and progression—the induction of a tumor vasculature, termed the "angiogenic switch" (Bergers and Benjamin, 2003; Hanahan and Weinberg, 2000). Proangiogenic gene expression is increased by physiologic stimuli, such as hypoxia, which results from increased tissue mass, and also by oncogene activation or tumor-suppressor mutation. Although it seems to be a paradox that blood vessels first regress as tumors progress, the hypoxic conditions eventually induce the formation of new blood vessels. The most prominent hypoxia-induced angiogenic factors are VEGF and VEGF receptor-2, which, in conjunction with angiopoietin-2, promote vascular remodeling and sprouting (Holash *et al.,* 1999). The clinical importance of VEGF is emphasized by the fact that VEGF inhibition has been shown to significantly inhibit angiogenesis and tumor growth in *in vivo* models (Kim *et al.,* 1993). Consequently anti-VEGF agents are being developed as therapeutic strategies to inhibit angiogenesis and progression.

It has recently reported that cancer cells with p53 mutations are selected for their ability to survive under hypoxic conditions (Yu *et al.,* 2002). As well as their increased resistance to apoptosis, cells with p53 defects have been shown to down-regulate the expression of thrombospodin-1 (TSP1), an endogenous angiogenesis inhibitor, and up-regulate the expression of VEGF (Bergers and Benjamin, 2003). This is supported by the finding that wild-type p53 inhibits VEGF transcription and that p53 promotes Mdm2-mediated ubiquitylation and proteosomal degradation of hypoxia-inducible factor-1 alpha (HIF-α)—the main transcriptional activator of VEGF under hypoxic conditions (Ravi *et al.,* 2000).

Protocol

Numerous studies have been published to determine the frequency of p53 and VEGF staining in gastric carcinoma and to relate the presence or absence of p53 nuclear staining and VEGF cytoplasmic staining to patient outcome or treatment outcomes.

Different antibodies have been used; tissue preparation and immunohistochemical detection techniques have varied. Some investigators use antigen-retrieval methods, whereas others do not, and the methods used

for antigen retrieval vary. Finally, criteria for judging a reaction to be positive or negative vary (Fenoglio-Preiser *et al.,* 2003). Here we describe our protocol for p53 and VEGF immunohistochemical detection and assessment.

MATERIALS

1. Xylene (PANREAC)
2. Formaldehyde 35–40% w/v (Panreac, Barcelona, Spain)
3. Ethyl alcohol 100% (Panreac)
4. Toluene (Panreac)
5. Paraffin for histology 58–60°C, Cymit Quimica SL. (Barcelona, Spain) Code N° 0587
6. Tissue-Tek II embedding cassette, Sakura. (Torrance, CA) Code N° 4187TT2
7. CITADEL 2000 Shandon (Thermo Electron Corporation, Waltham, MA)
8. Microtome MICROM (Walldorf, Germany) HM 325
9. Microtome Blades, FEATHER (Osaka, Japan) S 35
10. TechMate 500+, DakoCytomation Code N° S 230530
11. Capillary Gap Microscope Slides 75 µm ChemMate DakoCytomation Code N° S 2024
12. Micro coverglasses (Marienfeld, Baden-Württemberg, Germany) 24 × 36 N° 1
13. Pressure cooker, RAPID/SPLENDID 4 L
14. ChemMate Target Retrieval Solution 10×. DakoCytomation Code N° S 2031 (Glostrup, Denmark)
15. EDTA (ethylene diamine tetra-acetic acid) 1 mM (pH 8,0) 100×
16. Phosphate-buffered saline (PBS) 10×, (pH 7.4), Roche, Code N° S 2023
17. ChemMate Antibody Diluent, DakoCytomation Code N° S 2022
18. ChemMate Peroxidase-Blocking Solution, Dakocytomation Code N° S 2023
19. ChemMate Buffer Kit, DakoCytomation Code N° K 5006
20. Labeled Polymer HRP (horseradish peroxidase) Mouse, Dakocytomation Code N° K 4007.
21. Labeled Polymer HRP Rabbit, DakoCytomation Code N° K 4011.
22. Liquid DAB+ (diaminobenzidine) Substrate Chromogen System, DakoCytomation Code N° K 3468.
23. ChenMate Hematoxylin, DakoCytomation code N° S 2020.
24. Micromount (Mounting Medium) SURGIPATH Code N° 01730.
25. Antibodies:

Antibody	Manufacturer	Code N°	Origin	Clone	Retrieval	Working dilution
VEGF (A20)	Santa Cruz	Sc-152	Rabbit	—	PC/EDTA	1:300
p53	Novocastra	Ncl-p53-BP	Mouse	BP53-12	PC/citrate	1:50

PC, pressure cooker.

METHODS

Tissue Sections and Deparaffinization

Cut sections from paraffin blocks at 4 µm thickness on a microtome are floating on a 45°C waterbath containing distilled water. Transfer the sections onto a capillary gap microscope slide. Allow the slides to dry overnight in a oven at 37°C. Next day, deparaffinize sections in xylene and rehydrate them. Deparaffinize slide in 4 changes of xylene of 10 min each. Transfer slides to 100% ethyl alcohol, 1 change for 10 min and 2 changes for 3 min, and transfer once through 95%, 70%, 40%, and 20% alcohol for 1 min each. Finally place the slides into distilled water for 5 min.

Antigen Retrieval

Heat 2 L of the buffer solution (1 mM EDTA, pH 8.0 or 0.01 M sodium citrate buffer, pH 6.0) to boiling by using a stainless pressure cooker. Do not lock lid at this moment. When the buffer boils, put a maximum of 30 rehydrated sections in glass racks into the pressure cooker and make sure slides are well immersed in buffer solution, then lock the lid and bring to full pressure. The heating time begins only when full pressure is reached. Heating times of 2 min (citrate buffer) or 5 min (EDTA) are used. Remove the pressure cooker from heat source, depressurize, and cool it down under running water. Remove the lid and rinse the slides in PBS 3×, 5 min each for EDTA buffer. When using citrate buffer we leave the slides 15 min in buffer and then transfer them to PBS 3×, 5 min each.

Immunohistochemical Staining of Paraffin-Embedded Tissues

We use a semiautomated immunohistochemistry (IHC) stainer, TechMate 500+ (Dako, Carpinteria, CA) together with the Dako EnVision system. In brief:

1. Wash with ChemMate buffer N° 1.
2. Incubate with primary antibody (see Table in number 25 of previous list of materials) for 30 min.

3. Wash with ChemMate buffer N° 1 (3×).
4. Block endogenous peroxidase activity: ChenMate peroxidase blocking solution (3×).
5. Wash with ChemMate buffer N° 2 (3×).
6. Incubate with labeled polymer HRP mouse or rabitt for 30 min.
7. Wash with ChemMate buffer N° 1 (2×).
8. Wash with ChemMate buffer N° 3 (3×).
9. Substrate-Chromogen: DAB + Chromogen N° 3 (3×).
10. Wash with ChemMate N° 3 (3×).
11. Nuclear counterstain: hematoxylin 1 min
12. Wash with ChemMate buffer N° 4 (1×).
13. Wash with ChemMate buffer N° 3 (2×).
14. Wash with ChemMate buffer N° 2 (2×).
15. Wash with ChemMate buffer N° 3 (3×).
16. Controls:
    a. Positive control: Colon or breast carcinoma.
    b. Negative control: We replace the primary antibody for PBS.

Dehydration, Clearing, and Mounting Tissue Section on Slides

Dehydrate slides with ethyl alcohol	5× for 1 min each
Clearing slides with Xylene I	3 min
Xylene II	1 min
Xylene III	1 min

The sections are coverslipped with Micromount.

p53 Staining Analysis

Using a light microscope, a visual grading system based on the number of positively stained nuclei of the malignant cells in each tissue is used (Figure 18). If 10% or more of the malignant nuclei are stained, the slide is scored as positive. If fewer than 10% of the nuclei are stained, the slide is scored as negative, in accordance with other authors (Kakeji *et al.,* 1993; Maehara *et al.,* 1999). All specimens are usually analyzed by two separate investigators who are blinded to all clinical information. Conflicts in scores are resolved by consensus.

Vascular Endothelial Growth Factor Staining Analysis

Immunostaining with VEGF is considered positive when unequivocal cytoplasmic staining is seen in tumor cells, regardless of the number of cells stained. VEGF expression is analyzed in the invasive front of the tumor away from the tumor center where necrosis and hypoxia may induce VEGF expression. Intensity of staining for VEGF is graded as follows: –, no detectable expression; +, moderate stain; ++, strongest stain under a 250X field (Figure 19). As described by Inoue, we use smooth-muscle cells as positive internal control (Inoue *et al.,* 1997). Two different investigators usually assess the degree of staining without knowledge of the clinical data.

RESULTS AND DISCUSSION

Complete surgical resection is the mainstay of treatment with hope of cure for patients with gastric cancer. However, the prognosis after resection of gastric cancer has remained unsatisfactory because of a high incidence of postoperative recurrence. It has been suggested that identification of variables in gastric tumor biology may lead to more precise assessment of outcome and response to therapy. In a 2004 study, we investigated the potential prognostic value of p53

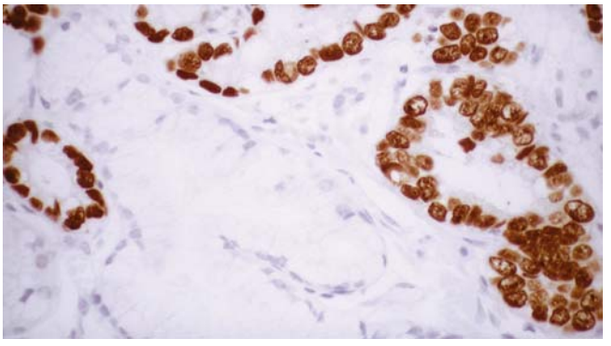

Figure 18. Intense and diffuse nuclear staining for p53 in tumor cells of an intestinal-type adenocarcinoma. By contrast the nuclei of normal glands are negative (400X).

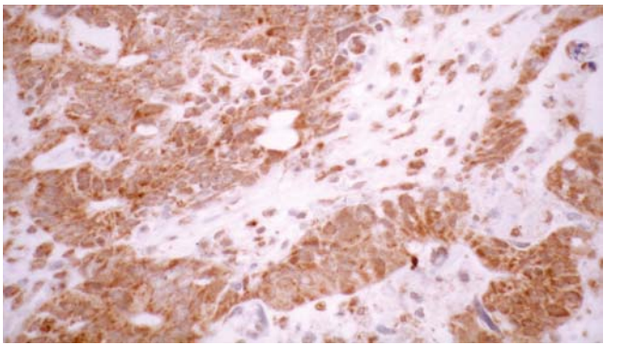

Figure 19. Cytoplasmic granular positivity for Vascular endothelial growth factor (VEGF) in tumor cells of a poorly differentiated intestinal-type adenocarcinoma (400X).

expression and VEGF expression in patients with gastric cancer operated on for cure (Fondevila *et al.,* 2004). In all, 156 patients with curatively resected gastric cancer constituted the basis of this blinded retrospective evaluation. Patients were treated with either surgery alone (n = 53) or surgery plus adjuvant chemotherapy (n = 103). After a mean follow-up of 43 months, 64 (41%) patients had died and 55 (35%) patients had developed tumor recurrence. Multivariate analysis confirmed that, in addition to the pathologic tumor stage, lymph-node ratio, the extent of lymphadenectomy and perineural invasion, p53 expression, and VEGF expression were independently associated with both disease-free survival and overall survival. Finally, patients whose tumors did not show p53 expression had a survival benefit compared to those expressing p53 when treated with adjuvant chemotherapy.

Expression of p53 was detected in 46% of patients, which falls within the range (40–60%) of previously published series in gastric cancer (Gabbert *et al.,* 1995; Joypaul *et al.,* 1994; Victorzon *et al.,* 1996). Evaluation of the immunohistochemical detection of p53 as a prognostic marker has yielded conflicting results (Fenoglio-Preiser *et al.,* 2003). These discrepancies may be the result of the limitations of p53 immunodetection at least in part. In fact, p53 immunoreactivity correlates with the presence or absence of gene mutations examined by direct sequencing in 50% of advanced gastric cancers when exons 5 through 9 are examined (Tolbert *et al.,* 1999). Most antibodies used in immunohistochemical studies detect both the wild-type as well as the mutant form of the protein and thus physiologic accumulations. In addition, technical issues can also contribute to divergent results. To overcome these limitations, we followed a meticulous methodology by using monoclonal antibody BP53-12, which is similar to antibody DO7 (recognizes amino acids 19–26), antigen retrieval, and a standard way of counting. p53 nuclear staining can be seen in both intestinal- and diffuse-type gastric tumors, although it is more common in intestinal- than in diffuse-type tumors (Fenoglio-Preiser *et al.,* 2003). The degree of p53 expression correlates with the proliferative rate of the tumors, perhaps explaining the higher incidence of p53 positivity in intestinal versus diffuse gastric cancer (diffuse gastric cancer tends to have low proliferative rates) (Fenoglio-Preiser *et al.,* 2003). There is often heterogeneity in the p53 staining pattern within a given tumor. In approximately 50% of p53-positive gastric carcinomas, 75% or more of the tumor cells are stained. In some studies, expression of p53 has been associated with a more aggressive progression manifested by higher frequency of serosal, vascular, and lymphatic invasion; increased number of lymph-node metastases; and, consequently, a more advanced tumor stage (Kakeji *et al.,* 1993; Kim *et al.,* 1997; Maehara *et al.,* 1999). In contrast, other authors have not shown association of p53 expression with lymph-node metastases or serosal invasion (Baba *et al.,* 1998; Maeda *et al.,* 1998). Our study confirms these latter results because p53 expression did not correlate to a more advanced tumor stage. In agreement with these results, p53 mutations have been found in 37% of patients with early gastric cancer (Uchino *et al.,* 1993), and p53 expression has even been detected in metaplastic gastric mucosa (Ochiai *et al.,* 1996). p53 abnormalities are common in dysplasia. The incidence of positivity varies with the degree of dysplasia that is present, increasing with increasing degrees of dysplasia (Fenoglio-Preiser *et al.,* 2003). Hence, it seems that p53 inactivation appears in an early step of gastric carcinogenesis, thus explaining the fact that p53 expression determined a worse prognosis independently of the lymph-node ratio or the depth of invasion (pT). Finally, the worse prognosis of patients whose tumors expressed p53 may actually reflect a higher rate of recurrence. In our study, recurrence rate in patients who were p53 negative was 28%, whereas the corresponding figure for patients who were p53 positive was 44% ($p < 0.05$), in a similar manner as in Japanese series (Maeda *et al.,* 1996; Maehara *et al.,* 1999).

Tumor angiogenesis is a complex, highly regulated process depending on the balance between activator and inhibitor factors (Castells and Rustgi, 2003). One of the most powerful and specific inducers of new vasculature in several neoplasms is VEGF. We used a standardized method to detect VEGF expression and, according to these results, patients were classified in two categories (presence or absence of staining reaction). This approach can justify the relatively low proportion of patients whose tumor were considered negative for VEGF (22%) in the present study because other authors also considered tumors with small amounts of VEGF as negatives (Tanigawa *et al.,* 1997).

Vascular endothelial growth factor induces the formation of new immature vessels with basal membrane holes, favoring the progression of tumor cells into the vascular space. VEGF expression in gastric cancer has been associated with various clinicopathologic parameters such as differentiation degree (Tanigawa *et al.,* 1997), intestinal-type tumors (Takahashi *et al.,* 1996), lymphatic invasion, and vascular invasion (Maeda *et al.,* 1996). Maehara *et al*. (2000) demonstrated that VEGF expression was an independent risk factor for vascular invasion, and, consequently, this fact could account for the existence of a large number of metastases. This correlation was not observed in our series, but it should be taken into account that it corresponded to curatively resected patients who had a lower probability of

metastatic dissemination. Actually, in our study, VEGF expression was not associated with any tumor-related characteristic, in a similar manner as in the series of Baba *et al*. (1998). These results, in addition to the demonstration of the independent predictive value of VEGF expression with respect to tumor recurrence, disease-free survival, and overall survival, suggested that this parameter could be a useful and powerful prognostic marker in patients with gastric cancer operated on for cure.

In the multivariate analysis, p53 expression and VEGF expression were independent prognostic factors. Similarly, concurrence of p53 expression and VEGF expression occurred in only 38% of patients, and there was no correlation between both markers. These observations suggested that, although p53 and VEGF influence tumor angiogenesis, they appear to act through different pathways. However, it is important to point out that this interpretation is not supported by all experimental studies, some have shown that mutated *p53* gene could stimulate tumor angiogenesis via up-regulation of VEGF (Mukhopadhyay *et al.,* 1995).

Preliminary studies suggested that the determination of p53 status and angiogenesis may be useful to predict response to chemotherapy. Indeed, *p53* gene inactivation by either mutation or deletion often results in resistance to antineoplastic drugs. In these *in vitro* studies, gastric and esophageal cancer cells with p53 expression were resistant to 5-Fu, mitomycin-C, and cisplatin (Lowe *et al.,* 1994; Nabeya *et al.,* 1995). Two clinical studies have evaluated the influence of p53 status in patients with locally advanced gastric cancer receiving neoadjuvant treatment. In one of them, patients with negative p53 expression had a greater tumor response to chemotherapy using 5-Fu (72% versus 12%, $p < 0.004$) (Cascinu *et al.,* 1998). Similarly, the second study found that patients who were p53 negative and VEGF positive responded better to chemotherapy with 5-Fu and cisplatin (Boku *et al.,* 1998). Finally, Diez *et al*. (2000) reported in a series of 46 patients with gastric cancer receiving adjuvant chemotherapy that absence of p53 overexpression was associated with longer survival. In agreement with these observations, we demonstrated that chemotherapy was less effective in patients whose tumors showed p53 expression, whereas VEGF expression did not have any predictive value in these settings. To our knowledge, this is the largest series assessing the relationship of p53 alteration to clinical outcome following adjuvant chemotherapy in gastric cancer, and its results may have noteworthy clinical implications.

In summary, the results of many of the studies evaluating the immunohistochemical detection of p53 in gastric carcinoma are contradictory. However, the methodology presented in this chapter may be useful for the future development of standardized protocols to assess the expression of p53 in gastric cancer. We have found that p53 and VEGF expression are independent prognostic factors for overall and disease-free survival in patients undergoing curative gastric resection. This information may allow us to select patients for additional postoperative therapies and to design better follow-up programs.

Acknowledgment

This work was supported by a research grant from "La Caixa" (02/126 = 00).

References

Ashcroft, M., Kubbutat, M.H., and Vousden, K.H. 1999. Regulation of p53 function and stability by phosphorylation. *Mol. Cell Biol. 19*:1751–1758.

Averbach, A.M., and Jacquet, P. 1996. Strategies to decrease the incidence of intra-abdominal recurrence in resectable gastric cancer. *Br. J. Surg. 83*:726–733.

Baba, M., Konno, H., Maruo, Y., Tanaka, T., Kanai, T., Matsumoto, K., Matsuura, M., Nishino, N., Maruyama, K., Nakamura, S., and Baba, S. 1998. Relationship of p53 and vascular endothelial growth factor expression of clinicopathological factors in human scirrhous gastric cancer. *Eur. Surg. Res. 30*: 130–137.

Bergers, G., and Benjamin, L.E. 2003. Tumorigenesis and the angiogenic switch. *Nat. Rev. Cancer 3*:401–410.

Boku, N., Chin, K., Hosokawa, K., Ohtsu, A., Tajiri, H., Yoshida, S., Yamao, T., Kondo, H., Shirao, K., Shimada, Y., Saito, D., Haseba, T., Mukai, K., Seki, S., Saito, H., and Johnston, P.G. 1998. Biological markers as a predictor for response and prognosis of unresectable gastric cancer patients treated with 5-fluorouracil and cis-platinum. *Clin. Cancer Res. 4*: 1469–1474.

Cascinu, S., Graziano, F., Del Ferro, E., Staccioli, M.P., Ligi, M., Carnevali, A., Muretto, P., and Catalano, G. 1998. Expression of p53 protein and resistance to preoperative chemotherapy in locally advanced gastric carcinoma. *Cancer 83*:1917–1922.

Castells, A., and Rustgi, A.K. 2003. Tumor growth, invasion and metastasis. In: Rustgi, A.K., and Crawford, J.M. (eds.) *Gastrointestinal Cancers.* Philadelphia: W.B. Saunders, 69–80.

Diez, M., Medrano, M.J., Gutierrez, A., Lopez, A., Muguerza, J.M., Hernández, P., Lazano, O., Noguerales, F., Ruiz, A., and Granell, J. 2000. p53 protein expression in gastric adenocarcinoma: negative predictor of survival after postoperative adjuvant chemotherapy. *Anticancer Res. 20*:3929–3933.

Fenoglio-Preiser, C.M., Wang, J., Stemmermann, G.N., and Noffsinger, A. 2003. TP53 and gastric carcinoma: a review. *Hum. Mutat. 21*:258–270.

Fondevila, C., Metges, J.P., Fuster, J., Grau, J.J., Palacin, A., Castells, A., Volant, A., and Pera, M. 2004. p53 and VEGF expression are independent predictors to tumour recurrence and survival following curative resection of gastric cancer. *Br. J. Cancer 90*:206–215.

Gabbert, H.E., Muller, W., Schneiders, A., Meier, S., and Hommel, G. 1995. The relationship of p53 expression to the prognosis of 418 patients with gastric carcinoma. *Cancer 76*:720–726.

Greenlee, R.T., Hill-Harmon, M.B., Murray, T., and Thun, M. 2001. Cancer statistics, 2001. *CA Cancer J. Clin. 51*:15–36.

Hanahan, D., and Weinberg, R.A. 2000. The hallmarks of cancer. *Cell 100*:57–70.

Harris, A.L. 1997. Antiangiogenesis for cancer therapy. *Lancet* 349 Suppl. *2*:SII13–SII15.

Holash, J., Maisonpierre, P.C., Compton, D., Boland, P., Alexander, C.R., ZagZag, D., Yancopoulos, G.D., and Wiegand, S.J. 1999. Vessel cooption, regression, and growth in tumors mediated by angiopoietins and VEGF. *Science 284*: 1994–1998.

Hollstein, M., Sidransky, D., Vogelstein, B., and Harris, C.C. 1991. p53 mutations in human cancers. *Science 253*:49–53.

Hundahl, S.A., Philips, J.L., and Menck, H.R. 2000. The National Cancer Data Base Report on poor survival of U.S. gastric carcinoma patients treated with gastrectomy: Fifth Edition American Joint Committee on Cancer staging, proximal disease, and the "different disease" hypothesis. *Cancer 88*:921–932.

Inoue, K., Ozeki, Y., Suganuma, T., Sugiura, Y., and Tunaka, S. 1997. Vascular endothelial growth factor expression in primary esophageal squamous cell carcinoma. Association with angiogenesis and tumor progression. *Cancer 79*:206–213.

Joypaul, B.V., Hopwood, D., Newman, E.L., Qureshi, S., Grant, A., Ogston, S.A., Lane, D.P., and Cuschieri, A. 1994. The prognostic significance of the accumulation of p53 tumor-suppressor gene protein in gastric adenocarcinoma. *Br. J. Cancer 69*:943–946.

Kakeji, Y., Korenaga, D., Tsujitani, S., Baba, H., Anai, H., Maehara, Y., and Sugimachi, K. 1993. Gastric cancer with p53 overexpression has high potential for metastasising to lymph nodes. *Br. J. Cancer 67*:589–593.

Kim, J.H., Uhm, H.D., Gong, S.J., Shin, D.H., Choi, J.H., Lee, H.R., Noh, S.H., Kim, B.S., Cho, J.Y., Rha, S.Y., Yoo, N.C., Chung, H.C., Roh, J.K., Min, J.S., Lee, K.S., and Kim, B.S. 1997. Relationship between p53 overexpression and gastric cancer progression. *Oncology 54*:166–170.

Kim, K.J., Li, B., Winer, J., Armanini, M., Gillett, N., Phillips, H.S., and Ferrara, N. 1993. Inhibition of vascular endothelial growth factor-induced angiogenesis suppresses tumor growth *in vivo*. *Nature 362*:841–844.

Levine, A.J. 1997. p53, the cellular gatekeeper for growth and division. *Cell 88*:323–331.

Lowe, S.W., Bodis, S., McClatchey, A., Remington, L., Ruley, H.E., Fisher, D.E., Housman, D.E., and Jacks, T. 1994. p53 status and the efficacy of cancer therapy *in vivo*. *Science 266*:807–810.

Maeda, K., Chung, Y.S., Ogawa, Y., Takatsuka, S., Kang, S.M., Ogawa, M., Sawada, T., and Sowa, M. 1996. Prognostic value of vascular endothelial growth factor expression in gastric carcinoma. *Cancer 77*:858–863.

Maeda, K., Kang, S.M., Onoda, N., Ogawa, M., Sawada, T., Nakata, B., Kato, Y., Chung, Y.S., and Sowa, M. 1998. Expression of p53 and vascular endothelial growth factor associated with tumor angiogenesis and prognosis in gastric cancer. *Oncology 55*:594–599.

Maehara, Y., Kabashima, A., Kago, T., Tokunaga, E., Takeuchi, H., Kakeji, Y., and Sugimachi, K. 2000. Vascular invasion and potential for tumor angiogenesis and metastasis in gastric carcinoma. *Surgery 128*:408–416.

Maehara, Y., Tomoda, M., Hasuda, S., Kabashima, A., Tokunaga, E., Kakeji, Y., and Sugimachi, K., 1999. Prognostic value of p53 protein expression for patients with gastric cancer: a multivariate analysis. *Br. J. Cancer 79*:1255–1261.

Mukhopadhyay, D., Tsiokas, L., and Sukhatme, V.P. 1995. Wild-type p53 and v-Src exert opposing influences and human vascular endothelial growth factor gene expression. *Cancer Res. 55*: 6161–6165.

Nabeya, Y., Loganzo, F., Jr., Maslak, P., Lai, L., de Oliveira, A.R., Schwartz, G.K., Blundell, M.L., Altorki, N.K., Kelsen, D.P., and Albino, A.P. 1995. The mutational status of p53 protein in gastric and esophageal adenocarcinoma cell lines predicts sensitivity to chemotherapeutic agents. *Int. J. Cancer 64*: 37–46.

Ochiai, A., Yamauchi, Y., and Hirohashi, S. 1996. p53 mutations in the non-neoplastic mucosa of the human stomach showing intestinal metaplasia. *Int. J. Cancer 69*:28–33.

Parkin, D.M., Pisani, P., and Ferlay, J. 1999. Estimates of the worldwide incidence of 25 major cancers in 1990. *Int. J. Cancer 80*:827–841.

Ravi, R., Mookerjee, B., Bhujwalla, Z.M., Sutter, C.H., Artemov, D., Zeng, Q., Dillehay, L.E., Madan, A., Semenza, G.L., and Bedi, A. 2000. Regulation of tumor angiogenesis by p53-induced degradation of hypoxia-inducible factor 1alpha. *Genes Dev. 14*: 34–44.

Takahashi, Y., Cleary, K.R., Mai, M., Kitadai, Y., Bucana, C.D., and Ellis, L.M. 1996. Significance of vessel count and vascular endothelial growth factor and its receptor (KDR) in intestinal-type gastric cancer. *Clin. Cancer Res. 2*:1679–1684.

Tanigawa, N., Amaya, H., Matsumura, M., and Shimomatsuya, T. 1997. Correlation between expression of vascular endothelial growth factor and tumor vascularity, and patient outcome in human gastric carcinoma. *J. Clin. Oncol. 15*:826–832.

Tolbert, D.M., Noffsinger, A.E., Miller, M.A., DeVoe, G.W., Stemmermann, G.N., Macdonald, J.S., and Fenoglio-Preiser, C.M. 1999. p53 immunoreactivity and single-strand conformational polymorphism analysis often fail to predict p53 mutational status. *Mod. Pathol. 12*:54–60.

Uchino, S., Noguchi, M., Ochiai, A., Saito, T., Kobayashi, M., and Hirohashi, S. 1993. p53 mutation in gastric cancer: a genetic model for carcinogenesis is common to gastric and colorectal cancer. *Int. J. Cancer 54*:759–764.

Victorzon, M., Nordling, S., Haglund, C., Lundin, J., and Roberts, P.J. 1996. Expression of p53 protein as a prognostic factor in patients with gastric cancer. *Eur. J. Cancer 32A*:215–220.

Vousden, K.H., and Lu, X. 2002. Live or let die: the cell's response to p53. *Nat. Rev. Cancer 2*:594–604.

Yoo, C.H., Noh, S.H., Shin, D.W., Choi, S.H., and Min, J.S. 2000. Recurrence following curative resection for gastric carcinoma. *Br. J. Surg. 87*:236–242.

Yu, J.L., Rak, J.W., Coomber, B.L., Hicklin, D.J., and Kerbel, R.S. 2002. Effect of p53 status on tumor response to antiangiogenic therapy. *Science 295*:1526–1528.

This Page Intentionally Left Blank

4

Role of Immunohistochemical Expression of p150 in Gastric Carcinoma: The Association with p53, Apoptosis, and Cell Proliferation

Gaoping Chen and Max M. Burger

Introduction

p150 is a novel mouse protein with an estimated molecular weight of 150 kDa, which was partially purified, and the complementary deoxyribonucleic acid (cDNA) was cloned in our laboratory (Bachmann *et al.,* 1997). We found that p150 was preferentially expressed in mouse cells transformed by a virus or by an oncogene and was specifically overexpressed in human breast carcinoma tissue, both in Western blot and in immunohistochemical analyses, in contrast to the low expression in normal breast tissue, indicating that p150 might be a new tumor marker.

The exact molecular function of p150 is as yet unknown. Sequence alignments indicated that it is the murine homolog of p180, the largest subunit of human eukaryotic translation initiation factor 3 (eIF3) (Johnson and Merrick, 1997) and of p110, its yeast counterpart (Vomlocher *et al.,* 1999). Database mining identified homologous sequences from *Caenorhabditis elegans, Nicotiana tabacum, Drosophila melanogaster, Arabidopsis thaliana,* and *Zea mays,* which are likely to be the corresponding eIF3 subunits in these organisms. By using the yeast 2-hybrid genetic screen, we found that a portion of p150 interacts with hPrt1 (hypoxanthine phosphoribosyltransferase 1), another subunit of eIF3, and cytokeratin 7, an intermediate-filament protein, suggesting that p150 acts as an adapter molecule between the translation initiation apparatus and the cytoskeleton structure in the cell in translation initiation (Lin *et al.,* 2001).

Our additional analyses in human cervical (Dellas *et al.,* 1998) and esophageal (Chen and Burger, 1999) carcinomas have revealed a correlation between high p150 expression and well-differentiated cancers. Furthermore, patients with high p150 expression in tumors showed better survival, which suggests that p150 might be a new tumor marker with prognostic value.

Handbook of Immunohistochemistry and *in situ* Hybridization of Human Carcinomas, Volume 4: Molecular Genetics, Gastrointestinal Carcinoma, and Ovarian Carcinoma

More recently, studies in human gastric carcinomas indicated a close relationship between p150 expression and tumor cell apoptosis (Chen and Burger, 2004).

Gastric carcinoma is one of the most frequent cancers worldwide, and until recently it was the second leading cause of cancer death (Fuchs and Mayer, 1995; Meyer *et al.,* 1994). Japan, China, South America, and Eastern Europe are the countries with the highest incidence of gastric cancer (Fuchs and Mayer, 1995; Parkin *et al.,* 2005). Gastric carcinoma can be histologically divided into an intestinal type and a diffuse type, with differences in their morphologic structures, their location and growth patterns, as well as their prognosis of the patients (Borchard, 1990; Hattori *et al.,* 1990; Lauren, 1965; Lim *et al.,* 1996; Tahara *et al.,* 1996; Wright *et al.,* 1992). Molecular biologic data on this cancer are relatively scarce and poorly understood. Searching for molecular markers in gastric cancer remains of major importance for improving early diagnosis, clinical management, outcome, and hence survival of the patients.

In this chapter, we describe p150 expression and its clinicopathologic relevance in human gastric carcinoma. We also investigate the significance of p150 expression in tumor cell progression and compare it with apoptosis, the proliferative marker Ki-67, and p53 immunoreactivity in human gastric carcinoma.

MATERIALS

Immunohistochemistry

1. Xylene (Fisher).
2. 75%, 80%, 90%, and 100% Ethanol.
3. 30% H_2O_2 (Sigma). Working concentration: 0.3% diluted with ddH_2O (double distilled water).
4. Bovine serum albumin (BSA) (Sigma).
5. Normal goat serum (Vector Laboratories).
6. 10 mM sodium citrate buffer, pH 6.0: Add 2.94 g sodium citrate trisodium salt dehydrate (Sigma) to 1 L ddH_2O. Adjust pH to 6.0.
7. Anti-p150 anti-serum.
8. Biotinylated goat anti-chicken immunoglobulin G (IgG) (Vector Laboratories).
9. Vectastain Elite ABC kit (Vector Laboratories).
10. DAB (diaminobenzidine) single solution (Zymed Laboratories).
11. Tris buffered saline (TBS). Stock solution A (10X saline): Add 42.5 g sodium chloride into 500 ml ddH_2O. Store at 4°C. Stock solution B (10X Tris/HCl): 30.5 g Tris and 215 ml 1N HCl in ddH_2O up to 500 ml, pH to 7.6. Store at 4°C. Working solution: 100 ml stock solution A and 100 ml B were made up to 1000 ml with ddH_2O. pH to 7.6.
12. TBST, (TBS Tween 20) washing buffer: add 1 ml Tween-20 to 1 liter of TBS buffer and mix.
13. Permount mounting media (Fisher).
14. Pan pen (Zymed Laboratories).

In situ Detection of Apoptotic Cells—TdT-Mediated dUTP Nick End Labeling Assay (TUNEL)

15. PBS buffer, pH 7.6: add 8 g sodium chloride, 0.2 g potassium chloride, 1.44 g sodium phosphate, dibasic, 0.24 g potassium phosphate, monobasic to 1 L of ddH_2O. Adjust pH to 7.4.
16. Xylene.
17. Ethanol 100%.
18. DAB kit (Vector Laboratories).
19. Permount mounting media (Fisher).
20. Proteinase K (Boehringer).
21. Apop Tag *in situ* apoptosis detection kit (Oncor), containing: equilibration buffer, terminal deoxynucleotidyl transferase (TdT) enzyme, stop/wash buffer, and anti-digoxigenin-peroxidase solution.
22. Methyl green (Vector Laboratories).

Immunoblot

23. Sodium chloride Tris EDTA (STE) buffer (0.1 M NaCl, 0.01 M Tris-HCl, pH 7.6, and 1 mM ethylenediamine tetracetic acid [EDTA]) with proteinase inhibitors (1 mM PMSF, [phenylmethylsulfonyl fluoride] leupeptin 1 µg/ml, and aprotine 2 µg/ml) for tissue homogenizing.
24. Polytron homogenizer (Brinkmann).
25. Running buffer: Dissolve 3.03 g Tris-base, 18.8 g glycine, and 1 g SDS (sodium dodecyl sulfate) in 1 L ddH_2O. pH to 8.3.
26. Sample buffer (4% SDS, 20% glycerol, and 0.1 M Tris-HCl, pH 6.8).
27. Transfer buffer: Dissolve 3.03 g Tris-base, 18.8 g glycine in up to 900 ml ddH_2O and add 100 ml methanol. pH to 8.3.
28. 5% sodium dodecyl (lauryl) sulfate-polyacrylamide gel electrophoresis (SDS-PAGE) minigels for electrophoresis.
29. Ponceau-S: 0.1% Ponceau-S in 5% acetic acid.
30. BCA protein assay kit (Pierce).
31. Polyvinylidene difluoride membrane (Millipore).
32. Blocking solution (0.5% Tween 20, 1% Triton X-100, 5% FCS [fetal calf serum], 1% BSA and 0.1 M Tris-HCl, pH 7.4).
33. PBS buffer: given previously.
34. ECL (enhanced chemiluminescence system) (Amersham).
35. Whatman blotting paper.

36. Autoradiography films.
37. Photographic developer and fixer.

METHODS

Immunohistochemistry

Deparaffinization and Rehydration

1. Xylene I 8 min.
2. Xylene II 8 min.
3. Xylene III 8 min.
4. 100% Ethanol I 2 min.
5. 100% Ethanol II 2 min.
6. 90% Ethanol 2 min.
7. 80% Ethanol 2 min.
8. 70% Ethanol 2 min.
9. ddH_2O, then, running water 5 min each.
10. Circle tissue section with Pan pen.

Antigen Retrieval

11. Put slides in a jar with 10 mM sodium citrate buffer (pH 6.0) and microwave to boiling, then maintain at a sub-boiling temperature for 10 min.
12. Cool down the slides at room temperature for 30 min.

Staining

13. Wash slides in ddH_2O 2× for 5 min each.
14. Wash slides in TBST buffer for 5 min.
15. Incubate slides in 0.3% H_2O_2 for 30 min.
16. Wash slides in ddH_2O 2× for 5 min.
17. Wash slides in TBST buffer for 5 min.
18. Incubate slides with normal 1% goat serum for 45 min.
19. Remove the serum and add primary antibodies (chicken antibody against p150 at 1:10,000 dilution; monoclonal mouse anti-human p53 at 1:100, dilution and rabbit anti-human Ki-67 antibody) to each section; incubate at 4°C overnight.
20. Remove antibody and wash slides in TBST buffer 3× for 5 min each.
21. Add secondary (biotinylated goat anti-chicken antibody for p150; goat anti-mouse for p53, and goat anti-rabbit for Ki-67, all at 1:200 dilution) to section and incubate for 45 min at room temperature.
22. Prepare ABC solution: one drop reagent A and one drop reagent B into 5 ml TBST buffer; let it stand for at least 30 min before use.
23. Remove secondary antibody and wash slides 3× with TBST buffer for 5 min each.
24. Add ABC reagent to the section and incubate for 30 min at room temperature.
25. Add DAB solution to section and monitor staining closely under microscope.
26. As soon as staining develops well, stop the staining by putting slides into ddH_2O.
27. Lightly counterstain slides in hematoxylin for a few seconds.
28. Wash slides in ddH_2O 2× for 5 min each.

Dehydration

29. Incubate slides in 70% ethanol for 30 sec.
30. Incubate slides in 80% ethanol for 30 sec.
31. Incubate slides in 90% ethanol for 30 sec.
32. Incubate slides in 100% ethanol I for 30 sec.
33. Incubate slides in 100% ethanol II for 30 sec.
34. Incubate slides in xylene I for 30 sec.
35. Incubate slides in xylene II for 30 sec.
36. Mount slides with Permonut media and cover with coverslip.

Evaluation

Each slide was examined by light microscopy without any prior knowledge of the patient's data. Ten high-power (200X) fields of homogeneous staining were reviewed for each case. p150 positivity was defined as strong cytoplasmic staining and was graded statistically by counting the population of positive tumor cells. The median value (10%) was used as the cutoff point to define p150-positive and -negative cancers. When more than 10% of the tumor cells were positively stained, tumors were scored as positive, and when less than 10% of the cells were stained, tumors were scored as negative (Chen and Burger, 1999, 2004; Dellas *et al.,* 1998). For analysis, tumors were divided into p150 immunoreactivity categories of low level (negative or <50% positive cells) and high level (50% positive cells). As negative controls, slides were incubated with PBS instead of primary antibodies. Slides with tissue specimens of breast carcinoma served as positive controls for p150. Selected cases of esophageal cancer known to be positive for p53 and the germinal center cells of lymph nodes were used as positive controls for p53 and Ki-67 immunostaining, respectively.

Determination of Ki-67 Labeling Index (KI) and Expression of p53

The KI and the expression of p53 were determined and calculated under 400-fold magnification. Ten high-power fields, a minimum of 3000 nuclei, were counted

in those tumor areas showing the highest density of cells with positive staining nuclei. Ki-67- and p53-positive cells were defined as cells with brown staining on the nucleus, regardless of staining intensity. The cutoff point to define p53-positive specimen (Lim *et al.,* 1996) was 5%. Ki-67 was expressed as the ratio of positive cells to all tumor cells as a percentage (Mueller *et al.,* 1996).

In situ Detection of Apoptotic Cells with TUNEL Method

Dewax and Rehydration

37. Xylene I 8 min.
38. Xylene II 8 min.
39. Xylene III 8 min.
40. 100% ethanol I 2 min.
41. 100% ethanol II 2 min.
42. 90% ethanol 2 min.
43. 80% ethanol 2 min.
44. 70% ethanol 2 min.
45. Wash in PBS 2×, for 5 min each.
46. Circle tissue section with Pan pen.

Staining

47. Digest sections with 20 µg/ml proteinase K for 15 min at 37°C.
48. Wash with ddH_2O 2× for 5 min each.
49. Incubate the slides with 2% H_2O_2 (30% H_2O_2 solution in ddH_2O) for 5 min in the dark to inactivate the endogenous peroxidase activity.
50. Wash with PBS 2× for 5 min each.
51. Add equilibration buffer to slides for 10 min.
52. Remove the equilibration buffer and add TdT enzyme to slides for 1 hr at 37°C.
53. Put the slides into stop/wash buffer for 10 min.
54. Add anti-digoxigenin–peroxidase solution on the slides and incubate for 30 min at room temperature.
55. Add DAB solution to section and monitor staining closely under microscope.
56. As soon as staining develops well, stop the staining by putting slides into ddH_2O.
57. Lightly counterstain slides in methyl green for a few seconds.
58. Wash slides in ddH_2O 2× for 5 min each.

Dehydration

59. Incubate slides in 70% ethanol for 30 sec.
60. Incubate slides in 80% ethanol for 30 sec.
61. Incubate slides in 90% ethanol for 30 sec.
62. Incubate slides in 100% ethanol I for 30 sec.
63. Incubate slides in 100% ethanol II for 30 sec.
64. Incubate slides in xylene I for 30 sec.
65. Incubate slides in xylene II for 30 sec.
66. Mount slides with Permount media and cover with coverslip.

A specimen known to be positive for apoptotic cells was used as positive control for subsequent staining. Substitution of TdT with distilled water was used as a negative control.

Determination of Apoptotic Index

The apoptotic index (AI) was expressed as the ratio of positive staining tumor cells to all tumor cells, given as a percentage (Lu and Tanigawa, 1997). A minimum of 3000 cells were counted under 400-fold magnification in the area without necrosis. Homogeneous brown or granular brown nuclear staining was considered as positive cells. Positive cells located in the stroma and lumen were excluded because these apoptotic cells may have originated from other cell types.

Immunoblot

1. Prepare 5% SDS-PAGE minigel.
2. Cut frozen tissue of both tumor and normal stomach of the same patient into small pieces, suspended in STE buffer with proteinase inhibitors, and homogenize with Polytron homogenizer.
3. Spin down the homogenates for 15 min at 1000 g at 4°C and collect the supernatants.
4. Add one volume of 2X sample buffer to the supernatants of the homogenates and incubate for 30 min at 56°C.
5. Spin down the mixture at 15,000 g for 10 min.
6. Determine the protein concentration spectrophotometrically with a BCA protein assay kit following the manufacturer's instructions.
7. Load the extracts of each tissue containing 40 µg protein on 5% SDS-PAGE minigel for electrophoresis.
8. Gel electrophoresis is performed at 120 V with constant cooling, until the front dye reaches the end of the gel.
9. Gel, membrane, and six pieces of Whatman paper, cut to the size of the gel, are pre-equilibrated in transfer buffer and mounted for blotting. Transfer the proteins to polyvinylidene difluoride membrane for 2 hr at 200 mV.
10. Immerse the membrane in Ponceau-S to check transfer efficiency, then wash with ddH_2O.
11. Immerse the membrane in blocking solution for 1 hr on the shaker.

12. Wash 2× for 5 min each with PBS.
13. Incubate the membrane with chicken antibody against p150 at 1:2000 overnight at 4°C.
14. Wash the membrane with blocking solution 2× for 10 min each.
15. Incubate with goat anti-chicken antibody at 1:2000 for 1 hr at room temperature on the shaker.
16. Wash with the blocking solution, PBS, then with ddH_2O for 10 min each.
17. Visualize with ECL solution following the manufacturer's instructions and expose to X-ray film in dark room.
18. Scan the film with a photoscanner.
19. Measure the intensity of the appropriate bands that represent the relative amount of p150 with Image Quant software.

RESULTS AND DISCUSSION

We have performed immunohistochemistry (IHC) and immunoblot analysis of p150 expression, its association with p53, apoptosis, and cell proliferation on a series of 102 patients (86 male, 16 female) who underwent gastrectomy for gastric adenocarcinoma at several university hospitals of northern China, the area with highest incidence of gastric cancer (Chen and Burger, 2004). An example of the IHC and Western blot analysis of the gastric carcinoma compared with the normal gastric tissues is shown in Figure 20.

Of all 102 gastric cancer samples, 86 (84%) showed p150 positive staining immunohistochemically, and 59 (58%) cases were found to show high expression of p150 (Table 5), whereas no positive staining was found in the normal gastric epithelium, indicating that p150 specifically overexpressed in the gastric cancer tissues, which is consistent with our previous findings in the cancers of breast (Bachmann *et al.,* 1997), esophagus (Chen and Burger, 1999), and cervix (Dellas *et al.,* 1998).

In the analyses of the relationship between p150 overexpression and the clinicopathologic parameters of gastric cancer, we found that p150 overexpression is correlated with histologic type (intestinal type versus diffuse type, $p < 0.005$), location (noncardia versus cardia area, $p < 0.005$), tumor invasion (muscularis versus serosa, $p < 0.005$), metastases (both local and distant, $p < 0.005$), and TNM stage ($p < 0.005$) (see Table 5).

It is well known that gastric carcinoma can be histologically divided into two distinct groups: intestinal type characterized by cohesive neoplastic cells forming glandlike tubular structures and a diffuse type in which cell cohesion is absent and where individual cells infiltrate and thicken the stomach wall without forming a discrete mass (Borchard, 1990; Lauren, 1965). The intestinal variant is thought to arise from gastric mucosa cells that have undergone intestinal metaplasia. This more differentiated form of gastric cancer is common in high-risk populations, often seen in the setting of chronic gastritis, and frequently located in the distal stomach. It generally occurs after age 50 and displays a male predominance of about 2:1. The diffuse form is thought to rise *de novo* from native gastric epithelial cells and is poorly differentiated in general. It tends to occur more often in young patients, develops throughout the stomach but especially in the cardia, and has no preference for males but frequently involves a heritable susceptibility. Accumulating evidence indicates that different genetic pathways may exist for these two types of gastric cancer (Fuchs and Mayer, 1995; Hattori *et al.,* 1990; Tahara, 1996; Wright *et al.,* 1992). The prognosis of gastric cancer is still very poor, with a 5-year survival rate ranging from 10% to 25% and a recurrence rate of at least 80% (Lim *et al.,* 1996; Meyer *et al.,* 1994; Parkin *et al.,* 2005). Little is known about the molecular mechanism of gastric carcinogenesis. In the present study, a good correlation between p150 expression and higher differentiated histologic type of gastric cancer was established. Our results showed that a significant higher expression of p150 was observed in the intestinal type (78.2%, 43/55 cases) as compared to the diffuse types of gastric cancer (32.0%, 15/47 cases, $p < 0.005$). The clear-cut difference in p150 expression between the intestinal and diffuse variants of gastric cancer provides supportive evidence for the hypothesis that these two types of cancer may arise as a consequence of different genetic alterations (Tahara *et al.,* 1996; Wright *et al.,* 1992). This result is also consistent with the fact that higher p150 expression was demonstrated also in less invasive (81.2% in the cancers with invasion of muscularis propria compared with 42.2% in the cancers with invasion of serosa, $p < 0.005$) and poorly metastasizing gastric cancer (38.5% and 18.2% in the cancer with lymph-node and distant metastases, respectively, compared with 89.2% and 61.5% in the cancers without lymph-node and distant metastases, $p < 0.001$), indicating an association of p150 expression with less aggressive behavior of the tumor cells. Indeed, all 16 of the p150 negative tumors observed in the current study were of the poorly differentiated diffuse type, which normally displays more aggressive behavior.

The location of gastric cancer appears to predict the outcome (Fuchs and Mayer, 1995; Shun *et al.,* 1997). Previous studies showed that the 5-year survival is approximately 2- to 2.5-fold higher for patients with noncardia tumors than for patients with cardia tumors.

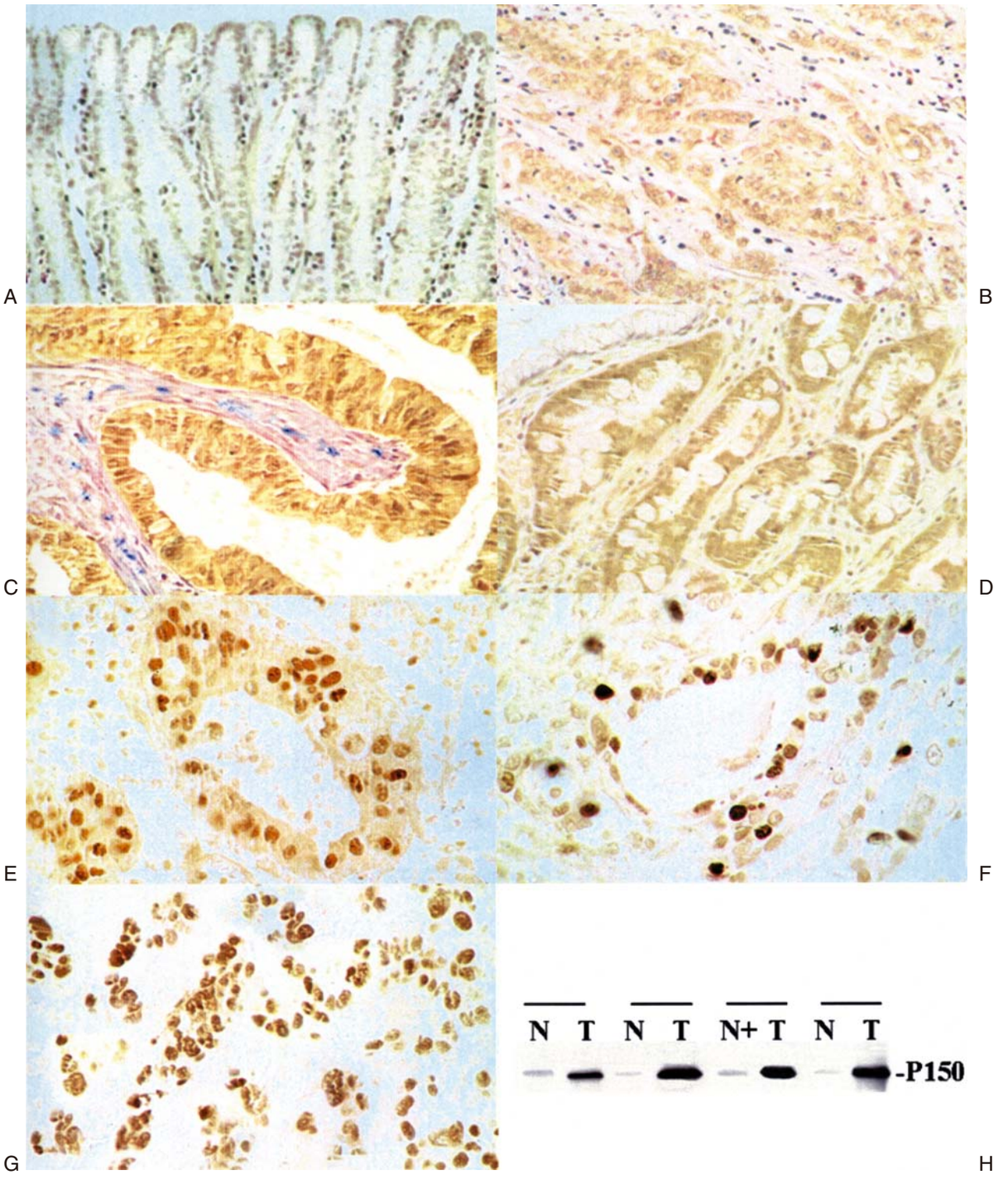

Figure 20. Expression of p150 protein in gastric carcinomas. p150 expression was determined either by immunohistochemistry **(A–D)** or by Western blot **(H)**. Normal gastric mucosa show no p150 expression **(A),** whereas diffuse-type **(B)** and intestinal-type **(C)** and intestinal-type gastric metaplasia **(D)** have some p150 expression. Representative pictures of Western blot from 4 patients correlated with the immunohistochemical study show much more p150 expression in the tumor tissues (T) than that in the normal tissue (N) of the same patients. Immunohistochemistry for p53 and Ki-67 expression and for apoptosis detected by TUNEL are shown in **E, F, and G,** respectively.

Table 5. Relationship between p150, p53 Expression, and Clinicopathologic Variables

Variables	p150 Overexpression/ Total Cases	p-value	p53-positive/ Total Cases	p-value
Total cases	59/102	—	42/102	—
Location				
Cardia	19/47	<0.005	18/47	NS
Noncardia	39/55		23/55	
Histologic type				
Intestinal	43/55	<0.005	28/55	<0.05
Diffuse	15/47		13/47	
Tumor invasion				
Muscularis propria	31/38	<0.005	16/38	NS
Serosa	27/64		25/64	
Lymph-node metastases				
Positive	25/65	<0.005	27/65	NS
Negative	33/37		14/37	
Distant metastases				
Positive	2/11	<0.001	4/11	NS
Negative	56/91		37/91	
TNM stages				
I, II	38/44	<0.005	17/44	NS
III, IV	20/58		24/58	

Therefore, the fact that distinctly more p150 high-expression cases (39 out of 55, 70.9%) were seen in noncardia gastric cancer than in the cardia area (19 out of 47, 40.4%, $p < 0.005$) raises the possibility that p150 expression may also have a prognostic value for patients of gastric carcinoma as we previously have shown for carcinomas of the cervix (Dellas *et al.,* 1998) and the esophagus (Chen and Burger, 1999). Indeed, the current results for gastric carcinoma indicate a clear link between high p150 expression and high differentiation, less invasion, reduced metastasis and early tumor-node-metastasis (TNM) stages of the tumor.

The immunohistochemical p150 expression correlated with the immunoblot results. The tumors with immunohistochemically high p150 expression also had stronger p150 expression on Western analysis and vice versa. The bands at MW 150 kDa were much stronger in all 30 tumors than in the normal esophageal tissues of the same patient (Figure 20H). The difference between tumor and normal samples was statistically significant ($p < 0.005$).

The current results do agree with our earlier observations in cervical (Dellas *et al.,* 1998) and esophageal (Chen and Burger, 1999) cancer, and they support the previous proposal that p150 overexpression could provide a certain protection against the final stages of malignancy, or the loss of p150 may simply reflect deterioration in higher malignancy (Chen and Burger, 1999). Although the two squamous cell carcinomas (cervix, Dellas *et al.,* 1998; esophagus, Chen and Burger, 1999) investigated showed the same link between less p150 expression and higher malignancy, no such correlation could be detected for breast adenocarcinoma (Bachmann *et al.,* 1997). Studies of p150 in other adenocarcinomas are therefore needed.

Tumor growth results from the balance between cell proliferation and cell death, most of which occur through apoptosis (Burger and Harris, 1995; Evan, 1997; Hanahan and Folkman, 1996; Marx, 1993; Thompson, 1995). Therefore, alterations in the control of apoptosis are just as important as those of proliferation (Marx, 1993; Thompson, 1995). Many studies have documented a possible role of apoptosis in the development and progression of malignant neoplasms, including cervical (Shoji *et al.,* 1996), esophageal (Ohbu *et al.,* 1995), and colorectal carcinomas (Kobayashi *et al.,* 1995). In gastric cancer, apoptosis occurred more frequently in the intestinal type of this cancer (Ikeda *et al.,* 1998; Shinohara *et al.,* 1996). This observation was confirmed in the current study by the finding that apoptosis was seen more frequently in the intestinal type than in the diffuse type of gastric carcinoma ($p < 0.05$). Demonstrated by TUNEL staining (Figure 20G), apoptosis of the tumor cells was clearly correlated with p150 expression. The AI (the percentage of apoptotic tumor cells to all tumor cells) (Lu and Tanigawa, 1997) was 5.0 in the group of all 59 cancers with higher p150 expression, compared with the AI of 1.9 in the group of 43 cancers with low p150 expression ($p < 0.01$) (Figure 21A). Accumulative evidence

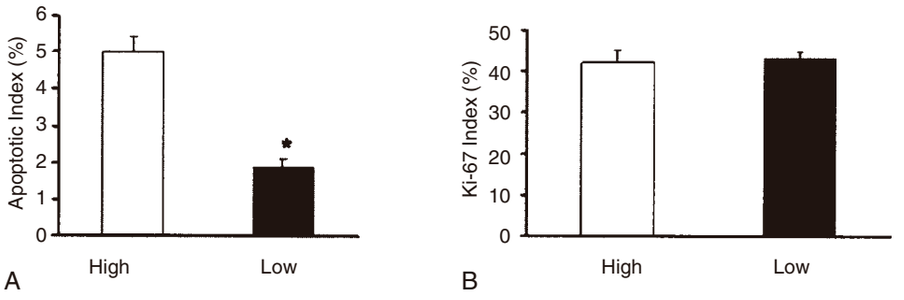

Figure 21. Relationship between p150 expression and apoptosis as well as Ki-67. Apoptosis **(A)** and Ki-67 **(B)** were evaluated in gastric cancer of low and high p150 expression groups. Each bar represents the mean standard deviation of total cases in the group. The asterisk indicates a significant difference in the apoptotic index of the low p150 group *(Low)* compared with the high p150 group *(High)*.

suggests that apoptosis can be divided into at least two distinct types: p53-dependent and p53-independent (Bellamy *et al.,* 1997; Clarke *et al.,* 1993; Ikeda *et al.,* 1998). If p150 would in any way be linked to the apoptosis process, it would have to be through the p53-independent pathway.

The determination of the Ki-67 index has been used to estimate the proliferative activity of cancer cells (Cattoretti *et al.,* 1992; Grabsch *et al.,* 2003). The failure to establish a correlation between Ki-67 and p150 with our current data (Figure 21B) suggests that p150 does not simply reflect increased growth or proliferation in tumor cells. No obvious relationship between apoptosis and the Ki-67 index is visible from our data, which is consistent with several other studies showing that tumor cell proliferation does not correlate with apoptosis (Holmgren *et al.,* 1995; Lu and Tanigawa, 1997; Parangi *et al.,* 1996).

One of the most commonly mutated gene in human cancers is p53 (Hollstein *et al.,* 1991; Liu and Gelmann, 2002; Soussi *et al.,* 1994). P53 positivity occurs in gastric carcinoma with a frequency of 23–60% (Gabbert *et al.,* 1995; Lim *et al.,* 1996; Martin *et al.,* 1992; Shun *et al.,* 1997; Starzynska *et al.,* 1996), a range into which our 41% fits. However, it is still controversial whether p53-positive staining is associated with changes in differentiation, metastasis, stage, or prognosis of gastric cancer (Fondevila *et al.,* 2004; Gabbert *et al.,* 1995; Martin *et al.,* 1992; Starzynska *et al.,* 1996; Victorzon *et al.,* 1996;). While the AI correlated with p150 expression, no such correlation could be found for p53 and either apoptotic index or Ki-67 index (Figure 22A and B).

In the current study, we demonstrate that p150 overexpression begins in gastric metaplasia, a pre-cancerous change of the stomach (Fuchs and Mayer, 1995; Mutoh *et al.,* 2004; Ochiai *et al.,* 1996) and increases to the stage of gastric carcinoma, especially for the intestinal type. This agrees with our previous findings in cervix (Dellas *et al.,* 1998) and esophageal cancer (Chen and Burger, 1999) and supports our earlier hypothesis that the level of p150 expression may possibly help in stabilizing the tumor transformation process. Later on, p150 overexpression begins to regress and then breaks down when the process reaches high malignancy stages and metastasis.

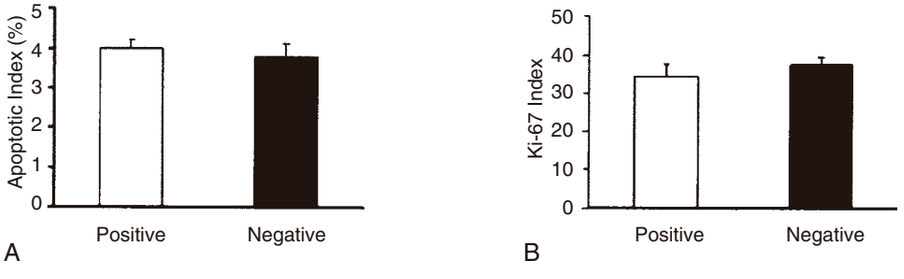

Figure 22. Relationship between p53 expression and apoptosis **(A)** as well as Ki-67 **(B)**. Apoptosis **(A)** and Ki-67 **(B)** were evaluated in gastric cancer of p53 positive and negative groups. Each bar represents the mean standard deviation of total cases in the group.

References

Bachmann, F., Baenziger, R., and Burger, M.M. 1997. Cloning of a novel protein overexpressed in human mammary carcinoma. *Cancer Res. 57*:988–994.

Bellamy, C.O.C., Malcomson, R., and Wyllie, A.H. 1997. The roles of p53 in apoptosis and cancer. In: Martin S.J. (ed.) *Apoptosis and Cancer.* London: Karger Landes Systems, 116–140.

Borchard, F. 1990. Classification of gastric carcinoma. *Hepato-Gastroenterology. 37*:223–232.

Burger, M.M., and Harris, C. 1995. UICC study group on basic and clinical cancer research: apoptosis in normal and tumor cells. *Int. J. Cancer 60*:590–592.

Cattoretti, G., Becker, M.G.H., Key, G., Duchrow, M., Schlueter, C., Galle, J., and Gerdes, J. 1992. Monoclonal antibodies against recombinant parts of the Ki-67 antigen (MIB 1 and MIB 3) detect proliferating cells in microwave-processed formalin-fixed paraffin sections. *J. Pathol. 168*:357–363.

Chen, G., and Burger, M.M. 1999. p150 expression and its prognostic value in squamous cell carcinoma of esophagus. *Int. J. Cancer (Pred. Oncol.) 84*:95–100.

Chen, G., and Burger, M.M. 2004. p150 overexpression in gastric carcinoma: the association with p53, apoptosis and cell proliferation. *Int. J. Cancer 112*:393–398.

Clarke, A.R., Purdie, C.A., Harrison, D.J., Morris, R.G., Bird, C.C., Hooper, M.L., and Wyllie, A.H. 1993. Thymocyte apoptosis induced by p53-dependent and independent pathways. *Nature 362*:849–852.

Dellas, A., Torhorst, J., Bachmann, F., Baenziger, R., Schultheiss, E., and Burger, M.M. 1998. Expression of p150 in cervical neoplasia and its potential prognostic value for survival. *Cancer 83*:1376–1383.

Evan, G. 1997. Cancer: A matter of life and cell death. *Int. J. Cancer 71*:709–711.

Fondevila, C., Metges, J.P., Fuster, J., Grau, J.J., Palacin, A., Castells, A., Volant, A., and Pera, M. 2004. p53 and VEGF expression are independent predictors of tumour recurrence and survival following curative resection of gastric cancer. *Br. J. Cancer 90*:206–215.

Fuchs, C.S., and Mayer, R.J. 1995. Gastric carcinoma. *N. Engl. J. Med. 333*:32–41.

Gabbert, H.E., Mueller, W., Schneiders, A., Meier, S., and Hommel, G. 1995. The relationship of p53 expression to the prognosis of 418 patients with gastric carcinoma. *Cancer 76*:720–726.

Grabsch, H., Takeno, S., Parsons, W.J., Pomjanski, N., Boecking, A., Gabbert, H.E., and Mueller, W. 2003. Overexpression of the mitotic checkpoint genes BUB1, BUBR1, and BUB3 in gastric cancer: association with tumour cell proliferation. *J. Pathol. 200*:16–22.

Hanahan, D., and Folkman, J. 1996. Patterns and emerging mechanisms of the angiogenic switch during tumorigenesis. *Cell 86*:353–364.

Hattori, Y., Odagiri, H., Nakatani, H., Miyagawa, K., Naito, K., Sakamoto, H., Kotoh, O., Yoshida, T., Sugimura, T., and Terada, M. 1990. *K-sam,* an amplified gene in stomach cancer, is a member of the heparin-binding growth factor receptor genes. *Proc. Natl. Acad. Sci. USA 87*:5983–5987.

Hollstein, M., Sidransky, D., Vogelstein, B., and Harris, C.C. 1991. p53 mutations in human cancers. *Science 253*:49–53.

Holmgren, L., O'Reilly, M.S., and Folkman, J. 1995. Dormancy of micrometastases: balanced proliferation and apoptosis in the presence of angiogenesis suppression. *Nat. Med. 1*:149–153.

Hsu, S.M., Raine, L., and Fanger, H. 1981. Use of avidin-biotin-peroxidase complex (ABC) in immunoperoxidase techniques: a comparison between ABC and unlabeled antibody (PAP) procedures. *J. Histochem. Cytochem. 29*:557–580.

Ikeda, M., Shomori, K., Endo, K., Makino, T., Matsuura, T., and Ito, H. 1998. Frequent occurrence of apoptosis is an early event in the oncogenesis of human gastric carcinoma. *Virch. Arch. 432*:43–47.

Johnson, K.R., and Merrick, W.C. 1997. Identification of cDNA clones for the large subunit of eukaryotic translation initiation factor 3. *J. Biol. Chem. 272*:7106–7113.

Kobayashi, M., Watanabe, H., Ajioka, Y., Yoshida, M., Hitomi, J., and Asakura, H. 1995. Correlation of p53 protein expression with apoptotic incidence in colorectal neoplasia. *Virch. Arch. 427*:27–32.

Lauren, P. 1965. The two histological main types of gastric carcinoma: diffuse and so-called intestinal-type carcinoma. *Acta. Pathol. Microbiol. Scand. 64*:31–49.

Lim, B.H., Soong, R., Grieu, F., Robbins, P.D., House, A.K., and Iacopetta, B.J. 1996. *p53* accumulation and mutation are prognostic indicators of poor survival in human gastric carcinoma. *Int. J. Cancer (Pred. Oncol.). 69*:200–204.

Lin, L., Holbro, T., Alonso, G., Gerosa, D., and Burger, M.M. 2001. Molecular interaction between human tumor marker protein p150, the largest subunit of eIF3, and intermediate filament protein K7. *J. Cell. Biochem. 80*:483–490.

Liu, M.C., and Gelmann, E.P. 2002. p53 gene mutations: case study of a clinical marker for solid tumors. *Semin. Oncol. 29*:246–257.

Lu, C., and Tanigawa, N. 1997. Spontaneous apoptosis is inversely related to intratumoral microvessel density in gastric carcinoma. *Cancer Res. 57*:221–224.

Martin, H.M., Filipe, M.I., Morris, R.W., Lane, D.P., and Silvestre, F. 1992. p53 expression and prognosis in gastric carcinoma. *Int. J. Cancer 50*:859–862.

Marx, J. 1993. Cell death studies yield cancer clues. *Science 259*:760–761.

Meyer, H.J., Jaehne, J., and Pichlmayr, R. 1994. Strategies in the surgical treatment of gastric carcinoma. *Ann. Oncol. 5(Suppl 3)*: S33–S36.

Mueller, W., Schneiders, A., Meier, S., Hommel, G., and Gabbert, H.E. 1996. Immunohistochemical study on the prognostic value of MIB-l in gastric carcinoma. *Br. J. Cancer 74*:759–765.

Mutoh, H., Sakurai, S., Satoh, K., Tamada, K., Kita, H., Osawa, H., Tomiyama, T., Sato, Y., Yamamoto, H., Isoda, N., Yoshida, T., Ido, K., and Sugano, K. 2004. Development of gastric carcinoma from intestinal metaplasia in Cdx2-transgenic mice. *Cancer Res. 64*:7740–7747.

Ochiai, A., Yamauchi, Y., and Hirohashi, S. 1996. P53 mutations in the non-neoplastic mucosa of the human stomach showing intestinal metaplasia. *Int. J. Cancer (Pred. Oncol.). 69*:28–33.

Ohbu, M., Saegusa, M., and Okayasu, I. 1995. Apoptosis and cellular proliferation in esophageal squamous cell carcinomas: differences between keratinizing and nonkeratinizing types. *Virch. Arch. 427*:271–276.

Parangi, S., O'Reilly, M., Christofori, G., Holmgren, L., Grosfeld, J., Folkman, J., and Hanahan, D. 1996. Antiangiogenic therapy of transgenic mice impairs *de novo* tumor growth. *Proc. Natl. Acad. Sci. USA 93*:2002–2007.

Parkin, D.M., Bray, F., Ferlay, J., and Pisani, P. 2005. Global cancer statistics, 2002. *CA Cancer J. Clin. 55*:*74–108.*

Shinohara, T., Ohshima, K., Murayama, H., Kikuchi, M., Yamashita, Y., and Shirakusa, T. 1996. Apoptosis and proliferation in gastric carcinoma: the association with histological type. *Histopathology 29*:123–129.

Shoji, Y., Saegusa, M., Takano, Y., Ohbu, M., and Okayasu, I. 1996. Correlation of apoptosis with tumor cell differentiation, progression, and HPV infection in cervical carcinoma. *J. Clin. Pathol. 49*:134–138.

Shun, C.T., Wu, M.S., Lin, J.T., Chen, S.Y., Wang, H.P., Lee, W.J., Wang, T.H., and Chuang, S.M. 1997. Relationship of p53 and c-erbB-2 expression to histopathological features, helicobacter pylori infection and prognosis in gastric cancer. *Hepato-Gastroenterology 44*:604–609.

Soussi, T., Legros, Y., Lubin, R., Ory, K., and Schlichtholz, B. 1994. Multifactorial analysis of *p53* alteration in human cancer: a review. *Int. J. Cancer 57*:1–9.

Starzynska, T., Markiewski, M., Domagala, W., Marlicz, K., Mietkiewski, J., Roberts, S.A., and Stern, P.L. 1996. The clinical significance of p53 accumulation in gastric carcinoma. *Cancer 77*:2005–2012.

Tahara, E., Semba, S., and Tahara, H. 1996. Molecular biological observations in gastric cancer. *Semin. Oncol. 23*:307–319.

Thompson, C.B. 1995. Apoptosis in the pathogenesis and treatment of disease. *Science 267*:1456–1462.

Victorzon, M., Nordling, S., Haglund, C., Lundin, J., and Roberts, P.J. 1996. Expression of p53 protein as a prognostic factor in patients with gastric cancer. *Eur. J. Cancer 32A*: 215–220.

Vomlocher, H.P., Hanachi, P., Ribeiro, S., and Hershey, J.W. 1999. A 110-kilodalton subunit of translation initiation factor eIF3 and an associated 135-kilodalton protein are encoded by the *Saccharomyces cerevisiae* TIF32 and TIF31 genes. *J. Biol. Chem. 274*:16802–16812.

Wright, P.A., Quirke, P., Attanoos, R., and Williams, G.T. 1992. Molecular pathology of gastric carcinoma: progress and prospects. *Hum. Pathol. 23*:848–859.

5

Role of Immunohistochemical Expression of Ki-67 in Adenocarcinoma of Large Intestine

Piotr Dziegiel and Maciej Zabel

Introduction

Cancer of the large intestine represents one of the most frequently developing malignant tumors. In approximately 90% of cases it involves tumors of adenocarcinoma histology. The morbidity varies with geographic location and is the highest in Western Europe and North America. In the United States such tumors represent the second most frequent cause of death from neoplastic diseases (Stewart *et al.,* 2004). Despite extensive progress in detection and diagnosis, fully satisfying results for treatment of large-intestine carcinomas are difficult to obtain. The prognosis reflects advancement of the neoplastic process, and clinicopathologic variables dictate selection of appropriate type of treatment. The most important clinicopathologic prognostic factors include stage of clinical advancement, histologic type of tumor, and grade of tumor malignancy. The clinical advancement stage is defined by the anatomic spread of the disease (depth of intestinal wall infiltration) and status of lymph nodes, whereas such evaluation most frequently takes advantage of the classification of Dukes and TNM (Jass, 2000).

Clinical observations indicate that, despite similar advancement of the disease, its course in some patients is more distinct than that indicated by prognostic evaluation (Henrique-Filho *et al.,* 2004). Therefore, the need arises to conduct additional studies useful in prognostic evaluation of large-intestine carcinoma. One of such studies involves immunohistochemical appraisal of tumor-cell proliferative activity using detection of Ki-67 nuclear antigen.

The immunohistochemical technique, using specific antibodies directed to antigenic determinants, allows evaluation of the site of protein expression in the cell (Ki-67 protein is localized in the nucleus). This technique is routinely used in histopathologic diagnoses to estimate expression of many types of receptors and variety of markers useful in delineation of prognosis as well as those required for determination of tumor histologic types. Using immunohistochemical reaction for detection of selected tumor antigens, its intensity is evaluated in line with a number of positive cells. This seems to represent a more advantageous approach, as compared to quantitative biochemical data, which do not document the site of antigen manifestation.

Handbook of Immunohistochemistry and *in situ* Hybridization of Human Carcinomas, Volume 4: Molecular Genetics, Gastrointestinal Carcinoma, and Ovarian Carcinoma

Ki-67 consists of two polypeptide chains of ~360 kDa and 320 kDa, respectively, localized in the cell nucleus (Endl and Gerdes, 2000; Starborg *et al.,* 1996). The protein was first identified by Gerdes *et al.* (1984) using monoclonal antibody directed against the nuclear antigen of proliferating non-Hodgkin lymphoma cells. Ki-67 antigen is expressed both in normal cells and in tumor cells. It appears in the active phases G1, S, and G2 in cell cycle and during mitosis. It is absent from the cells in the resting G0 phase (Duchrow *et al.,* 1996). Expression of the nuclear Ki-67 antigen positively correlates with the immunohistochemically detectable incorporation of bromodeoxyuridine (BrdU, a synthetic analog of thymidine), which enters DNA (deoxyribonucleic acid) structure during phase S of the cell cycle (Muskhelishvili *et al.,* 2003; Wilson *et al.,* 1996). Demonstration of Ki-67 antigen expression, followed by determination of the number of positive cells, allows evaluation of proliferative activity in tissues (Munakata and Hendricks, 1994; Rudolph *et al.,* 1998; Spyratos *et al.,* 2002). The original reports on cell-proliferation studies with the use of anti-Ki-67 cells pertained to non-Hodgkin lymphomas and breast cancer (Gerdes *et al.,* 1983, 1984; Gerdes, 1990). These studies were followed by numerous investigations on mitotic activity of various tumor cells as a potential prognostic variable.

Between 1992 and 2001 about 3500 articles were published involving Ki-67 protein (Brown and Gatter, 2002). Among them, a significant portion dealt with prognostic value of Ki-67 antigen expression in various malignant processes in humans. In the studies on mammary cancer most of the authors confirmed prognostic significance of Ki-67 detection. Expression of the protein has been found to correlate with advancement of the disease, grade of malignancy, and expression of other prognostic indices (e.g., status of estrogen receptor [ER] and progesterone receptors [PgR], HER-2 receptor, and proliferating cell nuclear antigen [PCNA]). Similar results have been reached in studies of the type conducted on malignant tumors of soft tissues, lung carcinomas, and brain tumors. However, in uterine cervix carcinoma and prostate carcinoma expression of Ki-67 has been found less important for prognostic course of the disease (Brown and Gatter, 2002; Dziegiel *et al.,* 2005). For a general review of Ki-67, the reader should consult Hayat (2002).

Similarly, most of the published reports have not confirmed the prognostic significance of Ki-67 expression in large intestine carcinoma. Only about 25% of publications have suggested that Ki-67 antigen expression in cells of large-intestine carcinoma is taken into account in prognosis of the disease course (Brown and Gatter, 2002). Some authors have reported a positive relationship between Ki-67 expression and spread or with relapse of the neoplastic process in the large intestine (Chen *et al.,* 1997; Lanza *et al.,* 1990). Application of Ki-67 antigen has also been suggested as an index of sensitivity to chemotherapy (Shepherd *et al.,* 1988). Tumors of a high proliferative index and exhibiting intense Ki-67 expression have been found to be more sensitive to chemotherapy and radiotherapy. Thus, using the assays of proliferative activity, the group of patients could be selected in whom positive reaction to the previously mentioned therapeutic modalities would be highly probable (Kim *et al.,* 2001). Evaluation of Ki-67 antigen immunoreactivity (using the immunohistochemical technique) could also be incorporated in the selection of patients with already-diagnosed large-intestine adenocarcinoma using the simple method of evaluating large-intestine biopsies, provided the sampled material contains a representative fragment of the tumors.

In this chapter, results of our multiannual studies on large intestine carcinoma are presented, describing the role of Ki-67 antigen expression in correlation with selected clinicopathologic parameters. In the studies, expression of metallothionein (MT), the protein affecting proliferation and differentiation of cells, has also been evaluated. In addition, intensities of Ki-67 and MT antigen expression are compared with intensity of apoptosis in cells of large intestine adenocarcinoma (Dumanska *et al.,* 2004; Dziegiel *et al.,* 2003, 2004).

MATERIALS

1. Fragments of tumors (large intestine adenocarcinoma) fixed in buffered formalin (10%) and embedded in paraffin.
2. Microscope glass slides SuperFrost Plus (Menzel, Branau, Germany).
3. Coverslips.
4. Permanent mounting medium (DPX—Fluka, Buchs, Switzerland).
5. Monoclonal mouse antibody anti-human Ki-67 antigen (clone MIB-1, DakoCytomation, Glostrup, Denmark).
6. Antibody diluent (DakoCytomation).
7. Xylene.
8. 70%, 96%, and 100% Ethanol.
9. Distilled H_2O.
10. Citrate buffer (pH 6) (Target Retrieval Solution—DakoCytomation).
11. Phosphate buffered saline (PBS).
12. Humid chamber.
13. Waterbath.
14. Container for incubation of preparations in the waterbath.

15. Reagent for universal negative controls (Dako Cytomation).
16. Reagent set for visualization of immunohistochemical reaction (LSAB [labeled streptavidin biotin]+ System-horseradish peroxidase [HRP], Dako Cytomation).
17. Mayer's hematoxylin.

METHODS

1. Fix the material (samples of large intestine adenocarcinomas) in buffered formalin and embed in paraffin blocks.
2. Deparaffinize sections (4 μm thick) in xylene (10 min) and then rehydrate in a series of decreasing ethanol concentrations: 100%, 96%, and 70% (5 min in each); rinse in distilled H_2O for 10 min.
3. Unblock the antigenic determinants in cells by incubating the sections in the container for incubation filled with the citrate buffer (Target Retrieval Solution) and placed in the waterbath (95–99°C) for 20 min.
4. Leave the incubated sections in the citrate buffer until they cool down.
5. Wash the sections in distilled water for 10 min.
6. Carefully drain excess water from the glass slide (wipe in the vicinity of the section).
7. Block endogenous peroxidase by applying 3% hydrogen peroxide (in LSAB+ System-HRP DakoCytomation) in sufficient amount to cover the sections. Incubate for 5 min.
8. Wash the sections in distilled water for 10 min and then in PBS for 5 min.
9. Remove excess buffer from the glass slide (wipe it around the section).
10. Cover one of the sections with the antibody (monoclonal mouse antibody anti-human Ki-67 antigen; diluted to 1:100 or ready to apply without diluting it) and another with the negative control reagent in an amount sufficient to cover the section; incubate for 1 hr at room temperature.
11. Wash in PBS for 10 min.
12. Remove excess buffer (as earlier).
13. Apply the biotinylated antibodies of the LSAB+ System-HRP kit (DakoCytomation) in amounts sufficient to cover the section and incubate for 20 min.
14. Wash in PBS for 10 min.
15. Remove excess buffer.
16. Apply sufficient amount of streptavidin–peroxidase complex to cover the section; incubate for 15–20 min.
17. Wash in PBS for 10 min.
18. Remove excess buffer.
19. Apply the substrate-chromogen solution (20 μl DAB chromogen per 1 ml buffer—the substrate buffer) contained in the LSAB+ System-HRP kit (DakoCytomation) in the amount sufficient to cover the section, and incubate for 5–10 min.
20. Wash in distilled water for 5 min.
21. Counterstain sections with hematoxylin (duration appropriate for the applied hematoxylin).
22. Wash in distilled water for 10 min, pass through a series of ethanols (70%, 96%, 100%), and immerse in xylene (5 min).
23. Mount under a covership using a drop of mounting medium (DPX—Fluka).

Concentrations of the applied antibodies and duration of any incubation should be selected individually for every laboratory and adjusted to the objective of the study.

Evaluation of Microscope Preparations

Slides are evaluated with light microscope. The entire section is screened under 200X magnification, and the proportion is calculated of tumor-cell nuclei manifesting brown deposits (diaminobenzidine [DAB]). Use the following scale points (the more positive cells the more points):

1. Absence of positive cells—0 points
2. 1–10% positive cells—1–2 points (expression of low intensity)
3. 11–30% positive cells—3–5 points (expression of average intensity)
4. 31–50% positive cells—6–9 points (expression of pronounced intensity)
5. More than 50% positive cells—10–12 points (expression of highly pronounced intensity).

The analysis and scoring of positive cells in large intestine adenocarcinoma can also be performed using computer-assisted image analysis (e.g., AnalySis software using OLYMPUS microscope equipped with video channel; Olympus UK Ltd). The software allows the user to score stained objects as related to cell nuclei presenting no reaction and to calculate the proportion of positive cells in a given visual field.

RESULTS AND DISCUSSION

Tissue specimens were collected from 81 cases during surgery. In 27 cases high intensity of the reaction was observed, in 35 cases it was average, in 17 cases the reaction was weak, and no such reaction was demonstrated in two cases (Figure 23A–C). The expression of Ki-67 antigen was compared in various grades of malignancy of the tumor and in various depths of tumor infiltration of the intestinal wall. In both cases the two

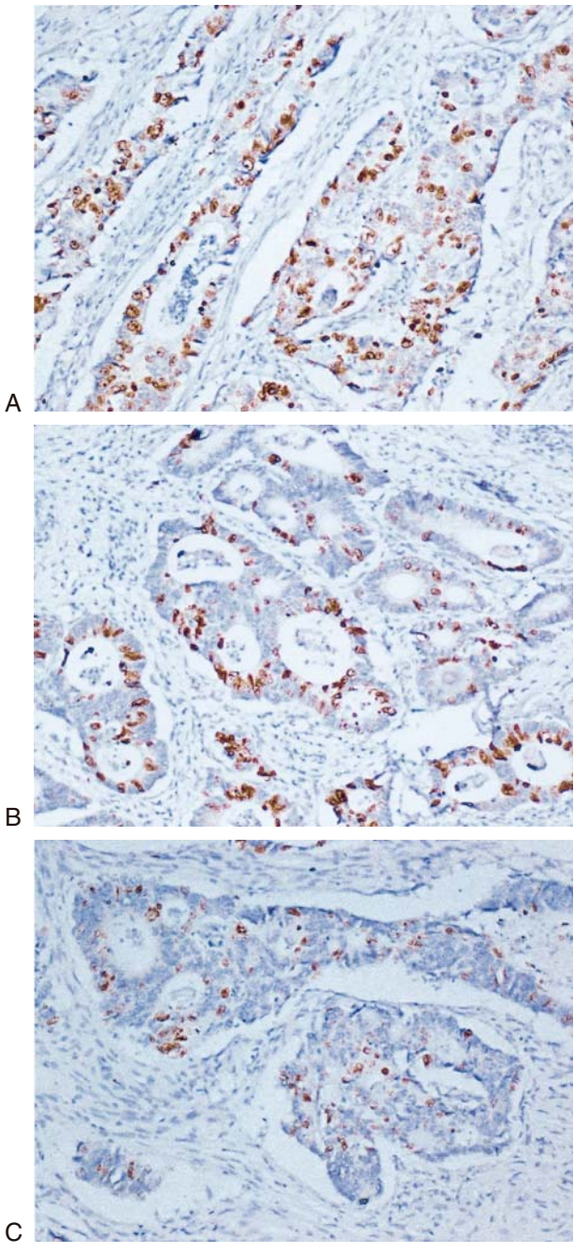

Figure 23. Intensity of Ki-67 expression in adenocarcinoma of large intestine (cell nuclei). **A:** Intense; **B:** Average; and **C:** Low. Couterstaining with hematoxylin. Magnification 100X.

variables were found to correlate. A higher intensity of Ki-67 expression was noted in adenocarcinomas of G3 grade as well as in tumors involving the surrounding lymph nodes and infiltrating the peri-intestinal adipose tissue (grade C according to Dukes) (Figure 24). Examining survival of the patients as related to intensity of Ki-67 antigen expression (analysis of Kaplan-Meier), we demonstrated that patients with primary large intestine adenocarcinoma, in whom the highest proportion of positive cells was disclosed, died earlier than patients with a lower proportion of positive cells (Figure 25). Patients with primary large-intestine adenocarcinoma, in whom the highest proportion of positive cells was disclosed, were found to die earlier than the remaining patients (see Figure 25). The differences were significant ($p < 0.05$) (Dziegiel *et al.,* 2003).

In conjunction with Ki-67 antigen expression, manifestation of MT protein was also examined in cells of large-intestine adenocarcinomas. The MT protein represents a low molecular weight protein that may be of significance for proliferation and differentiation of both neoplastic and normal cells (Dziegiel, 2004). Analysis of expression intensities of the two proteins (Ki-67, MT) indicated a relatively strong correlation of the two markers ($r = 0.536$; $p < 0.05$) (Dziegiel *et al.,* 2003).

In another investigation using 39 cases of primary large-intestine adenocarcinomas, we evaluated intensity of Ki-67 antigen expression as compared to selected clinicopathologic prognostic parameters (grade of malignancy G, depth of wall infiltration in the large intestine), MT expression, and markers of apoptotic process (Dumanska *et al.,* 2004). The results unequivocally demonstrated that Ki-67 expression was related to the previously mentioned variables. The higher amounts of Ki-67 protein were present in adenocarcinoma cells, the intensity of expression of MT and caspase-3 (cas-3) was higher, and apoptotic cells were more frequent. The same relation was also noted when G grade was compared with the infiltration depth (Dumanska *et al.,* 2004).

In another study we reexamined the expression of Ki-67 antigen, cas-3, and MT as well as their prognostic significance expressed in the analysis of survival in patients with primary large intestine adenocarcinomas. Only in the case of Ki-67 antigen did the patients with pronounced intensity of expression survive shorter post-surgery periods of time (Dziegiel *et al.,* 2004).

During the last 15 years we have witnessed a marked increase in publications related to prognostic significance of Ki-67 antigen expression in various neoplastic tumors. Most of these studies were conducted with breast cancers, soft-tissue tumors, lung cancer, prostate cancer, uterine cervix carcinoma, brain tumors, and large-intestine carcinoma. In most of the tumors, prognostic importance of Ki-67 antigen expression was unequivocally confirmed (Brown and Gatter, 2002).

In cases of large-intestine carcinoma and adenocarcinoma in particular, results of such studies proved disputable and occasionally contradictory. Therefore, the question arises whether Ki-67 antigen expression carries any prognostic value in primary adenocarcinomas

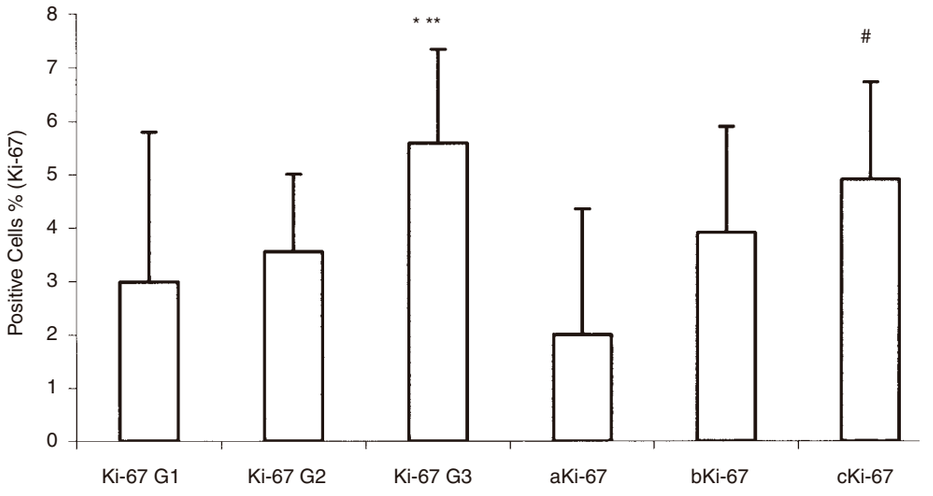

Figure 24. Extent of expression of Ki-67 in large intestine adenocarcinomas of individual grades of histologic malignancies (G). *: $p < 0.05$ (Ki-67 G3 versus Ki-67 G1); **: $p < 0.001$ (Ki-67 G3 versus Ki-67 G2). Kruskall-Wallis test. Extent of expression of Ki-67 as related to the depth of large intestine wall infiltration by adenocarcinoma. **a:** Mucosa and submucosa. **b:** Mucosa, submucosa, and muscle layer. **c:** Mucosa, submucosa, muscle layer, and adipose tissue. #: $p < 0.05$ (cKi-67 versus bKi-67 and cKi-67 versus aKi-67). Kruskall-Wallis test.

of the large intestine. In the series of our investigations (Dumanska *et al.,* 2004; Dziegiel *et al.,* 2003, 2004) the data have pointed to a strong positive correlation between expression of Ki-67 protein and grade of malignancy, G, or depth of infiltration in the intestinal wall by the tumor. Similarly, duration of survival of patients with large intestine adenocarcinoma of an elevated expression of Ki-67 antigen was significantly shorter. Certain divergencies in results obtained by various authors might reflect application of different antibodies (different clones) directed toward different antigenic determinants of Ki-67 protein.

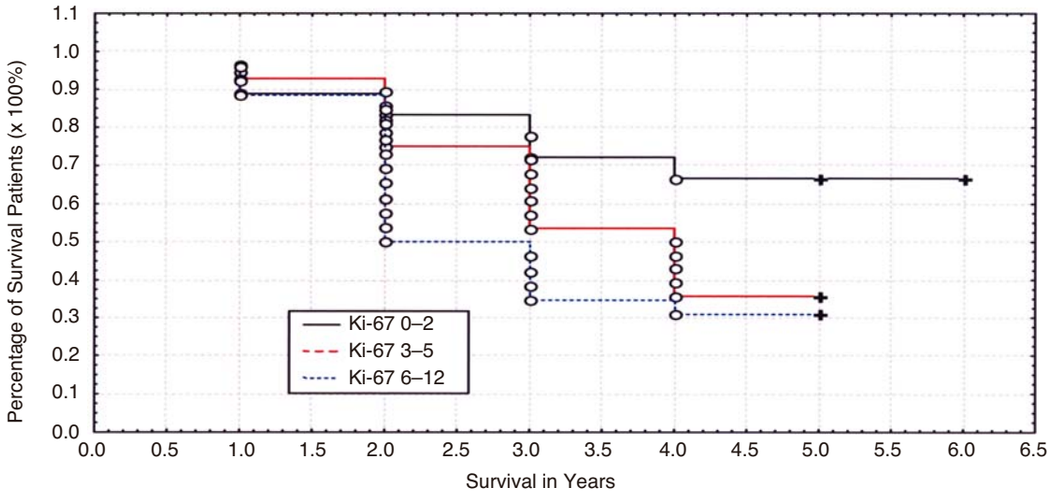

Figure 25. Survival of patients with large intestine adenocarcinomas as related to extent of expression of Ki-67 antigen (score 1–2: low expression; score 3–5: moderate expression; score 6–12: pronounced expression). Significant differences: low versus average expression: $p < 0.05$; low versus pronounced expression: $p < 0.01$. Kaplan-Meier test, F test of Cox, and χ^2 test.

Experience has shown that the most reliable and widely used antibodies are MIB-1 and Ki-S5 clones (Leong *et al.,* 2003; Lindboe and Torp, 2002; Schmidt *et al.,* 2002). The antibodies manifest reaction patterns most consistent with expression of other proliferation markers in various tumors (e.g., with PCNA, number of mitoses and the quantity of BrdU incorporated to cellular DNA in the phase S of the cell cycle) (Muskhelishvili *et al.,* 2003; Zacchetti *et al.,* 2003). This has been confirmed by some reports of recent years, pertaining to the evaluation of Ki-67 antigen expression with the use of MIB-1 antibodies in establishing prognosis of the disease resulting from large-intestine adenocarcinoma. Similarly, our data have shown that Ki-67 antigen carries prognostic significance in various advanced stages of the neoplastic disease (Allegra *et al.,* 2003; Chen *et al.,* 1997; Ishida *et al.,* 2004; Kirmura *et al.,* 2000; Kitabatake *et al.,* 2002; Palmqvist *et al.,* 1999). Examination of intensity of Ki-67 antigen expression may also help in evaluating the extent of mucosal dysplasia in ulcerative colitis, which when untreated results in development of cancer (Andersen *et al.,* 1998; Wong *et al.,* 2000).

Another important factor that might lead to divergencies in prognosis as to the course of disease, resulting from large-intestine adenocarcinoma, based on analysis of intensity in Ki-67 antigen expression may include the variable way in which advancement of the disease is evaluated. The classifications according to Dukes and Astler Coller are widely applied inaccurately to appraise the depth of neoplastic infiltrate, delimiting anatomic structures of the wall in large intestine (Jass, 2000). In our studies involving evaluation of the depth to which adenocarcinoma cells penetrate the wall of large intestine, we have classified advancement of wall infiltration into three groups. In the first group the infiltration is restricted to mucosa and submucosa, in the second it also involves the muscle layer, and in the third group the infiltrate reaches the peri-intestinal adipose tissue (Dziegiel *et al.,* 2003). In our opinion, this approach has simplified appraisal of advancement in the disease particularly in the cases with no metastases to regional lymph nodes. This approach of evaluating the depth of cancer cell penetration has resulted in selection of three groups of patients, in whom expression of Ki-67 antigen increased in parallel to the depth to which the tumor penetrated the large-intestine wall (Dziegiel *et al.,* 2003).

In the analysis of patient survival (method of Kaplan-Meier) with primary adenocarcinoma of large intestine, the significant variable involves the way in which the cells are scored, which demonstrates positive reaction with anti-Ki-67 antibodies. In such an appraisal, quality of analyzed microscope preparations with the color reaction (brown cell nuclei) is of utmost importance. The most frequently used technique for evaluation of intensity in the color nuclear reaction involves its grading, related to the percentage of positive cells as compared with cells demonstrating no expression of the protein in the entire tumor preparation. Various scales were used in the present study that may also be of certain significance in comparing the obtained results. In our studies, the five-grade scale was used, which is described in the Methods section (Dziegiel *et al.,* 2003). It seems that the more precise the classification of the expression intensity, the more accurate the evaluation scale of Ki-67 antigen, also the grouping of patients to individual catgories is easier.

The categories may be subjected to a more accurate statistical analysis, evaluating patients' survival time. This has been corroborated by several reports, indicating prognostic importance of Ki-67 expression intensity evaluation in primary adenocarcinomas of large intestine (similar to our data) (Allegra *et al.,* 2003; Chen *et al.,* 1997; Ishida *et al.,* 2004; Kimura *et al.,* 2000; Kitabatake *et al.,* 2002; Palmqvist *et al.,* 1999). Patients with the highest number of cancer cells containing Ki-67 protein have survived definitely shorter post-operative periods of time. New hopes for accurate evaluation of expression intensity of various prognostic indices (including Ki-67) result from application of computer-assisted image analysis, permitting scoring color objects. Nevertheless, few investigations have used such analysis, and the principal problem involves quality of analyzed microscope preparations, which need to be perfect.

In our studies of large-intestine adenocarcinomas several other markers were examined in addition to Ki-67 antigen expression. One of them was MT. Documentation of the positive correlation between Ki-67 and MT expression as well as their increase in cases more malignant (G3) and more advanced of the studied large intestine adenocarcinomas again has confirmed prognostic significance of the two proteins (Dziegiel *et al.,* 2003).

Tumor growth and progression represent the result of its proliferative activity and the capacity of eliminating cancer cells by apoptosis, necrosis, or both. Intensified proliferation of neoplastic cells leads to augmented volume and mass of the tumor, which, in turn, may induce within the tumor processes leading to apoptosis and necrosis. Therefore, exponents of apoptosis may indirectly provide markers of intensity of tumor cell proliferation. In large-intestine adenocarcinomas we have examined in parallel expression of Ki-67 antigen, intensity of apoptotic process (terminal deoxynucleotidyl transferase biotin-dUTP nick end labeling [TUNEL]), and immunohistochemical

expression of cas-3. The results have shown that the parameters have been weakly correlated with each other. Nevertheless, it is significant that, similar to Ki-67 antigen expression, the intensity of apoptosis and expression of cas-3 is most pronounced in G3 tumors and in tumors most deeply infiltrating the intestinal wall (Dumanska *et al.,* 2004; Dziegiel *et al.,* 2004).

Determination of survival period in a tumor patient represents the most important criterion of the aggressive nature of the tumor, its advancement, and effective treatment of the disease. Also, in cases of primary adenocarcinomas of large intestine this variable provides an index for decisions as to the type of applied treatment (chemotherapy, radiotherapy, or both before or after surgery, or at both times) (Verweij and Stoter, 1997). In large-intestine adenocarcinomas the most important prognostic factors include morphologic traits of the tumor: its size, histologic type, grade of malignancy (differentiation of cancer cells, number of mitotic figures, proportion of necrosis), and depth to which the intestinal wall is infiltrated (Jass, 2000).

Until now, no precise indices of tumor cell biology that would promote prognostic evaluation and choice of treatment modality have been identified in cases of large-intestine adenocarcinoma. Immunohistochemical indices of tumor growth dynamics, including Ki-67 antigen, seem to be useful in establishing prognosis in this disease.

Results obtained by us and presented in the series of articles are in part divergent from those of earlier studies of the similar type conducted by other authors. Nevertheless, application of Ki-67 antigen expression evaluation for prognosis in primary large intestine adenocarcinomas may play a role. Further standardized studies are needed, encompassing higher number of cases to unequivocally confirm the role of Ki-67 in tumors of this type.

References

Allegra, C.J., Paik, S., Colangelo, L.H., Parr, A.L., Kirsch, I., Kim, G., Klein, P., Johnston, P.G., Wolmark, N., and Wieand, H.S. 2003. Prognostic value to thymidylate synthase, Ki-67, and p53 in patients with Dukes' B and C colon cancer: a National Cancer Institute—National Surgical Adjuvant Breast and Bowel Project Collaborative Study. *J. Clin. Oncol. 21*:241–250.

Andersen, S.A., Rognum, T.O., Bakka, A., and Clausen, O.P.F. 1998. Ki-67: A useful marker for the evaluation of dysplasia in ulcerative colitis. *J. Clin. Pathol: Mol. Pathol. 51*:327–332.

Brown, D.C., and Gatter, K.C. 2002. Ki67 protein: the immaculate deception? *Histopathology 40*:2–11.

Chen, Y.T., Henk, M.J., Carrney, K.J., Wong, W.D., Rothenberger, D.A., Zheng, T., Feygin, M., and Madoff, R.D. 1997. Prognostic significance of tumor markers in colorectal cancer patients: DNA index, S-phase fraction, p53 expression, and Ki-67 index. *J. Gastrointest. Surg. 1*:266–273.

Duchrow, M., Schlüter, C., Wohlenberg, C., Flad, H.-D., and Gerdes, J. 1996. Molecular characterization of the gene locus of the human cell proliferation-associated nuclear protein defined by monoclonal antibody Ki-67. *Cell Prolif. 29*:1–12.

Dumanska, M., Dziegiel, P., Sopel, M., Wojnar, A., Zabel, M. 2004. Evaluation of apoptosis, proliferation intensity and metallothionein (MT) expression in comparison with selected clinicopathological variables in primary adenocarcinomas of the large intestine. *Folia Morphol. 63*:107–110.

Dziegiel, P. 2004. Expression of metallothionein in tumor cells. *Pol. J. Pathol. 55*:3–12.

Dziegiel, P., Dumanska, M., Forgacz, J., Wojnar, A., and Zabel, M. 2004. Intensity of apoptosis as related to the expression of matellothionein (MT), caspase-3 (cas-3) and Ki-67 antigen and the survival time of patients with primary colorectal adenocarcinomas. *Rocz. Akad. Med. Bialymst. 49* Suppl.:5–7.

Dziegiel, P., Forgacz, J., Suder, E., Surowiak, P., Kornafel, J., and Zabel, M. 2003. Prognostic significance of metallothionein expression in correlation with Ki-67 expression in adenocarcinomas of large intestine. *Histol. Histopathol. 18*:401–407.

Dziegiel, P., Salwa-Zurawska, W., Zurawski, J., Wojnar, A., and Zabel, M. 2005. Prognostic significance of augmented metallothionein (MT) expression correlated with Ki-67 antigen expression in selected soft tissue sarcomas. *Histol. Histopathol. 20*:83–89.

Endl, E., and Gerdes, J. 2000. The Ki-67 protein: fascinating forms and an unknown function. *Exp. Cell Res. 257*:231–237.

Gerdes, J. 1990. Ki-67 and other proliferation markers useful for immunohistological diagnostic and prognostic evaluations in human malignancies. *Semin. Cancer Biol. 1*:199–206.

Gerdes, J., Dallenbach, F., Lennert, K., Lemke, H., and Stein, H. 1984. Growth fractions in malignant non-Hodgkin's lymphomas (NHL) as determined *in situ* with the monoclonal antibody Ki-67. *Hematol. Oncol. 2*:365–371.

Gerdes, J., Schwab, U., Lemke, H., and Stein, H. 1983. Production of a mouse monoclonal antibody reactive with a human nuclear antigen associated with cell proliferation. *Int. J. Cancer 31*:13–20.

Hayat, M.A. 2002. *Microscopy, Immunohistochemistry, and Antigen Retrieval Methods.* New York: Kluwer Academic/Plenum Publishers.

Henrique-Filho, C., Bromberg, S.H., Barreto, E., Godoy, A.C., and Mattosinho-France, L.C. 2004. Prognostic value of the grade of cellular differentiation, of mucus presence and the growth pattern of the invasive margin in colorectal adenocarcinomas Dukes B. *Arq. Gastroenterol. 41*:185–189.

Ishida, H., Miwa, H., Tatsuta, M., Masutani, S., Imamura, H., Shimizu, J., Ezumi, K., Kato, H., Kawasaki, T., Furukawa, H., and Kawakami, H. 2004. Ki-67 and CEA expression as prognostic markers in Dukes' C colorectal cancer. *Cancer Lett. 207*:109–115.

Jass, J.R. 2000. Tumors of the small and large intestines (including the anal region). In Fletcher, C.D.M. (ed.) *Diagnostic Histopathology of Tumors,* Vol. 1. 2nd ed. London: Churchill Livingstone, 369–409.

Kim, N.K., Park, J.K., Lee, K.J., Yang, W.I., Yun, S.H., Sung, J.S., and Min, J.S. 2001. p53, BCL-2, and Ki-67 expression according to tumor response after concurrent chemoradiotherapy for advanced rectal cancer. *Ann. Surg. Oncol. 8*:418–424.

Kimura, T., Tanaka, S., Haruma, K., Sumii, K., Kajiyama, G., Shimamoto, F., and Kohno, N. 2000. Clinical significance of MUC1 and E-cadherin expression, cellular proliferation, and angiogenesis AT the deepest invasive portion of colorectal cancer. *Int. J. Oncol. 16*:55–64.

Kitabatake, T., Kojima, K., Fukasawa, M., Beppu, T., and Futagawa, S. 2002. Correlation of thymidine phosphorylase

staining and the Ki-67 labeling index to clinicopathologic factors and hepatic metastasis in patients with colorectal cancer. *Surg. Today 32*:322–328.

Lanza, G., Cavazzini, L., Borghi, L., Ferretti, S., Buccoliero, F., and Rubbini, M. 1990. Immunohistochemical assessment of growth fractions in colorectal adenocarcinomas with monoclonal antibody Ki-67: relation to clinical and pathological variables. *Pathol. Res. Pract. 186*:608–618.

Leong, A.S.Y., Cooper, K., and Leong, F.J.W.M. 2003. Ki-67 (MIB-1, Ki-S5). In Leong, A.S.Y., Cooper, K., and Leong, F.J.W.M. (eds.) *Manual of Diagnostic Antibodies for Immunohistochemistry,* 2nd ed. London: Greenwich Medical Media Ltd., 289–291.

Lindboe, C.F., and Torp, S.H. 2002. Comparison of Ki-67 equivalent antibodies. *J. Clin. Pathol. 55*:467–471.

Munakata, S., and Hendricks, J.B. 1994. A multilabeling technique for simultaneous demonstration and quantification of Ki-67 and nucleolar organizer regions (AgNORs) in paraffin-embedded tissue. *J. Histochem. Cytochem. 42*:789–793.

Muskhelishvili, L., Latendresse, J.R., Kodell, R.L., and Henderson, E.B. 2003. Evaluation of cell proliferation in rat tissues with BrdU, PCNA, Ki-67 (MIB-5) immunohistochemistry and *in situ* hybridization for histone mRNA. *J. Histochem. Cytochem. 51*:1681–1688.

Palmqvist, R., Sellberg, P., Oberg, A., Tavelin, B., Rutegard, J.N., and Stenling, R. 1999. Low tumour cell proliferation at the invasive margin is associated with poor prognosis in Dukes' stage B colorectal cancers. *Br. J. Cancer 79*:577–581.

Rudolph, P., Peters, J., Lorenz, D., Schmidt, D., and Parwaresch, R. 1998. Correlation between mitotic and Ki-67 labeling indices in paraffin-embedded carcinoma specimens. *Hum. Pathol. 29*:1216–1222.

Schmidt, M.H.H., Broll, R., Bruch, H.-P., and Duchrow, M. 2002. The proliferation marker pKi-67 becomes masked to MIB-1 staining after expression of its tandem repeats. *Histochem. Cell Biol. 118*:415–422.

Shepherd, N.A., Richman, P.I., and England, J. 1988. Ki-67 derived proliferative activity in colorectal adenocarcinoma with prognostic correlation. *J. Pathol. 155*:213–219.

Spyratos, F., Ferrero-Poüs, M., Trassard, M., Hacène, K., Phillips, E., Tubiana-Hulin, M., and Le Doussal, M. 2002. Correlation between MIB-1 and other proliferation markers. Clinical implications of the MIB-1 cutoff value. *Cancer 94*: 2151–2159.

Starborg, M., Gell, K., Brundell, E., and Höög, C. 1996. The murine Ki-67 cell proliferation antigen accumulates in the nucleolar and heterochromatic regions of interphase cells and at the periphery of the mitotic chromosomes in a process essential for cell cycle progression. *J. Cell Sci. 109*:143–153.

Stewart, S.L., King, J.B., Thompson, T.D., Friedman, C., and Wingo, P.A. 2004. Cancer mortality surveillance—United States. 1990–2000. *MMWR Surveill. Summ. 53*:1–108.

Verweij, J., and Stoter, G. 1997. Principles of systemic therapy of cancer. In Cavalli, F., Hansen, H.H., and Kaye, S.B. (ed.) *Textbook of Medical Oncology,* 1st ed. London: Martin Dunitz Ltd., 23–40.

Wilson, G.D., Saunders, M.I., Dische, S., Daley, F.M., Robinson, B.M., Martindale, C.A., Joiner, B., and Richman, P.I. 1996. Direct comparison of bromodeoxyuridine and Ki-67 labelling indices in human tumors. *Cell Prolif. 29*:141–152.

Wong, N.A.S.C., Mayer, N.J., MacKell, S., Gilmour, H.M., and Harrison, D.J. 2000. Immunohistochemical assessment of Ki67 and p53 expression assist the diagnosis and grading of ulcerative colitis-related dysplasia. *Histopathology 37*: 108–114.

Zacchetti, A., Van Garderen, E., Teske, E., Nederbragt, H., Dierendonck, J.H., and Rutterman, G.R. 2003. Validation of the use of proliferation markers in canine neoplastic and non-neoplastic tissues: comparison of Ki-67 and proliferating cell nulear antigen (PCNA) expression versus *in vivo* bromodeoxyuridine labelling by immunohistochemistry. *APMIS 111*:430–438.

6

Role of Immunohistochemical Expression of KIT/CD117 in Gastrointestinal Stromal Tumors

Tadashi Hasegawa

Introduction

Primary mesenchymal tumors arising in the gastrointestinal (GI) tract of adults form a large, diverse group; that differ in their histologic features and clinical behavior but sometimes pose diagnostic problems. Gastrointestinal stromal tumors (GISTs) comprise the majority of this tumor group. In the early literature, GISTs were described as smooth-muscle tumors: leiomyomas, cellular leiomyomas, leiomyoblastomas, and leiomyosarcomas (Appelman, 1990). Since the term "gastric stromal tumor" was first used to describe mesenchymal tumors of the stomach, formerly defined as leiomyomas lacking smooth-muscle differentiation immunohistochemically and ultrastructurally (Mazur and Clark, 1983), GIST has become the most widely used designation for specific mesenchymal tumors of the GI tract.

The *c-kit* protooncogene, located on human chromosome 4, is a 145-kD type III transmembrane receptor tyrosine kinase that is structurally similar to platelet-derived growth factor receptors (PDGFRs) A and B and to colony stimulating factor 1 receptor and is thought to play an important role in hematopoiesis, spermatogenesis, and melanogenesis (Heinrich *et al.,* 2002). Specific mutations in the *c-kit* protooncogene leading to its ligand-independent activation have been detected in GISTs (Hirota *et al.,* 1998). These genomic mutations encode structurally abnormal proteins with constitutive enzymatic activity (Rubin *et al.,* 2001), which in turn usually leads to expression of the *c-kit* protein KIT/CD117 and hence to the recognition of a new and reliable phenotypic marker for GISTs. Most of the *c-kit* mutations in GISTs occur within the juxtamembrane region, encoded by exon 11. In addition, mutations in other regions of the *c-kit* gene, including exons 9, 13, and 17, have been detected, although they occur at a much lower frequency than those in exon 11 (Hirota *et al.,* 2001; Kinoshita *et al.,* 2003; Lasota *et al.,* 2000; Lux *et al.,* 2000; Rubin *et al.,* 2001). Use of the *c-kit* tyrosine kinase inhibitor STI-571 (Glivec; imatinib mesylate) in the treatment of GISTs has proved promising for clinical management (Demetri *et al.,* 2002; Heinrich *et al.,* 2003; van Oosterom *et al.,* 2001). Accordingly, it has become more important for pathologists to diagnose GISTs accurately on the basis of standardized procedures and interpretation of KIT immunostaining.

Handbook of Immunohistochemistry and *in situ* Hybridization of Human Carcinomas, Volume 4: Molecular Genetics, Gastrointestinal Carcinoma, and Ovarian Carcinoma

This chapter outlines the pathologic features of GISTs, including their definition and the features of other spindle cell tumors from which they need to be differentiated, and discusses the validated KIT immunohistochemistry (IHC).

MATERIALS

- Primary antibody: rabbit polyclonal anti-human c-kit/CD117 antibody (DakoCytomation, Glostrup, Denmark, Code No. A4502) diluted in 0.05 mol/L; Tris buffered saline (TBS), pH 7.6, containing 1% bovine serum albumin (BSA), or Dako Antibody Diluent (DakoCytomation, Code No. S0809).
- Negative control reagent: normal/nonimmune rabbit serum, immunoglobulin fraction (DakoCytomation, Code Nos. X0903/X0936).
- Detection system: Dako EnVision + anti-rabbit peroxidase-labeled polymer (DakoCytomation, Code Nos. K4002/K4003).
- Substrate-chromogen: liquid 3,3′-diaminobenzidine (DAB+) substrate-chromogen solution (DakoCytomation, Code Nos. K3467/K3468).
- Antigen retrieval solution: Dako Target Retrieval Solution, pH 6.0, (DakoCytomation, Code Nos. S1699/S1700), or 0.01 mol/L citrate buffer, pH 6.0.
- Wash buffer solution: 0.05 mol/L Tris buffered saline T (TBST), containing 0.05% Tween 20 and 0.15 mol/L NaCl, pH 7.6, 10× concentrate (DakoCytomation, Code No. S3006).
- Peroxidase block: Dako Peroxidase Block, Code Nos. S2001/S2023, or 3% hydrogen peroxide.

METHODS

Standard manual immunohistochemical staining methods were used on formalin-fixed, paraffin-embedded tissues at room temperature and consisted of the following steps:

1. Deparaffinize and rehydrate as follows:
   a. 2 changes for 5 min each with xylene.
   b. 2 changes for 3 min each with 100% ethanol.
   c. 2 changes for 3 min each with 95% ethanol.
   d. Rinse in distilled water or tap water.
2. Retrieve target by immersion of tissue sections in a buffer solution (Dako Target Retrieval Solution, or 0.01 mol/L citrate buffer, pH 6.0) and heating either in a waterbath (95–99ºC) for 20 min or in an autoclave (121ºC) for 5 min, followed by a 20-min cooldown period.
3. Rinse slides with distilled water or tap water.
4. Block with peroxidase block or 3% hydrogen peroxide for 5 min.
5. Rinse slides with distilled water or tap water.
6. Place in wash buffer (TBST) for 5 min.
7. Incubate with enough 1/50–1/100 diluted polyclonal rabbit anti-human c-kit/CD117 (DakoCytomation, A4502) or negative control reagent for 30 min in a humid chamber at room temperature.
8. Rinse slides 3× with wash buffer for 5 min.
9. Incubate with enough EnVision + peroxidase-labeled polymer for 30 min in a humid chamber at room temperature.
10. Rinse slides 3× with wash buffer for 5 min.
11. Incubate with enough DAB+ substrate-chromogen solution for 10 min.
12. Rinse slides with distilled water or tap water.
13. Stain with hematoxylin for 30 sec.
14. Rinse slides with distilled water or tap water.
15. Cover the stained tissue with a coverslip.

RESULTS AND DISCUSSION

Morphologic Features of Gastrointestinal Stromal Tumors

Owing to the recent appreciation of the central role of *c-kit* mutations and KIT expression in GISTs, GIST can be defined as a mesenchymal spindle or epithelioid cell tumor arising in the wall of the GI tract that shows consistent immunoreactivity for KIT (Hasegawa *et al.,* 2002). In 211 GISTs diagnosed and treated at our institution, 177 tumors (84%) occurred in the stomach, 22 (10%) in the small intestine, 8 (4%) in the rectum, 3 (1%) in the esophagus, and one (1%) in the omentum (Yamaguchi *et al.,* 2004). In accordance with the predominant histologic pattern, 158 (75%) GISTs were classified as spindle cell type (Figure 26A), 39 (18%) as mixed (combination of spindle and epithelioid cell) type, and 14 (7%) as epithelioid cell type. The spindled GISTs usually were composed of uniform spindle cells forming interlacing bundles, whorls, or a storiform pattern, with a varying amount of interstitial collagen. The neoplastic cells had eosinophilic cytoplasm and elongated blunt-ended nuclei, often with nuclear palisading reminiscent of that of nerve sheath tumors and prominent vacuolization, which is a characteristic feature of gastric tumors.

The epithelioid GISTs consisted of round epithelioid cells with eosinophilic vacuolated or clear cytoplasm. They were often arranged in a nested paraganglioma-like or carcinoid-like growth pattern, enhancing the risk of confusion with an epithelial or melanocytic tumor. Mixed-type GISTs exhibited an abrupt transition between spindle cell and epithelioid areas, or they had an “intermediate” cytologic appearance of these cell types throughout. Epithelioid GISTs or predominantly

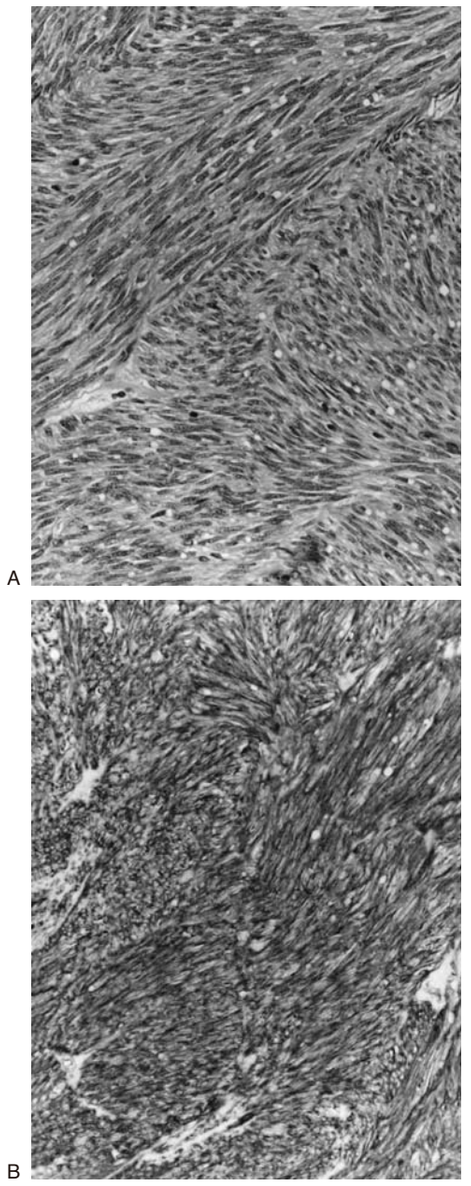

Figure 26. Gastrointestinal stromal tumors. A gastric stromal tumor of spindle cell type is composed of uniform cells with cytoplasmic vacuoles arranged in short fascicles. Diffuse and strong immunoreactivity for KIT/CD117 in the membrane **(A)** and cytoplasm of most tumor cells **(B)**.

epithelioid mixed-type GISTs occurred far more often in the stomach than elsewhere. The stroma was hyalinized, or even calcified in some tumors, and prominent myxoid change was observed in 9 (4.3%) GISTs. Cytologic pleomorphism was rare for GISTs: only three (1.4%) tumors had this feature. Of the 22 small intestinal GISTs 11 (50%) contained whorled or globular extracellular collagen bundles (called skeinoid fibers) in the spindle cell areas.

Immunophenotype of Gastrointestinal Stromal Tumors

Aside from KIT immunoreactivity, CD34 positivity was observed in almost all (98%) gastric GISTs but in only 32% of small intestinal tumors (Table 6). Positivity for smooth–muscle actin (SMA) was expressed in 31% of GISTs—most often in the small intestine (82%). Immunoreactivity for S-100 was infrequent (8%) in GISTs, but a proportion of tumors involving the small intestine (41%) were S-100 positive. Although staining for desmin was rare in GISTs (4%), the frequency of desmin positivity tended to be higher in epithelioid cell GISTs (21%) than in spindle cell GISTs (2.5%) and mixed-type GISTs (2.6%). No significant differences were observed among these three types of GIST in immunostaining patterns for the remaining markers. Knowing these immunohistochemical variations among anatomic locations and morphologic types, although none of these antigens is diagnostically specific, is helpful for differential diagnosis of GIST from other spindle cell tumors that may involve the GI tract.

In terms of KIT immunostaining, GISTs were consistently positive for KIT, and the reactivity usually was diffuse and strong in the cytoplasm and membranes of most tumor cells (see Figure 26). The pattern of KIT immunostaining was cytoplasmic reactivity in 54% and cytoplasmic dotlike reactivity (the so-called "Golgi-pattern") in 46% of tumors. In 7.6% of tumors, KIT immunoreactivity for epithelioid cells was weaker than in spindle cells in the same tissue sections or other tumors. The significance of this heterogeneity of KIT staining in GISTs remains to be investigated, but it is necessary to be aware of these patterns when carrying out immunostaining on small biopsy samples in suspected cases of GIST. Rarely, tumors with all of the morphologic and other phenotypic features of GIST do not express KIT. In such cases, accurate diagnosis of GISTs might be difficult.

Mutations of the *platelet-derived growth factor receptor alpha (PDGFRA)* gene encoding PDGFRA have been reported in some of these tumors, suggesting that, instead of KIT, PDGFRA plays an important role in the development of (GISTs without *c-kit* mutations (Debiec-Rychter *et al.,* 2004; Heinrich *et al.,* 2003a; Hirota *et al.,* 2003). We analyzed a series of GISTs that were immunohistochemically weak or negative for KIT; these tumors consisted at least partly of epithelioid cells. Two-thirds contained loosely arranged epithelioid cells and multinucleated tumor giant cells accompanied by

Table 6. Frequency of Immunostaining for Each Antibody in Gastrointestinal Stromal Tumors (GISTs) and Other Spindle Cell Tumors of the Gastrointestinal Tract

Tumor Type	KIT/CD117 (%)	CD34 (%)	Desmin (%)	Smooth-Muscle Actin (%)	S-100 (%)
GIST (n = 211)	100	91	4	31	8
Stomach (n = 177)	100	98	5	24	3
Small intestine (n = 22)	100	32	0	82	41
Smooth-muscle tumor					
Leiomyoma (n = 12)	0	0	100	100	0
Leiomyosarcoma (n = 18)	0	0	100	100	0
Peripheral nerve sheath tumor					
Schwannoma (n = 14)	0	50	0	0	100
Fibrous tumor					
Solitary fibrous tumor (n = 17)	0	100	0	0	24
Desmoid-type fibromatosis (n = 25)	0	0	20	84	0

a prominent myxoid stroma, often with mast cell infiltrate within the tumor nodules; we termed these myxoid epithelioid GISTs. As described earlier, a minority of GISTs show a variably prominent myxoid stroma (Suster *et al.,* 1995). We have found by mutational analyses that 90% of myxoid epithelioid GISTs, which occur mostly in the stomach, have *PDGFRA* mutations, primarily at exon 18 and rarely at exon 12 (Sakurai *et al.,* 2004). These results suggest that myxoid epithelioid GISTs are a distinct subtype with a special molecular background. Recognition of such morphologic characteristics will help to avoid confusion of these tumors with others that appear similar microscopically.

Differential Diagnosis

Leiomyomas and leiomyosarcomas are the main tumors of the GI tract that are often confused with GISTs. Leiomyomas are paucicellular and composed of elongated spindle cells with abundant eosinophilic, fibrillary cytoplasm. Leiomyosarcoma are characterized by long fascicles of eosinophilic spindle cells with elongated nuclei with rounded ends. Focal pleomorphism is common. Their well-differentiated smooth-muscle cells are negative for KIT and CD34 and positive for SMA and, usually, for desmin (Lasota *et al.,* 1999; Miettinen *et al.,* 1995; 2000a,b; 2001; 2003; Wieczorek *et al.,* 2001). Our findings were similar to those of previous studies and confirmed that all leiomyomas and leiomyosarcomas were immunoreactive for desmin and SMA (see Table 6). The immunostaining was diffuse and strong in leiomyomas but tended to be less intense and heterogeneous in leiomyosarcomas. KIT, CD34, and S-100 were negative in all leiomyomas and leiomyosarcomas.

Schwannomas rarely occur in the GI tract and are characterized microscopically by the presence of peripheral lymphoid cuffs and short fascicles of spindle cells and bizarre cells. Unlike conventional soft-tissue schwannomas, they usually have regular whorls or a storiform pattern and lack distinct palisading (Daimaru *et al.,* 1988). All schwannomas show strong nuclear and cytoplasmic staining for S-100. Of our cases, 50% were focally CD34-positive. This positive CD34 immunostaining was detected not only in tumors located in the stomach (as in our findings) but also in tumors occurring in other locations (Hirose *et al.,* 2003). Positivity for S-100 and negativity for smooth-muscle markers and KIT can be used to separate schwannomas from GISTs.

Solitary fibrous tumors (SFTs) may occur in the GI tract, mesentery, or retroperitoneum and become a diagnostic problem because they mimic GISTs to some extent histologically. Microscopically, SFTs have been described as showing "patternless" growth, with a haphazard arrangement of bland-looking short spindle or polygonal cells, alternating hypercellular and hypocellular sclerotic foci, keloid-like stromal hyalinization, and a prominent branching vasculature. All SFTs stained positively for CD34 but not for KIT (Miettinen *et al.,* 2000b; Sarlomo-Rikala *et al.,* 1998; Shidham *et al.,* 2002). Staining for CD34 was generally strong and diffuse in the cytoplasm of spindle cells of SFTs. None of the SFTs showed immunostaining for smooth-muscle markers (desmin or SMA). These findings suggest that a combination of immunostaining for KIT, CD34, and smooth-muscle markers might be helpful for differentiating GISTs from SFTs. We detected S-100 positivity in 24% of SFTs, as described previously (Hasegawa *et al.,* 1999).

Intraabdominal desmoid-type fibromatoses (DTFs) are uncommon tumors that affect primarily the mesentery or retroperitoneum and often invade the wall of the

GI tract. DTFs were infiltrative and locally aggressive, characterized by a loose fascicular arrangement of spindle cells in a predominantly collagenous background. Of DTFs, 84% showed moderate-to-strong positivity for SMA, and we detected scattered desmin immunoreactivity in 20% of DTFs. This supports the finding that DTFs consist mainly of neoplastic myofibroblasts (Hasegawa *et al.,* 1990). None of the DTFs were CD34-positive. S-100 was negative in DTFs.

It is well known that DTFs usually have mutations of the *APC* and *beta-catenin* genes (Giarola *et al.,* 1998; Miyoshi *et al.,* 1998; Shitoh *et al.,* 1999; Tejpar *et al.,* 1999) and that APC-truncating mutations confer a proliferative advantage on aggressive fibromatosis cells through *beta-catenin* (Li *et al.,* 1998). In all specimens of DTF, we recognized immunoreactivity for beta-catenin in the nuclei, and staining for beta-catenin was uniformly distributed throughout the sections, despite variability in the proportions of positive cells. This finding suggests the usefulness of beta-catenin for distinguishing this tumor from GISTs, as reported previously (Montgomery *et al.,* 2002). However, careful evaluation should be done because there is an overlap in the nuclear accumulation of beta-catenin in DTFs and SFTs. We noted that 24% of SFTs showed nuclear accumulation of beta-catenin. In this situation, additional CD34 immunostaining might be helpful for separating SFTs from DTFs.

Metastatic melanoma and primary clear cell sarcoma may occur in the walls of the intestine or stomach and should be separated from GIST because of their histologic resemblance. Positivity for melanocytic markers (tyrosinase, melan-A, and HMB-45) in combination with the results for combinations of other markers such as KIT, CD34, and S-100, or the use of molecular cytogenetic methods to detect the chromosomal translocations t(12;22)(q13;q12) or the *EWS-ATF1* fusion transcript are diagnostic (Zambrano *et al.,* 2003).

KIT Immunohistochemistry

Given the potential therapeutic significance of KIT immunopositivity and hence the desirability of avoiding false-positive or false-negative results, it is important to carefully titrate the most widely used polyclonal KIT antibodies using appropriate positive and negative controls. The results of KIT immunostaining in other bone and soft-tissue sarcomas are, at times, conflicting (Barisella *et al.,* 2002; Hornick and Fletcher, 2002; Sabah *et al.,* 2003; Smithey *et al.,* 2002), and at least a small number of these tumors are KIT positive with results ranging from weak, focal staining to occasionally strong staining. These findings suggest the possibility that KIT immunostaining would lead to diagnostic confusion because KIT positivity has been detected in other morphologically similar tumors, including intraabdominal DTFs (Lucas *et al.,* 2003; Yantiss *et al.,* 2000) and other mesenchymal tumors such as leiomyosarcoma, fibrosarcoma, and synovial sarcoma (Sabah *et al.,* 2003; Smithey *et al.,* 2002).

We assessed the intensity of KIT staining as the proper immunohistochemical score of the tumor on the basis of strength: 0, negative; 1+, weak staining; 2+, moderate staining; 3+, strong staining. We used tissue mast cells, which stain 2+, on 3+, as internal positive controls for KIT. We also recorded the distribution of positive cells in an effort to define the diffuse or focal nature of the positive cells: sporadic (positive cells <10%); focal (≥10% positive cells <50%); diffuse (positive cells ≥50%). Immunohistochemical scores of 2+ and 3+ with focal to diffuse distribution were considered to be positive for KIT. As a result, KIT staining in a series of other bone and soft-tissue sarcomas was limited (Table 7). We observed positive staining for KIT in 25% of Ewing sarcoma and primitive neuroectodermal tumors, 13% of angiosarcomas, 9% of neuroblastomas, 7% of clear cell sarcomas, and 5% of synovial sarcomas. In DTFs, KIT staining was frequent (60%) by the labeled streptavidin–biotinylated antibody (LSAB) method with 1/50 diluted polyclonal rabbit anti-human KIT/CD117 antibody (DakoCytomation, A4502). In this situation, the KIT staining in DTFs was exclusively cytoplasmic with a coarse granular pattern, but, unlike in GIST, there was no staining of the cell membrane. It is interesting that, moderate (2+) or strong (3+) KIT staining was eliminated or significantly reduced when 1/100 diluted antibody was used.

Such false positivity did not occur when we used a peroxidase-labeled polymer-based detection system with either 1/50 or 1/100 diluted antibody. It has been pointed out that the use of an avidin–biotinylated peroxidase complex or LSAB method with heat-induced antigen retrieval causes frequent nonspecific (false-positive) KIT staining in other non-GIST tumors (Sabah *et al.,* 2003), and, therefore, there are claims that antigen retrieval should not be performed for KIT immunostaining (Lucas *et al.,* 2003). In routine diagnostic pathology, however, we cannot skip the heat-induced antigen retrieval procedure if we wish to achieve reproducible and reliable immunohistochemical results on formalin-fixed, paraffin-embedded tissues. Our findings suggest that the dextran polymer-based detection system can be highly recommended as a standard protocol of KIT IHC, not only as a prerequisite for the diagnosis of GIST but also for determining the eligibility of the tumor for imatinib mesylate treatment. Moreover, further polymerase chain reaction analysis revealed that neither

Table 7. KIT Immunoreactivity in Non-GIST 418 Bone and Soft-Tissue Sarcomas

Tumor Type	Number	KIT/CD117 0	1+	2+	3+	Negative (0/1+)	Positive (2+/3+)
Fibrosarcoma	11	11	0	0	0	11 (100%)	0
Leiomyosarcoma	11	8	3	0	0	11 (100%)	0
Myxoid liposarcoma	52	52	0	0	0	52 (100%)	0
Well-differentiated liposarcoma	50	50	0	0	0	50 (100%)	0
Myxofibrosarcoma	53	52	1	0	0	53 (100%)	0
Malignant peripheral nerve sheath tumor	18	17	1	0	0	18 (100%)	0
Pleomorphic malignant fibrous histiocytoma	44	44	0	0	0	44 (100%)	0
Synovial sarcoma	42	40	0	2	0	40 (95%)	2 (5%)
Ewing sarcoma/primitive neuroectodermal tumor	20	8	7	4	1	15 (75%)	5 (25%)
Desmoplastic small round cell tumor	6	6	0	0	0	6 (100%)	0
Neuroblastoma	11	10	0	0	1	10 (91%)	1 (9%)
Clear cell sarcoma	15	14	0	0	1	14 (93%)	1 (7%)
Angiosarcoma	30	26	0	4	0	26 (87%)	4 (13%)
Osteosarcoma	20	20	0	0	0	20 (100%)	0
Rhabdomyosarcoma	35	35	0	0	0	35 (100%)	0
Total	418					405 (97%)	13 (3%)

mutations of *c-kit* nor *PDGRA* were detected in DTFs. KIT-positive non-GIST tumors, in the absence of any accompanying mutation such as *c-kit* and *PDGFRA* gene mutation, are not suitable for treatment with imatinib mesylate.

Summary

The extent and patterns of KIT immunostaining in GISTs are varied, and KIT immunostaining is also detected in a limited number of other mesenchymal tumors that may involve the GI tract and abdominal cavity. Thus, it is essential for the diagnosis of GISTs to use an immunohistochemical panel along with appropriate morphologic evaluation. In this context, consistent (100% positive) immunoreactivity for KIT, CD34, desmin, and S-100 and nuclear accumulation of beta-catenin in GISTs, SFTs, smooth-muscle tumors, schwannomas, and DTFs suggest that these are key markers for the clinical diagnosis of GISTs and other spindle cell tumors that can arise in the GI tract.

References

Appelman, H.D. 1990. Mesenchymal tumors of the gut: histological perspectives, new approaches, new results, and does it make any difference? *Monogr. Pathol. 31*:220–246.

Barisella, M., Andreola, S., and Rosai, J. 2002. CD117 in soft tissue sarcomas. *Am. J. Clin. Pathol. 118*:470–471.

Daimaru, Y., Kido, H., Hashimoto, H., and Enjoji, M. 1988. Benign schwannoma of the gastrointestinal tract: a clinicopathologic and immunohistochemical study. *Hum. Pathol. 19*:257–264.

Debiec-Rychter, M., Wasag, B., Stul, M., De Wever, I., Van Oosterom, A., Hagemeijer, A., and Sciot, R. 2004. Gastrointestinal stromal tumours (GISTs) negative for KIT (CD117 antigen) immunoreactivity. *J. Pathol. 202*:430–438.

Demetri, G.D., von Mehren, M., Blanke, C.D., Van den Abbeele, A.D., Eisenberg, B., Roberts, P.J., Heinrich, M.C., Tuveson, D.A., Singer, S., Janicek, M., Fletcher, J.A., Silverman, S.G., Silberman, S.L., Capdeville, R., Kiese, B., Peng, B., Dimitrijevic, S., Druker, B.J., Corless, C., Fletcher, C.D., and Joensuu, H. 2002. Efficacy and safety of imatinib mesylate in advanced gastrointestinal stromal tumors. *N. Engl. J. Med. 347*:472–480.

Giarola, M., Wells, D., Mondini, P., Pilotti, S., Sala, P., Azzarelli, A., Bertario, L., Pierotti, M.A., Delhanty, J.D., and Radice, P. 1998. Mutations of adenomatous polyposis coli (APC) gene are uncommon in sporadic desmoid tumors. *Br. J. Cancer 78*: 582–587.

Hasegawa, T., Hirose, T., Kudo, E., Abe, J., and Hizawa, K. 1990. Cytoskeletal characteristics of myofibroblasts in benign neoplastic and reactive fibroblastic lesions. *Virchows Archiv. A. Pathol. Anat. 416*:375–382.

Hasegawa, T., Matsuno, Y., Shimoda, T., Hasegawa, F., Sano, T., and Hirohashi, S. 1999. Extrathoracic solitary fibrous tumors: their histological variability and potentially aggressive behavior. *Hum. Pathol. 30*:1464–1473.

Hasegawa, T., Matsuno, Y., Shimoda, T., and Hirohashi, S. 2002. Gastrointestinal stromal tumor: consistent CD117 immunostaining for diagnosis, and prognostic classification based on tumor size and MIB-1 grade. *Hum. Pathol. 33*:669–676.

Heinrich, M.C., Corless, C.L., Demetri, G.D., Blanke, C.D., von Mehren, M., Joensuu, H., McGreevey, L.S., Chen, C.J., Van den Abbeele, A.D., Druker, B.J., Kiese, B., Eisenberg, B., Roberts, P.J., Singer, S., Fletcher, C.D., Silberman, S., Dimitrijevic, S., and Fletcher, J.A. 2003b. Kinase mutations and imatinib response in patients with metastatic gastrointestinal stromal tumor. *J. Clin. Oncol. 21*:4342–4349.

Heinrich, M.C., Corless, C.L., Duensing, A., McGreevey, L., Chen, C.J., Joseph, N., Singer, S., Griffith, D.J., Haley, A.,

Town, A., Demetri, G.D., Fletcher, C.D., and Fletcher, J.A. 2003a. PDGFRA activating mutations in gastrointestinal stromal tumors. *Science 299*:708–710.

Heinrich, M.C., Rubin, B.P., Longley, B.J., and Fletcher, J.A. 2002. Biology and genetic aspects of gastrointestinal stromal tumors: KIT activation and cytogenetic alterations. *Hum. Pathol. 33*:484–495.

Hirose, T., Tani, T., Shimada, T., Ishizawa, K., Shimada, S., and Sano, T. 2003. Immunohistochemical demonstration of EMA/Glut1-positive perineurial cells and CD34-positive fibroblastic cells in peripheral nerve sheath tumors. *Mod. Pathol. 16*:293–298.

Hirota, S., Isozaki, K., Moriyama, Y., Hashimoto, K., Nishida, T., Ishiguro, S., Kawano, K., Hanada, M., Kurata, A., Takeda, M., Tunio, G.M., Matsuzawa, Y., Kanakura, Y., Shinomura, Y., and Kitamura, Y. 1998. Gain-of-function mutations of c-kit in human gastrointestinal stromal tumors. *Science 279*:577–580.

Hirota, S., Nishida, T., Isozaki, K., Taniguchi, M., Nakamura, J., Okazaki, T., and Kitamura, Y. 2001. Gain-of-function mutation at the extracellular domain of KIT in gastrointestinal stromal tumours. *J. Pathol. 193*:505–510.

Hirota, S., Ohashi, A., Nishida, T., Isozaki, K., Kinoshita, K., Shinomura, Y., and Kitamura, Y. 2003. Gain-of-function mutations of platelet-derived growth factor receptor alpha gene in gastrointestinal stromal tumors. *Gastroenterology 125*:660–667.

Hornick, J.L., and Fletcher, C.D.M. 2002. Immunohistochemical staining for KIT (CD117) in soft tissue sarcomas is very limited in distribution. *Am. J. Clin. Pathol. 117*:188–193.

Kinoshita, K., Isozaki, K., Hirota, S., Nishida, T., Chen, H., Nakahara, M., Nagasawa, Y., Ohashi, A., Shinomura, Y., Kitamura, Y., and Matsuzawa, Y. 2003. C-kit gene mutation at exon 17 or 13 is very rare in sporadic gastrointestinal stromal tumors. *J. Gastroenterol. Hepatol. 18*:147–151.

Lasota, J., Jasinski, M., Sarlomo-Rikara, M., and Miettinen, M. 1999. C-kit mutations occur preferentially in malignant versus benign GISTs and do not occur in leiomyomas and leiomyosarcomas. *Am. J. Pathol. 154*:53–60.

Lasota, J., Wozniak, A., Sarlomo-Rikara, M., Rys, J., Kordek, R., Nassar, A., Sobin, L.H., and Miettinen, M. 2000. Mutations in exons 9 and 13 of KIT gene are rare events in gastrointestinal stromal tumors: a study of two hundred cases. *Am. J. Pathol. 157*:1091–1095.

Li, C., Bapat, B., and Alman, B.A. 1998. Adenomatous polyposis coli gene mutation alters proliferation through its beta-catenin-regulatory function in aggressive fibromatosis (desmoid tumor). *Am. J. Pathol. 153*:709–714.

Lucas, D.R., Al-Abbadi, M., Tabaczka, P., Hamre, M.R., Weaver, D.W., and Mott, M.J. 2003. c-Kit expression in desmoid fibromatosis. *Am. J. Clin. Pathol. 119*:339–345.

Lux, M., Rubin, B.P., Biase, T.L., Chen, C.J., Maclure, T., Demetri, G., Xiao, S., Singer, S., Fletcher, C.D., and Fletcher, J.A. 2000. KIT extracellular and kinase domain mutations in astrointestinal stromal tumors. *Am. J. Pathol. 156*:791–795.

Mazur, M.T., and Clark, H.B. 1983. Gastric stromal tumors: reappraisal of histogenesis. *Am. J. Surg. Pathol. 7*:507–519.

Miettinen, M., Furlong, M., Sarlomo-Rikala, M., Burke, A., Sobin, L.H., and Lasota, J. 2001. Gastrointestinal tumors, intramural leiomyomas, and leiomyosarcomas in the rectum and anus: a clinicopathologic, immunohistochemical, and molecular genetic study of 144 cases. *Am. J. Surg. Pathol. 25*:1121–1133.

Miettinen, M., Kopczynski, J., Makhlouf, H.R., Sarlomo-Rikala, M., Gyorffy, H., Burke, A., Sobin, L.H., and Lasota, J. 2003. Gastrointestinal stromal tumors, intramural leiomyomas, and leiomyosarcomas in the duodenum: a clinicopathologic, immunohistochemical, and molecular genetic study of 167 cases. *Am. J. Surg. Pathol. 27*:625–641.

Miettinen, M., Sarlomo-Rikara, M., Sobin, L.H., and Lasota, J. 2000a. Gastrointestinal stromal tumors and leiomyosarcomas in the colon: a clinicopathologic, immunohistochemical, and molecular genetic study of 44 cases. *Am. J. Surg. Pathol. 24*:1339–1352.

Miettinen, M., Sobin, L.H., and Sarlomo-Rikara, M. 2000b. Immunohistochemical spectrum of GISTs at different sites and their differential diagnosis with a reference to CD117 (KIT). *Mod. Pathol. 13*:1134–1142.

Miettinen, M., Virolainen, M., and Sarlomo-Rikara, M. 1995. Gastrointestinal stromal tumors: value of CD34 antigen in their identification and separation from true leiomyomas and schwannomas. *Am. J. Surg. Pathol. 19*:207–216.

Miyoshi, K., Iwao, K., Nawa, G., Yoshikawa, H., Ochi, T., and Nakamura, Y. 1998. Frequent mutation in the beta-catenin gene in desmoid tumors from patients without familial adenomatous polyposis. *Oncol. Res. 10*:591–594.

Montgomery, B., Torbenson, M.S., Kaushal, M., Fisher, C., and Abraham, S.C. 2002. Beta-catenin immunohistochemistry separates mesenteric fibromatosis from gastrointestinal stromal tumor and sclerosing mesenteritis. *Am. J. Surg. Pathol. 26*:1296–1301.

Rubin, B.P., Singer, S., Tsao, C., Duensing, A., Lux, M.L., Ruiz, R., Hibbard, M.K., Chen, C.J., Xiao, S., Tuveson, D.A., Demetri, G.D., Fletcher, C.D., and Fletcher, J.A. 2001. KIT activation is a ubiquitous feature of gastrointestinal stromal tumors. *Cancer Res. 61*:8118–8121.

Sabah, M., Leader, M., and Kay, E. 2003. The problem with KIT: clinical implications and practical difficulties with CD117 immunostaining. *Appl. Immunohistochem. Mol. Morphol. 11*:56–61.

Sakurai, S., Hasegawa, T., Sakuma, Y., Takazawa, Y., Motegi, A., Nakajima, T., Saito, K., Fukayama, M., Shimoda, T. 2004. Myxoid epithelioid gastrointestinal stromal tumor (GIST) with mast cell infiltrations: a subtype of GIST with mutations of platelet-derived growth factor receptor alpha gene. *Hum. Pathol. 35*:1223–1230.

Sarlomo-Rikala, M., Kovatich, A.J., Barusevicius, A., and Miettinen, M. 1998. CD117: a sensitive marker for gastrointestinal stromal tumors that is more specific than CD34. *Mod. Pathol. 11*:728–734.

Shidham, V.B., Chivukula, M., Gupta, D., Rao, R.N., and Komorowski, R. 2002. Immunohistochemical comparison of gastrointestinal stromal tumor and solitary fibrous tumor. *Arch. Pathol. Lab. Med. 126*:1189–1192.

Shitoh, K., Konishi, F., Iijima, T., Ohdaira, T., Sakai, K., Kanazawa, K., and Miyaki, M. 1999. A novel case of a sporadic desmoid tumor with mutation of the beta-catenin gene. *J. Clin. Pathol. 52*:695–696.

Smithey, B.E., Pappo, A.S., and Hill, D.A. 2002. c-kit expression in pediatric solid tumor: a comparative immunohistochemical study. *Am. J. Surg. Pathol. 26*:486–492.

Suster, S., Sorace, D., and Moran, C.A. 1995. Gastrointestinal stromal tumors with prominent myxoid matrix: clinicopathologic, immunohistochemical, and ultrastructural study of nine cases of a distinctive morphological variant of myogenic stromal tumor. *Am. J. Surg. Pathol. 19*:59–70.

Tejpar, S., Nollet, F., Li, C., Wunder, J.S., Michils, G., dal Cin, P., Van Cutsem, E., Bapat, B., van Roy, F., Cassiman, J.J., and Alman, B.A. 1999. Predominance of beta-catenin mutations and beta-catenin dysregulation in sporadic aggressive fibromatosis (desmoid tumor). *Oncogene 18*:6615–6620.

van Oosterom, A.T., Judson, I., Verweij, J., Stroobants, S., Donato di Paola, E., Dimitrijevic, S., Martens, M., Webb, A., Sciot, R., Van Glabbeke, M., Silverman, S., and Nielsen, O.S. 2001. Safety and efficacy of imatinib (STI-571) in metastatic gastrointestinal stromal tumors: a phase I study. *Lancet 358*: 1421–1423.

Wieczorek, T.J., Faquin, W.C., Rubin, B.P., and Cibas, E.S. 2001. Cytologic diagnosis of gastrointestinal stromal tumor with emphasis on the differential diagnosis with leiomyosarcoma. *Cancer (Cancer Cytopathol.) 93*:276–287.

Yamaguchi, U., Hasegawa, T., Masuda, T., Sekine, S., Kawai, A., Chuman, H., and Shimoda, T. 2004. Differential diagnosis of gastrointestinal stromal tumor and other spindle cell tumors in the gastrointestinal tract based on immunohistochemical analysis. *Virchows Arch. 445*:142–150.

Yantiss, R.K., Spiro, I.J., Compton, C.C., and Rosenberg, A.E. 2000. Gastrointestinal stromal tumor versus intra-abdominal fibromatosis of the bowel wall: a clinically important differential diagnosis. *Am. J. Surg. Pathol. 24:*947–957.

Zambrano, E., Reyes-Mugica, M., Franchi, A., and Rosai, J. 2003. An osteoclast-rich tumor of the gastrointestinal tract with features resembling clear cell sarcoma of soft parts: reports of 6 cases of a GIST simulator. *Int. J. Surg. Pathol. 11*:75–81.

7

Role of Immunohistochemical Expression of BUB1 Protein in Gastric Cancer

Wolfram Mueller and Heike Grabsch

Introduction

Genetic instability is thought to play a key role in the multistage process leading to cancer (Hanahan and Weinberg, 2000) and has been classified into two categories: microsatellite instability (MSI) and chromosomal instability (CIN) (Lengauer *et al.,* 1998). Investigations have demonstrated that DNA (deoxyribonucleic acid) ploidy can be used as a surrogate marker CIN (Furuya *et al.,* 2000; Lengauer *et al.,* 1997; Miyazaki *et al.,* 1999). The very nature of the CIN phenotype suggests that aneuploidy in cancer may develop from persistent missegregation of chromosomes resulting from defects of the mitotic spindle checkpoint (Cahill *et al.,* 1998).

BUB1 is a key component of this regulatory pathway and was first identified in budding yeast (Hoyt *et al.,* 1991; Li and Murray, 1991). Initially, *BUB1* mutations were identified in a subset of aneuploid colorectal cancer cell lines (Cahill *et al.,* 1998). However, subsequent studies in different human cancer tissues have revealed that mutations of *BUB1* are extremely rare (Imai *et al.,* 1999) or not identifiable at all (Olesen *et al.,* 2001).

Most gastric cancers exhibit various levels of MSI ranging between 10% and 50% (Hayden *et al.,* 1998; Simpson *et al.,* 2001). In the form of aneuploidy, CIN is much more common than MSI in gastric cancer and has been found in up to 89% of the cases (Baba *et al.,* 2002). Numerous studies have been published describing DNA ploidy patterns in gastric cancer (Kim and Cho, 2000; Ming, 1998), but the molecular mechanisms leading to aneuploidy in gastric cancer are still unknown.

So far, mutations of *BUB1* have not been identified in gastric cancer cell lines (Mimori *et al.,* 2001) or in gastric cancer tissue samples (Shigeishi *et al.,* 2001). However, cell cycle arrest as a result of activation of the mitotic spindle checkpoint seems to depend on the amount of BUB1 protein available at the kinetochore (Ouyang *et al.,* 1998; Sharp-Baker and Chen, 2001; Taylor and McKeon, 1997). We have shown previously that the majority of gastric cancers expressed *BUB1* messenger ribonucleic acid (mRNA) at a higher level than corresponding normal gastric mucosa. Although we were unable to demonstrate a correlation of *BUB1* mRNA expression level with histopathologic parameters or DNA ploidy (Grabsch *et al.,* 2003), it is possible that the BUB1 protein expression level may be related to the high prevalence of aneuploidy in gastric cancer. To address this question we extended our previous

Handbook of Immunohistochemistry and *in situ* Hybridization of Human Carcinomas, Volume 4: Molecular Genetics, Gastrointestinal Carcinoma, and Ovarian Carcinoma

BUB1 mRNA study by analyzing BUB1 protein expression in 80 gastric cancer cases by immunohistochemistry (IHC) and explored the association of BUB1 protein expression with tumor progression (pT, pN), tumor differentiation (grading), tumor type according to Laurén classification, MSI, and DNA ploidy.

MATERIALS AND METHODS

Patients

This study was performed according to the local ethics regulations. Eighty patients with gastric adenocarcinoma, all of whom underwent gastrectomy at the Department of Surgery, University of Duesseldorf, Germany, between 1996 and 2000, were included in this study. The median age of the patients was 64.5 years, ranging from 35 to 88 years. Forty-eight patients (60%) were male.

All tumor specimens were fixed in 4% paraformaldehyde, and tissue blocks were embedded in paraffin using a standard protocol. Approximately 4 µm thick tissue sections stained with haematoxylin/eosin were used for histopathologic classification. The following histopathologic parameters were recorded: depth of invasion (pT category) and lymph-node involvement (pN category) according to the tumor, node, metastasis (TNM) classification (Sobin and Wittekind, 1997), tumor differentiation (grading) according to the World Health Organization (Hamilton and Aaltonen, 2000), morphologic tumor type according to Laurén classification (Laurén, 1965), and lymphatic and blood vessel invasion. Because tissue for histopathologic diagnosis of distant metastasis (pM category) was received in 9 cases only, this parameter was excluded from further analysis.

Production of Anti-BUB1 Antibodies

A synthetic peptide was used for the immunization of rabbits. The sequence of the peptide, CVNKSTHEFKPQSGA (aa 407-412, GenBank AF046078), was compared with the aa sequences in GenBank using BLASTP 2.2.3 (Altschul *et al.,* 1997). Only mouse and human BUB1 fragments were identified and shown to be highly similar or identical to the synthetic peptide sequence. Peptide synthesis, immunization of rabbits, and affinity purification of the final bleed serum were performed by Eurogentec, Belgium.

Evaluation of Specificity and Sensitivity of Anti-BUB1 Antibodies

Enzyme linked immunosorbent assay (ELISA) testing of the antiserum against the peptide and the carrier protein was carried out by Eurogentec using standard protocols. Cell extractions, SDS-PAGE, and Western blotting using BUB1 anti-serum were performed essentially as described previously (Morrison *et al.,* 1998).

HeLa cells, previously demonstrated to be spindle checkpoint-competent (Li and Benezra, 1996; Takahashi *et al.,* 1999), were obtained from European Collection of Cell Cultures (ECACC) and maintained in Dulbecco's Modified Eagle Medium (DMEM) containing Glutamax, 10% (v/v) fetal calf serum and penicillin/streptomycin (Life Technologies). Cells were seeded on coverslips and allowed to grow for 72 hr. Cells were washed in 0.01 M phosphate buffer saline (PBS), pH 7.4, before fixation either in 4% paraformaldehyde/PBS at 18°C for 20 min or in methanol at −18°C for 10 min. After washing in PBS, the fixed cells were permeabilized with 0.1% Triton X-100/PBS at 18°C for 5 min. All cells were then incubated in 1% Marvel (nonfat dried milk)/PBS at 18°C for 15 min to block nonspecific binding. Cells were incubated with anti-BUB1 (1:50 in 1% Marvel/PBS) at 18°C for 1 hr. After washing in PBS, cells were incubated with goat anti-rabbit Alexa 488 1:300 (Molecular Probes) plus DAPI (4′,6-diamino-2-phenylindole 5 µg/ml, Sigma St. Louis, MO) in 1% Marvel/PBS at 18°C for 1 hr and mounted on glass slides. Confocal immunofluorescence microscopy was performed with a Leica TCS-SP spectral confocal microscope using the 488 nm line of an Argon laser and an Argon UV (ultraviolet) laser. The fluorophore and DAPI were imaged sequentially to eliminate any bleed-through artefacts.

BUB1 Immunohistochemistry in Gastric Cancer Tissues

One paraffin block from each case was processed for BUB1 immunohistochemistry (IHC) as follows: 4 µm tissue sections were mounted on adhesive slides, deparaffinized, and rehydrated. After antigen retrieval in 10 mM citrate buffer (pH 6.0) for 10 min using a microwaveable pressure cooker (Nordic Houseware, Minneapolis, MN), endogenous peroxidase was blocked by immersing the slides in 3% H_2O_2/distilled water at room temperature for 15 min. This was followed by incubating the slides with a solution of 2 egg white/200 ml distilled water at room temperature for 30 min, rinsing in tap water, and incubating with 0.02% biotin (Sigma)/PBS at room temperature for 30 min to block endogenous avidin-binding activity (Miller and Kubier, 1997). Anti-BUB1 serum was diluted with antibody diluent (1:4000, Zymed, San Francisco, CA) and tissue sections were incubated overnight at 4°C.

For immunohistochemical detection a modification of the ImmunoMax method (Merz *et al.,* 1995) was used.

Briefly, sections were incubated with biotinylated goat anti-rabbit immunoglobulin G (IgG) (Vector Laboratories, Burlingame, CA) diluted 1:200 in PBS plus 50 µl human serum/ml at 37°C for 30 min, rinsed, and incubated with ABC complex (Vectastain Elite ABC Kit, Vector Laboratories) diluted 1:100 in PBS at 37°C for 30 min. This was followed by incubating the slides with biotinylated tyramine working solution 1:100 in PBS plus 0.03% H_2O_2 at 37°C for 15 min, rinsing, and incubating with ABC complex again as described earlier. Biotinylated tyramine stock solution was prepared as described by Merz *et al.* (1995). The peroxidase substrate used was 3,3′-diaminobenzidine hydrochloride (DAB ready-to-use, ScyTek, Lugan, UT). Sections were counterstained with Mayer's hematoxylin, blued with 0.5% lithium carbonate, and mounted with Entellan (Merck, Whitehouse Station, NJ) after dehydration. Because of persistent technical problems, one of the gastric cancer cases could not be evaluated.

The following control experiments were performed: instead of incubating the slides with anti-BUB1, slides were incubated with 1) antibody diluent alone or 2) rabbit preimmune serum diluted 1:4000 or 3) a primary antibody solution (anti-BUB1 1:4000) that had been preincubated overnight at 4°C with different concentrations of the free peptide used for immunization.

Evaluation of BUB1 expression was done independently by two pathologists (HG, WM) both blinded to any histopathologic parameters, results of DNA cytophotometry, and microsatellite analysis. The number of BUB1-postive tumor cells of the entire tissue section was counted, resulting in one overall score per case. Values were categorized into five groups: Score I: 1–4% positive tumor cells; II: 5–25%; III: 26–50%; IV: 51–75% and V: 76–100%. Staining intensity was not considered.

Nuclear DNA Content Analysis (DNA Image Cytometry)

Nuclear DNA content was measured after preparation of nuclear suspensions of formalin-fixed, paraffin-embedded tumor and matching nonneoplastic gastric mucosa from all cases (n = 80) as previously described (Boecking *et al.,* 1995; Grabsch *et al.,* 2003). On average, 346 tumor cell nuclei (range: 230–466) were evaluated. DNA histograms were first categorized into four groups according to the position of stemlines (Haroske *et al.,* 200l): 1) peridiploid; 2) peritetraploid; 3) X-ploid (i.e., single stemline alone or additionally to a peridiploid/peritetrapioid stemline), and 4) multiploid: (i.e., more than one nonperidiploid or nonperitetraploid stemline). Cases with a peridiploid stemline were defined as DNA diploid, and all other groups were summarized as being DNA aneuploid. In addition, the modal DNA value of the stemline (i.e., the mean value of the most common DNA histogram class) was recorded for each case.

Microsatellite Analysis

DNA from tumor and paired nonneoplastic gastric mucosa was extracted from formalin-fixed, paraffin-embedded tissue sections after microdissection using the QIAamp DNA Mini Kit (QIAGEN Valencia, CA) according to the manufacturer's protocol. After purification on QIAamp spin columns, eluted DNA was tested for concentration and quality by measuring absorbance at 260 nm and determining the A260/A280 ratio using a spectrophotometer. The mononucleotide marker BAT26, located in intron 5 of *hMSH2* (GenBank U41210), was investigated using primer sequences, polymerase chain reaction (PCR) protocols, and denaturing polyacrylamide gel electrophoresis as described previously (Wirtz *et al.,* 1998). MSI was scored as present when a novel, abnormal-sized band occurred in the tumor sample in comparison to the corresponding normal DNA sample. Three cases could not be evaluated as a result of persistent technical problems.

Statistical Analysis

The statistical analysis was conducted using SPSS for Windows, release 11.0.1 (SPSS Inc., Chicago). Associations between percentage of BUB1-positive tumor cells, histopathologic parameters, ploidy, and microsatellite analysis were studied using Spearman's Rank correlation, Kruskal-Wallis Test, or Mann-Whitney Test where appropriate. P values less than 0.05 were considered significant.

RESULTS

Specificity and Sensitivity of Anti-BUB1 Antibodies

Positive staining was blocked after preincubation of anti-BUB1 serum with the peptide that had been used for immunization of the rabbits. No staining was visible when either rabbit preimmune serum or antibody diluent was used instead of primary antibody solution (data not shown).

SDS-PAGE and Western blotting of HeLa cell extracts using affinity-purified BUB1-311a antibodies revealed a single immunoreactive band with a molecular weight consistent with that expected for human BUB1 (122 kDa) (data not shown).

Proliferating HeLa cells were immunostained and confocal microscopy was performed to assess the

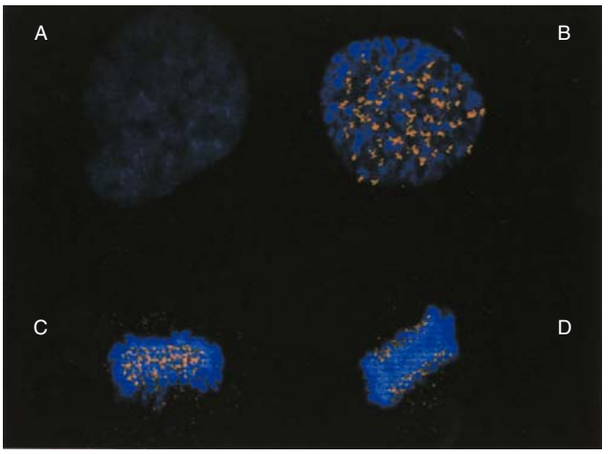

Figure 27. BUB1 immunocytochemistry *(red)* in HeLa cells; DAPI counterstain of DNA *(blue)*. **A:** No BUB1 staining in interphase nuclei or cytoplasm. **B:** Granular BUB1 staining within the nucleus in prophase. **C:** Strong BUB1 immunoreactivity on both sides of the kinetochores of chromosomes in metaphase. **D:** Decrease in BUB1 immunoreactivity at the kinetochores of chromosomes in metaphase–anaphase transition.

subcellular localization of BUB1 in different phases of the cell cycle (Figure 27). The staining results in HeLa cells were independent of the fixation method used. In interphase cells, no staining was detectable. In prophase, granular BUB1 staining was observed randomly distributed throughout the nucleus. In prometaphase, paired foci of strong BUB1 staining were indicative of an association with nascent kinetochores. In anaphase, BUB1 staining decreased significantly. These staining results in HeLa cells were entirely consistent with previously reported observations (Jablonski *et al.,* 1998; Taylor and McKeon, 1997) and together with the results from the blocking experiments as well as the Western blot test confirmed the high specificity and sensitivity of our newly generated BUB1 antibodies.

Expression of BUB1 in Nonneoplastic Gastric Mucosa and Gastric Cancer

In tumor-adjacent, nonneoplastic gastric mucosa nuclear expression of BUB1 was observed in some of the epithelial cells as well as in many lymphocytes. The number of positively stained epithelial cells did not vary significantly between cells of the surface epithelium, the proliferation zone, or gastric glands nor between different areas of the stomach, (i.e., gastric fundus, body, or antrum).

In gastric cancer, immunoreactivity for BUB1 was observed in all cases always showing a nuclear staining pattern (Figure 28). Mitotic figures were either negative for BUB1 or diffusely BUB1 positive throughout the cytoplasm. No difference regarding the number of positively stained tumor cells was seen when different parts of the same tumor (i.e., superficial or central parts) or tumor cells located at the invasion front were evaluated separately (data not shown).

The number of BUB1-positive tumor cells varied considerably between different gastric cancer cases, ranging from 1–99%. In detail, 19% (n = 15) of the cases were categorized score I; 28% (n = 22) of the cases were categorized score II; 23% (n = 18) were categorized score III; 23% (n = 18) of the cases were categorized score IV; and 7% (n = 6) of the cases were categorized score V (Figure 29).

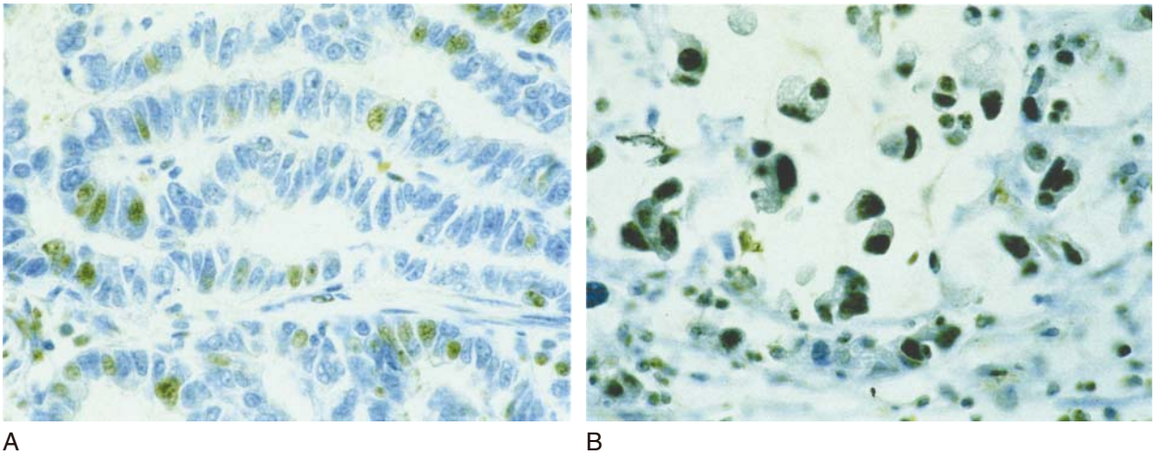

Figure 28. BUB1 immunohistochemistry *(brown-black)* in gastric cancer; Mayer's hematoxylin counterstain *(blue)*. Original magnification 1500X. **A:** Few BUB1 positive cell nuclei in intestinal-type gastric cancer. **B:** A large number of BUB1 positive cell nuclei in diffuse-type gastric cancer.

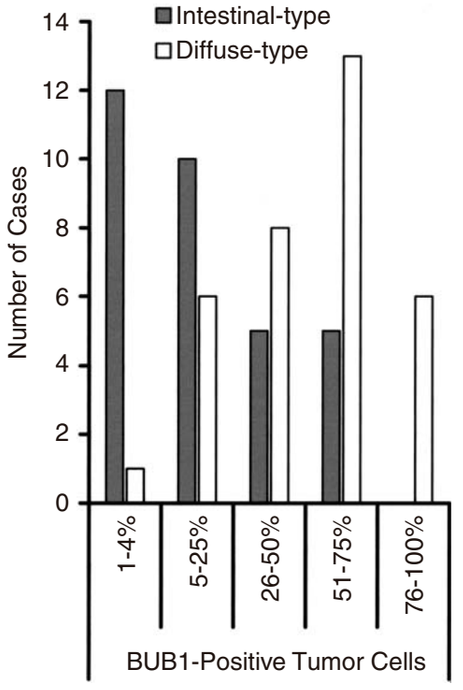

Figure 29. Number of gastric cancer cases in each BUB1 expression scoring group. Comparison of intestinal-type and diffuse-type gastric cancer. Data of mixed-type gastric cancer not shown.

Nuclear DNA Content Analysis

In nonneoplastic gastric mucosa, no DNA aneuploid peaks were detected by cytometric analysis. Peridiploid histograms were found in 13 gastric cancer cases (16%). A peritetraploid histogram was seen in one case only (1%). Histograms with one atypical stemline were observed in 24 cases (30%), with multiple atypical stemlines in 42 cases (53%). In total, our measurements identified DNA aneuploidy in 66 gastric cancer cases (84%). Of the diploid carcinomas, 71% (n = 10) were classified as diffuse-type and 14% (n = 2) were classified as intestinal-type according to Laurén classification.

The median modal DNA value was 2.75c ranging from 1.49c to 6.18c. A significant difference was found comparing the modal DNA value of intestinal-type and diffuse-type gastric cancer [modal value (95% CI [confidence interval]): intestinal-type 3.05c (2.72c–3.39c); diffuse-type 2.54c (2.30c–2.79c); difference of the means (95% CI): 0.51c (0.29c–0.73c); $p = 0.007$].

Microsatellite Analysis

Of the gastric cancer cases, 88.3% (n = 68) were stable at locus BAT26. In 11.7% of the cases (n = 9) MSI at this locus was detected. Of gastric cancers that showed MSI, 88.8% (n = 8) were DNA aneuploid. Of BAT26 unstable carcinomas, 66.6% (n = 6) were classified as intestinal type and 22.2% (n = 2) as diffuse type according to Laurén classification.

Correlation of BUB1 Expression with Nuclear DNA Content, Microsatellite Stability, and Histopathologic Parameters

Several cutoff levels, (i.e., more or less than 5%, 25%, 50%, or 75%) were explored statistically. The 25% cutoff value was used for further analysis because dichotomizing at this level resulted in an almost equal number of cases in each of the two groups. Tumors with less than 25% BUB1-positive cells (i.e., score I and II) were summarized as tumors with low expression of BUB1 (n = 37, 47% of cases), whereas cases with score III–V were summarized as tumors with high expression of BUB1 (n = 42, 53% of cases).

A highly significant correlation was observed between BUB1 expression and tumor type according to Laurén classification. The number of BUB1-positive tumor cells was significantly lower in intestinal-type gastric cancer ($p < 0.001$). In 69% of intestinal-type gastric cancer cases, BUB1 expression was observed in less than 25% of tumor cells, whereas only 21% of the diffuse-type gastric cancer cases expressed BUB1 in less than 25% of tumor cells (see Figures 28 and 29). No statistically significant association was found between BUB1 expression, DNA ploidy status, microsatellite analysis, pT, pN, grading, blood or lymphatic vessel invasion, or DNA modal value (see text).

DISCUSSION

Numerous studies have shown that DNA aneuploidy is a common feature in gastric cancer (Kim and Cho, 2000; Ming, 1998). The frequency of DNA aneuploidy and MSI identified in our study as well as the phenomenon that both types of genetic instability occur simultaneously in gastric cancer are in accordance with the current literature in gastric cancer (dos Santos *et al.,* 1996; Tsujimoto *et al.,* 1997). Inactivation of the mitotic spindle checkpoint has been predicted to result in chromosome missegregation and aneuploidy, and it has been shown that breast cancer cell lines with the highest levels of chromosome numeric instability, all have a defective mitotic spindle checkpoint (Yoon *et al.,* 2002). It has been demonstrated that low levels of BUB1 protein significantly compromised full execution of the spindle checkpoint in *Xenopus* and mice (Sharp-Baker and Chen, 2001; Taylor and McKeon, 1997).

Our study revealed a significantly higher expression of BUB1 protein in diffuse-type gastric cancer

compared to intestinal-type gastric cancer. This is in contrast to our previous *BUB1* mRNA expression study using the same gastric cancer cases (Grabsch *et al.,* 2003), where no differences between different histologic tumor types were found. These findings may suggest that posttranscriptional regulatory processes, protein degradation, or both may be important in controlling the amount of BUB1 available at the kinetochore during mitosis and warrant further investigation in gastric cancer. In addition, different BUB1 protein expression levels in intestinal- and diffuse-type gastric cancer may provide further evidence of a potential link between different genetic pathways and morphologic phenotype in gastric carcinogenesis.

Unexpectedly, this study revealed that there was no relationship between BUB1 protein expression level and DNA ploidy in gastric cancer. However, the significantly different BUB1 expression pattern in different histologic subtypes prompted us to analyze the DNA ploidy status of these tumor types in more detail. No significant difference between histologic tumor subtypes was observed when the cases were classified as diploid or aneuploid. Yet, the analysis of the modal DNA value revealed that intestinal-type gastric cancers had a significantly higher modal DNA value than diffuse-type cancers. This may indicate that the two histologic subtypes of gastric cancer have different "levels" of chromosomal instability. Nevertheless, no statistical association was observed between the modal DNA value and BUB1 expression level, which may partly be explained by the fact that the total number of cases investigated in this study was relatively small.

It is currently not clear at all whether BUB1 protein expression level does reflect mitotic spindle checkpoint function. It seems to be necessary to test the functional significance of high and low BUB1 protein expression levels in different gastric cancer cell lines in more detail to validate a potential link between BUB1 protein expression level, mitotic spindle checkpoint function, and CIN in different gastric cancer subtypes.

References

Altschul, S., Madden, T., Schaeffer, A., Zhang, J., Zhang, Z., Miller, W., and Lipman, D. 1997. Gapped BLAST and PSI-BLAST: a new generation of protein database search programs. *Nucleic Acids Res. 25*:3389–3402.

Baba, H., Korenaga, D., Kakeji, Y., Haraguchi, M., Okamura, T., and Maehara, Y. 2002. DNA ploidy and its clinical implications in gastric cancer. *Surgery 131*:S63–S70.

Boecking, A. 1995. DNA image cytometry. When and why? In Wied, G.L., Keebler, C.M., Rosentnal, D.L., Schemek, U., Sonirak, T.M., and Vooijs, G.P. (eds.). *Compendium on Quality Assurance, Proficiency Testing and Workload Limitations.* Chicago: Tutorials of Cytology, 170–188.

Cahill, D.P., Lengauer, C., Yu, J., Riggins, G.J., Willson, J.K.V., Markowitz, S.D., Kinzler, K.W., and Vogelstein, B. 1998. Mutations of mitotic checkpoint genes in human cancers. *Nature 392*:300–303.

dos Santos, N.R., Seruca, R., Constancia, M., Seixas, M., and Sobrinho-Simoes, M. 1996. Microsatellite instability at multiple loci in gastric carcinoma: clinicopathologic implications and prognosis. *Gastroenterology 110*:38–44.

Furuya, T., Uchiyama, T., Murakami, T., Adachi, A., Kawauchi, S., Oga, A., Hirano, T., and Sasaki, K. 2000. Relationship between chromosomal instability and intratumoral regional DNA ploidy heterogeneity in primary gastric cancers. *Clin. Cancer Res. 6*:2815–2820.

Grabsch, H., Takeno, S., Parsons, W.J., Pomjanski, N., Boecking, A., Gabbert, H.E., and Mueller, W. 2003. Overexpression of mitotic checkpoint genes BUB1, BUBR1 and BUB3 in gastric cancer: association with tumor cell proliferation. *J. Pathol. 200*:16–22.

Hamilton, S.R., and Aaltonen, L.A. (eds.) 2000. *Pathology and Genetics of Tumors of the Digestive System.* Lyon: IARC Press, 37–52.

Hanahan, D., and Weinberg, R.A. 2000. The hallmarks of cancer. *Cell 100*:57–70.

Haroske, G., Baak, J.P.A., Danielsen, H., Gschwendtner, F.G.A., Oberholzer, M., Reith, A., Spieler, P., and Boecking, A. 2001. Fourth updated ESACP consensus report on diagnostic DNA image cytometry. *Anal. Cell Pathol. 23*:89–95.

Hayden, J.D., Martin, I.G., Cawkwell, L., and Quirke, P. 1998. The role of microsatellite instability in gastric carcinoma. *Gut 42*: 300–303.

Hoyt, M., Totis, L., and Roberts, B. 1991. S. cerevisiae genes required for cell cycle arrest in response to loss of microtubule function. *Cell 66*:507–517.

Imai, Y., Shiratori, Y., Kato, N., Inoue, T., and Omata, M. 1999. Mutational inactivation in mitotic checkpoint genes, *hsMAD2* and *hBUB1,* is rare in sporadic digestive tract cancers. *Jpn. J. Cancer Res. 90*:837–840.

Jablonski, S.A., Chan, G.K.T., Cooke, C.A., Earnshaw, W.C., and Yen, T.J. 1998. The hBUB1 and hBUBR1 kinases sequentially assemble onto kinetochores during prophase with hBUBR1 concentrating at the kinetochore plates in mitosis. *Chromosoma 107*:386–396.

Kim, J.Y., and Cho, H.J. 2000. DNA ploidy patterns in gastric adenocarcinoma. *J. Korean Med. Sci. 15*:159–166.

Lauren, P. 1965. The two histological main types of gastric carcinoma: diffuse and so called intestinal-type carcinoma. *Acta. Pathol. Microbiol. Scand. 64*:31–49.

Lengauer, C., Kinzler, K.W., and Vogelstein, B. 1997. Genetic instability in colorectal cancer. *Nature 386*:623–627.

Lengauer, C., Kinzler, K.W., and Vogelstein, B. 1998. Genetic instabilities in human cancers. *Nature 396*:643–649.

Li, R., and Murray, A. 1991. Feedback control of mitosis in budding yeast. *Cell 66*:519–531.

Li, Y., and Benezra, R. 1996. Identification of a human mitotic checkpoint gene: *hsMAD2*. *Science 274*:246–248.

Merz, H., Malisius, R., Mannweiler, S., Zhou, R., Hartmann, W., Orscheschek, K., Moubayed, P., and Feller, A.C. 1995. ImmunoMax: a maximized immunohistochemical method for the retrieval and enhancement of hidden antigens. *Lab. Invest. 73*:149–156.

Miller, R., and Kubier, P. 1997. Blocking of endogenous avidin-binding activity in immunohistochemistry: the use of egg whites. *Appl. Immunohistochem. Molec. Morphol. 5*:63–66.

Mimori, K., Inoue, H., Alder, H., Ueo, H., Tanaka, Y., and Mori, M. 2001. Mutation analysis of *hBUB1,* human mitotic checkpoint gene in multiple carcinomas. *Oncol. Rep. 8*:39–42.

Ming, S.-C. 1998. Cellular and molecular pathology of gastric carcinoma and precursor lesions: a critical review. *Gastric Cancer 1*:31–50.

Miyazaki, M., Furuya, T., Shiraki, A., Sato, T., Oga, A., and Sasaki, K. 1999. The relationship of DNA ploidy to chromosomal instability in primary human colorectal cancers. *Cancer Res. 59*:5283–5285.

Morrison, E., Wardleworth, B., Askham, J., Markham, A., and Meredith, D. 1998. EB1, a protein which interacts with the APC tumor suppressor, is associated with the microtubule cytoskeleton throughout the cell cycle. *Oncogene 17*:3471–3477.

Olesen, S.H., Thykjaer, T., and Orntoft, T.F. 2001. Mitotic checkpoint genes hBUB1, hBUB1B, hBUB3 and TTK in human bladder cancer, screening for mutations and loss of heterozygosity. *Carcinogenesis 22*:813–815.

Ouyang, B., Lan, Z., Meadows, J., Pan, H., Fukasawa, K., Li, W., and Dai, W. 1998. Human Bub1: a putative spindle checkpoint kinases closely linked to cell proliferation. *Cell Growth Differ. 9*:877–885.

Sharp-Baker, H., and Chen, R.-H. 2001. Spindle checkpoint protein Bub1 is required for kinetochore localization of Mad1, Mad2, Bub3, and CENP-E, independently of its kinase activity. *J. Cell Biol. 153*:1239–1249.

Shigeishi, H., Yokozaki, H., Kunlyasu, H., Nakagawa, H., Ishikawa, T., Tahara, E., and Yasui, W. 2001. No mutations of the BUB1 gene in human gastric carcinomas. *Oncol. Rep. 8*:791–794.

Simpson, A.J.G., Caballero, O.L., and Pena, S.D.J. 2001. Microsatellite instability as a tool for the classification of gastric cancer. *Trends Molec. Med. 7*:76–80.

Sobin, L.H., and Wittekind, Ch. (eds.) 1997. *International Union Against Cancer. TNM Classification of Malignant Tumor*s, 5th ed. New York: Wiley-Liss, 59–65.

Takahashi, T., Haruki, N., Nomoto, S., Masuda, A., Saji, S., and Osada, H. 1999. Identification of frequent impairment of the mitotic checkpoint and molecular analysis of the mitotic checkpoint genes, *hsMAD2* and *p55CDC*, in human lung cancers. *Oncogene 18*:4295–4300.

Taylor, S.S., and McKeon, F. 1997. Kinetochore localization of murine Bub1 is required for normal mitotic timing and checkpoint response to spindle damage. *Cell 89*:727–735.

Tsujimoto, H., Sugihara, H., Hattori, T., and Hagiwara, A. 1997. Microsatellite instability, DNA ploidy, and mutation of transforming growth factor-beta receptor type II gene in sporadic gastric cancer. *Cancer J. 10*:211–216.

Wirtz, H.C., Mueller, W., Noguchi, T., Scheven, M., Rueschoff, J., Hommel, G., and Gabbert, H.E. 1998. Prognostic value and clinicopathological profile of microsatellite instability in gastric cancer. *Clin. Cancer Res. 4*:1749–1754.

Yoon, D.-S., Wersto, R.P., Zhou, W., Chrest, F.J., Garrett, E.S., Kwon, T.K., and Gabrielson E. 2002. Variable levels of chromosomal instability and mitotic spindle checkpoint defects in breast cancer. *Am. J. Pathol. 161*:391–397.

This Page Intentionally Left Blank

8

Role of Immunohistochemical Expression of Epidermal Growth Factor in Gastric Tumors

Luis Alberto Espinoza

Introduction

The application of methods, such as immunohistochemistry (IHC), to gastric tumor analysis can increase diagnostic precision, as well as provide valuable information regarding therapy selection and monitoring of residual tumors. In the last three decades, IHC has proven to be a cost-effective test in gastric cancer diagnosis. Stomach cancer is the most frequent cause of cancer death in men older than 50 years, and it is considered to be the second most common cause of worldwide annual cancer mortality (Pisani *et al.,* 1999). The prognosis for gastric cancer is related to the features of the primary tumors, but the histologic classification of these tumors is difficult because structural variability is high. Although several classifications have been proposed based on the morphologic features of gastric tumors (Lauren, 1991; Sobin and Wittekind, 1997), metastases to regional lymph nodes can increase difficulty in characterizing stomach adenocarcinoma subtypes. Therefore, the use of IHC in tumor analysis has had significant influence on clinical management of tumor pathology as well as in the clinical diagnosis of tumors by surgical pathologists (Hsi, 2001; Wick *et al.,* 1999). In fact, application of diagnostic IHC to gastric tumors has made it possible to identify the presence of micrometastases in lymph nodes, providing an accurate prognosis of gastric carcinomas (Karube *et al.,* 2004; Luebke *et al.,* 2005).

Abnormal expression of epidermal growth factor (EGF) detected by IHC in many types of human cancers, including gastric adenocarcinomas, has been associated with poor prognosis (Seth *et al.,* 1999; Tokunaga *et al.,* 1995). This is because EGF competes with the transforming growth factor-alpha (TGFα) for the same membrane-bound receptor sites of the epidermal growth factor receptor (EGFR). Interaction of EGFR with EGF or TGFα stimulates deoxyribonucleic acid (DNA) synthesis and cell growth in various systems, including the gastrointestinal (GI) tract. However, altered co-expression of these proteins has been associated with tumor development in several types of cancers including gastric tumors. In particular, in gastric cancer cells, augmented levels of EGF, TGFα, and EGFR have been proposed to influence various processes that determine tumor progression such as continuous cell proliferation, cell migration, cell adhesion, cell survival, and angiogenesis (Barnard *et al.,* 1995). In addition, increased expression of EGF, TGFα, and EGFR in GI cancer determined by IHC analysis is thought to be a mechanism for tumor cells to escape from normal growth regulation (Messa *et al.,* 1998), which promotes tumor aggressiveness and consequently poor prognosis in patients with gastric carcinomas (Werner *et al.,* 2001).

Handbook of Immunohistochemistry and *in situ* Hybridization of Human Carcinomas, Volume 4: Molecular Genetics, Gastrointestinal Carcinoma, and Ovarian Carcinoma

In this chapter, particular emphasis has been placed on the strategies to analyze the occurrence of altered expression of EGF as well as TGFα and EGFR in primary gastric tumors. Because of its easy applicability and reliability, we have used IHC analysis to evaluate the prognostic value of the increased expression of these growth factors in patients with gastric cancer. Because not all the available antibodies may work well in IHC, it is necessary to determine the limitations of each antibody used so as to optimize immunoreactivity. Therefore, both polyclonal and monoclonal antibodies, if available, should be tested to identify which one provides a minimal background and increased immunostaining.

In a routine biopsy the extracted tissue is divided in halves. One half is immediately snap-frozen to preserve the genomic and protein content and the other half is fixed by immersion in a buffered-formalin solution for further morphologic studies after being embedded in paraffin. Immunohistochemical studies can be carried out in both snap-frozen and formalin-fixed and paraffin-embedded (FFPE) sections. Because preservation of tissue morphology is important to compare the immunostaining results with the pathologic features, the FFPE tissue procedure is the most suitable method to use in IHC assays. The main disadvantage of using formalin is that it decreases tissue antigen epitopes' availability to primary antibodies, resulting in loss of immunoreactivity. Antibody sensitivity depends on the accessibility of the epitope of the protein target; therefore the use of antigen retrieval techniques does improve the working condition for the first antibody in FFPE tissues (Shi *et al.,* 2001). Optimizing other factors such as secondary antibody concentration, incubation time, temperature, and amplification and detection systems are also necessary to enhance the efficiency of the staining. To establish the optimum conditions to support the clinical diagnosis, we evaluated immunoreactivity in both snap-frozen and FFPE tissues. We also tested different variations of the unmasking antigen technique on the formalin-fixed tissues to determine the variance of effectiveness (Figure 30).

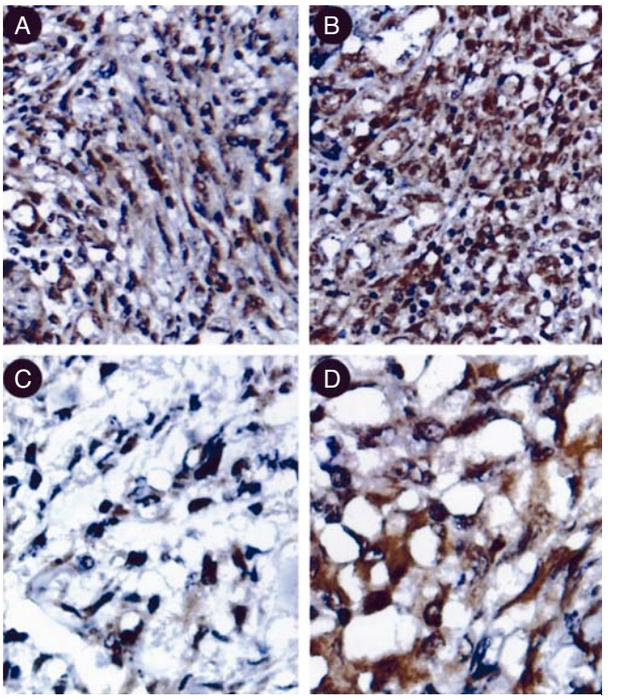

Figure 30. Comparison of epidermal growth factor (EGF) immunohistochemical detection protocols on frozen and paraffin sections of stomach adenocarcinomas. Fresh frozen **(A)** and formalin-fixed and paraffin-embedded **(B)** tissues showed similar intensity for EGF cytoplasmic staining. However, frozen tissues have their morphology deteriorated compared to embedded sections (original magnification, 200X). Comparison between immunohistochemical analyses on fomalin-fixed and paraffin-embedded samples pretreated with saponin **(C)** or microwave heated **(D)**. Note the increased EGF immunoreactivity on microwave-treated samples compared to detergent treatment (original magnification, 400X).

MATERIALS

1. Xylene.
2. Double-distilled water (ddH_2O).
3. Humid chamber and absorbent paper towels.
4. 50%, 70%, 95%, and 100% Ethanol.
5. PBS (phosphate buffer saline): (0.15 M NaCl, 0.01 M Na Phosphate, pH 7.4).
6. Microwave oven.
7. Plastic jars.
8. Citrate buffer (10 mM sodium citrate buffer, 0.05% Tween 20, pH 6.0). Mix to dissolve 2.94 g of Tris-sodium citrate in 1000 ml of dH_2O. Adjust to pH 6.0 using concentrated NaOH.
9. 0.05% of Saponin (Sigma, St. Louis, MO) in ddH_2O. Adjust pH to 7.4 with NaOH.
10. 0.1% Trypsin (Sigma) and 4 mM $CaCl_2$ (Sigma) in PBS. Adjust pH 7.8 with NaOH.
11. 3% hydrogen peroxide (H_2O_2) solution in PBS.
12. Blocking serum: 10% serum derived from the same species used to produce the primary antibody; 5% nonfat dry milk (Bio-Rad, Hercules, CA) or 1% BSA (bovine serum albumin) dissolved in PBS.
13. 3,3′ diaminobenzamide tetrahydrochloride (DAB) substrate (Sigma).

14. Vectastain ABC Kit (Vector Laboratories, Burlingame, CA).
15. Hematoxylin counterstain reagent (Zymed Laboratories, San Francisco, CA)
16. Coverslip.
17. Permanent mounting medium.
18. Light microscope.

METHODS

Cryostat Sections

1. Let frozen slides air-dry at room temperature.
2. Fix slides by immersion in cold acetone (–20°C) or other suitable fixative for 2–10 min.
3. Air-dry slides at room temperature for 10 min.
4. Incubate specimens for 5–10 min with 3% H_2O_2 in PBS to neutralize endogenous peroxidase activity.
5. Wash the slides 2× in fresh PBS, 5 min for each wash.
6. Follow standard procedures used for FFPE sections starting with blocking.

Paraffin-Embedded Sections

Deparaffinization

1. Incubate the tissue sections at 37°C overnight.
2. Deparaffinize tissue sections by incubating in xylene 2× for 10 min each.
3. Rehydrate tissue sections by passing slides through graded alcohols: 100%, 95%, 70%, and 50%, 2 changes for 5 min each.
4. Rinse the slides in ddH_2O for 2 min.
5. Immerse specimens for 5–10 min in 3% H_2O_2 in PBS to neutralize endogenous peroxidase activity.
6. Wash slides in PBS for 10 min at room temperature with occasional agitation.

Unmasking Antigen

A. Detergent Retrieval Method

1. Incubate the rehydrated sections with 0.05% saponin in PBS for 30 min at room temperature.
2. Wash the slides 2× with fresh PBS for 5 min each time.
3. Follow standard procedures starting with blocking.

B. Enzyme Retrieval Method

1. Prewarm the trypsin solution (0.1%) at 37°C in a waterbath.
2. Place the rehydrated sections in a container with ddH_2O at 37°C for 5 min.
3. Transfer the slides to the jar containing the warmed trypsin solution and incubate for 10 min.

Note: Incubation can oscillate between 10–30 min.

4. Rinse the slides in running ddH_2O for 10 min.
5. Follow standard procedures starting with blocking.

C. Microwave Retrieval Method

1. Heat a Coplin jar filled with citrate buffer in a microwave for 1 min at high potency. Buffer should be hot (95–99°C) but not boiling.
2. Place sections into the preheated jar with citrate buffer and set the microwave to full power. Wait until the solution comes to a boil. Boil the tissue sections for 10 min. Antigens are retrieved once the temperature has reached 98°C.

Note: Incubation can oscillate between 10–30 min.

Note: The levels of the buffer have to be replenished by the addition of heated ddH_2O.

3. Stop the reaction by removing jar with slides from the microwave and allow it to cool at room temperature for at least 20 min.
4. Rinse sections with 3 changes of PBS, 5 min each round.
5. Follow standard procedures starting with blocking.

Blocking

1. Incubate section with 10% of blocking serum, 5% skim milk, or 2% BSA in PBS at room temperature for 30 min in a humidified chamber.

Note: It is recommended to include the blocking reagent during the incubation of sections with primary and secondary antibodies.

Note: The skim milk should be used in all these steps at the concentration of 1%.

Immunoperoxidase Staining

1. Incubate slides with primary antibody solution and 10% of normal blocking serum in a humidified chamber for a minimum of 2 hr at room temperature or overnight at 4°C.

Note: The dilutions of antibodies used in our experiments were 1:50 (EGF), 1:100 (EGFR), and 1:50 (TGFα).

Note: The dilution titer for each antibody was determined empirically.

Note: Negative controls were performed using the same conditions, except that the primary or secondary antibody was replaced with PBS.

2. Wash slides 3× with PBS solution, 5 min each time.
3. Incubate with the secondary antibody solution and 10% normal blocking serum for a minimum of 30 min at room temperature in the humidified chamber.

4. Wash the slides in fresh PBS 3×, 5 min each round.

5. Prepare the ABC reagent according to the manufacturer's instructions. Vector Laboratories suggest that Vectastain ABC solution be prepared 30 min before use. Add 100 µl of reagent A to 5.0 ml of PBS and mix immediately, and then add 100 µl of reagent B and mix. Incubate slides in this solution for 30 min at room temperature in the humidified chamber.

6. Wash sections in PBS solution 3×, 5 min each time.

7. Wipe off the excess of PBS from the slide before adding the substrate.

Counterstaining and Visualization

1. During the last wash, prepare the diaminobenzidine tetrahydrochloride (6 mg of DAB in 10 ml of 0.05 M PBS, pH 7.4, and 0.1 ml of 3% H_2O_2 in ddH_2O).

Note: If a precipitate appears, filter DAB solution.

Note: If a gray/black stain is desired, add 1 ml of 0.3% w/v stock solution of nickel chloride in ddH_2O, and mix well. For this developing procedure, use a different counterstain (5% methyl green).

Note: DAB is a suspected carcinogen. Use disposable gloves, lab coat, and safety goggles.

2. Apply the DAB solution to the slide. Stop the reaction when the desired black precipitate is visible and before the background has begun to change (between 1–10 min).

Note: Monitor staining of sections under the microscope.

Note: The time for developing sections may differ depending on the level of antigen.

3. Stop the reaction by washing the slides in ddH_2O.

4. Wash the section 1× in PBS for 5 min.

5. Counterstain sections with hematoxylin (5–10 min).

Note: We have obtained similar results using Mayer's hematoxylin solution (Sigma).

6. Rinse slides 5× in ddH_2O, 2 min each wash.

7. Dehydrate the sections by passing slides through graded alcohols of 95% and 100%, 4 changes for 2 min each.

8. Clear specimens with xylene, 4 changes, 2 min each. Blot off excess xylene.

9. Add a drop of aqueous mounting media and carefully apply a coverslip. Avoid trapping air bubbles under the coverslip.

10. Blot off excess mounting media.

11. Seal coverslip with nail polish.

12. Slides can be stored at room temperature.

Immunohistochemistry Analysis and Image Capture

Samples for IHC were evaluated independently by two investigators without any prior knowledge of the clinicopathologic data of patients using a Nikon Eclipse TE200 microscope. Staining scores in tumor gastric sections were established by semi-quantitative analysis, using the product of percentage of positive cells and the intensity of staining. The relative intensities of the immunostaining for tumors were graded as follows: negative (−), low (+; positive for >10 and <25%), moderate (++; positive for >25 and <50%), and high (+++; positive for >50%) staining. Standard methods, such as the Chi-squared, *t* test, or Fisher's exact test, were used to evaluate the statistical significance of expression pattern of antibody immunoreactivity with the clinical–pathology or final clinical diagnosis. For all statistical analyses, a $p < 0.05$ was considered significant. The images were captured with a Sony Digital Photo Camera, DKC5000, and edited using the Adobe Photoshop 7.0 software (Adobe Systems, San Jose, CA).

RESULTS AND DISCUSSION

To classify the gastric tumor, histologic analysis was performed in all frozen and fixed sections used in this study. Thus, according to the morphologic characteristics, stomach adenocarcinomas were classified into either diffuse or intestinal adenocarcinoma, using the criteria of Lauren (Lauren, 1991). Then, immunohistochemical staining was performed in all of these samples. Because IHC is routinely used in diagnosis of human cancers, it is necessary to improve this technique to decrease cross-reactivity of antibodies that may generate false-positive results. All three antibodies (anti-EGF, anti-TGFα, and anti-EGFR) have worked relatively well in frozen tissues; however, it was clearly evident that the tissue morphology was much better preserved in FFPE tissue samples. Diminished preservation of the morphology as a result of the fragility of frozen sections is a frequent limitation when using these samples for IHC (Beckstead, 1994; Warford *et al.,* 2004). Conversely, FFPE tissues maintain the architecture of cellular constituents, avoid limitations of freezing and storage, and can be used for retrospective studies (Behan *et al.,* 2002; Dressler *et al.,* 1999).

Although formalin is the most reliable fixative used to preserve tissue specimens, it can have adverse effects on immunohistochemical staining because of the structural modifications that are introduced in the three-dimensional structure of epitopes, resulting in the masking of tissue antigens. Masked epitopes show reduced immunoreactivity, and therefore, in most cases, the use of antigen retrieval methods is necessary to increase the quality of staining. Until now, different protocols that include detergent, enzymatic, or high-temperature procedures have been developed to unmask

antigen in formalin-fixed tissues. We have found that all the antibodies used in this study had a higher efficiency on paraffin sections when using microwave treatment compared to those samples treated with proteolitic enzymes (trypsin digestion) or detergents (saponin). Antigen retrieval for EGF and TGFα required microwave treatment of 20 min, whereas EGFR retrieval required 30 min, respectively. The optimization of heating temperature in antigen retrieval is critical for this method. Longer treatments can damage the surface or even destroy sections and increase background staining after antigen retrieval. Therefore, appropriate tests have to be performed to reach the optimal conditions to improve antigen retrieval.

The immunohistochemical analysis revealed that immunoreactivity for EGF and TGFα staining was located in the cytoplasm, whereas EGFR was confined to the cell membrane. Nonneoplastic adjacent tissues consistently revealed very low or undetectable expression levels for EGF, TGFα, and EGFR. The immunoreactivity for these proteins was higher in tumors infiltrating the muscularis propria or subserosa (T2), the serosa (T3), and adjacent structure (T4) than in tumors invading only the mucosa and submucosa (T1). Increased expression of these proteins was also observed in samples of early stages with lymph-node metastases (Ishida *et al.,* 1997). These observations imply that tumor cells with high proliferative activity could have a greater potential for metastases.

Several reports have found that the complex EGF–EGFR, TGFα–EGFR, or both function as an autocrine mechanism involved in the growth and metastasizing potential of gastric carcinomas (Ishida *et al.,* 1997; Koyama *et al.,* 1997; Suzuki *et al.,* 1995). Because EGF contributes to increased synthesis, synthesis stabilization of EGFR messenger ribonucleic acid (mRNA), and *de novo* EGFR protein synthesis (McCulloch *et al.,* 1998; Seth *et al.,* 1999), the results presented here indicate that enhanced EGF expression in gastric cancer also contributes to the uncontrolled proliferation of tumor cells. Furthermore, the intensity of EGF and TGFα and EGFR immunoreactivity is significantly higher in advanced carcinomas as compared with low-grade tumors (Espinoza *et al.,* 2004). This suggests that overexpression of these growth factors and growth factor receptors contributes to the development and tumor growth as well as invasiveness of these tumors. This interpretation is entirely compatible with previous reports showing higher BrdU labeling index in gastric tumors co-expressing EGF-EGFR and TGFα-EGFR (Suzuki *et al.,* 1995). Comparative studies have demonstrated the higher potency of TGFα compared to EGF in a variety of processes such as stimulation of DNA synthesis and anchorage-independent growth. This implies that the augmented proliferation rate occurring in cells expressing EGF and TGFα can be modulated by TGFα, which has been indicated to be a superagonist of EGF. It can also explain the increased expression of TGFα compared to EGF in advanced gastric tumors at a frequency of 87% and 42%, respectively.

The accumulation of EGF protein facilitates the selective growth advantage of tumor cells, which may promote the development of malignant phenotype in gastric tumors. In this respect, increased expression of TGFα is correlated with infiltrating and poorly differentiated tumors. A biologic relationship has been postulated between the augmented levels of these growth factors and an invasive phenotype in gastric tumors (Messa *et al.,* 1998; Werner *et al.,* 2001). Therefore, it is conceivable that the deregulated expression of EGF and TGFα contributes to the progression for a highly malignant and metastatic state. Previous reports have also found a direct correlation between increased expression of EGF with poor differentiation, high proliferative activity of tumor cells, and the occurrence of lymph-node metastases (Kopp *et al.,* 2002; Tokunaga *et al.,* 1995). More recent studies also detected elevated expression of EGFR and higher kinase activity of EGFR in late-stage gastric tumors, suggesting that this receptor is involved in tumor progression (Kopp *et al.,* 2002; Masaki *et al.,* 2003). Taken together, our data confirm that co-expression of EGF, TGFα, and EGFR is closely associated with uncontrolled cell proliferation, thus playing a key role in the acceleration of tumor progression and aggressiveness, and may serve as an indicator of poor prognosis in gastric tumors.

The involvement of various genes encoding for growth factors, growth factor receptors, oncogenes, and tumor-suppressor genes in the origin of a tumor is a consequence of a multistep process and possibly reflects complex genetic changes as seen previously in gastric tumors (Yasui *et al.,* 1999). We and others have previously demonstrated that gastric tumors show heterogeneity in chromosomal abnormalities that have correlation with tumor progression (Espinoza *et al.,* 1999; Rao *et al.,* 1995). These events could also modulate to varying degrees the phenotypic differences between tumors of the same histologic class. Consequently, tumors that become more advanced show undifferentiated histologic patterns. Gastric tumors with poorly differentiated subtypes show a pattern of loss of differentiation as well as increased aggressiveness and a higher rate of genetic abnormalities. The varying histologic data found in our series suggest that this is a heterogeneous group of stomach carcinomas with a common clinical phenotype. Therefore, the use of IHC technique in the study of gastric cancer may provide information that can have prognostic significance for early diagnosis, novel treatments, and monitoring the efficacy of a therapeutic or preventive intervention.

Independently of tumor stage, we have observed that the biologic significance of EGF-positive tumor samples might be indicative of tumor progression. Moreover, increased TGFα/EGFR expression may contribute to increase proliferative activity of early-stage gastric carcinoma in advanced tumors as well as to a poor prognosis of the disease in patients. Altogether, the results obtained in the current study using IHC analysis may have clinical relevance for implications in the treatment of locally advanced gastric carcinoma where tumor stage and grade of differentiation at diagnosis are considered to be prognostic indicators.

References

Barnard, J.A., Beauchamp, R.D., Russell, W.E., Dubois, R.N., and Coffey, R.J. 1995. Epidermal growth factor-related peptides and their relevance to gastrointestinal pathophysiology. *Gastroenterology 108*:564–580.

Beckstead, J.H. 1994. A simple technique for preservation of fixation-sensitive antigens in paraffin embedded tissues. *J. Histochem. Cytochem. 42*:1127–1134.

Behan, W.M., Cossar, D.W., Madden, H.A., and McKay, I.C. 2002. Validation of a simple, rapid, and economical technique for distinguishing type 1 and 2 fibres in fixed and frozen skeletal muscle. *J. Clin. Pathol. 55*:375–380.

Dressler, L.G., Geradts, J., Burroughs, M., Cowan, D., Millikan, R.C., and Newman, B. 1999. Policy guidelines for the utilization of formalin-fixed, paraffin-embedded tissue sections: the UNC SPORE experience. University of North Carolina Specialized Program of Research Excellence. *Breast Cancer Res. Treat. 58*:31–39.

Espinoza, L.A., Barbieri Neto, J., and Casartelli, C. 1999. Pathological and karyotypic abnormalities in advanced gastric carcinomas. *Cancer Genet. Cytogenet. 109*:45–50.

Espinoza, L.A., Tone, L.G., Neto, J.B., Costa, R.S., Wang, Q.J., and Ballejo, G. 2004. Enhanced TGFalpha-EGFR expression and P53 gene alterations contributes to gastric tumors aggressiveness. *Cancer Lett. 212*:33–41.

Hsi, E.D. 2001. A practical approach for evaluating new antibodies in the clinical immunohistochemistry laboratory. *Arch. Pathol. Lab. Med. 125*:289–294.

Ishida, K., Katsuyama, T., Sugiyama, A., and Kawasaki, S. 1997. Immunohistochemical evaluation of lymph node micrometastases from gastric carcinomas. *Cancer 79*:1069–1076.

Karube, T., Ochiai, T., Shimada, H., Nikaidou, T., and Hayashi, H. 2004. Detection of sentinel lymph nodes in gastric cancers based on immunohistochemical analysis of micrometastases. *J. Surg. Oncol. 87*:32–38.

Kopp, R., Ruge, M., Rothbauer, E., Cramer, C., Kraemling, H.J., Wiebeck, B., Schildberg, F.W., and Pfeiffer, A. 2002. Impact of epidermal growth factor (EGF) radioreceptor analysis on long-term survival of gastric cancer patients. *Anticancer Res. 22*:1161–1167.

Koyama, S., Ikeda, K., Sato, M., Shibahara, K., Yuhara, K., Fukutomi, H., Fukunaga, K., Kanazawa, N., Yuzawa, K., Fukao, K., Iijima, T., Kikuchi, M., Tomiya, T., and Fujiwara, K. 1997. Transforming growth factor-alpha (TGF alpha)-producing gastric carcinoma with acanthosis nigricans: an endocrine effect of TGF alpha in the pathogenesis of cutaneous paraneoplastic syndrome and epithelial hyperplasia of the esophagus. *J. Gastroenterol. 32*:71–77.

Lauren, P. 1991. Histogenesis of intestinal and diffuse types of gastric carcinoma. *Scand. J. Gastroenterol. Suppl. 180*:160–164.

Luebke, T., Baldus, S.E., Zirbes, T.K., Pham, T.D., Schneider, P.M., Dienes, H.P., Holscher, A.H., and Monig, S.P. 2005. Lymph node revealing solution in gastric carcinoma does not provide upstaging of the N-status. *Oncol. Rep. 13*:361–365.

Masaki, T., Hatanaka, Y., Nishioka, M., Tokuda, M., Shiratori, Y., Reginfo, W., and Omata, M. 2000. Activation of epidermal growth factor receptor kinase in gastric carcinoma: a preliminary study. *Am. J. Gastroenterol. 95*:2135–2136.

McCulloch, R.K., Walker, C.E., Chakera, A., Jazayeri, J., and Leedman, P.J. 1998. Regulation of EGF-receptor expression by EGF and TGF alpha in epidermoid cancer cells is cell type-specific. *Int. J. Biochem. Cell. Biol. 30*:1265–1278.

Messa, C., Russo, F., Caruso, M.G., and Di Leo, A. 1998. EGF TGF-alpha, and EGF-R in human colorectal adenocarcinoma. *Acta. Oncol. 37*:285–289.

Pisani, P., Parkin, D.M., Bray, F., and Ferlay, J. 1999. Estimates of the worldwide mortality from 25 cancers in 1990. *Int. J. Cancer 83*:18–29.

Rao, P.H., Mathew, S., Kelsen, D.P., and Chaganti, R.S. 1995. Cytogenetics of gastric and esophageal adenocarcinomas. 3q deletion as a possible primary chromosomal change. *Cancer Genet. Cytogenet. 81*:139–143.

Seth, D., Shaw, K., Jazayeri, J., and Leedman, P.J. 1999. Complex post-transcriptional regulation of EGF-receptor expression by EGF and TGF-alpha in human prostate cancer cells. *Br. J. Cancer 80*:657–669.

Shi, S.R., Cote, R.J., and Taylor, C.R. 2001. Antigen retrieval techniques: current perspectives. *J. Histochem. Cytochem. 49*:931–937.

Sobin, L.H., and Wittekind, C. 1997. *International Union Against Cancer (UICC). TNM Classification of Malignant Tumors,* 5th ed. New York: John Wiley & Sons, Inc.

Suzuki, T., Tsuda, T., Haruma, K., Yoshihara, M., Sumii, K., and Kajiyama, G. 1995. Growth of human gastric carcinomas and expression of epidermal growth factor, transforming growth factor-alpha, epidermal growth factor receptor and p185c-erbB-2. Oncology *52*:385–391.

Tokunaga, A., Onda, M., Okuda, T., Teramota, T., Fujita, I., Mizutani, T., Kiyama, T., Yoshiyuki, T., Nishi, K., and Matsukura, N. 1995. Clinical significance of epidermal growth factor (EGF), EGF receptor, and c-erbB-2 in human gastric cancer. *Cancer 75*:1418–1425.

Warford, A., Howat, W., and McCafferty, J. 2004. Expression profiling by high-throughput immunohistochemistry. *J. Immunol. Methods 290*:81–92.

Werner, M., Becker, K.F., Keller, G., and Hofler, H. 2001. Gastric adenocarcinoma: pathomorphology and molecular pathology. *J. Cancer Res. Clin. Oncol. 127*:207–216.

Wick, M.R., Sayadi, H., Ritter, J.H., Hill, D.A., Reddy, V.B., and Gattuso, P. 1999. Low-stage carcinoma of the male breast: a histologic, immunohistochemical, and flow cytometric comparison with localized female breast carcinoma. *Am. J. Clin. Pathol. 111*:59–69.

Yasui, W., Yokozaki, H., Shimamoto, F., Tahara, H., and Tahara, E. 1999. Molecular-pathological diagnosis of gastrointestinal tissues and its contribution to cancer histopathology. *Pathol. Int. 49*:763–774.

9

Role of Immunohistochemical Expression of Beta-Catenin and Mucin in Stomach Cancer

Ryoji Kushima, Shizuki Tsukashita, and Takanori Hattori

Introduction

Beta-catenin plays important roles in the cell–cell adhesion system and in the wingless/Wnt cell–cell signaling system (Peifer *et al.,* 1993). Beta-catenin, in the former, acts as E-cadherin–binding protein mostly on the cell membrane (Barth *et al.,* 1997). Concerning the latter, beta-catenin is decomposed in the normal system (i.e., this abnormal function makes it accumulate in the cell). Abnormally accumulated beta-catenin subsequently causes cell proliferation and carcinogenesis. Intracellular levels of beta-catenin are mainly regulated by degradation, which is probably initiated by interaction with the adenomatous polyposis coli (APC) protein and glycogen synthase kinase (GSK)-3 beta (Rubinfeld *et al.,* 1996). Abnormality in exon 3 of the *beta-catenin* gene may result in accumulation of beta-catenin, or phosphorylation of these residues may inhibit degradation (Orford *et al.,* 1997). *Beta-catenin* mutations and expression have been analyzed in various common cancers.

Gastric carcinomas have been classified into two main types according to their gland-forming tendency: intestinal and diffuse types (Lauren, 1965). The category gland-forming intramucosal carcinoma was accepted as the early lesion of an advanced carcinoma according to the Vienna Classification (Schlemper *et al.,* 2000), and Western pathologists use this term. We histologically assigned the hematoxylin and eosin (H & E)–stained gland-forming lesions to one of three groups according to the Vienna Classification system: group A (low-grade adenoma/dysplasia, Category 3); group B (high-grade adenoma/dysplasia, Category 4.1); and group C (intramucosal carcinoma, Categories 4.2 and 4.3), which can be histochemically analyzed (Tsukashita *et al.,* 2003).

MATERIALS

1. Endoscopically or surgically resected tissues from patients.
2. Neutral buffered 10% formalin: 100 ml formalin (37% formaldehyde), 4.4 g monobasic sodium phosphate·$2H_2O$, 25.9 g dibasic sodium phosphate·$12H_2O$; bring vol to 1 L with distilled water (pH 7.2).
3. MAS-coated glass slides (Matsunami, Osaka, Japan).
4. 0.05 M citrate buffer: l.99 g citric acid·H_2O, 12.21 g sodium citrate·$2H_2O$; bring vol to 1 L with distilled water (pH 6.0).

5. 0.1 M phosphate buffer saline (PBS): 6.1 g monobasic sodium phosphate·$2H_2O$, 21.8 g dibasic sodium phosphate.$12H_2O$; bring vol to 1 L with distilled water (pH 7.0).
6. Beta-catenin monoclonal antibody (clone 14, Novocastra, Newcastle-upon-Tyne, UK).
7. LSAB-kit (Dako, Glostrup, Denmark).

METHODS

Immunohistochemistry

1. Fix the samples in neutral buffered 10% formalin for 24 hr.
2. The fixed tissue is cut into 3–5 mm slices.
3. Embed the tissue slices in paraffin and cut into 3-μm–thick sections for H & E staining and subsequent immunohistochemical processing.
4. Dry the slides with sections at 69°C for 20 min.
5. Deparaffinize the sections with 100% xylene followed by 100% ethanol.
6. Wash the sections in distilled water.
7. For the purpose of antigen retrieval, pretreat the sections in 0.05 M citrate buffer in an autoclave at 121°C for 10 min.
8. After cooling to room temperature, rinse the sections in 10% methanol in water solution for 20 min.
9. Incubate the sections in the blocking serum for 30 min at room temperature.
10. Incubate the sections in beta-catenin monoclonal antibody (diluted 1:100 with 0.1 M PBS) overnight at 4°C.
11. Wash the sections in 0.1 M PBS.
12. Incubate the sections in the secondary antibody with biotin at room temperature for 30 min.
13. Wash the sections in 0.1 M PBS.
14. Incubate the sections in the streptavidin-peroxidase at room temperature for 15 min.

(Use LSAB-kit from **Step 9** to **Step 14.**)

15. Wash the sections in 0.1 M PBS.
16. Visualize the peroxidase binding sites with diaminobenzidine, and counterstain the section with hematoxylin.

Scoring of Immunostaining

The intensity of beta-catenin expression is scored by comparing it to adjacent normal gastric mucosa. Nucleus and cytoplasm are essentially negative; lateral cell membrane is essentially positive but negative for basal membrane.

Nuclear expression is evaluated as the strength and the percentage of neoplastic cell nuclear region. When strong and weak expressions co-exist in one lesion, priority is given to the higher grade:

Grade 0, no positive cells or very few (<10%)
Grade 1, some positive cells with weak expression (10–50%)
Grade 2, well-defined areas of positive cells with weak expression (>50%)
Grade 3, some positive cells with strong expression (10–50%)
Grade 4, well-defined areas of positive cells with strong expression (>50%)

Cytoplasmic expression is evaluated as a percentage of positive cells:

Score 0, no positive cells or very few (<10%)
Score 1, some positive cells (10–50%)
Score 2, well-defined areas of positive cells (>50%)

Membranous staining is evaluated as a percentage of lateral membrane of positive cells:

LOM (loss of membranous) staining (–), extensive continuous areas of positive cells (>70%)
LOM (+), discontinuous areas of positive cells (<70%)
Examples of staining are showed in Figure 31.

RESULTS AND DISCUSSION

Beta-Catenin Expression, Histopathologic Characteristics, and Stages

Miyazawa *et al.* (2000) reported that 12% and 7% of gastric carcinomas showed beta-catenin localization of nucleus and cytoplasm, respectively, and all of them were intestinal-type adenocarcinomas. All of the nuclear localized cases except one were in the early clinical stage, and the remaining cases showed strong nuclear staining at the invasive front. These data suggest that high intranuclear levels of beta-catenin protein play an important role in early tumor growth and may function in initiation of invasive processes in intestinal-type gastric carcinoma. However, our study, which targeted adenoma/dysplasia and intramucosal adenocarcinoma (much earlier stages), showed no obvious difference in nuclear, cytoplasmic, or membranous beta-catenin expression (Tsukashita *et al.,* 2003) (Figure 31). *Beta-catenin* mutations were detected in other noncancerous lesions (Tamura *et al.,* 1994).

These data suggest that beta-catenin expression does not always reflect the malignant transformation in the early stage of gastric tumorigenesis, and *beta-catenin* abnormality is only one particular aspect of malignant

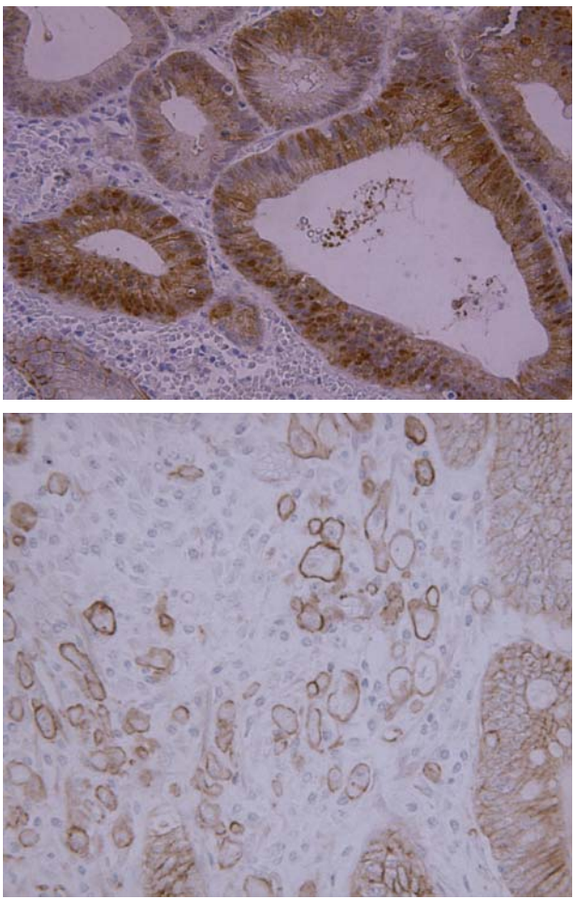

Figure 31. Immunohistochemical staining of beta-catenin in stomach tumors (Tsukashita *et al.,* 2003; modified). **A:** Group A lesion (low-grade adenoma/dysplasia), corresponding to the Category 3 of the Vienna Classification, shows high rate and strong expression in cytoplasm and nuclei, and continuous membranous staining is preserved. Cytoplasm: Score 2; nuclei: Grade 4, LOM(–). **B:** Signet-ring cell carcinoma. Neither cytoplasm nor nuclei is positive for beta-catenin, but the continuous membranous staining is preserved around the tumor cells, showing dissociated growth pattern. Cytoplasm: Score 0; nuclei: Grade 0, LOM(–).

transformation. Mutations of the *APC* gene occur and have been detected during early stages of gastric adenoma development (Tamura *et al.,* 1994) but not in gastric carcinomas (Ogasawara *et al.,* 1994). The nuclear beta-catenin expression in group A lesions might indicate an *APC* gene mutation, although the possibility of *beta-catenin* mutation remains.

Regarding membranous beta-catenin expression, LOM was detected in groups A, B, and C with no significant differences detected between them, but Ougolkov *et al.* (2000) indicated that loss of membranous beta-catenin correlated with invasion.

Concerning diffuse-type adenocarcinoma, however, neither nuclear nor cytoplasmic beta-catenin localization was observed (Tsukashita *et al.,* 2003).

These observations provide supporting evidence that intestinal- and diffuse-type carcinomas may be derived from different genetic pathways (Machado *et al.,* 1999). Frequent somatic mutations of the *APC* gene are detected in signet-ring cell carcinoma (Nakatsuru *et al.,* 1992). Therefore, it is suggested that mutations of the *APC* gene are not always a reflection of beta-catenin expression.

Ougolkov *et al.* (2000) reported that 47% of mucosal carcinoma showed abnormal beta-catenin expression, whereas 84% of submucosal carcinoma without lymph-node metastasis and 96% of submucosal carcinoma with lymph-node metastasis showed it. The LOM staining was seen in higher frequency in submucosal carcinoma than in mucosal carcinoma. They also reported that there were significant differences of membranous beta-catenin expression between mucosal and submucosal carcinomas in both intestinal-type and diffuse-type gastric carcinomas. As to 5-year survival and lymph-node metastasis, no obvious difference is detected in beta-catenin expression (Miyazawa *et al.,* 2000; Ougolkov *et al.,* 2000). Grabsch *et al.* (2001) also reported that beta-catenin expression was not correlated with tumor progression or prognosis in gastric cancer. They suggested that the extent of beta-catenin expression was related to that of tumor invasion but not to prognosis.

Beta-Catenin and Phenotypic Expression of MUC

The importance of mucin histochemical analyses of gastrointestinal (GI) carcinomas has been indicated. Mucins are heavily glycosylated glycoproteins that are the major components of the mucous viscous gel covering the surface of epithelial tissues. We targeted three of these mucins—MUC2, MUC5AC, and MUC6—which are specifically expressed in intestinal goblet cells, gastric surface mucous cells, and pyloric gland cells of the mature GI tract, respectively. CD10 was used to detect brush border of small intestinal absorptive cells. We analyzed intramucosal neoplastic lesions from phenotypical point of view and demonstrated that most group A lesions displayed complete intestinal phenotype, whereas many group C lesions retained gastric phenotype (Tsukashita *et al.,* 2001).

We also analyzed the relationship between beta-catenin expression and phenotype of group C lesion (Tsukashita *et al.,* 2003). Koseki *et al.* (2000) also analyzed the relationship between beta-catenin expression and phenotype of the tumor. This study showed

that significant beta-catenin accumulation was seen in tumors with intestinal phenotype. However, in our study, cytoplasmic beta-catenin expression was detected in gastric phenotype. Generic alteration in microsatellites linked to the *APC* gene is a very early event in gastric carcinomas with intestinal differentiation but a relatively late event in those with gastric differentiation (Wu *et al.,* 1998). Thus, it is suggested that the nuclear beta-catenin expression is related to the *APC* gene as mentioned earlier, whereas the cytoplasmic beta-catenin expression of group C lesions is not. It is possible that beta-catenin gene mutations could explain this, but this does not correspond to reports in which immunohistochemical beta-catenin expression rarely corresponds to the beta-catenin mutation of exon 3 (Rimm *et al.,* 1999).

References

Barth, A.I., Nathke, I.S., and Nelson, W.J. 1997. Cadherins, catenins and APC protein: interplay between cytoskeletal complexes and signaling pathways. *Curr. Opin. Cell. Biol. 9*:683–690.

Grabsch, H., Takeno, S., Noguchi, T., Hommel, G., Gabbert, H.E., and Mueller, W. 2001. Different patterns of beta-catenin expression in gastric carcinomas: relationship with clinicopathological parameters and prognostic outcome. *Histopathology 39*: 141–149.

Koseki, K., Takizawa, T., Koike, M., Ito, M., Nihei, Z., and Sugihara, K. 2000. Distinction of differentiated type early gastric carcinoma with gastric type mucin expression. *Cancer 89*:724–732.

Lauren, P. 1965. The two histological main types of gastric carcinoma: diffuse and so-called intestinal-type carcinoma. *Acta. Pathol. Microbiol. Scand. 64*:31–39.

Machado, J.C., Soares, P., Carneiro, F., Rocha, A., Beck, S., Blin, N., Berx, G., and Sobrinho-Simoes, M. 1999. E-cadherin gene mutations provide a genetic basis for the phenotypic divergence of mixed gastric carcinomas. *Lab. Invest. 79*:459–465.

Miyazawa, K., Iwaya, K., Kuroda, M., Harada, N., Serizawa, H., Koyanagi, Y., Sato, Y., Mizokami, Y., Matsuoka, T., and Mukai, K. 2000. Nuclear accumulation of beta-catenin in intestinal-type gastric carcinoma: correlation with early tumor invasion. *Virchows Arch. 437*:508–513.

Nakatsuru, S., Yanagisawa, A., Ichii, S., Tahara, E., Kato, Y., Nakamura, Y., and Horii, A. 1992. Somatic mutation of the APC gene in gastric cancer: frequent mutations in very well differentiated adenocarcinoma in signet-ring cell carcinoma. *Hum. Mol. Genet. 1*:559–563.

Ogasawara, S., Maesawa, C., Tamura, G., and Satodate, R. 1994. Lack of mutations of the adenomatous polyposis coli gene in oesophageal and gastric carcinomas. *Virch. Arch. 424*:607–611.

Orford, K., Crockett, C., Jensen, J.P., Weissmann, A.M., and Byers, S.W. 1997. Serine phosphorylation-regulated ubiquitination and degradation of beta-catenin. *J. Biol. Chem. 272*: 24735–24738.

Ougolkov, A., Mai, M., Takahashi, Y., Omote, K., Bilim, V., Shimizu, A., and Minamoto, T. 2000. Altered expression of beta-catenin and c-erbB-2 in early gastric cancer. *J. Exp. Clin. Cancer Res. 19*:340–355.

Peifer, M., Orsulic, S., Pai, L.M., and Loureiro, J. 1993. A model system for cell adhesion and signal transduction in *Drosophilia. Dev. Suppl.* 163–176.

Rimm, D.L., Caca, K., Hu, G., Harrison, F.B., and Fearon, E.R. 1999. Frequent nuclear/cytoplasmic localization of beta-catenin without exon 3 mutations in malignant melanoma. *Am. J. Pathol. 154*:325–329.

Rubinfeld, B., Albert, I., Porfiri, E., Fiol, C., Munemitsu, S., and Polakis, P. 1996. Binding of GSK3beta to the APC-beta-catenin complex and regulation of complex assembly. *Science 272*:1023–1026.

Schlemper, R.J., Riddell, R.H., Kato,Y., Borchard, F., Cooper, H.S., Dawsey, S.M., Dixon, M.F., Fenoglio-Preiser, C.M., Flejou, J.F., Geboes, K., Hattori, T., Hirota, T., Itabashi, M., Iwafuchi, M., Iwashita, A., Kim, Y.I., Kirchner, T., Klimpfinger, M., Koike, M., Lauwers, G.Y., Lewin, K.J., Oberhuber, G., Offner, F., Price, A.B., Rubio, C.A., Shimizu, M., Shimoda, T., Sipponen, P., Solcia, E., Stolte, M., Watanabe, H., and Yamabe, H. 2000. The Vienna classification of gastrointestinal epithelial neoplasia. *Gut. 47*:251–255.

Tamura, G., Maesawa, C., Suzuki, Y., Tamada, H., Satoh, M., Ogasawara, S., Kashiwaba, M., and Satodate, R. 1994. Mutations of the APC gene occur during early stages of gastric adenoma development. *Cancer Res. 54*:1149–1151.

Tsukashita, S., Kushima, R., Bamba, M., Nakamura, E., Mukaisho, K.I., Sugihara, H., and Hattori, T. 2003. Beta-catenin expression in intramucosal neoplastic lesions of the stomach: comparative analysis of adenoma/dysplasia, adenocarcinoma and signet-ring cell carcinoma. *Oncology 64*:251–258.

Tsukashita, S., Kushima, R., Bamba, M., Sugihara, H., and Hattori, T. 2001. MUC gene expression and histogenesis of adenocarcinoma of the stomach. *Int. J. Cancer 94*:166–170.

Wu, L.B., Kushima, R., Borchard, F., Molsberger, G., and Hattori, T. 1998. Intramucosal carcinomas of the stomach: phenotypic expression and loss of heterozygosity at microsatellites linked to the APC gene. *Pathol. Res. Pract. 194*:405–412.

10

Loss of Cyclin D2 Expression in Gastric Cancer

Jun Yu and Wai K. Leung

Introduction

Cell cycle is universal process by which cells divide and grow. The G1-phase is precisely regulated to coordinate cell division with cell growth, whereas deoxyribonucleic acid (DNA) replication during S phase is precisely ordered to prevent inadvertent events that will lead to genomic instability and cancer. The D-type cyclins are involved in regulation of transition from G1 to S phase (Sherr, 1995) by activating cdk4 and cdk6, which in turn leads to phosphorylation of the retinoblastoma tumor-suppressor protein and release of transcription factors involved in DNA synthesis. Thus, D-type cyclins trigger the onset of S-phase (Zhang, 1999) and are implicated as one of the earliest events leading to cell division (Tetsu and McCormick, 1999). Transcriptional induction of the D-type cyclins occurs in response to growth factors (Guttridge *et al.,* 1999), nuclear receptors (Sabbah *et al.,* 1999), and a variety of mitogenic stimuli including the Ras signaling cascade (Peeper *et al.,* 1997) and the adenomatous polyposis coli(APC)-β-catenin pathway (Tetsu and McCormick, 1999). Transcription and translation synthesis of D-type cyclins are highest in mid to late G1 and lowest during S phase (Takano *et al.,* 2000). Because uncontrolled cyclin/cdk regulation is most often the underlying cause of many diseases including human cancer, cyclin/cdk complexes are tightly regulated by extracellular or intracellular signals and the levels of cdks will remain constant throughout the cell cycle.

However, different D-type cyclins exhibit a number of distinctive properties with differential expressions in various cell lineages (Palmero *et al.,* 1993), different induction kinetics (Ajchenbaum *et al.,* 1993), and different behaviors with respect to their interaction with retinoblastoma protein (Dowdy *et al.,* 1993) cyclins D1, D2 and D3 also exhibit unique cell- and tissue-specific expression patterns, and various combinations of three D-type cyclins are induced in G1 phase (Zhang, 1999).

Among the D-type cyclins, cyclin D2 acts as a rate-limiting controller of G1 phase progression in mammalian cells. Induction of cyclin D2 is growth factor dependent and tightly regulated at the level of transcriptional activation, protein expression, or cellular localization (Sherr, 1995). Accumulation of cyclin D2 contributes to sequestration of the cell cycle inhibitor p27 and cell cycle progression (Perez-Roger *et al.,* 1999). However, cyclin D2 has also been implicated as a negative regulator of growth during the G0 and early G1 phases of normal human and murine fibroblast cell cycle and maintaining cells in a nonproliferative state (Meyyappan *et al.,* 1998).

Handbook of Immunohistochemistry and *in situ* Hybridization of Human Carcinomas, Volume 4: Molecular Genetics, Gastrointestinal Carcinoma, and Ovarian Carcinoma

Overexpression of Cyclin D2 and Cancer

Abnormal or untimely expression or loss of expression of D-type cyclins could disrupt the cell cycle and render them growth promoting. Overexpression of D-type cyclins effectively shortens the G1 phase (Resnitzky *et al.,* 1994) and is found in many human cancers. The most common genetic abnormality affecting cyclin Dl is DNA amplification (Peters, 1994). Overexpression and rearrangement of the cyclin D1 gene have been reported to be associated with tumor progression or poor prognosis in carcinomas of the breast (Gillett *et al.,* 1994), esophagus (Gramlich *et al.,* 1994), pancreas (Gansauge *et al.,* 1997), head and neck (Michalides *et al.,* 1997), and mantle cell lymphomas (Nakamura *et al.,* 1997).

Similar to cyclin Dl, overexpression of cyclin D2 has been noted in human squamous carcinoma cells (Liu *et al.,* 2002), human B-cell malignancies (Delmer *et al.,* 1995), testicular germ cell tumor (Sicinski *et al.,* 1996), and gastric cancer (Yu *et al.,* 2001). Up-regulation of cyclin D2 is shown to correlate with disease progression and poor prognosis of gastric cancer (Takano *et al.,* 2000). It has been suggested that cyclin D2 is a direct target of Myc and that accumulation of cyclin D2 contributes to sequestration of the cell cycle inhibitor p27 and to cell cycle entry (Perez-Roger *et al.,* 1999). Cyclin D2 is thereby considered to be a protooncogene because its up-regulation correlated with tumor progression and prognosis (Takano *et al.,* 2000).

Low or Absent Cyclin D2 Expression in Gastric Cancer

However, high levels of cyclin D2 expression are noted in a variety of normal human tissues, including brain, breast, and lymphoid tissues. In murine fibroblast cells, cyclin D2 may function as a negative regulator of growth (Meyyappan *et al.,* 1998). Hence, cyclin D2 may have different roles depending on the levels of expression and the particular cell type. Cyclin D2 has also been shown to induce a senescence-like phenotype (Meyyappan *et al.,* 1996) and to inhibit cell proliferation (Meyyappan *et al.,* 1996, 1998).

In this regard, reduced or lack of expression of cyclin D2 has been reported in human breast cancer (Lehmann *et al.,* 2002), prostate cancer (Padar *et al.,* 2003), pancreatic cancer (Matsubayashi *et al.,* 2003), and testicular germ cell tumor (Sicinski *et al.,* 1996). Lack of cyclin D2 messenger ribonucleic acid (mRNA) or protein expression was also demonstrated in 30–70% of primary gastric cancer cases (Takano *et al.,* 2000). The fact that cyclin D2 expression is lost in human tumor strongly suggests that the function of this gene is not limited to its well-known role in G1-S transition during the cell cycle.

Possible Mechanisms of Cyclin D2 Gene Silencing

Various mechanisms of gene silencing such as loss of heterozygosity, point mutations, and homozygous deletions have been reported in cancer development (Shapiro *et al.,* 1995). In addition, tumor-related genes can be functionally inactivated without alterations in the primary sequence by methylation of the cytosine residues of the promoter region (Wajed *et al.,* 2001). Aberrant promoter methylation, as an epigenetic mechanism of gene silencing, is increasingly recognized to be an important mechanism in the process of malignant transformation (Jones *et al.,* 1999). Through the recruitment of histone-modifying enzymes to the DNA, the cytosine residue methylation initiates the formation of a closed chromatin conformation, thereby repressing transcription (Bird and Wolffe, 1999). Cytosine methylation of CpG islands located within the promoter region is generally associated with delayed replication, condensed chromatin, and inhibition of transcription initiation (Jones *et al.,* 1999).

Studies including ours indicated that aberrant hypermethylation of CpG islands is one of the crucial mechanisms in the transcriptional silencing of tumor-related genes in gastric cancer (Leung *et al.,* 2001). Although the cyclin D2 gene possesses a CpG-rich island in the 5′ region (Evron *et al.,* 2001), we studied the methylation status of the CpG sites in the cyclin D2 promoter region of gastric cancer to elucidate the role of promoter hypermethylation in silencing of cyclin D2.

METHODS

We examined gastric cancer cell lines, primary human gastric cancer, and their corresponding normal tissues for aberrant methylation of cyclin D2 and their expression. Promoter hypermethylation was determined by methylation-specific polymerase chain reaction (MSP) and bisulfite sequencing, whereas expression of cyclin D2 mRNA and protein was assessed by reverse transcriptase-polymerase chain reaction (RT-PCR), Western blot, and immunohistochemistry (IHC), respectively.

Gastric Cancer Cell Lines

The human gastric cancer cell lines KATO III, MKN45, MKN28, AGS, and NCI-N87 (N87) were obtained from Riken Cell Bank (Tsukuba, Japan) or

American Type Culture Collection (ATCC; Rockville, MD, USA). All cell lines, except AGS, were maintained in RPMI medium (Gibco BRL, Rockville, MD) with 10% fetal bovine serum (Gibco BRL). AGS cell line was kept in F-12K medium (ATCC) with 10% fetal bovine serum.

Human Gastric Tissues

Gastric cancers were obtained at the time of surgery from 47 patients undergoing gastrectomy. In addition, normal endoscopic gastric biopsies from 23 subjects who did not have cancer were used as control. The samples were immediately snap-frozen in liquid nitrogen and stored at −80°C.The remaining tissue specimens were fixed in 10% formalin and embedded in paraffin for routine histologic examination and immunohistochemical analysis.

Expression of Cyclin D2

Expression of cyclin D2 mRNA and protein was determined by RT-PCR, Western blot, and IHC.

Reverse Transcriptase-Polymerase Chain Reaction Protocol

1. Gastric tissue specimens were homogenized with an ultrasound homogenizer at 30,000 rpm (KINEMATICA, Lucerne, Switzerland).
2. Total RNA was extracted by using RNA Tri Reagents (CINNA/MRC, Cincinnati, Ohio, USA) according to the manufacturer's protocol.
3. One μg of total RNA was reverse transcribed into cDNA (complementary DNA) by using dNTP (deoxyribonucleotide triphosphate) (1 mM), 5X reverse transcription buffer (500 mM Tris-HC1 [pH 8.3], 250 mM KC1, 50 mM $MgCl_2$ and 50 mM DTT), 16 units RNasin, and 2.5 units of AMV reverse transcriptase (GibcoBRL).
4. The cyclin D2 primer sequences were 5′-CATGGAGCTGCTGTGCCACG-3′ (sense) and 5′-CCGACCTACCTCCAGCATCC-3′ (anti-sense) (Evron *et al.,* 2001).
5. The reaction was performed at 95°C for 1.5 min and followed by 35 cycles of denaturating at 95°C for 24 sec annealing at 58°C for 48 sec, and extension at 72°C for 1 min.
6. The PCR products were separated on 1.5% agarose gel and saved as digital images (Uvigrab; UVItec, Cambridge, UK).

Western Blot Analysis

1. Proteins were extracted from cell pellets using Trizol Reagents (Gibco BRL).
2. Protein concentrations were measured by the method of Bradford (Bio-Rad, Hercules, CA).
3. Twenty micrograms of protein was loaded per lane, separated by 10% sodium dodecyl sulfate (SDS)-polyacrylamide gel electrophoresis under reducing conditions, and transferred onto equilibrated polyvinylidene difluoride membrane (Amersham Health, Buckinghamshire, UK) by electroblotting.
4. Membranes were blocked by 5% nonfat dry milk and then incubated with anti-cyclin D2 antibody (dilution 1:1000; sc-181-G, goat polyclonal antibodies; Santa Cruz Biotechnology, Santa Cruz, CA) for 2.5 hr at room temperature.
5. After secondary antibody incubation, cyclin D2 was detected by the enhanced chemiluminescence detection system (Amersham Health).

Immunohistochemistry

1. Expression of cyclin D2 protein was examined by avidin-biotin complex (ABC) immunoperoxidase method.
2. Five-micron sections were cut from the paraffin-embedded block, placed on charged glass slides, deparaffinized, rehydrated, rinsed with distilled water, and washed with Tris-buffered saline (TBS).
3. The slides were treated with 3% hydrogen peroxide (H_2O_2) to block endogenous peroxidase activity.
4. After blocking with 5% normal serum for 20 min, polyclonal antibody against cyclin D2 (dilution 1:200, sc181, Santa Cruz, CA) was applied and incubated overnight at 4°C.
5. After rinsing, the biotinylated secondary antibody and ABComplex horseradish peroxidase (HRP) (Dako A/S, Denmark) was applied.
6. Peroxidase activity was visualized by the diaminobenzidine (DAB) chromogen with 0.05% H_2O_2. The sections were counterstained with hematoxylin, dehydrated, cleared, and mounted.

Detection of Promoter Hypermethylation

Promoter hypermethylation of cyclin D2 was detected by MSP (Herman *et al.,* l996). Genomic DNA was first modified by sodium bisulfite to convert all unmethylated cytosine into uracil. This was followed by amplification with primers that selectively amplifies either the uracil or cytosine nucleotide of the promoter regions (Figure 32).

Bisulfite Modification

1. Genomic DNA from cell lines or frozen gastric tissues was extracted by using the High Pure PCR Template Preparation kit (Roche, Germany).
2. One μg of genomic DNA was treated with the CpGenome DNA Modification Kit (Intergen, Purchase, NY) according to the manufacturer's instructions.

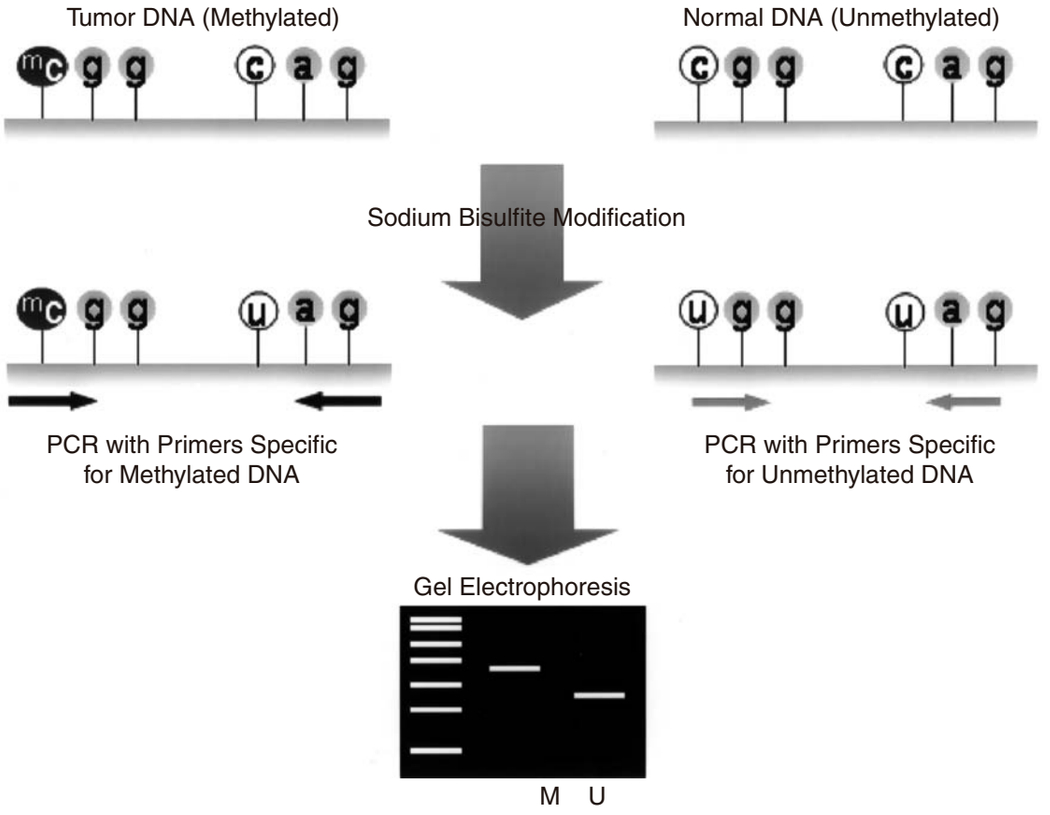

***Figure 32.* Methylation-specific polymerase chain reaction (PCR).** Normal unmethylated cytosine residue will be converted by sodium bisulfite treatment into uracil, whereas methylated cytosine will remain unchanged. Subsequent PCR amplification by specific sets of primers that target the segments containing the unchanged cytosine or altered uracil will enable the differentiation of methylated from unmethylated promoter region.

3. Differentiation between methylated and unmethylated sequences can be made by amplification using specific primers that target either the uracil or the cytosine nucleotide.

Methylation-Specific Polymerase Chain Reaction

1. The methylated and unmethylated primer sequences were based on the report by Evron *et al.,* and the region of primers were numbered from the transcriptional start site (Evron *et al.,* 2001): unmethylated reaction, 5′-GTTATGTTATGTTTGTTGTATG-3′ (sense, −1372 to −1350) and 5′-TAAAATCCACCAACACAAT CA-3′ (anti-sense, −1150 to −1170), 223-bp product; and methylated reaction, 5′-TACGTGTTAGGGTCGA TCG-3′ (sense, −1183 to −1165) and 5′-CGAAATAT CTACGCTAAACG-3′ (anti-sense, –908 to –927), 276-bp product.

2. Hot start PCR was conducted in a 25 μL reaction solution containing 1X PCR buffer, 0.25 mM each of the deoxynucleoside triphosphates, 1 mM of each primer, and 1 unit of Taq polymerase (AmpliTaq Gold; PE Applied Biosystems, Foster City, CA).

3. The temperature profile for the amplification was as follows: 12 min at 95°C, 35 cycles of denaturing at 95°C for 30 sec, 45 sec annealing at 52°C, 60 sec extension at 72°C, and final extension step of 5 min at 72°C.

4. *In vitro* methylated control (positive control; Intergen) and DNA template-negative control (water) were included in each PCR.

5. PCR products were analyzed in 2% agarose gels and stained with ethidium bromide.

Bisulfite DNA Sequencing

Bisulfite DNA sequencing was used to elucidate the comprehensive methylation patterns of the promoter region of cyclin D2.

1. PCR primers were designed to amplify a CpG-rich region spanning from -1220 to -883 from the transcriptional start site, which contains 27 CpG sites. Primer sequences were 5′-TTTGTAAAGAT AGTTTTGATTAAGG-3′ (sense, −1220 to −1195)

and 5′-CCCCTACATCTACTAACAAAC-3′ (antisense, −883 to −903).

2. The PCR product was cloned into the pCR4-TOPO vector using the TOPO TA Cloning Kit (Gibco/Invitrogen, Carlsbad, CA). Multiple clones (minimum of 5) from each PCR product were sequenced using the ABI Prism Dye Terminator Cycle Sequencing Kit (PE Biosystems, Foster City, CA) and the ABI Prism 310 DNA Sequencer (PB Biosystems).

Treatment of Cells with 5-aza-2′-deoxycytidine (5-azaDC)

1. Gastric cancer cells were seeded at a density of 1×10^6 cells/6 mm dish.

2. After 24 hr, (cells were treated with 1, 5, or 10 μM 5-azaDC (Sigma Chemical Co., St. Louis, MO, USA). The same concentration of DMSO (demethyl sulfoxide) was used as a control for nonspecific solvent effect on cells.

3. Total cellular RNA and protein were isolated 3 and 5 days after addition of 5-azaDC, as described previously.

RESULTS

Methylation of Cyclin D2 is Associated with Transcriptional Silencing in Gastric Cancer Cell Lines

We first examined the promoter methylation status and the expression of cyclin D2 in five gastric cancer cell lines. Three gastric cancer cell lines (KATOIII, AGS, and NCI-N87) with dense methylation at the CpG islands do not express cyclin D2 mRNA and protein. The MKN28 cell line had almost no methylation and displayed strong cyclin D2 expression. It is interesting that the MKN45 cell line was noticed to have a reduced level of cyclin mRNA expression but no protein expression.

By bisulfite DNA sequencing, the CpG islands exhibited extensive methylation in the three cell lines without cyclin D2 expression (KATOIII, AGS, N87). In contrast, there was no methylation in the MKN28 cell lines with positive cyclin D2 expression. Notably, the percentage of methylation ranged from 18.5% to 88.9% in the MKN45 cell line. This partial methylation may explain the low cyclin D2 mRNA expression in the MKN45 cell line.

Treatment with 5-azaDC restored the cyclin D2 expression in the three cell lines with cyclin D2 methylation (KATOIII, AGS, N87). These findings indicate that an appropriate conformation of the chromatin in which the cyclin D2 promoter is embedded for transcription can override the effects of DNA hypermethylation.

Hypermethylation Leads to Cyclin D2 Silencing in Primary Gastric Tumors

The same observation was found in primary human gastric cancers in which the density of methylation appears to have an inverse association with the expression of cyclin D2. Twenty-three (48.9%) of the 47 primary gastric cancers had cyclin D2 methylation detected by MSP. Of the methylation-positive cases, 15 (65.2%) had complete loss of cyclin D2 mRNA expression. In contrast, only 3 of 24 (12.5%) methylation-negative cases had lost cyclin D2 mRNA expression. There was a strong association between the lack of cyclin D2 mRNA expression and promoter hypermethylation ($p < 0.001$). To further demonstrate that promoter methylation of cyclin D2 is a tumor-specific phenomenon, DNA from 23 histologically normal gastric mucosa were tested and none of these normal samples had methylation detected by MSP.

Western blot analysis was performed in 28 randomly selected gastric cancers. Ten (66.7%) of the 15 cases with promoter hypermethylation in cyclin D2 did not express the corresponding protein. However, only 2 of the 13 unmethylated tumors did not express cyclin D2 protein ($p = 0.006$). In keeping with the findings by Western blot analysis, cyclin D2 immunoreactivity was detected in the cytoplasm at nucleus of gastric cancers without methylation (Figure 33). There was no cyclin D2 immunoreactivity detected in tumors with promoter hypermethylation and in normal gastric tissues.

Bisulfite sequencing was also performed in seven randomly selected gastric cancers. The three cases that showed hypermethylation by MSP had densely methylated alleles by bisulfite sequencing, whereas the two cases with low cyclin D2 expression had partially methylated CpG sites. In contrast, the two tumors with strong cyclin D2 expression had virtually no methylation detected. In addition, bisulfite sequencing of normal gastric mucosa showed the absence of methylation in the promoter region.

DISCUSSION

Our results suggest that cyclin D2 promoter methylation is an important regulator of cyclin D2 expression in gastric cancer cells. Promoter hypermethylation is associated with loss of cyclin D2 expression in gastric cancer cell lines. Moreover, the density of CpG island methylation appears to have an inverse association with the expression of cyclin D2. Treatment with 5-azaDC induced demethylation of the CpG islands with reactivation of gene expression in these cyclin

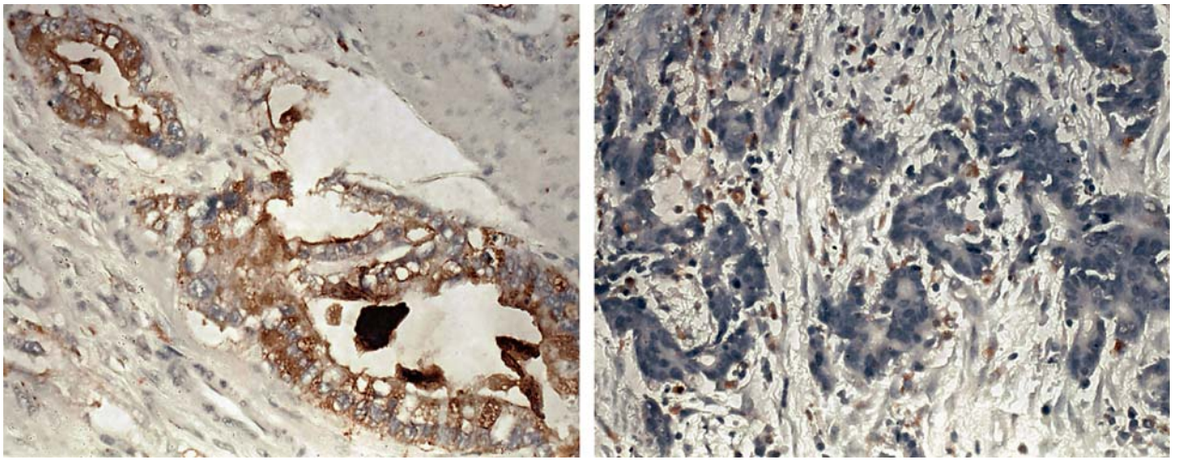

***Figure* 33. Cyclin D2 expressions in gastric cancer.** Expression of cyclin D2 was determined by immunohistochemistry. **A:** Intense cyclin D2 immunoreactivity was noted in the cytoplasm of gastric tumor cells (40X). **B:** Loss of cyclin D2 expression in gastric tumor with methylation in cyclin D2 promoter. Mild immunoreactivity was noted in adjacent myofibroblasts (40X)

D2–negative hypermethylated cell lines. In primary gastric cancer, the majority of tumors with cyclin D2 promoter hypermethylation had no cyclin D2 expression, whereas most of the tumors with unmethylated cyclin D2 promoter had cyclin D2 expression. This finding also confirmed a previous observation that expression of cyclin D2 is lost in a subset of gastric cancer (Takano *et al.,* 2000; Yu *et al.,* 2001).

Promoter methylation, if it involves tumor-suppressor genes, usually results in selective growth advantage favoring the survival of tumor cells. However, it is increasingly recognized that promoter hypermethylation can also be detected in genes other than tumor-suppressor genes. We have shown that the cyclooxygenase-2 gene (COX2) could also be silenced by promoter hypermethylation (Yu *et al.,* 2003). Moreover, it is important to recognize that cytosine methylation can also influence tumorigenicity by mechanisms other than gene silencing. Methylated cytosines can undergo spontaneous deamination resulting in C→T transitions and they are also preferred targets for G→T transversion mutations (Jones and Baylin, 2002). Thus, further studies are necessary to characterize the consequences of cyclin D2 methylation in the process of gastric carcinogenesis.

In this study, methylation of cyclin D2 promoter region appears to be a tumor-specific event because methylation was detected only in gastric cancer and cancer cell lines but not in any normal gastric mucosa. Our results also showed that cyclin D2 methylation was more frequent in older patients, suggesting that cyclin D2 methylation may play a more important role in gastric carcinogenesis of elderly patients. However, we believe that methylation in cyclin D2 is not an age-related phenomenon because methylation is not detected in normal gastric mucosa. Moreover, previous studies in breast cancer and Burkitt's lymphoma suggest that methylation in cyclin D2 is a tumor-specific event (Evron *et al.,* 2001; Sinclair *et al.,* 1995).

The detection of cyclin D2 mRNA expression in tumors with promoter hypermethylation may be related to the extreme sensitivity of MSP, which can theoretically detect as little as 0.1% of methylated cells (Herman *et al.,* 1996). Alternatively, a tumor may exhibit heterogeneity in cyclin D2 expression such that not 100% of tumor cells may demonstrate promoter hypermethylation and hence repression of transcriptional activity. In this regard, partial methylation may reduce the level of transcriptional repression, resulting in partial loss of gene expression only (Hsieh, *et al.,* 1994).

MSP provides qualitative data on the methylation status of the region analyzed. This may mask potential quantitative differences between samples from different patients and also dynamic changes in the extent of methylation during tumor evolution. For these reasons, several groups have developed quantitative assay for the density of CpG methylation by using quantitative real-time PCR in the rapid and sensitive quantitative detection of gene promoter hypermethylation (Eads *et al.,* 2000). This technology combines the advantages of high throughput with superior sensitivity and accuracy (Lie and Petropoulos, 1998).

Notably, we showed that three cancer samples did not express cyclin D2 in the absence of methylation. This finding suggests that alternative pathways, such

as homozygous deletion or genetic mutations, may account for loss of cyclin D2 in some tumors. Both of these events, however, have not been reported in gastric cancer, and further study may be necessary to clarify the role of genetic events leading to loss of cyclin D2 expression in tumors. In conclusion, transcriptional silencing by promoter hypermethylation of the cyclin D2 gene is detected in a subset of gastric cancers, suggesting that the development of a subset of gastric cancer is independent of cyclin D2 expression. Nonetheless, the functional significance underlying the methylation-mediated transcriptional loss of cyclin D2 in gastric carcinogenesis remains to be determined.

References

Ajchenbaum, F., Ando, K., DeCaprio, J.A., and Griffin, J.D. 1993. Independent regulation of human D-type cyclin gene expression during G1 phase in primary human T lymphocytes. *J. Biol. Chem. 268*:4113–4119.

Bird, A.P., and Wolfe, A.P. 1999. Methylation-induced repression: belts, braces, and chromatin. *Cell 99*:451–454.

Delmer, A., Ajchenbaum-Cymbalista, F., Tang, R., Ramond, S., Faussat, A.M., Marie, J.P., and Zittoun, R. 1995. Overexpression of cyclin D2 in chronic B-cell malignancies. *Blood 85*:2870–2876.

Dowdy, S.F., Hinds, P.W., Louie, K., Reed, S.I., Arnold, A., and Weinberg, R.A. 1993. Physical interaction of the retinoblastoma protein with human D cyclins. *Cell 73*:499–511.

Eads, C.A., Danenberg, K.D., Kawakami, K., Saltz, L.B., Blake, C., Shibata, D., Danenberg, P.V., and Laird, P.W. 2000. MethyLight: a high-throughput assay to measure DNA methylation. *Nucleic Acids Res. 28*:E32.

Evron, E., Umbricht, C.B., Korz, D., Raman, V., Loeb, D.M., Niranjan, B., Buluwela, L., Weitzman, S.A., Marks, J., and Sukumar, S. 2001. Loss of cyclin D2 expression in the majority of breast cancers is associated with promoter hypermethylation. *Cancer Res. 61*:2782–2787.

Gansauge, S., Gansauge, F., Ramadani, M., Stobbe, H., Rau, B., Harada, N., and Beger, HG. 1997. Overexpression of cyclin Dl in human pancreatic carcinoma is associated with poor prognosis. *Cancer Res. 57*:1634–1637.

Gillett, C., Fantal, V., Smith, R., Fisher, C., Bartek, J., Dickson, C., Barnes, D., and Peters, G. 1994. Amplification and overexpression of cyclin D1 in breast cancer detected by immunohistochemical staining. *Cancer Res. 54*:1812–1817.

Gramlich, T.L., Fritsch, C.R., Maurer, D., Eberle, M., and Gansler, T.S. 1994. Differential polymerase chain reaction assay of cyclin D1 gene amplification m esophageal carcinoma. *Diagn. Mol. Pathol. 3*:255–259.

Guttridge, D.C., Albanese, C., Reuther, J.Y., Pestell, R.G., and Baldwin, A.S. Jr. 1999. NF-kappaB controls cell growth and differentiation through transcriptional regulation of cyclin D1. *Mol. Cell Biol. 19*:5785–5789.

Herman, J.G., Graff, J.R., Myohanen, S., Nelkin, B.D., and Baylin, S.B. 1996. Methylation-specific PCR: a novel PCR assay for methylation status of CpG islands. *Proc. Natl. Acad. Sci. USA 93*:9821–9826.

Hsieh, C.L. 1994. Dependence of transcriptional repression on CpG methylation density. *Mol. Cell Biol. 14*:5487–5494.

Jones, P.A., and Baylin, S.B. 2002. The fundamental role of epigenetic events in cancer. *Nat. Rev. Genet. 3*:415–428.

Jones, P.A., and Laird, P.W. 1999. Cancer epigenetics comes of age. *Nat. Genet. 21*:163–167.

Lehmann, U., Langer, F., Feist, H., Glockner, S., Hasemeier, B., and Kreipe, H. 2002. Quantitative assessment of promoter hypermethylation during breast cancer development. *Am. J. Pathol. 160*:605–612.

Leung, W.K., Yu, J., Ng, E.K., To, K.F., Ma, P.K., Lee, T.L., Go, M.Y., Chung, S.C., and Sung, J.J. 2001. Concurrent hypermethylation of multiple tumor-related genes in gastric carcinoma and adjacent normal tissues. *Cancer 91*:2294–2301.

Lie, Y.S., and Petropoulos, C.J. 1998. Advances in quantitative PCR technology: *5′* nuclease assays. *Curr. Opin. Biotechnol. 9*:43–48.

Liu, S.C., Bassi, D.E., Zhang, S.Y., Holoran, D., Conti, C.J., and Klein-Szanto, A.J. 2002. Overexpression of cyclin D2 is associated with increased *in vivo* invasiveness of human squamous carcinoma cells. *Mol. Carcinog. 34*:131–139.

Matsubayashi, H., Sato, N., Fukushima, N., Yeo, C.J., Walter, K.M., Brune, K., Sahin, F., Hruban, R.H., and Goggins, M. 2003. Methylation of cyclin D2 is observed frequently in pancreatic cancer but is also an age-related phenomenon in gastrointestinal tissues. *Clin. Cancer Res. 9*:1446–1452.

Meyyappan, M., Atadja, P.W., and Riabowol, K.T. 1996. Regulation of gene expression and transcription factor binding activity during cellular aging. *Biol. Signals 5*:130–138.

Meyyappan, M., Wong, H., Hull, C., and Riabowol, K.T. 1998. Increased expression of cyclin D2 during multiple states of growth arrest in primary and established cells. *Mol. Cell Biol. 18*:3163–3172.

Michalides, R.J., van Veelen, N.M., Kristel, P.M., Hart, A.A., Loftus, B.M., Hilgers, F.J., and Balm, A.J. 1997. Overexpression of cyclin D1 indicates a poor prognosis in squamous cell carcinoma of the head and neck. *Arch. Otolaryngol. Head Neck Surg. 123*:497–502.

Nakamura, S., Yatabe, Y., and Seto, M. Cyclin 1997. Dl overexpression in malignant lymphomas. *Pathol. Int. 47*:421–429.

Padar, A., Sathyanarayana, U.G., Suzuki, M., Maruyama, R., Hsieh, J.T., Frenkel, E.P., Minna, J.D., and Gazdar, A.F. 2003. Inactivation of cyclin D2 gene in prostate cancers by aberrant promoter methylation. *Clin. Cancer Res. 9*:4730–4734.

Palmero, I., Holder, A., Sinclair, A.J., Dickson, C., and Peters, G. 1993. Cyclins D1 and D2 are differentially expressed in human B-lymphoid cell lines. *Oncogene 8*:1049–1054.

Peeper, D.S., Upton, T.M., Ladha, M.H., Neuman, E., Zalvide, J., Bernards, R., DeCaprio, J.A., and Ewen, M.E. 1997. Ras signalling linked to the cell-cyle machinery by the retinoblastoma protein. *Nature 386*:177–181.

Perez-Roger, I., Kim, S.H., Griffiths, B., Sewing, A., and Land, H. 1999. Cyclins D1 and D2 mediate myc-induced proliferation via sequestration of p27Kip1 and p21Cip1. *EMBO J. 18*:53l0–5320.

Peters, G. 1994. The D-type cyclins and their role in tumorigenesis. *J. Cell Sci. 8*:89–96.

Resnitzky, D., Gossen, M., Bujard, H., and Reed, S.I. 1994. Acceleration of the G1/S phase transition by expression of cyclins Dl and E with an inducible system. *Mol. Cell Biol. 14*:1669–1679.

Sabbah, M., Courilleau, D., Mester, J., and Redeuilh, G. 1999. Estrogen induction of the cyclin D1 promoter: involvement of a cAMP response-like element. *Proc. Natl. Acad. Sci. USA 96*:11217–11222.

Shapiro, G.I., Park, J.E., Edwards, C.D., Mao, L., Merlo, A., Sidransky, D., Ewen, M.E., and Rollins, B.J. 1995. Multiple mechanisms of p16INK4A inactivation in non-small cell lung cancer cell lines. *Cancer Res. 55*:6200–6209.

Sherr, C.J. 1995. D-type cyclins. *Trends Biochem. Sci. 20*:l87–190.
Sinclair, A.J., Palmero, I., Holder, A., Peters, G., and Farrell, P.J. 1995. Expression of cyclin D2 in Epstein-Barr virus-positive Burkitt's lymphoma cell lines is related to methylation status of the gene. *J. Virol.* 69:1292–1295.
Takano, Y., Kato, Y., van Diest, P.J., Masuda, M., Mitomi, H., and Okayasu, I. 2000. Cyclin D2 overexpression and lack of p27 correlate positively and cyclin E inversely with a poor prognosis in gastric cancer cases. *Am. J. Pathol. 156*:585–594.
Tetsu, O., and McCormick, F. 1999. Beta-catenin regulates expression of cyclin D1 in colon carcinoma cells. *Nature 398*:422–426.
Wajed, S.A., Laird, P.W., and DeMeester, T.R. 2001. DNA methylation: an alternative pathway to cancer. *Ann. Surg. 234*:10–20.
Yu, J., Leung, W.K., Lee, T.L., Tse, P.C., To, K.F., and Sung, J.J. 2003. Promoter hypermethylation of cyclooxygenase-2 in gastric carcinoma. *Int. J. Oncol. 22*:1025–1031.
Yu, J., Leung, W.K., Ng, E.K., To, K.F., Ebert, M.P., Go, Y., Chan, W.Y., Chan, F.K., Chung, S.C., Malfertheiner, P., and Sung, J.J. 2001. Effect of *Helicobacter pylori* eradication on expression of cyclin D2 and p27 in gastric intestinal metaplasia. *Aliment Pharmac. Ther. 15*:1505–1511.
Zhang, P. 1999. The cell cycle and development: redundant roles of cell cycle regulators. *Curr. Opin. Cell Biol. 11*:655–662.

11

Role of Immunohistochemical Expression of E-Cadherin in Diffuse-Type Gastric Cancer

Birgit Luber, Armando Gamboa-Dominguez, Karl-Friedrich Becker, Falko Fend, and Heinz Höfler

Introduction

E-cadherin is a cell-adhesion molecule expressed in epithelial cells. It plays an important role in maintenance of tissue architecture, normal development, and tumor progression (Birchmeier and Behrens, 1994). In gastric cancer, expression and distribution of E-cadherin is frequently deranged. E-cadherin staining ranges from normal membrane localization at cell–cell contacts to abnormal cytoplasmic staining combined with partial membrane staining to pure cytoplasmic staining to negative staining. Heterogeneous staining patterns with positive and negative malignant cells in the same tumor are also frequently detected. In addition, E-cadherin mutations are frequently observed in diffuse-type gastric carcinoma (Becker *et al.,* 1994). Mutation-specific antibodies reacting with mutant E-cadherin variants lacking exon 8 or 9 are available and can be used to screen for the most frequent mutations in this malignancy (Becker *et al.,* 1999; Becker *et al.,* 2002). The impact of the expression and mutation status of E-cadherin determined by immunohistochemistry (IHC) in diffuse-type gastric cancer specimens on patient survival will be discussed.

Biological Background

An anti-invasive role of E-cadherin is well-established in experimental tumor cell systems (Kremer *et al.,* 2003; Meiners *et al.,* 1998). A link between loss of E-cadherin or catenin expression and invasive tumor growth has been demonstrated in a variety of human malignancies (Birchmeier and Behrens, 1994; Van Aken *et al.,* 2001). The adhesive receptor consists of an extracellular domain that mediates calcium-dependent homophilic interactions between cells, a transmembrane region, and a cytoplasmic domain that binds to catenins (Gumbiner, 2000). α-, β- and γ-catenin and $p120^{ctn}$ link E-cadherin with the actin cytoskeleton (Gumbiner, 2000; Thoreson *et al.,* 2000). Beside playing an important role in cell adhesion, β-catenin also participates in the regulation of gene expression by forming a complex with members of the T cell factor/lymphoid enhancer factor 1 (TCF/LEF1) transcription factor family (Behrens *et al.,* 1996; Huber *et al.,* 1996; Molenaar *et al.,* 1996). Target genes comprise among others *c-myc* (He *et al.,* 1998) and *cyclin D1* (Shtutman *et al.,* 1999; Tetsu and McCormick, 1999), *MDR1* (multi-drug resistance gene 1)

Handbook of Immunohistochemistry and *in situ* Hybridization of Human Carcinomas, Volume 4: Molecular Genetics, Gastrointestinal Carcinoma, and Ovarian Carcinoma

(Yamada *et al.,* 2000), *jun* and *fra-1* (Mann *et al.,* 1999) and the gene coding for MMP-7 (matrix metalloproteinase-7, matrilysin) (Crawford *et al.,* 1999). Alterations of adherens junction components range from abnormal gene expression and altered subcellular localization to gene mutations in human cancer (Van Aken *et al.,* 2001). Somatic E-cadherin mutations have been described in gastric, breast, gynecologic, and thyroid carcinomas (Becker *et al.,* 1994; Berx *et al.,* 1998; Risinger *et al.,* 1994; Soares *et al.,* 1997), and germline E-cadherin mutations were found in familial gastric cancer (Gayther *et al.,* 1998; Guilford *et al.,* 1998; Keller *et al.,* 1999). Several stabilizing β-catenin mutations were detected among others in colon carcinoma and melanoma (Morin *et al.,* 1997; Rubinfeld *et al.,* 1997).

E-Cadherin Expression as Prognostic Marker in Gastric Cancer

Accumulating evidence suggests that E-cadherin–mediated adherens junctions can be dynamically modulated in circumstances where cells become motile—for instance, during wound healing or developmental morphogenesis. E-cadherin is removed from the cell membrane and subsequently recycled to sites of newly formed cell–cell contacts (Gumbiner, 2000). Receptor and nonreceptor tyrosine kinases such as epidermal growth factor receptor (EGFR), Met receptor, and Src kinase can play a role in these processes because they phosphorylate E-cadherin, which subsequently leads to internalization by endocytosis (Fujita *et al.,* 2002; Kamei *et al.,* 1999). These changes can result in epithelial–mesenchymal transition (Lu *et al.,* 2003). In gastric cancer, E-cadherin immunoreactivity patterns vary between normal membrane localization at sites of cell–cell contact to abnormal cytoplasmic staining combined with partial membrane staining to pure cytoplasmic staining to negative staining. Heterogeneous staining of tumors with positive and negative malignant cells are also detectable. Besides post-translational processes, E-cadherin expression can be regulated on the transcriptional level by transcription factors such as snail and sip1 (Batlle *et al.,* 2000; Comijn *et al.,* 2001; Rosivatz *et al.,* 2002). The E-cadherin promoter can be silenced by DNA (deoxyribonucleic acid) hypermethylation (Machado *et al.,* 2001).

The prognostic significance of E-cadherin has been investigated in gastric cancer in a variety of studies during the last few years. Abnormal E-cadherin expression is frequently found in gastric cancer, especially in the diffuse-type according to the Laurén classification (Jawhari *et al.,* 1997; Zhou *et al.,* 2002). A number of studies point to a possible association between abnormal E-cadherin expression and poor prognosis. Loss of E-cadherin expression has been found to be a marker of poor survival in gastric cancer in some reports (Gabbert *et al.,* 1996; Mayer *et al.,* 1993; Shino *et al.,* 1995; Yonemura *et al.,* 1995). In other studies, no correlation between abnormal E-cadherin expression and patient survival was found (Gamboa-Dominguez *et al.,* 2005; Jawhari *et al.,* 1997; Zhou *et al.,* 2002).

Somatic and Germline E-Cadherin Mutations in Gastric Cancer

Somatic E-cadherin mutations have been described in the diffuse- but not in the intestinal-type of gastric cancer according to the Laurén classification (Becker *et al.,* 1994; Machado *et al.,* 1999). The predominant type of mutations in gastric cancer were splice-site mutations and in-frame deletions, and most of the mutations were located in exon 8 or 9 (Becker *et al.,* 1993; Berx *et al.,* 1998). This region is therefore considered to be a mutational hot-spot region in gastric carcinoma. Diffuse-type gastric carcinoma is characterized by a noncohesive growth pattern, and the impairment of E-cadherin function by mutation might be an explanation for the diffusely infiltrative cell morphology observed in this tumor. Functional consequences of E-cadherin mutations, such as loss of cell adhesion and gain of cell motility, have been shown previously in cell-culture models (Fuchs *et al.,* 2002; Handschuh *et al.,* 1999; Luber *et al.,* 2000). E-cadherin inactivation by mutation seems to be an early event in diffuse-type gastric cancer formation because loss of E-cadherin expression associated with the presence of mutations is already found in early gastric carcinomas (Becker *et al.,* 1996).

Germline E-cadherin mutations have been reported in families with diffuse-type gastric carcinoma (Gayther *et al.,* 1998; Guilford *et al.,* 1998). In one family, a patient with an E-cadherin mutation developed both a diffuse-type gastric carcinoma and a lobular breast cancer (Keller *et al.,* 1999). The human E-cadherin gene at chromosome 16q22.1 comprises a region of 100 kbp and contains 16 exons (Berx *et al.,* 1995; Mansouri *et al.,* 1988; Natt *et al.,* 1989). Loss of heterozygosity (LOH) has been observed in gastric carcinogenesis (Becker *et al.,* 1994; Becker and Hofler, 1995), but besides LOH, E-cadherin promoter methylation has been identified as the second hit in sporadic and hereditary diffuse-type gastric cancer (Grady *et al.,* 2000; Machado *et al.,* 2001).

Mutation-Specific Antibodies Recognizing Mutant E-Cadherin Lacking Exon 8 or 9

In diffuse-type gastric carcinoma, in-frame deletions of exon 8 or 9 are present with a frequency depending on geographic influences (Becker *et al.,* 1994; Gamboa-Dominguez *et al.,* 2005). Mutation-specific monoclonal antibodies have been generated that recognize mutant E-cadherin variants lacking exon 8 (Becker *et al.,* 2002) or exon 9 (Becker *et al.,* 1999). Monoclonal antibody E-cad delta 8-1 was shown to react only with the mutant protein lacking exon 8 but not with wild-type E-cadherin (Becker *et al.,* 2002). It is interesting that antibody HECD-1 was found to react with an epitope present at least in part in exon 8. Combined use of E-cad delta 8-1 and HECD-1 allows the allele-specific examination of mutant and wild-type E-cadherin expression in tumor samples (Becker *et al.,* 2002). Similarly, antibody E9, which reacts with an epitope present at least in part in exon 9, can be used in combination with mutation-specific antibody E-cad delta 9-1 E-cad, which specifically reacts with mutant E-cadherin lacking exon 9 but not with the wild-type protein for allele-specific examination of wild-type and mutant E-cadherin.

Mutant E-Cadherin as a Therapeutic Target

Mutant E-cadherin variants could serve as targets for individualized cancer therapy (Becker and Hofler, 2001). As a cancer-associated mutant cell-surface molecule, E-cadherin is an attractive candidate to target tumor cells. Monoclonal antibodies against E-cadherin lacking exon 8 or 9 (Becker and Hofler, 2001; Becker *et al.,* 1999) could be linked to toxins or drugs or could be radiolabeled to enable selective and effective tumor-cell killing in a subgroup of patients expressing the respective E-cadherin mutations. A monoclonal antibody directed against a mutant E-cadherin lacking exon 9 was conjugated with the high-linear–energy transfer α-emitter 213Bi and tested for its binding specificity in s.c. and i.p. nude mice tumor models (Huber *et al.,* 2003; Senekowitsch-Schmidtke *et al.,* 2001). The therapeutic efficacy of the 213Bi conjugated monoclonal antibody together with a low bone marrow toxicity support the potential of locoregional therapy for the subgroup of patients expressing E-cadherin lacking exon 9.

MATERIALS

Required materials are slides (Dako Cytomation, Glostrup, Denmark), xylene, 70%, 96% and 100% ethanol; 3% hydrogen peroxide; 1% bovine serum albumin; and hemalaun. Required buffers are citric acid (2.1 g citric acid monohydrate in 1 L ddH_2O, pH 6.0) and PBS (phosphate buffer saline). The following antibodies are used for immunohistochemical detection of E-cadherin: monoclonal antibodies against wild-type E-cadherin clone 36 (Transduction Laboratories, Lexington, KY, dilution 1:1000) and HECD-1 (Alexis Deutschland, Grünberg, Germany, dilution 1:500); monoclonal rat E-cad delta 8-1 antibody, reacting with mutant E-cadherin protein lacking exon 8 (*del 8* mutation); clone 6D8 (Becker *et al.,* 2002), dilution 1:5 in 1% bovine serum albumin; monoclonal rat E-cad delta 9-1 detecting mutant E-cadherin protein lacking exon 9 (*del 9* mutation); and clone 7E6 (Becker *et al.,* 1999), undiluted, E9 (undiluted hybridoma supernatant, a gift from Margaret Wheelock, University of Nebraska Medical Center, Omaha, NE). For IHC, the avidin-biotin complex (ABC) peroxidase method (ABC Elite Kit, Vector, Burlingame, CA, USA) was applied and the Sigma FAST DAB peroxidase substrate kit (Sigma, Deisenhofen, Germany) was used.

METHODS

Staining of Paraffin-Embedded Tumor Sections with Antibody Directed to Wild-Type E-Cadherin or Mutant E-Cadherin Lacking Exon 8 or 9

1. Incubate tissue sections overnight at 44–60°C in an incubator.
2. Deparaffinize and hydrate tissue sections through xylene and graded alcohol:
   - 2 × 10 min Xylene
   - 2 × 2 min 100% ethanol
   - 2 × 2 min 96% ethanol
   - 2 × 2 min 70% ethanol
   - ddH_2O
3. Pretreatment: cook for 4 min in citrate buffer under high pressure or heat in microwave 3 × 5 min in citrate buffer.
4. Allow to cool down for 5–10 min.
5. Rinse 3× with PBS.
6. Quench endogenous peroxidase activity by incubation with 3% H_2O_2 for 10 min.
7. Rinse 3× with PBS.
8. Dilute the primary antibodies in PBS with 1% bovine serum albumin as described in Materials, and incubate for 1 hr in a humid chamber at room temperature.

9. Rinse 3× with PBS.
10. Incubate sections for 30 min with the diluted biotinylated secondary antibody.
11. Rinse 3× with PBS.
12. Incubate sections with Vectastain Elite ABC reagent at room temperature.
13. Rinse 3× with PBS.
14. Incubate sections in peroxidase substrate solution DAB (diaminobenzidene) until desired stain intensity develops.
15. Rinse sections in water.
16. Counterstain with hemalaun for 7 sec.
17. Rinse sections in water.
18. Dehydrate in an alcohol line:
    2 × 2 min 70% ethanol
    2 × 2 min 96% ethanol
    2 × 2 min 100% ethanol
    2 × 10 min Xylene
19. Mount sections, and cover the slides (Pertex).
20. If quantification of E-cadherin staining is envisaged, 10 representative high-power fields are counted for each antibody staining and the percentage of positive tumor cells is calculated (Fricke *et al.,* 2003). For qualitative analysis of the E-cadherin staining pattern, three different staining patterns are analyzed: 1) normal, 2) abnormal (including *atypical* with partial membrane staining and cytoplasmic staining and *heterogeneous* staining with positive and negative tumor cells in the same slide), or 3) negative staining (Gamboa-Dominguez *et al.,* 2005).
21. Immunohistochemical evaluation should be performed by at least two pathologists with experience in gastrointestinal pathology.

RESULTS AND DISCUSSION

Expression of Mutant E-Cadherin Lacking Exon 8 or 9 Correlates with Poor Survival in Diffuse-Type Gastric Carcinoma

We have performed immunohistochemical examination of wild-type and mutant E-cadherin expression in 177 gastrectomies from Mexican mestizo patients (Gamboa-Dominguez *et al.,* 2005). Of gastric carcinomas, 53 were of the intestinal type, 55 were mixed, and 69 were of the diffuse type according to the Laurén classification. In addition, 101 endoscopic biopsies from patients with gastric cancer without surgery were investigated.

The IHC test was performed with antibody clone 36, which reacts with wild-type E-cadherin. This antibody recognizes the intracellular part of E-cadherin and allows the classification of the E-cadherin staining pattern into the categories normal (membranous), abnormal (atypical or heterogeneous), or negative. However, use of this antibody does not allow discrimination between wild-type E-cadherin or mutant E-cadherin variants lacking exon 8 or 9 or harboring other genetic alterations in the extracellular domain of the molecule. Therefore, IHC was also performed with two mutation-specific antibodies recognizing the exon 8 or 9 deletion mutants (Becker *et al.,* 1999; Becker *et al.,* 2002). All cases that were positive with antibody E-cad delta 8-1 were investigated subsequently with HECD-1 antibody to show if the wild-type allele is present or lost. Similarly, cases positive with antibody E-cad delta 9-1 were investigated also with E9 antibody to determine allelic loss of the second allele. Figure 34 shows an example of gastric cancer samples with normal E-cadherin staining both in tumor cells and in residual normal glands *(A),* heterogeneous staining for wild-type E-cadherin *(B),* absence of wild-type E-cadherin in the tumor *(C),* tumor cell staining with E-cad delta 8-1 *(D),* and E-cad delta 9-1 *(E,F)* antibodies.

As reported previously (Gamboa-Dominguez *et al.,* 2005), E-cadherin staining was correlated with histotype, nodal status, and follow-up. Abnormal or absent E-cadherin expression determined with E-cadherin antibody clone 36 was identified in 84% of the investigated gastric cancer samples, predominantly in tumors of the diffuse or mixed type ($p = 0.004$) in advanced stages ($p = 0.003$). This result is in accordance with previous reports that irregular E-cadherin staining is more prevalent in diffuse- or mixed-type gastric cancer than in the intestinal type (Jawhari *et al.,* 1997; Zhou *et al.,* 2002).

One major aim of this study was to determine whether normal, abnormal, or negative E-cadherin expression have an impact on patient survival. No survival differences at 1 and 2 years were detectable among patients showing normal, abnormal, or absent E-cadherin expression as determined with E-cadherin clone 36 antibody. These results support previous findings that abnormal E-cadherin expression has no major impact on survival (Jawhari *et al.,* 1997; Zhou *et al.,* 2002).

As discussed earlier, E-cadherin mutations might escape from detection using E-cadherin clone 36 antibody. Therefore, immunohistochemical detection with antibodies E-cad delta 8-1 and E-cad delta 9-1 were performed. Overall reactivity with these antibodies was detected in 5.6% of patients treated with surgery. In 140 patients, dead from the disease or alive with the disease, the survival at 1 and 2 years was 37% versus 17% and 14% versus 0 for patients without and with positivity for E-cadherin lacking exon 8 or 9, respectively (log rank $p = 0.01$). delta 8-1 and E-cad delta 9-1

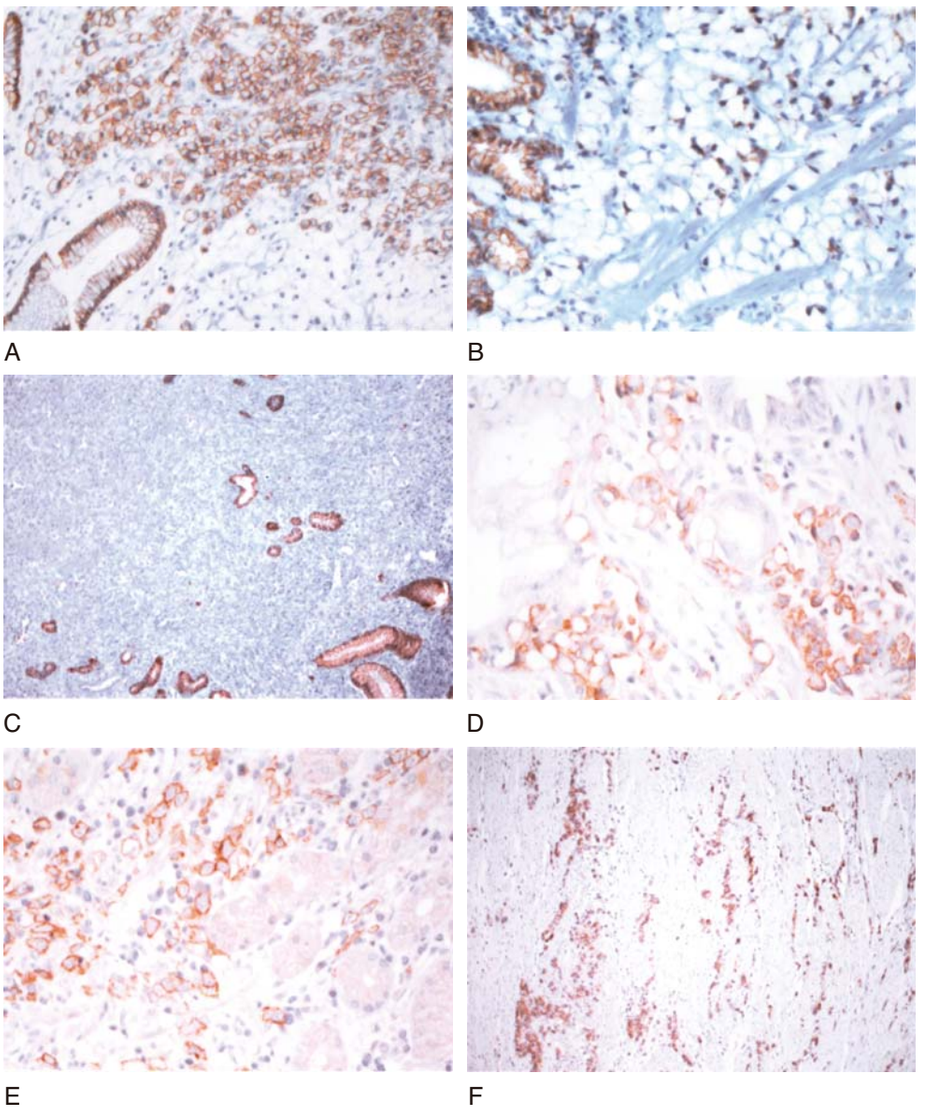

Figure 34. Immunohistochemical staining of E-cadherin in diffuse-type gastric cancer. **A:** Normal membrane staining for wild-type E-cadherin (clone 36) in the neoplastic cells and in residual normal glands *(lower left)*. **B:** Heterogeneous staining for wild-type E-cadherin in a carcinoma with predominance of signet ring cells. Note the normal glands on the left. **C:** Complete absence of wild-type E-cadherin; only residual glands show positive staining. **D:** Staining with delta 8-1 antibody recognizing E-cadherin lacking exon 8. Note negativity of residual normal glands. **E, F:** Staining with delta 9-1 antibody recognizing E-cadherin lacking exon 9. Both intramucosal and intramural tumor cells show strong membrane staining, whereas normal glands remain negative.

reactivity in biopsies from patients with inoperable gastric cancer was 4.95%. These data show for the first time that expression of mutant E-cadherin variants lacking exon 8 or 9 is associated with a worse prognosis. The results also indicate the value of IHC for a rapid determination of mutant E-cadherin variants as a screening method for patients who may benefit from an antibody-based therapy.

References

Batlle, E., Sancho, E., Franci, C., Dominguez, D., Monfar, M., Baulida, J., and Garcia De Herreros, A. 2000. The transcription factor snail is a repressor of E-cadherin gene expression in epithelial tumour cells. *Nat. Cell Biol. 2*:84–89.

Becker, I., Becker, K.F., Rohrl, M.H., Minkus, G., Schutze, K., and Hofler, H. 1996. Single-cell mutation analysis of tumors from stained histologic slides. *Lab. Invest. 75*:801–807.

Becker, K.F., Atkinson, M.J., Reich, U., Becker, I., Nekarda, H., Siewert, J.R., and Hofler, H. 1994. E-cadherin gene mutations provide clues to diffuse type gastric carcinomas. *Cancer Res. 54*:3845–3852.

Becker, K.F., Atkinson, M.J., Reich, U., Huang, H.H., Nekarda, H., Siewert, J.R., and Hofler, H. 1993. Exon skipping in the E-cadherin gene transcript in metastatic human gastric carcinomas. *Hum. Mol. Genet. 2*:803–804.

Becker, K.F., and Hofler, H. 1995. Frequent somatic allelic inactivation of the E-cadherin gene in gastric carcinomas. *J. Natl. Cancer Inst. 87*:1082–1084.

Becker, K.F., and Hofler, H. 2001. Mutant cell surface receptors as targets for individualized cancer diagnosis and therapy. *Curr. Cancer Drug Targets 1*:121–128.

Becker, K.F., Kremmer, E., Eulitz, M., Becker, I., Handschuh, G., Schuhmacher, C., Muller, W., Gabbert, H.E., Ochiai, A., Hirohashi, S., and Holler, H. 1999. Analysis of E-cadherin in diffuse-type gastric cancer using a mutation-specific monoclonal antibody. *Am. J. Pathol. 155*:1803–1809.

Becker, K.F., Kremmer, E., Eulitz, M., Schulz, S., Mages, J., Handschuh, G., Wheelock, M.J., Cleton-Jansen, A.M., Holler, H., and Becker, I. 2002. Functional allelic loss detected at the protein level in archival human tumours using allele-specific E-cadherin monoclonal antibodies. *J. Pathol. 197*: 567–574.

Behrens, J., von Kries, J.P., Kuhi, M., Bruhn, L., Wedlich, D., Grosschedl, R., and Birchmeier, W. 1996. Functional interaction of beta-catenin with the transcription factor LEF-1. *Nature 382*: 638–642.

Berx, G., Becker, K.F., Hofler, H., and van Roy, F. 1998. Mutations of the human E-cadherin (CDH1) gene. *Hum. Mutat. 12*:226–237.

Berx, G., Staes, K., van Hengel, J., Molemans, F., Bussemakers, M.J., van Bokhoven, A., and van Roy, F. 1995. Cloning and characterization of the human invasion suppressor gene E-cadherin (CDH1). *Genomics 26*:28l–289.

Birchmeier, W., and Behrens, J. 1994. Cadherin expression in carcinomas: role in the formation of cell junctions and the prevention of invasiveness. *Biochim. Biophys. Acta 1198*:11–26.

Comijn, J., Berx, G., Vermassen, P., Verschueren, K., van Grunsven, L., Bruyneel, E., Mareel, M., Huylebroeck, D., and van Roy, F. 2001. The two-handed E box binding zinc finger protein SlP1 downregulates E-cadherin and induces invasion. *Mol. Cell 7*:1267–1278.

Crawford, H.C., Fingleton, B.M., Rudolph-Owen, L.A., Goss, K.J., Rubinfeld, B., Polakis, P., and Matrisian, L.M. 1999. The metalloproteinase matrilysin is a target of beta-catenin transactivation in intestinal tumors. *Oncogene 18*:2883–2891.

Fricke, E., Keller, G., Becker, I., Rosivatz, E., Schott, C., Plaschke, S., Rudelius, M., Hermannstadter, C., Busch, R., Hofler, H., Becker, K.F., and Luber, B. 2003. Relationship between E-cadherin gene mutation and p53 gene mutation, p53 accumulation, Bcl-2 expression and Ki-67 staining in diffuse-type gastric carcinoma. *Int. J. Cancer 104*:60–65.

Fuchs, M., Hutzler, P., Brunner, I., Schlegel, J., Mages, J., Reuning, U., Hapke, S., Duyster, J., Hirohashi, S., Genda, T., Sakamoto, M., Uberall, F., Hofler, H., Becker, K.F., and Luber, B. 2002. Motility enhancement by tumor-derived mutant E-cadherin is sensitive to treatment with epidermal growth factor receptor and phosphatidylinositol 3-kinase inhibitors. *Exp. Cell Res. 276*:129–141.

Fujita, Y., Krause, G., Scheffner, M., Zechner, D., Leddy, H.E., Behrens, J., Sommer, T., and Birchmeier, W. 2002. Hakai, a c-Cbl-like protein, ubiquitinates and induces endocytosis of the E-cadherin complex. *Nat. Cell Biol. 4*:222–231.

Gabbert, H.E., Mueller, W., Schneiders, A., Meier, S., Moll, R., Birchmeier, W., and Hommel, G. 1996. Prognostic value of E-cadherin expression in 413 gastric carcinomas. *Int. J. Cancer 69*:184–189.

Gamboa-Dominguez, A., Dominguez-Fonseca, C., Chavarri-Guerra, Y., Vargas, R., Reyes-Gutierrez, E., Green, D., Quintanilla-Martinez, L., Luber, B., Busch, R., Becker, K.F., Becker, I., Hofler, H., and Fend, F. 2005. E-cadherin expression in sporadic gastric cancer from Mexico: Exon 8 and 9 deletions are infrequent events associated with poor survival. *Hum. Pathol. 36*:29–35.

Gayther, S.A., Gorringe, K.L., Ramus, S.J., Huntsman, D., Roviello, F., Grehan, N., Machado, J.C., Pinto, E., Seruca, R., Hailing, K., MacLeod, P., Powell, S.M., Jackson, C.E., Ponder, B.A., and Caldas, C. 1998. Identification of germ-line E-cadherin mutations in gastric cancer families of European origin. *Cancer Res. 58*:4086–4089.

Grady, W.M., Willis, J., Guilford, P.J., Dunbier, A.K., Toro, T.T., Lynch, H., Wiesner, G., Ferguson, K., Eng, C., Park, J.G., Kim, S.J., and Markowitz, S. 2000. Methylation of the CDH 1 promoter as the second genetic hit in hereditary diffuse gastric cancer. *Nat. Genet. 26*:16–I7.

Guilford, P., Hopkins, J., Harraway, J., McLeod, M., McLeod, N., Harawira, P., Taite, H., Scoular, R., Miller, A., and Reeve, A.E. 1998. E-cadherin germline mutations in familial gastric cancer. *Nature 392*:402–405.

Gumbiner, B.M. 2000. Regulation of cadherin adhesive activity. *J. Cell Biol. 148*:399–404.

Handschuh, C., Candidus, S., Luber, B., Reich, U., Schott, C., Oswald, S., Becke, H., Hutzler, P., Birchmeier, W., Hofler, H., and Becker, K.F. 1999. Tumour-associated E-cadherin mutations alter cellular morphology, decrease cellular adhesion and increase cellular motility. *Oncogene 18*:4301–4312.

He, T.C., Sparks, A.B., Rago, C., Hermeking, H., Zawel, L., da Costa, L.T., Morin, P.J., Vogelstein, B., and Kinzler, K.W. 1998. Identification of c-MYC as a target of the APC pathway. *Science 281*:1509–1512.

Huber, O., Korn, R., McLaughlin, J., Ohsugi, M., Herrmann, B.G., and Kemler, R. 1996. Nuclear localization of beta-catenin by interaction with transcription factor LEF-1. *Mech. Dev. 59*:3–10.

Huber, R., Seidl, C., Schmid, E., Seidenschwang, S., Becker, K.F., Schuhmacher, C., Apostolidis, C., Nikula, T., Kremmer, E., Schwaiger, M., and Senekowitsch-Schmidtke, R. 2003. Locoregional alpha-radioimmunotherapy of intraperitoneal tumor cell dissemination using a tumor-specific monoclonal antibody. *Clin. Cancer Res. 9*:3922S–3928S.

Jawhari, A., Jordan, S., Poole, S., Browne, P., Pignatelli, M., and Farthing, M.J. 1997. Abnormal immunoreactivity of the E-cadherin-catenin complex in gastric carcinoma: relationship with patient survival. *Gastroenterology 112*:46–54.

Kamei, T., Matozaki, I., Sakisaka, T., Kodama, A., Yokoyama, S., Peng, Y.F., Nakano, K., Takaishi, K., and Takai, Y. 1999. Coendocytosis of cadherin and c-Met coupled to disruption of cell-cell adhesion in MDCK cells: regulation by Rho, Rac and Rab small G proteins. *Oncogene 18*:6776–6784.

Keller, G., Vogelsang, H., Becker, I., Hutter, J., Ott, K., Candidus, S., Grundei, T., Becker, K.F., Mueller, J., Siewert, J.R., and Hofler, H. 1999. Diffuse type gastric and lobular breast carcinoma in a familial gastric cancer patient with an E-cadherin germline mutation. *Am. J. Pathol. 155*:337–342.

Kremer, M., Quintanilla-Martinez, L., Fuchs, M., Gamboa-Dominguez, A., Haye, S., Kalthoff, H., Rosivatz, E., Hermannstadter, C., Busch, R., Hofler, H., and Luber, B. 2003. Influence of tumor-associated E-cadherin mutations on tumorigenicity and metastasis. *Carcinogenesis 24*:1879–1886.

Lu, Z., Ghosh, S., Wang, Z., and Hunter, I. 2003. Downregulation of caveolin-1 function by EGF leads to the loss of E-cadherin, increased transcriptional activity of beta-catenin, and enhanced tumor cell invasion. *Cancer Cell 4*:499–515.

Luber, B., Candidus, S., Handschuh, G., Mentele, E., Hutzler, P., Feller, S., Voss, J., Hofler, H., and Becker, K.F. 2000. Tumor-derived mutated E-cadherin influences beta-catenin localization and increases susceptibility to actin cytoskeletal changes induced by pervanadate. *Cell Adhes. Commun. 7*:391–408.

Machado, J.C., Oliveira, C., Carvalho, R., Soares, P., Berx, G., Caldas, C., Seruca, R., Carneiro, F., and Sobrinho-Simoes, M. 2001. E-cadherin gene (CDH1) promoter methylation as the second hit in sporadic diffuse gastric carcinoma. *Oncogene 20*: 1525–1528.

Machado, J.C., Soares, P., Carneiro, F., Rocha, A., Beck, S., Blin, N., Berx, G., and Sobrinho-Simoes, M. 1999. E-cadherin gene mutations provide a genetic basis for the phenotypic divergence of mixed gastric carcinomas. *Lab. Invest. 79*:459–465.

Mann, B., Gelos, M., Siedow, A., Hanski, M.L., Gratchev, A., Ilyas, M., Bodmer, W.F., Moyer, M.P., Riecken, E.O., Buhr, H.J., and Hanski, C. 1999. Target genes of beta-catenin-T cell-factor/lymphoid-enhancer-factor signaling in human colorectal carcinomas. *Proc. Natl. Acad. Sci. USA 96*:1603–1608.

Mansouri, A., Spurr, N., Goodfellow, P.N., and Kemler, R. 1988. Characterization and chromosomal localization of the gene encoding the human cell adhesion molecule uvomorulin. *Differentiation 38*:67–71.

Mayer, B., Johnson, J.P., Leitl, F., Jauch, K.W., Heiss, M.M., Schildberg, F.W., Birchmeier, W., and Funke, I. 1993. E-cadherin expression in primary and metastatic gastric cancer: down-regulation correlates with cellular dedifferentiation and glandular disintegration. *Cancer Res. 53*:1690–1695.

Meiners, S., Brinkmann, V., Naundorf, H., and Birchmeier, W. 1998. Role of morphogenetic factors in metastasis of mammary carcinoma cells. *Oncogene 16*:9–20.

Molenaar, M., van de Wetering, M., Oosterwegel, M., Peterson-Maduro, J., Godsave, S., Korinek, V., Roose, J., Destree, O., and Clevers, H. 1996. XTcf-3 transcription factor mediates beta-catenin-induced axis formation in Xenopus embryos. *Cell 86*:391–399.

Morin, P.J., Sparks, A.B., Korinek, V., Barker, N., Clevers, H., Vogelstein, B., and Kinzler, K.W. 1997. Activation of beta-catenin-Tcf signaling in colon cancer by mutations in beta-catenin or APC. *Science 275*:1787–1790.

Natt, E., Magenis, R.E., Zimmer, J., Mansouri, A., and Scherer, G. 1989. Regional assignment of the human loci for uvomorulin (UVO) and chymotrypsinogen B (CTRB) with the help of two overlapping deletions on the long arm of chromosome 16. *Cytogenet. Cell Genet. 50*:145–148.

Risinger, J.I., Berchuck, A., Kohler, M.F., and Boyd, J. 1994. Mutations of the E-cadherin gene in human gynecologic cancers. *Nat. Genet. 7*:98–102.

Rosivatz, E., Becker, I., Specht, K., Fricke, E., Luber, B., Busch, R., Hofler, H., and Becker, K.F. 2002. Differential expression of the epithelial-mesenchymal transition regulators snail, SIP1, and twist in gastric cancer. *Am. J. Pathol. 161*:1881–1891.

Rubinfeld, B., Robbins, P., El-Gamil, M., Albert, I., Porfiri, E., and Polakis, P. 1997. Stabilization of beta-catenin by genetic defects in melanoma cell lines. *Science 275*:1790–1792.

Senekowitsch-Schmidtke, R., Schuhmacher, C., Becker, K.F., Nikula, T.K., Seidl, C., Becker, I., Miederer, M., Apostolidis, C., Adam, C., Huber, R., Kremmer, E., Fischer, K., and Schwaiger, M. 2001. Highly specific tumor binding of a 213Bi-labeled monoclonal antibody against mutant E-cadherin suggests its usefulness for locoregional alpha-radioimmunotherapy of diffuse-type gastric cancer. *Cancer Res. 61*:2804–2808.

Shino, Y., Watanabe, A., Yamada, Y., Tanase, M., Yamada, T., Matsuda, M., Yamashita, J., Tatsumi, M., Miwa, T., and Nakano, H. 1995. Clinicopathologic evaluation of immunohistochemical E-cadherin expression in human gastric carcinomas. *Cancer 76*:2193–2201.

Shtutman, M., Zhurinsky, J., Simcha, I., Albanese, C., D'Amicó, M., Pestell, R., and Ben-Ze'ev, A. 1999. The cyclin D1 gene is a target of the beta-catenin/LEF-1 pathway. *Pro. Natl. Acad. Sci. USA 96*:5522–5527.

Soares, P., Berx, G., van Roy, F., and Sobrinho-Simoes, M. 1997. E-cadherin gene alterations are rare events in thyroid tumors. *Int. J. Cancer 70*:32–38.

Tetsu, O., and McCormick, F. 1999. Beta-catenin regulates expression of cyclin D1 in colon carcinoma cells. *Nature 398*: 422–426.

Thoreson, M.A., Anastasiadis, P.Z., Daniel, J.M., Ireton, R.C., Wheelock, M.J., Johnson, K.R., Hummingbird, D.K., and Reynolds, A.B. 2000. Selective uncoupling of p120(ctn) from E-cadherin disrupts strong adhesion. *J. Cell Biol. 148*:189–202.

Van Aken, E., De Wever, O., Correia da Rocha, A.S., and Mareel, M. 2001. Defective E-cadherin/catenin complexes in human cancer. *Virchows Arch. 439*:725–751.

Yamada, T., Takaoka, A.S., Naishiro, Y., Hayashi, R., Maruyama, K., Maesawa, C., Ochiai, A., and Hirohashi, S. 2000. Transactivation of the multidrug resistance 1 gene by T-cell factor 4/beta-catenin complex in early colorectal carcinogenesis. *Cancer Res. 60*:4761–4766.

Yonemura, Y., Ninomiya, I., Kaji, M., Sugiyama, K., Fujimura, T., Tsuchihara, K., Kawamura, T., Miyazaki, I., Endou, Y., Tanaka, M., and Sasaki, T. 1995. Decreased E-cadherin expression correlates with poor survival in patients with gastric cancer. *Anal. Cell Pathol. 8*:177–190.

Zhou, Y.N., Xu, C.P., Han, B., Li, M., Qiao, L., Fang, D.C., and Yang, J.M. 2002. Expression of E-cadherin and beta-catenin in gastric carcinoma and its correlation with the clinicopathological features and patient survival. *World J. Gastroenterol. 8*:987–993.

This Page Intentionally Left Blank

12

Role of Immunohistochemical Expression of Adenomatous Polyposis Coli and E-Cadherin in Gastric Carcinoma

Christian Gulmann, Anthony O'Grady, and Elaine Kay

Introduction

Several lines of evidence link abnormalities in expression of adenomatous polyposis coli (APC) and epithelial (E)-cadherin proteins with gastric carcinogenesis (Gulmann *et al.,* 2003). As outlined later in this chapter, the two molecules interact and are involved in both tumor initiation and progression (Shino *et al.,* 1995). Immunohistochemical staining for both proteins is well established, and many reliable commercial antibodies are available. Mutation-specific antibodies to E-cadherin have been described (Becker *et al.,* 1999) and may eventually have diagnostic and even therapeutic potentials (Becker *et al.,* 2000). So far, however, they are not widely used.

The protein APC is a 312-kDa protein that is expressed in most normal somatic tissues (Midgley *et al.,* 1997). It is engaged in several cellular processes, including cell cycle regulation, apoptosis, cell adhesion, cell migration, and signal transduction (Polakis, 1997). A key function is down-regulation of the Wnt signaling pathway via degradation of beta-catenin, and mutations of the APC gene are reflected in increased intracellular levels of beta-catenin (Kikuchi, 2003). Mutations of the APC gene are frequent in gastric cancer, and most known mutations of the APC gene generate a truncated protein product that lacks the carboxy-terminal sequences. This is similar to the germline mutation found in familial adenomatous polyposis (FAP) syndrome (Midgley *et al.,* 1997). It is interesting that this region includes the binding site for beta-catenin (Ilyas and Tomlinson, 1997).

Up to 50% of well-differentiated cancers show APC gene mutations (Nakatsuru *et al.,* 1992), and a previous study from this institution showed lack of immunohistochemical staining in 78% of gastric cancers (Grace *et al.,* 2002). The APC mutations are thought to be of particular importance in initiation of gastric carcinogenesis (Grace *et al.,* 2002). Tamura *et al.* (1994) found mutations of the APC gene in 6 of 30 gastric adenomas. According to Correa's multistep model, intestinal metaplasia is believed to be an important early step in gastric carcinogenesis (Correa, 1992). It is therefore of interest that some studies demonstrate mutations of the APC gene at the stage of intestinal metaplasia (Tahara *et al.,* 1994). In a study by Nishimura *et al.* (1995), 6% of cases of intestinal metaplasia showed *APC* gene mutations. Another study found loss of heterozygosity

Handbook of Immunohistochemistry and *in situ* Hybridization of Human Carcinomas, Volume 4: Molecular Genetics, Gastrointestinal Carcinoma, and Ovarian Carcinoma

(LOH) within the region coding for APC in 6 of 33 cases of intestinal metaplasia adjacent to cancer (Kobayashi *et al.,* 2000). Inactivation of APC may also be more frequent in intestinal-type than in diffuse-type cancers (Nakatsuru *et al.,* 1992), although the reason for this is not well explained.

E-cadherin, a 120 kDa protein, is a calcium-dependent cell-adhesion molecule located in the cytoplasmic membrane and is found mainly in epithelial cells. It is a member of the cadherin family and plays an essential role in maintaining epithelial tissue integrity (Birchmeier and Behrens, 1994), and abnormal E-cadherin function has been linked with increased invasiveness of carcinomas. Mutations in the gene coding for E-cadherin usually result in either in-frame deletions (removing parts of the extracellular portions of the transmembrane protein) or point mutations. In contrast to APC inactivation, epigenetic changes appear to play significant roles in E-cadherin inactivation (Ascano *et al.,* 2001), and hypermethylation of promoter regions has been recorded in the majority of diffuse-type gastric cancers (Strathdee, 2002). Given the role of E-cadherin in cell–cell adhesion, loss of expression is more common in diffuse-type cancers (Karayiannakis *et al.,* 1998). Mutations in the gene encoding for E-cadherin have been identified in up to 50% of diffuse gastric cancers (Becker *et al.,* 1994), and in a study of 83 cancer specimens, Karayiannakis *et al.* (1998) found abnormal E-cadherin immunohistochemical expression in 96% of diffuse versus 47% of intestinal cancers. Reduced expression may be related to increased invasiveness and lymph-node metastases (Shino *et al.,* 1995), although this is not noted by all workers (Blok *et al.,* 1999). Several groups have found that reduced E-cadherin expression in gastric cancer correlates with poor survival (Jawhari *et al.,* 1997, Shino *et al.,* 1995). Although most research has focused on the role of E-cadherin in suppression of invasiveness and metastases (i.e., in established cancers), there is evidence that it may play a role at a much earlier stage of tumor development. E-cadherin inactivation is often found at an early stage in cancer invasion (Chan *et al.,* 2003). Germline mutations in the gene coding for E-cadherin are associated with familial forms of gastric cancer (Guilford *et al.,* 1998), and some groups have reported loss of expression of E-cadherin in preneoplastic conditions including in intestinal metaplasia (Blok *et al.,* 1999). In a study by Chan *et al.* (2003), methylation of the E-cadherin gene was found in 12 of 21 cases of intestinal metaplasia associated with cancer, although this corresponded poorly to lack of E-cadherin staining. This suggests that E-cadherin has a role in tumor initiation via regulation of cell cycle control, which may be via interaction between E-cadherin and α- and β-catenins. E-cadherin forms a complex with both, and through α-catenin it is anchored to the cytoskeleton (Ilyas and Tomlinson, 1997). Loss of E-cadherin function may therefore lead to increased release of β-catenin into the cytoplasm, thus modulating Wnt-mediated signaling (Strathdee, 2002).

As mentioned earlier, the functions of E-cadherin and APC are interlinked via competition for the interaction with beta-catenin and the cytoskeleton (Hulsken *et al.,* 1994). In the steady state, free beta-catenin is thought to be in equilibrium with APC and E-cadherin. Truncated APC may still bind beta-catenin, rendering the latter incapable of engaging in a complex with E-cadherin and thereby altering E-cadherin function (Ilyas and Tomlinson, 1997). This may be important in tumor initiation. It would also explain why some studies fail to detect loss of E-cadherin expression in early carcinogenesis because the molecule is still expressed at normal levels.

MATERIALS

1. Adhesive slides (Snowcoat X-tra slides cat# 00201, Surgipath, Richmond, IL).
2. Hydrogen peroxide solution: add 6 ml of 30% w/v hydrogen peroxide (BDH 10128) to 194 ml of methanol and mix well before adding to the slides.
3. 0.01M Sodium citrate buffer, pH 6.0: add 8.82 g Tri-sodium citrate (BDH 10242) to 2.9 L of deionized water. Adjust pH to 6.0 with HCl. Make up to 3 L with deionized water.
4. 0.05 M Tris buffered saline (TBS): add 6.06 g Tris (BDH 103156X) and 8.76 g sodium chloride (BDH 102415K) to 900 ml distilled water. Adjust pH to 7.6 with HCl. Add 500 µl Tween 20 (BDH 663684B) and make up to 1 L with deionized water.
5. Normal goat serum (Cat No.X0907, Dako Cytomation, Glostrup, Denmark).
6. E-Cadherin Clone 36B5 (Novocastra Laboratories Ltd., Newcastle-upon-Tyne, UK). Dilute 1:30 with TBS.
   Other E-cadherin antibodies:
   - Mouse anti-E-Cadherin Clone 6F9 (Abcam Ltd. Cat No. ab167).
   - Mouse anti-E-Cadherin Clone 5H9 (Research Diagnostics Inc., Flanders, NJ, Cat No. RDI-PRO10028).
   - Mouse anti-E-Cadherin Clone 4A2C7 (Zymed Laboratories Inc., San Francisco, CA, Cat No. 18-0223).
   - Mouse anti-E-Cadherin Clone ECH-6 (Cell Marque Corporation Hot Springs, Ar, Cat No. CMA580).
   - Rabbit anti-E-Cadherin (Labvision Corporation, Fremont, CA, Cat No. RB-9214-P).
7. APC Clone sc-896 K (Santa Cruz Biotechnology Inc., Santa Cruz, CA). Dilute 1:500 with TBS.

Other APC antibodies:

Rabbit anti-APC (Labvision Corporation, Fremont, CA, Cat No. RB-9276-P; also available from Spring BioScience, Cat No. E4084).

8. Secondary antibody and ABC (avidin-bistin complex): Vector Elite kit cat No. PK-6200 (Vector Laboratories, Burlingame, CA).

9. DAB (3,3′-diaminobenzidine) tablets Cat No. S3000, DakoCytomation. Prepare working solution by adding 1 tablet to 10 ml 0.05 M Tris buffer containing 75 µl 3% hydrogen peroxide.

10. Harris' hematoxylin Cat No. RBA4213-00A (CellPath plc, Newtown, U.K.).

METHODS

The same method is used for both antibodies.

1. Cut sections onto adhesive slides, allow to drain, and dry overnight at 55°C.
2. Immerse the slides in 2 changes of xylene for 5 min each with agitation to dewax the sections.
3. Immerse the slides in 2 changes of absolute alcohol for 5 min each with agitation to dehydrate the sections.
4. Rinse the slides in distilled water for 5 min.
5. Immerse the slides for 10 min in hydrogen peroxide solution to block endogenous peroxidase.
6. Rinse the slides in distilled water for 5 min.
7. Carry out heat-induced epitope retrieval as follows:
   a. Bring 3 L of 0.01 M sodium citrate buffer to the boil in a pressure cooker.
   b. Lower a 24-slot metal rack containing a maximum of 12 evenly spaced slides beneath the buffer.
   c. Incubate the sections at full pressure for 1.5 min.
   d. Cool the slides by filling the pressure cooker with cold distilled water.
8. Place the slides in an incubation tray and wash 2× in TBS for 3 min, ensuring the whole section is covered at all times.
9. Carefully dry around the sections with a tissue, and apply normal goat serum diluted 1/10 with TBS. Replace the immuno tray lid, and incubate the sections for 40 min.
10. Drain the excess serum from the slides, and apply the primary antibody (rabbit anti-APC or mouse anti-E-cadherin) to the test sections. Cover the negative control sections with TBS. Replace the immuno tray lid, and incubate the sections for 1 hr at room temperature.
11. Wash the slides in TBS for 10 min.
12. Prepare the secondary antibody solution by adding 20 µl biotinylated universal antibody and 20 µl normal goat serum to 1 ml TBS.
13. Carefully dry around the sections with a tissue, and apply the secondary antibody to all sections. Replace the immuno tray lid and incubate the sections for 40 min.
14. Rinse as in **Step 11.**
15. Prepare the ABC complex solution by adding 20 µl reagent A and 20 µl reagent B to 1 ml TBS. **The ABC complex solution must be prepared 30 min before use.**
16. Carefully dry around the sections with a tissue and apply the ABC complex to all sections. Incubate the sections for 40 min.
17. Rinse as in **Step 11.**
18. Prepare the DAB working solution and incubate all sections in the solution for 10 min.
19. Rinse the slides with distilled water.
20. Counterstain the sections in Harris' hematoxylin.
21. Dehydrate, clear, and coverslip the sections.

RESULTS

In tissues with normal APC expression, immunohistochemical staining for APC shows a diffuse cytoplasmic pattern. In the normal stomach, APC can be detected using antibodies, which typically decorate epithelial cells in a diffuse cytoplasmic pattern with accentuation of luminal and basal cells in the glandular mucosa (Midgley *et al.,* 1997). Abnormal APC function is associated with loss of staining (Grace *et al.,* 2002; Gulmann *et al.,* 2003). An important caveat is that truncated APC may be expressed. Because this most frequently involves the carboxy-terminal of the molecule (Nagase and Nakamura, 1993), antibodies designed to detect abnormalities in APC expression should target that region to be able to equate loss of immunohistochemical expression with loss of function of APC.

Immunohistochemical staining for E-cadherin reflects its subcellular location and shows a strong membranous pattern in normal epithelium. Abnormal patterns show either absent, diffuse cytoplasmic or occasionally coarse granular cytoplasmic staining of cells (Carpenter *et al.,* 2002). A study of 173 gastric cancers revealed paranuclear E-cadherin immunostaining in 24% of cases, most frequently in diffuse or mixed-type cancers (Carpenter *et al.,* 2002). This may reflect a defect in transport of molecules to the cell surface. Numerous antibodies to E-cadherin have been described (Shimoyama *et al.,* 1989), and although detectable E-cadherin immunoreactivity suggests a functional protein, this may not always be the case. Defective, mutant E-cadherin may be transcribed and has been reported to retain its antigenicity to various commercially available antibodies (Becker *et al.,* 2000).

Most studies describe homogeneous immunohistochemical expression patterns of both molecules in

normal mucosa as well as in intestinal metaplasia (Jawhari *et al.,* 1997). Cancers may be more heterogeneous. Mixed-diffuse and intestinal-type cancers often show absent E-cadherin staining in the diffuse component combined with preserved expression in the intestinal component (Jawhari *et al.,* 1997). Homogeneous gastric tumors may also, however, display focal E-cadherin staining (Carpenter *et al.,* 2002). Studies on colonic carcinoma have shown focal APC expression in 9% of cases (Iwamoto *et al.,* 2000), and this, in our experience, is seen in a similar proportion of gastric carcinomas (Figure 35).

DISCUSSION

Abnormalities in APC and E-cadherin expression play significant roles in gastric carcinogenesis, both in tumor initiation and progression. Because the main role of APC is control of cell cycle via inhibition of beta-catenin, it is frequently described in tumor initiation. In contrast, E-cadherin predominantly acts as a cell–cell adhesion molecule and is therefore involved in tumor invasiveness. The APC and E-cadherin functions are interlinked via their competition for binding of beta-catenin, presumably helping to keep the intracellular concentration of the molecule in steady state.

As a diagnostic tool, E-cadherin immunohistochemistry plays a more important role. Loss of immunohistochemical E-cadherin expression has been clearly linked to diffuse gastric carcinomas (Becker *et al.,* 2000). It may be premature at this stage to link abnormal E-cadherin expression to poor prognosis, and so far E-cadherin immunohistochemical staining has not been implemented in common histopathology practice (Dixon, 2000). However, an increasing number of reports show that abnormal E-cadherin expression

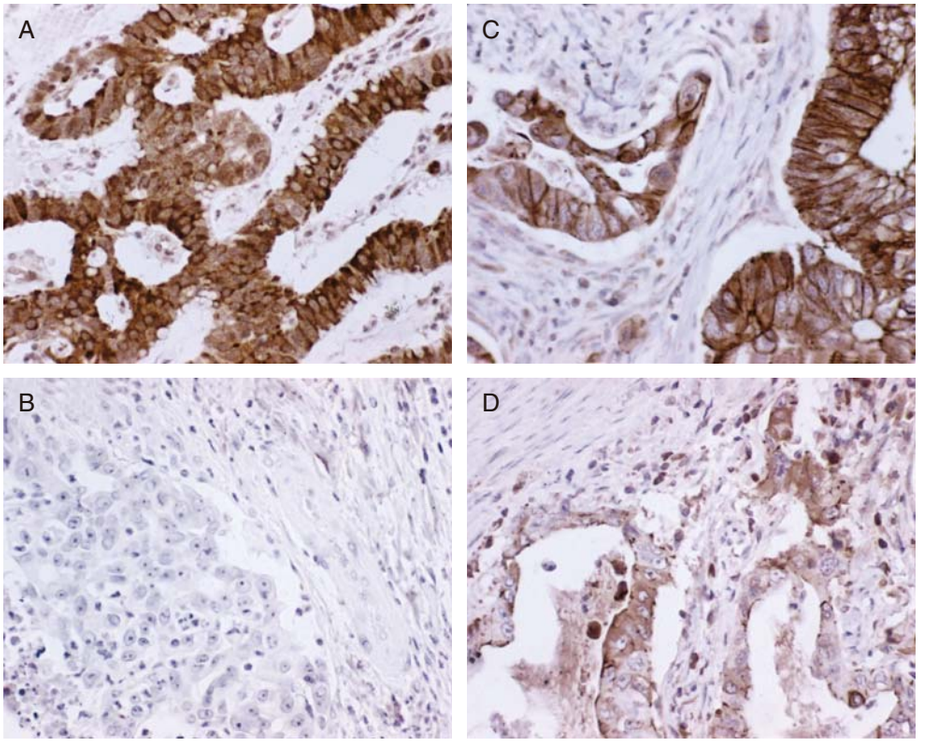

Figure 35. **A–B:** APC (adenomatous polyposis coli) staining in well-differentiated intestinal-type gastric carcinomas. **A:** This tumor shows a strong cytoplasmic signal indicating normal APC expression. **B:** Complete loss of staining indicates loss of APC expression. **C–D:** E-cadherin staining in well-differentiated intestinal-type gastric carcinomas. **C:** Normal staining pattern consisting of a strong cytoplasmic membrane signal. **D:** Abnormal staining pattern characterized by a weak, predominantly cytoplasmic signal. Other types of abnormal E-cadherin patterns include complete absence of staining *(not shown)*. APC and E-cadherin staining shown here was performed as described under methods using an APC polyclonal rabbit antibody (Clone sc-896 K) and an E-cadherin monoclonal mouse antibody (Clone 36B5). Counterstained with hematoxylin. Original magnification 400X.

correlates with increased tumor growth and poor overall survival (Shino *et al.,* 1995). It is of interest that Jawhari *et al.* (1997) found that in patients with tumors showing dual abnormal E-cadherin and beta-catenin expression, the mean survival was shortened to less than 4 months compared with more than 27 months in tumors with normal expression of both molecules. In conclusion, immunohistochemical staining for both APC and E-cadherin continues to play significant roles in gastric cancer research. Although more data are needed, it seems likely that E-cadherin status may provide additional prognostic information for patients with cancer.

References

Ascano, J.J., Frierson, H., Jr., Moskaluk, C.A., Harper, J.C., Roviello, F., Jackson, C.E., El Rifai, W., Vindigni, C., Tosi, P., and Powell, S.M. 2001. Inactivation of the E-cadherin gene in sporadic diffuse-type gastric cancer. *Mod. Pathol. 14*:942.

Becker, K.F., Atkinson, M.J., Reich, U., Becker, I., Nekarda, H., Siewert, J.R., and Hofler, H. 1994. E-cadherin gene mutations provide clues to diffuse type gastric carcinomas. *Cancer Res. 54*:3845.

Becker, K.F., Keller, G., and Hoefler, H. 2000. The use of molecular biology in diagnosis and prognosis of gastric cancer. *Surg. Oncol. 9*:5.

Becker, K.F., Kremmer, E., Eulitz, M., Becker, I., Handschuh, G., Schuhmacher, C., Muller, W., Gabbert, H.E., Ochiai, A., Hirohashi, S., and Hofler, H. 1999. Analysis of E-cadherin in diffuse-type gastric cancer using a mutation-specific monoclonal antibody. *Am. J. Pathol. 155*:1803.

Birchmeier, W., and Behrens, J. 1994. Cadherin expression in carcinomas: role in the formation of cell junctions and the prevention of invasiveness. *Biochim. Biophys. Acta. 1198*:11.

Blok, P., Craanen, M.E., Dekker, W., and Tytgat, G.N. 1999. Loss of E-cadherin expression in early gastric cancer. *Histopathology 34*:410.

Carpenter, P.M., Al Kuran, R.A., and Theuer, C.P. 2002. Paranuaclear E-cadherin in gastric adenocarcinoma. *Am. J. Clin. Pathol. 118*:887.

Chan, A.O., Lam, S.K., Wong, B.C., Wong, W.M., Yuen, M.F., Yeung, Y.H., Hui, W.M., Rashid, A., and Kwong, Y.L. 2003. Promoter methylation of E-cadherin gene in gastric mucosa associated with Helicobacter pylori infection and in gastric cancer. *Gut. 52*:502.

Correa, P. 1992. Human gastric carcinogenesis: a multistep and multifactorial process—First American Cancer Society Award Lecture on Cancer Epidemiology and Prevention. *Cancer Res. 52*:6735.

Dixon, M.F. 2000. *Minimum Dataset for Gastric Cancer Histopathology Reports*. London: The Royal College of Pathologists.

Grace, A., Butler, D., Gallagher, M., Al Agha, R., Xin, Y., Leader, M., and Kay, E. 2002. APC gene expression in gastric carcinoma: an immunohistochemical study. *Appl. Immunohistochem. Mol. Morphol. 10*:221.

Guilford, P., Hopkins, J., Harraway, J., McLeod, M., McLeod, N., Harawira, P., Taite, H., Scoular, R., Miller, A., and Reeve, A.E. 1998. E-cadherin germline mutations in familial gastric cancer. *Nature 392*:402.

Gulmann, C., Grace, A., Leader, M., Butler, D., Patchett, S., and Kay, E. 2003. Adenomatous polyposis coli gene, beta-catenin, and E-cadherin expression in proximal and distal gastric cancers and precursor lesions: an immunohistochemical study using tissue microarrays. *Appl. Immunohistochem. Mol. Morphol. 11*:230.

Hulsken, J., Birchmeier, W., and Behrens, J. 1994. E-cadherin and APC compete for the interaction with beta-catenin and the cytoskeleton. *J. Cell Biol. 127*:2061.

Ilyas, M., and Tomlinson, I.P. 1997. The interactions of APC, E-cadherin and beta-catenin in tumour development and progression. *J. Pathol. 182*:128.

Iwamoto, M., Ahnen, D.J., Franklin, W.A., and Maltzman, T.H. 2000. Expression of beta-catenin and full-length APC protein in normal and neoplastic colonic tissues. *Carcinogenesis 21*:1935.

Jawhari, A., Jordan, S., Poole, S., Browne, P., Pignatelli, M., and Farthing, M.J. 1997. Abnormal immunoreactivity of the E-cadherin-catenin complex in gastric carcinoma: relationship with patient survival. *Gastroenterology 112*:46.

Karayiannakis, A.J., Syrigos, K.N., Chatzigianni, E., Papanikolaou, S., and Karatzas, G. 1998. E-cadherin expression as a differentiation marker in gastric cancer. *Hepatogastroenterology 45*:2437.

Kikuchi, A. 2003. Tumor formation by genetic mutations in the components of the Wnt signaling pathway. *Cancer Sci. 94*:225.

Kobayashi, K., Okamoto, T., Takayama, S., Akiyama, M., Ohno, T., and Yamada, H. 2000. Genetic instability in intestinal metaplasia is a frequent event leading to well-differentiated early adenocarcinoma of the stomach. *Eur. J. Cancer 36*:1113.

Midgley, C.A., White, S., Howitt, R., Save, V., Dunlop, M.G., Hall, P.A., Lane, D.P., Wyllie, A.H., and Bubb, V.J. 1997. APC expression in normal human tissues. *J. Pathol. 181*:426.

Nagase, H., and Nakamura, Y. 1993. Mutations of the APC (adenomatous polyposis coli) gene. *Hum. Mutat. 2*:425.

Nakatsuru, S., Yanagisawa, A., Ichii, S., Tahara, E., Kato, Y., Nakamura, Y., and Horii, A. 1992. Somatic mutation of the APC gene in gastric cancer: frequent mutations in very well differentiated adenocarcinoma and signet-ring cell carcinoma. *Hum. Mol. Genet. 1*:559.

Nishimura, K., Yokozaki, H., Haruma, K., Kajiyama, G., and Tahara, E. 1995. Alterations of the APC gene in carcinoma cell lines and precancerous lesions of the stomach. *Int. J. Oncol. 7*:587.

Polakis, P. 1997. The adenomatous polyposis coli (APC) tumor suppressor. *Biochim. Biophys. Acta. 1332*:F127.

Shimoyama, Y., Hirohashi, S., Hirano, S., Noguchi, M., Shimosato, Y., Takeichi, M., and Abe, O. 1989. Cadherin cell-adhesion molecules in human epithelial tissues and carcinomas. *Cancer Res. 49*:2128.

Shino, Y., Watanabe, A., Yamada, Y., Tanase, M., Yamada, T., Matsuda, M., Yamashita, J., Tatsumi, M., Miwa, T., and Nakano, H. 1995. Clinicopathologic evaluation of immunohistochemical E-cadherin expression in human gastric carcinomas. *Cancer 76*:2193.

Strathdee, G. 2002. Epigenetic versus genetic alterations in the inactivation of E-cadherin. *Semin. Cancer Biol. 12*:373.

Tahara, E., Kuniyasu, H., Yasui, W., and Yokozaki, H. 1994. Gene alterations in intestinal metaplasia and gastric cancer. *Eur. J. Gastroenterol. Hepatol. 6* Suppl *1*:S97.

Tamura, G., Maesawa, C., Suzuki, Y., Tamada, H., Satoh, M., Ogasawara, S., Kashiwaba, M., and Satodate, R. 1994. Mutations of the APC gene occur during early stages of gastric adenoma development. *Cancer Res. 54*:1149.

This Page Intentionally Left Blank

13

Immunohistochemical Expression of Chromogranin A and Leu-7 in Gastrointestinal Carcinoids

Tomáš Jirásek and Václav Mandys

Introduction

Carcinoid Tumors, Chromogranin A, and Leu-7

Carcinoid tumors of the gastrointestinal (GI) tract represent a group of relatively rare malignant epithelial neoplasms characterized by less aggressive biological behavior and better prognosis compared to GI carcinomas, distinctive histologic appearance, and expression of markers suggesting neuronal and neuroendocrine differentiation of neoplastic cells. Precise histopathologic diagnosis of carcinoid tumors is important in selection of adequate oncologic strategy because of possible disposal of somatostatine receptor analog drugs in clinical diagnostics and therapy of these neoplasms.

Carcinoid tumors were first described in the small intestine in 1888 by Lubarsch. The term "karzinoide" (e.g., carcinoid) was used for the first time by Oberndorfer in 1907 to exempt a new entity characterized by typical histologic appearance, locally unlimited growth, and less aggressive biologic behavior in comparison with intestinal adenocarcinomas. Carcinoid tumors mainly appear in the GI and respiratory tract. Neuroendocrine differentiation of carcinoid tumor cells was discovered later; however, histogenetic background of these tumors has not been fully clarified yet. The histogenetic relation of these tumors to enterochromaffine epithelial cells (Kultschitski cells), which belong to amine precursor uptake and decarboxylation (APUD) system diffuse or to neuroendocrine system (DNES) or to their precursor stem cells, is widely accepted (Andrew *et al.,* 1998). Carcinoid tumors represent about 2% of all malignant neoplasms of the GI tract. According to primary localization, carcinoids of stomach represent 4%, duodenal 2%, small intestinal (i.e., jejunal and ileal) 49%, appendical 34%, large intestinal 7%, and rectal 4% of all GI carcinoids (Wilander, 1995).

Histologic techniques play an essential role in diagnostics of carcinoid tumors. Optical microscopy allows recognizing different characteristic histologic features, which are considered to be essential to the final diagnosis of carcinoid tumor (Fenoglio-Preiser *et al.,* 1999). Carcinoid tumor cells are smaller, polygonal, and uniform with obviously low mitotic rate. They form 1) solid nests, often with palisade at the edges; 2) tubular and rosette-like structures; 3) trabecular or ribbon-like anastomosing structures; and 4) acinary patterns. Tumors composed of these structures are referred to as

Handbook of Immunohistochemistry and *in situ* Hybridization of Human Carcinomas, Volume 4: Molecular Genetics, Gastrointestinal Carcinoma, and Ovarian Carcinoma

typical carcinoids. Some carcinoid tumors display more prominent cytologic irregularities and higher mitotic rate. Such tumors are usually bigger than 5 cm in diameter, often with foci of necrosis. These tumors are usually classified as atypical carcinoids, and they are in the intermediate position between typical carcinoids and carcinomas, according to their biologic behavior.

According to histologic features, the classification of carcinoids that divides carcinoid tumors into five distinctive groups, named alphabetically as A, B, C, D, and E, was introduced (Fenoglio-Preiser *et al.,* 1999; Soga and Tazawa, 1971). Group A includes tumors with solid, nodular, or insular morphologic patterns, group B is characterized by trabecular or ribbon-like structures, group C has with tubular, glandular, or rosette-like patterns, group D represents atypical and poorly differentiated tumors, and group E is formed of mixed tumors. New World Health Organization (WHO) classification of endocrine tumors was introduced in 2000 (Solcia *et al.,* 2000). Gastrointestinal endocrine tumors were divided in this classification into three groups, according to their cytologic characteristics, histologic features, depth of invasion, size of tumor, and mitotic rate/proliferation index. The well-differentiated endocrine tumors (1st) are characterized by no or only mild cellular atypia, growth in solid nests, trabeculae or pseudoglandulae, and tumor restriction to mucosa or submucosa. The behavior of nonangioinvasive tumors measuring ≤1 cm in size with ≤2 mitotic figures per 10 HPF (high power fields) is considered to be benign.

The term "carcinoid" is used as a synonym for these tumors. The group of well-differentiated endocrine carcinomas (2nd) is characterized by moderate cellular atypia; histologic pattem of solid nests; trabeculae or larger, less well-defined cellular aggregates; more progressed invasion (to lamina muscularis propria or deeper); or presence of liver or regional lymph-nodes metastases. These tumors larger than 1 cm in diameter, displaying moderately elevated mitotic index (>2 mitotic figures per 10 HPF) or higher proliferation index (>2% of Ki-67 positive tumor cells) are alternatively classified as "malignant carcinoids." Poorly differentiated endocrine carcinomas (small cell carcinoma) represent the 3rd group of endocrine tumors. These neoplasms are composed of highly atypical, small to intermediate-size cells that form not–well-defined aggregates. Necrosis, angioinvasion, perineural invasion, and distant metastases are often present. Poorly differentiated endocrine carcinomas show high mitotic rate (>10 mitotic figures per 10 HPF) as well as high proliferation index (>15% of Ki-67 positive tumor cells).

As mentioned earlier, histopathologic diagnosis of carcinoid tumors is based on characteristic arrangement and cytologic features of tumor cells. However, additional histologic and immunohistochemical methods have been used to confirm the final diagnosis of carcinoid tumor. *Argyrophil reaction* (Grimelius) allows visualization of neurosecretory granules in cytoplasm of carcinoid tumor cells. Although the chemical basis of argyrophil reaction remains unclear, its positivity in carcinoid tumors located within the entire GI tract makes it very useful. Argyrophil reaction is still widely used in carcinoid tumor diagnostics. Neurosecretory granules represent characteristic structure of carcinoid tumor cells. Electronmicroscopically they are observed in cytoplasm in endocrine and some neuronal cells as round-shaped membrane-bound vesicles with a mean size of ~60 nm and characterized by a dense central core. This typical appearance gave them the alternative name "dense core vesicles." The granular matrix of neurosecretory granules contains endocrine-acting polypeptide substances, often in prohormone/prepro-hormone storage form, as well as other polypeptidic substances. In normal nonneoplastic GI mucosa, neurosecretory granules could be detected in the cytoplasm of several types of differentiated cells, which belong to DNES (Fenoglio-Preiser *et al.,* 1999; Wilander, 1995).

Immunohistochemistry constitutes the most important diagnostic approach recently widely used in routine diagnostics of carcinoid tumors. Numerous antigens have been already detected in carcinoid tumor cells. Among them, markers of neuronal and neuroendocrine differentiation as chromogranin A (CgA), Leu-7 antigen, neuron-specific enolase (NSE), and synaptophysin are the most important for diagnostic purposes. NSE represents an enzyme molecule distributed within cell cytoplasm of many different cell types; synaptophysin belongs to proteins associated with neuronal praesynaptic vesicles membrane. Immunohistochemical positivity of NSE and synaptophysin in carcinoid tumors reflects neuronal differentiation of tumor cells. CgA and Leu-7 are the components of neurosecretory granules matrix. They represent specific immunomarkers of these granules, and their positive immunostaining denotes neuroendocrine differentiation of tumor cells.

Chromogranins (granins) belong to the group of acidic polypeptides, which are located in the matrix of neurosecretory granules. Historically, three different members of the chromogranin family are known, namely chromogranin A, B (also known as secretogranin I), and C (secretogranin II). Four different proteins have been proposed to belong among the members of the granin family: secretogranin III–VI (Taupenot *et al.,* 2003). Granin polypeptides consist of a single polypeptide chain of approximately 180–700 amino-acid residues. Granins' amino-acid end is bearing a signal peptide molecule that directs their movement from ribosomes to endoplasmatic reticulum and then to the

Golgi complex, where post-translational processing mediated by prohormone convertase 1 and 2 appears (Doblinger *et al.,* 2003; Laslop *et al.,* 2000). After that, granins form, together with different other substances, the matrix of neurosecretory granules (vesicles) and are secreted from the cells by exocytosis in a regulated manner (Halban and Irminger, 1994) (so-called regulated secretory pathway; granules release their contents only in response to a specific stimulus, while they can remain in cell cytoplasm containing a condensed cargo of peptides or amine hormones or neurotransmitters for an extended time).

The exact mechanism of granins sorting in the Golgi network before they enter the regulated secretion pathway has not been understood yet; however, granins tend to bind calcium ions with low affinity but high capacity and then aggregate *in vitro* at low pH in the presence of calcium. This mechanism together with mildly acidic pH probably segregates in trans-Golgi network the regulated cargo from other proteins, which are excreted constitutively (Gerdes *et al.,* 1989). Some authors (Arvan and Castle, 1998) also proposed that a specific sorting signal in the secretory protein that binds to a sorting receptor can facilitate the movement of the protein to the regulated pathway of secretion.

Post-translational proteolytic processing gives rise to several bioactive peptides derived from CgA and CgB and secretogranins II, V, and VI. These peptides have different autocrine, paracrine, endocrine, and antimicrobial activities—namely, CgA-derived peptide pancreastatin (Tatemoto *et al.,* 1986) inhibits glucose-stimulated insulin release from beta cells of pancreatic Langerhans' islets and diminishes glucose uptake by skeletal muscle, as well as inhibits the release of amylase from exocrine pancreas, the release of gastric acid from parietal cells, and the release of parathyroid hormone from parathyroid chief cells (Sanchez-Margalet *et al.,* 2000). Different CgA-derived fragments—vasostatin I and II—inhibit constriction of isolated human blood vessels and modulate the adhesion of fibroblasts and coronary artery smooth-muscle cells (Ratti *et al.,* 2000). Another CgA fragment named catestatin inhibits the release of catecholamines from sympatoadrenal chromaffine cells and probably contributes to an autocrine negative feedback that modulates catecholamine release within the sympatoadrenal system (Mahata *et al.,* 1997). Some findings also provide the evidence of a link between a diminished level of catestatin and hypertension (O'Connor *et al.,* 2002).

Regional-specific anti-sera raised against synthetic peptides and detecting different CgA fragments were described (Portela-Gomes *et al.,* 2001). According to their observation in different human neuroendocrine tumors including a group of carcinoid tumors of the GI tract, most carcinoid neoplastic cells showed immunohistologic positivity for all investigated CgA fragments. In contrast, the malignant ileal carcinoids either lacked one or more fragments or expressed the fragments in only a few tumor cells. The lack of expression of some fragments can result from abnormal splicing of CgA or from masking of detected epitopes. The exact mechanisms of how granins' fragments affect their target endocrine cells have not been elucidated yet. Cystatin probably acts by binding to the nicotinic cholinergic receptor (Mahata *et al.,* 1999). Some suggestions of G-protein–coupled receptors' role in granins' derived endocrine active peptides function have been already made; nevertheless, unique receptors have not been identified for most granins fragments (Sanchez-Margalet *et al.,* 2000). Anti-bacterial and anti-fungal activities of CgA fragments prochromacin, chromacin I, and chromacin II have been described, resulting from the ability of these fragments to form ion channels through membranes (Lugardon *et al.,* 2001). In summary, granins participate in different intracellular processes, namely in formation of secretory granules and in modulation of peptide hormone and neuropeptide processing, and can also play extracellulary an important role as hormonally acting substances.

Leu-7 (also known as CD 57) was originally described in natural killer cells in the immune system using monoclonal antibody clone HNK-1. This antibody also stains different types of neural cells of the central and the peripheral nervous system. In peripheral nerves, however, the myelin-associated glycoprotein was detected with HNK-1 antibody. Many different tissues react with this antibody, namely cells of small-cell lung carcinoma, different thyroid gland carcinomas, hyperplastic and tumorous prostatic tissue, and neoplastic and nonneoplastic cells of adrenal medulla and many different tumors raised from the APUD/DNES system (Sanno *et al.,* 1997; Wieczorek *et al.,* 1998). According to findings of some authors, HNK-1 antibody detects also pancreatic noninsulin–producing islet cells. HNK-1 antibody probably detects carbohydrate epitope, which is associated with cell membrane. Some authors suggest that this epitope belongs to neural cell adhesion molecules (NCAM), namely NCAM-140 (Wieczorek *et al.,* 1998). Immunogold staining in electron microscopy discovered the positive staining with HNK-1 in the matrix of dense core vesicles (neurosecretory granules) (see Tischler *et al.,* 1986). According to these findings, the 75 kDa protein antigen connected with dense core vesicles' membrane was recognized by the HNK-1 antibody. Thus, detection of Leu-7 antigen represents the novel possibility to identify dense core vesicles in carcinoid diagnostics. The majority of GI carcinoids reveal Leu-7 immunoreactivity, and its detection allows

recording of the neuroendocrine differentiation even in the case of CgA negativity.

MATERIALS

1. Primary antibodies:
   ▲ Mouse monoclonal anti-human CgA (clone DAK A3 Dako, Glostrup, Denmark).
   ▲ Mouse monoclonal anti-human CD 57 (clone NK-1 Dako).
2. Primary anti-serum:
   ▲ Rabbit polyclonal anti-human CgA (DAKOPATTS A 430 Dako).
3. Visualization agents (secondary antibodies):
   ▲ LSAB+ Peroxidase Kit (Dako).
   ▲ EnVision Peroxidase Kit (Dako).
   ▲ Secondary anti-rabbit immunoglobulin (IgG) antibody, conjugated with FITC (fluorescein isothyocyanate) (Jackson, West Grove, PA).
   ▲ Secondary anti-mouse IgG antibody, conjugated with Cy-3 (Jackson).
4. Phosphate buffer saline (PBS): 100 mg anhydrous calcium chloride, 200 mg potassium chloride, 200 mg monobasic potassium phosphate, 100 mg magnesium chloride $\times$ $6H_2O$; 8 g sodium chloride, and 2.16 g dibasic sodium phosphate $\times$ $7H_2O$; bring vol to 1 L with deionized glass-distilled water (pH 7.4).
5. Tris-buffered saline (TBS): 2.4 g Tris-HCl and 8.76 g NaCl; bring vol to 1 L with deionized glass-distilled water (pH 7.4).
6. 5% fetal calf serum: 5 g fetal calf serum and 100 mL TBS, add fetal calf serum to buffer with stirring.
7. Primary antibody/anti-serum diluted in 5% fetal calf serum.
8. Secondary antibodies (IgG conjugated with FITC or Cy-3) diluted in PBS.
9. 0.2 *M* Tris: 2.42 g Tris; bring vol to 100 mL with deionized glass-distilled water, adjust pH to 7.4 with HCl.
10. Mowiol: 3.0 g glycerol, 2.4 g Mowiol (Mowiol 4-88, Hoechst, Germany), 0.6 g 2,5% DABCO (1,4-diazobicyclo[2,2,2]octan), 12 ml 0.2 *M* Tris; add glycerol to Mowiol with stirring for 1 hr at room temperature, then add 6 mL of deionized glass-distilled water with stirring for 2 hr at room temperature, then add 0.2 *M* Tris with stirring for 10 min at 50°C, then centrifuge for l5′/4800 RPM, then add DABCO with stirring.
11. 0.05 *M* Tris: 6.05 g Tris; bring vol to 1 L with deionized glass-distilled water, adjust pH to 7.6 with HCl.
12. DAB: 30 mg 3, 3′-diaminobenzidine (Fluka, Buchs, Schweiz); bring vol to 80 ml with 0.05 *M* Tris for 1 hr at 60°C; add 40 µl 30% hydrogen peroxide before use.
13. Pertex, Histolab AB, Goteborg, Sweden.
14. Graded alcohols (increasing): ethylalcohol 70%, ethylalcohol 95%, isopropylalcohol, xylene.
15. Graded alcohols (decreasing): xylene, isopropylalcohol, ethylalcohol 95%, ethylalcohol 70%.
16. Harris's hematoxylin.

METHOD

Postembedding Labeling with Primary Antibodies/Anti-Sera for Immunohistology

1. Deparaffinise 5 µ-thick tissue sections in decreasing graded alcohols.
2. Rinse the sample once in TBS for 10 min.
3. Incubate the sample with primary antibody/anti-serum diluted in 5% fetal calf serum for 24 hr at 4°C.
4. Rinse the sample once in TBS for 10 min with stirring.
5. Incubate the sample with EnVision Peroxidase Kit/LSAB+ Peroxidase Kit following original instructions.
6. Rinse as in **Step 4.**
7. Incubate the sample with DAB for exactly 5 min.
8. Rinse as in **Step 4.**
9. Counterstain the sample with Harris's hematoxylin for exactly 20 sec.
10. Rinse as in **Step 4.**
11. Dehydrate the sample in backward graded alcohols.
12. Mount the sample to Pertex. Sample is now ready for final examination in optical microscope.

Postembedding Double Immunofluorescence Labeling for CgA and Leu-7 with Primary Antibodies/Anti-Sera for Confocal Laser Scanning Microscopy

1. Deparaffinise 5 µg-thick tissue sections in graded alcohol.
2. Rinse the sample once in TBS for 10 min.
3. Incubate the sample with primary antibody clone NK-1 as well as with primary rabbit anti-serum A 430 diluted in 5% fetal calf serum for 24 hr at 4°C.
4. Rinse the sample once in TBS for 10 min with stirring.
5. Incubate the sample with both secondary antibodies (FITC and Cy-3) diluted in PBS consequently for 1 hr at 37°C.
6. Rinse as in **Step 4.**
7. Mount the sample to Mowiol. Sample is now ready for final examination in confocal laser scanning microscope (recommended with oil immersion objectives),

an argon–ion laser at a wavelength of 488-nM can be used for excitation of FITC and a helium–neon laser at a wavelength of 543-nM for excitation of Cy-3, respectively. Simultaneous or consequent mode of excitation of FITC and Cy-3 can be used to evaluate double staining within the slides.

RESULTS AND DISCUSSION

The diagnosis of carcinoid tumors is based on morphologic features. However, confirmation of the diagnosis relies on the detection of markers of neuroendocrine differentiation of tumor cells (Fenoglio-Preiser *et al.,* 1999; Wilander, 1995). Among them, chromogranin A and Leu-7 (CD57), being the markers of neurosecretory granules, are widely used (Burke *et al.,* 1997; Tischler *et al.,* 1986).

The results of immunohistochemical detection of CgA and Leu-7 within individual tumor cells show diffuse, finely granular pattern, located within the cytoplasm of carcinoid tumor cells. In individual reports (Burke *et al.,* 1989a), Leu-7 stained predominantly luminal cytoplasmic borders. In carcinoid tumors, accumulation of CgA positive neurosecretory granules was immunohistochemically detected at the periphery or in the basal part of cytoplasm in carcinoid tumor cells (Burke *et al.,* 1989a; Burke *et al.,* 1989b). In our series of carcinoids (Jirásek *et al.,* 2003), we observed similar phenomenon especially in solid nests of typical carcinoids located in the midgut (Figure 36). To our experience, such phenomenon could reflect residual polarization of tumor cells and thus indicates higher degree of differentiation of particular tumor.

According to primary tumor site, various percentages of CgA- and Leu-7–positive tumors can be observed. In the group of gastric carcinoids (Thomas *et al.,* 1994), CgA was positive in all investigated tumors, whereas 94% of investigated tumors were simultaneously Leu-7 positive; CgA and Leu-7 together with synaptophysin were found as sensitive markers of gastric carcinoids. Similar results were obtained in the group of duodenal carcinoids (Burke *et al.,* 1989) indicating similar histogenetic origin of both these tumor groups in the foregut.

Carcinoid tumors of jejunum and ileum also revealed frequent immunopositivity for CgA (92%) and Leu-7 (100%) (Figure 37) (Burke *et al.,* 1997). In contrast, various histologic types of appendical carcinoids showed strong CgA immunopositivity, whereas more than 50% of appendical carcinoids were Leu-7 negative (Burke *et al.,* 1989). In the group of rectal and colonic carcinoids the majority (58%) of carcinoid tumors showed CgA positivity; Leu-7 was detected only in 53% of tumors (Federspiel *et al.,* 1990). In our study (Jirasek *et al.,*

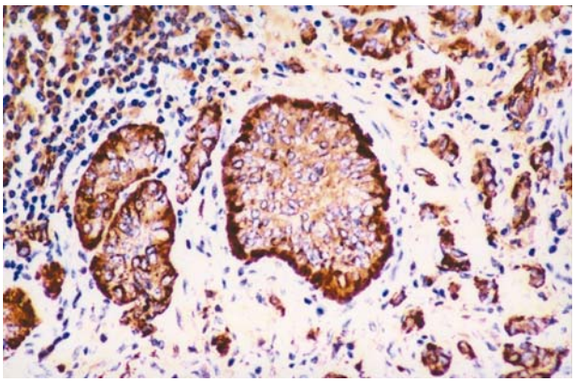

Figure 36. Immunohistochemical detection of CgA in typical carcinoid of the appendix. Diffuse immunostaining for CgA accentuated at the periphery of nests of tumor cells: polyclonal rabbit anti-serum; original magnification 100X.

2003), including the group of 32 carcinoid tumors of GI tract, all tumors revealed positive immunoreactivity for at least one marker of neurosecretory granules; however, detailed morphologic analysis showed that the distribution of positive areas as well as the intensity of staining of CgA and Leu-7 did not correspond in individual tumors. This finding was prominent mainly in appendical and rectal carcinoids, where regular distribution of CgA-positive tumor cells within the whole tumor mass was present, whereas Leu-7–positive tumor cells showed irregular, patchy distribution within the tumor. We also detected five carcinoid tumors, where immunoreactivity for CgA was observed in individual scattered tumor cells only or the entire tumor was CgA negative, but relatively large portion of tumor cells showed Leu-7 positivity. This finding indicates the importance of Leu-7 detection in CgA-negative tumor samples for recognition of neuroendocrine differentiation of tumor cells in routine bioptical examinations.

Different results of detection of CgA can be obtained using monoclonal antibodies and polyclonal anti-sera. To our experience, more carcinoid tumors reveal prominent and intensive staining with polyclonal anti-CgA anti-sera than with monoclonal antibodies. Such differences were described previously in laboratory conditions (Gill *et al.,* 1992), as well as in different human endocrine tumors (Portela-Gomes *et al.,* 2001). These observations reflect the fact that polyclonal displays a wider-binding capacity, and thus covers a wider spectrum of CgA epitops than does monoclonal antibody. Absence of different CgA fragments in human endocrine tumors (including carcinoid tumors) was referred to previously (Portela-Gomes *et al.,* 2001). This phenomenon could also explain different results of CgA detection observed by other authors (Burke *et al.,* 1997; Thomas *et al.,* 1994).

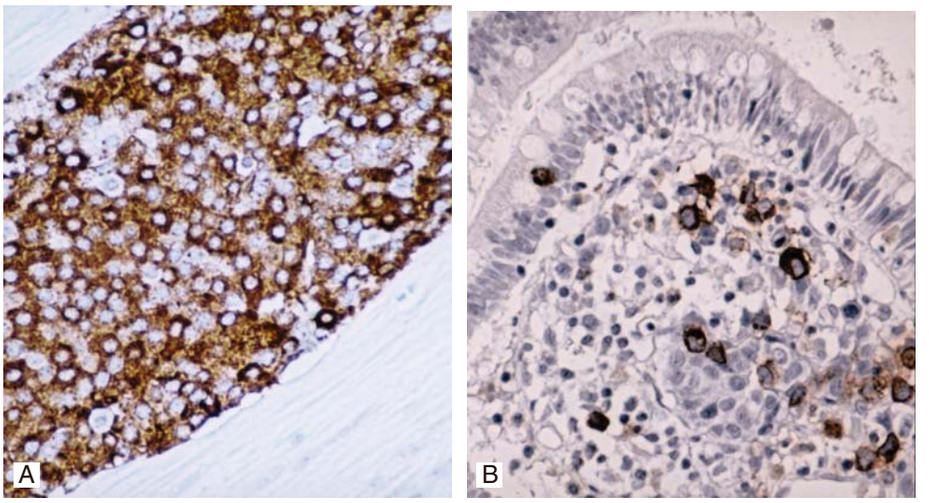

Figure 37. Immunohistochemical detection of CD57 in carcinoids of small intestine. **A:** Typical carcinoid of small intestine. Strong diffuse immunostaining for CD57; original magnification 100X. **B:** Atypical carcinoid of small intestine. Irregular patchy immunostaining for CD57; original magnification 100X.

Leu-7 antigen represents a newer possibility to detect neuroendocrine differentiation of tumor cells of GI carcinoids. Differences in distribution of positive staining between CgA and Leu-7 within individual tumors have already been described (Martin and Maung, 1987; Tischler *et al.,* 1986). In our study we also observed such differences, namely in the group of atypical carcinoids, where either cells positive only for CgA or cells positive only for Leu-7 were observed. Our results are in accordance with previous findings in primary carcinoid tumors of duodenum, large intestine, and rectum, where foci of tumor tissue displaying Leu-7 positivity but negative for CgA were identified (Burke *et al.,* 1989; Federspiel *et al.,* 1990). To explain these differences, the existence of different subpopulations (subtypes) of neurosecretory granules was suggested (Tischler *et al.,* 1986).

Confocal laser scanning microscopy allows the study of relations between CgA and Leu-7 antigens present in neurosecretory granules (Figure 38). This method enables evaluation in thin layers (i.e., optical sections), focused on a chosen plane in a thick specimen while rejecting the light that comes from out-of-focus regions above and below the plane. From a series of such optical sections taken at different depths of tissue section it is possible to reconstruct—using a special computer software—a three-dimensional image. We used this approach for characterization of distribution of CgA and Leu-7–positive cells and for detailed analysis of spatial arrangement of neurosecretory granules within individual tumor cells. Double fluorescent staining together with merged image analysis allowed us precise identification of populations of neurosecretory granules containing either one or both investigated antigens. We identified three different subpopulations of neurosecretory granules. Apart from the subgroup of only Leu-7–positive granules described previously (Tischler *et al.,* 1986), we also identified only the CgA-positive population of neurosecretory granules, as well as the granules containing both CgA and Leu-7. Our observation indicates that the majority of granules located within the basal (abluminal) and perinuclear compartments of nonneoplastic Kultschitski cells co-express both CgA and Leu-7. Scattered granules containing Leu-7 only are present within the cytoplasm at the luminal pole of these cells. Neuroendocrine tumors are composed of at least four cell subtypes. The first one resembling Kultschitski cells contains neurosecretory granules that co-express CgA and Leu-7 and scattered granules expressing either CgA or Leu-7. The second subtype is characterized by the predominance of CgA-positive neurosecretory granules; some of these cells also contain Leu-7–positive neurosecretory granules. The third cell subtype contains Leu-7–positive neurosecretory granules only. Finally, the fourth cell subtype does not contain neurosecretory granules detectable by studied markers. The first and second subtypes, usually revealing the signs of polarization, predominate in typical carcinoids. The presence of the second, third, and fourth type of cells was characteristic for atypical tumors. This observation suggests altered features of neurosecretory granules in neuroendocrine tumors related to the degree of differentiation

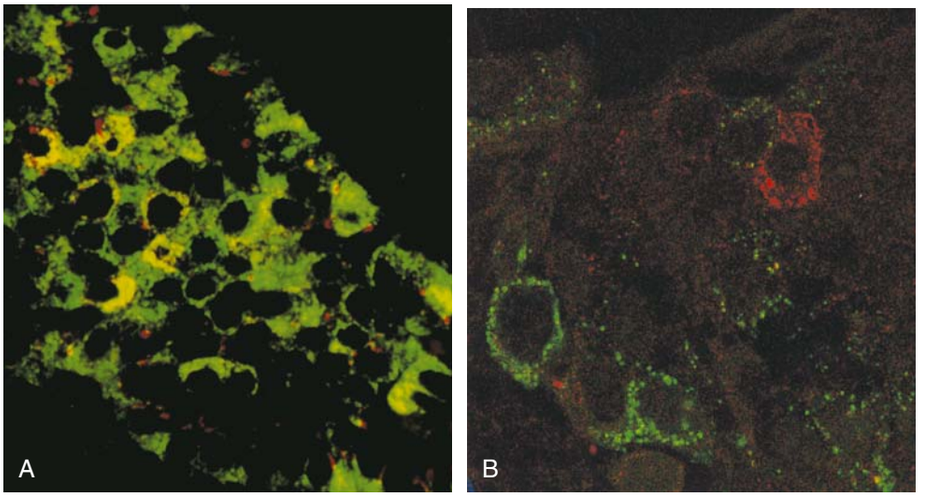

Figure 38. Confocal laser scanning microscopy results. **A:** Atypical carcinoid of small intestine. Cells containing predominantly CgA-positive *(green)* granules and cells containing granules positive for both markers *(yellow)*. Scattered CD57-positive granules *(red)* randomly distributed within the tumor cells; original magnification 400X. **B:** Atypical carcinoid of small intestine. Irregularly distributed cells containing either CgA-positive *(green)* or CD57-positive *(red)* granules; original magnification 630X.

of neoplastic cells and could explain the differences in the expression of neuroendocrine markers in individual tumors.

In summary, we found that different cell subtypes characterized by neurosecretory granules containing CgA, Leu-7, or both are present in neuroendocrine tumors of the GI tract. The patterns of neurosecretory granules distribution within the cytoplasm and the signs of polarization of neoplastic cells in typical carcinoids resemble to some extent Kultschitski cells. In contrast, atypical carcinoids are composed of less-differentiated cells that contain frequently either CgA or Leu-7–positive granules and a bigger proportion of cells are negative for both these markers.

References

Andrew, A., Kramer, B., and Rawdon, B.B. 1998. The origin of gut and pancreatic neuroendocrine (APUD) cells—the last word? *J. Pathol. 186*:117–118.

Arvan, P., and Castle, D. 1998. Sorting and storage during secretory granule biogenesis: looking backward and looking forward. *Biochem. J. 15*:593–610.

Burke, A.P., Federspiel, B.H., Sobin, L.H., Shekitka, K.M., and Helwig, E.B. 1989a. Carcinoids of the duodenum: a histologic and immunohistochemical study of 65 tumors. *Am. J. Surg. Pathol. 13*:828–837.

Burke, A.P., Sobin, L.H., Federspiel, B.H., and Shekitka, K.M. 1989b. Appendical carcinoids: correlation of histology and immunohistochemistry. *Mod. Pathol. 2*:630–637.

Burke, A.P., Thomas, R.M., Elsayed, A.M., and Sobin, L.H. 1997. Carcinoids of the jejunum and ileum: an immunohistochemical and clinicopathological study of 167 cases. *Cancer 79*: 1086–1093.

Doblinger, A., Becker, A., Seidah, N.G., and Laslop, A. 2003. Proteolytic processing of chromogranin A by the prohormone convertase PC2. *Regul. Pept. 28*:111–116.

Federspiel, B.H., Burke, A.P., Sobin, L.H., and Shekitka, K.M. 1990. Rectal and colonic carcinoids: a clinicopathologic study of 84 cases. *Cancer 65*:135–140.

Fenoglio-Preiser, C.M., Noffsinger, A.E., Stemmermann, G.N., Lanz, P.E., Listrom, M.B., and Rilke, F.O. 1999. Neoplastic lesions of the small intestine. In Fenoglio-Preiser C.M. (ed.) *Gastrointestinal Pathology*: *An Atlas and Text.* Philadelphia, New York: Lippincott-Raven, 481–495.

Gerdes, H.H., Rosa, P., Phillips, E., Baeuerle, P.A., Frank, R., Argos, P., and Huttner, W.B. 1989. The primary structure of human secretogranin II, a widespread tyrosine-sulfated secretory granule protein that exhibits low pH- and calcium-induced aggregation. *J. Biol. Chem. 15*:12009–12015.

Gill, B.M., Barbosa, J.A., Hogue-Angeletti, R., Varki, N., and O'Connor, D.T. 1992. Chromogranin A epitopes: clues from synthetic peptides and peptide mapping. *Neuropeptides 21*:105–118.

Halban, P.A., and Irminger, J.C. 1994. Sorting and processing of secretory proteins. *Biochem. J. 1*:1–18.

Jirásek, T., Hozák, P., and Mandys, V. 2003. Different patterns of Chromogranin A and Leu-7 (CD57) expression in gastrointestinal carcinoids: immunohistochemical and confocal laser scanning microscopy study. *Neoplasma 50*:1–7.

Laslop, A., Doblinger, A., and Weiss, U. 2000. Proteolytic processing of chromogranins. *Adv. Exp. Med. Biol. 482*:55–166.

Lugardon, K., Chasserot-Golaz, S., Kieffer, A.E., Maget-Dana, R., Nullans, G., Kieffer, B., Aunis, D., and Metz-Boutigue, M.H. 2001. Structural and biological characterization of chromofungin, the antifungal chromogranin A-(47-66)-derived peptide. *J. Biol. Chem. 21*:35875–35882.

Mahata, S.K., Mahata, M., Parmer, R.J., and O'Connor, D.T. 1999. Desensitization of catecholamine release: the novel

catecholamine release-inhibitory peptide catestatin (chromogranin a344-364) acts at the receptor to prevent nicotinic cholinergic tolerance. *J. Biol. Chem. 29*:2920–2928.

Mahata, S.K., O'Connor, D.T., Mahata, M., Yoo, S.H., Taupenot, L., Wu, H., Gill, B.M., and Parmer, R.J. 1997. Novel autocrine feedback control of catecholamine release: a discrete chromogranin a fragment is a noncompetitive nicotinic cholinergic antagonist. *J. Invest. 15*:1623–1633.

Martin, J.M.E., and Maung, R.T. 1987. Differential immunohistochemical reactions of carcinoid tumors. *Hum. Pathol. 18*:941–945.

O'Connor, D.T., Kailasam, M.T., Kennedy, B.P., Ziegler, M.G., Yanaihara, N., and Parmer, R.J. 2002. Early decline in the catecholamine release-inhibitory peptide catestatin in humans at genetic risk of hypertension. *J. Hypertens. 20*:1335–1345.

Portela-Gomes, G.M., Grimelius, L., Johansson, H., Wilander, E., and Stridsberg, M. 2001. Chromogranin A in human neuroendocrine tumors: an immunohistochemical study with region-specific antibodies. *Am. J. Surg. Pathol. 25*:1261–1267.

Ratti, S., Curnis, F., Longhi, R., Colombo, B., Gasparri, A., Magni, F., Manera, E., Metz-Boutigue, M.H., and Corti, A. 2000. Structure-activity relationships of chromogranin A in cell adhesion: identification of an adhesion site for fibroblasts and smooth muscle cells. *J. Biol. Chem. 22*:29257–29263.

Sanchez-Margalet, V., Gonzalez-Yanes, C., Santos-Alvarez, J., and Najib, S. 2000. Pancreastatin. Biological effects and mechanisms of action. *Adv. Exp. Med. Biol. 482*:247–262.

Sanno, N., Itoh, J., Teramoto, A., Itoh, Y., Hori, S., and Osamura, R.Y. 1997. Immunohistochemical detection of human natural killer cell like immunoreactivity in human pituitary adenomas, using monoclonal antibody NK-1. *J. Neuro. Oncol. 35*:29–38.

Soga, J., and Tazawa, K. 1971. Pathologic analysis of carcinoids. Histologic reevaluation of 62 cases. *Cancer 28*:990.

Solcia, E., Klöppel, G., and Sobin, L.H. 2000. *Histological Typing of Endocrine Tumours*, 2nd ed. Berlin-New York. Springer.

Tatemoto, K., Efendic, S., Mutt, V., Makk, G., Feistner, G.J., and Barchas, J.D. 1986. Pancreastatin, a novel pancreatic peptide that inhibits insulin secretion. *Nature 10*:476–478.

Taupenot, L., Harper, K.L., and O'Connor, D.T. 2003. The chromogranin-secretogranin family. *Engl. J. Med. 20*: 1134–1149.

Thomas, R.M., Baybick, J.H., Elsayed, A.M., and Sobin, L.H. 1994. Gastric carcinoids: an immunohistochemical and clinicopathological study of 104 patients. *Cancer 73*:2053–2058.

Tischler, A.S., Mobtaker, H., Mann, K., Nunnemacher, G., Jason, W.J., Dayal, Y., Delellis, R.A., Adelman, L., and Wolfe, H.J. 1986. Anti-lymphocyte antibody Leu-7 (HNK-1) recognizes a constituent of neuroendocrine granule matrix. *J. Histochem. Cytochem. 34*:1213–1216.

Wieczorek, G., Pospischil, A., and Perentes, E. 1998. A comparative immunohistochemical study of pancreatic islets in laboratory animals (rats, dogs, minipigs, nonhuman primates). *Exp. Toxic. Pathol. 50*:151–172.

Wilander, E. 1995. Whitehead, R. (ed.) Endocrine cell tumors. *Gastrointestinal and Oesophageal Pathology*, 2nd ed. New York: Churchill Livingstone, 741–754.

14

Role of Immunohistochemical Expression of MUC5B in Gastric Carcinoma

João Pinto de Sousa and Leonor David

Introduction

Mucins are high molecular weight glycoproteins that are synthesized by secretory epithelial cells as membrane or secreted proteins and are the major component of the mucous layer that protects the gastric epithelium from chemical and mechanical aggressions. In humans, at least 14 mucin genes have been identified that code for mucin proteins. They are designated as MUC1 (Gendler *et al.,* 1990; Lan *et al.,* 1990), MUC2 (Gum *et al.,* 1989), MUC3 (Gum *et al.,*1990), MUC4 (Porchet *et al.,* 1991), MUC5AC (Guyonnet-Duperat *et al.,* 1995), MUC5B (Dufosse *et al.,* 1993), MUC6 (Toribara *et al.,* 1993), MUC7 (Bobek *et al.,* 1993), MUC8 (Shankar *et al.,* 1997), MUC9 (Lapensee *et al.,* 1997), MUC11, MUC12, MUC13 (Williams *et al.,* 1999), and MUC16 (Yin *et al.,* 2001). Mucins share a common feature of a tandem-repeat domain rich in serine and threonine residues. These amino-acid residues are potential O-glycosylation sites for attachment of the O-glycan chains that constitute up to 80% of the molecular weight of the final mucin glycoprotein (Gendler and Spicer, 1995). Mucin genes are expressed in a regulated cell- and tissue-specific manner. Mucin expression is altered during the process of gastric carcinogenesis, and its expression pattern in gastric carcinoma is very heterogeneous (Gendler and Spicer, 1995). In gastric cancer we can observe the presence of the mucins normally expressed in the stomach, MUC1, MUC5AC, and MUC6, as well as *de novo* expression of the intestinal mucin MUC2 (Reis *et al.,* 1998, 2000). The pattern of mucin expression, including the expression of the intestinal mucin MUC2, may therefore provide new insights into the differentiation pathways of gastric carcinoma.

In a series of 94 cases of gastric carcinoma, we have analyzed the role of mucins MUC1, MUC2, MUC5AC, and MUC6 expression in the evaluation of differentiation and clinicobiologic behavior (Pinto-de-Sousa *et al.,* 2002). According to the results observed, we showed that mucin expression is associated with the characteristics of differentiation of the carcinomas. The expression of normal gastric mucins is modified at different levels in gastric carcinomas. We observed that the expression of MUC5AC is associated with diffuse-type gastric carcinomas according to the classification of Laurén and also with infiltrative carcinomas according to Ming. These results are in agreement with some studies that indicate that diffuse gastric carcinomas keep features of gastric differentiation. The low level of MUC6 expression in gastric carcinomas is consistent with previous histochemical, immunohistochemical,

and ultrastructural observations showing that mucopeptic cells occur only in a few gastric carcinomas (Fiocca *et al.,* 1987). In the same series, we showed that the expression of MUC2 was associated with the subset of mucinous carcinomas (Pinto-de-Sousa *et al.,* 2002). Because MUC2 expression is closely associated with globet cells both in normal and neoplastic gastric mucosa, our results suggest that globet cells are common in mucinous carcinomas, which is in keeping with previous histochemical and ultrastructural observations (Fiocca *et al.,* 1987).

Mucin expression can also be a useful tool providing some relevant insights concerning the location of gastric carcinomas. Considering gastric carcinomas classified as cardia, fundus/body, and antrum according to criteria previously defined (Pinto-de-Sousa *et al.,* 2001), we showed that the pattern of mucin expression was different in the clinicopathologic entities identified in accordance with the tumor location. The expression of intestinal mucin MUC2 was more frequent in carcinomas localized in the cardia compared to the other locations. This observation is consistent with the hypothesis that *de novo* expression of nongastric mucins can occur in advanced gastric cancer. In the same study, gastric carcinomas localized in the antrum had a significantly higher percentage of MUC5AC-expressing cases than those located in the fundus/body. These observations reinforce the use of mucins as differentiation markers of gastric carcinomas.

In the series evaluated we observed that the pattern of mucin expression did not influence the biologic behavior of gastric carcinoma (Pinto-de-Sousa *et al.,* 2002). Thus we were not able to confirm other results indicating that MUC5AC was more frequent in "early" gastric carcinomas (Reis *et al.,* 1997) and that MUC1 overexpression was associated with poor outcome of patients with gastric carcinoma (Lee *et al.,* 2001).

Immunohistochemical Evaluation of MUC5B Expression in Gastric Carcinoma

Four of the mucin genes, MUC2, MUC5AC, MUC5B, and MUC6, have been mapped to 11p15.5 on a single band of 400 kilobases (Pigny *et al.,* 1996). MUC5B gene is 39.09 kb in length, contains 49 exons, and encodes a 5701-amino-acid polypeptide with a molecular range of approximately 627,000 (Desseyn *et al.,* 1997; Van Seuningen *et al.,* 2000). The mucin MUC5B is expressed mainly in trachea and bronchus glands and also in submaxillary glands, endocervix, gallbladder, and pancreas (Balague *et al.,* 1995; Desseyn *et al.,* 1998). Under normal conditions, there is no MUC5B expression in the adult stomach. According to some studies, MUC5B was detected in the period between 8 and 27 weeks of gestation in the embryonic stomach, but after that no MUC5B could be consistently detected (Buisine *et al.,* 2000). It is interesting that, MUC5B is expressed *de novo* in the stomach only in cases of gastric carcinoma (Buisine *et al.,* 2000). The full coding sequence of the *MUC5B* gene has been obtained, but, despite the recent ongoing investigation, the role played by MUC5B in the evaluation of differentiation and biologic behavior of gastric carcinoma still remains partially unknown (Perrais *et al.,* 2001; Van Seuningen *et al.,* 2000).

The expression of MUC5B immunohistochemically detected with a monoclonal antibody is described in detail in a 2004 study (Pinto-de-Sousa *et al.,* 2004). The monoclonal antibody EU-MUC5Ba was used to detect MUC5B (Rousseau *et al.,* 2003). In that study, surgical specimens from 50 gastric carcinomas were evaluated retrospectively. The 50 patients were submitted to surgical resection of gastric carcinoma, in Serviço Cirurgia B, Hospital S. João, between January 1988 and December 1990. Sections from the surgical specimens representative of the carcinomas were immunostained by the avidin-biotin complex staining. The paraffin sections were dewaxed and rehydrated. Sections were treated with 0.3% hydrogen peroxide in methanol for 30 min, to block endogenous peroxidase, followed by incubation with normal nonimmune serum for 20 min. Sections were rinsed with Tris-buffered saline (TBS) and incubated with primary antibodies overnight at 4°C. Sections were rinsed and incubated with a biotin-labeled rabbit anti-mouse secondary antibody, diluted 1:200 in TBS for 30 min, then rinsed and incubated with avidin-biotin-peroxidase complex for 1 hr. Sections were rinsed and stained for 7 min with 0.05% 3,3′-diaminobenzidine tetrahydrochloride (DAB) that was freshly prepared in 0.05M Tris/hydroxymethylaminomethane buffer (pH 7.6) containing 0.1% hydrogen peroxide. Sections were counterstained with hematoxylin, dehydrated, and mounted. All series included normal human tissues as positive controls (minor salivary glands were used as a positive control for MUC5B). Negative controls were performed using conjugate alone.

Association between MUC5B Expression and Clinicopathologic Parameters of Gastric Carcinoma

MUC5B expression was never detected in normal adult human gastric mucosa or in mucosa with intestinal metaplasia in the vicinity of gastric carcinomas.

In the series evaluated, the mucin MUC5B was expressed in 11 of the 50 (22%) surgical specimens of gastric carcinomas analyzed by immunohistochemistry (Pinto-de-Sousa *et al.,* 2004). Because in human stomach MUC5B is expressed only during a brief period of fetal life (Buisine *et al.,* 2000), its expression in human stomach is always aberrant, or *de novo,* and is only observed in cases of gastric carcinoma (Buisine *et al.,* 2000; Perrais *et al.,* 2001). Thus, MUC5B expression might be considered an oncofetal marker and should be viewed as a tool in the diagnosis of gastric carcinoma in the near future (Pinto-de-Sousa *et al.,* 2004). In our study the percentage of carcinomas expressing MUC5B was lower compared to that described in other studies evaluating a small number of cases (Buisine *et al.,* 2000; Perrais *et al.,* 2001).

In the series we have analyzed, the expression of MUC5B was associated with the histologic differentiation of gastric carcinomas (Pinto-de-Sousa *et al.,* 2004). Significant differences were observed according to MUC5B expression and Laurén's classification of gastric carcinomas. The expression of MUC5B in unclassified gastric carcinomas was higher than in intestinal or diffuse carcinomas. Significant differences were also observed in the distribution of cases according to the expression of MUC5B and to venous invasion. The percentage of carcinoma cases with venous invasion expressing MUC5B was significantly lower than that of cases without venous invasion, and it was observed that in gastric carcinomas with venous invasion, 95% did not express MUC5B. No previous studies have established such an association between venous invasion and MUC5B expression. Five-year survival for patients with carcinomas not expressing MUC5B was not significantly different than that of those with carcinomas expressing MUC5B. To the best of our knowledge, our study was the first addressing the influence of MUC5B expression in the biologic behavior of gastric carcinoma and in the cumulative survival of patients.

Association between MUC5B Expression and That of Mucins MUC1, MUC2, MUC5AC, and MUC6

In the same series of cases of gastric carcinoma (Pinto-de-Sousa *et al.,* 2004) we addressed co-expression of MUC5B and mucins MUC1, MUC2, MUC5AC, and MUC6. A significant association in the expression of MUC5B and MUC5AC in gastric carcinoma cases was observed. Of the cases without expression of MUC5AC, 92% also did not express MUC5B. In the group of carcinomas with expression of MUC5AC, nine cases (36%) also expressed MUC5B. The significant association between MUC5B and MUC5AC expression is in accordance with the speculation that both genes may have evolved from a common ancestral gene and therefore might share common mechanisms of gene expression (Desseyn *et al.,* 1997; Escande *et al.,* 2001).

No significant association or agreement was observed in the study between the expression of MUC5B and that of MUC2 and MUC6 in gastric carcinoma cases. These observations may indicate that although closely located in the same chromosome these genes are probably regulated by mechanisms that are different and also not yet known with accuracy (Desseyn *et al.,* 2000; Perrais *et al.,* 2002).

We have further addressed the association between the mucin "phenotype" and immunoreactivity for MUC5B (Pinto-de-Sousa *et al.,* 2004). No significant association was observed between MUC5B expression and the presence of gastric mucin "phenotype." None of the cases with the so-called complete intestinal "phenotype" (MUC2 immunoreactivity with absent MUC5AC and MUC6 expression) expressed MUC5B. No significant association was observed between MUC5B and the so-called incomplete intestinal phenotype (MUC2 and MUC5AC or MUC6 expression) as well as between MUC5B and the absence of MUC2, MUC5AC, and MUC6 expression. In our study, MUC5B expression was present both in cases with gastric and incomplete intestinal "phenotype."

Summing up, our results showed that MUC5B expression was associated with gastric carcinoma differentiation, and we described for the first time an association between MUC5B expression and the lack of venous invasion. We observed an association between the expression of MUC5B and the co-expression of MUC5AC, but not with the MUC1, MUC2, and MUC6. None of the cases with the so-called complete intestinal "phenotype" of mucin expression expressed MUC5B. The expression of the mucins evaluated, namely MUC5B, was not associated with cumulative survival of patients with gastric cancer.

References

Balague, C., Audie, J.P., Porchet, N., and Real, F.X. 1995. *In situ* hybridization shows distinct patterns of mucin gene expression in normal, benign, and malignant pancreas tissues. *Gastroenterology 109*:953–964.

Bobek, L.A., Tsai, H., Biesbrock, A.R., and Levine, M.J. 1993. Molecular cloning, sequence, and specificity of expression of the gene encoding the lower molecular weight human salivary mucin (MUC7). *J. Biol. Chem. 268*:20563–20569.

Buisine, M.P., Devisme, L., Maunoury, V., Deschodt, E., Gosselin, B., Copin, M.C., Aubert, J.P., and Porchet, N. 2000. Developmental mucin gene expression in the gastroduodenal

tract and accessory digestive glands. I. Stomach: a relationship to gastric carcinoma. *J. Histochem. Cytochem. 48*:1657–1666.

Desseyn, J.L., Aubert, J.P., Porchet, N., and Laine, A. 2000. Evolution of the large secreted gel-forming mucins. *Mol. Biol. Evol. 17*:1175–1184.

Desseyn, J.L., Buisine, M.P., Porchet, N., Aubert, J.P., Degand, P., and Laine, A. 1998. Evolutionary history of the 11p15 human mucin gene family. *J. Mol. Evol. 46*:102–106.

Desseyn, J.L., Guyonnet-Duperat, V., Porchet, N., Aubert, J.P., and Laine, A. 1997. Human mucin gene MUC5B, the 10.7-kb large central exon encodes various alternate subdomains resulting in a super-repeat: structura1 evidence for a 11p15.5 gene family. *J. Biol. Chem. 272*:3168–3178.

Dufosse, J., Porchet, N., Audie, J.P., Guyonnet-Duperat, V., Laine, A., Van-Seuningen, I., Marrakchi, S., Degand, P., and Aubert, J.P. 1993. Degenerate 87-base-pair tandem repeats create hydrophilic/hydrophobic alternating domains in human mucin peptides mapped to 11p15. *Biochem. J. 293*:329–337.

Escande, F., Aubert, J.P., Porchet, N., and Buisine, M.P. 2001. Human mucin gene MUC5AC: Organization of its 5′-region and central repetitive region. *Biochem. J. 358*:763–772.

Fiocca, R., Villani, L., Tenti, P., Solcia, E., Cornaggia, M., Frigerio, B., and Capella, C. 1987. Characterization of four main cell types in gastric cancer: foveolar, mucopeptic, intestinal columnar and globet cells: an histopathologic, histochemical and ultrastructural study of "early" and "advanced" tumours. *Pathol. Res. Pract. 182*:308–325.

Gendler, S.J., Lancaster, C.A., Taylor-Papadimitriou, J., Duhig, J., Peat, T., and Burchell, J. 1990. Molecular cloning and expression of human tumor-associated plymorphic epithelial mucin. *J. Biol. Chem. 265*:15286–15293.

Gendler, S.J., and Spicer, A.P. 1995. Epithelial mucin genes. *Annu Rev Physiol 57*:607–634.

Gum, J.R., Byrd, J.C., Hicks, J.W., Toribara, N., Lamport, D.T., and Kim, Y.S. 1989. Molecular cloning and expression of human intestinal mucins cDNAs. *J. Biol. Chem. 264*:6480–6487.

Gum, J.R., Hicks, J.W., Swallow, D.M., Lagace, R.E., Byrd, J.C., Lamport, D.T., Siddiki, B., and Kim, Y.S. 1990. Molecular cloning of cDNAs derived from a novel human intestinal mucin gene. *Biochem. Biophys. Res. Commun. 171*:407–415.

Guyonnet-Duperat, V., Audie, J.P., Debailleul, V., Laine, A., Buisine, M.P., Galiegue-Zouitina, S., Pigny, P., Degand, P., Aubert, J.P., and Porchet, N. 1995. Characterization of the human mucin gene MUC5AC: a consensus cysteine-rich domain for 11p15 mucin genes? *Biochem. J. 305*:211–219.

Lan, M.S., Batra, S.K., Qi, W.N., Metzgar, R.S., and Hollingsworth, M.A. 1990. Cloning and sequencing of a human pancreatic tumor mucin. *J. Biol. Chem. 265*:15294–15299.

Lapensee, L., Paquette, Y., and Bleau, G. 1997. Allelic polymorphism and chromosomal localization of a human pancreatic tumor mucin cDNA. *J. Biol. Chem. 265*:15294–15299.

Lee, H.S., Lee, H.K., Kim, H., Yang, H., Kim, Y., and Kim, W. 2001. MUC1, MUC2, MUC5AC, and MUC expressions in gastric carcinomas: their roles as prognostic indicators. *Cancer 92*:1427–1434.

Perrais, M., Pigny, P., Buisine, M.P., Porchet, N., Aubert, J.P., and Van Seuningen-Lempire, I. 2001. Aberrant expression of human mucin gene MUC5B in gastric carcinoma and cancer cells: identification and regulation of a distal promoter. *J. Biol. Chem. 276*:15386–15396.

Perrais, M., Pigny, P., Copin, M.C., Aubert, J.P., and Van Seuningen, I. 2002. Induction of MUC2 and MUC5AC mucins by factors of the epidermal growth factor (EGF) family is mediated by EGF receptor/Ras/Raf/extracellular signal-regulated kinase cascade and Sp1. *J. Biol. Chem. 227*:32258–32267.

Pigny, P., Van Seuningen, I., Desseyn, J.L., Nollet, S., Porchet, N., Laine, A., and Aubert, J.P. 1996. Identification of a 42-kDa nuclear factor (NF1-MUC5B) from HT-29 MTX cells that binds to the 3′ region of human mucin gene MUC5B. *Biochem. Biophys. Res. Commun. 220*:186–191.

Pinto-de-Sousa, J., David, L., Reis, C.A., Gomes, R., Silva, L., and Pimenta, A. 2002. Mucins MUC1, MUC2, MUC5AC and MUC6 expression in the evaluation of differentiation and clinico-biological behaviour of gastric carcinoma. *Virchows Arch. 440*:304–310.

Pinto-de-Sousa, J., David, L., Seixas, M., and Pimenta, A. 2001. Clinicopathologic profiles and prognosis of gastric carcinomas from the cardia, fundus/body and antrum. *Dig. Surg. 18*:102–110.

Pinto-de-Sousa, J., Reis, C.A., David, L., Pimenta, A., and Cardoso-de-Oliveira, M. 2004. MUC5B expression in gastric carcinoma: relationship with clinico-pathological parameters and with expression of mucins MUC1, MUC2, MUC5AC and MUC6. *Virchows Arch. 444*:224–230.

Porchet, N., Van Cong, N., Dufosse, J., Audie, J.P., Guyonnet-Duperat, V., Gross, M.S., Denis, C., Degand, P., Bernhein, A., and Aubert, J.P. 1991. Molecular cloning and chromosomal localization of a novel human tracheo-bronchial mucin cDNA containing tandemly repeated sequences of 48 base pairs. *Biochem. Biophys. Res. Commun. 175*:414–422.

Reis, C.A., David, L., Carvalho, F., Mandel, U., Bolós, C., Mirorodskaya, M., Clausen, H., and Sobrinho-Simoes, M. 2000. Immunohistochemical study of the expression of MUC6 mucin and co-expression of other secreted mucins (MUC5AC and MUC2) in human gastric carcinomas. *J. Histochem. Cytochem. 48*:377–388.

Reis, C.A., David, L., Nielsen, P.A., Clausen, H., Mirorodskaya, M., Roepstorff, P., and Sobrinho-Simões, M. 1997. Immunohistochemical study of MUC5AC expression in human gastric carcinomas using a novel monoclonal antibody. *Int. J. Cancer 74*:112–121.

Reis, C.A., David, L., Seixas, M., Burschell, J., and Sobrinho-Simões, M. 1998. Expression of fully and under-glycosylated forms of MUC1 mucin in gastric carcinoma. *Int. J. Cancer 79*:402–410.

Rousseau, K., Wickstrom, C., Whitehouse, D.B., Carlstedt, I., and Swallow, D.M. 2003. New monoclonal antibodies to non-glycosylated domains of the secreted mucins MUC5B and MUC7. *Hybrid Hybridomics 22*:293–299.

Shankar, V., Pichan, P., Eddy, R.L., Tonk, V., Nowak, N., Sait, S.N., Shows, T.B., Schultz, R.E., Gotway, G., Elkins, R.C., Gilmore, M.S., and Sachdev, G.P. 1997. Chromosomal localization of a human mucin gene (MUC8) and cloning of the cDNA corresponding to the carboxy terminus. *Am. J. Resp. Cell. Mol. Biol. 16*:232–241.

Toribara, N.W., Roberton, A.M., Ho, S.B., Kuo, W.L., Gum, E., Hicks, J.W., Gum, J.R., Byrd, J.C., and Siddiki, B. 1993. Human gastric mucin. Identification of a unique species by expressing cloning. *J. Biol. Chem. 268*:4879–4885.

Van Seuningen, I., Perrais, M., Pigny, P., Porchet, N., and Aubert, J.P. 2000. Sequence of the 5′-flanking region and promoter activity of the human mucin gene MUC5B in different phenotypes of colon cancer cells. *Biochem. J. 348* Pt 3:675–686.

Williams, S.J., McGuckin, M.A., Gotley, D.C., Eyre, H.J., Sutherland, G.R., and Antalis, T.M. 1999. Two novel mucin genes down-regulated in colorectal cancer identified by differential display. *Cancer Res. 59*:4083–4089.

Yin, B.W.T., and Lloyd, K.O. 2001. Molecular cloning of the CA125 ovarian cancer antigen: identified as a new mucin (MUC16). *J. Biol. Chem. 276*:27371–27375.

15

Angiogenin in Gastric Cancer and Its Roles in Malignancy

Shouji Shimoyama

Introduction

Angiogenesis, a process of new blood-vessel formation, is critical for tissue maintenance and the support of its growth. Tissues require oxygen and nutrient support for their survival and therefore must recruit new blood vessels to grow beyond the size of the diffusion limit of these substrates. Angiogenesis consists of a complex biologic process involving endothelial cells and surrounding extracellular matrix components. For these reasons, angiogenesis requires a precise coordination of multiple steps including the degradation of the basement membrane, outgrowth of endothelial cells from preexisting vessels, migration of endothelial cells toward the stimulus, endothelial cell proliferation to form a new capillary vessel, maturation of nascent vessels by forming a new basement membrane as a capillary bed, recruitment of mesenchymal cells capable to differentiate into smooth-muscle cells or pericytes, and maturation of provisional extracellular matrix around nascent vessels (Folkman, 1986). Angiogenesis is a key event in a broad range of physiologic and pathologic conditions. It can be observed in embryogenesis and during adult reproduction cycles as well as at sites of tissue remodeling during wound healing or inflammation (Kawano *et al.,* 2003; Kolben *et al.,* 1997). Also, tumor development, invasion, and metastasis are critically dependent on angiogenesis.

Considering that angiogenesis occurs only at sites or during periods requiring a new vascular formation, angiogenesis is regulated by a delicate balance of angiogenic and anti-angiogenic factors. In a normal adult, most vasculature is quiescent. It is now widely accepted that the angiogenic switch is "off" while the effects of antiangiogenic factors are predominant and is "on" when angiogenic stimuli overcome the effects of anti-angiogenic factors and the net balance of these two factors is tipped in favor of angiogenesis. Since the pioneering investigations by Folkman (1971), who proposed that tumor growth and metastasis were angiogenesis dependent, various signals that trigger this switch on or off in these vital processes have been discovered. These findings have stimulated intensive research on the roles and regulations of angiogenic factors, including vascular endothelial growth factor (VEGF), angiopoietin, acidic and basic fibroblast growth factors, platelet-derived growth factor, and angiogenin. This chapter describes the biologic significance of angiogenin in human malignancies, especially in gastric cancer.

MATERIALS

Studies concerning the distribution and expression of angiogenin in gastric cancer have been scanty. Research on the detailed distribution of angiogenin and its clinical implications has remained unavailable,

Handbook of Immunohistochemistry and *in situ* Hybridization of Human Carcinomas, Volume 4: Molecular Genetics, Gastrointestinal Carcinoma, and Ovarian Carcinoma

partly because of a relatively lower incidence of the disease and higher frequency of an unresectable disease at presentation in Western countries. This limitation hinders researchers from obtaining a sufficient number and amount of samples. In contrast, patients with gastric cancer are more common in Japan and most of the cases are resectable, allowing research to concentrate on the clinical implications of angiogenin in a relatively large series as well as at various stages of gastric cancer.

Preoperative serum samples were obtained from patients with gastric cancer and healthy volunteers. Gastric cancer tissues and corresponding normal gastric tissues were obtained from patients undergoing surgical resection for the disease. These were snap frozen immediately after resection or fixed in formalin and embedded in paraffin wax. Frozen tissues were stored at –80°C until determination of tissue angiogenin amount. Five μm sections were cut from the formalin-fixed and paraffin embedded (FFPE) tissue blocks for immunohistochemistry and *in situ* hybridization.

METHODS

Immunohistochemistry

First Day

1. Five μm sections from FFPE blocks.
2. Rehydrated in xylol and graded alcohols (each 5 min).
3. Soak in distilled water (5 min).
4. Microwave treatment in citrate buffer (pH 6.0) (20 min).
5. Cool to room temparature.
6. Soak in Tris-buffered saline (TBS) (pH 7.6) (5 min).
7. Incubate with 1% bovine serum albumin (20 min).
8. Wash in TBS (5 min).
9. Incubate with normal rabbit serum (1:5) at room temperature (20 min).
10. Incubate with monoclonal mouse anti-human angiogenin (1:500) at 4°C (overnight).

For negative control: normal mouse immunoglobulin M (IgM) at 4°C (1:500) (overnight).

Second Day

11. Wash in TBS 3×(each 5 min).
12. Incubate with biotinylated rabbit anti-mouse IgM secondary antibody (1:100) (30 min).
13. Wash in TBS 3×(each 5 min).
14. Incubate with Strept AB Complex (Dako, Glostrup, Denmark).
15. Develop by DAB (diamino benzidine) 10 min.
16. Wash in distilled water (10 min).
17. Counterstain by hematoxylin (10 sec).
18. Wash in running tap water.
19. Graded with alcohol and xylol (each 5 min).
20. Mounting.

***In situ* Hybridization (MicroProbe Staining System, Fisher Scientific, Pittsburgh, PA)**

1. Five μm sections from FFPE blocks.
2. Mount on clean coated slides (Probe On Plus slides, Fisher Scientific).
3. Dewax by xylol, and rehydrate with alcohol.
4. Wash in 1X Universal Buffer (Research Genetics, now Invitrogen Corp., Carlsbad, CA) (3 min).
5. Digest by pepsin solution (0.12N HCl) at 105°C (3 min).
6. Wash in 1X Immuno/DNA (deoxyribonucleic acid) buffer (Research Genetics) (3×).
7. Perform hybridization with the angiogenin complementary DNA (cDNA) probe* (500ng/ml)
   At 105°C for 3 min.
   At room temperature (cool down) for approximately 1 min.
   At 37°C for 60 min.
8. Wash in 2X SSC (saline-sodium citrate) 2×.
9. Repeat step 6.
10. Incubate with alkaline phosphatase-conjugated streptavidin (Research Genetics) at 50°C (10 min).
11. Wash in alkaline phosphatase chromogen buffer (Research Genetics) 3×.
12. Incubate with a mixture of fast red and naphtol phosphate at 50°C (10 min).
13. Wash in distilled water (3×).
14. Conterstain with hematoxylin.
15. Wash in running tap water.
16. Air-dry.
17. Mount by Pristine Mount (Research Genetics).

Note: *Commercially synthesized cDNA sequence (Research Genetics): 5′-GAT GGC CTT GAT GCT GCG CTT GTT GCC-3′ with Brigati tail at the 3′ end ($[TAG]_5$-biotin-biotin-biotin- $[TAG]_2$-biotin-biotin-biotin-3′) (Montone and Brigati, 1994).

RESULTS

We first demonstrated an increased angiogenin protein expression in gastric cancer (Shimoyama and Kaminishi, 2000, 2003). Immunohistochemical analyses have revealed that angiogenin immunoreactivity can be detected in gastric cancer cells as well as in inflammatory cells in the stroma adjacent to cancer cells. It is interesting that angiogenin has also been detected in some nonneoplastic glandular cells. Furthermore, the intensity of the immunoreaction was stronger in cancer cells as compared with that in the nonneoplastic

glandular cells. Consistently, enzyme-linked immunosorbent assays have revealed that angiogenin in sera is also elevated in patients with gastric cancer as compared with those in healthy volunteers and patients who are nonneoplastic. Furthermore, levels of serum angiogenin significantly decrease after gastric cancer resection, whereas those of nonneoplastic patients do not alter after surgery, suggesting that changes in serum angiogenin levels are attributable, at least in part, to cancer resection but not to the surgery itself. Moreover, the amount of tissue angiogenin was found to correlate with serum angiogenin concentration.

We have further investigated the angiogenin message in gastric cancer tissues. *In situ* hybridization analysis has proved strong angiogenin signals in gastric cancer cells and surrounding stromal cells, findings that are in agreement with those obtained by immunohistochemistry (Figure 39).

Survival analyses have revealed that patients with higher serum angiogenin (≥400 ng/ml) levels exhibit worse disease-specific and disease-free survivals as compared with those with lower (<400 ng/ml) serum angiogenin levels. Furthermore, angiogenin in sera was found to be an independent prognostic factor, together with cancer depth, histologic type of cancer, and degrees of nodal involvement. Besides angiogenin, the latter three factors have been found to be well-known prognostic factors by many investigators, including us

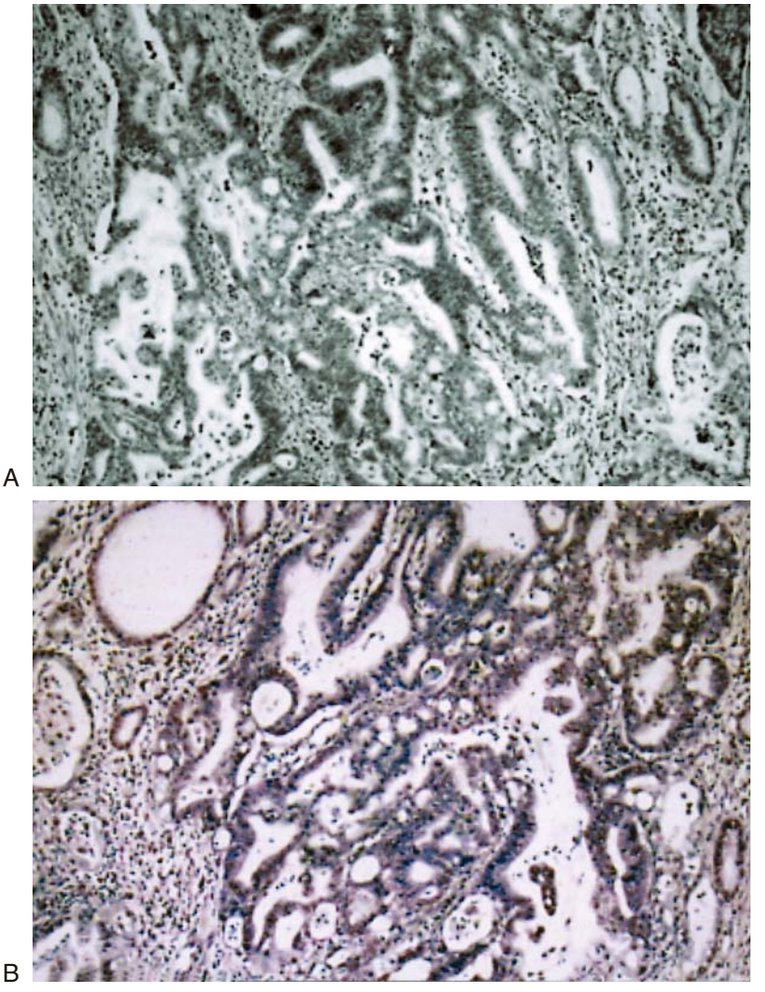

Figure 39. Angiogenin protein and messenger ribonucleic acid (mRNA) distribution in gastric cancer tissues by immunohistochemistry **(A)** and *in situ* hybridization **(B)**. Both angiogenin protein and mRNA signals are observed in cancer cells as well as in stromal cells adjacent to the cancer cells. Original magnification, 25X.

(Moormann *et al.,*1986; Shimoyama *et al.,* 1994). Our findings suggest that angiogenin is produced by gastric cancer cells as well as by cancer surrounding stromal cells, sheds into the circulation, contributes to gastric cancer aggressiveness, and finally becomes a significant prognostic factor.

DISCUSSION

Biologic Properties of Angiogenin

Angiogenin, a 14 kDa potent blood-vessel–inducing protein, was originally discovered in the conditioned media of the human colon carcinoma cell line HT-29 (Fett *et al.,* 1985). Human angiogenin consists of 123 amino acids with 35% homology with human pancreatic ribonuclease A (RNAse A) and is considered to be a member of the ribonuclease superfamily (Kurachi *et al.,* 1985). Besides the requirements of enzymatic activities for angiogenesis, evidence has been accumulated concerning the involvement of angiogenin *per se* in individual events during the process of angiogenesis. Angiogenin binds to endothelial cells (Badet *et al.,* 1989), is endocytosed and translocated in proliferating endothelial cells (Moroianu and Riordan, 1994), stimulates second messengers (Bicknell and Vallee, 1989), supports cell adhesion through extracellular matrix components (Soncin *et al.,* 1994), and organizes tubular formation from cultured endothelial cells (Jimi *et al.,* 1995).

These biologic activities are mediated by the endothelial cell-surface protein that is a member of the muscle actin family (Hu *et al.,* 1993). Interaction of angiogenin with an actin-like protein activates cell-associated protease cascades such as the plasminogen activator/plasmin serine protease system (Hu and Riordan, 1993). This protease cascade leads to degradation of the extracellular matrix and basement membrane, resulting in easier migration of endothelial cells through the architecture (Hu *et al.,* 1994).

In 1997, 170 kDa protein was discovered as another putative angiogenin receptor (Hu *et al.,* 1997). Binding of angiogenin to this receptor exhibits mitogenic activity of human umbilical cord vein endothelial cells and human microvascular endothelial cells. It is interesting that the two receptors, one an actin-like protein and the other a 170 kDa protein, are not concurrently expressed on the endothelial cells (Hu *et al.,* 1997). Furthermore, the expression of the 170 kDa receptor on the cell surface depends on the cell density on which the receptor is expressed. Angiogenin stimulates endothelial cell proliferation through the 170 kDa receptor in a cell-sparse condition, whereas the proliferative response diminishes when the cell number exceeds a certain density level. The discovery of these two receptors and their unique but distinct biologic profiles provide the following conceivable mechanisms of angiogenin-related angiogenesis. Once the condition in which neovascularization is required occurs, angiogenin and the cell-surface actin receptor bind and activate protease cascades that facilitate the mobilization of endothelial cells, which are initial events of neovascularization. The endothelial cell density becomes sparse at the migration front, which is the condition that triggers the expression of 170 kDa receptor on the endothelial cells. The interaction of angiogenin with the 170 kDa receptor stimulates endothelial cell proliferation, with the resultant sufficient number of endothelial cells for neovascularization. Once the endothelial cell density exceeds a certain threshold, the 170 kDa receptor diminishes and endothelial cell proliferation begins to subside, whereas subsequent processes of neovascularization, such as tube formation and the maturation of the perivascular architecture, progress. The two kinds of angiogenin receptors presumably play stage-specific roles on angiogenin-related angiogenesis throughout all events of neovascularization.

Angiogenin Expression in Gastric Cancer and Its Clinical Relevance

The clinical relevance of angiogenin expression in gastric cancer can be explained by the same scenario envisioned during the angiogenin-related angiogenesis. As mentioned earlier, angiogenin contributes to the activation of the protease system that can facilitate endothelial cell migration. In the same manner, it is plausible that angiogenin on tumor cells enhances tumor-vessel formation as well as degradation of the extracellular matrix architecture, which, as a consequence, facilitates tumor growth, tumor-cell invasion, tumor-cell entry into the bloodstream, and metastasis. Angiogenin on gastric cancer cells therefore promotes the invasive ability of the cancer cells and fosters growth and metastasis.

Another important finding is angiogenin expression in stromal cells in the vicinity of gastric cancer cells. Angiogenin expression both in cancer cells and in surrounding cells has also been observed in other malignancies. Angiogenin expression was also detected in endothelial cells, fibroblasts, and neutrophils adjacent to colorectal cancer (Etoh *et al.,* 2000). In addition, angiogenin expression was increased in chronic pancreatitis associated with pancreatic cancer but not in pure chronic pancreatitis (Shimoyama *et al.,* 1999a).

The clinical relevance of angiogenin expression on the stromal cells remains unclear. Tumor cells can

release cytokines (Pekarek *et al.,* 1993), which stimulate the production of a myriad of angiogenic factors from the cancer stromal cells such as leukocytes, macrophages, and mast cell (Coussens *et al.,* 1999; Seljelid *et al.,* 1999). Several lines of evidence also support the notion that interstitial cells recruited in tumor stroma participate in angiogenin production triggered by the cytokine network. Interleukin (IL)-6 is an inducer of angiogenin in HepG2 culture supernatant (Verselis *et al.,* 1999). In addition, the degree of macrophage aggregation also correlates with increased angiogenin expression (Etoh *et al.,* 2000). These observations suggest that stromal cells are also one of the sources of angiogenin, which may be up-regulated by cytokine stimulation, and the net amount of angiogenin in the stromal cells as well as on the tumor cells are conducive to cancer cell invasion and metastasis.

Helicobactor pylori infection, one of the risk factors of gastric cancer development, has been associated with the increased expression of several angiogenic factors such as angiogenin, VEGF, and IL-8 (Kitadai *et al.,* 2003). Gene expression of the urokinase type plasminogen activator is also up-regulated by *H. Pylori* infection. The protease activation may occur as a result of the up-regulation of angiogenin gene expression. Alternatively, *H. pylori* infection independently activates the expression of these genes. The detailed mechanisms of the up-regulation of these genes in relation to *H. pylori* infection remain unclear, but *H. pylori* appears to promote the invasive ability of gastric cancer cells via angiogenin expression.

Angiogenin Expression in Other Malignancies

The distributions of angiogenin and mechanisms of its action in other malignancies have remained poorly understood. However, intensive research has been carried out during the last decade concerning the distribution and role of angiogenin, degrees of its expression, and expression profiles responding to treatment. Clinical implications of angiogenin in malignancy have been previously reviewed (Shimoyama and Kaminishi, 2001), and the extent of this field of study has been increasing rapidly. An association between angiogenin and human malignancies has been observed in more than 20 publications to date, and results confirm that angiogenin expression is up-regulated in a wide variety of human malignancies. Angiogenin message or protein levels are elevated in colorectal, gastric, pancreatic, breast, prostate, liver, and urothelial cancer tissues as well as in melanoma as compared with normal counterparts (Table 8). It is striking that angiogenin is also detected in healthy human circulation at concentrations ranging from 100 to 362 ng/ml. In sera from patients with a malignancy, circulating angiogenin has been found to be elevated and the degree of its elevation correlates with aggressiveness of the tumor (Table 9). In some investigations, angiogenin in sera decreased after surgical resection or chemotherapy, and it was again elevated according to the disease recurrence (Hisai *et al.,* 2003). These observations suggest that at least the tumor cell is the source of circulating angiogenin and that the degree of net angiogenin expression correlates

Table 8. Angiogenin Expression in Tissues

Malignancies	Message/Protein[a]	Correlation Findings	Authors
Gastroenterologic			
Stomach	↑	Tumor stage progression	Shimoyama and Kaminishi, 2002
Colorectal	↑	Elevated serum angiogenin values	Shimoyama *et al.,* 2002
Colorectal	↑	Poor survival	Etoh *et al.,* 2000
Pancreas	↑	Poor survival	Shimoyama *et al.,* 1996
HCC	↑	Histologically less differentiated	Hisai *et al.,* 2003
Urologic			
Urothelial	↑	Cancer progression	Miyake *et al.,* 1999
Prostate	+	Not available[b]	Olson *et al.,* 2002
Others			
Breast	↑	Better disease-free survival	Montero *et al.,* 1998
Breast	↑	Poor disease-free survival	Eppenberger *et al.,* 1998
Melanoma	+	Not available	Hartmann *et al.,* 1999
Brain	↑	Higher tumor grade	Eberle *et al.,* 2000

HCC, hepatocellular carcinoma.

[a]↑: Increased in malignancy as compared with normal counterparts; +: positive in malignancy.

[b]Positive in established tumor by cell line s.c. injection.

Table 9. Angiogenin Values In Sera in Solid Malignancies and Normal Counterparts

Malignancies	In Sera[a]	Normal Mean (range)	Patients Mean (range)	Correlation Findings	Authors
Gastroenterologic					
Stomach	↑	334	378	Poor survival	Shimoyama *et al.,* 2003
Colorectal	↑	322 (246–446)	412 (215–640)	Poor survival	Shimoyama *et al.,* 1999b
Pancreas	↑	359 (258–481)	567 (271–1267)	Poor survival	Shimoyama *et al.,* 1996
HCC	↑	362 (NA)	405[b] (NA)	Poor survival	Hisai *et al.,* 2003
HCC	→	341 (NA)	247 (NA)	No correlation	Chao *et al.,* 2003
Gynecologic					
Ovary	↑	327 (92–472)	643 (100–2000)	Not available	Barton *et al.,* 1997
Ovary	↑	100[c] (NA)	NA (241–378)	Progression	Chopra *et al.,* 1996
Endometrial	↑	113 (NA)	NA (150–350)[c]	No correlation	Chopra *et al.,* 1997
Cervial	↑	104 (NA)	NA (249–381)	Progression	Chopra *et al.,* 1998
Choriocarcinoma	↑	343 (NA)	1092 (NA)	Progression	Shaarawy *et al.,* 2003
Urologic					
Renal cell	↑	284 (180–432)	433 (264–841)	No correlation	Wechsel *et al.,* 1999
Urothelial	↑	338 (183–532)	382[d], 515[e] (177–895)	Poor survival	Miyake *et al.,* 1999
Wilms	↑	196 (0–698)	296 (71–629)	Not available	Sköldenberg *et al.,* 2001
Others					
Breast	↑	206 (110–785)	401 (18–1845)	No correlation	Montero *et al.,* 1998
Melanoma	↑	362 (NA)	439 (NA)	Marginally poor survival	Ugurel *et al.,* 2001

HCC, Hepatocellular carcinoma; NA, not available.
[a]Serum angiogenin levels in malignancy as compared with normal counterpart, ↑: elevated; →: not elevated.
[b]Very hypervascular.
[c]Approximate value.
[d]Noninvasive cancer.
[e]Invasive cancer.

with tumor aggressiveness. The contribution of angiogenin seems, however, to differ according to tumor type.

Angiogenin in Cancer Therapy

Considerable evidence from clinical studies, as summarized in Tables 8 and 9, has prompted many researchers to use angiogenin inhibitors as targets for anti-cancer therapy. For these purposes, potential angiogenin inhibitors are being screened, modified anti-angiogenin monoclonal antibodies are being tested, and the discovery of candidates capable of inhibiting angiogenin activities has stirred a growing interest in using these molecules for anti-cancer applications.

As stated earlier, the angiogenic activity of angiogenin is mediated through a cell-surface receptor. Angiogenin has a cell-surface–binding site that is distinct from the site of its enzymatic activity (Hallahan *et al.,* 1991). This evidence led to the development of inhibitors against the cell-surface–binding site as candidates for antiangiogenin agents. The 11-amino-acid peptide developed from the anti-sense RNA (ribonucleic acid) sequence corresponding to the receptor binding site of angiogenin effectively inhibits the interaction of angiogenin with its putative receptor actin, and blocks angiogenesis induced by exogenous angiogenin or tumor-derived angiogenin. Subsequently, the peptide inhibits plasmin activity and hinders both the invasion of angiogenin-secreting human fibrosarcoma HT 1080 cells and the establishment of hepatic metastasis of angiogenin-secreting HM7 colon carcinoma cells. The peptide itself does not show any direct cytotoxicity against these tumor cells, suggesting that the peptide possesses anti-cancer activities via anti-angiogenin and anti-plasmin activities (Gho *et al.,* 2002).

A high-throughput screening assay has identified a variety of small molecules that bind to the ribonucleolytic active site of angiogenin. Among them, 15 molecules were selected that inhibit the enzymatic activity of angiogenin with Ki values of <100 μM. One of these, called N65828, was found to have an ability to delay the tumor appearance in human tumor xenograft models in athymic mice. The absence of abnormalities in liver and kidney at sacrifice in the N65828-treated mice recommends this compound as an attractive candidate

for cancer therapy without any apparant toxicities (Kao *et al.,* 2002).

Olson *et al*. (2002) have demonstrated that the neutralizing monoclonal antibody 26-2F to human angiogenin has the ability to prevent establishment of PC-3 prostate cancer in athymic mice, to prolong survival of PC-3–bearing mice more effectively than conventional chemotherapeutic agents, and to suppress dramatically the formation of metastasis by prophylactic 26-2F administration. Because angiogenin expression was confirmed in the PC-3 tumor in their experimental model, suppression of angiogenin activities could serve as a useful therapeutic target for preventing the progression and metastasis of an angiogenin-expressing tumor. It is important to note that one of the aminoglycoside antibiotic agents, neomycin, has inhibitory effects on the nuclear translocation of angiogenin (Hu, 1998). Neomycin inhibits angiogenin-induced human endothelial cell proliferation, whereas other aminoglycoside antibiotics do not. Although the detailed mechanisms are unknown, it may represent a new class of anti-angiogenic compounds.

More recently, an angiogenin-binding DNA sequence (angiogenin-binding element) has been identified and the sequence has been shown to exhibit an angiogenin-dependent promotor activity in a luciferase reporter system (Xu *et al.,* 2003). These observations further imply that angiogenin stimulates a number of gene expressions not restricted to angiogenesis through the binding of angiogenin and an angiogenin-binding element. As a consequence, it can be speculated that such interaction and gene activation accelerate tumor-cell invasion and metastasis.

Future Perspectives

Insights into the molecular basis of angiogenin have promoted the development of anti-angiogenin agents as therapeutic tools. The approaches seem to be promising; however, they are still in their infancy and many questions remain unanswered. The members and roles of angiogenin receptors have not been fully understood; thus, the molecular mechanisms of how angiogenin governs endothelial cells are still under investigation. What are the roles of angiogenin in the nonneoplastic gastric mucosa? In the same way, why is circulating angiogenin in healthy humans silent? It can be hypothesized that the angiogenin in this site(s) acts as a pooled angiogenic factor. Still, which factors regulate the on/off switch of angiogenin-related angiogenesis and how? In anti-angiogenin therapies, can we extrapolate the success of animal models to patients? Tumors may easily find routes to switch on alternative angiogenic factors; thus, anti-angiogenic therapies that inhibit both angiogenin and other angiogenic factors may be more effective. Long-term adverse effects of anti-angiogenin therapies on normal tissues or physiologic angiogenesis are unknown. Considering that angiogenin-expression profiles differ among tumor types and individuals, angiogenin expression may depend on genetic constitution, and thereby anti-angiogenin therapies may be tailored to individual pharmacogenetic profiles. Finally, tumors do not shrink with anti-angiogenin therapies because they may not be cytotoxic. For this reason, new evaluation systems are needed to monitor the effectiveness of anti-angiogenin therapy. The solution of these problems should be achieved with carefully designed animal experiments and clinical studies.

Conclusions

Angiogenin distributes in gastric cancer cells, in cancer stromal cells, and in nonneoplastic grandular cells. The degrees of angiogenin expression in gastric cancer cells and in stromal cells in the vicinity of cancer cells are increased as compared with those in the normal counterparts. Consistently, angiogenin in sera is elevated in patients with gastric cancer. Clinically, angiogenin in sera was found to be an independent prognostic factor, suggesting that angiogenin expression reflects gastric cancer aggressiveness. These findings can be explained, at least in part, by the proteolytic activity of angiogenin. Angiogenin activates protease cascade, which promotes cancer-cell migration more easily through extracellular matrix; therefore, it renders the invasive ability of gastric cancer cells and fosters growth and metastasis. Although the clinical relevance of angiogenin expression in stromal cells and nonneoplastic grandular cells remain unclear, angiogenin in these stromal cells adjacent to cancer cells presumably contributes cancer cell invasiveness. Inhibition of angiogenin activity can be one of the attractive targets for gastric cancer therapy.

References

Badet, J., Soncin, F., Guitton, J.-D., Lamare, O., Cartwright, T., and Barritault, D. 1989. Specific binding of angiogenin to calf pulmonary artery endothelial cells. *Proc. Natl. Acad. Sci. USA 86*:8427–8431.

Barton, D.P.J., Cai, A., Wendt, K., Young, M., Gamero, A., and De Cesare, S. 1997. Angiogenic protein expression in advanced epithelial ovarian cancer. *Clin. Cancer Res. 3*:1579–1586.

Bicknell, R., and Vallee, B.L. 1989. Angiogenin stimulates endothelial cell prostacyclin secretion by activation of phospholipase A_2. *Proc. Natl. Acad. Sci. USA 86*:1573–1577.

Chao, Y., Li, C.-P., Chau, G.-Y., Chen, C.-P., King, K.-L., Lui, W.-Y., Ten, S.-H., Chang, F.-Y., Chan, W.-K., and Lee, S.-D. 2003. Prognostic significance of vascular endothelial growth factor, basic fibroblast growth factor, and angiogenin in patients with resectable hepatocellular carcinoma after surgery. *Ann. Surg. Oncol. 10*:355–362.

Chopra, V., Dinh, T.V., and Hannigan, E.V. 1996. Angiogenin, interleukins, and growth-factor levels in serum of patients with ovarian cancer: correlation with angiogenesis. *Cancer J. Sci. Am. 2*:279–285.

Chopra, V., Dinh, T.V., and Hannigan, E.V. 1997. Serum levels of interleukins, growth factors and angiogenin in patients with endometrial cancer. *J. Cancer Res. Clin. Oncol. 123*:167–172.

Chopra, V., Dinh, T.V., and Hannigan, E.V. 1998. Circulating serum levels of cytokines and angiogenic factors in patients with cervical cancer. *Cancer Invest. 1*:152–159.

Coussens, L.M., Raymond, W.W., Bergers, G., Laig-Webster, M., Behrendtsen, O., Werb, Z., Caughey, G.H., and Hanahan, D. 1999. Inflammatory mast cells up-regulate angiogenesis during squamous epithelial carcinogenesis. *Genes Dev. 13*:1382–1397.

Eberle, K., Oberpichler, A., Trantakis, C., Krupp, W., Knüpfer, M., Tschesche, H., and Seifert, V. 2000. The expression of angiogenin in tissue samples of different brain tumors and cultures glioma cells. *Anticancer Res. 20*:1679–1684.

Eppenberger, U., Kueng, W., Schlaeppi, J.-M., Roesel, J.L., Benz, C., Mueller, H., Matter, A., Zuber, M., Luescher, K., Litschgi, M., Schmitt, M., Foekens, J.A., and Eppenberger-Castori, S. 1998. Markers of tumor angiogenesis and proteolysis independently define high- and low-risk subsets of node-negative breast cancer patients. *J. Clin. Oncol. 16*:3129–3136.

Etoh, T., Shibuta, K., Barnard, G.F., Kitano, S., and Mori, M. 2000. Angiogenin expression in human colorectal cancer: the role of focal macrophage infiltration. *Clin. Cancer Res. 4*:3545–3551.

Fett, J.W., Strydom, D.J., Lobb, R.R., Alderman, E.M., Lemuel Bethune, J., Riordan, J.F., and Vallee, B.L. 1985. Isolation and characterization of angiogenin, an angiogenic protein from human carcinoma cells. *Biochemistry 24*:5480–5486.

Folkman, J. 1971. Tumor angiogenesis: therapeutic implications. *N. Engl. J. Med. 285*:1182–1186.

Folkman, J. 1986. How is blood vessel growth regulated in normal and neoplastic tissue? G.H.A. Clowes Memorial Award Lecture. *Cancer Res. 46*:467–473.

Gho, Y.S., Yoon, W.-H., and Chae, C.-B. 2002. Antiplasmin activity of a peptide that binds to the receptor binding site of angiogenin. *J. Biol. Chem. 277*:9690–9694.

Hallahan, T.W., Shapiro, R., and Vallee, B.L. 1991. Dual site model for the organogenic acivity of angiogenin. *Proc. Natl. Acad. Sci. USA 88*:2222–2226.

Hartmann, A., Kunz, M., Köstlin, S., Gillitzer, R., Toksoy, A., Bröcker, E.-B., and Klein, C.E. 1999. Hypoxia-induced up-regulation of angiogenin in human malignant melanoma. *Cancer Res. 59*:1578–1583.

Hisai, H., Kato, J., Kobune, M., Murakami, T., Miyanishi, K., Takahashi, M., Yoshizaki, N., Takimoto, R., Terui, T., and Niitsu, Y. 2003. Increased expression of angiogenin in hepatocellular carcinoma in correlation with tumor vascularity. *Clin. Cancer Res. 9*:4852–4859.

Hu, G.-F. 1998. Neomycin inhibits angiogenin-induced angiogenesis. *Proc. Natl. Acad. Sci. USA 95*:9791–9795.

Hu, G.-F., and Riordan, J.F. 1993. Angiogenin enhances actin acceleration of plasminogen activation. *Biochem. Biophys. Res. Comm. 197*:682–687.

Hu, G.-F., Riordan, J.F., and Vallee, B.L. 1994. Angiogenin promotes invasiveness of cultured endothelial cells by stimulation of cell-associated proteolytic activities. *Proc. Natl. Acad. Sci. USA 91*:12096–12100.

Hu, G.-F., Riordan, J.F., and Vallee, B.L. 1997. A putative angiogenin receptor in angiogenin-responsive human endothelial cells. *Proc. Natl. Acad. Sci. USA 94*:2204–2209.

Hu, G.-F., Strydom, D.J., Fett, J.W., Riordan, J.F., and Vallee, B.L. 1993. Actin is a binding protein for angiogenin. *Proc. Natl. Acad. Sci. USA 90*:1217–1221.

Jimi, S., Ito, K., Kohno, K., Ono, M., Kuwano, M., Itagaki, Y., and Ishikawa, H. 1995. Modulation by bovine angiogenin of tubular morphogenesis and expression of plasminogen activator in bovine endothelial cells. *Biochem. Biophys. Res. Comm. 211*:476–483.

Kao, R.Y.T., Jenkins, J.L., Olson, K.A., Key, M.E., Fett, J.W., and Shapiro, R. 2002. A small molecule inhibitor of the ribonucleolytic activity of human angiogenin that possesses antitumor activity. *Proc. Natl. Acad. Sci. USA 99*:10066–10071.

Kawano, Y., Hasan, K.Z., Fukuda, J., Mine, S., and Miyakawa, I. 2003. Production of vascular endothelial growth factor and angiogenic factor in human follicular fluid. *Mol. Cell. Endocrinol. 202*:19–23.

Kitadai, Y., Sasaki, A., Ito, M., Tanaka, S., Oue, N., Yasui, W., Aihara, M., Imagawa, K., Haruma, K., and Chayama, K. 2003. Helicobactor pylori infection influences expression of genes related to angiogenesis and invasion in human gastric carcinoma cells. *Biochem. Biophys. Res. Comm. 311*:809–814.

Kolben, M., Bläser, J., Ulm, K., Schmitt, M., Schneider, K.T.M., Tschesche, H., and Graeff, H. 1997. Angiogenin plasma levels during pregnancy. *Am. J. Obstet. Gynecol. 176*:37–41.

Kurachi, K., Davie, E.W., Strydom, D.J., Riordan, J.F., and Vallee, B.L. 1985. Sequence of the cDNA and gene for angiogenin, a human angiogenesis factor. *Biochemistry 24*:5494–5499.

Miyake, H., Hara, I., Yamanaka, K., Gohji, K., Arakawa, S., and Kamidono, S. 1999. Increased angiogenin expression in the tumor tissue and serum of urothelial carcinoma patients is related to disease progression and recurrence. *Cancer 86*:316–324.

Montero, S., Guzmán, C., Cortés-Funes, H., and Colomer, R. 1998. Angiogenin expression and prognosis in primary breast carcinoma. *Clin. Cancer Res. 4*:2161–2168.

Montone, K.T., and Brigati, D.J. 1994. *In situ* molecular pathology: instrumentation, oligonucleotides, and viral nucleic acid detection. *J. Histochem. 17*:195–201.

Moormann, P.S., Pohl, C., Himmelmann, G.W., and Newmann, K. 1986. Morphological predictors of survival in advanced gastric carcinoma univariate and multivariate analysis. *J. Cancer Res. Clin. Oncol. 112*:156–164.

Moroianu, J., and Riordan, J.F. 1994. Nuclear translocation of angiogenin in proliferating endothelial cells is essential to its angiogenic activity. *Proc. Natl. Acad. Sci. USA 91*:1677–1681.

Olson, K.A., Byers, R., Key, M.E., and Fett, J.W. 2002. Inhibition of prostate carcinoma establishment and metastatic growth in mice by an antiangiogenin momoclonal antibody. *Int. J. Cancer 98*:923–929.

Pekarek, L.A., Weichselbaum, R.R., Beckett, M.A., Nachman, J., and Schreiber, H. 1993. Footprinting of individual tumors and their variants by constitutive cytokine expression patterns. *Cancer Res. 53*:1978–1981.

Seljelid, R., Jozefowski, S., and Sveinbjornsson, B. 1999. Tumor stroma. *Anticancer Res. 19*:4809–4822.

Shaarawy, M., El-Mallah, S.Y., and Sheiba, M. 2003. Angiogenin and gestational trophoblastic tumors, a promising prognostic marker. *Clin. Chem. Lab. Med. 41*:306–310.

Shimoyama, S., Gansauge, F., Gansauge, S., Negri, G., Oohara, T., and Beger, H.G. 1996. Increased angiogenin expression in

pancreatic cancer is related to cancer aggressiveness. *Cancer Res. 56*:2703–2706.

Shimoyama, S., Gansauge, F., Gansauge, S., Oohara, T., Kaminishi, M., and Beger, H.G. 1999a. Increased angiogenin expression in obstructive chronic pancreatitis surrounding pancreatic cancer but not in pure chronic pancreatitis. *Pancreas 18*:225–230.

Shimoyama, S., and Kaminishi, M. 2000. Increased angiogenin expression in gastric cancer correlated with cancer progression. *J. Cancer Res. Clin. Oncol. 126*:468–474.

Shimoyama, S., and Kaminishi, M. 2001. Angiogenin: its clinical implications in malignancy. *Asian J. Cancer 1*:32–36.

Shimoyama, S., and Kaminishi, M. 2003. Angiogenin in sera as an independent prognostic factor in gastric cancer. *J. Cancer Res. Clin. Oncol. 129*:239–244.

Shimoyama, S., Kaminishi, M., Joujima, Y., Oohara, T., Hamada, C., and Teshigawara, W. 1994. Lymph node involvement correlation with survival in advanced gastric carcinoma: univariate and multivariate analyses. *J. Surg. Oncol. 57*:164–170.

Shimoyama, S., Shimizu, N., Tsuji, E., Yamasaki, K., Kawahara, M., and Kaminishi, M. 2002. Distribution of angiogenin and its gene message in colorectal cancer patients and their clinical relevance. *Anticancer Res. 22*:1045–1052.

Shimoyama, S., Yamasaki, K., Kawahara, M., and Kaminishi, M. 1999b. Increased serum angiogenin concentration in colorectal cancer is correlated with cancer progression. *Clin. Cancer Res. 5*:1125–1130.

Sköldenberg, E.G., Christiansson, J., Sandstedt, B., Larsson, A., Läckgren, G., and Christofferson, C. 2001. Angiogenesis and angiogenic growth factors in wilms tumor. *J. Urol. 165*: 2274–2279.

Soncin, F., Shapiro, R., and Fett, J.W. 1994. A cell-surface proteoglycan mediates human adenocarcinoma HT-29 cell adhesion to human angiogenin. *J. Biol. Chem. 269*: 8999–9005.

Ugurel, S., Rappi, G., Tilgen, W., and Reinhold, U. 2001. Increased serum concentration of angiogenic factors in malignant melanoma patients correlates with tumor progression and survival. *J. Clin. Oncol. 19*:577–583.

Verselis, S.J., Olson, K.A., and Fett, J.W. 1999. Regulation of angiogenin expression in human HepG2 hepatoma cells by mediators of the acute-phase response. *Biochem. Biophys. Res. Comm. 259*:178–184.

Wechsel, H.W., Bichier, K.-H., Feil, G., Loeser, W., Lahme, S., and Petri, E. 1999. Renal cell carcinoma: relevance of angiogenic factors. *Anticancer Res. 19*:1537–1540.

Xu, Z.-P., Tsuji, T., Riordan, J.F., and Hu, G.-F. 2003. Identification and characterization of an angiogenin binding DNA sequence that stimulates luciferase reporter gene expression. *Biochemistry 42*:121–128.

This Page Intentionally Left Blank

16

Role of *Helicobacter pylori* in Gastric Cancer

Gerardo Nardone

Introduction

Despite the decreasing incidence and mortality rates observed worldwide over the last 50 years, gastric cancer still ranks as a leading cause of cancer-related deaths in many parts of the world. After lung cancer, gastric cancer kills more people than any other malignant tumors. The International Agency for the Research on Cancer (IARC) reported 934,000 new gastric cancer cases and 700,000 annual deaths in 2002. The estimated 5-year relative survival rate is less than 20%. The incidence of gastric cancer varies considerably worldwide, occurring more frequently in developing countries than in industrialized countries, and tends to show a predilection for urban and lower socioeconomic groups. Today, the estimated crude rates of gastric cancer incidence accounts for ~10% of cancers worldwide, with the highest incidence rates occurring in Costa Rica, Japan, South America, and Central and Eastern Europe and the lowest rates occurring in the United States, parts of Africa (Uganda), and Southeast Asia (Parkin *et al.,* 2005).

Gastric cancers are often resistant to radiotherapy and chemotherapy, and, indeed, surgery represents the only treatment with a curative potential. However, two-thirds of Western patients with gastric cancer are still diagnosed in advanced stages, when surgery can only be palliative. The only exception to these dismal statistics is Japan, where, for various reasons, the condition is often identified at an early stage and in younger and healthier patients (Hohenberger and Gretschel, 2003). At present, preventive measures are likely to be the most effective means of reducing the incidence and mortality from this disease. However, to be successful this strategy depends on knowledge of the etiologic factors and pathogenetic mechanisms involved in gastric carcinogenesis.

Topographically, gastric cancer may arise in the cardia of the stomach or more distally (noncardia cancer). Epidemiologic data show that the etiologic factors and possibly the pathogenesis of these two types of cancer are completely different (Fuchs and Mayer, 1995). Cardia cancer appears to be closely associated with gastroesophageal reflux, whereas noncardia cancer results from the interaction of several factors, including diet, environment, and individual genetic susceptibility. Histologically, noncardia cancer is prevalently divided into two types according to Laurén's classification. (Laurén, 1965). The intestinal type consists of a gland-like structure that mimics intestinal glands and recognizes a series of precancerous lesions. The diffuse type, more prevalent in women younger than 50 years, lacks any glandular structure and arises closer to the advancing border of inflammation but without any identifiable

histologic precursor lesions. During the last few years, it has become apparent that the most important single factor responsible for the development of both intestinal and diffuse-type gastric cancer is *Helicobacter pylori (H. pylori)* infection (Huang *et al.,* 1998). *H. pylori* is a curved, motile, Gram-negative organism that probably represents one of the most common infections, affecting more than 50% of the world population. It is acquired during childhood and colonizes the gastric epithelial cells where it may persist without appropriate treatment for life, inducing a chronic inflammatory reaction (Miyaji *et al.,* 2000).

Since the accidental discovery of *H. pylori* (Warren and Marshall, 1983), much has been learned about this bacterium and its associated disease states. In 1994, after just 10 years the NIH Consensus Conference recognized *H. pylori* as a cause of gastric and duodenal ulcers. Soon afterward, the IARC declared *H. pylori* to be a group I human carcinogen for gastric adenocarcinoma (IARC, 1994). The relationship between *H. pylori* and gastric cancer has been postulated to exist mainly on the basis of epidemiologic investigations and animal models studies.

Epidemiologic Studies

The exact prevalence of *H. pylori* infection in patients with gastric cancer remains difficult to estimate because (as a result of modified gastric microenvironment) the infection can be lost locally and serology becomes negative (Karnes *et al.,* 1991). Nonetheless, many epidemiologic studies have shown a close correlation between *H. pylori* seropositivity and gastric cancer. The EUROGAST study, including 17 populations from 13 different countries (11 European countries, Unites States, and Japan), found a six-fold increased risk of gastric cancer in *H. pylori*-infected populations compared with uninfected populations (EUROGAST Study Group, 1993). A meta-analysis of cohort and case-control studies found that *H. pylori* infection was associated with a two-fold increased risk for developing gastric adenocarcinoma (Huang *et al.,* 1998). The relative risk for gastric cancer was greatest for younger patients (9.29 at age <29 years), suggesting that infection with *H. pylori* during childhood is an important prerequisite condition. A nested controlled study combining 12 studies (6 from Europe, 4 from Asia, 2 from the United States) and involving 1228 gastric cancer cases and 3406 control found that the association of *H. pylori* infection with gastric cancer was restricted to noncardia cancers (odd ratio [OR] 2.97; 95% CI [confidence interval] 2.3–3.7) and was stronger when blood samples for *H. pylori* serology were collected 10 years or more before cancer diagnosis (OR 5.9; 95% CI 3.4–10.3) (*Helicobacter* and Cancer Collaborative Group, 2001). However, the most powerful evidence is the 2001 prospective study including 1526 Japanese patients, of whom 1246 were *H. pylori* positive (Uemura *et al.,* 2001). The authors found that 36 infected patients (2.9%) developed gastric cancer in contrast with none of 280 noninfected patients during a mean follow-up of 7.8 years. The association between *H. pylori* infection and gastric cancer may also be modified by the level of exposure to other environmental factors. The prevalence of gastric cancer caused by a combination of *H. pylori* and salted foods has been shown to be lower in a tea-drinking population compared to a non–tea-drinking control population (Weisburger and Chung, 2002). The relative risk for gastric cancer was 2.6 for nonsmokers infected with CagA-positive *H. pylori* strain and 7.2 for smokers infected with a CagA-positive *H. pylori* strains (Sasazuki *et al.,* 2002). The interaction between *H. pylori* and cigarette or alcohol consumption may contribute to explain the so-called *H. pylori*-related African and Asian enigmas (i.e., high *H. pylori* prevalence and low gastric cancer rate) (Holcombe, 1992). Significant difference exists in the availability of alcohol and tobacco between developing and developed countries; thus the expected gastric cancer incidence per 100,000 in the different geographic areas would be 5.7 in Africa, 7.0 in Asia and Oceania, 16.0 in North America, and 26 in Europe (Lunet and Barros, 2003).

Animal Models

Many kinds of animal models have been used to examine the effect of *H. pylori* infection in gastric disorders. The animal model best reproducing *H. pylori*-related human disease is the Mongolian gerbil. The Mongolian gerbils infected with human isolates of *H. pylori* developed histopathologic gastric changes that closely mimic the mucosal changes caused by *H. pylori* infection in humans. *H. pylori* infection alone may induce well-differentiated adenocarcinoma at very high incidences (37%) in the gerbils at week 62 (Watanabe *et al.,* 1998). Furthermore, using the same animal model, eradication of *H. pylori* was shown to be effective in reducing the incidence of stomach adenocarcinomas (Shimizu *et al.,* 2000).

In a mouse model treated with the combination of N-methyl-N-nitrosurea (MNU) and *H. pylori* infection, the latter alone caused only chronic atrophic gastritis, whereas the combination of MNU and *H. pylori* infection resulted in a significantly higher incidence of gastric adenoma and adenocarcinoma (80%) than MNU alone (27%) (Han *et al.,* 2002). In INS-GAS mouse model, *H. pylori* infection accelerated the development

of gastric cancer. In addition, male mice showed a greater incidence of cancer when compared with females (Fox *et al.,* 2003). In 2003, a comprehensive review of animal models in gastric carcinogenesis concluded that *H. pylori* infection and high-salt diet act synergistically to promote the development of stomach cancer (Tatematsu *et al.,* 2003).

Mechanisms Responsible for *Helicobacter pylori*-Related Gastric Cancer

Despite evidence of a close relationship between *H. pylori* infection and gastric cancer, the mechanisms underlying the carcinogenetic process still remain to be elucidated. *H. pylori* infection starts by colonizing the gastric epithelium where it induces an inflammatory reaction that may persist throughout the patient's life despite local immune reaction (Crabtree, 1996). The extent and severity of gastric mucosa inflammation, as well as the clinical outcome of the infection, depend on a number of factors, including virulence of the bacterium, host genetic susceptibility, immune response, age at the time of initial infection, and environmental factors. The complex interplay between these factors may explain why only a minority (<1%) of those infected ultimately develop gastric cancer (Correa, 1995).

Helicobacter pylori Strains

H. pylori is genetically more diverse than most bacterial species with significant geographic differences. A genetic, strain-specific difference has been suggested to be involved in the ability of the organism to cause different diseases. *H. pylori* is characterized by several putative virulence factors (i.e., *vacA; iceA;* and particularly *cagA;* with the cag pathogenicity island [PAI]) that are variously associated with the risk of gastric disease (Atherton, 1997a).

The *vacA* gene, which encodes a vacuolating cytotoxin, is present in ~50% of *H. pylori* isolates. This gene comprises two variable regions: the s region, namely, s1a, s1b, s1c, or s2 allele, and the m region, namely, m1 m2a, or m2b allele (van Doorn *et al.,* 1998). The vacAs1 and vacAm1 strains appear to be more virulent than type s2 strains, presenting a higher degree of inflammation and higher risks for peptic ulcer disease, gastric atrophy, and gastric carcinoma (Atherton *et al.,* 1997b).

The *cagA* gene is a marker for the presence of the cag PAI (Censini *et al.,* 1996). Only half of Western isolates carry the *cag* PAI, whereas nearly all East Asian strains carry the *cag* PAI (van Doorn *et al.,* 1999). The CagA protein is translocated by a type IV secretion system encoded by the *cag* PAI into the gastric epithelial cells where it induces changes in the tyrosine phosphorylation states of distinct cellular proteins (Odenbreit *et al.,* 2000). Several genes of the *cag* PAI encode proteins that increase the production of pro-inflammatory interleukin 8 (IL-8) by the gastric epithelium (Shimoyama and Crabtree, 1997). Infection with *cagA*-positive *H. pylori* strains is associated with higher levels of mononuclear and neutrophilic infiltrates, more severe atrophy, intestinal metaplasia, and alterations in the gastric epithelial cell cycle (Nogueira *et al.,* 2001). Pooled data have shown that cagA-positive strains of *H. pylori* are associated with a higher risk of gastric cancer (OR 2.01, 95% CI 1.21–3.32) than those infected with cagA-negative strains. (Huang *et al.,* 1998). Two studies conducted in the United States and one in Japan have shown that the CagA-positive strain was more closely related to intestinal-type gastric cancer than the CagA-negative strain (Blaser *et al.,* 1995a; Kikuchi *et al.,* 1999; Parsonnet *et al.,* 1997). A large population-based case-control study from Los Angeles County confirmed this positive association demonstrating a close relationship between distal gastric cancer and infection with CagA-positive *H. pylori* strains (Wu *et al.,* 2003). *H. pylori* strains isolated from patients with gastric cancer were more often characterized by the presence of *vacA* s1 allelotype, the presence of *iceA,* and an expanded 3′ region of the *cagA* gene, indicating that disease outcome may be related to subtle differences in the infecting strains a (Koehler *et al.,* 2003; Louw *et al.,* 2001).

In contrast with previous studies, no difference in seroprevalence for antibodies against CagA antigen was observed in China between patients with gastric cancer and asymptomatic subjects (Mitchell *et al.,* 1996). The presence of a functional *cagA* PAI has no predictive value for the presence or future development of a clinically significant outcome (Graham and Yamaoka, 2000). Using detailed DNA (deoxyribonucleic acid) fingerprints and *vacA, cagA,* and *iceA* genotyping, no definite or consistent relationship between the pattern of gastric diseases and the relatedness of the *H. pylori* strain has been reported (Li *et al.,* 2002). Therefore, the question of whether certain *H. pylori* strains are more carcinogenic than others still remains to be elucidated and may vary in relation to the different geographic areas.

Host Genetic Susceptibility

Early studies revealed that gastric cancer was less common in patients with blood group O but was frequently associated with blood group A, which increases the risk by 16–20%. Blood group A is more closely

associated with diffuse-type gastric cancer than with the intestinal type (Fuchs and Mayer, 1995). A positive family history of gastric cancer has been associated with an increased (~three-fold) risk of gastric cancer (Zanghieri *et al.,* 1990), but subjects with both a positive family history and infection with cagA+ *H. pylori* strains had a 16-fold increased risk of noncardiac gastric carcinoma (Brenner *et al.,* 2000).

Polymorphisms in a wide variety of genes, present in a significant proportion of the normal population, may affect the activity of key inflammatory molecules and modify the effect of environmental exposures. Thus, gene–environmental interactions could explain the high interindividual or geographic variations in the gastric cancer incidence. Interleukin-1 beta (IL-1beta) and IL-I receptor antagonists (IL-1ra) are potent cytokines that play a key role in regulating gastric acid secretion, showing a 100-fold greater potency than proton pump inhibitors (Beales and Calam, 1998). An important case-control study conducted in Scotland and Poland showed that individuals with particular *IL-1 beta* gene polymorphism presented an increased risk of gastric carcinoma in the presence of *H. pylori* infection (El-Omar *et al.,* 2000). Polymorphic sequences, associated with increased gastric cancer risk (up to 2.6-fold), were detected at position -31 and -511 of the IL-1 beta promoter region and at IL-1RN*2. The *H. pylori* genotype may also synergistically interact with individual polymorphisms in determining the clinical outcomes of *H. pylori* infection. The chances of having gastric carcinoma were greatest in those individuals both with high-risk bacterial and host genotypes (i.e., vacAs1/IL-1B-511*T carrier [OR = 87, 95% CI = 11–679], vacAs1/IL-1RN*2/*2 [OR = 32, 95% CI = 7.8–134], and cagA-positive/IL-1B-511*T carrier [OR = 25, 95% CI = 8.2–77]) (Figueiredo *et al.,* 2002).

A review on genetic susceptibility and gastric cancer risk found that IL-IB and NATI variants are associated with an increased gastric cancer risk, whereas polymorphisms at human leukocyte antigen-DQ proteins (HLA-DQ), tumor necrosis factor (TNF), and CYP2E genes may confer protection (Gonzales *et al.,* 2002). HLA antigens are cell-surface proteins that bind to the antigen-specific T-cell receptor, forming an important signaling event for the cell-inducing or -suppressing immune response. There are two classes of HLA genes: HLA class I *(HLA-A)* and HLA class II *(HLA-DR, HLA-DQ,* and *HLA-FP)*. All these genes are highly polymorphic, with varying alleles of putative functional significance. A variety of associations between gastric cancer risk, *H. pylori* infection, and specific HLA alleles have been described. In a case-control study in the United States, the *HLA-DQB1**0301 allele was more common in gastric cancer than in controls (OR 3.2) (Lee *et al.,* 1996). Paradoxically, the same *HLA-DQB1**0301 allele was protective against *H. pylori* infection, leaving the possibility open for an increased risk through an independent *H. pylori* pathway. Another case-control study suggested that the absence *of HLA-DQA1**0102 may be a host genetic risk factor for *H. pylori* infection and the intestinal type of gastric cancer (Azuma *et al.,* 1998). A European study has confirmed absence of the *HLA-DQA1**0102 allele as a risk factor for *H. pylori* infection, but it did not find any association with gastric cancer risk (Magnusson *et al.,* 2001). On the contrary, the HLA-DRB1*1601 allele was positively associated with gastric cancer risk, being stronger in the *H. pylori*-negative and diffuse type of gastric cancer. Taken together, these results appear to indicate the existence of a variable genetic susceptibility that may confer differential risk for *H. pylori* infection and gastric cancer. Cohort studies, taking into account both the different genetic and environmental factors, are needed to establish not only the relative contribution of these factors to tumor development but also the contribution of their putative interaction.

Host-Immune Response

The gastroduodenal tract represents an important barrier between the human host and the microbial populations. The ability to distinguish pathogenetic bacteria from commensals is regulated through T-cell–dependent responses. Despite a vigorous humoral response against *H. pylori* antigens, most infected subjects fail to eliminate the pathogen spontaneously (D'Elios *et al.,* 2003). The gastric epithelium, following contact with *H. pylori,* expresses IL-8, which triggers the initial host immune response to the bacterium (Baggiolini *et al.,* 1994). Stimulation of macrophages induces natural immunity with the activation of T-helper cell response and the release of cytokines and chemokines (Crabtree, 1996). This is the first important step in the natural history of *H. pylori* infection because the release of local cytokines, particularly IL-12, is a crucial event in driving the specific T-cell response into a more or less polarized Th1 pattern. Th1 cells secrete interferon gamma (IFN-γ), TNF-α, and IL-12 cytokines, which are associated with a cell-mediated response. In contrast, Th2 cells secrete cytokines, such as IL-4, IL-5, IL-13, and transforming growth factor beta (TGF-β), which are associated with induction of humoral immune responses (Del Prete, 1998). However, most T-cell responses, which depend on the *H. pylori* strain and host characteristics, do not express a polarized type-1 or type-2 profile representing a heterogeneous population (designated Th0), which secretes different combinations of both Th1- and Th2-type cytokines (D'Elios *et al.,* 2003).

The major factor in disease progression appears to be a strong host Th1 immune response in the setting of a permissive environment. The importance of IFN-γ (a Th1 cytokine) is illustrated in the IFN-γ-knockout mouse, where lack of IFN-γ protects infected mice from atrophy, whereas the knockout of IL-10, a Th2 cytokine, leads to severe atrophic gastritis (Smythies *et al.,* 2000). In addition, a shift in the Th1/Th2 immune response may explain, at least in part, the Africa enigma. Parasitic infestations or a genetic predisposition selected by malaria, both endemic in these areas, induce a Th2 immune response secreting IL-4, which inhibits the Th1 response and may protect these subjects from ulcers (Fox *et al.,* 2000). A Th1-polarized pattern was consistently observed in patients with chronic gastritis complicated by peptic ulcer (Houghton *et al.,* 2002). Conversely, in nonulcer chronic gastritis and in gastric cancer, the pattern of cytokine secretion was more heterogeneous, including both Th1 and Th0 cells (Blaser and Atherton, 2004). This implies a shift of the gastric T-cell response in gastric carcinoma development (Ren *et al.,* 2001).

Age and Time of Infection

It has been proposed that age, at the time of onset of *H. pylori* infection, may be another determinant of disease outcome. Onset of *H. pylori* infection early in life has been associated with an increased risk of gastric cancer (Blaser *et al.,* 1995b). Epidemiologic studies have revealed a high incidence of adult gastric cancer in areas with a high prevalence of *H. pylori* infection in childhood (Mitchell *et al.,* 1992; Parsonnet *et al.,* 1991). In the younger Japanese generation, a high OR of 13.3 was shown for the relationship between *H. pylori* infection and gastric cancer (Kikuchi *et al.,* 1995). In subjects from a well-defined Japanese ethnic group, a case-control study (787 patients with gastric cancer versus 1007 control subjects) showed similar results (Huang *et al.,* 1998).

Gastric cancer tends to occur in older people, and it seems more likely to occur in a stomach that has been inflamed for many years. *H. pylori* infection generally induces an inflammatory response characterized by chemotaxis and release of inflammatory mediators (Crabtree, 1996). As a consequence, long-lasting *H. pylori* infection may induce mucosal atrophy with decreased gastric acid secretion and mutations in epithelial DNA (Farinati *et al.,* 1998). Continuous infection with *H. pylori* during childhood, or the teenage years, may induce in adulthood irreversible harm to the gastric mucosa. Therefore, it is mandatory that *H. pylori* be eradicated in childhood or early teens because eradication after the irreversible gastric mucosa lesions have been inflicted does not prevent carcinogenesis at all.

In developing countries, the age of acquisition of *H. pylori* infection in most individuals is in early childhood, thus resulting in a prolonged infection and increased risk of gastric cancer. Conversely, in the Western world, as a result of improved socioeconomic status, there is a shift in the age of acquisition to a later time. This delay may decrease the risk of gastric cancer and increase the possibility of a disease requiring a shorter latency period, such as duodenal ulcer disease.

Helicobacter pylori-Associated Gastric Inflammatory Reaction

The overwhelming majority of patients with *H. pylori* infection are asymptomatic and never develop overt disease or symptoms. In contrast, in some patients, *H. pylori* infection elicits an inflammatory response with infiltration of the mucosa by polymorphonuclear leukocytes, macrophages, T lymphocytes, and B lymphocytes (Crabtree, 1996). CD11a/CD18 and CD11b/CD18 lymphocytes, induced by *H. pylori* infection, interact with the intercellular adhesion molecule (ICAM-1), resulting in the migration of neutrophils to the site of infection and adhesion to the surface epithelium. The infiltration of inflammatory cells into the lamina propria causes the release of reactive oxygen species (ROS) such as superoxide and hydroxyl ions. These ROS metabolites are partly responsible for increased oxidative stress of the gastric epithelial cells that can induce DNA mutations (Farinati *et al.,* 1998). Furthermore, prolonged gastric mucosal inflammation may induce progressive loss of acid-secreting parietal cells progressing to gastric atrophy with hypochlorhydria and increased intragastric pH. Hypochlorhydria enhances the growth of nitrosating bacteria, which can then catalyze the production of carcinogenic N-nitroso compounds (Sanduleanu *et al.,* 2001).

The normal stomach secretes ascorbic acid into the lumen, which scavenges the free oxygen metabolites and inhibits the conversion of nitrate to nitrite and nitrite to N-nitrosamines. Furthermore, it has been demonstrated that *H. pylori* infection inhibits the gastric secretion of ascorbic acid, which in turn influences the extension of the mucosal inflammation (O'Connor, 1992). An important host factor, increasing the relative risk of gastric cancer, is the presence of the IL-1 polymorphism, which in the presence of *H. pylori* infection powerfully inhibit gastric acid secretion (El-Omar *et al.,* 2000) (see also previous paragraph). Patients presenting high acid secretion tend to have mucosal inflammation limited to the antrum, whereas those with relative hypochlorhydria tend to develop pangastritis (Stolte *et al.,* 1998). Gastric cancer occurs most commonly in

patients presenting pangastritis or corpus-predominant gastritis associated with gastric atrophy and intestinal metaplasia (Correa, 1995).

The generation of ROS and nitric oxide can deaminate cellular DNA and cause mutation, thus initiating the genetic changes underlying the gastric carcinogenetic process (Li *et al.,* 2001). Higher concentrations of 8-hydroxydeoxy-guanosine (8-OH-dG), a well-known marker of oxidative DNA damage, have frequently been detected in patients who are *H. pylori*-positive with atrophic gastritis and intestinal metaplasia (Farinati *et al.,* 1998). The inflammatory process produced by infection and associated with the release of free oxygen metabolites may cause a reversible increase in the proliferation of gastric epithelial cells (Drake *et al.,* 1998; Lynch *et al.,* 1995). The dynamic balance between cell proliferation and apoptosis is essential for maintaining normal mucosal integrity. Sustained stimulation of apoptosis could ultimately result in excessive cell loss and ulcer development (i.e., the acute phase of *H. pylori* infection), whereas inhibition of apoptosis has been reported to be associated with the early phases of carcinogenesis (Rokkas *et al.,* 1999; Scotiniotis *et al.,* 2000). Prolonged survival of abnormal cells can favor the accumulation of sequential genetic mutations that would result in tumor promotion (Everett *et al.,* 2002). Moss (1988) reported an increase in the cell-proliferation rate and a decrease in the apoptotic index in *H. pylori* infection. The expression of c-fos (messenger ribonucleic acid [mRNA] and protein), which regulates the transcription of genes related to cell cycle control, was significantly higher in the *H. pylori*-infected mucosa and precancerous gastric lesions than in normal mucosa (Yang *et al.,* 2003). Mounting evidence shows that cyclooxygenase-2 (COX-2), which induces cell proliferation and inhibits apoptosis, is overexpressed in *H. pylori*-positive gastritis, precancerous lesions, and gastric cancer (Nardone *et al.,* 2004). These inflammatory reactions may induce a cascade of sequential events leading ultimately to intestinal-type gastric cancer or directly promoting diffuse-type gastric cancer.

Multistep Process of Intestinal-Type Gastric Cancer "Correa's Model"

According to Correa (1995), intestinal-type gastric cancer may be considered to be a multistep process starting from chronic gastritis and progressing through chronic atrophic gastritis, intestinal metaplasia, and dysplasia. This sequence is usually triggered by *H. pylori* infection and affected by a variety of genetic and environmental factors that may act synergistically (Ming, 1998).

Chronic Atrophic Gastritis

Long-standing *H. pylori*-induced gastric inflammation often leads to atrophic gastritis, which is considered the first important step in the histogenesis of gastric cancer. In a large population study on 2455 subjects in Japan, gastric atrophy was detected in 80% of patients with *H. pylori* compared to 10% of patients without *H. pylori* (Asaka *et al.,* 2001). According to previous European studies, the overall prevalence of gastric atrophy in asymptomatic adults ranges from 22% to 37%, with a gastric cancer incidence ranging from 7% to 13% after a follow-up of more than 11 years (Borchard, 1986; Cheli *et al.,* 1984). In a study, observing 5375 subjects for a 10-year follow-up period, 117 gastric cancers were identified. The risk was greatest in subjects with moderate atrophy at baseline (hazard ratio [HR] 2.22; 95% CI 1.08–4.58) and 4–6 years of follow-up (HR 4.6–5.0) (Inoue *et al.,* 2000). Gastric atrophy, particularly when it affects a large part of the gastric body, is associated with acid hyposecretion and impaired pepsinogen levels (McColl *et al.,* 1997). The low acidity of the gastric juice will, moreover, allow colonization with other bacteria, that, in turn, may promote the formation of carcinogenic factors (i.e., N-nitroso formation), inducing cellular DNA methylation. This finding is particularly important because in chronic atrophic gastritis, the proliferative activity increases in the mucosal epithelium, resulting in the presence of relatively immature cells in the glands. Ornithine decarboxylase (ODC), the first and rate-limiting enzyme in the biosynthesis of polyamines, is required for normal and neoplastic growth (Russo *et al.,* 1997). ODC is up-regulated by *H. pylori* and strongly expressed in atrophic and intestinal metaplasia areas (Konturek *et al.,* 2003). Therefore, expression of ODC may be considered an important marker of premalignancy in the stomach.

Intestinal Metaplasia

Chronic atrophic gastritis is often associated with intestinal metaplasia, both lesions being closely related to *H. pylori* infection and gastric cancer risk (Leung and Sung, 2002; Testino *et al.,* 2000). Indeed, the prevalence of intestinal metaplasia was significantly higher in *H. pylori*-positive (43%) than in *H. pylori*-negative subjects (6.2%) (Asaka *et al.,* 2001). In Japan, using a gastric cancer index, intestinal metaplasia was the only criterion associated with the development of intestinal-type gastric cancer (Shimoyama *et al.,* 2000).

Intestinal metaplasia has been classified, according to Jass and Filipe, into complete, or type I, and incomplete, which comprises types II and III (Jass and Filipe, 1980).

Based on retrospective data, the risk of gastric cancer is related to the type of intestinal metaplasia. In a 10-year follow-up study from Slovenia, patients with intestinal metaplasia showed an overall 10-fold increased risk of gastric cancer compared with those without intestinal metaplasia (Filipe *et al.,* 1994). In another study, the risk of gastric cancer was four-fold higher in patients with intestinal metaplasia type III than in those with type I (You *et al.,* 1999). The association between the risk of gastric cancer development and intestinal metaplasia subtypes is, however, not universally accepted. Intestinal metaplasia involving the lesser curvature, from the cardia to the pylorus, or the entire stomach, was associated with a higher risk of gastric cancer than focal or antral predominant intestinal metaplasia (Cassaro *et al.,* 2000). Thus, the distribution of intestinal metaplasia, rather than intestinal metaplasia subtype, may provide a higher predictive value of cancer risk. In a cohort study of 4655 healthy asymptomatic subjects observed for a mean period of 7.7 years, the risk of gastric cancer increased in a stepwise fashion from the *H. pylori*-positive chronic gastritis group (HR 7.13; 95% CI: 0.95–53.33) to the *H. pylori*-positive chronic atrophic gastritis group (HR 14.85; 95% CI: 1.96–107.7) and, finally, to severe chronic atrophic gastritis with extensive intestinal metaplasia (HR 61.85; 95% CI: 5.6–682.64) (Ohata *et al.,* 2004).

Molecular alterations could be involved in the progression of intestinal metaplasia to gastric cancer. The pattern of gene expression determining the cell phenotype is under the control of a complex hierarchy of transcription factors of which homeodomain proteins are important members. The homeobox genes *CDX1* and *CDX2* are intestinal transcription factors regulating the proliferation and differentiation of intestinal epithelial cells. CDX1 and CDX2 proteins are expressed predominantly in the small intestine and colon but not in the normal adult stomach (Silberg *et al.,* 1997). In a 2002 study from Japan, CDX2 expression was found in patients with chronic gastritis, closely associated with intestinal metaplasia (Satoh *et al.,* 2002). It is interesting that type III intestinal metaplasia, carrying a higher risk for gastric cancer, is harboring more genetic changes than type I and II (Moss, 1998; Nardone, 2003; Sepulveda, 2001).

Dysplasia

The next step in the cascade of morphologic changes in gastric carcinogenesis is dysplasia that usually develops in the intestinal metaplasia setting. This process includes a continuum of progressively dedifferentiated phenotypes, which may result in a new cell. According to the definition of the World Health Organization, dysplasia is now called noninvasive gastric neoplasia, indicating a preinvasive neoplastic change in the gastric glands (Fenoglio-Preiser *et al.,* 2000). In dysplasia cell morphology is characterized by uncontrolled growth and the potential to migrate and implant in other areas. The higher the grade of dysplasia, the greater the risk of developing invasive gastric cancer (Genta and Rugge, 1991). *H. pylori* is clearly associated with the onset of gastric inflammation and the progressive development of metaplastic changes.

From a molecular viewpoint, dysplastic cells are endowed with an increased amount of DNA, partly as a result of the increased number of proliferating cells (Abdel-Wahab, 1996). A mixture of polyploidy and aneuploidy cells, as well as many markers of genomic instability in high-grade dysplasia, have been demonstrated (Li *et al.,* 1994). According to our current knowledge, dysplastic cells resemble malignant cells and in fact may sometimes already be malignant. The majority of carcinomas found in follow-up studies and that were discovered within 1 year of the diagnosis of dysplasia may indicate that the carcinoma was already present at the time of diagnosis of dysplasia (Ming, 1998).

Are Precancerous Lesions Reversible?

The risk of gastric cancer is related to the severity and extent of atrophy, intestinal metaplasia, and dysplasia. *H. pylori* is the initial triggering factor, but its role in further progression still remains to be elucidated. This leads to the critical question of whether eradication of *H. pylori* can reverse these precancerous lesions and thus interrupt the gastric carcinogenic process. Many studies have focused on the issue of reversibility, and results have been controversial. According to one randomized 1-year follow-up study, *H. pylori* eradication was beneficial in preventing progression of atrophy and intestinal metaplasia of the gastric mucosa (Sung *et al.,* 2000). In a prospective study, there was no significant change in antral intestinal metaplasia during 4-year follow-up, although antral atrophy decreased significantly (Tepes *et al.,* 1999). The indexed literature on the effects of *H. pylori* cure on the dynamics of gastric atrophy or intestinal metaplasia, from 1992 to June 2001, have been evaluated (Hojo *et al.,* 2002). Focusing on the changes in atrophy, 11 out of 25 reports described a significant improvement, one reported a significant worsening, and the remaining 13 found no significant change. However, of 28 studies focusing on intestinal metaplasia changes, only 4 described a significant improvement. A review of data collected only from Japan revealed that there were more studies

showing regression following eradication than progression (Satoh, 2000).

To fully understand the effect of eradication therapy, diet style should be taken into account. Indeed, in an Italian study, co-administration of ascorbic acid with *H. pylori* eradication led to a significant improvement in intestinal metaplasia of the gastric mucosa (Zullo *et al.,* 2000). Likewise in Columbia, anti-*H. pylori* treatment and dietary supplementation with antioxidant micronutrients induced regression of cancer precursor lesions (Correa *et al.,* 2000). Finally, in a large, population-based, prospective study with a 10-year follow-up, vegetable and fruit intake, even in low amounts, was associated with a lower risk of gastric cancer (Kobayashi *et al.,* 2002).

A critical revision of the data obtained from various studies raises major questions: 1) How representative are the studies? 2) How accurate is the diagnosis of atrophy? 3) What is the biologic function of molecular markers in preneoplastic lesions? Selection of the study population, age of patients, genetic makeup of the host, *H. pylori* strains, and diet, together with biopsy protocols and follow-up time, account for major differences that may explain the significant discrepancies between the data emerging from the various studies. The literature is largely biased by the inconsistency of the histologic criteria used to classify atrophy, particularly when a dense inflammatory infiltrate is present (Rugge *et al.,* 2002; Staibano *et al.,* 2002). A large study from Houston showed that intestinal metaplasia was missed in more than 50% of biopsies from patients with confirmed intestinal metaplasia on multiple site sampling (El-Zimaity and Graham, 1999). Moreover, major differences exist between the Western and Japanese systems concerning terminology and definition of dysplasia (Schlemper *et al.,* 1997).

Atrophy is defined as the loss of specialized glands as a result of a prolonged inflammatory process. There are two principal pathways leading to atrophy, one in which the stem cell compartment or glands are destroyed and the second in which the selective destruction of specialized epithelial cells occurs with preservation of stem cells (Dixon, 2001). If the stem cell compartment is preserved by the inflammatory process, the removal of the injurious factor (i.e., *H. pylori*) could lead to regeneration of parietal and chief cells with full restoration of function. In contrast, if glands and their associated stem cells have been completely destroyed, regeneration of parietal cells is impossible.

Intestinal metaplasia represents a nonneoplastic change in cell phenotype, which is usually the result of selection pressures exerted by the modified microenvironment. Cytokines from chronic inflammatory cells and in particular Th2 helper lymphomonocytes may be responsible for adaptive intestinal metaplasia in *H. pylori* infection (Ishikawa *et al.,* 1997). Intestinal metaplasia is more likely to be reversible if it develops as an adaptation to an adverse factor that can be identified and removed. However, the change in phenotype is either a consequence of genetic mutations in stem cells or of epigenetic events that produce divergent differentiation in progeny cells (Dixon, 2001). If intestinal metaplasia is a consequence of stable genetic mutations in stem cells, changes in the immediate mucosal environment are unlikely to lead to reversal of intestinal metaplasia. Genetic stable mutations, generally found in type III intestinal metaplasia, are similar to those found in gastric dysplasia, whereas epigenetic mutations are detected in all types of intestinal metaplasia (Tahara, 1995).

In an attempt to overcome the discrepancies regarding gastric dysplasia, a consensus was reached in Vienna in 1998 (Schlemper *et al.,* 2000). Gastric dysplasia, now defined as "noninvasive neoplasia" is classified in a 5-tier system: 1) negative for neoplasia/dysplasia; 2) indefinite for neoplasia/dysplasia; 3) noninvasive neoplasia, low grade; 4) noninvasive neoplasia, high grade; and 5) invasive neoplasia. In agreement with this classification, a long-term prospective follow-up study on the clinicopathologic outcome of gastric dysplasia confirmed that high-grade dysplasia never regresses. Lesions, indefinite for dysplasia, are the only entities suitable for regression after eradication therapy (Rugge *et al.,* 2003). This may be explained by the fact that by lowering the inflammatory infiltrate of the gastric mucosa, the regenerative epithelial changes may regress.

Helicobacter pylori and Diffuse-Type Gastric Cancer

Diffuse gastric cancer, often associated with familial distribution, is more prevalent in younger females and patients with blood group A. The cancer develops in the stomach, following chronic inflammation, without passing through the intermediate steps of atrophic gastritis or intestinal metaplasia. The severity of the mucosal inflammation and host characteristics may directly induce mutagenetic events, ultimately leading to cancer (Asaka *et al.,* 1998). Many molecular alterations have been detected in diffuse-type gastric cancer that differ substantially from those found in the intestinal type (i.e., MSI-H phenotype, implicated in the repair of spontaneous and toxic DNA damage; SC-1 antigen, an apoptotic receptor; E-cadherin mutation and the growth factors c-met and k-sam) (Moss, 1998; Nardone, 2003; Tahara, 1995). The onset of these molecular alterations is strongly associated with *H. pylori* infection. A 1998 meta-analysis showed a close correlation between

diffuse-type gastric cancer and *H. pylori* infection, similar to that found between the intestinal type and *H. pylori* (OR 2.58, 95% CI: 1.47–4.53; OR 2.49; 95% CI: 1.41–4.43, respectively) (Huang *et al.,* 1998). Therefore, even if intestinal- and diffuse-type gastric cancer are characterized by a different genetic and morphologic pathway, they depend prevalently on the same triggering factor. Eradication of *H. pylori* might immediately reduce the risk of diffuse cancer, whereas cancers of the intestinal type may be less effectively prevented if patients are treated later in the evolution of their carcinogenic process. A prospective, randomized, placebo-controlled, population study has been carried out in a high-risk area of China (Wong *et al.,* 2004). Healthy carriers of *H. pylori* infection (1630 subjects) were observed from 1994 until 2002. A comparable incidence of gastric cancer development was found in the subjects receiving *H. pylori* eradication treatment and those receiving placebo. However, in a subgroup of *H. pylori* carriers not presenting precancerous lesions, eradication of *H. pylori* significantly decreased the development of gastric cancer.

Personal Experience in *Helicobacter pylori*-Related Gastric Carcinogenesis

Since 1993, we have analyzed some aspects of *H. pylori* gastric carcinogenesis. Initially, we demonstrated the effect of *H. pylori* infection on the gastric mucosa barrier. We found significant quantitative and qualitative variations in mucosal phospholipid composition, in particular a decrease in phosphatidylcholine and phosphatidylethanolamine classes, in infected compared to noninfected patients (Nardone *et al.,* 1993). These variations were hypothesized to be the consequence of an increased phospholipase activity. Thus, we investigated the activity and the molecular expression of cytosolic phospholipase A_2 ($cPLA_2$) in *in vivo* and *in vitro* systems. The $cPLA_2$ is involved in cellular signaling and growth and has even been implicated in the pathogenesis of malignant transformation. We found total PLA_2 activity (enzymatic assay) and $cPLA_2$ levels (mRNA by RT-PCR [reverse transcriptase-polymerase chain reaction] and protein expression by immunohistochemistry, Figure 40) increased in gastric biopsies of patients who were *H. pylori*-positive but not in patients who were *H. pylori*-negative. Conversely, in the *in vitro* system, represented by co-culture of microorganisms with an established epithelial cell target of *H. pylori* (HEp-2 cells), we found that the RNA level and protein expression of $cPLA_2$ were unchanged during *H. pylori* infection independently of their cellular adhesion or invasion. Thus, the increase in $cPLA_2$ expression and PLA_2 activity observed in the gastric mucosa of patients with *H. pylori* infection likely reflects an indirect manifestation mediated by the inflammatory response.

Another important issue that we studied concerns the expression of some markers of genomic instability in gastric mucosal samples in children, in adults, and in relatives of patients with familial gastric cancer.

We found overexpression of p53 and c-myc oncogenes and an altered DNA content in a subgroup of patients with *H. pylori* infection and gastric atrophy, particularly in the presence of metaplasia and dysplasia (Nardone *et al.,* 1999). The same study was repeated in

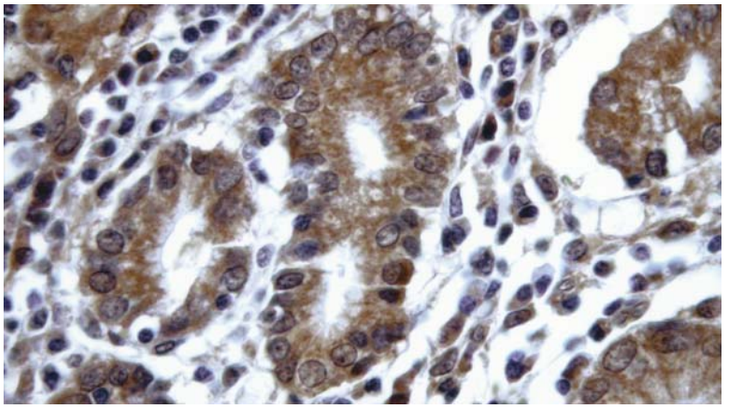

Figure 40. Immunohistochemical expression of cPLA2. *H. pylori*-positive chronic gastritis showing strong, definite immunostaining for cPLA2 (ABC standard; original magnification, 400X).

a pediatric population from the same geographic area. Unlike adults, *H. pylori* infection in children was, in some cases, associated with normal gastric histology, whereas intestinal metaplasia, dysplasia, p53 overexpression, and altered DNA content were always absent (Nardone *et al.,* 2001). Cell transformation takes a long time to progress to cancer, and neoplastic clonal expansion is generally anticipated by the appearance of markers of genomic instability. This could explain the morphologic and genomic alterations detected in adults but not in children, where a shorter period of infection is conceivable. Finally, we found markers of genomic instability in relatives of patients with familial gastric cancer only in the presence of *H. pylori* infection. These alterations disappeared 12 months after *H. pylori* eradication (Rocco *et al.,* 2003). This finding suggests that a hereditary predisposition may be, at least partly, mediated by environmental toxic agents (i.e., *H. pylori* infection).

The latest research on this issue has focused on a possible molecular pathway by which *H. pylori* could be implicated in gastric cancer development. In patients with *H. pylori,* the expression of COX-2 and $mPGES_1$ significantly correlated ($p < 0.0001$) with that of P-gp and Bcl-x_L, both implicated in blocking of apoptosis. High levels of COX-2, $mPGES_1$, P-gp, and Bcl-x_L expression were found, prevalently, in patients who were *H. pylori* positive, in nonresponders to eradication therapy, and in intestinal-type gastric cancer samples (Figures 41 and 42) (Nardone *et al.,* 2004).

Most of our investigations have been performed by means of immunohistochemistry according to the following protocol.

MATERIALS

1. Fixative: 10% neutral formol-saline: 100 ml of 40% formaldehyde, 900 ml of distilled water; 35 g of anhydrous dihydrogen phosphate (NaH_2PO_4); 6.5 g of anhydrous disodium-hydrogen-phosphate (Na_2HPO_4). Adjust pH using 1N HCl and 1N NaOH.
2. Tris-buffered saline (TBS): hydoxymethylaminomethane hydrochloride; distilled water; 1N HCl.
3. Blocking solution: nonimmune horse serum (Dakopatts, Hamburg, Germany); Tris/bovine serum albumin (1%).
4. Sodium citrate buffer, pH 6.0: Trisodium citrate; distilled water; 1.0 M HCl heated for 5 min in a Moulinex FM A735A.
5. 850 W microwave oven: Moulinex FM A735A.
6. 3% H_2O_2: 30% Hydrogen peroxide, Fisher Scientific, Pittsburgh, PA (200 ml: 30% hydrogen peroxide, 20 ml; distilled water, 180 ml).
7. Primary antibodies: $cPLA_2$ (polyclonal, C20, Santa Cruz, CA); p53 (monoclonal, NCL-p53-CM1, Ylem Italia); anti c-myc protein product (monoclonal, c-myc p62, Oncogene Science, San Diego, CA); COX-2 (polyclonal, H-62, Santa Cruz, CA); mPGE synthase (polyclonal, C-20, Santa Cruz, CA); *MDR1*-glycoprotein p (monoclonal, C129, Oncogene Science, San Diego, CA); Bcl-x_L (monoclonal, 2H12, Oncogene Science, San Diego, CA).
8. Secondary antibodies: Biotinylated rabbit F(Ab′) 2 fragment of anti-mouse IgG (or goat anti-rabbit for polyclonal Ab, Dako Corp., Carpinteria, CA).
9. Streptavidin conjugated with horseradish peroxidase (Dako Corp., Carpinteria, CA).

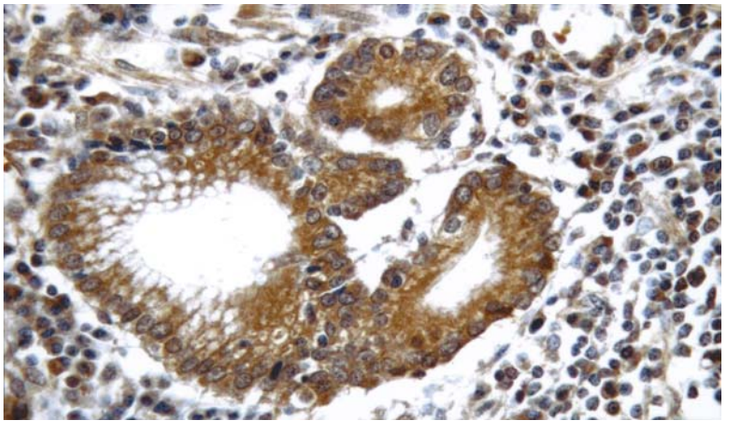

Figure 41. A case of *H. pylori*-positive gastritis showing uniform cytoplasmic immunostaining for cyclooxygenase-2 (COX-2) in glandular epithelium with membrane positivity. Staining is also visible in the inflammatory infiltrate (ABC standard; original magnification, 250X).

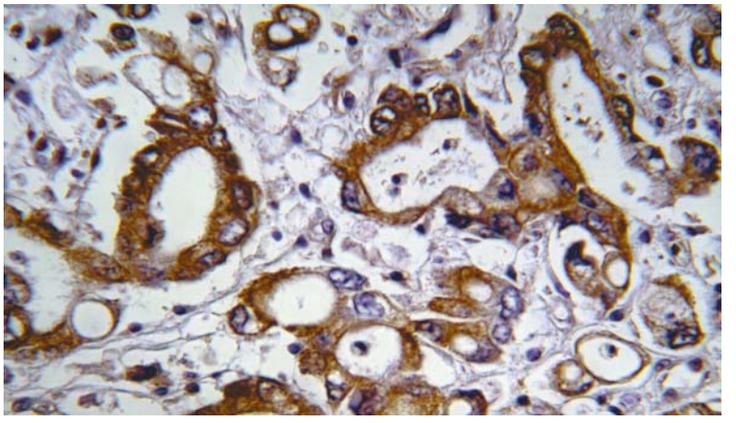

Figure 42. A case of intestinal-type gastric cancer showing strong immunostaining of gastric glands cyclooxygenase-2 (COX-2) (ABC standard; original magnification, 400X).

10. DAB (diaminobenzidene): liquid DAKO DAB Chromagen, containing 0.02% H_2O_2, (Dako Corp., Carpinteria, CA).

11. Hematoxylin Allegience (VWR), cat. # 72711 Richard Allen.

12. Mounting medium, Eukitt, Kindler GmbH & Co, Freiburg, Germany.

METHODS

1. Cut 4-µm-thick sections and place them onto poly-L-lysine (or gelatin)–coated slides, and dry overnight at 50°C.

2. Warm paraffinized tissue sections: 20 min at 40°C.

3. Deparaffinize with xylene, 5 min (2×) at room temperature.

4. Dip and blot 2 min (10×) at room temperature.

5. TBS: Add 30.5 g of Tris (hydroxymethyl-aminomethane hydrochloride) to 4 L of distilled H_2O. Add 185.3 ml of 1N HCl. Adjust pH using 1N HCl. Makeup to 5 L with distilled H_2O, magnetically stirred in a Coplin jar.

6. Dip and blot: 2 min (10×), room temperature, 100% ethanol.

7. Dip and blot: 2 min (10×), room temperature, 95% aqueous ethanol.

8. Dip and blot: 2 min (10×) room temperature, 80% aqueous ethanol.

9. Dip and blot: 2 min (10×) room temperature, deionized water.

10. Dip and blot: 2 min (10×) room temperature, TBS.

11. Quench tissue peroxidase, 15 min, room temperature, 3% H_2O_2 in distilled water.

12. Antigen retrieval: 40 min., 40°C: sections floated with 0.01 mol/L sodium-citrate buffer, pH 6.0. (Add 2.94 g of Trisodium citrate to 1 liter of distilled water. Adjust pH using 1N HCl). Heat for 5 mm in a Moulinex FM A735A, 850 W microwave oven.

13. Wash: 2 min, room temperature, TBS.

14. Block nonspecific bindings: 30 min, room temperature, nonimmune horse serum (1:20, Dakopatts, Hamburg, Germany) diluted in Tris/bovine serum albumin (1%) for 25 minutes. Slides held horizontally to limit nonspecific, edge staining of the sections. Wipe excess reagent from around tissue section.

15. Primary antibodies: (16 hr in a moist chamber, 4°C). Antibody diluted in TBS with 1 drop of Dako protein blocker/ml. The optimal working dilution of each antibody was determined by incubating sections with varying concentrations of antibody, ranging from 0.1–10 µg/ml; $cPLA_2$: 1:100; p53: 1:100; c-myc: 1:50; COX-2: 1:400; mPGEs: 1:800; *MDR1*-glycoprotein p: 1:150; Bcl-x_L: 1:100. Hold slides horizontally. As a rule, 150 µl of diluted primary antibody solution is applied to each tissue section. Perform negative controls by replacing the appropriate primary antibody by preimmune serum (isotype matched immunoglobulin (IgG) serum) to allow for the assessment of the nonspecific binding of the secondary antibody. Normalize the protein concentration of the normal mouse (or rabbit) serum to the protein concentration of the primary antibody. Incubate for 1 hr at room temperature. Positive controls: for $cPLA_2$ and c-myc: a normal lymph node; for p53 and *MDR1*-glycoprotein p, COX-2, and mPGEs: a case of colon adenocarcinoma; for Bcl-x_L: a low-grade follicular lymphoma.

16. Wash: 2 min, room temperature, TBS. (slides held horizontally).

17. Secondary antibody: 30 min, room temperature, biotinylated rabbit F(Ab′)2 fragment of anti-mouse IgG, 1:200 (or goat anti-rabbit) diluted in Tris. Slide held horizontally.

18. Wash: 2 min (2×), room temperature, TBS. Slides held horizontally.

19. Peroxidase: 30 min, room temperature, streptavidine-biotin complex: 1:200 in Tris (streptavidin conjugated with horseradish peroxidase). Slides held horizontally.

20. Wash: 2 min, room temperature, TBS. Slides held horizontally.

21. Peroxidase substrate: 6 min, room temperature, DAB (liquid, 3,3′ diaminobenzidine reagent from Dako). Slides held horizontally. Incubate in the dark.

22. Wash: 3 min, room temperature, distilled water, magnetically stirred distilled water in a Coplin jar.

23. Counterstaining: 45 sec, room temperature, modified Hams hematoxylin.

24. Wash: 3 min, room temperature, distilled water. Rinse until water is clean.

25. Dehydrate: dip and blot, 3 min, room temperature, 95% aqueous ethanol.

26. Dip and blot: 3 min (3×), room temperature, 100% ethanol.

27. Dip and blot: 5 min (2×), room temperature, xylene.

28. Mount and dry slides: 20 min, room temperature, Eukitt.

29. Evaluate staining localization: $cPLA_2$: cytoplasmic; p53 protein: nuclear; c-myc: cytoplasmic; COX-2 and mPGEs: cytoplasmic; *MDR1*-glycoprotein p: cytoplasmic; Bcl-x_L: cytoplasmic.

30. For each antibody, evaluate semiquantitatively the immunostaining, as follows: 0 (absence of staining) to + (up to 30% cell with positive staining), ++ (>30–60% cell with positive staining), +++ (>60% cell with positive staining).

31. Statistical analysis: k-statistics for interobserver agreement (a κ coefficient >0.75 denotes excellent reproducibility, a κ value between 0.4 and 0.75 denotes moderate reproducibility, and a κ value <0.4 denotes marginal or poor reproducibility) (Landis *et al.,* 1977); Chi-square test or Fisher's/Fisher exact test for categoric variables; Mann-Whitney U-test to evaluate differences among the average of the continuous variables; Kruskal-Wallis-ANOVA one-way analysis of variance to compare more than two groups of parameters; and nonparametric Spearman's coefficient to establish the significance among associations.

Concluding Remarks

In conclusion, the discovery of *H. pylori* infection ranks as one of the most important medical discoveries of the 20th century. The most dramatic impact of *H. pylori* infection has been in the treatment of peptic ulcer disease; however, epidemiologic studies have also shown that *H. pylori* is probably the most important single factor responsible for gastric cancer. The recognition of *H. pylori* as a key risk factor for gastric cancer has contributed to advancing our understanding of gastric carcinogenesis and also offered the exciting prospect of preventing this lethal disease through elimination of the infection. Indeed, eradication of *H. pylori* infection leads to resolution of inflammation, elimination of DNA damage by ROS, reduction in cell turnover, increase in acid output, and ascorbic acid secretion into gastric juice. A positive relationship has been established in some geographic areas where only a minority of *H. pylori*-infected individuals developed gastric cancers, but it has not been confirmed in some other countries (i.e., Africa), which has been described as the African enigma (Holcombe, 1992). Therefore, to determine whether *H. pylori* eradication would be a logical measure to prevent gastric cancer development, much more evidence needs to be collected, including the variation of virulence factors in the bacteria, host responses to inflammation, and side effects after eradication. One study that economically modeled the cost of screening per year of life saved estimated that in selected populations such as Japanese American, serologic screening for *H. pylori* beginning at age 50 years was more beneficial than breast cancer screening (Parsonnet *et al.,* 1996).

At present, there are insufficient data to recommend general screening for *H. pylori* of asymptomatic patients to prevent gastric cancer. However, the decision to screen should be based on individual risk factors, such as race, diet, and family history of gastric cancer. According to the Maastricht guidelines, search for and eventually eradication of *H. pylori* is strongly recommended after early gastric cancer resection and in patients with identified atrophic gastritis. Furthermore, eradication is recommended in individuals with a family history of gastric cancer and in patients who are first-degree relatives of patients with gastric cancer (Malfertheiner *et al.,* 2002). Development of an effective vaccine against *H. pylori* is the most logical approach to decrease the incidence of gastric adenocarcinoma worldwide and to achieve enormous benefits.

References

Abdel-Wahab, M., Attallah, A.M., Elshal, M.F., Eldousoky, I., Zalata, K.R., el-Ghawalby, N.A., Gad el-Hak, N., el-Ebidy, G.,

and Ezzat, F. 1996. Correlation between endoscopy, histopathology, and DNA flow cytometry in patients with gastric dyspepsia. *Hepatogastroenterology 43*:1313–1320.

Asaka, M., Kudo, M., Kato, M., Sugiyama, T., and Takeda, H. 1998. Review article: long-term *Helicobacter pylori* infection—from gastritis to gastric cancer. *Aliment. Phannacol. Ther. 12*:9–15.

Asaka, M., Sugiyama, T., Nobuta, A., Kato, M., Takeda, H., and Graham, D.Y. 2001. Atrophic gastritis and intestinal metaplasia in Japan: results of a large multicenter study. *Helicobacter 6*:294–299.

Atherton, J.C. 1997. The clinical relevance of strain types of *Helicobacter pylori. Gut. 40*:701–703.

Atherton, J.C., Peek, R.M., Tham, K.T., Cover, T.L., and Blaser, M.J. 1997. Clinical and pathological importance of heterogeneity in vacA, the vacuolating cytotoxin gene of *Helicobacter pylori. Gastroenterology 112*:92–99.

Azuma, T., Ito, S., Sato, F., Yamazaki, Y., Miyaji, H., Ito, Y., Suto, H., Kuriyama, M., Kato, T., and Kohli, Y. 1998. The role of the HLA-DQA1 gene in resistance to atrophic gastritis and gastric adenocarcinoma induced by *Helicobacter pylori* infection. *Cancer 82*:1013–1018.

Baggiolini, M., Dewald, D., and Moser, B. 1994. Interleukin-8 and related chemotactic cytokines: CXC and CC chemokines. *Adv. Immunol. 55*:97–179.

Beales, I.L., and Calam, J. 1998. Interleukin 1beta and tumour necrosis factor alpha inhibit acid secretion in cultured rabbit parietal cells by multiple pathways. *Gut. 42*:227–234.

Blaser, M.J., and Atherton, J.C. 2004. *Helicobacter pylori* persistence: biology and disease. *J. Clin. Invest. 113*:321–333.

Blaser, M.J., Chyou, P.H., and Nomura, A. 1995b. Age at establishment of *Helicobacter pylori* infection and gastric carcinoma, gastric ulcer, and duodenal ulcer risk. *Cancer Res. 55*:562–565.

Blaser, M.J., Perez-Perez, G.I., Kleanthous, H., Cover, T.L., Peek, R.M., Chyou, P.H., Stemmermann, G.N., and Nomura, A. 1995a. Infection with *Helicobacter pylori* strains possessing cagA is associated with an increased risk of developing adenocarcinoma of the stomach. *Cancer Res. 55*:2111–2115.

Borchard, F. 1986. Precancerous conditions and lesions of stomach. In Rugge, M., Arslan-Pagnini, C. and Di Mario, F. (eds.) Milano: *Edizioni Uniscop*, 175.

Brenner, H., Arndt, V., Sturmer, T., Stegmaier, C., Zeigtec, H., and Dhom, G. 2000. Individual and joint contribution of family history and *Helicobacter pylori* infection to the risk of gastric carcinoma. *Cancer 88*:274–279.

Cassaro, M., Rugge, M., Gutierrez, O., Leandro, G., Graham, D.Y., and Genta, R.M. 2000. Topographic patterns of intestinal metaplasia and gastric cancer. *Am. J. Gastroenterol. 95*:1431–1438.

Censini, S., Lange, C., Xiang, Z., Crabtree, J.E., Ghiara, P., Borodovsky, M., Rappuoli, R., and Covacci, A. 1996. Cag, a pathogenicity island of *Helicobacter pylori,* encodes type I-specific and disease-associated virulence factors. *Proc. Natl. Acad. Sci. USA 93*:14648–14653.

Cheli, R., Giacosa, A., and Pirasso, A. 1984. Chronic gastritis: a dynamic process toward cancer. In Ming, S.C. (ed.) *Precursor of gastric cancer.* New York: Praeger Scientific, *117.*

Correa, P. 1995. *Helicobacter pylori* and gastric carcinogenesis. *Am. J. Surg. Pathol. 19*:S37–43.

Correa, P., Fontham, E.T., Bravo, J.C., Bravo, L.E., Ruiz, B., Zarama, G., Reale, J.L., Malcom, G.T., Li, D., Johnson, W.D., and Mera, R. 2000. Chemoprevention of gastric dysplasia: randomized trial of antioxidant supplements and anti-*Helicobacter pylori* therapy. *J. Natl. Cancer. Inst. 92*:1881–1888.

Craanen, M.E., Blok, P., Dekker, W., Offerhaus, G.J.A., and Tytgat, G.N.J. 1995. Chronology of p53 protein accumulation in gastric carcinogenesis. *Gut. 36*:848–852.

Crabtree, J.E. 1996. Gastric mucosal inflammatory response to *Helicobacter pylori. Aliment. Pharmacol. Ther. 10*:29–37.

Del Prete, G. 1998. The concept of Type-1 and Type-2 helper T cells and their cytokines in humans. *Intern. Rev. Immunol. 16*:427–455.

D'E1ios, M.M., Amedei, A., and Del Prete, G. 2003. *Helicobacter pylori* antigen-specific T-cell responses at gastric level in chronic gastritis, peptic ulcer, gastric cancer and low-grade mucosa-associated lymphoid tissue (MALT) lymphoma. *Microb. Infect. 5*:723–730.

Dixon, M.F. 2001. Prospects for intervention in gastric carcinogenesis: reversibility of gastric atrophy and intestinal metaplasia. *Gut. 49*:2–4.

Drake, I.M., Mapstone, N.P., Schorah, C.J., White, K.L., Chalmers, D.M., Dixon, M.F., and Axon, A.T. 1998. Reactive oxygen species activity and lipid peroxidation in *Helicobacter pylori* associated gastritis: relation to gastric mucosal ascorbic acid concentrations and effect *of Helicobacter pylori* eradication. *Gut. 42*:768–771.

El-Omar, E.M., Carrington, M., Chow, W.H., McColl, K.E., Bream, J.H., Young, H.A., Herrera, J., Lissowska, J., Yuan, C.C., Rothman, N., Lanyon, G., Martin, M., Fraumeni, J.F. Jr., and Rabkin, C.S. 2000. Interleukin-1 polymorphisms associated with increased risk of gastric cancer. *Nature 404*:398–402.

El-Zimaity, H.M., and Graham, D.Y. 1999. Evaluation of gastric mucosal biopsy site and number for identification *of Helicobacter pylori* or intestinal metaplasia: role of the Sydney System. *Hum. Pathol. 30*:72–77.

EUROGAST Study Group. 1993. An international association between *Helicobacter pylori* infection and gastric cancer. *Lancet 341*:1359–1363.

Everett, S.M., White, K.L., Drake, L.M., Schorah, C.J., Calvert, R.J., Skinner, C., Stringer, M.D., Miller, D., Dixon, M.F., Chalmers, D.M., and Axon, A.T. 2002. The effect of *Helicobacter pylori* infection on levels of DNA damage in gastric epithelial cells. *Helicobacter 7*:271–280.

Farinati, F., Cardin, R., Degan, P., Rugge, M., Mario, F.D., Bonvicini, P., and Naccarato, R. 1998. Oxidative DNA damage accumulation in gastric carcinogenesis. *Gut. 42*:351–356.

Fenoglio-Preiser, C., Carneiro, F., and Cornea, P. 2000. Gastric carcinoma. In Hamilton S.R. and Aaltonen L.A. (eds.) *Pathology and genetics, tumors of the digestive system*. Lyon: IARC, 39.

Figueiredo, C., Machado, J.C., Pharoah, P., Seruca, R., Sousa, S., Carvaiho, R., Capelinha, A.F., Quint, W., Caldas, C., Van Doorn, L.J., Carneiro, F., and Sobrinho-Simoes, M. 2002. *Helicobacter pylori* and interleukin 1 genotyping: an opportunity to identify high-risk individuals for gastric carcinoma. *J. Natl. Cancer Inst. 94*:1680–1687.

Filipe, M.I., Munoz, N., Matko, I., Kato, I., Pompe-Kirn, V., Jutersek, A., Teuchmann, S., Benz, M., and Prijon, T. 1994. Intestinal metaplasia types and the risk of gastric cancer: a cohort study in Slovenia. *Int. J. Cancer 57*:324–329.

Fox, J.G., Beck, P., Dangler, C.A., Whary, M.T., Wang, T.C., Shi, H.N., and Nagler-Anderson, C. 2000. Concurrent enteric helminth infection modulates inflammation and gastric immune responses and reduces *Helicobacter*-induced gastric atrophy. *Nat. Med. 6*:536–542.

Fox, J.G., Rogers, A.B., Ihrig, M., Taylor, N.S., Whary, M.T., Dockray, G., Varro, A., and Wang, T.C. 2003. *Helicobacter pylori*-associated gastric cancer in INS-GAS mice is gender specific. *Cancer Res. 63*:942–950.

Fuchs, C.S., and Mayer, R.J. 1995. Gastric carcinoma. *N. Engl. J. Med. 333*:32–41.

Genta, R.M., and Rugge, M. 1999. Gastric precancerous lesions: heading for an international consensus. *Gut. 45*:15–18.

Gonzalez, C.A., Sala, N., and Capella, G. 2002. Genetic susceptibility and gastric cancer risk. *Int. J. Cancer 100*:249–260.

Graham, D.Y., and Yamaoka, Y. 2000. Disease-specific *Helicobacter pylori* virulence factors: the unfulfilled promise. *Helicobacter 5*:S279–282.

Han, S.U., Kim, Y.B., Joo, H.J., Hahm, K.B., Lee, W.H., Cho, Y.K., Kim, D.Y., and Kim, M.W. 2002. *Helicobacter pylori* infection promotes gastric carcinogenesis in a mice model. *J. Gastroenterol. Hepatol. 17*:253–261.

Helicobacter and Cancer Collaborative Group. 2001. Gastric cancer and *Helicobacter pylori*: a combined analysis of 12 case control studies nested within prospective cohorts. *Gut. 49*:347–351.

Hohenberger, P., and Gretschel, S. 2003. Gastric cancer. *Lancet 362*:305–315.

Hojo, M., Miwa, H., Ohkusa, T., Ohkura, R., Kurosawa, A., and Sato, N. 2002. Alteration of histological gastritis after cure of *Helicobacter pylori* infection. *Aliment. Pharmacol. Ther. 16*:1331–1332.

Holcombe, C. 1992. *Helicobacter pylori*: the African enigma. *Gut. 33*:429–433.

Houghton, J., Fox, J.G., and Wang, T.C. 2002. *Helicobacter pylori* and other causes of gastric ulceration. *J. Gastroenterol. Hepatol. 17*:495–499.

Huang, J.Q., Sridhar, S., Chen, Y., and Hunt, R.H. 1998. Meta-analysis of the relationship between *Helicobacter pylori* seropositivity and gastric cancer. *Gastroenterology* 114:1169–1172.

Inoue, M., Tajima, K., Matsuura, A., Suzuki, T., Nakamura, T., Ohashi, K., Nakamura, S., and Tominaga, S. 2000. Severity of chronic atrophic gastritis and subsequent gastric cancer occurrence: a 10-year prospective cohort study in Japan. *Cancer Lett. 161*:105–112.

International Agency for Research on Cancer. 1994. Schistosomes, liver flukes and *Helicobacter pylori*. *IARC 61*:177.

Ishikawa, N., Wakelin, D., and Mahida, Y.R. 1997. Role of T helper 2 cells in intestinal goblet cell hyperplasia in mice infected with Trichinella spiralis. *Gastroenterology 113*:542–549.

Jass, J.R., and Filipe, M.I. 1980. Suiphomucins and precancerous lesions of the human stomach. *Histopathology 4*:271–279.

Karnes, W.E. Jr., Samloff, I.M., Siurala, M., Kekki, M., Sipponen, P., Kim, S.W., and Walsh, J.H. 1991. Positive serum antibody and negative tissue staining for *Helicobacter pylori* in subjects with atrophic body gastritis. *Gastroenterology 101*:167–174.

Kikuchi, S., Crabtree, J.E., Forman, D., and Kurosawa, M. 1999. Association between infections with CagA-positive or -negative strains of *Helicobacter pylori* and risk for gastric cancer in young adults: Research Group on Prevention of Gastric Carcinoma Among Young Adults. *Am. J. Gastroenterol. 94*:3455–3459.

Kikuchi, S., Wada, O., Nakajima, T., Nishi, T., Kobayashi, O., Konishi, T., and Inaba, Y. 1995. Serum *anti-Helicobacter pylori* antibody and gastric carcinoma among young adults: Research Group on Prevention of Gastric Carcinoma Among Young Adults. *Cancer 75*:2789–2793.

Kobayashi, M., Tsubono, Y., Sasazuki, S., Sasaki, S., and Tsugane, S. 2002. Vegetables, fruit and risk of gastric cancer in Japan: a 10-year follow-up of the JPHC study Cohort I. *Int. J. Cancer 102*:39–44.

Koehler, C.I., Mues, M.B., Dienes, H.P., Kriegsmann, J., Schirmacher, P., and Odenthal, M. 2003. *Helicobacter pylori* genotyping in gastric adenocarcinoma and MALT lymphoma by multiplex PCR analyses of paraffin wax embedded tissues. *Mol. Pathol. 56*:36–42.

Konturek, P.C., Rembiasz, K., Konturek, S.J., Stachura, J., Bielanski, W., Galuschka, K., Karcz, D., and Hahn, E.G. 2003. Gene expression of ornithine decarboxylase, cyclooxygenase-2, and gastrin in atrophic gastric mucosa infected with *Helicobacter pylori* before and after eradication therapy. *Dig. Dis. Sci. 48*:36–46.

Landis, J.R., Koch, G.G. 1977. The measurement of observer agreement for categorical data. *Biometrics 33*:159–174.

Lauren, P. 1965. The two histological main types of gastric carcinoma: diffuse and so-called intestinal-type carcinoma. *Acta Path. Microbiol. Scand. 64*:31–38.

Lee, J.E., Lowy, A.M., Thompson, W.A., Lu, M., Loflin, P.T., Skibber, J.M., Evans, D.B., Curley, S.A., Mansfield, P.F., and Reveille, J.D. 1996. Association of gastric adenocarcinoma with the HLA class II gene DQB10301. *Gastroenterology 111*: 426–432.

Leung, W.K., and Sung, J.J**.** 2002. Review article: intestinal metaplasia and gastric carciogenesis. *Aliment. Pharmacol. Ther. 16*: 1209–1216.

Li, C.Q., Pignatelli, B., and Ohshima, H. 2001. Increased oxidative and nitrative stress in human stomach associated with cagA+ *Helicobacter pylori* infection and inflammation. *Dig. Dis. Sci. 46*:836–844.

Li, J., Zhao, A., Lu, Y., and Wang, Y. 1994. Expression of p185erbB2 and p21ras in carcinoma, dysplasia, and intestinal metaplasia of the stomach: an immunohistochemical and *in situ* hybridization study. *Semin. Surg. Oncol. 10*:95–99.

Li, L., Genta, R.M., Go, M.F., Gutirrez, O., Kim, J.G., and Graham, D.Y. 2002. *Helicobacter pylori* strain and the pattern of gastritis among first-degree relatives of patients with gastric carcinoma. *Helicobacter 7*:349–355.

Louw, J.A., Kidd, M.S., Kummer, A.F., Taylor, K., Kotze, U., and Hanslo, D. 2001. The relationship between *Helicobacter pylori* infection, the virulence genotypes of the infecting strain and gastric cancer in the African setting. *Helicobacter 6*:268–273.

Lunet, N., and Barros, H. 2003. *Helicobacter pylori* infection and gastric cancer: facing the enigmas. *Int. J. Cancer 106*:953–960.

Lynch, D.A., Mapstone, N.P., Clarke, A.M., Sobala, G.M., Jackson, P., Morrison, L., Dixon, M.F., Quirke, P., and Axon, A.T. 1995. Cell proliferation in *Helicobacter pylori* associated gastritis and the effect of eradication therapy. *Gut. 36*:346–350.

Magnusson, P.K.E., Enroth, H., Eriksson, I., Held, M., Nyren, O., Engstrand, L., Hansson, L.E., and Gyllensten, U.B. 2001. Gastric cancer and human leukocyte antigen: distinct DQ and DR alleles are associated with development of gastric cancer and infection by *Helicobacter pylori. Cancer Res. 61*:2684–2689.

Malfertheiner, P., Megraud, F., O'Morain, C., Hungin, A.P., Jones, R., Axon, A., Graham, D.Y., and Tytgat, G., European *Helicobacter Pylori* Study Group (EHPSG) 2002. Current concepts in the management of *Helicobacter pylori* infection: the Maastricht 2-2000 Consensus Report. *Aliment. Pharmacol. Ther. 16*:167–180.

McColl, K.E., El-Omar, E., Gillen, D., and Banerjee, S. 1997. The role of *Helicobacter pylori* in the pathophysiology of duodenal ulcer disease and gastric cancer. *Semin. Gastrointest. Dis. 8*:142–155.

Ming, S.C. 1998. Cellular and molecular pathology of gastric carcinoma and precursor lesions: a critical review. *Gastric Cancer 1*:31–50.

Mitchell, H.M., Hazell, S.L., Li, Y.Y., and Hu, P.J. 1996. Serological response to specific *Helicobacter pylori* antigens: antibody against CagA antigen is not predictive of gastric cancer in a developing country. *Am. J. Gastroenterol. 2*:1785–1788.

Mitchell, H.M., Li, Y.Y., Hu, P.J., Liu, Q., Chen, M., Du, G.G., Wang, Z.J., Lee, A., and Hazell, S.L. 1992. Epidemiology of *Helicobacter pylori,* in Southern China: identification of early childhood as the critical period for acquisition. *J. Infect. Dis. 166*:149–153.

Miyaji, H., Azuma, T., Ito, S., Abe, Y., Gejyo, F., Hashimoto, N., Sugimoto, H., Suto, H., Ito, Y., Yamazaki, Y., Kohli, Y., and Kuriyama, M. 2000. *Helicobacter pylori* infection occurs via close contact with infected individuals in early childhood. *J. Gastroenterol. Hepatol*. *15*:257–262.

Moss, S.F. 1998. Cellular markers in the gastric precancerous process. *Aliment. Pharmacol. Ther. 12 Suppl. 1*:91–109.

Nardone, G. 2003. Review article: molecular basis of gastric carcinogenesis. *Aliment. Pharmacol. Ther. 17 Suppl*. *2*:75–81.

Nardone, G., D'Armiento, P., Corso, G., Coscione, P., Esposito, M., and Budillon, G. 1993. Lipids of human gastric mucosa: effect of *Helicobacter pylori* infection and nonalcoholic cirrhosis. *Gastroenterology 107*:362–368.

Nardone, G., Rocco, A., Vaira, D., Staibano, S., Budillon, A., Tatangelo, F., Scialli, M.G., Perna, F., Salvatore, G., Di Benedetto, M., De Rosa, G., and Patrignani, P. 2004. Expression of COX-2, mPGE-synthase$_1$, MDR-1 (P-gp), and Bcl-x_L: a molecular pathway of *Helicobacter pylori*-related gastric carcinogenesis. *J. Pathol. 202*:305–312.

Nardone, G., Staibano, S., Rocco, A., Mezza, E., Balzano, T., Salvatore, G., Staiano, A., Donofrio, V., Grazioli, B., De Rosa, G., and Budillon, G. 2001. Effect of *Helicobacter pylori* infection on gastric cell proliferation and genomic instability in a paediatric population of Southern Italy. *Digest. Liver. Dis. 33*: 743–749.

Nardone, G., Staibano, S., Rocco, A., Mezza, E., D'armiento, F.P., Insabato, L., Coppola, A., Salvatore, G., Lucariello, A., Figura, N., De Rosa, G., and Budillon, G. 1999. Effect of *Helicobacter pylori* infection and its eradication on cell proliferation, DNA status, and oncogene expression in patients with chronic gastritis. *Gut. 44*:789–799.

Nogueira, C., Figueiredo, C., Carneiro, F., Gomes, A.T., Barreira, R., Figueira, P., Salgado, C., Belo, L., Peixoto, A., Bravo, J.C., Bravo, L.E., Reale, J.L., Plaisier, A.P., Quint, W.G., Ruiz, B., Cornea, P., and Van Doorn, L.J. 2001. *Helicobacter pylori* genotypes may determine gastric histopathology. *Am. J. Pathol*. *158*:647–654.

O'Connor, H.J. 1992. *Helicobacter pylori* and gastric cancer: a review and hypothesis. *Eur. J. Gastroenterol. Hepathol. 4*:103.

Odenbreit, S., Puls, J., Sedlmaier, B., Gerland, E., Fischer, W., and Haas, R. 2000. Translocation of *Helicobacter pylori* CagA into gastric epithelial cells by type IV secretion. *Science 287*: 1497–1500.

Ohata H., Kitauchi, S., Yoshimura, N., Mugitani, K., Iwane, M., Nakamura, H., Yoshikawa, A., Yanaoka, K., Arii, K., Tamai, H., Shimizu, Y., Takeshita, T., Mohara, O., and Ichinose, M. 2004. Progression of chronic atrophic gastritis associated with *Helicobacter pylori* infection increases risk of gastric cancer. *Int. J. Cancer.* 109:138–143.

Parkin, D.M., Bray, F., Ferlay, J., and Pisani, P. 2005. Global cancer statistics. *CA Cancer J. Clin. 55*:74–108.

Parsonnet, J., Friedman, G.D., Orentreich, N., and Vogelman, H. 1997. Risk for gastric cancer in people with CagA positive or CagA negative *Helicobacter pylori* infection. *Gut. 40*:297–301.

Parsonnet, J., Friedman, G.D., Vandersteen, D.P., Chang, Y., Vogelman, J.H., Orentreich, N., and Sibley, R.K. 1991. *Helicobacter pylori* infection and the risk of gastric carcinoma. *N. Engl. J. Med. 325*:1127–1131.

Parsonnet, J., Harris, R.A., Hack, H.M., and Owens, D.K. 1996. Modelling cost-effectiveness of *Helicobacter pylori* screening to prevent gastric cancer: a mandate for clinical trials. *Lancet 348*:150–154.

Ren, Z., Pang, G., Clancy, R., Li, L.C., Li, C.S., Batey, R., Borody, T., and Dunkley, M. 2001. Shift of the gastric T-cell response in gastric carcinoma. *J. Gastroenterol. Hepatol. 16*:142–148.

Rocco, A., Staiano, S., Ottini, L., Mezza, E., Somma, P., Mariani-Costantini, R., Budillon, G., and Nardone, G. 2003. Is there a link between environmental factors and a genetic predisposition to cancer? A lesson from a familial cluster of gastric cancers. *Eur. J. Cancer 39*:1619–1624.

Rokkas, T., Ladas, S., Liatsos, C., Petridou, E., Papatheodorou, G., Theocharis, S., Karameris, A., and Raptis, S. 1999. Relationship of *Helicobacter pylori* CagA status to gastric cell proliferation and apoptosis. *Dig. Dis. Sci. 44*:487–492.

Rugge, M., Cassaro, M., Di Mario, F., Leo, G., Leandro, G., Russo, V.M., Pennelli, G., and Farinati, F. 2003. The long term outcome of gastric non-invasive neoplasia. *Gut. 52*:1111–1116.

Rugge, M., Correa, P., Dixon, M.F., Fiocca, R., Hattori, T., Lechago, J., Leandro, G., Price, A.B., Sipponen, P., Solcia, E., Watanabe, H., and Genta, R.M. 2002. Gastric mucosal atrophy: interobserver consistency using new criteria for classification and grading. *Aliment. Pharmacol. Ther. 16*:1249–1259.

Russo, F., Linsalata, M., Giorgio, I., Caruso, M.L., Armentano, R., and Di Leo, A. 1997. Polyamine levels and ODC activity in intestinal-type and diffuse-type gastric carcinoma. *Dig. Dis. Sci. 42*:576–579.

Sanduleanu, S., Jonkers, D., De Bruine, A., Hameeteman, W., and Stockbrugger, R.W. 2001. Double gastric infection with *Helicobacter pylori* and *non-Helicobacter pylori* bacteria during acid-suppressive therapy: increase of pro-inflammatory cytokines and development of atrophic gastritis. *Aliment. Pharmacol. Ther. 15*:1163–1175.

Sasazuki, S., Sasaki, S., and Tsugane, S. 2002. Cigarette smoking, alcohol consumption and subsequent gastric cancer risk by subside and histologic type. *Int. J. Cancer 101*:560–566.

Satoh, K. 2000. Does eradication of *Helicobacter pylori* reverse atrophic gastritis or intestinal metaplasia? Data from Japan. *Gastroenterol. Clin. North Am. 29*:829–835.

Satoh, K., Mutoh, H., Eda, A., Yanaka, I., Osawa, H., Honda, S., Kawata, H., Kihira, K., and Sugano, K. 2002. Aberrant expression of CDX2 in the gastric mucosa with and without intestinal metaplasia: effect of eradication of *Helicobacter pylori*. *Helicobacter 7*:192–198.

Schlemper, R.J., Itabashi, M., Kato, Y., Lewin, K.J., Riddell, R.H., Shimoda, T., Sipponen, P., Stolte, M., Watanabe, H., Takahashi, H., and Fujita, R. 1997. Differences in diagnostic criteria for gastric carcinoma between Japanese and western pathologists. *Lancet 349*:1725–1729.

Schlemper, R.J., Riddell, R.H., Kato, Y., Borchard, F., Cooper, H.S., Dawsey, S.M., Dixon, M.F., Fenoglio-Preiser, C.M., Flejou, J.F., Geboes, K., Hattoni, T., Hirota, T., Itabashi, M., Iwafuchi, M., Iwashita, A., Kim, Y.I., Kirchner, T., Klimpfinger, M., Koike, M., Lauwers, G.Y., Lewin, K.J., Oberhuber, G., Offner, F., Price, A.B., Rubio, C.A., Shimizu, M., Shimoda, T., Sipponen, P., Solcia, E., Stolte, M., Watanabe, H., and Yamabe, H. 2000. The Vienna classification of gastrointestinal epithelial neoplasia. *Gut. 47*: 251–255.

Scotiniotis, I.A., Rokkas, T., Furth, E.E., Rigas, B., and Shiff, S.J. 2000. Altered gastric epithelial cell kinetics in *Helicobacter pylori*-associated intestinal metaplasia: implications for gastric carcinogenesis. *Int. J. Cancer 85*:192–200.

Sepulveda, A.R. 2001. Molecular testing of *Helicobacter pylori*-associated chronic gastritis and premalignant gastric lesions: clinical implications. *J. Clin. Gastroenterol*. *32*:377–382.

Shimizu, N., Ikehara, Y., Inada, K., Nakanishi, H., Tsukamoto, T., Nozaki, K., Kaminishi, M., Kuramoto, S., Sugiyama, A., Katsuyama, T., and Tatematsu, M. 2000. Eradication diminishes enhancing effects of *Helicobacter pylori* infection on glandular stomach carcinogenesis in Mongolian gerbils. *Cancer Res. 60*: 1512–1514.

Shimoyama, T., and Crabtree, J.E. 1997. Mucosal chemokines in *Helicobacter pylori* infection. *J. Physiol. Pharmacol. 48*:315.

Shimoyama, T., Fukuda, S., Tanaka, M., Nakaji, S., and Munakata, A. 2000. Evaluation of the applicability of the gastric carcinoma risk index for intestinal type cancer in Japanese patients infected with *Helicobacter pylori*. *Virchows Arch. 436*:585–587.

Silberg, D.G., Furth, E.E., Taylor, J.K., Schuck, T., Chiou, T., and Traber, P.G. 1997. CDX1 protein expression in normal, metaplastic, and neoplastic human alimentary tract epithelium. *Gastroenterology 113*:478–486.

Smythies, L.E., Waites, K.B., Lindsey, J.R., Harris, P.R., Ghiara, P., and Smith, P.D. 2000. *Helicobacter pylori*-induced mucosal inflammation is Th1 mediated and exacerbated in IL-4 but not IFN-gamma, gene-deficient mice. *J. Immunol. 165*: 1022–1029.

Staibano, S., Rocco, A., Mezza, E., De Rosa, G., Budillon, G., and Nardone, G. 2002. Diagnosis of chronic atrophic gastritis by morphometric image analysis: a new method to overcome the confounding effect of the inflammatory infiltrate. *J. Pathol. 198*:47–54.

Stolte, M., Meining, A., Schmitz, J.M., Alexandridis, T., and Seifert, E. 1998. Changes in *Helicobacter pylori*-induced gastritis in the antrum and corpus during 12 months of treatment with omeprazole and lansoprazole in patients with gastroesophageal reflux disease. *Aliment. Pharmacol. Ther. 12*: 247–253.

Sung, J.J., Lin, S.R., Ching, J.Y., Zhou, L.Y., To, K.F., Wang, R.T., Leung, W.K., Ng., E.K., Lau, J.Y., Lee, Y.T., Yeung, C.K., Chao, W., and Chung, S.C. 2000. Atrophy and intestinal metaplasia one year after cure of *H. pylori* infection: a prospective, randomized study. *Gastroenterology 119*:7–14.

Tahara, B. 1995. Molecular biology of gastric cancer. *World J. Surg. 19*:484–488.

Tatematsu, M., Nozaki, K., and Tsukamoto, T. 2003. *Helicobacter pylori* infection and gastric carcinogenesis in animal models. *Gastric Cancer 6*:1–7.

Tepes, B., Kavcic, B., Zaletel, L.K., Gubina, M., Ihan, A., Poljak, M., and Krizman, I. 1999. Two-to four-year histological follow-up of gastric mucosa after *Helicobacter pylori* eradication. *J. Pathol. 188*:24–29.

Testino, G., Valentini, M., Cornaggia, M., and Testino, R. 2000. Chronic atrophic gastritis and gastric cancer. *Digest. Liver Dis. 32*:544.

Uemura, N., Okamoto, S., Yamamoto, S., Matsumura, N., Yamaguchi, S., Yamakido, M., Taniyama, K., Sasaki, N., and Schlemper, R.J. 2001. *Helicobacter pylori* infection and the development of gastric cancer. *N. Engl. J. Med. 345*:784–789.

van Doorn, L.J., Figueiredo, C., Megraud, F., Pena, S., Midolo, P., Queiroz, D.M., Carneiro, F., Vanderborght, B., Pegado, M.D., Sauna, R., De Boer, W., Schneeberger, P.M., Correa, P., Ng, E.K., Atherton, J., Blaser, M.J., and Quint, W.G. 1999. Geographic distribution of *vacA* allelic types of *Helicobacter pylori*. *Gastroenterology 116*:823–830.

Van Doorn, L.J., Figueiredo, C., Sanna, R., Pena, S., Midolo, P., Ng, E.K., Atherton, J.C., Blaser, M.J., and Quint, W.G. 1998. Expanding allelic diversity of *Helicobacter pylori* vacA. *J. Clin. Microbiol. 36*:2597–2603.

Warren, J.R., and Marshall, B.J. 1983. Unidentified curved bacilli on gastric epithelium in active chronic gastritis. *Lancet 1*:1273–1277.

Watanabe, T., Tada, M., Nagai, H., Sasaki, S., and Nakao, M. 1998. *Helicobacter pylori* infection induces gastric cancer in Mongolian gerbils. *Gastroenterology 115*:642–648.

Weisburger, J.H., and Chung, F.L. 2002. Mechanisms of chronic disease causation by nutritional factors and tobacco products and their prevention by tea polyphenols. *Food Chem. Toxicol. 40*:1145–1154.

Wong, B.C., Lam, S.K., Wong, W.M., Chen, J.S., Zheng, T.T., Feng, R.E., Lai, K.C., Hu, W.H., Yuen, S.T., Leung, S.Y., Fong, D.Y., Ho, J., Ching, C.K., and Chen, J.S. 2004. *Helicobacter pylori* eradication to prevent gastric cancer in a high-risk region of China: a randomized controlled trial. *JAMA 291*:187–l94.

Wu, A.H., Crabtree, J.E., Bernstein, L., Hawtin, P., Cockburn, M., Tseng, C.C., and Forman, D. 2003. Role of *Helicobacter pylori* CagA+ strains and risk of adenocarcinoma of the stomach and esophagus. *Int. J. Cancer 103*:815–821.

Yang, Y.L., Xu, B., Song, Y.G., and Zhang, W.D. 2003. Overexpression of c-fos in *Helicobacter pylori*-induced gastric precancerosis of Mongolian gerbil. *World J. Gastroenterol. 9*:521–524.

You, W.C., Li, J.Y., Blot, W.J., Chang, Y.S., Jin, M.L., Gail, M.H., Zhang, L., Liu, W.D., Ma, J.L., Hu, Y.R., Mark, S.D., Cornea, P., Fraumeni, J.F. Jr., and Xu, G.W. 1999. Evolution of precancerous lesions in a rural Chinese population at high risk of gastric cancer. *Int. J. Cancer 83*:615–619.

Zanghieri, G., Di Gregorio, C., Sacchetti, C., Fante, R., Passatelli, R., Canonizzo, G., Carriero, A., and Ponz de Leon, M. 1990. Familial occurrence of gastric cancer in the 2-year experience of a population-based registry. *Cancer 66*:2047–2051.

Zullo, A., Rinaldi, V., Hassan, C., Diana, F., Winn, S., Castagna, G., and Attili, A.F. 2000. Ascorbic acid and intestinal metaplasia in the stomach: a prospective, randomized study. *Aliment. Pharmacol. Ther. 14*:1303–1309.

17

Protein Alterations in Gastric Adenocarcinoma

Qing-Yu He

Introduction

Gastric cancer is a common malignant tumor, representing the second major cause of cancer-related deaths worldwide (Pisani *et al.,* 2002). Gastric adenocarcinoma constitutes approximately 90% of all gastric cancers. *Helicobacter pylori (H. pylori)*-induced chronic gastritis has been recognized as the major risk for the development of gastric cancer (Ebert *et al.,* 2000). Clinically, surgical resection is still the best choice, but it works better for patients with small and early cancer lesions. Unfortunately, most patients are diagnosed at an advanced stage and thus have a very low 5-year survival rate (less than 10%) (Peddanna *et al.,* 1995). This is partially because of the lack of specific and sensitive biomarkers for diagnosis and monitoring of disease progress. The most frequently used gastric tumor markers, carcinoembryonic antigen and CA19-9, are far from satisfactory in terms of sensitivity, and only a modest proportion of patients with gastric cancer has elevated levels of these proteins.

Like most cancers, gastric carcinogenesis is a multistep process and many proteins are altered in expression and modification during this process. Vast efforts have been made to identify the protein alterations by using conventional biochemical methods, which usually study the proteins individually. Technologic advancements, especially the establishment of proteomics, offer a great opportunity to systematically search for tumor-associated protein alterations in gastric cancer. Proteomic analysis is a powerful technology used to comprehensively inspect protein expression in bodily fluids, tissues, and cells (He and Chiu, 2003). In a typical proteomic experiment, total proteins or fractions of proteins are extracted from specimens or cells and then separated according to their isoelectric points (p*I*s) in the first dimension and their molecular weights in the second dimension to generate two-dimensional protein profiles. By comparing the proteomic profiles between a health or control sample and a diseased or drug-treated sample with a computer-aided special software, proteins altered in their expression levels and patterns can be identified and characterized. This approach is especially useful in the discovery of disease-associated proteins, which change in expression and modification corresponding to a disease condition. These disease-related proteins can be used as biomarkers for diagnosis and disease monitoring and as targeted proteins for further mechanistic studies.

Two-dimensional gel electrophoresis (2-DE)-based proteomic technology has been used extensively to discover protein alterations in various diseases including gastric cancer (He *et al.,* 2004b). Proteomics has also been used to identify specific proteins or antigens that reflect the chemo- and thermo-resistant properties of stomach cancer (Sinha *et al.,* 1998, 2001; Yoo *et al.,* 2004) and that are associated with *H. pylori* infection (Baek *et al.,* 2004; Haas *et al.,* 2002; Nilsson, *et al.,* 2000).

Handbook of Immunohistochemistry and *in situ* Hybridization of Human Carcinomas, Volume 4: Molecular Genetics, Gastrointestinal Carcinoma, and Ovarian Carcinoma

The altered proteins were correlated to their functions and expression in gastric cancer, which produced informative clues for identifying biomarkers with a potential clinical value and for better understanding the carcinogenesis of the disease. As an example, this chapter describes the proteomic analysis conducted in our laboratory to globally search for protein alterations in gastric adenocarcinoma. Ten cases of gastrectomy specimens were included in the study. Two-dimensional protein profiles were compared between primary gastric adenocarcinoma and their paired adjacent nontumor mucosae, and altered protein spots were identified, cut off, and subjected to in-gel digestion and protein identification through peptide mass fingerprinting (PMF). A number of clusters of altered proteins in gastric carcinoma were found to be associated with tumorigenesis. These diverse protein alterations were discussed in terms of their reported functions and the potential utility as biomarkers to assess gastric adenocarcinoma.

MATERIALS

Ten pairs of gastrectomy specimens: five with tumor site in antrum and normal mucosa site in body (four males and one female).

Five with tumor site in body and normal mucosa site in antrum (four males and one female).

For Protein Extraction (2-DE)

1. Double distilled water (ddH_2O).
2. Extraction buffer (ReadyPrep Sequential Extraction Kit, Reagent 3, Bio-Rad, Hercules, CA).
3. Pellet Pestle Motor (Kimble/Kontes, Vineland, NJ).

For Protein Extraction (Enzyme Activity)

1. Cold physical saline (0.9% NaCl).
2. 20 mM Tris-HCl buffer (pH 7.5) containing 1 mM EDTA (ethylenediamine tetraacetic acid) and 1 mM β-mercaptoethanol.
3. Pellet Pestle Motor (Kimble/Kontes).

For Two-Dimensional Electrophoresis

IPGphor IEF (isoelectric focusing) and Hoefer SE600 Ruby electrophoresis units (Amersham Biosystems, Uppsala, Sweden).

First-Dimension Isoelectric Focusing—Rehydration of Immobilized pH Gradient Strip

8 M Urea.
3-[(3-Cholamidopropyl)dimethylammonio]-1-propanesulfonate (CHAPS) 2% (w/v).
Bromophenol blue 0.002% (w/v).
ddH_2O.
DL-Dirhiothreitol (DTT).
Pharmalyte pH 3–10.
Immobilized pH gradient (IPG) strip, 13 cm, pH 3–10 (Amersham Bioscience).
13 cm strip holder.
IPGphor system.

Second-Dimension Sodium Dodecyl Sulfate (SDS)/ Polyacrylamide Gel Electrophoresis (PAGE)

12.5% single-percentage gel solution.
30% acrylamide, 0.8% N,N′-methylenebisacrylamide.
1.5 M Tris-HCl, pH 8.8.
10% SDS (Sodium dodecyl sulfate).
10% ammonium persulfate.
TEMED (N,N,N′,N′-Tetramethylethylenediamine).
ddH_2O.
SDS electrophoresis buffer.
Water saturated butanol-1.
SDS equilibration buffer:
- Tris-HCl, pH 8.8, 50 mM
- Urea, 6 M
- Glycerol, 30% v/v
- SDS, 2%
- Bromophenol blue, 2% w/v
- ddH_2O

Sealing solution:
- 0.5% Low melting agarose and 0.2% bromophenol blue in SDS electrophoresis buffer.

For Silver Staining

1. Ethanol.
2. Acetic acid.
3. Na Acetate anhydrous.
4. Na Thiosulfate.
5. ddH_2O.
6. Silver nitrate.
7. Formaldehyde.
8. EDTA-Na•$2H_2O$.
9. Na-carbonate.
10. Formaldehyde.
11. 87% Glycerol.

For Image Analysis and Peptide Mass Fingerprinting

1. ImageScanner (Amersham Biosciences).
2. ImageMaster 2D Elite software (Amersham Biosciences).
3. Voyager-DE STR MALDI-TOF-mass spectrometer (Applied Biosystems, Foster City, CA).

For In-Gel Digestion

1. ddH_2O.
2. 30 mM Potassium ferricyanide.
3. 100 mM Sodium thiosulphate.
4. 50 mM Ammonium bicarbonate (ABC).
5. Trypsin (10 μg/ml in 25 mM ABC).
6. α-Cyano-4-hydroxycinnamic acid (CHCA).
7. Formic acid.
8. Acetonitrile (ACN).

For Two-Dimensional Western Blotting

1. Immobilon-P transfer membrane (Millipore, Bedford, MA).
2. 100% methanol.
3. Transfer buffer.
4. Nonfat milk powder.
5. Tris-buffered saline (TBS; pH 7.6) with 0.1% Tween 20 (TBS-T).
6. Primary monoclonal or polyclonal antibody:
   - 1:500, 18 kDa antrum mucosa protein (AMP-18), gift from Dr. T. Martin, University of Chicago.
   - 1:1000, Heat-shock protein 60 (HSP60), Enolase, alpha1-antitrypsin (α1-AT) (Santa Cruz, CA).
7. Secondary horseradish peroxidase conjugated antibody:
   - 1:10,000, Anti-mouse antibody (Amersham Biosciences).
   - 1:10,000, Anti-rabbit antibody (Amersham Biosciences).
8. ELC (Amersham Biosciences).

For Enzyme Activity Assessment

Triosephosphate Isomerase Activity

1. Triethanolamine buffer (0.16 M triethanolamine, 0.12 M KCl, 21 mM $MgSO_4$, 1.3 mM EDTA, pH 7.5).
2. 0.3 M GAP, 0.14 M NADH, 2.4 M GDH and 200 μg of tissue extract.
3. Wavelength was set at 340 nm with 1 cm light path, and final volume was confined to 0.5 ml at 25°C.
4. All chemicals from Sigma, St. Louis, MO, or Fluka, Switzerland.

Phosphoglycerate Mutase Activity

1. Tris buffer (0.1 M, pH 7.6), 0.1 M $MgSO_4$, 0.01 M NADH, ADP (10 mg/ml). Glycerate-2-3-P2 (6 mg/ml), LDH (5 mg/ml), pyruvate kinase (2 mg/ml), enolase (10 mg/ml), and 200 μg of tissue extract.

All chemicals from Sigma.

Enolase Activity

1. Tris buffer (0.1 M, pH 7.6), 0.1 M $MgSO_4$, NADH (10 mg/ml).
2. Glycerate-2-P (10 mg/ml), ADH (10 mg/ml), LDH (5 mg/ml).
3. Pyruvate kinase (2 mg/ml) and 200 μg of tissue extract.

All chemicals from Sigma.

For Immunohistochemistry Staining

1. Xylene.
2. Ethanol.
3. Tap water.
4. 3% Hydrogen peroxide.
5. 0.01 M Sodium citrate buffer (pH 6.0).
6. 10% Normal goat serum.
7. TBS (pH 7.4).
8. Primary polyclonal antibody: rabbit anti-human AMP-18, 1:1000 (gift from Dr. T. Martin, University of Chicago).
9. Secondary antibody: peroxidase-labeled (goat) anti-rabbit antibody (Dako, Glostrup, Denmark).
10. 3,3′-Diaminobenzine (DAB) (Sigma).
11. Hematoxylin.
12. ddH_2O.
13. Mounting media.

METHODS

Protein Extraction for 2-DE

1. Tissue (200 mg) is cut into about 2 mm^3 in size.
2. Add 0.5 ml extraction buffer (Biorad, ReadyPrep Sequential Extraction Kit, Reagent 3).
3. Homogenize for 5 min on ice using Pellet Pestle Motor (Kimble/Kontes).
4. Spin down at 14,000 rpm for 10 min at 4°C. Keep the supernatant, and measure the protein concentration by the method of Bradford. Aliquot the protein lysates and store at −70°C.

Protein Extraction for Enzyme Activity

1. Wash tissue by cold physical saline (0.9% NaCl) 2×.
2. Homogenize in 2 vol (w/v) of cold 20 mM Tris-HCl buffer (pH 7.5), containing 1 mM EDTA and 1 mM β-mercaptoethanol with Pellet Pestle Motor (Kimble/Kontes), for 1 min over ice.
3. Remove cellular debris by centrifugation at 4°C for 30 min at 12,600 g, and collect supernatant for enzyme activities.

4. Determine protein concentrations by the method of Bradford.

Two-Dimensional Electrophoresis for Protein Separation

For First-Dimension Isoelectric Focusing

1. DTT (2.8 mg/ml) and Pharmalyte (5 µl/ml) are added just prior to use.
2. First, rinse off the strip holder. Use a toothbrush with cleaning solution and vigorous agitation to clean the strip holder.
3. Rinse well with distilled or deionized water. Thoroughly air-dry the strip holders or use lint-free tissue prior to use.
4. Load 250 ml of total volume of rehydration solution and sampled into strip holder.
5. Remove the protective cover foil from the IPG strip starting at the acidic (pointed) end. Position the IPG strip with *gel side down* and the pointed (anodic) end of the strip directed toward the pointed end of the strip holder.
6. Apply 1 ml IPG cover fluid (mineral oil) to minimize evaporation and urea crystallization.
7. Place the cover on the strip holder.
8. Position the strip holders with the pointed end over the anode (follow the guidemark).
9. Rehydrate at 20°C for at least 12 hr and IEF for another 10 hr.

S1	30 V	12 hr
S2	500 V	1 hr
S3	1000 V	1 hr
S4	8000 V	64,000 Vhr (~8 hr)
S5	0 V	0 hr

10. After IEF, proceed to the SDS or store the IPG strips at −70°C in screw-cap tubes.

For Second Dimension

1. Place gel tank horizontally on sink and unscrew.
2. Wash each plate with detergent and rinse with ddH_2O.
3. Use 1.5 mm thick spacers gel system. Prepare 12.5% single-percentage gel solution (each gel requires 15 ml gel solution).
4. Add TEMED and ammonium persulfate and gently swirl the flask to mix, being careful not to generate bubbles. Immediately pour the gel.
5. Fill the gel cassette and overlay each gel with a layer of butanol-1 (1 ml) immediately after pouring to minimize gel exposure to oxygen and to create a flat gel surface.
6. Allow polymerization for a minimum of 30 min. Remove the overlay and rinse the gel surface with running buffer.

For SDS Equilibration

1. Place the IPG strips in individual tubes with the support film toward wall.
2. 1st EQ: Add 100 mg DTT to 10 ml of equilibration buffer with 10 µl bromophenol blue for 15 min.
3. 2nd EQ: Add 250 mg IAA to 10 ml of equilibration buffer with 10 µl bromophenol blue for 15 min.

Position the Immobilized pH Gradient Strip and Two-Dimensional Electrophoresis

1. Dip the equilibrated strip in the SDS electrophoresis buffer to lubricate it.
2. Position the IPG strip between the plates on the surface of the second-dimension gel with the plastic backing against one of the glass plates with the point end towards positive terminal. Push the IPG strip down to contact the gel slab by a thin plastic ruler.
3. Prepare agarose sealing solution. Heat in a microwave oven until completely dissolved. Allow the agarose to cool until it can be held by finger (60°C) and then slowly pipette the amount required to seal the IPG strip in place (1–1.5 per gel). Allow at least 1 min for the agarose to cool and solidify.
4. Electrophoresis condition: set 15 mA/gel for 15 min. Then 30 mA/gel for 4 hr. Set voltage and watt in maximum.
5. Ready for blotting or to be visualized by silver staining.

Silver Staining

Stain the gel according to the table.

Solution	Time (min)	Composition	250 ml
1. Fixation	30	Ethanol	100 ml
	or O/N	Acetic acid	25 ml
2. Incubation	30	Ethanol	75 ml
	or O/N	Na acetate anhydrous	10.25 g
		Na thiosulfate	0.5 g/*0.79 g
3. Washing	3 × l0	dd H_2O	
4. Silver nitrate	40	Silver nitrate	0.25 g
		Formaldehyde	50 µl
5. Development	15	Na-carbonate	6.25 g
		Formaldehyde	25 µl
6. Stop solution	10	EDTA-Na·2H_2O	3.65 g
7. Washing	3 × 5	dd H_2O	
8. Preservation	60	87% glycerol	11.5 ml
		Ethanol	75 ml

*Indicates the weight of Na thiosulfate with two water molecules.

Image Analysis

1. Scan stained gels by using an Image Scanner (Amersham Biosciences), operated by the software program LabScan 3.00.
2. Create an Experiment. Import scanned images.
3. Spot Detection by selecting spot detection wizard. Adjust the sensitivity, operator size, and background factor.
4. Then follow by spot filtering, manual editing, and spot renumbering.
5. Create reference gel with highest number of spots of nontumor gels.
6. Create average gel by grouping into tumor gel and nontumor gel.
7. Match the spots in the average gels to the nontumor reference gel.
8. Follow background subtraction in the "mode of nonspot."
9. Normalize total spot volume with 100X mode.
10. Finally, cut the spots with changes of more than two folds and p-values <0.05 and subject them to in-gel digestion.

In-Gel Digestion

1. Excise protein spots and put in a siliconized 1.5 ml Eppendorf tube.
2. Soak gel chips in 0.5 ml of a 1:1 mixture of 30 mM potassium ferricyanide: 100 mM sodium thiosulfate for 5 min until silver stain disappears (agitation at 700 rpm).
3. Rinse gel pieces with 1 ml of ddH_2O 2× until the yellow color disappears.
4. Equilibrate the gel chips in 0.5 ml of 50 mM ABC 5–10 min, then discard the liquid (agitation at 700 rpm).
5. Add 250 µl 50 mM ABC and then add further 250 µl 100% ACN and soak for 30 min (agitation at 700 rpm).
6. Replace supernatant with 200 µl of ACN to completely dehydrate (gel slices should turn opaque white, ~5 min).
7. Remove ACN and dry gel chips in a Speed Vac.
8. Rehydrate the gels with a minimal volume of trypsin solution (10 µg/ml in 25 mM ABC buffer pH 8.0). Add 15 µl for small gel slices, use more (15 µl) if needed for larger gels to cover entire gel surface.
9. Incubate at 37°C overnight.
10. Spin down the solution, agitate at 1000 rpm for 5 min, and spin down again, ready for spotting on mass spectrometry (MS) sample plate (Applied Biosystems).
11. Prepare matrix solution: CHCA 4 mg/ml in 35% ACN and 1% TFA.
12. Apply 1 µl of trypsinized sample onto the plate until dry. Then coat 1 µl of matrix solution on top.

Peptide Mass Fingerprinting for Protein Identification

1. Voyager-DE STR MALDI-TOF mass spectrometer (Applied Biosystems) produce mass spectra in reflector mode with 175 ns delay extraction time, 60–65% grid voltage, and 20 K accelerating voltage.
2. Set mass ranges from 0.5 to 4.0 kDa.
3. Search the database in MS-Fit (http://prospector.ucsf.edu/).
4. Matching criteria: 25 ppm, at least 4 matched peptides, close molecular mass and p*I*.
5. Species limited to *Homo sapiens.*

Two-Dimensional Western Blotting

1. Prepare transfer membrane (PVDF). Immerse in 100% methanol for 1–2 sec to hydrate it.
2. Equilibrate the membrane in transfer buffer for 10 min.
3. Equilibrate the separating gel with transfer buffer for 10 min.
4. Place 3 sheets of filter paper saturated with transfer buffer on the anode.
5. Place membrane on top of filter paper stack.
6. Remove all bubbles between membrane and filter paper by rolling a test tube over surface of membrane.
7. Place gel on top of membrane, and roll a test tube again.
8. Complete the surface stack by putting the 3 remaining sheets of filter paper on top of the gel.
9. Place top electrode onto transfer stack.
10. Connect constant high-voltage and apply 0.8 mA per cm^2 for 1 hr. Set voltage and watt at maximum.
11. Turn off supply and disassemble unit. Remove membrane from transfer stack and note orientation by cutting a corner.
12. Place membrane in plastic box with 5 ml 5% blocking buffer (5% nonfat milk in 0.1% Tween 20 TBS) and incubate at 4°C for overnight with constant agitation.
13. Dilute primary antibody (patient serum) to 1:200 in blocking buffer (5% nonfat milk in 0.1% Tween 20 TBS), (50 µl patient serum + 9950 µl blocking buffer).
14. Pour out blocking buffer. Replace with diluted primary antibody and incubate at 4°C overnight.
15. Wash 3× by agitating with TTBS for 15 min each.
16. Dilute secondary antibody (rabbit anti-human IgG horseradish peroxidase) in blocking buffer (5% nonfat milk in 0.1% Tween 20 TBS) in 1/10,000.

17. Incubate secondary antibody at room temperature for 1 hr with constant agitation.
18. Wash with TTBS for 3 times, 15 min each time. And proceed to detection by enhanced chemiluminescence (Pierce, Rock Ford, IL) (ELC).

Enzyme Activity Assessment

Enzyme activity was determined by using UV-Vis spectrophotometer. The absorbance of the final product that converted by target enzyme was read against time.

1. Set wavelength at 340 nm with 1 cm light path.
2. Mix reagents and final volume confined to 0.5 ml at 25°C.
3. Equilibrate assay mixture at 25°C for 15 min and add tissue extract just prior to measurement.

Immunohistochemistry Staining

1. Mount paraffin sections (4–6 μm thick) onto poly-L-lysine-coated glass slides.
2. Bake the slides in an oven at 60°C for 15 min.
3. Deparaffinize the slides in xylene.
4. Rehydrate the slides in graded ethanol.
5. Wash the slides in tap water.
6. Incubate the slides with 3% H_2O_2 to block endogenous peroxidase.
7. Place in a steam cooker filled with 0.01 M sodium citrate buffer (pH 6.0) for antigen retrieval.
8. Cool the slides in 0.01 M sodium citrate buffer (pH 6.0) solution at room temperature.
9. Treat the slides with 10% normal goat serum for 10 min to block nonspecific protein binding.
10. Wash the slides with TBS 3× for 2 min each.
11. Apply rabbit polyclonal antibodies AMP-18 to the slides at 4°C for overnight.
12. Wash the slides with TBS 3× for 2 min each.
13. Incubate with peroxidase-labeled anti-rabbit antibody for 1 hr.
14. Wash the slides with TBS 3× for 2 min each.
15. Apply DAB.
16. Wash the slides with distilled water.
17. Conterstain with hematoxylin for 3–5 min.
18. Dehydrate and mount.

RESULTS AND DISCUSSION

Protein Extraction, Separation, and Identification

Primary gastric adenocarcinoma and their adjacent nontumor mucosae were collected from 10 gastrectomy specimens with sex and age matched. Tissues were snap frozen in liquid nitrogen and stored in a deep freezer (−80°C) until use. All specimens were intestinal-type tumors according to Laurén's classification. Detailed clinicopathologic data including tumor stage (according to the American Joint Committee on Cancer [AJCC] system), site, differentiation, and histologic data on the tissue samples are listed in Table 10. Histologically, areas of tumor with purity more than 70% were chosen after assessment by cryostat sectioning for protein extraction. The nontumor mucosae were dissected free of muscle wall in fresh state and confirmed by cryostat section before protein extraction. If necessary, laser capture microdissection can be used to select pure tumor and normal cells for protein extraction.

Protein separation was performed in nonlinear 13 cm two-dimensional gels with p*I* ranges of 3–10 and molecular weight ranges of 6–200 K. Around 1300 protein spots were well separated in the gels (He *et al.,* 2004b). Significant and consistent alterations of protein expression were identified through image analysis by a computer-aided sophisticated software. These altered proteins distributed evenly throughout the entire gel, indicating that multiple clusters of proteins are involved in the process of tumorigenesis of gastric cancer. Table 11 lists all of the proteins identified through PMF matching, together with their accession numbers, fold differences in expression, and p-values for the protein alterations in gastric cancer. These proteins can be classified into several categories based on their functions, including cytoskeleton proteins, stress-related and chaperoning proteins, acute-phase proteins, glycolytic enzymes, enzymes involved in metabolism and cell proliferation, tumor-suppressor protein, and stomach-specific proteins. As in most cancers, tumorigenesis of gastric adenocarcinoma involves multiple steps and factors (Ming, 1998). It is therefore not surprising that many proteins performing various functional processes were found to be differently expressed between tumor and nontumor tissues.

In protein identification, MALDI-TOF (matrix-assisted laser desorption ionization-time of flight) MS is a common tool to obtain peptide mass fingerprints, which are then matched to known proteomic or genomic databases to deduce protein identities. There are several online PMF algorithms available (Reinders *et al.,* 2004), and one of the commonly used is http://prospector.ucsf.edu/. During the data matching using this program, a number of parameters including missed cleavage, peptides matched, sequence coverage, total mass error and MOWSE (*mo*lecular *w*eight *se*arch) score should be examined and ranked for matching confidence. For those no-confident matching, tandem MS/MS or *de novo* sequencing (Reinders *et al.,* 2004)

Table 10. Patients' Information and Histologic Data for the Tissue Samples Used

Patient Code	Sex/Age	Tumor Site	Normal Mucosa Site	T Stage	Sample Pairs	Tumor Cells (%)	Normal Mucosal Cells (%)	Muscle Cells (%)	Connective Tissue Cells Lymphocytes, Vessel Cells, Fibroblast (%)
SX390	F/90	Antrum	Body	pT3N3	Tumor	95	0	0	5
					Nontumor	0	95	0	5
SX426	M/72	Antrum	Body	pT2N0	Tumor	90	0	0	10
					Nontumor	0	95	0	5
SX437	M/62	Antrum	Body	pT3N3	Tumor	95	0	0	5
					Nontumor	0	95	0	5
SX452	M/63	Antrum	Body	pT2N2	Tumor	75	5	5	15
					Nontumor	0	90	0	10
SX471	M/66	Antrum	Body	pT3N3	Tumor	70	0	5	25
					Nontumor	0	95	0	5
SX409	M/79	Body	Antrum	pT3N2	Tumor	90	0	0	10
					Nontumor	0	90	0	10
SX415	M/85	Body	Antrum	pT2N0	Tumor	90	0	0	10
					Nontumor	0	70	10	20
SX423	M/56	Body	Antrum	pT3N2	Tumor	80	0	10	10
					Nontumor	0	90	0	10
SX442	M/82	Body	Antrum	pT3N1	Tumor	80	0	0	20
					Nontumor	0	90	0	10
SX453	F/52	Body	Antrum	pT3N1	Tumor	75	0	5	20
					Nontumor	0	80	10	10

Relative percentage (%) of cells was rounded up to 5%; cells less than 5% were counted as 0 because the number was too small.

can be performed for further confirmation. Alternatively, Western blot analysis with specific antibodies can be carried out to validate the identities of proteins that have low matching scores or are particularly interesting in designed studies. Table 12 summarizes parameters in PMF for current protein identification in gastric tissues. Most database matching has a very low total mass error (<25 ppm) and high overall MOWSE score (>300). For HSP60 and α1-AT, which had scores lower than 200, enolase that has typical isoforms, and AMP-18, the specific stomach protein, two-dimensional Western blot analysis was performed to confirm the protein identification. Specific and positive immunochemical interactions occurred for the four proteins evaluated, and similar patterns of protein isoforms were observed in both silver staining and Western blot analysis for all the proteins (He *et al.,* 2004b), indicating an overall confidence in protein identification.

Cytoskeletal Protein Alterations in Gastric Cancer

The advantage of proteomic analysis is its ability to simultaneously detect global protein alterations corresponding to a given disease condition so that all the protein alterations can be correlated and considered in an integrated way. For the current gastric adenocarcinoma, diverse protein alterations were first found in cytoskeleton proteins between tumor and nontumor tissues from the same patients. Both cytokeratin 8 (CK8) and tropomyosin isoform were significantly up-regulated in tumor samples, whereas cytokeratin 20 (CK20) had decreased expression in tumor tissues (see Table 11). Tropomyosin is a cytoskeletal microfilament binding protein. Many studies have shown that different tropomyosin isoforms play distinct physiologic roles, allowing isoform-specific regulation in response to cell transformation (Braverman, *et al.,* 1996; Gunning *et al.,* 1997). High molecular weight tropomyosin isoforms were suppressed, whereas low molecular weight isoforms were up-regulated in cancers and transformed cells (He *et al.,* 2004a; Novy *et al.,* 1993). The observed overexpression of the low molecular weight tropomyosin isoform (29 kDa) suggests that tropomyosin-related cell transformation was also involved in gastric cancer.

Cytokeratins are main structural proteins in epithelial cells. They comprise the intermediate filaments of the cytoskeletons and are expressed in various combinations depending on the epithelial type and the degree of differentiation. The various and restricted expressions of CKs can help in determining the origin of many epithelial tumors, and thus CKs are potential diagnostic and prognostic biomarkers for epithelial

Table 11. Proteins and Their Alterations in the Tissues of Gastric Cancer. Change Folds Were Calculated Based on the Image Analysis of Silver-Staining Gels

Protein ID (MW/p*I*)	Experimental (MW/p*I*)	Accession (NCBI)	Reported Function	Change (Fold)	P-Value
Cytokeratin 8 (CK8), (54 kD/5.5)	55 kD/5.5	2506774	Cytoskeleton protein of intermediate filaments	+3	0.0023
Cytokeratin 20 (CK20), (48 kD/5.5)	50 kD/5.5	547750	Cytoskeleton protein of intermediate filaments	–2	0.0107
Tropomyosin isoform (TPM), (29 kD/4.8)	30 kD/4.6	9508585	Cytoskeletal microfilament binding protein	+2	0.0056
Enolase 1, (47 kD/7.0)	48 kD/7.0	693933	Glycolysis	+2	0.0003
Triosephosphate isomerase (TPI), (27 kD/6.4)	26 kD/6.5	136060	Glycolysis	+2.5	0.0021
Phosphoglycerate mutase 1 (PGM), (29 kD/6.7)	30 kD/6.6	130348	Glycolysis	+2.5	0.0052
Pyruvate kinase (PK), (58 kD/8.0)	56 kD/8.0	478822	Glycolysis	+3.5	0.0093
Chaperonin containing TCP1 (CCT), (58 kD/6.2)	60 kD/6.2	627402	Stress-related, chaperone	+2	0.0016
Heat shock protein 60 (HSP60), (61 kD/5.7)	60 kD/5.5	129379	Stress-related, chaperone	+3	0.0009
Heat shock cognate 71 protein (HSP70), (71 kD/5.4)	70 kD/5.5	123648	Stress-related, chaprone	+2	0.0085
Protein disulfide isomerase (PDI), (57 kD/6.2)	55 kD/6.3	2135267	Chaperone, isomerase, and redox activities	+1.5	0.0099
Translation elongation factor EF-Tu (EF-Tu), (49 kD/7.7)	50 kD/7.4	7443384	Translation factor, cell growth, chaperone activity	+1.7	0.0133
Alpha-1-antitrypsin (α1 -AT), (47 kD/5.4)	51 kD/5.2	15990507	Acute-phase protein	–2	0.0045
Apolipoprotein A-1 (ApoA1), (31 kD/5.6)	30 kD/5.7	4557321	Acute-phase protein	–1.8	0.0039
Guanosine monophosphate reductase 2 (GMPR) (Fragment), (38 kD/6.8)	22 kD/7.1	25008511	Promote monocytic differentiation	–2	0.0011
Creatine kinase B (CK-B), (43 kD/5.3)	42 kD/5.2	180570	Proliferation-transformation, energy buffering	–1.6	0.0071
Selenium-binding protein 1 (SeBP), (52 kD/5.9)	51 kD/6.0	16306550	Detoxification, inhibition of premalignant cells	–2	0.0008
Prohibitin (30 kD/5.6)	30 kD/5.4	4505773	Tumor suppressing, inhibition of cell proliferation	+1.8	0.0017
Carbonic anhydrase I (CA-I), (29 kD/6.6)	31 kD/7.0	115449	CO_2 hydration for intermediate metabolism	–2.5	0.0006
Carbonic anhydrase II (CA-II), (29 kD/6.9)	31 kD/7.1	115456	CO_2 hydration for intermediate metabolism	–5	0.0005
18 kDa Antrum mucosa protein (AMP-18), (22 kD/5.9)	20 kD/6.0	26000208	Human stomach-specific, epithelial cell mitogen	–19	0.0001

MW, molecular weight; NCBI, National Center for Biotechnology Information; p*I*, isoelectric points.

Table 12. Results of MALDI-TOF Mass Spectra and Database Searching for Protein Identification

Protein	Peptides Matched	Sequence Coverage (%)	Total Mass Error (ppm)	MOWSE Score
Cytokeratins 8 (CK8)	36	59	20	1.16e+06
Cytokeratins 20 (CK 20)	24	39	19	4.55e+05
Tropomyosin isoform (TPM)	13	45	20	336
Enolase 1 (47 kD/7.0)	16	41	14	5325
Triosephosphate isomerase (TPI)	12	38	31	6524
Phosphoglycerate mutase 1 (PGM)	12	41	18	5.08e+05
Pyruvate kinase (PK)	7	12	22	632
Chaperonin containing TCP1 (CCT)	6	10	24	359
Heat shock protein 60 (HSP60)	5	10	15	172
Heat shock cognate 71 protein (HSP70)	5	11	16	345
Protein disulfide isomerase (PDI)	16	28	17	7446
Translation elongation factor EF-Tu (EF-Tu)	12	20	12	1376
Alpha-1-antitrypsin (α1-AT)	6	10	15	165
Apolipoprotein A-1 (ApoA1)	11	35	12	2739
Guanosine monophosphate reductase 2 (GMPR) (Fragment)	6	8	30	1556
Creatine kinase B (CK-B)	11	35	14	8.88e+05
Selenium-binding protein 1 (SeBP)	13	27	13	1.74e+05
Prohibitin	7	19	10	625
Carbonic anhydrase I (CA-I)	7	39	19	2.94e+04
Carbonic anhydrase II (CA-II)	8	45	28	4993
18 kDa Antrum mucosa protein (AMP-18)	16	27	15	5.06e+04

MALDI-TOF, matrix-assisted laser desorption ionization-time of flight; MOWSE, *mo*lecular *w*eight *se*arch.

cancers including those in the gastrointestinal (GI) tract (Ormsby *et al.,* 2001; Scheuemann *et al.,* 2001). A CK7+/CK20-immunophenotype has been suggested to be a useful diagnostic tool for classifying esophageal adenocarcinoma (Ormsby *et al.,* 2001; Taniere *et al.,* 2002) and especially for discriminating primary carcinomas from metastatic cancers of colon and gastric origins (Tot, 2002; Wauters *et al.,* 1995). However, cancer cells are known to secrete CK8-containing protein complex *in vitro* and *in vivo* (Gonias *et al.,* 2001). Positive correlations have been demonstrated between high levels of CK8 expression and increased migration and invasion of certain cancer cells (Gonias *et al.,* 2001). In particular, CK8 was found to be highly expressed in ductal and other GI malignances (Herzig *et al.,* 1994; Lam *et al.,* 1995). The detected up-regulation of CK8 and down-regulation of CK20 in this study confirm the diversified expression of different CKs, which may be used to specifically define gastric cancer.

Active Glycolysis in Gastric Tumorigenesis

Substantial co-overexpression of glycolytic enzymes in gastric tumor tissues indicates increased energy consumption during tumorigenesis in gastric cancer. The increased glycolytic enzymes include enolase, triosephosphate isomerase (TPI), phosphoglycerate mutase 1 (PGM), and pyruvate kinase (PK) (see Table 11). To test whether the enzymatic activities of these proteins are also higher in tumor tissue than in nontumor tissues, three glycolytic enzymes (enolase, TPI, and PGM) were selected to assess their activities in paired gastric tissues. To simplify the procedure, protein mixtures with equal aliquots respectively from each normal and tumor tissue extract were used in the assessment. Table 13 lists the enzyme activities of the three proteins in paired tissue samples. Evidently, these glycolytic enzymes have activities 1–3-fold higher in tumor than in nontumor tissues, corresponding to the higher expressions of the proteins in tumor compared to control tissues.

The four co–up-regulated proteins—TPI, PGM, enolase, and PK–are involved in the triose stage of glycolytic pathway. In glycolysis, glucose is converted to pyruvate, which is accompanied by the net production of two molecules of ATP. This energy-generating pathway is active in all differentiated cell types in multicellular organisms. Over-expression of glycolytic enzymes may be a reflection of active glycolysis, producing energy for the growth of gastric tumor cells. The fact that enolase, TPI, and PGM have higher enzyme activities in gastric tumor than in normal tissue reinforces the increased energy generation during carcinogenesis. Moreover, higher enzymatic activities of PGM and enolase have been detected in various tumor

Table 13. Activity Levels of Glycolytic Enzymes in Gastric Normal Tissue and Adenocarcinoma

Enzyme	Normal Tissue (U g^{-1})	Tumor Tissue (U g^{-1})
Enolase	3.65	5.43
Triosephosphate isomerase (TPI)	1.67	4.78
Phosphoglycerate mutase 1 (PGM)	1.80	3.53

tissues including lung, colon, liver, and breast carcinoma (Durany *et al.,* 2000; Usuba *et al.,* 2001). Significant over-expression of TPI has also been found in lung adenocarcinoma (Chen *et al.,* 2002) and in squamous cell carcinoma of the bladder (Montgomerie *et al.,* 1997). Our observation of increased expression of glycolytic enzymes in gastric cancer strengthens the association between glycolysis and carcinogenesis.

Coherent Stress Responses in Gastric Carcinogenesis

Another observation corresponding to the pathologic feature of gastric cancer is the alterations of stress-related and acute-phase proteins (see Table 11). Whereas the stress proteins that have molecular chaperone activity, including chaperonine containing TCP1 (CCT), HSP60, heat-shock cognate protein 70 (HSP70), protein disulfide isomerase (PDI), and translation elongation factor EF-Tu protein (EF-Tu) were up-regulated, acute-phase proteins including α1-AT and apolipoprotein A1 (ApoA1) were obviously suppressed in gastric adenocarcinoma.

Numerous studies *in vivo* and *in vitro* have shown that the production of heat-shock proteins (HSPs) are transiently increased in response to harmful insults such as environmental stresses and infection (Kiang and Tsokos, 1998). Increased expression of HSPs has been proved to have protective effects in cells and tissues as a result of the capacity of HSPs to function as molecular chaperones to regulate appropriate protein folding and packaging. The over-expression of a group of HSPs including HSP70, HSP60, and CCT found in the present gastric tumor tissues reflects the coherent stress response and self-protective effort of the cells during malignant transformation. The cytosolic molecular chaperone, CCT can assist the folding of actin, tubulin, and other proteins. It is a member of the HSP60 family. Although similar enhanced expression has been observed for HSP70 in gastric cancer (Canoz *et al.,* 2002; Isomoto *et al.,* 2003; Maehara *et al.,* 2000), HSP60 in *H. pylori*-related gastric carcinoma (Kamiya *et al.,* 1998; Yamaguchi *et al.,* 1998), and CCT in colonic cancer cells (Yokota *et al.,* 2001), the simultaneous up-regulation of these HSPs makes perfect mechanistic sense. In many cellular processes, HSPs work cooperatively to fulfill their functions as molecular chaperones. Research has shown that HSP70 acts to promote substrate binding to CCT (Melville *et al.,* 2003) and to pass the newly synthesized, unfolded proteins to HSP60 for final polypeptide folding (Kiang and Tsokos, 1998).

The multifunctional redox chaperone PDI localizes in the endoplasmic reticulum. As a result of its ability to catalyze the oxidation, reduction, and isomerization of protein disulfides, PDI plays a role in the regulation of receptor function, cell–cell interaction, gene expression, and actin filament polymerization. Considering its activity as a chaperone involved in the proper folding and formation of proteins, it is reasonable that PDI expression is often up-regulated under stress conditions. For example, elevated expression of PDI has been found in mouse F9 teratocarcinoma cells treated with retinoic acid and dibutyryl cAMP (cyclic adenosine monophosphate) (Miyaishi *et al.,* 1998), in primary-cultured glial cells in response to hypoxia (Tanaka *et al.,* 2000), in human prostate epithelial tumor cells subjected to ionizing radiation-induced apoptosis (Prasad *et al.,* 1999) and in human breast ductal carcinoma tissues (Bini *et al.,* 1997). Translation elongation factor-Tu (EF-Tu) also displays PDI activity and chaperone-like properties, in addition to its known role in translation elongation. It is therefore not surprising that increased EF-Tu expression was observed in response to heat stress in maize line (Bhadula *et al.,* 2001) and ischemia-reperfusion injury in rat hearts (Sakai *et al.,* 2003). Overall, our present findings indicate that coordinated regulation of molecular chaperones exists in gastric carcinoma.

In contrast to the increased expression of chaperone proteins, decreased expression was observed for the acute-phase proteins α1-AT and ApoA1. Acute-phase proteins are produced mainly by the liver in response to inflammation or a toxic challenge. These proteins can be regulated individually under different inflammatory conditions, presenting in enhanced (positive) or suppressed (negative) expression in plasma. ApoA1 is a negative acute-phase protein. The current observation, together with a similar finding from a 2003 study (Ryu *et al.,* 2003), indicates that this negative acute response can also be found in tissues of gastric cancer. However, α1-AT, as a positive acute-phase protein, usually increased expression during inflammatory stress and carcinogenesis (Lee *et al.,* 2004), reflecting its protective property by inhibiting apoptosis and caspase activity (Van Molle *et al.,* 1999). The observed

underexpression of α1-AT therefore appears in controversy. However, the same phenomenon of α1-AT down-regulation in gastric cancer has been reported (Ryu *et al.,* 2003). The underlying mechanism may be unique and interesting.

Alterations of Proteins Involved in Cell Proliferation

Diverse protein alterations also occurred with proteins involved in cell proliferation (see Table 11). In contrast to the underexpression of guanosine monophosphate reductase 2 (GMPR), creatine kinase B (CK-B), and selenium-binding protein 1 (SeBP), an increased level of prohibitin was detected in gastric cancer. CK-B and GMPR are enzymes that promote cell differentiation. The expression of CK-B has been long related to malignant tumors of the gastrointestinal tract (Hirata *et al.,* 1989; Koven *et al.,* 1983). The down-regulation of these two enzymes may reflect the poor differentiation state at the late stages of gastric cancer. In contrast, the observed up-regulation of prohibitin is a reciprocal indicator for the inhibition of cell proliferation. Prohibitin has been shown to be a potential tumor-suppressor protein, and its increased levels have been found in various carcinomas (Byrjalsen *et al.,* 1999; Srisomsap *et al.,* 2002; Williams *et al.,* 1998). However, accumulated evidence (see review article Harrison *et al.,* 1997) convincingly demonstrated that selenium is a growth inhibitor and can prevent tumor cell growth. Yang and Sytkowski also showed that human selenium-binding protein gene *(hsp56)* was differently expressed in prostate cancer cells (Yang and Sytkowski, 1998). The protein is expressed in the slow-growing prostate cancer cell line LNCaP but not in the rapidly growing cancer cells PC-3 and Du145. These results support the finding of underexpression of SeBP in gastric adenocarcinoma.

Down-Regulation of Metabolism Enzymes and Growth Factor

The significant down-regulation of the metabolism enzymes, carbonic anhydrase (CA) I and II, and a normal growth factor, AMP-18, comprise the final protein alterations observed in the present gastric cancer study (see Table 11). Because AMP-l8 is a stomach-specific protein and has the most significant expression change in gastric adenocarcinoma, this protein was selected for immunohistochemistry staining in tissue samples to further verify its altered expression. Figure 43 is a typical AMP-18 antibody staining picture, clearly indicating the strong positive staining in nontumor cells *(left)* and the negative staining in the matched tumor cells *(right).*

The zinc-containing enzyme CA has nine isoforms that catalyze the hydration of CO_2 for intermediate metabolism and to maintain pH and ion equilibrium in the body (Nogradi, 1998). Although the presence of the enzyme has been proven essential in almost every organ, no evidence has so far been found to show a direct relationship between malignant transformation and CA expression for CAs I through VII (Nogradi, 1998). Nevertheless, two earlier studies revealed that the expression of both CA-I and CA-II was significantly reduced in colorectal tumors when compared to normal colorectal epithelium or mucosa (Gramlich *et al.,* 1990; Mori *et al.,* 1993). This was supported by the finding that CA-I messenger ribonucleic acid (mRNA) was considerably reduced in colon carcinoma (Sowden *et al.,* 1993). A 2000 report also presented results showing that reduced expression of CA-I and CA-II correlated with the biologic aggressiveness of colorectal cancer and synchronous distant metastasis (Bekku *et al.,* 2000). The decreased expression levels of CA-I and CA-II in the present gastric tumor tissues reveal a similar correlation, implying that gastric and colorectal carcinomas may share a similar mechanism of cell proliferation and mucosa malignancy.

More interestingly, AMP-18, a recently identified gastric-specific protein (Martin *et al.,* 2003; Toback *et al.,* 2003), was found to be dramatically down-regulated in cancer tissues. The gastric complementary deoxyribonucleic acid (cDNA), *CA11,* which encodes an amino acid sequence that differs from AMP-18 in only a single residue (Shiozaki *et al.,* 2001), should refer to the gene that produces the same protein, AMP-18. Both *CA11* gene and AMP-18 were found to be intensively expressed in normal stomach tissue but not in most gastric cancers (Martin *et al.,* 2003; Shiozaki *et al.,* 2001). Immunohistochemical studies demonstrated that AMP-18 appears to be present in mucosal epithelial cells of normal human gastric antrum and duodenum (Martin *et al.,* 2003). AMP-18 is a growth factor at least partly responsible for maintaining normal functional gastric epithelium (Martin *et al.,* 2003). Our current data further validate the high expression of AMP-18 in both normal antrum and stomach body tissues and the substantial suppression of the protein in gastric adenocarcinoma, indicating that AMP-18 growth factor participates in the maintenance of normal differentiation and the growth of gastric mucosal epithelium but not in tumor cells after neoplastic transformation. In addition, this protein has been suggested to be a secreted rather than an integral membrane protein (Shiozaki *et al.,* 2001), implying that the protein may also be detected in serum. If so, a substantial decrease of AMP-18 in patients' sera compared to the average level of the protein in normal

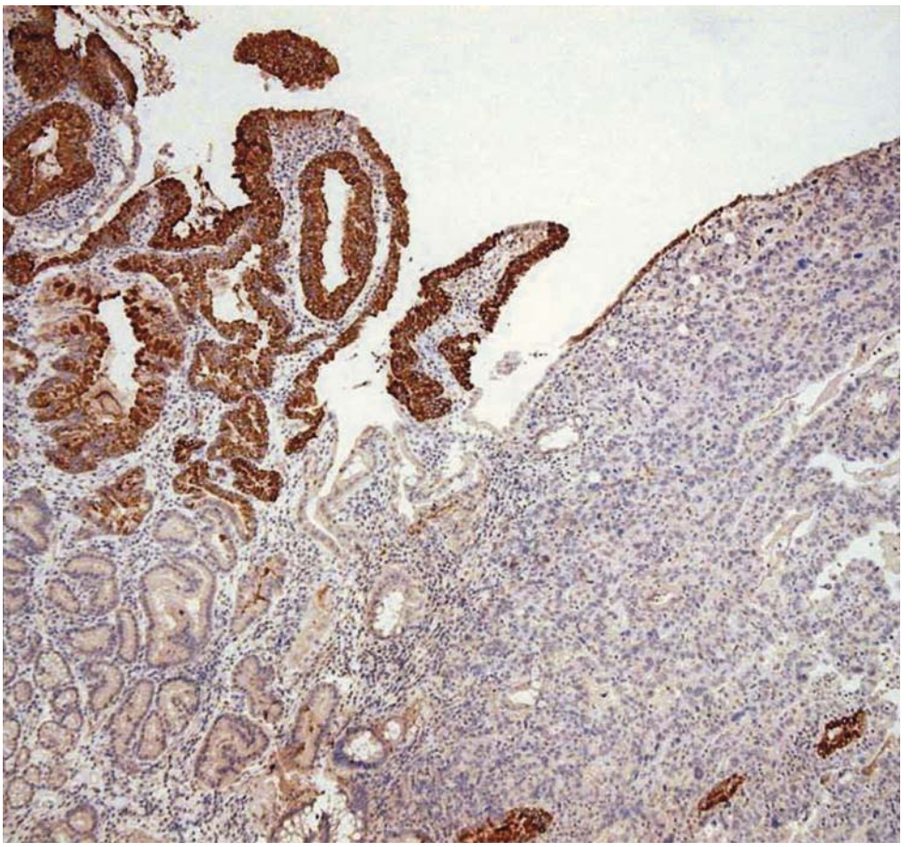

Figure 43. Immunohistochemical staining of AMP-18 (18 kDa antrum mucosa protein) showed strong positive staining in the foveolar antral mucosal cells *(left side)* but completely negative in the gastric carcinoma cells *(right side)*.

serum may be informative for the assessment of the gastric cancer.

Concluding Remarks

Multiple alterations in protein expression were concurrently detected in gastric adenocarcinoma by using proteomic analysis. Some of these protein alterations were confirmed by immunochemical reactions or correlated with enzyme activities corresponding to the changes. Overall, gastric carcinogenesis involved protein alterations that may be common in malignant transformation such as variations in cytoskeletal proteins, acute-phase proteins, molecular chaperones, and energy-producing enzymes. Gastric cancer also involved tumor-associated proteins that presented a unique pattern of variation. A combination strategy simultaneously targeting different pathways should be an effective remedy to counter this disease. In addition, a stomach-specific protein, AMP-18, was found to be greatly down-regulated in gastric adenocarcinoma. The identification of alterations of specific proteins has great significances because these proteins can be the potential biomarkers for specific assessment of the disease and for mechanism study of carcinogenesis. This also depends on the improvement of resolution in protein separation. Prefractionation or subcellular compartment fractionation of proteins prior to two-dimensional electrophoresis is a promising procedure in increasing the resolution in proteomios (Stasyk and Huber, 2004). Other improvement methods include the application of narrow pH isoelectronic focusing and affinity protein concentration and the increase of mass detecting sensitivity (Gorg *et al.,* 2004). Moreover, it should be pointed out that the identification of protein alterations is only a starting step in understanding carcinogenesis. The follow-up functional study of the altered proteins will elucidate the pathogenetic implication underlying the protein alterations. Further combinational evaluation

by co-currently considering these alteration factors and their functions may result in a specific index for the assessment of the disease and may also provide in-depth information for better understanding the pathogenesis of diseases including gastric adenocarcinoma.

References

Baek, H.Y., Lim, J.W., Kim, H., Kim, J.M., Kim, J.S., Jung, H.C., and Kim, K.M. 2004. Oxidative-stress-related proteome changes in *Helicobacter pylori*-infected human gastric mucosa. *Biochem. J. 379*:291–299.

Bekku, S., Mochizuki, H., Yamamoto, T., Ueno, H., Takayama, E., and Tadakuma, T. 2000. Expression of carbonic anhydrase I or II and correlation to clinical aspects of colorectal cancer. *Hepatogastroenterology 47*:998–1001.

Bhadula, S.K., Elthon, T.E., Habben, J.E., Helentjaris, T.G., Jiao, S., and Ristic, Z. 2001. Heat-stress induced synthesis of chloroplast protein synthesis elongation factor (EF-Tu) in a heat-tolerant maize line. *Planta 212*:359–366.

Bini, L., Magi, B., Marzocchi, B., Arcuri, F., Tripodi, S., Cintorino, M., Sanchez, J.C., Frutiger, S., Hughes, G., Pallini, V., Hochstrasser, D.F., and Tosi, P. 1997. Protein expression profiles in human breast ductal carcinoma and histologically normal tissue. *Electrophoresis 18*:2832–2841.

Braverman, R.H., Cooper, H.L., Lee, H.S., and Prasad, G.L. 1996. Anti-oncogenic effects of tropomyosin: isoform specificity and importance of protein coding sequences. *Oncogene 13*: 537–545.

Byrjalsen, I., Mose, L.P., Fey, S.J., Nilas, L., Larsen, M.R., and Christiansen, C. 1999. Two-dimensional gel analysis of human endometrial proteins: characterization of proteins with increased expression in hyperplasia and adenocarcinoma. *Mol. Hum. Reprod. 5*:748–756.

Canoz, O., Belenli, O., and Patiroglu, T.E. 2002. General features of gastric carcinomas and comparison of HSP70 and NK cell immunoreactivity with prognostic factors. *Pathol. Oncol. Res. 8*:262–269.

Chen, G., Gharib, T.G., Huang, C.C., Thomas, D.G., Shedden, K.A., Taylor, J.M., Kardia, S.L., Misek, D.E., Giordano, T.J., Iannettoni, M.D., Orringer, M.B., Hanash, S.M., and Beer, D.G. 2002. Proteomic analysis of lung adenocarcinoma: identification of a highly expressed set of proteins in tumors. *Clin. Cancer Res. 8*:2298–2305.

Durany, N., Joseph, J., Jimenez, O.M., Climent, F., Fernandez, P.L., Rivera, F., and Carreras, J. 2000. Phosphoglycerate mutase, 2,3-bisphosphoglycerate phosphatase, creatine kinase and enolase activity and isoenzymes in breast carcinoma. *Br. J. Cancer 82*:20–27.

Ebert, M.P., Yu, J., Sung, J.J., and Malfertheiner, P. 2000. Molecular alterations in gastric cancer: the role of *Helicobacter pylori*. *Eur. J. Gastroenterol. Hepatol. 12*:795–798.

Gonias, S.L., Hembrough, T.A., and Sankovic, M. 2001. Cytokeratin 8 functions as a major plasminogen receptor in select epithelial and carcinoma cells. *Front. Biosci. 6*:D1403–D141l.

Gorg, A., Weiss, W., and Dunn, M.J. 2004. Current two-dimensional electrophoresis technology for proteomics. *Proteomics 4*: 3665–3685.

Gramlich, T.L., Hennigar, R.A., Spicer, S.S., and Schulte, B.A. 1990. Immunohistochemical localization of sodium-potassium-stimulated adenosine triphosphatase and carbonic anhydrase in human colon and colonic neoplasms. *Arch. Pathol. Lab. Med. 114*:415–419.

Gunning, P., Weinberger, R., and Jeffrey, P. 1997. Actin and tropomyosin isoforms in morphogenesis. *Anal. Embryol. (Berl) 195*:311–315.

Haas, G., Karaali, G., Ebermayer, K., Metzger, W.G., Lamer, S., Zimny-Arndt, U., Diescher, S., Goebel, U.B., Vogt, K., Roznowski, A.B., Wiedenmann, B.J., Meyer, T.F., Aebischer, T., and Jungblut, P.R. 2002. Immunoproteomics of Helicobacter pylori infection and relation to gastric disease. *Proteomics 2*:313–324.

Harrison, P.R., Lanfear, J., Wu, L., Fleming, J., McGarry, L., and Blower, L. l997. Chemopreventive and growth inhibitory effects of selenium. *Biomed. Environ. Sci. 10*:235–245.

He, Q.Y., Chen, J., Kung, H.F., Yuen, A.P., and Chiu, J.F. 2004a. Identification of tumor-associated proteins in oral tongue squamous cell carcinoma by proteomics. *Proteomics 4*:271–278.

He, Q.Y., Cheung, Y.H., Leung, S.Y., Yuen, S.T., Chu, K.M., and Chiu, J.F. 2004b. Diverse proteomic alterations in gastric adenocarcinoma. *Proteomics 4*:3276–3287.

He, Q.Y. and Chiu, J.F. 2003. Proteomics in biomarker discovery and drug development. *J. Cell Biochem. 89*:868–886.

Herzig, K.H., Altmannsberger, M., and Folsch, U.R. 1994. Intermediate filaments in rat pancreatic acinar tumors, human ductal carcinomas, and other gastrointestinal malignancies. *Gastroenterology 106*:1326–1332.

Hirata, R.D., Hirata, M.H., Strufaldi, B., Possik, R.A., and Asai, M. 1989. Creatine kinase and lactate dehydrogenase isoenzymes in serum and tissues of patients with stomach adenocarcinoma. *Clin. Chem. 35*:1385–1389.

Isomoto, H., Oka, M., Yano, Y., Kanazawa, Y., Soda, H., Terada, R., Yasutake, T., Nakayama, T., Shikuwa, S., Takeshima, F., Udono, H., Murata, I., Ohtsuka, K., and Kohno, S. 2003. Expression of heat shock protein (Hsp) 70 and Hsp 40 in gastric cancer. *Cancer Lett. 198*:219–228.

Kamiya, S., Yamaguchi, H., Osaki, T., and Taguchi, H. 1998. A virulence factor of Helicobacter pylori: role of heat shock protein in mucosal inflammation after *H. pylori* infection. *J. Clin. Gastroenterol. 27 Suppl 1*:S35–S39.

Kiang, J.G., and Tsokos, G.C. 1998. Heat shock protein 70 kDa: molecular biology, biochemistry, and physiology. *Pharmacol. Ther. 80*:183–201.

Koven, I.H., Freedman, M., Miller, D., Reece, S., Maitland, A., Sigurdson, E., and Blackstein, M.E. 1983. Macro–creatine kinase 2: a possible marker of gastrointestinal cancer? *Surgery 94*:631–635.

Lam, K.Y., Loke, S.L., Shen, X.C., and Ma, L.T. 1995. Cytokeratin expression in non-neoplastic oesophageal epithelium and squamous cell carcinoma of the oesophagus. *Virchows Arch. 426*: 345–349.

Lee, K., Kye, M., Jang, J.S., Lee, O.J., Kim, T., and Lim, D. 2004. Proteomic analysis revealed a strong association of a high level of alpha1-antitrypsin in gastric juice with gastric cancer. *Proteomics 4*:3343–3352.

Maehara, Y., Oki, E., Abe, T., Tokunaga, B., Shibahara, K., Kakeji, Y., and Sugimachi, K. 2000. Overexpression of the heat shock protein HSP70 family and p53 protein and prognosis for patients with gastric cancer. *Oncology 58*:144–151.

Martin, T.E., Powell, C.T., Wang, Z., Bhattacharyya, S., Walsh-Reitz, M.M., Agarwal, K., and Toback, F.G. 2003. A novel mitogenic protein that is highly expressed in cells of the gastric antrum mucosa. *Am. J. Physiol. Gastrointest. Liver Physiol. 285*:G332–G343.

Melville, M.W., McClellan, A.J., Meyer, A.S., Darveau, A., and Frydman, J. 2003. The Hsp70 and TRiC/CCT chaperone systems cooperate *in vivo* to assemble the von Hippel-Lindau tumor suppressor complex. *Mol. Cell Biol. 23*:3141–3151.

Ming, S.C. 1998. Cellular and molecular pathology of gastric carcinoma and precursor lesions: a critical review. *Gastric Cancer 1*:31–50.

Miyaishi, O., Kozaki, K., Iida, K., Isobe, K., Hashizume, Y., and Saga, S. 1998. Elevated expression of PDI family proteins during differentiation of mouse F9 teratocarcinoma cells. *J. Cell Biochem. 68*:436–445.

Montgomerie, J.Z., Gracy, R.W., Holshuh, H.J., Keyser, A.J., Bennett, C.J., and Schick, D.G. 1997. The 28K protein in urinary bladder, squamous metaplasia and urine is triosephosphate isomerase. *Clin. Biochem. 30*:613–618.

Mori, M., Staniunas, R.J., Barnard, G.F., Jessup, J.M., Steele, G.D., Jr., and Chen, L.B. 1993. The significance of carbonic anhydrase expression in human colorectal cancer. *Gastroenterology 105*:820–826.

Nilsson, C.L., Larsson, T., Gustafsson, E., Karlsson, K.A., and Davidsson, P. 2000. Identification of protein vaccine candidates from *Helicobacter pylori* using a preparative two-dimensional electrophoretic procedure and mass spectrometry. *Anal. Chem. 72*:2148–2153.

Nogradi, A. 1998. The role of carbonic anhydrases in tumors. *Am. J. Pathol. 153*:1–4.

Novy, R.E., Lin, J.L., Lin, C.S., and Lin, J.J. 1993. Human fibroblast tropomyosin isoforms: characterization of cDNA clones and analysis of tropomyosin isoform expression in human tissues and in normal and transformed cells. *Cell Motil. Cytoskeleton 25*:267–281.

Ormsby, A.H., Goldblum, J.R., Rice, T.W., Richter, J.E., and Gramlich, T.L. 2001. The utility of cytokeratin subsets in distinguishing Barrett's-related oesophageal adenocarcinoma from gastric adenocarcinoma. *Histopathology 38*:307–311.

Peddanna, N., Holt, S., and Verma, R.S. 1995. Genetics of gastric cancer. *Anticancer Res. 15*:2055–2064.

Pisani, P., Bray, F., and Parkin, D.M. 2002. Estimates of the worldwide prevalence of cancer for 25 sites in the adult population. *Int. J. Cancer 97*:72–81.

Prasad, S.C., Soldatenkov, V.A., Kuettel, M.R., Thraves, P.J., Zou, X., and Dritschilo, A. 1999. Protein changes associated with ionizing radiation-induced apoptosis in human prostate epithelial tumor cells. *Electrophoresis 20*:1065–1074.

Reinders, J., Lewandrowski, U., Moebius, S., Wagner, Y., and Sickmann, A. 2004. Challenges in mass spectrometry-based proteomics. *Proteomics 4*:3686–3703.

Ryu, J.W., Kim, H.J., Lee, Y.S., Myong, N.H., Hwang, C.H., Lee, G.S., and Yom, H.C. 2003. The proteomics approach to find biomarkers in gastric cancer. *J. Korean Med. Sci. 18*:505–509.

Sakai, J., Ishikawa, H., Kojima, S., Satoh, H., Yamamoto, S., and Kanaoka, M. 2003. Proteomic analysis of rat heart in ischemia and ischemia-reperfusion using fluorescence two-dimensional difference gel electrophoresis. *Proteomics 3*:1318–1324.

Scheuemann, P., Hosch, S.B., and Izbicki, J.R. 2001. Cytokeratins and other sensitive markers for esophageal cancer and metastases. *Dis. Esophagus 14*:85–90.

Shiozaki, K., Nakamori, S., Tsujie, M., Okami, J., Yamamoto, H., Nagano, H., Dono, K., Umeshita, K., Sakon, M., Furukawa, H., Hiratsuka, M., Kasugai, T., Ishiguro, S., and Monden, M. 2001. Human stomach-specific gene, CA11, is down-regulated in gastric cancer. *Int. J. Oncol. 19*:701–707.

Sinha, P., Hutter, G., Kottgen, E., Dietel, M., Schadendorf, D., and Lage, H. 1998. Increased expression of annexin I and thioredoxin detected by two-dimensional gel electrophoresis of drug resistant human stomach cancer cells. *J. Biochem. Biophys. Methods 37*:105–116.

Sinha, P., Poland, J., Schnolzer, M., Celis, J.E., and Lage, H. 2001. Characterization of the differential protein expression associated with thermoresistance in human gastric carcinoma cell lines. *Electrophoresis 22*:2990–3000.

Sowden, J., Leigh, S., Talbot, I., Delhanty, J., and Edwards, Y. 1993. Expression from the proximal promoter of the carbonic anhydrase 1 gene as a marker for differentiation in colon epithelia. *Differentiation 53*:67–74.

Srisomsap, C., Subhasitanont, P., Otto, A., Mueller, E.C., Punyarit, P., Wittmann-Liebold, B., and Svasti, J. 2002. Detection of cathepsin B up-regulation in neoplastic thyroid tissues by proteomic analysis. *Proteomics 2*:706–712.

Stasyk, T., and Huber, L.A. 2004. Zooming in: fractionation strategies in proteomics. *Proteomics 4*:3704–3716.

Tanaka, S., Uehara, T., and Nomura, Y. 2000. Up-regulation of protein-disulfide isomerase in response to hypoxia/brain ischemia and its protective effect against apoptotic cell death. *J. Biol. Chem. 275*:10388–10393.

Taniere, P., Borghi-Scoazec, G., Saurin, J.C., Lombard-Bohas, C., Boulez, J., Berger, F., Hainaut, P., and Scoazec, J.Y. 2002. Cytokeratin expression in adenocarcinomas of the esophagogastric junction: a comparative study of adenocarcinomas of the distal esophagus and of the proximal stomach. *Am. J. Surj. Pathol. 26*:1213–1221.

Toback, F.G., Walsh-Rejtz, M.M., Musch, M.W., Chang, E.B., Del Valle, J., Ren, H., Huang, E., and Martin, T.E. 2003. Peptide fragments of AMP-18, a novel secreted gastric antrum mucosal protein, are mitogenic and motogenic. *Am. J. Physiol. Gastrointest. Liver Physiol. 285*:G344–G353.

Tot, T. 2002. Cytokeratins 20 and 7 as biomarkers: usefulness in discriminating primary from metastatic adenocarcinoma. *Eur. J. Cancer 38*:758–763.

Usuba, T., Ishibashi, Y., Okawa, Y., Hirakawa, T., Takada, K., and Ohkawa, K. 2001. Purification and identification of monoubiquitin-phosphoglycerate mutase B complex from human colorectal cancer tissues. *Int. J. Cancer 94*:662–668.

van Molle, W., Denecker, G., Rodriguez, I., Brouckaert, P., Vandenabeele, P., and Libert, C. 1999. Activation of caspases in lethal experimental hepatitis and prevention by acute phase proteins. *J. Immunol. 163*:5235–5241.

Wauters, C.C., Smedts, F., Gerrits, L.G., Bosman, F.T., and Ramaekers, F.C. 1995. Keratins 7 and 20 as diagnostic markers of carcinomas metastatic to the ovary. *Hum. Pathol. 26*:852–855.

Williams, K., Chubb, C., Huberman, E., and Giometti, C.S. 1998. Analysis of differential protein expression in normal and neoplastic human breast epithelial cell lines. *Electrophoresis 19*:333–343.

Yamaguchi, H., Osaki, T., Taguchi, H., Hanawa, T., Yamamoto, T., and Kamiya, S. 1998. Relationship between expression of HSP60, urease activity, production of vacuolating toxin, and adherence activity of *Helicobacter pylori. J. Gastroenterol. 33 Suppl 10*:6–9.

Yang, M., and Sytkowski, A.J. 1998. Differential expression and androgen regulation of the human selenium-binding protein gene hSP56 in prostate cancer cells. *Cancer Res. 58*:3150–3153.

Yokota, S., Yamamoto, Y., Shimizu, K., Momoi, H., Kamikawa, T., Yamaoka, Y., Yanagi, H., Yura, T., and Kubota, H. 2001. Increased expression of cytosolic chaperonin CCT in human hepatocellular and colonic carcinoma. *Cell Stress. Chaperones 6*:345–350.

Yoo, B.C., Ku, J.L., Hong, S.H., Shin, Y.K., Park, S.Y., Kim, H.K., and Park, J.G. 2004. Decreased pyruvate kinase M2 activity linked to cisplatin resistance in human gastric carcinoma cell lines. *Int. J. Cancer 108*:532–539.

18

Vesicle Proteins in Neuroendocrine and Nonendocrine Tumors of the Gastrointestinal Tract

Anne-Marie Levin-Jakobsen and Ola Nilsson

Introduction

Neuroendocrine tumors of the gastrointestinal (GI) tract are rare, accounting for a small percentage of all GI tumors (Sandor and Modlin, 1998). Most neuroendocrine tumors occur as sporadic lesions, but 5–20% of the tumors occur in a clinical setting of inherited neoplastic syndrome (e.g., multiple endocrine neoplasia1 [MEN 1], MEN 2, von Recklinghausen disease, and von Hippel Lindau disease; Calender, 1999; Hoff *et al.,* 2000). The neuroendocrine tumors comprise a wide range of tumors, from benign lesions detected incidentally to highly malignant tumors with distant metastases and severe hormonal symptoms. To account for the wide spectrum of neuroendocrine tumors, the classification of neuroendocrine tumors of the GI tract has been upgraded (Solcia *et al.,* 2000). Five tumor categories are now recognized, including well-differentiated endocrine tumors, well-differentiated endocrine carcinomas, poorly differentiated (small cell) endocrine carcinomas, mixed exocrine–endocrine tumors, and tumor-like lesions. Neuroendocrine tumors of the GI tract are thought to originate from the "diffuse neuroendocrine cell system" of the GI mucosa. The reason for this assumption is that neuroendocrine tumors have morphologic and functional similarities with the cells of the "diffuse neuroendocrine cell system."

Neuroendocrine tumors have been shown to share a number of markers with normal neuroendocrine cells and nerve cells—that is, cytosolic enzymes (neuron-specific enolase [NSE], protein gene product [PGP] 9.5), synaptic vesicle proteins (synaptophysin), secretory granule components (chromogranins), and neurotransmitters or hormones (Bishop *et al.,* 1982; Lloyd and Wilson, 1983; Rode *et al.,* 1985; Rindi *et al.,* 1986, 1999). The diagnosis of neuroendocrine tumors relies on the identification of a neuroendocrine phenotype (i.e., demonstration of one or several of the markers known to be expressed by the "diffuse neuroendocrine cell system"). In diagnostic histopathology indentification of the neuroendocrine phenotype has been achieved by different methods (i.e., silver impregnation techniques, ultrastructural demonstration of secretory granules, or immunocytochemistry using antibodies against neuroendocrine markers). A number of novel vesicle proteins have been identified in normal neurons and endocrine cells, which has increased our understanding of the complexity of the secretory processes in these cell systems. Subsequent studies have demonstrated expression of the same vesicle proteins in many of the neuroendocrine tumors. In this

Handbook of Immunohistochemistry and *in situ* Hybridization of Human Carcinomas, Volume 4: Molecular Genetics, Gastrointestinal Carcinoma, and Ovarian Carcinoma

chapter, we review the current knowledge of vesicle proteins in neuroendocrine tumors and the practical use of antibodies against vesicle proteins in the diagnosis of neuroendocrine tumors of the GI tratct.

Neuroendocrine Differentiation—Secretory Granules and Synaptic Vesicles

Neurons and neuroendocrine cells contain two types of secretory vesicles, which are crucial for the regulated secretory process and represent cell-specific compartments of these cells. Peptide hormones and neuropeptides are mainly contained within the *secretory granules* or *large dense core vesicles* (LDCV). These vesicles are characterized morphologically by an electron dense core and a vesicle diameter of 100–150 nm. They are formed by budding of clathrin-coated vesicles from the *trans* Golgi network. In addition to peptide hormones/neuropeptides, these vesicles contain high concentrations of matrix proteins of the granin family such as chromogranin, CgB, and CgC. The membranes of LDCV contain cytochrome b651, an integral membrane protein, as well as the v-SNARE proteins, synaptobrevin, and syntagmin. Packaging of secretory proteins in LDCV is the standard way of release in the regulated secretory pathway.

Some neuroendocrine cells and nerve cells use another type of specialized secretory vesicles, the *synaptic-like microvesicles* (SLMV). These vesicles are ~50 nm in diameter and lack an electron dense core. Neurotransmitter molecules stored in SLMVs are acetylcholine, glutamate, gamma aminobutyric acid (GABA), epinephrine, and norepinephrine. The membrane components of the SLMVs include carrier proteins specialized for the uptake of neurotransmitter from the cytosol. SLMVs are devoid of granins but have synaptophysin in the vesicle membrane as well as v-SNARE proteins. A schematic presentation of the synaptic vesicle/secretory granule is given in Figure 44. Demonstration of secretory granules/large dense core vesicles or synaptic-like microvesicles in tumors cells provides strong evidence for classifying a tumor as a neuroendocrine (Solcia *et al.,* 1993). Electron microscopy can be used to demonstrate the secretory granules and synaptic vesicles and to subclassify neuroendocrine tumors according to the morphology of these organelles. A schematic representation of the secretory granules is given in Figure 44.

Neuroendocrine Differentiation—Secretory Granule Proteins

Secretory granules/large dense core vesicles are present in the majority of neuroendocrine cells and neuroendocrine tumors. These organelles are characterized by high concentrations of matrix proteins such as the chromogranins. The chromogranin family includes CgA, CgB, CgC, secretogranin III, and neuroendocrine secretory protein 55 (NESP55) (Laslop *et al.,* 2000). Chromogranin is the major acidic protein of secretory granules and represents 40% of the soluble protein of adrenal medullary chromaffin cells (Stefaneanu *et al.,* 2000). The largest store of chromogranin is found in the adrenal medulla, but smaller amounts are also found

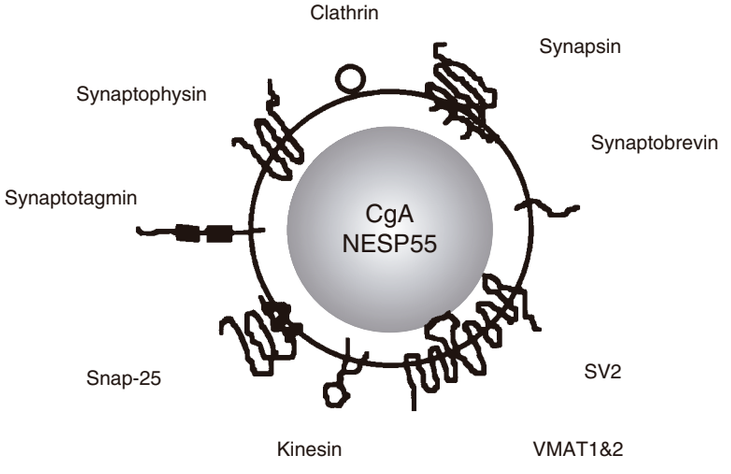

Figure 44. Schematic presentation of secretory granule from a neuroendocrine (NE) cell. Major proteins of the granule are indicated. ACTH, adrenocorticotropic hormone; NESP, neuroendocrine secretory protein; NSE, neuro-specific enolase; PGP, protein gene product; PP, pancreatic polypeptide; VMAT, vesicular monoamine transporter.

in the pituitary, pancreas, stomach, intestine, and other endocrine organs (Winkler and Fischer-Colbrie, 1992). Chromogranin is not restricted to granules of chromaffin cells, but it is present in most neuroendocrine cells and neuroendocrine tumor granules and vesicles. Both chromogranin and CgB are heat-stable proteins, probably because of their hydrophilic nature and random coil properties (Winkler and Fischer-Colbrie, 1992). After synthesis, chromogranin is converted into smaller bioactive peptides such as pancreastatin, vasostatin, and secretoneurin by prohormone convertases (Laslop *et al.,* 2000). However, the proteolytic processing of chromogranin varies between different tissues and may also take place after the release from neuroendocrine cells (Winkler and Fischer-Colbrie, 1992). CgA is colocalized with transmitters or neuropeptides within secretory granules and also cosecreted at exocytosis. The functional role of CgA in neuroendocrine cells and neuroendocrine tumors is not fully understood. Apart from being a precursor of bioactive peptides, CgA interacts with Ca^{2+} and catecholamines in the secretory granules. Studies in 2001 established CgA as the key regulator of secretory granule biosynthesis and hormone sequestration in endocrine cells (Kim *et al.,* 2001).

The protein NESP55, the latest member of the chromogranin family, is a heat-stable, acidic protein localized to the soluble content of secretory granules of adrenal chromaffin cells. Although NESP55 is present in secretory granules of endocrine cells and neurons, it is less widely distributed than CgA. The functional role of NESP55 is yet unknown. It is expressed in a subset of neuroendocrine tumors, such as endocrine pancreatic tumors, pheochromocytomas, and neuroblastomas, and may be useful in the classification of neuroendocrine tumors (Jakobsen *et al.,* 2003).

Neuroendocrine Differentiation—Synaptic Vesicle Proteins

Synaptic vesicles are present in the majority of neurons, neuroendocrine cells, and neuroendocrine tumors (Wiedenmann *et al.,* 1986). These organelles are characterized by a large number of highly specialized membrane proteins. Most of the synaptic vesicles proteins are members of gene families containing multiple isoforms (e.g., synaptotagmin, synaptophysin, synapsin, synaptic vesicle protein 2-[SV2], vesicular monoamine transporter, and vesicular amino acid transporters) (Bajjalieh *et al.,* 1993; Gras *et al.,* 2002; Janz and Sudhof, 1999; Janz *et al.,* l999; Kao *et al.,* 1998; Takamori *et al.,* 2002).

Synaptophysin is an abundant vesicle membrane glycoprotein with four transmembrane domains (Elferink and Scheller, 1995). It is thought to play a role in recovery and reconstitution of the synaptic vesicle SLVMs via Ca^{2+} binding (Daly and Ziff, 2002). Synaptophysin is widely distributed in both neurons and neuroendocrine cell and in neuroendocrine tumors **(**Wiedenmann and Huttner, 1989; Wiedenmann *et al.,* 1986). Monoclonal antibodies against synaptophysin are widely used as a marker for neuroendocrine differentiation in diagnostic histopathology.

The membrane protein SV2 is universally present in synaptic vesicles of neurons and neuroendocrine cells (Buckley and Kelly, 1985; Lowe *et al.,* 1988). It is among the most abundant and conserved components of synaptic vesicles (Janz and Sudhof, 1999) and comprises three isoforms (Bajjalieh *et al.,* 1993; Janz and Sudhof, 1999). All isoforms are integral membrane proteins with 12 transmembrane regions and intravesicular consensus sites for N-glycosylation (Bajjalieh *et al.,* 1993; Janz and Sudhof, 1999). The function of SV2 in neurons and neuroendocrine cells is poorly understood. However, the N-terminal region of SV2A has been shown to bind to synaptotagmin I, a Ca^{2+} binding protein. Experiments with knockout mice indicate that SV2A plays a role in Ca^{2+} transport and is essential for survival and normal function of the nervous system. Using monoclonal antibodies, SV2A was demonstrated in neuroendocrine cells of the human GI tract, pancreas, anterior pituitary gland, thyroid, parathyroid, and adrenal medulla, as well as in a selected series of neuroendocrine tumors (Portela-Gomes *et al.,* 2000). In a study on GI endocrine and nonendocrine tumors we found that SV2 is widely expressed in neuroendocrine tumors and that SV2 can be used as a general marker of neuroendorine differentiation (Jakobsen *et al.,* 2002).

Vesicular monoamine transporter (VMAT) is a vesicle membrane protein that functions as a transporter of amine neurotransmitters from the cytoplasm into synaptic vesicles and secretory granules of neurons, neuroendocrine cells, platelets, and mast cells (Erickson and Eiden, 1993; Erickson *et al.,* 1996). Sequestration of amines into secretory granules and vesicles is a prerequisite for regulated secretion of amine transmitters via exocytosis. The VMAT protein exists in two different isoforms—VMAT 1 and 2 bind and transport amines (but also other substances (e.g., the neurotoxin MPP^+ and the norepinephrine analog meta-iodobenzylguanidine [MIBG]) (Henry *et al.,* 1994). The VMAT proteins are differentially expressed in normal tissues, with VMAT 2 present in cells of the amine-containing nuclei of the brain stem, in dopaminergic cells of substantia nigra, and in abundant nerve fibers and terminals in the cerebral cortex, whereas no VMAT 1 can be detected in the human brain. In the peripheral nervous system VMAT 1 is present in SIF (small intensely fluorescent)

cells of sympathetic ganglia, whereas VMAT 2 was found in sympathetic principal ganglion cells and ganglion cells of the myenteric plexus. Enterochromaffin-like (ECL) cells of the oxyntic stomach expressed VMAT 2, whereas the majority of the enterochromaffin (EC) cells of the small and large intestine expressed VMAT 1. In the endocrine pancreas only VMAT 2 is expressed, whereas both VMAT 1 and VMAT 2 were expressed in the chromaffin cells of the adrenal medulla (Erickson *et al.,* 1996). The expression of VMAT in neuroendocrine tumors has only recently been studied. Expression of VMAT 2 has been demonstrated in gastric ECL–cell tumors, paragangliomas, and in occasional EC–cell tumors and endocrine pancreatic tumors (EPT) (Rindi *et al.,* 2000). The protein VMAT 2 is also expressed in hyperplastic ECL cells ("precursor lesions") of the gastric mucosa in patients suffering from chronic atrophic gastritis, or the Zollinger-Ellison (ZE) syndrome. The protein VMAT 2 has therefore been suggested to be a specific marker of ECL cell hyperplasia/neoplasia (Eissele *et al.,* 1999; Rindi *et al.,* 2000). An analysis of a larger series of GI tumors demonstrated VMAT 2 in gastric endocrine tumors and VMAT 1 in ileal and appendiceal endocrine tumors (carcinoids). There was no expression of VMAT 1 and 2 in nonendocrine tumors of the gastrointestinal tract or pancreas (Jakobsen *et al.,* 2001). From this we conclude that VMAT 1 and 2 can be used to identify amine-producing endocrine tumors and may be helpful in subclassifying neuroendocrine tumors.

METHODS

Advances in Immunocytochemistry

The introduction of immunocytochemistry in diagnostic histopathology has greatly facilitated the classification of neuroendocrine tumors. Advances made in immunocytochemistry during the past few decades include increased number of antibodies against different neuroendocrine markers and improved sensitivity, specificity, and reproducibility of the immunocytochemical detection systems. Another advance is the introduction of automated immunostaining machines, which have facilitated the introduction of immunocytochemistry in routine histopathology. Automated immunostaining is also important for standardization, reproducibility, and ergonomics. Although care is taken to standardize and optimize the conditions of the immunocytochemical procedures, the final results still depend on a number of "preanalytical" parameters that are difficult to control, (e.g., handling of tumor material prior to fixation, choice of fixation medium and fixation time). These parameters may vary between different laboratories and must be considered when comparing the immunocytochemical results from different studies.

Novel Neuroendocrine Markers

Synaptic vesicle proteins and secretory granule proteins, such as synaptophysin and CgA, have long been important diagnostic tools for neuroendocrine tumors. Both CgA and synaptophysin are expressed by the majority of neuroendocrine tumors and are therefore used as general neuroendocrine markers. New antibodies secretory granule/vesicle proteins have been applied in the diagnosis of neuroendocrine tumors. Among these new antibodies are SV2, VMAT 1 and 2, soluble NSF, (*N*-ethylmaleimide-sensitive factor) attachment proteins (SNAP25), synaptobrevin (VAMP2), and syntaxin (Grabowski *et al.,* 2002; Graff *et al.,* 2001; Jakobsen *et al.,* 2001, 2002; Kumaki *et al.,* 2002). We have shown that all neuroendocrine tumors of the GI tract and pancreas express SV2 and that monoclonal antibodies against SV2 can be used to identify these tumors (Jakobsen *et al.,* 2002). From these data, and from unpublished data on neuroendocrine tumors from other organs, we concluded that SV2 may serve as a general neuroendocrine marker and that monoclonal antibodies against SV2 have a sensitivity comparable to that of monoclonal antibodies against synaptophysin and CgA. The potential role of SV2 in the diagnostic workup of neuroendocrine tumors is indicated in Figure 45.

Two other vesicle proteins, VMAT 1 and 2, have also been demonstrated in GI endocrine tumors. However, differential expression of VMAT isoforms was demonstrated in neuroendocrine tumors of the GI tract and pancreas (Jakobsen *et al.,* 2001). Expression of VMAT 2 primarily was found in amine-producing carcinoid tumors of the stomach, whereas VMAT 1 was found in carcinoids of the small bowel and appendix, reflecting the cellular composition of these tumors. Isoforms of VMAT can therefore be regarded as markers of cell lineage, and antibodies against specific isoforms may be used to classify neuroendocrine tumors. A potential role of VMAT in the diagnosis of neuroendocrine tumors is indicated in Figure 45.

A novel chromaffin granule marker NESP55, has been shown to be expressed in neuroendocrine tumors of the GI tract. It has a more limited expression than CgA and is found in certain, but not all, of the neuroendocrine tumors of the GI tract, pancreas, and adrenals (Jakobsen *et al.,* 2003). The protein NESP55 can therefore not be used as a general neuroendocrine tumor marker, but it may be used to identify subtypes of neuroendocrine tumors, which may be of particular importance when a patient presents with metastatic disease and the origin of the primary tumor is unknown. As yet, NESP55 positivity does not seem to have any prognostic significance in neuroendocrine tumors. A list of some of the available antibodies against secretory granule proteins and vesicle proteins is given in Table 14.

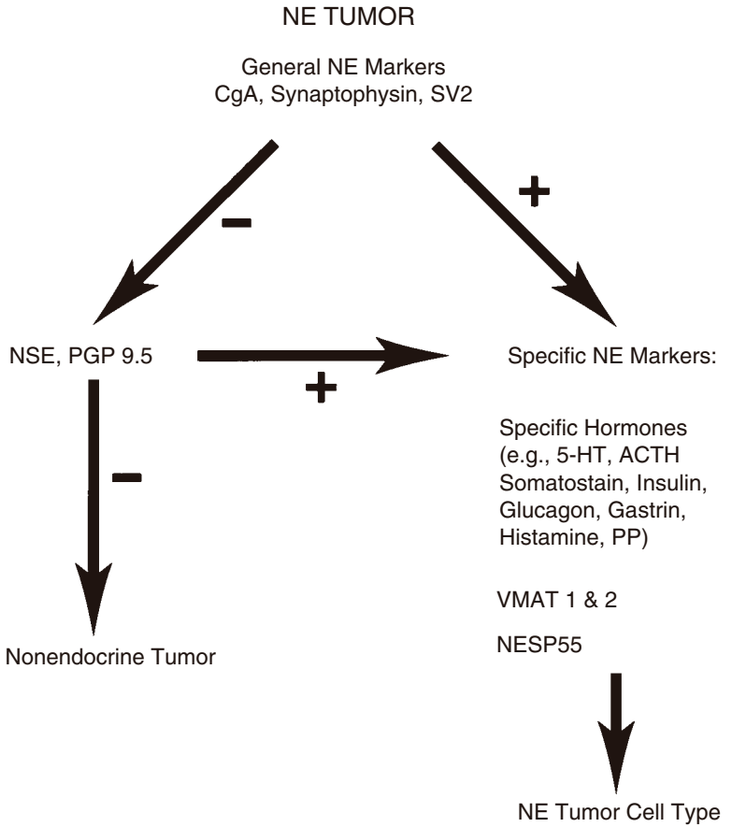

Figure 45. Suggested use of vesicle proteins in the diagnosis of neuroendocrine tumors of the gastrointestinal tract. ACTH, Adrenocorticotropic hormone; CgA, chromogranin A; NE, nonendocrine; NESP, nonendocrine secretory protein; NSE, neurospecific enolase; PGP, protein gene product; PP, pancreatic polypeptide; VMAT, vesicular monoamine transporter.

Methods of Antigen Retrieval in Immunocytochemistry

Processing of surgical specimens for routine pathology includes fixation in formalin and embedding in paraffin wax. This procedure denatures tissue proteins and may lead to masking of epitopes. Antigen retrieval is a method to reexpose hidden antigens in formalin-fixed and paraffin-embedded specimens, so that antigens can be detected by antibodies. Developed methods for antigen retrieval have greatly improved the sensitivity and reproducibility of immunocytochemical staining of routinely processed surgical specimens. Antigen retrieval is one of the most important factors affecting the results of immunocytochemical staining; it is generally more important than the sensitivity of the detection system.

The two most important methods for antigen retrieval are *enzymatic digestion* and *heat-induced epitope retrieval* (HIER). Antigen retrieval by *enzymatic digestion* of tissue sections is achieved by proteolytic enzymes such as trypsin, pepsin, or protease (Battifora and Kopinski, 1986). Regardless of the enzyme used, longer fixation time requires longer enzymatic digestion, and this makes the enzymatic digestion procedure difficult to standardize.

Antigen retrieval by HIER is achieved by heating tissue sections in a buffer using a microwave oven or pressure cooker. This method is very effective in demasking antigens in formalin-fixed tissues. The exact mode of action of HIER is not clear. Putative mechanisms are as follows: 1) breaking of formalin-induced cross-links between epitopes and unrelated proteins; 2) extraction of diffusible blocking proteins, and 3) precipitation of proteins and rehydration of the tissue section allowing better penetration of antibody and increasing accessiblity of epitopes (Boon and Kok, 1994). Many different types of retrieval solution can be used for HIER (e.g., citrate buffer [pH 6], EDTA [ethylenediamine tetra-acetic acid]-NaOH [pH 8], Tris-HCL [pH 8], and commercial target retrieval fluids. The pH appears to be more important than the chemical composition of the antigen-retrieval fluids for the effectiveness of HIER (Shi *et al.,* 1995). Studies have shown that retrieval solution with an alkaline pH is a much more effective general retrieval

Table 14. Available Antibodies against Secretory Granule Proteins and Vesicle Proteins

Antibody	Species	Clone	Source[a]
Anti-SV2	mouse	SP2/0	Development Studies, Hybridoma Bank, University of Iowa, IA, USA
Anti-CgA	mouse	LK2H10 DAK-A3	Temecula, CA, USA DAKO, Copenhagen, Denmark
Anti-Synaptophysin	mouse	SY38	DAKO
Anti-CgA-CgB	rabbit	—	Eurodiagnostica
Anti-SNAP 25	mouse	SP12	Oncogene Research Products, MA, USA Synaptic Systems, Göttingen, Germany
Anti-Synaptobrevin	mouse	SP11	Oncogene Research Products Synaptic Systems
Anti-Synapsin I	mouse	A1OC	Oncogene Research Products
Anti-Synapsin IIa	mouse	—	Transduction Laboratories, Lexington, KY, USA
Anti-Syntaxin	mouse	—	Synaptic Systems
Anti-VMAT1	goat	—	Santa Cruz Biotechnology, CA, USA
Anti-VMAT2	rabbit	—	Chemicon International, CA, USA
Anti-NESP55	rabbit	—	R. Fischer-Colbrie, Innsbruck, Austria

[a]Suppliers of antibodies used by the authors.

solution than is acidic fluid (Pileri *et al.,* 1997). There is not a single HIER method that is considered optimal for all antibodies and epitopes. Instead it is recommended that maximal retrieval for a given antibody must be tried out by a "test-battery," which includes pH, temperature and time. A summary of available antigen-retrieval methods is given in Tables 15 and 16.

Antigen Retrieval of Vesicle Proteins in Neuroendocrine Tumors

The optimal conditions for antigen retrieval have to be determined for each antigen and each antibody. This is particularly important when analyzing "routinely" processed material, where the preanalytical conditions (i.e., handling of specimen prior to arrival in the laboratory) are difficult to control. Although there are studies describing the effect of antigen retrieval on a wide range of antigens, there is little information regarding optimal methods for vesicle proteins. Our experience is that the majority of vesicle proteins do benefit from HIER prior to immunocytochemical analysis (Shi *et al.,* 1997, 1998). Standard protocols with citrate buffer (pH 6) or Tris-EDTA (pH 8) will give excellent immunocytochemical demonstration of most vesicle proteins.

Immunocytochemical Detection Systems

Many of the immunocytochemical detection systems in practice today are based on streptavidin/avidin and biotin. A strong amplification of immunolabeling is achieved in the streptavidin-biotin methods as compared to the peroxidase anti-peroxidase (PAP) method. The basic protocol includes primary antibody, biotinylated secondary antibody, followed either by the preformed (strept)avidin-biotin-enzyme complex (avidin-biotin complex, ABC method) or by the enzyme-labeled streptavidin (LSAB). Development of new detection systems has improved the sensitivity and specificity of immunocytochemistry, (e.g., the tyramide signal amplification [TSA] system and the dextran polymer visualization systems/labeled polymer methods. (EnVision, EnVision+). The tyramide signal amplification system, which is based on the CARD principle (catalyzed reporter deposition), is used to enhance the signal from horseradish peroxidase (HRP)-labeled primary or secondary antibodies (Bobrow *et al.,* 1989). The principle of the tyramide signal amplification is the capacity of HRP to catalyze the activation of tyramide to a free radical, which in turn binds to electron-rich amino acids in the tissue. In this way high amounts of biotin are bound to tissue proteins via tyramide, which is then detected by adding HRP-conjugated streptavidin and a chromogen. In the dextran polymer visualization systems (Sabattini *et al.,* 1998) the former three-step

Table 15. Antigen Retrieval Methods

Enzymatic Digestion by Proteolytic Enzymes:
a) Trypsin (5–20 min at 37°C, depending on time of fixation in NBF)
b) Pepsin (10–120 min at 37°C, depending on time of fixation in NBF)
c) Protease XIV (5–15 min at 37°C, depending on time of fixation in NBF)

Heat Induced Epitope Retrieval (HIER)
a) Microwave oven
b) Pressure cooker

Table 16. Test Battery for Optimization of Antigen Retrieval According to Shi *et al.*, 1997

Buffer[a]	pH l	pH 6	pH 10
120°C, 10 min[b]	Slide 1	Slide 4	Slide 7
100°C, 10 min	Slide 2	Slide 5	Slide 8
90°C, 10 min	Slide 3	Slide 6	Slide 9

[a]10 mM Tris-HCl is used at pH 1, 10mM Citrate is used at pH6 and 100 mM Tris-HCl at pH 10.

[b]To get a temperature of l20°C, pressure cooker is used. The same effect is obtained by microwave treatment for 20 min.

visualization method, based on the affinity between avidin and biotin, is replaced by a dextran polymer (enzyme-labeled inert "spine" molecule of dextran) coupled to HRP, or alkaline phosphatase (AP), and either directly to the primary or the secondary antibody. An example of an immunocytochemical incubation protocol used by the authors is given in the following.

METHOD

Fixation and Embedding of Specimens

1. Cut fresh specimens into small pieces.
2. Place specimens immediately in fixative (4% formaldehyde in phosphate buffer saline, or PBS). Allow to fix at room temperature for 24–48 hr (depending on size).
3. Dehydrate specimens in graded ethanol (70% for 1 hr, 95% for 1 hr 2X, 99.5% for 1 hr 2X. Clear in xylene (15 min and 30 min) and place in paraffin wax at 58–60°C (30 min 2X, 1 hr).
4. Place specimens in cassettes and fill with paraffin wax (58–60°C). Cool on ice.

Antigen Retrieval with Microwave Treatment

1. Cut 3–5 μm sections on a microtome. Stretch sections by placing sections in a waterbath at room temperature and at 45°C.
2. Place sections on positive charged glass slides (SuperFrost).
3. Heat slides at 60°C for 30 min. Allow to cool to room temperature.
4. Deparaffinize sections in xylene (10 min 2×) and rehydrate in graded ethanol (99.5% for 5 min 2×, 95% for 5 min l×, 70% for 5 min 1X) and distilled water (1 min).
5. Place sections in containers with antigen retrieval buffer (e.g., Tris-EDTA pH 9 or citrate buffer pH 6). Sections should be completely covered with buffer and must not dry during microwave treatment.
6. Heat containers with sections in a microwave oven set at 800W for 5–10 min (depending on number of slides). Replace evaporated liquid with distilled water. Repeat microwave treatment. Allow to cool at room temperature for 20 min.

Immunocytochemical Incubation Procedure

The following steps are performed at room temperature, except for **Step 5.**

1. Rinse sections in distilled water (1 min).
2. Treat sections with 3% hydrogen peroxide in distilled water for 10 min (blocks endogenous peroxidase).
3. Rinse sections in distilled water (1 min).
4. Place sections in PBS-Tween 20.
5. Incubate overnight with diluted primary antibody at 4°C.
6. Rinse in PBS 3 min 3X, with 1 drop of Tween 20 added in the last rinse.
7. Incubate with EnVision+ for 30 min.
8. Rinse in PBS 3 min 3X and PBS-Tween 20 in the last rinse.
9. Incubate sections with substrate solution (hydrogen peroxide-DAB [diaminobenzidine]) for 2 min.
10. Rinse in distilled water (1 min).
11. Counterstain with Mayer's hematoxylin for 5 min.
12. Rinse in tap water for 15 min.
13. Dehydrate in graded ethanol, clear in xylene, and mount.

MATERIALS

1. PBS: 2.3 g monobasic sodium phosphate, 8.2 g dibasic sodium phosphate, 4 g sodium chloride; bring volume to 1 L with deionized distilled water, pH 7.4.
2. Fixative: 4% paraformaldehyde in PBS (pH 7.4).
3. Paraffin wax: purified paraffins and microcrystallizing waxes, melting point 56°–58°C.
4. Positively charged glass slides: SuperFrost Plus (cat. no. 041300), Menzel-Gläser, Germany.
5. Tris-EDTA buffer: 1.21 g Tris, 0.372 g EDTA; bring volume to 1 L with deionized distilled water (pH 9).
6. Sodium citrate buffer: 2.1 g sodium citrate, bring volume to 1 L with deionized distilled water (pH 6.0).
7. 3% hydrogen peroxidase: freshly add 20 ml of 30% H_2O_2 to 180 ml of deionized distilled water (final volume 200 ml).
8. PBS-Tween 20: add 1 drop of Tween 20 to 200 ml PBS.
9. Antibody solution: primary antibodies are diluted in antibody diluent (cat. no. Dako Cytomation Glostrup, Denmark).

10. Secondary antibodies: EnVision+ (anti-rabbit, cat. no. K4002, anti-mouse, cat. no. K4007, Dako Cytomation).
11. Substrate chromogen: freshly prepare 0.75 µl of 30% H_2O_2 in 1 ml of DAB solution (cat. no. K3468, Dako).

RESULTS

Expression Patterns of Vesicular Proteins in Gastrointestinal Neuroendocrine and Nonneuroendocrine Tumors

Secretory granule proteins and vesicle proteins are expressed in neuroendocrine tumors of the GI tract. In general, all neuroendocrine tumors express one or several granule/vesicle proteins, whereas nonneuroendocrine tumors do not express vesicle proteins (Solcia *et al.,* 1993). Because neuroendocrine tumors may differentiate toward different endocrine cell types, the pattern of vesicle proteins may also vary. In one study, we analysed the expression of several vesicle proteins in neuroendocrine and nonneuroendocrine tumors of the GI tract. General neuroendocrine markers/vesicle proteins such as CgA, SV2, and synaptophysin were strongly expressed in all neuroendocrine tumors of the GI tract, whereas no or only focal expression was observed in nonneuroendocrine tumors. Some vesicle proteins such as VMAT 1 and 2, and NESP55 were only found in a subset of neuroendocrine tumors and may therefore be regarded as tumor-type specific (Table 17). Gastrointestinal stromal tumors (GIST), which are thought to originate from the intertitial cell of Cajal, were also shown to express one of the general neuroendocrine markers, which indicates that these tumors have a neuroendocrine phenotype (Kindblom *et al.,* 1998). Examples of immunocytochemical demonstration of vesicle proteins in neuroendocrine tumors are given in Figure 46.

DISCUSSION

Antibodies against SV proteins have proved to be powerful tools for the study of neuroendocrine differentiation in tumor tissue. New proteins, such as SV2, VMAT 1 and 2, and NESP55 have been explored, and many more vesicle proteins are waiting to be studied regarding their expression profiles in tumor tissue (Jakobsen *et al.,* 2001, 2002, 2003). New and more sensitive immunocytochemical detection systems together with better antigen retrieval have also improved diagnosis of neuroendocrine tumors.

Prognosis and Neuroendocrine Differentiation

Identification of the neuroendocrine phenotype carries prognostic implications. For example, well-differentiated neuroendocrine tumors of the GI tract and pancreas have better prognosis than their nonendocrine counterparts, but carcinoids in general have better prognosis than EPT of similar stage (Johanson *et al.,* 1999). Poorly differentiated endocrine carcinomas (PDEC), however, have a very aggressive clinical course (Saclarides *et al.,* 1994). Identification of the neuroendocrine phenotype also carries therapeutic implications. Besides surgical and medical treatment, many neuroendocrine tumors can be treated with radiation therapy, targeted via somatostatin receptors on the cell surface or via intracellular amine transporters (Wängberg *et al.,* 1997).

Importance of the Secretory Granule Proteins and Synaptic Vesicle Proteins in Tumor Biology and Therapy

The protein CgA is of crucial importance for the biogenesis of secretory granules and storage of hormones (Kim *et al.,* 2001). Processing of this granule protein by prohormone convertases results in biologically active peptides. Plasma measurements of CgA in patients with

Table 17. Expression Pattern of Vesicle Proteins in Tumors of the Gastrointestinal Tract

Tumor Type	SV2	Synaptophysin	VMAT1	VMAT2	CgA
NE Tumors					
Gastric endocrine tumors	Yes	Yes	No	Yes	Yes
Ileal endocrine tumors	Yes	Yes	Yes	Yes	Yes
Appendiceal endocrine tumors	Yes	Yes	Yes	No	Yes
Rectal endocrine tumors	Yes	Yes	No	No	Yes
Pancreatic endocrine tumors	Yes	Yes	No	No	Yes
Non-NE Tumors					
Gastric carcinoma	No	No	No	No	No
Colorectal carcinoma	No	No	No	No	No
Pancreatic carcinoma	No	No	No	No	No
GIST	Yes	No	No	No	No

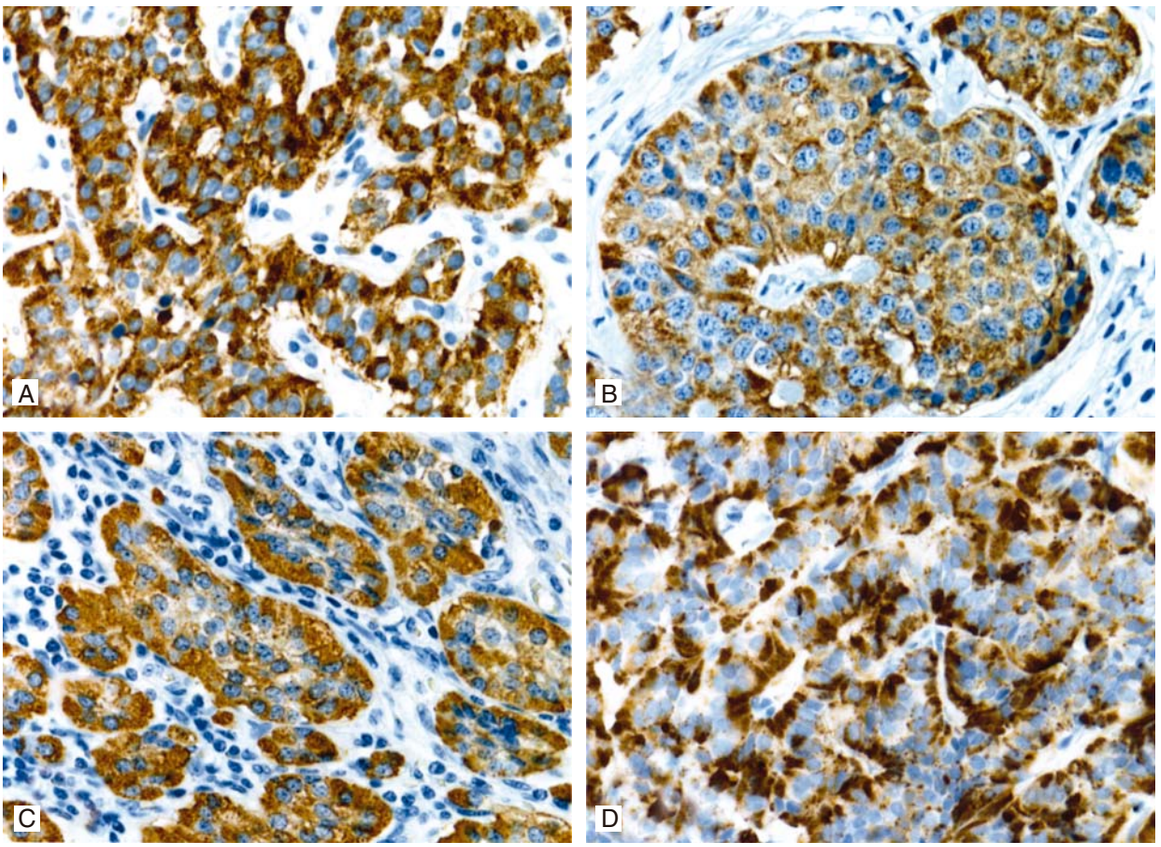

Figure 46. Immunocytochemical demonstration of synaptic vesicle proteins in neuroendocrine tumors of the gastrointestinal tract. **A:** Vesicular monamine transports (VMAT2) expression in a gastric (enterochromaffin-like cell) carcinoid. **B:** VMAT1 expression in an ileal (enterochromaffin cell) carcinoid. **C:** Chromogranin A (CgA) expression in an appendiceal carcinoid. **D:** Synaptic vesicle protein 2 (SV2) expression in a rectal (L cell) carcinoid. EnVision and DAB (diaminobenzidine).

neuroendocrine tumors have proved to be sensitive and specific tumor markers correlated with hormonal activity and tumor burden (Baudin *et al.,* 1998; Hsiao *et al.,* 1990). Well-differentiated tumors with high density of granules have high CgA levels versus tumors with low density of granules (Giovanella *et al.,* 1999). Synaptophysin is widely expressed in neurons and neuroendocrine cells, but its function is still not clearly understood. It may have a function in the biogenesis of synaptic vesicles/SLMV and the recycling of these vesicles (Daly and Ziff, 2002). The biologic function of synaptophysin in neuroendocrine tumors has not been studied, but a similar function as in normal neurons may be assumed. The protein SV2 is also present in SLMV of neurons and neuroendocrine cells and functions as a Ca^{2+} regulator. Together with synaptotagmin, SV2 participates in the control of exocytosis in neurons. The function of SV2 in neuroendocrine tumors has not been studied, but it can be assumed that SV2 has a regulatory role in the secretory processes. If so, it may be a therapeutic target to control hormone secretion and symptoms in patients with metastatic neuroendocrine tumors.

The protein NESP55 was shown to be expressed in certain neuroendocrine tumors of the pancreas and adrenals (Jakobsen *et al.,* 2003). At the present time very little is known about the function of NESP55 in normal tissues. In patients with neuroendocrine tumors, NESP55 might be of value in the follow-up (i.e., monitoring circulating NESP55), which may relate to tumor burden and prognosis.

The proteins VMAT 1 and 2 are differentially expressed in neuroendocrine tumors of the GI tract and pancreas (Jakobsen *et al.,* 2001). The VMAT isoform

expression was clearly related to tumor type and cellular composition. The function of monoamine transporters in neuroendocrine cells is to transport different amines and amine analog from the cytosol into vesicles, where they are kept until an external signal initiates the process of exocytosis. Storage of different amines in vesicles could also be a way of protecting the cell from toxic effects. Studies on the uptake of MIBG (meta-iodobenzylguanidine) in neuroendocrine tumors suggests that VMAT has similar functions in neuroendocrine tumors as in normal neuroendocrine cells (Kölby *et al.,* 2003). The norepinephrine analog MIBG is a substrate for VMAT and can thus be used in its radiolabeled form for scintigraphy and therapy of pheochromocytomas, neuroblastomas, and ileal carcinoids. Radiolabeled MIBG is internalized in secretory granules and vesicles by VMAT, which means that tumor cells can be targeted for radiation therapy. In the future VMAT expression can be an important tool to select candidates for uptake studies prior to radiation therapy with ^{123}I-MIBG for residual tumor disease.

Acknowledgments

This work was supported by the Swedish Cancer Society (3911), the Assar Gabrielsson Foundation, Göteborg Medical Society, the King Gustav the Fifth Jubilee Clinic Cancer Fund, Göteborg, Sahlgrenska University Hospital Research Funds, the Serena Ehrenströms Foundation, and the Camilla Landgren Memorial Fund.

References

Bajjalieh, S.M., Peterson, K., Linial, M., and Scheller, R.H. 1993. Brain contains two forms of synaptic vesicle protein 2. *Proc. Natl. Acad. Sci. USA 90*:1550–2l54.

Battifora, H., and Kopinski, M. 1986. The influence of protease digestion and duration of fixation on the immunostaining of keratins. A comparison of formalin and ethanol fixation. *J. Histochem. Cytochem. 34*:1095–1100.

Baudin, E., Gigliotti, A., Ducreux, M., Ropers, J., Comoy, E., Sabourin, J.C., Bidart, J.M., Cailleux, A.F., Bonacci, R., Ruffie, P., and Schlumberger, M. 1998. Neuron-specific enolase and chromogranin A as markers of neuroendocrine tumours. *Br. J. Cancer 78*:1102–1107.

Bishop, A.E., Polak, J.M., Facer, P., Fern, G.L., Marangos, P.J., and Pearse, A.G. 1982. Neuron specific enolase: a common marker for the endocrine cells and innervation of the gut and pancreas. *Gastroenterology 83*:902–915.

Bobrow, M.N., Harris, T.D., Shaughnessy, K.J., and Litt, G.J. 1989. Catalyzed reporter deposition, a novel method of signal amplification. Application to immunoassays. *J. Immunol. Meth. 125*:279–285.

Boon, M.E., and Kok, L.P. 1994. Microwaves for immunohistochemistry.

Buckley, K., and Kelly, R.B. 1985. Identification of a transmembrane glycoprotein specific for secretory vesicles of neural and endocrine cells. *J. Cell. Biol. 100*:1284–l294.

Calender, A. 1999. New insights in genetics of digestive neuroendocrine tumors. In M. Mignon and J.F. Colmbel (eds.) *Recent Advances in the Pathophysiology and Management of Inflammatory Bowel Diseases and Digestive Endocrine Tumors.* Montrouge, John Libbey, 155–176.

Daly, C., and Ziff, E.B. 2002. Ca2+-dependent formation of a dynamin-synaptophysin complex: potential role in synaptic vesicle endocytosis. *J. Biol. Chem. 277*:9010–90l5.

Eissele, R., Anlauf, M., Schafer, M.K., Eiden, L.E., Arnold, R., and Weihe, E. 1999. Expression of vesicular monoamine transporters in endocrine hyperplasia and endocrine tumors of the oxyntic stomach. *Digestion 60*:428–439.

Elferink, L.A., and Scheller, R.H. 1995. Synaptic vesicle proteins and regulated exocytosis. *Prog. Brain. Res. 105*:79–85.

Erickson, J.D., and Eiden, L.E. 1993. Functional identification and molecular cloning of a human brain vesicle monoamine transporter. *J. Neurochem. 61*:2314–2317.

Erickson, J.D., Schafer, M.K., Bonner, T.I., Eiden, L.E., and Weihe, E. 1996. Distinct pharmacological properties and distribution in neurons and endocrine cells of two isoforms of the human vesicular monoamine transporter. *Proc. Natl. Acad. Sci. USA 93*:166–l71.

Giovanella, L., La Rosa, S., Ceriani, L., Uccella, S., Erba, P., and Garancini, S. 1999. Chromogranin-A as a serum marker for neuroendocrine tumors: comparison with neuron-specific enolase and correlation with immunohistochemical findings. *Int. J. Biol. Markers 14*:160–166.

Grabowski, P., Schonfelder, J., Ahnert-Hilger, G., Foss, H.D., Heine, B., Schindler, I., Stein, H., Berger, G., Zeitz, M., and Scherubl, H. 2002. Expression of neuroendocrine markers: a signature of human undifferentiated carcinoma of the colon and rectum. *Virchows Arch. 441*:256–263.

Graff, L., Castrop, F., Bauer, M., Hofler, H., and Gratzl, M. 2001. Expression of vesicular monoamine transporters, synaptosomal-associated protein 25 and syntaxin 1: a signature of human small cell lung carcinoma. *Cancer Res. 61*:2138–2144.

Gras, C., Herzog, E., Bellenchi, G.C., Bernard, V., Ravassard, P., Pohl, M., Gasnier, B., Giros, B., and El Mestikawy, S. 2002. A third vesicular glutamate transporter expressed by cholinergic and serotoninergic neurons. *J. Neurosci. 22*:5442–545l.

Henry, J.P., Gasnier, B., Desnos, C., Scherman, D., Krejci, E., and Massoulie, J. 1994. The catecholamine transporter of adrenal medulla chromaffin granules. *Ann. N.Y. Acad. Sci. 733*:185–192.

Hoff, A.O., Cote, G.J., and Gagel, R.F. 2000. Multiple endocrine neoplasias. *Annu. Rev. Physiol. 62*:377–411.

Hsiao, R.J., Neumann, H.P., Parmer, R.J., Barbosa, J.A., and O′Connor, D.T. 1990. Chromogranin A in familial pheochromocytoma: diagnostic screening value, prediction of tumor mass, and post-resection kinetics indicating two-compartment distribution. *Am. J. Med. 88*:607–613.

Jakobsen, A.M., Ahlman, H., Kölby, L., Abrahamsson, J., Fischer-Colbrie, R., and Nilsson, O. 2003. NESP55, a novel chromogranin-like peptide, is expressed in endocrine tumours of the pancreas and adrenal medulla but not in ileal carcinoids. *Br. J. Cancer 88*:1746–1754.

Jakobsen, A.M., Ahlman, H., Wängberg, B., Kölby, L., Bengtsson, M., and Nilsson, O. 2002. Expression of synaptic vesicle protein 2 (SV2) in neuroendocrine tumours of the gastrointestinal tract and pancreas. *J. Pathol. 196*:44–50.

Jakobsen, A.M., Andersson, P., Saglik, G., Andersson, E., Kölby, L., Erickson, J.D., Forssell-Aronsson, E., Wangberg, B., Ahlman, H., and Nilsson, O. 2001. Differential expression of vesicular monoamine transporter (VMAT) 1 and 2 in gastrointestinal endocrine tumours. *J. Pathol. 195*:463–472.

Janz, R., Goda, Y., Geppert, M., Missler, M., and Südhof, T.C. 1999. SV2A and SV2B function as redundant Ca2+ regulators in neurotransmitter release. *Neuron 24*:1003–1016.

Janz, R., and Sudhof, T.C. 1999. SV2C is a synaptic vesicle protein with an unusually restricted localization: anatomy of a synaptic vesicle protein family. *Neuroscience 94*:1279–1290.

Johanson, V., Tisell, L.E., Olbe, L., Wangberg, B., Nilsson, O., and Ahlman, H. 1999. Comparison of survival between malignant neuroendocrine tumours of midgut and pancreatic origin. *Br. J. Cancer 80*:1259–1261.

Kao, H.T., Porton, B., Czernik, A.J., Feng, J., Yiu, G., Haring, M., Benfenati, F., and Greengard, P. 1998. A third member of the synapsin gene family. *Proc. Natl. Acad. Sci. USA 95*:4667–4672.

Kim, T., Tao-Cheng, J.H., Eiden, L.E., and Loh, Y.P. 2001. Chromogranin A, an "on/off" switch controlling dense-core secretory granule biogenesis. *Cell 106*:499–509.

Kindblom, L.G., Remotti, H.E., Aldenborg, F., and Meis-Kindblom, J.M. 1998. Gastrointestinal pacemaker cell tumor (GIPACT): gastrointestinal stromal tumors show phenotypic characteristics of the interstitial cells of Cajal. *Am. J. Pathol. 152*:1259–1269.

Kölby, L., Bernhardt, P., Levin-Jakobsen, A.M., Johanson, V., Wängberg, B., Ahlman, H., Forssell-Aronsson, E., and Nilsson, O. 2003. Uptake of meta-iodobenzylguanidine in neuroendocrine tumours is mediated by vesicular monoamine transporters. *Br. J. Cancer 89*:1383–1388.

Kumaki, N., Kajiwara, H., Kameyama, K., DeLellis, R.A., Asa, S.L., Osamura, R.Y., and Takami, H. 2002. Prediction of malignant behavior of pheochromocytomas and paragangliomas using immunohistochemical techniques. *Endocr. Pathol. 13*:149–l56.

Laslop, A., Doblinger, A., and Weiss: U. 2000. Proteolytic processing of chromogranins. *Adv. Exp. Med. Biol. 482*:155–l66.

Lloyd, R.V., and Wilson, B.S. 1983. Specific endocrine tissue marker defined by a monoclonal antibody. *Science 222*:628–630.

Lowe, AW., Madeddu, L., and Kelly, R.B. 1988. Endocrine secretory granules and neuronal synaptic vesicles have three integral membrane proteins in common. *J. Cell. Biol. 106*:51–59.

Pileri, S.A., Roncador, G., Ceccarelli, C., Piccioli, M., Briskomatis, A., Sabattini, E., Ascani, S., Santini, D., Piccaluga, P.P., Leone, 0., Damiani, S., Ercolessi, C., Sandri, F., Pieri, F., Leoncini, L., and Falini, B. 1997. Antigen retrieval techniques in immunohistochemistry: comparison of different methods. *J. Pathol. 183*: 116–123.

Portela-Gomes, G.M., Lukinius, A., and Grimelius, L. 2000. Synaptic vesicle protein 2: a new neuroendocrine cell marker. *Am. J. Pathol. 157*:1299–3309.

Rindi, G., Buffa, R., Sessa, F., Tortora, O., and Solcia, E. 1986. Chromogranin A, B and C immunoreactivities of mammalian endocrine cells. Distribution, distinction from costored hormones/prohormones and relationship with the argyrophil component of secretory granules. *Histochemistry 85*:19–28.

Rindi, G., Capella, C., and Solcia, E. 1999. Pathobiology and classification of gut endocrine tumors. In M. Mignon and J.F. Colombel (eds.) *Recent Advances in the Pathophysiology and Management of Inflammatory Bowel Diseases and Digestive Endocrine Tumors.* Montrouge; John Libbey, 177–191.

Rindi, G., Paolotti, D., Fiocca, R., Wiedenmann, B., Henry, J.P., and Solcia, E. 2000. Vesicular monoamine transporter 2 as a marker of gastric enterochromaffin-like cell tumors. *Virchows Arch. 436*:217–223.

Rode, J., Dhillon, A.P., Doran, J.F., Jackson, P., and Thompson, R.J. 1985. PGP 9.5, a new marker for human neuroendocrine tumours. *Histopathology 9*:147–158.

Sabattini, E., Bisgaard, K., Ascani, S., Poggi, S., Piccioli, M., Ceccarelli, C., Pien, F., Fraternali-Orcioni, G., and Pileri, S.A. 1998. The EnVision++system: a new immunohistochemical method for diagnostics and research. Critical comparison with the APAAP, ChemMate, CSA, LABC, and SABC techniques. *J. Clin. Pathol. 51*:506–511.

Saclarides, T.J., Szeluga, D., and Staren, E.D. 1994. Neuroendocrine cancers of the colon and rectum. Results of a ten-year experience. *Dis. Colon Rectum. 37*:635–642.

Sandor, A., and Modlin, I.M. 1998. A retrospective analysis of 1570 appendiceal carcinoids. *Am. J. Gastroenterol. 93*:422–428.

Shi, S.R., Cote, R.J., Chaiwun, B., Young, L.L., Shi, Y., Hawes, D., Chen, T., and Taylor, C.R. 1998. Standardization of immunohistochemistry based on antigen retrieval technique for routine formalin-fixed tissue sections. *Appl. Immmunohistochem. 6*:89–96.

Shi, S.R., Cote, R.J., and Taylor, C.R. 1997. Antigen retrieval immunohistochemistry: past, present, and future. *J. Histochem. Cytochem. 45*:327–343.

Shi, S.R., Imam, S.A., Young, L., Cote, R.J., and Taylor, C.R. 1995. Antigen retrieval immunohistochemistry under the influence of pH using monoclonal antibodies. *J. Histochem. Cytochem. 43*:193–201.

Solcia, B., Fiocca, R., Rindi, G., Villani, L., Cornaggia, M., and Capella, C. 1993. The pathology of the gastrointestinal endocrine system. *Endocrinol. Metab. Clin. North. Am. 22*:785–821.

Solcia, E., Klöppel, G., and Sobin, L.H. 2000. *Histological Typing of Endocrine Tumours,* New York: Springer-Verlag.

Stefaneanu, L., Sasano, H., and Kovacs, K. (eds.). 2000. *Molecular and Cellular Endocrine Pathology.* London: Arnold.

Takamori, S., Malherbe, P., Broger, C., and Jahn, R. 2002. Molecular cloning and functional characterization of human vesicular glutamate transporter 3. *EMBO Rep. 3*:798–803.

Wängberg, B., Nilsson, O., Johanson, V., Kölby, L., Forssell-Aronsson, E., Andersson, P., Fjälling, M., Tisell, L.E., and Ahlman, H. 1997. Somatostatin receptors in the diagnosis and therapy of neuroendocrine tumors. *Oncologist 2*:50–58.

Wiedenmann, B., Franke, W.W., Kuhn, C., Moll, R., and Gould, V.E. 1986. Synaptophysin: a marker protein for neuroendocrine cells and neoplasms. *Proc. Natl. Acad. Sci. USA 83*:3500–3504.

Wiedenmann, B., and Huttner, W.B. 1989. Synaptophysin and chromogranins/secretogranins—widespread constituents of distinct types of neuroendocrine vesicles and new tools in tumor diagnosis. *Virch. Arch. B. Cell Pathol. Incl. Mol. Pathol. 58*:95–121.

Winkler, H., and Fischer-Colbrie, R. 1992. The chromogranins A and B: the first 25 years and future perspectives. *Neuroscience 49*:397–528.

This Page Intentionally Left Blank

19

Role of Immunohistochemical Expression of Caspase-3 in Gastric Carcinoma

Naoki Isobe and Hisashi Onodera

Introduction

Apoptosis plays a critical role in the development and homeostasis of normal tissues. One object of apoptosis is to remove harmful cells, such as virus-infected and genetically altered cells, from an organism. It is conceivable that cancer cells possess a mechanism to avoid apoptosis and the molecules involved in the cascade influence the activity of the disease.

The study of nematode Caenorhabiditis elegans provided the insight into the molecular control of apoptosis. *Ced-3, Ced-4,* and *Ced-9* were found to be core components required for the control of apoptosis. The *Ced-3* gene encodes a cysteine protease with homology to a family of mammalian proteases termed "caspase." The *Ced-9* gene encodes protein with homology to *Bcl-2,* which is a mitochondrial membrane protein that protects cells from apoptosis. *Ced-4* is homologous to *Apaf-1,* which plays a key role in the activation of caspase-9 (Krajewska *et al.,* 1997a, 1997b).

Apoptosis is known to occur by at least two pathways. One is the pathway activated by the Fas receptor, which alternatively activates caspase-8, and the other is the pathway activated by the release of cytochrome-C from the mitochondria, which activates caspase-9. In either pathway, nonactive procaspase-3 is processed into the activated form by catalytic cleavage. Activated caspase-3 exists as a tetrameric enzyme and is deeply involved in DNA (deoxyribonucleic acid) fragmentation by cleaving the DNA repair enzymes such as poly (ADP-ribose) polymerase (Budihardjo *et al.,* 1999; Nicholson *et al.,* 1995; Shinoura *et al.,* 2000).

Because caspase-3 is the most downstream caspase and is reported to best correlate with apoptosis, there have been many reports describing the relationship between caspase-3 and prognosis. Non–small-cell lung cancer, neuroblastomas, and acute lymphoblastic leukemia had better prognoses when caspase-3 expression was stronger (Estrov *et al.,* 1998; Koomagi and Volm, 2000; Nakagawara *et al.,* 1997; Volm and Koomagi, 2000). However, Jonges *et al*. reported that caspase-3 activity positively correlated with a risk of distant recurrence in colorectal cancer (Jonges *et al.,* 2001). Peiro *et al*. reported that survival was shorter in endometrial carcinoma when tumors showed a high rate of caspase-3, and Estrov *et al*. reported that high levels of both caspase-2 and caspase-3 predicted poor outcomes in acute myelogenous leukemia (Estrov *et al.,* 1998; Peiro *et al.,* 2001).

In this chapter, we will describe how we evaluated the expression level of caspase-3 in gastric cancer using the immunohistochemical method (Isobe *et al.,* 2004).

Handbook of Immunohistochemistry and *in situ* Hybridization of Human Carcinomas, Volume 4: Molecular Genetics, Gastrointestinal Carcinoma, and Ovarian Carcinoma

Immunohistochemistry is one of the most reliable methods to distinguish cancer cells from nonneoplastic cells, but it is difficult to evaluate protein expression quantitatively because the staining intensity differs within slight modifications. To overcome this problem and quantify the caspase-3 expression, we evaluated the intensity by comparing cancer cells with nonneoplastic cells in the same specimen. Germinal center lymphocytes of the lymphoid follicle are known to express a high level of caspase-3 (Krajewska *et al.*, 1997). For the quantification and to assure the result of caspase-3 staining, we used these nonneoplastic cells as an internal positive control.

MATERIALS

1. Formalin-fixed and paraffin-embedded tissue sections with a thickness of 4 μm
2. 70%, 90%, and 100% Ethanol.
3. Xylene.
4. 0.01 M PBS (phosphate buffer saline).
5. 3,3′-diaminobenzidine (DAB).
6. 0.05M Tris HCl (pH 7.2).
7. Mayer's hematoxylin solution.
8. Vectastain ABC (avidin-biotin complex) kit (Vector Laboratories, Burlingame, CA).
9. Target Retrieval Solution (pH 6.0) (Dako, Glostrup, Denmark).
10. Goat polyclonal antibody against human caspase-3 (Santa Cruz Biotechnology, Santa Cruz, CA).
11. Block Ace (Dainihon Seiyaku, Osaka, Japan).

METHODS

1. For deparaffinization, immerse slides in 3 changes of xylene for 5 min each at room temperature.
2. Dyhydrate slides by immersing them successively in Coplin jars containing 100%, 90%, and 70% ethanol at room temperature for 1 min each.
3. Immerse slides in 3 changes of 0.01 M PBS for 5 min each at room temperature.
4. Incubate slides with Target Retrieval Solution (pH 6.0) (Dako) in a 95°C waterbath for 40 min.
5. Block endogenous peroxidase activity by 0.3% H_2O_2 in methanol for 30 min.
6. Place slides in moist chamber and incubate with protein-blocking solution Block Ace (Dainihon Seiyaku) for 30 min at room temperature.
7. Incubate slides at 4°C overnight with antibody against caspase-3 (Santa Cruz Biotechnology, sc-1226) at a dilution of 1:200.
8. Immerse slides in 3 changes of 0.01 M PBS at room temperature for 5 min each.
9. Incubate slides with biotinylated secondary antibodies (Vector Laboratories, Vectastain ABC kit) for 40 min at room temperature.
10. Immerse slides in 3 changes of 0.01 M PBS at room temperature for 5 min each.
11. Incubate slides with avidin-biotin-peroxidase complex (Vector Laboratories) for 50 min at room temperature.
12. Immerse slides in 3 changes of 0.01 M PBS at room temperature for 5 min each.
13. Immerse slides in 0.03% 3,3′-DAB tetrahydrochloride (Wako, Osaka, Japan) in 0.05 M Tris HCl (pH 7.2) for 15 min.
14. For color-reaction development, immerse slides in 0.03% DAB in 0.05 M Tris HCl (pH 7.2) with 0.1% H_2O_2 for 2 min.
15. Immerse slides in water for at least 15 min.
16. Counterstain slides with Mayer's hematoxylin solution.

The caspase-3 staining intensity of the cancer cells compared with that of the germinal center was graded as follows: 0 points for nonstaining, 1 point for lower staining, 2 points for even staining, and 3 points for stronger staining. The total addition of each score multiplied by the occupational percentage of each group represented the caspase-3 expression index (C3EI), resulting in scores ranging from 0 to 300 (Figure 47).

RESULT AND DISCUSSION

Germinal center lymphocytes of the lymphoid follicle in the gastric wall and plasma cells showed intense caspase-3 immunostaining, and mantle zone lymphocytes exhibited little or no staining. Caspase-3 expression was located in the cytoplasm, and no nuclear staining was seen. These findings were universally recognized and served as a good internal control. Cancer cells also exhibited immunoreactivity in the cytoplasm, but the intensity in each cell varied and showed a heterogeneous pattern. C3EI was determined by comparing the germinal center intensities in each specimen as described. The study population we evaluated includes 109 males and 42 females, with ages ranging from 34 to 84 years (mean 62.8).

The C3EI was 125.4 ± 77.4 in the mean ± SD (standard deviation) with a median of 130. A comparison of the clinicopathologic features with the C3EI was performed, and significance was seen in lymph-node metastasis (negative 105.5 ± 78.7, positive 153.8 ± 66.1 $P = 0.001$) examined by the Mann-Whitney U test. Variables such as gender, age, stage, histologic type of gastric carcinoma, invasion depth, and operation curability were not significant. When the patient was classified

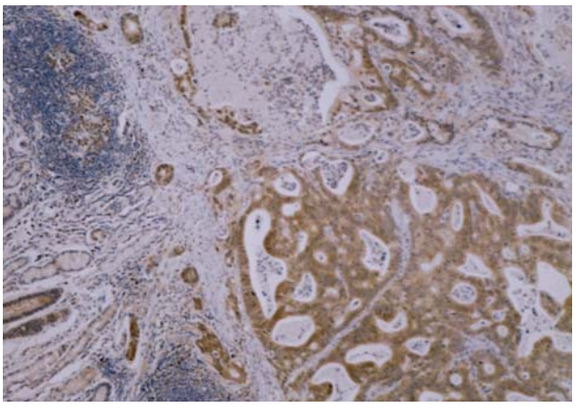

Figure 47. Representative example of caspase-3 immunohistochemical staining. In this case caspase-3 expression index is calculated as $0 \times 0 + 1 \times 10 + 2 \times 10 + 3 \times 80 = 270$.

into two groups by the median value of C3EI (higher group >130, lower group <129), the number of patients belonging to the stages in two groups showed no difference (χ^2 P = 0.215). Postoperative intravenous chemotherapy was administered to 12 cases of the C3EI lower group and 11 cases of the C3EI higher group. The statistical differences between the stage and the number of patients who received the chemotherapy were not seen (chi-square test $P = 0.157$). However, the lower C3EI group had significantly better prognosis than the higher group (log-rank test P = 0.0001). To determine the independent prognostic value in overall survival, C3EI was included in the Cox proportional hazards model, together with age, gender, liver metastasis, lymph-node metastasis, histologic type, and tumor invasion. Multivariate analysis showed that age (P = 0.0021), liver metastasis (P = 0.0008), tumor invasion depth (P = 0.0001), and caspase-3 expression (P = 0.0478) were significant determinants in overall survival.

There may be several reasons for the C3EI showing as a negative prognostic factor. According to the manufacturer's information, the caspase-3 antibody we used for evaluating the C3EI detects both active and procaspase-3.

We performed the immunohistochemistry of activated caspase-3 using monoclonal antibody (BD Bioscience, San Jose, CA) and found that most caspase-3 in the cancer cells was not activated, indicating the accumulation of procaspase-3 in cancer cells.

It is conceivable that those tumors having the ability to escape apoptosis by inactivating caspase-3 are able to metastasize with more ease and have worse prognosis. These results are consistent with those reported by Estrov *et al.* They reported that a high level of uncleaved caspase-3 was associated with a lower survival rate in acute myelogenous leukemia, but a high level of cleaved caspase-3 indicated a higher survival rate (Estrov *et al.,* 1998). To identify the molecule actually regulating the caspase-3 activation, we examined the expression of *Bcl-2,* which is a crucial participant in the prevention of the apoptosis cascade (Chao and Korsmeyer, 1998). Our results showing a *Bcl-2*-positive rate (13.7% n = 11/80) was in line with other reports on gastric cancer (11.4%, Muller *et al.,* 1998; 14%, Saegusa *et al.,* 1996). However, we could not find any correlation between *Bcl-2* and the C3EI. These results are in accord with those of Muller *et al.,* who reported that the survival of gastric cancer patients showed no significant correlation with *Bcl-2* expression. In gastric cancer, other caspase-3 regulating factors such as inhibitor of apoptosis family protein may predominantly participate in the behavior determination (Deveraux and Reed, 1999). Other molecules such as vascular endothelial growth factor, COX2, and transforming growth factor-β1 are also reported to inhibit caspase-3 activation and, interestingly, they are also reported to correlate with lymph-node metastasis and worsen the prognosis (Dempke *et al.,* 2001; Jin *et al.,* 2001; Zhu *et al.,* 2001).

Considering that various molecules are involved in caspase-3 regulation and the existence of other possibilities, the C3EI serves as a useful indicator of the degree of caspase-3 inhibition.

Further investigation on the inhibition mechanism of caspase-3 would provide an efficient approach to developing new therapeutic strategies for human gastric cancer.

References

Budihardjo, I., Oliver, H., Lutter, M., Luo, X., and Wang, X. 1999. Biochemical pathways of caspase activation during apoptosis. *Annu. Rev. Cell Dev. Biol. 75*:269–290.

Chao, D.T., and Korsmeyer, S.J. 1998. BCL-2 family: regulators of cell death. *Annu. Rev. Immunol. 16*:395–419.

Dempke, W., Rie, C., Grothey, A., and Schmoll, H.J. 2001. Cyclooxygenase-2: a novel target for cancer chemotherapy? *J. Cancer Res. Clin. Oncol. 127*:411–417.

Deveraux, Q.L., and Reed, J.C. 1999. IAP family proteins—suppressors of apoptosis. *Genes Dev. 73*:239–252.

Estrov, Z., Thall, P.F., Talpaz, M., Estey, E.H., Kantarjian, H.M., Andreeff, M., Harris, D., Van, Q., Walterscheid, M., and Kornblau, S.M. 1998. Caspase 2 and caspase 3 protein levels as predictors of survival in acute myelogenous leukemia. *Blood 92*:3090–3097.

Isobe, N., Onodera, H., Mori, A., Shimada, Y., Yang, W., Yasuda, S., Fujimoto, A., Ooe, H., Arii, S., Kitaichi, M., and Imamura, M. 2004. Caspase-3 expression in human gastric carcinoma and its clinical significance. *Oncology 66*:201–209.

Jin, K., Mao, X.O., Batteur, S.P., McEachron, E., Leahy, A., and Greenberg, D.A. 2001. Caspase-3 and the regulation of hypoxic neuronal death by vascular endothelial growth factor. *Neuroscience 108*:351–358.

Jonges, L.E., Nagelkerke, J.F., Ensink, N.G., van der Velde, E.A., Tollenaar, R.A., Fleuren, G.J., van de Velde, C.J., Morreau, H., and Kuppen, P.J. 2001. Caspase-3 activity as a prognostic factor in colorectal carcinoma. *Lab. Invest. 81*:681–688.

Koomagi, R., and Volm, M. 2000. Relationship between the expression of caspase-3 and the clinical outcome of patients with non-small cell lung cancer. *Anticancer Res. 20*:493–496.

Krajewska, M., Wang, H.G., Krajewski, S., Zapata, J.M., Shabaik, A., and Gascoyne, R.D., and Reed, J.C. 1997a. Immunohistochemical analysis of *in vivo* patterns of expression of CPP32 (Caspase-3), a cell death protease. *Cancer Res. 57*:1605–1613.

Krajewski, S., Gascoyne, R.D., Zapata, J.M., Krajewska, M., Kitada, S., Chhanabhai, M., Horsman, D., Berean, K., Piro, L.D., Fugier-Vivier, I., Liu, Y.J., Wang, H.G., and Reed, J.C. 1997b. Immunolocalization of the ICE/Ced-3-family protease, CPP32 (Caspase-3), in non-Hodgkin's lymphomas, chronic lymphocytic leukemias, and reactive lymph nodes. *Blood 15*:3817–3825.

Muller, W., Schneiders, A., Hommel, G., and Gabbert, H.E. 1998. Prognostic value of bcl-2 expression in gastric cancer. *Anticancer Res. 18*:4699–4704.

Nakagawara, A., Nakamura, Y., Ikeda, H., Hiwasa, T., Kuida, K., Su, M.S., Zhao, H., Cnaan, A., and Sakiyama, S. 1997. High levels of expression and nuclear localization of interleukin-1 beta converting enzyme (ICE) and CPP32 in favorable human neuroblastomas. *Cancer Res. 15*:4578–4584.

Nicholson, D.W., Ali, A., Thornberry, N.A., Vaillancourt, J.P., Ding, C.K., Gallant, M., Gareau, Y., Griffin, P.R., Labelle, M., Lazebnik, Y.A., Munday, N.A., Raju, S.M., Smuison, M.E., Yamin, T., Yu, V.L., and Miller, D.K. 1995. Identification and inhibition of the ICE/CED-3 protease necessary for mammalian apoptosis. *Nature 376*:37–43.

Peiro, G., Diebold, J., Baretton, G.B., Kimmig, R., and Lohrs, U. 2001. Cellular apoptosis susceptibility gene expression in endometrial carcinoma: correlation with Bcl-2, Bax, and caspase-3 expression and outcome. *Int. J. Gynecol. Pathol. 20*:359–367.

Saegusa, M., Takano, Y., Kamata, Y., and Okayasu, J. 1996. Bcl-2 expression and allelic loss of the p53 gene in gastric carcinomas. *J. Cancer Res. Clin. Oncol. 122*:427–432.

Shinoura, N., Yamamoto, N., Asai, A., Kirino, T., and Hamada, H. 2000. Adenovirus-mediated transfer of Fas ligand gene augments radiation-induced apoptosis in U-373MG glioma cells. *Jpn. J. Cancer Res. 91*:1044–1050.

Volm, M., and Koomagi, R. 2000. Prognostic relevance of c-Myc and caspase-3 for patients with non-small cell lung cancer. *Oncol. Rep. 7*:95–98.

Zhu, Y., Ahlemeyer, B., Bauerbach, E., and Krieglstein, J. 2001. TGF-beta1 inhibits caspase-3 activation and neuronal apoptosis in rat hippocampal cultures. *Neurochem. Int. 38*:227–235.

20

Role of Immunohistochemical Expression of PRL-3 Phosphatase in Gastric Carcinoma

Hiroshi Yokozaki, Upik Anderiani Miskad, Yasuko Matsukawa, Hirotaka Kato, and Shuho Semba

Introduction

The incidence and mortality of stomach cancer have fallen dramatically over the last 50 years. However, it still remains one of the most common malignancies worldwide (Alberts *et al.,* 2003; Roder, 2002). Moreover, mortality from gastric cancer is second only to lung cancer. Metastasis of gastric cancer to the lymph nodes, peritoneum, or other organs is often responsible for the high mortality rate; even the primary tumors can usually be surgically removed (Buchholtz *et al.,* 1978; Hawley *et al.,* 1970). Regional lymph-node involvement is an important prognostic factor for this malignancy. When lymph nodes are found to be negative, more than 50% of patients may be expected to survive for 5 years. However, the survival rate drops to less than 10% with nodal involvement. The mechanisms for stomach cancer metastasis are not fully clarified because it involves multiple pathobiologic steps and requires the accumulation of many genetic and epigenetic alterations (Hippo *et al.,* 2001).

Protein tyrosine phosphatases play a fundamental role in regulating diverse proteins that essentially participate in every aspect of cellular physiologic and pathogenic processes (Zhang *et al.,* 2002). The proteins PRL-1, -2, and -3 represent a novel class of protein tyrosine phosphatase superfamily members in that they possess a unique COOH-terminal prenylation motif with a protein tyrosine phosphatase–active site signature sequence CX5R (Cates *et al.,* 1996; Zeng *et al.,* 1998). The PRLs were found to be associated with the early endosome and plasma membrane in their prenylated state, whereas nuclear localization of these phosphatases may occur in the absence of prenylation (Zeng *et al.,* 2000). Although the PRLs share 75% amino-acid sequence similarity, the ScanProsite analysis revealed that the potential sites of phosphorylation by several kinases are quite different (Diamond *et al.,* 1994; Zeng *et al.,* 1998). Moreover, Northern blot analysis has demonstrated that the preferential messenger ribonucleic acid (mRNA) expression pattern of these PRLs also differed among organs, indicating that PRLs are quite divergent in their functions (Matter *et al.,* 2001; Zeng *et al.,* 1998).

The founding member of PRL phosphatases, PRL-1, was originally identified as an immediate early gene, the expression of which was induced in mitogen-stimulated cells and in the regenerating liver (Mohn *et al.,* 1991; Montagna *et al.,* 1995). Overexpression of PRL-1 and PRL-2 has been found to transform mouse fibroblasts and hamster pancreatic epithelial cells in culture and

Handbook of Immunohistochemistry and *in situ* Hybridization of Human Carcinomas, Volume 4: Molecular Genetics, Gastrointestinal Carcinoma, and Ovarian Carcinoma

to promote tumor growth in nude mice, suggesting that both of these PRLs may participate in tumorigenesis (Cates *et al.,* 1996; Diamond *et al.,* 1994).

One of the PRL family tyrosine phosphatases, PRL-3 (also known as PTP4A3), has been found to enhance growth of human embryonic kidney fibroblasts (Matter *et al.,* 2001). Among normal human adult tissues, it is expressed predominantly in the heart and striated and smooth-muscle cells, with lower expression in the pancreas, and this expression pattern is distinct from the wider expression of PRL-1 and PRL-2 (Matter *et al.,* 2001). Gene expression profiling using serial analysis of gene expression revealed that among 144 up-regulated genes detected in metastatic colorectal liver samples, *PRL-3* is the only gene consistently overexpressed in all 18 of the cancer metastases examined, with lower levels in nonmetastatic tumors and normal colorectal epithelium (Saha *et al.,* 2001). In addition, overexpression of PRL-3 in nonmetastatic CHO cells enhanced the motility and invasive ability of the cells (Zeng *et al.,* 2003). These results suggest that high expression of PRL-3 phosphatase is a key alteration contributing to the metastasis of tumor cells. In this chapter, we introduce our results on the role of immunohistochemical detection of PRL-3 in human gastric carcinomas (Miskad *et al.,* 2004).

MATERIALS

1. Rabbit polyclonal antibody to human PRL-3 (Cat. No. 18-2324, Zymed Laboratories Inc., San Francisco, CA).
2. Biotinylated goat anti-rabbit immunoglobulin (Ig) G (DakoCytomation).
3. Streptavidin conjugated to horseradish peroxidase (DakoCytomation).
4. Avidin-biotin blocking solution (DakoCytomation).
5. Chromogen fixation substrate, such as diaminobenzidine (DAB) Tablet or DAB Liquid System (DakoCytomation).
6. 0.03% H_2O_2 in methanol.
7. 0.01 M citrate buffer, pH 6.0.
8. PBS, pH 7.2.
9. Mayer's hematoxylin solution.
10. Formalin-fixed and paraffin-embedded tissue of surgically removed human stomach cancer sectioned into 4 μm in thickness, mounted on silane-coated slide glass.
11. Xylene.
12. Ethanol (99%, 90%, 80%, 70%).
13. Mounting medium, such as Eukitt (O. Kindler, Freiburg, Germany) or Entellan New (Merck, Darmstadt, Germany).
14. Coverglass.

METHODS

Dewaxing and Dehydration of Sections

1. Dewax sections with fresh xylene.
2. Rehydrate sections with graded ethanol.
3. Wash sections with deionized water.

Heat-Induced Epitope Retrieval

4. Place the sections in a glass box filled with 0.01 M citrate buffer (pH 6.0).
5. Autoclave the sections in citrate buffer for 15 min at 125°C.
6. Allow the sections to cool in the box at room temperature for 60 min.

Blocking the Endogenous Peroxidase Activity and Avidin

7. Immerse the sections in methanol containing 0.03% H_2O_2 for 15 min to block endogenous peroxidase activity.
8. Wash the sections with deionized water.
9. Wash the sections with phosphate buffer saline (PBS).
10. Incubate the sections in avidin-biotin blocking solution to block avidin in the tissue.
11. Wash the sections 3× with PBS.

Primary Antibody Reaction

12. Apply primary polyclonal rabbit anti-human PRL-3 antibody (1:100 dilution) to the sections and incubate overnight at 4°C in a moist chamber.
13. Wash the sections 3× with PBS.

Secondary Antibody Reaction and Fixation of Horseradish Peroxidase with Avidin-Biotin Reaction

14. Apply biotinylated goat anti-rabbit IgG to the sections and incubate at room temperature for 30 min.
15. Wash the sections 3× with PBS.
16. Apply streptavidin conjugated horseradish peroxidase to the sections and incubate at room temperature for 30 min.
17. Wash the sections 3× with PBS.

Chromogen Fixation

18. Immerse the sections in 3,3′-DAB tetrahydrochloride solution prepared using DAB Tablet or

DAB Liquid System (DakoCytomation, Glostrup, Denmark) at room temperature for 10 min until a distinct reaction product is evident microscopically.

19. Wash the sections 3× with PBS.

Counterstaining and Posttreatment of the Sections

20. Counterstain the sections with Mayer's hematoxylin solution for 5 sec.
21. Wash the sections in running water.
22. Dehydrate the sections with graded ethanol.
23. Immerse the sections in xylene.
24. Apply mounting medium on each section and mount a coverglass.

Grading of PRL-3 Immunoreactivity in Human Gastric Carcinomas

25. Immunoreactivity of anti-PRL-3 antibody is graded according to the number of stained cells and the staining intensity in individual cells as follows: negative, almost no positive cells; low, 5 to 50% of tumor cells show weak to moderate immunoreactivity; high, more than 50% of tumor cells show strong immunoreactivity (Figure 48). Smooth-muscle cells of muscular layer or

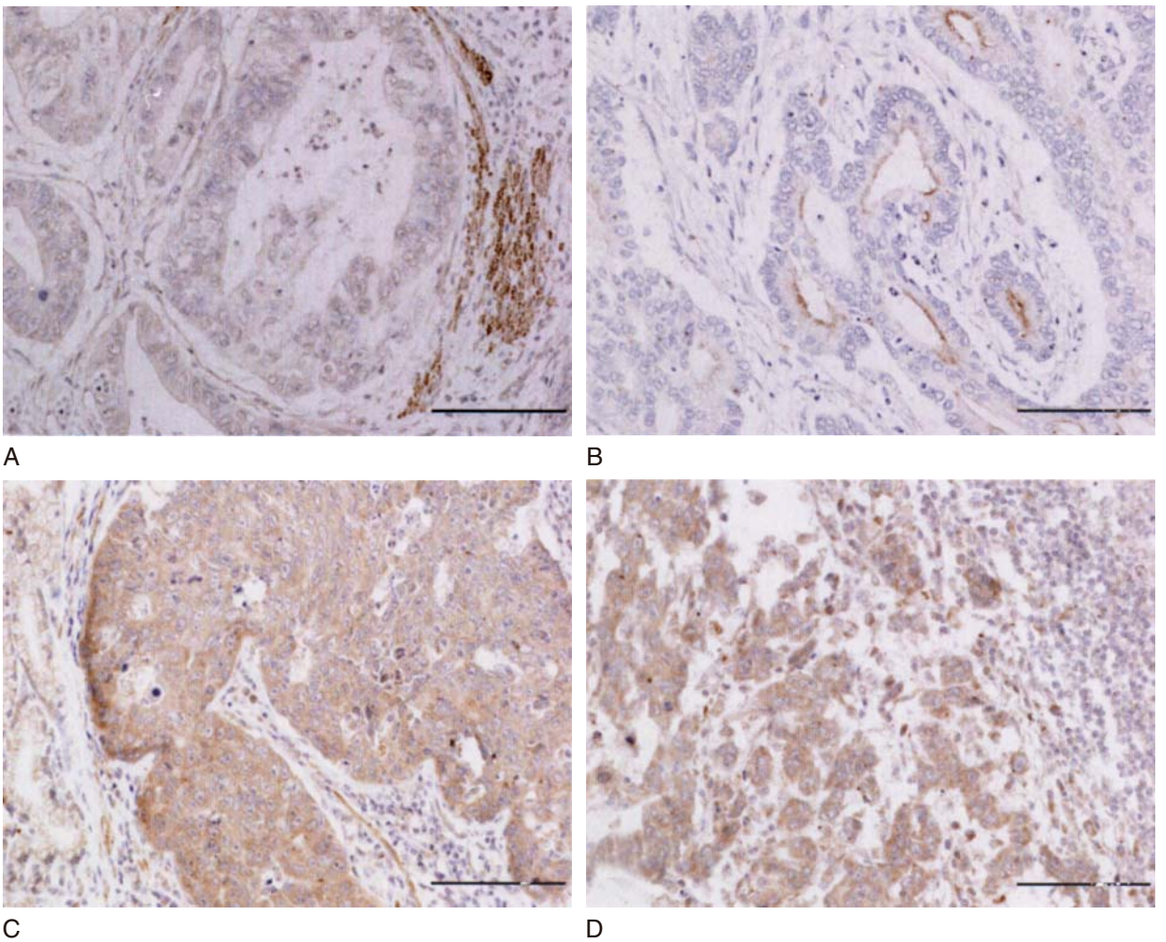

Figure 48. Grading of PRL-3 immunoreactivities in human gastric carcinomas. **A:** Negative. PRL-3 immunoreactivity is not detected in cancer cells. Smooth-muscle cells, showing strong staining, can be used for positive internal control of the reaction. **B:** Low level of PRL-3 expression. Immunoreactivity is observed at cell membrane of some cancer cells. **C:** High level of PRL-3 expression. Cancer cells reveal strong immunoreaction in the cytoplasm. **D:** High level of PRL-3 expression is observed in lymph-node metastasis of the case shown in **C**. Bars: 100 µm.

vascular wall, which show strong immunoreactivity, are used for positive internal control.

RESULTS AND DISCUSSION

The expression and localization of immunoreactive PRL-3 in 148 cases of gastric carcinomas and metastatic tumor in the lymph nodes were examined. In nonneoplastic gastric mucosa, foveolar epithelia as well as fundic and pyloric gland cells demonstrated weak to negative PRL-3 immunoreactivity. Fibroblasts, endothelial cells, and some inflammatory cells showed weak to moderate PRL-3 expression.

In gastric cancer cells, PRL-3 immunoreactivity was mainly located in the cytoplasm that was intense at the cell membrane. Sixty-four (68.1%) of 94 cases of gastric carcinomas revealed positive immunoreactivity to PRL-3. Among them, 37 (39.4%) and 27 (28.7%) showed low and high expression, respectively. The expression of PRL-3 was significantly associated with the tumor stage ($p = 0.045$), lymphatic vessel invasion ($p = 0.002$), and extent of lymph-node metastasis ($p = 0.002$). In contrast, no significant correlation was observed between PRL-3 expression and histologic type, tumor size, venous invasion, or depth of tumor invasion.

Expression of PRL-3 was observed in 44 (81.5%) primary tumors of 54 gastric carcinomas with lymph-node metastasis; the incidence was 50% (20/40) in those without nodal metastasis ($p = 0.004$). Finally, we investigated the expression of PRL-3 in regional lymph-node metastases. It is interesting that, out of 54 cases with lymph-node metastases, PRL-3 immunoreactivity was detected in 50 cases (92.6%), of which 7 (12.9%) and 43 (79.6%) showed low and high expression, respectively. PRL-3 expression was detected more frequently in matched lymph-node metastases than primary gastric carcinomas ($p < 0.001$). High PRL-3 expression was also detected in other metastatic sites, such as the liver and peritoneum.

Results of histochemical detection of PRL-3 in human cancer tissues have been reported mainly on colorectal carcinomas. Bardelli *et al*. (2003) developed *in situ* hybridization methods for the study of paraffin-embedded colorectal cancer sections and reported that *PRL-3* expression was elevated in nearly all metastatic lesions derived from colorectal cancers, regardless of the site of metastasis. In contrast, they observed little or no *PRL-3* expression in normal colon, nonmetastatic primary cancers or metastatic lesions derived from cancers of pancreas, stomach, or esophagus. However, Kato *et al*. (2004), also using *in situ* hybridization methods on paraffin-embedded specimens, detected *PRL-3* mRNA expression in primary colorectal cancers of which the frequency of up-regulated *PRL-3* expressions in cases with liver or lung metastasis was statistically higher than that in cases without either type of metastasis. Peng *et al*. (2004) prepared a specific monoclonal antibody against PRL-3 and detected PRL-3 immunoreactivity in 7% of normal colorectal epithelia, 23.9% of primary colorectal cancers, 53.7% of metastatic lymph nodes, and 66.7% of liver metastases. The present immunohistochemical examination on human gastric carcinomas revealed that expression of PRL-3 was closely associated with the stage of tumor and carcinoma progression, such as invasion of lymphatic vessels and extent of lymph-node metastasis. Furthermore, expression of PRL-3 was significantly more frequent in primary gastric carcinoma with nodal metastasis than in those without nodal metastasis. Consistent with the elevated expression of PRL-3 in colorectal cancer metastasis, increased expression of PRL-3 was significantly more frequently detected in regional lymph-node metastasis than in primary gastric carcinoma. Our findings suggest that PRL-3 has an important role in invasion and metastasis of gastric carcinomas.

Stable transfection of *PRL-3* in nonmetastatic CHO cells has been reported to induce the acquisition of metastasis-associated properties, such as enhanced invasiveness and motility, and to confer metastatic ability (Zeng *et al.,* 2003). Moreover, nude mice injected with *PRL-3*–expressing cells exhibited tumor formation with metastasis (Pathak *et al.,* 2002; Zeng *et al.,* 2003), and the growth of the tumors was markedly inhibited by pentamidine at tolerable dose (Pathak *et al.,* 2002). Like other phosphatases, PRL-3 has a catalytic active signature motif (C104S) (Matter *et al.,* 2001; Zhao *et al.,* 1996). It has been shown that stable expression of wild-type active PRL-3 dramatically enhanced cell migration, whereas a catalytically inactive PRL-3 (C104S) mutant greatly reduced the effect on promoting cell migration (Zeng *et al.,* 2003). These results indicate that phosphatase activity is required for optimization of PRL-3 to promote cell migration. Wu *et al*. (2004) reported that *PRL-3* was also highly expressed in metastatic melanoma B16-BL6 cells but not in its lowly metastatic parental cell line, B16 cells. B16 cells transfected with *PRL-3* complementary deoxyribonucleic acid (cDNA) displayed morphologic transformation from epithelial-like shape to fibroblast-like shape. *PRL-3*–overexpressed cells showed much higher migratory ability, which could be reversed by specific antisense oligodeoxynucleotide and the phosphatase inhibitors sodium orthovanadate or potassium bisperoxo oxovanadate V. Meanwhile, the expression of the catalytically inactive PRL-3 mutations (D72A or C104S) significantly reduced the cell migratory capability.

In addition, *PRL-3* transfectants demonstrated altered extracellular matrix adhesive property and up-regulated integrin-mediated cell-spreading efficiency. Furthermore, they confirmed that PRL-3 could facilitate lung and liver metastasis of B16 cells in an experimental metastasis model in mice, consistent with accelerated proliferation and growth rate both *in vitro* and *in vivo.* Kato *et al*. (2004) reported that transfection of *PRL-3*–specific small interfering RNA (siRNA) into DLD-1 human colon cancer cells abrogated *in vitro* motility without affecting the proliferation of these cells. Moreover, when *PRL-3*–specific siRNA transfected DLD-1 cells were injected into the spleen of nude mice, *in vivo* hepatic colonization was markedly suppressed in comparison with nontreated controls. This phenomenon suggests that PRL-3 may contribute to the establishment of liver metastasis, especially at the step in which cancer cells leave the circulation to extravasate into the liver tissue.

Protein prenylation is important in targeting proteins to intracellular membranes and in protein–protein interactions (Seabra, 1998; Si *et al.,* 2001). PRL-3 has been reported to be a member of the prenylated protein phosphatases, and the metastatic properties of PRL-3 are dependent on prenylation activity (Zeng *et al.,* 2000, 2003). PRL-3 phosphatase is located at the cytoplasmic membrane and the early endosome when prenylated, and it is shifted into the nucleus when unprenylated or lacking the C-terminal prenylation signal (Zeng *et al.,* 2000). A previous study has shown that cells expressing PRL-3 were enriched in several membrane processes including protrusions, ruffles, and some vacuolar-like membrane extensions, which have been reported to play a role in invasion and cell movement (Zeng *et al.,* 2003). In this study, although PRL-3 protein was detected diffusely in the cytoplasm of the tumor cells, some tumors with high expression of PRL-3 and nodal metastases exhibited more intense PRL-3 protein expression in the cytoplasmic membranes. The distribution pattern of PRL-3 in the cell membranes may correlate with the metastatic ability of the tumor cells. This finding supports the previous report that localization of PRL-3 in the cytoplasmic membrane enhanced the migration and invasion properties of cells.

High expression of PRL-3 in lymph-node metastasis and advanced gastric cancer with nodal metastasis provides further evidence for the role of this gene in metastasis. Up-regulated PRL-3 in cancer provides an excellent target for developing novel therapeutics, especially for tumors that are intractable as a result of cancer metastasis. Although the specific protein substrate for PRL-3 has not been identified yet, blocking or reducing the functions of PRL-3 in metastasis could be achieved by inhibition of prenylation or inactivating the catalytic function of the PRL-3 phosphatase active site (Zeng *et al.,* 2003). Actually, pentamidine has been reported to be an inhibitor of PRL phosphatases with anti-cancer activity (Pathak *et al.,* 2002). However, further experiments are still required to determine monospecific inhibitors of PRL-3 and to elucidate the biochemical mechanisms through which PRL-3 influences neoplastic growth and metastasis.

References

Alberts, S.R., Cervantes, A., and van de Velde, C.J. 2003. Gastric cancer: epidemiology, pathology and treatment. *Ann. Oncol. 14* Suppl *2*:ii31–36.

Bardelli, A., Saha, S., Sager, J.A., Romans, K.E., Xin, B., Markowitz, S.D., Lengauer, C., Velculescu, V.E., Kinzler, K.W., and Vogelstein, B. 2003. PRL-3 expression in metastatic cancers. *Clin. Cancer Res. 9*:5607–5615.

Buchholtz, T.W., Welch, C.E., and Malt, R.A. 1978. Clinical correlates of resectability and survival in gastric carcinoma. *Ann. Surg. 188*:711–715.

Cates, C.A., Michael, R.L., Stayrook, K.R., Harvey, K.A., Burke, Y.D., Randall, S.K., Crowell, P.L., and Crowell, D.N. 1996. Prenylation of oncogenic human PTP (CAAX) protein tyrosine phosphatases. *Cancer Lett. 110*:49–55.

Diamond, R.H., Cressman, D.E., Laz, T.M., Abrams, C.S., and Taub, R. 1994. PRL-1, a unique nuclear protein tyrosine phosphatase, affects cell growth. *Mol. Cell. Biol. 14*:3751–3762.

Hawley, P.R., Westerholm, P., and Morson, B.C. 1970. Pathology and prognosis of carcinoma of the stomach. *Br. J. Surg. 57*:877–883.

Hippo, Y., Yashiro, M., Ishii, M., Taniguchi, H., Tsutsumi, S., Hirakawa, K., Kodama, T., and Aburatani, H. 2001. Differential gene expression profiles of scirrhous gastric cancer cells with high metastatic potential to peritoneum or lymph nodes. *Cancer Res. 61*:889–895.

Kato, H., Semba, S., Miskad, U.A., Seo, Y., Kasuga, M., and Yokozaki, H. 2004. High expression of *PRL-3* promotes cancer cell motility and liver metastasis in human colorectal cancer: a predictive molecular marker of metachronous liver and lung metastases. *Clin. Cancer Res. 10*:7318–7328.

Matter, W.F., Estridge, T., Zhang, C., Belagaje, R., Stancato, L., Dixon, J., Johnson, B., Bloem, L., Pickard, T., Donaghue, M., Acton, S., Jeyaseelan, R., Kadambi, V., and Vlahos, C.J. 2001. Role of PRL-3, a human muscle-specific tyrosine phosphatase, in angiotensin-II signaling. *Biochem. Biophys. Res. Commun. 283*:1061–1068.

Miskad, U.A., Semba, S., Kato, H., and Yokozaki, H. 2004. Expression of PRL-3 phosphatase in human gastric carcinomas: close correlation with invasion and metastasis. *Pathobiology 71*:176–184.

Mohn, K.L., Laz, T.M., Hsu, J.C., Melby, A.E., Bravo, R., and Taub, R. 1991. The immediate-early growth response in regenerating liver and insulin-stimulated H-35 cells: comparison with serum-stimulated 3T3 cells and identification of 41 novel immediate-early genes. *Mol. Cell. Biol. 11*:381–390.

Montagna, M., Serova, O., Sylla, B.S., Feunteun, J., and Lenoir, G.M. 1995. A 100-kb physical and transcriptional map around the EDH17B2 gene: identification of three novel genes and a pseudogene of a human homologue of the rat PRL-1 tyrosine phosphatase. *Hum. Genet. 96*:532–538.

Pathak, M.K., Dhawan, D., Lindner, D.J., Borden, E.C., Farver, C., and Yi, T. 2002. Pentamidine is an inhibitor of PRL

phosphatases with anticancer activity. *Mol. Cancer Ther. 1*:1255–1264.

Peng, L., Li, Y., Meng, L., and Shou, C. 2004. Preparation and characterization of monoclonal antibody against protein tyrosine phosphatase PRL-3. *Hybrid. Hybridomics 23*:23–27.

Roder, D.M. 2002. The epidemiology of gastric cancer. *Gastric Cancer* 5 Suppl *1*:5–11.

Saha, S., Bardelli, A., Buckhaults, P., Velculescu, V.E., Rago, C., St. Croix, B., Romans, K.E., Choti, M.A., Lengauer, C., Kinzler, K.W., and Vogelstein, B. 2001. A phosphatase associated with metastasis of colorectal cancer. *Science 294*:1343–1346.

Seabra, M.C. 1998. Membrane association and targeting of prenylated Ras-like GTPases. *Cell Signal. 10*:167–172.

Si, X., Zeng, Q., Ng, C.H., Hong, W., and Pallen, C.J. 2001. Interaction of farnesylated PRL-2, a protein-tyrosine phosphatase, with the beta-subunit of geranylgeranyltransferase II. *J. Biol. Chem. 276*:32875–32882.

Wu, X., Zeng, H., Zhang, X., Zhao, Y., Sha, H., Ge, X., Zhang, M., Gao, X., and Xu, Q. 2004. Phosphatase of regenerating liver-3 promotes motility and metastasis of mouse melanoma cells. *Am. J. Pathol. 164*:2039–2054.

Zeng, Q., Dong, J.M., Guo, K., Li, J., Tan, H.X., Koh, V., Pallen, C.J., Manser, E., and Hong, W. 2003. PRL-3 and PRL-1 promote cell migration, invasion, and metastasis. *Cancer Res. 63*: 2716–2722.

Zeng, Q., Hong, W., and Tan, Y.H. 1998. Mouse PRL-2 and PRL-3, two potentially prenylated protein tyrosine phosphatases homologous to PRL-1. *Biochem. Biophys. Res. Commun. 244*: 421–427.

Zeng, Q., Si, X., Horstmann, H., Xu, Y., Hong, W., and Pallen, C.J. 2000. Prenylation-dependent association of protein-tyrosine phosphatases PRL-1, -2, and -3 with the plasma membrane and the early endosome. *J. Biol. Chem. 275*: 21444–21452.

Zhang, Z.Y., Zhou, B., and Xie, L. 2002. Modulation of protein kinase signaling by protein phosphatases and inhibitors. *Pharmacol. Ther. 93*:307–317.

Zhao, Z., Lee, C.C., Monckton, D.G., Yazdani, A., Coolbaugh, M.I., Li, X., Bailey, J., Shen, Y., and Caskey, C.T. 1996. Characterization and genomic mapping of genes and pseudogenes of a new human protein tyrosine phosphatase. *Genomics 35*:172–181.

21

Role of Immunohistochemical Expression of DNA Methyltransferase 1 Protein in Gastric Carcinoma

Yae Kanai, Eri Arai, and Tsuyoshi Etoh

Introduction

Deoxyribonucleic acid (DNA) methylation plays an important role in transcriptional regulation and chromatin remodeling in mammalian cells. Both overall DNA hypomethylation and more regional DNA hypermethylation have been well documented in various cancers (Jones and Baylin, 2002). Aberrant DNA methylation may be involved in carcinogenesis as a result of 1) increased gene mutagenicity from deamination of 5-methylcytosine to thymine; 2) a possible association of aberrant DNA methylation with genetic instability; and 3) repression of gene transcription through methylation of CpG islands in regulatory regions of specific genes, including tumor-suppressor genes. Furthermore, accumulating evidence suggests that aberrant DNA methylation is involved even in the early and precancerous stages of human carcinogenesis (Eguchi *et al.,* 1997; Kanai *et al.,* 1996, 1997, 1998, 1999, 2000; Kondo *et al.,* 2000).

To date, three enzymes, DNA methyltransferase l (DNMT1) (Bestor *et al.,* 1988), DNMT3a, and DNMT3b (Okano *et al.,* 1998), have been confirmed to possess DNMT activity. Of these, DNMT1 is the most major and best known. Increased messenger ribonucleic acid (mRNA) or protein expression of DNMT1 has been reported in various human precancerous conditions and cancers. For example, we observed that mRNA expression of DNMT1 is significantly increased in chronic hepatitis or liver cirrhosis, which are considered to be precancerous conditions for hepatocellular carcinomas (HCCs), compared with normal liver tissues, and is further increased in HCCs (Saito *et al.,* 2001; Sun *et al.,* 1997). Immunohistochemically detected protein overexpression of DNMT1 in HCCs was significantly correlated with poorer tumor differentiation and with portal-vein involvement. Moreover, the recurrence-free survival rate and overall survival rate of patients with HCCs with increased protein expression of DNMT1 were significantly lower than those of patients with HCCs without such increased expression (Saito *et al.,* 2003). Increased expression of DNMT1 is a biologic predictor both of the recurrence of HCCs and of a poorer prognosis for patients with HCC.

With regard to urothelial carcinogenesis, even noncancerous urothelia showing no marked histologic changes obtained from patients with bladder cancers can be considered precancerous because they may have

Handbook of Immunohistochemistry and *in situ* Hybridization of Human Carcinomas, Volume 4: Molecular Genetics, Gastrointestinal Carcinoma, and Ovarian Carcinoma

been exposed to carcinogens in the urine. Indeed, increased protein expression of DNMT1 preceding an increase in proliferating cell nuclear antigen (PCNA) labeling index was observed in such noncancerous urothelia from patients with bladder cancers. The incidence and intensity of nuclear immunoreactivity for DNMT1 further and progressively increased from dysplastic urothelia to transitional cell carcinomas (Nakagawa *et al.,* 2003). The increased protein expression of DNMT1 was particularly associated with the development of widely spreading flat carcinomas *in situ* of the urinary bladder, which are considered to be precursors of nodular invasive carcinomas with aggressive clinical courses (Nakagawa *et al.,* 2003). Protein expression levels of DNMT1 correlated significantly with accumulation of DNA hypermethylation on multiple CpG islands during multistage urothelial carcinogenesis (Nakagawa *et al.,* 2005). These data suggest that increased expression of DNMT1 may participate in both the precancerous stage and the malignant progression of human cancers originating from various organs.

In gastric carcinomas, we have reported that mRNA expression levels of DNMT1 were significantly higher than in noncancerous gastric mucosae and that the increased mRNA expression of DNMT1 correlated significantly with the CpG island methylator phenotype (CIMP) (Kanai *et al.,* 2001). CIMP is defined as frequent DNA hypermethylation of C-type CpG islands, which are methylated in a cancer-specific but not an age-dependent manner (Toyota *et al.,* 1999). In this chapter, we describe the methodology of immunohistochemistry for DNMT1 and discuss the significance of protein overexpression of DNMT1 in gastric carcinomas.

MATERIALS

1. Five-µm-thick sections of formalin-fixed and paraffin-embedded tissue specimens mounted on silane-coated glass slides.
2. Xylene.
3. 100% Ethanol.
4. 3% and 30% H_2O_2; store at 4°C.
5. 0.3% H_2O_2: immediately before use, add 1 ml of 30% H_2O_2 to 99 ml of 100% methanol.
6. Phosphate buffer saline (PBS): dissolve 8 g of NaCl, 0.2 g of KCl, 1.44 g of Na_2HPO_4, and 0.24 g of KH_2PO_4 in 800 ml of distilled water. Adjust the pH to 7.4 and add water to 1 L.
7. 10 mM citric acid: dilute the commercially available stock solution of citric acid with distilled water.
8. 2% normal swine serum (NSS): add 1 ml of NSS (Dako Glostrup, Denmark) to 49 ml of PBS.
9. Anti-human DNMT1 antibody (goat polyclonal antibody, sc-10219; Santa Cruz Biotechnology, Santa Cruz, CA): for staining 50 slides at a dilution of 1:1000, add 12 µl of the antibody to 12 ml of 2% NSS. It is recommended that the primary antibody is diluted immediately before use.
10. Biotinylated anti-goat immunoglobulin G (IgG) (Vector Laboratories, Burlingame, CA): for staining 50 slides at a dilution of 1:200, add 60 µl of the antibody to 12 ml of 2% NSS. It is recommended that the secondary antibody is diluted immediately before use.
11. Avidin-biotin peroxidase complex (ABC) solution: add 50 µl of Reagent A and 50 µl of Reagent B (both supplied in the Vectastain Elite ABC kit, Vector Laboratories) to 10 ml of 2% NSS. Allow the ABC solution to stand at room temperature for 30 min before use.
12. 3,3′-Diaminobenzidine tetrahydrochloride (DAB) solution: immediately before use, dissolve 3 DAB-Tris tablets (MUTO Pure Chemicals, Tokyo, Japan) to 150 ml of distilled water. Keep the solution on ice throughout the incubation.
13. Hematoxylin solution.

METHODS

1. Deparaffinize the sections in xylene for 30 min, and clear them through 5 changes of xylene for 1 min each.
2. Rehydrate the sections through 5 changes of 100% ethanol for 1 min each.
3. To block endogenous peroxidase activity, incubate the sections in freshly prepared 0.3% H_2O_2 solution in methanol at room temperature for 30 min.
4. Rinse the sections in PBS 3× for 5 min each.
5. For antigen retrieval, heat the sections in 10 mM citric acid for 10 min at 120°C in an autoclave.
6. Cool the sections, and rinse them in PBS 2× for 5 min each.
7. To block nonspecific reactions, apply 200 µl of 2% NSS to each section and incubate the sections at 4°C for 30 min.
8. Drain the serum solution from the sections. Do not rinse the sections between serum blocking and primary antibody incubation. Apply 200 µl of the diluted anti-DNMT1 antibody to each section and incubate the sections at 4°C overnight.
9. Rinse the sections in PBS 4× for 5 min each.
10. Apply 200 µl of the diluted biotinylated secondary antibody to each section, and incubate the sections at room temperature for 30 min.
11. Rinse the sections in PBS 4× for 5 min each.
12. Apply 200 µl of the freshly prepared ABC solution to each section, and incubate at room temperature for 30 min.

13. Rinse the sections in PBS 4× for 5 min each.
14. Add 30 µl of 3% H_2O_2 to 150 ml of ice-cold DAB solution. Then immediately incubate the sections with the mixture of H_2O_2 and ice-cold DAB solution for ~7 min.
15. After microscopic confirmation of the staining intensity, rinse the sections in running tap water for several minutes.
16. Counterstain the sections with hematoxylin solution for 1 min.
17. Rinse the sections in running tap water for several minutes.
18. Incubate the sections with PBS for 1 min.
19. Rinse the sections in running tap water for several minutes.
20. Dehydrate the sections through 4 changes of 100% ethanol, and clear them through 4 changes of xylene.
21. Mount coverslips onto the sections.

RESULTS AND DISCUSSION

We evaluated the significance of aberrant DNMT1 protein expression during gastric carcinogenesis. Immunoreactivity for DNMT1 was detected in the nuclei, but not in the cytoplasm or cell membranes, of cells in the proliferating zones of foveolar epithelia, lymphocytes, and gastric carcinoma cells. If more than 30% of the cells in a tissue sample exhibited nuclear staining, the sample was considered to show positive immunoreactivity. None (0%) of the examined noncancerous epithelia exhibited DNMT1 immunoreactivity (except in the proliferative zones, which acted as the positive internal control for the analysis), whereas 72% of the corresponding gastric carcinomas were DNMT1-positive (Etoh *et al.,* 2004). We have also confirmed at the mRNA level the increased expression of DNMT1 in gastric carcinomas compared with the corresponding noncancerous mucosae (Kanai *et al.,* 2001). Taken together, these observations indicate that increased expression of DNMT1 has some significance during gastric carcinogenesis.

DNMT1 protein overexpression was significantly associated with poorer tumor differentiation (Figure 49), suggesting that DNMT1 may be particularly involved in the stage of malignant progression of gastric carcinomas (Etoh *et al.,* 2004). However, in a previous study that used quantitative reverse transcription-polymerase chain reaction analysis to examine DNMT1 mRNA expression levels in HCCs, overexpression was detected even in precancerous conditions (Saito *et al.,* 2001; Sun *et al.,* 1997). By analogy with hepatocarcinogenesis, we cannot rule out the possibility that a small elevation in DNMT1 expression had already occurred in the earlier stages of gastric carcinogenesis, before the DNMT1 expression level reached the threshold of detection for the immunohistochemical methods used.

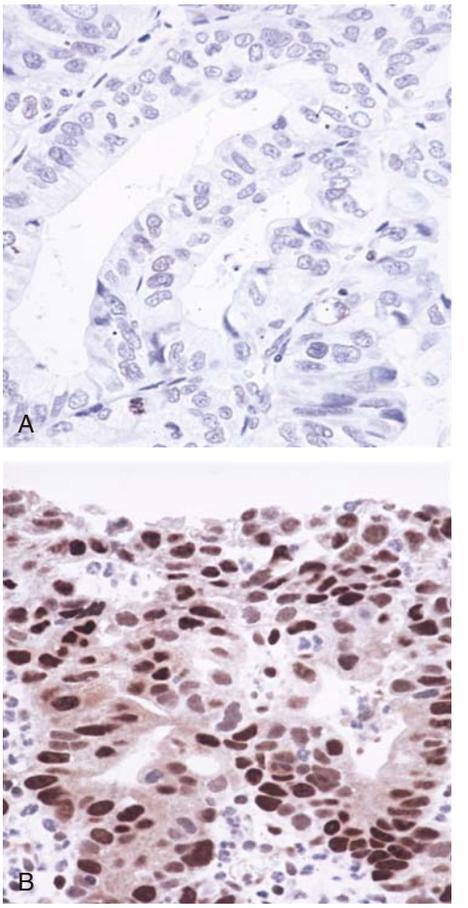

Figure 49. Immunohistochemical examination using anti-human DNA methyltransferase 1 (DNMT1) goat polyclonal antibody. Although most cancer cells in a well-differentiated adenocarcinoma lacked nuclear immunoreactivity for DNMT1 **(A),** a moderately differentiated adenocarcinoma of the stomach showed strong nuclear DNMT1 immunoreactivity **(B)** (360X).

We also examined DNA methylation status on C-type CpG islands in noncancerous mucosae and the corresponding gastric carcinomas. Regional DNA hypermethylation on C-type CpG islands was detected even in the noncancerous mucosae, which can contain precursor cells for cancers or precancerous lesions such as intestinal metaplasia (Etoh *et al.,* 2004). However, the incidence and degree of DNA hypermethylation was increased in the gastric carcinomas compared with the noncancerous mucosae. When DNA hypermethylation was seen on three or more C-type CpG islands, we regarded the cancer as being CIMP-positive, according

to previously described criteria (Toyota *et al.,* 1999). Of the gastric carcinomas, 24% were CIMP-positive, confirming that aberrant DNA methylation is associated with the multistage development of certain subgroups of gastric carcinomas (Etoh *et al.,* 2004).

We have previously reported that the increased mRNA expression of DNMT1 correlates significantly with CIMP in gastric and colorectal carcinomas (Kanai *et al.,* 2001). In addition, we demonstrated a significant correlation between DNMT1 expression at the protein level and CIMP in gastric carcinomas. Although DNMT1 has been considered to be a "maintenance" form of DNMT that copies methylation patterns after DNA replication, targeting of the substrate DNA by DNMT1 may be disrupted by mechanisms such as dysfunction of p21WAF1 (Baylin, 1997), which competes with DNMT1 for binding to PCNA (Chuang *et al.,* 1997), in cancer cells. Moreover, it has been suggested that DNMT1 is capable of *de novo* methylating activity, and it may have a maintenance function (Rhee *et al.,* 2002). Therefore, it is feasible that, in cancers, DNMT1 participates in DNA hypermethylation on CpG islands that are not methylated in normal cells.

The increased protein expression of DNMT1 correlated significantly with DNA hypermethylation on the CpG islands of the *hMLH1* and *THBS-1* genes (Etoh *et al.,* 2004). Among the C-type CpG islands examined, those of the *hMLH1* and *THBS-1* genes may be particularly targeted by overexpressed DNMT1. This is compatible with previous reports that silencing of the *hMLH1* gene results in frequent microsatellite instability in gastric carcinomas (Fleisher *et al.,* 2001). Reduced E-cadherin expression was significantly associated with poorer tumor differentiation and DNA hypermethylation on the CpG island of the *E-cadherin* gene in gastric carcinomas. Furthermore, there was a significant correlation between DNMT1 protein overexpression and reduced *E-cadherin* expression in gastric carcinomas, indicating that the *E-cadherin* gene may also be a target of overexpressed DNMT1 (Etoh *et al.,* 2004).

DNMT1 mRNA is expressed mainly during the S-phase and, because tumor tissue is presumed to contain a greater proportion of dividing cells than does normal tissue, some debate has arisen as to whether the increased DNMT1 expression is the result of an increase in the proportion of dividing cells or of a specific increase in DNMT1 expression per individual cell. However, in our study, the PCNA-labeling index was increased even in well-differentiated adenocarcinomas, in which the incidence of DNMT1 protein overexpression was low. Thus, the incidence of nuclear immunoreactivity for DNMT1 was not significantly associated with the PCNA-labeling index among all examined gastric carcinomas, suggesting that DNMT1 protein overexpression does not result entirely from the increased numbers of dividing cells during gastric carcinogenesis (Etoh *et al.,* 2004).

Finally, to clarify the background of DNMT1 protein overexpression, we focused on etiologic factors believed to be involved in gastric carcinogenesis. Although DNMT1 protein overexpression was not significantly associated with the incidence of *Helicobacter pylori* infection in the corresponding noncancerous mucosae, all of the Epstein-Barr virus (EBV)-positive cancers showed DNMT1 protein overexpression. EBV infection was significantly associated with the DNA hypermethylation of five or more C-type CpG islands, indicating that DNMT1 may play an important role in EBV-related gastric carcinogenesis via aberrant DNA methylation (Etoh *et al.,* 2004).

In summary, DNMT1 overexpression may not be just a secondary effect of increased cancer cell proliferate activity; it may be associated with EBV infection and other etiologic factors during gastric carcinogenesis. Furthermore, DNMT1 may play a significant role in the development of poorly differentiated gastric carcinomas by inducing frequent DNA hypermethylation of multiple CpG islands.

References

Baylin, S.B. 1997. Tying it all together: epigenetics, genetics, cell cycle, and cancer. *Science 277*:1948–1949.

Bestor, T., Laudano, A., Mattaliano, R., and Ingram, V. 1988. Cloning and sequencing of a cDNA encoding DNA methyltransferase of mouse cells: the carboxyl-terminal domain of the mammalian enzymes is related to bacterial restriction methyltransferases. *J. Mol. Biol. 203*:971–983.

Chuang, L.S., Ian, H.I., Koh, T.W., Ng, H.H., Xu, G., and Li, B.F. 1997. Human DNA-(cytosine-5) methyltransferase-PCNA complex as a target for p21WAF1. *Science 277*:1996–2000.

Eguchi, K., Kanai, Y., Kobayashi, K., and Hirohashi, S. 1997. DNA hypermethylation at the D17S5 locus in non-small cell lung cancers: its association with smoking history. *Cancer Res. 57*:4913–4915.

Etoh, T., Kanai, Y., Ushijima, S., Nakagawa, T., Nakanishi, Y., Sasako, M., Kitano, S., and Hirohashi, S. 2004. Increased DNA methyltransferase 1 (DNMT1) protein expression correlates significantly with poorer tumor differentiation and frequent DNA hypermethylation of multiple CpG islands in gastric cancers. *Am. J. Pathol. 164*:689–699.

Fleisher, A.S., Esteller, M., Tamura, G., Rashid, A., Stine, O.C., Yin, J., Zou, T.T., Abraham, J.M., Kong, D., Nishizuka, S., James, S.P., Wilson, K.T., Herman, J.G., and Meltzer, S.J. 2001. Hypermethylation of the hMLH1 gene promoter is associated with microsatellite instability in early human gastric neoplasia. *Oncogene 20*:329–335.

Jones, P.A., and Baylin, S.B. 2002. The fundamental role of epigenetic events in cancer. *Nat. Rev. Genet. 3*:415–428.

Kanai, Y., Hui, A.M., Sun, L., Ushijima, S., Sakamoto, M., Tsuda, H., and Hirohashi, S. 1999. DNA hypermethylation at the D17S5 locus and reduced HIC-1 mRNA expression are associated with hepatocarcinogenesis. *Hepatology 29*:703–709.

Kanai, Y., Ushijima, S., Hui, A.M., Ochiai, A., Tsuda, H., Sakamoto, M., and Hirohashi, S. 1997. The E-cadherin gene is silenced by CpG methylation in human hepatocellular carcinomas. *Int. J. Cancer 71*:355–359.

Kanai, Y., Ushijima, S., Kondo, Y., Nakanishi, Y., and Hirohashi, S. 2001. DNA methyltransferase expression and DNA methylation of CpG islands and peri-centromeric satellite regions in human colorectal and stomach cancers. *Int. J. Cancer 91*: 205–212.

Kanai, Y., Ushijima, S., Ochiai, A., Eguchi, K., Hui, A.M., and Hirohashi, S. 1998. DNA hypermethylation at the D17S5 locus is associated with gastric carcinogenesis. *Cancer Lett. 122*:135–141.

Kanai, Y., Ushijima, S., Tsuda, H., Sakamoto, M., and Hirohashi, S. 2000. Aberrant DNA methylation precedes loss of heterozygosity on chromosome 16 in chronic hepatitis and liver cirrhosis. *Cancer Lett. 148*:73–80.

Kanai, Y., Ushijima, S., Tsuda, H., Sakamoto, M., Sugimura, T., and Hirohashi, S. 1996. Aberrant DNA methylation on chromosome 16 is an early event in hepatocarcinogenesis. *Jpn. J. Cancer Res. 87*:1210–1217.

Kondo, Y., Kanai, Y., Sakamoto, M., Mizokami, M., Ueda, R., and Hirohashi, S. 2000. Genetic instability and aberrant DNA methylation in chronic hepatitis and cirrhosis: a comprehensive study of loss of heterozygosity and microsatellite instability at 39 loci and DNA hypermethylation on 8 CpG islands in microdissected specimens from patients with hepatocellular carcinoma. *Hepatology 32*:970–979.

Nakagawa, T., Kanai, Y., Saito, Y., Kitamura, T., Kakizoe, T., and Hirohashi, S. 2003. Increased DNA methyltransferase 1 protein expression in human transitional cell carcinoma of the bladder. *J. Urol. 170*:2463–2466.

Nakagawa, T., Kanai, Y., Ushijima, S., Kitamura, T., Kakizoe, T., and Hirohashi, S. 2005. DNA hypermethylation on multiple CpG islands associated with increased DNA methyltransferase DNMT1 protein expression during multistage urothelial carcinogenesis. *J. Urol. 173*:1767–1771.

Okano, M., Xie, S., and Li, E. 1998. Cloning and characterization of a family of novel mammalian DNA (cytosine-5) methyltransferases. *Nat. Genet. 19*:219–220.

Rhee, I., Bachman, K.E., Park, B.H., Jair, K.W., Yen, R.W., Schuebel, K.E., Cui, H., Feinberg, A.P., Lengauer, C., Kinzler, K.W., Baylin, S.B., and Vogelstein, B. 2002. DNMT1 and DNMT3b cooperate to silence genes in human cancer cells. *Nature 416*:552–556.

Saito, Y., Kanai, Y., Nakagawa, T., Sakamoto, M., Saito, H., Ishii, H., and Hirohashi, S. 2003. Increased protein expression of DNA methyltransferase (DNMT) 1 is significantly correlated with the malignant potential and poor prognosis of human hepatocellular carcinomas. *Int. J. Cancer 105*:527–532.

Saito, Y., Kanai, Y., Sakamoto, M., Saito, H., Ishii, H., and Hirohashi, S. 2001. Expression of mRNA for DNA methyltransferases and methyl-CpG-binding proteins and DNA methylation status on CpG islands and pericentromeric satellite regions during human hepatocarcinogenesis. *Hepatology 33*:561–568.

Sun, L., Hui, A.M., Kanai, Y., Sakamoto, M., and Hirohashi, S. 1997. Increased DNA methyltransferase expression is associated with an early stage of human hepatocarcinogenesis. *Jpn. J. Cancer Res. 88*:1165–1170.

Toyota, M., Ahuja, N., Ohe-Toyota, M., Herman, J.G., Baylin, S.B., and Issa, J.P. 1999. CpG island methylator phenotype in colorectal cancer. *Proc. Natl. Acad. Sci. USA 96*:8681–8686.

This Page Intentionally Left Blank

22

Role of Immunohistochemical Expression of Cytoplasmic Trefoil Factor Family-2 in Gastric Cancer

Dipok Kumar Dhar, Timothy C. Wang, Hideki Tabara, and Naofumi Nagasue

Introduction

Despite a precipitous drop in the incidence of gastric carcinoma worldwide and availability of flexible endoscope to identify the disease at a relatively early stage, gastric cancer remains one of the leading causes of death from malignant disease. Gastric carcinoma is the second most frequent malignancy in the world after lung carcinoma, with an estimated 876,000 new cases and 647,000 deaths reported in 2000 (Parkin, 2001). Irrespective of the treatment modalities, the reported 5-year survival is disappointing when the disease extends to adjacent organs or when it is diagnosed with widespread metastasis in the locoregional or distant regions (Dhar *et al.,* 2001). Despite a trend toward diagnosis at an early stage and increasing survival rates, the treatment of patients with gastric cancer still poses a major challenge for the clinicians. Early detection and surgical or endoscopic removal of small tumors have been reported to yield excellent results. However, the prognosis of patients with advanced-stage disease remains dismal.

The most probable initiators of gastric carcinoma formation from normal gastric mucosa include acquisition of *Helicobacter pylori* infection or repeated insult from dietary carcinogens, chronic gastritis followed by atrophic gastritis, intestinal metaplasia, dysplasia, and tumor formation. During this progression, an array of genetic mutations associated with dysregulation in cellular homeostasis increase the chance of uncontrolled cell growth and malignancy. Nevertheless, genetic instability or acquired defects in genes controlling cellular proliferation and apoptosis likely play a vital role in gastric carcinogenesis. It has been shown that chronic inflammation, with repeated injury and healing in gastric mucosa, secondary to *Helicobacter* infection, may promote the recruitment of bone marrow cell to the gastric mucosa (Houghton *et al.,* 2004). Over time, these cells may progress through metaplasia and dysplasia to epithelial cancer. This unique paradigm may change our understanding about the gastric carcinogenesis and may help to design authentic ways to stop the carcinogenesis process. Although significant progress has been made in the general understanding of the molecular and cellular biology of cancer development, progression, invasion, and metastasis, our understanding of gastric carcinoma remains quite limited.

Cancers can be thought of as "wounds that do not heal" (Dvorak, 1986), where dysregulated cells with

Handbook of Immunohistochemistry and *in situ* Hybridization of Human Carcinomas, Volume 4: Molecular Genetics, Gastrointestinal Carcinoma, and Ovarian Carcinoma

acquired genetic alterations accumulate during a continuous turnover of cells. In this process, the expression of numerous growth factor or oncogenes is constitutively switched on, resulting in dysregulated cellular growth. There is a battery of genes—including the epidermal growth factor (EGF), transforming growth factor-alpha, regenerating gene, and trefoil factors—which are overexpressed in gastric mucosa to restitute the breached area following a noxious injury and also in gastric carcinoma (Dhar *et al.,* 2003; Kawanami *et al.,* 1997). Among these genes, trefoil factors deserve special attention because of their rapid induction in the vicinity of injured mucosa (Alison *et al.,* 1997). The trefoil factor family (TFF) peptides are a group of protease-resistant proteins that all contain one or more trefoil domains, a characteristic three-leaved structure that has given the peptide family its name (Wright *et al.,* 1997). There are three known trefoil factors: TFF1 (also known as pS2) is an estrogen responsive peptide but expresses abundantly in the surface epithelium of the stomach; TFF2 (also known as spasmolytic polypeptide, SP) is expressed in mucous neck cells of the gastric mucosa and Brunner's glands of duodenum; and TFF3 (also known as intestinal trefoil factor or ITF) is expressed in the mucus-secreting goblet cells of the intestine. The genes encoding these TFFs are all clustered within a tandem of 55 kilobases on human chromosome 21q22.3 and are thought to have overlapping biologic activities (Seib *et al.,* 1997). Trefoil peptides are involved in several biologic functions including gastrointestinal (GI) cytoprotection, cellular proliferation, and increased cell motility (Hoosein *et al.,* 1989; Playford *et al.,* 1995). The role of TFFs in tumorigenesis remains controversial; in general, TFF1 appears to function as a gastric-specific tumor-suppressor gene, whereas TFF3 has been postulated to enhance tumor progression by increasing cellular invasion and metastasis (Lefebvre *et al.,* 1996; Yamachika *et al.,* 2002). It has been reported that TFF2 expression is associated with the development of gastric cancer formation in mouse and TFF2 became a poor prognostic marker in patients with gastric carcinoma (Dhar *et al.,* 2003; Wang *et al.,* 2000).

In this chapter, we will describe the methods used to identify expression and localization of TFF2 in gastric carcinoma samples. The results will be compared with the clinicopathologic characteristics of cancers; also, the impact of TFF2 expression on prognosis of patients with gastric carcinoma will be evaluated.

MATERIALS

1. A total of 144 patients with gastric carcinoma undergoing curative tumor resection between 1990 and 1998 were enrolled in this study. Among the 144 patients, 111 had advanced gastric carcinoma and 33 patients had early gastric carcinoma.

2. Glass slides precoated with 0.1% poly-L-lysine in water.

3. Tissue sections of 5 μm thickness from paraffin-embedded tissue blocks containing the most invasive portion of the tumor and adjacent normal mucosa. Regional metastatic lymph nodes containing metastatic tumor.

4. Slide warmer or 55–60°C incubator.

5. Xylene for deparaffinization and graded ethanol (100%, 95%, 90%, and 70%) for rehydration.

6. Phosphate buffer solution (PBS)—130 mM NaCl; 7 mM Na_2HPO_4; 3 mM NaH_2PO_4. For 10×PBS mix 75.97 g NaCl, 12.46 Na_2HPO_4, and 4.80 g NaH_2PO_4 should be used. Dissolve in less than 1 L of distilled water; adjust pH 7.4 and mess up to a final volume of 1 L. Store this solution at room temperature. Dilute 1:10 with distilled water before use and adjust pH if necessary.

7. Citrate buffer—trisodium citrate dihydrate 3.1 g/L, adjust pH to 6.0 (Dako ChemMate; Dako, Glostrup, Denmark).

8. 3% Hydrogen peroxide in water.

9. Autoclave machine for antigen retrieval.

10. Primary antibodies and nonimmune serum from the same species of primary antibody for reagent negative control.

11. Immunostaining kit (Histofine SAB-PO (M) kit; Nichirei, Tokyo, Japan):

   a. Blocking serum; 10% rabbit serum.

   b. Secondary antibody; biotin labeled anti-mouse rabbit immunoglobulin G (IgC) + IgA; IgM (10 μg/ml).

   c. Peroxidase or alkaline phosphatase-labeled streptavidin (100 μg/ml).

   d. Substrate chromogen for peroxidase—3,3′-diaminobenzidine (DAB) tetrahydrochloride, TBS buffer, and 0.6% hydrogen peroxide in separate containers. To be mixed immediately before use.

   e. Substrate chromogen for alkaline phosphatase—nitroblue tetrazolium/5-bromo-4-chloro-3-indolyl phosphate (NBT/BCIP) solution (Roche Diagnostics Incorporation, Indianapolis, IN).

12. Mayer's hematoxyline for counterstaining.

13. Mounting solution (Zymed Histomount, San Francisco, CA) and coverglass.

METHODS

Preparation of Tissue Sections

According to prospective protocol, formalin-fixed tumor and all lymph nodes were cut at several levels and embedded in paraffin. Sections were taken at 5 μm

thickness for routine hematoxylin and eosin (H&E) staining and also for immunohistochemical staining. An experienced pathologist checked all H&E stained slides and documented the pathologic characteristics of tumor and lymph nodes. Tumor stage was defined according to the International Union Against Cancer (UICC) Tumor Node Metastasis (TNM) 2002 staging system (Sobin *et al.,* 2002).

Trefoil Factor Family-2 Immunohistostaining Procedure

1. Prewarm slides in a 55–60°C incubator for 15 min.
2. Deparaffinze in xylene 3×10 min; incomplete removal of paraffin may result in increased nonspecific staining.
3. Rehydrate in graded series of ethanol: 100% for 3 min; 95% for 3 min; 90% for 3 min, and 70% for 3 min.
4. Do not allow tissue sections to dry from this point; dried part may display increased nonspecific staining.
5. Rinse slides in distilled water and submerge in PBS wash bath for 5 min.
6. Immerse sections in autoclavable Coplin jars filled with sufficient target retrieval solution (citrate buffer, pH 6.0). Autoclave for 10 min at 15 psi (121°C). Vent pressure under slow exhaust to prevent boilover.
7. Allow the Coplin jar containing tissue sections to cool to about 60°C before removing from the autoclave.
8. Decant target retrieval solution and rinse tissue sections 2× with room-temperature PBS buffer.
9. Tap off excess buffer and carefully wipe around the specimen using a folded Kimwipe or gauze pad, leaving a wet rim of area around the specimen. Do not allow the specimen to dry out at any time.
10. Add enough drops of 3% hydrogen peroxide in water to cover the whole section, and incubate for 30 min at room temperature.
11. Slides should be placed on a flat-surface humidity chamber to avoid drying out during the incubation period.
12. Rinse with distilled water and submerge in PBS wash bath for 5 min.
13. Apply enough drops of blocking serum to cover whole specimen, place slides in a sealed humidity chamber, and incubate at room temperature for 30 min.
14. Tap off excess blocking serum, apply enough anti-TFF2 primary antibody (GE16C clone; Novocastra Laboratories Ltd., Newcastle, UK; 1:50 dilution) to cover specimen, tilt each slide in two different directions to evenly spread the antibody, and incubate overnight at 4°C temperature.
15. Rinse gently with PBS from a wash bottle (avoid a direct jet, which may loosen tissue section) and wash with fresh PBS for 5 min 3×.
16. Incubate with rabbit anti-mouse antibody at room temperature for 30 min.
17. Rinse gently and place slides in PBS for 5 min 3×.
18. Incubate with peroxidase-labeled streptavidin at room temperature for 30 min.
19. Rinse gently and place slides in PBS for 5 min 3×.
20. Add 1 drop each of 3,3′-DAB tetrahydrochloride and TBS buffer to 1ml distilled water, mix well, and then add 1 drop of 0.6% hydrogen peroxide. Mix again and apply sufficient amount of reagent on specimens.
21. Incubate for 5 ± 1 min and monitor under a microscope for optimum staining. Initially, a positive control specimen should be used to fix the incubation time.
22. Rinse in running tap water and counterstain in Mayer's hematoxylin. Incubation period depends on strength of hematoxylin.
23. Dip slides in a waterbath to remove excess hematoxylin, shake off excess fluid, and mount the sections using aqueous base mounting medium such as glycerol gelatin. Coverslip may be sealed with clear nail polish.

Double Immunostaining for Trefoil Factor Family and α-Smooth-Muscle Actin

1. Repeat **Steps 1** through **21** for TFF2 staining.
2. Immerse sections in Coplin jars filled with sufficient target retrieval solution. Place slides in a microwave oven and operate the oven on high power (~700W) for 5 min 2×.
3. Allow slides to cool down for 20 min at room temperature and rinse with PBS for 5 min.
4. Repeat **Steps 12** through **23**.
5. Apply anti-α-SMA (α-smooth-muscle actin) antibody (Dako Inc., 1:50 dilution, overnight at 4°C) as primary antibody in **Step 14** and alkaline phosphatase-labeled streptavidin in **Step 18**.
6. In Step 20, add 20 µl of NBT/BCIP solution to 1 ml of distilled water in an Eppendorf tube, mix well, and apply sufficient amount on specimens.

Statistical Analysis

The correlation between TFF2 expression and various clinicopathologic parameters was determined by the Fisher's exact test or Mann-Whitney U test as appropriate. The survival curves were plotted using the Kaplan-Meier method, and the statistical significance between groups was determined by the log rank test. The end points for analysis were the disease-free survival and

the overall survival starting from the day of operation. Independent variables predicting survival were evaluated by the multiple stepwise regression analysis using the Cox model. The Statview 4.5J (Abacus Concepts, Barkley, CA) software was used for data analysis.

RESULTS AND DISCUSSION

In this study, we evaluated the immunohistochemical expression of TFF2 in gastric carcinoma samples and in corresponding adjacent gastric mucosa. Cytoplasmic expression of TFF2 by tumor cells had a strong correlation with poor prognostic variables and had an adverse impact on patient prognosis. Moreover, a double immunohistochemical staining with TFF2 and α-SMA showed that tumor cells invading beyond the muscularis mucosa layer (stained purple by α-SMA staining were frequently positive for TFF2. When properly used, immunohistochemistry (IHC) technique is an extremely powerful tool for analyzing patterns of protein expression in tissue sections, both temporally and spatially. Detecting the expression level of ribonucleic acid (RNA) transcripts in clinical materials diverse methodologies such as RT-PCR (real-time reverse transcriptase-polymerase chain reaction), RNase protection assay, or Northern Blot analysis is highly sensitive; however, these methods can sometimes be misleading as a result of sampling error or heterogeneity in expression of transcripts in different parts of the same tumor. Similar limitations hold true for other techniques such as Western blot analysis. These drawbacks can be overcome by using IHC to assess the pattern and level of expression and correlating such findings with other clinical parameters and prognostic markers.

As shown in Figure 50A, TFF2 staining in normal gastric fundic mucosa is largely restricted to the neck cells of the gastric glands, sparing the superficial foveolar epithelial cells and deep glands. In the normal gastric antrum, TFF2 tends to be restricted to the base of the gastric glands. In contrast to this normal pattern, in patients with gastric cancer the lower half of the fundic glands was frequently positive for TFF2 in the noncancerous gastric mucosa adjacent to the tumor (Figure 50B). These TFF2-positive fundic glandular cells had abundant mucous granules and had morphologic similarity with both antral glands and Brunner's gland of duodenum. As described by Schmidt *et al*. (1999), these altered fundic glands are well-known as a special type of metaplastic precancerous lesion (also known as spasmolytic polypeptide-expressing metaplasia [SPEM]) and are thought to be precancerous for gastric carcinoma. Nomura *et al*. (2005) reported that oxyntic atrophy induced by DMP-777 in C57BL/6 mice was accompanied by a rapid increase in proliferative cells and a second proliferative population emerged at the base of fundic glands along with the development of mucous cell metaplasia expressing TFF2/SPEM. In a *H. felis*–infected C57BL/6 mouse model of gastric carcinogenesis, the authors also showed that SPEM represents a precursor lineage for the development of dysplasia during gastric carcinogenesis (Nomura *et al.,* 2004). In this study, among the 144 tumors, the SPEM lineage cells were present in 135 (94%) gastric mucosae adjacent to the tumor which may indicate that SPEM is a precancous lesion, and TFF2 expression by gastric cells may imply a proliferative advantage for the gastric mucosal cells. Intestinal metaplasia is another well-known morphologic entity frequently associated with *H. pylori* infection and also considered to be a precancous lesion for intestinal type of gastric adenocarcinoma. In contrast to SPEM, we noticed that areas of intestinal metaplasia were always negative for TFF2 (see Figure 50A). In our clinical samples, SPEM lineage cells and intestinal metaplasia frequently coexisted and a mononuclear cell infiltration was commonly observed in proximity to the SPEM cells. As reported by others (Schmidt *et al*. 1999), we also found that the prevalence of SPEM (94%) was higher than that of intestinal metaplasia (70%) in gastric mucosa adjacent to the tumors.

In cancerous tissue, TFF2 staining was observed as cytoplasmic, apical or membranous staining, and mixed type of staining (Figure 50C, D, and E). Strong and distinct staining for TFF2 was seen in the cytoplasm predominantly in the diffuse type of cancers, whereas weak membranous staining was the characteristic feature of the intestinal tumors. In most of the tumors positive for TFF2, strong cytoplasmic staining was preferentially observed in the invasive cells sparing the superficial tumor cells (see Figure 50G and H). May *et al*. (2004) found a similar pattern of TFF2 expression in the invasive front of breast cancer samples. Double immunohistochemical staining for TFF2 and α-SMA showed that TFF2 expression was particularly notable in cases where the tumor cells had invaded beyond the muscularis mucosa layer (see Figure 50G). When both of the primary antibodies are raised in the same species of animal, double immunostaining is usually quite difficult because of cross immunoreactivity and background staining. As described by Lan *et al*. (1995), this cross-reactivity could be easily overcome in our studies by a simple microwave treatment of sections between the two primary antibody incubations. We used this method and found this technique very convenient for double immunostaining with TFF2 and α-SMA antibody, both of which are derived from mouse. Metastatic tumor cells in the regional lymph nodes of the TFF2-positive cases were strongly stained for TFF2 (see Figure 50H). In general, the staining was confined to the metastatic

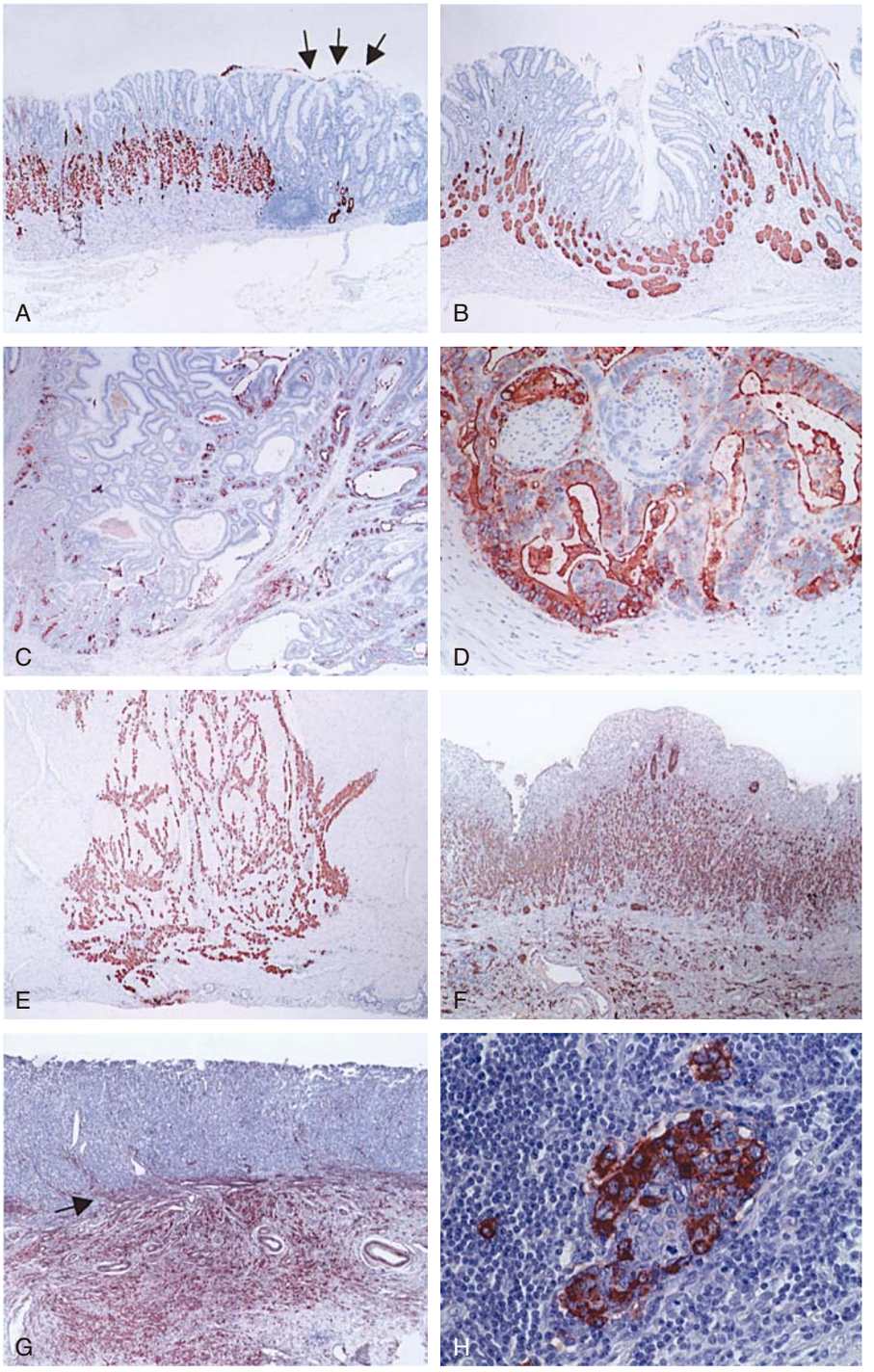

Figure 50. **A:** Normal staining of trefoil family factor (TFF2) was observed in the isthmus region of the gastric glands, and intestinal metaplastic region was negative for TFF2 *(arrow)*. **B:** The spasmolytic polypeptide-expressing metaplasia with abundant mucous granules had similarity with Brunner's gland of the duodenum. **C:** Weak membranous staining was the characteristic feature of intestinal tumors. **D:** A mixed type of staining in both cytoplasm and cell membrane is shown. **E:** Strong cytoplasmic staining in a diffuse type of tumor invading the muscularis propia layer is shown. **F:** Strong staining was noticed in the invasive front of the tumor sparing the superficial luminal tumor cells. **G:** Double immunostaining with α-smooth-muscle actin *(purple)* and TFF2 *(red)* shows that TFF2-positive tumor cells are invading the muscularis mucosa layer *(arrow)*. **H:** Metastatic tumor cells in a regional metastatic lymph node are strongly positive for TFF2, and lymphocytes are negative for TFF2.

tumor cells and was somewhat heterogeneous, with a large number of positive cells in the periphery of the tumor nodule.

Considering the strong cytoplasmic staining of TFF2 in SPEM and also in invasive gastric cancer cells, tumors having cytoplasmic or mixed type of staining were considered to be positive for TFF2. Tumors having weak membranous type of staining were classified as negative for TFF2. According to these criteria, among 144 cases, 43 cases (29.8%) were positive for TFF2. When TFF2 positivity was correlated with clinicopathologic parameters, we did not notice any correlation between TFF2 positivity and the sex or age of the patients. There was a strong correlation ($p < 0.001$) with the differentiation status of the tumor, with an increased prevalence of TFF2 expression in the diffuse type of tumors. Of the diffuse tumors, 48% (positive/negative, 30/32, 48%) were positive, whereas only 15% (positive/negative, 13/69) of the intestinal tumors were positive for TFF2. With respect to early gastric cancers, only two cases were positive and both of them were diffuse of tumors (2/7). Machado *et al*. (2002) reported that TFF2 was expressed by only 10.4% of gastric cancer specimens, with a trend (but no statistical difference) of higher expression in diffuse-versus intestinal-type tumors. Also it was reported that TFF2/SP was preferentially strongly expressed in diffuse type of gastric cancer cell lines (Kirikoshi and Katoh, 2002). Of note, the cellular localization for TFF2 was specific for each histologic type of cancer. This may indicate that the SPEM cells, which also have a strong cytoplasmic TFF2 expression, are the precursors of the diffuse type of cancers; however, further evidence is necessary to prove this speculation.

To date, several studies have suggested that TFF2 may promote cellular proliferation, and TFF2-deficient mice have been reported to decrease gastric mucosal proliferation (Farrell *et al.,* 2002). In this study, expression of TFF2 increased with the advancement of the T- ($p = 0.0011$) and N-stage ($p = 0.0001$) of the tumor. Also, similar correlation was observed with the lymphatic ($p = 0.0007$) and venous vessel invasions ($p = 0.0189$). The average tumor size of the TFF2-positive tumors (6.7 ± 3.6 cm, mean ± standard deviation) was significantly ($p = 0.0068$) greater than those of negative ones (4.5 ± 2.5 cm, mean ± standard deviation). These results may indicate that TFF2 may play a vital role in tumor growth, invasion, and metastasis.

TFF2 immunostaining was strongly positive in cancer cells at the invasive front of the tumor, sparing for the most part the superficial luminal cancer cells (see Figure 50F and G). Tumor cells located deep within the metastatic lymph nodes of the patients who were TFF2 positive tended to be strongly positive for TFF2 (see Figure 50H) indicating that TFF2-positive cell lineage may have metastasized to the regional lymph nodes and thus that the metastatic phenotype could be attributable in part to the TFF2 expression by the tumor cells. This finding further strengthens the conclusions of previous *in vitro* studies stating that TFF2 is intricately related with cancer cell motility and invasion (Emami *et al.,* 2001; Graness *et al.,* 2002, Playford *et al.,* 1995). In an *in vitro* wound-induced, cell migration assay using confluent rat intestinal epithelial cells, Dignass *et al*. (1994) showed that application of TFF2 enhanced migration of cells into the wound approximately fourfold. In addition, Playford *et al*. (1995) showed that TFF2 induced vertical invasion of HT29 cells into type I collagen gel in a dose-dependent manner. More recently, several authors showed that activation of several other signaling pathways involving the cellular transformation, survival, and motility—namely, src/RhoA, P13-K/Akt and phospholipase C/PKC, EGF receptors, MAP kinase, and APC/E-cadherin/β-catenins—play a crucial role in cellular invasion by TFFs (Emami *et al.,* 2001; Taupin *et al.,* 1999). Tumor angiogenesis and metastasis are intricately related phenotypes. Rodrigues *et al*. (2001) provided a concrete evidence of induction of angiogenesis by the TFFs in an *in vitro* study. Occasionally, strong TFF2 staining was observed in the endothelial cells of tumor-associated blood vessels. In a recent study, we found a significant correlation between strong expression of TFF2 and high microvessel density in gastric carcinoma samples (Dhar, 2005). Thus it is conceivable that TFF2 could be a potentially useful target for anti-angiogenic therapy.

Despite significant improvement in our understanding of gastric carcinogenesis, only a few genes are reported that may serve as potentially useful prognostic markers. Results from this study suggest that TFF2 expression should be investigated further as a useful indicator of patient's prognosis. According to the last follow-up, 30 (21%) patients out of 144 patients had disease recurrence. The follow-up was complete in all patients. The median follow-up period was 47.2 months. The data obtained at regular follow-up visits at the outpatient department were stored in a database specially designed for patients with gastric carcinoma. TFF2 expression had a significant ($p < 0.0001$, log rank test) impact on patient prognosis only in terms of the disease-free survival and had a trend ($p = 0.0973$, log rank test) of poor overall survival in the TFF2-positive cases but did not reach statistically significant level. The 5-year overall survival rates of patients with TFF2-negative and-positive status were 66.8% and 54.8%, whereas the 5-year disease-free survival rates for patients who were TFF2 negative and positive were 86.1% and 53.4%, respectively. A multivariate analysis was done to single

out the independent prognostic factors. All the conventional prognostic variables including the UICC stage, TFF2 expression, intraoperative blood loss, tumor differentiation status, tumor size, age, sex, and lymphatic and venous invasions were included in the analysis. Among the several factors analyzed, only the UICC tumor stage ($p < 0.0001$), TFF2 expression ($p = 0.0208$), and amount of intraoperative blood loss ($p = 0.0270$) remained significant for the disease-free survival.

Although the results from this study do require further validation and confirmation in independent prospective studies, immunohistochemical expression of TFF2 might be an effective tool for screening invasive phenotypes of gastric carcinoma and also may be a strong prognostic marker for this disease.

References

Alison, M.R., Chinery, R., Poulsom, R., Ashwood, P., Longcroft, J.M., and Wright, N.A. 1997. Experimental ulceration leads to sequential expression of spasmolytic polypeptide, intestinal trefoil factor, epidermal growth factor and transforming growth factor alpha mRNAs in rat stomach. *J. Pathol. 175*:405–414.

Dhar, D.K., Kubota, H., Tachibana, M., Kinugasa, S., Masunaga, R., Shibakita, M., Kohno, H., and Nagasue, N. 2001. Prognosis of T4 gastric carcinoma patients: an appraisal of aggressive surgical treatment. *J. Surg. Oncol. 76*:278–282.

Dhar, D.K., Wang, T.C., Maruyama, R., Udagawa, J., Kubota, H., Fuji, T., Tachibana, M., Ono, T., Otani, H., and Nagasue, N. 2003. Expression of cytoplasmic TFF2 is a marker of tumor metastasis and negative prognostic factor in gastric cancer. *Lab. Invest. 9*:1343–1352.

Dhar, D.K., Wang, T.C., Tabara, H., Tonomoto, Y., Maruyama, R., Tachibana, M., Kubota, H., and Nagasue, N. 2005. Expression of trefoil factor family members correlates with patient prognosis and neoangiogenesis. *Clin. Cancer Res. 11*:6472–6478.

Dignass, A., Lynch-Devaney, K., Kindon, H., Thim, L., and Podolsky, D.K. 1994. Trefoil peptides promote epithelial migration through a transforming growth factor-independent pathway. *J. Clin. Invest. 94*:376–383.

Dvorak, H.F. 1986. Tumors: wounds that do not heal. Similarities between tumor stroma generation and wound healing. *N. Engl. J. Med. 315*:1650–1659.

Emami, S., Floch, N.L., Bruyneel, E., Thim, L., May, F., Westley, B., Rio, M.C., Mareel, M., and Gespach, C. 2001. Induction of scattering and cellular invasion by trefoil peptides in src- and RhoA-transformed kidney and colonic epithelial cells. *Faseb. J. 15*:351–361.

Farrell, J.J., Taupin, D., Koh, T.J., Chen, D., Zhao, C.M., Podolsky, D.K., and Wang, T.C. 2002. TFF2/SP-defient mice show decreased gastric proliferation, increased acid secretion, and increased susceptibility to NSAID injury. *J. Clin. Invest. 109*:193–204.

Graness, A., Chwieralski, C.E., Reinhold, D., Thim, L., and Hoffmann, W. 2002. Protein kinase C and ERK activation are required for TFF-peptide-stimulated bronchial epithelial cell migration and tumor necrosis factor-alpha-induced interleukin-6 (IL-6) and IL-8 secretion. *J. Biol. Chem. 24*:18440–18446.

Hoosein, N.M., Thim, L., Jorgensen, K.H., and Brattain, M.G. 1989. Growth stimulatory effect of pancreatic spasmolytic polypeptide on culture colon and breast tumor cells. *Febs. Lett. 247*:303–306.

Houghton, J., Stoicov, C., Nomura, S., Rogers, A.B., Carlson, J., Li, H., Cai, X., Fox, J.G., Goldenring, J.R., and Wang, T.C. 2004. Gastric cancer originating from bone marrow-derived cells. *Science 306*:1568–1571.

Kawanami, C., Fukui, H., Kinoshita, Y., Nakata, H., Asahara, M., Matsushima, Y., Kishi, K., and Chiba, T. 1997. Regenerating gene expression in normal gastric mucosa and indomethacin-induced mucosal lesions of the rat. *J. Gastroenterol. 32*:2–8.

Kirikoshi, H., and Katoh, M. 2002. Expression of TFF1, TFF2 and TFF3 in gastric cancer. *Int. J. Oncol. 21*:655–659.

Lan, H.Y., Mu, W., Nikolic-Paterson, D.J., and Atkins, R.C. 1995. A novel, simple, reliable, and sensitive method for multiple immunoenzyme staining: use of microwave oven heating to block antibody crossreactivity and retrieve antigens. *J. Histochem. Cytochem. 43*:97–102.

Lefebvre, O., Chenard, M.P., Masson, R., Linares, J., Dierich, A., LeMeur, M., Wendling, C., Tomasetto, C., Chambon, P., and Rio, M.C. 1996. Gastric mucosa abnormalities and tumorigenesis in mice lacking the pS2 trefoil protein. *Science 274*: 259–262.

Machado, J.C., Nogueira, A.M.M.F., Carneiro, F., Reis, C.A., and Sobrinho-Simoes, M. 2002. Gastric carcinoma exhibit distinct types of cell differentiation: an immunohistochemical study of trefoil peptides (TFF1 and TFF2) and mucins (MUC1, MUC2, MUC5AC, and MUC6). *J. Pathol. 190*:437–443.

May, F.E.B., Semple, J.I., Prest, S.J., and Westley, B.R. 2004. Expression and motogenic activity of Tff2 in human breast cancer cells. *Peptides 25*:865–872.

Nomura, S., Baxter, T., Yamaguchi, H., Leys, C., Vartapetian, A.B., Fox, J.G., Lee, J.R., Wang, T.C., and Goldenring, J.R. 2004. Spasmolytic polypeptide expressing metaplasia to preneoplasia in H. felis-infected mice. *Gastroenterology 127*:582–594.

Nomura, S., Yamaguchi, H., Ogawa, M., Wang, T.C., Lee, J.R., and Goldenring, J.R. 2005. Alterations in gastric mucosal lineages induced by acute oxyntic atrophy in wild-type and gastrin-deficient mice. *Am. J. Physiol. Gastrointest. Liver Physiol. 288*: G362–375.

Parkin, D.M. 2001. Global cancer statistics in the year 2000. *Lancet. Oncol. 2*:533–543.

Playford, R.J., Marchbank, T., Chinery, R., Evison, R., Pignatelli, M., Boulton, R.A., Thim, L., and Hanby, A.M. 1995. Human spasmolytic polypeptide is a cytoprotective agent that stimulates cell migration. *Gastroenterology 108*:108–116.

Rodrigues, S., Nguyen, Q.D., Faivre, S., Bruyneel, E., Thim, L., Westley, B., May, F., Flatau, G., Mareel, M., Gespach, C., and Emami, S. 200l. Activation of cellular invasion by trefoil peptides and src is mediated by cyclooxygenase- and thromboxane A2 receptor-dependent signaling pathways. *FASEB. J. 15*: 1517–1528.

Schmidt, P.H., Lee, J.R., Joshi, V., Playford, R.J., Poulsom, R., Wright, N.A., and Goldenring, J.R. 1999. Identification of a metasplastic cell lineage associated with human gastric adenocarcinoma. *Lab. Invest. 79*:639–646.

Seib, T., Blin, N., Hilgert, K., Seifert, M., Theisinger, B., Engel, M., Dooley, S., Zang, K.D., and Welter, C. 1997. The three human trefoil genes TFF1, TFF2, and TFF3 are located within a region of 55 kb on chromosome 21q22.3. *Genomics 40*:200–202.

Sobin, I.H., and Wittekind, C.H. eds. 2002. *UICC TNM Classification of Malignant Tumors,* 6th ed. New York: John Wiley and Sons.

Taupin, D., Wu, D.C., Jeon, W.K., Devaney, K., Wang, T.C., and Podolsky, D.K. 1999. The trefoil gene family are coordinately

expressed immediate-early genes: EGF receptor and MAP kinase-dependent interregulation. *J. Clin. Invest. 103*:R31–R38.

Wang, T.C., Dangler, C.A., Chen, D., Goldenring, J.R., Koh, T., Raychowdhury, R., Coffey, R.J., Ito, S., Varro, A., Dockray, G.J., and Fox, J.G. 2000. Synergistic interaction between hypergastrinemia and helicobacter infection in a mouse model of gastric cancer. *Gastroenterology 118*:36–47.

Wright, N.A., Hoffmann, W., Otto, W.R., Rio, M.C., and Thim, L. 1997. Rolling in the clover: trefoil factor family (TFF)-domain peptides, cell migration and cancer. *FEBS Lett. 408*:121–123.

Yamachika, T., Werther, J.L., Bodain, C., Babyyatsky, M., Tatematsu, M., Yamamura, Y., Chen, A., and Itzkowitz, S. 2002. Intestinal trefoil factor: a marker of poor prognosis in gastric carcinoma. *Clin. Cancer Res. 8*:1092–1099.

23

Role of Immunohistochemical Expression of Cytokeratins in Small Intestinal Adenocarcinoma

Zong-Ming E. Chen and Hanlin L. Wang

Introduction

The small intestine constitutes approximately 75% of the length and almost 90% of the mucosal surface of the gastrointestinal (GI) tract. However, primary malignant neoplasms of the small intestine are extremely rare, accounting for only 1–3% of all malignancies of the GI tract (Frost *et al.,* 1994; O'Riordan *et al.,* 1996). Adenocarcinoma is the predominant histologic type and accounts for 30–50% of all primary small intestinal malignancies (Donohue, 1994; North and Pack, 2000). The annual incidence of small intestinal adenocarcinoma in the United States is estimated to be 0.37–1.4 per 100,000 population (Chow *et al.,* 1996; Howe *et al.,* 1999), approximately 1/50th as common as colorectal adenocarcinoma (Neugut *et al.,* 1998; O'Riordan *et al.,* 1996). The peak incidence occurs in the sixth and seventh decades of life (Abrahams *et al.,* 2002; Chen and Wang, 2004; Howe *et al.,* 1999), but it has been reported in children as young as 12 years of age (Dunsmore and Lovell, 1998). The clinical manifestations of small intestinal adenocarcinoma usually appear late in the course of the disease, often with local or distal metastasis when initially detected. The primary treatment modality is surgery. However, because these patients often present with advanced disease, the prognosis is usually poor, with an estimated overall 5-year survival rate of 30% (Dabaja *et al.,* 2004; Delaunoit *et al.,* 2004; Howe *et al.,* 1999).

Primary adenocarcinoma of the small intestine occurs more frequently in the duodenum, followed by the jejunum and ileum (Howe *et al.,* 1999). However, the majority of the duodenal tumors are seen at the vicinity of the ampulla of Vater (Ross *et al.,* 1991), constituting a special group of tumors (ampullary carcinoma) with two major histologic types: intestinal type arising from the duodenal mucosa overlying the papilla and pancreaticobiliary type originating from pancreatic or biliary ductal epithelium. The reason for ampullary/duodenal preponderance is unknown, but a link to the potential carcinogenic effect of bile acids has been suggested (Bernstein *et al.,* 2005; Stamp, 2002). In this chapter, we have included ampullary carcinoma in the discussion because the predominant histologic type, intestinal type, is morphologically indistinguishable from primary small intestinal adenocarcinoma of nonampullary origin.

Perhaps because of its rarity, the molecular mechanisms involved in small intestinal tumorigenesis are poorly understood. Existing data have shown that small

Handbook of Immunohistochemistry and *in situ* Hybridization of Human Carcinomas, Volume 4: Molecular Genetics, Gastrointestinal Carcinoma, and Ovarian Carcinoma

intestinal adenocarcinoma may share similar tumorigenic pathways with colorectal adenocarcinoma. Both types of tumors develop in an adenoma–carcinoma sequence, and some of the genetic abnormalities frequently detected in colorectal adenocarcinoma can also be demonstrated in small intestinal adenocarcinoma. Examples are mutations in the adenomatous polyposis coli (APC), β-catenin, K-*ras,* and *p53* genes; defects in the DNA (deoxyribonucleic acid) mismatch repair system, and mutations in genes involved in the TGF-β (transforming growth factor-beta)/Smad pathway (Delaunoit *et al.,* 2005). In addition, a number of identifiable risk factors thought to be important for the development of colorectal adenocarcinoma are also implicated in small intestinal tumorigenesis. These include familial adenomatous polyposis (FAP), hereditary nonpolyposis colorectal cancer syndrome (HNPCC), Peutz-Jeghers syndrome, Crohn disease, celiac disease, cystic fibrosis, cholecystectomy, and dietary factors. In fact, a significant number of patients with primary small intestinal adenocarcinoma may also concurrently develop colorectal cancers (Ripley and Weinerman, 1997).

In general, the histopathologic diagnosis of small intestinal adenocarcinoma is straightforward and does not require special ancillary tests. However, the rare and insidious nature of the disease may sometimes pose a diagnostic dilemma to pathologists, particularly when a metastasis is encountered, when the differential diagnosis is a colorectal adenocarcinoma, when the diagnostic material is a small biopsy, and when clinical information is incomplete. In addition, because it is not infrequent to have concurrent primary tumors in both the small intestine and the colorectum in the same patient, it may be similarly challenging to answer the question whether these two tumors represent two primaries or one primary with a metastasis. Furthermore, accurately categorizing ampullary carcinomas into either intestinal or pancreaticobiliary types may have important therapeutic and prognostic implications, but this may not always be easy based on histologic examination alone. In these scenarios, ancillary studies that may help delineate the tissue or cell origin would be very useful.

Cytokeratins (CK) are intracellular intermediate filaments consisting of more than 20 subtypes (Barak *et al.,* 2004; Chu and Weiss, 2002). They are selectively expressed during the course of differentiation in different types of epithelium, with a cell-type–specific expression pattern that usually remains unaltered during neoplastic transformation (Moll *et al.,* 1982). These characteristics make it possible to use unique CK expression profiles to facilitate differential diagnosis for tumors of unknown primary by suggesting potential cell origins. This is particularly true for CK7 and CK20, whose diagnostic value has been extensively explored (Chu *et al.,* 2000; Gown and Yaziji, 1999; Tot, 2002; Wang *et al.,* 1995). Specifically, immunohistochemical detection of CK20 expression in the absence of CK7 coexpression is relatively specific for colorectal adenocarcinoma, whereas a CK7-positive and CK20-negative pattern may suggest multiple possibilities but makes a colorectal origin highly unlikely.

MATERIALS

Equipment required to perform immunohistochemical staining described in this chapter includes a microtome, a waterbath, a drying oven, a microwave oven, a pH meter, a light microscope, a flat humid chamber, a timer, several staining jars and wash bottles, and an automated immunostainer (e.g., Dako autostainer, Carpinteria, CA). Other materials such as clean precoated glass slides (e.g., Snowcoat X-tra microslides from Surgipath, Winnipeg, Manitoba, Canada), coverslips (e.g., Gold Seal coverglass from Fisher Scientific, Pittsburgh, PA), and absorbent wipes are also needed.

Reagents needed for our protocol include xylene, ethanol (absolute and 95%), hydrogen peroxide (3%), distilled water, hematoxylin (e.g., hematoxylin 7211 from Richard-Allan Scientific, Kalamazoo, MI; or Mayer's hematoxylin), mounting medium (e.g., xylene-based Cytoseal XYL from Richard-Allan Scientific), 10 mM citrate buffer (pH 6.0), 0.05 M phosphate-buffered saline (PBS; pH 7.4), and 0.05 M Tris-buffered saline (TBS; pH 7.6). We use Dako LSAB+ kit, which contains link (secondary) antibodies that are biotinylated anti-mouse, anti-rabbit, and anti-goat immunoglobulins (Ig), and streptavidin conjugated to horseradish peroxidase. Dako liquid diaminobenzidine (DAB) + substrate–chromogen system is used for color visualization, which contains 3,3′-DAB in chromogen solution, and buffered substrate (imidazole-HCl buffer, pH 7.5, with hydrogen peroxide). Primary antibodies are mouse IgG_1 against CK7 (clone OV-TL 12/30) and mouse IgG_{2a} against CK20 (clone Ks20.8) purchased from Dako. Nonhuman reactive mouse IgG (e.g., from Dako) is used for negative controls. Antibodies are diluted using the antibody diluent obtained from Dako.

METHOD

1. Cut formalin-fixed and paraffin-embedded tissue blocks at 4-μM thickness onto precoated glass slides using a microtome and a waterbath.
2. Dry slides in 56°C oven for 45 min.
3. Deparaffinize sections in xylene with 3 changes of 3 min each.
4. Rehydrate sections as follows:
   a. Absolute ethanol with 3 changes, 15–20 dips each.

b. 95% Ethanol with 2 changes, 15–20 dips each.
c. Distilled water with 2 changes, 15–20 dips each.

5. Incubate slides in 3% hydrogen peroxide for 15 min at room temperature.
6. Rinse slides with distilled water.
7. Place slides in 10 mM citrate buffer (pH 6.0) and heat in a microwave oven for 10 min.
8. Allow slides to cool in the buffer for ~20 min.
9. Rinse slides with distilled water.
10. Incubate slides in 0.05 M PBS (pH 7.4) for 10 min at room temperature.
11. Drain slides and wipe carefully around the tissue with absorbent wipes. Leave a fine film of PBS and do not let tissue dry.
12. Apply enough (usually 100–200 µL depending on the size of the tissue section) primary antibody diluted in antibody diluent to each slide to cover the entire tissue (1:1200 dilution for anti-CK7 antibody and 1:30 for anti-CK20 antibody).
13. Place slides (with primary antibody) in a flat humid chamber lined with wet paper towels to maintain a moist environment, and incubate at room temperature for 1 hr.
14. Remove the primary antibody and wash slides with PBS in a wash bottle with 3 changes for 5 min each.
15. Drain and wipe slides as described in **Step 11.**
16. Apply enough biotinylated link (secondary) antibodies to each slide to cover the entire tissue.
17. Incubate in the flat humid chamber at room temperature for 30 min.
18. Remove the link antibodies and wash slides with PBS in a wash bottle with 3 changes for 5 min each.
19. Drain and wipe slides as described earlier.
20. Apply enough streptavidin-horseradish peroxidase solution to each slide to cover the entire tissue.
21. Incubate in the flat humid chamber at room temperature for 30 min.
22. Remove the streptavidin-horseradish peroxidase solution and wash slides with PBS in a wash bottle with 3 changes of 5 min each.
23. Drain and wipe slides as described earlier.
24. Apply enough substrate-chromogen solution to each slide to cover the entire tissue. This solution is prepared before use by mixing 1 drop (~20 µL) of DAB chromogen solution with 1 mL of buffered substrate.
25. Incubate at room temperature for 30 sec to 10 min until desired brown color is developed as determined by examination under a light microscope.
26. Wash slides with tap water for 5 min, with 2 changes, to completely remove DAB.
27. Counterstain slides with hematoxylin for 3 min in a staining jar.
28. Rinse in running tap water until water becomes clear.
29. Dehydrate slides as follows:
    a. 95% Ethanol with 2 changes, 15–20 dips each.
    b. Absolute ethanol with 3 changes, 15–20 dips each.
    c. Xylene with 3 changes of 3 min each.
30. Mount slides with xylene-based permanent medium (such as Cytoseal XYL) and coverslips, and analyze under a light microscope.

If an automated immunostainer is used, slides are loaded into the machine after deparaffinization and antigen retrieval with 10 mM citrate buffer. The procedure may then be programmed as 3% hydrogen peroxide treatment for 5 min, primary antibody incubation for 1 hr, link antibody 15 min, streptavidin-horseradish peroxidase 15 min, and substrate-chromogen 5 min. The volume used for each reagent is 200 µL. The wash solution used between steps is 0.05 M TBS instead of PBS. The counterstaining and mounting procedures are performed manually as described earlier.

Ideally, tissue sections selected for immunohistochemical studies should contain both tumor and histologically normal-appearing mucosa so that a comparison between tumor and normal tissue can be made. The normal intestinal mucosa also serves as "built-in" negative controls for the expression of CK7 and positive controls for CK20. Another negative control should also always be included in each run, in which the primary antibody is omitted (only antibody diluent is used) or replaced by nonhuman reactive mouse IgG.

RESULTS AND DISCUSSION

Positive immunoreactivity to anti-CK7 and anti-CK20 antibodies is evidenced by cytoplasmic staining. Similar to normal colorectal mucosa, normal small intestinal epithelial cells (including those lining the ampulla of Vater) do not express CK7 (Figure 51A) but exhibit strong and diffuse cytoplasmic staining for CK20 (see Figure 51B). This pattern is opposite to that seen in epithelial cells lining the pancreaticobiliary tree that express CK7 but not CK20.

A variation in the degree of immunoreactivity may be observed in tumors. The staining may be diffuse or focal, strong or weak. There has been no consensus regarding how many tumor cells are needed to show positive staining for a tumor to be considered positive. The criteria described in the literature vary widely, from any number of cells to 50%, depending on different investigators. As discussed later, this variation may be problematic in interpreting immunostaining data. In our laboratory, we usually use 10% as a cutoff—that is,

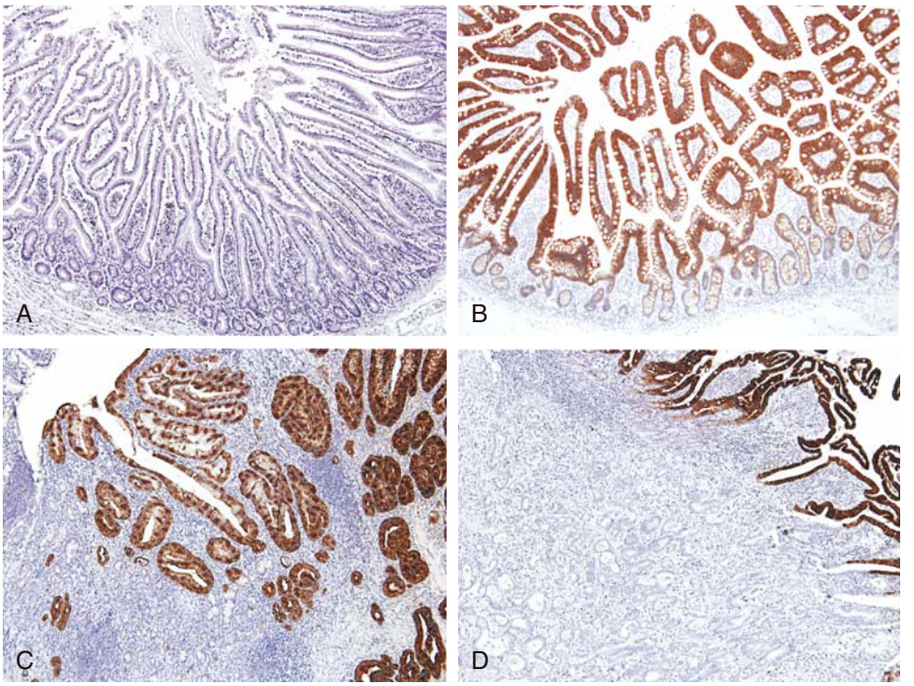

Figure 51. Immunohistochemistry showing negative staining for CK7 **(A)** but positive staining for CK20 **(B)** in normal small intestinal epithelium. This was in contrast to small intestinal adenocarcinoma that exhibited positive staining for CK7 **(C)** and negative staining for CK20 **(D)**. Note that the adjacent nonneoplastic small intestinal mucosa stained negative for CK7 (**C;** *left lower*) and positive for CK20 (**D;** *right upper*) (original magnification 100X).

a tumor is considered positive if greater than 10% of the tumor cells exhibit immunoreactivity to a specific antibody.

For the ease of discussion, we divide small intestinal adenocarcinomas into two subgroups: nonampullary and ampullary. For nonampullary tumors, we emphasize the role of CK7 and CK20 expression patterns in the distinction between small intestinal and colorectal adenocarcinomas. For ampullary tumors, we focus our discussion on whether CK7 and CK20 expression patterns can be used to facilitate an accurate histologic subcategorization of these tumors.

Role of CK7 and CK20 Expression Patterns in Distinguishing Small Intestinal Adenocarcinoma from Colorectal Adenocarcinoma

By studying 24 primary, nonampullary adenocarcinomas of the small intestine by immunohistochemistry (Chen and Wang, 2004), we demonstrated a unique CK7 and CK20 expression pattern that differed markedly from those observed in normal small intestinal mucosa from which these tumors originate and in colorectal adenocarcinoma. As mentioned earlier, normal small intestinal mucosa universally expressed CK20 but not CK7 (see Figure 51A and 51B). On the contrary, all small intestinal adenocarcinomas we examined exhibited a variable degree of CK7 expression (see Figure 51C). More specifically, 13 tumors (54%) showed diffuse cytoplasmic staining (greater than 50% of the tumor cells positively stained), and the remaining 11 cases exhibited focal immunoreactivity (at least 10% of the tumor cells stained). The staining intensity was strong in the majority of the cases (79%). It is interesting that, 8 tumors (33%) completely lost CK20 immunoreactivity when compared with adjacent nonneoplastic small intestinal mucosa (see Figure 51D). Although the other 16 tumors retained CK20 immunoreactivity, the staining was focal in 8 cases. Therefore, small intestinal adenocarcinomas either co-express CK7 and CK20 or express CK7 only.

For comparison, our study included 23 colorectal adenocarcinomas secondarily involving the small intestine by direct extension or metastasis. In these cases, 22 (96%) showed strong immunoreactivity to

anti-CK20 antibody, among which a diffuse staining pattern was observed in 19 cases. Only 1 case showed focal CK7 expression.

In summary, our study demonstrates a marked difference in CK7 and CK20 expression between small intestinal and colorectal adenocarcinomas. The expression patterns in small intestinal adenocarcinomas are similar to those reported for pancreaticobiliary carcinomas (Chu and Weiss, 2002)—that is, approximately two-thirds of the tumors express both CK7 and CK20, and the other one-third express CK7 only. In contrast, the vast majority of colorectal adenocarcinomas show a CK7-negative and CK20-positive staining pattern (Chu *et al.,* 2000; Gown and Yaziji, 1999; Tot, 2002; Wang *et al.,* 1995). These characteristic CK7 and CK20 expression profiles appear to be of diagnostic value in the distinction between adenocarcinomas of the small intestinal and colorectal origins.

An interesting finding in our study was that the reciprocal emergence of CK7 and loss of CK20 occurred early in small intestinal tumorigenesis, observed in adenomatous epithelium overlying the invasive adenocarcinoma. In those tumors where CK20 expression was completely lost, a sharp transition from CK7-negative, CK20-positive nonneoplastic, normal-appearing enterocytes to CK7-positive, CK20-negative adenomatous epithelial cells was evident. It remains unclear at the present, however, why enterocytes in the small intestine differ from those in the colorectum by gaining CK7 immunoreactivity while losing CK20 expression during neoplastic transformation. We suspect that it may be related to different regulatory mechanisms involved in the development of these two different types of intestinal tumors. In this sense, CK7 and CK20 may serve not only as diagnostic markers but also as important targets to investigate the molecular pathways critical to intestinal tumorigenesis.

In a study on the expression of cytokeratins and apomucins in primary carcinomas of the digestive system, Lee *et al.* (2003) also examined CK7 and CK20 expression in small intestinal adenocarcinomas. Although they also reported a higher frequency of CK7 expression and a lower frequency of CK20 expression in small intestinal adenocarcinomas relative to colorectal adenocarcinomas, their results appeared to differ somewhat from ours because only 8 of 23 small intestinal tumors (35%) they studied expressed CK7 and only 11 (48%) were positive for CK20. Moreover, these authors observed a marked variation in the frequency of CK20 expression based on tumor location in the small intestine; only 2 of 14 tumors (14%) from the duodenum showed positive CK20 staining in contrast to 9 of 9 tumors (100%) from the jejunum and ileum. This topographic variation was not evident in our study (Chen and Wang, 2004). However, we had only 2 duodenal tumors in our study because the majority of the duodenal adenocarcinomas were excluded because of their potential ampullary origin. Nevertheless, the discrepancy between our observations and those by Lee *et al.* may be partially explained by the fact that the immunohistochemical studies by Lee *et al.* were performed on tissue arrays, whereas ours used whole-tissue sections. It is conceivable that the validity of information derived from tissue-array studies may be relatively limited because only a tiny area from each tumor is examined. This is particularly true considering that a large fraction of the small intestinal adenocarcinomas in our study showed focal immunoreactivity in less than 50% of the tumor cells for both CK7 and CK20, seen in 46% and 67% of the cases, respectively. As we mentioned earlier, the interpretation of immunohistochemical results by different observers may also vary. Cases interpreted as weak or focal positive staining by some investigators may be considered negative by others.

Role of CK7 and CK20 Expression Patterns in Histologic Subclassification of Ampullary Adenocarcinomas

Ampullary carcinomas have been traditionally subclassified into several histologic types (Albores-Saavedra *et al.,* 2000). As mentioned in the Introduction, the intestinal and pancreaticobiliary types are the most common adenocarcinomas in this special anatomic region. From a clinical point of view, separating these two types may have important therapeutic significance because they may respond to different regimens of therapy. The intestinal type has also been shown to bear a better prognosis than the pancreaticobiliary type (Kimura *et al.,* 1994). The distinction may be facilitated by microscopic recognition of subtle histologic differences and identification of precursor lesions, such as adenomatous change or carcinoma *in situ,* present either on the mucosal surface of the duodenum or in the epithelium lining the pancreaticobiliary duct. In practice, however, this distinction may not always be straightforward based on histologic examination alone.

Zhou *et al.* (2004) studied 55 ampullary adenocarcinomas, among which 15 cases were classified as intestinal type and 24 as pancreaticobiliary type based on histologic analysis. On immunohistochemical examination, 27% and 80% of the tumors of intestinal type expressed CK7 and CK20, respectively. This was in marked contrast to the pancreaticobiliary type, in which 96% and 8% of the tumors showed CK7 and CK20 expression. Using CK7 and CK20 expression patterns

as arbitrary immunohistochemical classification criteria (i.e., CK7-negative/CK20-positive for intestinal type and CK7-positive/CK20-negative for pancreaticobiliary type), these authors demonstrated a good correlation between histologic and immunohistochemical classification criteria. In their series, 9 of 15 (60%) carcinomas of histologically intestinal type showed intestinal type cytokeratin pattern, and 21 of 24 (88%) tumors of histologically pancreaticobiliary type exhibited pancreaticobiliary pattern immunohistochemically. Using the same approach, the authors were also able to classify some of the ampullary carcinomas of unusual histologic type (such as signet-ring cell carcinoma and undifferentiated carcinoma) into either intestinal or pancreaticobiliary types. These data suggest that CK7 and CK20 are useful immunohistochemical markers for aiding in the subclassification of ampullary carcinomas, but additional markers, such as apomucins, appear to be necessary to achieve a higher accuracy for the distinction.

Chu *et al.* (2005) examined a number of immunohistochemical markers in pancreaticobiliary and ampullary adenocarcinomas. In this study, 18 ampullary adenocarcinomas were included, among which 7 were of intestinal type and 6 were of pancreaticobiliary type based on histologic analysis. Their results showed positive CK7 immunostaining in 5 of 7 (71%) tumors of intestinal type and all 6 tumors of pancreaticobiliary type. CK20 expression was observed in 6 (86%) intestinal type ampullary carcinomas but in only 1 (17%) pancreaticobiliary-type tumor. Although this study demonstrates that ampullary carcinomas of pancreaticobiliary type predominantly exhibit a CK7-positive/CK20-negative pattern, whereas those of intestinal type co-express CK7 and CK20 more frequently, their data again indicate the necessity to expand the immunomarker panel. Based on their results, the authors recommended adding CDX2, CK17, MUC1, and MUC2. The histologically intestinal-type tumors appear to correlate well with an immunophenotype of negative MUC1 and CK17 and positive CK20, MUC2, and CDX2. In contrast, the histologically pancreaticobiliary-type ampullary adenocarcinomas tend to show positive staining for MUC1, CK7, and CK17 and negative staining for CK20, MUC2, and CDX2. Based on this study, it appears that CK17, CDX2, MUC1, and MUC2 are more valuable markers when used in combination than CK7 and CK20 for the differential diagnosis. When an ampullary adenocarcinoma stains positive for both CK17 and MUC1, the positive predictive value for pancreaticobiliary origin is 83% and the negative predictive value for intestinal type is 100%. However, co-expressing MUC2 and CDX2 have a positive predictive value of 82% for intestinal type and a negative predictive value of 100% for pancreaticobiliary type.

Our own studies on ampullary adenocarcinomas also showed similar results and demonstrated that tumors with histologic features suggesting an intestinal origin expressed CK7 and CK20 in similar patterns to those observed in nonampullary small intestinal adenocarcinomas (Chen *et al.,* 2005). More specifically, CK7 and CK20 expression was detected in 22 (92%) and 16 (67%) of 24 ampullary tumors of intestinal type in our series. This is in contrast to tumors of pancreaticobiliary type, where all 7 cases showed CK7 expression but only 1 case (14%) showed positive CK20 staining. Similar to nonampullary small intestinal adenocarcinomas, intestinal-type ampullary carcinomas either co-expressed both types of cytokeratins (58%) or expressed CK7 only (33%). The classic colorectal pattern (i.e., CK7-negative/CK20-positive) was seen in only 2 tumors (8%) of this type. On the contrary, pancreaticobiliary-type ampullary carcinomas predominantly exhibited a CK7-positive and CK20-negative staining pattern. It is interesting that positive staining for CK7 was almost always diffuse, seen in 93% of the cases, irrespective of histologic type. Focal positivity was more common for CK20, observed in 47% of the cases. Therefore, our study confirms the value of CK7 and CK20 immunostains in separating ampullary carcinomas into different histologic types and further emphasizes the need for more specific immunomarkers.

SUMMARY

In conclusion, the current literature, albeit scarce, supports a role of immunohistochemical staining for cytokeratins, particularly CK7 and CK20, to help differentiate adenocarcinomas of small intestinal primary from colorectal origin and to help separate ampullary carcinomas into different histologic types. In addition, because the CK7 and CK20 expression pattern in normal small intestinal mucosa is uniquely altered in neoplasms, these molecules may serve as important tools to investigate molecular mechanisms involved in small intestinal tumorigenesis, which are apparently different from those occurring in colorectal tumorigenesis. These future investigations may not only enhance our understanding of intestinal tumorigenesis; they may also lead to the discovery of more useful biomarkers to assist differential diagnosis in our daily practice.

References

Abrahams, N.A., Halverson, A., Fazio, V.W., Rybicki, L.A., and Goldblum, J.R. 2002. Adenocarcinoma of the small bowel: a study of 37 cases with emphasis on histologic prognostic factors. *Dis. Colon Rectum 45*:1496–1502.

Albores-Saavedra, J., Henson, D.E., and Klimstra, D.S. 2000. Tumors of the gallbladder, extrahepatic bile ducts, and ampulla of Vater. In: J. Rosai and L. Sobin (eds.). *Atlas of Tumor Pathology, Third Series, Fascicle 27*. Armed Forces Institute of Pathology, Washington D.C., 259–316.

Barak, V., Goike, H., Panaretakis, K.W., and Einarsson, R. 2004. Clinical utility of cytokeratins as tumor markers. *Clin. Biochem. 37*:529–540.

Bernstein, H., Bernstein, C., Payne, C.M., Dvorakova, K., and Garewal, H. 2005. Bile acids as carcinogens in human gastrointestinal cancers. *Mutat. Res. 589*:47–65.

Chen, Z.M., Ritter, J.H., and Wang, H.L. 2005. Differential expression of α-methylacyl coenzyme A racemase in adenocarcinomas of the small and large intestines. *Am. J. Surg. Pathol. 29*: 890–896.

Chen, Z.M., and Wang, H.L. 2004. Alteration of cytokeratin 7 and cytokeratin 20 expression profile is uniquely associated with tumorigenesis of primary adenocarcinoma of the small intestine. *Am. J. Surg. Pathol. 28*:1352–1359.

Chow, J.S., Chen, C.C., Ahsan, H., and Neugut, A.I. 1996. A population-based study of the incidence of malignant small bowel tumours: SEER, 1973–1990. *Int. J. Epidemiol. 25*: 722–728.

Chu, P.G., Schwarz, R.E., Lau, S.K., Yen, Y., and Weiss, L.M. 2005. Immunohistochemical staining in the diagnosis of pancreatobiliary and ampulla of Vater adenocarcinoma: application of CDX2, CK17, MUC1, and MUC2. *Am. J. Surg. Pathol. 29*:359–367.

Chu, P.G., and Weiss, L.M. 2002. Keratin expression in human tissues and neoplasms. *Histopathology 40*:403–439.

Chu, P., Wu, E., and Weiss, L.M. 2000. Cytokeratin 20 expression in epithelial neoplasms: a survey of 435 cases. *Mod. Pathol. 13*:962–972.

Dabaja, B.S., Suki, D., Pro, B., Bonnen, M., and Ajani, J. 2004. Adenocarcinoma of the small bowel: presentation, prognostic factors, and outcome of 217 patients. *Cancer 101*:518–526.

Delaunoit, T., Neczyporenko, F., Limburg, P.J., and Erlichman, C. 2004. Small bowel adenocarcinoma: a rare but aggressive disease. *Clin. Colorectal Cancer 4*:241–251.

Delaunoit, T., Neczyporenko, F., Limburg, P.J., and Erlichman, C. 2005. Pathogenesis and risk factors of small bowel adenocarcinoma: a colorectal cancer sibling? *Am. J. Gastroenterol. 100*:703–710.

Donohue, J.H. 1994. Malignant tumours of the small bowel. *Surg. Oncol. 3*:61–68.

Dunsmore, K.P., and Lovell, M.A. 1998. Small bowel adenocarcinoma metastatic to the ovaries in a 12-year-old girl. *J. Pediatr. Hematol. Oncol. 20*:498–501.

Frost, D.B., Mercado, P.D., and Tyrell, J.S. 1994. Small bowel cancer: a 30-year review. *Ann. Surg. Oncol. 1*:290–295.

Gown, A.M., and Yaziji, H. 1999. Immunohistochemical analysis of carcinomas of unknown primary site. *Pathol. Case Rev. 4*:250–259.

Howe, J.R., Karnell, L.H., Menck, H.R., and Scott-Conner, C. 1999. The American College of Surgeons Commission on Cancer and the American Cancer Society: adenocarcinoma of the small bowel—review of the National Cancer Data Base, 1985–1995. *Cancer 86*:2693–2706.

Kimura, W., Futakawa, N., Yamagata, S., Wada, Y., Kuroda, A., Muto, T., and Esaki, Y. 1994. Different clinicopathologic findings in two histologic types of carcinoma of papilla of Vater. *Jpn. J. Cancer Res. 85*:161–166.

Lee, M.J., Lee, H.S., Kim, W.H., Choi, Y., and Yang, M. 2003. Expression of mucins and cytokeratins in primary carcinomas of the digestive system. *Mod. Pathol. 16*:403–410.

Moll, R., Franke, W.W., Schiller, D.L., Geiger, B., and Krepler, R. 1982. The catalog of human cytokeratins: patterns of expression in normal epithelia, tumors and cultured cells. *Cell 31*:11–24.

Neugut, A.I., Jacobson, J.S., Suh, S., Mukherjee, R., and Arber, N. 1998. The epidemiology of cancer of the small bowel. *Cancer Epidemiol. Biomarkers Prev. 7*:243–251.

North, J.H., and Pack, M.S. 2000. Malignant tumors of the small intestine: a review of 144 cases. *Am. Surg. 66*:46–51.

O'Riordan, B.G., Vilor, M., and Herrera, L. 1996. Small bowel tumors: an overview. *Dig. Dis. 14*:245–257.

Ripley, D., and Weinerman, B.H. 1997. Increased incidence of second malignancies associated with small bowel adenocarcinoma. *Can. J. Gastroenterol. 11*:65–68.

Ross, R.K., Hartnett, N.M., Bernstein, L., and Henderson, B.E. 1991. Epidemiology of adenocarcinomas of the small intestine: is bile a small bowel carcinogen? *Br. J. Cancer 63*:143–145.

Stamp, D.H. 2002. Three hypotheses linking bile to carcinogenesis in the gastrointestinal tract: certain bile salts have properties that may be used to complement chemotherapy. *Med. Hypotheses 59*:398–405.

Tot, T. 2002. Cytokeratins 20 and 7 as biomarkers: usefulness in discriminating primary from metastatic adenocarcinoma. *Eur. J. Cancer 38*:758–763.

Wang, N.P., Zee, S., Zarbo, R.J., Bacchi, C.E., and Gown, A.M. 1995. Coordinate expression of cytokeratins 7 and 20 defines unique subsets of carcinomas. *Appl. Immunohistochem. 3*:99–107.

Zhou, H., Schaefer, N., Wolff, M., and Fischer, H.P. 2004. Carcinoma of the ampulla of Vater: comparative histologic/immunohistochemical classification and follow-up. *Am. J. Surg. Pathol. 28*:875–882.

This Page Intentionally Left Blank

24

Quantitative Immunohistochemistry by Determining the Norm of the Image Data File

Kristina A. Matkowskyj, Randal Cox, and Richard V. Benya

Introduction

In the predigital period, quantitative immunohistochemistry (Q-IHC) relied exclusively on the interpretation of several investigators using a subjective scale to grade the intensity of chromogen staining. The information generated by the subjective scales was of a limited usefulness because most approaches used quantification scales ranging between 0 and 4 (Shi *et al.,* 1991; 1993). By this method a score of 0 indicated less than 20% of all cells stained with chromogen, whereas a score of 4 indicated that greater than 80% of the cells contained in the image stained with chromogen. However, the data generated using this approach suffered from investigator subjectivity, bias, and inter- and intra-observer variation. With the introduction of digital photomicroscopy these weaknesses could potentially be eliminated. However, most digital algorithms involve either counting the total numbers of pixels stained or determining the area occupied by pixels of relevant color (Goldlust *et al.,* 1996; Kohlberger *et al.,* 1996; Kuyatt *et al.,* 1993; Lehr *et al.,* 1999; Ruifrok, 1997). These approaches suffer from a number of problems, however. First, pixel counting algorithms only provide information as to the percentage of a tissue stained and as such are limited to providing information about the relative—but not absolute—amount of chromogen present. Second, a tissue specimen may have a very small amount of chromogen spread over a large area, whereas another specimen may have a large amount of chromogen concentrated to a particularly small region such as the nucleus. In either case, pixel-counting methods over-estimate or underestimate the amount of chromogen, thereby providing data that are inconsistent with the actual experimental results.

To perform true Q-IHC, we devised an algorithm that takes advantage of the fact that digital images are stored as matrix files of dimension N_1 pixels $\times$ N_2 pixels $\times$ 3 in size; where (N_1,N_2) represents the image size and 3 is for the separate red, green, and blue grayscale values for each pixel. In our algorithm we calculate matrix size of the digital file encoding the image by calculating its norm. To quantify the amount of chromogen present as a result of antigen–epitope interaction, we determine

Handbook of Immunohistochemistry and *in situ* Hybridization of Human Carcinomas, Volume 4: Molecular Genetics, Gastrointestinal Carcinoma, and Ovarian Carcinoma

the square root of the sum of the squares for each grayscale value encoding each pixel in the image from the antibody-treated slide. We then perform the same process on the image acquired from the negative control slide. By subtracting the data of the negative-control image from the antibody-treated image data, the amount of chromogen specifically attributed to the primary antibody is identified and expressed as a value per pixel evaluated. Finally, we show that, at least for an antibody directed to a transmembrane-spanning receptor, the amount of protein detected using our algorithm for Q-IHC correlates with the amount determined to be present using pharmacologic techniques.

MATERIALS

A polyclonal rabbit anti-peptide antibody directed to the distal third intracellular loop (CVEGNI-HVKKQIESRKR) of the gastrin-releasing peptide receptor (GRPR) was used in these studies. An aliquot of this antibody was affinity purified and directly conjugated to horseradish peroxidase (GRPR-HRP) for studies described separately. Balb 3T3 cells were obtained from ATCC (Rockville, MD), whereas all tissue culture reagents were purchased from Fisher Scientific (Hanover Park, IL). The vector pcDNA2.1 was purchased from Invitrogen (Carlsbad, CA), whereas radionucleotides were obtained from Amersham (Arlington Heights, IL). 10X wash buffer, 10X target retrieval buffer, antibody diluent, large-volume LSAB2 kit, liquid DAB (diaminobenzidine) substrate-chromogen system, and automated hematoxylin were purchased from DakoCytomation Corporation (Carpinteria, CA). Images were analyzed and processed using TIFFalyzer software that we have written to process our algorithm and that is available as freeware downloadable at www.uic.edu/com/dom/gastro/Freedownloads.html.

METHODS

Immunohistochemistry

We performed IHC analysis on 6 cell lines stably transfected to express variable but known numbers of GRPR (Benya *et al.,* 1995). A three-stage indirect immunoperoxidase technique was performed on 4-µm thick sections that were hydrated in graded alcohols and rinsed in a running waterbath. Antigen retrieval was used for tissue sections submerged in 1X target retrieval solution for 30 min at 100°C in a steamer; slides were then allowed to cool to room temperature, followed by incubation for 5 min in a 3% hydrogen peroxide solution to quench endogenous peroxidase activity. Slides were rinsed using wash buffer, and the sections were incubated for 1 hour with a 1:750 dilution of the primary GRPR antibody resuspended in antibody diluent. In all instances, control tissues were processed simultaneously as the experimental slide with the exception that primary antibody was not applied. After rinsing with wash buffer, slides were incubated with biotinylated immunoglobulin G (IgG) for 10 min, rinsed, and then incubated with streptavidin conjugated to HRP for 10 min. The tissue sections were then rinsed and incubated with liquid DAB substrate-chromogen system for 5 min to identify bound antibody. Slides were counterstained with automated hematoxylin for 2 min after a final rinse with wash buffer and water, followed by dehydration in graded alcohols, and coverslips were mounted using Permount.

A sizeable tertiary complex of primary and secondary antibodies in association with avidin–biotin molecules is generated when using the avidin-biotin complex (ABC). To determine the extent of reagent saturation or steric inhibition resulting from this complex, a second immunohistochemical method was evaluated. Here, sections were treated with a 1:800 dilution of the GRPR-HRP antibody in antibody diluent. The biotinylated anti-rabbit IgG and streptavidin steps were omitted, and the bound antibody was directly visualized following a 5-min incubation with liquid DAB substrate. Sections were stained using automated hematoxylin for 2 min, dehydrated in graded alcohols, and mounted with a coverslip. As in the first method, control tissues were processed simultaneously with the exception that the GRPR-HRP antibody was not applied.

Immunohistochemistry Quantification

All photomicrographs were obtained at 1000X magnification using a SPOT RT Digital Scanning Camera (Diagnostic Instrument, Sterling Heights, MI), attached to a E600 microscope system (Nikon, Florham Park, NJ), and saved in uncompressed TIFF format. After acquisition of the relevant digital image, the file was opened in Photoshop (Adobe, San Jose, CA). The region of interest—brown cytoplasmic staining indicative of the DAB chromogen—was selected using the "Magic Wand" tool. The tool was touched to one discrete point on the image to select and highlight the pixels of interest, remove them, and then store them in a new TIFF-format file for further analysis (Matkowskyj *et al.,* 2000a,b; 2003a,b). The image for the control slides was generated similarly.

As indicated previously the norm for an image that is represented as a series of discrete variables can be expressed as follows:

$$\text{norm} = \left[\sum_{N_1=1}^{N_1}\sum_{N_2=1}^{N_2}\left[f_{RED}(n_1, n_2)\right]^2\right]^{1/2} + \left[\sum_{N_1=1}^{N_1}\sum_{N_2=1}^{N_2}\left[f_{GREEN}(n_1, n_2)\right]^2\right]^{1/2} + \left[\sum_{N_1=1}^{N_1}\sum_{N_2=1}^{N_2}\left[f_{BLUE}(n_1, n_2)\right]^2\right]^{1/2}$$

where n_1,n_2 identifies a specific pixel within the matrix. To calculate the chromogen-specific mathematic energy or E_M, we subtract the data obtained for the norm of the control image from that of the antibody-treated image such that:

$$E_M = \left|\text{norm (antibody)} - \text{norm (negative control)}\right|$$

RESULTS

BALB 3T3 cell lines were treated with either GRPR antibody (Figure 52A) or wash buffer as a negative control (Figure 52C), and then images were acquired at 1000X magnification. The regions representing cytoplasm were selected using the Magic Wand tool, and the highlighted pixels were digitally removed and saved in a new file on a pure white background in uncompressed TIFF format (Figure 52B and D). The norm for each file was then calculated using TIFFalyzer, and the E_M was determined by subtracting the "control" data from the "experimental" data. Alterations in chromogen intensity between the cell lines with the highest and lowest number of GRPR-binding sites (as determined previously (Benya *et al.,* 1995; Matkowskyj *et al.,* 2003) could be appreciated with the naked eye; in contrast, small differences between cell lines containing intermediate numbers of GRPR were nearly impossible to distinguish. However, when chromogen quantity was determined using our novel algorithm, a tight correlation was observed with the number of GRPR present in each cell line (Figure 53; Table 18). Yet the data was best fit using a logarithmic plot (Figure 53A; Line 1, $r^2 = 0.98$). This plotting of E_M as a function of increasing GRPR is not physiologically relevant and suggests the possibility that excessive epitope sites might be unable to be detected as a result of the steric inhibition of the large ABC. Indeed, when the cell line with the highest number of GRPR binding sites was discarded from analysis, a nonlogarithmic linear fit was observed (see Figure 53A; Line 2, $r^2 = 0.84$).

To examine whether steric hindrance could be occurring, we used our GRPR antibody that was directly conjugated to HRP. Using this modified antibody obviated the need for using the large ABC. When data obtained using standard antibody and ABC for cell lines expressing known numbers of receptors was compared with data obtained using antibody directly conjugated to HRP for cell lines expressing high numbers of receptor, a tight linear fit between E_M and GRPR could be detected (Figure 53B; Line 3, $r^2 = 0.96$).

DISCUSSION

In digital photography each pixel (n) contained within an image is represented by separate grayscale values for each of the 3 primary colors: red, green, and blue. Thus, any specific color is a linear combination of the 3 primary colors so that $f_i(n)$ is the intensity of color "i" represented by the number of pixels with gray level n. For the DAB-generated staining in our IHC, any pixel (n) can be represented by the following equation with the unique predetermined set of coefficients α_i, where i = 1,2,3 correspond to the color "brown":

$$f_{\text{"BROWN"}}(n) = \alpha_1 f_{RED}(n) + \alpha_2 f_{GREEN}(n) + \alpha_3 f_{BLUE}(n)$$

The coefficients in this equation are used to characterize the perceived, or "brown," color component of the image. Yet it is important to point out that "color" refers to what we see with our eyes. The cones of the eyes are able to absorb red, green, and blue light. These three types of cone cells provide us with our entire visual interpretation of color. The different combinations of these colors produce the entire visual spectrum. Many different combinations (demonstrated by the α coefficients) can thus produce exactly the same color sensation in our eyes, making the precise identification of the visual spectrum difficult. Although the visual spectrum contains precise information about the different combinations that cannot be measured or interpreted by the eyes, this information is readily available and extractable from the image digital file.

One may attempt to use this equation to isolate a specific color for quantitative purposes, but to do this, one must first experimentally determine the α coefficients. Because the coefficients change with wavelength, they must be determined for each sample. The wavelength is often unknown, however, making experimental determination of the α coefficients nearly impossible

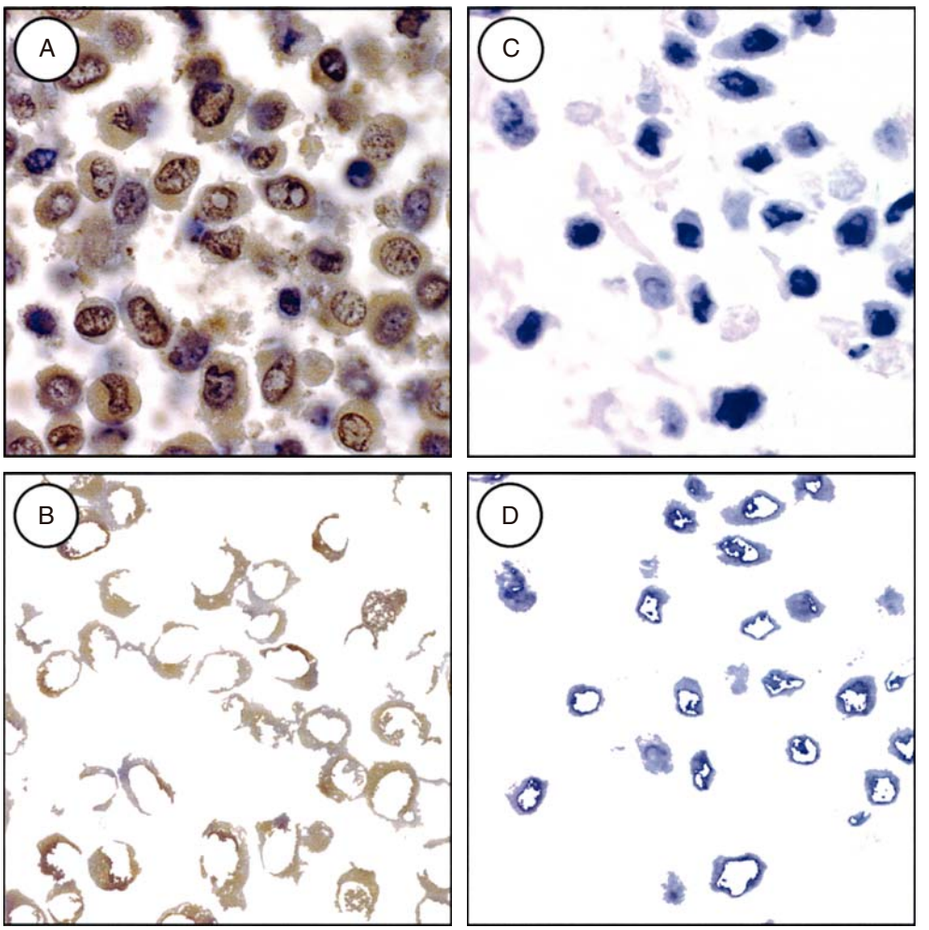

Figure 52. Overview of the Q-IHC (quantitative immunohistochemistry) algorithm for determining mathematic energy or E_M. Immunohistochemistry using an antibody to the GRPR (gastrin-releasing peptide receptor) was performed on cell lines, and the image was acquired at 1000X magnification using a digital scanning camera. The Photoshop Magic Wand tool was double-clicked to display the OPTIONS palette that permits tolerance values to be selected. Lower values, such as those between 0 and 50, identify colors similar in greyscale to the "index" pixel. Higher values, between 80 and 120, select a broader range of colors. We used a tolerance value of 30 by default. The "anti-aliasing" parameter was selected, but the "contiguous" parameter was deselected in the OPTIONS palette. These choices allowed for pixels of similar color that may not be immediately adjacent to the "index" pixel but perhaps farther away in the image to be included for quantitative analysis. **A:** Section from Balb 3T3 cells stably transfected to express 63,000 GRPRs were treated immunohistochemically with GRPR antibody. **B:** The digitally dissected image from Panel A has been saved as a new file on a white background and used for TIFFalyzer analysis. **C:** Section from Balb 3T3 cells stably transfected to express 63,000 GRPRs not treated with antibody, serving as a negative control. **D:** The digitally dissected image from Panel C has been saved as a new file on a white background and used for TIFFalyzer analysis.

and of limited usefulness. Chromogen-positive pixels in an experimental image represent the visual spectrum specified by the chromogen as well as the visual spectrum of the original specimen image (i.e., often dictated by the counterstain). Thus, identification of only the visual spectrum of the chromogen on the original image is not sufficient for true Q-IHC. Furthermore, if an algorithm for the detection of "brown" color could be established using the previous equation, its use would not be transferable for use in the quantification of other color-detection systems. As indicated previously, the visual spectrum and information regarding

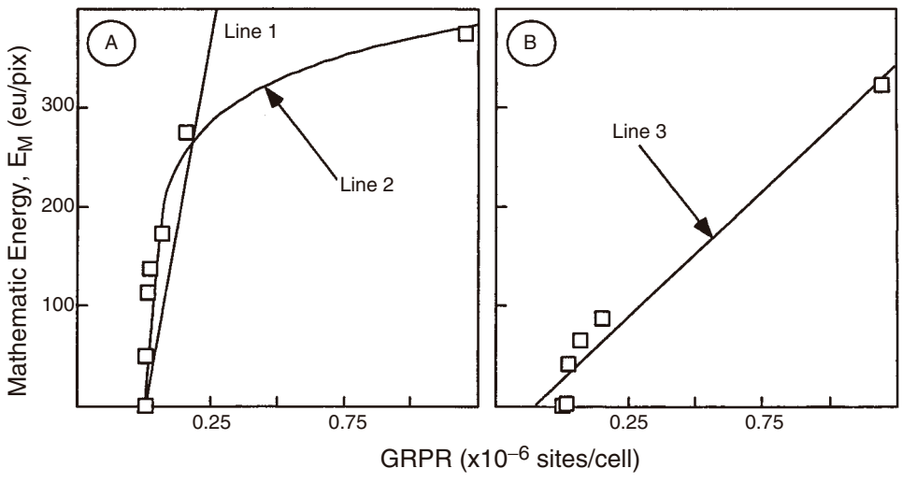

Figure 53. Mathematic energy or E_M is linearly associated with GRPR (gastin-releasing peptide receptor) number. Sections from Balb 3T3 cells stably transfected to express variable, but known numbers of GRP receptors were treated immunohistochemically with GRPR antibody. **A:** Chromogen quantity correlated logarithmically when all cell lines were evaluated using the unmodified GRPR primary antibody (Line 1; $r^2 = 0.98$). A linear fit was generated when data from the cell line expressing the highest number of receptors is eliminated (Line 2; $r^2 = 0.84$). **B:** In contrast, GRPR-HRP (horseradish peroxidase) antibody was necessary to achieve a tight linear fit when including the data from all the cell lines (Line 3; $r^2 = 0.96$). For graphic clarity, standard errors that were minimal are not shown.

the different combinations are contained in the image's digital data file. Using the digital data contained within the antibody-treated slide and subtracting the digital data obtained from the negative control allow for these limitations to be circumnavigated.

Using this algorithm for Q-IHC, we have successfully demonstrated the ability to quantify small and large concentrations of GRPR, a transmembrane-spanning receptor. An interesting observation was made regarding the ABC that is commonly used to amplify the chromogen signal. When small numbers of antigenic sites are evaluated, E_M values plateau as the GRPR number increased beyond 55,000 binding sites/cell. Direct conjugation of our GRPR antibody with HRP suggests that this plateau is the result of the large size of the primary antibody and ABC that inhibits the binding of additional molecules. It is possible to circumvent this obstacle by using a primary antibody that is directly conjugated to HRP. Hence, with appropriate antibodies, it is possible to assess protein quantity (i.e., receptor number) over a 10^4-fold range. In data not shown here, we evaluated archived human colon cancer specimens for GRPR expression. Our data demonstrate that well-differentiated tumor cells within any particular human colon had an E_M of 247.7 ± 5.7 eu/pix, moderately differentiated tumors expressed 161.1 ± 7.8 eu/pix, and poorly differentiated tumors had GRPR expression levels of 10.4 ± 1.1 eu/pix. Based on the data generated in this study and the type of antibody used, these results indicated that ~55,000 GRPR per cell are expressed by well-differentiated and 10,000 receptors by moderately differentiated colon cancers. In contrast, poorly differentiated colon cancers do not express significant numbers of GRPR. The ~50-fold difference in GRPR expression between well- and poorly differentiated colon cancers provides much more information than that obtained from analog images using a 0–4 grading scale; it also

Table 18. Determination of Cumulative Signal Strength (E_M) and Gastrin-Releasing Peptide Receptor (GRPR) Number

Cell Line	GRPR (B_{MAX})	E_M GRPR	E_M GRPR-HRP
1	5,800	49 ± 2	0.5 ± 0.2
2	13,000	114 ± 1	25 ± 1
3	21,000	138 ± 2	42 ± 1
4	63,000	173 ± 5	66 ± 2
5	150,000	276 ± 14	87 ± 1
6	1,200,000	286 ± 11	324 ± 10

B_{MAX}, maximal binding as determined by Scatchard analysis of the binding data; E_M, mathematic energy expressed in the unitless values of energy units per pixel (eu/pix); GRPR, data generated using the unmodified antibody; GRPR-HRP (horseradish peroxidase), data generated using the modified antibody.

permits precise quantification of protein at the cellular level from relatively rare, archived human tissues.

This algorithm also allows for the precise quantification of chromogen contained within small structures as well as subcellular regions. For example, we have used this algorithm to identify the amount of focal adhesion kinase (FAK) contained within the cytoplasm (Matkowskyj *et al.,* 2003), proliferating cell nuclear antigen (PCNA) staining in the nucleus (Carroll *et al.,* 2002), or *Her2/Neu* present in the cell membrane (data not published). Likewise, we have quantified chromogen in distinct cell populations such as galanin in colonic nerves and galanin-1 receptor in specific regions of small intestinal villi.

The use of a nonsubjective algorithm for quantitating immunohistochemically generated chromogen is increasingly more important in the clinical arena. For example, treatment of patients with breast cancer with trastuzumab (Herceptin) depends on the amount of tumor cell *HER2/Neu* expression as assessed immunohistochemically. This is currently determined using a 0–4 staining scale such that patients whose tumors are $\geq 2^+$ immunopositive receive chemotherapy treatment, whereas patients whose tumor cells are graded <2 do not (Nunes and Harris, 2002; Spigel and Burstein, 2002). Yet this approach is fraught with problems relating to interpretation consistency. One in five samples read at community hospitals for *HER2/Neu* immunopositivity is overinterpreted compared to those at a facility using a gold standard (Paik *et al.,* 2002), suggesting that the larger laboratories may have the advantage of image analysis systems that may not be available to smaller facilities. With algorithms such as the one we described herein now available as freeware, replacing subjective grading of immunohistochemically generated chromogen with true Q-IHC is now readily achievable and can be routinely and inexpensively accomplished.

References

Benya, R.V., Kusui, T., Pradhan, T.K., Battey, J.F., and Jensen, R.T. 1995. Expression and characterization of cloned human bombesin receptors. *Mol. Pharmacol. 147*:10–20.

Carroll, R.E., Matkowskyj, K., Saunthararajah, Y., Sekosan, M., Battey, J.F., and Benya, R.V. 2002. Contribution of gastrin-releasing peptide and its receptor to villus development in the murine and human gastrointestinal tract. *Mech. Dev. 113*:121–130.

Goldlust, E.J., Paczynski, R.P., He, Y.Y., Hsu, C.Y., and Goldberg, M.P. 1996. Automated measurement of infarct size with scanned images of triphenyltetrazolium chloride-stained rat brains. *Stroke 27*:1657–1662.

Jain, A.K. 1989. *Fundamentals of Digital Image Processing.* Englewood Cliffs, NJ: Prentice-Hall.

Kohlberger, P.D., Obermair, A., Sliutz, G., Heinzl, H., Koelbl, H., Breitenecker, G., Gitsch, G., and Kainz, C. 1996. Quantitative immunohistochemistry of factor VIII-related antigen in breast carcinoma. *Am. J. Clin. Pathol. 105*:705–710.

Kuyatt, B., Reidy, C.A., Hui, K.Y., and Jordan, W.H. 1993. Quantitation of smooth muscle proliferation in cutured aorta: a color image analysis method for the Macintosh. *Anal. Quant. Cytol. Histol. 15*:83–87.

Lehr, H.A., Mankoff, D.A., Corwin, D., Santeursanio, G., and Gown, A.M. 1997. Application of Photoshop-based image analysis to quantification of hormone receptor expression in breast cancer. *J. Histochem. Cytochem. 45*:1559–1565.

Lehr, H.A., Van der Loos, C.M., Teeling, P., and Gown, A.M. 1999. Complete chromogen separation and analysis in double immunohistochemical stains using Photoshop-based image analysis. *J. Histochem. Cytochem. 47*:119–125.

Matkowskyj, K.A., Cox, R., Jensen, R.T., and Benya, R.V. 2003a. Quantitative immunohistochemistry by measuring cumulative signal strength accurately measures receptor number. *J. Histochem. Cytochem. 51*:205–214.

Matkowskyj, K.A., Danilkovich, A., Marrero, J., Savkovic, S.D., Hecht, G., and Benya, R.V. 2000b. *Galanin-1 receptor up-regulation* mediates the excess colonic fluid production caused by infection with enteric pathogens. *Nat. Med. 6*:1048–1051.

Matkowskyj, K.A., Keller, K., Glover, S., Kornberg, L., Tran-Son-Tay, R., and Benya, R.V. 2003b. Expression of GRP and its receptor in well-differentiated colon cancer cells correlates with the presence of focal adhesion kinase phosphorylated at tyrosines 397 and 407. *J. Histochem. Cytochem. 51*: 1041–1048.

Matkowskyj, K.A., Schonfeld, D., and Benya, R.V. 2000a. Quantitative immunohistochemistry by measuring cumulative signal strength using commercially available software Photoshop and Matlab. *J. Histochem. Cytochem. 48*:303–311.

Nunes, R.A., and Harris, L.N. 2002. The HER2 extracellular domain as a prognostic and predictive factor in breast cancer. *Clin. Breast Cancer 3*:125–135.

Paik, S., Bryant, J., Tan-Chiu, E., Romond, E., Hiller, W., Park, K., Brown, A., Yothers, G., Anderson, S., Smith, R., Wickerham, D.L., and Wolmark, N. 2002. Real-world performance of HER2 testing: National Surgical Adjuvant Breast and Bowel Project experience. *J. Natl. Cancer Inst. 94*:852–854.

Ruifrok, A.C. 1997. Quantification of immunohistochemical staining by color translation and automated thresholding. *Anal. Quant. Cytol. Histol. 19*:107–113.

Shi, S.R., Chaiwun, B., Young, L., Cote, R.J., and Taylor, C.R. 1993. Antigen retrieval technique utilizing citrate buffer or urea solution for immunohistochemical demonstration of androgen receptor in formalin-fixed paraffin section. *J. Histochem. Cytochem. 41*:1599–1604.

Shi, S.R., Key, M.E., and Kalra, K.L. 1991. Antigen retrieval in formalin-fixed, paraffin-embedded tissues: an enhancement method for immunohistochemical staining based on microwave oven heating of tissue sections. *J. Histochem. Cytochem. 39*:741–748.

Spigel, D.R., and Burstein, H.J. 2002. HER2 overexpressing metastatic breast cancer. *Curr. Treat. Options Oncol. 3*:163–174.

III

Ovarian Carcinoma

This Page Intentionally Left Blank

1

Ovarian Carcinoma: An Introduction

M.A. Hayat

Ovarian carcinoma is the leading cause of death from gynecologic malignancies in the United States, with ~23,000 new cases diagnosed and 14,000 deaths annually. The death rates with this cancer exceed the death rates from cervical and endometrial carcinoma combined. Ovarian cancer is exceeded only by cancers of lung, breast, rectum, and colon. At the time of ovarian cancer diagnosis, ~70% of patients have advanced disease (stage III or VI) (International Federation of Gynecology and Obstetrics [FIGO]). At this stage, cancer levels have already spread to the pelvic and abdominal viscera, distant metastasis has developed, and the disease is rarely curable; at this stage the diagnosis-to-death ratio is ~1:64.

Only ~30% of ovarian tumors are diagnosed at an early stage (I or II); the rest are diagnosed at an advanced stage (III or IV). Five-year survival rates for patients with this cancer range from >80% for patients with stage I cancer to <20% for patients with stage III or IV cancer (Qazi and McGuire, 1995). Even when the tumor is clinically localized, the 5-year relative survival rate is <40%, regardless of the therapy received. The poor survival rate is mainly the result of late clinical manifestation and rapid development of chemoresistance. It is known, for example, that *p53* mutation and chemoresistance occur at very high frequencies in ovarian cancer (Fraser *et al.,* 2003). It is obvious that the high frequency, late diagnosis, and poor prognosis of ovarian cancer emphasize the need for both additional and improved diagnostic methods. Both early detection and early intervention are critical in improving the clinical outcome of patients with ovarian cancer.

As stated earlier, the key to significantly improving overall survival in ovarian cancer is early diagnosis so that curative surgery can be performed in a very small-volume disease. More importantly, however, large-scale studies evaluating both serologic and imaging techniques are ongoing and show progress in detecting early, small lesions. In addition, new methods of genomics and proteomics have resulted in identifying genes and proteins that may be associated with early-stage disease.

The majority of ovarian cancers are found in postmenopausal women, and the median age for ovarian adenocarcinoma, which accounts for 85–90% of all malignant ovarian tumors, is between 50 and 65 years. Familial or hereditary patterns account for only 5–l0% of all of the ovarian malignancies that are most commonly associated with mutations in *BRCA1* and *BRCA2* (Boyd *et al.,* 2000).

Approximately 90% of human ovarian neoplasms arise from the ovarian surface epithelium, a modified mesothelium that covers the peritoneal aspect of the ovary. Of these neoplasms, ~90% occur sporadically, whereas 10% are genetically linked. These neoplasms

are the most lethal among all gynecologic malignancies, with a 5-year survival rate of only 20%. The poor prognosis is mainly the result of lack of symptoms at the early stage of disease.

Nonepithelial ovarian tumors show a lower incidence than the 90% rate shown by epithelial tumors, although their clinical behavior is similar (Matias-Guin and Prat, 1996). Borderline ovarian tumors are usually of low malignant potential, have a better prognosis, and are histopathologically similar to epithelial tumors. In fact, borderline tumors usually do not fit clearly into benign or malignant category. When a tumor with borderline ovarian tumor morphologically invades its own stroma and the surrounding ovarian tissue, the condition is not called invasive—it is metastatic. Although invasive borderline ovarian tumors do not exist, pathologists reserve a category of microinvasive borderline ovarian tumor (Berman, 2004). In other words, a borderline ovarian tumor can show microinvasion, but it cannot have invasion. High–grade serous subtype might develop *de novo* from surface epithelium and its inclusions as well as from endosalpingeal tissues in the cortical stroma.

Carcinosarcomas of the ovary, a rare (only <1–2% of all malignant ovarian tumors) but aggressive variant of ovarian cancer has also been known. These carcinosarcomas pathologically consist of a mixture of malignant epithelial and malignant mesenchymal components. Microscopically these tumors are solid, cystic, or both; fleshy, and hemorrhagic; and they frequently spread beyond the ovary and over peritoneal surfaces by the time of surgery. They can occur throughout the female genital tract but are found most commonly in the uterus. According to a 2003 study (Harris *et al.,* 2003), its overall median survival of 8.7 months is poorer than 15–40% 5-year survival in epithelial ovarian carcinoma.

Ovarian Carcinoma Classification

Ovarian carcinomas comprise a heterogeneous group of tumors with distinctly different histologic types, molecular features, and clinical behavior. Because the histologic classification of these malignancies is diverse, the wide morphologic variation within and among the subtypes (discussed later) can result in diagnostic difficulties. Based on the appearance of the epithelium, these neoplasms are classified into distinct morphologic categories—that is, into tumors of serous, mucinous, endometrioid, clear-cell, transitional, squamous, mixed, and undifferentiated types. Each of these histologic subtypes is associated with distinct molecular genetic alterations.

The most common subtype of ovarian cancer is serous carcinoma, which is divided into high-grade serous carcinoma and a low-grade tumor and invasive micropapillary serous carcinoma (Singer *et al.,* 2002). All serous carcinomas and endometrioid carcinomas arise from surface epithelium or inclusion cysts with *TP53* mutations and dysfunction of *BRCA1* and *BRCA2*. Low- and high-grade serous carcinomas arise via different pathways. Low-grade serous carcinomas arise in a stepwise manner via an adenoma–borderline tumor carcinoma progression from typical to micropapillary serous borderline tumor to low-grade serous carcinoma, with alteration of the RAS–RAF signaling pathway secondary to mutations in *KRAS* and *BRAF*. High-grade serous carcinomas, however, arise from SEIG, with *TP53* mutations and *BRCA1* or *BRCA2* dysfunction (Bell, 2005).

The majority of mucinous ovarian carcinomas arise via an adenoma–borderline tumor–carcinoma sequence with activation of the RAS–RAF signaling pathway secondary to *KRAS* mutations. At least a subset of low-grade endometrioid adenocarcinomas arise from endometriosis, with mutations of *CTNNB1* (β-catenin) and *PTEN*. Clear-cell carcinomas probably also arise from endometriosis. It is also possible that most low-grade, relatively indolent ovarian carcinomas of serous, mucinous, and endometrioid type arise from preexisting cystadenomas or endometriosis, whereas most high-grade serous carcinomas arise without an easily identifiable precursor lesion (Bell, 2005).

Ovarian Cancer Genetics

It is evident that ovarian cancer is a malignancy of signaling and cellular networks that affect cell proliferation, cell survival, apoptosis, differentiation, cell interactions, and the acquisition of genomic instability. This paradigm incorporates the cell-intrinsic properties of tumor oncogenes and tumor-suppressor genes and also genes that influence and dictate the tumor microenvironment. It is obvious that the molecular genetic events underlying ovarian neoplasms are exceedingly complex. For example, loss of tumor-suppressor gene activity plays a crucial role in the origin and progression of malignant tumors, including ovarian tumors.

A commonly accepted mechanism leading to the loss of tumor-suppressor gene function requires the occurrence of at least two events: 1) one of the two alleles must contain a mutation (somatic or germline), rendering this allele incapable of producing a functional tumor-suppressor protein, and 2) the remaining allele must be lost, resulting in an overall absence of tumor-suppressor gene function. This loss can be detected in individuals heterozygous for a marker closely linked to the tumor-suppressor gene (loss of heterozygosity [LOH]),

which is a characteristic of tumor-suppressor genes. The LOH frequencies up to 80% in ovarian cancer occur on multiple chromosomes, most commonly involving chromosomes 3, 6, 9, 11, 17, 18, and 22, suggesting the involvement of many different tumor-suppressor genes (Pieretti *et al.,* 2002); LOH also occurs at chromosome X (Yang Feng *et al.,* 1992).

Most ovarian carcinomas also show complex chromosome aberrations with hypodiploid or near-triploid stemline chromosome numbers. The most common numeric changes are losses of chromosomes 4, 8, 11, 13, 14, 15, 17, and 22 and gains of chromosomes 1, 2, 3, 6, 7, 9, 12, and 20 (Taetle *et al.,* 1999). Comparative genomic hybridization analyses have revealed frequent gains of 3q, 6p, 8q, and chromosome 20 and losses of 4q, 6q, 12q, 13q, and 16q (Hauptmann *et al.,* 2002).

Telomere dysfunction and chromosomal breakage-fusion-breakage events are thought to play a role in the generation of complex chromosomal changes in ovarian carcinoma and other carcinomas. Höglund *et al.,* (2003) have shown that ovarian carcinomas develop through at least three phases of karyotypic evolution. At the early stage, phase I, the karyotypic evolution seems to proceed through stepwise acquisition of changes. The transition to phase II shows signs of an increased chromosomal instability, most probably caused by extensive telomere crises and the onset of breakage-fusion-breakage cycles. This process is linked to the presence of imbalances characteristic for the $6q^{-}/1q^{-}$ pathway (Höglund *et al.,* 2003). The transition to phase III involves triploidization and is also linked to the presence of the $6q^{-}/1q^{-}$ pathway. In short, the key element in the progression of ovarian carcinomas is the $6q^{-}/1q^{-}$ pathway.

As stated earlier, defects in cell-signaling pathways play a central role in cancer cell growth, survival, invasion, and metastasis. Altered expression or function of a number of kinases and phosphatases participates in the development and progression of ovarian cancer. For example, the phosphatidylinositol 3-kinase (P13K) pathway, associated with cell survival, plays an important role in the growth and invasion of tumors and is activated in a significant number of ovarian cancers (Philp *et al.,* 2001). Genes encoding subunits of P13K and its downstream target, Akt2, are amplified in primary ovarian tumors, and overexpression of the Akt2 kinase is associated with aggressive, advanced-stage cancers (Bellacosa *et al.,* 1995). Alterations in mitogenic signaling pathways, such as the mitogen-activated protein kinase (MAPK) pathway, have also been studied in the context of ovarian carcinogenesis.

Wulfkuhle *et al*. (2003) have used reverse-phase protein-array technology coupled with laser capture microdissection and phosphorspecific antibodies to examine the activation status of several key molecular "gates" involved in cell survival and proliferation signaling in human ovarian tumor tissue. This study indicates that the levels of activated extracellular-regulated kinase (ERK1/2) varies considerably in tumors of the same histotype, but no significant differences are observed between histotypes. Advanced-stage tumors have slightly higher levels of phosphorylated ERK1/2 compared to early-stage tumors. This and other evidence suggests that patterns in signal pathway activation in ovarian tumors may be patient-specific rather than type- or stage-specific. Each patient with ovarian cancer may have her own unique signal pathway activation portrait. Thus, effective targeting of the deranged pathways will need to be tailored to the specific derangements taking place (Wulfkuhle *et al.,* 2003).

Although the role of cell division in carcinogenesis is being increasingly recognized, the enormous efficiency with which clonal expansion of premalignant cells can lead to malignant transformation has not been fully appreciated. It is important to recognize the rapid spread of mutations in a clonally expanding population of cells. Similarly, clonally expansion of partially altered cells on the pathway to cancer can significantly increase the population of cells that have acquired some of the mutations critical for carcinogenesis, thus increasing the probability that at least one of these cells will acquire the remaining mutations required for malignant transformation.

In this multistage carcinogenesis model, environmental agents increase the rate of clonal expansion of partially altered cells; thus these agents are efficient carcinogens. It is important to note that some chemical agents administered to prevent cancer can cause cancer. Many of the chapters in this series of handbooks explain the aforementioned events as well as the impact that many genes have on the regulation of DNA (deoxyribonucleic acid) damage, repair, chromosome structure, and genomic instability.

Role of Loss of Heterozygosity

It is known that LOH is correlated with reduced survival in patients with ovarian cancer. Frequencies of LOH up to 80% have been found on multiple chromosomes in this cancer, most commonly involving chromosomes 3, 6, 9, 11, 17, 18, and 22 (Launonen *et al.,* 2000). Also LOH occurs on chromosomes Xp and Xq (Yang Feng *et al.,* 1992); and LOH at DXS538 (Xp 11.21-p21.1) has been reported to be associated with poor survival in patients with ovarian cancer (Høgdall *et al.,* 2004). Similarly, LOH at DXS454 (Xq) is associated with reduced survival in these patients.

Høgdall *et al*. (2004) have amplified polymorphic marker (microsatellite) regions (TP53, CACNLB1, DXS538, and DXS454) in 160 women with primary epithelial ovarian carcinoma by using polymerase chain reaction followed by separation using gel electrophoresis before identifying LOH. In this study, univariate survival analyses were limited to patients with advanced-stage ovarian cancer (FIGO stage III–IV) because the number of deaths was too small in stage I–II. The presence of a tumor-suppressor gene locus on the X chromosome (21q-23q) is likely, which may have prognostic value. Although the study by Høgdall *et al.* (2004) is fairly large for clarifying the prognostic value of LOH at chromosomes 17, 18, and X, it is important to evaluate the DXS454 marker as a prognostic factor in other, larger studies.

This and other studies suggest that loss of the X chromosome is a predisposing factor for developing an invasive ovarian tumor. Furthermore, loss of this chromosome may be a primary or an early event in ovarian tumorigenesis because LOH at DXS454 (Xq21-q23) occurs in both early and late stages of ovarian cancer. Some information is available suggesting that LOH is more common in ovarian tumors with more aggressive biologic behavior and in more advanced ovarian tumors (Otis *et al.,* 2000). However, in this respect, consensus is lacking. It is concluded that many different tumor-suppressor genes are involved in the initiation, progression, and metastatic stage of ovarian cancer.

Ovarian Metastasis

In the case of most human carcinomas, metastases occur by the spread of tumor cells through lymphatic channels or blood vessels to distant sites by means of multiple steps. In contrast, ovarian cancer cells spread by dissemination throughout the peritoneal cavity. For ovarian carcinoma metastases to occur, the following steps are required (Carpenter and Dao, 2003): 1) separation of cells from the primary tumor mass on the ovarian surface, 2) passive movement of the tumor cells through the peritoneal fluid, 3) adherence of the cells to the mesothelium that lines the peritoneal cavity, 4) migration of tumor cells past the mesothelium into the stroma, 5) enzymatic digestion or remodeling of the underlying stroma by proteinases, and 6) growth of the newly established tumor cells in their new location. Ovarian carcinoma cells must interact with the mesothelium where the tumor implants on the peritoneal surface.

Ovarian carcinoma, like most other malignant tumors, kills patients through the effects of metastatic disease rather than primary tumor growth. Dissemination and, therefore, tumor progression in ovarian carcinoma consists primarily of intraperitoneal spread, manifested as both malignant effusions and solid metastases, frequently with secondary extension to the pleural cavity. Pleural effusion is, in fact, the most common presentation of stage IV disease (Akahira *et al.,* 2001).

Biomarkers for Ovarian Carcinoma

The development of cancer is a relatively slow multistep process, and often it takes several years to become clinically manifested. During tumor progression, cancer cells acquire multiple alterations that render them increasingly competent to establish metastatic lesions in specific organs. However, primary tumors may already contain a gene(s) expression profile that is strongly predictive of metastasis and poor survival, thus challenging the notion that metastatic ability is acquired only late during tumor progression.

Presently, techniques are lacking that may possess the sensitivity and specificity to detect a tumor at its earliest stage. Because reduction of cancer mortality is dependent partly on the early detection, the importance of such detection of neoplasia is obvious. Early detection of tumor development also facilitates accurate clinical decisions such as risk assessment, monitoring course of disease, and positive or negative response to therapy. Thus, through early detection, longer disease-free survival, longer overall survival, and improved quality of life for the patient can be achieved. Early detection of certain tumor types can be ascertained by detecting specific biomarkers.

Biomarkers are molecular signatures of a cellular phenotype that facilitate early cancer detection, pathologic grading and staging, and risk assessment to help in the development and use of molecularly targeted therapies tailored to the patient and to increase the rate of survival resulting from early detection and/or improved therapies. In other words, tumor markers can help in at least six areas: 1) screening (finding cancer early), 2) diagnosis (is it really a cancer?), 3) prognosis (how will the cancer behave?), 4) monitoring (how is the treatment working?), 5) predicting a response (will a drug be effective?), and 6) surveillance (will the patient need more treatment?). Because early detection and effective prevention represent the most promising clinical approaches, the identification of biomarkers to stratify patients into different risk groups would be a potential strategy for clinical trials.

The ideal biomarker should be sensitive and specific for the given cellular entity, not detected anywhere else, and sufficiently sensitive, enabling optimal detection, especially at an early stage of the disease. An early detection increases the chances of curative treatment.

In addition, the marker should be relatively easily measurable and the test should be reproducible (reliable) and minimally invasive. Many new markers are being discovered based on several methods, including gene microarray, proteomics, and immunohistochemistry. Most of the known markers have not been yet tested clinically, although some of them in this respect appear to be promising (Table 19).

To guide the process of biomarker development, evaluation, and application, a five-phase program is recommended by the Early Detection Research Network (EDRN) of the National Cancer Institute (Pepe *et al.,* 2001). This program assists in defining the criteria to determine the current status of biomarkers in the published literature, assesses how close these markers are to clinical application, and serves as a guide for future marker development (Marrero and Lok, 2004). The program essentially is biomarker validation protocol: 1) preclinical exploratory studies, 2) clinical assay development for disease, 3) retrospective longitudinal study to detect preclinical disease, 4) prospective screening study, and 5) cancer control studies. There is an urgent need for clinical biomarkers for early detection of gastric carcinoma. A number of biomarkers, including those studied with IHC, fluorescence *in situ* hybridization (FISH), or both, for ovarian cancer are given in Table 19.

Table 19. Biomarkers for Ovarian Carcinomas

*cABL	Schmandt *et al.,* (2003)
Activins	Robertson *et al.,* (2002)
AKT2	Lynch *et al.,* (1998)
*Alpha-6 integrin	Givant-Horwitz *et al.,* (2003)
*Aminopeptidase	This volume
Androgen	Evangelou *et al.,* (2003)
*Angiopietins and Tie-2	This volume
Apolipoprotein A1	Zhang *et al.,* (2004)
*ARF protein	Iba *et al.,* (2004)
*Aurora-A kinase	Yang *et al.,* (2004)
*bcl-2	Piek *et al.,* (2003)
*Beta-catenin	This volume
BRAF	Singer *et al.,* (2003)
*BRCA1	Kato *et al.,* (2004)
BRCA1/2	Rutter *et al.,* (2003)
*CA125	McCluggage (2000)
CA125	This volume
*Calponin	Zamecnik and Michal (2003)
*Calretinin	Shah *et al.,* (2003)
*Carcinoembryonic antigen	Chhieng *et al.,* (2003)
*Caveolin-1	Wiechen *et al.,* (2001)
*CD24	Santin *et al.,* (2004)
*CD34	Ali-Fehmi *et al.,* (2003)
*CD40	Gallagher *et al.,* (2002)
CD44	Igarashi *et al.,* (2003)
*CDX2	Raspollini *et al.,* (2004)
*Cellular apoptosis susceptibility gene	Peiró *et al.,* (2002)
*Chromogranin	This volume
*C-Myc	Wisman *et al.,* (2003)
*COP1	Dornan *et al.,* (2004)
* Coxsackie-adenovirus receptor	Khuu *et al.,* (1999)
*Cyclin Dl	Peiró *et al.,* (2002)
*Cyclooxygenase-2	Ali-Fehmi *et al.,* (2003)
*Cyclooxygenase-2	Sakamoto *et al.,* (2004)
*Cytokeratins	McCluggage (2000)
*Cytokeratin 7	Strobel and Graham (2003)
*Dipeptidyl peptidase IV	Kajiyama *et al.,* (2003)
*E-cadherin	Kajiyama *et al.,* (2003)
eIF-5A2	Guan *et al.,* (2004)
*EphA2 (epithelial cell kinase)	Thaker *et al.,* (2004)
*Epidermal growth factor receptor	Ali-Fehmi *et al.,* (2003)
*Epithelial membrane antigen	Drapkin *et al.,* (2004)
*Estrogen receptor	Wisman *et al.,* (2003)
*Estrogen receptor beta	This volume
Estrogen receptor beta	Bardin *et al.,* (2004)
*Ets-1	Davidson *et al.,* (2001)
Eukaryotic initiation factor 2B	Fogli *et al.,* (2003)
EVII	Sonoda *et al.,* (1997)
FANCF	Olopade and Wei (2003)
*Fas	This volume
Fibroblast growth factor 2	De Cecco *et al.,* (2004)
Fibronectin	Franke *et al.,* (2003)
FLIP protein	Abedini *et al.,* (2004)
*Focal adhesion kinase	Grisaru-Granovsky *et al.,* (2005)
Follicle stimulating hormone	Ho *et al.,* (2003)
*ATA transcription factor	Rasola *et al.,* (2004)
*Glycodelin	Mandelin *et al.,* (2003)
HE4 (WFDC2)	Bingle *et al.,* (2002)

Continued

Selected Biomarkers

Biomarkers essentially are biologic markers of diseases, especially cancer. Tremendous efforts have been made to identify pathologic, biochemical, and genetic biomarkers of diseases so that diagnosis could be determined in earlier stages. The advantage of early detection of biomarkers is obvious considering the possibility of an early treatment and repression of the disease progression. Other advantages of detecting biomarkers include the prediction of the onset of the disease, overseeing the rate of disease progression, and response to treatment. These advantages can be realized only when biomarkers are specific and reliable and only when they will guide us to make more accurate diagnosis and better treatment of the disease.

It is widely recognized that early detection and subsequent assessment of recurrence of ovarian cancers are key steps for successful treatment. Therefore, there is a need to find early detection systems for this disease. Accumulation of genetic changes in ovarian cancer cells also allows them to evade chemotherapeutic drugs and become increasingly dangerous. In view of the high mortality rates associated with ovarian cancer, a better understanding of the molecular mechanisms

Table 19. Biomarkers for Ovarian Carcinomas—cont'd

Heparin-binding epidermal growth factor–like growth factor	Miyamoto *et al.,* (2004)
Hepatocyte growth factor	Capo-Chichi *et al.,* (2003)
*HER-2/neu	Bookman *et al.,* (2003)
*High-mobility group 1 proteins	Masciullo *et al.,* (2003)
*HMGA1	Masciullo *et al.,* (2003)
*hMLH1	Cai *et al.,* (2004)
*hMSH2	Cai *et al.,* (2004)
hTERT mRNA	Wisman *et al.,* (2003)
Human kallikrein 5 protein	Diamandis *et al.,* (2003)
Human kallikrein 13 protein	Scorlias *et al.,* (2004)
Hyaluronan	Carpenter and Dao (2003)
*I,25-Dihydroxyvitamin-D_3-receptors	This volume
* Inhibin	Shah *et al.,* (2003)
Inhibitor of differentiation or DNA binding	Zhang *et al.,* (2004)
Insulin-like growth factor II mRNA	Gu *et al.,* (2004)
Insulin-like growth factor binding protein	Baron-Hay *et al.,* (2004)
*Integrins	This volume
Interleukin-1 receptor antagonist	Sehouli *et al.,* (2003)
* Interleukin-18	Wang *et al.,* (2002)
Insulin-like growth factor II mRNA binding protein	Gu *et al.,* (2004)
Kallikreins 14	Yousuf *et al.,* (2003)
Kallikrein 11	Diamandis *et al.,* (2004)
Kallikrein 5	Kurlender *et al.,* (2004)
*kallikrein 6	Ni *et al.,* (2004)
*Ki-67	Iba *et al.,* (2004; this volume)
*cKIT	Schmandt *et al.,* (2003)
*K-ras	Singer *et al.,* (2003)
Laminin receptor	Givant-Horwitz *et al.,* (2003)
*Lewis-Y antigen	This volume
L-Myc	Wu *et al.,* (2003)
Matrix metalloproteinases	Manenti *et al.,* (2003)
*Matrix metalloproteinases	Määttä *et al.,* (2004)
*MCL-1	This volume
*Melan-A	Yao *et al.,* (2003)
Mesothelin	Scholler *et al.,* (1999)
MUC1	Obermair *et al.,* (2002)
MYBL2	Sonoda *et al.,* (1997)
MYO18B	Yanaihara *et al.,* (2004)
C-Myc	Iba *et al.,* (2004)
NES-1	Schvartsman *et al.,* (2001)
OVCA ½	Schultz *et al.,* (1996)
*Oxytocin receptor	Morita *et al.,* (2004)
*p21	Vassilopoulos *et al.,* (2003)
*p53	Wisman *et al.,* (2003)
*p53	This volume
p73	Concin *et al.,* (2004)
*PCNA	This volume
*PDGFRA	Lassus *et al.,* (2004)
*Peroxisome proliferator-activated receptor gamma	Zhang *et al.,* (2005)
*Peroxisome proliferator-activated receptor gamma	Sakamoto *et al.,* (2004)
*Platelet-derived growth factor receptor-beta	Schmandt *et al.,* (2003)
*Polo-like kinase	Weichert *et al.,* (2004)
*Progesterone receptor	Piek *et al.,* (2003)
Progesterone receptor	Whittemore and McGuire (2002)
Prostasin	Mok *et al.,* (2001)
*Protease activated receptor 1	Grisaru-Granovsky *et al.,* (2005)
PTEN	Schöndorf *et al.,* (2004)
PTPN 1	Watanabe *et al.,* (2002)
RB1	Dodson *et al.,* (1994)
*Relaxin-like factor	Bamberger *et al.,* (1999)
Retinoblastoma	Kim *et al.,* (1994)
SFRP1 gene	Takada *et al.,* (2004)
Smad 3	Symonds *et al.,* (2003)
Smad	This volume
* Survivin	Tringler *et al.,* (2004)
* Syndecan-1	Davies *et al.,* (2004)
Telomerase	Wisman *et al.,* (2003)
*Telomere	Deng *et al.,* (2003)
*Tetranectin	Høgdall *et al.,* (1993)
*Topoisomerase	Gotlieb *et al.,* (2001)
*TP53	Nezhat *et al.,* (2002)
Transforming growth factor-beta receptor	Chen *et al.,* (2001)
*Trop-1/Ep-CAM	Santin *et al.,* (2004)
Tumor necrosis factor-alpha	Yang *et al.,* (2004)
Urokinase-type plasminogen activator receptor	Sier *et al.,* (1998)
*Uroplakin III	Logani *et al.,* (2003)
*Vascular endothelial growth factor	Bamberger and Perrett (2002)
YKL-40	Dupont *et al.,* (2004)

The * indicates that these markers have been identified with IHC, ISH, or both.

underlying tumor progression in the disease would reveal novel pathways of important clinical relevance. Therefore, the importance of targeting biomarkers for early detection of ovarian cancer is obvious. Some of such markers are summarized next and are also listed in Table 19. Some of the markers listed in the table have not been proved clinically relevant as yet. Methods for detection of individual markers and their role in the initiation and progression of this cancer are also presented elsewhere in this volume.

Androgens

The ovarian steroidal milieu, including androgens, influences the initiation or progression of ovarian cancer. The majority of ovarian cancers are diagnosed after menopause, when the balance of ovarian steroid production shifts from estrogens to androgens. Women with high serum androgen levels have an increased risk of developing ovarian cancer. Androgens regulate the

growth of ovarian epithelial cells *in vitro* by preventing inhibition by transforming growth factor β1 and coordinately modulating its receptors and steroid receptor coativators in these cells (Evangelou *et al.,* 2003). This coordinated effect of androgen is lost in tumor cells and in some cells bearing a BRCA1/2 mutation, increasing the possibility that altered androgen response may result in the predisposition to cancer.

β-Catenin

β-Catenin has a critical role in the highly conserved Wnt signaling pathway. Wnts are secreted glycoproteins with important roles in regulating cell fate specification, proliferation, and differentiation during development and in various adult tissues (Zhai *et al.,* 2002). At least two distinct pools of β-catenin exist in cells: 1) plasma membrane–associated pool of β-catenin–E-cadherin, and 2) cytoplasmic/nuclear-associated pool of β-catenin in Wnt signaling. The latter pool is regulated in part by a multiprotein complex consisting of the adenomatous polyposis coli (APC) tumor suppressor, Axin, and glycogen synthase kinase 3β proteins (Polakis, 2001)

Inactivating mutations in the APC or Axin tumor-suppressor proteins or activating mutations in β-catenin elevate β-catenin levels, resulting in marked effects on T cell factor (TCF)-regulated transcription. Several candidate β-catenin/TCF-regulated genes in cancer have been proposed. Mutations leading to β-catenin deregulation were found in nearly half of ovarian endometrioid adenocarcinomas (OEAs) (Zhai *et al.,* 2002). Significantly elevated expression of the *MMP-7, CCNDI (cyclin D1), connexin 43,* and *ITF2* genes along with deregulated β-catenin were found in OEAs. Immunohistochemical studies have confirmed that overexpression of *cyclin D1* and *MMP-7* was highly associated with nuclear accumulation of β-catenin and mutational defects of the Wnt/β-catenin/TCF signaling pathway (Zhai *et al.,* 2002). The aforementioned genes play important roles in the pathogenesis of those OEAs that show defects in β-catenin regulation. However, these genes are not uniformly up-regulated in all OEAs with defective β-catenin regulation. Role of β-catenin in gastric cancer is discussed in chapter 1 in Part II in this volume.

BRCA1/BRCA2

Although *BRCA1/BRCA2* mutations usually are associated with familial breast cancer, these mutations also carry a significant risk for the development of ovarian cancers. In fact, mutations in these genes account for the majority of inherited predisposition to ovarian and breast cancers.

These mutations are responsible for approximately half of all cases of hereditary breast cancer and for almost all cases of combined hereditary breast and ovarian cancers. In fact, genetic predisposition to breast/ovarian cancer results from alterations of the *BRCA1/BRCA2* genes. The carriers of these mutations bear a lifetime risk of ~50–80% for breast cancer and 15–45% for ovarian cancer (Martinez *et al.,* 2004). The BRCA1/BRCA2 mutations are also linked to prostate cancer.

Germline mutations of these tumor-suppressor genes are responsible for 5–l0% of all epithelial ovarian cancers. Carriers of these germline mutations have an estimated lifetime risk of 2l–28% for developing ovarian cancer. Thus, a family history of ovarian cancer is a development of ovarian cancer. p53 and Rb (retinoblastoma) seem to have a secondary role. Immunohistochemical and FISH studies demonstrate high expression of the protein and amplification of the gene, respectively (Peiró *et al.,* 2002). These changes should become targets of molecular therapy for ovarian carcinoma.

The protein product of BRCA1/BRCA2 is necessary for the maintenance of genomic stability by regulating the homologous, recombination-based DNA repair processes. The deficiency of this protein in normal cells is a result of the accumulation of lethal chromosomal aberrations. Most deleterious mutations are small insertions or deletions, nonsense mutations, or splice-site mutations that result in a truncated protein.

The tumor-suppressor function of BRCA1 depends, at least partially, on its transcriptional activity, as explained next. BRCA1 is a nuclear protein that activates transcription and facilitates DNA damage repair. The changes in the core of BRCA1 C-terminus are involved in several of its functions, including modulation of the activity of several transcription factors, binding to the RNA, (ribonucleic acid) fused to a heterologous DNA-binding domain. It can be inferred that abolishing the transcriptional activation function of BRCA1 leads to tumor development.

It is important to determine which mutations in BRCA1 or BRCA2 do or do not abolish the transcription activation function of this gene. Such information is useful in predicting their cancer association. To obtain such information, Mirkovic *et al*. (2004) have used a three-dimensional structure of the human BRCA1 COOH-terminal domains to assess the transcriptional activation functions of BRCA1 mutants. Thus, mutations that predispose individuals to ovarian cancer can be identified.

The following series of events more clearly explain the involvement of BRCA1 in the regulation of cellular immortalization through the modulation of C-Myc

on the human telomerase reverse transcriptase (hTERT); this is a critical early step in carcinogenesis. The transcription of hTERT promoter is negatively regulated by normal BRCA1 in ovarian cancer cells, resulting in the transcription through the binding sites located on the hTERT promoter. The catalytic subunit of human telomerase, hTERT is responsible for the synthesis and telomerase expression is repressed in normal human cells and is activated in Myc. The question is whether BRCA1 inhibits hTERT transcription through its direct interation with C-Myc. In ovarian cancer cells, C-Myc increases hTERT expression threefold and BRCA1 completely abrogates this activity (Zhou and Liu, 2003). A mutation in the C-Myc-binding site (E-box) of the hTERT promoter results in the loss of activation by C-Myc and in the loss of inhibition by BRCA1. Deletion of the C-Myc-binding domain in BRCA1 results in the loss of BRCA1's ability to inhibit transcription of the hTERT promoter.

Although most ovarian cancers associated with germline mutations in BRCA1 have serous or endometrial histology, other types of ovarian tumors, including mucinous and transitional-cell ovarian tumors, are also linked to these mutations (1136 insA 538 and insC mutations). Studies have also indicated the association of malignant ovarian transitional cell tumors (stage III C) in patients carrying germline mutations with BRCA1 (Pautier *et al.,* 2004). The patient had a mutation in exon 5 of BRCA1 that resulted in an A-to-G substitution at nucleotide 330, which led to an R17G mutation.

CA-125

CA-125 is a high molecular weight (2,000,000) glycoprotein distributed on the endothelium of fallopian tubes, endometrium, and endocervix and also in the normal ovary. In addition, it is found on the mesothelial cells of the pleura, pericardium, and peritoneum. The serum concentration of CA-125 is elevated by the vascular invasion, tissue destruction, and inflammation associated with malignant disease and is elevated in ~90% of those women with advanced ovarian cancer and 40% of all patients with advanced intraabdominal malignancy (Tuxen *et al.,* 1995). Levels can also be elevated during menstruation or pregnancy and in other benign conditions such as endometriosis, peritonitis, or cirrhosis, especially with ascites (Meyer and Rustin, 2000).

Currently, the only well-accepted serologic marker for ovarian cancer is CA-125. According to some workers, this protein is sufficiently well-validated to be used in routine clinical care (Meyer and Rustin, 2000). According to this point of view, CA-125 is a fair test for ovarian cancer with a time perspective of ~l.5 years only (Bjørge *et al.,* 2004). This marker in combination with ultrasound has been reported to be promising in screening for early detection of ovarian cancer (Jacobs *et al.,* l999). This combination study was used because of the relatively low sensitivity of retrospective seroepidemiological study (Zurawski *et al.,* 1988). However, according to another study, intensive surveillance by using CA-125 and ultrasound has not proved to be an effective means of diagnosing early-stage ovarian cancer in women who are at high risk (Liede *et al.,* 2002).

Other studies also indicate that CA-125 has serious limitations as a diagnostic, prognostic, and screening tool (Holschneider and Berek, 2000). Based on the cumulative evidence, the sensitivity of using CA-l25 only as a screening test for ovarian cancer is low. Thus, the value of this marker in monitoring the treatment of patients with ovarian cancer is doubtful. A number of other putative markers, including inhibin prostasin, LASA, and OVX1, have been tried to compensate for the limitations of CA-125 (e.g., Lambert-Messerlian, 2000). These markers can be used in combination with CA-125 in the management of ovarian carcinoma. Another marker, KLK14, a member of the Kallikrein gene family, is a relatively new, independent, and favorable prognostic marker for ovarian cancer (Yousef *et al.,* 2003). This family resides on chromosomes 19q13.4 and includes 15 gene members, and the corresponding proteins are designated as hKl to hKl5 (Yousef and Diamandis, 2001). The expression of KLKI4 has been examined using quantitative reverse transcription polymerase chain reaction (RT-PCR) (Yousef *et al.,* 2003). The role of CA-125 in ovarian cancer is discussed comprehensively by Olivier and Van Beurden and Miyatake and Shroyer in this volume.

CAS

The cellular apoptosis susceptibility *(CAS)* gene is located on chromosome 20q13 region, which harbors several oncogenes. This is the human homolog of the essential yeast chromosome segregation gene (CSE1). The *CAS* gene could induce or advance neoplasia by interfering with the regulation of nuclear transport of other proteins necessary for cell cycle progression; these proteins include cyclin-dependent kinases and cyclin/cyclin-dependent kinase complexes, p53, and BRCA1. Deregulation of several genes at 20q13 (CAS and ZNF21) as well as of cyclin Dl represents one of the major pathways that leads to the development of ovarian cancer. p53 and Rb seem to have a secondary role. Immunohistochemical and FISH studies demonstrate high expression of the protein and amplification of the gene, respectively (Peiró *et al.,* 2002). These changes should become targets of molecular therapy for ovarian carcinoma.

CD40

CD40 plasma membrane protein belongs to the tumor necrosis factor receptor family and is expressed primarily in normal β cells where it regulates growth, survival, and differentiation. CD4O activation in resting β cells provides co-stimulatory signals for proliferation and isotype switching, enhances survival through up-regulation of various antiapoptotic proteins (e.g., Bcl-2, Bcl-xL, and A20), and induces homotypic cell adhesion and cytokine production (Noelle *et al.,* 1992). CD40 is also expressed in some carcinoma cells. A 2002 study suggests that the CD40 pathway is functional in ovarian carcinoma cells (Gallagher *et al.,* 2002). Further studies are required to provide insight into the role of this protein in the carcinogenic process and possible exploitation of this pathway for novel, more effective therapeutic approaches.

CDX-2

CDX genes are homebox genes necessary for intestinal organogenesis and encode for nuclear transcription factors involved in proliferation and differentiation of intestinal epithelial cells in fetal and adult tissues (Suh and Taber, 1996). CDX-2 is expressed in normal colonic epithelia and most colorectal adenocarcinomas.

Primary ovarian carcinomas can be confused with carcinomas metastatic to the ovary because these two types have similar histologic and morphologic appearance. Another problem is that mucinous adenocarcinomas of the pancreas, biliary tract, colon, appendix, and cervix can mimic ovarian mucinous carcinomas (Ronnet *et al.,* 1997). Approximately 40% of adenocarcinoma metastases of the ovary originate from the colon (Wauters *et al.,* 1995). In addition, the specificity of CEA, CK20, CK7, CA-125, and CA19.9 markers is not sufficiently high in distinguishing between these two types of ovarian carcinomas. The distinction between these two types is important because the management, including surgical and chemotherapeutic treatment, and prognosis of them are different. CDX-2 is a useful marker for differentiating these two types of carcinomas and thus can be added to a limited immunohistochemical panel for distinguishing these two entities from each other.

As stated earlier, CDX-2 is a highly sensitive and specific marker for distinguishing primary ovarian mucinous carcinomas from metastatic secondary (intestinal) ovarian tumors. Immunohistochemical studies have shown that almost all of the primary ovarian carcinomas lacked CDX-2 immunoreactivity, whereas 14 of the 16 (~87%) metastases to the ovary from intestinal primaries showed CDX-2 immunoexpression (Tornillo *et al.,* 2004). In this study prediluted CDX-2-88 monoclonal antibody (Biogenex, San Ramon, CA) was used. Another immunohistochemical study has also demonstrated that primary ovarian carcinomas are CDX-2-negative, whereas metastatic secondary ovarian tumors are CDX-2-positive (Raspollini *et al.,* 2004). It should be noted, however, that poorly differentiated intestinal carcinomas may lose their CDX-2 expression and rare primary ovarian tumors may become focally positive for CDX-2.

Cyclooxygenase

It is known that cyclooxygenase (COX) enzymes are overexpressed in various neoplastic lesions. Cyclooxygenase-2 expression is significantly correlated with survival in patients with high-grade, *high-stage serous* ovarian carcinoma (Ali-Fehmi *et al.,* 2003). Expression of this enzyme is associated with poor survival and is correlated with tumor angiogenesis but not with EGFR (epidermal growth factor receptor), HER-2/*neu*, or p53 expression. Some of the mechanisms by which COX-2 contributes to the process of carcinogenesis are increased proliferation, reduced apoptosis, and stimulation of angiogenesis and metastases.

Fas

The best-characterized cell-death receptor with respect to its signal transduction pathway is the Fas (Apo-1/CD95) protein. This receptor mediates apoptosis when triggered by antibodies or its ligand (FasL).

Immunohistochemical and flow cytometric studies have demonstrated changes in Fas/FasL expression in ovarian tumors (Van Haaften-Day *et al.,* 2003). Fas expression is significantly greater in borderline serous tumors than in either benign or malignant serous tumors, whereas FasL expression appears similar in benign and borderline tumors but markedly increases in malignant serous tumors. There is strong evidence for the role of Fas in apoptosis.

HE4

HE4 is considered to be the prototypic member of the whey acidic proteins (WAP) in the mammalian milk. It is located on chromosome 20q12-13 region. A number of studies have reported that HE4 is overexpressed in ovarian tumors and thus can be considered as a potential serum marker for these tumors (Schummer *et al.,* 1999). However, HE4 expression is also increased in some breast tumors and tumor cell lines of colon, renal, and melanoma. A number of normal human tissues also show the presence of HE4. Several studies

have reported that HE4 can undergo a complex series of alternative splicing that can yield five distinct WAP domain–containing protein isoforms. These and other results cast doubt on the potential role of HE4 as an independent serum tumor marker for ovarian cancer (Bingle *et al.,* 2002).

HER-2/*neu*

The clinical value of HER-2/*neu* receptor in ovarian and primary peritoneal carcinoma is limited because of the low overexpression of this marker (Bookman *et al.,* 2003). In contrast, according to Smith *et al.* (2002), ovarian cancer cells show HER-2/*neu* overexpression. This study also indicates that such cells show resistance to various drugs and agents, including cisplatin, the P13K inhibitor LY294002, and the tyrosine kinase inhibitor emodin. However, this study also reports that these cells, instead of being resistant to all anti-cancer drugs, show increased sensitivity to drugs such as geldanamycin. These and other studies show differences with regard to the role of HER-2/*neu* marker in the initiation and progression of ovarian cancer. Further large-scale studies, using various technologies such as ISH, FISH, and microarray, are required to possibly resolve the differences.

Hyaluronan

Diverse biologic molecules, including growth factors, cytokines, and extracellular matrix proteins, are known to induce motility in normal and malignant cells. In addition, hyaluronan, a glycosaminoglycan of alternating N-acetyl-D-glucosamine and D-glucuronic acid residues, induces cellular motility. Mesothelial cells are known to synthesize hyaluronan *in vitro* (Breborowicz *et al.,* 1998). Mesothelial cell hyaluronan induces ovarian carcinoma cell chemotaxis (Carpenter and Dao, 2003). Such hyaluronan is a potential paracrine motility factor for ovarian carcinoma. The presence of mesothelial cells on the peritoneal cavity may encourage the establishment of ovarian metastases. Because hyaluronan contributes to ovarian tumor motility, hyaluronan provides a mechanism for the prognostic significance of the expression of this molecule and a rationale for ovarian cancer therapy using hyaluronan-paclitaxel conjugates (Luo and Prestwich, 1999).

Inhibin

Inhibin, a dimeric 32 kDa peptide hormone, is produced by ovarian granulosa and theca cells. Inhibin is a product of the gonads and is present in at least two biologically active forms (inhibin A and inhibin B) as well as in a variety of alpha subunit precursor forms. Is inhibin a serum marker for ovarian cancer? The most convincing data in support of this protein being a useful marker of ovarian cancer was obtained from the serum of patients with granulosa cell tumors (GCTs) (Robertson *et al.,* 1999). As stated earlier, granulosa cells are the primary origin of inhibin synthesis. The level of inhibin is decreased in these tumors after surgery, whereas it is increased with recurrence of the disease (Lappöhn *et al.,* 1989). Antibodies against inhibin are useful immunohistochemical markers for GCTs (McCluggage *et al.,* 1997). Using immunohistochemistry (IHC), it has been demonstrated that patients who are negative for inhibin after surgery for GCT show far worse outcome than the patients with inhibin-positive tumors (Ala-Fossi *et al.,* 2000). Both alpha subunit and dimeric forms of inhibin are secreted in abundance in GCTs. However, the former is a better serum marker than the latter for all cases of epithelial ovarian tumors (Lambert-Messerlian, 2000). It should be noted that the specificity of inhibin with regard to other spindle-cell neoplasms that may mimic sarcomatoide adult granulosa cell tumor (AGCT) is uncertain. Calretinin, a 29 kDa calcium-binding protein, has also been suggested as an immunohistochemical marker for ovarian sex-cord stromal tumors (McCluggage and Maxwell, 2001) However, according to Shah *et al*. (2003), calretinin seems to be less specific than inhibin in immunohistochemical studies.

Despite the previous reports, in general, immunohistochemical staining with antibodies against epithelial and mesenchymal antigens is of little value in differentiating sarcomatoid AGCT of the ovary from real sarcomas because none of the markers are specific for AGCT. However, inhibin and calretinin are useful markers to some degree for AGCT. Calretinin appears to be a less specific marker than inhibin in the AGCT of the ovary (Shah *et al.,* 2003). Another study has concluded that calretinin is a more sensitive but less specific marker than alpha inhibin for ovarian sex-cord stromal neoplasms (Movahedi-Lankarani and Kumar, 2002). In conclusion, although inhibin is a promising marker for ovarian cancer, its specificity is yet to be confirmed. In fact, the question of inhibin's utility as a prognostic indicator for ovarian cancer is still in its infancy. The foregoing studies lay the groundwork for future studies of the molecular changes that contribute to the development of ovarian cancer including GCT.

KRAS-BRAF

The kinase cascade involving RAS, RAF, mitogen/extracellular signal/regulated kinase (MEK), extracellular signal-regulated kinase (ERK), and MAPK

mediates the transmission of growth signals into the nucleus (Peyssonnaux and Eychene, 2001). Activating mutation in KRAS and in one of its downstream mediators, BRAF, is found in a variety of human cancers, including ovarian cancer. BRAF is activated by somatic mutation in ovarian cancer. All known BRAF mutations occur within the kinase domain. Similarly, activating mutations in RAS occur frequently in carcinomas.

Singer *et al*. (2003) have determined the role of mutations in BRAF and KRAS in ovarian carcinoma; genes for three common mutations (at codon 599 of BRAF and codons [12 and 13] of KRAS) were analyzed. None of the tumors contained a mutation in both BRAF and KRAS. BRAF mutations occur during progression of serous borderline tumors. (Serous borderline tumors include a benign precursor and a noninvasive carcinoma.) Both BRAF and KRAS mutations are not found together in the same ovarian tumor. Furthermore, none of the conventional aggressive high-grade serous carcinomas contain the BRAF codon 599 mutation or either of the two KRAS mutations. The restriction of these BRAF and KRAS mutations to low-grade serous ovarian carcinoma and its precursors suggests that low-grade and high-grade ovarian serous carcinomas develop through independent pathways. Different histologic types of ovarian carcinomas may also have distinctive molecular pathways in tumor development. Thus, blocking BRAF–KRAS signaling may provide more effective therapy for ovarian cancer. A high frequency of KRAS mutations also occur in fallopian tube carcinoma (Mizuuchi *et al.,* 1995).

L-Myc

L-Myc is another oncogene that is amplified in ovarian cancer. This gene is located on chromosome 1p34-35, and its protein product is overexpressed in a subset of primary ovarian cancers. Alterations include genomic gains and amplifications on the short arm and chromosomal translocation at distal 1p.

The Myc protooncogene family consists of three major members: *C-Myc*, *L-Myc*, and *N-Myc*. These genes encode proteins that play distinct but overlapping roles in a wide range of normal and aberrant cellular processes such as cell proliferation, differentiation, apoptosis, and tumorigenesis (Morgenbesser *et al.,* 1995*).* All three Myc proteins bind to the CACGT (E-box) motif, a function that is critical for the transforming activity of these proteins.

Restriction landmark genome scanning in combination with virtual genome scans has been used for identifying these three genes in ovarian carcinoma (Wu *et al.,* 2003). This study indicates increased *L-Myc* gene copy number in ~15% of primary ovarian carcinomas and overexpression of this gene protein product even more frequently (~40%). L-Myc protein is thought to be more frequently overexpressed than that shown by C-Myc or N-Myc relative to ovarian surface epithelium.

MUC1

The *MUC1* gene encodes, as its major isoform, a cell-surface glycoprotein with a complex cytoplasmic domain involved in signal transduction. This gene is often overexpressed in epithelial cancers, including epithelial ovarian cancer, and overexpression is associated with poor survival. The *MUC1* gene is also implicated as an important modulator of adhesion and metastasis. A number of other MUC1 isoforms generated by alternative messenger RNA (mRNA) have been described: MUC1 splice variants A, B, C, D, X, Y, Z, REP, and SEC. Using RT-PCR it was determined that primary ovarian cancer was positive for variant REP but negative for variant SEC (Obermair *et al.,* 2002). Expression of MUC1 splice variants A, D, X , Y, Z, and REP is associated with the presence of malignancy, whereas expression of MUC1/SEC is associated with the absence of malignancy. Unfortunately, antibodies reactive specifically with various MUC1 isoforms are not available. Such antibodies need to be developed to demonstrate the presence of various protein isoforms encoded by the mRNA variants present in ovarian cancers.

PTEN

Phosphatase and tensin homolog on chromosome 10 *(PTEN)* gene plays a pivotal role in signal transduction, and it is thought to be the missing link between the biology of primary and recurrent ovarian cancers. This gene is located on chromosome 10q23.3. By assessing the PTEN content in both the primary and recurrent specimens from each category of patients, it has been shown that a prolonged progression-free interval follows an increase in the PTEN protein (Schöndorf *et al.,* 2003). There are a number of other genes (e.g., HER-2/*neu*, *Ki-ras*, *p53*, and *CTNNB1*) that play a role in the ovarian carcinogenesis. However, none of these genes mutates in such a high frequency in this carcinoma compared to *PTEN*. Many of these genes are discussed in this volume.

PTEN acts as a tumor-suppressor phosphatase with specificity for both lipid and protein substrates. The gene is differentially regulated in ovarian cancer, because its decreased expression accompanies the progression of the cancer. Declining PTEN expression results in a shortened relapse-free interval, whereas an increase of this gene prolongs the time to progression. A complete

loss of PTEN function in early-stage tumors appears to be unique for ovarian and endometrial cancers. Most often complete inactivation of this gene is associated with late-stage, aggressive, usually metastatic tumors.

The *PTEN* gene is most common in the endometroid subtype of the ovarian cancer. When present, *PTEN* is functionally active. Point mutations and microdeletions or insertions in one allele are likely to be early crucial events in the development of endometrioid carcinoma of the ovary, whereas LOH of the other allele occurs at later stages.

The *PTEN* gene is also known to be involved in the suppression of several sporadic cancers, including tumors of the brain, prostate, and endometrium (Di Cristofano and Pandolfi, 2000). In fact, alteration of *PTEN* expression is thought to be a major, general event in the progression of carcinomas derived from different origins. For example, *PTEN* is a reliable molecular marker to distinguish between ovarian and uterus carcinomas, especially when the patient is suffering from synchronous endometrioid carcinomas of the ovary and uterus.

Although histopathology is the standard method to process tumor specimens from these patients, exclusive use of this method is often insufficient and sometimes misleading. Mutation screening, however, for PTEN and LOH analysis at chromosome l0q23.3 provides helpful genetic tools to establish a correct diagnosis. For example, mutation screening indicates the location of two point mutations and one frameshift mutation in exon 5 and two frameshift mutations in exon 8 in the uterine tumors, whereas ovarian carcinomas show 1 point mutation in exon 5 and 1 frameshift mutation in exon 6 (Ricci *et al.,* 2003). Thus, histopathology together with genetic screening at the PTEN locus provides a more reliable final diagnosis, which influences the prognosis and therapy of the patients. A therapeutic regimen leading to increased PTEN might be a useful additive treatment for women with advanced ovarian cancer to prolong their time to progression. However, PTEN is not the only mechanism to suppress tumor progression in ovarian cancer.

Immunohistochemical studies provide some evidence that several mechanisms of PTEN silencing contribute to ovarian carcinogenesis (Kurose *et al.,* 2001). This effect is mediated via phosphorylation and thus activation of the downstream effector protein kinase B (PKB) in ovarian cancer (Schöndorf *et al.,* 2003). PTEN negatively regulates the PKB-dependent cell survival. It is also accepted that ovarian cancer cells lacking PTEN have high PKB activity, intensifying the ce1l-survival signal-transduction pathway. In conclusion, PTEN is differentially regulated in ovarian cancer, which is linked to the clinical outcome.

PTPN1

PTPN1 is one of the genes that has been proposed as a target for the 20q amplification. This gene encodes a nonreceptor tyrosine phosphatase that is often overexpressed in ovarian cancer (Wiener *et al.,* 1994). Expression levels of PTPN1 and ZNF217 are significantly correlated with their copy numbers determined by FISH analysis in the primary ovarian cancer (Watanabe *et al.,* 2002). Amplifications of 20q in ovarian cancers appear to be extensive and complex, probably as a result of synergistic or nonsynergistic amplifications of separate regions involving multiple, independently amplified targets (Watanabe *et al.,* 2002).

TP53

The *TP53* gene found on the short arm of chromosome 17 (17 p13) encodes a nuclear protein that normally acts to restrain inappropriate cellular proliferation. It functions as a tumor-suppressor gene and negatively regulates cell division. Mutated p53 accumulates in cells and is commonly detected with immunohistochemical staining because of the increased stability of the mutated form of the protein. Mutation of TP53 is a frequent event in many tumor types including epithelial ovarian cancer. Molecular genetic alteration of TP53, such as overexpression or mutation, is common in advanced epithelial ovarian carcinoma. Immunohistochemical studies demonstrate that staining for mutated p53 is essentially negative in benign endometriotic cysts but positive in malignant ovarian epithelial tumors (Nezhat *et al.,* 2002). Further larger series studies of this marker might identify those women with endometriosis who are at risk for developing ovarian carcinoma.

Vascular Endothelial Growth Factor

Vascular endothelial growth factor (VEGF) is one of the most potent angiogenic factors in solid tumors. As is true in the case of tumors in general, ovarian tumor progression is related to the expression of VEGF and microvessel density. The factor VEGF and its receptors fit-1 and flk-1 (KDR) (VEGFR) have been detected at mRNA or protein levels, or both, in ovarian cancer. High levels of VEGF are also found in serum or plasma and in ascetic fluid of patients with ovarian cancer (Yamamoto *et al.,* 1997). The influence of VEGF expression on prognosis becomes clear considering that its expression is significantly associated with disease state ($p = 0.002$), histologic grade ($p = 0.0004$), and patient outcome ($p = 0.0002$) (Shen *et al.,* 2000). These and other studies indicate that VEGF and VEGFR

expression is associated with ovarian cancer growth and invasion.

The survival of patients with high VEGF expression is significantly worse than that of patients with low or negative VEGF expression. Even patients with early-stage ovarian carcinoma and increased VEGF have poor prognosis. Analysis by RT-PCR has shown that VEGF isoforms 121, 165, and 189 are uniformly expressed in all ovarian tissues, with the predominant isoforms being 165 and 121 (Shen *et al.,* 2000). Enough evidence is available suggesting that disease stage and VEGF expression can be considered as independent prognostic indicators of overall survival time ($p = 0.008$ and $p = 0.006$, respectively). It is further suggested that in conjunction with the established clinicopathologic prognostic parameters of ovarian cancer, VEGF expression can help to more accurately predict patients at high risk for tumor progression who are potential candidates for aggressive therapy.

Chemotherapy

Although the subject of treatment of patients with ovarian cancer is outside the scope of this volume, a summary of the use of chemotherapy is presented next. The majority of patients with epithelial ovarian cancer require chemotherapy. Chemotherapy response is the most important prognostic factor in ovarian cancer. Platinum-based combination chemotherapy, currently the standard treatment for this cancer, has achieved a high response rate, but it is limited by the development of resistance to chemotherapy; the resistance could be intrinsic, acquired, or both.

In the 1990s the first-line therapy for ovarian cancer was a paclitaxel–platinum combination (McGuire *et al.,* 1996). The International Collaborative Ovarian Neoplasm (ICON) group reported a benefit when paclitaxel is added to platinum in patients with potentially platinum-sensitive relapsed disease (Parmar *et al.,* 2003). Overall tumor response rates associated with this combined treatment are reported to be relatively high and range from ~70% to 80%. However, other subsequent studies failed to confirm the benefit of this combination of drugs (Muggia *et al.,* 2002). Approximately 50–75% of responders relapse within ~18 months after completing first-line therapy and require further systemic therapy. A negative interaction between these two drugs is thought to be responsible for the reduced efficacy of these two drugs. Although a potential benefit of paclitaxel chemotherapy for some patients with ovarian cancer has been reported, it is associated with significant toxicity (Markman *et al.,* 2003). In fact, because only 10–15% of patients who present with advanced disease experience long-term remission, most patients are subject to repetitive treatment cycles, tumor responses, and disease recurrences or unchecked disease progression.

Treatment with a platinum compound, carboplatin, is also being used. This compound has been shown to have equivalent efficacy but less toxicity than cisplatin (Ozols *et al.,* 2003). However, carboplatin may cause thrombocytopenia, which can be reduced by short infusions with taxanes. Platinum and taxanes can be given sequentially rather than concurrently.

Despite some benefits observed in the trials using the previously mentioned drugs, patients eventually die from their disease, thus underscoring the need to improve the results achieved. This has been attempted by adding other potentially noncross-resistant drugs such as paclitabine, docetaxel, etoposide, gemcitabine, topotecan, and liposomal doxorubicin. These active agents provide various clinical benefit–risk profiles. This treatment of recurrent disease is palliative and is initiated with the goals of controlling disease-related symptoms, limiting treatment-related toxicity, maintaining or improving quality of life, delaying time to progression, and prolonging survival.

Gemcitabine, a pyrimidine analog in a phase II study produced a modest overall response in patients with ovarian cancer that was recurrent platinum- and paclitaxel-resistant (D'Agostino *et al.,* 2003). Gemcitabine generally well-tolerated, but results in common toxicities, including myelosuppression, lethargy, flu-like symptoms, peripheral edema, and skin rashes. The use of gemcitabine in combination with platinum and paclitaxel has also been explored as first-line therapy for patients with ovarian cancer (Hansen, 2002). In this study, although the response rate was highly favorable, hematologic toxicity was significant.

In 2004, Harries *et al.* (2004) evaluated the addition of gemcitabine to carboplatin and paclitaxel in a sequential regimen, with carboplatin monotherapy followed by gemcitabine and paclitaxel to chemonaive patients with ovarian cancer. This sequential treatment is feasible and the efficacy data are encouraging, but the incidence of pulmonary toxicity is a problem, thus limiting the use of this weekly regimen. Considering this side effect, evaluation of sequential carboplating followed by the combination of gemcitabine/paclitaxel, but with a more conventional 3-week taxane dosing was proposed.

Although epithelial ovarian cancer is a relatively chemosensitive disease, the disease ultimately relapses and leads to the death of most patients. The median duration of remission following first-line chemotherapy with platinum–taxame combinations for patients with advanced disease is between 12 and 24 months. A variety of strategies have been used to maintain the benefits achieved with chemotherapy in advanced

ovarian cancer. Such strategies include increasing the dose and duration of chemotherapy to enhance the benefits of chemotherapy in patients with advanced ovarian cancer. However, the resulting increases in response rates are not associated with improvement in survival (McGuire *et al.,* 2000). For example, although interferon-α has limited activity in active advance ovarian cancer, Hall *et al.* (2004) carried out a randomized phase III trial to reassess the role of interferon-α in maintaining the response following surgery or chemotherapy in patients with epithelial ovarian carcinoma. This study showed that this chemical was ineffective in maintaining chemotherapy benefits in women with ovarian cancer. It is concluded that despite the modern chemotherapy combination, as mentioned earlier, the natural pattern of ovarian carcinoma remains one of relapse following initial positive response to chemotherapy. The need for an effective nontoxic maintenance therapy is apparent.

Many mechanisms have been postulated to explain chemoresistance, including decreased drug accumulation, increased cellular detoxification, and increased DNA repair. Apoptosis is also related to chemoresistance. Anti-tumor properties of vitamin E compounds are effective in inducing apoptosis in human breast, prostate, colon, lung, endometrial, ovarian, and cervical tumor cells. Two compounds of vitamin E, vitamin E analog (α-TEA) and vitamin E succinate (VES) are potent growth inhibitors of a wide variety of cancer cell lines *in vitro* and effective tumor growth inhibitors *in vivo* (Kline *et al.,* 2001).

As an inducer of apoptosis in human ovarian and cervical tumor cells, α-TEA is superior to VES, although both compounds signal DNA synthesis arrest and promote apoptosis. When administered to human ovarian cancer cells, α-TEA is structurally stable and acts as a potent proapoptotic agent (Anderson *et al.,* 2004). Thus, α-TEA can be considered a potential chemotherapeutic agent against ovarian cancer.

Some information is available regarding the role of *C-Myc* gene overexpression and *p53* gene mutation in response to chemotherapy. A cell-cycle checkpoint protein, *p53* plays a regulatory role in the control of cell proliferation and apoptosis. The transcription–regulatory oncoprotein C-Myc directly induces apoptosis via ARF, whereas ARF also regulates *p53*-dependent apoptosis through *mdm-2* (Tsuji *et al.,* 2002).

The critical role of *p53* in executing cell death in response to anti-cancer drugs is well known. Mutations of the *p53* gene are associated with lack of response to such drugs in many types of tumors, including ovarian tumors (Sato *et al.,* 1999). Regardless of *p53* gene status, apoptosis is increased after exposure to cisplatin, and apoptosis parallels cytotoxicity in cell lines (Takahashi *et al.,* 2000). Apoptosis induced by cisplatin seems to occur through both p53-dependent and p53-independent pathways. A 2004 study suggests that *C-Myc* contributes to chemotherapy (platinum-induced) apoptosis via ARF (Iba *et al.,* 2004). Responders to chemotherapy show a significantly higher expression of *C-Myc* than that shown by nonresponders. This and other studies also indicate that *C-Myc* expression is related to chemoresponse regardless of the *p53* status in ovarian cancer. *C-Myc* gene expression and whether or not *p53* and *C-Myc* have interacting roles in apoptosis is controversial. McCarthy *et al.,* (2001) indicate the mutual interaction of p53 and C-Myc pathways in apoptosis. In contrast, Iba *et al.* (2004) did not find a relationship between the expression of these two genes in ovarian cancer.

As stated earlier, to overcome the drug resistance in ovarian cancer, it is necessary to elucidate the mechanisms responsible for such resistance and to develop ways to treat resistant disease effectively or prevent its occurrence. To investigate the mechanism of drug resistance in human ovarian carcinoma, Li *et al.* (2004) have developed and characterized five human ovarian carcinoma cell models for chemoresistance studies of cisplatin, carboplatin, and taxol. These models included two models for cisplatin resistance, two models for carboplatin, and one model for taxol resistance. The expression of *p53*, *lrp-1*, and *mrp-1* was decreased, while the expression of *pkc*, *topo-1*, and *topo 11* beta was increased in the drug resistant tumor cells as compared with the parental cells. In contrast, no significant alterations were observed in *gst-pi* and *topo 11* alpha expression. The levels of *mdr-1* expression were elevated in some models, but were reduced in others.

The above-mentioned results suggest that different pathways are involved in the development of drug resistance in different cell model systems, and that different mechanisms are responsible for the emergence of different drug resistances in tumor cells. The cell models developed by Li *et al*. (2004) and other similar cell model systems are useful in assessing the biochemical and genetic mechanisms responsible for drug resistance in human cancers.

References

Abedini, M.R., Qiu, Q., Yan, X., and Tsang, B.K. 2004. Possible role of FLICE-like inhibitory protein (FLIP) in chemoresistant ovarian cancer cells *in vitro. Oncogene 23*:6997–7004.

Akahira, J.I., Yoshikawa, H., Shimizu, Y., Tsunematsu, R., Hirakawa, T., Kuramoto, H., Shiromizu, K., Kuzuya, K., Kamura, T., Kikuchi, Y., Kodama, S., Yamamoto, K., and Sato, S. 2001. Prognostic factors of stage IV epithelial ovarian cancer: a multicenter retrospective study. *Gynecol. Oncol. 81*:398–403.

Ala-Fossi, S.L., Aine, R., Punnonen, R., and Maenpaa, J. 2000. Is potential to produce inhibins related to prognosis in ovarian granulosa cell tumors? *Eur. J. Gynaecol. Oncol. 21*:187–189.

Ali-Fehmi, R., Che, M., Khalifeh, I., Malone, J.M., Morris, R., Lawerence, W.D., and Munkarah, A.R. 2003. The effect of cyclooxygenase-2 expression on tumor vascularity in advanced stage ovarian serous carcinoma. *Cancer 98*:1423–1429.

Anderson, K., Simmons-Menchaca, M., Lawson, K.A., Atkinson, J., Sanders, B.G., and Kline, K. 2004. Differential response of human ovarian cancer cells to induction of apoptosis by vitamin E succinate and vitamin E analogue, alpha-TEA. *Cancer Res. 64*:4263–4269.

Bamberger, A.M., Ivell, R., Balvers, M., Kelp, B., Bamberger, C.M., Riethdorf, L., and Loning, T. 1999. Relaxin-like factor (RLF): a new specific marker for Leydig cells in the ovary. *Int. J. Gynecol. Pathol. 18*:163–168.

Bamberger, E.S., and Perrett, C.W. 2002. Angiogenesis in epithelial ovarian cancer. *Mol. Pathol. 55*:348–359.

Bardin, A., Hoffman, P., Boulle, N., Katsaros, D., Vignon, F., Pujol, P., and Lazennec, G. 2004. Involvement of estrogen receptor beta in ovarian carcinogenesis. *Cancer Res. 64*:586l–5869.

Baron-Hay, S., Boyle, F., Ferrier, A., and Scott, C. 2004. Elevated serum insulin-like growth factor binding protein-2 as a prognostic marker in patients with ovarian cancer. *Clin. Cancer Res. 10*:1796–1806.

Bell, D.A. 2005. Origins and molecular pathology of ovarian cancer. *Mod. Pathol. 18*:519–532.

Bellacosa, A., de Feo, D., Godwin, A.K., Bell, D.W., Cheng, J.Q., Altomare, D.A., Wan, M., Dubeau, L., Scambia, G., and Masciullo, V. 1995. Molecular alterations of the AKT2 oncogene in ovarian and breast carcinomas. *Int. J. Cancer 64*:280–285.

Berman, J.J. 2004. Borderline ovarian tumor workshop. *Hum. Pathol. 35*:907–909.

Bingle, L., Singleton, V., and Bingle, C.D. 2002. The putative ovarian tumour marker gene HE4 (WFDC2) is expressed in normal tissues and undergoes complex alternative splicing to yield multiple protein isoforms. *Oncogene 21*:2768–2773.

Bjørge, T., Lie, A.K., Hovig, E., Gislefoss, R.E., Hansen, S., Jellum, E., Langseth, H., Nustad, K., Trope, C.G., and Dørum, A. 2004. BRCA1 mutations in ovarian cancer and borderline tumours in Norway: a nested case-control study. *Br. J. Cancer 91*:1829–1834.

Bookman, M.A., Darcy, K.M., Clarke-Pearson, D., Boothby, R.A., and Morowitz, I.R. 2003. Evaluation of monoclonal humanized anti-HER2 antibody, trastuzumab, in patients with recurrent or refractory ovarian or primary peritoneal carcinoma with overexpression of HER2: a phase II trial of the Gynecologic Oncology Group. *J. Clin. Oncol. 21*:283–290.

Boyd, J., Sonoda, Y., Federici, M.G., Bogomolniy, F., Rhei, E., Maresco, D.L., Saigo, P.E., Almadrones, L.A., Barakat, R.R., Brown, C.L., Chi, D.S., Curtin, J.P., Poynor, E.A., and Hoskins, W.J. 2000. Clinicopathologic features of BRCA-linked and sporadic ovarian cancer. *JAMA 283*:2260–2265.

Breborowicz, A., Wisniewska, J., Polubinska, A., Wieczorowska-Tobis, K., Martis, L., and Oreopoulos, D.G. 1998. Role of peritoneal mesothelial cells and fibroblasts in the synthesis of hyaluronan during peritoneal dialysis. *Perit. Dial. Int. 18*: 382–386.

Cai, K.Q., Albarracin, C., Rosen, D., Zhong, R., Zheng, W., Luthra, R., Broaddus, R., and Liu, J. 2004. Microsatellite instability and alteration of the expression of hMLH1 and hMSH2 in ovarian clear cell carcinoma. *Hum. Pathol. 35*:553–559.

Capo-chichi, C.D., Roland, I.H., Vanderveer, L., Bao, R., Yamagata, T., Hirai, H., Cohen, C., Hamilton, T.C., Godwin, A.K., and Xu, X.X. 2003. Anomalous expression of epithelial differentiation-determining GATA factors in ovarian tumorigenesis. *Cancer Res.* 63:4967–4977.

Carpenter, P.M., and Dao, A.V. 2003. The role of hyaluronan in mesothelium-induced motility of ovarian carcinoma cells. *Anticancer Res. 23*:3985–3990.

Chen, T., Triplett, J., Dehner, B., Hurst, B., Colligan, B., Pemberton, J., Graff J.R., and Carter, J.H. 2001. Transforming growth factor-beta receptor type I gene is frequently mutated in ovarian carcinomas. *Cancer Res. 61*:4679–4682.

Chhieng, D.C., Rodriguez-Burford, C., Talley, L.I., Sviglin, H., Stockard, C.R., Kleinberg, M.J., Barnes, M.N., Partrigde, E.E., Khazaeli, M.B., and Grizzle, W.E. 2003. Expression of CEA, Tag-72, and Lewis-Y antigen in primary and metastatic lesions of ovarian carcinoma. *Hum. Pathol. 34*:1016–1021.

Concin, N., Becker, K., Slade, N., Erster, S., Mueller-Holzner, E., Ulmer, H., Daxenbichler, G., Zeimet, A., Zeillinger, R., Marth, C., and Moll, U.M. 2004. Transdominant DeltaTAp73 isoforms are frequently up-regulated in ovarian cancer. Evidence for their role as epigenetic p53 inhibitors *in vivo. Cancer Res. 64*:2449–2460.

D'Agostino, G., Amant, F., Berteloot, P., Scambia, G., and Vergote, I. 2003. Phase II study of gemcitabine in recurrent platinum- and paclitaxel-resistant ovarian cancer. *Gynecol. Oncol. 88*: 266–269.

Davidson, B., Risberg, B., Goldberg, I., Nesland, J.M., Berner, A., Trope, C.G., Kristensen, G.B., Bryne, M., and Reich, R. 2001. Ets-l mRNA expression in effusions of serous ovarian carcinoma patients is a marker of poor outcome. *Am. J. Surg. Pathol. 25*:1493–1500.

Davies, E.J., Blackhall, F.H., Shanks, J.H., David, G., McGown, A.T., Swindle, R., Slade, R.J., Martin-Hirsch, P., Gallagher, J.T., and Jayson, G.C. 2004. Distribution and clinical significance of heparan sulfate proteoglycans in ovarian cancer. *Clin. Cancer Res. 10*:5178–5186.

De Cecco, L., Marchionni, L., Gariboldi, M., Reid, J.F., Lagonigro, M.S., Caramuta, S., Ferrario, C., Bussani, E., Mezzanzanica, D., Turatti, F., Delia, D., Daidone, M.G., Oggionni, M., Bertuletti, N., Ditto, A., Raspagliesi, F., Pilotti, S., Pierotti, M.A., Canevari, S., and Schneider, C. 2004. Gene expression profiling of advanced ovarian cancer: characterization of a molecular signature involving fibroblast growth factor 2. *Oncogene 23*:8174–8183.

Deng, W., Tsao, S.W., Guan, X.Y., Lucas, J.N., and Cheung, A.L. 2003. Role of short telomeres in inducing preferential chromosomal aberrations in human ovarian surface epithelial cells: a combined telomere quantitative fluorescence *in situ* hybridization and whole-chromosome painting study. *Genes Chromos. Cancer 37*:92–97.

Diamandis, E.P., Borgoño, C.A., Scorilas, A., Harbeck, N., Dorn, J., and Schmitt, M. 2004. Human kallikrein 11: an indicator of favorable prognosis in ovarian cancer patients. *Clin. Biochem. 37*:823–829.

Diamandis, E.P., Borgoño, C.A., Scorilas, A., Yousef, G.M., Harbeck, N., Dorn, J., Schmalfeldt, B., and Schmitt, M. 2003. Immunofluorometric quantification of human kallikrein 5 expression in ovarian cancer cytosols and its association with unfavorable patient prognosis. *Tumour Biol. 24*:299–309.

Di Cristofano, A., and Pandolfi, P.P. 2000. The multiple roles of PTEN tumour suppression. *Cell 100*:387–390.

Dodson, M.K., Cliby, W.A., Xu, H.J., DeLacey, K.A., Hu, S.X., Keeney, G.L., Li, J., Podratz, K.C., Jenkins, R.B., and Benedict, W.F. 1994. Evidence of functional RB protein in epithelial ovarian carcinomas despite loss of heterozygosity at the RB locus. *Cancer Res. 54*:610–613.

Dornan, D., Bheddah, S., Newton, K., Ince, W., Frantz, G.D., Dowd, P., Koeppen, H., Dixit, V.M., and Frenchi, D.M. 2004.

COP1, the negative regulator of p53, is overexpressed in breast and ovarian adenocarcinoma. *Cancer Res. 64*:7226–7230.

Drapkin, R., Crum, C.P., and Hecht, J.L. 2004. Expression of candidate tumor markers in ovarian carcinoma and benign ovary: evidence for a link between epithelial phenotype and neoplasia. *Hum. Pathol. 35*:1014–102l.

Dupont, J., Tanwar, M.K., Thaler, H.T., Fleisher, M., Kauff, N., Hensley, M.L., Sabbatini, P., Anderson, S., Aghajanian, C., Holland, E.C., and Spriggs, D.R. 2004. Early detection and prognosis of ovarian cancer using serum YKL-40. *J. Clin. Oncol. 22*:3330–3339.

Evangelou, A., Letarte, M., Jurisica, I., Sultan, M., Murphy, K.J., Rosen, B., and Brown, T.J. 2003. Loss of coordinated androgen regulation in nonmalignant ovarian epithelial cells with *BRCA1/2* mutations and ovarian cancer cells. *Cancer Res. 63*:2416–2424.

Fogli, A., Rodriguez, D., Eymard-Pierre, E., Bouhour, F., Labauge, P., Meaney, B.F., Zeesman, S., Kaneski, C.R., Schiffmann, R., and Boespflug-Tanguy, O. 2003. Ovarian failure related to eukaryotic initiation factor 2B mutations. *Am. J. Hum. Genet. 72*:1544–1550.

Franke, F.E., Von Georgi, R., Zygmunt, M., and Munstedt, K. 2003. Association between fibronectin expression and prognosis in ovarian carcinoma. *Anticancer Res. 23*:426l–4267.

Fraser, M., Leung, B.M., Yan, X., Dan, H.C., Cheng, J.Q., and Tsang, B.K. 2003. p53 is a determinant of X-linked inhibitor of apoptosis protein/Akt-mediated chemoresistance in human ovarian cancer cells. *Cancer Res. 163*:7081–7088.

Gallagher, N.J., Eliopoulos, A.G., Agathangelo, A., Oates, J., Crocker, J., and Young, L.S. 2002. CD40 activation in epithelial ovarian carcinoma cells modulates growth, apoptosis, and cytokine secretion. *Mol. Pathol. 55*:110–l20.

Givant-Horwitz, V., Davidson, B., van de Putte, G., Dong, H.P., Goldberg, I., Amir, S., Kristensen, G.B., and Reich, R. 2003. Expression of the 67 kDa laminin receptor and the α 6 integrin subunit in serous ovarian carcinoma. *Clin. Exp. Metastasis 20*:599–609.

Gotlieb, W.H., Goldberg, I., Weisz, B., Davidson, B., Novikov, I., Kopolovic, J., and Ben-Baruch, G. 2001. Topoisomerase II immunostaining as a prognostic marker for survival in ovarian cancer. *Gynecol. Oncol. 82*:99–l04.

Grisaru-Granovsky, S., Salah, Z., Maoz, M., Pruss, D., Belier, U., and Bar-Shavit, R. 2005. Differential expression of protease activated receptor 1 (Par1) and pY397FAK in benign and malignant human ovarian tissue samples. *Int. J. Cancer 113*: 372–378.

Gu, L., Shigemasa, K., and Ohama, K. 2004. Increased expression of IGF II mRNA-binding protein 1 mRNA is associated with an advanced clinical stage and poor prognosis in patients with ovarian cancer. *Int. J. Oncol. 24*:671–678.

Guan, X.Y., Fung, J.M., Ma, N.F., Lau, S.H., Tai, L.S., Xie, D., Zhang, Y., Hu, L., Wu, Q.L., Fang, Y., and Sham, J.S. 2004. Oncogenic role of eIF-5A2 in the development of ovarian cancer. *Cancer Res. 64*:4197–4200.

Hall, G.D., Brown, J.M., Coleman, R.E., Stead, M., Metcalf, K.S., Peel, K.R., Poole, C., Crawford, M., Hancock, B., Selby, P.J., and Perren, T.J. 2004. Maintenance treatment with interferon for advanced ovarian cancer: results of the Northern and Yorkshire gynaecology group randomised phase III study. *Br. J. Cancer 191*:621–626.

Hansen, S.W. 2002. Gemcitabine, platinum, and paclitaxel regimens in patients with advanced ovarian carcinoma. *Semin. Oncol. 29*:17–19.

Harries, M., Moss, C., Perren, T., Gore, M., Hall, G., Everard, M., A'Hem, R., Gibbens, I., Jenkins, A., Shah, R., Cole, C., Pizzada, O., and Kaye, S. 2004. A phase II feasibility study of carboplatin followed by sequential weekly paclitaxel and gemcitabine as first-line treatment for ovarian cancer. *Br. J. Cancer 91*:627–632.

Harris, M.A., Delap, L.M., Sengupta, P.S., Wilkinson, P.M., Welch, R.S., Swindell, R., Shanks, J.H., Wilson, G., Slade, R.J., Reynolds, K., and Jayson, G.C. 2003. Carcinosarcoma of the ovary. *Br. J. Cancer 88*:654–657.

Hauptmann, S., Denkert, C., Koch, I., Petersen, S., Schluns, K., Reles, A., Dietel, M., and Petersen, I. 2002. Genetic alterations in epithelial ovarian tumors analyzed by comparative genomic hybridization. *Hum. Pathol. 33*:632–641.

Ho, S.M., Lau, K.M., Mok, S.C., and Syed, V. 2003. Profiling follicle stimulating hormone-induced gene expression changes in normal and malignant human ovarian surface epithelial cells. *Oncogene 22*:4243–4256.

Høgdall, C.K., Christensen, L., and Clemmensen, I. 1993. The prognostic value of tetranectin immunoreactivity and plasma tetranectin in patients with ovarian cancer. *Cancer 72*:24l5–2422.

Høgdall, E.V., Ryan, A., Kjaer, S.K., Blaakaer, J., Christensen, L., Bock, J.E., Glud, E., Jacobs, I.J., and Hogdall, C.K. 2004. Loss of heterozygosity on the X chromosome is an independent prognostic factor in ovarian carcinoma. *Cancer 100:*2387–2395**.**

Höglund, M., Gisselsson, D., Hansen, G.B., Sall, T., and Mitelman, F. 2003. Ovarian carcinoma develops through multiple modes of chromosomal evolution. *Cancer Res. 63*:3378–3385.

Holscneider, C.H., and Berek, J.S. 2000. Ovarian cancer: epidemiology, biology, and prognostic factors. *Semin. Surg. Oncol. 19*:3–l0.

Iba, T., Kigawa, J., Kanamori, Y., Itamochi, H., Oishi, T., Simada, M., Uegaki, K., Naniwa, J., and Terakawa, N. 2004. Expression of the c-myc gene as a predictor of chemotherapy response and a prognostic factor in patients with ovarian cancer. *Cancer Sci. 95*:418–423.

Igarashi, M., Ikuma, K., Yamada, Y., Abe, Y., Igarashi, S., and Minegishi, T. 2003. High CD44 content in ovarian endometriotic cysts. *Fertil. Steril. 80*:1065–l066.

Jacobs, I.J., Skates, S.J., McDonald, N., Menon, U., Rosenthal, A.N., Davies, A.P., Woolas, I., Jayarajah, A.R., Sibley, K., Lowe, D.J., and Oraru, D.H. 1999. Screening for ovarian cancer: a pilot randomized controlled trial. *Lancet 353*:1207–1210.

Kajiyama, H., Kikkawa, F., Khin, E., Shibata, K., Ino, K., and Mizutani, S. 2003. Dipeptidyl peptidase IV overexpression induces up-regulation of E-cadherin and tissue inhibitors of matrix metalloproteinases, resulting in decreased invasive potential in ovarian carcinoma cells. *Cancer Res. 63*:2278–2283.

Kato, H., Arakawa, A., Suzumori, K., Kataoka, N., and Young, S.R. 2004. FISH analysis of BRCA1 copy number in paraffin-embedded ovarian cancer tissue samples. *Exp. Mol. Pathol. 76*: 138–142.

Khuu, H., Conner, M., Vanderkwaak, J., Shultz, J., Gomez-Navarro, J., Alvarez, R.D., Curiel, D.T., and Siegel, G.P. 1999. Detection of coxasackie-adenovirus receptor (CAR) immunoreactivity in ovarian tumors of epithelial derivation. *AIMM 7*:266–270.

Kim, T.M., Benedict, W.F., Xu, H.J., Hu, S.X., Gosewehr, J., Velicescu, M., Yin, E., Zheng, J., D'Ablaing, G., and Dubeau L. 1994. Loss of heterozygosity on chromosome 13 is common only in the biologically more aggressive subtypes of ovarian epithelial tumors and is associated with normal retinoblastoma gene expression. *Cancer Res. 54*:605–609.

Kline, K., Yu, W., and Sanders, B.G. 2001. Vitamin E: mechanisms of action as tumor cell growth inhibitors. *J. Nutr. 131*:161S–163S.

Kurlender, L., Yousef, G.M., Memari, N., Robb, J.D., Michael, I.P., Borgono, C., Katsaros, D., Stephan, C., Jung, K., and

Diamandis, E.P. 2004. Differential expression of a human kallikrein 5 (KLK5) splice variant in ovarian and prostate cancer. *Tumor Biol. 25*:149–156.

Kurose, K., Zhou, X.-P., Araki, T., Cannistra, S.A., Maher, E.R., and Eng, C. 2001. Frequent loss of PTEN expression is linked to elevated phosphorylated. Akt levels, but not associated with p27 and cyclin Dl expression, in primary epithelial ovarian carcinomas. *Am. J. Pathol. 158*:2097–2106.

Lappöhn, R.E., Burger, H.G., Bouma, J., Bangah, M., Krans, M., and de Bruijn, W.A. 1989. Inhibin as a marker for granulose-cell tumors. *N. Engl. J. Med. 321*:790–793.

Lambert-Messerlian, G.M. 2000. Is inhibin a serum marker for ovarian cancer? *Eur. J. Endocrinol. 142*:33l–333.

Lassus, H., Sihto, H., Leminen, A., Nordling, S., Joensuu, H., Nupponen, N.N., and Butzow, R. 2004. Genetic alterations and protein expression of KIT and PDGFRA in serous ovarian carcinoma. *Br. J. Cancer 91*:2048–2055.

Launonen, V., Mannermaa, A., Stenback, F., Kosma, V.M., Puistola, U., Huusko, P., Anttila M., Bloigu, R., Saarikoski, S., Kauppila, A., and Winquist, R. 2000. Loss of heterozygosity at chromosomes 3, 6, 8, 11, 16, and 17 in ovarian cancer: correlation to clinicopathological variables. *Cancer Genet. Cytogenet. 122*:49–54.

Li, L., Luan-Wang, G., Tang, B., Li, D., Zhang, W., Li, X., Zhao, J., Ding, H., Reed, E., and Li, Q.Q. 2004. Development and characterization of five cell models for chemoresistance studies of human ovarian carcinoma. *Int. J. Mol. Med. 14*:257–264.

Liede, A., Karlan, B.Y., Baldwin. R.L., Platt, L.D., Kuperstein, G., and Narod, S.A. 2002. Cancer incidence in a population of Jewish women at risk of ovarian cancer. *J. Clin. Oncol. 20*:l570–1577.

Logani, S., Oliva, E., Amin, M.B., Folpi, A.L., Cohen, C., and Young, R.H. 2003. Immunoprofile of ovarian tumors with putative transitional cell (urothelial) differentiation using novel urothelial markers: histogenetic and diagnostic implications. *Am. J. Surg. Pathol. 27*:1434–1441.

Luo, Y., and Prestwich, G.D. 1999. Synthesis and selective cytotoxicity of a hyaluronic acid-antitumor bioconjugate. *Bioconjug. Chem. 10*:755–763.

Lynch, H.T., Casey, M.J., Lynch, J., White, T.E., and Godwin, A.K. 1998. Genetics and ovarian carcinoma. *Semin. Oncol. 25*: 265–280.

Määttä, M., Santala, M., Soini, Y., Talvensaari-Mattila, A., and Turpeenniemi-Hujanen, T. 2004. Matrix metalloproteinases 2 and 9 and their tissue inhibitors in low malignant potential ovarian tumors. *Tumour Biol. 25*:188–192.

Mandelin, E., Lassus, H., Seppala, M., Leminen, A., Gustafsson, J.A., Cheng, G., Butzow, R., and Koistinen, R. 2003. Glycodelin in ovarian serous carcinoma: association with differentiation and survival. *Cancer Res. 63*:6258–6264.

Manenti, L., Paganoni, P., Floriani, I., Landoni, F., Torri, V., Buda, A., Taraboletti, G., Labianca, R., Belotti, D., and Giavazzi, R. 2003. Expression levels of vascular endothelial growth factor, matrix metalloproteinases 2 and 9 and tissue inhibitor of metalloproteinases 1 and 2 in the plasma of patients with ovarian carcinoma. *Eur. J. Cancer 39*:l948–1956.

Markman, M., Webster, K., Zanotti, K., Kulp, B., Peterson, G., and Belinson, J. 2003. Phase 2 trial of single-agent gemcitabine in platinum-paclitaxel refractory ovarian cancer. *Gynecol. Oncol. 90*:593–596.

Marrero, J.A., and Lok, A.S. 2004. Newer markers for hepatocellular carcinoma. *Gastroenterology 127*:S113–S119.

Martinez, S.L., Herzog, J., and Weitzel, J.N. 2004. Loss of five amino acids in BRCA2 is associated with ovarian cancer. *J. Med. Genet. 41*:1–3.

Masciullo, V., Baldassarre, G., Pentimalli, F., Berlingieri, M.T., Boccia, A., Chiappetta, G., Polazzo, J., Manfioletti, G., Giancotti, V., Viglietto, G., Scambia, G., and Fusco, A. 2003. HMGA 1 protein over-expression is a frequent feature of epithelial ovarian carcinomas. *Carcinogenesis 24*:1191–1198.

Matias-Guiu, X., and Prat, J. 1996. Molecular pathology of ovarian carcinomas. *Virchows Arch. 433*:103–111.

McCarthy, N., Mercer, J., and Bennett, M. 2001. Apoptotic proteins, p53 and c-myc related pathways. *Cardiol. Dis. 19*:75–89.

McCluggage, W.G. 2000. Recent advances in immunohistochemistry in the diagnosis of ovarian neoplasms. *J. Clin. Pathol. 53*:327–334.

McCluggage, W.G., and Maxwell, P. 2001. Immunohistochemical staining for calretinin is useful in the diagnosis of ovarian sex cord stromal tumors. *Histopathol. 38*:403–408.

McCluggage, W.G., Maxwell, P., and Sloan, J.M. 1997. Immunohistochemical staining of ovarian granulosa cell tumors with monoclonal antibody against inhibin. *Hum. Pathol. 28*:1034–1038.

McGuire, W.P., Blessing, J.L., Bookman, M.A., Lentz, S.S., and Dunton, C.J. 2000. Topotecan has substantial antitumor activity as first line salvage therapy in platinum-sensitive epithelial ovarian carcinoma: a gynecologic oncologic study. *J. Clin. Oncol. 18*:1062–1067.

McGuire, W.P., Hoskins, W.J., Brady, M.F., Kucera, P.R., Partridge, E.E., Look, K.Y., Clarke-Pearson, D.L., and Davidson, M. 1996. Cyclophosphamide and cisplatin compared with paclitaxel and cisplatin in patients with stage III and stage IV ovarian cancer. *N. Engl. J. Med. 334*:1–6.

Meyer, T., and Rustin, G.J. 2000. Role of tumour markers in monitoring epithelial ovarian cancer. *Br. J. Cancer 82*: 1535–1538.

Miyamoto, S., Hirata, M., Yamazaki, A., Kageyama, T., Hasuwa, H., Mizushima, H., Tanaka, Y., Yagi, H., Sonoda, K., Kai, M., Kanoh, H., Nakano, H., and Mekada, E. 2004. Heparin-binding EGF-like growth factor is a promising target for ovarian cancer therapy. *Cancer Res. 64*:5720–5727.

Mizuuchi, M., Mori, Y., Sato, K., Kamiya, H., Okamura, N., Nasim, S., Garrett, C.T., and Kudo, R. 1995. High incidence of point mutation in K-ras codon 12 in carcinoma of the fallopian tube. *Cancer 76*:86–90.

Mok, S.C., Chao, J., Skates, S., Wong, K., Yiu, G.K., Muto, M.G., Berkowitz, R.S., and Cramer, D.W. 2001. Prostasin, a potential serum marker for ovarian cancer: identification through microarray technology. *J. Natl. Cancer Inst. 93*:1458–1464.

Morgenbesser, S.D., Schreiber-Agus, N., Bidder, M., Mahon, K.A., Overbeek, P.A., Horner, J., and DePinho, R.A. 1995. Contrasting roles for c-Myc and L-Myc in the regulation of cellular growth and differentiation *in vivo*. *EMBO J. 14:*743–756.

Morita, T., Shibata, K., Kikkawa, F., Kajiyama, H., Ino, K., and Mizutani, S. 2004. Oxytocin inhibits the progression of human ovarian carcinoma cells *in vitro* and *in vivo*. *Int. J. Cancer 109*:525–532.

Movahedi-Lankarani, S., and Kumar, R.J., 2002. Calretinin, a more sensitive but less specific marker than α-inhibin for ovarian sex cord-stromal neoplasms. *Am. J. Surg. Pathol. 26*: 14277–14283.

Muggia, F.M., Braly, P.S., Brady, M.F., Sutton, G., Niemann, T.H., Lentz, S.L., Alvarez, R.D., Kucera, P.R., and Small, J.M. 2000. Phase III randomized study of cisplatin versus paclitaxel versus cisplatin and paclitaxel in patients with suboptimal stage III or IV ovarian cancer: a gynecologic oncology group study. *J. Clin. Oncol. 18*:106–115.

Nezhat, F., Cohen, C., Rahaman, J., Gretz, H., Cole, P., and Kalir, T. 2002. Comparative immunohistochemical studies of bcl-2 and

p53 proteins in benign and malignant ovarian endometriotic cysts. *Cancer 94*:2935–2940.

Ni, X., Zhang, W., Huang, K.C., Wang, Y., Ng, S.K., Mok, S.C., Berkowitz, R.S., and Ng, S.W. 2004. Characterisation of human kallikrein 6/protease M expression in ovarian cancer. *Br. J. Cancer 91*:725–731.

Noelle, R.J., Ledbetter, J.A., and Aruffo, A. 1992. CD40 and its ligand, an essential ligand-receptor pair for thymus-dependent B-cell activation. *Immunol. Today 13*:431–433.

Obermair, A., Schmid, B.C., Packer, L.M., Leodolter, S., Birner, P., Ward, B.G., Crandon, A.J., McGuckin, M.A., and Zeillinger, R. 2002. Expression of MUC1 splice variants in benign and malignant ovarian tumours. *Int. J. Cancer 100*:l66–171.

Olopade, O.I., and Wei, M. 2003. FANCF methylation contributes to chemoselectivity in ovarian cancer. *Cancer Cell 3*:417–420.

Otis, C.N., Krebs, P.A., Quezado, M.M., Albuquerque, A., Bryant, B., San Juan, X., Kleiner, D., Sobel, M.E., and Menrno, M.J. 2000. Loss of heterozygosity in P53, BRCA1, and estrogen receptor genes and correlation to expression of p53 protein in ovarian epithelial tumors of different cell types and biological behavior. *Hum. Pathol. 31*:233–238.

Ozols, R.F., Bundy, B.N., Greer, B.E., Fowler, J.M., Clarke-Pearson, D., Burger, R.A., Mannel, R.S., DeGeest, K., Hartenbach, E.M., and Baergen, R. 2003. Phase III trial of carboplatin and paclitaxel compared with cisplatin and paclitaxel in patients with optimally resected stage III ovarian cancer: a Gynecologic Oncology Group Study. *J. Clin. Oncol. 21*: 3l94–3200.

Parmar, M.K., Ledermann, J.A., Colombo, N., du Bois, A., Delaloye, J.F., Kristensen, G.B., Wheeler, S., Swart, A.M., Qian, W., Torri, V., Floriani, I., Jayson, G., Lamont, A., and Trope, C. 2003. Paclitaxel plus platinum-based chemotherapy versus conventional platinum-based chemotherapy in women with relapsed ovarian cancer: the ICON4/AGO-OVAR-2.2 trial. *Lancet 361*:2099–2106.

Pautier, P., Morice, P., Delaloge, S., Bressac-de Paillerets, B., and Spatz, A. 2004. Is systemic disease in the coelomic epithelium associated with BRCA1 germline mutations? *J. Natl. Cancer Inst. 96*:488–489.

Peiró, G., Diebold, J., and Lohrs, U. 2002. CAS (cellular apoptosis susceptibility) gene expression in ovarian carcinoma: correlation with 20q 13.2 copy number and cyclin Dl, p53, and Rb protein expression. *Am. J. Clin. Pathol. 118*: 922–929.

Pepe, M., Etzioni, R., Feng, Z., Potter, J.D., Thompson, M.L., Thornquist, M., Winget, M., and Yasui, Y. 2001. Phases of biomarker development for early detection of cancer. *J. Natl. Cancer Inst. 93*:1054–l06l.

Peyssonnaux, C., and Eychene, A. 2001. The Raf/MEK/ERK pathway: new concepts of activation. *Biol. Cell 9*3:53–62.

Philp, A.J., Campbell, I.G., Leet, C., Vincan, E., Rockman, S.P., Whitehead, R.H., Thomas, R.J., and Phillips, W.A. 2001. The phosphatidylinositol 3′-kinase p85alpha gene is an oncogene in human ovarian and colon tumors. *Cancer Res. 61*:7426–7429.

Piek, J.M., Verheijen, R.H., Menko, F.H., Jongsma, A.P., Weegenaar, J., Gille, J.J., Pals, G., Kenemans, P., van Diest, P.J. 2003. Expression of differentiation and proliferation related proteins in epithelium of prophylactically removed ovaries from women with a hereditary female adnexal cancer predisposition. *Histopathol. 43*:26–32.

Pieretti, M., Hopenhayn-Rich, C., Khatar, N.H., Cao, Y., Huang, B., and Tucker, T.C. 2002. Heterogeneity of ovarian cancer: relationships among histological group, stage of disease, tumor markers, patient characteristics, and survival. *Cancer Invest. 20*:11–23.

Polakis, M. 2001. More than one way to skin a catenin. *Cell 105*: 563–566.

Qazi, F., and McGuire, W.P. 1995. The treatment of epithelial ovarian cancer. *CA Cancer J. Clin. 45*:88–101.

Rasola, A., Anguissola, S., Ferrero, N., Gramaglia, D., Maffe, A., Maggiora, P., Comoglio, P.M., and Di Renzo, M.F. 2004. Hepatocyte growth factor sensitizes human ovarian carcinoma cell lines to paclitaxel and cisplatin. *Cancer Res. 64*:1744–1750.

Raspollini, M.R., Amunni, G., Villanucci, A., Baroni, G., Taddei, A., and Taddei, G.L. 2004. Utility of CDX-2 in distinguishing between primary and secondary (intestinal) mucinous ovarian carcinoma: an immunohistochemical comparison of 43 cases. *Appl. Immunohistochem. Mol. Morphol. 12*:127–131.

Ricci, R., Komminoth, P., Bannwart, F., Torhorst, J., Wight, E., Heitz, P.U., and Caduff R.F. 2003. PTEN as a molecular marker to distinguish metastatic from primary synchronous endometrioid carcinomas of the ovary and uterus. *Diag. Mol. Pathol. 12*:71–78.

Robertson, D.M., Cahir, N., Burger, H.G., Mamers, P., and Groome, N. 1999. Inhibin forms in serum from post menopausal women with ovarian cancers. *Clin. Endocrinol. 50*:381–386.

Robertson, D.M., Stephenson, T., Pruysers, E., Burger, H.G., McCloud, P., Tsigos, A., Groome, N., Mamers, P., McNeilage, J., Jobling, T., and Healy, D. 2002. Inhibins/activins as diagnostic markers for ovarian cancer. *Mol. Cellular Endocrinol. 191*:97–103.

Ronnett, B.M., Kurman, R.J., Shmookler, B.M., Sugarbaker, P.H., and Young, R.H. 1997. The morphologic spectrum of ovarian metastases of appendiceal adenocarcinomas: a clinicopathologic and immunohistochemical analysis of tumors often misinterpreted as primary ovarian tumors or metastatic tumors from other gastrointestinal sites. *Am. J. Surg. Pathol. 21*:1144–1155.

Rutter, J.L., Wacholder, S., Chetrit, A., Lubin, F., Menczer, J., Ebbers, S., Tucker, M.A., Struewing, J.P., and Hartge, P. 2003. Gynecologic surgeries and risk of ovarian cancer in women with BRCA1 and BRCA2 Ashkenazi founder mutations: an Israeli population-based case-control study. *J. Natl. Cancer Inst. 95*:1072–1078.

Sakamoto, O.A., Yokoyama, Y., Umemoto, M., Futagami, M., Sakamoto, T., Bing, X., and Mizunuma, H. 2004. Clinical implication of expression of cyclooxygenase-2 and peroxisome proliferator activated-receptor gamma in epithelial ovarian tumours. *Br. J. Cancer 91*:633–638.

Santin, A.D., Zhan, F., Bellone, S., Palmieri, M., Cane, S., Bignotti, B., Anfossi, S., Gokden, M., Dunn, D., Roman, J.J., O'Brien, T.J., Tian, E., Cannon, M.J., Shaughnessy, J. Jr., and Pecorelli, S. 2004. Gene expression profiles in primary ovarian serous papillary tumors and normal ovarian epithelium: identification of candidate molecular markers for ovarian cancer diagnosis and therapy. *Int. J. Cancer 112*:14–25.

Sato, S., Kigawa, J., Minagawa, Y., Okada, M., Shimada, M., Takahashi, M., Kamazawa, S., and Terakawa, N. 1999. Chemosensitivity and p53-dependent apoptosis in epithelial ovarian carcinoma. *Cancer 86*:1307–1313.

Schmandt, R.E., Broaddus, R., Lu, K.H., Shvartsman, H., Thornton, A., Malpica, A., Sun, C., Bodurka, D.C., and Gershenson, D.M. 2003. D.M. Expression of c-ABL, c-KIT, and platelet-derived growth factor receptor-beta in ovarian serous carcinoma and normal ovarian surface epithelium. *Cancer 98*:758–764.

Scholler, N., Fu, N., Yang, Y., Ye, Z., Goodman, G.E., Hellstrom, K.E., and Hellstrom, I. 1999. Soluble member(s) of the mesothelin/megakaryocyte potentiating factor family are detectable in sera from patients with ovarian carcinoma. *Proc. Natl. Acad. Sci. USA 96*:1153l–11536.

Schöndorf, T., Gohring, U.J., Roth, G., Middel, I., Becker, M., Moser, N., Valter, M.M., and Hoopmann, M. 2003. Time to progression is dependent on the expression of the tumour suppressor PTEN in ovarian cancer patients. *Eur. J. Clin. Invest. 33*:256–260.

Schultz, D.C., Vanderveer, L., Berman, D.B., Hamilton, T.C., Wong, A.J., and Godwin, A.K. 1996. Identification of two candidate tumor suppressor genes on chromosome l7p 13.3. *Cancer Res. 56*:1997–2002.

Schummer, M., Ng, W.V., Bumgarner, R.E., Nelson, P.S., Schummer, B., Bednarski, D.W., Hassell, L., Baldwin, R.L., Karlan, B.Y., and Hood, L. 1999. Comparative hybridization of an array of 21,500 ovarian cDNA for the discovery of genes over expressed in ovarian carcinomas. *Gene 238*:375–385.

Schvartsman, H.S., Lu, K.H., Le, J., Lillie, J., Deavers, M.T., and Clifford, S.L. 2001. *Overexpression of NES-1 in epithelial ovarian carcinoma* (abstract). Society of Gynecologic 32nd Annual Meeting. Abstract 103.

Scorilas, A., Borgono, C.A., Harbeck, N., Dorn, J., Schmalfeldt, B., Schmitt, M., and Diamandis, E.P. 2004. Human kallikrein 13 protein in ovarian cancer cytosols: a new favorable prognostic marker. *J. Clin. Oncol. 22*:678–685.

Sehouli, J., Mustea, A., Koensgen, D., and Lichtenegger, W. 2003. Interleukin-1 receptor antagonist gene polymorphism in epithelial ovarian cancer. *Cancer Epidemiol. Biomark. Prev. 12*:1205–1208.

Shah, V.I., Freites, O.N., Maxwell, P., and McCluggage, W.G. 2003. Inhibin is more specific than calretinin as an immunohistochemical marker for differentiating sarcomatoid granulosa cell tumour of the ovary from other spindle cell neoplasms. *J. Clin. Pathol. 56*:221–224.

Shen, G.H., Ghazizadeh, M., Kawanami, O., Shimizu, H., Jin, E., Araki, T., and Sugisaki, Y. 2000. Prognostic significance of vascular endothelial growth factor expression in human expression in human ovarian carcinoma. *Brit. J. Cancer 83*:196–203.

Sier, C.F.M., Stephens, R., Bizik, J., Mariani, A., Bassan, M., Pedersen, N., Frigerio, L., Ferrari, A., Dano, K., Brunner, N., and Blasi, F. 1998. The level of urokinase-type plasminogen activator receptor is increased in serum of ovarian cancer patients. *Cancer Res. 58*:1843–1849.

Singer, G., Kurman, R.J., Chang, H.W., Cho, S.K., and Shih, I.M. 2002. Diverse tumorigenic pathways in ovarian serous carcinoma. *Am. J. Pathol. 160*:1223–1228.

Singer, G., Oldt, R. 3rd, Cohen,Y., Wang, B.G., Sidransky, D., Kurman, R.J., and Shih, I.M. 2003. Mutations in BRAF and KRAS characterize the development of low-grade ovarian serous carcinoma. *J. Natl. Cancer Inst. 95*:484–486.

Smith, V., Hobbs, S., Court, W., Eccles, S., Workman, P., and Kelland, L.R. 2002. ErbB2 overexpression in an ovarian cancer cell line confers sensitivity to the HSP9O inhibitor geldanamycin. *Anticancer Res. 22*:1993–1999.

Sonoda, G., Palazzo, J., du Manoir, S., Godwin, A.K., Feder, M., Yakushiji, M., and Testa, J.R. 1997. Comparative genomic hybridization detects frequent overrepresentation of chromosomal material from 3q26, 8q24, and 20q13 in human ovarian carcinomas. *Genes Chromos. Cancer 20*:320–328.

Strobel, L., and Graham, R. 2003. Primary non-small cell neuroendocrine carcinoma of the ovary. *J. Histotechnol. 26*:73–76.

Suh, E., and Traber, P.G. 1996. An intestine-specific homeobox gene regulates proliferation and differentiation. *Mol. Cell Biol. 16*:619–625.

Symonds, D., Tomic, D., Borgeest, C., McGee, E., and Flaws, J.A. 2003. Smad 3 regulates proliferation of the mouse ovarian surface epithelium. *Anat. Rec. 273A*:681–686.

Taetle, R., Aickin, M., Yang, J.M., Panda, L., Emerson, J., Roe, D., Adair, L., Thompson, F., Liu, Y., Wisner, L., Davis, J.R., Trent, J., and Alberts, D.S. 1999. Chromosome abnormalities in ovarian adenocarcinoma: I, nonrandom chromosome abnormalities from 244 cases. *Genes Chromos. Cancer 25*:290–300.

Takada, T., Yagi, Y., Maekita, T., Imura, M., Nakagawa, S., Tsao, S.W., Miyamoto, K., Yoshino, O., Yasugi, T., Taketani, Y., and Ushijima, T. 2004. Metbylation-associated silencing of the Wnt antagonist SFRP1 gene in human ovarian cancers. *Cancer Sci. 95*:741–744.

Takahashi, M., Kigawa, J., Minagawa, Y., Itamochi, H., Shimada, M., Kamazawa, S., Sato, S., Akeshima, R., and Terakawa, N. 2000. Sensitivity to paclitaxel is not related to p53-dependent apoptosis in ovarian cancer cells. *Eur. J. Cancer 36*:1863–1868.

Thaker, P.H., Deavers, M., Celestino, J., Thorton, A., Fletcher, M.S., Landen, C.N., Kinch, M.S., Kiener, P.A., and Sood, A.K. 2004. EphA2 expression is associated with aggressive features in ovarian carcinoma. *Clin. Cancer Res. 10*:5145–5150.

Tornillo, L., Moch, H., Diener, P.A., Lugli, A., and Singer, G. 2004. CDX-2 immunostaining in primary and secondary ovarian carcinomas. *J. Clin. Pathol. 51*:641–643.

Tringler, B., Lebner, R., Shroyer, A.L., and Shroyer, K.R. 2004. Immunohistochemical localization of survivin in serous tumors of the ovary. *Appl. Immunohistochem. Mol. Morphol.12*:40–43.

Tsuji, K., Mizumoto, K., Sudo, H., Kouyama, K., Ogata, E., and Matsuoka, M. 2002. p53-independent apoptosis is induced by the p19ARF tumor suppressor. *Biochem. Biophys. Res. Commun. 295*:621–629.

Tuxen, M.K., Soletormos, G., and Dombernowsky, P. 1995. Tumor markers in the management of patients with ovarian cancer. *Cancer. Treat. Rev. 21*:215–245.

Van Haaften-Day, C., Russell, P., Davies, S., King, N.J., and Tattersall, M.H. 2003. Expression of FAS and FasL in human serrous ovarian epithelial tumors. *Hum. Pathol. 34*:74–79.

Vassilopoulos, I., Korkolopoulou, P., Konstantinidou, A.E., Patsouris, E., Eftichiadis, C., Thymara, I., Perdiki, M., Pavlakis, K., Agapitos, E., and Davaris, P.S. 2003. Evaluation of the cyclin-dependent kinase inhibitor p21 Cip 1 in epithelial ovarian tumors of low malignant potential and adenocarcinomas. *Histol. Histopathol. 18*:761–770.

Wang, Z.Y., Gaggero, A., Rubartelli, A., Rosso, O., Miotti, S., Mezzanzanica, D., Canevari, S., and Ferrini, S. 2002. Expression of interleukin-18 in human ovarian carcinoma and normal ovarian epithelium: evidence for defective processing in tumor cells. *Int. J. Cancer 98*:873–878.

Watanabe, T., Imoto, I., Katahira, T., Hirasawa, A., Ishiwata, I., Emi, M., Takayama, M., Sato, A., and Inazawak, J. 2002. Differentially regulated genes as putative targets of amplifications at 20q in ovarian cancers. *Jpn. J. Cancer Res. 93*: 1114–1122.

Wauters, C.C., Smedts, F., Gerrits, L.G., Bosman, F.T., and Ramaekers, F.C. 1995. Keratins 7 and 20 as diagnostic markers of carcinomas metastatic to the ovary. *Hum. Pathol. 26*: 852–855.

Weichert, W., Denkert, C., Schmidt, M., Gekeler, V., Wolf, G., Kobel, M., Dietel, M., and Hauptmann S. 2004. Polo-like kinase isoform expression is a prognostic factor in ovarian carcinoma. *Br. J. Cancer 90*:815–821.

Whittemore, A.S., and McGuire, V. 2002. Analysis of the human progesterone receptor gene polymorphism PROGINS in Austrian ovarian cancer patients. *Int. J. Cancer 101*:202.

Wiechen, K., Diatchenko, L., Agoulnik, A., Scharff, K.M., Schober, H., Arlt, K., Zhumabayeva, B., Siebert, P.D., Dietel, M., Schafer, R., and Sers, C. 2001. Caveolin-1 is down-regulated in human ovarian carcinoma and acts as a candidate tumor suppressor gene. *Am. J. Pathol.* 159:1635–1643.

Wiener, J.R., Hurteau, J.A., Kerns, B.J., Whitaker, R.S., Conaway, M.R., Berchuck, A., and Bast, R.C. 1994. Overexpression of the tyrosine phosphatase PTP1B is associated, with human ovarian carcinomas. *Am. J. Obstet. Gynecol. 170*:1177–1183.

Wisman, G.B., Hollema, H., Helder, M.N., Knol, A.J., van der Meer, G.T., Krans, M., De Jong, S., De Vries, E.G., van der Zee, A.G. 2003. Telomerase in relation to expression of p53, c-Myc and estrogen receptor in ovarian tumours. *Int. J. Oncol. 23*: l451–1459.

Wu, R., Lin, L., Beer, D.G., Ellenson, L.H., Lamb, B.J., Rouillard, J.M., Kuick, R., Hanash, S., Schwartz, D.R., Fearon, E.R., and Cho, K.R. 2003. Amplification and overexpression of the L-MYC proto-oncogene in ovarian carcinoma. *Am. J. Pathol. 162*:1603–1610.

Wulfkuhle, J.D., Aquino, J.A., Calvert, V.S., Fishman, D.A., Coukos, G., Liotta, L.A., and Petricoin, E.F. 2003. Signal pathway profiling of ovarian cancer from human tissue specimens using reverse-phase protein microarrays. *Proteomics 3*:2085–2090.

Yamamoto, S., Konishi, I., Mandai, M., Kuroda, H., Komatsu, T., Nanbu, K., Sakahara, H., and Mori, T. 1997. Expression of endothelial growth factor (VEGF) in epithelial ovarian neoplasms: correlation with clinicopathology and patient survival, and analysis of serum VEGF levels. *Br. J. Cancer. 76*:1221–1227.

Yanaihara, N., Nishioka, M., Kohno, T., Otsuka, A., Okamoto, A., Ochiai, K., Tanaka, T., and Yokota, J. 2004. Reduced expression of MYO 18B, a candidate tumor-suppressor gene on chromosome arm 22q, in ovarian cancer. *Int. J. Cancer 112*:150–154.

Yang, H., Ou, C.C., Feldman, R.I., Nicosia, S.V., Kruk, P.A., and Cheng, J.Q. 2004. Aurora-A kinase regulates telomerase activity through c-Myc in human ovarian and breast epithelial cells. *Cancer Res. 64:*463–467.

Yang Feng, T.L., Han, H., and Schwartz, P.E. 1992. Frequent loss of heterozygosity on chromosome Xp and l3q in human ovarian cancer. *Int. J. Cancer 52*:575–580.

Yao, D.X., Soslow, R.A., Hedvat, C.V., Leitao, M., and Baergen, R.N. 2003. Melan-A (Al03) and inhibin expression in ovarian neoplasms. *Appl. Immunohistochem. Mol. Morphol. 11*:244–249.

Yousef, G.M., and Diamandis, E.P. 2001. The new human tissue kallikrein gene family: structure, function, and association to disease. *Endocr. Rev. 22*:184–204.

Yousef, G.M., Fracchioli, S., Scorilas, A., Borgono, C.A., Iskander, L., Puopolo, M., Massobrio, M., Diamandis, E.P., and Katsaros, D. 2003. Steroid hormone regulation and prognostic value of the human kallikrein gene 14 in ovarian cancer. *Am. J. Clin. Pathol. 119*:346–355.

Zamecnik, M., and Michal, M. 2003. Ovarian carcinoma of hypercalcemic type: myoid features and lack of estrogen and progesterone receptors. *Virchows Arch. 442*:186–187.

Zhai, Y., Wu, R., Schwartz, D.R., Darrah, D., Reed, H., Kolligs, F.T., Nieman, M.T., Fearon, B.R., and Cho, K.R. 2002. Role of beta-catenin/T-cell factor-regulated genes in ovarian endometrioid adenocarcinomas. *Am. J. Pathol. 160*:1229–l238.

Zhang, G.Y., Ahmed, N., Riley, C., Oliva, K., Barker, G., Quinn, M.A., and Rice, G.E. 2005. Enhanced expression of peroxisome proliferator-activated receptor gamma in epithelial ovarian carcinoma. *Br. J. Cancer. 92*:113–119.

Zhang, Z., Bast, R.C. Jr., Yu, Y., Li, J., Sokoll, L.J., Rai, A.J., Rosenzweig, J.M., Cameron, B., Wang, Y.Y., Meng, X.Y., Berchuck, A., van Haaften-Day, C., Hacker, N.F., de Bruijn, H.W., van der Zee, A.G., Jacobs, I.J., Fung, E,T., and Chan, D.W. 2004. Three biomarkers identified from serum proteomic analysis for the detection of early stage ovarian cancer. *Cancer Res. 64*:5882–5890.

Zhou, C., and Liu, J. 2003. Inhibition of human telomerase reverse transcriptase gene expression by BRCA1 in human ovarian cancer cells. *Biochem. Biophys. Res. Commun. 303*:130–136.

Zurawski, V.R.J., Ørjaaseter, H., Andersen, A., and Jellum, E. 1988. Elevated serum CA 125 levels prior to diagnosis of ovarian neoplasia: relevance for early detection of ovarian cancer. *Int. J. Cancer 41*:677–680.

2

Methods for Detecting Genetic Abnormalities in Ovarian Carcinoma Using Fluorescence *in situ* Hybridization and Immunohistochemistry

Ngan F. Huang, Mala Gupta, and Sunny Luke

Introduction

Ovarian carcinoma (OC) is the fifth most common cancer in females (after cancers of the breast, lung, colon, and uterus). It is estimated that in the United States there were 22,220 new cases of OC in 2005, of which 16,210 people died (American Cancer Society, 2005). It is believed that OC arises from the surface epithelium of the ovary. The World Health Organization (WHO) classifies OC into several histologic subtypes, of which serous, mucinous and endometrioid subtypes constitute up to 90% of all cases. These subtypes can be further classified into borderline tumors (low malignant potential) and frankly invasive carcinomas. For prognostic purposes, invasive carcinomas are grouped into well-differentiated, moderately differentiated, and poorly differentiated carcinoma based on the degree of differentiation.

The presence of abnormal amounts of deoxyribonucleic acid (DNA) in tumor-cell nuclei was discovered as early as 1936, but only during the past 20 years has evidence emerged for the accumulation of different genetic abnormalities in various OC subtypes. This presumably explains the heterogeneity of OC, differences in tumor growth rates, and varied responses to chemotherapy. Changes in chromosomes, genes, and gene expressions play a pivotal role in tumor genesis and progression. The aggressiveness of OC depends on genetic abnormalities, which relates to the activation of oncogenes, inactivation of tumor-suppressor genes, changes in chromosome number and structure, loss of heterozygosity (LOH), and other epigenetic alterations. Some of the changes consistently occurring in a particular subtype can be exploited as tumor markers for early detection, diagnosis, prognosis, and therapeutic monitoring (Wang, 2002).

Of the two techniques discussed in this chapter, fluorescence *in situ* hybridization (FISH), or interphase cytogenetics, is gradually finding use in routine work. Examples of diagnostic use of FISH include *HER-2/neu*

Handbook of Immunohistochemistry and *in situ* Hybridization of Human Carcinomas, Volume 4: Molecular Genetics, Gastrointestinal Carcinoma, and Ovarian Carcinoma

detection in breast carcinoma prognosis and therapy, *N-myc* amplifications in neuroblastoma, trisomy 12 analysis in chronic lymphocytic leukemia (CLL), and *Bcr/Abl* gene fusion as a marker for Philadelphia (Ph) chromosome in chronic myelogenous leukemia (CML) (Gozzetti *et al.,* 2000; Kearney, 1999; Ross and Fletcher, 1999). Karyotypic analysis by high-resolution chromosome banding following tissue culture has not found widespread application in routine diagnostic work because of unacceptably long turnaround time and inherent technical problems in the methodology (John, 2003). However, FISH provides rapid results regarding the genetic status of interphase cancer cells, with the help of various chromosome- and gene-specific DNA probes. These genetic abnormalities include numeric anomalies such as chromosome aneuploidy, structural anomalies such as chromosome translocations, gene duplications, and losses by deletion. The application of FISH to formalin-fixed and paraffin-embedded (FFPE) tissue has also opened the possibility of using archival material (Luke *et al.,* 1997).

The second technique to be discussed in this chapter, immunohistochemistry (IHC), is well entrenched in diagnostic histopathology and is routinely used in all laboratories. Several antibodies are commonly used to narrow down the differential diagnosis in "metastatic carcinoma of unknown primary" or, less frequently, to aid in the primary diagnosis of various histologic subtypes of ovarian carcinoma (McCluggage, 2002). Thus, FISH and IHC can be performed on consecutive sections derived from the same tissue paraffin block.

In this chapter on technical methodology, we provide the protocols for FISH using different types of DNA probes and IHC detection of various antigens in a wide spectrum of specimens. These two techniques will shed light on the pathogenesis and progression of ovarian cancers as well as aid in diagnosis and prognosis in different clinical situations.

Ovarian Carcinoma Specimen Preparation

Various types of specimens can be used for FISH or IHC. These include tissue sections, cells grown in culture, and cells isolated from peritoneal fluids. Before carrying out FISH or IHC, the specimen must be preserved to maintain tissue morphology and mounted on glass slides. The sample preparation method can affect the quality of results, and the optimal protocol is best determined empirically. The primary types of prepared tissue samples are FFPE tissue sections, cytologic preparations, and cryosections (Brown *et al.,* 2000). Traditionally, paraffin-embedded sections have been the preferred sample type because of better resolution, preservation of morphology, and ease of storage (Jackson, 2002). Metaphase chromosomal analysis can be performed on cells derived from fresh samples grown in culture (Dracopoli *et al.,* 2001). Cell suspensions obtained from peritoneal fluid or other sources can be processed into cytospin specimens, and fresh tissues can be rapidly frozen for cryosectioning (Luke *et al.,* 1998).

Formalin-Fixed and Paraffin-Embedded Sections

Neutral-buffered formalin (10%) is a common choice for fixation in diagnostic pathology. Formalin preserves the tissue morphology by forming cross-links within and between protein molecules through hydroxymethylene bridges (Werner *et al.,* 1996). However, the drawback of formalin fixation is that the cross-links mask epitopes, so formalin-fixed samples usually require an epitope recovery step for IHC and a DNA demasking step for FISH. Prolonged fixation periods (>24 hr) may reduce antigenicity, so samples that are not immediately processed after formalin fixation should be stored in 70% ethanol at 4°C (Roche and Hsi, 2001). After fixation, the samples are dehydrated in alcohols and cleared in xylene before embedding in paraffin. On solidification, the paraffin-embedded tissue blocks are cut into 4 μm thick sections and applied to glass slides for FISH or IHC analysis.

Protocol 1: Preparation of Formalin-Fixed and Paraffin-Embedded Tissue Sections

MATERIALS

1. Dulbecco's phosphate buffered saline (PBS) (pH 7.4) (Fisher Scientific, Pittsburgh, PA)
2. 10% neutral-buffered formalin (pH 6.8–7.2), (Fisher Scientific)
3. 70%, 80%, and 95% ethanol, diluted from 100% ethanol in distilled water.
4. Xylene
5. Paraffin wax (Paraplast, Fisher Scientific)
6. Biopsy cassettes
7. Superfrost Plus glass slides
8. Embedding molds
9. Histology jars and containers
10. Rotary microtome
11. Tissue flotation bath
12. Cold plate, Tissue Tek II (VWR, Westchester, PA)
13. Forceps
14. Razor blade
15. Slide warmer
16. Shur/mark pen (Fisher Scientific)

METHOD

1. Place samples in tissue cassettes. Label cassettes using a Shur/mark pen.
2. Immerse cassettes in 10% formalin for 12–24 hr for tissue fixation.
3. Transfer cassettes to ethanol dehydration series for 45 min each in 70%, 80%, and 95% ethanol.
4. Immerse cassettes in 2 changes of 100% ethanol for 45 min each.
5. Clear samples in 2 changes of xylene for 45 min.
6. Soak cassettes in a glass jar of melted paraffin wax for 45 min for infiltration of tissue at the melting temperature of the paraffin (58–60°C).
7. Fill the depression of the metal embedding mold with paraffin wax, and allow it to harden slightly by cooling for 30 sec on a cold plate. Remove sample from biopsy cassette and place sample in desired position (orientation) on top of the paraffin with forceps.
8. Place the underside of the biopsy cassette on top of the embedding mold and pour melted paraffin wax through the cassette to fill the mold.
9. Transfer the mold with cassette onto a cold plate until the paraffin wax solidifies.
10. Remove embedding mold and trim the cutting surface of the paraffin block into a trapezoidal shape with a razor blade.
11. Mount the block onto a standard rotary microtome.
12. Cut 4 μm thick sections of the paraffin-embedded samples, which will produce serial sections of paraffin ribbon. Float the ribbon on a heated waterbath at 48°C. Separate the ribbon into one or two sections using forceps.
13. Submerge the lower half of a charged slide in the waterbath to attach the sections onto it.
14. Heat slides on a 60°C side warmer for 10 min to attach the sections on the slide.
15. Store slides at room temperature.
16. Slides with tissue sections can be processed for FISH and IHC.

Note: The procedure given here is ideal for research laboratories involved in low-volume sample preparations. In regular pathology laboratories, after formalin fixation of tissues, samples in tissue cassettes are dehydrated through alcohols, cleared in xylene, and infiltrated in molten paraffin through an automated processing system using tissue processors. After automated tissue processing, embedding is carried out in embedding stations with multiple temperature control systems (68°C, 58°C, 4°C, and –6°C).

Frozen Sections

Frozen sections can be prepared from samples immediately frozen after removal from the body. This method preserves antigenic reactivity and requires less processing time.

Protocol 2: Preparation of Fresh Frozen Sections

MATERIALS

1. Cryostat
2. Cryostat mounting disc
3. Optimal Cutting Temperature (OCT) freezing compound (Sakura Finetek, Torrance, CA)
4. Charged glass slides
5. Isopentane
6. Cryomold
7. Dry ice
8. Acetone
9. Forceps

METHOD

1. Prepare a bath of isopentane chilled over dry ice.
2. Fill half of cryomold with OCT compound and place in isopentane bath.
3. When OCT freezes, remove mold from isopentane bath and orient sample in the mold with forceps. Fill mold with more OCT to submerge the sample.
4. Keep mold in isopentane until frozen.
5. Allow samples to equilibrate at –20°C for at least 1 hr prior to cryosectioning.
6. Pour a layer of OCT onto a cryostat specimen disc. Remove cryomold and mount the OCT specimen block onto the cryostat specimen disk.
7. Allow the specimen disc to freeze in cryostat at –20°C for 5 min.
8. Cut 4 μm thick sections and transfer them to charged glass slides. Slides can be stored at –70°C until ready for use.
9. Fix slides at –20°C in acetone or other suitable fixatives for 2 min before starting FISH or IHC procedure.

Single-Cell Suspensions

Protocol 3: Preparation of Single-Cell Suspensions from FFPE Tissue

MATERIALS

1. Paraffin-embedded tissue blocks (see Protocol 1)
2. Microcentrifuge tube
3. Xylene
4. Ethanol
5. Deionized water
6. Pepsin (Gibco, Carlsbad, CA)
7. PBS (pH 7.4)
8. Dry ice
9. Glass slides
10. Centrifuge

11. Waterbath
12. Cotton gauze

METHOD

1. Cut paraffin-embedded tissue into 1–3 sections, each one 50-µm thick.
2. Transfer 1–2 50 µm tissue pieces into a microcentrifuge tube.
3. Deparaffinize the thick tissue sections by adding 1 ml of xylene into microcentrifuge tube. Incubate for 30 min at room temperature.
4. Continue dewaxing with a second change of xylene for an additional 10 min.
5. Rehydrate the tissue pieces sequentially in an ethanol series of 100%, 90%, 70%, and 50%. Add 1 ml of ethanol at each interval and incubate for 10 min.
6. Continue final dehydration through 1 ml of deionized water for 10 min.
7. Perform protein digestion of tissue pieces by incubating in 0.5% pepsin at pH 1.5 in a 37°C waterbath for 45–60 min. Vortex at 10 min intervals.
8. Remove the undigested fragments (by filtration through cotton gauze) and pellet the cells by centrifugation at 8000 X g for 8 min.
9. Wash the cell pellet 2× in PBS and finally resuspend in 350 µl of PBS.
10. Aliquot 10–20 µ1 of the cell suspension on histologic slides and spread the cell suspension evenly over the slide.
11. Dry at 65°C for 10 min before proceeding to FISH or IHC procedure.

Note: Refer to Schurter *et al.* (2002) for further information regarding this protocol.

Ovarian Tumor Cell Culture and Metaphase Chromosomes

Protocol 4: Ovarian Tumor Cell Culture and Metaphase Chromosome Preparation

To identify altered metaphase chromosomes, fresh ovarian tumor tissue can be grown in culture flasks for 10–15 days to yield sufficient mitotic cells for preparing analyzable chromosomes. These chromosomes can be used for conventional FISH, G-banding, chromosome painting, comparative genomic hybridization, microdissection, and spectral karyotyping.

Ovarian Tumor Cell Culture

MATERIALS

1. Culture medium: 500 ml RPMI 1640 (GIBCO Carlsbad, CA), 100 ml fetal bovine serum (FBS) (GIBCO), 6 ml L-glutamine (200 mM, l00×) (GIBCO), 12 ml penicillin/streptomycin, (pen/strep; 10,000 U/ml, 10,000 µg/ml, GIBCO)
2. Transport solution: 100 ml PBS (1×) (GIBCO)
3. Collagenase enzyme (0.8%) solution: 120 mg collagenase II (GIBCO), 15 ml RPMI 1640 (Collagenase is dissolved in RPMI 1640 incomplete medium by stirring at 37°C for 2 hr. The solution is sterilized by filtration stored frozen in small aliquots)
4. 100 ml Hank's Balanced Salt Solution (HBSS) (GIBCO)
5. Scalpels
6. Petri dishes
7. T-25 flasks
8. Laminar flow hood
9. Incubator
10. Centrifuge
11. Inverted microscope

METHOD (SHOULD BE CARRIED OUT ASEPTICALLY)

1. Obtain a minimum of 500 mg of a sterile ovarian tumor sample in PBS transport solution.
2. Rinse the sample in 3 successive Petri dishes containing HBSS with 2% pen/strep in a laminar flow hood.
3. Transfer tissue sample to Petri dish without any media and mince tissue with two crossed scalpels into small pieces of ~2 mm.
4. Add 5 ml of collagenase solution (0.8% collagenase in RPMI medium) to the Petri dish. Make sure the tumor pieces are immersed in the collagenase solution.
5. Incubate the Petri dish with tumor samples in a tissue culture incubator for 6–12 h at 37°C in 5% CO_2. If needed, check the progress of dissociation with the aid of an inverted microscope. The optimal incubation time will vary between samples.
6. After the desired incubation, triturate the samples by passing through a pipette for further disaggregation. (This mechanical disaggregation is optional.)
7. Transfer the disaggregated tissue with the entire collagenase solution to a sterile 15 ml centrifuge tube, and centrifuge the sample for 10 min at 800–1000 rpm.
8. Aspirate the supernatant and wash the cell pellet with 10 ml of culture medium by centrifuging the samples for 10 min at 800–1000 rpm.
9. Discard the suspension, suspend the cells in 9 ml of complete culture media, distribute the contents to 3 different T-25 flasks equally (3 ml each), and return it to the incubator. Culture at 37°C in 5% CO_2.
10. Examine the culture flasks after 48 hr for cell attachment. Discard the media and unattached cells.

Add 5 ml of complete media and return the flasks to the incubator.

11. Change media every 2 days. Significant growth can be observed by the end of the week, and colonies will be sufficient in size by the end of 10–12 days. These actively proliferating colonies can be harvested for chromosome preparations. (If growth is slow, allow a few more days for harvest.)

Harvesting and Chromosome Slide Preparation

MATERIALS

1. Colcemid solution (10 μg/ml) (GIBCO)
2. Cancer hypotonic solution: 3.0 g potassium chloride, 4.8 g HEPES (N-2-hybroxyethyl-piperazine-N-2-ethanesulfonic acid) (Sigma, St. Louis, MO), 0.2 g EGTA (ethylene-bis[oxyethylene nitrol] tetraacetic acid) (Sigma). (Dissolve in 1000 ml of distilled water and adjust pH to 7.0 using 10 N NaOH. Store at 4°C for 2–3 weeks.)
3. 100 ml Trypsin-ethylenediamine tetraacetic acid (EDTA) solution (1X) (GIBCO)
4. Fixative: 3 parts of methanol (Fisher), 1 part acetic acid (Fisher)
5. Microscope slides
6. Centrifuge tubes
7. Pasteur pipettes
8. Water bath at 37°C
9. Incubator at 37°C
10. Centrifuge
11. Old media containing 10% FBS, or prepare new 1 ml of FBS with 9 ml of HBSS (GIBCO)
12. Slide warmer

METHOD

1. Add colcemid solution to culture flask (T-25) at a final concentration of 0.02 μg/ml (10 μl/5 ml of medium) and incubate at 37°C for 4 hr (short-term colcemid treatment) or 0.01 μg/ml (5 μl/5 ml media) for overnight incubation (12 hr) to accumulate enough mitosis.
2. Remove the flask from the incubator and examine it under an inverted microscope for the presence and frequency of round cells, which generally indicates detached mitotic cells.
3. Save the detached mitotic cells by decanting the media into a 15 ml centrifuge tube. Wash the monolayer with 1 ml trypsin and decant the washed trypsin into the same centrifuge tube. Centrifuge for 10 min at 800 rpm.
4. While centrifuging, add 1 ml trypsin solution to the T-25 flask by returning it to incubator for 8–10 min for trypsinization.
5. By this time the first centrifugation will be completed. Discard the supernatant without disturbing the extremely small cell pellet.
6. Remove the trypsinized flask from the incubator and pour the cell suspension into the same centrifuge tube.
7. Wash the T-25 flask 2× with old media (~5 ml) containing fetal bovine serum (FBS) or HBSS with 10% FBS, and then transfer the contents to centrifuge tube from **Step 5.**
8. Centrifuge for 10 min at 800 rpm and then remove the supernatant without disturbing the cell pellet. Leave 0.5 ml of supernatant and gently resuspend the pellet.
9. Add 10 ml of cancer hypotonic solution, slowly, and then incubate the centrifuge tube for 20 min in a 37°C waterbath.
10. Add 5 drops of fixative (1:3 ratio of acetic acid to methanol) as a prefix to the hypotonic solution. Slowly mix.
11. Centrifuge for 10 min at 800 rpm.
12. Aspirate supernatant to 0.5 ml and resuspend the pellet slowly. Add 10 ml of fixative gently through the side of the centrifuge tube.
13. Leave at room temperature for 1 hr in the first fixative.
14. Repeat 2 more fixations with 30 min intervals between each change.
15. Proceed for slide preparation.

Chromosome Slide Preparation

16. Use frosted-end slides that have been rinsed with distilled water and stored at 4°C.
17. Centrifuge the cell suspension from **Step 14** at 800 rpm for 10 min.
18. Remove all but 0.2–0.4 ml of supernatant. Resuspend the cell pellet.
19. Add fresh and cold fixative to dilute the cell suspension; 0.2–0.5 ml of fresh fixative may be required depending on the quantity of cells. Gently resuspend the cells using a Pasteur pipette.
20. Using a Pasteur pipette, place 2 or 3 drops of cell suspension near the frosted end of the slide. Spread cells by tilting the slide and blowing gently. Wipe dry the back of the slide and place it on the slide warmer at 37°C for 1–2 min, until the slide is dry. It may be necessary to adjust the temperature of the wet slides and time on slide warmer to maximize cell spreading. If this technique does not yield good spreading, other cell-dropping techniques may be used, such as dropping cell suspension from a distance of 6–24 inches.
21. Label slides with culture identification, date of preparation, and slide number.

22. Note the number of slides made from each tube and record that number on the label of the tube. The slides can be used for conventional cytogenetic or molecular cytogenetic analysis.

23. After making slides, if needed, add a pipette full of fixative to each tube. Cap tightly and store at 4°C for the short term or –20°C for long term.

Note: Four to six slides with metaphase chromosomes can be obtained from each T-25 flask. If needed, one of these slides can be analyzed at 100X magnification for chromosome count, numeric chromosome alterations, structural chromosomes aberrations, and mosaic chromosome constitution (clonal selection). However, this conventional chromosome analysis is beyond the expertise of an ordinary researcher or pathologist without cytogenetic expertise. If needed, slides can be passed to the cytogenetic laboratory for further analysis. However, these slides are ideal for molecular cytogenetic analysis by FISH by an entry-level researcher, if appropriate DNA probes are carefully selected.

Cytospin Preparations from Effusions and Peritoneal Fluids

Protocol 5: Cytospin Preparations from Effusions and Peritoneal Fluids

MATERIALS

1. Cytospin 4 (Shandon/Thermo Electron Corp., Waltham, MA)
2. Cytoslides (Shandon/Thermo)
3. Cytofunnel (Shandon/Thermo)
4. Cytospin sealed head (Shandon/Thermo)
5. Cytospin filter card (Shandon/Thermo)
6. Cytoclips stainless steel slide clips (Shandon/Thermo)

METHOD

1. Place cytoslide, cytofunnel, and cytospin filter card into cytoclip assembly. Tighten the spring.
2. Place the assembled apparatus into the cytospin sealed head. Balance the samples.
3. Pour 0.5×10^6 cells in 200 µl into the cytofunnel. Cap the cytofunnel.
4. Spin samples at 800 rpm for 3 min.
5. Remove cytospin sealed head.
6. Carefully detach cytofunnel from slide.
7. Allow sample to dry overnight at room temperature.
8. Fix the cells in 95% ethanol or 3:1 methanol: glacial acetic acid for 5 min.

Note: This protocol is based on the use of a Thermo Shandon Cytospin 4 cytocentrifuge. For equipment from other manufacturers, refer to manufacturer's operating instructions.

Protocol 6: Preparation of Cell Smears

MATERIALS

1. Slide
2. Acetone
3. Cell suspension or solid tissue

METHOD

Cell Suspension

1. Place 100–200 µl of the fresh cell suspension on one end of a dry, clean slide.
2. Bring the narrow edge of a second slide into contact with the first slide. Orient the second slide at a 45-degree angle from the first slide.
3. Slowly glide the second slide toward the cell suspension until the suspension spreads along the bottom of the slide.
4. Allow the first slide to dry at room temperature.
5. Fix the slide with acetone or another appropriate fixative for 2–5 min.

Solid Tissue

1. Glide the fresh tissue along a slide.
2. Fix the slide with acetone or another appropriate fixative for 2–5 min.

Note: Sections derived from Protocol 1 are the most popular form of sample for FISH and IHC analyses. This technique is an adjunct to standard hematoxylin and eosin (H&E) staining because it provides analysis of genetic abnormalities after morphologic diagnosis in pathology laboratories. Although this protocol provides tissues with excellent cell morphology, demasking the target DNA is essential before FISH. Truncation of nuclei in thin FFPE sections can lead to underestimation of the true chromosome aneuploidy because some parts of the nucleus may be lost during microtomy. Some laboratories avoid the truncation effect by isolating single cells from 50 µm thick tissue pieces, as shown in Protocol 3, but tissue architecture is lost in the process. However, this technique is excellent for a comparative study of chromosome copy number differences by FISH with DNA aneuploidy using flow cytometry. This technique is also suitable for the isolation of genomic DNA from paraffin-embedded tissues for comparative genomic hybridization (CGH), a modified form of FISH technology. Protocols 1 and 2 are well-suited for IHC and FISH, but the former procedure requires antigen retrieval, whereas the latter does not.

Protocol 4 is used for the preparation of chromosomes for conventional cytogenetic analysis as well as for metaphase *in situ* hybridization for hidden cryptic changes, gene localization studies, and complex chromosome rearrangements. However, several instances were reported with normal karyotypes with abnormal flow cytometry results in DNA aneuploidy.

This discrepancy was found to be the result of overgrown stromal cell or the preparation of chromosomes from infiltrating lymphocytes. Excellent tissue-culture capability is needed to grow

tumor cells *in vitro*. Protocol 5 is suitable for exfoliated cells by cytocentrifugation as in malignant effusions. Tissues obtained from fresh samples as in Protocol 6 show poor cell morphology, but they have fast turnaround time.

Ovarian Carcinoma Chromosome and Gene Analysis with Fluorescence *in situ* Hybridization

Background

The molecular morphologic technique FISH used for the visualization of chromosomes, genes, and messenger ribonucleic acid (mRNA) of interest within the cells. The basic principle of FISH is that target DNA sequences are denatured to become single-stranded and then hybridized with complementary probe DNA sequences labeled with haptens (i.e., biotin, digoxigenin) or fluorochromes (i.e., fluorescein, rhodamine, coumarin, cy-3, cy-5, spectrum orange, spectrum green, etc.). The probe reanneals to the target at locations, where the base pairs are complementary, forming a double-stranded "hybrid molecule." Following the removal of unbound and loosely bound probe molecules by stringent washes, the hybridized signals are detected by a fluorescence microscope to identify the genetic changes in a variety of tumor cells (John, 2003).

The availability of a vast number and variety of commercial DNA probes, labeling techniques, fluorochromes, detection systems, and advances in image analysis makes this technology within the reach of a regular diagnostic pathology laboratory. Consequently, genetic alterations within nondividing cells, at chromosomal and gene levels, are analyzed on a "cell-by-cell" basis, while preserving the histologic and cytologic architecture. This newly emerging discipline of laboratory medicine to identify the chromosome and gene content on nondividing cells by FISH is called "interphase cytogenetics" (Ried, 1998).

Chromosome banding allows the entire analysis of chromosomes in a dividing cell (Dracopoli *et al.,* 2001). However, many tumor cells do not grow well in culture conditions to yield analyzable metaphase chromosomes (Teixeira, 2002). In such difficult situations, repetitive DNA probes and gene-specific probes can be used to tag chromosomes and genes in interphase nuclei in tissue sections, disaggregated cells, or touch preparations. Consequently, interphase cytogenetic analysis is used to analyze three general types of genetic alterations, which include chromosomal numeric changes, chromosomal structural aberrations, and some gene alterations (Kearney, 1999).

Numeric alterations of chromosomes increase with tumor progression and can be visualized at interphase cells by an increase or decrease in the number of fluorescent dots. Numeric alterations may result in addition or loss of a single copy of a particular autosome (aneuploidy or aneusomy) or the addition of complete haploid sets of chromosomes called polyploidy (triploidy or tetraploidy). Structural chromosome aberrations, however, result from breakage and fusion of chromosome segments, which may alter the location and expression of oncogenes and tumor-suppressor genes. Such altered genes, chromosomal segments, and break points confer growth advantages to tumor cells; FISH is also well-suited for gene amplification or deletion studies at interphase levels. Gene amplification is one of the mechanisms by which cancer cells achieve overexpression of some oncogenes, where the number of additional gene copies can range from four copies to several hundred copies per cell (Schwab, 1998).

The following genetic information about ovarian tumorigenesis, as listed in Table 20, can be provided by FISH on interphase cells or nondividing cells and chromosomes from dividing cells.

Principles and Methods of Fluorescence *in situ* Hybridization

Selection of DNA Probes

Different types of DNA probes targeting to several genomic regions of the chromosomes are available for FISH. The probes can be specific for centromeres, telomeres, chromosome bands, genes, translocation break points, interspersed repeated sequences, and whole chromosome–specific and whole genome-specific DNA sequences (Luke *et al.,* 1997). These probes are also classified based on the size of the DNA fragments that can be cloned using appropriate cloning vectors, such as plasmid (5–6 kb), phage (3–20 kb), cosmid (40 kb), P1 artificial chromosomes (150 kb), yeast artificial chromosomes (YAC) (100–200 kb), and bacterial artificial chromosomes (BAC). A variety of methods is now available for the labeling of cloned DNA with various nonisotopic labels, which include biotin, fluorescein, digoxigenin, spectrum orange, and spectrum green. The popular methods for introducing these reporter molecules into the cloned DNA are by nick translation and random primer labeling techniques (Fan, 2002). The labeled products, called probes, are now readily available from different vendors that can be used for routine uses.

Table 20. Types of Genetic Abnormalities Amenable to Fluorescence *in situ* Hybridization Technology

Genetic Abnormalities	Interphase Cells	Metaphase Chromosomes
Numeric chromosome anomalies	Y	Y
Structural chromosome aberrations	Y	Y
Analysis of increase in gene copy number (gene amplification)	Y	Y
Detection of gene deletions	Y	Y
Analysis of translocated or fused genes	Y	Y
Tracing the origin of marker chromosomes or derivative chromosomes	Y	Y
Detection of submicroscopic or cryptic translocations	Y	Y
Chromosomal origin of double minutes (DMs)	Y	Y
Chromosomal origin of homogenously staining regions (HSRs)	Y	Y
Abnormalities in genome organization	Y	Y
Cell cycle-dependent behavior of genes	Y	N
Viral presence	Y	Y
Viral integration sites in human chromosomes and their neighboring oncogenes	N	Y
Amplified gene location sites (chromosome bands)	N	Y
Gene mapping to appropriate chromosome bands	N	Y
RNA synthesis, transport, and expression	Y	N
Chromosome arm alterations	N	Y
Telomeric alterations	N	Y
Chromosome-specific telomeric alterations	Y	Y

Y, Yes; N, no.

Chromosome-specific, repetitive DNA probes, originated from the centromeric regions (alphoid DNA) and heterochromatic regions (satellite DNA), are exploited in detecting numeric alterations of the chromosomes in nondividing cells by *in situ* hybridization. The minisatellite family of the terminal regions of chromosomes as well as the subtelomeric repetitive DNA specific for each human chromosome have been cloned using YACs to produce telomeric and subtelomeric probes. These probes are used for characterizing chromosomal abnormalities in the terminal region of human chromosomes as well as disclosing the role of important genes lying close to the telomeric regions. Whole chromosome printing (WCP) probe is composed of numerous DNA sequences that are present along the entire chromosome, and they are used to identify structural aberrations, derivative chromosomes, gene amplified double minutes (DMs), and homogeneously staining regions (HSRs). Microdissection of specific chromosome bands followed by high-efficiency cloning resulted in the creation of clinically important locus-specific DNA probes (LSP). They are used in analyzing interchromosomal or intrachromosomal rearrangements as well as in tracing chromosome-specific markers in tumorigenesis and cancer progression using amplified, duplicated, or deleted chromosome segments or alterations. Chromosome translocation or specific break point probes contain unique sequences, which span or flank chromosome structural break points. Finally, gene probes cloned by positional cloning or forward genetics are available for many oncogenes and tumor-suppressor genes. In various genetic abnormalities, they are used in assessing oncogene amplification or deletion, tumor-suppressor gene rearrangement, and gene translocation or fusion (Tonnies, 2002).

A careful selection of specific probes or of probe sets is important before embarking on *in situ* hybridization to delineate specific chromosome or chromosomal regions, which are involved in numeric alterations or structural aberrations. To yield bright hybridization signals and avoid cross-hybridization, the chromosomal *in situ* suppression hybridization protocol should be followed for large probes derived from cloning vectors (i.e., YAC, BAC, P1) by introducing blocking DNA (i.e., human Cot-1, placental DNA) in the hybridization buffer (John, 2003).

Specimen Preparation

Interphase cytogenetic analysis with FISH can be successfully carried out with all forms of ovarian tissue preparations, including imprint preparation, single-cell suspensions obtained from solid tumors, frozen sections, FFPE, and cytospin preparations of effusions, and peritoneal fluids. Because frozen sections and paraffin sections are standard practice in most pathology laboratories, the FISH protocol will be limited to these two types of specimens. For paraffin-embedded tissue sections, deparaffinization should be carried out in xylene followed by dehydration in ethanol series before pretreatment (Huang *et al.,* 2002).

Pretreatment of Paraffin-Embedded Tissue Sections

For paraffin-embedded tissues, demasking the target DNA before denaturation is essential for probe penetration. This procedure also minimizes background over hybridization sites. Generally, unmasking is achieved by

boiling sections in citrate buffer or by using enzymatic digestion using pepsin or proteinase K. Ribonuclease treatment can also be used, if needed, to eliminate RNA molecules remaining in the cell that are homologous to the sequence of interest. It is important to optimize pretreatment conditions because insufficient tissue digestion prevents probe penetration, whereas overdigestion may degrade the target DNA. In both cases, hybridization failure occurs (Johnson *et al.,* 2000).

Denaturation and Hybridization

Immediately after pretreatment, the target DNA and probe DNA are denatured. Denaturation is the process in which the double-stranded DNA of the probe separates into single strands. For FFPE tissue specimens, denaturation of probe DNA and tissue DNA is performed simultaneously by applying probe mixture onto the specimen in an oven at 90°C for 10 min. Prior to denaturation, the probe (10–16 ng DNA probe per slide) is mixed with a hybridization buffer. The majority of hybridization buffers contain 50% (vol/vol) formamide, 10% dextran sulfate, 2XSSC (saline-sodium citrate), 0.1 mM EDTA, 0.5 mM Tris-HCl (pH 7.6), and 100 µg of blocking DNA (unlabeled Cot-1 DNA or placental DNA or sheared salmon sperm DNA). It is important to use blocking DNA when repetitive DNA probes are used. In the case of fresh cells, denaturation of probe DNA and target DNA can be carried out separately. Denaturing of probe DNA is generally carried out at 71°C in a probe mixture for 5 min, whereas the slide containing tumor cells can be denatured in a Coplin jar containing 70% formamide, 10% 2XSSC, and 20% distilled water, preheated in a waterbath to 71°C. The denatured probe is then applied to denatured cells coverslipped and sealed for hybridization. Hybridization is performed overnight in a humidified chamber at 37°C, and during this period duplex molecules are formed. Formamide and dextran sulphate promotes annealing at moderate temperature, where repetitive DNA probes anneal faster than cosmid gene or locus-specific probes (Luke *et al.,* 1997).

Post-Hybridization Washing

After hybridization, excess unhybridized, mismatched, or loosely attached probes are removed by extensive washing of the slides termed "stringency washes." Under such conditions, only the actual hybrid will be retained. Stringency washes are achieved by changing the formamide concentration, temperature, and salt concentration. High-stringency wash conditions are applied to gene probes as well as chromosome-specific alphoid and telomeric probes with elevated formamide concentration (65%), an increase in temperature (45°C), and low salt concentration. Low stringency washes are generally performed for pan centromeric, pan telomeric, and whole-genomic DNA probes (Luke *et al.,* 1997).

Hybrid Detection

Following post-hybridization wash, the site of hybridization in target cells is identified directly or indirectly, depending on the nature of haptens used during labeling. In directly labeled probes, counterstaining with appropriate fluorochromes such as propidium iodide (PI) or 6-diaminophenylindole (DAPI) is sufficient to visualize the site of hybridization using a fluorescent microscope. However, the sensitivity suffers and signals are usually weak. As a result, an indirect method is used for labels such as biotin- and digoxigenin-labeled probes, which produces brighter signals.

Biotinylated probes are detected by the avidin or streptavidin method, and the sensitivity can be further enhanced by the use of a bridging anti-avidin antibody followed by a second round with fluorescein-labeled avidin. Table 21 shows the various reporter molecules commonly used for laboratory, detection, amplification, and counterstaining methods. Various vendors, such as Vysis, have developed efficient and simplified detection systems for obtaining bright signals with their spectrum orange and spectrum green probes without requiring additional detection or amplification methodologies (Choo, 1994). Although FISH signals are enhanced (amplified) by the application of multi-immunologic layers, the tyramide-based detection system can be substituted for higher signal enhancement in this indirect detection technique (Qian *et al.,* 1996).

Note 1: Vector laboratories provides a panel of detection and amplification reagents with corresponding counterstains for each category of probe label (e.g., biotin, digoxigenin, dinotrophenol [DNP], TexasRed, or rhodamine labels).

Note 2: For detection reagents fluorescein (FITC) and TexasRed or rhodamine use counterstains PI or DAPI, respectively.

Visualization, Signal Resolution, and Evaluation

The FISH signals are analyzed with high-quality fluorescent microscopes with well-matched filters with the wavelength of the fluorochromes used during FISH. Single-band, double-band, triple-band, and quadruple-band pass filter sets are available from commercial sources (Omega Optical, Inc., Brattleboro, VT) for single-, double-, and triple-color hybridization experiments, respectively. For example, a probe with FITC on the conjugated fluorochrome with PI may require a

Table 21. Probe Labels, Detection Reagents, and Counterstains

Probe Label	1st Incubation	2nd Incubation	3rd Incubation	Counterstain
Biotin	Avidin/streptavidin conjugated fluorochrome (e.g., fluorescein avidin or TexasRed avidin)	Biotinylated anti-avidin antibody	Avidin/streptavidin conjugated fluorochrome (e.g., fluorescein avidin)	PI or DAPI
	Fluorochrome (e.g., fluorescein or Rhodamine)	Fluorochrome conjugated anti-sheep antibody	—	PI or DAPI
Digoxigenin	Conjugated sheep anti-digoxigenin antibody			
	Mouse anti-digoxigenin antibody	Digoxigenin-labeled anti-mouse antibody	Fluorochrome conjugated anti-digoxigenin antibody	PI or DAPI
Fluorescence	Biotinylated anti-fluorescein	Fluorochrome (e.g., fluorescein or TexasRed) conjugated avidin	—	PI or DAPI
DNP			—	PI or DAPI
	Biotinylated anti-DNP	Fluorescein avidin or TexasRed avidin)		

DAPI, Diaminophenylindole; DNP, dinotrophenol; PI, propidium iodide.
Fluorochromes include fluorescein (green), Texas red (red), rhodamine (red), cyanine 3/5 (red), AMCA (blue).

FITC-PI dual band pass filter to view hybridization signals in greenish yellow in the background of red interphase nuclei. Similarly, triple-band pass filter sets for FITC/TexasRed/DAPI allow simultaneous visualization of triple fluorescence combinations, whereas FITC and Tex-Red detect yellow and red hybridization signal, respectively, and DAPI stains the nuclei blue. Generally, double-color hybridization is the preferred method for detecting two different target DNA sequences in exploring genetic anomalies relating to chromosomal aberrations, gene translocations, and gene amplifications (Slovak *et al.,* 2001).

For data collection, 100–200 interphase nuclei are analyzed from each sample, where the exact number of cells needed is decided by the hybridization efficiency. Hybridization efficiency is directly related to the target size. The YAC and BAC probes provide very bright signals (100–250 kb), whereas single copy genes provide moderate to weak signals. Usually, the minimum detection level for a probe at interphase level is 3–5 kb. Signal resolution can be improved by using a cooled CCD (charge-coupled device) camera with sophisticated FISH software. The sensitivity and specificity of a probe can be quantified if both positive and negative control slides are included during the experiment. Sensitivity is defined as [(true positive)/(true positive + false negative)], whereas specificity is calculated as [(true negative)/(true negative + false positive)]. The accuracy of the test is confirmed if both values are close to 1.

Care should be taken to exclude cells with loss of signals or cells with monosomy because of the truncation of nuclei in tissue sections. Consequently, establish a baseline frequency for monosomic population to control "truncation" artifacts (Qian *et al.,* 1996). Similarly, exclude overlapping nuclei during data collection to avoid overestimation of hybridization signals resulting from overlapping nuclei. Most tissue sections are cut to 4–6 μm thicknesses, but thinner sections reduce the chance of overlapping nuclei. Data should be taken from areas showing uniform fluorescence intensity, where split signals should be considered as one hybridization site. Photographs preparations can be taken by Kodochrome 400 daylight film for prints or Ektachrome 1600 for slides.

Fluorescence *in situ* Hybridization Assay Procedure

Commercial DNA Probes and Probe Labeling

Labeled DNA probes are available from different commercial sources. They are generally labeled with

biotin, digoxigenin, spectrum orange, spectrum green, and spectrum aqua. Consequently, probe labeling is not a usual practice in standard cancer diagnostic laboratory. Additionally, commercial probes are validated and their sensitivity and specificity are already established.

When a probe is not commercially available for a specific use, contact several research laboratories for obtaining DNA fragments, containing the sequences or genes of interest. The YAC clones can be selected based on sequence tagged site (STS) markers that map to the chromosomal area of interest from Whitehead Institute for Biomedical Research (www.genome.wi.mit.edu), Dr. D.C.Ward's laboratory at Yale University School of Medicine, and other sources. Once the cloned DNA of interest is secured, they can be labeled by nick translation or random priming methods. Excellent labeling kits are commercially available. Examples are the BioNick kit (Life Technologies, Gaithersburgh, MD) for introducing digoxigenin or biotin by nick translation, Bio Prime kit (GIBCO) for random priming, and photoprobe biotin labeling kit (Vector Labs). Generally, a translation kit contains nucleotide (dNTP) mixture, bio-II-dUTP or dig-11-dUTP and enzyme mixture containing DNase and DNA polymerase I and EDTA; it also carries the nick translation labeling reaction as follows.

Protocol 7: Probe Labeling via Nick Translation

Prepare the following solutions in advance and store on ice. These solutions can be stored at −20°C until use.

MATERIALS

1. 10X nick reaction buffer (add the following reagents to a microcentrifuge tube labeled A): 500 µl 1.5 M Tris-HCl (pH 8.0), 50 µl 50 mM $MgCl_2$, 25 µl 0.5 mg/ml BSA (bovine serum albumin), 425 µl distilled water
2. Nucleotide stock solution (add the following reagents in a microcentrifuge tube labeled B): 10 µl 0.5 mM dATP, 10 µl 0.5 mM dGTP, 10 µl 0.5 mM dCTP, 10 µl 0.5 mM dTTP, label of choice (7 µl 0.5 mM biotin-21-dUTP or 7 µl 0.5 mM digoxigenin-11-dUTP), 4 µl 20 mM Tris 7.4, and 126 µl distilled water
3. 0.01 M β-mercaptoethanol 4.10 µg/ml of DNase I.

METHOD

1. Prepare the labeling mixture in a centrifuge tube on ice as follows.

10X Nick reaction buffer	10 µl
Nucleotide stock solution containing biotin or digoxigenin	10 µl
β-mercaptoethanol	10 µl
DNase I	1 µl
dsDNA template (2–10 µg of probe DNA)	5 µl
Escherichia coli DNA polymerase (10 U/ml)	1 µl
Sterile water	63 µl
Total volume	100 µl

2. Vortex to mix using a 4°C microcentrifuge for 30 sec.
3. Incubate the centrifuge tube by placing into a 15°C waterbath for 70–120 min **(Note 1)**.
4. Stop the reaction by keeping the tube on ice and adding 1 µl of 0.1 M EDTA.
5. Add 20 µl of 3 M sodium acetate and 200 µl of ice-cold 100% ethanol and precipitate probe DNA at −80°C for 1 hr.
6. Centrifuge at 12,000x g for 10 min at room temperature and carefully aspirate the supernatant. Be careful that the pellet is not removed with the supernatant.
7. Briefly, rinse the DNA pellet with 1 ml of 70% ethanol (optional).
8. Dry the DNA pellet under vacuum for 10 min or by speedvac for 5 min. Avoid overdrying of the sample.
9. Dissolve the labeled DNA in 20 µl TE buffer for a final concentration of ~100 ng/ml.
10. Store at −20°C for future use **(Note 2)**.

Note 1: The probe size should be between 100 and 300 bps. To verify this, take 5 µl sample from **Step 7** after 60–70 min of labeling reaction, and run on 1% agarose gel between 70 and 90 V for 50 min. If the probe size is not between 100 and 300 bps, allow the reaction to continue for an additional 20 min by allowing further digestion.

Note 2: This protocol is adapted from Langer *et al.* (1981).

Protocol 8: Dewaxing and Pretreatment of Sections

Tissue sections that are FFPE should be dewaxed and hydrated before protease digestion, RNase digestion (for DNA *in situ* hybridization), and DNase digestion (for RNA *in situ* hybridization). These steps are essential for probe penetration. An appropriate protein digestion protocol is essential for FFPE tissue sections for unmasking the DNA by removing some cross-linked proteins from the cells and extracellular network. This procedure makes the DNA accessible for FISH and improves signal quality by reducing the background. The duration of protein digestion should be optimized for each specimen type.

MATERIALS

1. Paraffin-embedded tissue sections
2. Xylene
3. Ethanol
4. Proteinase K (1 mg/ml in 50 mM TrisHCl, pH 7.5)

5. Pepsin solution (2 mg/ml in distilled water, pH 2.0): 40 mg pepsin in 19 ml distilled water + 1 ml 2 N HCl

6. Trypsin solution (2 mg/ml in distilled water): 40 mg of trypsin in 19 ml distilled water + 1 ml 2 N HCl

7. 2X Saline sodium citrate (2XSSC): Dilute from 20X with distilled water. (See reagent preparations in Protocol 9.)

8. Propidium Iodide

9. DAPI (Molecular Probes)

10. HCl (Fisher)

11. 2XSSC/0.05% Tween 20 (50 ml 20XSSC + 450 ml distilled water + 0.25 ml Tween 20)

12. Coplin jars

13. Waterbath

14. Fluorescence microscope with filter sets for DAPI or PI (Chroma Technology)

15. TEN buffer (0.05 M Tris-HCl, pH 7.8, 0.01 M EDTA and 0.01 M NaC1) (for alternative pretreatment protocol treatment only)

METHOD

1. Obtain 4–6 µm thick paraffin-embedded tissue sections using a standard rotary microtome. Transfer the sections onto poly-L-lysine coated slides. Incubate overnight in a 60°C oven.

2. Prepare 5 Coplin jars by labeling 3 of the jars for xylenes and 2 for 100% ethanol.

3. Dewax the sections using 3 changes of xylene for 5 min each.

4. Dehydrate the tissue by passing through 100% ethanol for 5 min each.

5. Remove the slides from ethanol and air-dry.

6. Prepare protein digestion solution at this time. Three types of protease solutions can be prepared to decide which works best for your tissue. Protease solutions can be stored at –20°C for up to 3 weeks **(Note 1)**.

7. Place slides in a Coplin jar of protein digestion solution for 15–25 min at room temperature or incubate at 45°C. Alternatively, overlay the tissue sections with appropriate volumes of the protease solution (60 µl/5 cm^2). Generally, a Coplin jar containing protein digesting solution is prewarmed in a 45°C water bath and the slides are incubated for 15–20 min **(Note 2)**.

8. Rinse the slides in 2XSSC for 10–20 sec.

9. Evaluate the tissue sections for under, over, or at optimal digestion **(Note 3)** by applying 10 µl of propidium iodide or DAPI and viewing under a fluorescent microscope. Sometimes, additional trouble shooting steps can be implemented adopting alternative protocol, as described in Note 4 **(Note 4)**.

10. Wash slides 3× in 2XSSC (pH 7) for 10 sec in each rinse.

11. Dehydrate in 70%, 80%, 95%, and 100% alcohol series for 1 min in each wash.

12. Air-dry slides at room temperature, and proceed for DNA *in situ* hybridization. (Store for a day, if needed, at room temperature.)

Note 1: Various vendors provide a number of protease solutions. Some need additional pretreatment before protein digestion in a pretreatment solution, such as sodium thiosulphate, which ranges from 10% to 30% concentration at 45°C for 15–20 min. If pretreatment is recommended, then the slides should be washed in 2XSSC before proceeding to protein digestion.

Note 2: Protein digestion is different for each enzyme. It is necessary to inactivate the enzymes after digestion by washing properly. Otherwise, overdigestion may result. Pepsin and trypsin can be inactivated more easily than proteinase K.

Note 3: Overdigested tissue may show loss of nuclear borders or in extreme cases appears as "ghosts." In this case, start with a different slide and follow from **Step 3.** Undigested tissue shows persistent green autofluorescence and poor PI staining. If further digestion is needed, proceed from **Step 7.** Optimal duration of digestion must be determined in individual laboratories.

Note 4: Some laboratories perform a combination of acid treatment (0.2 N HCl, 10–20 min), heat treatment (2XSSC at 80°C), and enzyme treatment (proteinase K at 37°C) before hybridization. The optimal duration of all the three different treatments must be determined depending on the sturdiness of the section. If needed, alternative protocol can be followed from **Step 6,** as shown as follows.

Alternative Pretreatment Protocol (Optional)

6. Following **Step 5,** treat slides with 0.2 M HCl for 20 min. This duration can be changed by ±10 min depending on the sturdiness of the section.

7. Dip slides in distilled water. Rinse in 2XSSC/0.05% Tween 20 for 5 min.

8. Treat with 2XSSC for 20 min at 80°C. (This duration can be changed.)

9. Dip slides in distilled water for 1 min. Rinse in 2XSSC/0.05% Tween 20 for 5 min.

10. Treat with 0.05 mg/ml proteinase K in TEN buffer for 10 min at 37°C. (The duration can be changed depending on the tissue.)

11. Rinse in 2XSSC/0.05% Tween 20 for 5 min.

12. Post-fix the specimen in 10% buffered formalin or 4% formaldehyde in PBS for 10 min.

13. Rinse in 2XSSC/0.05% Tween 20 for 5 min.

14. Dehydrate slides in 70%, 80%, and 100% ethanol for 2 min each.

(**Note:** This protocol is adapted from Johnson, 2000)

Protocol 9: Fluorescence *in situ* Hybridization

MATERIALS

1. Tissue sections, chromosome preparations, or exfoliated cells on microscope slides as appropriate

2. Epifluorescence microscope

3. Filter sets (Chroma Technology)

4. Incubator
5. Oven
6. Waterbath
7. Slide warmer
8. Humidified slide chamber
9. Microcentrifuge and microcentrifuge tubes
10. Micropipettes and tips
11. Glass Coplin jars
12. Glass coverslips
13. Plastic coverslips
14. Biotinylated DNA probes
15. Formamide (Sigma)
16. Fluorescein-labeled avidin (Vector Labs)*
17. Biotinylated anti-avidin (Vector Labs)
18. Vectashield anti-fade mounting medium (Vector Labs)
19. Propidium Iodide (Vector Labs and Molecular Probes)*
20. DAPI (Vector Labs and Molecular Probes)
21. Ice cold ethanol (60%, 70%, 95%, 100%)
22. 20xSSC (see reagent preparation)
23. Herring sperm DNA (Sigma)
24. Placental DNA (Sigma)
25. Nonidet P-40 (Sigma)
26. PN Buffer (see reagent preparation)
27. Modified PN Buffer (see reagent preparation)
28. Dextran sulphate (Sigma)
29. Sodium citrate (Sigma)
30. Icebath
31. Sodium azide
32. Nonfat dry milk
33. BSA
34. Distilled water
35. Rubber cement
36. Color films (Kodochrome 400 for prints or Ektachrome 1600 for slides) or Imaging system with CCD camera (Vysis)

Substitute appropriate detection reagents and counterstains as indicated in the reagent preparation as well as in the footnotes of FISH protocol. Where necessary, detection reagents for digoxigenin label and double color hybridization are indicated in the current procedure.

REAGENT PREPARATION

1. 20XSSC: Dissolve 175.3 g NaCl in 800 ml distilled water. Add 88.2 g of trisodium citrate, bring to a final volume of 1000 ml, and adjust the pH to 5.

2. 2XSSC: 1 part of 20XSSC in 9 parts of sterile water. Adjust pH to 7. When 20XSSC is diluted, pH will be close to 7.

*Indicates that materials will vary depending on the probe labels used for hybridization.

3. Probe DNA: Obtain probe DNA from commercial sources and prepare the probe mixture as instructed, or label the probe DNA with biotin or digoxigenin (as indicated in Protocol 7).

4. Hybridization mixture: Prepare by mixing 5 ml formamide, 2 ml 50% (wt/vol) dextran sulfate, and 1ml 20XSSC. Adjust the pH to 7.0. It can be stored at 4°C for several weeks.

5. Blocking DNA: Cot1 DNA or placental DNA at a concentration of 1 mg/ml.

6. Carrier DNA: Dissolve herring sperm DNA in distilled water to obtain a final concentration of 1 mg/ml. Sonicate to 400 base pairs in length.

7. Probe solution (probe cocktail): Prepare the probe solution in a microcentrifuge tube by adding the following **(Note 1)**:

Hybridization mixture	105 µl
Human placental DNA (blocking DNA)	15 µl
Herring sperm DNA (carrier DNA)	15 µl
Probe DNA (labeled DNA)	15 µl

8. Vortex and mix. Store aliquots of 30 µl at −20°C or proceed for *in situ* hybridization.

Note 1: Follow the supplier's instructions if commercially prepared probes are used.

Note 2: When pipetting the probe DNA, care should be given to the concentration of DNA in 15 µl of probe solution. It varies considerably depending on the source of the probe. For single cosmids/plasmids or phage, this concentration may be 40 ng; for purified YAC DNA this may be 60 ng. For chromosome band–specific probe, the concentration can be 200 ng. However, DNA obtained from sorted chromosomes can have concentrations as high as 500 ng.

9. Denaturation solution (70% formamide/2XSSC):

Prepare as follows:

Formamide	35 ml
20XSSC	5 ml
Double-distilled water	10 ml

Adjust the pH to 7. This solution can be stored for a month at 4°C.

10. PN buffer (washing buffer): Add 25.2 g $Na_2HPO_4.7H_2O$ and 0.83 $NaH_2PO_4.H_2O$ in 1000 ml of distilled water. Add 0.6 ml of Nonidet P-4 (NP-40). Mix and adjust to pH 8.0. This buffer can be kept at room temperature for a year.

11. Modified PN buffer (blocking buffer): Prepare by adding 2% nonfat dry milk (Carnation) and 0.02% sodium azide to PN buffer in a beaker. Mix well and spin in a centrifuge to collect the supernatant, which can be stored at 4°C for several months.

12. For post-hybridization wash solution I, prepare as follows:

Formamide	25 ml (50%)
Distilled water	20 ml (40%)
20XSSC	5 ml (10%)

13. For post-hybridization wash solution II, prepare as follows:

Formamide	32.5 ml (65%)
Distilled water	12.5 ml (25%)
20XSSC	4.0 ml (10%)

14. Detection molecules: (Varies according to probe labels used. Select as appropriate.)

a. Biotinylated Probes:
   Fluorescein Avidin D Cell Sorting (DCS) grade (5 µg/ml)
   OR
   Texas Red Avidin DCS (for first incubation)
   Biotinylated anti-avidin D (5 µg/ml) (second incubation)
b. Digoxigenin-labeled probes:
   Fluorescein/anti-digoxigenin
   OR
   Rhodamine/anti-digoxigenin (for first incubation)
   Rabbit anti-sheep antibody (second incubation)
c. Fluorescein-labeled probes:
   Biotinylated anti-fluorescein (10 µg/ml) (first incubation)
   Fluorescein avidin DCS (10 µg/ml) (second incubation)
d. DNP (dinitrophenyl)-labeled probes:
   Biotinylated anti-DNP (10 µg/ml) (first incubation)
   Fluorescein avidin DCS or Texas Red Avidin DCS (10 µg/ml) (second incubation)
e. Texas Red- or Rhodamine-labeled probes:
   Biotinylated anti-Rhodamine (10 µg/ml) (first incubation)
   Texas Red Avidin DCS or Fluorescein avidin DCS (l0 µg/ml)
f. For double-color hybridization, select biotin- and digoxigenin-labeled probes and use Fluorescein avidin DCS and Rhodamine anti-digoxigenin during the first incubation. Use DAPI as the counterstain.
g. For triple color hybridization, select biotin-digoxigenin- and fluorescein-labeled probes.

Note 3: The current FISH protocol is optimized for DNA probes labeled with biotin or digoxigenin. For other labels, select the appropriate detection reagents and counterstains from the list provided in **Steps 14** and **15.**

15. Counterstains: use DAPI or PI from commercial sources as appropriate.

Note 4: Use DAPI for fluorochromes, Texas Red or Rhodamine, but PI for fluorescein.

16. Anti-fade mounting media: anti-fade mounting media with or without counterstains from commercial sources (e.g., Vectashield).

METHOD

A. Denaturation

Two types of denaturation are described, depending on sample type.

Denaturation I (co-denaturation for tissue sections)

1. Prewarm 30 µl of probe cocktail (see probe preparation) at 37°C for 5 min in a microcentrifuge. This probe mixture contains 10 ng/µ of biotin-labeled alphoid DNA.

Note 5: Instead of biotin, other labeled probes can be used.

2. Pipette 30 µl of the probe solution and place onto a specific area on the pretreated slide from the previous protocol (Protocol 8).
3. Cover the area of hybridization with a glass coverslip and carefully seal all four slides with rubber cement.
4. Denature the probe and the specimen simultaneously by placing in an oven (co-denaturation) at 92°C for 15 min.

Note 6: The denaturation temperature and duration of denaturation varies from sample to sample. Generally, FFPE tissue samples require higher temperature and more time for denaturation, whereas frozen sections, smears, and touch preparations require lower temperature and lesser time. In various laboratories, the denaturation temperature varied from 75°–95°C, whereas the length of duration varied from 5–20 min. This leads to the performance of an optimization experiment to determine the ideal temperature and duration of denaturation for the specimen in question.

5. Proceed for hybridization.

Denaturation II (separate denaturation for metaphase chromosomes, tissue culture cells, and exfoliated cells)

1. Dehydrate the slides carrying tissue culture cells, metaphase chromosomes (Protocol 4), and exfoliated cells through a series of ice-cold 60%, 70%, and 95% ethanol for 2 min each.
2. Denature the slides in denaturation buffer containing 70% formamide. The denaturation buffer prepared (see reagent preparation) should be transferred to a Coplin jar and prewarmed to 70°C in a waterbath. Once the temperature reaches 70°–72°C, incubate the slide in denaturation buffer for 2–3 min. (The optimum denaturation time varies within the narrow window of 2–3 min).
3. Dehydrate the denatured slide in 80%, 90%, and 100% ethanol kept at 4°C for 2 min each step and allow the slide to air-dry.

4. Add ~1.5 µl of biotin- (or digoxigenin-) labeled alpha satellite probe in 40 µl of probe mixture (hybridization mixture) in a microcentrifuge tube. (See reagent preparation.)

5. Denature the probe cocktail at 70°–74°C for 5–7 min in a waterbath. Chill quickly in an icebath. (Some probes need a preannealing step. In such cases, after the denaturation of the probe, transfer the centrifuge tube to 37°C oven or waterbath for 60 min for annealing.)

6. Apply the probe cocktail to the slide and cover with a coverslip. Seal the coverslip with rubber cement and proceed for hybridization.

B. Hybridization

Hybridization is carried out by transferring the slides to a humidified chamber at 37°C overnight.

Note 7: The presence of moisture in the oven is necessary to prevent the drying of the specimen and probe DNA. The hybridization duration varies according to the specimen and probe. For gene probes, as well as low copy no sequences, incubation of 2–3 days may be needed. For repetitive DNA probes, 3–18 hr will be sufficient because they reanneal with template strands of DNA quickly.

C. Post-Hybridization Wash

Note 8: Prepare materials and reagents for post-hybridization washes (see reagent preparations). The concentration of the post-hybridization wash solutions will vary based on the type of the probe under study. Low-stringency wash condition at lower temperature is preferred for genomic and gene probes (i.e., pan-centromeric and pan-telomeric probes, low-copy number sequences), whereas high-stringency wash conditions are required for chromosome-specific probes. An optimization experiment is required to determine the concentration of the wash solutions and the temperature of incubation. Before starting the experiment, preheat the Coplin jars with 50 ml of post-hybridization wash solutions to 43°C or 37°C, depending on the samples and probes.

1. Take slides from the hybridization chamber. While holding one corner of the coverslip, remove the rubber cement from slides with forceps without disturbing the sample.

2. Soak slides with coverslips in 2XSSC until coverslips come off.

Note 9: Stringency wash conditions will vary, as shown as follows in **Step 3** a–d.

3. Determine which section is applicable to your probe and specimens. Then, follow the wash conditions, according to specimen type, as follows:

a. Chromosome-Specific Probes on Metaphase Chromosomes

1. Place slides in preheated **high-stringency** wash buffer in a shaking waterbath at 43°C for 20 min. If a shaking waterbath is not available, shake the Coplin jar gently every 5 min.

2. Wash slides in a 2XSSC solution at 37°C for 8 min, agitating the Coplin jar after 4 min.

3. Transfer slides to 40 ml of PN buffer and proceed for detection. From this point on, the slides should not be allowed to dry.

b. Genomic Probes on Metaphase Chromosomes

1. Place slides in preheated **low-stringency** wash buffer in a shaking waterbath at 37°C for 20 min. If a shaking waterbath is not available, shake the Coplin jar gently every 5 min.

2. Wash slides in a 2XSSC solution at 37°C for 8 min, agitating the jar after 4 min.

3. Transfer slides to 40 ml of PN buffer and proceed for detection. From this point on, the slides should not be allowed to dry.

c. Gene Probes on Metaphase Chromosomes

1. Place slides in preheated **low-stringency** wash buffer in a shaking waterbath at 37°C for 20 min. If a shaking waterbath is not available, shake the Coplin jar gently every 5 min.

2. Wash slides in a 2XSSC solution at 37°C for 8 min, agitating the jar after 4 min.

3. Transfer slides to 40 ml of PN buffer and proceed for detection. From this point on, the slides should not be allowed to dry.

d. Probes on Paraffin-Embedded Tissue Section, Cytologic Preparations, Cells from Frozen Tissue, and Exfoliated Cells

Option 1

1. Place slides in preheated 1XSSC solution in a shaking waterbath at 72°C for 5 min. (Never place a cold Coplin jar into a hot waterbath. Allow the Coplin jar to rise in temperature to 72°C while warming the water bath.)

2. Transfer slides to 40 ml of PN buffer and proceed for detection.

Option 2

1. Place slides in 2XSSC 10 min at 42°C.

2. Wash slides 2× in 2XSSC/50% formamide for 5 min each at 42°C.

3. Wash slides in 2XSSC for 5 min at 42°C.

4. Transfer slides to 40 ml of PN buffer and proceed for detection.

Option 3

1. Place slides in 2XSSC/50% formamide at 45°C and wash 3× for at 2-min intervals.

2. Wash slides in 2XSSC at 45°C for 2 min.

3. Wash slides in 2XSSC/0.1% NP-40 at 45°C for 2 min.

4. Wash slides in 2xSSC/0.1% NP-40 at room temperature and proceed for counterstaining with DAPI or PI. (This option is for Vysis probes with direct detection capability labeled with spectrum orange, spectrum green, or spectrum aqua.)

D. Detection

The detection system should be carefully selected, based on the labeling haptens used during the labeling procedure or based on the commercial source of labeled probes (Table 22). For spectrum orange, spectrum green, and spectrum aqua-labeled probes from Vysis, proceed to hybrid visualization (Section F) for counterstaining and visualization. For biotin-, digoxigenin-, fluorescein-, DNP-, and Rhodamine-labeled probes, follow the following detections systems. (Consult "detection molecules" in the reagent preparation of this protocol for selection of appropriate reagents for indirect detection procedures.)

1. Remove slides from PN buffer and place 100–200 µl of blocking solution (modified PN buffer, which contains 5% nonfat dry milk or 4% BSA). Cover with plastic coverslips and incubate at room temperature for 10–20 min. The blocking step is performed before detection of bound probe DNA. This reduces any nonspecific binding.
2. Wash 2× twice in PN buffer at 5-min intervals.
3. Add 100 µl of fluorescein-labeled avidin (Fluorescein Avidin DCS solution 5 µg/ml) for biotin-labeled probes (or biotinylated anti-fluorescein [10 µg/ml] for fluorescein-labeled probes, or fluorescein-labeled anti-digoxigenin for digoxigenin-labeled probes) to each slide. Cover with plastic coverslips and incubate at 37°C in a humidified chamber for 20–30 min in the dark.
4. Carefully remove the coverslip and wash 3× in PN buffer at room temperature.

Note 9: If needed, mount the slide in 20 µl anti-fade solution, containing PI or DAPI. Evaluate the result under a fluorescence microscope. If the signals are unsatisfactory, wash in PN buffer and proceed for signal amplification. If satisfactory sensitivity has been achieved, then proceed to data analysis.

Table 22. Probe Labels

Hapten-Labeled Nucleotides	Fluorescent-Labeled Nucleotides
Bio-dUTP	FITC-dUTP
Dig-dUTP	Cy3-dUTP
DNP-dUTP, etc.	AMCA-dUTP
	Spectrum orange-dUTP
	Spectrum green-dUTP
	Spectrum red-dUTP
	Spectrum aqua-dUTP

E. Amplification of Signals (Optional)

1. The intensity of fluorescence can be amplified by adding anti-avidin solution (5 µg/ml) to biotin-labeled probes, fluorescein-labeled probes or rabbit anti-sheep antibody for digoxigenin-labeled probes. Incubate for 20 min at 37°C in a humidified chamber in the dark.
2. Carefully, remove the coverslip and wash 3× in PN buffer for 2 min each at room temperature.
3. Apply another layer of fluorescein-labeled avidin DCS (for biotin labeled probes) or fluorescein-labeled anti-rabbit antibody (for digoxigenin-labeled probes). Coverslip and incubate in the dark for 15 min at 37°C in a humidified chamber.
4. Carefully, remove the coverslip and wash 3× in PN buffer for 2 min each at room temperature.
5. Wash slides in 4XSSC + 0.1% Tween 20 for 10 min (4XSSC is 0.6 M NaC1, 60 mM sodium citrate, pH 7.0) and proceed for counterstaining.

F. Hybrid Visualization

1. Counterstain the slides in the dark with Vectashield mounting medium with DAPI or PI as appropriate, and view with an epifluorescence microscope with filter sets as appropriate for signal detection.
2. Proceed to Protocol 10 for microscopic scoring and data analysis.

Double and Multicolor Fluorescence *in situ* Hybridization

The platform technology of FISH can be extended to include more than one DNA probe for the simultaneous detection of two to three hybridization sites in a single interphase nucleus or a metaphase spread. In this technology, the differently labeled haptens (e.g., biotin and digoxigenin) can be co-hybridized, and after stringency washes can be detected simultaneously if antibodies conjugated with appropriate fluorochromes are used during the detection procedure (e.g., avidin conjugated with fluorescein for biotin hapten and anti-digoxigenin conjugated with rhodamine for digoxigenin). In such a hybridization experiment, FITC yields green fluorescent dots, whereas rhodamine gives red fluorescent dots in the background of blue if DAPI is the counterstain. By using the principle of combinatorial labeling, a triple or multicolor FISH procedure can be introduced if the fluorescent microscope is equipped with the appropriate filter sets, allowing excitation and detection of three or more fluorescent colors. Combinatorial labeling uses the simultaneous labeling strategy, in which a single probe is labeled with two different fluorochromes, such as FITC-dUTP (green) and rhodamine-dUTP (red), which on hybridization

provide a yellow signal by the merging of red and green fluorescence. As a result, if three probes are introduced (e.g., biotin [probe 1] + digoxigenin [probe 2] + FITC rhodamine [probe 3]) during hybridization, a triple-color FISH can be achieved. Consequently, many of the commercial probes are suitable for double- or triple-color FISH procedure for detecting anomalies involving chromosome number using centromeric probes, and gene anomalies or locus anomalies using gene or locus probes.

A double- or triple-color FISH procedure can be introduced in the laboratory by modifying the existing FISH protocol according to the following suggestions:

1. Identify the commercially available hapten- or fluorescent-labeled nucleotides for selecting the appropriate combination probes for the experiment under consideration.
2. Select the appropriate detection system and filter sets and counterstains (DAPI or PI).
3. Use the matching filter sets for the visualization of the hybridization sites that will appear as green, red, yellow, white, blue, etc.

Double-color FISH procedure is generally used for translocation analysis between chromosomes, fusion of oncogenes, gene amplification, gene deletion, and chromosome enumeration. In such cases, alpha satellite DNA sequences are used for chromosome enumeration, whereas differently labeled genes or tumor-suppressor genes are used for genotypic analysis of tumor cells.

Note 10: Refer to the Web sites of Vysis, Ventana, and Cytocell for the availability of differently labeled commercial probes and their corresponding detection systems for implementing double- or triple-color FISH. During visualization, use a triple-band filter to visualize a green fluorescent dot (from FITC) and red fluorescent dot (from rhodamine) in the background of either blue (DAPI Counterstain) or red (PI counterstain).

Protocol 10: Microscopic Scoring and Data Analysis

MATERIALS

1. Epifluorescence microscope with appropriate filter combination
2. Test slides, positive control slides, and negative control slides
3. Scan slides at 40X and perform testing at 60X or 100X magnifications
4. Camera for photomicrography or digital fluorescence imaging system using CCD camera
5. A copy of the International System for Human Cytogenetics (ISCN) for FISH nomenclature
6. Figure 54 as a visual standard for expected interphase hybridization signals

METHOD

A. Interphase Enumeration

1. Perform an analytic sensitivity assay using the normal tissue by scoring 200 interphase nuclei from the different parts of the slide. The signals should be bright and distinct, with an analytic sensitivity higher than 90%.
2. Check for cross-hybridization, background, and visual quality. Before performing interphase enumeration of tumor cells, establish a baseline frequency for monosomic cell population in normal tissue by counting 200 interphase nuclei to establish the truncation artifact frequency. Subtract this artifact percentage from the original monosomic population of the tumor cells. Similarly, perform a trisomy check for hyperdiploid population for cross-hybridization or for splitting signals. Subtract this from the original trisomy population of the tumor cells for truncation effect and cutoff values (Huang *et al.,* 2002).
3. For tumor-cell analysis, avoid stromal cells from data collection.
4. Select well-separated malignant cells with well-defined borders for interphase data collection.
5. Avoid clumps, giant cells, or infiltrating leukocytes from data collection.
6. Avoid signals from fragmented nuclei.
7. Count diffuse signal as one if it has an acceptable boundary.
8. Avoid overlapped nuclei from data collection.
9. Do not evaluate interphase nuclei with split signals, weak signals, broken signals, signals from the periphery, and floating signals.
10. If two small signals are connected by a fluorescent link, consider it as one signal.
11. For interphase chromosome enumeration, consider a nucleus with a single spot as monosomy, double spots as disomy (diploid = control), triple spots as trisomy, and four spots as tetrasomy for each centromeric probe.
12. Signals for gene amplification should be carefully evaluated as they appear diffuse rather than distinct. In such cases, determination of gene copy number is difficult but can be interpreted subjectively.
13. The shape of the signals may vary depending on the cell cycle phase. In G2 cells, paired signals can be seen and should be considered as one signal. In the S phase, an oval signal instead of a round signal can be seen.

B. Metaphase Enumeration

Metaphase enumeration is straightforward as signals are distinct on the particular region of the chromosome. Select well-separated chromosomes and avoid short counts, pulverized chromosomes, and overlapping chromosomes from data collection. Knowledge of

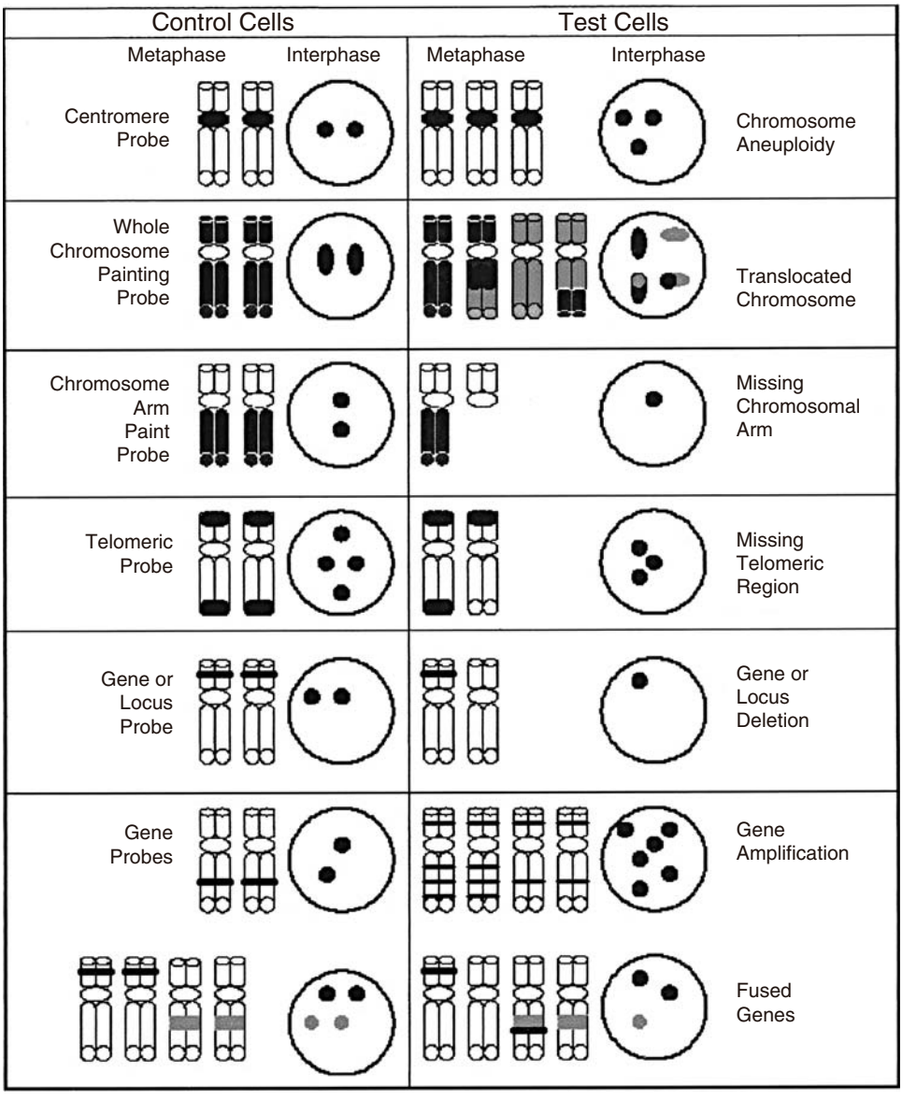

Figure 54. Schematic representation of genetic abnormalities detected by DNA probes with metaphase and interphase cells.

probe size and signal quality is essential during data collection.

14. Perform photomicrography using Kodak (Ektachrome P1600 for slides or Ektachrome 400 for prints) professional color reversal film or digitally using charge-coupled device array cameras (cooled CCD camera).

Troubleshooting the Fluorescence *in situ* Hybridization Procedure

The procedure FISH is an excellent analytic tool in analyzing the genetic abnormalities visually on a single-cell basis, if the protocols are followed carefully. However, in the some situations, excellence can be compromised resulting in the need for troubleshooting that may span in three core areas, which include 1) tissue preparation, 2) FISH methodologies, and 3) microscopic scoring and interpretation.

Pitfalls in tissue preparations include poor-quality slides; high slide background; and distorted tissue, cell, or chromosome morphology. Other difficulties include overdigestion or underdigestion of tissues during protease treatment and proper selection of tissues as positive or negative controls. Pitfalls associated with FISH methodologies are numerous. Some of their problems

include 1) errors in probe selection, identification of specific label, probe concentration, probe mixing, and difficulties in identifying the corresponding detection systems; 2) cross-hybridization of the probe with nonspecific targets; 3) weak or absence of hybridization signals; and 4) diffuse signals. During microscopic analysis, problems are encountered as a result of the faulty alignment of microscope, overlapping of signals, truncation effect on nuclei, signal pattern for each probe, and other problems associated with photomicroscopy and image analysis.

Some trouble-shooting tips are as follows:

1. Weak and absence of hybridization signals indicate inadequate denaturation; poor specimen preparation; inadequate probe cocktail preparation; and inappropriate hybridization, wash, or detection methodologies.
2. If both positive control and tumor tissues are negative, it may be the result of overdigestion or underdigestion of tissues during protein digestion. Optimize protein digestion protocols.
3. Presence of signals in nonspecific nuclear targets may be the result of inadequate stringency posthybridization in identifying the type of the probe (alpha satellite *versus* gene probes) and washing conditions to avoid cross-hybridization.
4. Excessive background may be because of the poor slide preparation, poor quality slides, or cellular debris.

It is difficult to mention all the potential problems that can be encountered and their solution. In some cases, one has to adapt a detective role in identifying the underlying cause and to suggest a possible solution. However, by self-study, consulting with experts and calling the helpline of many vendors like Vysis, a solution usually can be found.

Ovarian Carcinoma Immunohistochemistry

Background

Analysis by IHC is based on the formation of antigen-antibody complexes. A labeled antibody for a target antigen is applied onto a specimen, and the resulting antigen-antibody reaction is then visualized under a microscope. Obtaining optimal coloring intensity involves careful processing and preparation of the tissue as well as the blocking of nonspecific antibody binding. In fixation methods that suppress antigens, an additional unmasking step is required. When no staining is observed, a number of troubleshooting methods are used to identify the cause of the problem.

This section provides an overview of sample preparation and methodology for IHC detection of OC-related markers.

Principles of Immunohistochemistry

The principle of the IHC staining procedure is to visualize target antigens through antigen-antibody interactions that are visualized by enzymatic reactions. The IHC staining protocol consists of several key steps: 1) blocking, 2) epitope recovery, and 3) detection. The blocking steps prevent background staining as a result of nonspecific binding of the antibody to endogenous peroxidase, alkaline phosphatase, avidin, and biotin. For FFPE samples, an antigen-retrieval step is often required to unmask epitopes that are altered during fixation and processing. A number of heat-based treatments have been developed, including waterbaths, microwaves, autoclaves, and pressure cookers. The addition of heat unmasks epitopes by disrupting crosslinks formed by formalin fixation and by changing the tertiary protein structure (Hayat, 2002). Among these heating methods, the waterbath system has shown fairly good results for a wide range of antibodies and tissues. For certain antibodies in which heating is not recommended, enzymatic treatment using trypsin or pepsin may be an alternative. Some antibodies require both heat retrieval and enzymatic treatment for adequate epitope unmasking. Next, the target antigen is detected by direct or indirect enzyme-based techniques such as horseradish peroxidase (HRP) or alkaline phosphatase (AP). The antigen-antibody complex is finally visualized by the addition of a chromogen such as 3,3′ diaminobenzidine (DAB) or 3-amino-9-ethylcarbazole (AEC), which stains brown and red, respectively. The choice of chromogen depends on color preference and solubility. Whereas DAB requires a nonaqueous mounting media, AEC requires an aqueous mounting media. Where not specified, steps are performed in room temperature. Positive and negative controls should be used in each assay to ensure the quality of staining. Tissue sections with known expression of the target antigen should be used as a positive control sample. For a negative control, the primary antibody should be replaced with an isotype control.

General IHC staining protocols for paraffin-embedded and frozen sections are described in the following. Table 23 lists a number of relevant markers for IHC detection as well as information regarding positive control tissues and dilutions. The primary antibody dilutions are only suggested starting points for determining the optimal dilution for each specimen type.

Table 23. Monoclonal Primary Antibodies for Immunohistochemistry Staining

Monoclonal Antibody	Catalog # (Clone)	Vendor	Sample Type	Antigen Retrieval for FFPE Samples	Positive Human Control	Primary Antibody Dilution
Mouse anti-Cyclin D1	08-0220 (AM29)	Zymed	FFPE, FS	HIER3	Mantle cell lymphoma	1:50–1:200
Mouse anti-RB gene product	28-0007 (MAb1)	Zymed	FS	HIER1	Normal tonsil tissue	1:10–1:25
Mouse anti-retinoblastoma protein	18-0159 (Rb1;1F8)	Zymed	FFPE, FS	Trypsin or pepsin or HIER1	Normal tonsil tissue	1:50
Mouse anti-p53	18-7251 (DO-7)	Zymed	FFPE	HIER1	Colorectal carcinoma	1:50–1:100
Mouse anti-p21 (Cip1/WAF1)	33-7000 (EA 10)	Zymed Zymed	FFPE, FS	Not required	Ultraviolet irradiated skin	1:100
Mouse anti-p27	18-2370 (57)	Zymed	FFPE, FS	HIER1	Normal colon	1:50–1:200
Mouse anti-proliferating cell nuclear antigen (PCNA)	18-0110 (PC 10)	Zymed	FFPE, FS	Not required	Normal tonsil	1:50
Mouse anti-Ki-67 antigen	18-0192 (7B11)	Zymed	FFPE, FS	HIER1 then trypsin	Normal tonsil or spleen; breast carcinoma	1:50–1:200
Mouse anti-epidermal growth factor receptor (EGFR)	28-0005 (31G7)	Zymed	FFPE, FS	Pepsin	Normal skin epidermis, glioblastoma	1:20–1:80
Mouse anti-C-Myc protein	NCL-cMYC (9E11)	Novo Castra	FFPE, FS	Trypsin	SkBr3 breast cancer cell line	1:150–1:250
Mouse anti-CA-125	18-7242 (OC 125)	Zymed	FFPE, FS	HIER1	Normal epithelial cells in colon and stomach	1:100–1:200
Mouse anti-carcinoembryonic antigen (CEA)	M7072 (11-7)	Dako Corp	FFPE, FS	HIER1	Colon adenocarcinoma	1:50–1:100
Mouse cellular apoptosis susceptibility (CAS)	NCL-CAS (30F12)	Novo Castra	FFPE, FS	HIER1	Tonsil	1:40–1:80
Mouse anti-E-cadherin	18-0223 (4A2C7)	Zymed	FFPE, FS	Not required	Nonneural epithelia	1:100–1:200
Mouse anti-N-cadherin	18-0224 (3B9)	Zymed	FFPE, FS	HIER1	Neural tissue, heart	1:100
Mouse Anti-Fas (CD95/Apo-1),	NCL-FAS-310 (GM30)	Novo Castra	FFPE, FS	HIER1	Small intestine	1:40–1:80

FFPE, Formalin-fixed and paraffin-embedded; FS, frozen section; HIER, heat-induced epitope recovery; HIER1,10 mM sodium citrate buffer, pH 6.0; HIER2, 10 mM sodium citrate buffer, pH 6.0; HIER3, ethylenediamine tetraacetic acid, pH 8.

Protocol 11: Immunohistochemistry of Paraffin-Embedded Tissue Sections

MATERIALS

1. Staining dish
2. Water bath
3. Xylene
4. Ethanol
5. Distilled water
6. 0.01 M PBS
7. 0.01 M citrate buffer (pH 6.0)
8. EDTA
9. Enzymes (i.e., pepsin, trypsin)
10. Primary antibody
11. Isotype control
12. Detection kit
13. Blocking reagents (i.e., serum blocking solution, peroxidase quenching solution)

14. Hematoxylin
15. Bluing reagent (dilute ammonium hydroxide in water, pH 8.5)
16. Chromogen (i.e., AEC, DAB, or Fast-Red)
17. Mounting solution

REAGENT PREPARATION

All reagent preparation should be prepared according to the manufacturer's directions.

METHOD

1. Incubate slides in a dry incubator at 37°C for 1 hr, followed by 30 min at 60°C.
2. Soak slides in xylene for 10 min 2×.
3. Rehydrate samples in a series of 100%, 95%, 80%, and 70% ethanol for 5 min each.
4. Immerse slides in distilled water 3 min.
5. Perform epitope recovery by 1) heat or 2) enzyme methods as necessary.
   a. Heat-induced epitope recovery: Immerse slides in a plastic staining dish of 0.01 M citrate or EDTA at 95°C in a waterbath for 20–30 min or over a hot plate. Transfer slides into a dish of 95°C distilled water for 10 min. Transfer distilled water solution with slides to room temperature until cooled to room temperature.
   b. Enzyme digestion: Prewarm enzyme (trypsin or pepsin) to 37°C and apply onto slide. Incubate at 37°C for 10 min.
6. Rinse in PBS for 2 min.
7. Place slides in a peroxidase-quenching solution for 5 min. Soak in distilled water for 2 min 2×.
8. Wipe around perimeter of the sample. Apply serum blocking solution for 10 min. Wash in PBS 2 min 2×.
9. Repeat for other blocking reagents as necessary.
10. Wipe around sample perimeter and apply on sample primary antibody diluted in PBS (see Table 23). Incubate for 1–2 hr in humidified chambers at 37°C. Wash in PBS for 2 min 2×.
11. Wipe around perimeter of the sample. Apply sufficient secondary antibody to cover entire sample and incubate for 10–30 min. Wash in PBS for 2 min 2×.
12. Wipe around perimeter of the sample. Apply sufficient enzyme conjugate antibody to cover entire tissue, and incubate for 10–30 min. Wash in PBS 2 min 2×.
13. Wipe around perimeter of the sample. Apply sufficient chromogen to cover entire tissue, and incubate for 5–10 min. Wash in slow running tap water for 2 min 2×. Soak in distilled water for 2 min 2×.
14. To counterstain, dip slides in hematoxylin solution for 1 min. Wash in slow running tap water for 2 min 2×. Soak in distilled water for 2 min 2×.
15. Soak in bluing reagent for 1 min. Wash in distilled water for 2 min 2×.
16. Samples should be mounted according to the type of chromogens used as follows:
   a. For AEC and Fast-Red chromogens, add 1 drop of aqueous mounting media on the slide and apply coverslips
   b. For DAB chromogen, dehydrate samples through 4 changes of ethanol (80%, 95%, 100%, and 100%) for 3 min each, and then clear in 2 changes of xylene for 5 min each.
17. Allow slides to dry before visualizing under light microscope.

Protocol 12: Immunohistochemistry of Frozen Sections, Cytospin Preparations, Cell Suspensions, and Cell Smears

MATERIALS

1. Staining dish
2. Water bath
3. Xylene
4. Ethanol
5. Distilled water
6. 0.01 M PBS
7. Primary antibody
8. Isotype control
9. Detection kit
10. Blocking reagents (i.e., serum blocking solution, peroxidase quenching solution)
11. Hematoxylin
12. Bluing reagent (dilute ammonium hydroxide in water, pH 8.5)
13. Chromogen (i.e., AEC, DAB, or Fast-Red)
14. Mounting solution

METHOD

1. Rinse in PBS for 2 min.
2. Place slides in a peroxidase quenching solution for 5 min. Soak in distilled water for 2 min 2×.
3. Wipe around perimeter of the sample. Apply serum blocking solution for 10 min. Wash in PBS for 2 min 2×.
4. Repeat for other blocking reagents as necessary.
5. Wipe around sample perimeter and apply sample primary antibody diluted in PBS (see Table 23). Incubate for 1–2 hr in humidified chambers. Wash in PBS for 2 min 2×.
6. Wipe around perimeter of the sample. Apply sufficient secondary antibody to cover entire sample and incubate for 10–30 min. Wash in PBS for 2 min 2×.

7. Wipe around perimeter of the sample. Apply sufficient enzyme conjugate antibody to cover entire tissue, and incubate for 10–30 min. Wash in PBS for 2 min 2×.

8. Wipe around perimeter of the sample. Apply sufficient chromogen to cover entire tissue, and incubate for 5–10 min. Wash in slow running tap water for 2 min 2×. Soak in distilled water for 2 min 2×.

9. To counterstain, dip slides in hematoxylin solution for 1 min. Wash in slow running tap water for 2 min 2×. Soak in distilled water for 2 min 2×.

10. Soak in bluing reagent for 1 min. Wash in distilled water for 2 min 2×.

11. Samples should be mounted according to the type of chromogens used as follows:

a. For AEC and Fast Red chromogens, add 1 drop of aqueous mounting media on the slide and apply coverslips.

b. For DAB chromogen, dehydrate samples through 4 changes of ethanol (80%, 95%, 100%, and 100%) for 3 min each, and then clear in 2 changes of xylene for 5 min each.

12. Allow slides to dry before visualizing under light microscope.

Detection of Multiple Antigens

Two antigens can be visualized on the same tissue by using two different enzyme–substrate reactions such as alkaline phosphatase (AP)/Vector Red (VR) and peroxidase/Vector SG. After incubating the specimen with the primary and secondary antibody, apply avidin- and biotin-conjugated alkaline phosphatase solution (ABC–AP), followed by VR substrate solution. After these steps are done, the sections are blocked with Avidin D and biotin and then incubated in the primary antibody directed against the second protein of interest. After the secondary antibody incubation, the specimen is incubated with avidin- and biotin-conjugated peroxidase (ABC–HRP) solution. Alternatively, peroxidase-antiperoxidase (PAP) can be used instead of ABC methods, but the sensitivity of ABC technique may be higher than PAP (Sternberger and Sternberger, 1986).

Troubleshooting

If no staining is seen on both the experimental and control samples, some sources of error could be inadequate sample fixation, incorrect or defective reagents, or incorrect antibodies. Samples fixed for more than 24 hr generally become less sensitive to IHC staining, so overfixation may reduce or eliminate staining intensity. Make sure all reagents are prepared in the correct dilution and used in the proper order according to the manufacturer's directions. Check expiration dates to ensure that the antibodies and chromogen are still in good use.

Weak staining can be interpreted as nonspecific background staining or weak specific staining. If observed on the positive control sample, it is an indication of weak specific staining. Weak staining can be the result of overly dilute primary antibody concentration or incubation time. It can also be the result of insufficient chromogen incubation time. If weak staining is only seen on the experimental sample and not the positive control sample, the final interpretation between true and nonspecific staining requires careful microscopy. Background staining can result from nonspecific reactions with endogenous tissue proteins, so it is important to make sure that serum blocks and hydrogen peroxide quenching solutions are applied. Drying of samples during the assay can also cause background staining, so care should be taken to carry out incubations in moist chambers. If the negative control exhibits background staining, whereas the experimental and positive control samples do not, most likely the source of error is in the isotype serum. The isotype serum may contain cross-reacting immunoglobulin components, and this problem can be corrected by purification or replacing the serum with a better match.

Comparison between Fluorescence *in situ* Hybridization and Immunohistochemistry

The techniques of FISH and IHC are powerful tools for identifying genomic alterations in ovarian carcinoma. Their consistent results and quick turnaround time make them a mainstay in pathologic analysis. In particular, both techniques have distinctive advantages and disadvantages for detection of abnormalities. The technique FISH is highly specific for identifying chromosomal aberrations, as well as gene amplifications, deletions, and translocations on a cell-by-cell basis. However, FISH is limited by nonspecific binding and false-positive or false-negative results because of inappropriate assay conditions. Furthermore, the truncation of nuclei during sectioning of tissues introduces a source of error. The technique IHC visualizes antigen expression while revealing morphologic details on a tissue level. However, the occurrence of nonspecific background staining can lead to improper interpretation. The efficacy of both FISH and IHC have been evaluated with *HER-2/neu* in breast cancer specimens, and in one study, it was shown that 34 out of 61 (51%) of the tumor samples stained positive for *HER-2/neu* overexpression by FISH, of which 9 of the cases were negative by IHC with monoclonal antibody (Cianciulli *et al.,* 2002). The false-positive nature of IHC has also

been reported by Tubbs *et al.,* who reported that 15% of breast cancer cases with negative FISH results were erroneously graded as positive by IHC (Tubbs *et al.,* 2001). Regarding the reliability of data among various observers, Kakar *et al.* (2000) reported an 88% agreement between IHC and FISH results. The results indicated that combined use of both techniques is more accurate for therapeutic treatment planning in breast cancer, and similar studies are under way for ovarian carcinoma. Therefore, FISH and IHC can have significant value for ovarian carcinoma diagnosis and prognosis. The methods FISH and IHC have also been compared by Hayat (2004) in volume 1 of this series of handbooks.

Applications of Fluorescence *in situ* Hybridization in Ovarian Tumors

Karyotype analysis by chromosome banding and tumor-cell culture is not frequently performed in epithelial ovarian tumors because of several technical problems. This includes low cell viability, overgrowth of nonneoplastic cells, use of malignant effusions rather than solid tissues for culturing, low mitotic index, and poor chromosome morphology. However, close to 500 untreated epithelial ovarian carcinomas were fully karyotyped by various authorities. Classic cytogeneticists reported gains and losses of several chromosomes (chromosome aneuploidy) and several complex (karyotypic) morphologies. Nonrandom cytogenetic abnormalities involving chromosomes 1, 3, 6, 5, 9, 11, and 12 were reported. Chromosome gains were frequent with 12, whereas chromosome losses were common with 8, 13, 14, 22, and X (van Dekken *et al.,* 1997). Karyotype analysis, in general, supported that gains and losses of large segments of chromosomes occurred in sporadic ovarian carcinomas, and more complex karyotypes were associated with advanced or poorly differentiated tumors. However, it is unclear from karyotype analysis whether chromosome abnormalities are the result of general genomic instability or are specifically required to activate or inactivate multiple oncogenes and tumor suppressor genes. The technique FISH and a modified form of this procedure called CGH later addressed this lag in cytogenetic characterization of ovarian carcinomas with additional well-defined chromosome markers.

Combining classic cytogenetics with FISH, Tibiletti *et al.* (1999) proposed that chromosome band 6q27 plays a critical role in ovarian tumor development and detection of this band supports early events in ovarian tumor development. The procedure CGH further showed chromosomal loss of 16q and 17p and chromosome gains of 3q and 8q with various ovarian carcinomas (Iwabuchi *et al.,* 1995). Similarly, by FISH, it was shown that the gain of chromosome band 20q13.2, overexpression of oncogenes *HER-2/neu* on chromosome 17q21, and amplification of oncogene *myc* at 8q24 all indicated poor survival of patients (Fukushi *et al.,* 2001).

Interphase cytogenetic study supported the loss of specific chromosomes 17, 20 and X, whereas gain was reported with chromosomes 1, 7, 8, 11, and 12. Chromosome aneuploidy resulting from the loss or gain of chromosomes showed heterogenous distribution with growth advantages. Table 24 provides the list of chromosome rearrangements that may have clinical relevance (Wang, 2002).

In general, gains are twice as common as losses. The average number of changes in OC is about 7 (Gallion *et al.,* 1990). Poorly differentiated or advanced stages of OC have more genetic alterations than early-stage or borderline cases (Dodson *et al.,* 1993). Studies of LOH are useful in detecting deletion of one allele. Such deletions have been noted in several chromosome arms such as 5q, 6q, 7p, 8p, 11p, 11q, 13q, 14q, 17p, 17q, and 22q. It is unclear whether these are a result of general genomic instability or are specifically required to inactivate multiple-tumor-suppressor genes (Pihan and Doxsey, 1999).

Markers for Ovarian Carcinoma

Some of the antigens used to diagnose and confirm OC include CA-125, p53, CAS, E-cadherin, N-cadherin, and FAS. CA-125, raised in 80% of patients, is a serum tumor marker for OC (Bast *et al.,* 1983). It has a well-established role in following the response to treatment and detecting relapse in patients with OC, although very little is known about its biochemistry and genetics (Kaneko *et al.,* 2003). As a tumor-suppressor gene, *p53* is mutated in 30–80% of ovarian cancers and OC cell lines. Loss of functional *p53* from either point mutation or allelic deletions leads to unrestrained cellular proliferation. Mutation of *p53* is probably an early event because it is seen in both primary and metastatic sites, but there is a higher incidence of overexpression of mutant *p53* in advanced-stage disease as compared with early-stage disease. The cellular apoptosis susceptibility gene (*CAS*) is the human homolog of yeast chromosome segregation gene (CSE1). The CAS protein is a nuclear transport factor needed in the mitotic spindle checkpoint that ensures genomic stability during cell division. Amplification of *CAS* leads to protein overexpression, which in turn interferes with the regulation of cyclin-dependent kinases and other proteins involved in cell cycle progression.

Table 24. Altered Chromosomes in Ovarian Cancer Cells Detected by Fluorescence *in situ* Hybridization

	Types of Chromosomal Anomalies						
	Numerical Alterations (FISH)		Genetic Inbalances (LOH and Amplifications)	Locus Anomaly	Structural Alterations or Derivative Chromosomes (FISH) and Spectral Karyotyping)	Gene Alterations (FISH and IHC)	
Chromosome Number	Gain	Loss	(CGH)	(FISH)		Amplifications	Deletions
1	X		1q		X		
2	X						
3	X		3q	dup 3q26			
4		X	4p				
5			5q				
6	X		6q	del 6q27	X		
7	X					7p12(EGFR)	
8			8p, 8q			8q24 (C-Myc)	
9	X						9p21 (p16)
10							
11		X				11q13 (cyclin D1)	
12	X						
13		X					l3ql4 (Rb1)
14							
15		X					
16			16q			.	
17		X	17p, 17q			17p13 (p53) 17q21 (HER- 2/neu)	17p13 (p53)
18			18q				
19			19p				
20			20q			20q13(ZNF 217)	
21							
22		X					
X		X	Xp				
Others (DMs, HSRs)							

CGH, Comparative genomic hybridization; DMs, double minutes; EGFR, epidermal growth factor receptor; FISH, fluorescence *in situ* hybridization; HSRs, homogenously staining regions; IHC, immunohistochemistry; LOH, loss of heterozygosity.

E-cadherin and N-cadherin are two glycoproteins in the cadherin family that are found in epithelial cells. Studies of E- and N-cadherins in ovarian carcinoma help distinguish serous and endometrioid carcinomas from mucinous carcinomas (Peralta Soler *et al.,* 1997). The protein FAS is a transmembrane molecule belonging to the tumor necrosis factor family with a role in the apoptotic pathway. It induces apoptosis by cross-linking with CD95 ligand or FAS ligand (CD95L/FASL), resulting in a functional trimeric structure of the FAS protein. The intracellular domain of FAS, also known as "death domain," interacts with the FAS-associated death domain protein to transduce the death signal.

Tumor-suppressor and cancer susceptibility oncogenes detected by IHC or FISH include *BRCA1*, *BRCA2,* and *HER-2/neu*. *BRCA1* is a tumor-suppressor gene, as evidenced by LOH studies (Miki *et al.,* 1994). It is believed that, for mutational inactivation of *BRCA1* to contribute to ovarian tumorigenesis, it has to have occurred early in fetal development of the ovary and not in the adult ovarian epithelium. In fact, somatic mutations of *BRCA1* are not a feature of sporadic ovarian carcinoma. However, *BRCA2* is a cancer-susceptibility gene (Wooster *et al.,* 1995). It has a lower penetrance than *BRCA1*, and inherited mutations of *BRCA2* actually confer a higher risk for breast carcinoma than ovarian carcinoma. *HER-2/neu* is a member of a transmembrane receptor gene family that includes EGFRs. About 30% of breast cancers and 20% of OC overexpress *HER-2/neu,* and it is unclear if it is associated with a more aggressive behavior. In addition, to distinguish between histologic subtypes of OC, IHC for antibodies against CK7, CK20, HAM56, CA125, and CEA may be useful. The review article by McCluggage *et al.* (2002) provides accurate information about various antibodies of diagnostic relevance.

Table 25. Emerging Antibodies in Ovarian Cancers

Category	Examples (Many Tumors)
Oncogenes	Many mutated oncogenes specific to ovarian cancer
Tumor-suppressor genes	*BRCA*, *p53, Rb,* etc.
Overexpression of oncogenes	*HER-2/neu, myc, fos ras*
Growth factor related (cytokines)	EGF, TGF, BMP 4, endothelin, etc.
Invasion related	Cadherins, integrins, ICAMs, cytoskeleton, laminin, CD44, etc.
Angiogenesis related	VEGF, bFGF, Von Willebrand factor, etc.
Metabolic and proteolytic enzymes	Matrix metalloproteinases (MMP), plasminogen activators, catapsins
Blood group antigens	Lewis Y, Lewis X
Apoptosis related	*Bcl-2, bax,* etc.
Proliferation related	Cyclin D, nuclear protein p120, topoisomerase 11, MPM2, etc.
Heat-shock proteins	Hsp70, Hsp90
Metastasis-related gene expression	Nm23, KiSS1, CAD1, BRMS1, MKK4

bFGF, Basic fibroblast growth factor; BMP, bone morphogenetic protein; EGF, epidermal growth factor; ICAM, intracellular adhesion molecule; TGF, transforming growth factor; VEGF, vascular endothelial growth factor.

Although antibodies of prognostic importance are not well-documented in ovarian neoplasms, the emerging antibodies with great research potential are documented in Table 25. In the future, it is hoped that some of these antibodies may emerge as prognostic markers.

In conclusion, FISH has shown that different ovarian tumor histotypes have nonrandom chromosome gains and losses, as well as "hot spots" for gene rearrangements, amplifications, and chromosome deletions, which may play an important role in tumor progression. In the future, genetic markers may help to identify patients falling in various molecular subtypes with different prognosis (Pieretti *et al.,* 2002).

Acknowledgments

We thank Nameeta Chimanji (research associate) and Rachel Tewari (research scientist) at Ortec International, Inc. for technical assistance in the preparation of this manuscript.

References

American Cancer Society. 2005. Cancer Facts and Figures. Atlanta, GA: American Cancer Society.

Bast, R.C. Jr., Klug, T.L., St. John, E., Jenison, E., Niloff, J.M., Lazarus, H., Berkowitz, R.S., Leavitt, T., Griffiths, C.T., Parker, L., Zurawski, V.R. Jr., and Knapp, R.C. 1983. A radioimmunoassay using a monoclonal antibody to monitor the course of epithelial ovarian cancer. *N. Engl. J. Med*. *309*:883–887.

Brown, G., Wong, A., and Beesley, J. 2000. Preservation of tissue for immunocytochemistry. In Beesley, J. (ed) *Immunocytochemistry and in situ Hybridization in the Biomedical Sciences.* Boston: Birkhauser, 30–54.

Choo, K. 1994. *In situ Hybridization Protocols*. Totowa, NJ, Humana Press.

Cianciulli, A.M., Botti, C., Coletta, A.M., Buglioni, S., Marzano, R., Benevolo, M., Cione, A., and Mottolese, M. 2002. Contribution of fluorescence *in situ* hybridization to immunohistochemistry for the evaluation of HER-2 in breast cancer. *Cancer Genet. Cytogenet*. *133*:66–71.

Dodson, M.K., Hartmann, L.C., Cliby, W.A., DeLacey, K.A., Keeney, G.L., Ritland, S.R., Su, J.Q., Podratz, K.C., and Jenkins, R.B. 1993. Comparison of loss of heterozygosity patterns in invasive low-grade and high-grade epithelial ovarian carcinomas. *Cancer Res*. *53*:4456–4460.

Dracopoli, N., Haines, J., Korf, B., Moir, D., Morton, C., Seidman, C., Seidman, J., and Smith, D. (eds). 2001. *Current Protocols in Human Genetics*. New York: John Wiley & Sons, Inc.

Fan, Y.-S. (ed). 2002. *Molecular Cytogenetics*. Totowa, NJ, Humana Press. Inc.

Gallion, H.H., Powell, D.E., Smith, L.W., Morrow, J.K., Martin, A.W., van Nagell, J.R., and Donaldson, E.S. 1990. Chromosome abnormalities in human epithelial ovarian malignancies. *Gynecol. Oncol*. *38*:473–477.

Gozzetti, A., and Le Beau, M.M. 2000. Fluorescence *in situ* hybridization: uses and limitations. *Semin. Hematol*. 37:320–333.

Hayat, M. 2002. *Microscopy, Immunohistochemistry, and Antigen Retrieval Methods*. New York: Kluwer/Academic.

Hayat, M.A. 2004. Comparison of immunohistochemistry, *in situ* hybridization, fluorescence *in situ* hybridization, and chromogenic *in situ* hybridization. In Hayat, M. (ed). *Handbook of Immunohistochemistry and in situ Hybridization of Human Carcinomas*: *Molecular Genetics, Lung Carcinoma and Breast Carcinoma*. San Diego and London: Elsevier.

Huang, N.F., Gupta, M., Varghese, S., Rao, S., and Luke, S. 2002. Detection of numerical chromosomal abnormalities in epithelial ovarian neoplasms by fluorescence *in situ* hybridization (FISH) and a review of the current literature. *Appl. Immunohistochem. Mol. Morphol*. *10*:187–193.

Iwabuchi, H., Sakamoto, M., Sakunaga, H., Ma, Y.Y., Carcangiu, M.L., Pinkel, D., Yang-Feng, T.L., and Gray, J.W. 1995. Genetic analysis of benign, low-grade, and high-grade ovarian tumors. *Cancer Res*. *55*:6172–6180.

Jackson, L. 2002. Cytogenetics and molecular cytogenetics. *Clin. Obstet. Gynecol*. *45*:622–639; discussion 730–732.

John, S. (ed). 2003. *Cancer Cytogenetics*: *Methods and Protocols*. Totowa, NJ: Humana Press.

Johnson, K.L., Zhen, D.K., and Bianchi, D.W. 2000. The use of fluorescence *in situ* hybridization (FISH) on paraffin-embedded tissue sections for the study of microchimerism. *Biotechniques 29*:1220–1224.

Kakar, S., Puangsuvan, N., Stevens, J.M., Serenas, R., Mangan, G., Sahai, S., and Mihalov, M.L. 2000. HER-2/neu assessment in breast cancer by immunohistochemistry and fluorescence *in situ* hybridization: comparison of results and correlation with survival. *Mol. Diagn*. *5*:199–207.

Kaneko, S.J., Gerasimova, T., Smith, S.T., Lloyd, K.O., Suzumori, K., and Young, S.R. 2003. CA125 and UQCRFS1 FISH studies of ovarian carcinoma. *Gynecol. Oncol*. *90*:29–36.

Kearney, L. 1999. The impact of the new FISH technologies on the cytogenetics of haematological malignancies. *Br. J. Haematol. 104*:648–658.

Langer, P.R., Waldrop, A.A., and Ward, D.C. 1981. Enzymatic synthesis of biotin-labeled polynucleotides: novel nucleic acid affinity probes. *Proc. Natl. Acad. Sci. USA 78*:6633–6637.

Luke, S., Belogolovkin, V., Varkey, J.A., and Ladoulis, C.T. 1997. Fluorescence *in situ* hybridization. In Gu, J. (ed). *Analytical Morphology*. Boston: Eaton Publishing Co., 139–173.

Luke, S., Huang, N.F., Goyal, N., Varkey, J.A., Alsay-Oculam, A.A., Gupta, M., and Ladoulis, C.T. 1998. Optimization of fluorescence *in situ* hybridization (FISH) in cytological specimens. *Cell Vis*. *5*:85–86.

McCluggage, W.G. 2002. Recent advances in immunohistochemistry in gynaecological pathology. *Histopathology 40*: 309–326.

Miki, Y., Swensen, J., Shattuck-Eidens, D., Futreal, P.A., Harshman, K., Tavtigian, S., Liu, Q., Cochran, C., Bennett, L.M., Ding, W. 1994. A strong candidate for the breast and ovarian cancer susceptibility gene BRCA1. *Science 266*:66–71.

Peralta Soler, A., Knudsen, K.A., Tecson-Miguel, A., McBrearty, F.X., Han, A.C., and Salazar, H. 1997. Expression of E-cadherin and N-cadherin in surface epithelial-stromal tumors of the ovary distinguishes mucinous from serous and endometrioid tumors. *Hum. Pathol*. *28*:734–739.

Pieretti, M., Hopenhayn-Rich, C., Khattar, N.H., Cao, Y., Huang, B., and Tucker, T.C. 2002. Heterogeneity of ovarian cancer: relationships among histological groups, stage of disease, tumor markers, patient characteristics, and survival. *Cancer Invest*. *20*:11–23.

Pihan, G.A., and Doxsey, S.J. 1999. The mitotic machinery as a source of genetic instability in cancer. *Semin. Cancer Biol*. *9*:289–302.

Qian, J., Bostwick, D.G., Takahashi, S., Borell, T.J., Brown, J.A., Lieber, M.M., and Jenkins, R.B. 1996. Comparison of fluorescence *in situ* hybridization analysis of isolated nuclei and routine histological sections from paraffin-embedded prostatic adenocarcinoma specimens. *Am. J. Pathol. 149*:1193–1199.

Ried, T. 1998. Interphase cytogenetics and its role in molecular diagnostics of solid tumors. *Am. J. Pathol*. *152*:325–327.

Roche, P., and Hsi, E. 2001. Immunohistochemistry: theory and practice. In Lloyd, R. (ed). *Morphology Methods*: *Cell and Molecular Biology Techniques*. Totowa, NJ: Humana Press.

Ross, J.S., and Fletcher, J.A. 1999. The HER-2/neu oncogene: prognostic factor, predictive factor and target for therapy. *Semin. Cancer Biol*. *9*:125–138.

Schurter, M.J., LeBrun, D.P., and Harrison, K.J. 2002. Improved technique for fluorescence *in situ* hybridisation analysis of isolated nuclei from archival, B5 or formalin fixed, paraffin wax embedded tissue. *Mol. Pathol*. *55*:121–124.

Schwab, M. 1998. Amplification of oncogenes in human cancer cells. *Bioessays 20*:473–479.

Slovak, M.L., Tcheurekdjian, L., Zhang, F.F., and Murata-Collins, J.L. 2001. Simultaneous detection of multiple genetic aberrations in single cells by spectral fluorescence *in situ* hybridization. *Cancer Res. 61*:831–836.

Sternberger, L.A., and Sternberger, N.H. 1986. The unlabeled antibody method: comparison of peroxidase-antiperoxidase with avidin-biotin complex by a new method of quantification. *J. Histochem. Cytochem*. *34*:599–605.

Teixeira, M.R. 2002. Combined classical and molecular cytogenetic analysis of cancer. *Eur. J. Cancer 38*:1580–1584.

Tibiletti, M.G., Bernasconi, B., Dionigi, A., and Riva, C. 1999. The applications of FISH in tumor pathology. *Adv. Clin. Path. 3*:111–118.

Tonnies, H. 2002. Modern molecular cytogenetic techniques in genetic diagnostics. *Trends Mol. Med*. *8*:246–250.

Tubbs, R.R., Pettay, J.D., Roche, P.C., Stoler, M.H., Jenkins, R.B., and Grogan, T.M. 2001. Discrepancies in clinical laboratory testing of eligibility for trastuzumab therapy: apparent immunohistochemical false-positives do not get the message. *J. Clin. Oncol. 19*:2714–2721.

van Dekken, H., Rosenberg, C., Krijtenburg, P.J., and Alers, J.C. 1997. Interphase cytogenetics and comparative genomic hybridization of human epithelial cancers and precursor lesions. *Histochem. Cell Biol*. *108*:419–430.

Wang, N. 2002. Cytogenetics and molecular genetics of ovarian cancer. *Am. J. Med. Genet. 115*:157–163.

Werner, M., Von Wasielewski, R., and Komminoth, P. 1996. Antigen retrieval, signal amplification and intensification in immunohistochemistry. *Histochem. Cell Biol. 105*:253–260.

Wooster, R., Bignell, G., Lancaster, J., Swift, S., Seal, S., Mangion, J., Collins, N., Gregory, S., Gumbs, C., and Micklem, G. 1995. Identification of the breast cancer susceptibility gene BRCA2. *Nature 378*:789–792.

3

Role of Immunohistochemical Expression of HER2/neu in High-Grade Ovarian Serous Papillary Cancer

Alessandro D. Santin

Introduction

Epithelial ovarian carcinoma (OC) remains the cancer with the highest mortality rate among gynecologic malignancies with an estimated 25,580 cases and 16,090 deaths in the United States in 2004 (Jemal *et al.,* 2004). Two-thirds of patients have advanced disease when diagnosed, and although many patients with disseminated tumors respond initially to standard combinations of surgical and cytotoxic therapy, nearly 90% will develop recurrence and inevitably succumb to their disease. Novel diagnostic and therapeutic markers useful for early ovarian cancer diagnosis and for the effective therapy of chemotherapy resistant or residual disease are urgently needed.

The morphologic and biologic heterogeneity of OC has contributed to difficulties in defining the molecular alterations associated with its development and progression. On the basis of morphologic criteria, several major types of epithelial OC have been described, with ovarian serous papillary cancer (OSPC) representing the most common histologic variant of ovarian tumor. It is important to note that the exact nature of the normal cell type from which ovarian epithelial tumor cells originate remains unclear (Dubeau, 1999). The currently favored hypothesis is that ovarian epithelial tumors arise from the single mesothelial cell layer lining the ovarian surface, which is often referred to as surface epithelium, after a process of metaplasia to become müllerian-like. This is because the most common subtypes of ovarian cancers are morphologically indistinguishable from neoplasms arising from those organs of the female genital tract that are embryologically derived from müllerian ducts. Indeed, the serous type is similar to the tumors arising in the fallopian tubes, the endometrioid type is similar to the tumors of the endometrium, and the mucinoid type resembles neoplasms of the endocervix. However, an alternative hypothesis has been proposed in which components of the secondary müllerian system, which include paraovarian or paratubal cysts, rete ovarii, endosalpingiosis, endomucinosis, and endometriosis may instead represent the cell source of ovarian tumorogenesis (Dubeau, 1999).

Handbook of Immunohistochemistry and *in situ* Hybridization of Human Carcinomas, Volume 4: Molecular Genetics, Gastrointestinal Carcinoma, and Ovarian Carcinoma

In the last two decades much of the cancer research has focused on identifying the molecular and genetic changes that cause malignant transformation. Protooncogenes are a group of normal genes that play important roles in the regulation of cell proliferation. Abnormalities in the expression, structure, or activity of protooncogene products contribute to the development and maintenance of the malignant phenotype. These genes and their expression products may be used as attractive targets for the development of novel anti-cancer treatments.

The human *HER2/neu (c-erbB2)* gene product, like the epidermal growth factor receptor (EGFR), is a transmembrane receptor protein that includes an intracellular tyrosine kinase domain (Graus-Porta *et al.,* 1997). With no direct ligand identified to date, *HER2/neu* functions as a preferred partner for heterodimerization with other members of the EGFR family (namely, HER-1 or ErbBl, HER-3 or ErbB3, and HER-4 or ErbB4) and thus plays an important role in coordinating the complex ErbB signaling network (Graus-Porta *et al.,* 1997). In normal cells, two copies of the gene per cell (one on each chromosome 17) are present. However, in the presence of *HER2/neu* amplification there may be as many as 50 or 100 *HER2/neu* genes per tumor cell (Busse *et al.,* 2000). This gene amplification results in overexpression of p185 HER2/neu at both the messenger ribonucleic acid (mRNA) and protein levels. As a result, instead of ~20,000 to 50,000 HER2/neu molecules per cell, there can be as many as 2 million molecules per cell in neoplastic tissues (Busse *et al.,* 2000). When *HER2/neu* is overexpressed at such high levels, the kinases become constitutively activated, possibly as a result of auto-activation caused by crowding of adjacent *HER2/neu* receptor molecules within the cell membrane. The final result of this phenomenon appears to be ligand-independent activation of the *HER2/neu* receptor, resulting in an increased mitogen-activated protein kinase (MAPK) and phosphatidylinositol-3 kinase (PI-3K) cell signaling, leading to increased cell proliferation (Yarden and Sliwkowski, 2001).

High levels of *HER2/neu* in human tumors have been associated with shorter patient survival, resistance to hormonal therapy, and resistance to tumor necrosis factor alpha (TNF-α) activated macrophages and lymphocyte-activated killer cells (Busse *et al.,* 2000). In addition, *HER2/neu* overexpression on tumor cells has been correlated with down-regulation of E-cadherin (a condition associated with invasiveness of tumor cells) and with the secretion of vascular endothelial growth factor (one of the more important mediators of tumor angiogenesis) (Sliwkowski *et al.,* 1999). In breast, ovarian, and endometrial cancers, several, but not all, studies have reported that the amplification of this gene is associated with resistance to chemotherapeutic treatment and poor survival, suggesting that cells overexpressing *HER2/neu* may manifest a more aggressive biologic behavior and may have a selective growth advantage over *HER2/neu*-negative tumor cells (Berchuck *et al.,* 1990; Hetzel *et al.,* 1992). Consistent with this view, previous studies have reported a significantly higher expression of *HER2/neu* in OC that relapsed after chemotherapy when compared to chemotherapy-naïve ovarian disease (Meden *et al.,* 1998). However, these results have not been confirmed in other studies (Bookman *et al.,* 2003). Although *HER2/neu* overexpression in ovarian cancer was initially reported in 25–30% of the cases, with figures ranging from 9% to 65% in different series (Hellstrom *et al.,* 2001), *HER2/neu* overexpression today is considered to be a rare event in ovarian cancer. Indeed, the largest study reported to date by the Gynecologic Oncology Group (GOG) (n = 837) found only 11.4% 2+/3+ overexpressing tumors (Bookman *et al.,* 2003). Similarly, a low percentage of *HER2/neu* overexpression has been reported in another large OC series (Mano *et al.,* 2004).

In this chapter we describe how we use immunohistochemical assay to determine *HER2/neu* protein overexpression in OSPC tissues routinely processed for histologic evaluation as well as in other high-grade serous papillary gynecologic tumors histologically indistinguishable from ovarian carcinomas (i.e., uterine serous papillary carcinoma, USPC), which may commonly spread to the ovaries, abdominal cavity, or both. As discussed later in the chapter, this differential diagnosis might have important clinical and therapeutic implications.

MATERIALS

1. Peroxidase-blocking reagent: 3% hydrogen peroxide (H_2O_2) containing 15 mmol sodium azide (NaN_3) (Dako Corp., Carpenteria, CA).
2. Rabbit anti-human *HER2/neu* protein: Ready-to-use affinity-isolated antibody in 0.05 mol/L Tris/HCl, 0.1 mol/L NaCl, 15 mmol/L NaN_3, (pH 7.2) containing stabilizing protein (Dako).
3. Visualization reagent: Dextran polymer conjugated with horseradish peroxidase and affinity-isolated goat anti-rabbit immunoglobulins in Tris/HCl buffer containing stabilizing protein and an anti-microbial agent (Dako).
4. Negative control reagent: Immunoglobulin fraction of normal rabbit serum at an equivalent protein concentration as the antibody to *HER2/neu* protein in 0.05 mol/L TrislHCl, 0.1 mol/L NaCl, 15 mmol/L NaN_3, (pH 7.2) containing stabilizing protein (Dako).

5. *Diaminobenzidine* (DAB) buffered substrate: Substrate buffer solution (pH 7.5) containing H_2O_2, stabilizers, enhancers, and an anti-microbial agent (Dako).

6. Ammonium hydroxide, 15 mol/L diluted to 37 mmol/L.

7. DAB chromogen: 5% 3,3′-DAB tetrahydrochloride chromogen solution (Dako).

8. Distilled or deionized water (washing water).

9. Ethanol, absolute and 95%.

10. Epitope retrieval solution (10×): 0.1 mol/L citrate buffer with an anti-microbial agent (Dako).

11. Xylene, toluene, or xylene substitutes.

12. Absorben wipes.

13. Counterstain: Hematoxylin.

14. Slides, SuperFrost, poly-L-lysine-coated slides.

15. Wash Buffer (10×): Tris/HCl buffer with a detergent and an anti-microbial agent (Dako).

16. Staining jars or baths.

17. Wash bottles.

18. Mounting medium (Dako).

19. Drying oven, capable of maintaining 60°C.

20. Light microscope (4–40 objective magnification).

21. Coverslips.

22. Positive control slides: Each slide contains sections of three formalin-fixed and paraffin embedded breast carcinoma cell lines representing different levels of HER2/neu protein expression: MDA-231 (0), MDA-l75 (1+), and SK-BR-3 (3+) (Dako).

23. Negative control slides: *HER2/neu* protein–negative tissues to use as control tissue fixed, processed, and embedded in a manner identical to the patient samples with each staining run to verify the specificity of the primary antibody and to provide indication of specific background staining.

METHODS

1. Tissues preserved in neutral buffered formalin or Boulin's fixative for routine processing and paraffin embedding are suitable.

2. Tissue specimens should be cut into sections of 4–5 μm.

3. A specific epitope retrieval method, boiling in 10 mmol/L citrate buffer in a waterbath, must be used for optimal assay performance. Epitope retrieval solution used in this study was purchased by Dako.

4. Prior to staining, tissue slides must be deparaffinized to remove embedding medium and rehydrated at room temperature:

   a. Place slides in xylene bath and incubate for 5 min.

   b. Place slides in absolute ethanol for 3 min.

   c. Place slides in 95% ethanol for 3 min.

   d. Place slides in deionized water for at least 30 sec.

5. Staining of epitope-retrieved slides:

   a. Apply 100 μl of peroxidase-blocking reagent (Dako) to cover specimen, and incubate 5 min. Rinse gently with deionized water.

   b. Apply 100 μl of primary antibody anti-*HER2/neu* or negative control reagents (Dako) and incubate for 30 min, and rinse gently with wash buffer (Dako).

   c. Cover specimen with 100 μl of visualization reagent (Dako), incubate for 30 min, and rinse gently with wash buffer (Dako).

   d. Cover specimen with 100 μl of substrate-chromogen solution (DAB) (Dako), incubate for 10 min, and rinse gently with deionized water.

6. For counterstain, immerse slides in a bath of hematoxylin and incubate for 2–5 min, depending on the strength of hematoxylin used.

7. Specimens may be mounted and coverslipped with a water-based mounting medium (Dako).

Interpretation of Staining

Only the membrane-staining intensity and pattern should be evaluated. Cytoplasmic staining should be considered nonspecific staining and was not included in the assessment of membrane-staining intensity. For evaluation of the immunocytochemical staining and scoring, an objective of 10 magnification is appropriate.

Slides were scored as follows:

0 = Negative: No staining is observed, or membrane staining is less than 10% of the tumor cells). 1+ = Light staining: A faint partial membrane staining is detected in more than 10% of the tumor cells.

2+ = Moderate staining: A weak to moderate membrane staining is observed in more than 10% of the tumor cells.

3+ = Heavy staining: A strong complete membrane staining is observed in more than l0% of the tumor cells.

RESULTS AND DISCUSSION

Formalin-fixed tumor tissue blocks from 30 specimens (i.e., 15 OSPC and 15 USPC) derived from patients with advanced stage ovarian and uterine cancer (i.e., stage III and IV) were tested for *HER2/neu* expression. Moderate to heavy staining for *HER2/neu* protein (i.e., score 2+ and 3+) was noted in 9 out of 15 (60%) of UPSC specimens, whereas only 2 of the 15 (13%) ovarian cancer samples showed moderate to heavy staining for *HER2/neu* protein expression (Table 26, $p = 0.02$ USPC versus OSPC by Fisher exact text).

Table 26. *HER2/neu* Expression in OSPC and USPC

HER2/neu Expression:	OSPC N 15	USPC N 15	P-Value
Staining intensity:			
0 (none)	6	2	
1+ (light)	7	4	
2+ (moderate)	1	3	
3+ (heavy)	1	6	0.0082[a]
Dichotomized:			
None–low (0/1+)	13 (87)	6 (40)	
Moderate–heavy (2+/3+)	2 (13)	9 (60)	0.0209[b]

OSPC, ovarian serous papillary cancer, USPC, uterine serous papillary cancer.
[a]Cochran-Armitage trend test.
[b]Fisher exact test.

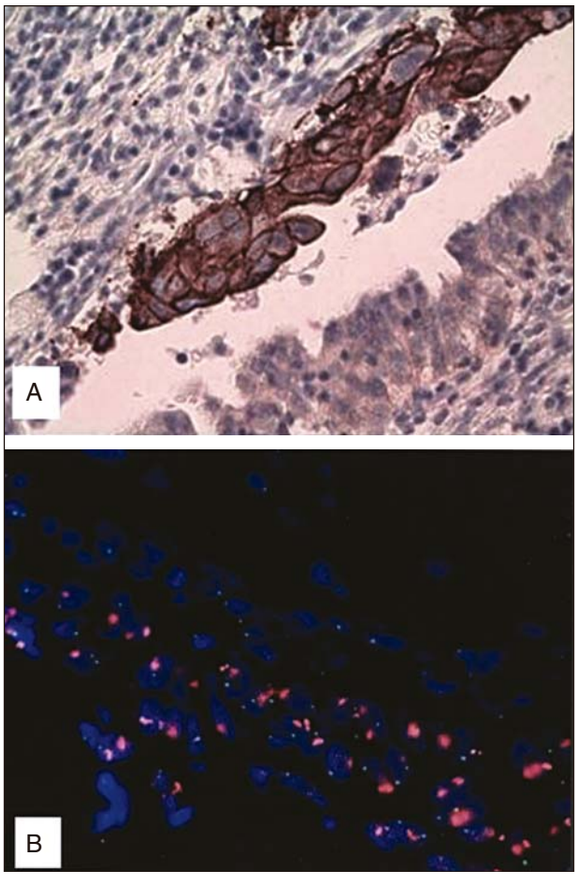

Figure 55. Immunohistochemistry (IHC) and fluorescence *in situ* hybridization (FISH) result in a representative case of uterine serous papillary cancer (USPC). **A:** Heterogeneous *HER2/neu* staining by IHC in a high-grade serous papillary tumor sample. **B:** *HER2/neu* gene amplification was present in pockets of tumor cells amid nonamplified tumor cells (orange signals are for *HER2/neu* gene, and the green signals are for chromosome 17 centromere; PathVysion FISH assay).

In agreement with previous reports (Lassus *et al.,* 2004; Santin *et al.,* 2002), all USPC and OSPC specimens positive for *HER2/neu* protein expression were high-grade tumors. The majority (i.e., 7 out of 9) of the 2+/3+ USPC cases and 1 out of 2 OSPC samples showed moderate or strong membrane staining uniformly distributed among all areas of the cancer. In contrast, heterogeneity in the staining patterns was observed in the sections of 2 USPC samples and 1 OSPC sample. We initially thought these heterogeneous staining patterns were an artifact resulting from the tissues being fixed in formalin and embedded in paraffin. However, the presence of fluorescence *in situ* hybridization (FISH) amplification only in those clusters of tumor cells found moderately or strongly positive by immunohistochemistry (IHC) (Figure 55) suggests an alternative hypothesis. Indeed, although the significance of the presence of these small, amplified foci reported in other epithelial tumors (i.e., breast cancer; Varshney *et al.,* 2004) is not clear at the present time, in previous studies we and others have reported that small fractions of *HER2/neu*-positive tumor cells may be selected and become the overwhelming tumor cell population during *in vitro* culture (Santin *et al.,* 2002).

On the basis of these findings, we are therefore tempted to speculate that, because of the known high resistance to chemotherapy of *HER2/neu*-overexpressing tumors cells *in vivo* (Berchuck *et al.,* 1990), these small clusters of *HER2/neu*-positive cells may have a growth advantage over *HER2/neu*-negative cells and become the predominant tumor population at the time of the development of chemotherapy-resistant disease after multiple courses of cytotoxic therapy. This hypothesis is supported by the findings of Meng *et al.* (2004), who found that 37.5% of breast cancers whose primary tumor was apparently *HER2/neu* negative developed *HER2/neu* gene amplification during cancer progression. It is important to note that such foci of amplifications may be easily missed if only FISH analysis is performed because only a limited sample of the tumor is analyzed. In these cases, prior screening by IHC and selection of appropriate areas for FISH analysis may become crucial for the correct classification of the sample.

Our group has used high-throughput comprehensive technologies for assaying gene expression such as high-density oligonucleotide microarrays to identify and compare the genetic fingerprints of OSPC and USPC (Santin *et al.,* 2004). In this regard, advanced or metastatic serous papillary gynecologic tumors, regardless of

their ovarian or uterine origin, are treated with a combined cisplatinum-based chemotherapy. However, given that: 1) USPC likely arises from metaplastic müllerian epithelium, whereas OSPC likely derives from the ovarian surface epithelium, and 2) a dramatic difference in response to standard chemotherapy regimens is commonly reported among these histologically indistinguishable serous carcinomas (Nicklin and Copeland, 1996); a significant diversity in gene expression among these tumors is probable. Consistent with this hypothesis and in confirmation of the low and high *HER2/neu* expression reported in the literature for OSPC and USPC, respectively (Bookman *et al.,* 2003; Santin *et al.,* 2004), in this pilot study *HER2/neu* gene was found to be the most highly differentially expressed gene in USPC, with more than 17-fold up-regulation compared to OSPC (Santin *et al.,* 2004). Furthermore, the growth factor receptor-bound protein 7 *(GRB7)*, a gene tightly linked to *HER2/neu* and previously reported co-amplified and co-expressed with this gene in several cancer types (Janes *et al.,* 1997), was also highly differentially expressed in USPC compared with OSPC. Thus, it is likely that the striking overexpression of the *HER2/neu* gene, as well as its protein product, on USPC may represent a distinctive molecular marker useful for differentiation of these histologically similar serous tumors and may also provide insight into the dramatically different response to chemotherapy and the disproportionately poor prognosis of USPC relative to OSPC.

A humanized monoclonal antibody (mAb) to *HER2/neu* (Herceptin [Trastuzumab], Genentech, San Francisco, CA) as been reported to have significant therapeutic effects in patients with strongly (i.e., score 2+ and 3+) *HER2/neu*-positive breast carcinomas, particularly when combined with chemotherapeutic drugs (Cobleigh *et al.,* 1999; Slamon *et al.,* 2001). In an analysis of these studies, a positive correlation was shown between the degree of overexpression of *HER2/neu* and the effect of Herceptin: Patients with a score of 3+ had a greater benefit from the addition of the antibody than patients with a score of 2+. On the basis of these findings, in ovarian cancer as well as in other solid human tumors, clinical studies are currently investigating the efficacy of Herceptin in patients whose tumors exhibit moderate to strong plasmalemmal immunoreactivity for this protein.

The group GOG has reported the results of a large study evaluating the potential clinical benefit of Herceptin administration in patients with recurrent or refractory, OC overexpressing *HER2/neu* (Bookman *et al.,* 2003). The overall response rate of 7.3% is lower than the 12–15% response rates reported for the single-agent phase II trials in patients with breast cancer (Baselga *et al.,* 1996). On the basis of these results, the GOG authors concluded that because of the low frequency of *HER2/neu* overexpression and low rate of objective responses among patients with ovarian cancer, the value of Herceptin may be limited (Bookman *et al.,* 2003). It is worth noting, however, that in this trial FISH assays were not used to confirm the amplification of the *HER2/neu* gene in any of the patients treated with Herceptin. This point is noteworthy because FISH is considered a superior method for selecting patients likely to benefit from Herceptin therapy (Vogel *et al.,* 2002). Furthermore, from previous reports investigating the anti-tumor effects of MAb *in vivo,* it is well known that their clinical efficacy is primarily dependent on immune activation through the Fc receptor (Clynes *et al.,* 2000). Patients with ovarian cancer harboring large amounts of recurrent disease resistant to multiple regimens of chemotherapy have been shown to be profoundly immunocompromised (Merogi *et al.,* 1997). Thus, treatment-induced immunosuppression combined with tumor-induced subversion of the immune system may impose severe limitations on the efficacy of Herceptin therapy in heavily pretreated patients with ovarian cancer. These observations may at least in part explain the low response rate to herceptin observed in this group of patients with ovarian cancer and suggest that, as in patients with breast cancer (Slamon *et al.,* 2001), herceptin will likely be more effective when administered as first-line treatment in combination with chemotherapy to patients with ovarian cancer harboring tumors with amplification of the *HER2/neu* gene.

The aggressiveness of HER2/neu-positive serous papillary tumors including high-grade OSPC and USPC and the poor prognosis of women developing these diseases demand the availability of accurate and reliable tests for evaluating *HER2/neu* status and the optimization of *HER2/neu*-targeted therapy. Several techniques are available today to assess *HER2/neu* status, including those that measure gene amplification (Southern blot analysis, polymerase chain reaction, and FISH), protein expression (IHC and Western blot analysis), or mRNA levels (Northern blot analysis). However, tissue-based detection of *HER2/neu* alterations by IHC, FISH, or both offers a clear advantage over other approaches, which suffer from cumbersome laboratory procedures and artifacts produced by dilution of malignant tissue with normal cells. Thus, although there is still debate about which of the two methods is better, our findings that small clusters of tumor cells overexpressing *HER2/neu* may be present in the original high-grade serous papillary tumors and that such foci of amplifications may be easily missed during FISH analysis suggest that the combination of the two techniques (i.e., prior screening by IHC and selection of appropriate areas for FISH analysis) may become the gold standard for the selection

of the totality of patients with OSPC or USPC likely to benefit from Herceptin therapy.

References

Baselga, J., Tripathy, D., Mendelsohn, J., Baughman, S., Benz, C.C., Dantis, L., Sklarin, N.T., Seidman, A.D., Hudis, C.A., Moore, J., Rosen, P.P., Twaddell, T., Henderson, I.C., and Norton, L. 1996. Phase II study of weekly intravenous recombinant humanized anti-p185HER2 monoclonal antibody in patients with HER2/neu-overexpressing metastatic breast cancer. *J. Clin. Oncol. 14*:737–744.

Berchuck, A., Kamel, A., Whitaker, R., Kerns, B., Olt, G., Kinney, R., Soper, J.T., Dodge, R., Clarke-Pearson, D.L., and Marks, P. 1990. Overexpression of HER-2/neu is associated with poor survival in advanced epithelial ovarian cancer. *Cancer Res. 50*:4087–4091.

Bookman, M.A., Darcy, K.M., Clarke-Pearson, D., Boothby, R.A., and Horowitz, IR. 2003. Evaluation of monoclonal humanized anti-HER2 antibody, trastuzumab, in patients with recurrent or refractory ovarian or primary peritoneal carcinoma with over-expression of HER2: a phase II trial of the Gynecologic Oncology Group. *J. Clin. Oncology 21*:283–290.

Busse, D., Doughty, R.S., and Arteaga, C.L. 2000. HER-2/neu (erbB-2) and the cell cycle. *Semin. Oncol. 27*:3–8.

Clynes, R.A., Towers, T.L., Presta, L.G., and Ravetch, J.V. 2000. Inhibitory Fc receptors modulate *in vivo* cytoxicity against tumor targets. *Nat. Med. 6*:443–446.

Cobleigh, M.A., Vogel, C.L., Tripathy, D., Robert, N.J., Scholl, S., Fehrenbacher, L., Wolter, J.M., Paton, V., Shak, S., Lieberman, G., and Slamon, D.J. 1999. Multinational study of the efficacy and safety of humanized anti-HER2 monoclonal antibody in women who have HER2-overexpressing metastatic breast cancer that has progressed after chemotherapy for metastatic disease. *J. Clin. Oncol. 17*:2639–2648.

Dubeau, L. 1999. The cell of origin of epithelial tumors and the ovarian surface epithelium dogma: does the emperor have no clothes? *Gynecol. Oncol. 72*:437–442.

Graus-Porta, D., Beerli, R.R., Daly, J.M., and Hynes, N.E. 1997. ErbB-2, the preferred heterodimerization partner of all erbB receptors is a mediator of lateral signaling. *EMBO J. 16*:1647–1655.

Hellstrom, I., Goodman, G., Pullman, J., Yang, Y., and Hellstrom, K.E. 2001. Overexpression of HER-2 in ovarian carcinomas. *Cancer Res. 61*:2420–2423.

Hetzel, D.J., Wilson, T.O., Keeney, G.L., Roche, P.C., Cha, S.S., and Podratz, K.C. 1992. HER-2/neu expression: a major prognostic factor in endometrial cancer. *Gynecol. Oncol. 47*:179–185.

Janes, P.W., Lackmarin, M., Church, W.B., Sanderson, G.M., Sutherland, R.L., and Daly, R.J. 1997. Structural determinants of the interaction between the erbB2 receptor and the Src homology 2 domain of Grb7. *J. Biol. Chem. 272*:8490–8497.

Jemal, A., Tiwari, R.C., Murray, T., Ghafoor, A., Samuels, A., Ward, E., Feuer, E.J., and Thun, M.J. 2004. Cancer Statistics, 2004. *CA Cancer J. Clin. 54*:8–29.

Lassus, H., Leminen, A., Vayrynen, A., Cheng, G., Gustafsson, J.A., Isola, J., and Butzow, R. 2004. ERBB2 amplification is superior to protein expression status in predicting patient outcome in serous ovarian carcinoma. *Gynecol. Oncol. 92*:31–39.

Mano, M.S., Awada, A., Di Leo, A., Durbecq, V., Paesmans, M., Cardoso, F., Larsimont, D., and Piccart, M. 2004. Rates of topoisomerase II-alpha and HER-2 gene amplification and expression in epithelial ovarian carcinoma. *Gynecol. Oncol. 92*:887–895.

Meden, H., Marx, D., Roegglen, T., Schauer, A., and Kuhn, W. 1998. Overexpression of the oncogene c-erbB-2 (HER2/neu) and response to chemotherapy in patients with ovarian cancer. *Int. J. Gynecol. Pathol. 17*:61–65.

Meng, S., Tripathy, D., Shete, S., Ashfaq, R., Haley, B., Perkins, S., Beitsch, P., Khan, A., Euhus, D., Osborne, C., Frenkel, E., Hoover, S., Leitch, M., Clifford, E., Vitetta, E., Morrison, L., Herlyn, D., Terstappen, L.W., Fleming, T., Fehm, T., Tucker, T., Lane, N., Wang, J., and Uhr, J. 2004. I-IER-2 gene amplification can be acquired as breast cancer progresses. *Proc. Natl. Acad Sci. USA 101*:9393–9398.

Merogi, A.J., Marrogi, A.J., Ramesh, R., Robinson, W.R., Fermin, C.D., and Freeman, C.M. 1997. Tumor–host interaction: analysis of cytokines, growth factors, and tumor infiltrating lymphocytes in ovarian carcinomas. *Hum. Pathol. 28*:321–331.

Nicklin, J.L., and Copeland, L.J. 1996. Endometrial papillary serous carcinoma: pattern of spread and treatment. *Gun. Obstet. Gynecol. 39*:686–695.

Santin, A.D., Bellone, S., Gokden, M., Palmieri, M., Dunn, D., Agha, J., Roman, J.J., Hutchins, L., Pecorelli, S., O'Brien, T., Cannon, M.J., and Parham, G.P. 2002. Overexpression of HER-2/neu in uterine serous papillary cancer. *Clin. Cancer Res. 8*:1271–1279.

Santin, A.D., Zhan, F., Bellone, S., Palmieri, M., Cane, S., Gokden, M., Roman, J.J., O'Brien, T.J., Tian, E., Cannon, M.J., Shaughnessy, J. Jr., and Pecorelli, S. 2004. Discrimination between uterine serous papillary carcinomas and ovarian serous papillary tumours by gene expression profiling. *Brit. J. Cancer 90*:1814–1824.

Slamon, D.J., Leyland-Jones, B., Shak, S., Fuchs, H., Paton, V., Bajamonde, A., Fleming, T., Eiermann, W., Wolter, J., Pegram, M., Baselga, J., and Norton, L. 2001. Use of chemotherapy plus a monoclonal antibody against HER2 for metastatic breast cancer that overexpresses HER2. *New Engl. J. Med. 344*:783–792.

Sliwkowski, M.X., Lofgren, J.A., Lewis, GD., Hotaling, T.E., Fendly, B.M., and Fox, J.A. 1999. Nonclinical studies addressing the mechanism of action of trastuzumab (Herceptin). *Semin. Oncol. 26*:60–70.

Varshney, D., Zhou, Y.Y., Geller, S.A., and Alsabeh, R. 2004. Determination of HER-2 status and chromosome 17 polysomy in breast carcinomas comparing HercepTest and PathVysion FISH assay. *Am. J. Clin. Pathol. 121*:70–77.

Vogel, C.L., Cobleigh, M.A., Tripathy, D., Gutheil, J.C., Harris, L.N., Fehrenbacher, L., Slamon, D.J., Murphy, M., Novotny, W.F., Burchmore, M., Shak, S., Stewart, S.J., and Press, M. 2002. Efficacy and safety of trastuzumab as a single agent in first-line treatment of HER2-overexpressing metastatic breast cancer. *J. Clin. Oncol. 20*:719–726.

Yarden, Y., and Sliwkowski, M.X. 2001. Untangling the ErbB signalling network. *Nature Rev. Mol. Cell Biol. 2*:l27–137.

4

Role of Immunohistochemical Expression of BRCA1 in Ovarian Carcinoma

Yoichi Aoki and Kenichi Tanaka

Introduction

Ovarian cancer is caused by genetic alterations that disrupt proliferation, apoptosis, senescence, and DNA (deoxyribonucleic acid) repair and is a characteristic of the phenotype of two distinct familial cancer syndromes: hereditary breast/ovarian cancer syndrome and Lynch syndrome. Approximately 10% of ovarian cancers arise in women who have inherited mutations in cancer susceptibility genes (*BRCA1* or *BRCA2*). No gene that confers increased susceptibility to ovarian cancer alone has yet been isolated, so site-specific familial ovarian cancer and the hereditary breast/ovarian cancer syndrome are considered to be part of the same spectrum.

BRCA1 is a putative tumor-suppressor gene linked to breast cancer in families with dominant inheritance of the disease (Miki *et al.,* 1994). Many tumors with germline BRCA1 mutations display loss of heterozygosity (LOH) at this locus, with loss of the wild-type BRCA1 as allele, indicating a role for *BRCA1* as a tumor-suppressor gene (Smith *et al.,* 1992). BRCA1 spans ~80 kb of genomic DNA and is thought to produce a protein of 1863 amino acids. Approximately 60% of the coding sequence is contained with a single exon (exon 11), whereas the remaining 21 exons are relatively small. The protein has a RING finger domain at its N-terminus and a BRCT motif at its C-terminus, which functions as a transactivator (Monteiro *et al.,* 1996). The function of the BRCA1 protein is not fully elucidated, but it probably plays an important role in DNA repair, apoptosis, or cell cycle arrest, interacting with p53 and RAD51 in response to DNA damage (Kote-Jarai and Eeles, 1999).

In this chapter we discuss the specificity of anti-BRCA1 antibodies, subcellular localization of BRCA1, and the role of this gene in ovarian carcinoma using immunohistochemistry (IHC).

BRCA1 Antibodies for Immunohistochemical Analysis

There is controversy regarding the size and localization of the BRCA1 protein, mainly as a result of differences in fixation, the antigen-retrieval method used, and the specificity of anti-BRCA1 antibodies (Table 27). The D-20, I-20, C-20, and K-18 antibodies have been

Handbook of Immunohistochemistry and *in situ* Hybridization of Human Carcinomas, Volume 4: Molecular Genetics, Gastrointestinal Carcinoma, and Ovarian Carcinoma

Table 27. Primary Antibodies to BRCA1

Antibody	Location of Immunogen (Amino Acid)	Isotype	Fixative Used in IHC	Working Dilution or Concentration Used in IHC
N-terminal Ab				
MS13 (Ab-2)	1–304	mAb (IgG1)	PLP	1:1000
D-20	2–21	PAb	PLP	0.1 µg/ml
K-18	70–89	PAb	PLP	0.5 µg/ml
Ab-1	1–304	mAb (IgG2a)	PLP	10 µg/ml
Ab-A	2–20	PAb		
Exon 11 Ab				
8F7	341–748	mAb (IgG1)	NBF, MW	2 µg/ml
17F8	762–1315	mAb (IgG1)		5 µg/ml
Ab-C	768–793	PAb		
C-terminal Ab				
AP16	1313–1863	mAb (IgG1)	PLP	0.5 µg/ml
I-20	1823–1842	PAb	PLP	0.5 µg/ml
C-20	1843–1862	PAb	PLP	0.1 µg/ml
D-9	1843–1862	mAb (IgG1)		1 µg/ml
SG11 (Ab-3)	1847–1863	mAb (IgG2b)	NBF, MW	0.2 µg/ml
VALY	1842–1844	PAb	NBF	1:100
GLK-2	1839–1863	mAb	PLP	1:10,000

IgG, Immunoglobulin G; IHC, immunohistochemistry; mAb, monoclonal antibody; MW, microwave treatment; NBF, neutral-buffered formalin; PAb, polyclonal antibody; PLP, periodate–lysine–paraformaldehyde.

reported to show cytoplasmic staining only, the nucleus being constantly nonimmunoreactive either in cancer or normal mammary gland cells on paraffin-embedded samples (Perez-Valles *et al.,* 2001). Jarvis *et al*. (1998) found differences in nuclear staining of tumor cells with the D-20 antibody, the cytoplasm being positive in all sporadic breast cancers tested. Using the C-terminal I-20 polyclonal antibody, with no differences in staining between tumoral and nontumoral mammary epithelial cells, uniform cytoplasmic staining was seen in all samples with heterogeneous nuclear staining.

In cell lines lacking the C-terminal portion of the BRCA1 protein, I-20 antibody showed false-positive immunostaining (Yoshikawa *et al.,* 1999); furthermore, the I-20 antibody probably recognizes proteins other than BRCA1 or products of alternative splicing of the *BRCA1* gene (Wilson *et al.,* 1997). The value of these polyclonal antibodies (D-20, I-20, and K-18) for IHC on frozen or paraffin-embedded samples has been questioned (Wilson *et al.,* 1999). The C-20 antibody has been reported to cross-react with the epidermal growth factor receptor (EGFR) and *HER-2* protein, which are frequently overexpressed in human breast and ovarian cancers and malignant cell lines (Wilson *et al.,* 1996). Yoshikawa *et al.* (1999) have demonstrated, using normal mammary epithelium, breast tumor cells, and breast cancer cell lines, that the different fixation methods gave drastically different immunostaining results, depending on the antibody used. Antibodies 17F8 and D-9 showed no immunoreactivity in the nucleus, but some immunoreactivity was found in the cytoplasm with any fixation method used. Antibodies MS13 and AP16 reacted with nucleus in only an extremely small number of scattered cancer cells. False-positive nuclear staining was observed with C-terminal antibodies I-20, C-20, SG11, and VALY in BRCA1-associated breast cancer cells that should lack the C-terminus of the BRCA1 protein.

Ab-1 specificity was validated in four ovarian cancers containing germline BRCA1 del185AG mutations. This mutation results in the deletion of most of the protein, including the Ab-1 epitope, which maps between an 89–222. No signal was detected in the malignant cells of these specimens, whereas staining was observed in normal cells in the same section. Eventually, the monoclonal antibodies Ab-1 and 8F7 are considered to be appropriate for staining paraffin-embedded tissue sections. Wilson *et al.* (1999) have comprehensively characterized 19 anti-BRCA1 antibodies and concluded that Ab-1 antibody is the only reliable antibody when working with paraffin sections with antigen retrieval.

When used on formalin-fixed and paraffin-embedded material, the monoclonal antibody Ab-1 appeared to be

the most accurate, reliable, and reproducible (Wilson *et al.,* 1999). The Ab-1 antibody reacts with the N-terminal portion of the BRCA1 protein only after antigen retrieval by microwave, producing an almost exclusively nuclear staining pattern in normal mammary cells and breast and ovarian cancer cell lines (MCF-7 and SKOV-3).

Subcellular Localization of BRCA1 Assessed by Immunohistochemistry

The subcellular localization of BRCA1 has been described as exclusively nuclear, predominantly nuclear, nuclear in most cell types but cytoplasmic in breast and ovarian cancer cells, and a secreted protein (Chen *et al.,* 1995; Jensen *et al.,* 1996). There is much controversy with regard to the importance and localization of BRCA1 protein expression. Although the link between the *BRCA1* tumor-suppressor gene and hereditary breast and ovarian cancer is established, the role, if any, of BRCA1 in nonfamilial cancers is unclear. BRCA1 mutations are rare in sporadic cancers, but loss of BRCA1 resulting from reduced expression or incorrect subcellular localization is postulated to be important in nonfamilial breast and ovarian cancers. Epigenetic loss, however, has not received general acceptance because of controversy regarding the subcellular localization of BRCA1 proteins, reports of which have ranged from exclusively nuclear, to conditionally nuclear, to the endoplasmic reticulum/Golgi, to cytoplasmic invaginations into the nucleus. Chen *et al.* (1995) reported that the BRCA1 protein was found in the nuclei of normal epithelial cells but was aberrantly located in the cytoplasm of most breast and ovarian cancer cell lines. In contrast, Scully *et al.* (1996) found the BRCA1 protein in the nuclei of both normal and malignant cells. Jensen *et al.* (1996) reported that BRCA1 was located in the cytoplasm and the plasma membrane, whereas Coene *et al.* (1997) proposed that it was located in cytoplasmic tubelike invaginations in the nucleus. One possible explanation for these differences regarding localization of the BRCA1 protein is mainly the result of differences in fixation, the antigen retrieval method used, and the specificity of anti-BRCA1 antibodies.

To resolve this issue, Wilson *et al.* (1999) have shown that immunoreactivity specific for BRCA1 is a 220-kD molecule located in nuclear foci of all cell types, including malignant ovarian cells. They could not confirm the existence of a secreted or membrane-localized 190-kD BRCA1. It is more likely that the secreted protein previously identified is the EGFR protein (Wilson *et al.,* 1996).

Immunohistochemical Expression of BRCA1 as a Prognostic Factor in Sporadic Ovarian Carcinoma

In the field of breast cancer, Thompson *et al.* (1995) demonstrated that BRCA1 messenger ribonucleic acid (mRNA) expression decreases with breast cancer progression in a small number of breast cancer cell lines. Jarvis *et al.* (1998) found a significant inverse correlation between nuclear BRCA1 and expression of the proliferation marker Ki-67, suggesting that tumors with a germline mutation in one of the breast cancer genes may be highly proliferative and a more aggressive tumor phenotype. Wilson *et al.* (1999) demonstrated that BRCA1 expression was reduced or undetectable in the majority of high-grade, ductal carcinomas, suggesting that absence of BRCA1 may contribute to the pathogenesis of a significant percentage of sporadic breast cancers. Yoshikawa *et al.* (1999) also showed that reduction of BRCA1 protein expression in sporadic breast carcinomas was associated with solid-tubular phenotype, with poor tubular differentiation, and with an overexpression of c-erbB-2 protein, which is one of the prognostic factors in breast cancer. They concluded that reduced expression of BRCA1 protein might play an important role in mammary carcinogenesis, not only in BRCA1-associated breast carcinomas but also in sporadic carcinomas. Yang *et al.* (2001) have shown, using immunohistochemical analyses, that positive BRCA1 emerged as an independent prognostic indicator for disease-free survival in sporadic breast cancers.

For ovarian cancers, Wilson *et al.* (1999) evaluated BRCA1 localization and relative expression levels in normal and malignant human breast and ovarian tissues using the Ab-1 antibody. Paraffin-embedded tissues from 32 normal human ovaries displayed punctate nuclear BRCA1 staining, and no significant differences in expression were noted between cell types in the ovary. Most normal ovarian samples displayed moderate signal intensity with the remainder equally split between weak and strong staining. BRCA1 immunoreactivity in normal ovary cells was concentrated in the nuclei of granulosa and theca interna cells of the developing follicles, the vast majority of which were BRCA1 positive; this is consistent with observations made on mouse ovaries (Phillips *et al.,* 1997). They also analyzed BRCA1 expression and localization in a series of ovarian cancer specimens. Reduced BRCA1 levels in malignant compared with benign cells was observed in 14 of 35 (40%) ovarian cancers. Several histologic types were represented in that study; however, similar to breast cancers, a correlation ($p < 0.01$) between loss of expression and nuclear grade was observed.

Their critical observation is the correlation between the loss of BRCA1 protein expression and high nuclear grade in sporadic breast and ovarian cancers. This observation could be the result of the convergence of several genetic and epigenetic phenomena. BRCA1 mutations are rare in sporadic breast and ovarian malignancies (Futreal *et al.,* 1994; Merajver *et al.,* 1995), but allelic losses of chromosome 17q markers including the BRCA1 region are relatively common (Futreal *et al.,* 1992). This cannot fully explain the absence of BRCA1 in intermediate- and high-grade tumors; however, the wild-type gene presumably remains intact. There is evidence suggesting that epigenetic loss of BRCA1 may occur at the level of transcription or a subsequent process affecting RNA accumulation. In addition, hypermethylation of the BRCA1 regulatory region, which could inhibit transcription, has been observed in DNA from sporadic breast cancers (Dobrovic and Simpfendorfer, 1997).

Zheng *et al.* (2000) have suggested that normal BRCA1 might be expressed at very low levels in ovarian epithelial cancers that have negative results for BRCA1 using IHC, rather than its complete loss of function. These results confirm and extend the finding of Wilson *et al.* (1999) of reduced BRCA1 expression in ovarian carcinomas. The mechanisms of the reduced levels of BRCA1 expression in sporadic ovarian cancers are unknown, which could be the result of a combination of several genetic and epigenetic changes. Although mutations of BRCA1 are rare in sporadic ovarian cancers, LOH of chromosome 17q markers, including the BRCA1 region, is relatively common. Alternatively, lower BRCA1 activity may be related to epigenetic changes such as methylation of its promoter region (Laird and Jaenisch, 1996). Methylation of the BRCA 1 promoter has been shown to be associated with reduced gene activity in sporadic breast cancers (Rice *et al.,* 1998). Rice *et al.* (1998) reported that BRCA1 immunoreactivity in normal ovary was concentrated in the nuclei, the vast majority of which were BRCA1 positive, and BRCA1 immunoreactivity was also observed mainly in the nuclei of ovarian epithelial tumor cells. However, they found occasional cytoplasmic staining in epithelial ovarian cancers. This is in contrast to the report of Wilson *et al.* (1999) who, using the same antibody (Ab-1), found BRCA1 immunoreactivity exclusively in the nucleus. Further studies are needed to clarify these issues.

Russell *et al.* (2000) have shown that reduced or absent protein expression was observed in 90% of 57 sporadic ovarian cancers, and decreased protein expression was significantly associated with a reduction in the levels of RNA expression. They suggested that expression of BRCA1 is down-regulated at the level of transcription during the development of sporadic ovarian cancers. In their study, there was a tendency for loss of BRCA1 protein expression associated with higher tumor stage; 4/5 BRCA1-positive tumors were stage I or II compared with 6/28 and 8/21 tumors classified as having intermediate or low levels of staining.

A critical observation in previous studies using IHC has shown the correlation between the loss of BRCA1 protein expression and tumor progression in sporadic ovarian cancers. Further investigation should clarify loss or reduced expression of BRCA1 protein, which may be used as a prognostic indicator for disease-free survival in sporadic ovarian cancers.

Prediction for *BRCA1* Mutation in Ovarian Carcinoma by Immunohistochemistry

Perez-Valles *et al.* (2001) have tried to detect the mutated *BRCA1* gene in breast cancer using IHC, but they concluded that commercially available BRCA1 antibodies lack the specificity required to identify the BRCA1 protein and are not useful for establishing differences between familial and sporadic breast tumors or between BRCA1-associated and non-BRCA1–associated breast tumors.

We also tried prediction of BRCA1 mutation using immunohistochemical staining. Because BRCA1 has a high frequency of truncating mutations, a C-terminal antibody may be unable to detect the truncated BRCA1. Therefore, we performed immunohistochemical analyses using the following two monoclonal antibodies: The GLK-2 monoclonal antibody (PhenoPath Laboratory, Seattle, WA) was directed against peptides corresponding to C-terminal amino acids 1839–1863 of the human BRCA1 protein. The Ab-2 monoclonal antibody (Oncogene Research Products, Cambridge, MA) was raised against epitopes of N-terminal amino acids 1–304 of the human BRCA1 protein. Immunohistochemical studies were carried out on 5-μm thick resections that were placed on polylysine-coated slides. The sections were depapaffinized in xylene and rehydrated through graded alcohol series. Forty-four patients with familial ovarian cancer were in 20 site-specific ovarian cancer families and 10 breast–ovarian cancer families; the BRCA1 mutation analyses were previously described in detail (Sekine *et al.,* 2001). In 24 patients from 20 families, we found 13 independent germline mutations of BRCA1, consisting of 9 frameshifts, 3 nonsense, and 1 missense mutation. Also, 20 patients with nonfamilial ovarian cancer were examined in this study. LOH assays were performed at three microsatellite markers, D17S855, D17S1322, and D17S1323, located in the BRCA1 gene. In familial ovarian cancers with a germline

mutation of BRCA1, LOH was detected in at least one of the BRCA1 microsatellite markers in all 21 informative tumors. In 20 sporadic ovarian cancers, the frequencies of allelic losses found at the markers D17S855, D17S1322, and D17S1323 were 53% (8 of 15 informative tumors), 36% (5 of 14), and 31% (5 of 16 tumors), respectively.

We analyzed 24 familial ovarian cancer specimens by IHC, in which 16 cases had BRCA1 mutation in exon 11 and 8 cases in an exon other than exon 11. In 15 of 16 tumors (93.8%) with mutation in exon 11, cytoplasmic staining was observed with GLK-2 antibody, whereas in all 8 tumors with mutation in exons other than exon 11, BRCA1 staining was absent. BRCA1 protein was visualized by GLK-2 antibody immunohistochemical analysis in the majority of tumor cells. When immunohistochemical staining was performed with Ab-2 antibody, both nuclear and cytoplasmic staining were observed in 14 of 16 tumors (87.5%) with mutation in exon 11. Of great interest, using Ab-2 antibody, nuclear staining was observed in 3 of 3 tumors (100%) with mutation downstream of exon 11, but no staining was detected in 5 of 5 tumors (100%) with mutation upstream of exon 11. Nuclear staining with Ab-2 antibody was noted in more than 70% of the tumor cells and the surrounding lymphocytes, and the intensity in the nucleus was different in each tumor cell. In 20 familial ovarian cancers with no BRCA1 mutations, nuclear staining or both nuclear and cytoplasmic staining was observed in 18 of 20 specimens with GLK-2 antibody and all 20 specimens with Ab-2 antibody. The BRCA1 immunoreactivities were detected in 90% or more of the cancer cells, and the intensity of the nuclear dot pattern varied in each tumor cell. In 20 sporadic ovarian cancers, 9 samples (45%) showed only nuclear staining, 6 tumors (30%) showed both nuclear and cytoplasmic staining, and one sample showed only cytoplasmic staining with both the GLK-2 and Ab-2 antibodies. In 4 tumors, different staining patterns with these two monoclonal antibodies (mAbs) were observed. Two samples showed both nuclear and cytoplasmic immunoreactivity with Ab-2 antibody and only nuclear with GLK-2 antibody. Immunoreactivity in both the nucleus and cytoplasm with Ab-2 antibody and cytoplasm with GLK-2 antibody was detected in one tumor. The one remaining sample reacted with Ab-2 antibody in the nucleus but did not react with GLK-2 antibody at all. The staining intensity in the cytoplasm was homogeneous in all samples, whereas the nuclear intensity differed in each cancer cell as well as in tumor samples in familial ovarian cancer without BRCA1 mutation. In 5 normal ovarian tissues, BRCA1 was detected in the nucleus or in both the nucleus and cytoplasm of epithelial cells and the adjacent stromal cells with Ab-2 or GLK-2 antibodies. Nuclear expression was demonstrated in about 70% of normal epithelial cells and stromal cells. The intensity of the staining was relatively low.

Previous studies have demonstrated that a splice variant protein lacking most exon 11 (BRCA1-Δ exon 11) exists in a number of normal or tumor cells, including ovarian tissues. Although the function of these transcripts remains elusive, it has been shown that they are localized in the cytoplasm (Wilson *et al.,* 1997). Subcellular fractionation analysis revealed p120BRCA1 in the cytoplasmic fraction in both normal and malignant mammary and ovarian epithelial cell lines. Because p120BRCA1 was immunoprecipitated not with the exon 11–specific antibody but with most C-terminal antibodies, p120BRCA1 seems to correspond to the product of the BRCA1 splicing variant that lacks almost all of exon 11, including nuclear localization signals (NLSs). Previous studies demonstrated that weak cytoplasmic staining and nuclear staining were immunohistochemically observed in some breast and ovarian cancer cell lines, but such a predominant cytoplasmic staining in any breast and ovarian cancer tissues was not found. Some data from previous studies have shown that the BRCA1 protein is present in the cytoplasm. Splice variant isoforms that lack exon 11 along with the nuclear localization signal are located exclusively in the cytoplasm. However, Perez-Valles *et al.* (2001) found no cytoplasmic staining with the Ab-1 antibody in the 45 breast cancers tested. One possible explanation for the discrepancy in results between cultured cells and the tissues may lie in the difficulty of preserving the epitope of p120BRCA1 or the p120BRCA1 itself in the immunohistochemical procedures. Another possible reason is that nuclear staining is more intense because BRCA1 may be densely localized in the nucleus and diffused in the cytoplasm. Actually, we observed cytoplasmic staining, presumably because of the splice variant, in normal ovarian tissues. Cytoplasmic staining may represent detection of BRCA1-Δ exon 11 variant proteins with GLK-2 antibody. In addition, nuclear staining with GLK-2 antibody was found in the majority of tumor samples from patients with familial ovarian cancer without BRCA1 mutations (90%) and patients with sporadic ovarian cancer (85%), as well as normal ovarian tissues (100%). Correlation between the immunohistochemical staining pattern with GLK-2 antibody and the position of the BRCA1 mutation revealed that cytoplasmic staining of BRCA1 indicates for exon 11 mutation of the BRCA1, absence of BRCA1 immunoreactivity for the BRCA1 mutation in other than exon 11, and nuclear BRCA1 immunoreactivity for wild-type BRCA1 with more than 90% of sensitivity and specificity (Table 28). Using immunohistochemical analysis with Ab-2 antibody, nuclear staining was

Table 28. Prediction of Germline Mutation of BRCA1 Using Immunohistochemistry with GLK-2 Antibody

BRCA1 Mutation	Immunohistochemistry	Sensitivity (%)	Specificity (%)	PPV (%)
Exon 11	Cytoplasm	93.8	92.9	88.2
Others	Absence	100	97.2	88.9
Negative or both	Nucleus	90.0	100	100

PPV, Positive predictive value.

detected in 17 of 19 ovarian cancers with BRCA1 mutation downstream of exon 11 in which the NLSs were located, whereas BRCA1 immunoreactivity was not found in tumors with BRCA1 mutation upstream of exon 11. Thakur *et al.* (1997) reported that two putative NLSs—amino acids 501 to 507 (NLS1; KCKRKRR) and 607 to 614 (NLS2; KKNRLRRK)—are present in exon 11, and only NLS1 is necessary for nuclear transport.

It may be possible to predict germline mutation of the BRCA1 on the basis of the immunoreactivity pattern with Ab-2 and GLK-2 antibodies (Figure 56). These findings are consistent with the notion that full-length BRCA1 protein resides in the nucleus, and aberrant proteins may exist in two forms—first as truncated protein in the nucleus in cases that the NLSs are conserved, and second as splice variant protein lacking the NLSs in exon 11 in the cytoplasm. These results suggest that an immunohistochemical assay in combination with use of the C-terminal and the N-terminal antibodies appears to have potential as a reliable and useful technique for the screening of BRCA1 mutations, at least to predict the status of mutation, upstream or downstream of exon 11. Two possible advantages of this analysis exist in clinical practice. A positive test may indicate that other family members are at risk for ovarian or breast cancers and also may alert a woman with ovarian cancer that she has an increased susceptibility to breast cancer. Immunohistochemical analyses require tumor samples, so the test can be applied only to women with ovarian cancer; individuals at risk for ovarian cancer cannot be identified. The prospect of a project that

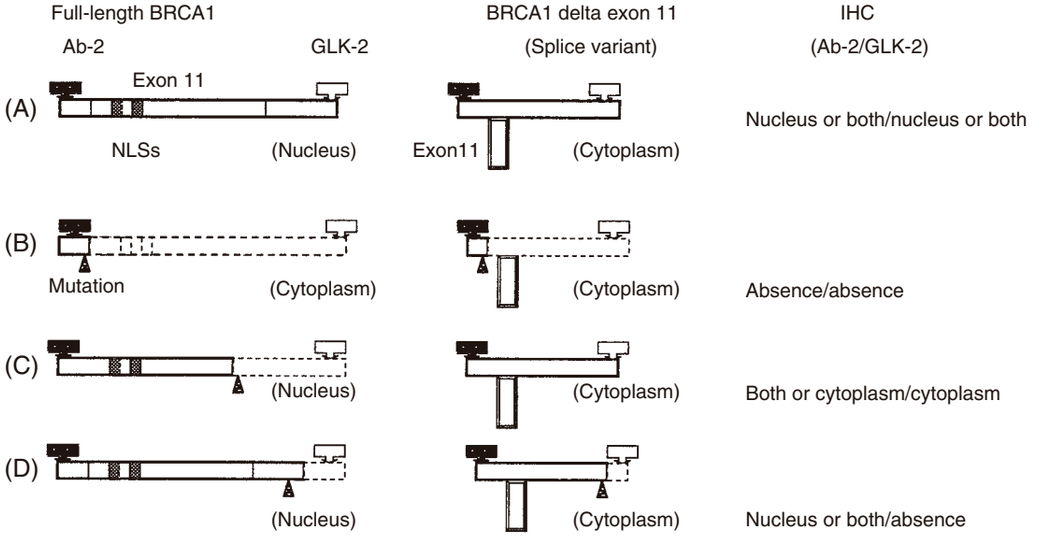

Figure 56. Immunohistochemical staining patterns of BRCA1 (full-length BRCA1 and BRCA1-D exon 11) with Ab-2 antibody and GLK-2 antibody. The predicted subcellular localization of the protein is indicated in brackets *(lower right)* **A:** Tumor with no BRCA1 mutations. **B:** Tumor with mutation in exons upstream of exon 11. **C:** Tumor with mutation in exon 11 downstream of the two putative nuclear localization signals (NLSs). **D:** Tumor with mutation in exons downstream of exon 11. Closed triangles indicate the mutation points of the BRCA1. IHC; Immunohistochemistry.

screens ovarian cancer tissues with IHC, including those of hereditary ovarian cancer families, offers an attractive model for further investigation.

RESULTS AND DISCUSSION

1. When used on formalin-fixed and paraffin-embedded material, the mAb Ab-1 appeared to be the most accurate, reliable, and reproducible for BRCA1 immunohistochernistry. The Ab-1 antibody reacts with the N-terminal portion of the BRCA1 protein only after antigen retrieval by microwave, producing an almost exclusively nuclear staining pattern in normal mammary cells and breast and ovarian cancer cell lines.

2. In subcellular localization analysis of BRCA1 protein, immunoreactivity specific for BRCA1 is a 220-kD molecule located in nuclear foci of all cell types, including malignant ovarian cells. The existence of a secreted or membrane-localized 190-kD BRCA1 could not be confirmed. It is more likely that the secreted protein previously identified is the EGFR protein.

3. A critical observation in previous studies using IHC has shown the correlation between the loss of BRCA1 protein expression and tumor progression in sporadic ovarian cancers. Further investigation may demonstrate that loss or reduced expression of BRCA1 protein emerges as a prognostic indicator for disease-free survival also in sporadic ovarian cancers.

4. An immunohistochemical assay in combination with use of the C-terminal and the N-terminal antibodies appears to have potential as a reliable and useful technique for the screening of BRCA1 mutations, at least to predict the status of mutation, upstream or downstream of exon 11. The prospect of a project that screens ovarian cancer tissues with IHC, including those of hereditary ovarian cancer families, offers an attractive model for further investigation.

References

Chen, Y., Chen, C.F., Riley, D.J., Allred, D.C., Chen, P.L., Von Hoff, D., Osborne, C.K., and Lee, W.H. 1995. Aberrant subcellular localization of BRCA1 in breast cancer. *Science 270*:789–791.

Coene, E., Van Oostveldt, P., Willems, K., van Emmelo, J., and De Potter, C.R. 1997. BRCA1 is localized in cytoplasmic tube-like invaginations in the nucleus. *Nat. Genet. 16*:122–124.

Dobrovic, A., and Simpfendorfer, D. 1997. Methylation of the BRCA1 gene in sporadic breast cancer. *Cancer Res. 57*:3347–3350.

Futreal, P.A., Liu, Q., Shattuck-Eidens, D., Cochran, C., Harshman, K., Tavtigian, S., Bennett, L.M., Haugen-Strano, A., Swensen, J., and Mild, Y. 1994. BRCA1 mutations in primary breast and ovarian carcinomas. *Science 266*:120–122.

Futreal, P.A., Soderkvist, P., Marks, J.R., Iglehart, J.D., Cochran, C., Barrett, J.C., and Wiseman, R.W. 1992. Detection of frequent allelic loss on proximal chromosome 17q in sporadic breast carcinoma using microsatellite length polymorphisms. *Cancer Res. 52*:2624–2627.

Jarvis, E.M., Kirk, A., and Clarke, C.L. 1998. Loss of nuclear BRCA1 expression in breast cancers is associated with a highly proliferative tumor phenotype. *Cancer Genet. Cytogenet. 101*: 109–115.

Jensen, R.A., Thompson, M.E., Jetton, T.L., Szabo, C.I., van der Meer, R., Helou, B., Tronick, S.R., Page, D.L., King, M.C., and Holt, J.T. 1996. BRCA1 is secreted and exhibits properties of a granin. *Nat. Genet. 12*:303–308.

Kote-Jarai, Z., and Eeles, R.A. 1999. BRCA1, BRCA2 and their possible function in DNA damage response. *Br. J. Cancer 81*:1099–1102.

Laird, P.W., and Jaenisch, R. 1996. The role of DNA methylation in cancer genetic and epigenetics. *Ann. Rev. Genet. 30*:441–464.

Merajver, S.D., Pham, T.M., Caduff, R.F., Chen, M., Poy, E.L., Cooney, K.A., Weber, B.L., Collins, F.S., Johnston, C., and Frank, T.S. 1995. Somatic mutations in the BRCA1 gene in sporadic ovarian tumours. *Nat. Genet. 9*:439–443.

Miki, Y., Swensen, J., Shattuck-Eidens, D., Futreal, P.A., Harshman, K., Tavtigian, S., Liu, Q., Cochran, C., Bennett, L.M., and Ding, W. 1994. A strong candidate for the breast and ovarian cancer susceptibility gene BRCA1. *Science 266*:66–71.

Monteiro, A.N., August, A., and Hanafusa, H. 1996. Evidence for a transcriptional activation function of BRCA1 C-terminal region. *Proc. Natl. Acad. Sci. USA 93*:13595–13599.

Perez-Valles, A., Martorell-Cebollada, M., Nogueira-Vazquez, E., Garcia-Garcia, J.A., and Fuster-Diana, E. 2001. The usefulness of antibodies to the BRCA1 protein in detecting the mutated BRCA1 gene: an immunohistochemical study. *J. Clin. Pathol. 54*:476–480.

Phillips, K.W., Goldsworthy, S.M., Bennett, L.M., Brownlee, H.A., Wiseman, R.W., and Davis, B.J. 1997. Brca1 is expressed independently of hormonal stimulation in the mouse ovary. *Lab. Invest. 76*:419–425.

Rice, J.C., Massey-Brown, K.S., and Futscher, B.W. 1998. Aberrant methylation of the BRCA1 CpG island promoter is associated with decreased BRCA1 mRNA in sporadic breast cancer cells. *Oncogene 17*:1807–1812.

Russell, P.A., Pharoah, P.D.P., De Foy, K., Ramus, S.J., Symmonds, I., Wilson, A., Scorr, I., Ponder, B.A.J., and Gayther, S.A. 2000. Frequent loss of BRCA1 mRNA and protein expression in sporadic ovarian cancers. *Int. J. Cancer 87*:317–321.

Scully, R., Ganesan, S., Brown, M., De Caprio, J.A., Cannistra, S.A., Feunteun, J., Schnitt, S., and Livingston, D.M. 1996. Location of BRCA1 in human breast and ovarian cancer cells. *Science 272*:123–125.

Sekine, M., Nagata, H., Tsuji, S., Hirai, Y., Fujimoto, S., Hatae, M., Kobayashi, I., Fujii, T., Nagata, I., Ushijima, K., Obata, K., Suzuki, M., Yoshinaga, M., Umesaki, N., Satoh, S., Enomoto, T., Motoyama, S., and Tanaka, K. Japanese Familial Ovarian Cancer Study Group. 2001. Mutational analysis of BRCA1 and BRCA2 and clinicopathologic analysis of ovarian cancer in 82 ovarian cancer families: two common founder mutations of BRCA1 in Japanese population. *Clin. Cancer Res. 7*:3144–3150.

Smith, S.A., Easton, D.F., Evans, D.G., and Ponder, B.A. 1992. Allele losses in the region 17q12-21 in familial breast and ovarian cancer involve the wild-type chromosome. *Nat. Genet. 2*:128–131.

Thakur, S., Zhang, H.B., Peng, Y., Le, H., Carroll, B., Ward, T., Yao, J., Farid, L.M., Couch, F.J., Wilson, R.B., and Weber, B.L. 1997. Localization of BRCA1 and a splice variant identifies the nuclear localization signal. *Mol. Cell. Biol. 17*:444–452.

Thompson, M.E., Jensen, R.A., Obermiller, P.S., Page, D.L., and Holt, J.T. 1995. Decreased expression of BRCA1 accelerates growth and is often present during sporadic breast cancer progression. *Nat. Genet. 9*:444–450.

Wilson, C.A., Payton, M.N., Elliott, G.S., Buaas, F.W., Cajulis, E.E., Grosshans, D., Ramos, L., Reese, D.M., Slamon, D.J., and Calzone, F.J. 1997. Differential subcellular localization, expression and biological toxicity of BRCA1 and the splice variant BRCA1-delta11b. *Oncogene 14*:1–16.

Wilson, C.A., Payton, M.N., Pekar, S.K., Zhang, K., Pacifici, R.E., Gudas, J.L., Thukral, S., Calzone, F.J., Reese, D.M., and Slamon, D.I. 1996. BRCA1 protein products: antibody specificity. *Nat. Genet. 13*:264–265.

Wilson, C.A., Ramos, L., Villasenor, M.R., Anders, K.H., Press, M.F., Clarke, K., Karlan, B., Chen, J.J., Scully, R., Livingston, D., Zuch, R.H., Kanter, M.H., Cohen, S., Calzone, F.J., and Slamon, D.J. 1999. Localization of human BRCA1 and its loss in high-grade, non-inherited breast carcinomas. *Nat. Genet. 21*:236–240.

Yang, Q., Sakurai, T., Mori, I., Yoshimura, G., Nakamura, M., Nakamura, Y., Suzuma, T., Tamaki, T., Umemura, T., and Kakudo, K. 2001. Prognostic significance of BRCA1 expression in Japanese sporadic breast carcinomas. *Cancer 92*:54–60.

Yoshikawa, K., Honda, K., Inamoto, T., Shinohara, H., Yamauchi, A., Suga, K., Okuyama, T., Shimada, T., Kodama, H., Noguchi, S., Gazdar, A.F., Yamaoka, Y., and Takahashi, R. 1999. Reduction of BRCA1 protein expression in Japanese sporadic breast carcinomas and its frequent loss in BRCA1-associated cases. *Clin. Cancer Res. 5*:1249–1261.

Zheng, W., Luo, F., Lu, J.J., Baltayan, A., Press, M.F., Zhang, Z.F., and Pike, M.C. 2000. Reduction of BRCA1 expression in sporadic ovarian cancer. *Gynecol. Oncol. 76*:294–300.

5

Role of BRCA1/BRCA2 in Ovarian, Fallopian Tube, and Peritoneal Papillary Serous Carcinoma

R.I. Olivier and M. van Beurden

Introduction

Germline mutations in the *BRCA1* and *BRCA2* genes are the most important causes of inherited susceptibility to familial ovarian, fallopian tube, and peritoneal papillary serous carcinoma (PPSC). In this chapter, we discuss the contribution of *BRCA1* and *BRCA2* to ovarian and fallopian-tube carcinomas and PPSC incidence. Furthermore, strategies involved in ovarian cancer risk reduction in *BRCA1* and *BRCA2* mutation carriers are explained. The pathology and clinical outcome of these tumors are also described.

The Contribution of BRCA1/2 Germline Mutations to Ovarian and Fallopian Tube Carcinomas and Peritoneal Papillary Serous Carcinoma Incidence

Identification of BRCA1 and BRCA2

In 1990 the *BRCA1* gene was first localized and was identified in 1994 using linkage analysis and cloning (Hall *et al.,* 1990; Miki *et al.,* 1994). BRCA1 is present on the long arm of chromosome 17 at locus 21. The *BRCA2* gene was discovered in 1995, and it is present on chromosome 13 (Wooster *et al.,* 1995). The *BRCA* genes function as tumor-suppressor genes, with loss of function of both alleles required for tumor development (Boyd *et al.,* 2000). In 2003, 1237 *BRCA1* and 1381 *BRCA2* mutations, required for carcinogenesis, were recorded in the Breast Cancer Information Core database. Most of these mutations include splice-site mutations, small insertions or deletions resulting in a frame shift causing a truncated protein (Thompson and Easton, 2004). Deoxyribonucleic acid (DNA) analysis has been performed using denaturing gradient gel electrophoresis, denaturing high-performance liquid chromatography, protein truncation tests, multiplex ligation-dependent probe amplification, or mutation-specific tests (Hogervorst *et al.,* 2003). The majority of the mutations are being found randomly throughout the population. However, certain mutations are found more frequently in certain populations and are called founder mutations. For example, in Ashkenazi Jews three mutations are often found: 185delAG *BRCA1*, 5382insC *BRCA1,* and 6174delT *BRCA2* (Hartge *et al.,* 1999).

Handbook of Immunohistochemistry and *in situ* Hybridization of Human Carcinomas, Volume 4: Molecular Genetics, Gastrointestinal Carcinoma, and Ovarian Carcinoma

Epidemiology of Ovarian Carcinoma

Cancer of the ovary is the sixth most common cancer in women, affecting approximately 1 in 70 women in the developed world, and is the leading cause of death from a gynecologic malignancy (Cannistra, 2004). Of ovarian cancer cases, 90–95% are sporadic and 5–10% are hereditary, of which the majority are associated with germline mutations, including *BRCA1* and *BRCA2* (Risch *et al.,* 2001). In an analysis of 237 families, each with at least four cases of breast cancer, it was estimated that in 52% of the families the disease was linked to *BRCA1* and it was linked to *BRCA2* in 32% of the families (Ford *et al.,* 1998). The lifetime risk for ovarian cancer has been calculated in a study of 8139 index case patients. Of these patients, unselected for a positive family history, 86% had female breast cancer, 2% had male breast cancer, and 12% had epithelial ovarian cancer. In total, 500 (6%) were carriers of a *BRCA1* or *BRCA2* mutation. The estimated risk of ovarian cancer has been reported to have a range of 11–39%, depending on the penetrance of the germline mutation (Antoniou *et al.,* 2003).

Epidemiology of Fallopian Tube Carcinoma

Carcinoma of the fallopian tube comprises 0.5% of all gynecologic tumors in the general population (Schneider *et al.,* 2000). The true incidence of both early- and late-stage fallopian-tube carcinomas is unknown and may be underestimated. In a screening study of 22,000 women, three cases of early-stage primary fallopian-tube carcinoma were diagnosed. This number was 25-fold higher than expected by national incidences figures. Several explanations were given. First, it was possible that the selected population was at high risk for developing fallopian-tube carcinoma. Second, the screening test CA-125 may be especially effective in detecting fallopian-tube carcinoma. Finally, it was stated that in general clinical practice it could be possible that the primary site of some ovarian carcinomas (OCs) is in fact in the fallopian tubes (Woolas *et al.,* 1994). A primary fallopian-tube carcinoma can be diagnosed when the main tumor is present in the fallopian tube, and if the wall is involved, a transition of dysplastic tubal epithelium to carcinoma is observed (Figure 57; Woolas *et al.,* 1997). Both the clinical and histopathologic diagnosis of fallopian-tube carcinoma and OC is usually made at an advanced stage. However, fallopian-tube carcinoma is characterized by a number of signs and symptoms, most frequently abnormal vaginal bleeding, discharge, and abdominal pain, whereas patients with OC have fewer signs (Baekelandt *et al.,* 2000).

The association between BRCA1/2 mutations and fallopian-tube carcinomas has been recognized. In the last few years there have been a growing number of articles reporting fallopian-tube carcinomas in proven mutation carriers (Agoff *et al.,* 2002; Colgan *et al.,* 2001; Hartley *et al.,* 2000; Kauff *et al.,* 2002; Leeper *et al.,* 2002; Lu *et al.,* 2000; Olivier *et al.,* 2004; Paley *et al.,* 2001; Zweemer *et al.,* 2000). These fallopian tumors were occult carcinomas found in prophylactic oophorectomy specimens. Zweemer *et al*. (2000) published molecular evidence linking fallopian-tube carcinoma to a *BRCA1* mutation. In two patients with a *BRCA1* mutation, a loss of the wild-type allele was shown in both tumors. A population-based study of fallopian-tube carcinoma has revealed the presence of *BRCA1/2* germline mutation in more than 15% of fallopian-tube carcinomas (Aziz *et al.,* 2001). Furthermore, a mutation frequency of 17% (5/29 patients) was reported by Levine *et al.* (2003). Finally, a 120-fold increased risk of fallopian-tube carcinoma in *BRCA1* mutation carriers has been published by Brose *et al*. (2002).

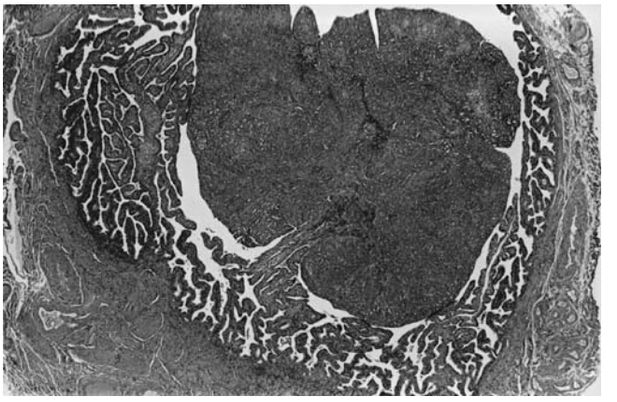

Figure 57. A tumor embolus with a diameter of 2.5 mm nearly completely obliterating the lumen of the left fallopian tube.

Epidemiology of Peritoneal Papillary Serous Carcinoma

Each year in the United States PPSC is diagnosed in 1000 women. It is diffusely spread on the peritoneal surfaces, and the ovaries are either not involved or superficially involved (Schorge *et al.,* 1998). For the diagnosis of PPSC, the criteria are strict according to the Gynecologic Oncology Group (Bloss *et al.,* 1993). First, both ovaries are either normal in size or enlarged by a benign cause. Judged by the surgeon and the pathologist, the bulk of the tumor is in the peritoneum and the extent of extra ovarian tumor is greater than on the surface of either ovary. Second, microscopic examination of the ovaries reveals one of the following: 1) no tumor; 2) tumor confined to the surface epithelium and no cortical invasion; 3) tumor involving the surface

and the cortical stroma but less than 5 × 5 mm in diameter; or 4) tumor less than 5 × 5 mm within the ovarian substance, with or without surface involvement. Third, pathologic characteristics of the tumor are predominantly serous and similar or identical to those of ovarian serous papillary carcinomas of any grade. Finally, cases in which an oophorectomy has been done before the diagnosis of PPSC must have the pathology report of the oophorectomy to document the absence of carcinoma with review of all slides (or an attempt to remove them).

The question of PPSC being a primary carcinoma or a metastasis of OC has been discussed. Reasons for PPSC being a primary carcinoma can be summarized as follows: First, the clinical behavior of patients with PPSC was compared with that of patients with high-stage ovarian cancer. In the study by Bloss *et al*. (1993), median survival for the PPSC group was 20 months compared to 28 months in the ovarian carcinoma group, although this was not significantly different and can be explained by the small size of the cohort. However, in the study by Killackey and Davis (1993), patients with PPSC had more limited cytoreduction (65.5% versus 79% in sporadic cases), shorter disease-free interval (3.4 months versus 11.7 months), and shorter overall survival time (19 versus 31 months). Second, there is evidence that some cases of PPSC have a multifocal origin as compared to the unifocal origin of advanced-stage epithelial OC. Muto *et al.* (1995) reported that in four out of six PPSC cases different patterns of allelic loss at different localizations were found. Also a p53 mutation was found in one of these patients but not at all anatomic sites. A possible explanation for these findings is that PPSC arises as synchronous primaries within multifocal rests of the müllerian epithelium, and spreads throughout the peritoneal cavity. Furthermore, PPSC has been diagnosed after prophylactic surgery of the ovaries. In 1982, three (11%) cases of intraabdominal adenocarcinoma that were indistinguishable histopathologically from ovarian carcinoma were described for the first time in patients 1–11 years after oophorectomy for a family history of ovarian cancer was performed (Tobacman *et al.,* 1982). Piver *et al*. (1993) described 9 (2.8%) cases of PPSC after abdominal total hysterectomy and salpingo-oophorectomy in women with one or more family members with ovarian cancer. In an analysis of 551 women, 2 of 259 (0.8%) mutation carriers had PPSC 3.8 and 8.6 years after bilateral prophylactic oophorectomy (Rebbeck *et al.,* 2002). An argument for PPSC being a metastasis is the immunohistochemical similarity between PPSC and OC. Thirteen patients with PPSC and 31 with ovarian carcinoma were analyzed with immunohistochemistry (IHC). Both groups of carcinomas were positive for cytokeratin and epithelial membrane antigen; in addition, they had similar reactions to B72.3 antigen; carcinoembryonic antigen; Leu M1; CA-125 antigen; LN1, LN2, MB2, and S100 protein; placental alkaline phosphatase; and amylase (Wick *et al.,* 1989).

The cancer PPSC has been described in BRCA1 mutation carriers. The incidence of PPSC found by Kauff *et al.* (0.5 in 100 women-years) was lower than the 3.4 in 100 BRCA1 women-years found in our cohort, but this may be because of a shorter mean follow-up duration (respectively 23.4 months versus 45; Kauff *et al.,* 2002; Olivier *et al.,* 2004). The cancer PPSC is also related to BRCA2 mutations. The first report of PPSC occurring in two BRCA2 carriers after hysterectomy and salpingo-oophorectomy has been published; clearly, it is too early to conclude that BRCA2 carriers face a lower risk than BRCA1 carriers of developing PPSC. The authors mention that BRCA2 mutation carriers, besides a known delayed onset of OC, also have a delayed onset of PPSC (Foulkes *et al.,* 2003). Furthermore, six BRCA2 mutation carriers were found in 22 cases of PPSC by Levine *et al.* (2003), but whether these cases developed after a prophylactic procedure is not mentioned.

In general, besides OC, fallopian tube carcinoma and PPSC should also be considered as malignancies expressed in the hereditary ovarian cancer syndrome. Higher risks of OC, fallopian-tube carcinoma, and PPSC in women with a proven *BRCA1* and *BRCA2* mutation compared to women with sporadic carcinomas have stimulated counseling toward carriers regarding screening and an optional prophylactic salpingo-oophorectomy.

Gynecologic Management of BRCA1 and BRCA2 Mutation Carriers

Screening

There are some important considerations concerning screening high-risk women. First, because of a lack of premalignant lesions, early-stage detection is of crucial importance in the surveillance; therefore, it is hoped that screening will achieve a longer overall survival of patients. Second, because of the high ovarian cancer risk, randomized controlled trials in these women are unethical. Annual or semi-annual screening with transvaginal ultrasound (TVU) and CA-125 determination and an optional prophylactic surgery of the ovaries and fallopian tubes (bilateral prophylactic salpingo-oophorectomy, or BPSO) is recommended by a taskforce of the Cancer Genetics Studies Consortium (CGSC; Burke *et al.,* 1997). These recommendations were also applied in the Netherlands. Despite these clear guidelines, there are limited data regarding the

application of these guidelines. The efficiency of annual screening in low- and high-risk patients by assessing serum CA-125 and TVU monitoring is not clear.

The largest studies on screening are mostly performed in the general population and low-risk women. Screening with CA-125 resulted in the diagnosis of mainly advanced tumors (Hogg and Friedlandes, 2004). Although the specificity of CA-125 for early-stage disease is high (96–100%), the sensitivity is poor (Einhorn *et al.,* 1992; Jacobs *et al.,* 1996). Another screening tool advocated for ovarian cancer is TVU. In the largest study of women at general population risk, mostly early-stage carcinomas were detected. The majority of these carcinomas, however, were of nonserous epithelial origin (van Nagell *et al.,* 2000). The combination of CA-125 and TVU was also tested in the general population. The performance of the combination was assessed in an analysis of 22,000 women. A sensitivity of 58% and a specificity of 100% at 2-year follow-up was achieved. However, failure to detect 73% of early-stage disease and high false-positive rates of CA-125 and TVU are the major limitations of this type of screening (Jacobs *et al.,* 1993). Menon *et al.* (1999) showed that if the elevated CA-125 was associated with an abnormal TVU, then the risk of developing a cancer in the subsequent year was increased approximately 300-fold, supporting the use of these screening tests in combination. This multi-modality screening concept was further tested in the general population in a randomized way, but it failed to show a difference in the number of deaths from ovarian cancer between the control and screened group (Jacobs *et al.,* 1999). Furthermore, the low prevalence of ovarian cancer in the general population may limit the potential cost-effectiveness of screening. Presently, routine screening of low-risk women is unlikely to be effective. Bourne *et al.* (1991) used TVU to screen 776 women for familial ovarian cancer. A sensitivity of TVU of 100% and a specificity of 97% after finding three stage I OCs was reported. The major limitation of this study is that only 2% of the cohort had two first-degree affected relatives and no data on DNA analysis are given.

A screening study using CA-125 and TVU as screening tools in high-risk women was done by Laframboise *et al.* (2002). In these 311 women, 2.7% of the CA-125 results and 16.8% of the TVUs were abnormal. Nine patients underwent surgery because of an abnormal screening test. Only 1 (0.3%) patient appeared to have a stage 1a ovarian carcinoma, grade 1 and endometrioid adenocarcinoma. The reason that the detection rate is so low may be because only 13 (10%) of the patients were known mutation carriers, which was the main limitation of this study. Furthermore, sensibility and specificity were not calculated. Hogg *et al.* (2004) reviewed studies about screening in low- as well as in high-risk groups published between 1988 and 2003. In this review 15 interval carcinomas were documented in 12 different published studies. The occurrence of interval carcinomas shows the incapacity of this type of screening. This unpredictable character OC makes it hard to make guidelines and recommendations for the frequency of screening. Finally, studies are lacking data demonstrating a significant survival advantage for a screened population.

Prophylactic Surgery

There is insufficient evidence for the efficacy of screening in high-risk women, and these women should be counseled that BPSO is an option that will substantially lower their risk. In 1995 a National Institutes of Health consensus was published: Prophylactic oophorectomy should be offered after completion of childbearing or at age 35 years. Since then, a growing number of manuscripts reporting the incident findings of tumors at prophylactic salpingo-oophorectomy including patients with fallopian-tube cancer have been published (Table 29). Occult carcinomas within the fallopian tubes have changed the standard procedure from bilateral oophorectomy into salpingo-oophorectomy. The prevalence of published occult carcinomas including OCs varies depending on the cohort studied from 3.0% to 18% (Agoff *et al.,* 2002; Colgan *et al.,* 2001; Hartley *et al.,* 2000; Kauff *et al.,* 2002; Leeper *et al.,* 2002; Lu *et al.,* 2000; Olivier *et al.,* 2004; Paley *et al.,* 2001; Salazar *et al.,* 1996). These studies show the importance of attentiveness to occult tumors.

The procedure BPSO has been shown to reduce the ovarian cancer risk in *BRCA1* or *BRCA2* mutation carriers. Rebbeck *et al.* (2002) studied 259 oophorectomized and 259 nonoophorectomized high-risk women. Two cases of PPSC after BP(S)O were diagnosed versus 58 ovarian carcinomas in the nonsurgery group. This resulted in a risk reduction of 96% with a hazard ratio (HR) of 0.04 (95% confidence interval [CI] 0.01–0.16). This hazard ratio could be an overestimation as a result of unclear surveillance of the control group.

As noted before, removal of the ovaries and the fallopian tubes does not eliminate the development of PPSC (Rebbeck *et al.,* 2002). Piver *et al.* (1993) reported nine cases of PPSC after abdominal total hysterectomy and salpingo-oophorectomy. The cumulative risk of developing PPSC subsequent to risk reducing BPSO may be as high as 10% based on the study by Tobacman *et al.* (1982); however, an update of the same group of patients later showed that no additional cancers were found (Struewing *et al.,* 1995).

Rates of BPSO after genetic testing have been reported in the literature. In a Dutch family cancer clinic,

Table 29. Review of the Literature for Occult Tumors at Prophylactic Surgery

Author(s)	Age (yr)	Diagnosis	BRCA Mutation	Follow-Up (Months)	Design
Salazar *et al*., 1996	50	Ovary	N.D.	—	Retrospective
	44	Ovary	BRCA1	—	N = 20
Zweemer *et al.,* 2000	61	Fallopian tube	2804delAA(BRCA1)	—	Retrospective
	50	Fallopian tube	1410insT(BRCA1)	—	N = 23
Hartley *et al.,* 2000	49	Fallopian tube	BRCA1	—	Retrospective Case report
Lu *et al.,* 2000	49	Fallopian tube/ovary	BRCA1	—	Retrospective
	65	Fallopian tube	BRCA2	—	N = 50
	40	Borderline	BRCA1	—	
	49	Borderline	BRCA1	—	Retrospective
Colgan *et al.,* 2001	—	Ovary	185delAG(BRCA1)	DOD <36	N = 60
	—	Fallopian tube/ovary	5382insC(BRCA1)	NED 36	
	—	Fallopian tube/ovary	5083del19(BRCA1)	NED 12	
	—	Fallopian tube *in situ*	G4236T(BRCA1)	NED 12	
	—	Fallopian tube	5382insC(BRCA1)	—	
Paley *et al.,* 2001	47	Fallopian tube *in situ*	2800delAA(BRCA1)	—	Retrospective
	62	Fallopian tube	2800delAA(BRCA1)	—	Case report
Agoff *et al.,* 2002	63	Fallopian tube	2800delAA(BRCA1)	NED 7	Retrospective
	47	Fallopian tube	2800delAA(BRCA1)	NED 6	Case reports
	65	Fallopian tube	2558insA(BRCA1)	—	
	74	Fallopian tube	—	—	
	43	Fallopian tube	—	Metastatic breast cancer	
	48	PPSC	3795del4(BRCA1)	Rec. 7	
	48	Borderline fibroma	—	—	Retrospective
Leeper *et al.,* 2002	48	PPSC	3795dell4(BRCA1)	NED 23	N = 30
	47	Fallopian tube *in situ*	2800delAA(BRCA1)	NED 24	
	62	Fallopian tube	2800delAA(BRCA1)	Rec. 21	
	65	Fallopian tube *in situ*	2558insA(BRCA2)	NED 16	
	48	Borderline fibroma	N.D.	NED 19	
Kauff *et al.,* 2002	—	Ovary	—	—	Retrospective
	—	Ovary	—	—	N = 98
	—	Fallopian tube	—	—	
Olivier *et al.,* 2004	33	Fallopian tube	3875del4(BRCA1)	NED 46	Retrospective
	49	Fallopian tube	BRCA1*	Rec. 20	N = 128
	45	Fallopian tube/ovary	2312del5(BRCA1)	Rec. 11	
	47	Ovary	1411insT(BRCA1)	NED 35	
	37	Ovary	exon11stop(BRCA1)	NED 11	

Abbreviations:

DOD, Dead of disease; N.D., not determined; NED, no evidence of disease; PPSC, peritoneal papillary serous carcinoma; Rec, recurrence; *, not further specified; —, not available.

64% of unaffected women with a *BRCA1* or *BRCA2* mutation chose prophylactic oophorectomy (Meijers-Heijboer *et al.,* 2000). However, Schwartz *et al.* (2003) reported a lower risk-reducing surgery rate of 27% in mutation carriers compared to women with no proven mutation (5%) after 1 year, whereas 58 of 79 (73%) *BRCA1/2* carriers were being screened 1 year after testing. Besides this, a positive DNA test result was associated with a more frequent use of TVU and CA-125. Regarding the timing and age at which women should decide to undergo preventive surgery, the age-specific cumulative probability of developing ovarian cancer suggests an increased risk of OC after the age of 40 for BRCA1 carriers and after the age of 50 for BRCA2 mutation carriers (Antoniou *et al.,* 2003). Therefore, in the future a longer period of fertility can be preserved with eventually changing guidelines with respect to the discussion of an optional BPSO.

Ovarian ablation also has disadvantages. As with every operation it has its own complications; it also leads to a surgical menopause and infertility with related symptoms such as flushes, night sweats, depression, vaginal dryness, and vaginal atrophy caused by estrogen deficiency (Rozenberg *et al.,* 2000). Only one study has compared quality of life (QOL) effects of BPSO and screening. Women who have had an oophorectomy reported a significantly worse QOL. However, the sample size of this single center study was small (n = 57).

Furthermore, BPSO was not found to relieve cancer-specific distress or to worsen sexual functioning in this cohort (Fry *et al.,* 2001).

At the Netherlands Cancer Institute, an additional bilateral prophylactic salpingectomy (BPS) is offered to high-risk women who underwent risk-reducing bilateral prophylactia oophorectomy (BPO) only. Although no (pre)malignant lesions were found in 15 patients, we believe that an additional risk reduction of fallopian tube carcinoma may be achieved with BPS in high-risk women after previous BPO, based on 1) a 120-fold increased risk in *BRCA1* mutation carriers found by Brose *et al*. (2002), 2) findings of occult fallopian-tube carcinomas and premalignant lesions in previous reports (see Table 29), and 3) the failure of early detection at screening (Olivier, *et al.,* 2005).

Pathology of BRCA1/2-Related Gynecologic Malignancies

Surface epithelial tumors account for 90% of all malignant ovarian tumors in the Western world. The six epithelial subtypes are serous, mucinous, endometrioid, clear, transitional, and squamous. The serous subtype that is often associated with rings of calcification known as psammoma bodies, represents 60% of all sporadic malignant epithelial tumors (Heintz *et al.,* 2003). Furthermore, serous carcinomas are characterized by extensive cellular budding. The extent of papillarity varies greatly (Scully *et al.,* 2003). Histologically, fallopian-tube carcinoma and PPSC are identical to invasive epithelial ovarian carcinoma. In a clinicopathologic study of 151 women with fallopian-tube carcinoma, 82% had a histologic serous subtype (Baekelandt *et al.,* 2000). The frequency of serous carcinomas among cases with PPSC (80%) carcinomas was not significantly different to that of OCs (66%) in the cohort study (Barda *et al.,* 2004). These similarities between PPSC and OC support the probability of a common molecular pathogenesis. BRCA1/2 carcinomas as compared to sporadic tumors are histologically different. Serous tumors are more common (81%) in patients with a *BRCA1* or *BRCA2* mutation than in sporadic tumors (Rubin *et al.,* 1996). This is further supported by the finding that OCs arising in women from *BRCA1*-positive families are more likely to be nonmucinous than cancers arising in women from *BRCA1*-negative families. Furthermore, none of the 66 tumors were borderline tumors in *BRCA* mutation carriers, whereas 10 (6.9%) of the 148 primary OCs from BRCA1-negative patients were borderline tumors (Werness *et al.,* 2000a). This low frequency of borderline tumors in *BRCA1* carriers was also found by Lakhani *et al.* (2004), who found 1% borderline tumors in *BRCA1* carriers as compared to 10% borderline tumors in the control group. Only one single case of a primary ovarian dysgermimoma has been reported in a *BRCA1* mutation carrier (Werness *et al.,* 2000b).

Serous carcinomas are commonly bilateral, have spread beyond the ovaries at the time of diagnosis, and have probably no recognizable precursor. The absence of these recognizable precursor lesions in serous cancers may reflect a rapid progression that makes it difficult to identify any premalignant changes. Hogg *et al.* (2004) suggest that stage I OCs are biologically different from advanced-stage carcinomas. Two separate models were proposed for the development and progression of epithelial OC. In the first model, well-differentiated serous and other epithelial carcinomas are included, and early-stage detection with screening appears to be possible. In the second model, high-grade serous carcinomas are included and then screening is of limited value.

There might be an *in situ* form of fallopian-tube carcinoma because others have reported dysplastic changes in the fallopian tubes of women at high risk for developing ovarian cancer (Carcangiu *et al.,* 2004; Piek *et al.,* 2001). Carcangiu *et al.* (2004) reported that in the 22 women who were *BRCA1*-mutated, two *in situ* carcinomas and two cases of atypical hyperplasia of the tubal epithelium were found. In the study by Piek *et al.* (2001), the fallopian tubes of women predisposed to develop ovarian cancer harbored dysplastic changes, indicating an increased risk of developing tubal cancer. Of 12 women with a predisposition for ovarian cancer, 6 showed dysplasia and 5 had hyperplasic lesions in the tubes.

Other histologic and molecular features of *BRCA1* and *BRCA2* mutated carcinomas have also been reported. In a systematic review of 178 *BRCA1* mutation carriers, 29 *BRCA2* mutation carriers, and 235 controls both *BRCA1* and *BRCA2* OCs were of higher grade than controls ($p = 0.001$ and $p = 0.028$, respectively). Furthermore, a higher frequency of p53 staining was found in BRCA1 and BRCA2 compared to sporadic ovarian tumors (respectively, 70% for BRCA1, 67% for BRCA2, and 39% for sporadic tumors (Lakhani *et al.,* 2004). This is consistent with earlier published data on p53 staining in *BRCA1* breast carcinomas. The percentage of breast carcinomas showing a high p53 staining (34%) was higher than in controls (17%; Lakhani *et al.,* 2002). The increased frequency regarding a higher grade and p53 staining has raised the possibility that these women may have poor survival (Lakhani *et al.,* 2004). Cell proliferation and apoptosis did not differ between *BRCA1*- and *BRCA2*-associated tumors, which indicates that *BRCA*-related tumors have a higher growth fraction than sporadic carcinomas (Levine *et al.,* 2002). It has been suggested that histologic and

immunohistochemical analysis can provide information on a possible *BRCA1* or *BRCA2* mutation status, which could help genetic testing programs, given the higher frequency of serous carcinomas, p53 staining, and higher grade (Lakhani *et al.,* 2004).

Clinical Aspects of BRCA1/2-Related Gynecologic Malignancies

Age at diagnosis in sporadic ovarian carcinoma differs from the age at diagnosis in *BRCA1* mutation carriers. Age at onset was 8 years younger for *BRCA1*-associated cases compared with sporadic cases (54 years versus 63 years, respectively) in the cohort studied by Boyd *et al*. (2000). Mean age for *BRCA2* carriers was not different compared with women with sporadic OC. In another study these data were supported. Thirty-four *BRCA1* and *BRCA2* carriers were significantly 9 years younger than 37 patients with sporadic tumors. Of these 34 *BRCA* mutation carriers, 12 were carriers of a *BRCA2* mutation of which none was diagnosed at an age younger than 45 years, whereas 36% of *BRCA1* carriers were diagnosed before the age of 45 years (Cass *et al.,* 2003). The different age-specific risk of ovarian cancer in *BRCA1* versus *BRCA2* mutation carriers is consistent with earlier published estimates in breast and ovarian cancer families. The estimated penetrance of *BRCA2* up to 50 years is lower compared to the penetrance of *BRCA1*, but at the age of 70 the penetrance is similar (88% versus 83% respectively; Ford *et al.,* 1998). This may have important implications with regard to counseling of these women and deciding when to undergo an optional prophylactic surgery.

The management of sporadic and high-risk patients is similar. Total abdominal hysterectomy with salpingo-oophorectomy and staging (examination of all peritoneal surfaces, biopsy of paraaortic lymph nodes when appropriate, random biopsies of clinically involved areas, and peritoneal washings) is the standard treatment in patients with sporadic OC. Furthermore, the combination of paclitaxel and platinum-based postoperative chemotherapy is standard for patients at high risk for relapse. A randomized trial has shown that the combination of cisplatin–paclitaxel prolongs the progression-free survival compared to cisplatin–cyclophosphamide (median, 18 versus 13 months) and overall survival (median, 38 versus 24 months; McGuire *et al.,* 1996). Patients at high risk are those with stage I, grade 3, and those with higher stages (Cannistra, 2004).

Survival is high in all patients with ovarian cancer with a stage I or II OC who have a 5-year survival rate of 88% and 48%, respectively, after 5 years of the diagnosis. In approximately 75% of all cases, the disease is disseminated beyond the ovary at diagnosis. Only 25% of women with a stage III or IV disease are alive after 5 years (Cannistra, 2004). Boyd *et al.* (2000) found a longer disease-free interval in stage III patients with germline mutations compared with a matched control group of noncarriers with a median time to recurrence of 14 months and 7 months, respectively. *BRCA* advanced cases also had a significantly longer survival ($p = 0.04$) than advanced sporadic cases. Other published data supported Boyd's data (Ben David *et al.,* 2002; Cass *et al.,* 2003). In the study by Cass *et al.* (2003), overall survival had improved in BRCA patients with advanced stage: 91 months in *BRCA* patients versus 54 months in sporadic patients. Ben David *et al.* (2002) reported a significant survival pattern between carriers and noncarriers with ovarian cancer (median survival 53.4 months versus 37.8 months). *BRCA* mutation status was a good prognostic factor and independent of age at diagnosis or stage. The fact that this better survival was seen in all stages shows that the results are not the effect of early detection. The hypothesis explaining this improved survival could be associated with a potential indolent clinical behavior through a slower rate of cell division or with a better response to platinum-based chemotherapy. This latter idea is also supported by the knowledge that *BRCA* proteins are involved in DNA damage recognition and repair and that BRCA-mutated OCs could be more sensitive to chemotherapy (Boyd *et al.,* 2000).

Although most data suggest a better outcome for *BRCA* patients, there are contradictory data as well. According to the data by Cass *et al.* (2003), success of cytoreductieve surgery seemed to be similar in hereditary and sporadic cases. A population-based study from southern Sweden noted an initial survival advantage for *BRCA1*-associated ovarian cancers that disappeared with time. However, compared with the age- and stage-matched control group, survival appeared equal or worse (HR, 1.2; 95% CI, 0.5 to 2.8). This is in agreement with the earlier mentioned adverse histopathologic gynecologic characteristics (e.g., higher frequency of serous carcinomas, p53 staining, and higher grade) of the tumors (Johannsson *et al.,* 1998).

Advanced fallopian-tube carcinomas and PPSC have a clinical behavior similar to epithelial OCs. Therefore, Baekelandt *et al.* (2000) recommended that the treatment and follow-up strategies for patients with ovarian cancer can be used in the management of patients with fallopian-tube carcinoma.

CONCLUSIONS

Women with a *BRCA1* or *BRCA2* mutation should be fully informed about the issues and dilemmas raised in this chapter. Women electing screening should be

aware of the lack of proven benefit of screening and the low likelihood of detecting early-stage cancer. Findings of occult carcinomas and interval carcinomas show the incapacity of screening as well.

Bilateral prophylactic salpingo-oophorectomy is presently the most effective approach to the management in these women. However, the risk of developing PPSC remains unaltered. At this moment there are discrepancies in the results of published studies of survival in *BRCA*-associated ovarian cancer, although they clearly exhibit a number of histopathologic and molecular generic features usually associated with a poorer survival as compared to sporadic ovarian cancer.

Genetic analysis should soon give us more data on the biology of a *BRCA1* OC. Jazaeri *et al.* (2002) revealed that *BRCA1* and *BRCA2* germline mutations have different gene-expression profiles, suggesting different pathways to carcinogenesis. Furthermore, in sporadic tumors both *BRCA1* as *BRCA2* expression patterns were seen. Therefore, many of the overexpressed genes involved in *BRCA*-pathways were interferon inducible; some were members of the major histocompatibility complex class II family. These genes could be used in the future as an immunotherapeutic target.

Proteomics may provide us with early detection of the tumors. One study has already shown that discrimination between serum of normal individuals and serum of patients diagnosed with ovarian cancer is possible. If these results are more firmly confirmed, a possible survival benefit can also be sorted out (Petricoin *et al.,* 2002).

References

Agoff, S.N., Mendelin, J.E., Grieco, V.S., and Garcia, R.L. 2002. Unexpected gynecologic neoplasms in patients with proven or suspected BRCA-1 or -2 mutations: implications for gross examination, cytology, and clinical follow-up. *Am. J. Surg. Pathol. 26*:171–178.

Antoniou, A., Pharoah, P.D., Narod, S., Risch, H.A., Eyfjord, J.E., Hopper, J.L., Loman, N., Olsson, H., Johannsson, O., Borg, A., Pasini, B., Radice, P., Manoukian, S., Eccles, D.M., Tang, N., Olah, E., Anton-Culver, H., Warner, E., Lubinski, J., Gronwald, J., Gorski, B., Tulinius, H., Thorlacius, S., Eerola, H., Nevanlinna, H., Syrjakoski, K., Kallioniemi, O.P., Thompson, D., Evans, C., Peto, J., Lalloo, F., Evans, D.G., and Easton, D.F. 2003. Average risks of breast and ovarian cancer associated with BRCA1 or BRCA2 mutations detected in case series unselected for family history: a combined analysis of 22 studies. *Am. J. Hum. Genet. 72*:1117–1130.

Aziz, S., Kuperstein, G., Rosen, B., Cole, D., Nedelcu, R., McLaughlin, J., and Narod, S.A. 2001. A genetic epidemiological study of carcinoma of the fallopian tube. *Gynecol. Oncol. 80*:341–345.

Baekelandt, M., Jorunn Nesbakken, A., Kristensen, G.B., Trope, C.G., and Abeler, V.M. 2000. Carcinoma of the fallopian tube. *Cancer 89*:2076–2084.

Barda, G., Menczer, J., Chetrit, A., Lubin, F., Beck, D., Piura, B., Glezerman, M., Modan, B., and Sadetzki, S. 2004. Comparison between primary peritoneal and epithelial ovarian carcinoma: a population-based study. *Am. J. Obstet. Gynecol. 190*:1039–1045.

Ben David, Y., Chetrit, A., Hirsh-Yechezkel, G., Friedman, E., Beck, B.D., Beller, U., Ben Baruch, G., Fishman, A., Levavi, H., Lubin, F., Menczer, J., Piura, B., Struewing, J.P., and Modan, B. 2002. Effect of BRCA mutations on the length of survival in epithelial ovarian tumors. *J. Clin. Oncol. 20*:463–466.

Bloss, J.D., Liao, S.Y., Buller, R.E., Manetta, A., Berman, M.L., McMeekin, S., Bloss, L.P., and DiSaia, P.J. 1993. Extraovarian peritoneal serous papillary carcinoma: a case-control retrospective comparison to papillary adenocarcinoma of the ovary. *Gynecol. Oncol. 50*:347–351.

Bourne, T.H., Whitehead, M.I., Campbell, S., Royston, P., Bhan, V., and Collins, W. P. 1991. Ultrasound screening for familial ovarian cancer. *Gynecol. Oncol. 43*:92–97.

Boyd, J., Sonoda, Y., Federici, M.G., Bogomolniy, F., Rhei, E., Maresco, D.L., Saigo, P.E., Almadrones, L.A., Barakat, R.R., Brown, C.L., Chi, D.S., Curtin, J.P., Poynor, E.A., and Hoskins, W.J. 2000. Clinicopathologic features of BRCA-linked and sporadic ovarian cancer. *JAMA 283*:2260–2265.

Brose, M.S., Rebbeck, T.R., Calzone, K.A., Stopfer, J.E., Nathanson, K.L., and Weber, B.L. 2002. Cancer risk estimates for BRCA1 mutation carriers identified in a risk evaluation program. *J. Natl. Cancer Inst. 94*:1365–1372.

Burke, W., Daly, M., Garber, J., Botkin, J., Kahn, M.J., Lynch, P., McTieman, A., Offit, K., Perlman, J., Petersen, G., Thomson, E., and Varricchio, C. 1997. Recommendations for follow-up care of individuals with an inherited predisposition to cancer. II. BRCA1 and BRCA2. Cancer Genetics Studies Consortium. *JAMA 277*:997–1003.

Cannistra, S.A. 2004. Cancer of the ovary. *N. Engl. J. Med. 351*: 2519–2529.

Carcangiu, M.L., Radice, P., Manoukian, S., Spatti, G., Gobbo, M., Pensotti, V., Crucianelli, R., and Pasini, B. 2004. Atypical epithelial proliferation in fallopian tubes in prophylactic salpingo-oophorectomy specimens from BRCA1 and BRCA2 germline mutation carriers. *Int. J. Gynecol. Pathol. 23*:35–40.

Cass, I., Baldwin, R.J., Varkey, T., Moslehi, R., Narod, S.A., and Karlan, B.Y. 2003. Improved survival in women with BRCA-associated ovarian carcinoma. *Cancer 97*:2187–2195.

Colgan, T.J., Murphy, J., Cole, D.E., Narod, S., and Rosen, B. 2001. Occult carcinoma in prophylactic oophorectomy specimens: prevalence and association with BRCA germline mutation status. *Am. J. Surg. Pathol. 25*:1283–1289.

Einhorn, N., Sjovall, K., Knapp, R.C., Hall, P., Scully, R.E., Bast, R.C., Jr., and Zurawski, V.R., Jr. 1992. Prospective evaluation of serum CA 125 levels for early detection of ovarian cancer. *Obstet. Gynecol. 80*:14–18.

Ford, D., Easton, D.F., Stratton, M., Narod, S., Goldgar, D., Devilee, P., Bishop, D.T., Weber, B., Lenoir, G., Chang-Claude, J., Sobol, H., Teare, M.D., Struewing, J., Arason, A., Scherneck, S., Peto, J., Rebbeck, T.R., Tonin, P., Neuhausen, S., Barkardottir, R., Eyfjord, J., Lynch, H., Ponder, B.A., Gayther, S.A., Zelada-Hedman, M., *et al.* 1998. Genetic heterogeneity and penetrance analysis of the BRCA1 and BRCA2 genes in breast cancer families. The Breast Cancer Linkage Consortium. *Am. J. Hum. Genet. 62*:676–689.

Foulkes, W.D., Narod, S.A., Swenerton, K., Panabaker, K., and Gilbert, L. 2003. Re: Gynecologic surgeries and risk of ovarian cancer in women with BRCA1 and BRCA2 Ashkenazi founder mutations: an Israeli population-based case-control study. *J. Natl. Cancer Inst. 95*:1640.

Fry, A., Busby-Earle, C., Rush, R., and Cull, A. 2001. Prophylactic oophorectomy versus screening: psychosocial outcomes in

women at increased risk of ovarian cancer. *Psychooncology 10*:231–241.

Hall, J.M., Lee, M.K., Newman, B., Morrow, J.E., Anderson, L.A., Huey, B., and King, M.C. 1990. Linkage of early-onset familial breast cancer to chromosome 17q21. *Science 250*:1684–1689.

Hartge, P., Struewing, J.P., Wacholder, S., Brody, L.C., and Tucker, M.A. 1999. The prevalence of common BRCA1 and BRCA2 mutations among Ashkenazi Jews. *Am. J. Hum. Genet. 64*:963–970.

Hartley, A., Rollason, T., and Spooner, D. 2000. Clear cell carcinoma of the fimbria of the fallopian tube in a BRCA1 carrier undergoing prophylactic surgery. *Clin. Oncol. (R. Coll. Radiol.) 12*:58–59.

Heintz, A.P., Odicino, F., Maisonneuve, P., Beller, U., Benedet, J.L., Creasman, W.T., Ngan, H.Y., and Pecorelli, S. 2003. Carcinoma of the ovary. *Int. J. Gynaecol. Obstet. 83 Suppl 1*:135–166.

Hogervorst, F.B., Nederlof, P.M., Gille, J.J., McElgunn, C.J., Grippeling, M., Pruntel, R., Regnerus, R., van Welsem, T., van Spaendonk, R., Menko, F.H., Kluijt, I., Dommering, C., Verhoef, S., Schouten, J.P., van't Veer, L.J., and Pals, G. 2003. Large genomic deletions and duplications in the BRCA1 gene identified by a novel quantitative method. *Cancer Res. 63*: 1449–1453.

Hogg, R., and Friedlander, M. 2004. Biology of epithelial ovarian cancer: implications for screening women at high genetic risk. *J. Clin. Oncol. 22*:1315–1327.

Jacobs, I., Davies, A.P., Bridges, J., Stabile, I., Fay, T., Lower, A., Grudzinskas, J.G., and Oram, D. 1993. Prevalence screening for ovarian cancer in postmenopausal women by CA 125 measurement and ultrasonography. *BMJ 306*:1030–1034.

Jacobs, I.J., Skates, S., Davies, A.P., Woolas, R.P., Jeyerajah, A., Weidemann, P., Sibley, K., and Oram, D.H. 1996. Risk of diagnosis of ovarian cancer after raised serum CA 125 concentration: a prospective cohort study. *BMJ 313*:1355–1358.

Jacobs, I.J., Skates, S.J., MacDonald, N., Menon, U., Rosenthal, A.N., Davies, A.P., Woolas, R., Jeyarajah, A.R., Sibley, K., Lowe, D.G., and Oram, D.H. 1999. Screening for ovarian cancer: a pilot randomised controlled trial. *Lancet 353*:1207–1210.

Jazaeri, A.A., Yee, C.J., Sotiriou, C., Brantley, K.R., Boyd, J., and Liu, E.T. 2002. Gene expression profiles of BRCA1-linked, BRCA2-linked, and sporadic ovarian cancers. *J. Natl. Cancer Inst. 94*:990–1000.

Johannsson, O.T., Ranstam, J., Borg, A., and Olsson, H. 1998. Survival of BRCA1 breast and ovarian cancer patients: a population-based study from southern Sweden. *J. Clin. Oncol. 16*:397–404.

Kauff, N.D., Satagopan, J.M., Robson, M.E., Scheuer, L., Hensley, M., Hudis, C.A., Ellis, N.A., Boyd, J., Borgen, P.I., Barakat, R.R., Norton, L., Castiel, M., Nafa, K., and Offit, K. 2002. Risk-reducing salpingo-oophorectomy in women with a BRCA1 or BRCA2 mutation. *N. Engl. J. Med. 346*:1609–1615.

Killackey, M.A., and Davis, A.R. 1993. Papillary serous carcinoma of the peritoneal surface: matched-case comparison with papillary serous ovarian carcinoma. *Gynecol. Oncol. 51*:171–174.

Laframboise, S., Nedelcu, R., Murphy, J., Cole, D.E., and Rosen, B. 2002. Use of CA-125 and ultrasound in high-risk women. *Int. J. Gynecol. Cancer 12*:86–91.

Lakhani, S.R., Manek, S., Penault-Llorca, F., Flanagan, A., Arnout, L., Merrett, S., McGuffog, L., Steele, D., Devilee, P., Klijn, J.G., Meijers-Heijboer, H., Radice, P., Pilotti, S., Nevanlinna, H., Butzow, R., Sobol, H., Jacquemier, J., Lyonet, D.S., Neuhausen, S.L., Weber, B., Wagner, T., Winqvist, R., Bignon, Y.J., Monti, F., Schmitt, F., Lenoir, G., Seitz, S., Hamman, U., Pharoah, P., Lane, G., Ponder, B., Bishop, D.T., and Easton, D.F. 2004. Pathology of ovarian cancers in BRCA1 and BRCA2 carriers. *Clin. Cancer Res. 10*:2473–2481.

Lakhani, S.R., Van De Vijver, M.J., Jacquemier, J., Anderson, T.J., Osin, P.P., McGuffog, L., and Easton, D.F. 2002. The pathology of familial breast cancer: predictive value of immunohistochemical markers estrogen receptor, progesterone receptor, HER-2, and p53 in patients with mutations in BRCA1 and BRCA2. *J. Clin. Oncol. 20*:2310–2318.

Leeper, K., Garcia, R., Swisher, E., Goff, B., Greer, B., and Paley, P. 2002. Pathologic findings in prophylactic oophorectomy specimens in high-risk women. *Gynecol. Oncol. 87*:52–56.

Levine, D.A., Argenta, P.A., Yee, C.J., Marshall, D.S., Olvera, N., Bogomolniy, F., Rahaman, J.A., Robson, M.E., Offit, K., Barakat, R.R., Soslow, R.A., and Boyd, J. 2003. Fallopian tube and primary peritoneal carcinomas associated with BRCA mutations. *J. Clin. Oncol. 21*:4222–4227.

Levine, D.A., Federici, M.G., Reuter, V.E., and Boyd, J. 2002. Cell proliferation and apoptosis in BRCA-associated hereditary ovarian cancer. *Gynecol. Oncol. 85*:431–434.

Lu, K.H., Garbe, J.E., Cramer, D.W., Welch, W.R., Niloff, J., Schrag, D., Berkowitz, R.S., and Muto, M.G. 2000. Occult ovarian tumors in women with BRCA1 or BRCA2 mutations undergoing prophylactic oophorectomy. *J. Clin. Oncol. 18*:2728–2732.

McGuire, W.P., Hoskins, W.J., Brady, M.F., Kucera, P.R., Partridge, E.E., Look, K.Y., Clarke-Pearson, D.L., and Davidson, M. 1996. Cyclophosphamide and cisplatin compared with paclitaxel and cisplatin in patients with stage III and stage IV ovarian cancer. *N. Engl. J. Med. 334*:1–6.

Meijers-Heijboer, E.J., Verhoog, L.C., Brekelmans, C.T., Seynaeve, C., Tilanus-Linthorst, M.M., Wagner, A., Dukel, L., Devilee, P., van den Ouweland, A.M., van Geel, A.N., and Klijn, J.G. 2000. Presymptomatic DNA testing and prophylactic surgery in families with a BRCA1 or BRCA2 mutation. *Lancet 355*:2015–2020.

Menon, U., Talaat, A., Jeyarajah, A.R., Rosenthal, A.N., MacDonald, N.D., Skates, S.J., Sibley, K., Oram, D.H., and Jacobs, I.J. 1999. Ultrasound assessment of ovarian cancer risk in postmenopausal women with CA125 elevation. *Br. J. Cancer 80*:1644–1647.

Miki, Y., Swensen, J., Shattuck-Eidens, D., Futreal, P.A., Harshman, K., Tavtigian, S., Liu, Q., Cochran, C., Bennett, L.M., Ding, W. *et al.* 1994. A strong candidate for the breast and ovarian cancer susceptibility gene BRCA1. *Science 266*:*66–71.*

Muto, M.G., Welch, W.R., Mok, S.C., Bandera, C.A., Fishbaugh, P.M., Tsao, S.W., Lau, C.C., Goodman, H.M., Knapp, R.C., and Berkowitz, R.S. 1995. Evidence for a multifocal origin of papillary serous carcinoma of the peritoneum. *Cancer Res. 55*:490–492.

Olivier, R.I., Lubsen-Brandsma, L.A., van Boven, H., and Van Beurden, M. 2005. Additional salpingectomy after previous prophylactic oophorectomy in high-risk women: sense or nonsense? *Gynecol. Oncol. 96*:439–443.

Olivier, R.I., Van Beurden, M., Lubsen, M.A., Rookus, M.A., Mooij, T.M., Van De Vijver, M.J., and van't Veer, L.J. 2004. Clinical outcome of prophylactic oophorectomy in BRCÀ1/BRCA2 mutation carriers and events during follow-up. *Br. J. Cancer 90*:1492–1497.

Paley, P.J., Swisher, E.M., Garcia, R.L., Agoff, S.N., Greer, B.E., Peters, K.L., and Goff, B.A. 2001. Occult cancer of the fallopian tube in BRCA-1 germline mutation carriers at prophylactic oophorectomy: a case for recommending hysterectomy at surgical prophylaxis. *Gynecol. Oncol. 80*:176–180.

Petricoin, E.F., Ardekani, A.M., Hitt, B.A., Levine, P.J., Fusaro, V.A., Steinberg, S.M., Mills, G.B., Simone, C., Fishman, D.A.,

Kohn, E.C., and Liotta, L.A. 2002. Use of proteomic patterns in serum to identify ovarian cancer. *Lancet 359*:572–577.

Piek, J.M., van Diest, P.J., Zweemer, R.P., Jansen, J.W., Poort-Keesom, R.J., Menko, F.H., Gille, J.J., Jongsma, A.P., Pals, G., Kenemans, P., and Verheijen, R.H. 2001. Dysplastic changes in prophylactically removed fallopian tubes of women predisposed to developing ovarian cancer. *J. Pathol. 195*: 451–456.

Piver, M.S., Jishi, M.F., Tsukada, Y., and Nava, G. 1993. Primary peritoneal carcinoma after prophylactic oophorectomy in women with a family history of ovarian cancer: a report of the Gilda Radner Familial Ovarian Cancer Registry. *Cancer 71*:2751–2755.

Rebbeck, T.R., Lynch, H.T., Neuhausen, S.L., Narod, S.A., Van't Veer, L., Garber, J.E., Evans, G., Isaacs, C., Daly, M.B., Matloff, E., Olopade, O.I., and Weber, B.L. 2002. Prophylactic oophorectomy in carriers of BRCA1 or BRCA2 mutations. *N. Engl. J. Med. 346*:1616–1622.

Risch, H.A., McLaughlin, J.R., Cole, D.E., Rosen, B., Bradley, L., Kwan, E., Jack, E., Vesprini, D.J., Kuperstein, G., Abrahamson, J.L., Fan, I., Wong, B., and Narod, S.A. 2001. Prevalence and penetrance of germline BRCA1 and BRCA2 mutations in a population series of 649 women with ovarian cancer. *Am. J. Hum. Genet. 68*:700–710.

Rozenberg, S., Fellemans, C., Kroll, M., and Vandromme, J. 2000. The menopause in Europe. *Int. J. Fertil. Womens Med. 45*: 182–189.

Rubin, S.C., Benjamin, I., Behbakht, K., Takahashi, H., Morgan, M.A., LiVolsi, V.A., Berchuck, A., Muto, M.G., Garber, J.E., Weber, B.L., Lynch, H.T., and Boyd, J. 1996. Clinical and pathological features of ovarian cancer in women with germ-line mutations of BRCA1. *N. Engl. J. Med. 335*: 1413–1416.

Salazar, H., Godwin, A.K., Daly, M.B., Laub, P.B., Hogan, W.M., Rosenblum, N., Boente, M.P., Lynch, H.T., and Hamilton, T.C. 1996. Microscopic benign and invasive malignant neoplasms and a cancer-prone phenotype in prophylactic oophorectomies. *J. Natl. Cancer Inst. 88*:1810–1820.

Schneider, C., Wight, E., Perucchini, D., Haller, U., and Fink, D. 2000. Primary carcinoma of the fallopian tube: a report of 19 cases with literature review. *Eur. J. Gynecol. Oncol. 21*:578–582.

Schorge, J.O., Muto, M.G., Welch, W.R., Bandera, C.A., Rubin, S.C., Bell, D.A., Berkowitz, R.S., and Mok, S.C. 1998. Molecular evidence for multifocal papillary serous carcinoma of the peritoneum in patients with germline BRCA1 mutations. *J. Natl. Cancer Inst. 90*:841–845.

Schwartz, M.D., Kaufman, E., Peshkin, B.N., Isaacs, C., Hughes, C., DeMarco, T., Finch, C., and Lerman, C. 2003. Bilateral prophylactic oophorectomy and ovarian cancer screening following BRCA1/BRCA2 mutation testing. *J. Clin. Oncol. 21*:4034–4041.

Scully, R., Young, R., and Clement, P. 2003. Tumors of the fallopian tube: histologic classification and cancer staging epithelial and mixed epithelial-mesenchymal tumors. In: Rosai, J., and Sobin, L. (eds.) *Tumors of the Ovary, Maldeveloped Gonads, Fallopian Tube, and Broad Ligament.* Washington, DC: Armed Forces Institute of Pathology, 461–476.

Struewing, J.P., Watson, P., Easton, D.F., Ponder, B.A., Lynch, H.T., and Tucker, M.A. 1995. Prophylactic oophorectomy in inherited breast/ovarian cancer families. *J. Natl. Cancer Inst. Manogr. 17*:33–35.

Thompson, D., and Easton, D. 2004. The BRCA1 and BRCA2 genes. In: Eeles, R.A., Easton, D., Ponder, B., Eng, C. (eds). *Genetic Predisposition to Cancer*. New York: Oxford University Press, 256–276.

Tobacman, J.K., Greene, M.H., Tucker, M.A., Costa, J., Kase, R., and Fraumeni, J.F., Jr. 1982. Intra-abdominal carcinomatosis after prophylactic oophorectomy in ovarian-cancer-prone families. *Lancet 2*:795–797.

van Nagell, J.R., Jr., DePriest, P.D., Reedy, M.B., Gallion, H.H., Ueland, F.R., Pavlik, E.J., and Kryscio, R.J. 2000. The efficacy of transvaginal sonographic screening in asymptomatic women at risk for ovarian cancer. *Gynecol. Oncol. 77*:350–356.

Werness, B.A., Ramus, S.J., Whittemore, A.S., Garlinghouse-Jones, K., Oakley-Girvan, I., DiCioccio, R.A., Tsukada, Y., Ponder, B.A., and Piver, M.S., 2000a. Histopathology of familial ovarian tumors in women from families with and without germline BRCA1 mutations. *Hum. Pathol. 31*:1420–1424.

Werness, B.A., Ramus, S.J., Whittemore, A.S., Garlinghouse-Jones, K., Oakley-Girvan, I., DiCioccio, R.A., Tsukada, Y., Ponder, B.A., and Piver, M.S. 2000b. Primary ovarian dysgerminoma in a patient with a germline BRCA1 mutation. *Int. J. Gynecol. Pathol. 19*:390–394.

Wick, M.R., Mills, S.E., Dehner, L.P., Bollinger, D.J., and Fechner, R.E. 1989. Serous papillary carcinomas arising from the peritoneum and ovaries: a clinicopathologic and immunohistochemical comparison. *Int. J. Gynecol. Pathol. 8*:179–188.

Woolas, R., Jacobs, I., Davies, A.P., Leake, J., Brown, C., Grudzinskas, J.G., and Oram, D. 1994. What is the true incidence of primary fallopian tube carcinoma? *Int. J. Gynecol. Cancer 4*:384–388.

Woolas, R., Smith, J., Saharnis, P., Paterson, M., and Sharp, F. 1997. Fallopian tube carcinoma: an under-recognized primary neoplasm. *Int. J. Gynecol. Cancer 7*:284–288.

Wooster, R., Bignell, G., Lancaster, J., Swift, S., Seal, S., Mangion, J., Collins, N., Gregory, S., Gumbs, C., and Micklem, G. 1995. Identification of the breast cancer susceptibility gene BRCA2. *Nature 378*:789–792.

Zweemer, R.P., van Diest, P.J., Verheijen, R.H., Ryan, A., Gille, J.J., Sijmons, R.H., Jacobs, I.J., Menko, F.H., and Kenemans, P. 2000. Molecular evidence linking primary cancer of the fallopian tube to BRCA1 germline mutations. *Gynecol. Oncol. 76*:45–50.

6

K-Ras Mutations in Serous Borderline Tumors of the Ovary

Joachim Diebold

Introduction

The Ras proteins, which are low molecular weight GTPases, function as components of the Ras-RAF-MAPK (mitogen-activated protein kinase) signal-transduction pathway that regulates differentiation and proliferation by extracellular stimuli. Normal Ras signaling can be disturbed by mutations of the *Ras* genes. Point mutations, usually concerning codons 12, 13, or 61, result in persistent activation of the Ras proteins.

They have been found in a variety of cancers with different frequencies, depending on the histologic tumor type (Waldmann and Rabes, 1996). Which of the three *Ras* genes (*K-Ras, H-Ras,* or *N-Ras*) is preferentially mutated is also dependent on the tumor type. In ovarian tumors, mutations most often involve codon 12 or 13 of K-Ras. The frequency of these K-Ras mutations strongly depends on the histologic phenotype of the neoplasms; in general the fraction of cases with mutations is higher in mucinous than in serous tumors. Regarding serous tumors, mainly the so-called borderline tumors harbor K-Ras alterations.

Serous borderline tumors of the ovary (SBOT), also called tumors of low malignant potential, are characterized by increased epithelial proliferation and structural and cytologic atypia that distinguish these tumors from serous cystadenomas of the ovary. In contrast to serous carcinomas, borderline tumors are noninvasive neoplasms (Lauchlan, 1990). However, 30–40% of patients with SBOT have bilateral or multifocal lesions at the time of diagnosis (Chambers *et al.,* 1988; Leake *et al.,* 1992). These foci comprise a spectrum from clearly benign müllerian inclusion cysts to so-called implants with strong resemblance to the ovarian tumors. Implants are subclassified into noninvasive and invasive. Presence of invasive serous implants is associated with poor prognosis (Kennedy and Hart, 1996; Kurman and Trimble, 1993). The optimal treatment of patients with extraovarian lesions of serous borderline tumors is a topic of ongoing discussion (Sutton *et al.,* 1991). Noninvasive implants show little response to conventional chemotherapy. They seem to be indolent lesions that can be stable for a long time without therapeutic intervention. In contrast, invasive implants are treated like advanced ovarian carcinomas (OCs) with peritoneal metastases.

The genesis and pathobiology of extraovarian lesions of SBOT remain enigmatic. Some investigators regard them as independent foci of serous epithelial proliferation that are derived from the mesothelial cell layer, which covers the ovarian surface and the pelvic peritoneum—the so-called secondary müllerian system (Kadar and Krumerman, 1995). In contrast, others favor the notion that extraovarian foci of SBOT are the result of metastatic spread from the ovarian tumor (Moore *et al.,* 2000). This theory may be suitable for those ovarian borderline tumors located on the surface of

Handbook of Immunohistochemistry and *in situ* Hybridization of Human Carcinomas, Volume 4: Molecular Genetics, Gastrointestinal Carcinoma, and Ovarian Carcinoma

the ovary; however, it cannot easily explain those extraovarian lesions associated with cystic ovarian borderline tumors that are clearly separated from the ovarian surface and peritoneal cavity (Segal and Hart, 1992).

In two consecutive studies we determined the frequency of K-Ras mutations in SBOT and in associated ovarian and extraovarian lesions. The investigation aimed at a better understanding of the role of Ras in SBOT. In addition, we hypothesized that analysis of the K-Ras mutation status might further help to clarify the relation of ovarian and extraovarian lesions of serous borderline tumors.

MATERIALS

Two studies were performed. In a first step, 20 serous borderline tumors were analyzed for the presence of K-Ras mutations. The mutation status was compared with results of an analysis of 7 serous cystadenomas, 6 well-differentiated serous carcinoma samples, and 11 poorly differentiated serous carcinoma samples. In a second step the investigation was extended in 10 cases. Multiple samples were taken from the ovarian tumor, contralateral tumors, and extraovarian lesions to test for intratumoral heterogeneity, monoclonality, and multifocality.

METHOD

Lasermicrodissection and DNA Extraction

Paraffin blocks bearing ovarian borderline tumor tissue or extraovarian lesions were sectioned at 2 µm thickness, mounted on microscope slides previously covered with a 1,35-µm PEN membrane (P.A.L.M. Mikrolaser Technology, Bernried, Germany), and dried at 55°C. Sections were stained with methylene blue. Microdissection was carried out by means of a laser (P.A.L.M. Mikrolaser Technology). Dissected tissue was transferred directly into 25 µl lysis buffer (50 mM Tris-HC1, pH 8.5/1 mM EDTA [ethylenediamine], pH 8.0/0.5% Tween-20/200 pg/µl proteinase K) and incubated at 55°C overnight.

Proteinase K was heat inactivated by a 10-min incubation at 95°C. Subsequently, tissue debris was pelleted by centrifugation at 14,000 rpm for 5 min, and the supernatant was transferred to a fresh Eppendorf tube. Deoxyribonucleic acid (DNA) was extracted by using the EZNA Tissue DNA extraction Kit II (Peqlab, Erlangen, Germany).

K-Ras Analysis

For denaturing gradient gel electrophoresis (DGGE), exon 1 of K-Ras was amplified by polymerase chain reaction (PCR) in a reaction mixture containing 10 mM Tris-HCl (pH 8.3), 50 mM KCl, 2 mM $MgCl_2$, 200 µM of each deoxynucleotide trisphosphate (Amersham Pharmacia, Uppsala, Sweden), 0.2 pmol/µl of each primer, and 0.025 U/µl AmpliTaq Gold (Applied Biosystems, Foster City, CA). The primer sequences have been described (Imai *et al.,* 1994). Conditions for PCR were as follows: 10 min at 94°C followed by 40–45 cycles of 94°C for 2 min, 52°C for 2 min, and 72°C for 2 min. After the final cycle another 8 min at 72°C was added. The PCR products were then run on a 10% polyacrylamide gel with a vertical denaturing gradient from 20% to 60% (100% denaturant corresponds to 7 M urea and 40% formamide). Electrophoresis was performed on a Dcode System (BioRad, Hercules, CA) at 60°C with constant voltage (150 V) for 6 hr. Finally, the gel was stained with ethidium bromide and evaluated on an ultraviolet screen.

For sequencing, the DNA was amplified under the same PCR conditions as described by Sarkar *et al.* (1995). The PCR products were purified with a PCR purification kit (Quiagen, Hilden, Germany). After cycle sequencing with a dye terminator cycle sequencing kit (Applied Biosystems) according to the manufacturer's instructions, the products were purified with centri-sep columns (Princeton Separations, Adelphia, NJ). The sequences were analyzed on an ABI PRISM 310 genetic analyzer (Applied Biosystems). For each sample up-and- down sequences were determined.

RESULTS AND DISCUSSION

K-Ras in Serous Borderline Ovarian Tumors

In 7 of 20 SBOTs (35%) a mutation of codon 12 of the K-Ras gene was detected. Four of these mutations were GGT → GTT transversions and three were GGT → GAT transitions. No mutations were found in any of the 7 serous cystadenomas. The 6 well-differentiated carcinoma samples included 2 (33%) that were mutated at codon 12, one having a GGT → GTT transversion and one having a GGT → GAT transition. No mutations were found in the poorly differentiated carcinomas.

In Table 30 the type of K-Ras mutation of 34 SBOT (including own cases) reported in the literature is summarized.

It is evident that the GGT → GTT transversion is the most frequent aberration followed by the GGT → GAT transition. Furthermore there is consensus in the literature that K-RAS mutations are particularly characteristic for the borderline type of serous ovarian tumors (Table 31).

Table 30. K-Ras Point Mutations at Codon 12 in Serous Borderline Ovarian Tumors

	Type of Mutation					
	GGT → GTT	GGT → GCT	GGT → GAT	GGT → CGT	GGT → TGT	GGT → GGC
Teneriello *et al.,* 1993			3/3 (100%)			
Mok *et al.,* 1993	7/9 (78%)		1/9 (12%)		1/9 (12%)	
Haas *et al.,* 1999	4/7 (57%)		3/7 (43%)			
Ortiz *et al.,* 2001	2/4 (50%)			2/4 (50%)		
Alvarez *et al.,* 2001	2/3 (67%)		1/3 (33%)			
Diebold *et al.,* 2003	5/8 (63%)	1/8 (13%)	1/8 (13%)			1/8 (13%)
Total	20/34 (59%)	1/34 (3%)	9/34 (26%)	2/34 (6%)	1/34 (3%)	1/34 (3%)

Regarding carcinomas, our observations show that Ras mutations are often associated with a prominent papillary growth pattern and little nuclear atypia (i.e., well-differentiated tumors). For serous ovarian tumors the results do not support the assumption of a progression of serous ovarian low malignant potential (LMP) tumors to poorly differentiated carcinomas. Rather, a *de novo* development of highly malignant OCs seems to be probable. However, progression of some serous LMP tumors to well-differentiated serous carcinomas seems to occur. This result has been also supported by a study by Singer *et al.* (2003) that arrived at the same conclusion by analyzing BRAF mutations in ovarian tumors.

K-Ras in Associated Ovarian and Extraovarian Lesions of Serous Borderline Tumors of the Ovary

To elucidate the role of K-Ras mutations in associated ovarian and extraovarian lesions of SBOT, a second investigation comprised 8 cases of SBOT with known K-Ras mutation (RAS+) and 2 cases with wild-type K-Ras (Ras-) for comparison (Diebold *et al.,* 2003). A total of 97 samples of 58 paraffin-embedded and laser-microdissected ovarian and extraovarian lesions (10 ovarian tumors, 8 ovarian tumors, 25 noninvasive implants, 15 müllerian inclusion cysts) were analyzed. Five of 8 Ras+ ovarian borderline tumors contained a GGT → GTT mutation (Gly to Val), 2 ovarian tumors had a GGT → GAT mutation (Gly to Asp), and 1 case had a GGT → GCT mutation (Gly to Ala) at codon 12 of the *K-Ras* gene.

To address the question of whether papillary serous epithelial lesions of borderline malignancy consist of polyclonal or monoclonal cell populations, multiple samples from the same site were analyzed in 16 ovarian and extraovarian lesions. Between 2 and 5 samples were studied per lesion. In 12 of 14 ovarian borderline tumors and in 2 of 2 extraovarian implants identical K-Ras mutations could be found in different areas of the same lesion. The demonstration of identical mutations in the vast majority of cases clearly suggests that SBOT and their implants consist of monoclonal cell populations, which is in agreement with the results of X-chromosome inactivation studies (Gu *et al.,* 2001; Lu *et al.,* 1998). Although it has been suggested that induction of müllerian metaplasia may be an early step in the development of SBOT (Feeley and Wells, 2001), these data show that SBOT and associated implants do not represent reactive alterations of the secondary müllerian epithelium but clearly are neoplastic lesions.

Table 31. K-Ras Mutations in Serous Ovarian Tumors

	Serous Cystadenoma	Serous Borderline Ovarian Tumors	Serous Carcinoma
Varras *et al.,* 1999	0/8 (0%)	1/1 (100%)	7/29 (24%)
Mandai *et al.,* 1998	0/2 (0%)	0/2 (0%)	1/22 (5%)
Cuatrecasas *et al.,* 1998	4/30 (14%)	3/11 (27%)	15/38 (39%)
Ichikawa *et al.,* 1994	0/22 (0%)	0/8 (0%)	0/17 (6%)
Teneriello *et al.,* 1993	0/11 (0%)	3/11 (27%)	1/21 (5%)
Mok *et al.,* 1993		9/25 (36%)	1/14 (29%)
Haas *et al.,* 1999	0/7 (0%)	7/20 (35%)	2/17 (11%)
Total	4/80 (5%)	23/78 (29%)	31/15 (21%)

In 7 of 8 RAS+ cases additional lesions could be analyzed. In 6 borderline tumors, tumor tissue was available from the second ovary. All contralateral tumors (6/6) harbored an identical mutation. In 1 case (case 322) the bilateral cystic borderline tumor was characterized by a GGT → GCT mutation, and a separate surface borderline tumor component contained a GGT → GTT mutation in addition. Extraovarian lesions were available in 5 RAS+ cases. In 4 of these, RAS mutations were also found in implants (15/21 implants, 71%) and in müllerian inclusion cysts (3/12 lesions, 25%). The extraovarian mutations were always identical to the one in the ovary (18/18, 100%).

The demonstration of identical K-Ras mutations in inclusion cysts and implants by us and one other group (Alvarez *et al.,* 2001) suggests that they may be related like metastases of invasive carcinomas to their primary in the ovary. In this regard, it is noteworthy that Moore *et al.* (2000) found a statistically significant association of müllerian inclusion cysts in lymph nodes with SBOT but not with other tumors of the female genital tract. They concluded that this might indicate a metastatic mechanism of development. However, a field effect acting on the pelvic peritoneum could conceivably lead to independent multifocal proliferation of müllerian epithelium, too. The identification of identical K-Ras mutations at different localizations is not completely incompatible with multifocality. Because the spectrum of K-Ras mutations in SBOT is small (see Table 30) this mutation might develop independently in separate lesions by chance. Supporting this notion, we could demonstrate a codon 12 glycine-to-valine mutation in an implant associated with one SBOT without Ras mutation.

Investigations of advanced SBOT that determined the X-chromosome inactivation pattern suggested multifocal development of bilateral tumors and extraovarian implants. Lu *et al.* (1998) found different patterns of X-chromosome inactivation in three of eight cases. However, in five cases the inactivation pattern was identical at different sites, which can have happened by chance or may suggest a common origin. Using the same assay, Gu *et al.* (2001) found different inactivation patterns in six of seven tumors comparing implants and ovarian lesions and in three of seven bilateral ovarian tumors. Although these findings indicate multifocality, they do not rule out that at least some lesions are derived from a common progenitor cell. In addition, the technique of X-chromosome inactivation analysis is only applicable to a minority of cases of SBOT.

In case 322 with two different K-Ras mutations, the glycine-to-alanine mutation of the bilateral cystic borderline tumor was also found in five implants located next to the uterus on both sides, whereas the glycine-to-valine mutation of the surface borderline tumor of the right ovary was also detected in four implants on the right uterine and parasalpingeal peritoneum and in two müllerian inclusion cysts in right pelvic lymph nodes. In this puzzling case at least the lesions containing the relatively rare glycine-to-alanine mutation seem to be related to the surface SBOT of the right ovary. Furthermore, the other cases of the present study, which demonstrated rarer types of codon 12 K-Ras mutations (glycine to asparagines and glycine to alanine), both in the ovarian tumor and in extraovarian lesions, are difficult to explain by multifocality.

CONCLUDING REMARKS

Regarding our observations, the designation of extraovarian lesions as "implants" may be justified in at least some cases. The determination of the clonal origin of contralateral and peritoneal lesions of SBOT may have important clinical implications. The prognosis of advanced SBOT is much more favorable than for invasive OCs. However, a 15-year mortality rate of 27% has been reported (Leake *et al.,* 1992). Our data could be interpreted as indication that some patients might benefit from heightened surveillance, adjuvant therapy, or both. However, at present chemotherapy is reserved for those women with invasive implants. It has not been proved that adjuvant therapy has a positive effect in patients with noninvasive implants (Sutton *et al.,* 1991). Apparently because of their low proliferation rate, SBOTs have an indolent course and respond poorly to chemotherapy. Therefore, even if some extraovarian lesions represent true metastases, adjuvant chemotherapy is not necessarily indicated.

The results of the present study and published data suggest that on the molecular genetic level SBOTs are a heterogenous group of tumors. K-Ras mutations are found only in one-third of cases. However, Singer *et al.* (2003) found BRAF point mutations in an additional 28% of SBOT. Ras and RAF mutations were mutually exclusive phenomena. Thus, the Ras–RAF–ERK–MAPK pathway is activated in the majority of cases, suggesting a pivotal role of Ras signaling for the development of serous epithelial lesions of ovarian surface epithelium and extraovarian peritoneal epithelium.

The pathways leading to the development of extraovarian manifestations of the disease might be variable. As evidenced by one case in our series, multifocal development and metastatic spread from the ovarian tumor might even occur at the same time. Apparently, these two possible pathways are not mutually exclusive. Even without having solved this question it can be speculated that blocking K-Ras–BRAF signaling may be an effective therapeutic option in the future for patients with advanced SBOT.

References

Alvarez, A.A., Moore, W.F., Robboy, S.J., Bentley, R.C., Gumbs, C., Futreal, P.A., and Berchuck, A. 2001. K-ras mutations in Müllerian inclusion cysts associated with serous borderline tumors of the ovary. *Gynecol. Oncol. 80*:201–206.

Chambers, J.T., Merino, M.J., Kohorn, E.I., and Schwartz, P.E. 1988. Borderline ovarian tumors. *Am. J. Obstet. Gynecol. 37*:1088–1094.

Cuatrecasas, M., Erill, N., Musulen, E., Costa, I., Matias-Guiu, X., and Prat, J. 1998. K-ras mutations in nonmucinous ovarian epithelial tumors: a molecular analysis and clinicopathologic study of 144 patients. *Cancer 82*:1088–1095.

Diebold, J., Seemüller, F., and Löhrs, U. 2003. K-ras mutations in ovarian and extraovarian lesions of serous tumors of borderline malignancy. *Lab. Invest. 83*:251–258.

Feeley, K.M., and Wells, M. 2001. Precursor lesions of ovarian epithelial malignancy. *Histopathol. 38*:87–95.

Gu, J., Roth, L.M., Younger, C., Michael, H., Abdul-Karim, F.W., Zhang, S., Ulbright, T.M., Eble, J.N., and Cheng, L. 2001. Molecular evidence for the independent origin of extra-ovarian papillary serous tumors of low malignant potential. *J. Natl. Cancer Inst. 93*:1147–1152.

Haas, C.J., Diebold, J., Hirschmann, A., Rohrbach, H., and Löhrs, U. 1999. In serous ovarian neoplasms the frequency of K-ras mutations correlates with their malignant potential. *Virchows Arch. 434*:117–120.

Ichikawa, Y., Nishida, M., Suzuki, H., Yoshida, S., Tsunoda, H., Kubo, T., Uchida, K., Miwa, M. 1994. Mutation of K-ras protooncogene is associated with histological subtypes in human mucinous ovarian tumors. *Cancer Res. 54*:33–35.

Imai, M., Hoshi, T., and Ogawa, K. 1994. K-ras codon 12 mutations in biliary tract tumours detected by polymerase chain reaction denaturing gradient gel electrophoresis. *Cancer 73*:2727–2733.

Kadar, N., and Krumerman, M. 1995. Possible metaplastic origin of lymph node "metastases" in serous ovarian tumor of low malignant potential (borderline serous tumor). *Gynecol. Oncol. 59*:394–397.

Kennedy, A.W., and Hart, W.R. 1996. Ovarian papillary serous tumors of low malignant potential (serous borderline tumors): a long-term follow-up study, including patients with microinvasion, lymph node metastasis, and transformation to invasive serous carcinoma. *Cancer 78*:278–286.

Kurman, R.J., and Trimble, C.L. 1993. The behaviour of serous tumors of low malignant potential: are they ever malignant? *Int. J. Gynecol. Pathol. 12*:120–127.

Lauchlan, S.C. 1990. Non-invasive ovarian carcinoma. *Int. J. Gynecol. Pathol. 9*:158–169.

Leake, J.F., Currie, J.L., Rosenshein, N.B., and Woodruff, J.D. 1992. Long-term follow-up of serous ovarian tumors of low malignant potential. *Gynecol. Oncol. 47*:150–158.

Lu, K.H., Bell, D.A., Welch, W.R., Berkowitz, R.S., and Mok, S.C. 1998. Evidence for the multifocal origin of bilateral and advanced human serous borderline ovarian tumors. *Cancer Res. 58*:2328–2330.

Mandai, M., Konishi, I., Kuroda, H., Komatsu, T., Yamamoto, S., Nanbu, K., Matsushita, K., Fukumoto, M., Yamabe, H., Mori, T. 1998. Heterogeneous distribution of K-ras-mutated epithelia in mucinous ovarian tumors with special reference to histopathology. *Hum. Pathol. 29*:34–40.

Mok, S.H., Bell, D.A., Knapp, R.C., Fishbaugh, P.M., Welch, W.R., Muto, M.G., Berkowitz, R.S., and Tsao, S.W. 1993. Mutation of K-ras protooncogene in human ovarian epithelial tumors of borderline malignancy. *Cancer Res. 53*:1489–1492.

Moore, W.F., Bentley, R.C., Berchuck, A., and Robboy, S.J. 2000. Some Müllerian inclusion cysts in lymph nodes may sometimes be metastasis from serous borderline tumors of the ovary. *Am. J. Surg. Pathol. 24*:710–718.

Ortiz, B.H., Ailawadi, M., Colitti, C., Muto, M.G., Deavers, M., Silva, E.G., Berkowitz, R.S., Mok, S.C., and Gershenson, D.M. 2001. Second primary or recurrence? Comparative patterns of p53 and K-ras mutations suggest that serous borderline ovarian tumors and subsequent serous carcinomas are unrelated tumors. *Cancer Res. 61*:7264–7267.

Sarkar, F.H., Valdivieso, M., Borders, J., Yao, K.L., Raval, M.M.T., Madan, S.K., Sreepathi, P., Shimoyama, R., Steiger, Z., Visscher, D.W., and Crissman, J.D. 1995. A universal method for the mutational analysis of K-ras and p53 gene in non-small cell lung cancer using formalin-fixed paraffin-embedded tissue. *Diagn. Mol. Pathol. 4*:266–273.

Segal, G.H., and Hart, W.R. 1992. Ovarian serous tumors of low malignant potential (serous borderline tumors). The relationship of exophytic surface tumor to peritoneal "implants." *Am. J. Surg. Pathol. 16*:577–583.

Singer, G., Oldt, R., Cohen, Y., Wang, B.G., Sidransky, D., Kurman, R.J., and Shih, I.M. 2003. Mutations in BRAF and KRAS characterize the development of low-grade ovarian serous carcinoma. *J. Natl. Cancer Inst. 19*:484–486.

Sutton, G.P., Bundy, B.N., Omura, G.A., Yordan, E.L., Beecham, J.B., and Bonfiglio, T. 1991. Stage III ovarian tumors of low malignant potential treated with cisplatin combination therapy (a Gynecologic Oncology Group study). *Gynecol. Oncol. 41*:230–233.

Teneriello, M.G., Ebina, M., Linnoila, R.I., Henry, M., Nash, J.D., Park, R.C., and Birrer, M.J. 1993. p53 and K-ras gene mutations in epithelial ovarian neoplasms. *Cancer Res. 53*: 3103–3108.

Varras, M.N., Sourvinos, G., Diakomanolis, E., Koumantakis, E., Flouris, G.A., Lekka-Katsouli, J., Michalas, S., and Spandidos, D.A. 1999. Detection and clinical correlations of ras gene mutations in human ovarian tumors. *Oncology 56*:89–96.

Waldmann, V., and Rabes, H.M. 1996. What's new in ras genes? Physiological role of ras genes in signal transduction and significance of ras gene activation in tumourigenesis. *Pathol. Res. Pract. 192*:883–891.

This Page Intentionally Left Blank

7

Role of Immunohistochemical Expression of Ki-67 in Ovarian Carcinoma

Yoshihiro Ohishi, Eisuke Kaneki, Sadafumi Tamiya, Yoshinao Oda, Toshio Hirakawa, Shingo Miyamoto, Tsunehisa Kaku, Hitoo Nakano, and Masazumi Tsuneyoshi

Introduction

The malignant phenotype of carcinoma can be characterized based on a number of criteria, including extreme proliferative activity, drug resistance, or invasive or metastatic potency. Extreme proliferative activity is one of the most important measures of the malignant potency of carcinoma. Ki-67 antigen has been used as an important tool for evaluation of the proliferative activity because this nuclear protein is preferentially expressed during all active phases of the cell cycle (G1, S, G2, and M phase). The percentage of Ki-67–positive neoplastic cells characterizes benign–borderline–malignant serous neoplasm of ovary, cystadenoma (0–2.1%), atypical proliferating tumor (1.3–7%), and cystadenocarcinoma (4.7–20.3%) (Frigerio *et al.,* 1997).

Cattoretti *et al.* (1992) introduced a monoclonal antibody (MIB 1) against recombinant parts of the Ki-67 antigen (MIB 1) for detecting proliferating cells in microwave-processed, formalin–fixed paraffin sections. Because they had successfully applied this new method to sections obtained from paraffin blocks stored for a long time, the assessment of cell kinetics through the detection of Ki-67 antigen became possible on archival material collected in histopathology departments all over the world.

In the field of ovarian cancer, there have been various reports regarding the correlation between Ki-67 expression and clinical feature, but the results are still confusing. Some investigators reported that high expression of Ki-67 is correlated with poor prognosis (Garzetti *et al.,* 1995), and another one reported opposite results (Itamochi *et al.,* 2002). More current data have shown that aberration of the components of cell cycle checkpoints, which play an important role in cell proliferation, is a common feature of many neoplasms. The first checkpoint of the cell cycle controls the transition between G1 and S phase, beyond which mitogenic signaling is no longer required and the cell is committed to complete a cycle of replication. The major factors controlling cell transition to the S phase are the D-type cyclins and cyclin-dependent kinases (CDKs) 4 and 6 (McKay *et al.,* 2002; Sherr, 1996). Complexes formed between cyclin D1 and either CDK4 or CDK6 are activated by CDK-activating kinase, leading to hyperphosphorylation of retinoblastoma protein (pRb) and derepression

Handbook of Immunohistochemistry and *in situ* Hybridization of Human Carcinomas, Volume 4: Molecular Genetics, Gastrointestinal Carcinoma, and Ovarian Carcinoma

of E2F-responsive promotors. The net effect of this pathway is transcription of genes necessary for progression through the S phase (Sellers and Kaelin, 1997). In contrast, the CIP (e.g., p2l, p27) and INK (e.g., p16) families of CDK inhibitors (CKIs) negatively regulate the action of cyclin/CDK complexes, preventing cell cycle progression (Grana and Reddy, 1995; McKay *et al.,* 2002).

In the field of ovarian cancer, loss of CKIs such as p16 or p21 expression is reported to be associated with prognosis or chemoresponse (Havrilesky *et al.,* 2001). Konstantinidou *et al.* (2003) demonstrated that diminished pRb levels are related to several clinicopathologic indicators of aggressiveness in ovarian adenocarcinomas. They also demonstrated that pRb expression coupled with the percentage of Ki-67–positive cells is a better prognostic marker than pRb, Ki-67, or other G1 interacting proteins. Although several publications have evaluated the role of cell cycle proteins or Ki-67 expression for ovarian carcinoma (OC), little is known in detail.

The aim of this manuscript is 1) to clarify the optimal method of immunohistochemistry (IHC) for Ki-67 antigen using formalin-fixed and paraffin-embedded tissue specimen, and 2) to clarify the value of the Ki-67 expression in patients with (OC) using the previously mentioned method. First, we attempted to set up the optimal method of Ki-67 immunostaining by using tonsilar tissue as a positive control tissue specimen. Two different methods of antigen retrieval such as enzyme predigestion or heat treatment were tested. Second, using the previously mentioned optimal method, we evaluated the Ki-67 expression of the tumor samples taken from 29 patients with serous papillary adenocarcinoma treated by debulking surgery and platinum-based chemotherapy, and the results were compared with prognosis. We also examined the expression of p16, cyclin D1, and pRb, which are the G1–S phase cell cycle checkpoint proteins, to clarify the co-regulation of them. Furthermore, we evaluated expression of the proteins (Ki-67, p16, cyclin D1, and pRb) in the tumor samples taken from 20 patients with clear cell adenocarcinoma to compare with that of serous phenotype.

MATERIALS AND METHODS

Patients and Specimens

A total of 49 patients with primary untreated OC (30 patients with serous papillary adenocarcinoma and 20 patients with clear cell adenocarcinoma), who had undergone debulking surgery before chemotherapy at Kyushu University Hospital between 1994 and 2000, were examined. The performance status of all the patients was less than grade 1. Patients with borderline malignancy, mixed epithelial carcinoma, and peritoneal carcinoma were excluded from this study. All the patients were staged according to the International Federation of Obstetrics and Gynecology (FIGO) classification (International Federation of Gynecology and Obstetrics, 1987) and were treated with chemotherapy containing at least cisplatin or carboplatin. Of the 29 patients with serous papillary adenocarcinoma, 23 were treated by cisplatin (CDDP) (70 mg/m^2 body surface/day 1), epirubicin (Epi) (50 mg/m^2 body surface/day 1) and cyclophosphamide (Cyclo) (500 mg/m^2 body surface/day 1), whereas 6 were treated with paclitaxel (180 mg/m^2 body surface/day 1) and carboplatin (CBDCA/day 1). The dose of CBDCA was calculated by Calverts formula (Calvert *et al.,* 1989):

$$\text{dose (mg/body)} = \text{target area under curve (AUC)} \times (\text{glomerular filtration rate [GFR]} + 25)$$

We set the target AUC at 5 mg/ml × min (Calvert *et al.,* 1989). All 20 patients with clear cell adenocarcinoma were treated with cisplatin (60 mg/m^2 body surface/day 1) and irinotecan hydrochloride (CPT- 11) (60 mg/m^2 body surface/day 1, 8, and 15). Each course comprised 28 days. For the patients with advanced-stage cancer, chemotherapy was repeated for a maximum of 6 courses, provided the treatment continued to be effective. The effect of chemotherapy was evaluated 3–4 weeks after each administration of chemotherapy by ultrasonography or computed tomography. After chemotherapy, all patients were followed up every 2 months for the first year, every 3 months for the next year, every 4 months for the next year, every 6 months for the next 2 years, and every year thereafter. For routine histologic studies, adequate numbers of 3 μm sections of tissue specimens were fixed with 10% formalin, embedded in paraffin, and stained with hematoxylin and eosin. Tumors were classified according to World Health Organization classification (World Health Organization, 1979) and were graded into grade 1, 2, or 3 as proposed by Silverberg (2000).

Immunohistochemistry

The following monoclonal antibodies were used as the primary antibody: anti-Ki-67 (MIB-1, [Dako, Glostrup, Denmark]). Optimal dilutions were determined by testing serial 1:2 dilutions of each antibody from 1:25 to 1:400, using tissue specimens of chronic tonsilitis. Sections of tissue samples fixed with 10% formalin and embedded in paraffin were cut at 4 μm. The following procedures were tested. The same procedures were performed for the following antibodies: anti-p16 (F-12 [Santa Cruz Biotechnology, Inc., Santa Cruz CA]), anti-cyclin D1 (P2D11F11 [Novocastra Laboratories Ltd,

Newcastle, UK]), anti-pRb (G3-245 [Fujisawa Pharmaceutical Co., Ltd., Tokyo, Japan]).

Procedure A: Universal Immuno-Peroxidase Polymer Method

1. Cut and mount sections on slides (MAS-coated slides, Matsunami, Osaka, Japan).
2. Deparaffinize sections and rehydrate to distilled water. Xylene (5 min) 2× and 99% alcohol (5 min) 2×.
3. Place sections in 3% hydrogen peroxide/methanol (15 ml of 30% hydrogen peroxide is mixed with 150 ml of methanol) for 30 min at room temperature. This step is necessary to inhibit the effect of endogenous peroxidase.
4. Wash slides in phosphate buffered saline (PBS) for 5 min.
5. Pretreat for antigen retrieval (as stated elsewhere*).
6. Wash slides in running water for 5 min.
7. Wash slides in PBS for 5 min.
8. Cover sections with primary antibody for 12 hr at 4°C. Slides should be placed in a moist chamber so the sections will not dry up.
9. Wash slides in PBS buffer for 3× 5 min.
10. Cover sections with 2 drops of secondary antibody labeled with horseradish peroxidase (Histofine Simple Stain PO [M], Nichirei, Tokyo) for 20 min at room temperature. Slides should be placed on the waterish paper on a plate with a tight-fitting cap so sections will not dry up.
11. Wash slides in PBS buffer for 3× 5 min.
12. Incubate slides in 3,3′-diaminobenzidine (DAB); DAB reaction solution is composed of 40 mg of DAB, 150 ml of PBS buffer, and a few drops of 3% hydrogen peroxide.
13. Wash 5× in distilled water for 30 sec each time.
14. Counterstain with hematoxylin for 30 sec.
15. Wash slides in running water for 25 min.
16. Perform dehydration procedure (95% ethanol, 99% ethanol, 100% ethanol, xylene 3×).
17. Coverslip and mount.

Procedure B: Streptavidin–Biotin–Peroxidase (SAB-PO) Method with Endogenous Biotin Blocking Procedure

1–7. Same procedures as Procedure A.

a. Inhibition of nonspecific adsorption of secondary antibody taken from immunized rabbit.

i. Place sections in 10% of normal rabbit serum (10% Normal Rabbit Serum, Nichirei, Tokyo) for 10 min.

ii. Wash slides in PBS for 5 min.

b. Procedure for blocking endogenous biotin.

i. Cover sections with 2 drops of reagent A of endogenous avidin/biotin blocking kit (Nichirei, Tokyo).

ii. Incubate for 10 min at room temperature.

iii. Wash slides in PBS buffer for 3× 5 min.

iv. Cover sections with 2 drops of reagent B of endogenous avidin/biotin blocking kit (Nichirei, Tokyo).

v. Incubate for 10 min at room temperature.

vi. Wash slides in PBS buffer for 3× 5 min.

8–9. Same procedure as Procedure A.

c. SAB-PO method following procedure instead of **Step 10.**

i. Cover sections with 2 drops of biotinylated secondary antibody (Biotinylated Anti-Mouse IgG + IgA + IgM, Nichirei, Tokyo).

ii. Wash slides in PBS buffer for 3× 5 min.

iii. Cover sections with 2 drops of solution of peroxidase-conjugated streptavidin (Peroxidase Conjugated Streptavidin, Nichirei, Tokyo).

iv. Incubate for 20 min at room temperature.

10–17. Same procedures as Procedure A.

*Following I-III pretreatment procedures were tested.

I. Trypsin pretreatment. Incubate slides in the trypsin solution composed of 50 mg of trypsin and 50 ml of PBS for 30 min in the constant-temperature bath at 37°C.

II. Microwave heating using H2800 microwave processor (Energy Beam Science, Inc., Agawan, MA). Incubate slides in the PBS buffer for 15 min at 99°C using-microwave processor. Citric acid buffer (pH 6.0, 0.01 M) and citric acid + Tween 20 (Katayama Chemistry, Osaka, Japan) buffer (pH 6.0, 0.01 M + 0.01% Tween 20) were also tested.

III. No pretreatment. Pretreatment procedures were omitted for one section.

Evaluation of Immunohistochemistry

Nuclear staining in tumor cells was regarded as positive in sections subjected to immunohistochemical staining. Cytoplasmic reactivity was disregarded, and only nuclear staining above a cytoplasmic background was considered as evidence of expression because cytoplasmic staining is controversial and regarded as nonspecific by some investigators (Reed *et al.,* 1995).

Sections immunostained for p16, cyclin D1, and pRb were scored semi-quantitatively by scanning the entire section and estimating the percentage of stained tumor cell nuclei. More than 5% of positive tumor cells were defined as positive expression according to previously published reports (McKay *et al.,* 2002). All immunoreactive nuclei were regarded as positive, irrespective of

the intensity of staining. The Ki-67 labeling index (Ki-67 LI) was caluculated as the percentage of positive nuclei in 300–500 tumor cells. We have selected the area with highest density of immunoreactive cells in each sections for counting. The Ki-67 LI above (below) 30 was regarded as high (low) expression (Marcelli *et al.,* 1996). Ki-67 expression was also assessed solely by the distribution of positive cells; if the distribution of the positive cells is more (less) than 50% areas of the tissue specimens, the case was regarded as diffuse (focal) irrespective of the density of immunoreactive cells.

Statistical Analysis

We used the statistical software StatView version 4.5 (Abacus Concepts Inc., Berkeley, CA). Contingency tables were analyzed by chi-square statistics or Fisher's exact test. The differences of Ki-67 LI between groups were analyzed by Mann-Whitney U test. The differences in progression-free survival were analyzed using log-rank statistics. The influences of possible confounding factors for progression-free survival were analyzed by Cox proportional hazards regression model, nonstepwise method. Only p values <0.05 were considered significant.

RESULTS

Determination of Optimal Methods for Immunohistochemistry

Optimal dilution of Ki-67, p16, pRb, and cyclin D1 antibodies were as follows: (1:100, 1:50, 1:800, and 1:25, respectively).

Optimal pretreatments for antigen retrieval were as follows:

Ki-67: Microwave heating, citric acid (pH 6.0, 0.01 M) + Tween 20 (0.01%) buffer, 20 min.
p16: Microwave heating, citric acid (pH 6.0, 0.01 M) buffer, 20 min.
pRb: Microwave irradiation, citric acid (pH 6.0, 0.01 M) + Tween 20 (0.01%) buffer, 15 min.
Cyclin D1: Microwave irradiation, citric acid (pH 6.0, 0.01 M) buffer, 30 min.

Figure 58 shows the tonsilar tissue with lymphoid follicles of which germinal centers were highlighted by Ki-67 immunostaining using the previously mentioned optimal method (A, B). Representative sections of OC stained by Ki-67 were also presented (C, D).

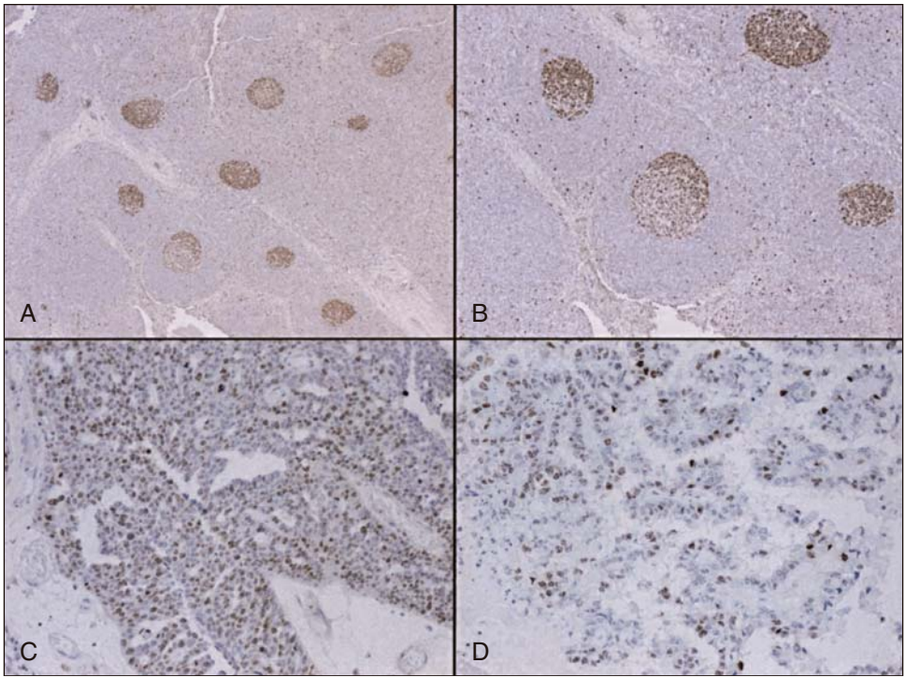

Figure 58. Ki-67 expression in tonsilar **(A)** 20X, **(B)** 40X, and ovarian carcinoma tissue **(C)** serous **(D)** clear cell. The dark zone of the germinal center was highlighted by immunoreactive nuclei in tonsilar tissue. Both serous and clear cell adenocarcinoma were diffusely stained.

Patients

Of the 29 patients with ovarian serous papillary adenocarcinoma, median progression-free survival was 432 days (range, 0–1939), and median survival was 839 days (range, 86–1939**)**.

Immunohistochemistry

Immunohistochemical analysis of p16, cyclin D1, pRb, and Ki-67 protein expression was carried out on 49 primary OC specimens (29 for serous/20 for clear cell). Briefly, the number of samples with positive/negative results of IHC for p16, cyclin D1, and pRb was as follows: p16 (+: 35/total, 19/serous, 16/clear, −: 14/total, 10/serous, 4/clear), pRb (+: 38/t, 20/s, 18/c, −: 11/t, 9/s, 2/c), cyclin D1 (all of 49 samples were negative). Although all of the results for cyclin D1 were negative using 5% cutoff; 10 of 49 samples had minor areas of cyclin D1–positive nuclei (6/serous, 4/clear cell), and we classified these 10 samples into cyclin D1–present group. The remaining 39 were put into the cyclin D1 absent group in this manuscript. Various levels of Ki-67 expression were observed in both serous and clear cell phenotype (LI: total; median, 22.1, 0–75.1, serous; median, 23.4, 0–62.5, clear cell; median, 20.9, 1.2–75.1). The number of the samples with high/low or diffuse/focal categories was as follows: high 22/t, 14/s, 8/c; low: 27/t, 15/s, 12/c; diffuse: 26/t, 14/s, 12/c; focal: 23/t, 15/s, 8/c.

Correlation between Cell Cycle Proteins and Ki-67 Expression

Cell Cycle Proteins and Ki-67 LI

In clear cell phenotype, Ki-67 LI in the p16-positive group showed a significantly higher correlation than those in p16-negative group (Mann-Whitney-U test: $p = 0.038$). There was no significance or tendency in any other data sets in clear cell phenotype.

In serous phenotype, Ki-67 LI in cyclin D1–absent group were significantly higher than those in cyclin D1–present group (Mann-Whitney-U test: $p = 0.041$). There was no significance or tendency in any other data sets in serous phenotype.

After analyzing all 49 samples, no significance or tendency was found in any data sets.

Cell Cycle Proteins and Ki-67 High/Low Category

There was no significance or tendency in any other data sets in serous and clear cell phenotype and total samples.

Cell Cycle Proteins and Ki-67 Diffuse/Focal Category

There was no significance or tendency in any other data sets in serous and clear cell phenotype and total samples.

Correlation between Ki-67 Labeling Index and Ki-67 Diffuse/Focal Category

The Ki-67 LI in diffuse Ki-67 category was significantly higher than that in focal Ki-67 category in both serous and clear cell phenotype (Mann-Whitney-U test: $p = 0.0024$, and $p = 0.025$, respectively).

Clinicopathologic Data and Cell Cycle Proteins or Ki-67 Expression

In this chapter, patient's age, FIGO stage, histologic grade, the size of the residual lesion, and chemotherapy regimen were included for possible confounding factors. Cell cycle proteins and Ki-67 expression were compared with these factors in serous and clear cell phenotype, respectively, and there was no significant correlation in any data sets.

Cell Cycle Proteins/Ki-67 Expression and Progression-Free Survival Analysis

Progression-free survival analyses were performed in only 29 patients with serous phenotype. The interval of progression-free survival of patients with diffuse Ki-67 expression was significantly longer than that found in patients with focal Ki-67 expression (log-rank statistic: $p = 0.0072$). The other parameters, such as p16, pRb, cyclin D1, high Ki-67 LI, had no significance. There were no independent prognostic factors found by using multivariate analysis.

Comparison between Serous and Clear Cell Phenotype

There was no significant correlation in any data sets between serous and clear cell phenotype.

DISCUSSION

In the current manuscript, we have set up the optimal method for immunohistochemical expression of Ki-67. Serial dilutions of the antibody and various types of

pretreatment for antigen retrieval were tested, and we defined that the optimal dilution was 1:100, and the optimal pretreatment was microwave heating with citric acid + Tween 20 buffer. The sections of chronic tonsilitis were used as the positive control tissue for Ki-67 expression because chronic tonsilitis was histologically characterized by lymphoid follicles and the cells in the dark zone of the germinal center are known to proliferate rapidly. This optimal method highlights the dark zone of lymphoid follicles and indicates that IHC of Ki-67 expression, by our assay, could demonstrate the localization of rapidly proliferating cells.

There are various methods of antigen retrieval such as enzyme predigestion or microwave irradiation. Enzyme predigestion using proteases, such as trypsin or pepsin, is believed to knock down the steric hindrance as a result of intramolecular or intermolecular cross-linkage. We tested the effectiveness of trypsin predigestion for IHC of Ki-67 and found that ineffective. This suggests that trypsin-sensitive cross-linkage is not the reason for Ki-67 antigen masking after formalin fixation. Contrary to enzyme predigestion, microwave heating, which was introduced by Shi *et al.* (1991), could successfully unmask the Ki-67 antigen. Knocking down the steric hindrance caused by molecular cross-linkage may underly this method. Microwave heating can be substituted by autoclave heating for the purpose of high-temperature treatment (Hayat, 2002).

Although we introduced the universal immunoperoxidase polymer method, whose reaction is not mediated by streptavidin–biotin binding, streptavidin–biotin complex peroxidase method (SAB-PO method) is also widely used. If using the SAB-PO method, we should bear in mind that endogenous biotin confounds the judgment for positive staining. Endogenous biotin is known to be present in hepatocytes, renal tubules, and colonic mucosal epithelium. In our experiences, high-temperature heat treatment by microwave irradiation enhances the effect of endogenous biotin, and streptavidin–biotin blocking kit (Nichirei, Tokyo) can eliminate such confounding. Using skim milk as the diluted solution for primary antibodies has also been reported to reduce the effects of endogenous biotin. In addition, we recommend that optimization should be performed in each situation because the optimal procedures we introduced earlier are illustrative only.

Second, we evaluated the Ki-67 expression in primary OC samples using the previous optimal immunohistochemical methods and then compared these results with clinical outcome. Cell cycle regulators such as p16, pRb, and cyclin D1 were also tested. The data was compared with Ki-67 expression and clinical data.

In the current manuscript, we demonstrate that Ki-67 LI in p16-positive group was significantly higher than those in p16-negative group in clear cell phenotype. Generally, p16 protein is known to be a cell cycle inhibitor, which inhibits the cell cycle G1–S transition by inhibition of CDK activation, and some researchers have reported that loss of p16 expression was associated with tumorigenesis or prognosis in a variety of malignant tumors (Liggett and Sidransky, 1998). In such tumors, the aberrant expression of p16 is regarded as the cause of increased proliferative activity. However, Milde-Langosch *et al*. has reported that overexpression of p16 in breast cancer is associated with a more malignant phenotype, and a significant association of p16 staining with high Ki-67 expression was found (Milde-Langosch *et al.,* 2001). Our results are consistent with the latter, and we suppose that the positive correlation between p16 and Ki-67 expression may be explained by the existence of a homeostatic feedback mechanism that may prevent the inapropriate proliferative activity, as described in previous literature (Doki *et al.,* 1997; Migita *et al.,* 2002), although this is a matter for speculation. In latter cases, including ours, p16 expression may be the results of abnormally increased proliferative activity of these tumors. The possible homeostatic feedback regulation between Ki-67 and p16 may be phenotype-specific regulation for clear cell phenotype because the correlation was not observed in the serous phenotype.

In serous phenotype, Ki-67 LI in cyclin D1-absent group showed a significantly higher correlation than in cyclin D1-present group. Cyclin D1 is well-known to be a positive regulator of the G1–S phase cell cycle checkpoint, and a correlation between the overexpression of cycin D1 and cellular proliferative activity has been noted in some human cancers (Sugimachi *et al.,* 2001). However, Shoker *et al.* have reported that there was negative association between cyclin D1 and Ki-67 expression in breast cancer (Shoker *et al.,* 2001). These negative correlations, including ours, may be explained by the hypothesis of negative feedback regulation, although this is a mere assumption. Our result conflicts with the general perception, and further analysis is necessary to resolve the contradiction.

As for the prognosis, only diffuse Ki-67 expression group showed significant correlation with longer progression-free survival in patients with serous phenotype. We did not analyze progression-free survival for 20 patients with clear cell adenocarcinoma because 14 patients were stage I and all of them were presently progression free. It is impossible for patients who are stage I to determine whether favorable clinical outcome depends on the lack of aggressive biological behavior, excellent drug response, or excellent surgical removal. Therefore, we only used the data of clear cell phenotype for evaluation of the differences between serous and clear cell phenotype.

In general, Ki-67 expression is known to be a useful measure of proliferative activity, and, in a variety of tumors, high expression is reported to correlate with a more malignant phenotype or worse prognosis. In the field of OC, the Ki-67 expression has been reported to escalate during tumor progression through benign cystadenoma–borderline–adenocarcinoma sequence, and higher expression of Ki-67 expression has been reported to be an independent worse prognostic factor (Garzetti *et al.,* 1995) that is consistent with the general perception that the more proliferative activity, the worse the prognosis. However, Itamochi *et al.* demonstrated that low proliferation activity measured by Ki-67 expression level is associated with chemoresistance and poor prognosis in OC (Itamochi *et al.,* 2002). They demonstrated that 1) Ki-67 LI of clear cell adenocarcinoma was significantly lower than that of serous adenocarcinoma, 2) the estimated 5-year survival rate for patients with clear cell carcinoma was significantly poorer than that for those with serous adenocarcinoma, 3) the estimated 5-year survival rate for higher Ki-67 LI patients was significantly greater than that for lower Ki-67 LI patients in clear cell carcinoma, and 4) Ki-67 LI of chemoresponders was significantly higher than that of nonresponders in both serous and clear cell phenotype.

It is known that rapidly proliferating cells are the most chemosensitive, whereas cells that slowly proliferate are generally less sensitive to cytotoxic agents (Itamochi *et al.,* 2002); and intracellular drug accumulation has been reported to decrease in resting cells (Dimanche-Boitrel *et al.,* 1992). It is also known that platinum-based combination chemotherapy plays a major role in the treatment of OC and that resistance to anti-cancer drugs is a major obstacle in attempts to improve clinical outcome.

Considering Itamochi's results and the general perception, low proliferation activity measured by Ki-67 LI is associated with chemoresistance, which is a major obstacle for the favorable outcome of patients with ovarian carcinoma. Additionally, the chemoresistant nature of clear cell phenotype may be explained by low proliferative activity.

In our manuscript, only the diffuse Ki-67 expression group showed significant correlation with longer progression-free survival in patients with serous phenotype, whereas the high Ki-67 LI group did not. Regarding only the data for Ki-67 LI, Itamochi's results were not the same as ours. From a broader perspective, however, we could say that Itamochi's results have a certain similarity with ours in that high or diffuse Ki-67 expression is associated with favorable prognosis, probably as a result of effectiveness of chemotherapy. Furthermore, we demonstrated that Ki-67 LI of the diffuse Ki-67 group was significantly higher than that of the local Ki-67 group, suggesting that classification as diffuse or focal has a certain amount of correlation with proliferative activity measured by conventional Ki-67 LI method. We believe that the distribution of the positive cells can reflect the proliferative activity of the tumor cells in the whole section examined, and LI can reflect the proliferative activity of the tumor cells in the selected areas. We believe that both methods for evaluating Ki-67 expression (classifying into diffuse or focal category/LI) can represent the proliferative activity of the tumor, and evaluating whole areas of sections for the distribution of Ki-67 positive cells can also be useful from the viewpoint of prognostic marker for advanced ovarian cancer after chemotherapy.

It is natural that proliferative activity itself can be a component of multifactorial malignant biological behavior of cancer, and, in fact, most papers demonstrate that high expression of Ki-67 correlates with poor prognosis or malignant phenotype. However, chemoresistance is also a component of multifactorial malignant biological behavior, particularly in tumors whose major treatment is chemotherapy. It is intresting that the more proliferative activity, the more likely it is for the tumor to be sensitive, and this may lead to the results that high Ki-67 expression correlates with favorable outcome. Taking the previous facts into consideration, the effect of proliferative activity on prognosis may be conflicting. Further analysis is necessary to resolve this contradiction. According to our data, diffuse staining of Ki-67 antigen, which may represent high proliferative activity, may be a useful marker for a longer progression-free interval in patients with advanced serous papillary adenocarcinoma treated by platinum-based chemotherapy.

As for the comparison between clear and serous phenotype, there was no significant correlation in any data sets. Contrary to our data, Itamochi *et al.* (2002) demonstrated that there is significantly lower Ki-67 LI in clear cell phenotype than that in serous phenotype. One possible reason may be the difference of the selected areas for counting immunoreactive cells.

In conclusion, we have demonstrated the possible optimal immunohistochemical method for Ki-67 expression. Using the previous optimal method, we have also shown that the diffuse Ki-67 expression group indicated a significantly longer interval of progression-free survival than the focal Ki-67 expression group in patients with advanced ovarian cancer. Furthermore, phenotype-specific correlation between cell cycle proteins and Ki-67 expression may exist.

We should bear in mind that the diffuse/focal categorization for Ki-67 expression is not conventional,

and further analysis is necessary to clarify the utility of this category as a prognostic marker.

References

Calvert, A.H., Newell, D.R., Gumbrell, L.A., O'Reilly, S., Burnell, M., Boxall, F.E., Siddik, Z.H., Judson, I.R., Gore, M.E., and Wiltshaw, E. 1989. Carboplatin dosage: prospective evaluation of a simple formula based on renal function. *J. Clin. Oncol. 7*:1748–1756.

Cattoretti, G., Becker, M.H., Key, G., Duchrow, M., Schluter, C., Galle, J., and Gerdes, J. 1992. Monoclonal antibodies against recombinant parts of the Ki-67 antigen (MIB 1 and MIB 3) detect proliferating cells in microwave-processed formalin-fixed paraffin sections. *J. Pathol. 168*:357–363.

Dimanche-Boitrel, M.T., Pelletier, H., Genne, P., Petit, J.M., Le Grimellec, C., Canal, P., Ardiet, C., Bastian, G., and Chauffert, B. 1992. Confluence-dependent resistance in human colon cancer cells: role of reduced drug accumulation and low intrinsic chemosensitivity of resting cells. *Int. J. Cancer 50*: 677–682.

Doki, Y., Imoto, M., Han, E.K., Sgambato, A., and Weinstein, I.B. 1997. Increased expression of the P27KIP1 protein in human esophageal cancer cell lines that over-express cyclin D1. *Carcinogenesis 18*:1139–1148.

Frigerio, L., Agnello, A., Sassi, I., Mangili, F., Taccagni, G., Mariani, A., and Ferrari, A. 1997. Adjuvant role of MIB 1 index in differentiating serous ovarian tumors—preliminary report. *Anticancer Res. 17*:1287–1292.

Garzetti, G.G., Ciavattini, A., Goteri, G., De Nictolis, M., Stramazzotti, D., Lucarini, G., and Biagini, G. 1995. Ki-67 antigen immunostaining (MIB 1 monoclonal antibody) in serous ovarian tumors: index of proliferative activity with prognostic significance. *Gynecol. Oncol. 56*:169–174.

Grana, X., and Reddy, E.P. 1995. Cell cycle control in mammalian cells: role of cyclins, cyclin dependent kinases (CDKs), growth suppressor genes and cyclin-dependent kinase inhibitors (CKIs). *Oncogene 11*:211–219.

Havrilesky, L.J., Alvarez, A.A., Whitaker, R.S., Marks, J.R., and Berchuck, A. 2001. Loss of expression of the p16 tumor suppressor gene is more frequent in advanced ovarian cancers lacking p53 mutations. *Gynecol. Oncol. 83*:491–500.

Hayat, M.A. 2002. *Microscopy, Immunohistochemistry and Antigen Retrieval Methods*. New York: Kluwer Academic/ Plenum Publishers.

International Federation of Gynecology and Obstetrics. 1987. Changes in definitions of clinical staging for cancer of the cervix and ovary. *Am. J. Obstet. Gynecol. 156*:236–241.

Itamochi, H., Kigawa, J., Sugiyama, T., Kikuchi, Y., Suzuki, M., and Terakawa, N. 2002. Low proliferation activity may be associated with chemoresistance in clear cell carcinoma of the ovary. *Obstet. Gynecol. 100*:281–287.

Konstantinidou, A.E., Korkolopoulou, P., Vassilopoulos, I., Tsenga, A., Thymara, I., Agapitos, E., Patsouris, E., and Davaris, P. 2003. Reduced retinoblastoma gene protein to Ki-67 ratio is an adverse prognostic indicator for ovarian adenocarcinoma patients. *Gynecol. Oncol. 88*:369–378.

Liggett, W.H. Jr., and Sidransky, D. 1998. Role of the p16 tumor suppressor gene in cancer. *J. Clin. Oncol. 3*:1197–1206.

Marcelli, A.R., Demopoulos, R.I., Goswami, S., and Mittal, K.R. 1996. Comparison of p53 and MIB 1 expression in benign and borderline areas of ovarian serous tumors. *Int. J. Gynecol. Pathol. 15*:39–44.

McKay, J.A., Douglas, J.J., Ross, V.G., Curran, S., Loane, J.F., Ahmed, F.Y., Cassidy, J., McLeod, H.L., and Murray, G.I. 2002. Analysis of key cell-cycle checkpoint proteins in colorectal tumours. *J. Pathol. 196*:386–393.

Migita, T., Oda, Y., Naito, S., and Tsuneyoshi, M. 2002. Low expression of p27KIP1 is associated with tumor size and poor prognosis in patients with renal cell carcinoma. *Cancer 94*: 973–979.

Milde-Langosch, K., Bamberger, A.M., Rieck, G., Kelp, B., and Loning, T. 2001. Overexpression of the p16 cell cycle inhibitor in breast cancer is associated with a more malignant phenotype. *Breast Cancer Res. Treat. 67*:61–70.

Reed, J.A., Loganzo, F., Jr., Shea, C.R., Walker, G.J., Flores, J.F., Glendening, J.M., Bogdany, J.K., Shiel, M.J., Haluska, F.G., and Fountain, J.W. 1995. Loss of expression of the p16/cyclin-dependent kinase inhibitor 2 tumor suppressor gene in melanocytic lesions correlates with invasive stage of tumor progression. *Cancer Res. 55*:2713–2718.

Sellers, W.R., and Kaelin, W.G. 1997. Role of the retinoblastoma protein in the pathogenesis of human cancer. *J. Clin. Oncol. 15*: 3301–3312.

Sherr, C.S. 1996. Cancer cell cycles. *Science 274*:1672–1677.

Shi, S.R., Key, M.E., and Kalra, K.L. 1991. Antigen retrieval in formalin-fixed, paraffin-embedded tissues: an enhancement method for immunohistochemical staining based on microwave oven heating of tissue sections. *J. Histochem. Cytochem. 39*: 741–748.

Shoker, B.S., Jarvis, C., Davies, M.P., Iqbal, M., Sibson, D.R., and Sloane, J.P. 2001. Immunodetectable cyclin D(1) is associated with oestrogen receptor but not Ki-67 in normal, cancerous and precancerous breast lesions. *Br. J. Cancer 84*: 1064–1069.

Silverberg, S.G. 2000. Histopathologic grading of ovarian carcinoma: a review and proposal. *Int. J. Gynecol. Pathol. 19*:7–15.

Sugimachi, K., Aishima, S., Taguchi, K., Tanaka, S., Shimada, M., Kajiyama, K., Sugimachi, K., and Tsuneyoshi, M. 2001. The role of overexpression and gene amplification of cyclin D1 in intrahepatic cholangiocarcinoma. *J. Hepatol. 35*:74–79.

World Health Organization. 1979. *WHO Handbook for Reporting Results of Cancer Treatment*. Geneva, Switzerland: World Health Organization.

8

Role of Expression of Estrogen Receptor β, Proliferating Cell Nuclear Antigen, and p53 in Ovarian Granulosa Cell Tumors

Stefania Staibano and Gaetano De Rosa

Introduction

Ovarian granulosa cell tumor (OGCT) represents the largest group of sex-cord stromal tumors and comprises 1.5–3% of primary ovarian malignancies (Costa *et al.,* 1994; Savage *et al.,* 1998; Scully, 1997). These tumors are almost always unilateral (>95%) and localized in the ovary (Miller *et al.,* 1997). Two different histologic subtypes of OGCTs are described: the "adult" (OGCTA) and "juvenile" (OGCTJ) forms (Kurman, 1989; Scully, 1999; Serov *et al.,* 1973; Sternberg, 1994). The former represents 95% of all OGCTs (Costa *et al.,* 1994; Savage *et al.,* 1998). The adult form of this tumor may arise after menopause, the highest incidence occurring between ages 50 to 55 years (Young and Scully, 2002), but it may be diagnosed before puberty and sometimes during childbearing age.

Cases of OGCTJ are generally diagnosed during the first two decades of life, and most patients present with isosexual precocity (Rosai, 1996). Histologically, this subgroup is characterized by larger tumor cells and more frequent nuclear atypia and mitotic activity with respect to the adult form (Rosai, 1996).

Clinically, endocrine changes related to increased estrogen production are frequently observed in OGCTA (in about three-fourths of cases) (Rosai, 1996), whereas only two-thirds of OGCTJ are associated with endocrine derangement (Young *et al.,* 2002). Usually, both subtypes of OGCT are immunoreactive for inhibin, a peptide hormone normally produced by ovarian granulosa cells (Flemming *et al.,* 1995). These tumors may show heterogeneous genetic aberrations, only partially known. Up until now, mainly numeric chromosomal aberrations have been described. A comprehensive study on paraffin-embedded material of 20 OGCTS, (17 adult, 3 juvenile) (Mayr *et al.,* 2002) confirm earlier reports that trisomy 12 and 14 are frequent aberrations; however, monosomy 22 seemingly is even more prevalent, revealing a distinctive pattern of cytogenetic alterations in OGCT.

Surgery is required for definitive tissue diagnosis, staging, and tumor debulking. In older women, a total abdominal hysterectomy and bilateral salpingo-oophorectomy usually are performed. In women of childbearing age, a more conservative unilateral salpingo-oophorectomy may be performed, assuming that careful

Handbook of Immunohistochemistry and *in situ* Hybridization of Human Carcinomas, Volume 4: Molecular Genetics, Gastrointestinal Carcinoma, and Ovarian Carcinoma

staging reveals that the disease has not extended outside the involved ovary (Schumer and Cannistra, 2003).

Most cases of OGCT are characterized by a relatively good outcome, with a trend toward late relapse, metastasis, or both. However, some tumors behave aggressively and some tend to recur many years after the initial diagnosis. Five-year survival figures are not accurate predictors of permanent cure: metastases have been reported in a percentage varying from 7–53% in a 5-year interval, and studies encompassing a long-term follow-up have shown high mortality rates, with about 50% of death for disease within 20 years of diagnosis. Stage is the most important prognostic factor, with a higher risk of relapse being associated with stages II–IV disease. In addition, patients with stage I disease associated with features such as large tumor size, high mitotic index, tumor rupture, or more than 40 years of age at the time of diagnosis may also be at higher risk of adverse clinical behavior. Nevertheless, to date none of these parameters can supply accurate indications on the biological behavior of OGCTs (Costa *et al.,* 1994; Savage *et al.,* 1998; Schumer and Cannistra, 2003; Young *et al.,* 2002).

Proliferative indices and microvessel density have been studied to determine possible valuable methods to assess the outcome of a patient with an OGCT. Unfortunately, angiogenesis did not seem to be a useful determinant parameter of a possible aggressive behavior (Juric *et al.,* 2001). These findings support instead the importance of proliferative factors, beyond tumor size and histologic patterns, as possible prognostic indicators for estimating the biologic behavior of patients with OGCT.

In the ovary, which is the principal source of estrogens and one of their target organs, cell proliferation is strongly influenced by estrogens. Estrogens exert their wide range of functions through two estrogen receptors (ERα and ERβ) that are encoded by separate genes (Enmark *et al.,* 1997). These two receptors, which share both structural and functional homology, are members of the steroid/thyroid/retinoid superfamily of ligand-dependent transcription factors (Matthews and Gustafsson, 2003).

The major site of *estrogen receptor β* (*ERβ*) *gene* expression is the ovary, where its expression clearly predominates over that of ERα and is localized, in particular, in granulosa cells of the developing follicle (Enmark *et al.,* 1997; Kuiper *et al.,* 1997). It has been suggested then that ERβ constitutes the main mediator of estrogen effects on growth and maturation of the ovarian follicles (Sar and Welsch, 1999).

Expression of ER has been demonstrated in different benign and malignant ovarian tumors (Lanita, 1984; Toppila *et al.,* 1986). Nevertheless, data on the relationship between ER and ovarian tumor progression are still not conclusive. In particular, the localization of ERβ prevalently in granulosa cells has stimulated great interest, both for its physiologic role and for the eventual involvement in the multistep neoplastic process in estrogen-target organs.

We sought to evaluate immunohistochemically the ERβ expression in a selected series of granulosa cell tumors of the ovary and to compare the findings with the expression of proliferating cell nuclear antigen (PCNA), p53 protein, and follow-up data of patients. The aim of our study was to determine the role of these parameters in the prognostic evaluation of OGCT.

MATERIALS

1. Fixative: 10% neutral formol-saline: 100 ml of 40% formaldehyde, 900 ml of distilled water; 35 g of anhydrous dihydrogen phosphate (NaH_2PO_4); 6.5 g of anhydrous disodium-hydrogen-phosphate (Na_2HPO_4). Adjust pH using 1 N HCl and 1 N NaOH.
2. Tris buffered saline (TBS): hydroxymethyl-aminomethane hydrochloride; distilled water; HCl 1 N.
3. Blocking solution: nonimmune horse serum (Dakopatts, Hamburg, Germany); Tris/bovine serum albumine (1%).
4. Sodium citrate buffer, pH 6.0: trisodium citrate; distilled water; 1.0 M HC1 heated for 5 min in a Moulinex FM A735A.
5. 850 W microwave oven: Moulinex FM A735A.
6. 3% H_2O_2: 30% hydrogen peroxide, Fisher Scientific, Pittsburgh, PA (200 ml: 30% hydrogen peroxide, 20 ml; distilled water, 180 ml).
7. Primary antibodies: ERβ: polyclonal rabbit antibody, PAI310, directed against a synthetic peptide corresponding to C-terminal amino acids 467–485 of mouse ERβ, Affinity Bioreagents, Inc., Golden, CO; anti-ERα (monoclonal, 1D5) Dako Corp., Carpinteria, CA; PCNA: (monoclonal, PC10) DBA Italia, Milan; p53: (monoclonal, NCL-p53-CM1), Ylem, Italia.
8. Secondary antibodies: Biotinylated rabbit F(Ab′)2 fragment of anti-mouse immunoglobulin G (IgG) (or goat anti-rabbit for polyclonal Ab) (Dako).
9. Streptavidin conjugated with horseradish peroxidase (Dako).
10. DAB: liquid Dako DAB Chromagen, containing 0.02% H_2O_2 (Dako).
11. Hematoxylin Allegience (VWR), cat # 72711, Richard Allen.
12. Mounting medium, Eukitt, Kindler GmbH & Co, Freiburg, Germany.

METHODS

1. Cut 4 μm thick sections and place them onto poly-L-lysine (or gelatin)-coated slides, and dry overnight at 50°C.

2. Warm paraffinized tissue sections: 20 min, 40°C.

3. Deparaffinize with xylene, 5 min (2×), room temperature.

4. Dip and blot 2 min (10×), room temperature.

5. Tris buffered saline: Add 30.5 g of Tris (hydroxymethylaminomethane hydrochloride) to 4 L of distilled H_2O. Add 185.3 ml of HCl 1 N. Adjust pH using HCl 1 N. This made up to 5 L with distilled H_2O, magnetically stirred in a Coplin jar.

6. Dip and blot 2 min (10×), room temperature: 100% ethanol.

7. Dip and blot 2 min (10×), room temperature: 95% aqueous ethanol.

8. Dip and blot 2 min (10×), room temperature: 80% aqueous ethanol.

9. Dip and blot 2 min (10×) room temperature: de-ionized water.

10. Dip and blot 2 min (10×), room temperature: TBS.

11. Quench tissue peroxidase, 15 min, room temperature, 3% H_2O_2 in distilled water.

12. Antigen retrieval: 40 min, 40°C: sections floated with 0.01 mol/L sodium-citrate buffer, pH 6.0 (add 2.94 g of trisodium citrate to 1 L of distilled water. Adjust pH using 1.0 M HCl), heated for 5 min in a Moulinex FM A735A, 850 W microwave oven.

13. Wash: 2 min, room temperature, TBS.

14. Block nonspecific bindings: 30 min, room temperature: nonimmune horse serum (1:20, Dakopatts) diluted in Tris/bovine serum albumin (1%) for 25 min.

Hold slides horizontally to limit nonspecific edge staining of the sections. Wipe excess reagent from around tissue section. Do not rinse sections with buffer.

15. Primary antibodies: (16 hr in a moist chamber, 4°C). Antibody diluted in Tris with 1 drop of Dako protein blocker/ml: ERβ: 10 μg/ml; ERα: 2 μg/ml (the Optimal working dilution of each antibody was determined by incubating sections with varying concentrations of antibody, ranging from 0.1 to 10 μg/ml); PCNA: 1:200; p53: 1:100. Hold slides horizontally. As a rule, 150 μl of diluted primary antibody solution is applied to each tissue section. Perform negative controls by replacing the appropriate primary antibody with preimmune serum (isotype-matched IgG serum) to allow for the assessment of the nonspecific binding of the secondary antibody. Normalize the protein concentration of the normal mouse (or rabbit) serum to the protein concentration of the primary antibody. Incubate for 1 hr at room temperature. Positive controls: for ERα and ERβ, normal ovarian tissue; for PCNA: palatine tonsil; for p53: low-differentiated breast cancer (or colon cancer).

16. Wash: 2 min, room temperature: TBS (hold slides horizontally).

17. Secondary antibody: 30 min, room temperature: Biotinylated rabbit F(Ab′) 2 fragment of anti-mouse IgG, 1:200 (or goat anti-rabbit) diluted in Tris. Hold slides horizontally.

18. Wash: 2 min, room temperature: TBS (hold slides horizontally).

19. Peroxidase: 30 min, room temperature: Streptavidine–biotin complex: 1:200 in Tris (streptavidin conjugated with horseradish peroxidase). Hold slides horizontally.

20. Wash: 2 min, room temperature: TBS (hold slides horizontally).

21. Peroxidase substrate: 6 min, room temperature: DAB (liquid, 3,3′-diaminobenzidine reagent from Dako), hold slides horizontally. Incubate in the dark.

22. Wash: 3 min, room temperature: Distilled tap water, magnetically stirred distilled water in a Coplin jar.

23. Counterstaining: 45 sec, room temperature: Modified Harris hematoxylin.

24. Wash: 3 min, room temperature: Distilled tap water. Rinse until water is clear.

25. Dehydrate: Dip and blot, 3 min, room temperature: 95% Aqueous ethanol.

26. Dip and blot: 3 min (3×), room temperature: 100% ethanol.

27. Dip and blot: 5 min (2×), room temperature: xylene.

28. Mount and dry slides: 20 min, room temperature: Eukitt.

29. Evaluate staining localization: ERα and ERβ: nuclear; PCNA: it is dependent on the cell cycle stage: G0: no staining, G1: nuclear, 1+ above the background, S: nuclear, intense, G2: nuclear + cytoplasmic, 2+ above the background, M: cytoplasmic, granular, P53 protein: nuclear (wild-type p53 protein cannot be detected by immunohistochemistry in normal, undamaged cells. The presence of immunohistochemically detectable p53 levels is always associated with genetic mutations or abnormal stabilization of the protein; Levine *et al.,* 1991).

30. For each antibody, evaluate semi-quantitatively the immunostaining, as follows: 0 (absence of staining) to + (up to 30%), ++ (> 30–60%), +++ (more than 60%).

31. Statistical analysis: k-statistics for interobserver agreement (a k coefficient greater than 0.75 denotes excellent reproducibility, a k value between 0.4 and 0.75 denotes moderate reproducibility, and a k value below 0.4 denotes marginal or poor reproducibility; Landis and Koch, 1997; Chi square test or Fisher's exact test, for categorical variables; Kruskal–Wallis–Anova one-way analysis of variance to compare more than two groups of parameters; nonparametric Spearman's coefficient to establish the significance among associations.

RESULTS

Clinical-Pathologic Findings

The age of patients ranged from 1 up to 63 years (mean age: 36.43 years). The tumors involved the left ovary in 20 cases and the right ovary in 10 cases. Monolateral salpingo-oophorectomy was performed in 22 cases, and a hysterectomy with bilateral ovariectomy was performed in 8 cases. All the tumors were clinically staged as IA FIGO (International Federation of Gynecology and Obstetrics; Staibano *et al.,* 2003).

The largest diameter of tumors (LTD) ranged from 1 to 25 cm (mean LTD: 8.3 cm). Grossly, a combination of cystic and solid areas was observed. Cystic spaces were prevalently filled by serous liquid, with blood-filled spaces frequently observed in OGCTJ.

Histopathologically, 19 cases were diagnosed as OGCTA and 11 cases as OGCTJ. The interobserver reproducibility of the diagnosis was excellent (κ coefficient: 0.90). In OGCTA, the pattern of growth was microfollicular, macrofollicular, and trabecular in 14 cases and solid (diffuse) in 5 cases. The characteristic nuclear grooves were always observed.

The OGCTJ group showed prevalently a lobular pattern of growth, with frequent macrocystic and microcystic areas lined by stratified neoplastic cells. Rarely, myxoid areas were found, in which neoplastic large cells with hyperchromatic nuclei were observed. Nuclear grooves were clearly detectable only in three cases. Areas of stromal cell luteinization were observed in all OGCT cases. Cytologic atypia was found slight in 56.6% of cases, moderate in 36.6%, and severe in 6.6% of tumors.

Mitotic index (MI) ranged from 3 up to 20 mitoses/10 HPF (high power field; mean value: 9.96 mitoses/10 HPF). The follow-up time ranged from 2 years to 15 years (mean follow-up: 5.39 years). At the end of follow-up, 90% of patients (n = 27) were alive, in two cases with omental metastasis. In 3 cases (10%), patients died after having developed omental and hepatic metastasis (respectively at 12, 24, and 48 months after diagnosis).

Immunohistochemistry

Estrogen Receptor Alpha

Controls.

ERα expression was observed in stromal, thecal, and interstitial cells and rarely in granulosa cells of the antral follicle of control ovaries.

OGCT

ERα was not expressed in 27 cases of OGCT examined. Three cases (all OGCT of adult type, OGCTA) showed only a focal, low expression (+/–).

Estrogen Receptor Beta

Controls.

ERβ expression was found in granulosa cells of primary, secondary, and mature (preovulatory) follicles (++/+++). The intensity of immunoreactivity was higher (+++) in late stages of follicle maturation. Most of the atresic follicles, on the contrary, did not show ERβ positivity. Thecal, interstitial, and germinal cells and germinal epithelium were found negative.

OGCT

ERβ expression was scored as +++ in 7 cases (23.3%) (Figure 59A), all OGCTA; ++ in 10 cases (33.3%), 6 OGCTA and 4 OGCT of juvenile type (OGCTJ); + in 8 cases (26.6%, 3 OGCTA and 5 OGCTJ); 0 in four cases (13.3%) (see Figure 59D), 3 OGCTA, and 2 OGCTJ.

PCNA Expression (Proliferation Index)

The proliferation index (PI) was scored, according to the nuclear positivity for PCNA, as + in 16 cases (53.3%, 13 OGCTA and 3 OGCTJ, see Figure 59B); ++ in 8 cases (26.6%, 3 OGCTA and 5 OGCTJ), and +++ in 6 cases (20%, 3 OGCTA and 3 OGCTJ, see Figure 59E).

p53

p53 protein expression was scored as + in 7 cases (23.3%, 2 OGCTA and 5 OGCTJ); ++ in 1 case of OGCTA (3.33%); +++ in 4 cases (13.3%, 2 OGCTA and 2 OGCTJ) (see Figure 59F), and 0 in 18 cases (60%), 14 OGCTA, and 4 OGCTJ (see Figure 59C).

Statistical Analysis Results

The agreement level for the interobserver evaluations, expressed by the κ coefficient, was 0.9 for histologic diagnosis and was comprised of between 0.7 and 0.75 for the semi-quantitative evaluation of immunohistochemical staining for all the antibodies used in the study.

A positive correlation emerged between mitotic rate and PCNA positivity ($p < 0.05$) and between low PCNA levels and absence of p53 overexpression ($p < 0.05$) in both the subgroups of tumors. An inverse correlation was found between overexpression of ERβ and the occurrence of metastasis or death from disease ($p < 0.05$). High PCNA values and p53 overexpression were directly associated with the occurrence of metastasis or death ($p < 0.05$), as well as the absence of ERβ expression ($p < 0.01$). In particular, OGCTJ presented a significant p53 overexpression and high values of PCNA. In all OGCT, an inverse correlation was found between high expression of ERβ and overexpression of p53 and PCNA ($p < 0.05$). Of great relevance is the finding that among the four sections examined for each tumor, we found minimal, nonsignificant differences among

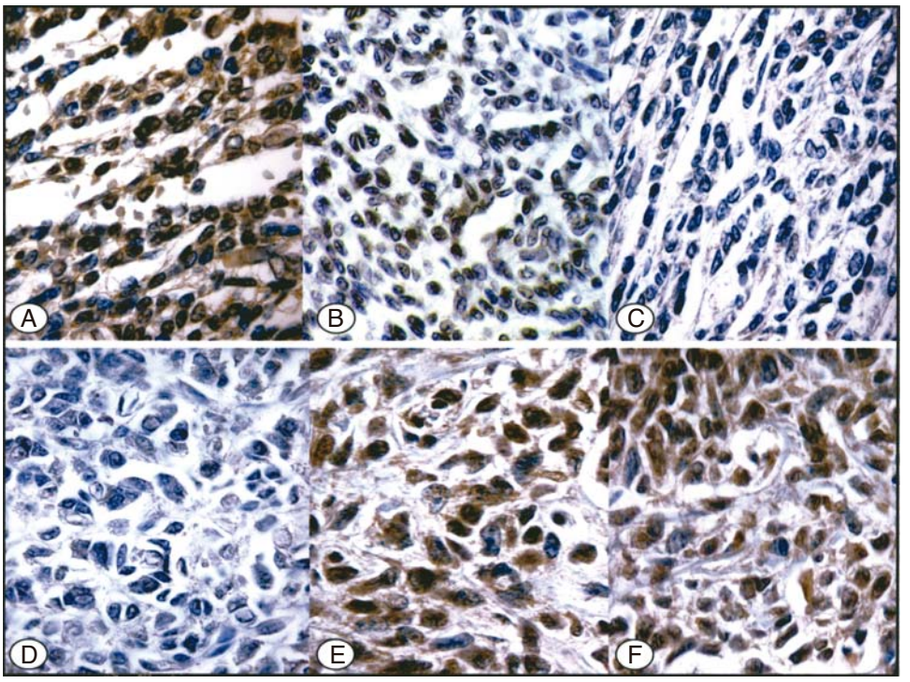

Figure 59. **A:** Ovarian granulosa cell tumor, adult histotype (OGCTA): most of neoplastic cells show immunostaining for estrogen receptor beta (ERβ) (immunoperoxidase, 400X). **B:** Ovarian granulosa cell tumor, adult histotype (OGCTA): only a minority of neoplastic cells show immunostaining for proliferating cells nuclear antigen (PCNA) (immunoperoxidase, 400X). **C:** Ovarian granulosa cell tumor, adult histotype (OGCTA): absent immunopositivity of neoplastic cells for p53 protein (immunoperoxidase, 400X). **D:** Ovarian granulosa cell tumor, juvenile-type (OGCTJ): neoplastic cells show absence of immunostaining for estrogen receptor beta (ERβ) (immunoperoxidase, 400X). **E:** Ovarian granulosa cell tumor, juvenile-type (OGCTJ): the majority of neoplastic cells show immunostaining for proliferating cells nuclear antigen (PCNA) (immunoperoxidase, 400X). **F:** Ovarian granulosa cell tumor, juvenile-type (OGCTJ): most of neoplastic cells show immunostaining for p53 protein (immunoperoxidase, 400X).

the counts. *This finding indicates the absence of significant intratumoral heterogeneity in OCGT of our series.* There was no significant difference in clinical behavior of tumors for age of patients, endocrine state, or LTD.

DISCUSSION

Ovarian granulosa cell tumors behave unpredictably. Patients with stage I disease may suffer recurrences many years after surgery, and histopathologic evaluation of the primary tumor offers only a few clues. Grading, in particular, is largely ineffective (Costa *et al.,* 1996). The factors involved in the pathogenesis of OGCT still remain unclear. Despite the attempts made to correlate histologic and clinicopathologic parameters with their biological behavior, there is still the need to find sensible and reliable prognostic markers for these tumors. Cellular atypia, pattern of growth, and mitotic rate, generally considered features of unfavorable outcome, have no actual discriminating value, influencing only partially the prognosis (Young *et al.,* 2002).

The identification of a second estrogen receptor gene *(ERβ),* expressed predominantly in ovarian granulosa cells, has dramatically changed our understanding of the biological functions of estrogens and the mechanisms through which they bring about them (Hurst *et al.,* 1995; Pettersson *et al.,* 2001). Until 1995, in fact, it was assumed that there was only one ER, responsible for mediating all of the biological effects of natural and synthetic estrogens and anti-estrogens (Greene *et al.,* 1984; Jensen, 1962; Kumar *et al.,* 1987; Nilsson *et al.,* 2001; Stumpf, 1969; Suzuki *et al.,* 1994; Webster *et al.,* 1988). This hypothesis contrasted with that observed for other members of the nuclear receptor superfamily, where multiple forms have been reported (Katzenellenbogen and Korach, 1997). In 1996, a second ER, ERβ, was cloned from a rat prostate cDNA (complementary deoxyribonucleic acid) library (Kuiper, 1996). How had

this second ER eluded investigators for so many years? A possible explanation may be that only a limited number of major estrogen target cell cDNA libraries had been screened (Katzenellenbogen and Korach, 1997). Since then, several groups have cloned ERβ from various species (Enmark *et al.,* 1997; Tremblay *et al.,* 1997) and have identified several ERβ isoforms (Chu and Fuller, 1997; Sar and Welsch, 1999; Petersen *et al.,* 1998).

The discovery of ERβ has forced a reevaluation of the biology of estrogen in normal human tissues as in their neoplastic counterparts (Nilsson *et al.,* 2001; Foegh and Ramwell, 1998). It is well-known that the binding of a ligand to ER triggers conformational changes in the receptor, leading to a number of events, changes in the rate of transcription of estrogen-regulated genes; nonetheless, these events and the order in which they occur in the overall process are only partially understood (Nilsson *et al.,* 2001; Ogawa *et al.,* 1998). They include receptor dimerization, receptor–DNA interaction, recruitment of and interaction with co-activators and other transcription factors, and formation of a preinitiation complex (Nilsson *et al.,* 2001; Grosemeyer, 1991).

It is particularly relevant that the characterization of mice lacking the classical ERα, ERβ, or both has revealed that both receptor subtypes have overlapping but also unique roles in estrogen-dependent action *in vivo.* Moreover, ERα and ERβ have different transcriptional activities in certain ligand, cell-type, and promoter contexts (Matthews and Gustafsson, 2003) and may be co-expressed in a number of tissues, forming functional heterodimers whose biological role still remains largely unknown (Cowley *et al.,* 1997; Dechering *et al.,* 2000).

Intriguing considerations may derive from this finding. As has been shown, many of the epithelial ovarian tumors co-express ERα and ERβ, although whether this co-expression also occurs at a cellular level has not yet been systematically examined (Chu *et al.,* 2000). This suggests first that estrogens may have a role in ovarian cancer pathogenesis, and second that appropriate agonists or antagonists may have a therapeutic role (Chu *et al.,* 2000; Clinton *et al.,* 1997). Previous studies on the therapeutic effects of anti-estrogens, particularly tamoxifen, may have been confounded by the relative heterogeneity of the tumors being examined, particularly with regard to ERα *versus* ERβ expression. Some evidence suggests tissue- and promoter-specific differences in the way in which ERα and ERβ respond to ligands, particularly antagonists (Barkhem *et al.,* 1998). With this postulate as a basis, consideration of the types and isoforms of ER expressed in an ovarian tumor in future clinical studies may enable the therapeutic agents to be tailored to the specific tumor.

The discovery of a prevalent expression of ERβ in granulosa cells of the ovary led many researchers to explore its role in normal ovary development, follicular maturation, and ovarian cancer, particularly in granulosa cell tumors. It has been shown that ERβ mRNA (messenger ribonucleic acid) is most abundant in human fetal ovaries, suggesting that it might play an important role in ovarian development (Brandenberger *et al.,* 1998). In females, follicular and stromal ovarian cells undergo periodic changes in distribution of both ERs according to the phases of the menstrual cycle, with different expression in granulosa cells compared to thecal and stromal cells (Iwai *et al.,* 1990).

Several integrated approaches (Western Blotting, indirect immunofluorescence, reverse transcription-polymerase chain reaction, and transient transfection) have determined the expression and function of estrogen receptor ERα/β subtypes and ERβ variants in granulosa cells, showing that ERβ is the predominant type of estrogen receptor in the ovary, with a pivotal physiologic role in reproductive female functions (Byers *et al.,* 1997), and that the function of the ovaries is severely impaired in its absence (Chu *et al.,* 2000). In particular, it has been shown that ERβ protein is preferentially expressed in immature granulosa cells, is functionally active (binds DNA), can transactivate (either as a homodimer or heterodimer with ERα) ERE-containing promoter constructs, and might be associated with increased expression of the endogenous gene encoding c-*Jun.*

Reports seem to confirm the involvement of ERβ in ovarian cancerogenesis (Brandenberger *et al.,* 1998). Chu *et al.* (2000) found a widespread expression of ERα in all types of ovarian tumor types (epithelial and stromal) but at relatively low levels. ERβ instead resulted predominantly expressed in OGCT. This finding confirms the reported presence of ERβ mRNA in human OGCT (Speirs *et al.,* 1999). The prevalent expression of ERβ in the granulosa cell tumors parallels the patterns of expression for ERα and ERβ in normal granulosa cells. Our data support previous reports of a striking prevalence of ERβ expression in the major part of these tumors. This may account for the generally relatively indolent biological behavior of these tumors, considering the reported ability of ERβ to inhibit proliferation by repressing *c-myc, cyclin D1* and *cyclin A* gene transcription, increasing the expression of $p21^{Cip1}$ and $p27^{Kip1}$, which leads to a G_2 cell cycle arrest in cell lines of breast cancer (Paruthiyil *et al.,* 2004).

These findings appear of even more interest if compared with those concerning the expression of p53 protein and PCNA in our series of cases. p53 monoclonal antibodies and PCNA provide insight into nuclear proliferation and control, respectively. In the last decade, various authors have hypothesized that p53 and the

molecular markers of proliferation will help predict the clinical behavior of GCTs. In particular, it has been pointed out that OGCT with an elevated PI are characterized by the presence of p53 mutations and a poorer prognosis (Costa *et al.,* 1996; Horny *et al.,* 1999). This is not surprising because the p53 protein is involved in the regulation of the transition from G1 to S phase of the cell cycle and is a key sentinel protein for the human genome. A large body of literature indicates that a deregulated expression of p53 is strongly related to cellular transformation (Levine *et al.,* 1991). It has been reported that high mitotic index and PI were inversely related with survival of patients with OGCT (Milner, 1991). Costa *et al.* (1996) reported a transformation of molecular markers to increased proliferative activity and overexpression of p53 in recurrent OGCT, different than the primary tumor, hypothesizing that factors other than proliferation of the primary OGCT either extrinsic to the neoplasm (host dependent) or as yet undetectable must determine malignant behavior of this tumor.

The PCNA is an essential processivity factor for deoxyribonucleic acid (DNA) polymerases delta and epsilon (Hindges and Hübscher, 1997). It functions in DNA replication, acting as a clamp to keep the replicative DNA polymerase delta attached to DNA, increasing the processivity of DNA synthesis (Scott *et al.,* 2001). It is highly conserved evolutionarily and essential for viability and cell proliferation. An abundance of papers has described the interactions of PCNA with various proteins involved in processes as different as cell cycle control, DNA replication, nucleotide excision repair, postreplicational mismatch repair, base excision repair, apoptosis, and most recently cytosine methylation (Scott *et al.,* 2001; Koundrioukoff *et al.,* 2000). The promiscuity of PCNA points toward a much wider role in coordinating the cell cycle and DNA replication with various types of DNA repair (Jónsson *et al.,* 1998). We found that the ERβ-expressing OGCTs were characterized by good prognosis, absent or low p53 expression, and low values of PCNA and mitotic index. On the contrary, the subset of OGCT characterized by the loss or hypoexpression of ERβ, p53 overexpression, high mitotic index, and elevated levels of PCNA expression in all cases showed an unfavorable biological behavior, thus constituting a definite prognostic category.

It is very interesting, in our series, the level of expression of ERβ showed no appreciable variation among the samples examined for each tumor, both in OGCT with favorable clinical behavior and in aggressive ones. This finding indicates the absence of a relevant intratumoral cell population heterogeneity, contrasting with the otherwise-reported considerable variation in ERβ expression by ovarian epithelial tumors (Chu *et al.,* 2000), for which a wide tumor sampling is indicated.

The major novel finding of this study is the strict association between loss of expression of ERβ, and an unfavorable biological behavior of OGCT, independent from the classical clinicopathologic parameters and histologic subtypes of the primary tumor. This is further supported by the contemporaneous hyperexpression of both p53 protein and PCNA in the same "aggressive" cases. This finding is of great interest if one considers that, to date, surgery represents the primary therapy for early-stage disease (local disease, FIGO stage I), but management of women with advanced disease, relapses, or metastasis is less clear. Because of their relative rarity, evidence to support decisionmaking in the management of granulosa cell tumors is limited. Thus, a better understanding of the molecular pathology may assist treatment of OGCT that remains a tumor of unquestionable malignant potential.

CONCLUDING REMARKS

The results of this study obviously need to be confirmed on a larger series of cases. A number of ERβ isoforms have also been described, many of which alter estrogen-mediated gene expression (Matthews *et al.,* 2003), and these will be necessary to verify their expression and relative role in OGCT. However, collectively our results depict a scenario in which one may assume that a loss of ERβ expression is associated with a high proliferation rate and hyperexpression of p53 protein in a subset of OGCT with unfavorable behavior, besides the histologic subtype or classical clinico pathologic features. This suggests that the immunohistochemical evaluation of ERβ expression may represent a precious tool for the biological evaluation of OGCT.

In other words, a simple *immunohistochemical screening* of routinely fixed, paraffin-embedded tumor sections could lead to an effective postsurgical prognostic subtypization of OGCT, enabling us to identify subclasses of tumors with different biological behavior. Identification of a high-risk OGCT, characterized by loss of ERβ expression, high mitotic index, elevated PCNA values and overexpression of p53 protein, may be of primary importance in addressing appropriate therapeutic strategies, with closer follow-up protocols, offering the chance to prevent or delay relapses and metastases by using adjunctive, specifically targeted, more aggressive therapies.

References

Barkem, T., Bo, C., Nilsson, Y., Enmark, E., Gustafsson J.A., and Nilsson, S. 1998. Differential response of estrogen receptor α and estrogen receptor β to partial estrogen agonist/antagonist. *Mol. Pharmacol. 54*:105–112.

Brandenberger, A.W., Tee, M.K., and Jaffe, R.B. 1998. Oestrogen receptor alpha (ERα) and beta (ERβ) mRNAs in normal ovary, ovarian serous cystadenocarcinoma and ovarian cancer lines: down-regulation of ERβ in neoplastic tissues. *J. Clin. End. Met. 83*:1025–1028.

Byers, M., Kuiper, G.G.J.M., Gustafsson, J.A., and Park-Sarge, O.K. 1997. Oestrogen receptor β mRNA expression in rat ovary: down regulation by gonadotropin. *Mol. Endocrinol. 11*: 172–182.

Chu, S., and Fuller, P.J. 1997. Identification of a splice variant of the rat estrogen receptor beta gene. *Mol. Cell. Endocrinol. 132*:195–199.

Chu, S., Mamers, P., Burger, H.G., and Fuller, P.J. 2000. Estrogen receptor isoform gene expression in ovarian stromal and epithelial tumors. *J. Clin. Endocrinol. Metab. 85*:1200–1205.

Clinton, G.M., and Hua, W. 1997. Estrogen action in human ovarian cancer. *Crit. Rev. Oncol. Hematol. 25*:1–9.

Costa, M.J., Derose, P.B., Roth, L.M., Brescia, R.J., Zaloudek, C.U., and Cohen, C. 1994. Immunohistochemical phenotype of ovarian granulosa cell tumors. *Hum. Pathol. 25*:60–66.

Costa, M.J., Walls, J., Ames, P., and Roth, L.M. 1996. Transformation in recurrent ovarian granulosa cell tumors: Ki67 (MIB-1) and p53 immunohistochemistry demonstrates a prediction of clinical behavior. *Hum. Pathol. 27*:274–281.

Cowley, S.M., Hoare, S., Mosselman, S., and Parker, M.G. 1997. Estrogen receptors α and β form heterodimers on DNA. *J. Biol. Chem. 272*:19858–19862.

Dechering, K., Boersma, C., and Mosselman, S. 2000. Estrogen receptors α and β: two receptors of a kind? *Curr. Med. Chem. 7*:561–576.

Enmark, E., Pelto-Huikko, M., Grandien, K., Lagercrantz, S., Lagercrantz, J., Fried, G., Nordenskjold, M., and Gustafsson, J.A. 1997. Human estrogen receptor β gene structure, chromosomal localization and expression pattern. *J. Clin. Endocrinol. Metab. 82*:4258–4265.

Flemming, P., Wellmann, A., Maschjek, H., Lang, H., and Georgii, A. 1995. Monoclonal antibodies against inhibin represent key markers of adult granulosa cell tumors of the ovary even in their metatastes. A report of three cases with late metastasis, being previously misinterpreted as hemangiopericytoma. *Am. J. Surg. Pathol. 19*:927–933.

Foegh, M.L., and Ramwell, P.W. 1998. Cardiovascular effects of estrogen: implications of the discovery of the estrogen receptor subtype β. *Curr. Opin. Nephrol. Hyperten. 7*:83–89.

Greene, G.L., King, S.B., and Jensen, W.J. 1984. Immunocytochemical studies in oestrogen receptors. *J. Steroid. Biochem. 20*:51–56.

Grosemeyer, H. 1991. Transcription activation by estrogen and progesterone receptors. *Annu. Rev. Genet. 25*:89–123.

Hindges, R., and Hübscher, U. 1997. DNA polymerase δ, an essential enzyme for DNA transactions. *J. Biol. Chem. 378*:345–362.

Horny, H.P., Marx, L., Krober, S., Luttges, J., Kaiserling, E., and Dietl, J. 1999. Granulosa cell tumor of the ovary. Immunohistochemical evidence of low proliferative activity and virtual absence of mutation of p53 tumor-suppressor gene. *Gynecol. Obstet. Invest. 47*:133–138.

Hurst, B.S., Zilberstein, M., Chou, J.Y., Litman, B., Stephens, J., and Leslie, K.K. 1995. Estrogen receptors are present in human granulosa cells. *J. Clin. Endocrinol. Metab. 89*:229–232.

Iwai, T., Nanbu, Y., Iwai, M., Taii, S., Fujii, S., and Mori, T. 1990. Immunohistochemical localization of oestrogen receptors and progesterone receptors in human ovary throughout the menstrual cycle. *Virchows Arch. A Pathol. Anat. 417*:369–375.

Jensen, E.V., and Jacobsen, H.I. 1962. Basic guides to the mechanism of estrogen action. *Rec. Prog. Horm. Res. 18*:387–414.

Jónsson, Z.O., Hindges, R., and Hübscher, U. 1998. Regulation of DNA replication and repair proteins through interaction with the front side of proliferating cell nuclear antigen. *EMBO J. 17*:2412–2425.

Juric, G., Zarkovic, N., Nola, M., Tillian, M., and Jukic, S. 2001. The value of cell proliferation and angiogenesis in the prognostic assessment of ovarian granulosa cell tumors. *Tumori 87*:47–53.

Katzenellenbogen, B.S., and Korach, K.S. 1997. A new actor in the estrogen receptor drama—enter ER beta. *Endocrinology 138*:861–862.

Koundrioukoff, S., Jónsson, Z.O., Hasan, S., de Jong, R.N., van der Vliet, P.C., Hottiger, M.O., and Hübscher, U. 2000. A direct interaction between proliferating cell nuclear antigen (PCNA) and Cdk2 targets PCNA-interacting proteins for phosphorylation. *J. Biol. Chem. 275*:22882–22887.

Kuiper, G.G., Carisson, B., Grandien, K., Enmark, E., Haggblad, J., Nilsson, S., and Gustafsson, J.A. 1997. Comparison of the ligand binding specify and transcription tissue distribution of oestrogen receptors α and β. *Endocrinology 138*:863–870.

Kuiper, G.G.J.M., Enmark, E., Pelto-Hnikko, M., Nilsson, S., and Gustafsson, J. 1996. Cloning of a novel oestrogen receptor expressed in rat prostate and ovary. *Proc. Natl. Acad. Sci. USA 93*:5925–5930.

Kumar, V., Green, S., Stack, G., Berry, M., Jin, J.R., and Chambon, P. 1987. Functional domains of the human estrogen receptor. *Cell 51*:941–951.

Kurman, R.J. 1989. *Blaustein's Pathology of the Female Genital Tract,* 3rd ed. Berlin: Springer-Verlag.

Landis, J.R., and Koch, G.G. 1997. The measurement of observer agreement for categorical data. *Biometrics 33*:159–174.

Lanita, M. 1984. Estradiol and progesterone receptors in normal ovary and ovarian tumors. *Acta Obstet. Gynecol. Scand. 63*: 497–503.

Levine, A., Momand, J., and Finlay, C. 1991. The p53 tumor suppressor gene. *Nature 351*:453–456.

Matthews, J., and Gustafsson, J.A. 2003. Estrogen signaling: a subtle balance between ERα and ERβ. *Mol. Interven. 3*:281–292.

Mayr, D., Kaltz-Wittmer, C., Arbogast, S., Amann, G., Aust, D.E., and Diebold, J. 2002. Characteristic pattern of genetic aberrations in ovarian granulosa cell tumors. *Mod. Pathol. 15*:951–957.

Miller, B.E., Barron, B.A., Wan, J.Y., Delmore, J.E., Silva, E.G., and Gershenson, D.M. 1997. Prognostic factors in adult granulosa cell tumor of the ovary. *Cancer 79(10)*:1951–1955.

Milner, J. 1991. The role of p53 in normal control of cell proliferation. *Curr. Opin. Cell Biol. 3*:282–286.

Nilsson, S., Mäkelä, S., Treuter, E., Tujague, M., Thomsen, J., Andersson, G., Enmark, E., Pettersson, K., Warner, M., and Gustafsson, J.A. 2001. Mechanisms of estrogen action. *Physiol. Rev. 81*:1535–1565.

Ogawa, S., Inoue, S., Watanabe, T., Orimo, A., Hosoi, T., Ouchi, Y., and Muramatsu, M. 1998. Molecular cloning and characterization of human estrogen receptor βcx: a potential inhibitor of estrogen action in human. *Nucleic Acids Res. 26*: 3505–3512.

Paruthiyil, S., Parmar, H., Kerekatte, V., Cunha, G.R., Firestone, G.L., and Leitman, D.C. 2004. Estrogen receptor β inhibits human breast cancer cell proliferation and tumor formation by causing a G2 cell cycle arrest. *Cancer Res. 64*:423–428.

Petersen, D.N., Tkalcevic, G.T., Koza-Taylor, P.H., Turi, T.G., and Brown, T.A. 1998. Identification of estrogen receptor beta2, a functional variant of estrogen receptor beta expressed in normal rat tissues. *Endocrinology. 139*:1082–1092.

Petterson, K., Gustafsson, J.A., 2001. Role of estrogen receptor beta in estrogen action. *Annu. Rev. Physiol. 63*:165–192.

Rosai, J. 1996. *Ackerman's Surgical Pathology,* vol II. St. Louis: Mosby-Year Book, 1505–1509.

Sar, M., and Welsch, F. 1999. Differential expression of oestrogen receptor α and oestrogen receptor β in the rat ovary. *Endocrinology 140*:964–970.

Savage, P., Constenla, D., Fisher, C., Shepherd, J.H., Barton, D.P., Blake, P., and Gore, M.E. 1998. Granulosa cell tumour of the ovary: demographics, survival and the management of advanced disease. *Clin. Oncol. 10*:242–245.

Schumer, S.T., and Cannistra, S.A. 2003. Granulosa cell tumor of the ovary. *J. Clin. Oncol. 21*:1180–1189.

Scott, M., Bonnefin, P., Vierya, D., Boisvert, F.M., Young, D., Bazett-Jones, D.P., and Riabowol, K. 2001. UV-induced binding of ING1 to PCNA regulates the induction of apoptosis *Cell 114*:3455–3462.

Scully, R.E. 1997. Ovarian tumors. A review. *Am. J. Pathol. 87*: 686–720.

Scully, R.E. 1999. Granulosa cell tumours. In: *Histological Typing of Ovarian Tumors.* Geneva: World Health Organization, 19–21.

Serov, S.P., Scully, R.E., and Sobin, L.H. 1973. In: *International Histological Classification of Tumors.* No. 9. Histological typing of ovarian tumors. Geneva: World Health Organization.

Speirs, V., Parkers, A.T., Kerin, M.J., Walton, D.S., Carleton, P.J., and Fox, J.N. 1999. Coexpression of oestrogen receptor alfa and beta: poor prognostic human breast cancer? *Cancer Res. 59*:525–528.

Staibano, S., Franco, R., Mezza, E., Chieffi, P., Sinisi, A., Pasquali, D., Errico, M.E., Nappi, C., Tremolaterra, F., Somma, P., Mansueto, G., and De Rosa, G. 2003. Loss of estrogen receptor β, high PCNA and p53 expression and aneuploidy as markers of worse prognosis in ovarian granulosa cell tumors. *Histopathology 43*:254–262.

Sternberg, S. 1994. Female reproductive system. The ovary. In: Sternberg S. (ed.) *Diagnostic Surgical Pathology.* New York: Raven Press.

Stumpf, W.E. 1969. Nuclear concentration of [^{3}H]-Estradiol in target tissues. Drymout autoradiography of vagina, oviduct, ovary, testis, mammary gland and adrenal. *Endocrinology 85*: 31–37.

Suzuki, T., Sasano, H., Rimura, N., Tamura, M., and Fukaya, T. 1994. Immunohistochemical distribution of progesteron, androgen and oestrogen receptors in the rat ovary during the menstrual cycle: relationship to expression of steroid enzymes. *Hum. Reprod. 9*:1589–1595.

Toppila, M., Tyler, J.P.P., Fay, R., Baird, P.J., Crandon, A.J., Eastman, C.J., and Hudson, C.N. 1986. Steroid receptors in human ovarian malignancy. A review of four years tissue collection. *Br. J. Obstet. Gynecol. 93*:986–992.

Tremblay, G.B., Tremblay, A., and Copeland, N.G. 1997. Cloning, chromosomal localization, and functional analysis of murine oestrogen receptor β. *Mol. Endocrinol. 11*:353–365.

Webster, N.J.G., Green, S., Jin, J.R., and Chambon, P. 1988. The hormone-binding domains of the estrogen and glucocorticoid receptors contain an inducible transcription activation function. *Cell 54*:199–207.

Young, R.H., and Scully, R.E. 2002. Sex cord-stromal, steroid cell, and other ovarian tumors with endocrine, paraendocrine, and paraenoplastic manifestations. In: Kurman R.J. (ed.) *Blaustein's Pathology of the Female Genital Tract*, 3rd ed. Berlin: Springer-Verlag, 905–921.

This Page Intentionally Left Blank

9

Role of Immunohistochemical Expression of Cyclooxygenase-2 in Ovarian Serous Carcinoma

Adnan R. Munkarah and Rouba Ali-Fehmi

Introduction

The enzyme prostaglandin endoperoxide synthase (PES), also referred to as cyclooxygenase *(COX),* is responsible for the conversion of arachidonic acid to prostaglandins (PGs). Mammalian cells contain at least two *COX* isozymes: *COX-1* and *COX-2.* Cyclooxygenase-1 is a well-characterized enzyme that is constitutively expressed in most tissues; the protein levels do not fluctuate in response to stimuli such as cytokines or growth factors. Cyclooxygenase-2 is characterized as an immediate-early gene associated with cellular growth and differentiation. Its expression can be induced by a variety of agents, including growth factors, phorbol esters, and cytokines. The *COX-2* protein is membrane-bound with a molecular weight of 71 kDa; it localizes to the endoplasmic reticulum and nuclear envelope. Emerging data suggest that *COX-2* and PGs are involved at various steps of the process of malignant transformation and tumor progression.

Angiogenesis is a complex process that is regulated by a number of cellular pathways. Vascular endothelial growth factor *(VEGF),* a heparin-binding glycoprotein, is a critical regulator of the angiogenesis process during embryogenesis. It also plays an important role in cancer neoangiogenesis (Zhang *et al.,* 2003). Overexpression of *VEGF* has been described in a large number of malignancies. Although the process of angiogenesis regulation is complex, there is mounting evidence that prostaglandins and *COX-2* do play an active role (Williams *et al.,* 2000).

Immunohistochemical staining is a technique used for identifying cellular or tissue constituents (such as proteins) by means of antigen–antibody interactions. The site of antibody binding is identified either by direct labeling of the antibody, or by use of a secondary labeling method. This technique has given the researchers and clinicians the ability to identify specific substances that could not be characterized by conventional special stains. With time, the wide range of well-characterized specific anti-sera and the improvement in antibody–enzyme conjugates have eliminated many of the early problems associated with immunohistochemical staining. As a result, this technique has now found acceptance in most research and histology laboratories. Its value in diagnosis and accurate classification of disease processes has become widely accepted.

Immunohistochemistry (IHC) provides several advantages over the methods traditionally used in the laboratory to evaluate protein expression. In most instances, it is usable on archival paraffin-embedded histologic material. It provides the cellular localization of the protein of interest. Although it is not a quantitative method, it still allows a good assessment of the pattern and

Handbook of Immunohistochemistry and *in situ* Hybridization of Human Carcinomas, Volume 4: Molecular Genetics, Gastrointestinal Carcinoma, and Ovarian Carcinoma

extent of expression within the tissue evaluated. There are a number of limitations of IHC staining. Its specificity and sensitivity can be suboptimal, depending on the levels of the expression of the protein being evaluated, the specificity of the antibody used, and the quality of the tissue blocks. In addition, the staining procedure needs to be optimized before being used, a process that can be meticulous and time consuming. Finally, the interpretation of the staining results and their quantification can be subjective and open to interpreters' biases.

In this chapter, we will describe the materials and methods used in our laboratory to perform IHC staining for *COX-2* and *VEGF* in epithelial ovarian carcinoma (OC) specimens. We will also review some of the existing literature regarding *COX-2* overexpression in ovarian cancer and the correlation with tumor angiogenesis (see also Chapter 11 in Part III).

MATERIALS

Reagents

- Common lab reagent and solvents: xylene, ethanol's 100% and 95%, hematoxylin, eosin, bluing reagent, clarifier (Richard-Allan Scientific, Kalamazoo, MI), and mounting media.
- 0.01 mM (phosphate buffer saline [PBS]) (pH 7.4) (Sigma, St. Louis, MO).
- 3% Hydrogen peroxide (H_2O_2) for quenching of endogenous peroxidase.
- Antigen-retrieval solution: citrate buffer, pH 6.0 (Vector Laboratories, Burlingame, CA).
- 1 mM EDTA (ethylenediamine tetraacetic acid), antigen-retrieval solution (pH 8.0) (Sigma).
- Target retrieval solution: Dako (Glostrup, Denmark) (pH 9.0).
- Blocking serum, goat, horse, or rabbit for nonspecific staining (Vector Laboratories).
- Antibody diluent solution (Zymed, San Francisco).
- Biotinylated secondary antibody (Vector Laboratories).
- Avidin-biotin complex (ABC) (Vector Elite Kit).
- Chromagen, 3,3′-Diaminobenzidine (DAB) (Vector Laboratories).

Cyclooxygenase-2 Antibody

- The primary antibody, anti-COX-2 (Zymed Laboratories Inc., South San Francisco, CA), is a monoclonal mouse anti–COX-2 antibody intended to qualitatively detect COX-2 protein in frozen and formalin-fixed and paraffin-embedded tissue sections.
- Immunogen: Synthetic peptide from human COX-2.
- COX 229 clone.
- Isotype: IgG1 (immunoglobulin G1)-Kappa.
- Positive control tissue: colon carcinoma.
- Expected staining pattern: cytoplasmic.

Vascular Endothelial Growth Factor Antibody

- The monoclonal mouse anti-VEGF antibody (Santa Cruz Biotechnology, Santa Cruz, CA) is recommended for detection of precursor and mature VEGF of mouse, rat, and human origin by Western Blotting, immunoprecipitation, immunofluorescence, and IHC in paraffin-embedded tissue section.
- VEGF C-1 clone.
- IgG 2a isotype.
- Positive controls: human breast carcinoma tissue, normal human kidney.
- Expected staining pattern: cytoplasmic.

METHODS

High-affinity glycoprotein avidin for biotin and a mild biotinylation process makes the avidin-biotin method more sensitive than previous methods of IHC. Avidin has four binding sites, which form a tertiary structure possessing four biotin-binding hydrophobic pockets. In the ABC method a complex of avidin and biotinylated tracer, which contains free avidin-binding sites, is applied to the biotinylated antibody. The sequence of reagent application is primary antibody, biotinylated secondary antibody, preformed ABC, followed by the substrate–chromogen visualization. We used this method of IHC for *COX-2* and *VEGF* antibodies.

Cyclooxygenase-2 Immunohistochemistry

1. Deparaffinize and hydrate slides through xylene followed by graded alcohol to distilled water.
2. Block endogenous peroxidase with 3% H_2O_2 (20 min).
3. Rinse in MPBS (modified PBS), 2 changes for 3 min each.
4. Antigen retrieval: citrate buffer (pH 6.0). Warm solution for 30 min in steamer; immerse slides in hot buffer for 20 min followed by cooling on bench for 20 min.
5. Incubate in normal blocking (horse) solution (do not rinse slides after blocking) for 30 min.
6. Incubate in designated primary antibody anti-COX-2 1:400 (Zymed) 1 hr.

7. Rinse in MPBS, 3 changes for 3 min each.
8. Incubate in designated biotinylated secondary antibody, 1:200 anti-Mouse IgG (H+L) (Vector Laboratories) for 30 min.
9. Rinse in MPBS, 3 changes for 3 min each.
10. Incubate in ABC for 20–30 min.
11. Rinse in MPBS, 3 changes for 3 min each.
12. Wash in distilled water for 5 min.
13. Visualize substrate/chromogen: DAB. Watch intensity with microscope.
14. Counterstain with hematoxylin and dehydrate with gradient of ethanol to xylene, then place coverslip.

Vascular Endothelial Growth Factor Immunohistochemistry

Perform IHC on the Ventana automated instrument, BenchMark-XT (Ventana Medical Systems, Tucson, AZ). The parameters per VEGF optimal specific staining-to-background ratio are carried out using the Ventana Medical Systems detection kit.

1. Deparaffinization: apply EZ-Prep and then rinse.
2. Apply inhibitor solution to decrease the endogenous peroxidase activity.
3. Apply Protease1 enzyme for 10 min and then rinse.
4. Titration: apply 100 µl of VEGF-1 (Santa Cruz Biotechnology, Santa Cruz, CA) at 1:50 to slide and incubate for 32 min at 37°C, then rinse.
5. Apply biotinylated anti-mouse secondary antibody, incubate for 8 min at 37°C, and then rinse.
6. Apply avidin/streptavidin-enzyme conjugate for 8 min at 37°C, and then rinse.
7. Apply chromogenic substrate, then rinse.
8. Remove slides from instrument, counterstain, dehydrate, clarify, and place coverslip.

Evaluating/Scoring the Immunohistochemical for Cyclooxygenase-2 and Vascular Endothelial Growth Factor

For COX-2 and VEGF assessment, the staining intensity and the percentage of tumor cells stained were analyzed. Staining intensity was scored as 0 (negative), 1+ (weak), 2+ (medium), and 3+ (strong). A combined score based on the staining intensity and the percentage of cells stained was used to assign a final score. Low expression was defined as intensity 0, 1, 2, or 3 and <10% or intensity 0, 1, and <50% cells staining; high expression was defined as intensity 2, 3, and >10% or intensity 1, 2, 3, and >50% of cells staining.

Discussion

A number of studies have looked at the patterns of COX-2 expression in various human neoplasms and the clinical implications of overexpression. Some investigators have also tried to evaluate any potential correlation between the patterns of COX-2 expression and specific molecular and morphologic characteristics of the tumors. In ovarian cancer, COX-2 expression is noted in a significant percentage of tumors evaluated (Li *et al.,* 2004; Raspollini *et al.,* 2004a; Seo *et al.,* 2004).

In one study, overexpression of the protein by IHC was shown to correlate with the stage and grade of disease; the frequency of COX-2 overexpression was 9% in early-stage, low-grade tumors; 27% in early-stage, high-grade tumors; 70% in high-stage, low-grade tumors; and 63.3% in high-grade, high-stage tumors (Seo *et al.,* 2004). In another large study that only included patients with high-grade, high-stage ovarian serous carcinomas, *COX-2* overexpression was noted in 69% of cases. The staining was purely cytoplasmic and confined to the neoplastic cells; the stroma did not exhibit any significant COX-2 expression (Figures 60 and 61). There was no correlation between *COX-2* overexpression and the patients' age or race. However, *COX-2* expression did correlate with survival where *COX-2*–expressing tumors were associated with a worse prognosis. The median survival of patients with *COX-2*–positive cancers was 660 days compared to 890 days for those with COX-2–negative tumors (Ali-Fehmi *et al.,* 2003). Similar frequencies and patterns of COX-2 overexpression were noted in a cohort of patients with primary peritoneal serous carcinoma (Khalifeh *et al.,* 2004).

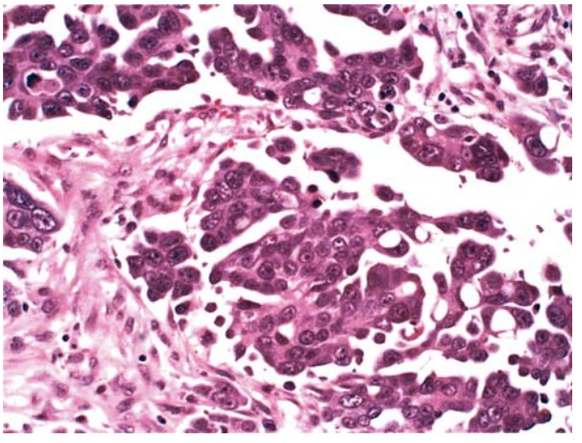

Figure 60. Hematoxylin and eosin representative section of high-grade ovarian serous carcinoma (200X).

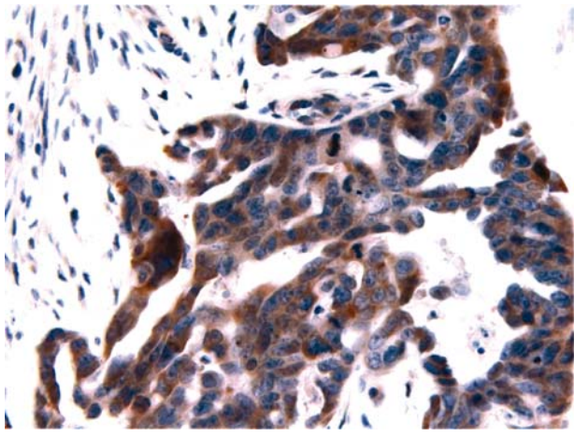

Figure 61. Immunohistochemical staining for cyclooxygenase-2 (COX-2) in a representative section of high-grade ovarian serous carcinoma is shown. High COX-2 expression was mainly in the tumor areas. No significant stain is seen in the stroma (200X).

Other investigators have similarly reported high rates of *COX-2* overexpression in ovarian cancer and correlated that with poor patient outcome (Ferrnadina *et al.,* 2002). Women with *COX-2*–positive tumors had a lower response to chemotheraphy and shorter time to progression and overall survival. It is interesting that a recent publication showed comparable rates of *COX-2* overexpression in benign, borderline, and malignant epithelial ovarian tumors. A significantly higher rate of *COX-2* positivity was found in serous compared to mucinous borderline and benign tumors. However, there was no difference in *COX-2* positivity by histology subtype in the invasive cancers (Ferrnadina *et al.,* 2004). Although the interpretation of *COX-2* positivity based on IHC varied among different investigators, many have used comparable scoring systems that combined the percentage of positively staining cells and the intensity of staining, thus limiting the variability and subjectivity of interpretation. It is worth noting that some investigators have refuted the finding of *COX-2* overexpression in ovarian cancer. In a study that evaluated *COX-1* and *COX-2* expression levels using Northern blot and immunoblot analysis, dramatic elevations of *COX-1,* but not *COX-2,* protein and messenger ribonucleic acid (mRNA) were seen in 11 epithelial ovarian cancers analyzed (Gupta *et al.,* 2003). Similarly, another group found that out of 18 carcinomas confined to the ovaries, only 2 cases were *COX-2* positive by IHC. However, many tumors that metastasized to the omentum were *COX-2* positive (Rolland *et al.,* 2003).

Through various mechanisms *COX-2* can contribute to the process of carcinogenesis and tumor progression. Experimental data have shown that forced *COX-2* expression might contribute to reduced apoptosis. Transfection of rat intestinal epithelial cells with a *COX-2*–expressing vector resulted in an increase in the intracellular levels of *COX-2* and *bcl-2* proteins. These changes were associated with resistance to butyrate-induced apoptosis. In addition, these cells exhibited higher levels of adhesion to the extracellular matrix. In a different experimental system, treatment of epithelial ovarian cancer cells with PGE_2 resulted in an increase in the *bcl*$_2$*/bax* mRNA levels, a molecular alteration that was associated with reduced apoptosis (Munkarah *et al.,* 2002). When IHC was used to evaluate serous ovarian carcinomas obtained from patients with advanced-stage disease, *bcl-2* overexpression was noted in 39% of cases. No correlation was found between *bcl-2* and *COX-2* expression in these tumors (Ali-Fehmi *et al.,* 2003).

Induction of angiogenesis is another mechanism by which *COX-2* contributes to tumor progression. Angiogenesis is a critical step in the process of cancer progression. Tumor neovascularization as reflected by tumor microvessel density (MVD) strongly correlates with the risk of invasion and metastasis. As one of the most potent angiogenic cytokines, VEGF plays a major role in tumor neovascularization (Ferrara *et al.,* 2003). Its production is regulated through a number of pathways. Mounting evidence from a number of studies indicates that PGs and their synthesizing enzyme, *COX*, play an important role in VEGF regulation and angiogenesis. In an *in vitro* experimental model, treatment of osteoblasts with PGE_1 and E_2 increased *VEGF* mRNA and protein levels. In another study, increased *VEGF* expression in human monocytic cells was seen in response to treatment with iloprost, a PGI_2-analog. Experiments using co-culture of endothelial cells with colon carcinoma cells showed that COX-2 overexpressing cancer cells produced proangiogenic factors and stimulated endothelial cell migration and tube formation; control cells had very little activity in these processes.

Treatment of epithelial ovarian cancer cells with PGE_2 was associated with an increase in VEGF mRNA levels (Zhu *et al.,* 2004). This association between *COX-2* and tumor neoangiogenesis in ovarian cancer was confirmed in a number of studies using IHC. Ali-Fehmi *et al.* (2003) evaluated tumor MVD in a cohort of patients with advanced-stage high serous carcinomas using IHC for CD34. They found a significant positive correlation between *COX-2* expression and tumor MVD. A strong positive correlation was also noted between the expression of *COX-2* and *VEGF* in the tumor cells. In fact, low VEGF expression was noted in 100% of low COX-2–expressing tumors. However, 96%

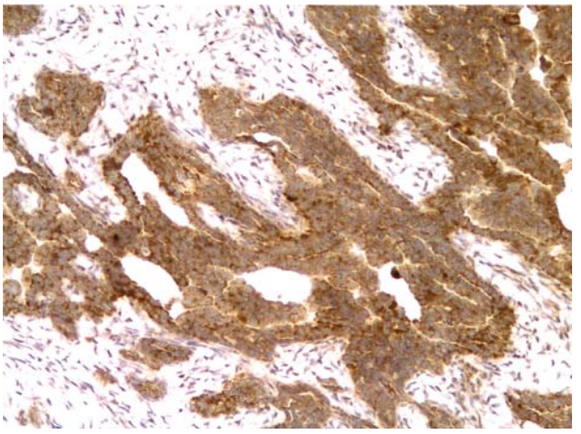

Figure 62. Immunohistochemistry staining for vascular endothelial growth factor (VEGF) showing strong positivity in high-grade ovarian serous carcinoma (100X).

high *COX-2*–expressing tumors exhibited high *VEGF* expression (Ali-Fehmi *et al.,* 2005) (Figure 62). Similar findings were reported by other groups also using IHC to assess *COX-2* and *VEGF* expression. Raspollini *et al.* (2004b) found a strong correlation between tumor MVD and the expression of *COX-2* and *VEGF* in 52 cases with metastatic OC (Raspollini *et al.,* 2004b). In a logistic regression analysis, *COX-2, VEGF,* and MVD had a significant impact on survival.

In conclusion, the evaluation of OC specimens by IHC has revealed high levels of *COX-2* expression in a significant number of advanced-stage tumors. These molecular changes correlated with increased tumor vascularity and *VEGF* overexpression. This supports the *in vitro* data showing that *COX-2* plays a role in regulating *VEGF* expression and tumor neoangiogenesis. In addition, the consistent association between *COX-2* expression and poor patient prognosis is clinically important. Targeting of *COX-2* may have a therapeutic role in cancer therapy. This needs to be weighed against the recent data suggesting that specific *COX-2* inhibitors may be associated with increased cardiovascular side effects.

References

Ali-Fehmi, R., Che, M., Khalifeh, I., Malone, J.M., Morris, R., Lawrence, D., and Munkarah, A.R. 2003. The effect of cyclooxygenase-2 expression on tumor vascularity in advanced stage ovarian serous carcinoma. *Cancer 98*:1423–1429.

Ali-Fehmi, R., Morris, R., Bandyotpadhyay, S., Che, M., Schimp, V., Malone, J., and Munkarah, A.R. 2005. Expression of cyclooxygenase-2 in advanced stage ovarian serous carcinoma: correlation with tumor cell proliferation, apoptosis, angiogenesis, and survival. *Am. J. Obstet. Gynecol. 192*:819–825.

Ferrandina, G., Lauriola, L., Zannoni, G.F., Fagotti, F., Fanfani, F., Legge, F., Maggiano, N., Gessi, M., Mancuso, S., Ranelletti, F.O., and Scambia, G. 2002. Increased cyclooxygenase-2 (COX-2) expression is associated with chemotherapy resistance and outcome in ovarian cancer patients. *Ann. Oncol. 13*: 1205–1211.

Ferrnadina, G., Zannoni, G.F., Ranelleti, F.O., Legge, F., Gessi, M., Salutari, V., Lauriola, L., and Scambia, G. 2004. Cyclooxygenase-2 expression in borderline ovarian tumors. *Gynecol. Oncol. 95*:46–51.

Ferrara, N., Gerber, H.P., and Le Couter, J. 2003. The biology of VEGF and its receptors. *Nat. Med. 9*:669–676.

Gupta, R.A., Lovella, V.T., Tong, B.J., Das, S.K., Morrow, J.D., Dey, S.K., and Dubois, R.N. 2003. Cyclooxygenase-1 is overexpressed and promotes angiogenic growth factor production in ovarian cancer. *Cancer Res. 63*:906–911.

Khalifeh, I., Munkarah, A.R., and Lonardo, F. 2004. Expression of Cox-2, CD34, Bcl-2, and p53 and survival in patients with primary peritoneal serous carcinoma and primary ovarian serous carcinoma. *Int. J. Gynecol. Pathol. 23*:162–169.

Li, S., Miner, K., and Fannin, R. 2004. Cyclooxygenase-l and 2 in normal and malignant human ovarian epithelium. *Gynecol. Oncol. 92*:622–627.

Munkarah, A.R., Morris, R., Baumann, P., Deppe, G., Malone, J., Diamond, M.D., and Saed, G.M. 2002. Effects of prostaglandin E2 on proliferation and apoptosis of epithelial ovarian cancer cells. *J. Soc. Gynecol. Investigat.* 9:168–173.

Raspollini, M.R., Amunni, G., and Villanucci, A. 2004a. Expression of inducible nitric oxide synthase and cyclooxygenase-2 in ovarian cancer: correlation with clinical outcome. *Gynecol. Oncol. 92*:806–812.

Raspollini, M.R., Amunni, G., and Villanucci, A. 2004b. COX-2 status in relation to tumor microvessel density and VEGF expression: analysis in ovarian carcinoma patients with low versus high survival rates. *Oncol. Rep. 11*:309–311.

Rolland, I.H., Yang, W.L., Daly, M.B., Ozols, R.F., Hamilton, T.C., Lynch, H.T., Godwin, A.K., and XU, X.X. 2003. Loss of surface and cyst epithelial basement membranes and preneoplastic morphologic changes in prophylactic oophorectomies. *Cancer 98*:2607–2623.

Seo, S.S., Song, Y.S., and Kang, D.H. 2004. Expression of cyclooxygenase-2 in association with clinicopathological prognostic factors and molecular markers in epithelial ovarian cancer. *Gynecol. Oncol. 92*:927–935.

Williams, C.S., Tsujii, M., Reese, J., Dey, S.K., and DuBois, R.N. 2000. Host cyclooxygenase-2 modulates carcinoma growth. *J. Clin. Invest. 105*:1589–1594.

Zhang, L., Yang, N., Park, J.W., Katsaros, D., Fracchioli, S., Cao, G., O'Brien-Jenkins, A., Randall, T.C., Rubin, S.C., and Coukos, G. 2003. Tumor-derived vascular endothelial growth factor up-regulates angiopoietin-2 in host endothelium and destabilizes host vasculature, supporting angiogenesis in ovarian cancer. *Cancer Res. 63*:3403–3412.

Zhu, G., Saed, G.M., Deppe, G., Wang, R., Diamond, M.P., and Munkarah, A.R. 2004. Hypoxia up-regulates the effects of prostaglandin E2 on tumor angiogenesis in ovarian cancer cells. *Gynecol. Oncol. 94*:422–426.

This Page Intentionally Left Blank

10

Role of Immunohistochemical Expression of Cyclooxygenase and Peroxisome Proliferator–Activated Receptor γ in Epithelial Ovarian Tumors

Yoshihito Yokoyama, Akiko Sakamoto, and Hideki Mizunuma

Introduction

Clinical Implication of Cyclooxygenase-2 Expression in Epithelial Ovarian Tumors

Cyclooxygenase (COX) is a rate-limiting enzyme in prostaglandin (PG) synthesis because of its rapid autoinactivation. The COX enzyme has two isoforms, the constitutive COX-1 and the inducible COX-2; COX-1 is expressed in most tissues, whereas COX-2 is largely absent but is responsible primarily for PGs produced in inflammatory sites, suggesting that COX-2 plays a critical role in inflammation (Smith *et al.,* 1996). Epidemiologic studies have shown a 40–50% reduction in mortality from colorectal carcinoma in continuous users of nonsteroidal anti-inflammatory drugs (NSAIDs) compared with that of noncontinuous users. An anti-tumour effect of NSAIDs was caused by inhibition of COX-2 (Taketo, 1998). The enzyme COX-2 is known to be a promoter of gastrointestinal (GI) carcinoma. Many studies suggest that overexpression of COX-2 might be involved in multistep carcinogenesis and tumor progression, especially in gastric and colorectal carcinoma (Prescott and White, 1996; van Rees *et al.,* 2002). A progressive development from ovarian serous tumors of low potential malignancy to invasive serous carcinoma has been suggested in parallel to the concept of adenoma–carcinoma sequence in colorectal carcinomas (Hauptmann and Dietel, 2001), although the concept that ovarian carcinogenesis is a linear pathway as for colorectal carcinoma is still contested. Shigemasa *et al.* (2003) reported that COX-2 expression might play an important role in ovarian carcinoma (OC) development. Ferrandina *et al.* (2002) described that increased COX-2 expression was associated with chemotherapy resistance and outcome in patients with OC, and then Denkert *et al.* (2002) reported that COX-2 expression was an independent prognostic factor in OC. In this chapter, we will describe association of COX-2 expression with ovarian carcinogenesis and progression of ovarian tumors by means of immunohistochemical technique (see also Chapter 9, Part III).

Handbook of Immunohistochemistry and *in situ* Hybridization of Human Carcinomas, Volume 4: Molecular Genetics, Gastrointestinal Carcinoma, and Ovarian Carcinoma

Relationship between Cyclooxygenase-2 and Peroxisome Proliferator–Activated Receptor γ Expression in Epithelial Ovarian Tumors

Peroxisome proliferator–activated receptor γ (PPARγ) is a member of a nuclear hormone receptor superfamily that can modulate gene expression on ligand binding (Subbaramaiah *et al.,* 2001). Ligand-mediated activation of PPARγ has been linked to cellular differentiation, apoptosis, and anti-inflammatory responses. In colon carcinoma cells, ligand activation of the receptor inhibits cell growth, induces a differentiation response, and reverses the malignant phenotype (Sarraf *et al.,* 1998). Agonists of PPARγ and PPARγ overexpression led to a drastic reduction of the cell growth rate in PPARγ-expressing thyroid carcinoma cells (Martelli *et al.,* 2002). The nuclear prostanoid 15-deoxy-$\Delta^{12,14}$ PGJ_2 (15d-PGJ_2) was identified as a potent natural ligand for the PPARγ. 15d-PGJ_2 was found to induce apoptosis, inhibit proliferation, and prevent the growth of human breast carcinoma cells in the nude mouse model (Clay *et al.,* 1999). Inhibition of COX-2 and activation of PPARγ inhibited the development of rat mammary-gland carcinogenesis (Harris *et al.,* 2000; Suh *et al.,* 1999). Additionally, independent studies showed that COX-2 and PPARγ are induced and inactivated, respectively, in human breast carcinoma (Jiang *et al.,* 2000; Ristimaki *et al.,* 2002). Inoue *et al*. (2000) proposed that expression of COX-2 was regulated by a negative feedback loop mediated through PPARγ in macrophages. Badawi and Badr (2003) reported that the altered expression of COX-2 and PPARγ might influence the development of human breast carcinoma and its progression to metastasis. In 2001, PPARγ was reported to be localized primarily to granulosa cells in ovarian tissue and to be involved in follicular development (Komar *et al.,* 2001). In this chapter, we will also describe the effect of COX-2 and PPARγ expression on ovarian carcinogenesis and progression of ovarian tumors by means of immunohistochemical technique.

MATERIALS

1. Ovarian carcinomas.
2. Borderline ovarian tumors.
3. Benign ovarian cystadenomas.
4. Anti-COX-2 antibody (Immuno-Biological Laboratories, Gunma, Japan).
5. Anti-PPARγ antibody (Cayman Chemical, Ann Arbor, MI).
6. 0.01 M Citrate buffer (pH 6.0).
7. 0.3% Hydrogen peroxide (H_2O_2) in methanol.
8. Biotinylated anti-rabbit immunoglobulin G (IgG) (Dako, Kyoto, Japan).
9. 1% Bovine serum albumin (BSA) and 20% heat-inactivated goat serum in phosphate buffer saline (PBS).
10. Normal rabbit serum.
11. PBS containing 0.1% Tween 20 (PBS/Tween).
12. Avidin-biotinylated-horseradish peroxidase (Vectastain Elite ABC kit, Vector Laboratories, Peterborough, UK).
13. 0.02% Diaminobenzidine tetrahydrochloride (DAB) (Sigma-Aldrich, St. Louis, MO) in Tris-HCl buffer (pH 7.6) containing 0.03% H_2O_2.

METHODS

1. Fix ovarian carcinoma tissues in 10% formaldehyde for 24 hr.
2. Embed tissues in paraffin and cut 6 μm thick sections.
3. Deparaffinize and hydrate tissue sections through xylene and a graded alcohol series (100%, 90%, 70%).
4. Rinse for 5 min in tap water.
5. Place the sections in 0.01 M citrate buffer (pH 6.0) and heat at 500 W in a microwave oven for 5 min to retrieve tissue antigen.
6. Incubate the sections with 0.3% H_2O_2 in methanol for 10 min to quench the endogenous peroxidase activity.
7. Wash in PBS for 5 min.
8. Incubate the sections with 1% BSA and 20% heat-inactivated goat serum in PBS for 30 min at room temperature to block nonspecific binding sites.
9. Blot excess serum from the sections.
10. This is a multi-step process.
    a. Apply anti-COX-2 antibody at a concentration of 5 μg/ml for 12 hr at 4°C in a moist chamber.
    b. Apply anti-PPARγ antibody at a concentration of 5 μg/ml for 1 hr at 37°C in a moist chamber.
    c. As negative control, use preimmune rabbit serum instead of both antibodies.
11. Wash slides with three changes for 1 hr in PBS containing PBS/Tween.
12. Incubate the sections for 1 hr with 2000 fold-diluted biotinylated anti-rabbit IgG solution at room temperature.
13. Wash slides for 15 min with three changes of PBS/Tween.
14. Incubate sections for 30 min with avidin-biotinylated-horseradish peroxidase complex.
15. Wash slides for 15 min with three changes of PBS/Tween.
16. Visualize the binding sites of peroxidase with 0.02% DAB as a chromogen in Tris-HCl buffer (pH 7.6) containing 0.03% H_2O_2.
17. Counterstain the sections with hematoxylin for microscopic examination.

18. Clear and mount.

19. Evaluate the results of immunohistochemical staining. Cases in which more than 10% of tumor cells are as strongly immunoreactive as positive control cells are considered positive.

20. Use formalin-fixed and paraffin-embedded sections of colon carcinoma and urinary bladder carcinoma as positive control for COX-2 and PPARγ staining, respectively.

Study Population

Immunohistochemical examination was performed retrospectively on 112 epithelial ovarian tumors obtained from women who were surgically treated at the Hirosaki University Hospital between 1989 and 2003 and who had given informed consent. The tissue specimens included 71 carcinomas, 18 borderline tumors, and 23 benign cystadenomas. All patients with epithelial OC were surgically staged in accordance with the 1988 International Federation of Gynecology and Obstetrics (FIGO) criteria. Patients included in this study had not received any preoperative chemotherapy. The breakdown for stages of OCs consisted of 40 patients with stage I, 7 with stage II, 18 with stage III, and 6 with stage IV. Histologic types were classified into 30 cases with serous cystadenocarcinoma, 11 with mucinous cystadenocarcinoma, 17 with endometrioid adenocarcinoma, 12 with clear cell adenocarcinoma, and 1 with undifferentiated adenocarcinoma. All patients with OC received postoperative chemotherapy combining cisplatin (60 mg/m^2), epirubicin (40 mg/m^2), and cyclophosphamide (300 mg/m^2). The duration of follow-up ranged from 8 to 156 months (median, 54 months). The mean age of patients with OC at surgery was 54.1 years (range, 28–78 years). Of the 18 borderline tumors, 4 were serous and 14 were mucinous. Of the 23 benign cystadenomas, 9 were serous and 14 were mucinous.

RESULTS

In the cytoplasm of tumor cells in positive cases COX-2 and PPARγ were homogeneously stained (Figure 63). The frequencies of COX-2 detection in benign tumor, borderline tumor, and carcinoma were 13%, 16.7%, and 39.4%, respectively, and those of PPARγ detection in benign tumor, borderline tumor, and carcinoma were 4.5%, 77.8%, and 43.7%, respectively. There was no significant difference in COX-2 positivity between samples of benign and borderline tumors. The incidence of COX-2 detected in carcinomas was significantly higher than that detected in benign tumors ($p < 0.02$) and higher with a marginal significance than that detected in borderline tumors ($p = 0.058$). However, the frequency of PPARγ detected in borderline tumors was significantly higher than that detected in benign tumors and carcinomas, respectively ($p < 0.0001$, $p < 0.01$, respectively). Positivity of COX-2 and PPARγ in carcinomas was not correlated with clinical factors such as stage, histologic type, lymph-node metastasis, and recurrence.

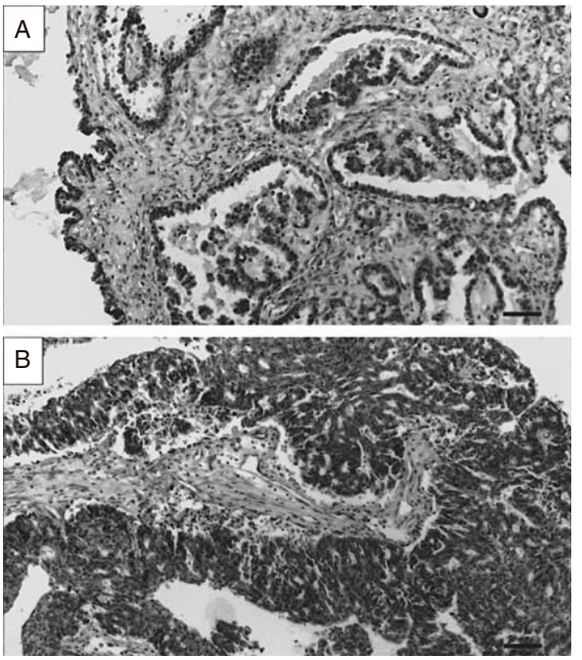

Figure 63. Immunohistochemical staining of cyclooxygenase-2 (COX-2) and peroxisome proliferator–activated receptor γ (PPARγ) in ovarian carcinoma. Positive staining of COX-2 **(A)** and PPARγ **(B)** in carcinoma tissues (scale bar, 50 μm). They are representative of all the positive samples. Tissues demonstrated in **A** and **B** are a clear cell adenocarcinoma and a serous adenocarcinoma, respectively.

DISCUSSION

Overexpression of COX-2 has been observed in many tumor types including gynecologic malignancies. Mechanistic study suggested that expression of COX-2 in uterine cervical carcinoma cells down-regulated apoptotic processes and thus enhanced tumor invasion and metastasis (Affney *et al.,* 2001). Li *et al.* (2004) described that, although COX-2 protein was not detected in normal epithelium of the ovary, its protein was frequently expressed in epithelial OC, suggesting that it might contribute to the carcinoma development or progression. Matsumoto *et al.* (2001) found a significant correlation between expression of vascular endothelial growth

factor (VEGF) and COX-2 in ovarian neoplasms and suggested that an increased expression of COX-2 might be associated with malignant transformation and tumorigenesis through the activation of VEGF. Denkert *et al.* (2002) reported that expression of COX-2 was immunohistochemically detected in 42% of OCs and in 37% of borderline tumors and described that COX-2 expression was an independent prognostic factor in human OC. Although we found high frequency of COX-2 expression in OC, we did not show the close relationship between expression of COX-2 and metastasis or recurrence in ovarian carcinoma. Large-scale prospective and retrospective studies are needed to clarify whether COX-2 expression is of practical utility as a prognostic factor.

It was clearly demonstrated that the frequency and the degree of PPARγ expression were significantly decreased as lesions progressed from a borderline tumor to carcinoma, and those of COX-2 expression were significantly increased as lesions progressed from a benign tumor to carcinoma, suggesting that low expression of PPARγ and high expression of COX-2 in precancerous lesions might be involved in progression of ovarian tumors to carcinoma. Independent studies have shown that induction of COX-2 and inactivation of PPARγ occurred during the development and progression of human breast carcinoma (Jiang *et al.,* 2000; Ristimaki *et al.,* 2002). However, inhibition of COX-2 and activation of PPARγ have been shown to prevent mammary carcinogenesis in experimental animals (Harris *et al.,* 2000; Suh *et al.,* 1999). Additionally, COX-2 selective inhibitors and PPARγ ligands could significantly attenuate the growth of human breast carcinoma cells (Elstner *et al.,* 1998; Howe *et al.,* 2001). Thus, it has been suggested that high expression of PPARγ and low expression of COX-2 in the tumors might be involved in attenuating the capacity of the tumors to develop into more malignant nature. Badawi and Badr (2003) described that an increase of COX-2 expression and a decrease of PPARγ expression in breast-carcinoma tissues were paralleled by increases in the tissue levels of PGE_2 and decreases in 15d-PGJ_2 and their altered expressions might influence the development of human breast carcinoma.

The receptor PPARγ plays a crucial role in apoptosis and differentiation of a variety of cells. Induction of differentiation has been observed in several malignant cells as a result of stimulation by PPARγ (Mueller *et al.,* 1998). Activation of PPARγ resulted in apoptosis of choriocarcinoma cells (Keelan *et al.,* 1999), prostate carcinoma cells (Kubota *et al.,* 1998), leukemic cells (Asou *et al.,* 1999), and gastric carcinoma (Sato *et al.,* 2000). More recently, Martelli *et al.* (2002) reported that arrest of G1 cell cycle was observed and apoptosis was induced in thyroid carcinoma cells transfected with PPARγ. Breast-carcinoma cells treated with PPARγ agonist show dramatic morphologic changes and express E-cadherin and b-casein, markers of breast-cell differentiation (Clay *et al.,* 1999; Elstner *et al.,* 1998). Furthermore, it has been reported that differentiation and reversal of malignant changes were induced in COX-1 colonic tumor cells treated with PPARγ agonist in Swiss nude mice (Sarraf *et al.,* 1998). Zander *et al.* (2002) described that activation of PPARγ transiently induced N-cadherin, the glioma differentiation marker, in human and rat glioma cells, and, in parallel, a subset of surviving cells showed *de novo* outgrowth of processes resembling astrocyte-like morphology based on PPARγ activation. Taking these results together, including ours, activation of PPARγ and inhibition of COX-2 may be favorable for guiding neoplastic cells toward redifferentiation.

In conclusion, the reciprocal correlation between COX-2 and PPARγ implicates that COX-2 and PPARγ may contribute to OC induction. The results suggest that high expression of PPARγ and low expression of COX-2 might play an important role in inhibiting ovarian carcinogenesis.

References

Affney, D.K., Holden, J., Davis, M., Zempolich, K., Murphy, K.J., and Dodson, M. 2001. Elevated cyclooxygenase-2 expression correlates with diminished survival in carcinoma of the cervix treated with radiotherapy. *Int. J. Radiat. Oncol. Biol. Phys. 49*: 1213–1217.

Asou, H., Verbeek, K., Williamson, E., Elstner, E., Kubota, T., Kamada, N., and Koeffler, H.P. 1999. Growth inhibition of myeloid leukemia cells by troglitazone, a ligand for peroxisome proliferation activated receptor gamma and retinoids. *Int. J. Oncol. 15*:1027–1031.

Badawi, A.F., and Badr, M.Z. 2003. Expression of cyclooxygenase-2 and peroxisome proliferator-activated receptor-γ and levels of prostaglandin E_2 and 15-deoxy-$\Delta^{12,14}$ PGJ_2 in human breast cancer and metastasis. *Int. J. Cancer 103*:84–90.

Clay, C.E., Namen, A.M., Atsumi, G., Willingham, M.C., High, K.P., Kute, T.E., Trimboli, A.J., Fonteh, A.N., Dawson, P.A., and Chilton, F.H. 1999. Influence of J series prostaglandins on apoptosis and tumorigenesis of breast cancer cells. *Carcinogenesis 20*:1905–1911.

Denkert, C., Kobel, M., Pest, S., Koch, I., Berger, S., Schwabe, M., Siegert, A., Reles, A., Klosterhalfen, B., and Hauptmann, S. 2002. Expression of cyclooxygenase-2 is an independent prognostic factor in human ovarian carcinoma. *Am. J. Pathol. 160*:893–903.

Elstner, E., Muller, C., Koshizuka, K., Williamson, E.A., Park, D., Asou, H., Shintaku, P., Said, J.W., Heber, D., and Koeffler, H.P. 1998. Ligands for peroxisome proliferator-activated receptor gamma and retinoic acid receptor inhibit growth and induce apoptosis of human breast cancer cells in vitro and in BNX mice. *Proc. Natl. Acad. Sci. USA 95*:8806–8811.

Ferrandina, G., Lauriola, L., Zannoni, G.F., Fagotti, A., Fanfani, F., Legge, F., Maggiano, N., Gessi, M., Mancuso, S., Ranelletti, F.O., and Scambia, G. 2002. Increased cyclooxygenase-2 (COX-2) expression is associated with chemotherapy resistance and outcome in ovarian cancer patients. *Ann. Oncol. 13*:1205–1211.

Harris, E.R., Alshafie, G.A., Abou-Issa, H., and Seibert, K. 2000. Chemoprevention of breast cancer in rats by celecoxib, a cyclooxygenase-2 inhibitor. *Cancer Res. 60*:2101–2103.

Hauptmann, S., and Dietel, M. 2001. Serous tumors of low malignant potential of the ovary-molecular pathology. II. *Virchows Arch. 438*:539–551.

Howe, L.R., Subbaramaiah, K., Brown, A.M., and Dannenberg, A.J. 2001. Cyclooxygenase-2: a target for the prevention and treatment of breast cancer. *Endocr. Relat. Cancer 8*:97–114.

Inoue, H., Tanabe, T., and Umesono, K. 2000. Feedback control of cyclooxygenase-2 expression through PPARγ. *J. Biol. Chem. 275*:28028–28032.

Jiang, W.G., Redferm, A., Bryce, R.P., and Mansel, R.E. 2000. Peroxisome proliferator activated receptor-γ (PPARγ) mediates the action of γ-linolenic acid in breast cancer cells. *Prostaglandin Leukot. Essent. Fatty Acids 60*:119–127.

Keelan, J.A., Sato, T.A., Marvin, K.W., Lander, J., Gilmour, R.S., and Mitchell, M.D. 1999. 15-Deoxy-Delta (12, 14)-prostaglandin J(2), a ligand for peroxisome proliferator-activated receptor-gamma, induces apoptosis in JEG3 choriocarcinoma cells. *Biochem. Biophys. Res. Commun. 262*:579–585.

Komar, C.M., Braissant, O., Wahli, W., and Curry, T.E. Jr. 2001. Expression and localization of PPARs in the rat ovary during follicular development and the periovulatory period. *Endocrinology 142*:4831–4838.

Kubota, T., Koshizuka, K., Williamson, I.A., Asou, H., Said, J.W., Holden, S., Miyoshi, I., and Koeffler, H.P. 1998. Ligand for peroxisome proliferator activated receptor γ (troglitazone) has potential anti-tumor effects against human prostate cancer both *in vitro* and *in vivo*. *Cancer Res. 58*:3311–3352.

Li, S., Miner, K., Fannin, R., Barrett, J.C., and Davis, B.J. 2004. Cyclooxygenase-1 and -2 in normal and malignant human ovarian epithelium. *Gynecol. Oncol. 92*:622–627.

Martelli, M.L., Iuliano, R., Pera, I.L., Sama, I., Monaco, C., Cammarota, S., Kroll, T., Chiariotti, L., Santoro, M., and Fusco, A. 2002. Inhibitory effects of peroxisome proliferator-activated receptor γ on thyroid carcinoma cell growth. *J. Clin. Endocrinol. Metab. 87*:4728–4735.

Matsumoto, Y., Ishiko, O., Deguchi, M., Nakagawa, E., and Ogita, S. 2001. Cyclooxygenase-2 expression in normal ovaries and epithelial ovarian neoplasms. *Int. J. Mol. Med. 8*:31–36.

Mueller, E., Sarraf, P., Tontonoz, P., Evans, R.M., Martin, K.J., Zhang, M., Fletcher, C., Singer, S., and Spiegelman, B.M. 1998. Terminal differentiation of human breast cancer through PPAR gamma. *Mol. Cell 1*:465–470.

Prescott, S.M., and White, R.L. 1996. Self-promotion? Intimate connection between APC and prostaglandin H synthase-2. *Cell 87*:783–786.

Ristimaki, A., Sivula, A., Lundin, J., Lundin, M., Salminen, T., Haglund, C., Joensuu, H., and Isola, J. 2002. Prognostic significance of elevated cyclooxygenase-2 expression in breast cancer. *Cancer Res. 62*:632–635.

Sarraf, P., Mueller, E., Jones, D., King, F.J., DeAngelo, D.J., Partridge, J.B., Holden, S.A., Chen, L.B., Singer, S., Fletcher, C., and Spiegelman, B.M. 1998. Differentiation and reversal of malignant changes in colon cancer through PPARγ. *Nature Med. 4*:1046–1052.

Sato, H., Ishihara, S., Kawashima, K., Moriyama, N., Suetsugu, H., Kazumori, H., Okuyama, T., Rumi, M.A.K., Fukuda, R., Nagasue, N., and Kinoshita, Y. 2000. Expression of peroxisome proliferator-activated receptor (PPAR) γ in gastric cancer and inhibitory effects of PPARγ agonists. *Br. J. Cancer 83*: 1394–1400.

Shigemasa, K., Tian, X., Gu, L., Shiroyama, Y., Nagai, N., and Ohama, K. 2003. Expression of cyclooxygenase-2 and its relationship to p53 accumulation in ovarian adenocarcinomas. *Int. J. Oncol. 22*:99–105.

Smith, W.L., Garavito, R.M., and DeWitt, D.L. 1996. Prostaglandin endoperoxide H synthases (cyclooxygenases)-1 and -2. *J. Biol. Chem. 271*:33157–33160.

Subbaramaiah, K., Lin, D.T., Hart, J.C., and Dannenberg, A.J. 2001. Peroxisome proliferator-activated receptor γ ligands suppress the transcriptional activation of cyclooxygenase-2. *J. Biol. Chem. 276*:12440–12448.

Suh, N., Wang, Y., Williams, C.R., Risingsong, R., Gilmer, T., Wilison, T.M., and Sporn, M.B. 1999. A new ligand for the peroxisome proliferator-activated receptor-γ (PPARγ) GW7845, inhibits rat mammary carcinogenesis. *Cancer Res. 59*: 5671–5673.

Taketo, M.M. 1998. Cyclooxygenase-2 inhibitors in tumorigenesis. I. *J. Natl. Cancer Inst. 90*:1529–1536.

van Rees, B.P., Saukkonen, K., Ristimaki, A., Polkowski, W., Tytgat, G.N.J., Drillenburg, P., and Offerhaus, G.J.A. 2002. Cyclooxygenase-2 expression during carcinogenesis in the human stomach. *J. Pathol. 196*:171–179.

Zander, T., Kraus, J.A., Grommes, C., Schlegel, U., Feinstein, D., Klockgether, T., Landreth, G., Koenigsknecht, J., and Heneka, M.T. 2002. Induction of apoptosis in human and rat glioma by agonists of the nuclear receptor PPARγ. *J. Neurochem. 81*:1052–1060.

This Page Intentionally Left Blank

11

CDX2 Immunostaining in Primary and Secondary Ovarian Carcinomas

Gad Singer and Luigi Tornillo

Introduction

Histologic subtypes of ovarian carcinoma (OC) include serous papillary, endometrioid, clear cell, and mucinous carcinomas (Lee *et al.,* 2003). Earlier studies concluded that mucinous carcinomas represent 10–12% of all OCs. Newer studies indicate that primary mucinous ovarian adenocarcinomas are rare, occurring in only about 2% of all OCs (Seidman *et al.,* 2003). Most mucinous carcinomas of the ovary are probably metastatic, with the majority of intestinal provenance. In a 2003 study of 124 consecutive ovarian mucinous carcinomas, only 24% were primary and nearly 60% were derived from the intestine or pancreas (Seidman *et al.,* 2003). On morphologic examination, many metastases to the ovary may also closely mimic other primary OCs (Young and Hart, 1992), many showing a so-called "pseudoendometrioid" pattern. The most challenging task is therefore the distinction between primary and metastatic OCs (Lee *et al.,* 2003). This distinction is crucial because of different implications for therapy and prognosis. Immunohistochemistry (IHC) plays a fundamental role in the differential diagnosis of adenocarcinomas of unknown origin. In regard to OC, mainly the combination of cytokeratin 7 (CK7) and CK20 is in wide use (Berezowski *et al.,* 1996; Dionigi *et al.,* 2000; Lagendijk *et al.,* 1998). CDX2 protein, the product of the homebox *cdx2* gene, is involved in the development of the gastrointestinal (GI) tract (Suh *et al.,* 1994; Suh and Traber, 1996) and has been shown to be a specific marker of intestinal-type differentiation (Moskaluk *et al.,* 2003).

The reported prevalence of *CDX2* expression in primary OCs is inconsistent (Barbareschi *et al.,* 2003; Fraggetta *et al.,* 2003; Moskaluk *et al.,* 2003; Werling *et al.,* 2003). We therefore decided to further investigate the role of *CDX2* in primary OC and to include metastases from carcinomas to the ovary (Tornillo *et al.,* 2004), to specifically assess the utility of CDX2 as a marker for the distinction between primary OCs and metastases to the ovary.

METHODS

A monoclonal antibody to CDX2 protein (clone CDX2-88 BioGenex, Norris Canyon Road, San Ramon, CA) was used, dilution 1/100.

For detection commercial kits (DAB [diaminobenzidine] detection kit, amplification kit, endogenous

biotin blocking kit [Ventana Medical Systems, Tucson, AZ]) were used.

Solutions

1. Phosphate buffer saline (PBS), 0.01 M (pH 7.4).
2. Citrate buffer (10 mM, pH 6.0) (Quartett Immunodiagnostika GmbH, Berlin, Germany).
3. 0.3% H_2O_2 in methanol.

Antibody

Monoclonal antibody to CDX2 protein, clone CDX2-88 (BioGenex), dilution 1/100.

Tissue

Fix tissue in 10% buffered formalin and embed in paraffin. Cut 5 μm thick sections and place them on sialinized slides.

Procedure

1. Dry overnight at 37°C.
2. Rinse in xylene 2× for 5 min each.
3. Rinse in absolute alcohol twice for 3 min each.
4. Rinse in 95% alcohol for 3 min.
5. Rinse in 80% alcohol for 3 min.
6. Rinse in running water for 5 min.
7. Pretreat in microwave oven at 98°C for 30 min in citrate buffer.
8. Wash in PBS buffer at 37°C.
9. Add 0.3% H_2O_2 in methanol at 37°C for 4 min.
10. Wash in PBS buffer at 37°C.
11. Add CDX2 antibody 37°C for 32 min.
12. Wash in PBS buffer at 37°C.
13. Add prediluted rabbit anti-mouse immunoglobulin G (IgG) heavy and light chains in PBS buffer at 37°C for 8 min.
14. Wash in PBS buffer at 37°C.
15. Add prediluted rabbit anti-mouse IgG heavy chains in PBS buffer at 37°C for 8 min.
16. Wash in PBS buffer at 37°C.
17. Add 2.5 mg egg-white avidin in 0.1 M PBS at 37°C for 4 min.
18. Wash in PBS buffer at 37°C.
19. Add 2.5 mg egg-free biotin in 0.1 M PBS at 37°C for 4 min.
20. Add anti-rabbit biotinylated antibody.
21. Wash in PBS buffer at 37°C (2×).
22. Add avidin horseradish peroxidase at 37°C for 8 min.
23. Wash in PBS buffer at 37°C.
24. Add chromogen (DAB) at 37°C for 8 min.
25. Wash in PBS buffer at 37°C.
26. Add copper sulphate at 37°C for 4 min.
27. Add haematoxylin for 2 min.
28. Wash in PBS buffer.
29. Add 0.1 M lithium carbonate in 0.5 M sodium carbonate and treat for 2 min.
30. Wash in PBS buffer at 37°C.
31. Rinse in 80% alcohol for 3 min.
32. Rinse in 95% alcohol for 3 min.
33. Rinse in 100% alcohol.
34. Rinse in xylene 2× for 3 min each.
35. Mount on slide.

RESULTS AND DISCUSSION

The CDX2 protein is a homebox transcription factor, which derives its name from the *Drosophila* homeotic *caudal (Cad)* gene (Hinoi *et al.,* 2003). *Cad* plays an important role in segmentation and formation of posterior structures in *Drosophila,* such as the posterior midgut and hindgut (Mlodzik and Gehring, 1987).

A number of *Cad*-related genes have been identified in mammals, including at least two homologs in humans, termed *cdx1* and *cdx2.* Although CDX2 protein is rather broadly expressed in embryogenesis and in adult tissues of mice and humans, its expression appears to be essentially restricted to epithelial cells in the small intestine and colon (Beck *et al.,* 1995). CDX2 protein is localized in the more differentiated epithelial cells of the villus or the crypt tip (James *et al.,* 1994), being involved in the control of differentiation (Suh *et al.,* 1994; Suh and Traber, 1996). Expression of CDX2 protein is very high in the small intestine and the cecum and decreases in the distal colon (Chawengsaksophak *et al.,* l997; Freund *et al.,* l998; Jin and Drucker, 1996). Its homeotic function is showed by experiments in mice: $cdx2^{-/-}$ animals die during development and $cdx2^{+/-}$ ones develop hamartomatous polyps and adenomas in the GI tract, with characteristic heteroplasias underlining the role of the protein in the determination of position along the anterior–posterior axis of the gut (Silberg *et al.,* 2002). *Cdx2* probably acts as a tumor-suppressor gene because forced expression of CDX2 in various intestinal epithelial cell lines increases cell differentiation and apoptosis and inhibits proliferation (Lorentz *et al.,* 1997; Mallo *et al.,* 1998; Suh and Traber, 1996), while its level is lowered in human colorectal cancer cells (Ee *et al.,* 1995; Hinoi *et al.,* 2003; Kaimaktchiev *et al.,* 2004; Mallo *et al.,* 1997). The detailed distribution of CDX2 immunohistochemical expression in normal tissues and in tumors has been shown in large series (Moskaluk *et al.,* 2003). CDX2 protein has been reported to be expressed in 85–100% of colon

adenocarcinomas (Kaimaktchiev *et al.,* 2004), 20–70% of oesophageal and gastric adenocarcinomas (Kaimaktchiev *et al.,* 2004), and 10–60% of pancreas and gallbladder adenocarcinomas (Werling *et al.,* 2003). Moreover, CDX2 immunoreactvity has been reported in well-differentiated neuroendocrine tumors of the GI tract (Barbareschi *et al.,* 2004; La Rosa *et al.,* 2004) and so-called goblet-cell–type mucinous carcinomas of the lung (Rossi *et al.,* 2004). These studies, together with the reported positive immunoexpression of CDX2 in Barret's esophagus (Groisman *et al.,* 2004; Moons *et al.,* 2004), underline its specificity as a marker of intestinal differentiation.

The most important differential diagnosis of OCs is metastatic disease that may present clinically as a primary ovarian tumor (Lee and Young, 2003). Most of metastases to the ovary arise in carcinomas of the intestines, pancreas, bilary tract, or uterine cervix (Seidman *et al.,* 2003).

Several morphologic patterns might be suggestive for metastatic disease. Metastatic tumors tend to occur bilaterally, usually measure below 10 cm, and show superficial involvement and vascular invasion (Lee *et al.,* 2003). Immunohistochemical markers that are in use for the distinction between primary and metastatic OCs include CK7, CK20, Dpc4, and beta-catenin (Chou *et al.,* 2003; Ji *et al.,* 2002), but no individual marker is entirely specific. Therefore, primary OCs and metastatic carcinomas to the ovary should be identifiable by a distinct pattern of markers or by more reliable markers.

To investigate the role of CDX2 for the differential diagnosis between primary and metastatic OCs, we have studied the expression of CDX2 protein in 237 primary ovarian tumors and 20 metastases to the ovary (Tornillo *et al.,* 2004). Only a clearcut nuclear staining was considered as positive. Serous (n = 129), endometrioid (n = 68), and clear cell (n = 24) OCs were negative for CDX2. Among primary mucinous tumors only one showed a focal weak nuclear positivity (<25% of tumor cells). Metastases from gastric, pancreatic, and cervical adenocarcinomas were negative for CDX2. On the contrary, 14 (all moderately differentiated adenocarcinomas) out of 16 (2 additional poorly differentiated adenocarcinomas) metastatic tumors to the ovary of intestinal origin as well as their primaries showed strong immunoreactivity for CDX2 in more than 75% (3+) of the tumor cells (Tornillo *et al.,* 2004) (Figure 64).

In the literature, two studies found a lack of immunostaining for CDX2 (Barbareschi *et al.,* 2003; Werling *et al.,* 2003) in "nonmucinous" and serous OCs, whereas one study found CDX2 immunoreactivity in 20% of endometrioid carcinomas (Moskaluk *et al.,* 2003). In ovarian mucinous carcinomas, CDX2 expression was detected in 20–100% of the neoplasms

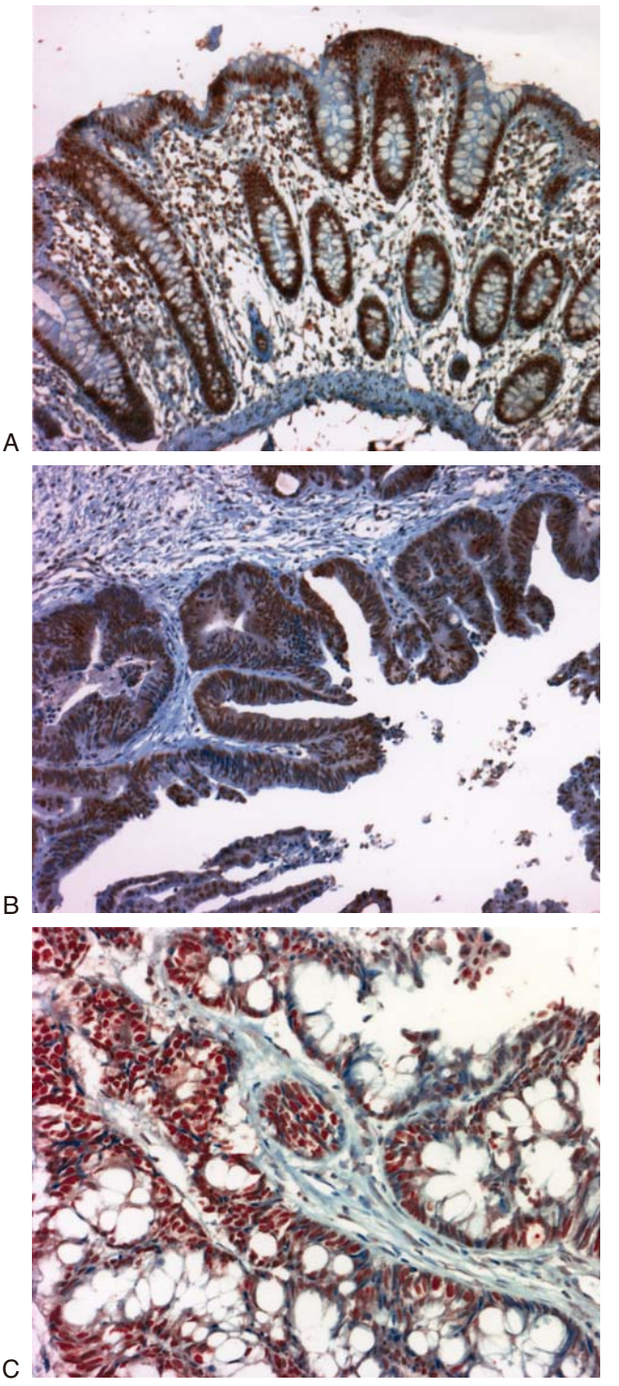

Figure 64. Nuclear staining of CDX-2. **A:** Normal colon mucosa. **B:** Primary carcinoma of the colon. **C:** Ovarian metastasis of colonic carcinoma.

(Barbareschi *et al.,* 2003; Werling *et al.,* 2003). Fraggetta *et al*. (2003) reported an investigation of CDX2 immunoexpression in a series of 62 mucinous tumors of the ovary, including 16 carcinomas. They found at least a focal CDX2 reactivity in 15 of the 16 carcinomas. In contrast, a 2004 fine-needle aspiration study (Saad *et al.,* 2004) found CDX2 expression only in metastatic carcinomas. Some contrasting reports of CDX2 immunopositivity in OCs might be partially explained by a misclassification of metastases as ovarian primaries. Conceivably, focal positivity of CDX2 (Fraggetta *et al.,* 2003) might be related to a partial "intestinal" differentiation.

In summary, CDX2 IHC is a useful and largely specific marker in the differential diagnosis between primary and metastatic tumors of the ovary. Although CDX2 appears to be an excellent marker for metastases to the ovaries from intestinal carcinomas, it should be noted that poorly differentiated intestinal carcinomas may lose their CDX2 expression and that rare primary ovarian tumors may be focally positive for CDX2. Ideally, it should be used in a panel with other markers such as CK7 or CK20.

References

Barbareschi, M., Murer, B., Colby, T.V., Chilosi, M., Macri, E., Loda, M., and Doglioni, C. 2003. CDX-2 homeobox gene expression is a reliable marker of colorectal adenocarcinoma metastases to the lungs. *Am. J. Surg. Pathol. 27*:141–149.

Barbareschi, M., Roldo, C., Zamboni, G., Capelli, P., Cavazza, A., Macri, E., Cangi, M.G., Chilosi, M., and Doglioni, C. 2004. CDX-2 homeobox gene product expression in neuroendocrine tumors: its role as a marker of intestinal neuroendocrine tumors. *Am. J. Surg. Pathol. 28*:1169–1176.

Beck, F., Erler, T., Russell, A., and James, R. 1995. Expression of Cdx-2 in the mouse embryo and placenta: possible role in patterning of the extra-embryonic membranes. *Dev. Dyn. 204*:219–227.

Berezowski, K., Grimes, M.M., Gal, A., and Kornstein, M.J. 1996. CD5 immunoreactivity of epithelial cells in thymic carcinoma and CASTLE using paraffin-embedded tissue. *Am. J. Clin. Pathol. 106*:483–486.

Chawengsaksophak, K., James, R., Hammond, V.E., Kontgen, F., and Beck, F. 1997. Homeosis and intestinal tumours in Cdx2 mutant mice. *Nature 386*:84–87.

Chou, Y.Y., Jeng, Y.M., Kao, H.L., Chen, T., Mao, T.L., and Lin, M.C. 2003. Differentiation of ovarian mucinous carcinoma and metastatic colorectal adenocarcinoma by immunostaining with beta-catenin. *Histopathology 43*:151–156.

Dionigi, A., Facco, C., Tibiletti, M.G., Bernasconi, B., Riva, C., and Capella, C. 2000. Ovarian metastases from colorectal carcinoma: clinicopathologic profile, immunophenotype, and karyotype analysis. *Am. J. Clin. Pathol. 114*:111–122.

Ee, H.C., Erler, T., Bhathal, P.S., Young, G.P., and James, R.J. 1995. Cdx-2 homeodomain protein expression in human and rat colorectal adenoma and carcinoma. *Am. J. Pathol. 147*:586–592.

Fraggetta, F., Pelosi, G., Cafici, A., Scollo, P., Nuciforo, P., and Viale, G. 2003. CDX2 immunoreactivity in primary and metastatic ovarian mucinous tumors. *Virchows Arch. 443*:782–786.

Freund, J.N., Domon-Dell, C., Kedinger, M., and Duluc, I. 1998. The Cdx-1 and Cdx-2 homeobox genes in the intestine. *Biochem. Cell. Biol. 76*:957–969.

Groisman, G.M., Amar, M., and Meir, A. 2004. Expression of the intestinal marker Cdx2 in the columnar-lined esophagus with and without intestinal (Barrett's) metaplasia. *Mod. Pathol. 17*:1282–1288.

Hinoi, T., Loda, M., and Fearon, E.R. 2003. Silencing of CDX2 expression in colon cancer via a dominant repression pathway. *J. Biol. Chem. 278*:44608–44616.

James, R., Erler, T., and Kazenwadel, J. 1994. Structure of the murine homeobox gene cdx-2. Expression in embryonic and adult intestinal epithelium. *J. Biol. Chem. 269*:15229–15237.

Ji, H., Isacson, C., Seidman, J.D., Kurman, R.J., and Ronnett, B.M. 2002. Cytokeratins 7 and 20, Dpc4, and MUC5AC in the distinction of metastatic mucinous carcinomas in the ovary from primary ovarian mucinous tumors: dpc4 assists in identifying metastatic pancreatic carcinomas. *Int. J. Gynecol. Pathol. 21*: 391–400.

Jin, T., and Drucker, D.J. 1996. Activation of proglucagon gene transcription through a novel promoter element by the caudal-related homeodomain protein cdx-2/3. *Mol. Cell. Biol. 16*:19–28.

Kaimaktchiev, V., Terracciano, L., Tornillo, L., Spichtin, H., Stoios, D., Bundi, M., Korcheva, V., Mirlacher, M., Loda, M., Sauter, G., and Corless, C.L. 2004. The homeobox intestinal differentiation factor CDX2 is selectively expressed in gastrointestinal adenocarcinomas. *Mod. Pathol. 17*:1392–1399.

La Rosa, S., Rigoli, E., Uccella, S., Chiaravalli, A.M., and Capella, C. 2004. CDX2 as a marker of intestinal EC-cells and related well-differentiated endocrine tumors. *Virchows Arch. 445*: 248–254.

Lagendijk, J.H., Mullink, H., Van Diest, P.J., Meijer, G.A., and Meijer, C.J. 1998. Tracing the origin of adenocarcinomas with unknown primary using immunohistochemistiy: differential diagnosis between colonic and ovarian carcinomas as primary sites. *Hum. Pathol. 29*:491–497.

Lee, K.R., Tavassoli, F.A., Prat, J., Dietel, M., Gersell, D.J., Karseladze, A.I., Hauptmann, S., Rutgers, J., Russell, P., Buckley, C.H., Pisani, P., Schwartz, P., Goldgar, D.E., Silva, E., Caduff, R., and Kubik-Huch, R.A., (eds). 2003. *Surface Epithelial-Stromal Tumors. World Health Classification of Tumors*. Lyon: IARC Press.

Lee, K.R., and Young, R.H. 2003. The distinction between primary and metastatic mucinous carcinomas of the ovary: gross and histologic findings in 50 cases. *Am. J. Surg. Pathol. 27*:281–292.

Lorentz, O., Duluc, I., Arcangelis, A.D., Simon-Assmann, P., Kedinger, M., and Freund, J.N. 1997. Key role of the Cdx2 homeobox gene in extracellular matrix-mediated intestinal cell differentiation. *J. Cell Biol. 139*:1553–l565.

Mallo, G.V., Rechreche, H., Frigerio, J.M., Rocha, D., Zweibaum, A., Lacasa, M., Jordan, B.R., Dusetti, N.J., Dagorn, J.C., and Iovanna, J.L. 1997. Molecular cloning, sequencing and expression of the mRNA encoding human Cdx1 and Cdx2 homeobox: down-regulation of Cdx1 and Cdx2 mRNA expression during colorectal carcinogenesis. *Int. J. Cancer 74*:35–44.

Mallo, G.V., Soubeyran, P., Lissitzky, J.C., Andre, F., Farnarier, C., Marvaldi, J., Dagorn, J.C., and Iovanna, J.L. 1998. Expression of the Cdx1 and Cdx2 homeotic genes leads to reduced malignancy in colon cancer-derived cells. *J. Biol. Chem. 273*: 14030–14036.

Mlodzik, M., and Gehring, W.J. 1987. Expression of the caudal gene in the germ line of Drosophila: formation of an RNA and protein gradient during early embryogenesis. *Cell 48*:465–478.

Moons, L.M., Bax, D.A., Kuipers, E.J., Van Dekken, H., Haringsma, J., Van Vliet, A.H., Siersema, P.D., and Kusters, J.G. 2004.

The homeodomain protein CDX2 is an early marker of Barrett's oesophagus. *J. Clin. Pathol. 57*:1063–1068.

Moskaluk, C.A., Zhang, H., Powell, S.M., Cerilli, L.A., Hampton, G.M., and Frierson, H.F., Jr. 2003. Cdx2 protein expression in normal and malignant human tissues: an immunohistochemical survey using tissue microarrays. *Mod. Pathol. 16*:913–919.

Rossi, G., Murer, B., Cavazza, A., Losi, L., Natali, P., Marchioni, A., Migaldi, M., Capitanio, G., and Brambilla, E. 2004. Primary mucinous (so-called colloid) carcinomas of the lung: a clinicopathologic and immunohistochemical study with special reference to CDX-2 homeobox gene and MUC2 expression. *Am. J. Surg. Pathol. 28*:442–452.

Saad, R.S., Essig, D.L., Silverman, J.F., and Liu, Y. 2004. Diagnostic utility of CDX-2 expression in separating metastatic gastrointestinal adenocarcinoma from other metastatic adenocarcinoma in fine-needle aspiration cytology using cell blocks. *Cancer 102*:168–173.

Seidman, J.D., Kunnan, R.J., and Ronnett, B.M. 2003. Primary and metastatic mucinous adenocarcinomas in the ovaries: incidence in routine practice with a new approach to improve intraoperative diagnosis. *Am. J. Surg. Pathol. 27*:985–993.

Silberg, D.G., Sullivan, J., Kang, E., Swain, G.P., Moffett, J., Sund, N.J., Sackett, S.D., and Kaestner, K.H. 2002. Cdx2 ectopic expression induces gastric intestinal metaplasia in transgenic mice. *Gastroenterology 122*:689–696.

Suh, E., Chen, L., Taylor, J., and Traber, P.G. 1994. A homeodomain protein related to caudal regulates intestine-specific gene transcription. *Mol. Cell. Biol. 14*:7340–7351.

Suh, E., and Traber, P.G. 1996. An intestine-specific homeobox gene regulates proliferation and differentiation. *Mol. Cell Biol. 16*:619–625.

Tornillo, L., Moch, H., Diener, P.A., Lugli, A., and Singer, G. 2004. CDX-2 immunostaining in primary and secondary ovarian carcinomas. *J. Clin. Pathol. 57*:641–643.

Werling, R.W., Yazji, H., Bacchi, C.E., and Gown, A.M. 2003. CDX2, a highly sensitive and specific marker of adenocarcinomas of intestinal origin: an immunohistochemical survey of 476 primary and metastatic carcinomas. *Am. J. Surg. Pathol. 27*:303–320.

Young, R.H., and Hart, W.R. 1992. Renal cell carcinoma metastatic to the ovary: a report of three cases emphasizing possible confusion with ovarian clear cell adenocarcinoma. *Int. J. Gynecol. Pathol. 11*:96–104.

This Page Intentionally Left Blank

12

Epithelial Ovarian Cancer and the E-Cadherin–Catenin Complex

Cristina Faleiro-Rodrigues, Isabel Macedo-Pinto, and Deolinda Pereira

Introduction

Ovarian carcinomas are a heterogeneous group of neoplasms with different biological potential and clinical outcome. The International Federation of Gynecology and Obstetries (FIGO) stage is a classical prognostic variable in ovarian cancer that allows a certain degree of tumor stratification, useful for clinical purposes, such as planning treatment and predicting patient survival. However, a considerable degree of heterogeneity remains within each group of FIGO stage, limiting its predictive value. In this respect, the identification of new prognostic markers that may allow a more thorough understanding of the biology of these tumors would be of great clinical value (Fox and Wells, 1999). The poor survival and significant morbidity associated with ovarian cancer primarily results from the fact that epithelial ovarian tumors are often asymptomatic until they have developed to a large size, causing distension of the abdomen. Consequently, a significant number of tumors are diagnosed in advanced stages, which results in poor prognosis. During the subsequent surgical removal of the tumor metastases are frequently observed in the peritoneal cavity and occasionally in the liver (Barns *et al.,* 2002).

Cell-adhesion molecules may play an important role in ovarian carcinogenesis because cell-to-cell adhesion plays a critical role in a wide variety of biological processes including embryogenesis, maintenance of cell polarity, cell growth, and cell differentiation (Birchmeier and Behrens, 1994; Takeichi, 1991). The loss of cell-adhesion molecules may lead to changes in cellular adhesion and to increased motility, processes that contribute to the invasive or metastatic potential of cells.

Epithelial cadherin (E-cadherin, 120 kDa; chromosome 16q22.1) (Natt *et al.,* 1989) is a transmembrane glycoprotein that mediates calcium-dependent homotypic intercellular adhesion and plays an important function in maintaining the histoarchitecture in adult tissues and forming the key functional component of adherence junctions between epithelial cells (Takeichi, 1991). Although the adhesive activity of E-cadherin resides in its extracellular domain, the function of E-cadherin depends on its ability to form an intracellular complex with the catenin proteins (Birchmeier and Behrens, 1994).

The catenins, α- (102 kDa, chromosome 5q21-22) (McPherson *et al.,* 1994), β- (92 kDa, chromosome 3p21) (Krauss *et al.,* 1994), and γ-catenin (plakoglobin, 83 kDa, chromosome 17q21) (Aberle *et al.,* 1995), are a set of peripheral membrane proteins that act as intermediates in the linkage between E-cadherin and the cytoskeleton. At adherens junctions, α-catenin links the E-cadherin–β-catenin complex or the

Handbook of Immunohistochemistry and *in situ* Hybridization of Human Carcinomas, Volume 4: Molecular Genetics, Gastrointestinal Carcinoma, and Ovarian Carcinoma

E-cadherin–γ-catenin complex to the actin cytoskeleton, thereby forming mutually exclusive complexes (Nagafuchi and Takeichi, 1988). In this way, the catenins are essential in association with E-cadherin in anchoring and organizing the cytoskeleton and stabilizing cell-to-cell adhesion (Kemler, 1993). Because the function of cadherin is dependent on the catenins for efficient cell-to-cell adhesion, alterations in the functionally active catenins may result in loss of cell adherence and facilitate the process of invasion and metastatic dissemination.

The purpose of these studies was first to describe the immunohistochemical expression of the proteins that make up the E-cadherin–catenin complex in epithelial ovarian tumors. Second, it was to evaluate whether an association between the immunoexpression of these proteins with clinicopathologic parameters could be established. The clinicopathologic parameters evaluated were the FIGO stage, histologic type and differentiation of the tumor, peritoneal metastasis, residual postoperative tumor, integrity of the tumor's serosal surface, peritoneal cytology, and lymphatic and vascular invasion. In addition, its purpose was to determine whether the immunoexpression of these proteins associated significantly with overall survival of the patients.

In this chapter, we summarize the results of our studies evaluating the immunohistochemical expression of the E-cadherin–catenin complex proteins in epithelial ovarian tumors.

MATERIALS

1. The study group consisted of 154 epithelial ovarian tumors, diagnosed at the Portuguese Institute of Oncology of Francisco Gentil, Porto, from January 1995 to December 2000.
2. Tissue samples were obtained from routine formalin-fixed and paraffin-embedded blocks.
3. All tissue specimens underwent microscopic confirmation of diagnosis; tumor classification (World Health Organization) and histologic grade and staging of tumors were assigned according to FIGO standards.
4. In the series of 154 epithelial ovarian tumors, 17 cases were benign tumors, 33 were borderline, and 104 were malignant tumors.
5. The series of carcinomas included 56 serous, 22 mucinous, 16 clear cell, 8 endometrioid, and 2 transitional tumors, graded into 26 well-differentiated, 27 moderately differentiated, and 51 poorly differentiated tumors.
6. In this series, 31 cases were diagnosed in FIGO stage I, 7 in FIGO stage II, 47 in FIGO stage III, and 19 in FIGO stage IV.

METHODS

Immunohistochemistry

1. Tissues were sectioned at 3 μm and mounted on poly-L-lysine–treated glass slides, deparaffinized, and rehydrated in a series of graded ethanols.
2. Endogenous peroxidase was blocked with 0.3% H_2O_2 for 30 min at room temperature.
3. For the antigen-retrieval procedure, sections were immersed in 0.01 M sodium citrate buffer solution (pH 6.0) and heated in a 600 W microwave oven for 4 cycles of 2 min; the slides were then left to cool for 30 min and rinsed in phosphate buffer saline (PBS) solution.
4. Nonspecific binding was reduced by incubation of the tissue section in normal rabbit serum diluted 1:5 in 12.5% bovine serum albumin for 30 min.
5. The slides were then incubated at 4°C overnight with the appropriate monoclonal antibodies diluted in 12.5% BSA, anti-E-cadherin (C20820) 1:2500, α-catenin (C21620) l:180, β-catenin (C19220) l:2000, and γ-catenin (C26220) 1:1000.
6. After washing in PBS for 10 min, the slides were incubated in biotinylated rabbit anti-mouse immunoglobulin (IgG) diluted 1:200 for 30 min and washed in PBS.
7. The slides were then incubated for another 30 min with the avidin-biotin complex labeling antibody at room temperature.
8. After washing in PBS, the detection system was achieved by a peroxidase substrate solution (0.05% diaminobenzidine [DAB] 3,3-tetrahydrochloride, and 0.03% H_2O_2 in PBS) added to the slides for 7 min.
9. The DAB reaction was stopped under running tap water.
10. The sections were counterstained with haematoxylin for 30 sec and mounted for microscopic examination.

To ensure accurate and reproducible staining, normal skin epithelium was used as a positive control. Strong and homogenous E-cadherin and α-, β-, and γ-catenin immunoexpression was observed at the cell-to-cell membranes of epithelial cells. Normal skin without the primary antibody was used as a negative control.

Evaluation and Quantification of Immunostaining

All slides were evaluated by light microscopy semi-quantitatively. The abundance of membranous E-cadherin and catenin-positive cells was scored from 0 to 3 (0 = complete absence of expression, 1 = <10%,

2 = 11–50%, 3 = 51–100%). Reduced expression consisted of positive staining in ≤50% of the tumor cell population. Preserved expression consisted of positive staining in >51% of the tumor cell population.

Statistical Analysis

The association between E-cadherin–catenin antigen expression and the clinicopathologic parameters were evaluated using the Chi-square test. The univariate survival analysis was based on the Kaplan-Meier method and probabilities were compared by the log-rank or the Breslow test. The multivariate analysis to determine the independent prognostic value of the various parameters was performed by the Cox regression. A value of $P < 0.05$ was considered statistically significant.

RESULTS AND DICSUSSION

Cell-to-cell adhesion participates in histiogenesis and plays a critical role in the establishment and maintenance of cell polarity. Reduced cell-to-cell adhesiveness allows cancer cells to disobey the social order, resulting in the destruction of the histologic structure, the morphologic hallmark of malignant tumors (Birchmeier *et al.,* 1993; Van Aken *et al.,* 2001; Hajra and Fearon, 2002; Takatsugu *et al.,* 2002).

E-cadherin is localized at specialized cell-to-cell adhesion sites termed adherens junctions. Adherens junctions play an adhesive as well as architectural role in the epithelium by providing a link between cell-surface adhesion molecules and the cytoskeleton. At the adherens junctions, E-cadherin establishes a linkage with the actin cytoskeleton through a group of intracellular proteins termed catenins, which mediate signal transduction mechanisms that regulate cell growth and differentiation (Kemler, 1993; Ozawa *et al.,* 1989; Takeichi, 1991; Shimoyama *et al.,* 1989). The interaction of the catenins to E-cadherin is a requirement for normal cell adhesion, and alterations of catenin molecules can lead to the disruption of cell-to-cell adhesion, resulting in tumor aggressiveness and invasiveness in neoplastic diseases (Behrens *et al.,* 1989; Frixen *et al.,* 1991; Takatsugu *et al.,* 2002; Wijnhoven *et al.,* 2000).

The biological relevance of the E-cadherin–catenin complex proteins in primary epithelial ovarian tumors was studied. This study used the immunohistochemical method to analyze the expression pattern of E-cadherin, α-catenin, β-catenin, and γ-catenin (reduced versus preserved phenotype) in epithelial ovarian tumors. In the borderline tumors, the immunoexpression pattern of E-cadherin and α-catenin associated with histologic type ($P = 0.014$, $P = 0.030$, respectively). In malignant tumors, the immunoexpression pattern of E-cadherin was related to histologic type ($P = 0.001$). The preserved phenotype of E-cadherin was most frequently observed in mucinous tumors, whereas reduced E-cadherin was most frequently observed in serous tumors. The immunoexpression pattern of β-catenin associated with histologic type and tumor differentiation ($P = 0.005$, $P = 0.025$, respectively). The preserved phenotype of β-catenin associated with endometrioid carcinomas, whereas reduced β-catenin expression associated with poorly differentiated serous and clear cell carcinomas. Although the reduced phenotype was the most frequent immunoexpression observed for all proteins of the E-cadherin-catenin complex in epithelial ovarian tumors, only β-catenin expression showed a significant difference between benign, borderline, and malignant tumors ($P = 0.045$). Borderline and malignant tumors most frequently showed the reduced phenotype. In this study, the immunohistochemical profile of β-catenin was shown to be of biological relevance because reduced β-catenin expression correlated with loss of tumor differentiation and serous carcinomas that are known to depict aggressive biological behaviour in epithelial ovarian tumors (Faleiro-Rodrigues *et al.,* 2005).

When we determined whether the immunoexpression pattern (reduced versus preserved phenotype) of E-cadherin and β-catenin correlated with the clinicopathologic features in the group of 104 primary malignant tumors, the immunoexpression pattern of E-cadherin associated with FIGO tumor stage ($P = 0.043$) histologic subtype ($P = 0.001$), peritoneal metastasis ($P = 0.006$), and residual tumor ($P = 0.036$). The immunoexpression pattern of β-catenin associated with histologic subtype ($P = 0.005$), tumor differentiation ($P = 0.025$), and peritoneal metastasis ($P = 0.041$). The immunoexpression pattern of E-cadherin correlated with that of β-catenin ($P = 0.001$). The reduced phenotype for both E-cadherin and β-catenin associated with histologic subtype ($P < 0.001$) and peritoneal metastasis ($P = 0.001$), suggesting that the immunohistochemical profile of E-cadherin and β-catenin may be useful in identifying a particular subpopulation of patients with ovarian cancer characterized by an adverse clinical outcome because the reduced phenotype of these molecules associated with poor tumor differentiation, peritoneal metastasis, and advanced FIGO stage tumors (Faleiro-Rodrigues *et al.,* 2004a).

When the classification of E-cadherin and β-catenin immunoexpression pattern was assessed into negative (total absence) versus positive (positive in 1–100% of tumor cell population) immunostaining in the primary malignant tumors, this immunoexpression pattern associated significantly with overall survival. Two separate studies, evaluating the significance of E-cadherin

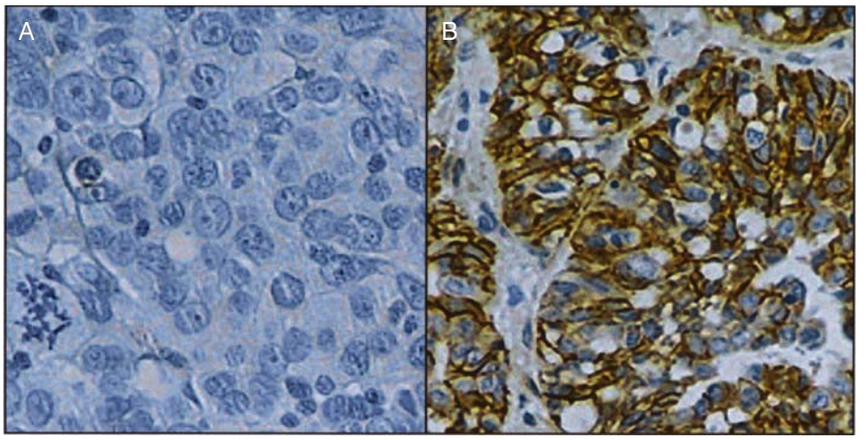

Figure 65. Immunoreactivity of β-catenin. Negative expression 400X, **(A)** and positive expression, **(B)** of β-catenin in a serous carcinoma 200X.

and the catenins as predictors of poorer overall survival, were performed. Negative expression of E-cadherin was observed in 7 (7%) tumors, and positive immunoexpression was seen in 97 (93%). In the univariate survival analysis, negative E-cadherin expression significantly predicted a poorer overall survival in patients when compared with positive expression ($P = 0.006$). In the multivariate analyses, immunoexpression of E-cadherin and the presence of residual tumor after cytoreductive surgery were independent prognostic factors for survival ($P = 0.014$, $P = 0.034$, respectively) (Faleiro-Rodrigues *et al.,* 2004b). In another study, the negative expression of β-catenin observed in 15 (14%) carcinomas associated with a poorer overall survival in the univariate analyses ($P = 0.022$). In the multivariate analysis, the immunoexpression of β-catenin and the presence of residual tumor after cytoreductive surgery were independent prognostic factors for survival ($P = 0.003$, $P = 0.019$, respectively) (Faleiro-Rodrigues *et al.,* 2004c). When both E-cadherin and β-catenin were analyzed further to determine whether the immunoexpression of these two proteins continued to be important independent prognostic factors in the same sample of malignant tumors, when assessed simultaneously in the Cox's multivariate regression analysis. The loss of β-catenin ($P = 0.0001$) was shown to be the strongest independent predictor of poor survival, together with residual tumor after cytoreductive surgery ($P = 0.016$), and FIGO stage ($P = 0.048$), when assessed with peritoneal metastasis, peritoneal cytology, and lymphatic or vascular invasion and E-cadherin expression (Faleiro-Rodrigues *et al.,* 2004c).

These results suggest that β-catenin is a crucial and indispensable component in the formation of the cadherin–catenin complex and that the loss of β-catenin alone is sufficient to render carcinoma cells more invasive. Although the prognostic value of β-catenin needs to be confirmed in a larger number of patients, our results suggest that the immunohistochemical assessment of β-catenin into negative *versus* positive expression (Figure 65, A and B) in primary ovarian carcinomas could prove to be a useful marker for selecting a small group of patients with a high risk of suffering an unfavorable clinical outcome. Whether this information can be used to stratify patients for therapeutic strategies also needs to be explored in future clinical studies.

References

Aberle, H., Bierkamp, C., Torchard, D., Serova, O., Wagner, T., Natt, E., Wirsching, J., Heidkämper, C., Montagna, M., Lynch, H.T., Lenoir, G.M., Schereer, G., Feunteun, J., and Kemler, R. 1995. The human plakoglobin gene localizes on chromosome 17q21 and is subjected to loss of heterozygosity in breast and ovarian cancers. *Proc. Natl. Acad. Sci. USA, 92*: 6384–6388.

Barns, M.N., Grizzle, W.E., Grubbs, C.J., and Patridge, E.E. 2002. Paradigms for primary prevention of ovarian carcinoma. *CA Cancer J. Clin. 52*:216–225.

Behrens, J., Mareel, M.M., Van Roy, F.M., and Birchmeier, W. 1989. Dissecting tumor cell invasion: epithelial cells acquire invasive properties after the loss of uvomorulin-mediated cell-cell adhesion. *J. Cell Biol. 108*:2435–2447.

Birchmeier, W., Weidner, K.M., Hulsken, J., Behrens, J. 1993. Molecular mechanisms leading to cell junction (cadherin) deficiency in invasive carcinomas. *Semin. Cancer Biol. 4*:231–235.

Birchmeier, W., and Behrens, J. 1994. Cadherin expression in carcinomas: Role in the formation of cell junctions and the prevention of invasiveness. *Bioch. Biophys. Acta. 1198*:11–26.

Faleiro-Rodrigues, C., Macedo-Pinto, I., Maia, S.S., Vieira, R.H., and Lopes, C.S. 2005. Biological relevance of the E-cadherin-catenin

complex proteins in primary epithelial ovarian tumors. *Gynecol. Obstet. Invest. 40*:75–83.

Faleiro-Rodrigues, C., Macedo-Pinto, I., Pereira, D., Ferreira, V.M., and Lopes, C.S. 2004a. Association of E-cadherin and β-catenin immunoexpression with clinicopathologic features in primary ovarian carcinomas. *Hum. Pathol. 35*:663–669.

Faleiro-Rodrigues, C., Macedo-Pinto, I., Pereira, D., and Lopes, C.S. 2004b. Prognostic value of E-cadherin immunoexpression in patients with primary ovarian carcinomas. *Ann. Oncol. 15*: 1532–1542.

Faleiro-Rodrigues, C., Macedo-Pinto, I., Pereira, D., and Lopes, C.S. 2004c. Loss of β-catenin is associated with poor survival in ovarian carcinomas. *Int. J. Gynecol. Pathol. 23*:337–346.

Fox, H., and Wells, M. 1999. Histopathology of epithelial ovarian cancer with particular reference to prognostic factors *CME. J. Gynecol. Oncol. 4*:142–150.

Frixen, U.H., Behrens, J., Sachs, M., Eberle, G., Voss, B., Warda, A., Lochner, D., and Birchmeier, W. 1991. E-cadherin-mediated cell-cell adhesion prevents invasiveness of human carcinoma cells. *J. Cell Biol. 113*:173–185.

Hajra, K.M., and Fearon, E.R. 2002. Cadherin and catenin alterations in human cancers. *Genes. Chromos. Cancer 34*:255–268.

Kemler, R. 1993. From cadherins to catenins: cytoplasmatic protein interactions and regulation of cell adhesion. *Trends Genet. 9*:317–321.

Krauss, C., Liehr, T., Hulsken, J., Behrens, J., Birchmeier, W., Grzeschik, K-H., and Ballhausen, W. 1994. Localization of the human beta-catenin gene (CTNNB1) to chromosome 3p21: a region implicated in tumor development. *Genomics 23*: 272–274.

McPherson, J.D., Morton, R.A., Ewing, C.M., Wasmuth, J.J., Overhauser, J., Nagafuchi A., Tsukita, S., and Isaacs, W.B. 1994. Assignment of the human alpha-catenin gene (CTNNA1) to chromosome 5q21-q22. *Genomics 19*:188–190.

Nagafuchi, A., and Takeichi, M. 1988. Cell binding function of E-cadherin is regulated by the cytoplasmic domain. *EMBO J. 7*:3679–3684.

Natt, E., Magenis, R.E., Zimmer, J., Mansouri, A., and Scherer, G. 1989. Regional assignment of the human loci for ovumorulin (UVO) and chymotrypsinogen B (CTRB) with the help of two overlapping deletions on the long arm of chromosome 16. *Cytogenet. Cell Genet. 50*:145–148.

Ozawa, M., Baribault, H., and Kemler, R. 1989. The cytoplasmic domain of the cell adhesion molecule ovumorulin associates with three independent proteins structurally related in different species. *EMBO J. 8*:1711–1717.

Shimoyama, Y., Hirohashi, S., Hirano, S., Noguchi, M., Shimsato, Y., Takeichi, M., and Abe, O. 1989. Cadherin celladhesion molecules in epithelial tissues and carcinomas. *Cancer Res. 49*:2128–2133.

Takatsugu, O., Yingming, L., Rey-Chen, P., and Jer-Tsong, H. 2002. Cell adhesion proteins as tumor suppressors. *J. Urol. 167*:1836–1843.

Takeichi, M. 1991. Cadherin cell adhesion receptors as a morphogenetic regulator. *Science 251*:1451–1455.

Van Aken, E., De Wever, O., Correia da Rocha, A.S., and Mareel, M. 2001. Defective E-cadherin/catenin complexes in human cancer. *Virchows Arch. 439*:725–751.

Wijnhoven, B.P.L., Dinjens, W.N.M., and Pignatelli, M. 2000. E-cadherin-catenin cell-cell adhesion complex and human cancer. *Br. J. Surg. 87*:992–1005.

This Page Intentionally Left Blank

13

Role of Cytokeratin Immunohistochemistry in the Differential Diagnosis of Ovarian Tumors

Helen P. Cathro and Mark H. Stoler

Introduction

Most ovarian tumors are readily diagnosable by routine hematoxylin and eosin (H&E) morphology without adjunctive immunohistochemical studies. However, immunohistochemical analysis is useful for some ovarian tumors, particularly sex-cord stromal and germ-cell tumors, and a few ovarian epithelial tumors that cannot be reliably diagnosed with H&E alone. The ovary is a fairly common target for metastatic tumors, and although the figures vary depending on the type of study, approximately 5–10% of explorations of an abdominal or pelvic mass in females prove to be metastases to the ovary (Ulbright *et al.,* 1984). Immunohistochemical staining can help determine whether a tumor is primary or metastatic, but it should always be used in the context of a detailed clinical history and pertinent radiologic and intraoperative data.

Certain tumors, when found in the ovary, should immediately cause one to consider a metastasis. For example, mucinous adenocarcinomas of colonic, gastric, and pancreatobiliary origin can produce lesions morphologically indistinguishable from primary ovarian tumors (Blaustein, 2002; Scully *et al.,* 1996). Metastatic breast carcinomas, carcinoid tumors, and lymphoma can also cause a problem in differential diagnosis. The gross findings (e.g., unilateral or bilateral involvement, single or multiple surface nodules, and cystic features) are not always reliable predictors of primary versus metastatic malignancy (Daya *et al.,* 1992; DeCostanzo *et al.*, 1997; Young and Hart, 1998). Serous carcinomas and undifferentiated ovarian tumors are more frequently bilateral than other ovarian primaries; when other light microscopic patterns are seen with bilateral involvement, metastatic disease should be considered (Blaustein, 2002). The light microscopic findings of mucinous tumors, columnar cell adenocarcinomas of various types, and small round-cell tumors can be particularly misleading. The fact that a mucinous tumor of the ovary is low grade is not supportive of a primary lesion because low-grade tumors of the appendix and pancreas can easily be mistaken for borderline or atypical proliferative mucinous tumors.

Although determination of the primary site may make little difference in choosing treatment modalities or particular chemotherapeutic regimens for some ovarian tumors, for others it may be critical. Determination of the primary site may also aid in prognostication.

Handbook of Immunohistochemistry and *in situ* Hybridization of Human Carcinomas, Volume 4: Molecular Genetics, Gastrointestinal Carcinoma, and Ovarian Carcinoma

For example, in one study, the 5-year survival rate for mucinous adenocarcinomas metastatic to the ovary versus primary mucinous adenocarcinomas of ovary was 11% versus 51% at all stages (Riopel *et a1.,* l999). Accurate determination of primary versus secondary ovarian tumors may also impact many databases used to profile ovarian neoplasia. Of course, primary ovarian tumors also metastasize and may require immunohistochemical analysis in this setting. Of the immunohistochemical stains used to help determine the primary or secondary nature of ovarian tumors, cytokeratin differential staining, particularly cytokeratins 7 (CK7) and 20 (CK2O), are among the most useful.

Cytokeratins are a group of polypeptides constituting the 7-ll nm intermediate filaments of the cytoskeleton of epithelial cells. Although 30 proteins have been identified, 20 keratins, the so-called epithelial or soft keratins, are the best characterized (Miettinen, 1993). The other 10 trichocytic or hard keratins are present almost exclusively in hair- and nail-forming epithelia. The soft keratins are coded by separate genes on chromosomes 12 and 17 and are expressed in differentiation-specific patterns. When carcinomas differentiate toward a particular type of epithelium, they express the cytokeratin characteristic of the nonneoplastic version of that epithelium, making cytokeratins particularly useful in classifying carcinomas (Moll *et al.,* l992).

The use of immunohistochemical markers in panels based on the light microscopic findings by H&E facilitates the diagnosis of primary poorly differentiated ovarian tumors. The distinction among poorly differentiated sex-cord stromal, surface-epithelial, and germ-cell tumors can be made using various cytokeratins, often in the form of a so-called keratin cocktail, along with an ever-expanding group of other antibodies. Ovarian surface epithelium, which gives rise to the majority of primary ovarian tumors, is a specialized form of mesothelium; however, it is distinguished from peritoneal and pleural mesothelium by its expression of estrogen and progesterone receptors. Not surprisingly, ovarian serous papillary carcinoma can be morphologically similar to papillary peritoneal mesothelioma. Although both tumors express cytokeratins characteristically found in simple epithelia (CK7, CK8, CK18, and CK19), mesotheliomas can be distinguished by their CK5 and CK6 positivity.

Although mucinous ovarian neoplasms are also surface epithelial in differentiation, they have a different cytokeratin expression pattern from the other ovarian surface-epithelial tumors. Up to 70% express CK20, as do the vast majority of lower gastrointestinal (GI) carcinomas, bladder tumors, and Merkel cell tumors. Many primary mucinous ovarian tumors also express CK7, although studies have demonstrated only a small majority with the CK7 positive/CK20 positive staining pattern (Cathro and Stoler, 2002). Most other ovarian surface-epithelial tumors, and nonovarian adenocarcinomas including those from the upper GI tract, are CK7 positive and CK20 negative.

It has now been unequivocally demonstrated that the type of tumor most commonly associated with pseudomyxoma peritonei, a low-grade, disseminated mucinous tumor involving the appendix and usually both ovaries, originates in the appendix (Guerrieri *et al.,* 1997; Ronnett *et al.,* 1997). For this reason, a majority of cases of low-grade pseudomyxoma peritonei express CK20 and a minority express CK7.

The differential diagnosis of small round-cell tumors involving the ovary can be broad and particularly difficult to unravel. It ranges from undifferentiated carcinoma, lymphoma, and small-cell carcinoma of hypercalcemic or pulmonary types, through the whole range of small round-cell tumors of childhood. Once again, cytokeratins singly or in a cocktail containing those characteristically expressed in both simple and complex epithelia can be among the most useful antibodies. As in the diagnosis of undifferentiated neoplasia at other sites, an excellent first-round immunohistochemical panel used to narrow the field may include a keratin cocktail, S-100 protein, and leukocyte common antigen (CD45RO) (DeYoung and Wick, 2000).

Hence, cytokeratins are virtually always used as part of an immunohistochemical panel, chosen in the context of the clinical, gross, and light microscopic findings on H&E. A panel approach protects against false interpretation of antigen expression and against misinterpretation of heterogeneous antigen expression and provides increased sensitivity and specificity. On occasion, the use of a panel approach may add tumors to the differential list that were not among the primary considerations. Immunohistochemistry (IHC) is also increasingly being used in the interpretation of cytologic specimens—for example in ascites fluid, both in cell blocks and now in the new liquid-based cytologic preparations. As with any adjunctive technique, the utility of cytokeratin IHC should be balanced against potentially misleading results caused by undirected immunoassay-based searches for primary sites.

MATERIALS

1. Xylene (Allegiance, McGaw Park, IL).
2. Absolute ethanol.
3. 95% Ethanol.
4. Hydrogen peroxide methanol. Mix 50 ml 3% hydrogen peroxide (Allegiance) and 75 ml methanol. Make fresh before each use.

5. Citrate Buffer Solution/Tissue Revival Solution (Cell Marque Corporation, Hot Springs, AZ).

6. APK Wash Concentrate 10× Solution (Ventana, Tuscon, AZ). Add 18 L of distilled water to a 20 L carboy. Add the 2 L bottle of APK Wash Concentrate and mix well. Adjust the pH if necessary to 7.6 ± 0.2. Store at room temperature.

7. Ventana Basic Diaminobenzidine (DAB) Detection Kit (Ventana). Store at 4°C.

8. Antibody Diluent (Ventana). Store at 4°C and warm to room temperature before use.

9. Endogenous Biotin Blocking Kit (Ventana). Store at 4°C.

10. Protease 1 (Ventana). Store at 4°C.

11. Protease 3 (Ventana). Store at 4°C.

12. Negative Control (Ventana). Store at 4°C.

13. Liquid Coverslip (Ventana).

14. Hematoxylin 1 (Richard Allen, Kalamazoo, MI).

15. Bluing agent (Richard Allen).

16. Pap pen (Zymed, South San Francisco, CA).

17. Cytoseal (Richard Allen).

18. Vectastain ELITE Avidin Biotin C Kit (Vector, Burlingame, CA). Store at 4°C.

The working solutions for all kits are good for 72 hrs.

a. Blocking serum (normal serum): Add 3 drops (150 µl) of stock to 10 ml of buffer in yellow working-solution bottle. The preferred serum for blocking is prepared from the same species from which the biotinylated antibody is made.

b. Biotinylated secondary antibody: Add 3 drops (150 µl) of blocking serum stock (yellow bottle) to 10 ml of buffer in blue working solution bottle and then add a single drop (50 µl) to biotinylated antibody stock (blue label).

c. Vectastain ELITE ABC Reagent: Add exactly 2 drops (100 µl) of Reagent A (gray label) to 5 ml of buffer in the ABC working solution bottle. Then add exactly 2 drops (100 µl) of Reagent B (gray label) to the same working solution bottle. Mix immediately and allow to stand for 10 min before use.

19. DAB Chromogen Solution (Dako, Carpinteria, CA). Store at 4°C

a. Stock solution: Allow bottle of DAB tablets to reach room temperature before opening. Place 10 ml of phosphate buffer saline (PBS) into a test tube. Carefully transfer a single tablet to the tube and allow to dissolve. *Caution: DAB is a suspected carcinogen and causes severe skin and eye irritation. Exercise caution and always use gloves when handling this agent.* Any fine particulate matter remaining undissolved will not interfere with staining. Store at 4°C.

b. Working substrate solution: Transfer 2 µ1 of DAB stock solution to another test tube. Add 15 µl of 3% hydrogen peroxide. This solution is only stable for 2 hr.

Primary Antibodies

1. Keratin cocktail.
   (800 µ1 of MAK-6 Mouse Monoclonal anti-Cytokeratin Cocktail (Zymed). Store at 4°C. Stains human cytokeratins 8, 14, 16, 18, and 19.
   40 µl of Anti-keratin AE1/AE3 (Boeringer Mannheim, Indianapolis, IN). Store at 4°C for up to a week; if longer, store in aliquots at –20°C. Stains human cytokeratins 1–8,10,14, 15,16, and 19.
   264 µl of CAM 5.2 (Enzo Diagnostics, New York, NY). Store at 4°C. Stains human cytokeratins 1,5,10, and 14.
   80 µl of Keratin-902 (35βH11) (Enzo Diagnostics). Store at 4°C. Stains human cytokeratin 8.
   80 µl of Keratin-903 (34βE12) (Enzo Diagnostics). Store at 4°C. Stains human cytokeratins 1,5,10, and 14.

Add all of the above to 9.6 ml of Antibody Diluent, mix well, and treat slides with Protease 3 for 4 min.

2. Cytokeratin 7. Clone OV-TL 12/30 (Dako). Store at 4°C. Use in a 1:400 dilution with Protease 1 for 4 min.

3. Cytokeratin 20. Clone Ks 20.8 (Dako). Store at 4°C. Use in a 1:400 dilution with Protease 1 for 4 min.

4. Cytokeratin 5/6/18. Clone LP34 (Novocastra Laboratories Ltd, Newcastle upon Tyne, United Kingdom). Store at 4°C. Use in a 1:200 dilution.

Note: All antibodies should be aliquoted in amounts necessary to add to a single dispenser, q.s. a total volume of 5 ml, placed in sealed tubes and stored at –80°C for up to 10 years.

METHODS

Deparaffinization

1. Dry paraffin-embedded slides cut 3–4 µm thick at 60°C for a minimum of 1 hr. Slides may then be held overnight at 37°C and stored at room temperature.

2. Immerse slides in reagents using a manual stain set up, in the following order:

a. Xylene 10 min.
b. Xylene 10 min.
c. Xylene 10 min.
d. Absolute alcohol 10 dips.
e. Absolute alcohol 10 dips.

f. Absolute alcohol 10 dips.
g. 95% Alcohol 10 dips.
h. 95% Alcohol 10 dips.
i. 95% Alcohol 10 dips.
j. Distilled water 10 dips.
k. Distilled water 10 dips.
l. Distilled water 10 dips.

3. Slides can then be subjected to an antigen retrieval procedure if necessary.

Antigen Retrieval Using Pressure Cooker

1. Fill a container with citrate buffer solution, place rack in buffer, and place container in the pressure cooker.
2. Set the timer for 15 min, after which it should be turned off and the pressure vented.
3. Once completely vented, open lid, remove container, and let cool for 15 min.

Counterstaining and Coverslipping Procedure

1. Immediately after the slides are rinsed in running tap water, using a manual stain set up, immerse the slides as follows

a.	Hematoxylin	1 min, 15 sec
b.	Tap water	Rinse until water is clear
c.	Bluing agent	1 min
d.	Distilled water	10 dips
e.	Distilled water	10 dips
f.	Distilled water	10 dips
g.	95% Alcohol	10 dips
h.	95% Alcohol	10 dips
i.	95% Alcohol	10 dips
j.	Absolute alcohol	10 dips
k.	Absolute alcohol	10 dips
l.	Absolute alcohol	10 dips
m.	Xylene	10 dips
n.	Xylene	10 dips
o.	Xylene	10 dips

2. Coverslip in the usual fashion.

Automated Immunoperoxidase Stain Procedure

These methods pertain to the use of a Ventana ES or Ventana NexES instrument.

Note: The manufacturers recommendations for balancing the instrument, aligning the reagent dispensers, and checking the rinsing jets should be rigorously followed because failure to do so can cause weak or uneven staining.

1. Attach barcode labels appropriate for the antibody protocol to each clinical/research and control slide. *Make sure that none of the edges of the barcode labels touch the edge of the slide, because this can affect the amount of antibody remaining on the slide during incubation.* Load the slides into the stain rack.
2. Deparaffinize and rehydrate to water according to the previous procedure. *It is important not to allow air-drying to prevent excess DAB staining.*
3. Immerse slides in hydrogen peroxide/methanol for 15 min.
4. Rinse in distilled water and follow antigen retrieval procedure described earlier.
5. Load the reagent carousel with the appropriate detection and primary dispensers needed.
6. If using an antibody dispenser for the first time, check for the presence of reagent in the tip. If none is present, follow the instructions for that particular dispenser. *Do not reprime if the dispenser has been previously used or if using an antibody kit.*
7. Load the barcode-labeled slides onto the slide carousel.
8. Apply APK Wash from a squeeze bottle to each slide to maintain moisture of the slide.
9. Close the chamber and begin the run by starting the computer.
10. When the run is completed, remove the slides in the rack and place the rack in a stain container filled with warm tap water and one drop of Dawn dishwashing detergent.
11. Rinse the slides in running tap water.
12. Counterstain, blue, dehydrate, clear, and coverslip according to the counterstaining and coverslipping procedure.

Manual Immunohistochemistry Staining Procedure

1. Take DAB tablets out of the refrigerator to reach room temperature.
2. Deparaffinize and rehydrate slides according to the previously described procedure.
3. Immerse slides in hydrogen peroxide/methanol for 15 min.
4. Rinse in distilled water and follow procedure for antigen retrieval.
5. If not using marked slides, circle the area of tissue to be stained with a Pap pen.
6. Lay slides flat in a humid incubating tray with a lid.
7. Apply working blocking serum (yellow bottle) to tissue area. Incubate at room temperature for 10 min.
8. Gently tap off excess serum, but do not rinse the slides.
9. Apply the appropriately diluted primary antibody and incubate at room temperature for 1 hr.
10. Rinse slides individually in APK Wash.
11. Apply the working biotinylated antibody secondary antibody solution to the tissue area and incubate at room temperature for 10 min.

12. Rinse the slides well with APK Wash.
13. Apply the working ABC solution (gray bottle) to the tissue area and incubate at room temperature for 10 min.
14. Make up a fresh batch of DAB while the slides are incubating.
15. Rinse slides individually in APK Wash.
16. Apply working DAB solution to the tissue area and incubate for approximately 7 min, checking microscopically for the correct stain level.
17. Rinse slides in tap water to stop the DAB reaction.
18. Counterstain, blue, dehydrate, and coverslip according to the previous procedures.

Processing of Cytologic Material for Immunohistochemistry

1. Liquid-based preparations fixed in 95% ethanol, agar-based cell blocks, and cellular smears fixed in 95% ethanol are all satisfactory IHC and are processed using standard protocols.
2. Antigen retrieval should not be performed on cytologic material.
3. Should immunohistochemical staining be required on either cell block slides or smeared slides previously stained with H&E or Papanicolaou stains, destaining is not required because the procedures for immunohistochemical staining will remove the previous stain.

Interpretive Guidelines

Primary versus Metastatic Ovarian Neoplasms

Lower GI tumors are among the most common tumors that metastasize to the ovary, with the reported rate varying from 4% to 10% (Birnkrant *et al.,*1986; Kaminski and Norris, 1984). These tumors typify the pitfalls of attempting to differentiate primary from metastatic disease in the ovary. Grossly, metastatic colonic lesions are often cystic and larger than the primary intestinal lesion (Daya *et al.,* 1992; Young and Hart, 1998). The signature microscopic findings of coloni carcinoma, so-called central "dirty necrosis" surrounded by a garland pattern of neoplastic glands, can often be seen focally in primary endometrioid carcinoma of the ovary (DeCostanzo, *et al.,* 1997). Although microscopic features such as focal endometriosis, an adjacent adenofibromatous tumor, or concurrent squamous metaplasia can support an ovarian origin, they are often absent. Mucinous intestinal adenocarcinoma can closely mimic mucinous ovarian adenocarcinoma (Riopel *et al.,* 1999). Paradoxically, metastatic mucinous intestinal adenocarcinomas can have a striking mixture of benign, borderline, and carcinomatous features, although the benign component will not be predominant (Scully *et al.,* 1996). An immunohistochemical panel using CK7, CK20, and carcinoembryonic antigen (CEA) may be helpful in this setting.

Nearly all primary nonmucinous ovarian carcinomas are likely to be CK7 positive and CK20 negative. A majority (up to 75%) of colonic adenocarcinomas are CK7 negative and CK20 positive (Cathro and Stoler, 2002; Loy *et al.,* 1996; Wang *et al.,* 1995). (See Figure 67). Rectal adenocarcinomas in particular may exhibit a CK7-positive, CK20-negative expression profile; however, dual positive colonic adenocarcinomas have also been rarely found. The immunohistochemical dogma states that the majority of ovarian mucinous tumors are CK7 and CK20 dual positive (Loy *et al.,* 1996; Wang *et al.,* l995). Some authors have suggested that a dual positive CK7/CK20 pattern is specific for mucinous ovarian tumors of low malignant potential (Ronnett *et al.,* 1997), and other authors have found all primary mucinous ovarian tumors to be CK7 positive (Guerrieri *et al.,* 1997). Another study, however, has found a small majority (56%) of ovarian mucinous adenocarcinomas expressing the CK7-positive/CK20-negative profile with the remainder having the "characteristic" CK7-positive/CK20-positive profile (Cathro and Stoler, 2002). These differences in staining profiles may be related to the often-patchy staining obtained with CK20, as well as the percentage of stained cells set as the cutoff for positivity in the CK7 studies. It should be noted that upper-GI and pancreatobiliary tumors can also have a CK7-positive/CK20-positive staining pattern (up to 65% for pancreatic tumors and 35% for gastric carcinomas) (Chu *et al.,* 2000; Wang *et al.,* 1995).

Other adenocarcinomas likely to metastasize to the ovary include gastric, pancreatic, breast, appendiceal, and biliary carcinomas. Endocervical and esophageal carcinomas do so more rarely. Metastatic *gastric carcinomas* often have signet-ring morphology, making the distinction from a primary ovarian tumor relatively easy. Primary ovarian signet-ring–cell tumors may be a real entity (Blaustein, *et al.,* 2002) but are difficult to separate from mucinous adenocarcinoma primary to the ovary with extensive signet-ring differentiation. Second and third in frequency for primary sites of Krukenberg-like tumors are the intestine and appendix (Scully, *et al.,* 1996). Gastric, pancreaticobiliary, and ampullary adenocarcinomas may demonstrate the CK7-positive CK 20-positive phenotype as discussed earlier (up to 65% for pancreatic and 35% for gastric carcinomas) but can often be CK7 positive/CK20 negative (up to 30% for pancreatic and 25% for gastric carcinomas),

as breast and endocervical carcinomas can also be. Appendiceal adenocarcinomas may express the CK7-negative/CK20-positive phenotype characteristic of lower-gastrointestinal carcinomas; however, up to 55% are both CK7 and CK20 positive (Cathro and Stoler, 2002; Ronnett *et al.,* l997).

Carcinoid tumors metastatic to the ovary usually originate in the small intestine and most often have a trabecular growth pattern, although a few are insular or mucinous (Scully *et al.,* 1996). Almost all of the rare carcinoids metastatic to the ovary from the appendix are of the mucinous or goblet-cell type. Appendiceal mucinous carcinoid tumors can have multiple different morphologic patterns and usually a minority endocrine cell population with chromogranin and serotonin expression. They can only be separated from the extremely rare mucinous carcinoids of the ovary based on the clinical and gross findings because they are morphologically and immunohistochemically similar. Cytokeratin expression in appendiceal carcinoid tumors appears to be restricted to a minority, with both CK7 and CK20 positivity having been demonstrated (Cai *et al.,* 2001; Chu *et al.,* 2000; Wilander and Scheibenpflug, 1993).

Most *breast carcinoma* metastatic to the ovary becomes clinically apparent after the primary breast diagnosis or as occult metastases found in up to 30% of oophorectomies subsequent to a primary breast tumor. Lobular breast carcinomas metastasize to the ovary significantly more frequently than ductal adenocarcinomas, and a keratin cocktail can be very helpful in finding the inconspicuous single-file cells of the lobular tumors. Breast carcinomas have a propensity to metastasize into a wide variety of other primary ovarian carcinomas, but the disparate morphologies usually facilitate this distinction. Because the majority of both breast and ovarian carcinomas are pankeratin/CK7 positive and CK20 negative, these antibodies will not be helpful in separating primary ovarian from metastatic breast tumors; however GCDFP-15 marks up to 71% (Monteagudo *et al.,* l991) of breast carcinomas in a paranuclear pattern (Chu *et al.,* 2000; Wang *et al.,* 1995).

Cervical carcinomas are reported to metastasize to the ovary in up to 7% of cases, with adenocarcinomas metastasizing much more frequently than squamous cell carcinomas (Kaminski and Norris 1984; Riopel *et al.,* 1999). In one study of mucinous ovarian tumors associated with mucinous cervical adenocarcinomas, 63% of the ovarian tumors were probably independent primary tumors (Young and Scully, 1988). Primary ovarian squamous cell carcinomas can nearly always be differentiated on the basis of an association with a benign dermoid tumor or endometriotic cyst. The distinction between synchronous ovarian and cervical primary mucinous tumors and metastases can be very difficult. Cytokeratin immunohistochemical stains will not be helpful unless the ovarian mucinous tumor happens to display the CK7-positive/CK20-positive pattern.

It is now widely accepted that mucinous ovarian tumors arising in association with *low-grade appendiceal tumors and pseudomyxoma peritonei* are metastatic from the appendix and not synchronous primary tumors (Blaustein, 2002). These tumors, as opposed to high-grade appendiceal adenocarcinomas, make up the preponderance of tumors metastatic to the ovary from the appendix (Ronnett *et al.,* 1995). The cytokeratin staining profile of these tumors is consistent with the appendiceal origin, with the vast majority of these sets of tumors having synchronous staining in the appendix and ovary and a majority (60–75%), being CK7 negative and CK20 positive. Most of the remaining tumors are CK7 positive and CK20 negative, analogous to the percentage of lower-GI tumors with that staining profile (Guerrieri *et al.,* 1997; Ronnett *et al.,* 1997).

Most ovarian *endometrioid carcinomas* arising in association with endometrioid carcinomas of the uterus represent synchronous primaries (Ulbright *et al.,* 1984). Because both tumors will have the common adenocarcinoma pattern of CK7 positivity and CK20 negativity, keratin, IHC will not be helpful. In this situation, attention to the depth of invasion of the uterus is likely to be more helpful in judging the likelihood of metastatic disease. On occasions where the ovarian versus uterine origin of a serous papillary carcinoma is being sought, WT 1 may be helpful because it usually demonstrates nuclear positivity in ovarian and negativity in uterine serous papillary carcinomas (Goldstein and Uzieblo, 2002). *Endometrial stromal sarcomas* are more likely to metastasize to the ovary than leiomyosarcomas (Young and Scully, 1990). The former may be confused with sex-cord stromal tumors (e.g., thecomas) or granulosa-cell tumors; however, the characteristic arterial pattern of endometrial stromal sarcomas can usually be found at least focally. Cytokeratins will be unhelpful in this scenario; however, CD10 appears to be a reliable marker of tumors of endometrial stroma if the staining is diffuse and strong (Chu and Arber, 2000). *Malignant mesodermal mixed tumors* (MMMT) metastasize to the ovary fairly commonly, with usually little difficulty in making this assessment. A keratin cocktail would be likely to highlight the glandular component in cases where it is scant. Rare MMMTs primary to the ovary would also be keratin positive.

Other carcinomas rarely spreading to the ovary include hepatocellular, transitional-cell, and renal-cell carcinomas. Cytokeratins may be helpful in identifying the first and last of these. *Hepatocellular carcinomas,*

which may be confused with both hepatoid ovarian yolk-sac tumors and metastatic gastric or pulmonary hepatoid tumors, are fairly often both CK7 and CK20 negative (79–93%), whereas the other tumors in the differential may have variable cytokeratin positivity (Chu *et al.,* 2000; Lau *et al.,* 2002; Maeda *et al.,* 1996). Both sets of tumors may have alpha fetoprotein (AFP) positivity. Analyses of *transitional-cell carcinomas* have produced conflicting results with a preponderance (63%) of CK7-positive/CK20-negative cases in one series and a preponderance (89%) of dual-positive cases in another large series (Chu *et al.,* 2000; Wang *et al.,* 1995). A third large study examining only urothelial carcinomas demonstrated high molecular weight cytokeratin in 80% and CK20 in 48% (Parker *et al.,* 2003). Because ovarian transitional cell carcinomas are rarely positive for CK20 and would usually be positive for CK7, the utility of differential cytokeratin staining in this situation is variable (Soslow *et al.,* 1996). *Renal-cell (clear-cell) carcinomas* are one of the rare groups of tumors that frequently demonstrate dual CK7/CK20 negativity, with 70–89% demonstrating this pattern (Chu *et al.,* 2000; Cathro and Stoler, 2002; Wang *et al.,* 1995). CD10 can be used as an immunohistochemical marker to support a diagnosis of renal-cell carcinoma because approximately 90% were positive in one large study (Chu and Arber, 2000). Clear-cell carcinomas of the ovary, however, are likely to display the usual CK7-positive/CK20-negative phenotype (Vang *et al.,* 2001).

Although the rate of ovarian metastases to the ovary is fairly high in *malignant melanoma,* the majority of cases are detected in autopsy specimens. The morphologic features of malignant melanoma are usually readily apparent; however, occasionally lymphoma, granulosa-cell tumor, or small-cell carcinoma of hypercalcemic type may prove problematic. S100 protein, HMB-45, or Melan-A (MART-1) positivity will allow a diagnosis of malignant melanoma, with cytokeratin providing a useful negative marker.

A keratin cocktail may also be useful as a negative marker for another group of tumors more commonly disseminated than primary to the ovary, *the non-Hodgkin lymphomas.* Burkitt's lymphoma has a particular propensity to involve the ovary, whether occurring in endemic or nonendemic areas. Among other lymphomas involving the ovaries, diffuse large B-lymphocytic lymphomas are the next most common group. Tumors difficult to distinguish morphologically can include dysgerminomas, small-cell carcinomas of various types, and poorly differentiated metastatic carcinomas. Virtually all lymphomas are leukocyte common antigen (LCA) positive (the exception being anaplastic large-cell lymphoma), with further confirmation being provided by expression of B- or T-lymphocytic markers in the vast majority. Once again, a keratin cocktail provides a reassuring negative marker. It is important to determine whether an ovarian lymphoma is primary or disseminated to the ovary for prognostic purposes. Disseminated disease presenting in the ovary, although uncommon, is actually more common than primary ovarian lymphoma. The largest group of ovarian lymphoma cases is those with occult involvement by node-based lymphoma. Leukemic involvement of the ovaries has similar features of occult involvement.

Cytokeratins 5/6 are a limited tool in the separation of ovarian involvement by *malignant mesothelioma* from papillary surface-epithelial neoplasms, in those cases where ovarian involvement predominates and the tumor lacks the typical tubular and low-grade papillary features of most mesotheliomas. Cytokeratins 5/6 are found in the cytoskeleton of basal cells, epidermal stratum spinosum, and mesothelial cells (Chu and Weiss, 2002). Mesotheliomas are keratin 5/6 positive in 56–l00% of cases, with sarcomatoid mesotheliomas less likely to be positive (33–77%), whereas serous carcinomas of the ovary and papillary serous carcinomas of the peritoneum taken together are likely to be positive in only 25% of cases (Chu and Weiss, 2002; Ordonez 1998). Positivity for CK5/6 in adenocarcinomas is likely to be focal, as opposed to the diffuse and strong staining characteristic of mesotheliomas (Ordonez, 1998). Calretinin and Ber-EP4 as positive markers for mesothelioma and adenocarcinoma respectively, may prove more useful in immunohistochemical panels used to make this distinction.

Ovarian metastatic lesions peculiar to *children* include the fairly common secondary involvement in adrenal neuroblastoma and rare secondary involvement by rhabdomyosarcomas. Although ovarian metastases of neuroblastomas do not usually present during life, such involvement is found in up to 50% of autopsies. Although IHC may be helpful in microscopically challenging cases, cytokeratin would be useful only as a negative marker. The distinctive histologic features of neuroblastoma usually preclude the need for immunohistochemical staining. Primary rhabdomyosarcomas of the ovary are usually embryonal in type with secondary cases including both the alveolar and embryonal types.

Primary Ovarian Neoplasms

Although very few immunohistochemical studies have included cases of undifferentiated or *poorly differentiated ovarian carcinomas,* these tumors often provide a diagnostic challenge. Undifferentiated or poorly differentiated carcinomas would usually be expected to retain some pancytokeratin or epithelial

membrane antigen (EMA) positivity and be inhibin negative (Pelkey *et al.,* 1998). Adult granulosa-cell tumors, one type of tumor that has to be distinguished from poorly differentiated carcinoma, are variably positive for cytokeratins, are fairly reliably inhibin positive and may be up to 100% calretinin positive (Movahedi-Lankarani and Kurman, 2002; Pelkey *et al.,* 1998; Riopel *et al.,* 1998; Rishi *et al.,* 1997). Poorly differentiated sex-card stromal tumors have been shown to retain inhibin positivity; (e.g., poorly differentiated Sertoli-Leydig cell tumor) (Pelkey *et al.,* 1998). Lymphomas involving the ovary have been described earlier in the section on metastatic lesions to the ovary and would obviously be cytokeratin/EMA negative, as would small-cell primitive neuroectodermal tumors, malignant melanomas, and endometrial-stromal sarcomas (usually CD10 positive). Small-cell carcinomas of hypercalcemic type and pulmonary type, as well as undifferentiated small-cell carcinomas, are likely to express cytokeratins, including CK7 and EMA (Riopel *et al.,* 1998). Another tumor likely to be difficult to differentiate from an undifferentiated carcinoma is a poorly differentiated transitional-cell carcinoma. As discussed earlier in the section on metastatic tumors to the ovary, differential cytokeratin staining is not necessarily helpful in this situation. CK20 positivity may, however, be suggestive of a transitional-cell carcinoma.

Another classic distinction that may have to be made is that between an *endometrioid carcinoma with Sertoliform features* and a *Sertoli cell tumor*. The endometrioid carcinoma, as one of the ovarian surface-epithelial tumors, should express cytokeratin, particularly CK7, and EMA (Aguirre *et al.,* 1989; Ordi *et al.,* 1999). Both inhibin and calretinin should be expressed in approximately 70% of Sertoli cell tumors and 90% of Sertoli-Leydig cell tumors (Kommoss *et al.,* 1998).

In childhood, *small round-cell tumors* have a differential diagnosis that includes juvenile granulosa-cell tumors, small-cell carcinomas of hypercalcemic type, lymphomas, and rare gonadoblastomas. As stated earlier the morphology of another tumor in this differential, rhabdomyosarcoma, may be helpful in deciding between primary and secondary involvement of the ovary. The alveolar subtype is rarely primary to the ovary; the embryonal subtype is the most common primary rhabdomyosarcoma of the ovary. Both subtypes should be cytokeratin negative. Another tumor in the small round-cell tumor category, more likely to occur in young women, is intraabdominal desmoplastic small round-cell tumor. Because these tumors exhibit multiple types of differentiation, they may co-express cytokeratin, desmin, and vimentin. Care should be taken because sex-cord stromal neoplasms can also display this pattern of positivity (McCluggage, 2002).

Pitfalls in the Use of Cytokeratin Immunohistochemical Staining

The major pitfall in the use of cytokeratin immunohistochemical stains, as in the use of any immunohistochemical stain, is using the marker in isolation. As should be clear from the previous discussion, no immunohistochemical stain is 100% sensitive or specific. The positive and negative predictive value of a panel is therefore always stronger than a single stain used alone. An example would be the so-called characteristic dual-negative staining pattern of renal-cell carcinomas with CK7 and CK20. A metastatic renal-cell carcinoma may on occasion be hard to differentiate from a clear-cell carcinoma primary to the ovary. If the cytokeratins are not used in an immunohistochemical panel with vimentin (usually positive in clear-cell carcinomas of the kidney) or CD10, an incorrect conclusion may be drawn because a significant proportion of various epithelial tumors may be dual CK7 and CK20 negative.

Another pitfall is the common misconception that the intensity of staining is more important than the proportion of tumor cells staining positively. Staining intensity is dependent not only on the individual tumor characteristics but also on the particular type of stain and various technical factors. Staining of less than 5–10% of tumor cells often correlates with aberrant or heterogeneous staining, which should produce caution in interpretation. Heterogeneous staining is particularly characteristic of CK20 among the cytokeratins, and can lead to erroneous conclusions in biopsy specimens, in cytologic specimens, or on tissue microarrays.

Molecular Correlates

As covered exhaustively in Volume I of the Handbook, molecular techniques are multiplying at a rate only equaled by the number of genes or proteins that can be analyzed on a single microchip. It will be some years before more than a few of these techniques will be readily applied to regular pathologic practice; however, molecular genetics is beginning to interface with the world of IHC in the setting of clinical trials where novel antibodies are tested immunohistochemically to direct molecularly based experimental treatment regimens.

Tissue microarrays are increasingly used to identify patterns of protein expression immunohistochemically in large series of tumors, without expending large amounts of tissue. Although heterogeneous protein expression can be problematic using this technique, the use of multiple cores per tumor, especially for the smallest diameter cores, can allow useful studies.

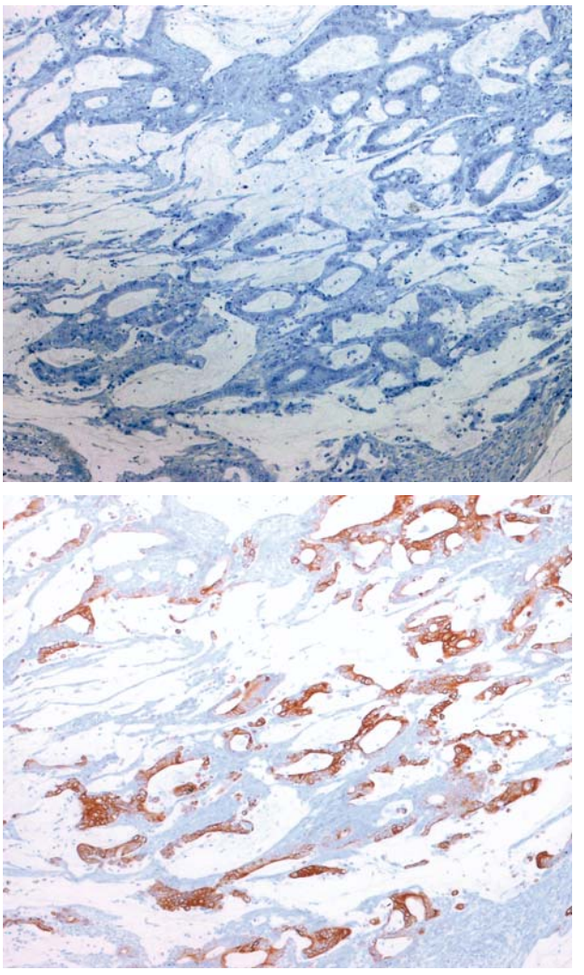

Figure 66. Colon carcinoma metastatic to the ovary with immunohistochemical staining negative for cytokeratin 7 (CK7) and positive for CK20 (100X both panels).

Cytokeratin 20 would be the cytokeratin stain most likely in our experience to demonstrate this heterogeneous pattern of expression. Tissue microarrays can also be used for *in situ* hybridization.

Gene-expression profiles of various types of carcinoma, including ovarian, are being characterized using oligonucleotide microarrays with reverse transcription-polymerase chain reaction used to validate the findings. Microdissection of frozen tissue is necessary to produce enough ribonucleic acid (RNA) for complementary RNA (cRNA) synthesis and production of an RNA microarray. After complex data analysis, information from one such study on ovarian tumors was used to separate classic histologic subgroups of ovarian tumors (Schwartz *et al.,* 2002). Another group has produced a novel high-throughput protocol that layers oligonucleotide microarray or microarray in a so-called "array-of-arrays" (Welsh *et al.,* 2001). Hierarchical cluster analysis of the data allows separation of normal and neoplastic ovarian tissue and subclassification of ovarian tumors into groups that correlate with classic histologic subtypes. Cytokeratins 7, 8, 18, and 19 were among the highly ranked genes in ovarian tumors. Giordano *et al.* (2001) have used high-density oligonucleotide arrays to obtain comprehensive gene-expression profiles of lung, colon, and ovarian tumors with immunohistochemical correlation. Two outlier tumors on gene-expression analysis, one of which was ovarian and one of which was colonic, proved to be a colonic metastasis in the case of the ovarian tumor, and the colonic tumor was confirmed as a sarcoma. Cytokeratin 20 was one of the top differentially expressed genes in this study of 50 colon carcinomas and one colon sarcoma.

Protein and gene expression of various tumor types are also being studied in an effort to provide improved prognostic information. For example, gene-expression profiles of early-stage lung adenocarcinomas using oligonucleotide microarray analysis has been analyzed to define a set of genes that predicts survival and allows delineation of a group of patients who may benefit from adjuvant therapy (Beer *et al.,* 2002). The gene for CK7 was among the top 100 genes identified as having a relationship between gene expression and worse outcome. The expression of CK5 and CK17 has been examined in tissue microarrays in an effort to provide an independent prognostic indicator of patient outcome in breast carcinoma (van de Rijn *et al.,* 2002). Specific isoforms of cytokeratins 7, 8, 18, and 19 determined by polyacrylamide gel electrophoresis and mass spectrometry have also been correlated with patient survival in one study of lung carcinoma (Gharib *et al.,* 2002). Gene-expression profiles have even been used to predict differing responses to chemotherapy in various neoplasms.

These techniques are exciting, with almost limitless potential for understanding the pathophysiology, behaviour, and responsiveness to chemotherapy of different tumors; however, they are time consuming, costly, technically complex, and bewildering in their variety and complexity. Most importantly, they are not yet clinically validated. Many of the molecular techniques produce unimaginably large amounts of information, the analysis of which depends on the correct application of complex statistical software. Because of this, IHC will remain useful in the diagnosis, classification, and perhaps in the prognostication of ovarian tumors for some years to come.

References

Aguirre, P., Thor, A.D., and Scully, R.E. 1989. Ovarian endometrioid carcinomas resembling sex cord-stromal tumors: an immunohistochemical study. *Int. J. Gynecol. Pathol. 8*:364–373.

Beer, D.G., Kardia, S.L., Huang, C.C., Giordano, T.J., Levin, A.M., Misek, D.E., Lin, L., Chen, G., Gharib, T.G., Thomas, D.G., Lizyness, M.L., Kuick, R., Hayasaka, S., Taylor, J.M., Iannettoni, M.D., Orrunger, M.B., and Hanash, S. 2002. Gene-expression profiles predict survival of patients with lung adenocarcinoma. *Nat. Med. 8*:816–824.

Birnkrant, A., Sampson, J., and Sugarbaker, P.H. 1986. Ovarian metastasis from colorectal cancer. *Dis. Colon. Rectum. 29*: 767–77l.

Blaustein, A. 2002. *Pathology of the Female Genital Tract.* New York: Springer-Verlag.

Cai, Y.C., Banner, B., Glickman, J., and Odze, R.D. 200l. Cytokeratin 7 and 20 and thyroid transcription factor 1 can help distinguish pulmonary from gastrointestinal carcinoid and pancreatic endocrine tumors. *Hum. Pathol. 32*:1087–1093.

Cathro, H.P., and Stoler, M.H. 2002. Expression of cytokeratins 7 and 20 in ovarian neoplasia. *Am. J. Clin. Pathol. 117*:944–951.

Chu, P., and Arber, D.A. 2000. Paraffin-section detection of CD10 in 505 nonhematopoietic neoplasms. Frequent expression in renal cell carcinoma and endometrial stromal sarcoma. *Am. J. Clin. Pathol. 113*:374–382.

Chu, P., Wu, E., and Weiss, L.M. 2000. Cytokeratin 7 and cytokeratin 20 expression in epithelial neoplasms: a survey of 435 cases. *Mod. Pathol. 13*:962–972.

Chu, P.G., and Weiss, L.M. 2002. Expression of cytokeratin 5/6 in epithelial neoplasms: an immunohistochemical study of 509 cases. *Mod. Pathol. 5*:6–10.

Daya, D., Nazerali, L., and Frank, G.L. 1992. Metastatic ovarian carcinoma of large intestinal origin simulating primary ovarian carcinoma: a clinicopathologic study of 25 cases. *Am. J. Clin. Pathol. 97*:751–758.

DeCostanzo, D.C., Elias, J.M., and Chumas, J.C. 1997. Necrosis in 84 ovarian carcinomas: a morphologic study of primary versus metastatic colonic carcinoma with a selective immunohistochemical analysis of cytokeratin subtypes and carcinoembryonic antigen. *Int. J. Gynecol. Pathol. 16*:245–249.

DeYoung, B.R., and Wick, M.R., 2000. Immnunohistologic evaluation of metastatic carcinomas of unknown origin: an algorithmic approach. *Semin. Diagn. Pathol. 17*:184–193.

Gharib, T.G., Chen, G., Wang, H., Huang, C.C., Prescott, M.S., Shedden, K., Misek, D.E., Thomas, D.G., Giordano, T.J., Taylor, J.M., Kardia, S., Yee, J., Orringer, M.B., Hanash, S., and Beer, D.G. 2002. Proteomic analysis of cytokeratin isoforms uncovers association with survival in lung adenocarcinoma. *Neoplasia 4*:440–448.

Giordano, T.J., Shedden, K.A., Schwartz, D.R., Kuick, R., Taylor, J.M.G., Lee, N., Misek, D.E., Greenson, J.K., Kardia, S.L.R., Beer, D.G., Rennert, G., Cho, K.R., Gruber, S.B., Fearon, E.R., and Hanash, S. 2001. Organ-specific molecular classification of primary lung, colon and ovarian adenocarcinomas using gene expression profiles. *Am. J. Pathol. 159*: 1231–1238.

Goldstein, N.S., and Uzieblo, A. 2002. WT1 immunoreactivity in uterine papillary serous carcinomas is different from ovarian serous carcinomas. *Am. J. Clin. Pathol. 117*:541–545.

Guerrieri, C., Franlund, B., Fristedt, S., Gillooley, J.F., and Boeryd, B. 1997. Mucinous tumors of the vermiform appendix and ovary, and pseudomyxoma peritonei: histogenetic implications of cytokeratin 7 expression. *Hum. Pathol. 28*:1039–1045.

Kaminski, P.J., and Norris, H.J. 1984. Coexistence of ovarian neoplasms and endocervical adenocarcinoma. *Obstet. Gynecol. 64*:553–556.

Kommoss, F., Oliva, E., Bhan, A.K., Young, R.L., and Scully, R.E. 1998. Inhibin expression in ovarian tumors and tumor-like lesions: an immunohistochemical study. *Mod. Pathol. 11*: 656–664.

Lau, S.K., Prakash, S., Geller, S.A., and Alsabeh, R.J. 2002. Comparative immunohistochemical profile of hepatocellular carcinoma, cholangiocarcinoma, and metastatic adenocarcinoma. *Hum. Pathol. 33*:1175–1181.

Loy, T.S., Calaluce, R.D., and Keeney, G.L. 1996. Cytokeratin immunostaining in differentiating primary ovarian carcinoma from metastatic colonic adenocarcinoma. *Mod. Pathol. 9*: 1040–1044.

Maeda, T., Kajiyama, K., Adachi, E., Takenaka, K., Sugimachi, K., and Tsuneyoshi, M. 1996. The expression of cytokeratins 7, 19, and 20 in primary and metastatic carcinomas of the liver. *Mod. Pathol. 9*:901–909.

McCluggage, W.G. 2002. Recent advances in immunohistochemistry in gynaecological pathology. *Histopathology 40*:309–326.

Miettinen, M. 1993. Keratin immunohistochemistry: update of applications and pitfalls. *Pathol. Annu. 28 Pt 2*:113–143.

Moll, R., Lowe, A., Laufer, J., and Franke, W.W. 1992. Cytokeratin 20 in human carcinomas: a new histodiagnostic marker detected by monoclonal antibodies. *Am. J. Pathol. 140*:427–447.

Monteagudo, C., Merino, M.J., LaPorte, N., and Neumann, R.D. 1991. Value of gross cystic disease fluid protein-15 in distinguishing metastatic breast carcinomas among poorly differentiated neoplasms involving the ovary. *Hum. Pathol. 22*:368–372.

Movahedi-Lankarani, S., and Kunnan, R.J. 2002. Cairetinin, a more sensitive but less specific marker than alpha-inhibin for ovarian sex cord-stromal neoplasms: an immunohistochemical study of 215 cases. *Am. J. Surg. Pathol. 26*:1477–1483.

Ordi, J., Schammel, D.P., Rasekh, L., and Tavassoli, F.A. 1999. Sertoliform endometrioid carcinomas of the ovary: a clinicopathologic and immunohistochemical study of 13 cases. *Mod. Pathol. 12*:933–940.

Ordonez, N.G. 1998. Role of immunohistochemistry in distinguishing epithelial peritoneal mesotheliomas from peritoneal and ovarian serous carcinomas. *Am. J. Surg. Pathol. 22*:1203–1214.

Parker, D.C., Folpe, A.L., Bell, J., Oliva, E., Young, R.H., Cohen, C., and Amin, M.B. 2003. Potential utility of uroplakin III, thrombomodulin, high molecular weight cytokeratin, and cytokeratin 20 in noninvasive, invasive, and metastatic urothelial (transitional cell) carcinomas. *Am. J. Surg. Pathol. 27*:1–10.

Pelkey, T.J., Frierson, H.F. Jr., Mills, S.E., and Stoler, M.H. 1998. The diagnostic utility of inhibin staining in ovarian neoplasms. *Int. J. Gynecol. Pathol. 17*:97–105.

Riopel, M.A., Perlman, E.J., Seidman, J.D., Kurman, R.J., and Sherman, M.E. 1998. Inhibin and epithelial membrane antigen immunohistochemistry assist in the diagnosis of sex cord-stromal tumors and provide clues to the histogenesis of hypercalcemic small cell carcinomas. *Int. J. Gynecol. Pathol. 17*: 46–53.

Riopel, M.A., Ronnett, B.M., and Kurman, R.J. 1999. Evaluation of diagnostic criteria and behavior of ovarian intestinal-type mucinous tumors: atypical proliferative (borderline) tumors and intraepithelial, microinvasive, invasive, and metastatic carcinomas. *Am. J. Sung. Pathol. 23*:617–635.

Rishi, M., Howard, L.N., Bratthauer, G.L., and Tavassoli, F.A. 1997. Use of monoclonal antibody against human inhibin as a marker for sex cord-stromal tumors of the ovary. *Am. J. Surg. Pathol. 21*:583-589.

Ronnett, B.M., Kurman, R.J., Zahn, C.M., Shmookler, B.M., Jablonski, K.A., Kass, M.E., and Sugarbaker, P.H. 1995. Pseudomyxoma peritonei in women: a clinicopathologic analysis of 30 cases with emphasis on site of origin, prognosis, and relationship to ovarian mucinous tumors of low malignant potential. *Hum. Pathol. 26*:509–524.

Ronnett, B.M., Shmookler, B.M., Diener-West, M., Sugarbaker, P.H., and Kurman, R.J. 1997. Immunohistochemical evidence supporting the appendiceal origin of pseudomyxoma peritonei in women. *Int. J. Gynecol. Pathol. 16*:1–9.

Ronnett, B.M., Zahn, C.M., Kurman, R.J., Kass, M.E., Sugarbaker, P.H., and Shmookler, B.M. 1995. Disseminated peritoneal adenomucinosis and peritoneal mucinous carcinomatosis: a clinicopathologic analysis of 109 cases with emphasis on distinguishing pathologic features, site of origin, prognosis, and relationship to "pseudomyxoma peritonei." *Am. J. Surg. Pathol. 19*:1390–1408.

Schwartz, D.R., Kardia, S.L., Shedden, K.A., Kuick, R., Michailidis, G., Taylor, J.M., Misek, D.E., Wu, R., Zhai, Y., Darrah, D.M., Reed, H., Ellenson, L.H., Giordano, T.J., Fearon, E.R., Hanash, S.M., and Cho, K.R. 2002. Gene expression in ovarian cancer reflects both morphology and biological behavior, distinguishing clear cell from other poor-prognosis ovarian carcinomas. *Cancer Res. 62*:4722–4729.

Scully, R., Young, R.H., and Clement, P. 1996. *Tumors of the Ovary, Maldeveloped Gonads, Fallopian Tube, and Broad Ligament.* Washington, D.C.: Armed Forces Institute of Pathology.

Soslow, R.A., Rouse, R.V., Hendrickson, M.R., Silva, E.G., and Longacre, T.A. 1996. Transitional cell neoplasms of the ovary and urinary bladder: a comparative immunohistochemical analysis. *Int. J. Gynecol. Pathol. 15*:257–265.

Ulbright, T.M., Roth, L.M., and Stehman, F.B. 1984. Secondary ovarian neoplasia: a clinicopathologic study of 35 cases. *Cancer 53*:1164–1174.

van de Rijn, M., Perou, C.M., Tibshirani, R., Haas, P., Kallioniemi, O., Kononen, J., Torhorst, J., Sauter, G., Zuber, M., Kochli, O.R., Mross, F., Dieterich, H., Seitz, R., Ross, D., Botstein, D., and Brown, P. 2002. Expression of cytokeratins 17 and 5 identifies a group of breast carcinomas with poor clinical outcome. *Am. J. Pathol. 161*:1991–1996.

Vang, R., Whitaker, B.P., Farhood, A.I., Silva, E.G., Ro, J.Y., and Deavers, M.T. 2001. Immunohistochemical analysis of clear cell carcinoma of the gynecologic tract. *Int. J. Gynecol. Pathol. 20*:252–259.

Wang, N., Zee, S., Zarbo, R., Bacchi, C., and Gown, A. 1995. Coordinate expression of cytokeratins 7 and 20 defines unique subsets of carcinomas. *Appl. Immunohistoch. 3*:99–l07.

Welsh, J.B., Zarrinkar, P.P., Sapinoso, L.M., Kern, S.G., Behling, C.A., Monk, B.J., Lockhart, D.J., Burger, R.A., and Hampton, G.M. 2001. Analysis of gene expression profiles in normal and neoplastic ovarian tissue samples identifies candidate molecular markers of epithelial ovarian cancer. *Proc. Natl. Acad. Sci. USA 98*:1176–4181.

Wilander, E., and Scheibenpflug, L. 1993. Cytokeratin expression in small intestinal and appendiceal carcinoids: a basis for classification. *Acta. Oncol. 32*:131–134.

Young, R.H., and Hart, W.R. 1998. Metastatic intestinal carcinomas simulating primary ovarian clear cell carcinoma and secretory endometrioid carcinoma: a clinicopathologic and immunohistochemical study of five cases. *Am. J. Surg. Pathol. 22*:805–815.

Young, R.H., and Scully, R.E. 1988. Mucinous ovarian tumors associated with mucinous adenocarcinomas of the cervix: a clinicopathological analysis of 16 cases. *Int. J. Gynecol. Pathol. 7*:99–111.

Young, R.H., and Scully, R.E. 1990. Sarcomas metastatic to the ovary: a report of 2l cases. *Int. J. Gynecol. Pathol. 9*:231–252.

This Page Intentionally Left Blank

14

Role of Immunohistochemical Expression of Cytokeratins and Mucins in Ampullary Carcinomas

Hans-Peter Fischer and Hui Zhou

Introduction

Papilla of Vater includes the border between two completely different types of mucosa: The intestinal mucosa of the ampullo-duodenum adjoins the mucosa of the ampullo-pancreaticobiliary duct respective common channel. This channel drains the ampullo-pancreatic duct segment coming from the main pancreatic duct and the ampullo-biliary duct segment coming from the choledochal duct. The periampullary region is a hot spot for adenomas and malignant tumors of the small intestine (Albores-Saavedra *et al.,* 2000b), and many carcinomas arise in the duct mucosa of the papilla and neighboring large ducts. The very special situation of this border between two different types of mucosa should be reflected in the classification of ampullary tumors. Consequently, Kimura *et al.* (1994) subdivided these carcinomas into intestinal-type tumors and pancreaticobiliary-type tumors. Albores-Saavedra *et al.* (2000a) defined the pancreaticobiliary and intestinal types as main types and added so-called "other types" such as signet-ring–cell carcinoma or undifferentiated carcinoma (Table 32).

Matsubayashi *et al.* (1999) separated intestinal-type and pancreaticobiliary-type carcinoma by the immunohistochemical expression of apomucin MUC2. Mucins (MUC) and glycoproteins characterized by high molecular mass, high carbohydrate content, and marked heterogeneity involving both the apoprotein and the oligosaccaride side chains (Carvalho *et al.,* (1999). The MUC genes are expressed in a regulated cell- and tissue-specific manner (Gendler and Spicer, 1995). In the gut, MUC5AC and MUC6 are expressed in the gastric mucosa, and MUC2 is expressed in goblet cells of the intestinal mucosa (Taylor *et al.,* 1998).

Zhou *et al.* (2004) correlated the different histologic subtypes of ampullary carcinomas as defined by Albores-Saavedra (2000a) with the different cytokeratin (CK) spectrum of these tumors. Cytokeratins are intracellular intermediate filaments consisting of 20 subtypes (Chu and Weiss, 2002). They are selectively expressed during the course of development and differentiation in different types of epithelium. The expression profile usually remains unaltered when an epithelium undergoes neoplastic transformation (Moll *et al.,* 1982). Colorectal mucosa and intestinal carcinomas usually express CK20 and lack CK7. However, mucosal epithelium of pancreatic and bile ducts as well as most carcinomas arising from these mucosal epithelium contain CK7 and lack CK20. Carcinomas of the small intestine might show a heterogeneous expression of bulk of

Handbook of Immunohistochemistry and *in situ* Hybridization of Human Carcinomas, Volume 4: Molecular Genetics, Gastrointestinal Carcinoma, and Ovarian Carcinoma

Table 32. Histological Classification of the Tumors of the Gallbladder and Extrahepatic Bile Ducts (WHO, Albores-Saavedra *et al.*, 2000b) and of the Benign and Malignant Tumors of the Ampullary Region (Albores-Saavedra *et al.*, 2000). Endocrine Tumors and Related Neoplasm are Left Out in This Comparison.

WHO Histological Classification	Classification According to Albores-Saavedra *et al.* (2000a)
Adenoma	Adenoma
Tubulary	Tubulary
Papillary	Papillary
Tubulopapillary	Tubulopapillary
Papillomatosis (adenomatosis)	
Intraepithelial neoplasia (dysplasia and carcinoma in situ)	Flat carcinoma in situ
Carcinoma	Carcinoma
Adenocarcinoma	Usual types
Papillary adenocarcinoma	Intestinal type adenocarcinoma
Adenocarcinoma, intestinal type	Pankreatobiliäry type adenocarcinoma
Adenocarcinoma, gastric-foveolar type	
Mucinous adenocarcinoma	Unusual histologic types
Clear cell adenocarcinoma	Papillary carcinoma (noninvasive)
Signet-ring cell carcinoma	Invasive papillary Carcinoma
Adenosquamous carcinoma	Mucinous Carcinoma
Squamous cell carcinoma	Signet-ring cell carcinoma
Small cell carcinoma	Clear cell Carcinoma
Large cell carcinoma	Adenocarcinoma with hepatoid differentiation
Undifferentiated carcinoma	Adenosquamous Carcinoma
Biliary cystadenocarcinoma	Small cell carcinoma
	Large cell neuroendocrine carcinoma
	Undifferentiated carcinoma

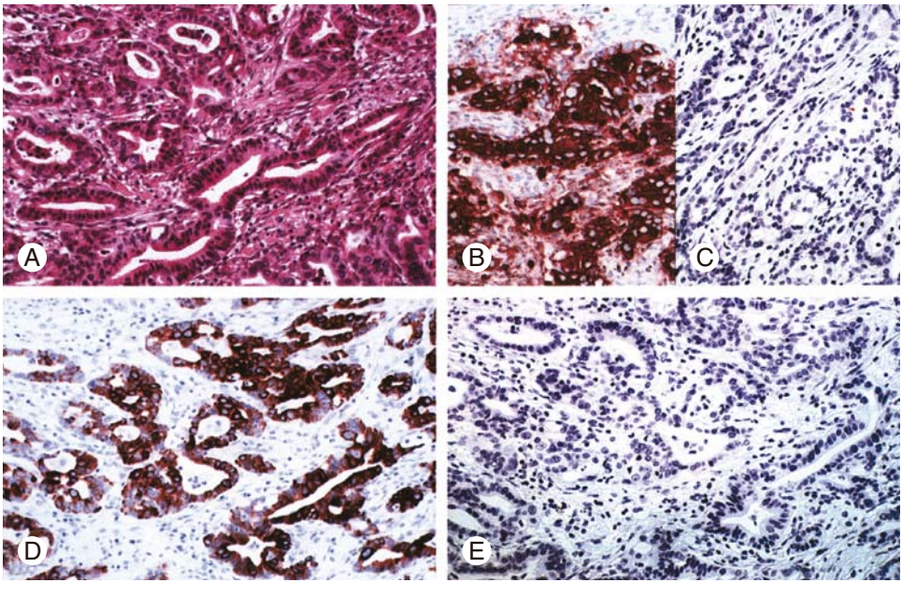

Figure 67. Ampullary carcinoma of pancreatobiliary type **(A-E)** with simple and branching glands **(A),** stained by MUC1-antibody **(B),** negative for MUC2-antibody **(C),** stained by CK7-antibody **(D),** negative for CK20-antibody **(E).**

these both keratin subtypes (Cheng and Wang, 2004). In the following review the role of MUC and keratin expression for a histogenetically based reproductible morphologic and immunohistologic classification of ampullary carcinomas will be discussed.

MATERIALS AND METHODS

Materials included 55 invasive carcinomas of Vater's ampulla (53 resection specimens of Whipple's operation and two transduodenal ampullectomy specimens). All tumors included in the study were limited to the ampulla or were mainly located in the ampulla and secondarily spreading into the neighboring structures. All specimens were gross anatomically prepared by a standard procedure including evaluation of all important anatomic structures (main and accessory pancreatic duct, ampulla of Vater, minor papilla, common bile duct, pancreatic head). Tumors were embedded completely after serial sections of the ampullary region perpendicular to the duodenal axis. For immunohistochemical study, 8 normal papillas of Vater from Whipple's operation specimens served as controls. All specimens were fixed in 4% buffered formaldehyde and embedded in paraffin.

Histologic and Immunohistochemical Staining

Tissue sections were stained with hematoxylin and eosin (H&E) and periodic acid-Schiff stain (PAS). Subsequently, all tissue samples bearing carcinomas were stained immunohistochemically with the following antibody panel: monoclonal antibodies to CK7 (OV-TL 12/30; dilution 1:500), CK20 (Ks 20.8; 1:250, both from Dako, Hamburg, Germany), apomucin MUC1 (mammary gland–type apomucin, Ma695; 1:100), apomucin MUC2 (apomucin of intestinal goblet–cell type, Ccp 58, 1:100), apomucin MUC5AC (apomucin of gastral foveolar cells type, CLH2, 1:1000, all antibodies to apomucins from Medac, Wedel, Germany).

Immunohistochemical staining was performed on an immunostainer (Techmate 500; Dako). The antigen–antibody binding was visualized with the avidin-biotin complex (ABC method) using AEC (3-amino-9-ethylcarbazol) as chromogen. To access the specifity of the antibodies, replacement of the first antibody by PBS was used as a negative control.

Morphologic Criteria for Tumor Classification

All tumors were classified histologically according to the criteria published by Albores-Saavedra *et al.* (2000a): The intestinal-type carcinoma is composed of well-formed tubular to elongate glands, complex cribriformed areas, and solid nests indistinguishable from colorectal adenocarcinoma, whereas the pancreaticobiliary-type carcinomas mostly consists of simple or branching glands and small solid nests of cells surrounded by a strikingly desmoplastic stroma. Tumors with mixed pattern were classified according to their predominant component into either the pancreaticobiliary- or the intestinal-type group. Carcinomas of "other types" included solid, invasive papillary, mucinous, and signet-ring–cell carcinomas.

The staining intensity of each immunohistochemical reaction was scored semi-quantitatively: no staining reaction = 0, <10% positive stained tumor cells = 1, 10–50% = 2, >50–80% = 3, >80% = 4. With the exception of correlation analyses between each immunohistochemical staining result, analyses were done by using a simplified scoring system (scores 0 and 1 were regarded as negative, and scores 2–4 were as positive) (Zhou *et al.,* 2004).

RESULTS

Keratin and Mucin Immunostaining of Normal Ampullas of Vater

Eight normal appearing ampullas of Vater were stained with the antibody panel as mentioned earlier (Table 33). The intestinal epithelia of the ampullo-duodenal part of the papilla was stained by the CK20 antibody, whereas the CK7 antibody stained the mucosal epithelia of all other parts of ampulla of Vater and the periampullary glands. The MUC2 antibody stained only the goblet cells of the duodenum. Few epithelia at the junction between the ampullo-duodenal part of ampulla and common channel express CK7 and MUC5AC. However, CK7 and CK20 were never co-expressed.

Histologic and Immunohistochemical Classification of Ampullary Carcinomas

Typing according to histologic criteria published by Albores-Saavedra *et al.* (2000a), we found 24/55 histologically pancreaticobiliary-type carcinomas, 15/55 histologically intestinal-type carcinomas, and 16/55 histologically "other"-type carcinomas (Tables 34 and 35). Based on this histologic classification of ampullary carcinomas, we found a high specifity of CK7 for pancreaticobiliary-type carcinomas and CK20 for intestinal-type carcinomas.

According to the different CK expression of intestinal mucosa and pancreaticobiliary mucosa, tumors expressing CK20 and lacking CK7 were defined as immunohistochemically intestinal type. Tumors expressing CK7 and lacking CK20 were defined of immunohistochemically pancreaticobiliary type. Carcinomas expressing

Table 33. Immunohistochemical Staining Characteristics of Eight Normal Ampullas of Vater

	Duodenum				Ampulla of Vater		Bile Duct and Main Pancreatic Duct	
	Surface Epithelia	Goblet Cells	Brunner Glands	Papilla	Common Channel	Periampullary Glands	Surface Epithelia	Periductal Glands
CK7	–	–	–	–	+	+	+	+
CK20	+	–	–	+	–	–	–	–
MUC2	–	+	–	–	(+)	(+)	–	–
MUC1	–	–	–	–	(+)	(+)	(+)	(+)
MUC5 AC	–	–	–	(+)	(+)	–	–	–

(+), Few cells.

CK7 and CK20 or lacking both antigens were defined as "other." Seven cases expressed CK7 as well as CK20; 5 cases were negative for these markers (see Table 35). In all subgroups, the number of males preceeded females, and the mean age of males was lower than of females.

Correlation Analysis of Histologic and Immunohistochemical Classification

In most tumors, histologic and immunohistochemical classifications were consistent. The pancreaticobiliary carcinomas were the most frequent carcinomas for both classifications. Of carcinomas of histologically pancreaticobiliary type 21 of 24 were of immunohistochemically pancreaticobiliary type and 9 of 15 carcinomas of histologically intestinal carcinomas showed the intestinal CK pattern. The 16 carcinomas of histologically "other" type could be immunohistochemically divided into 8 pancreaticobiliary-, 4 "other," and 4 intestinal-type carcinomas. The latter were signet-ring–cell carcinomas. Immunohistochemical classification correlated well with histologic classification (κ-coefficient = 0.398, $p < 0.001$).

The 7 carcinomas that expressed CK7 and CK20 were related to different histologic types. Of them 6, were MUC2 negative. None of our pancreatobiliary-type ampullary carcinomas expressed MUC2. Only 8 of 15 intestinal-type carcinomas showed this apomucin. Furthermore we found this apomucin especially in mucinous and signet-ring–cell carcinomas reflecting normal MUC2-positive intestinal goblet cells (see Table 35). Mucin1 was expressed in the majority of intestinal-type, pancreatobiliary-type and other type ampullary carcinomas. A relevant amount of carcinomas of these types expressed apomucin MUC5AC (see Table 34).

DISCUSSION

Histologic Classification of Ampullary Carcinomas

Following a proposal of Kimura *et al.* (1994), Albores-Saavedra *et al.* (2000b) emphasized the intestinal type and the pancreaticobiliary type of carcinoma as main histologic types of carcinoma of papilla of Vater. Furthermore, these authors listed unusual histologic types (e.g., mucinous, signet-ring–cell carcinomas, neuroendocrine or undifferentiated carcinomas). In the collective of the Memorial Sloan Kettering Cancer Center the intestinal type of adenocarcinoma comprised 49% and the pancreaticobiliary type comprised 21% of ampullary carcinomas (Albores-Saavedra *et al.* (2000b) (Table 36). Kimura *et al.* (1994) collected 38 pancreaticobiliary-type and 13 intestinal-type carcinomas. Also in our collective (Fischer and Zhou, 2004), the pancreaticobiliary type (44.8%) predominates the

Table 34. Immunohistochemical Expression Profile of the Three Histologically Defined Carcinoma Groups

	Intestinal Type (n = 15) (%)	Pancreaticobiliary Type (n = 24) (%)	Others (n = 16) (%)
CK7	27	96	62
CK20	80	8	37
MUC1	60	83	81
MUC2	47	0	44
MUC5AC	40	67	56

Table 35. Histologic Types, Expression of Keratin 7, 20, and of Intestinal Apomucin MUC2 in Carcinomas of the Papilla of Vater (Own Cases). Antibody-Staining in More Than 10% of Tumor Cells was Defined as Positive Reaction (Fischer and Zhou, 2004).

Histologic Type (AFIP)	Cases	CK7 + CK20 −	CK7− CK20 +	CK7 + CK20 +	CK7− CK20 −	MUC2 (+/−)
Intestinal	**15**	0	**10**	3	2	8/7
Pancreaticobiliary	**24**	**21**	0	2	1	**0/24**
Adenoca. nos	5	**4**	-	1	0	0/5
Mucinous	3	-	1	1	1	**3/0**
Signet ring cell	3	-	3	-	-	**3/0**
Papillary	4	3	0	-	1	**0/4**
Papillary, non-invasive	1	1	-	-	-	0/1
Sum	55	29	14	7	5	14/41
MUC 2 (+/−)	14/41	**0/29**	12/2	1/6	1/4	

intestinal type (26.9%) of adenocarcinoma. In World Health Organization classification, the intestinal type of adenocarcinoma is characterized as an "unusual variant" of the tumors of the gallbladder and extrahepatic bile ducts including the ampullary region (Albores-Saavedra *et al.,* 2000a). The considerable differencies in the frequency of the different histologic types of ampullary carcinomas make it obvious that there exists a considerable percentage of tumors that cannot be related undoubtedly to the main types of ampullary adenocarcinoma by histologic criteria alone.

Immunohistochemical Characterization of Ampullary Carcinomas

Immunohistochemically the different types of carcinomas can be characterized more objectively (Fischer and Zhou, 2004; Matsubayashi *et al.,* 1999). *Pancreaticobiliary-type adenocarcinomas* nearly always express keratin 7 and lack the intestinal apomucin MUC2. In most cases they are negative for keratin 20. This marker spectrum is according to that of the normal pancreaticobiliary epithelium and to the epithelium of the peripapillary glands of the papilla of Vater. *Intestinal-type adenocarcinomas* mostly contain keratin 20 and apumucin MUC2 and often lack keratin 7 according to normal intestinal epithelium. It is interesting that also many *other type carcinomas* of papillary region can be related to intestinal type or pancreaticobiliary type of mucusa: In our collective most poorly differentiated carcinomas as well as most papillary carcinomas showed the immunohistochemical pattern of pancreaticobiliary-duct mucosa. All mucinous and signet-ring–cell type carcinomas of our collective expressed intestinal apomucin MUC2. The signet-ring–type carcinomas reflected the keratin profile of intestinal epithelium. Some carcinomas that reacted negatively for keratins and apomucin 2 developed from precursor lesions with a line-specific marker pattern for intestinal or pancreaticobiliary-duct mucosa (Fischer and Zhou, 2004).

Histogenetic Aspects of Keratins and Apomucins in Ampullary Carcinomas

The strikingly correlated expression pattern of two unrelated types of immunohistochemical markers (keratins and apomucin 2) in pancreaticobiliary duct epithelium as well as in pancreaticobiliary-type carcinomas (CK7+, CK20–, MUC2–) versus intestinal epithelium and intestinal-type adenocarcinomas (CK7–, CK20+, MUC2+) indicate that these different tumor types develop from two different types of mucosa.

Table 36. Frequency of the Histological Main Types of Carcinomas of Papilla of Vater in Different Studies

Authors/Study	No of Cases	Intestinal Type (%)	Pancreaticobiliary Type (%)	Other Types (%)
Kimura *et al.* (1994)	51	25	75	
Matsubayashi *et al.* (1999)	52	58	42	
Albores-Saavedra *et al.* (2000a)	140	49	21	30
WHO classification (2000)		Unusual		
Zhou *et al.* (2004)	55	23	44	24

A topologic analysis of very small ampullary carcinomas underlines this hitogenetic concept: Noninvasive precursor lesions of intestinal-type carcinomas constantly involved the ampulloduodenal part of the papilla or are limited on this region. Intramucosal parts of pancreaticobiliary carcinomas often left out ampullo-duodenum. Apparently they arose in the deeper parts of Vater's papilla (Fischer and Zhou, 2004; Matsubayashi *et al.,* 1999).

Special Aspects of Mucin and Keratin Expression in Ampullary Carcinomas

A relevant part of ampullary carcinomas express the apomucin MUC 5AC reflecting metaplastic gastric respective foveolar changes (Fischer and Zhou, 2004; Matsubayashi *et al.,* 1999). This apomucin can be found in intestinal-type carcinomas as well as in pancreaticobiliary-type carcinomas. These tumors often bear *K-Ras* mutations on codon 12. The intramucosal parts of these carcinomas are found significantly more often in the ampullo-duodenum and the ampullo-pancreatic duct than in the ampullo-biliary part of the papilla. Therefore Matsubayashi *et al.* (1999) speculated that pancreatic juice may have influence on the development and morphology of these carcinomas. In 2004 MUC6, a further gastric mucin, and trefoil peptide 1 (TFF1), which is co-localized with MUC5AC in gastric epithelium, were demonstrated in 5 of 11 ampullary carcinomas (Gürbütz and Klöppel, 2004). Apparently in ampullary carcinomas but also in duodenal carcinomas that both develop from foregut structures, gastric differentiation in terms of mucin expression seems not to be unusual. This is in striking contrast to colorectal carcinomas, which do not express these mucins.

The histogenetic relation of ampulla to small intestinum might also explain the co-expression of CK7 and CK20 in a small minority of our ampullary carcinomas as well as in some ampullary carcinomas in the collection of Goldstein and Bassi (2001). In contrast to colorectal carcinomas (CK7 negative, CK20 positive) the expression of the keratins 7 and 20 in carcinomas of the small intestine is more heterogeneous, and a co-expression of both keratins was found in 67% of these tumors (Chen and Wang, 2004).

Histologic/Immunohistologic Type of Ampullary Carcinoma and Prognosis

Prognosis of ampullary carcinomas depends on operability, tumor stage, nodal stage, and histologic grade (Kayahara *et al.,* 1997; Klempnauer *et al.,* 1998; Yamaguchi and Enjoji, 1987; for review see Fischer and Zhou, 2000). Nodal stage was the most discriminating risk factor in our collective of resected ampullary carcinomas. The data relating histologic type to prognosis are inconsistent. Kimura *et al.* (1994) found a significantly better prognosis for patients with intestinal-type ampullary carcinomas than with pancreaticobiliary-type carcinomas. In their collective, pancreaticobiliary-type carcinomas had a significantly higher nodal stage than intestinal-type carcinomas. In the collective of Memorial Sloan Kettering Cancer Center, the outcome of intestinal-type tumors was somewhat more favorable than that of the pancreaticobiliary-type (Albores-Saavedra *et al.,* 2000b). Our collective did not show even a tendential difference in cumulative survival comparing pancreaticobiliary-type and intestinal-type carcinomas using histologic or immunohistochemical criteria based on keratin expression (Zhou and Fischer, 2004). Also comparing MUC2-positive and MUC2-negative carcinomas we did not find statistically significant differencies in cumulative survival time. Furthermore, our patients with intestinal-type ampullary carcinomas bore the same risk for nodal metastases as those with pancreaticobiliary-type carcinomas. The expression of MUC1 was not discriminative in terms of different histologic tumor types or prognosis. So, our findings are in contrast to the results of (Kitamura *et al.,* 1996), who found a positive correlation of MUC2 expression and survival rate and a negative one for MUC1.

In summary, this study and review support the concept of histogenetically different types of ampullary carcinomas, which develop from different types of ampullary mucosa. The separation of intestinal-type, carcinoma from pancreaticobiliary-type carcinoma is supported by their different CK polypeptide pattern. Furthermore, many histologically unusual subtypes of ampullary carcinomas can immunohistochemically be related to pancreaticobiliary or intestinal mucosa. In our German collection, neither the histopathologic classification nor the immunohistochemical classification based on CK profile or expression of apomucin MUC2 identifies a subgroup of tumors with a better or worse outcome (Zhou and Fischer, 2004).

References

Albores-Saavedra, J., Henson, D.E., and Klimstra, D.S. 2000a. Tumors of the gallbladder, extrahepatic bile ducts, and ampulla of Vater. *Atlas of Tumor Pathology,* Third series, Fascicle 27.

Albores-Saavedra, J., Menck, H.R., Scoazec, J.C., Soehendra, N., Wittekind, C., Sriram, P.V.J., and Sripa, B. 2000b. Tumours of the gallbladder and extrahepatic bile ducts. In: Hamilton S.R., Aaltonen L.A. (eds). *WHO Classification of Tumours*. Pathology and Genetics of the Digestive System. Lyon, IARC Press, 203–218.

Carvalho, F., David, I., Aubert, J.P., Lopez-Ferrer, A., De Bolos, C., Reis, C.A., Gartner, F., Peioxoto, A., Alves, P., and Sobrinho-Simoes, M. 1999. Mucins and mucin-associated

carbohydrate antigen expression in gastric carcinoma cell lines. *Virchows Arch. 435*:479–485.

Cheng, Z.M.E., and Wang, H.L. 2004. Alteration of cytokeratin 7 and cytokeratin 20 expression profile is uniquely associated with tumorigenesis of primary adenocarcinoma of the small intestine. *Am. J. Surg. Pathol. 28*:1352–1359.

Chu, P.G., and Weiss, L.M. 2002. Keratin expression in human tissues and neoplasms. *Histopathology 40*:403–439.

Cubilla, A.L., and Fitzgerald, P.J. 1980. Surgical pathology aspects of cancer of the ampulla-head of pancreas region. *Monogr. Pathol. 21*:67–81.

Fischer, H.P., and Zhou, H. 2000. Pathologie der Papilla Vateri. In: Doerr W., Seifert G., and Uehlinger E., (Hrsg). Spezielle *Pathologische Anatomie: Pathologie der Leber und der Gallenwege,* 2. Aufl. Berlin, Heidelberg, New York, Tokyo, Springer, 1219–1257.

Fischer, H.P., and Zhou, H. 2004. Pathogenesis of carcinoma of the papilla of Vater. *J. Hepatobiliary Pancreat. Surg. 11*: 301–309.

Gendler, S.J., and Spicer, A.P. 1995. Epithelial mucin genes. *Annu. Rev. Physiol. 57*:607–634.

Goldstein, N.S., and Bassi, D. 2001. Cytokeratins 7, 17, and 20 reactivity in pancreatic and ampulla of Vater adenocarcinomas: percentage of positivity and distribution is affercted by the cut-point threshold. *Am. J. Clin. Pathol. 115*:695–702.

Gürbüz, Y., and Klöppel, G. 2004. Differentiation pathways in duodenal and ampullary carcinomas: a comparative study on mucin and terfoil peptide expression, including gastric and colon carcinomas. *Virchows Arch. 444*:536–541.

Katoh, M. 2003. Trefoil factors and human gastric cancer (Review). *Int. J. Mol. Med. 12*:3–9.

Kayahara, M., Nagakawa, T., Ohta, T., Kitagawa, H., and Miyazaki, I. 1997. Surgical strategy for carcinoma of the papilla of Vater on the basis of lymphatic spread and mode of recurrence. *Surgery 121*:611–617.

Kimura, W., Futakawa, N., Yamagata, S., Wada, Y., Kuroda, A., Muto, T., and Esaki, Y. 1994. Different clinicpathologic findings in two histologic types of carcinoma of Papilla of Vater. *Jpn. J. Cancer Res. 85*:161–166.

Kitamura, H., Yonezawa, S., and Tanaka, S. 1996. Expression of mucin carbohydrates and core proteins in carcinomas of the ampulla of Vater: their relationship to prognosis. *Jpn. J. Cancer Res. 87*:631–640.

Klempnauer, J., Ridder, G.J., Maschek, H., and Pichlmayr, R. 1998. Carcinoma of the ampulla of Vater: determinants of long-term survival in 94 resected patients. *H.P.B. Surg. 11*:1–11.

Matsubayashi, H., Watanabe, H., Yamaguchi, T., Ajioka, Y., Nishikura, K., Kijima, H., and Saito, T. 1999. Differences in mucus and K-ras mutation in relation to phenotypes of tumors of the papilla of Vater. *Cancer 86*:596–607.

Moll, R., Franke, W.W., and Schiller, D.L. 1982. The catalog of human cytokeratins: pattern of expression in normal epithelia, tumors and cultured cells. *Cell 31*:11–24.

Taylor, K.L., Mall, A.S., Barnard, R.A., Ho, S.B., and Cruse, J.P. 1998. Immunohistochemical detection of gastric mucin in normal and disease states. *Oncol. Res. 10*:465–473.

Yamaguchi, K., and Enjoji. M. 1987. Carcinoma of the ampulla of Vater. *Cancer 59*:506–515.

Zhou, H., Schaefer, N., Wolff, M., and Fischer, H.P. 2004. Carcinoma of the ampulla of Vater: comparative histologic/immunohistochemical classification and follow-up. *Am. J. Surg. Pathol. 28*:875–882.

This Page Intentionally Left Blank

15

Role of Integrins in Ovarian Cancer

Nuzhat Ahmed

Introduction

Ovarian cancer is a major cause of cancer morbidity and mortality in women. It is the sixth most common cancer and the fourth most common cause of cancer-related death in American women of all ages. In spite of recent medical advances, the prognosis for a woman diagnosed with ovarian cancer has not changed over the last 30 years. The median age at diagnosis is about 62 years, and the 5-year survival for a woman diagnosed with ovarian cancer is only 30%. Poor survival from ovarian cancer can be attributed to the late-stage diagnosis. As a result of the lack of clinical symptoms, patients with ovarian cancer usually present with stage III or IV, when the cancer has spread from the pelvis and involves the peritoneal cavity and the surrounding organs. Yet, women diagnosed with stage I disease, when the cancer is restricted to ovaries, have good prognosis with a 5-year survival of approximately 90%. Ovarian cancer is very aggressive and readily spreads to the peritoneal cavity and invades the surrounding peritoneal organs. A critical feature of ovarian carcinoma (OC) development and growth is the ability of transformed epithelial cells to survive *in vivo* as single cells or small clumps in the tumor fluid of the peritoneum. Hence, a greater understanding of the biologic features determining the unusual growth pattern and metastasis of ovarian cancer is vital to design novel therapies.

Pathology and Staging

The ovarian stroma and epithelium are of the same mesodermal origin (Auersperg *et al.,* 2001). The epithelium lining of the ovary and the peritoneum is similar to the coelomic epithelium that gives rise to the fallopian tube, uterus, cervix, and müllerian duct from which approximately 75% of all primary ovarian neoplasms arise. Epithelial ovarian tumors are classified according to the cell type and behavior as benign, borderline (tumors of low malignant potential), or malignant.

The major cell types of epithelial tumors are serous, mucinous, endometriod, clear-cell, transitional, and undifferentiated. Different epithelial ovarian tumors have different biologic behaviors, likelihood of spread, and consequent variation in prognosis and treatment. However, for invasive epithelial carcinomas histologic subtype has limited prognostic significance and is independent of clinical stage, extent of residual disease, and pathologic grade.

Serous tumors: Serous tumors represent 50% of epithelial ovarian tumors, and of these 10% are borderline serous tumors.

Mucinous tumors: Mucinous tumors make up 8–10% of epithelial ovarian tumors. These tumors are usually enormous in size, filling the entire abdominal cavity. The mucinous lesions are intraovarian in 95–98% of cases.

Handbook of Immunohistochemistry and *in situ* Hybridization of Human Carcinomas, Volume 4: Molecular Genetics, Gastrointestinal Carcinoma, and Ovarian Carcinoma

Endometriod tumors: Of epithelial ovarian tumors, 6–8% resemble endometrial adenocarcinoma. Concurrent endometriosis occurs in 10% of cases. Although the malignant potential of endometriosis is very low, a transition from benign to malignant epithelium may occur.

Clear cell carcinomas: Clear cell carcinoma occurs in 5% of cases and may be associated with endometriosis or endometrial cancer. These tumors have a worse prognosis than others and are often associated with hypercalcemia or hyperpyrexia and other metastatic disease.

Transitional-cell tumors: Some primary OCs resemble transitional-cell carcinoma of the urinary bladder. Those that are more than 50% transitional-cell tumors are more sensitive to chemotherapy and have a favorable prognosis.

Undjfferentiated carcinomas: Undifferentiated carcinomas make up 17% of epithelial ovarian tumors, and the prognosis for patients with these tumors is poor.

Histologic Grading

Histologic grading of ovarian tumors generally depends on the microscopic appearance of a lesion. Lesions range from grade 1 (well-differentiated) to grade 2 (moderately differentiated and predominantly glandular) to grade 3 (poorly differentiated and predominantly solid). The value of grade as an independent prognostic variable has not been fully clarified. A number of reports have suggested that the tumor grade may be of value in early-stage ovarian cancer but that its value declines in patients with advanced-stage disease.

International Federation of Gynecology and Obstetrics Staging of Ovarian Cancer

International Federation of Gynecology and Obstetrics (FIGO) staging of ovarian cancer is well established and is used as a prognostic value in describing the cancer. The FIGO stages are described as follows:

1. Stage I: The growth of the tumor is limited to the ovaries and the patients have a 5-year survival rate of 80–90%. Stage I is further subdivided into the following:
   a. Stage IA: Growth is limited to only one ovary, no ascites or external tumor, capsules intact.
   b. Stage IB: Growth is limited to both ovaries, no ascites or external tumor, capsules intact.
   c. Stage IC: Stage IA or lB tumor, with tumor on the surface of one or both ovaries, and ascites present with malignant cells.

2. Stage II: Tumor growth involves both ovaries with pelvic extension, and the patients have a 5-year survival rate of 40–60%. Stage II is further subdivided into the following:
   a. Stage IIA: The metastases has spread to the uterus and/or fallopian tube.
   b. Stage IIB: The tumor has extended to other pelvic tissues.
   c. Stage IIC: The tumor is either stage IIA or IIB and is on the surface of one or both ovaries, capsule(s) ruptured, ascites present containing malignant cells.

3. Stage III: The tumor involves both ovaries and there are peritoneal implants outside the pelvis with superficial liver metastases with histologically proven malignant extension to small bowel or omentum. The 5-year survival rate in stage III ovarian cancer is 10–15%. Stage III is further divided into the following:
   a. Stage IIIA: The tumor is grossly limited to the pelvis with negative nodes, but there is a histologically confirmed microscopic seeding of abdominal peritoneal surfaces.
   b. Stage IIIB: Histologically confirmed implants of peritoneal seedings less than 2 cm in diameter can be seen in one or both ovaries; nodes are negative.
   c. Stage IIIC: Abdominal implants are greater than 2 cm diameter and/or positive retroperitoneal or inguinal nodes are present.

4. Stage IV: Tumor growth is present in both ovaries. Parenchymal liver metastases indicate stage IV ovarian cancer, and the patients have a 5-year survival rate of less than 5%.

Integrins in Ovarian Cancer

The ability of tumor cells to invade locally into host tissue and metastasize to distant organs is a major determinant of tumor progression. Invasion and subsequent dissemination require active interaction of tumor cells with matrix resulting in a loss of adhesion between tumor cells and extracellular matrix and the ability to bind and degrade extracellular matrix to migrate to distant organs. These processes are mediated by a large family of transmembrane receptors called integrins (Hynes, 1992).

Integrins are non-covalently linked heterodimers composed of α and β glycoprotein subunits (Hynes, 1992). Eighteen α and eight β integrin subunits can form at least 23 different heterodimers of which 15 are receptors for matrix protein. The ligand specificity for each heterodimer is determined by the specific combination of the α and β subunits (Ruoslahti, 1991). Most β subunits can associate with more than one α subunit. Integrins recognize components of extracellular matrix

and cell-adhesion co-receptors of the immunoglobulin and cadherin families (Kumar, 1998).

The role of integrins extends practically to all main aspects of cellular function (Mortarini and Anichini, 1993). Integrins are intimately associated with the cytoskeleton through the cytoplasmic domain of β subunit (Clark and Brugge, 1995; Kim and Yamada, 1997). The complex can bind several cytoskeletal proteins, including α-actinin, paxillin, talin, tensin, and vinculin. These proteins aggregate in discrete assemblies as focal adhesion sites. The focal adhesion is composed of numerous integrin heterodimers accumulating on the cell surface in response to ligand binding. This accumulation of integrins recruits the cytoskeleton proteins such as α-actinin, talin, and vinculin that may act as an anchor for F-actin (Gilmore and Burridge, 1996).

The stabilization of microfilaments recruits other cytoskeletal proteins such as paxillin and talin. In addition to these cytoskeletal proteins, the focal adhesion sites containing integrins include signaling complexes, such as focal adhesion kinase (FAK) (Zeng *et al.,* 2003), the integrin-linked kinase (ILK) (Mulrooney *et al.,* 2000), mitogen-activated protein (MAP) kinase (Ahmed *et al.,* 2002a), small GTPases (ras, rho, etc.) (Arthur *et al.,* 2002), liquid kinases (PI-3 kinase) (Ishida *et al.,* 2003), and phospholipids (phospholipase C and A2) (Milella *et al.,* 1999). This network of cytoskeletal and signaling complexes within the focal adhesion site allows for the control of integrin activity both inside and outside the cells and is commonly referred to as "inside-out" and "outside-in" signaling (Longhurst and Jennings, 1998). An integrin on the cell surface can respond to changes within the cell by increasing or decreasing its affinity for the ligand (inside-out signaling).

Alternatively, an integrin binding to its ligand can result in a conformational shift that leads to the activation of signal transduction pathways (outside-in signaling). Both outside-in and inside-out signaling are involved in cell adhesion, migration, growth, invasion, cellular transformation, and tumor progression. These effects are closely linked to the activation of metastasis-associated molecules such as urokinase plasminogen activator (uPA), matrix metalloproteinases (MMPs), and so on. Altered expression of integrins in the form of down- or up-regulated expression has been noted in the majority of tumors but vary considerably according to the origin of the neoplasm (Jones *et al.,* 1993).

Little is known about the expression and functional role of integrins in ovarian cancer. Hence, the prognostic roles of these molecules in ovarian cancer remain largely unknown. This primarily is because very few studies have analyzed integrin expression on clinical specimens. αvβ3 integrin expression was shown to be lower in tumors of low malignant potential compared to invasive carcinomas (Liapis *et al.,* 1997), inconsistent with the previous study where tumors of low malignant potential had high expression of αvβ3 integrin expression compared to invasive tumors (Carreiras *et al.,* 1995). It has been demonstrated that the expression of αvβ6 integrin increases with the increasing grade of tumors, and perturbing the function of this integrin as shown to result in the loss of matrix-degrading capability of ovarian cancer cell lines (Ahmed *et al.,* 2002c, 2002d). β1 and αvβ3 integrins have been shown to mediate *in vitro* adhesion to collagen, laminin, and fibronectin in ovarian cancer cell lines (Cannistra *et al.,* 1995).

Localization of the α6β4 laminin receptor within the cell membrane in poorly differentiated OCs is changed compared with normal epithelial (Bottini *et al.,* 1993). This change is associated with topologic alterations of laminin within the cell membrane of ovarian cancer cells, suggesting a relationship between altered production or degradation of extracellular matrix components of ovarian cancer cells and the α6β4 receptor. αvβ3, α5, and α6 showed higher immunoreactivity in ovarian cancer tissues and cell lines compared with α2, α3, and α4 subunits (Cannistra *et al.,* 1995). Furthermore, peritoneal seeding of ovarian cancer was successfully blocked by using RGD (arginyl-glucyl-aspartyl) binding peptide, suggesting a role for β integrin subunits in ovarian cancer metastasis (Yamamoto *et al.,* 1991). In short, αvβ6, αvβ3 and α6β4 integrin may have a role in ovarian cancer progression, but whether the expression of these integrin is an independent prognostic factor in survival and disease-free period remains to be known.

Immunohistochemical Localization of Integrins in Ovarian Cancer Tissues

Immunohistochemistry (IHC) is a technique that permits the localization of antigens in tissue preparations and also allows morphologic evaluation by light microscopy. The pathologic diagnosis of a tumor relies on its microscopic morphology. As the tumor progresses, a number of structural changes occur including loss of normal tissue architecture, variable shaped cells and nuclei, prominent nucleoli, enlarged cell nuclei, and so on. These morphologic changes can be correlated to tumor grading scheme. As ovarian tumors are heterogenous and highly variable, a morphologic grading system often presents a problem to pathologists because individual pathologists may vary in drawing the line between two specific grades of tumor. Hence, immunohistochemical staining techniques in conjunction with assessment of morphologic changes in a tumor are used to bring a precision of microscopic diagnosis and a concordance between the pathologists.

In cancer tissues, specific antibodies are used to detect tumor-associated antigens commonly characterized as "prognostic marker." The treatment and management of a disease relies very much on the presence or absence of these prognostic markers.

Immunohistochemical procedures are applicable to both cryostat and paraffin-embedded tissue sections. The fundamental of good IHC is ideal tissue processing (frozen or fixed) and preservation so that the tissue antigens are made insoluble, and yet the antigenic sites are available without alteration to their tertiary structure. Right choice of the specific antibody, optimum antibody titer, precise enzyme–substrate reaction conditions, and ideal choice of staining methods are also crucial. In addition to that, necessary controls are required for the validation of immunohistochemical staining results.

Choice of Antibody

Immunohistochemical technique requires specific binding of antibodies to antigens in the presence of high concentrations of other macromolecules. Two types of antibody preparations can be used for immunohistochemical staining, as explained in the following.

Staining with Polyclonal Antibody

A good polyclonal serum will contain multiple antibodies directed against different epitopes on the antigen. Although stearic competition may prevent large numbers of antibodies from binding to the same antigen molecule, several antibodies often will bind and a strong signal can be expected. However, the polyclonal sera contain relatively high concentrations of irrelevant antibodies of unknown specificity that can result in high background. However, satisfactory staining results can be obtained and nonspecific background staining can be decreased by careful titration of polyclonal antibodies.

As polyclonal sera usually contain antibodies specific for a broad range of epitopes on the antigen, including denaturation-resistant epitopes, they often work well on fixed samples such as paraffin sections of paraformaldehyde-fixed tissues.

Staining with Monoclonal Antibody

Monoclonal antibodies often work exceptionally well in immunohistochemical staining techniques. The purity and specificity of monoclonal antibodies yields low background over a wide range of antibody concentrations. Monoclonal antibodies work well on both frozen and paraffin-embedded tissues.

Immunohistochemical localization of integrins in ovarian tissues uses an indirect biotin-streptavidin conjugate method of visualization. In this method, integrin-specific primary unconjugated antibody binds to the antigen. A biotin-labeled secondary antibody directed against the primary antibody is then applied, followed by binding with streptavidin conjugated to horseradish peroxidase (HRP). The presence of HRP is detected by the use of the chromogenic substrate diaminobenzidine (DAB), which produces a visible brown to red color at the sites of antigen–antibody–enzyme complex. If the primary integrin antibody is made in mouse, the secondary antibody must be directed against mouse inmunoglobulins (Igs). This approach of integrin detection in ovarian tissues is very versatile because a variety of primary integrin antibodies from the same species can be used with the same secondary antibody. The procedure is sensitive, and nonspecific tissue reactions can be blocked with unconjugated nonimmune serum from the donor of the secondary antibody.

MATERIALS AND METHODS

1. Frosted microscope slides, preclean (76 × 26 mm).
2. Poly-L-Lysine.
3. Acetone (AR grade).
4. Methanol (AR grade).
5. Ethanol (AR grade).
6. Xylene (AR grade).
7. Isopentane (AR grade).
8. Hydrogen peroxide (AR grade).
9. OCT (Tissue Tek, Sakura, Japan).
10. Egg emulsion (one egg white in 100 ml of distilled water, mixed vigorously for 2–3 min).
11. Skim milk (5 g of skim milk in 100 ml of distilled water).
12. Tris buffered saline (TBS, 0.05 M Tris in 0.15 M NaCl, pH 7.6).
13. Citrate buffer (Citric acid, 0.1 M, pH 6.0).
14. Bovine serum albumin (BSA, 1 g in 100 ml of distilled water).
15. Primary antibody.
16. Dako LSAB kit (Dako, Glostrup, Denmark).
17. Liquid DAB kit (Dako).
18. Mayer's hematoxylin.
19. Scott's tap water or lithium carbonate (AR grade).
20. Resinous mounting medium.
21. Coplin jars.
22. Paper towels.
23. Microwave oven.
24. Microscope.
25. Phosphate buffer saline (PBS, 14 mM Na_2HPO_4, 6 mM NaH_2PO_4, 0.1 M NaCl pH 7.4).

26. Dimethylsulfoxide (DMSO).
27. Trypsin-EDTA (ethylene diamine tetraacetic acid).

Tissue Preparation and Storage

1. Divide ovarian tissue samples into small aliquot, and cut the sections 2–3 cm in thickness and 1 cm in dimension to enhance uniform freezing or permeation by buffer, fixative, antibody solution, etc.
2. Embed tissue sections in frozen-section embedding medium (Tissue Tek, OCT, Sakura Finetek, Torrance, CA) and freeze by immersion in isopentane cooled in dry ice.
3. Store tissues at −80°C until required.
4. Cut frozen tissue sections into 5 μm thickness and mount poly-L-lysine–coated slides. If not required immediately, store the slides at −20°C.

Preparation of Poly-L-Lysine–Coated Slides

Poly-L-lysine binds to most solid support through its charged side chains. The positively charged polymer provides a binding support for negatively charged cells. Although this cross-link is not covalent, it is sufficiently strong for cell staining techniques.

1. Prepare a solution of 1 mg/ml poly-L-lysine in distilled water.
2. Coat clean glass slides by dipping or incubating in this solution for 5 min.
3. Dry slides at room temperature overnight or at 37°C for 1 hr.
4. Store poly-L-lysine–coated slides at room temperature.

Tissue Fixation

1. Fix tissue sections in cold acetone (4°C) for 15 min.
2. Wash with TBS for 5 min.

Blockage of Endogenous Peroxidase Activity

1. Block endogenous peroxidase activity in the ovarian cancer tissues by immersing the tissue mounted slides into 3% H_2O_2 in methanol for 10 min.
2. Wash the slides with 2 changes of TBS for 5 min each to get rid of the methanol.

Blockage of Endogenous Biotin Activity

1. Prepare a diluted egg-white emulsion and mix vigorously for 2–3 min.
2. Filter through cheesecloth. This emulsion can be stored at 4°C for up to 2 weeks.
3. Immerse the slides in egg white emulsion for 10 min, and then wash under running tap water for 5 min.
4. Prepare fresh 5% skim milk solution. Immerse the slides into skim milk solution for 10 min, and then wash under running tap water for 5 min.
5. Wash the slides with 2 changes of TBS for 5 min each.

After the blocking steps it is important that the tissue sections remain hydrated at all times to ensure permeability of antibody and buffer solutions. To ensure that, maintain slides in a moist chamber. This can be achieved by putting a piece of damp cloth at the bottom of the slide chamber and keeping the slide chamber covered at all times.

Primary Antibody Treatment

1. Ring tissue sections on the slides with a water repellent pen to ensure retention of the antibody solution on the tissue section.
2. Dilute the primary antibody in TBS containing 1% BSA (optimum antibody titer should be determined by the user; the Chemicon integrin antibody works well at 1:200 dilution).
3. Incubate tissue sections with primary antibody (~100 μl) for 1 hr at room temperature in a moist chamber.
4. Wash with TBS using a wash bottle for a minute.
5. Immerse the slides in a dish in TBS for 5 min.
6. Repeat **Step 5.**

Secondary Antibody Treatment

1. Use Dako LSAB kit and follow the instructions given on the manual.
2. Briefly, incubate tissue sections at room temperature for 15 min with Link antibody (biotinylated anti-mouse-sheep-rabbit, ~100 μl).
3. Wash with TBS using a wash bottle for 1 min.
4. Immerse the slides in a dish in TBS for 5 min.
5. Repeat **Step 4.**
6. Incubate slides in streptavidin HRP for 15 min and repeat **Steps 3, 4,** and **5.**

Visualization of Antigen–Antibody Complex

1. Visualize the antigen–antibody complex by using Dako liquid DAB kit. Briefly, incubate tissue sections in 100 μl of diluted DAB (1 drop of DAB mixed with 1 ml of supplied buffer) for 5 min (monitor color development with a light microscope).
2. Wash with TBS as described in "Primary Antibody Treatment." (DAB is a potential carcinogen and should

be disposed accordingly. When using DAB, gloves, face mask, and a fume cupboard should be used. The waste should be polymerized with sodium hypochlorite before disposal).

3. Wash slides under running tap water for 2 min.
4. Stain nuclei with Mayer's hematoxylin stain in a Coplin jar for 20 sec.
5. Wash under running tap water for 2 min.
6. Blue the sections with dilute alkali (Scott's tap water substitute or saturated lithium carbonate solution).
7. Wash under running tap water for 2 min.
8. Dehydrate the tissue sections through 3 changes of absolute ethanol for 2 min each.
9. Clear the sections through 2 changes of xylene for 2 min each.
10. Mount and coverslip the sections with a resinous mounting medium (Fast Mount, Histolabs, Australia).
11. Assess the slides under the microscope.

Antigen-Retrieval Protocols

Antigen-retrieval is a term used for the identification of antigens in formalin-fixed, processed, and paraffin-embedded specimens. The procedure involves exposure of hydrated slides to elevated temperatures in a microwave oven while immersed in a fluid. The fluid may be various buffers or even distilled water. During the procedure, the solution in which the slides are immersed is brought to boiling and maintained at that temperature for several minutes. The slides are then allowed to cool down for an additional 10–20 min prior to continuing the staining procedure.

Antigen-retrieval pretreatment works with any microwave oven, but it is absolutely necessary that the oven be standardized and the procedure be performed exactly the same way each time. Because commercial microwave ovens are supplied in a variety of sizes and with various maximum power levels the heating effect is highly variable within the chamber of the oven. For standardization of microwave heating, it is recommended to place the same mass within the chamber each time. If the slides are being processed in a slide rack, the rack should be completely filled with slides to maintain the same load with each run. It is recommended to use 250 ml staining dishes rather than Coplin jars because the extra volume assists in evening out minor variations in output power and also helps to prevent evaporation and possible drying of the slides. In addition, improved reproducibility can be obtained by using a microwave oven with a rotating platform.

Preparation of Slides

1. Cut tissue sections at 5 µm thickness and mount them on poly-L-lysine–coated slides.
2. Dry slides overnight at 37°C or for 1 hr at 60°C (tissue sections must be completely dry).
3. Deparaffinize slides in xylene with 3 changes of slides in xylene for 5 min each.
4. Dehydrate slides through absolute ethanol with 3 changes of ethanol for 5 min each.
5. Wash in running tap water for 2 min to get rid of the alcohol.

Antigen Retrieval

1. Place 250 ml of citrate buffer (pH 6.0) in a plastic staining dish and bring it to boil.
2. Place slides in slide rack, filling any empty slots with blank slides.
3. Place the slide rack in heated citrate buffer in a plastic container with the lid loosely on the staining dish, and center the dish inside the microwave oven on a paper towel to absorb any liquid runover.
4. Heat slides with the buffer at low power for 10 min (the temperature of the buffer should be maintained near boiling point).
5. Stand the slides in warm citrate buffer for additional 20 min, transfer to TBS, and rinse slides with 3 changes of TBS for 5 min each.
6. Proceed with the blocking and immunostaining steps as described earlier.

The secret of reproducibility with the antigen-retrieval pretreatment technique is careful attention to details while operating the microwave. If the same mass of slides and solution is used each time, there will be little variation from run to run. As a quality-control measure, the oven calibration should be checked from time to time. The easiest way to check oven calibration is to load a staining dish with blank slides and buffer and check the time required to achieve boiling. As the microwave generating tubes inside the oven ages, its output power may change. Hence, by maintaining a quality-control log for the microwave, adjustments of times used in the antigen-retrieval pretreatment step can be made, and reproducible immunostaining will result.

Besides microwave ovens, alternative methods of antigen retrieval include the use of an autoclave, a pressure cooker, and a vegetable steamer. Comparative studies of these different methods have shown that the use of a pressure cooker with a microwave oven is the most effective (Taylor *et al.,* 1994). However, standardization of these protocols for immunostaining of

integrins in ovarian cancer tissues should be determined by the end user (Figure 68).

METHODS

Preparation of Cells

Ovarian cancer cells in ascites or effusion usually are presented in suspension, whereas those in culture can be either adherent or in suspension. Adherent cells normally are prepared for staining by growing on a suitable support. Suspension cells can be attached to a solid support by centrifugation or simply dehydration.

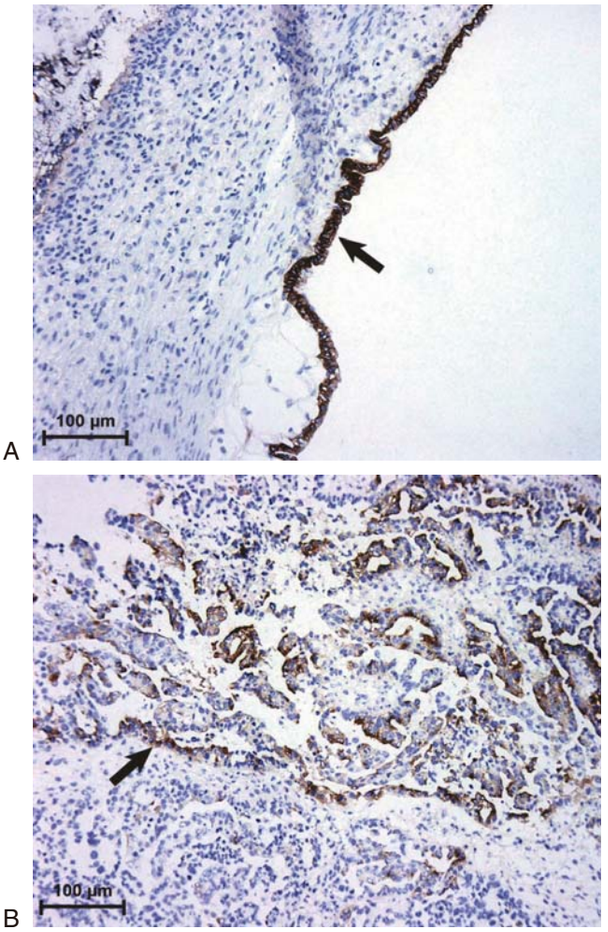

Figure 68. Immunohistochemical localization of αvβ6 integrin in ovarian cancer tissues. **A:** Mucinous borderline ovarian tumor. **B:** Grade 3 serous ovarian tumor tissue. Cryosections of ovarian tissues were stained by the immunoperoxidase method for the expression of αvβ6 integrin. Arrows in **(A)** indicate localized αvβ6 staining of epithelial layer, whereas in **(B)** they indicate αvβ6 staining of scattered tumor cells throughout the tissue.

Staining Adherent Cells on Coverslips, Slides, or Tissue Culture Dishes

For high-resolution studies, adherent cells should be grown on the highest available grade glass coverslips because the controlled thickness, flatness, and good optical properties of a proper coverslip are required to produce the best images. If many antibodies are required or different dilution of the antibodies are used or if one is using various controls, plating the cells onto multi-well slides can be helpful.

1. Prior to staining, sterilize the glass coverslips or slides. For small numbers of slides or coverslips, you can dip them in 70% ethanol and then flame while holding them loosely between forceps. For large batches, sterilize coverslips or slides by placing them in a glass petri dish and baking in an oven. Do not use the steam cycle of an autoclave, because this will cause them to stick to one another.
2. Place the dry coverslips or slides in suitable tissue culture dishes.
3. Place drops of ovarian cancer cell suspension from culture or ascites directly onto the coverslips or slides, and incubate that in sterile glass petri dishes for 4 hr at 37°C in a humid incubator containing 5% CO_2.
4. Fill the dish gently with growth medium and incubate for a further 24 hr. This way, most cells will be captured on the glass coverslips or slides and will spread properly to allow greater resolution for most antigens.

The cells are now ready for fixing, as described earlier.

Attaching Suspension Cells to Slides Using Cytocentrifuge

A simple method for detecting integrins in cells that grow in suspension or for adherent cells that have been made into suspension by harvesting in trypsin-EDTA is to attach the cells to a solid substrate before fixation. This can be achieved by the use of a cytocentrifuge. The centrifugal force spreads the cells, allowing better resolution of internal structures.

1. Resuspend cells at 1–2 × 10^6/ml in a medium containing 30% serum.
2. Mount microscope slides in cytocentrifuge with card covers. Add 0.1–0.5 ml (2–5 × 10^5 cells) of cell suspension to reservoir.
3. Centrifuge at 1200 g for 10 min.
4. Dry cell monolayer in air for 20–30 min.

Cells are now ready for fixation and can be handled in the same manner as the tissue section mounted on slides.

Preparing Cell Smear

1. Place a drop of cells in suspension (the suspension should be made in PBS buffer with 30% serum to preserve cell morphology) on one end of a clean glass slide.
2. Touch the edge of a slide containing the cell suspension with another slide to allow the liquid to be drawn by capillary action to the entire width of the slide.
3. Smoothly and evenly push the slide across the length of the slide, drawing the liquid in a film over the slide.
4. Allow the samples to air-dry for 20–30 min.

The samples are now ready for fixation.

Quality Control

The most critical and difficult aspect of IHC is the evaluation of the data. The reliability of an immunohistochemical procedure is dependent on the specificity of all the reactions that include reagents, antibodies, and their labels. A positive result may be genuine, but there are risks of nonspecific reactions that must be eliminated before the result can be accepted.

Polyclonal antibodies usually contain antibodies for several antigenic determinants on the antigen. Because many related molecules have components in common, false-positive result may occur. One can eliminate these problems using monoclonal antibodies, but epitope similarities are present and unwanted cross-reactivity can occur. Because the binding of antibodies to their specific antigenic determinant forms the basis of specificity in IHC, adequate controls are necessary.

Positive Tissue Control

Positive tissue control contains the material being investigated. Process that tissue identically to the unknown specimen. This will allow assessment of the sensitivity of immunohistochemical reactions. Duplicate sections of the test and positive control tissues should be included in each immunohistochemical run.

Negative Tissue Control

Negative tissue control samples do not contain the antigen under investigation and should be processed identically to the test specimen.

Serum Control

Staining should only occur in tissues known to contain the antigen being investigated. It should not be seen if any step in the procedure is omitted or if nonimmune serum is substituted for specific immune serum. Hence, for each IHC run prepare duplicate sections of the test and positive control tissues with nonimmune serum from the species immunized with the primary antigen. This will rule out any positive immunostaining by natural or cross-linking antibodies that interfere with interpretation of test anti-serum. The substituted nonimmune serum should contain an almost identical protein concentration to the primary antibody and should be diluted with identical buffers and with identical dilution.

Detection of Integrins in Ovarian Cancer Cells by Immunoprecipitation Techniques

Immunoprecipitation is a useful immunochemical technique by which the antigen present in the cells can be purified, allowing one to detect the presence of the antigen, and to determine the relative quantity of an antigen. This technique when combined with SDS-polyacrylamide gel electrophoresis determines the relative molecular weight of an antigen, rate of its synthesis and degradation, post-translational modifications, and protein–protein interactions. This technique has been widely used in integrin research and is used for detecting different integrin subunits in ovarian cancer cells. The immunoprecipitation procedure can be divided into six steps:

1. Labeling the antigen (optional).
2. Lysis of the cells to release the antigens.
3. Preclearing the cell lysate.
4. Formation of immune complex.
5. Purification of the immune complexes.
6. Identification of the antigen by resolving it on SDS-polyacrylamide gels and subsequently staining or immunoblotting.

Choice of Antibody

Two types of antibodies can be used for immunoprecipitations. These are either ploYclonal or monoclonal in origin.

Immunoprecipitation with Polyclonal Antibody

As polyclonal antibodies have multiple antigenic sites they have much higher avidity for the antigen and produce stable antigen–antibody complex that can sustain the harsh washing procedure. As the immune complexes are collected on a solid-phase matrices such as protein A beads, the availability of multiple binding sites for the protein A molecules provides a more stable

antigen–antibody–protein A complex. Hence, multiple antibody–antigen interactions and multiple antibody–protein A interactions provide a multivalent stable complex that can result in high nonspecific background. These problems are inherent with any immunochemical technique using polyclonal antibody and can be decreased by titrating the amount of anti-sera needed to immunoprecipitate the integrin. By providing the smallest amount of serum necessary for the quantitative recovery of the antigen, the background can be kept to a minimum. In addition, because of the stability of the complexes, more stringent washings may reduce nonspecific background.

Immunoprecipitation with Monoclonal Antibody

The biggest advantage of using monoclonal antibodies for immunoprecipitations is the specificity of their interactions. Because the immune complexes formed using monoclonal antibodies are not multimeric and are smaller than those formed using polyclonal antibodies, there is less of a problem with nonspecific backgrounds. However, not all monoclonal antibodies will work well in immunoprecipitation because the antibodies with affinities less than 10^7/mol are difficult to use for immunoprecipitation.

Another problem that is commonly encountered when using monoclonal antibodies is their varied affinities for the immunoadsorbant protein A. Unless the antigen is multimeric, there will be only one antibody bound to the antigen, so the antigen will be linked to the immunoadsorbant only through this single antibody molecule. This makes the affinity of the antibody–protein A interaction as critical for the detection of the antigen as the antibody–antigen interaction. Unfortunately, not all subclasses of IgG molecules bind well to protein A. Among the rat monoclonal antibodies, only the IgG2c subclass binds to protein A. Mouse monoclonal antibodies are better, IgG2a antibodies binds with high affinity, when IgG2b binds less well but with enough affinity to allow easy detection of the antigen. The lowest affinities are found with antibodies from the IgG1 subclass. Here, the immune complexes are difficult to purify by binding to protein A immunoadsorbants.

However, this problem can be circumvented by using intermediate antibodies such as rabbit anti-mouse or anti-rat immunoglobulin antibodies. Because rabbit antibodies have much higher affinity for protein A, this bridging layer will make the interaction stronger both by providing a higher affinity for protein A and by making the antibody–protein A interaction multivalent. The addition of rabbit antibodies to the immune complexes, however, adds the problem of dirtier background.

MATERIALS

1. [^{35}S] methione.
2. Biotin disulfide N-hydroxysuccinimide ester.
3. Protein A sepharose/protein G sepharose.
4. PBS.
5. Cell lysis buffer (150 mM NaCl, 1% NP-40, 0.1% SDS, 1 mM EDTA, 1 mM $CaCl_2$, 1 mM MgCl, 50 mM Tris, pH 7.5*).* Add phenyl methyl sulfonyl fluoride (PMSF, 1 mM) and aprotonin (5 µg/ml) just before use.
6. Rubber policeman.
7. Antigen-specific antibody.
8. Centrifuge.
9. Rotating wheel.
10. Trypsin-EDTA.

Labeling Integrins

[^{35}S] Methionine Labeling of Integrins

The most commonly used radioactive precursor for labeling integrins is [^{35}S] methionine. The [^{35}S] decay is easier to detect than either [^{3}H] or [^{14}C]. In addition, the intracellular pool of methionine is smaller than many other amino acids; therefore, exogenous methionine is easily incorporated into proteins. One other advantage to the use of [^{35}S] methionine is that its incorporation into proteins is linear over a wide range of added label. This means that the number of counts that are incorporated is dependent primarily on the amount of [^{35}S] methionine added to the culture. The optimum concentration of [^{35}S] methionine needed to label the cells depends on the abundance of integrins in the cells and should be determined by the end user. Exponentially growing cells should look healthy and be sub-confluent at the time of labeling.

For ***monolayer cultures,*** cells should be approximately 75% confluent. Remove the medium and wash the monolayer once with the medium without methionine (prewarmed to 37°C). Add approximately *2*.5 ml of medium without methionine per 25 cm^2 flask or 5 ml in a 75 cm^2 flask. Slightly larger volumes may be needed for a longer labeling period.

For ***suspension cultures,*** collect the cells by centrifugation at 400 g for 5 min. Resuspend the cell pellet in the medium without methionine (prewarmed to 37°C) and wash by centrifugation as before. Remove the wash medium as completely as possible. Resuspend the cells at approximately 10^6 cells/ml in medium without methionine, and transfer to a tissue culture flask (3–4 × $l0^6$ cells/25 cm^2 flask or 7–8 × $l0^6$ cells/75 cm^2 flask).

1. Add the [^{35}S] methionine. The amount of [^{35}S] methionine depends on the time of incubation and on

the abundance of the protein in the cells and should be determined by the user (incorporation of radiolabel into total protein will be linear for approximately 6–8 hr.)

2. Incubate at 37°C in a CO_2 incubator for 2–4 hr.

3. For ***monolayer cultures,*** remove the medium and wash the monolayer once with PBS. For suspension cultures, transfer the cells to a test tube and centrifuge at 400 g for 5 min. Remove the medium and wash the cells once by resuspending the cells in PBS and centrifuge at 400 g. The spent medium and the wash should be combined and disposed in accordance with your institution's procedure for handling radioactive waste.

4. Drain well and lyse the cells as described in the following section.

Biotin Labeling of Integrins

1. Cells should be rapidly growing and healthy at the time of labeling.

2. For monolayer cultures, remove the medium and wash the monolayer twice with PBS. Drain well and harvest cells with trypsin-EDTA. Centrifuge at 400 g for 5 min, discard the supernatant, resuspend cells in PBS, and wash again by centrifugation and resuspension in PBS. For suspension cultures, centrifuge cells at 5×10^6–10^7 cell/ml at 400 g for 5 min. Remove and discard the supernatant. Resuspend the cells in PBS and wash twice by centrifugation and resuspension in PBS.

3. After the last wash, resuspend cells in PBS containing 50–80 µg/ml of biotin-ester (stock solution of 10 mg/ml prepared in DMSO and stored at −20°C).

4. Rotate cells in a rotating wheel at a slow speed at 4°C for 30–40 min.

5. Centrifuge cells at 400 g for 5 min and resuspend in cell lysis buffer.

A number of different cell lysis buffers can be used to release integrins from cells. In general, the conditions used for lysis should be as gentle as possible to retain the antibody-binding sites and to avoid solubilization of background proteins but harsh enough to ensure quantitative release of the antigen. For optimum results choose nonionic detergents over ionic and single detergent over mixes. Variables that can drastically affect the release on integrins from cells include salt concentration, type of detergent, presence of divalent cations, and pH. Salt concentrations between 0–0.5 M, nonionic detergent concentration between 0.1–2%, divalent cation concentration between 0–5 mM, EDTA concentrations between 0–2 mM and pH 6–8 should be monitored to determine the optimal conditions of extraction of integrins. As the extraction conditions will release proteases, the lysis buffer should be supplemented with protease inhibitors and care should be taken to keep the samples at 4°C (4°C decreases the rate of degradation by the proteases). In immunoprecipitation the two most commonly used inhibitors are aprotonin and phenylmethylsulfonyl fluoride (PMSF). A cocktail of several different protease inhibitors can also be used.

Lysis of Cells

Monolayer Cultures

1. Wash the monolayer of cells with PBS. Drain well.

2. Place the tissue culture dish on ice and add 1.0 ml of cell lysis buffer (prechilled to 4°C) per 75 cm^2 flask.

3. Incubate the plate on ice for 30 min with occasional rocking.

4. Scrape the cells and debris from the plate with a rubber policeman, and transfer the lysis buffer and the cell debris to a 1.7 ml Eppendorf tube.

5. Centrifuge for 20 min at 10,000 g at 4°C. Remove the supernatant to a fresh tube and discard the pellet containing the debris.

The supernatant is now ready for preclearing.

Suspension Cultures

1. Collect the cells by centrifugation at 400 g for 5 min and wash with PBS by centrifugation.

2. Resuspend the cells in cell lysis buffer as described earlier.

3. Incubate the cells on ice for 30 min at 4°C.

4. Centrifuge for 20 min at 10,000 g at 4°C. Remove the supernatant to a fresh tube and discard the pellet containing the debris.

The supernatant is now ready for preclearing.

Preclearing the Cell Lysate

It is necessary to remove proteins in the cell lysate that bind nonspecifically to the immune complexes or the solid phase prior to adding the specific antibodies. Depending on the type of antibody the most common solid phase used for the immunoprecipitation of integrins is either protein A sepharose or protein G sepharose.

1. Add 50–70 µl slurry of protein A sepharose or protein G sepharose (0.1g/ml of lysis buffer) to 1.0 ml (1 mg of protein) of cell lysate.

2. Incubate the cell lysate at 4°C on a rotating wheel at a low speed for 1–4 hr.

3. Centrifuge at 10,000 g at 4°C for 20 min. Carefully remove the supernatant and discard the pellet.

Formation of Immune Complex

1. Add 4–10 µg of antibody to 1 ml (1 mg/ml) of cell lysate.
2. Incubate the cell lysate at 4°C on a rotating wheel at a low speed overnight.
3. Add 50–70 µl slurry of protein A sepharose or protein G sepharose (0.1 g/ml of lysis buffer) to 1.0 ml (1 mg of protein) of cell lysate.
4. Incubate at 4°C on a rotating wheel at a low speed for at least 4 hr.

Purifying Immune Complexes

1. Collect the beads containing the integrin bound to the antibody by centrifugation at 10,000 g for 20 min at 4°C.
2. Aspirate and discard the supernatant and wash the beads 3× by the centrifugation procedure described earlier.
3. Remove the final wash as completely as possible and re-suspend the beads in 100 µl of lysis buffer.
4. Transfer the beads in fresh tubes and resuspend in 1 ml of lysis buffer.
5. Remove the supernatant; the immune complex is now ready for appropriate assay.

For SDS-polyacrylamide gel electrophoresis, add 100 µl of Laemmli sample buffer (2% SDS, 10% glycerol, 100 mM DTT, 60 mM Tris pH 6.8 and 0.001% bromophenol blue). Heat at 95°C for 5 mM. Spin, remove supernatant, and load onto gel. Samples at this stage can be stored at −20°C. For the detection of biotin-labeled integrins see Ahmed and colleagues (2002d).

Detection of Integrins in Ovarian Cancer Cells by Immunoblotting Techniques

Immunoblotting is a technique that combines the resolution of proteins by gel electrophoresis to the specificity of immunochemical detection. The technique determines the presence of an antigen in the sample and also provides information on the relative molecular weight of the protein. The procedure can be divided into six steps:

1. Preparation of sample.
2. Resolution of sample by gel electrophoresis.
3. Transfer of the separated proteins to a membrane support.
4. Blocking of nonspecific binding sites on the membrane.
5. Formation of immune complex.
6. Detection.

MATERIALS

1. Polyacrylamide gels.
2. Electrophoresis and blotting apparatus.
3. Blotting membranes.
4. Whatman 3MM sheets.
5. Centrifuge.
6. Sonicator.
7. Homogenizer.
8. Tris buffer (10 mM Tris, 150 mM NaCl, 2 mM EGTA, 2 mM DTT, 1 mM orthovanadate (pH 7.0).
9. Protease inhibitors.
10. Gel running buffer (25 mM Tris, 192 mM glycine, 0.1% SDS (pH 8.3).
11. Transfer buffer (48 mM Tris, 39 mM glycine, 0.037% SDS, 20% methanol, make up to 1000 ml by distilled water).
12. Tris buffered saline with Tween 20 (TBST, 0.02 M Tris, 0.135 NaCl, 0.2% Tween 20, pH 7.6).

Preparation of Sample

In this procedure, samples of cells or tissues are disrupted in a buffer. For integrins usually Tris buffer is used. The buffer is supplemented with protease inhibitors (1 mM PMSF and 5 µg/ml of aprotonin) before use.

1. Measure the amount of sample to be lysed: For cells 10^6–10^7 cells/ml of buffer or for tissues 0.2 g/ml of buffer.
2. For cells, resuspend the cells in Tris buffer and sonicate for three bursts of 30 sec with an interval of 30 sec between. Between each sonication step the samples should be kept on ice. For tissues, homogenize the tissue section in Tris buffer. Using a small-size pestle, lyse the cells by repeated stokes (approximately 6). Even pressure will result in uniform lysis.
3. Centrifuge the sample at 10,000 g for 20 min. Recover the supernatant and discard any pellet. Determine the relative protein concentration. At this stage the samples can be stored at −20°C and are stable for months.

The samples are now ready for electrophoresis.

Resolution of Sample by Gel Electrophoresis

SDS-polyacrylamide gels are commonly used for separating integrins for immunoblotting. Before running a gel, decisions should be made on the total amount of

protein and the acrylamide concentration of the separating gel. The total amount of the protein loaded on the gel should not exceed more than 30 µg because that would result in the distortion of bands. Because the blotting requires transfer of proteins from gels to membrane, consideration of the percentage of acrylamide in the gel is important. The lower the percentage of acrylamide and cross-linker, the easier the transfer will be. Hence, a best resolution is obtained by selecting a percentage of gel on which the protein of interest will migrate at least one-third of the distance from the top of the separating gel to the bottom within the time it takes the dye front to reach the bottom. In general, proteins that run slower than this will be difficult to elute. Run the gels under standard conditions (150 volts for 10 min followed by 200 volts for 1 hr) using gel running buffer.

Transfer of the Separated Proteins to a Membrane Support

Nitrocellulose and polyvinylidene fluoride (PVDF) are used successfully to bind the transferred integrins in biological samples. Transfer of proteins from the gel to the membrane is achieved by electrophoretic elution either by complete immersion of a gel-membrane sandwich in a buffer (wet transfer) or by placing the gel-membrane sandwich between absorbent paper soaked in transfer buffer (semi-dry transfer). For wet transfer, the sandwich is placed in a buffer tank with platinum wire electrodes. For the semi-dry transfer the gel-membrane sandwich is placed between carbon-plate electrodes. Apparatus for both types of transfers are available commercially, and both systems can be effectively used for immunoblotting of integrins in biologic samples.

Semi-Dry Electrophoretic Transfer

1. Cut six sheets of absorbent paper (Whatman 3MM or equivalent) and one sheet of nitrocellulose membrane to the size of the gel. If the paper overlaps the edge of the gel, the current will bypass the gel, resulting in inefficient transfer.
2. Soak the nitrocellulose membrane, absorbent paper, and gel by soaking in transfer buffer for 15 min.
3. On the bottom plate of the apparatus (the anode), assemble the gel, nitrocellulose, and paper in the following order:
   - Bottom electrode.
   - Three layers of absorbent paper soaked in transfer buffer.
   - One nitrocellulose membrane soaked in transfer buffer.
   - Polyacrylamide gel soaked in transfer buffer.
   - Three layers of absorbent paper soaked in transfer buffer.
4. Check for air bubbles and gently remove them either by using a gloved hand or by rolling a pipet or pencil over the sandwich. Dry any buffers that may surround the gel-paper sandwich to reduce the chance of short circuit during transfer.
5. Carefully place the upper electrode on the top of the stack. Connect the electrodes and commence transfer by running for 30–45 min with a current of 0.8 mA/cm^2 of gel. Avoid running a longer time because this may cause drying out.
6. Disconnect the power source and carefully disassemble the apparatus. Mark membrane to follow orientation.
7. The blots can now be stained as required. The polyacrylamide gel can be stained with Coomassie to verify transfer.

Wet Electrophoretic Transfer

1. Cut one sheet of nitrocellulose paper and four sheets of absorbent filter paper (Whatman 3MM or equivalent) to the size of the gel.
2. Soak the nitrocellulose membrane in distilled H_2O. Nitrocellulose should be wetted by carefully laying it on the surface of water. Allow the nitrocellulose to wet by capillary action from the bottom, and then submerge the sheet for 2 min. Transfer the membrane to soak in transfer buffer (48 mM Tris, 39 mM glycine, 0.037% SDS, 20% methanol, make up to 1000 ml by distilled water) for 15 min. Wet the absorbent paper by soaking in transfer buffer.
3. Immerse gel, membrane, filter papers, and support pads in transfer buffer to ensure they are thoroughly soaked. Be careful to exclude air bubbles from the support pads.
4. Assemble the transfer sandwich as follows:
   - Negative electrode (cathode, black electrode).
   - Support pads soaked in transfer buffer.
   - Two layers of absorbent paper soaked in transfer buffer.
   - Polyacrylamide gel soaked in transfer buffer.
   - One nitrocellulose membrane soaked in transfer buffer.
   - Two layers of absorbent paper soaked in transfer buffer.
   - Support pads soaked in transfer buffer.
   - Positive electrode (anode, red electrode).
5. Place the complete sandwich in a transfer tank with the membrane closest to the positive electrode (anode, red electrode).
6. Transfer for 30 min at 100 volts. In all transfers, the temperature will rise, so use a cooling coil or transfer in a cold room to avoid the generation of gas bubbles in the sandwich.

7. After the completion of transfer, disconnect the power supply. Dissemble the sandwich and mark the nitrocellulose membrane by clipping one corner.

8. The polyacrylamide gel can now be stained with Coomassie or silver stain to verify transfer. Prepare the nitrocellulose membrane for blocking.

Note: To avoid background and interference with protein transfer, wear gloves during the whole procedure of transfer. For the detection of low-abundance proteins by immunoblotting dry the membrane completely before blocking. In such cases, there is a reduced chance of the transferred protein being lost during subsequent washing steps. After drying, rewet the membrane as described earlier.

Blocking Nonspecific Binding Sites on the Blot

Before the blot can be processed for antigen detection, it is essential to block the membrane to prevent nonspecific adsorption of immunologic reagents. The two blocking solutions that are compatible with integrin detection are nonfat dried milk and BSA.

1. Rinse the membrane 3× for 15 min each with TBST.
2. Add 5% nonfat milk or 0.1% BSA solution to the membrane.
3. Incubate at room temperature for 1 hr with gentle agitation or overnight at 4°C.

The membrane is now ready for the addition of antibody.

Formation of Immune Complex

Detecting the antigen in an immunoblot is achieved by binding antibodies to the proteins immobilized on the membrane. This can be done by either direct or indirect detection methods. In the direct method, labeled antibodies are used that can detect the location of the antigen directly; alternatively in the indirect method, antigens are first labeled with unlabeled antibodies and located by labeled secondary reagents. In integrin research most immunoblots are analyzed by indirect method where a secondary antibody compatible to the primary antibody is labeled with HRP or alkaline phosphatase (commercially available) and then detected using soluble substrates that can either yield enhanced chemiluminescence response or insoluble colored products. These methods are simple and provide immediate results. However, because of the nature of the enzymatic reactions involved, it is not possible to obtain quantitative results using such approach.

Antibody Binding

1. Remove the membrane from the blocking solution and wash 3× with TBST for 15 min each.
2. Prepare the primary antibody solution in TBST. Use 10 ml of diluted antibody (antibody dilution should be determined by the end user, but for most integrin antibodies a dilution of 1:1000 is used if the initial antibody concentration is 1 mg/ml) for 15 × 15 cm membrane. Incubations can be performed in shallow trays.
3. Incubate the blot with the antibody for at least 1 hr at room temperature with gentle agitation.
4. Wash the blot with four changes of TBST for 15 min each.
5. Incubate the blot in suitably diluted (usually 1:2000–1:10,000) alkaline phosphatase or HRP labelled secondary antibody for 30 min–1 hr at room temperature with gentle rocking.
6. Wash the blot with four changes of TBST for 15 min each.

The blot is now ready for detection.

Detection of Antigen

Using the Alkaline Phosphatase System

The bromochloroindolyl phosphate/nitro blue tetrazolium (BCIP/NBT) substrate generates an intense black-purple precipitate at the site of enzyme binding. The BCIP/NBT characteristically produces sharp bands with little background and is available in the form of a kit. The enzyme reaction can be monitored and stopped when the desired signal over background is observed. This method is easier to perform than the chemiluminescent detection method, but it is less sensitive and does not allow the multiple exposure of chemiluminescent method; however, it provides single end-point result.

1. Prior to developing the blot, prepare the solutions as instructed in the kit.
2. Place the washed immunoblot in a suitable container. Add the required volume of substrate solution. Develop the blot at room temperature with gentle agitation until the bands are suitably dark.
3. To stop reaction wash the blot with TBS containing 20 mM EDTA.

Using the Horseradish Peroxidase System

Chemiluminescent Western Blot is a highly sensitive technique in which enzyme-conjugated antibodies catalyze the oxidation of luminol, which produces a light signal that can be captured on film. An enhancer

intensifies the signal output, enabling the detection of picogram quantities of antigen.

Prior to developing the blot, prepare the stock solutions as instructed in the ECL Western Blotting kit. Follow the instructions as described in the kit. Multiple exposure can be obtained depending on the amount of target protein on the blot.

Using Biotin-Labeled Integrins

1. Block the membranes with 5% nonfat dry milk in TBST for 1 hr.
2. Wash the membrane with three changes of TBST for 15 min each.
3. Incubate the blot with streptavidin-conjugated HRP diluted in TBST for 60 min at room temperature with gentle rocking.
4. Wash the membrane with four changes of TBST for 15 min each with gentle rocking.
5. Develop the blot using the ECL Western Blotting kit.

Comments

The most frequently encountered problem in immunoprecipitation and immunoblotting is the presence of high background consisting either of extra discrete bands or a general background covering the entire membrane. Diffuse background results from insufficient blocking of the membrane or from the specific reaction of the detecting reagent with a component of the blocking buffer. Diffuse background can be eliminated by changing blocking buffer, by reducing the incubation time of primary and secondary antibodies, by increasing the duration of each washing step or by reducing the time of exposure to the substrate of the secondary antibody, or by using less of the substrate. Specific background bands are generated either by contaminating antibodies in the polyclonal sera or by specific cross-reactions between different antigens, which is more prevalent with monoclonal antibodies. These problems can be reduced by using an alternative available monoclonal antibody or by adsorbing the polyclonal serum with a protein preparation that does not contain the antigen of interest (Figure 69).

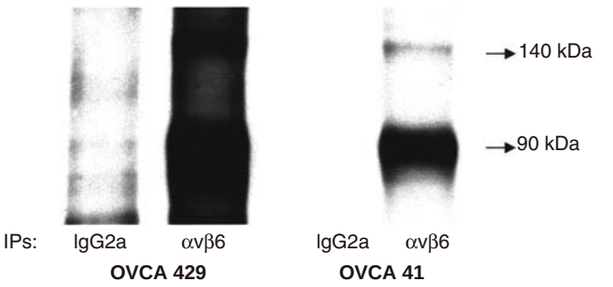

Figure 69. Immunoprecipitation and immunoblotting of αvβ6 integrin in OVCA 429 and OVCA 432 ovarian cancer cells. Cells were labeled with biotin, immunoprecipitated with anti- αvβ6 integrin (R6G9, Chemicon, CA), resolved on 10% SDS gel and then blotted with streptavidin-horseradish peroxidase. The bands at 140 kDa indicate α subunit, whereas that at 90 kDa is the β6 subunit of the complex.

RESULTS AND DISCUSSION

Of ovarian cancer, 75% arises from the malignant transformation of the ovarian surface epithelium. Tumor cells spread out and proliferate in an adhesive manner in the intraperitoneal cavity and often generate the accumulation of ascites. Although cancer cells adhere on the peritoneal surface, many cells still remain floating in the ascitic fluid. The presence of adhering and floating cells is a characteristic of ovarian cancer and suggests that the alteration in the adhesion process of the cells can be an important stage in development and phenotype of ovarian tumor. In spite of this, little is known about the adhesion receptors of ovarian tumors.

The present literature suggests that the expression and localization of α6β4 (Bottini *et al.,* 1993) and α3β1 (Bartolazzi *et al.,* 1993) integrins are to some extent correlated with the degree of tumor differentiation in OC. A gradual increase in the expression of αvβ6 integrin with the progression of OCs has been reported (Ahmed *et al.,* 2002d). The expression of αvβ3 integrin in ovarian cancer progression is controversial (Carreiras *et al.,* 1995; Liapis *et al.,* 1997) and has been shown in several ovarian adenocarcinoma cell lines (Ahmed *et al.,* 2002b; Carreiras *et al.,* 1995). Moreover, in human ovarian carcinomas α5 and α6 integrins showed higher immunoreactivity compared to α2, α3, and α4 subunits (Cannistra *et al.,* 1995).

Little is known about the expression and functional role of integrins in ovarian cancer, and the prognostic role of these molecules in ovarian cancer remains to be known. In a single study of 56 primary OCs and metastatic lesions from 34 patients diagnosed with advanced-stage ovarian carcinomas (stages III/IV) the expression of αv and β1 integrin was evaluated by IHC and *in situ* hybridization (Goldberg *et al.,* 2001). Expression of αv and β1 integrin messenger ribonucleic acid (mRNA) was observed in carcinoma and stromal cells with no significant differences between the primary and metastatic lesions. However, the αv integrin expression was found more often in tumors of short-term survivors compared with long-term survivors, whereas β1 integrin expression was comparable in the two groups (Goldberg *et al.,* 2001). This is the first

evidence associating αv integrin expression with poor survival in ovarian carcinomas. Thus αv integrin is the only prognostic marker so far known in ovarian carcinoma.

The presence of carcinoma cells in ascites is sufficient to classify the disease as stage III even in the absence of distant solid metastases. Yet no clinical data are available to show significant association between integrin expression and the progression of ovarian cancer. In conclusion, integrin literature in ovarian cancer is still in its infancy and much remains to be known about the correlation of different integrin subunit expression and clinicopathologic parameters.

References

Ahmed, N., Niu, J., Dorahy, D.J., Gu, X., Andrews, S., Meldrum, C.J., Scott, R.J., Baker, M.S., Macreadie, I.G., and Agrez, M.V. 2002a. Direct integrin alphavbeta6-ERK binding: implications for tumour growth. *Oncogene 21*:1370–1380.

Ahmed, N., Pansino, F., Baker, M., Rice, G., and Quinn, M. 2002b. Association between [alpha]v[beta]6 integrin expression, elevated p42/44 kDa MAPK, and plasminogen-dependent matrix degradation in ovarian cancer. *J. Cell. Biochem. 84*:675–686.

Ahmed, N., Pansino, F., Clyde, R., Murthi, P., Quinn, M.A., Rice, G.E., Agrez, M.V., Mok, S., and Baker, M.S. 2002c. Overexpression of alphavbeta6 integrin in serous epithelial ovarian cancer regulates extracellular matrix degradation via the plasminogen activation cascade. *Carcinogenesis 23*:237–244.

Ahmed, N., Riley, C., Rice, G.E., Quinn, M.A., and Baker, M.S. 2002d. Alpha(v)beta(6) integrin-A marker for the malignant potential of epithelial ovarian cancer. *J. Histochem. Cytochem. 50*:1371–1380.

Arthur, W.T., Noren, N.K., and Burridge, K. 2002. Regulation of Rho family GTPases by cell-cell and cell-matrix adhesion. *Biol. Res. 35*:239–246.

Auersperg, N., Wong, A.S., Choi, K.C., Kang, S.K., and Leung, P.C. 2001. Ovarian surface epithelium: biology, endocrinology, and pathology. *Endocr. Rev. 22*:255–288.

Bartolazzi, A., Kaczmarek, J., Nicolo, G., Risso, A.M., Tarone, G., Rossino, P., Defihippi, P., and Casteilani, P. 1993. Localization of the alpha 3 beta 1 integrin in some common epithelial tumors of the ovary and in normal equivalents. *Anticancer Res. 13*:1–11.

Bottini, C., Miotti, S., Fiorucci, S., Facheris, P., Menard, S., and Colnaghi, M.J. 1993. Polarization of the alpha 6 beta 4 integrin in ovarian carcinomas, *Int. J. Cancer 54*:261–267.

Cannistra, S.A., Ottensmeier, C., Niloff, J., Orta, B., and DiCarlo, J. 1995. Expression and function of beta 1 and alpha v beta 3 integrins in ovarian cancer. *Gynecol. Oncol. 58*:216–225.

Carreiras, F., Lehmann, M., Sichel, F., Marvaldi, J., Gauduchon, P., and Le Talaer, J.Y. 1995. Implication of the alpha v beta 3 integrin in the adhesion of the ovarian-adenocarcinoma cell line IGROV1. *Int. J. Cancer 63*:530–536.

Clark, E.A., and Brugge, J.S. 1995. Integrins and signal transduction pathways: the road taken. *Science 268*:233–239.

Gilmore, A.P., and Burridge, K. 1996. Molecular mechanisms for focal adhesion assembly through regulation of protein-protein interactions. *Structure 4*:647–651.

Goldberg, I., Davidson, B., Reich, R., Gotlieb, W.H., Ben-Baruch, G., Bryne, M., Berner, A., Nesland, J.M., and Kopolovic, J. 2001. Alphav integrin expression is a novel marker of poor prognosis in advanced-stage ovarian carcinoma. *Clin. Cancer Res. 7*: 4073–4079.

Hynes, R.O. 1992. Integrins: versatility, modulation, and signaling in cell adhesion. *Cell 69*:11–25

Ishida, K., Nagahara, H., Kogiso, T., Aso, T., Hayashi, N., and Akaike, T. 2003. Cell adhesion aside from integrin system can abrogate anoikis in rat liver cells by down-regulation of FasL expression, not by activation of PI-3K/Akt and ERK signaling pathway. *Biochem. Biophys. Res. Commun. 300*:201–208.

Jones, J., Sugiyama, M., Watt, F.M., and Speight, P.M. 1993. Integrin expression in normal, hyperplastic, dysplastic, and malignant oral epithelium. *J. Pathol. 169*:235–243.

Kim, L.T., and Yamada, K.M. 1997. The regulation of expression of integrin receptors. *Proc. Soc. Exp. Biol. Med. 214*:123–131

Kumar, C.C. 1998. Signaling by integrin receptors. *Oncogene 17*: 1365–1373.

Liapis, H., Adler, L.M., Wick, M.R., and Rader, J.S. 1997. Expression of *alpha(v)beta3* integrin is less frequent in ovarian epithelial tumors of low malignant potential in contrast to ovarian carcinomas. *Hum. Pathol. 28*:443–449.

Longhurst, C.M., and Jennings, L.K. 1998. Integrin-mediated signal transduction. *Cell Mol. Life Sci. 54*:514–526.

Milella, M., Gismondi, A., Roncaioli, P., Palmieri, G., Morrone, S., Piccoli, M., Frati, L., Cifone, M.G., and Santoni, A. 1999. Beta 1 integrin cross-linking inhibits CD16-induced phospholipase D and secretory phospholipase A2 activity and granule exocytosis in human NK cells: role of phospholipase D in CD16-triggered degranulation. *J. Immunol. 162*:2064–2072.

Mortarini, R., and Anichini, A. 1993. From adhesion to signalling: roles of integrins in the biology of human melanoma. *Melanoma Res. 3*:87–97.

Mulrooney, J., Foley, K., Vineberg, S., Barreuther, M., and Grabel, L. 2000. Phosphorylation of the *beta1* integrin cytoplasmic domain: toward an understanding of function and mechanism. *Exp. Cell Res. 258*:332–341.

Ruoslahti, E. 1991. Integrins. *J. Clin. Invest. 87*:1–5

Taylor, C.R., Shi, S.R., Chaiwun, B., Young, L., Imam, S.A., and Cote, R.J. 1994. Strategies for improving the immunohistochemical staining of various intranuclear prognostic markers in formalin-paraffin sections: androgen receptor, estrogen receptor, progesterone receptor, p53 protein, proliferating cell nuclear antigen, and Ki-67 antigen revealed by antigen retrieval techniques. *Hum. Pathol. 25*:263–270.

Yamamoto, K., Murae, M., and Yasuda, M. 1991. RGD-containing peptides inhibit experimental peritoneal seeding of human ovarian cancer cells. *Nippon Sanka Fujinka Gakkai Zasshi 43*: 1687–1692

Zeng, L., Si, X., Yu, W.P., Le, H.T., Ng, K.P., Teng, R.M., Ryan, K., Wang, D.Z., Ponniah, S., and Pallen, C.J. 2003. PTP alpha regulates integrin-stimulated FAK autophosphorylation and cytoskeletal rearrangement in cell spreading and migration. *J. Cell Biol. 160*:137–146.

This Page Intentionally Left Blank

16

Role of Immunohistochemical Expression of Vascular Endothelial Growth Factor C and Vascular Endothelial Growth Factor Receptor 2 in Ovarian Cancer

Naoyo Nishida, Hirohisa Yano, Kan Komai, Takashi Nishida, Toshiharu Kamura, and Masamichi Kojiro

Introduction

Immunohistochemical examination is a well-established technique to exhibit the tissue localization of an immunoreactive antigen. Recent advances in immunohistochemistry have assisted the differential diagnosis of a tumor from the wide variety of other neoplasms showing similar morphology and clarified the origin of some tumors that had difficulties in the classification.

Angiogenesis and lymphangiogenesis have an essential role in the proliferation of the vascular network to supply nutrition, oxygen, and immune cells and also to remove waste products. The mechanism, however, has not been clarified in detail until now. Families of vascular endothelial growth factors (VEGF) and the receptors (VEGFR) are now receiving increasing attention especially in the field of neoplastic vascularization. The growth factor VEGF is accepted as a powerful angiogenic agent in neoplastic tissues as well as in normal tissues. Under the influences of some cytokines and other growth factors, the VEGF family appears in the cancer tissue and the adjacent stroma and plays an important role in making the neovascularization (Folkman 1990, 1995). In the absence of vascular support, tumors may become necrotic or even apoptotic (Holmgren *et al.,* 1995). Among the family, VEGF-A, -B, and -C induce new blood-vessel proliferation, and VEGF-C and VEGF-D relate to lymphangiogenesis. These growth factors act with their own VEGF receptor. The receptors VEGFR-1 and VEGFR-2 are known to act as the receptors of VEGF-A, and VEGFR-2 and VEGFR-3 act as the receptors of VEGF-C (Mandriota *et al.,* 2001; Neufeld *et al.,* 1999; Rafii and Skobe, 2003; Veikkoa *et al.,* 2000). The factor VEGF-C consists of VEGF homology domain, which contains receptor-binding sites, and is 30% identical in amino-acid sequence to VEGF165 (Joukov *et al.,* 1997, 1998). Unlike VEGF-A, VEGF-C expression does not appear to be regulated by hypoxia (Enholm *et al.,* 1997). The factor VEGF-C appears to be restricted in early development and in certain pathologic settings such as tumor angiogenesis and lymphangiogenesis.

Handbook of Immunohistochemistry and *in situ* Hybridization of Human Carcinomas, Volume 4: Molecular Genetics, Gastrointestinal Carcinoma, and Ovarian Carcinoma

The ovary, however, is pliable in structure, which allows follicle development and movement for ovulation. This ever-changing structure also allows a variety of neoplastic development. The corpus luteum must accommodate a period of angiogenesis, controlled regression of the vasculature in the noninfertile cycle, or maintenance of the vasculature within a short period. In fact, there is increasing evidence that VEGF, which has been localized in the human ovary, is essential for luteal angiogenesis (Al-zi′abi *et al.,* 2003; Gaytan *et al.,* 1999). The angiogenic agent, such as VEGF-A and C, was expressed strongly in corpus luteum (Figure 70). Generally the tissue having active metabolism needs abundant nutrient. Proliferating cancer cells are similar.

Ovarian carcinoma has the poorest prognosis among cancers in the gynecologic field, and surgical staging of the International Federation of Gynecology and Obstetrics (FIGO) is regarded as the most important prognostic factor (Heintz *et al.,* 2001). When the tumor confines to the ovary, a better than 90% chance of 5-year survival is expected. If the disease extends to the peritoneal cavity, however, the prognoses are limited to 30% or lower (Greenlee *et al.,* 2000). Cytotoxic chemotherapy and maximal debulking are conventional prognostic methods of controlling ovarian cancer, on which the treatment policy is based. Despite the current progression of cytotoxic chemotherapy and surgical techniques, the consequence of ovarian carcinoma is unchanged. Therefore, new management strategies against the disease are required.

In this chapter, we will describe how we used the method of immunohistochemical examination to identify the expression of VEGF family and its receptors.

MATERIALS

1. Formalin-fixed and paraffin-embedded serial sections (4 μm) that were mounted on 3-aminopropyltriethoxysilane-coated slides (Matsunami Glass Ind., Ltd., Osaka, Japan).
2. Xylene and a graded series of ethanol (75%, 85%, 95%, 100%).
3. Primary antibodies:
   a. Rabbit polyclonal anti-VEGF-C (1.6 μg/ml, Zymed Laboratories, Inc., San Francisco, CA).
   b. Rabbit polyclonal anti-VEGF-A (2 μg/ml, Santa Cruz Biotechnology, Inc., Santa Cruz, CA).
   c. Rabbit polyclonal anti-VEGFR-3 (2 μg/ml, Santa Cruz).
   d. Rabbit polyclonal anti-VEGFR-2 (5 μg/ml, Upstate Cell Signaling Solutions, Charlottesville, VA).
   e. Mouse monoclonal anti-CD31 (1:40 dilution, Dako, Ltd., Copenhagen, Denmark).

These antibodies were stored at 4°C.

4. Catalyzed Signal Amplification (CSA) System (Dako, Ely, UK) included the following:
   a. 3% hydrogen peroxide (H_2O_2) in double-distilled water (ddH_2O).
   b. Serum-free protein in phosphate buffered saline (PBS) with 0.015 M sodium azide.
   c. Biotinylated rabbit anti-mouse immunoglobulins in Tris-HCl buffer containing carrier protein and 0.015 M sodium azide.
   d. Streptavidin in PBS buffer containing an anti-microbial agent.
   e. Biotin conjugated to horseradish peroxidase, (HRP) in PBS containing an anti-microbial agent.
   f. PBS buffer containing carrier protein and anti-microbial agent.
   g. Biotinyl tyramide and hydrogen peroxidase in PBS containing carrier protein and anti-microbial agent.
   h. Streptavidin-conjugated HRP in PBS containing carrier protein and anti-microbial agent.
5. PBS containing 0.1% Tween 20 (polyoxyethlene sorbitan monolaurate) (Bio-Rad Laboratories, Hercules, CA) (PBS/Tween).
6. 0.02% 3,3′-diaminobenzidine tetrahydrochloride (Nichirei, Tokyo, Japan) as a chromogen in Tris-HCl buffer (pH 7.6) containing 0.03% H_2O_2.
7. Hematoxylin was used to counterstain the nuclei.
8. Normal rabbit serum for negative control of primary antibody.
9. As positive controls, formalin-fixed and paraffin-embedded sections of human placenta were stained for VEGF-A and VEGF-C, and the sections of normal human umbilical cord were stained for VEGFR-2 and VEGFR-3 by using the same procedure.
10. Stat View version 5 (SAS Institute Inc., Cary, NC) was used for statistical analysis.

METHODS

Immunohistochemical Staining Using CSA System

The techniques used in the CSA system are based on avidin-biotin and peroxidase methodologies (Bobrow *et al.,* 1989; Hsu *et al.,* 1981).

1. Keep mounted sections in an oven at 37°C overnight.
2. To depraffinize, immerse sections in xylene and a series of ethanol for 3 min.
3. Prepare wash buffer solution.
4. Treat with 0.3% H_2O_2 in double-distilled water for 10 min at room temperature to quench the endogenous peroxidase activity within the tissue.

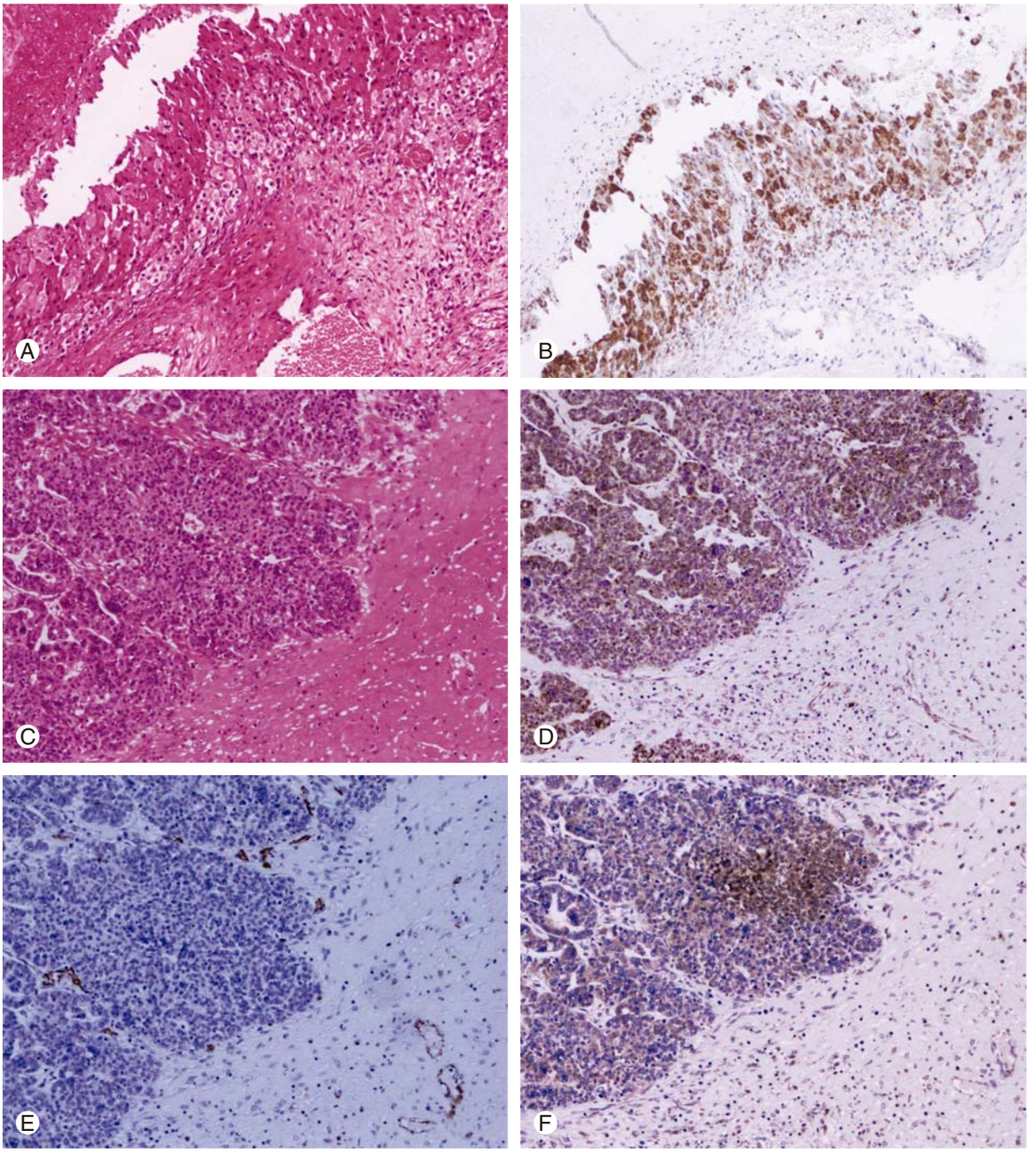

Figure 70. Immunohistochemical staining of vascular endothelial growth factor-C (VEGF-C) in corpus luteum and VEGF-C and VEGFR-2 in ovarian carcinoma. Corpus luteum **(A)**. Serous cystadenocarcinoma **(C)** was hematoxylin and eosin stained. VEGF-C was expressed in corpus luteum **(B)**, tumor cells, and adjacent endothelial cells **(D)**. VEGFR-2 was also expressed in tumor cells and adjacent endothelial cells **(E)**. CD31 was stained in the endothelial cells of blood and lymph vessels in the stroma **(F)**.

5. Rinse gently with wash buffer solution and place in fresh buffer bath for 5 min. Change the solution 3×.

6. Incubate the sections for 10 min at room temperature in the presence of the heat-inactivated nonserum protein to block nonspecific binding sites.

7. Incubate the sections for 15 min at room temperature in the presence of the primary antibody.

8. Rinse gently with wash buffer solution and place in fresh buffer bath for 5 min. Change the solution 3×.

9. Incubate the sections for 15 min at room temperature in the presence of the second antibody.

10. Rinse gently with wash buffer solution and place in fresh buffer bath for 5 min. Change the solution 3×.

11. Incubate the sections for 15 min at room temperature in the presence of the streptavidin-biotin complex (mixed material 4d–4f).

12. Rinse gently with wash buffer solution and place in fresh buffer bath for 5 min. Change the solution 3×.

13. Incubate the sections for 15 min at room temperature in the presence of biotinyl tyramide and H_2O_2 in PBS (material 4g-7).

14. Rinse gently with wash buffer solution and place in fresh buffer bath for 5 min. Change the solution 3×.

15. Incubate the sections for 15 min at room temperature in the presence of streptavidin-conjugated HRP in PBS (materials 4h-8).

16. Rinse gently with wash buffer solution and place in fresh buffer bath for 5 min. Change the solution 3×.

17. The reaction was visualized with 0.02% 3,3′-diaminobenzidine tetrahydrochloride as a chromogen in Tris-HC1 buffer (pH 7.6) containing 0.03% H_2O_2.

18. Immerse slides in a bath of hematoxylin to counterstain the nuclei.

19. Rinse slides in a bath of deionized water for 3 min.

20. To dehydrate and mount, immerse sections in series of ethanol and xylene.

21. Take coverslip on the sections.

Microscopic Assessment of VEGF-A, VEGF-C, VEGFR-2, and VEGFR-3 Expressions and Microvessel Density

Two pathologists independently evaluated and interpreted the results of immunostain without knowing the clinical data of each patient. The staining results in tumor cells were classified into three levels: negative when immunostain-positive tumor cells accounted for less than 10% of the tumor area on the section; low expression when the positive cells accounted for 10% to <50% of the area; and high expression when the positive cells accounted for more than 50% of the area. We used such criteria because the median of immunostain-positive tumor cells in the whole sample was about 50%. Faint or equivocal immunoreaction was not regarded as positive. Receptor VEGFR-2 and VEGFR-3 staining in endothelial cells was considered positive when at least 5% of endothelial cells in the area were strongly immunoreactive as seen in the positive control cells. Microvessel density (MVD) was assessed by counting CD31-positive microvessels under 200X magnification in a grid area of 0.16 mm^2 according to the criteria of Weidner (Weidner, 1993). Five areas of high vascular density (hot spots) were selected, and microvessels were counted on each section.

Statistical Analysis with Stat View Version 5

The significance of the relationship among the expression of VEGF-A, VEGF-C, VEGFR-2, or VEGFR-3; MVD; and clinicopathologic factors was evaluated by using univariate analysis (χ^2 test) and logistic regression analysis. Survival rates were calculated by using the Kaplan-Meier method, and the statistical significance of differences in the cumulative survival curves between the groups was evaluated by using the log-rank test. Multivariate survival analysis was conducted by using Cox's proportional hazard method. Other statistical analysis was carried out with the Mann-Whitney U test. The result was deemed significant at $P < 0.05$.

RESULTS AND DISCUSSION

In our previous study using immunohistochemistry to examine the expression of VEGF family and their own receptors in 80 ovarian carcinoma cases (Nishida *et al.,* 2004), VEGF-A, VEGF-C, VEGFR-2, and VEGFR-3 were expressed in the cytoplasm of tumor cells and also of endothelial cells of the blood and lymph vessels in the stroma adjacent to tumor nests (see Figure 70). In ovarian cancer, prognostic factors such as peritoneal spreads outside the pelvic cavity and lymph-node metastasis are determined by surgical staging (Heintz *et al.,* 2001). We examined the relationship between these prognostic factors and the expressions of VEGF-A, VEGF-C, VEGFR-2, and VEGFR-3 and MVD, and demonstrated that VEGF-C and VEGFR-2 showed significant effects on prognosis. Our study also showed a close relationship among the expressions of VEGF-C and their corresponding receptors, the prognostic factor, and MVD. These findings suggest that VEGF-C acts on the corresponding receptor and initiates angiogenesis in ovarian carcinoma. Survival curves determined by the Kaplan-Meier method and univariate analysis demonstrated that high expressions of VEGF-C

and VEGFR-2 were associated with the lower 5-year survival rate. In multivariate analysis, high expressions of VEGF-C and VEGFR-2 emerged as independent indicators for carcinoma-specific survival.

Histologic classification and grading are related to the patient's prognosis (Friedlander *et al.,* 1991; Malkasian *et al.,* 1984; Omura *et al.,* 1991; Shimizu *et al.,* 1998; Silverberg, 1989). Expressions of VEGF-C, VEGFR-3, VEGF-A, and VEGFR-2 were not related to the histologic type of ovarian carcinoma (Nishida *et al.,* 2004). However, histologic grade of cancer tissue generally reflects aggressiveness of the tumor and thus a prognostic factor. In FIGO's grading system, in which the tumor histologies were graded according to the ratio of solid components, there were no significant differences between the grade and the expressions of VEGF-C, VEGFR-3, VEGF-A, and VEGFR-2. When using Silverberg's grading system, which stands on the overall evaluation of architectural pattern, nuclear pleomorphism, and mitotic activity (Silverberg, 1989), no relationship was found between the system and the expressions of VEGF-C, VEGFR-3, VEGF-A, and VEGFR-2. These results suggest that histologic architecture and tumor-cell atypia are not related to angiogenesis and lymphangiogenesis.

Much has been described concerning the neoplastic or nonneoplastic angiogenesis since the identification of angiogenic agents in 1970s. In the field of ovarian cancer, Yeo *et al.* (1993) first demonstrated various levels of vascular permeability factor (VEGF), which is identified by an immunoassay in the ascites of patients with the disease. However, at present the prognostic significance of neoplastic angiogenic factors remains to be controversial. In uterine malignancies, Kaku *et al.* (1997, 1998) emphasized the prognostic significance of angiogenic factors and of MVD for endometrial cancer and for cervical adenocarcinoma. The prognostic importance of angiogenic factors in ovarian carcinoma has not been confirmed (Ogawa *et al.,* 2002; Shen *et al.,* 2000). The significance of VEGF-A expression is also uncertain. One supported that the factor was associated with poor prognosis (Shen *et al.,* 2000), whereas the other reported that the factor had no impacts on the prognosis in some histologic types (Ogawa *et al.,* 2002). In our previous study, the cases with positive expression of VEGF-A showed a higher propensity to have peritoneal metastasis outside the pelvic cavity and lymph-node metastasis and the positive ascitic cytology, but the differences were not statistically significant. For the reason of discrepancy, it is speculated that the growth of ovarian carcinoma does not depend on only VEGF-A; it relies on the existence of other factors affecting the proliferation and infiltration of the epithelial cancer cells.

It is reported that VEGF-A and VEGF-C are expressed not only on tumor cells but also on endothelial cells of blood and lymph vessels and on fibrous connective tissues of tumor stroma (Boocock *et al.,* 1995; Brown *et al.,* 1993; Gunningham *et al.,* 2000) This should be contributed by both paracrine and autocrine mechanisms: VEGF-A and VEGF-C produced by tumor cells act on their corresponding receptors on endothelial cells through a paracrine mechanism, promote angiogenesis and lymphangiogenesis, and should affect hematogenous and lymphogenous metastases. The factors may also act on the receptors on the tumor cells through an autocrine mechanism and promote the tumor proliferation (Nishida *et al.,* 2004; Yokoyama *et al.,* 2003).

By the method of immunohistochemical examination, VEGF-C expression has been demonstrated in about half of the human cancers (Salven *et al.,* 1998). The factor VEGF-C and their receptors are known to affect the prognosis of adenocarcinomas developed in the uterine cervix (Hashimoto *et al.,* 2001), endometrium, (Hirai *et al.,* 2001), ovary (Yokoyama *et al.,* 2003; Nishida *et al.,* 2004), stomach (Amioka *et al.,* 2002; Yonemura *et al.,* 1999), colorectal cancers (Andre *et al.,* 2000; Furudoi *et al.,* 2002; George *et al.,* 2001), breast cancer (Kinoshita *et al.,* 2001; Kurebayashi *et al.,* 1999; Skobe *et al.,* 2001), lung cancer (Decaussin *et al.,* 1999; Kajita *et al.,* 2001; Niki *et al.,* 2000), head and neck squamous cell carcinoma (O-charoenrat *et al.,* 2001), Kaposi sarcoma (Jussila *et al.,* 1998), and malignant mesothelioma (Ohta *et al.,* 1999).

High tissue expression of VEGF-C and VEGFR-2 reflects the aggressiveness of the spread of tumor in ovarian carcinoma, and thus both have a predictive value to identify the high-risk patients with poor prognosis. Suppression of VEGF-C and VEGFR-2 by using angiogenesis suppressors and receptor inhibitors can prohibit the neovascularization of cancer tissue as well as growth of the tumor and thus should take a certain place in the treatment of ovarian cancer.

References

Al-zi′abi, M.O., Watson, E.D., and Fraser, H.M. 2003. Angiogenesis and vascular endothelial growth factor expression in the equine corpos luteum. *Reproduction 123*:67–77.

Amioka, T., Kitadai, Y., Tanaka, S., Haruma, K., Yoshihara, M., Yasui, W., and Chayama, K. 2002. Vascular endothelial growth factor-C expression predicts lymph node metastasis of human gastric carcinomas invading the submucosa. *Eur. J. Cancer 38*: 1413–1419.

Andre, T., Kotelevets, L., Vaillant, J.C., Coudray, A.M., Weber, L., Prevot, S., Parc, R., Gespach, C., and Chastre, E. 2000. VEGF, VEGF-B, VEGF-C and their receptors KDR, FLT-1 and FLT-4 during the neoplastic progression of human colonic mucosa. *Int. J. Cancer 86*:174–181.

Bobrow, M.N., Harris, T.D., Shaughnessy, K.J., and Litt, G.J. 1989. Catalyzed reporter deposition, a novel method of signal amplification: application to immunoassays. *J. Immunol. Methods 125*:279–285.

Boocock, C.A., Charnock-Jones, D.S., Sharkey, A.M., McLaren, J., Barker, P.J., Wright, K.A., Twentyman, P.R., and Smith, S.K. 1995. Expression of vascular endothelial growth factor and its receptors flt and kdr in ovarian carcinoma. *J. Natl. Cancer Inst. 87*:506–516.

Brown, L.F., Berse, B., Jackman, R.W., Tognazzi, K., Manseau, E.J., Dvorak, H.F., and Senger, D.R. 1993. Increased expression of vascular permeability factor (vascular endothelial growth factor) and its receptors in kidney and bladder carcinomas. *Am. J. Pathol. 143*:1225–1262.

Decaussin, M., Sartelet, H., Robert, C., Moro, D., Claraz, C., Brambilla, C., and Brambilla, E. 1999. Expression of vascular endothelial growth factor (VEGF) and its two receptors (VEGF-R1-FLT1 and VEGF-R2-FLK1/KDR) in non-small cell lung carcinomas (NSCLCs): correlation with angiogenesis and survival. *J. Pathol. 188*:369–377.

Enholm, B., Paavonen, K., Ristimaki, A., Kumar, V., Gunji, Y., Klefstrom, J., Kivinen, L., Laiho, M., Olofsson, B., Joukov, V., Eriksson, U., and Alitalo, K. 1997. Comparison of VEGF, VEGF-B, VEGF-C and Ang-1 mRNA regulation by serum, growth factors, oncoproteins and hypoxia. *Oncogene 14*: 2475–2483.

Folkman, J. 1990. What is the evidence that tumors are angiogenesis dependent? *J. Natl. Cancer Inst. 82*:4–6.

Folkman, J. 1995. Angiogenesis in cancer, vascular, rheumatoid and other disease. *Nat. Med. 1*:27–31.

Friedlander, M.L., and Dembo, A.J. 1991. Prognostic factors in ovarian cancer. *Semin. Oncol.18*:205–212.

Furudoi, A., Tanaka, S., Haruma, K., Kitadai, Y., Yoshihara, M., Chayama, K., and Shimamoto, F. 2002. Clinical significance of vascular endothelial growth factor C expression and angiogenesis at the deepest invasive site of advanced colorectal carcinoma. *Oncology 62*:157–166.

Gaytan, F., Morales, C., Garcia-Pardo, L., Reymundo, C., Bellido, C., and Sanchez-Criado, J.E. 1999. A quantitative study of changes in the human corpus luteum microvasculature during the menstrual cycle. *Biol. Reprod. 60*:914–919.

George, M.L., Tutton, M.G., Janssen, F., Arnaout, A., Abulafi, A.M., Eccles, S.A., and Swift, R.I. 2001. VEGF-A, VEGF-C, and VEGF-D in colorectal cancer progression. *Neoplasia 3*:420–427.

Greenlee, R.T., Murray, T., Bolden, S., Wingo, P.A., Harris, A.L., and Fox, S. B. 2000. Cancer statistics. *Cancer J. Clin. 50*:7–33.

Gunningham, S.P., Currie, M.J., Han, C., Robinson, B.A., Scott, P.A., Harris, A.L., and Fox, S.B. 2000. The short form of the alternatively spliced FLT-4 but not its ligand vascular endothelial growth factor C is related to lymph node metastasis in human breast cancers. *Clin. Cancer Res. 6*:4278–4286.

Hashimoto, I., Kodama, J., Seki, N., Hongo, A., Yoshinouchi, M., Okuda, H., and Kudo, T. 2001. Vascular endothelial growth factor-C expression and its relationship to pelvic lymph node status in invasive cervical cancer. *Br. J. Cancer 85*:93–97.

Heintz, A.P., Odicino, F., Maisonneuve, P., Beller, U., Benedet, J.L., Creasman, W.T., Ngan, H.Y., Sideri, M., and Pecorelli, S. 2001. Carcinoma of the ovary. *J. Epidemiol. Biostat. 6*:107–138.

Hirai, M., Nakagawara, A., Oosaki, T., Hayashi, Y., Hirono, M., and Yoshihara, T. 2001. Expression of vascular endothelial growth factors (VEGF-A/VEGF-1 and VEGF-C/VEGF-2) in postmenopausal uterine endometrial carcinoma. *Gynecol. Oncol. 80*:l81–188.

Holmgren, L., O'Reilly, M. S., and Folkman, J. 1995. Dormancy of micrometastases: balance proliferation and apoptosis in the presence of angiogenesis suppression. *Nat. Med. 1*:149–153.

Hsu, S.M., Raine, L., and Fanger, H. 1981. The use of antiavidin antibody and avidin-biotin-peroxidase complex in immunoperoxidase technics. *Am. J. Clin. Pathol. 75*:816–821.

Joukov, V., Kumar, V., Sorsa, T., Arighi, E., Weich, H., Saksela, O., and Alitalo, K. 1998. A recombinant mutant vascular endothelial growth factor-C that has lost vascular endothelial growth factor receptor-2 binding, activation, and vascular permeability activities. *J. Biol. Chem. 20*:6599–6602.

Joukov, V., Sorsa, T., Kumar, V., Jeltsch, M., Claesson-Welsh, L., Cao, Y., Saksela, O., Kalkkinen, N., and Alitalo, K. 1997. Proteolytic processing regulates receptor specificity and activity of VEGF-C. *EMBO J. 16*:3898–3911.

Jussila, L., Valtola, R., Partanen, T.A., Salven, P., Heikkila, P., Matikainen, M.T., Renkonen, R., Kaipainen, A., Detmar, M., Tschachler, E., Alitalo, R., and Alitalo, K. 1998. Lymphatic endothelium and Kaposi sarcoma spindle cells detected by antibodies against the vascular endothelial growth factor receptor-3. *Cancer Res. 58*:1599–1604.

Kajita, T., Ohta, Y., Kimura, K., Tamura, M., Tanaka, Y., Tsunezuka, Y., Oda, M., Sasaki, T., and Watanabe, G. 2001. The expression of vascular endothelial growth factor C and its receptors in non-small cell lung cancer. *Br. J. Cancer 85*:255–260.

Kaku, T., Hirakawa, T., Kamura, T., Amada, S., Kinukawa, N., Kobayashi, H., Sakai, K., Ariyoshi, K., Sonoda, K., and Nakano, H. 1998. Angiogenesis in adenocarcinoma of the uterine cervix. *Cancer 83*:1384–1390.

Kaku, T., Kamura, T., Kinukawa, N., Kobayashi, H., Sakai, K., Tsuruchi, N., Saito, T., Kawauchi, S., Tsuneyoshi, M., and Nakano, H. 1997. Angiogenesis in endometrial adenocarcinoma. *Cancer 80*:741–747.

Kinoshita, J., Kitamura, K., Kabashima, A., Saeki, H., Tanaka, S., and Sugimachi, K. 2001. Clinical significance of vascular endothelial growth factor-C (VEGF-C) in breast cancer. *Breast Cancer Res. Treat. 66*:159–164.

Kurebayashi, J., Otsuki, T., Kunisue, H., Mikami, Y., Tanaka, K., Yamamoto, S., and Sonoo, H. 1999. Expression of vascular endothelial growth factor (VEGF) family members in breast cancer. *Jpn. J. Cancer Res. 90*:977–981.

Malkasian, G.D. Jr., Melton, L.J. III., O'Brien, P.C., and Greene, M.H. 1984. Prognostic significance of histologic classification and grading of epithelial malignancies of the ovary. *Am. J. Obstet. Gynecol.149*:272–284.

Mandriota, S.J., Jussila, L., Jeltsch, M., Compagni, A., Baetens, D., Prevo, R., Banerji, S., Huarte, J., Montesano, R., Jackson, D.G., Orci, L., Alitalo, K., Christofori, G., and Pepper, M.S. 2001. Vascular endothelial growth factor-C-mediated lymphangiogenesis promotes tumor metastasis. *EMBO J. 20*:672–682.

Neufeld, G., Cohen, T., Gengrinovitch, S., and Poltorak, Z. 1999. Vascular endothelial growth factor (VEGF) and its receptors. *FASEB J. 13*:9–22.

Niki, T., Iba, S., Tokunou, M., Yamada, T., Matsuno, Y., and Hirohashi, S. 2000. Expression of vascular endothelial growth factor A, B, C, and D and their relationships to lymph node status in lung adenocarcinoma. *Clin. Cancer Res. 6*:2431–2439.

Nishida, N., Yano, H., Komai, K., Nishida, T., Kamura, T., and Kojiro, M. 2004. Vascular endothelial growth factor C and vascular endothelial growth factor receptor 2 are related closely to the prognosis of ovarian carcinoma. *Cancer 101*:1364–1374.

O-charoenrat, P., Rhys-Evans, P., and Eccles, S.A. 2001. Expression of vascular endothelial growth factor family members in head and neck squamous cell carcinoma correlates with lymph node metastasis. *Cancer 92*:556–568.

Ogawa, S., Kaku, T., Kobayashi, H., Hirakawa, T., Ohishi, Y., Kinukawa, N., and Nakano, H. 2002. Prognostic significance of microvessel density, vascular endothelial growth factor expression in ovarian carcinoma: special review for clear cell adenocarcinoma. *Cancer Letters 176*:111–118.

Ohta, Y., Shridhar, V., Bright, R.K., Kalemkerian, G.P., Du, W., Carbone, M., Watanabe, Y., and Pass, H.I. 1999. VEGF and VEGF type C play an important role in angiogenesis and lymphangiogenesis in human malignant mesothelioma tumors. *Br. J. Cancer 81*:54–61.

Omura, G.A., Brady, M.F., Homesley, H.D., Yordan, E., Major, F.J., Buchsbaum, H.J., and Park, R.C. 1991. Long-term follow up and prognostic factor analysis in advanced ovarian carcinoma: the Gynecologic Oncology Group Experience. *J. Clin. Oncol. 9*:1138–1150.

Rafii, S., and Skobe, M. 2003. Splitting vessels: keeping lymph apart from blood. *Nature Med. 9*:166–168.

Salven, P., Lymboussaki, A., Heikkila, P., Jaaskela-Saari, H., Enholm, B., Aase, K., von Euler, G., Eriksson, U., Alitalo, K., and Joensuu, H. 1998. Vascular endothelial growth factors VEGF-B and VEGF-C are expressed in human tumors. *Am. J. Pathol. 153*:103–108.

Shen, G.H., Ghazizadeh, M., Kawanami, O., Shimizu, H., Jin, E., Araki, T., and Sugisaki, Y. 2000. Prognostic significance of vascular endothelial growth factor expression in human ovarian carcinoma. *Br. J. Cancer 83*:196–203.

Shimizu, Y., Kamoi, S., Amada, S., Akiyama, F., and Silverberg, S.G. 1998. Toward the development of Universal Grading System for ovarian epithelial carcinoma. *Cancer 82*:893–901.

Silverberg, S.G. 1989. Prognostic significance of pathologic features of ovarian carcinoma. *Curr. Top. Pathol. 78*:85–109.

Skobe, M., Hawighorst, T., Jackson, D.G., Prevo, R., Janes, L., Velasco, P., Riccardi, L., Alitalo, K., Claffey, K., and Detmar, M. 2001. Induction of tumor lymphangiogenesis by VEGF-C promotes breast cancer metastasis. *Nat. Med. 7*:192–198.

Veikkoa, T., Karkkainen, M., Claesson-Welsh, L., and Alitalo, K. 2000. Regulation of angiogenesis via vascular endothelial growth factor receptors. *Cancer Res. 60*:203–212.

Weidner, N. 1993. Tumor angiogenesis: review at current applications in tumor prognostication. *Semin. Diagn. Pathol. 10*: 302–313.

Yeo, K.T., Wang, H.H., Nagy, J.A., Sioussat, T.M., Ledbetter, S.R., Hoogewerf, A.J., Zhou, Y., Masse, E.M., Senger, D.R., Dvorak, H.F., and Yeo, T.K. 1993. Vascular permeability factor (vascular endothelial growth factor) in guinea pig and human tumor and inflammatory effusions. *Cancer Res. 53*: 2912–2918.

Yokoyama, Y., Charnock-Jones, D.S., Licence, D., Yanaihara, A., Hastings, J.M., Holland, C.M., Emoto, M., Umemoto, M., Sakamoto, T., Sato, S., Mizunuma, H., and Smith, S.K. 2003. Vascular endothelial growth factor D is an independent prognostic factor on epithelial ovarian carcinoma. *Br. J. Cancer. 88*:237–224.

Yonemura, Y., Endo, Y., Fujita, H., Fushida, S., Ninomiya, I., Bandou, E., Taniguchi, K., Miwa, K., Ohoyama, S., Sugiyama, K., and Sasaki, T. 1999. Role of vascular endothelial growth factor C expression in the development of lymph node metastasis in gastric cancer. *Clin. Cancer Res. 5*:1823–1829.

This Page Intentionally Left Blank

17

Use of Microarray in Immunohistochemical Localization of SMAD in Ovarian Carcinoma

Heini Lassus and Ralf Bützow

Introduction

Transforming growth factor-beta (TGF-β) inhibits the proliferation of most epithelial cells, and somatic alterations in TGF-β pathway have been implicated in the pathogenesis of many types of carcinomas including ovarian carcinoma (OC). Binding of TGF-β to its membrane receptors leads to phosphorylation of intracellular signaling molecules SMAD2 and SMAD3, which then form heterotrimeric complex with SMAD4. The complexes translocate into the nucleus, where they act as transcriptional activators or repressors of target genes (Massague, 1998). Originally, *SMAD4* was cloned as a candidate tumor-suppressor gene in pancreatic carcinoma (DPC4), and subsequent studies showed that the gene is lost or mutated in ~50% of these tumors (Hahn *et al.,* 1996a, b). *SMAD4* mutations also occur in colon carcinomas (Miyaki *et al.,* 1999) and in the germline of a subset of juvenile polyposis families (Howe *et al.,* 1998). In OC, mutations of *SMAD4* have been observed in <5% of primary tumors (Wang *et al.,* 2000). However, SMAD4 locus at 18q21.1 belongs to the most frequently lost chromosomal regions in OC (Lassus *et al.,* 2001b), and loss of SMAD4 protein was previously shown in 17 of 60 (28%) primary serous OCs (Lassus *et al.,* 2001b). However, the clinicopathologic correlations of lost SMAD4 expression in OC are unknown.

The second most common malignancy of the female genital tract is OC. The overall prognosis of OC is poor, reflecting the frequent finding of advanced disease at diagnosis (Heintz *et al.,* 200l). However, the biological behavior, response to available treatment, and outcome of apparently similar cases vary greatly. This suggests that OC is likely to be made up of a number of different entities, and, therefore, molecular markers that would define biologically and clinically relevant disease entities and predict disease outcome are needed.

The OCs consist of different histologic types, including serous, mucinous, endometrioid, and clear cell carcinomas. The histologic types show differences in their risk factors and biological characteristics (Risch *et al.,* 1996), as well as molecular pathogeneses (Lassus *et al.,* 2001a; Schwartz *et al.,* 2002). Because of these differences, we believe that to find biologically relevant disease entities, different histologic types should be analyzed separately. In the present study, we analyzed SMAD4 protein expression by immunohistochemistry (IHC) in tissue (Kononen *et al.,* 1998) array consisting of 522 primary serous OCs. Multivariate survival analysis was performed, and

Handbook of Immunohistochemistry and *in situ* Hybridization of Human Carcinomas, Volume 4: Molecular Genetics, Gastrointestinal Carcinoma, and Ovarian Carcinoma

clinicopathologic correlations of the SMAD4 expression were assessed.

MATERIALS

The study consisted of 522 patients treated for serous OC at the Department of Obstetrics and Gynecology of the Helsinki University Central Hospital between 1964 and 2000 (median of recruitment 28.8.1989). The study was approved by the Ethics Committee of the Department of Obstetrics and Gynecology. Consecutive patients treated for serous OC were searched according to pathologic records. The serous histology of all carcinomas had originally been determined by a gynecologic pathologist and was verified. The clinical information of the patients was extracted from the hospital records, and additional survival information was obtained from the Population Register Centre, where all death certificates are collected in Finland. To be included in the study, data of primary treatment and the survival status of the patient were required.

New treatment regimens were adopted as follows: platinum-based chemotherapy at the beginning of the 1980s, radical surgery at the end of the 1980s and paclitaxel/platinum chemotherapy after 1996. In 406 (78%) of the 522 patients included in the study, total abdominal hysterectomy and bilateral salpingo-oophorectomy were performed along with surgical removal of tumor masses, and in 173 of these also pelvic or para-aortic lymphadenectomy or both was performed. In 61 (12%) cases unilateral or bilateral salpingo-oophorectomy was performed, and in 55 (10%) cases only biopsies were obtained in the primary surgery. The tumor samples for the study were obtained from the primary surgery before patients received any chemotherapy. In 347 cases (66%) platinum-based combination therapy was given as first-line chemotherapy, and in 101 of these cases paclitaxel was given in combination with platinum compound. In 104 (20%) cases, the patient received something other than platinum-based chemotherapy or radiotherapy, and in 71 (14%) cases no adjuvant therapy was given. Response to therapy was evaluated after the initial six cycles of chemotherapy, and in cases where no chemotherapy was given the evaluation was performed 5–6 months after the surgery (the same time interval from the surgery as in patients receiving chemotherapy).

In 203 (39%) cases, second-look laparotomy was performed, and in these cases the evaluation of the response was based on pathologic findings. In other cases, the evaluation of the response was based on gynecologic examinations, pelvic ultrasonography, CA-125 measurements, and radiologic findings. Specific overall survival of patients with OC was calculated from the date of diagnosis to death from OC. Patients who died of intercurrent causes or were alive at follow-up were censored. Disease-free survival was calculated for patients who were disease free after the primary treatment (surgery and first-line chemotherapy, if given), and it was the time from the date of diagnosis to relapse of the disease. The median follow-up of patients alive at the end of the study period was 5.2 years (range, 0.4–36.1 years). The 5-year overall survival rate for the whole cohort was 49% (95% CI, 44–53%).

METHODS

1. Tumor and normal tissues were fixed in 10% neutral buffered formalin and embedded in paraffin, and 5-μm sections stained with hematoxylin and eosin (H&E) were obtained to select representative areas for biopsies.

2. Core tissue biopsy specimens (diameter 0.8 mm) were taken from these areas of individual donor paraffin blocks and precisely arrayed into a new recipient paraffin block with a custom-built instrument (Beecher Instruments, Silver Spring, MD). Tissue samples were taken from 34 normal ovarian and 23 normal fallopian tube (normal equivalent of serous epithelium) specimens and 522 serous ovarian carcinomas. Four core-tissue biopsies were obtained from each specimen. There were a total of 2306 samples in 6 recipient paraffin blocks. The presence of tumor tissue on the arrayed samples was verified on H&E stained section.

3. Five-μm sections of these tissue array blocks were cut and placed on coated Dako ChemMate Capillary Gap Microscope Slides (Dako A/S, Glostrup, Denmark) and dried overnight at +37°C. The tissue sections were deparaffinized in xylene and rehydrated through graded concentrations of ethanol to distilled water. The sections were boiled in 10 mM citrate buffer (pH 6.0) in a microwave oven for 20 min.

4. The sections were incubated with diluted (phosphate buffer saline, pH 7.2) primary monoclonal anti-human SMAD4 (final concentration 2 μg/ml; sc-7966, Santa Cruz Biotechnology Inc., Santa Cruz, CA) for 55 min at room temperature. An avidin-biotin immunoperoxidase system was used to visualize the bound antibody, and the procedure was carried out in a Techmate automated machine (Peroxidase DAB [diaminobenzidine] detection kit; Dako ChemMate, Denmark). The sections were counterstained with Mayer's hematoxylin. Omitting the primary antibody was used as negative control, and colon carcinoma cell lines shown to express SMAD4 by Western Blotting and reverse transcription-polymerase chain reaction

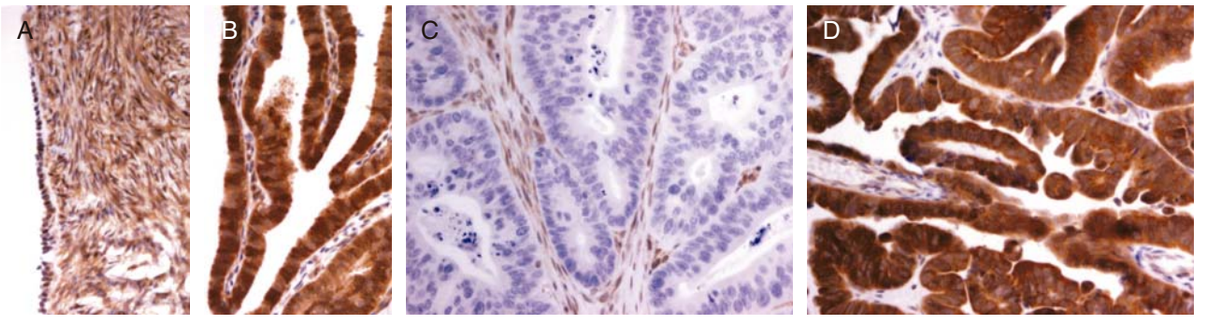

Figure 71. Examples of expression of SMAD4 protein by immunohistochemistry. Normal ovarian surface **(A)** and tubal epithelium **(B)** showing moderate to strong (positive) immunostaining of SMAD4 protein. Serous ovarian carcinomas showing negative **(C)** and positive **(D)** staining of SMAD4 protein.

(RT-PCR) were used as positive controls (Salovaara *et al.*, 2002).

5. Absence of any reactivity or very weak staining that diverged from that observed in the surface epithelium of normal ovaries and the general pattern of positive staining of the tumor samples were interpreted as negative. The evaluation of the immunohistochemical stainings was performed independently by the authors without knowledge of the clinicoopathologic information. The cases with discordant score by the two authors were reevaluated at the microscope, and a consensus score was formed.

6. Associations between factors were analyzed with the χ^2 and Fisher's exact tests. The overall and disease-free survival curves were constructed according to the Kaplan-Meier method and compared with the log-rank test. For multivariate survival analysis Cox proportional hazards model was used, with backward stepwise selection procedure, and entering the following as categorical co-variates: International Federation of Gynecology and Obstetrics (FIGO) stage (Stages I, II, III, and IV), grade (grades 1, 2, and 3), age at diagnosis (<57 years [median], ≥57 years), tumor size (≤10 cm, >10 cm), residual tumor size (≤1 cm, >1 cm), ascites (presence or absence), and p53 expression (normal, aberrant). A *P* value of 0.05 was adopted as the limit for inclusion of a co-variate. All *P* values are two-sided.

RESULTS AND DISCUSSION

SMAD4 Immunohistochemistry

In normal ovarian tissue moderate to strong immunoreactivity of SMAD4 was observed in surface epithelial cells and a proportion of stromal cells. Also the serous fallopian-tube epithelium was positive for SMAD4. Nuclear as well as cytoplasmic staining was seen. Tumors with moderate to strong immunoreactivity, similar to that found in normal epithelium (ovarian surface and fallopian tube), were considered to show positive SMAD4 expression (Figure 71). Absence of any reactivity or very weak staining that diverged from that observed in the surface epithelium of normal ovaries were interpreted as negative SMAD4 expression. SMAD4 staining was not interpretable in 18 (3%) of the 522 carcinomas as a result of loss of biopsy specimens, absence of tumor tissue, or staining artefacts. Positive SMAD4 expression was detected in 345 (68%) and negative SMAD4 expression was found in 159 (32%) of the interpretable 504 carcinomas. Heterogeneity in SMAD4 immunostaining between the biopsies from the same samples was seen in <10% of cases.

Clinicopathologic Characteristics

Negative SMAD4 expression was significantly associated with high tumor grade ($P < 0.0001$); large residual tumor size ($P = 0.0125$); size of the primary tumor ($P = 0.0194$); high mitotic index ($P = 0.0124$); aberrant p53 ($P < 0.0001$); and negative progesterone receptor ($P < 0.0001$), negative estrogen receptor α ($P = 0.0002$), and β ($P = 0.0008$) expression (Table 37). There was no significant association with tumor stage ($P = 0.0996$), patient age ($P = 0.2823$), presence of ascites ($P = 0.3434$), or response to therapy ($P = 0.1436$).

Disease-Free Survival

Patients with negative SMAD4 expression showed shorter disease-free survival time than patients with positive SMAD4 expression ($P = 0.0069$) (Figure 72). The 5-year disease-free survival rate was 73% (95% CI, 67–80%) for patients with positive SMAD4 and 52% (39–65%) for those with negative SMAD4 expression.

Table 37. Association of SMAD4 Protein Expression with Clinicopathologic Characteristics

Clinicopathologic Characteristics FIGO Stage	Positive	%	Negative	%	P Value
FIGO Stage					
I	81/342	24	23/159	14	NS; 0.0996
II	45/342	13	21/159	13	
III	179/342	52	92/159	58	
IV	37/342	11	23/159	14	
Grade					
1	153/339	45	34/157	22	<0.0001
2	87/339	26	41/157	26	
3	99/339	29	82/157	52	
Residual Tumor Size					
≤1 cm	161/303	53	61/150	41	0.0125
>1 cm	142/303	47	89/150	59	
Age					
<57 years	174/345	50	72/159	45	NS; 0.2823
≥57 years	171/345	50	87/159	55	
Tumor Size					
≤10 cm	130/339	38	43/156	28	0.0194
>10 cm	209/339	62	113/156	72	
Ascites					
No	128/341	38	51/154	33	NS; 0.3434
Yes	213/339	62	103/154	67	
Primary Response					
Complete response	170/331	51	66/155	43	NS; 0.1436
Partial response	73/331	22	33/155	21	
Stable disease	33/331	10	18/155	12	
Progressive disease	55/331	17	38/155	25	
p53					
Normal	168/340	49	33/157	21	<0.0001
Aberrant	172/340	51	124/157	79	
Ki-67					
<10%	188/338	56	75/157	48	0.0124
10–25%	76/338	22	55/157	35	
>25%	74/338	22	27/157	17	
PR					
Negative	208/345	60	134/159	84	<0.0001
Positive	137/345	40	25/159	16	
ERα					
Negative	125/345	36	86/159	54	0.0002
Positive	220/345	64	73/159	46	
ERβ					
Negative	246/345	71	135/159	85	0.0008
Positive	99/345	29	24/159	15	

ER, Estrogen receptor; NS, not significant; PR, progesterone receptor.

Overall Survival

Negative SMAD4 was associated with poor overall survival compared with tumors showing positive SMAD4 expression ($P < 0.0001$) (Figure 73). The 5-year overall survival rates for patients with tumors with positive and negative SMAD4 expression were 56% (95% CI, 50–61%) and 32% (24–40%). In multivariate analysis, SMAD4 expression status was identified as an independent prognostic factor, together with tumor grade, residual tumor size, FIGO stage, and patient age (Table 38).

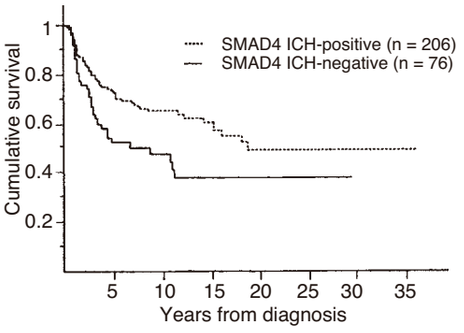

Figure 72. Disease-free survival in 282 patients with serous ovarian carcinoma in relation to SMAD4 expression detected by immunohistochemistry.

Discussion

To our knowledge, this is the first study to assess the clinicopathologic associations of SMAD4 expression in ovarian carcinoma. The success rate of immunohistochemical analysis of SMAD4 in the OC tissue array was high: 97% of the samples were interpretable. The question of tumor heterogeneity and representativeness of core biopsies in a tissue array is relevant. In the present study, heterogeneity in SMAD4 immunostaining between the biopsies was seen in a minority (<10%) of cases. We took four samples from each tumor, and in cases showing heterogeneity between the biopsies the staining score was determined by the average of the individual biopsies. Previously, three tissue cores per sample have been shown sufficient for two category distinction (Hoos *et al.,* 2001). Using normal ovarian surface epithelium as a reference, we observed loss of SMAD4 expression in 32% of the carcinomas. The result is consistent with our preliminary findings showing negative SMAD4 expression in 17 of 60 (28%) primary serous OCs (Lassus *et al.,* 2001b). In cancers with the highest frequency of SMAD4 alterations (i.e., pancreatic and colorectal carcinomas), SMAD4 protein down-regulation has been observed in up to 50% of tumors (Salovaara *et al.,* 2002; Wilentz *et al.,* 2000b).

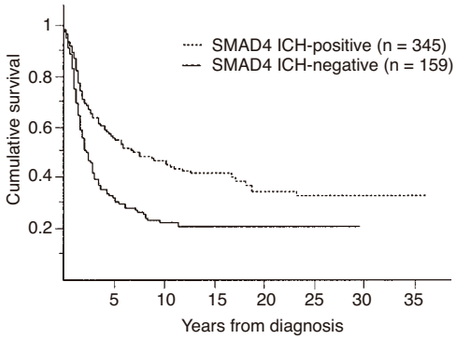

Figure 73. Overall survival in 504 patients with serous ovarian carcinoma in relation to SMAD4 expression detected by immunohistochemistry.

Because of its role in the TGF-β pathway, *SMAD4* has been categorized as a tumor-suppressor gene. In pancreatic carcinogenesis the first hit of the biallelic inactivation of SMAD4 occurs early by allelic loss. The second hit, by mutation or loss of the other allele, leading to loss of SMAD4 expression takes place later in high-grade dysplasia and invasive carcinoma (Hahn *et al.,* 1996a,b; Luttges *et al.,* 2001; Wilentz *et al.,* 2000a). SMAD4 IHC has been found to be a sensitive and specific marker for gene alterations detected in *SMAD4* (Wilentz *et al.,* 2000b). Mutant SMAD4 proteins are degraded more rapidly than their wild-type counterparts (Xu and Attisano, 2000), which should lead to decreased staining of the protein by IHC. In contrast to pancreatic carcinoma, SMAD4 mutations are infrequent in OC (Wang *et al.,* 2000), and the mechanisms causing down-regulated expression of SMAD4 are unclear. In our previous study, 10 of 17 (59%) tumors with negative SMAD4 expression showed allelic loss at 18q21.1 (Lassus *et al.,* 2001b). The analysis was performed by PCR-based amplification of microsatellite markers and, thus, evaluation of homozygous deletion could be done only indirectly. The PCR was performed using 30–35 cycles, where the reaction should not reach the plateau level and the result could be considered as semi-quantitative. Based on this estimation, homozygous loss of 18q21.1 was not detected. In addition to loss of chromosomal material or mutations, a gene can be inactivated at a transcriptional level (e.g., by promoter hypermethylation). To address this, we studied the methylation status of SMAD4 (for method see Roth *et al.,* 2000), but none of the 59 serous OCs showed promoter hypermethylation. Thus, besides allelic loss of one allele, the mechanisms causing the down-regulated expression of SMAD4 in OC remain unclear.

Different histologic subtypes of OC form biologically distinct entities. To better understand the pathogenesis, the histologic subtypes can be divided further into subgroups based on biological and molecular characteristics. The subgroup of serous OC with loss of SMAD4 expression was associated with characteristics of aggressive tumor behavior, such as high tumor grade, large residual tumor size, and large size of the primary tumor. In colon carcinomas, loss of SMAD4 expression is associated with aggressive characteristics as well (i.e., high tumor stage and presence of metastatic

Table 38. Cox Proportional Hazards Model of Independent Prognostic Factors for Overall Survival

Variable		β-Coefficient	Chi-Square	P Value	HR	95% CI
Grade	1				1	
	2	0.853	17.8	<0.0001	2.35	1.58–3.49
	3	1.070	28.8	<0.0001	2.92	1.97–4.31
Residual tumor >1 cm		0.798	23.6	<0.0001	2.22	1.61–3.07
FIGO Stage	I				1	
	II	0.856	6.2	0.0125	2.36	1.20–4.61
	III	1.228	15.5	<0.0001	3.41	1.85–6.29
	IV	1.639	21.6	<0.0001	5.15	2.58–10.29
Age >57 years		0.426	10.3	0.0013	1.53	1.18–1.99
Negative SMAD4		0.286	4.62	0.0315	1.331	1.03–1.73

CI, Confidence interval; HR, hazard ratio.

disease) (Maitra *et al.,* 2000; Miyaki *et al.,* 1999). The TGF-β signaling pathway is known to induce growth inhibition in epithelial cells. Consistent with this, serous OCs with negative SMAD4 expression showed high mitotic index. In addition, loss of SMAD4 expression was associated with aberrant p53 as well as negative status of progesterone receptor and estrogen receptor α and β. These associations may have functional significance or may be explained by loss of tissue differentiation. It is interesting that, in breast cancer cells a functional connection between SMAD4 and estrogen receptor α has been found: anti-estrogen ligands induce co-immunoprecipitation of SMAD4 and estrogen receptor α, and the complex formation inhibits estrogen downstream target gene transcription (Wu *et al.,* 2003).

The overall prognosis of OC is relatively poor (Heintz *et al.,* 2001). However, the biological behavior, response to treatment, and outcome of apparently similar cases of OC are variable, and there is a need for prognostic and predictive molecular markers. Loss of SMAD4 expression was associated with shorter disease-free and overall survival. The 5-year overall survival rates for patients with tumors with negative SMAD4 expression was 32% as compared with 56% associated with positive SMAD4 expression. In multivariate analysis, in addition to known clinicopathologic prognostic factors (tumor grade, residual tumor size, FIGO stage, and patient age) (Friedlander, 1998), SMAD4 expression status showed independent prognostic value. In pancreatic adenocarcinoma, SMAD4 expression has been found as an independent prognostic factor of overall survival as well (Tascilar *et al.,* 2001). In contrast, only a small proportion (2%) of breast carcinomas show loss of SMAD4 expression and there is no association with patient outcome (Xie *et al.,* 2002).

Tumor tissue array combined with clinical database is an efficient way to test clinicopathologic associations and prognostic value of candidate genes. In the present study on tissue array of 522 serous OC, loss of SMAD4 expression was associated with poor patient outcome, indicated by shorter overall and disease-free survival. Loss of SMAD4 expression was also associated with characteristics of aggressive tumor behavior, such as high tumor grade, large residual tumor size, and aberrant p53 and negative hormone receptor status. The results augment the classification of serous ovarian carcinoma into biologically and clinically meaningful entities, which is becoming increasingly important as new and more specific treatment modalities are developed.

Acknowledgments

We thank Arto Leminen and Pentti Lehtovirta for collecting the clinical information, Lauri Aaltonen and Reijo Salovaara for help with SMAD4 IHC, Stina Roth for advice with SMAD4 promoter hypermethylation analysis, Guojun Cheng and Jan-Åke Gustafsson for performing the hormone receptor analyses, and Gynel Arifdshan for technical assistance.

References

Friedlander, M.L. 1998. Prognostic factors in ovarian cancer. *Semin. Oncol. 25*:305–314.

Hahn, S.A., Hoque, A.T., Moskaluk, C.A., da Costa, L.T., Schutte, M., Rozenblum, E., Seymour, A.B., Weinstein, C.L., Yeo, C.J., Hruban, R.H., and Kern, S.E. 1996a. Homozygous deletion map at 18q21.1 in pancreatic cancer. *Cancer Res. 56*:490–494.

Hahn, S.A., Schutte, M., Hoque, A.T., Moskaluk, C.A., da Costa, L.T., Rozenblum, E., Weinstein, C.L., Fischer, A., Yeo, C.J., Hruban, R.H., and Kern, S.E. 1996b. DPC4, a candidate tumor suppressor gene at human chromosome 18q21.1. *Science 271*:350–353.

Heintz, A.P., Odicino, F., Maisonneuve, P., Beller, U., Benedet, J.L., Creasman, W.T., Ngan, H.Y., Sideri, M., Pecorelli, S. 2001. Carcinoma of the ovary. *J. Epidemiol. Biostat. 6*:107–138.

Hoos, A., Urist, M.J., Stojadinovic, A., Mastorides, S., Dudas, M.E., Leung, D.H., Kuo, D., Brennan, M.F., Lewis, J.J., and Cordon-Cardo, C. 2001. Validation of tissue microarrays for immunohistochemical profiling of cancer specimens using the example of human fibroblastic tumors. *Am. J. Pathol. 158*:1245–1251.

Howe, J.R., Roth, S., Ringold, J.C., Summers, R.W., Jarvinen, H.J., Sistonen, P., Tomlinson, I.P., Houlston, R.S., Bevan, S., Mitros, F.A., Stone, E.M., and Aaltonen, L.A. 1998. Mutations in the SMAD4/DPC4 gene in juvenile polyposis. *Science 280*: 1086–1088.

Kononen, J., Bubendorf, L., Kallioniemi, A., Barlund, M., Schraml, P., Leighton, S., Torhorst, J., Mihatsch, M.J., Sauter, G., and Kallioniemi, O.P. 1998. Tissue microarrays for high-throughput molecular profiling of tumor specimens. *Nat. Med. 4*:844–847.

Lassus, H., Laitinen, M.P., Anttonen, M., Heikinheimo, M., Aaltonen, L.A., Ritvos, O., and Butzow, R. 2001a. Comparison of serous and mucinous ovarian carcinomas: distinct pattern of allelic loss at distal 8p and expression of transcription factor GATA-4. *Lab. Invest. 81*:517–526.

Lassus, H., Salovaara, R., Aaltonen, L.A., and Butzow, R. 2001b. Allelic analysis of serous ovarian carcinoma reveals two putative tumor suppressor loci at 18q22-q23 distal to SMAD4, SMAD2, and DCC. *Am. J. Pathol. 159*:35–42.

Luttges, J., Galehdari, H., Brocker, V., Schwarte-Waldhoff, I., Henne-Bruns, D., Kloppel, G., Schmiegel, W., Hahn, S.A., Schutte, M., Hruban, R.H., Hedrick, L., Cho, K.R., Nadasdy, G.M., Weinstein, C.L., Bova, G.S., Isaacs, W.B., Cairns, P., Nawroz, H., Sidransky, D., Casero, R.A. Jr., Meltzer, P.S., Kern, S.E., Hoque, A.T., Moskaluk, C.A., da Costa, L.T., Rozenblum, E., Seymour, A.B., Yeo, C.J., and Fischer, A. 2001. Allelic loss is often the first hit in the biallelic inactivation of the p53 and DPC4 genes during pancreatic carcinogenesis DPC4 gene in various tumor types. *Am. J. Pathol. 158*:1677–1683.

Maitra, A., Molberg, K., Albores-Saavedra, J., and Lindberg, G. 2000. Loss of DPC4 expression in colonic adenocarcinomas correlates with the presence of metastatic disease. *Am. J. Pathol. 157*:1105–1111.

Massague, J. 1998. TGF-beta signal transduction. *Annu. Rev. Biochem. 67*:753–791.

Miyaki, M., Iijima, T., Konishi, M., Sakai, K., Ishii, A., Yasuno, M., Hishima, T., Koike, M., Shitara, N., Iwama, T., Utsunomiya, J., Kuroki, T., and Mori, T. 1999. Higher frequency of SMAD4 gene mutation in human colorectal cancer with distant metastasis. *Oncogene 18*:3098–3103.

Risch, H.A., Marrett, L.D., Jain, M., and Howe, G.R. 1996. Differences in risk factors for epithelial ovarian cancer by histologic type. Results of a case-control study. *Am. J. Epidemiol. 144*:363–372.

Roth, S., Laiho, P., Salovaara, R., Launonen, V., and Aaltonen, L.A. 2000. No SMAD4 hypermethylation in colorectal cancer. *Br. J. Cancer 83*:1015–1019.

Salovaara, R., Roth, S., Loukola, A., Launonen, V., Sistonen, P., Avizienyte, E., Kristo, P., Jarvinen, H., Souchelnytskyi, S., Sarlomo-Rikala, M., Aaltonen, L.A., and Laiho, P. 2002. Frequent loss of SMAD4/DPC4 protein in colorectal cancers. *Gut. 51*:56–59.

Schwartz, D.R., Kardia, S.L., Shedden, K.A., Kuick, R., Michailidis, G., Taylor, J.M., Misek, D.E., Wu, R., Zhai, Y., Darrah, D.M., Reed, H., Ellenson, L.H., Giordano, T.J., Fearon, E.R., Hanash, S.M., and Cho, K.R. 2002. Gene expression in ovarian cancer reflects both morphology and biological behavior, distinguishing clear cell from other poor-prognosis ovarian carcinomas. *Cancer Res. 62*:4722–4729.

Tascilar, M., Skinner, H.G., Rosty, C., Sohn, T., Wilentz, R.E., Offerhaus, G.J., Adsay, V., Abrams, R.A., Cameron, J.L., Kern, S.E., Yeo, C.J., Hruban, R.H., Goggins, M., Iacobuzio-Donahue, C., McCarthy, D.M., Brat, D.J., Iacobuzio-Donahue, C.A., Argani, P., Parsons, J.L., Su, G.H., Dai, J.L., Sparks, A.B., and Sohn, T.A. 2001. The SMAD4 protein and prognosis of pancreatic ductal adenocarcinoma. *Clin. Cancer Res. 7*:4115–4121.

Wang, D., Kanuma, T., Mizunuma, H., Takama, F., Ibuki, Y., Wake, N., Mogi, A., Shitara, Y., and Takenoshita, S. 2000. Analysis of specific gene mutations in the transforming growth factor-beta signal transduction pathway in human ovarian cancer. *Cancer Res. 60*:4507–4512.

Wilentz, R.E., Iacobuzio-Donahue, C.A., Argani, P., McCarthy, D.M., Parsons, J.L., Yeo, C.J., Kern, S.E., Hruban, R.H., Su, G.H., Dai, J.L., Sparks, A.B., and Sohn, T.A. 2000a. Loss of expression of DPC4 in pancreatic intraepithelial neoplasia: evidence that DPC4 inactivation occurs late in neoplastic progression. *Cancer Res. 60*:2002–2006.

Wilentz, R.E., Su, G.H., Dai, J.L., Sparks, A.B., Argani, P., Sohn, T.A., Yeo, C.J., Kern, S.E., and Hruban, R.H. 2000b. Immunohistochemical labeling for DPC4 mirrors genetic status in pancreatic adenocarcinomas: a new marker of DPC4 inactivation. *Am. J. Pathol. 156*:37–43.

Wu, L., Wu, Y., Gathings, B., Wan, M., Li, X., Grizzle, W., Liu, Z., Lu, C., Mao, Z., and Cao, X. 2003. SMAD4 as a transcription corepressor for estrogen receptor alpha. *J. Biol. Chem. 278*: 15192–15200.

Xie, W., Mertens, J.C., Reiss, D.J., Rimm, D.L., Camp, R.L., Haffty, B.G., and Reiss, M. 2002. Alterations of SMAD signaling in human breast carcinoma are associated with poor outcome: a tissue microarray study. *Cancer Res. 62*: 497–505.

Xu, J., and Attisano, L. 2000. Mutations in the tumor suppressors SMAD2 and SMAD4 inactivate transforming growth factor beta signaling by targeting SMADs to the ubiquitin-proteasome pathway. *Proc. Natl. Acad. Sci. USA 97*:4820–4825.

This Page Intentionally Left Blank

18

Role of Immunohistochemical Expression of Fas in Ovarian Carcinoma

Caroline Van Haaften

Introduction

Cell numbers in tissue are held constant by cell proliferation and growth-balancing cell elimination: programmed cell death or apoptosis. Disturbances of apoptotic processes caused by mutations of the controlling genes play a central role in the pathogenesis of human disease (Kam and Ferch, 2000).

The best-characterized "cell death" receptor with respect to its signal-transduction pathway is the Fas (Apo-1/CD95) protein. This M 45,000 type I transmembrane cell-surface receptor of the tumor necrosis factor (TNF)/nerve growth factor superfamily mediates apoptosis when triggered by antibodies or its ligand, FasL. This ligand, FasL/CD95L, a type II transmembrane molecule of M 40,000, is expressed on cell membranes or in soluble form and belongs to a co-evolved family of proteins of the TNF family (Itoh *et al.,* 1991; Nagata and Golstein 1995; Suda *et al.,* 1993).

Fas is expressed by a variety of cells. Recognized first in lymphoid tissue, it was later recognized in tissues of nonlymphoid origin. Studied often in relation to malignancy, where apoptosis is often considered to be intrinsic to malignant derailment, it is also to be found in relation to apoptotic processes of normal tissue. These include some of the cell lineages that together compose normal follicles in the ovaries (Leithauser *et al.,* 1993). In the process of follicular atresia, apoptosis eliminates thecal and granulosa cells, constituents of the follicle (Foghi *et al.,* 1998; Kondo *et al.,*1996; Quirk *et al.,* 1995). It also has been shown that ovarian surface epithelial cells of dispersed mouse corpora lutea undergo programmed cell death before ovulation. Rapid repair of the surface cells occurs after ovulation (Quirk *et al.,* 1997). FasL expression in normal tissue is largely restricted to T-lymphocyte and macrophage lineages. The primary function of the Fas/FasL system is thought to be the maintenance of homeostasis in the immune system (Nagata, 1997). Thus, expression of the Fas receptor, which on triggering activates the apoptotic process, may be limited to cells in specific phases of a biologically important process. This may include the ending of an immune response as well as development and reduction of cell masses as part of a cyclical process such as the menstrual cycle. It may, however, also affect cells as part of a continuous process such as the maturation of dermal keratinocytes and small bowel epithelium once they leave the tissue compartment of basal cells or cells lining crypts.

The biological spectrum of ovarian epithelial tumors includes benign, proliferating (borderline), and malignant neoplasms (Russell and Farnsworth, 1997; Scully *et al.,* 1998). Of the malignant epithelial ovarian tumors, which account for more than 90% of all ovarian

Handbook of Immunohistochemistry and *in situ* Hybridization of Human Carcinomas, Volume 4: Molecular Genetics, Gastrointestinal Carcinoma, and Ovarian Carcinoma

cancers, the serous papillary variants form the largest subgroup. Considered to be derived from ovarian surface lining epithelium, which shows cyclical changes, most likely involving alternating periods of proliferation and gene-controlled apoptotic involution. Thus the question as to a potential role for apoptosis modulation of tumors derived from this epithelium presents itself. Present treatment of these lesions, despite the introduction of novel, platinum-based drug moieties is still considered to be less effective compared to the results achieved in other lesion types. The potential for progress through exploiting possible treatment options within modulation of apoptosis requires a deeper understanding of the biology of this mechanism in this lesion type.

However, study of the clinical relevance of this antigen in histologic section material is compromised by its membrane location, resulting in very low epitope density and near-critical optical profile dimensions. This requires optimization of antigen detection with secondary use of amplification through use of avidin-biotin methodology supported by improvement of delicate structural features (i.e., intactness of cell membranes exposed to the space lined by the serous epithelial tumor tissue). Although optimal situations can be created using frozen sections, often follow-up studies require use of classic tissue resources (i.e., paraffin-embedded material), further emphasizing the need for optimization of immunocytochemical procedures. At this stage, however, the demonstration of the antigens detectable by novel monoclonal antibodies has not been systematically addressed to the level whereby relative advantages of frozen versus fixed tissues, and within that the relative benefits of various fixatives, have been fully detailed. Thus, we chose to assess the expression of Fas in normal ovarium (surface epithelium) and within the biological spectrum of epithelial neoplasms using immunocytochemistry. Within this the effect of various fixation alternatives and the effects of fixation time and the use of signal amplification were assessed within specific limitations.

MATERIALS AND METHODS

Ovarian Tissue

Study Populations

Study Group I. Formaldehyde-fixed and paraffin-embedded tissue from 86 patients with ovarian serous surface epithelial tumors and normal ovaries of 4 additional patients were analyzed. Thirty patients had benign tumors, 22 patients were histologically classified as having borderline tumors, and 34 patients had invasive cancer.

The surface epithelial tumors were typed and categorized according to the current protocols of the World Health Organization and the International Society of Gynecological Pathologists (Scully *et al.,* 1998) by two investigators not involved in the original diagnosis to achieve consistency throughout the study material. Although originally as part of the diagnostic process, tumors of borderline malignancy had been divided into low- and high-grade variants (according to the severity of architectural and cellular changes, mitotic activity, and nuclear atypia), for the purpose of this study lesions were combined into a single group mainly because of the limited number of cases.

Study Group II. In light of recent developments, suggesting better antigen preservation in the absence of cross-linking fixatives, an explorative series of ovarian tissue from six patients (four carcinoma, two of borderline malignancy) seen as part of routine diagnostic pathology services were included in the study using a series of different fixatives so as to allow for direct comparison of results.

Tissue Fixation, Processing

Study Group I. Study group I consisted of materials of lesions retrieved from the files of the Department of Anatomical Pathology, Royal Prince Alfred Hospital, Sydney Australia. Primary fixation was in 0.1 M phosphate buffer (pH 7.0), formalin 10% (3.6% formaldehyde, up to 1985), or formaldehyde/acetic acid/alcohol-ethanol (FAA) after 1985. All tissues in this study group were routinely processed for paraffin embedding. For each case, one slide considered representative for the lesion as a whole was selected. In cases with manifest heterogeneity, the slide with the most atypical area or highest grade of abnormality was chosen. For these the original paraffin blocks were retrieved for further study.

Study Group II. Tissue for cases in study group II was obtained from the Pathology Department of MCH, The Hague, and The Erasmus Medical Center, Rotterdam, The Netherlands. Tissue samples were fixed either in BoonFix (Finetec, Tokyo, Japan) or, for comparison, in classic 0.1 M phosphate-buffered 3.6% formaldehyde (pH 7.4). Tissues were processed to paraffin using microwave-enhanced rapid processing (RMS, Milestone, Sorisole, Italy). For all cases, sections (Australia, 5 μm; the Netherlands, 4 μm) were cut and mounted on silanized glass slides followed by hematoxylin and eosin (H & E) staining and coverslipping, staining by Papanicolau (trichrome stain), and cutting of 5/4 μm standard sections for immunocytochemistry.

Antibodies

For the detection of Fas protein in fixed, paraffin-embedded tissues, we used immunostaining kits obtained from Santa Cruz Biotechnology. The kit contains

prediluted rabbit polyclonal anti-serum to Fas (C20) (Santa Cruz product sc 715K), and a biotin–streptavidin–peroxidase detection system.

The same rabbit polyclonal anti-serum to Fas (C-20; sc-715) was diluted in a series of 1:50 till 1:800, with the final choice for a working dilution of 1:100 to assess the preservation and demonstration of this antigen in the tissue processed after BoonFix and formaldehyde fixation. A second antibody goat-anti-polyvalent/biotin was used (Labvision Corporation, Fremont, CA) and followed by streptavidin–peroxidase (Labvision Corporation). For comparison the ChemMate Envision K5007 (DakoCytomation, Glostrup, Denmark) was used. After the rabbit polyclonal anti-serum to Fas only a second step with ChemMate Envision was performed. Negative control serum (sc 715P) (Santa Cruz Biotechnology) was applied at the same protein concentrations as the primary anti-serum.

Immunohistochemistry

Newly cut paraffin sections (4 μm) of ovarian tissues (fixed in formaldehyde) were floated to silanized slides and dried at 65°C for 30 min. Prior to immunostaining, sections were subjected to heat-induced epitope retrieval (HIER). For this purpose, dewaxed, rehydrated sections were immersed in an ethylenediamine tetraacetic acid (EDTA)-Tris-citrate antigen-retrieval medium (pH 8.0) and boiled in a microwave oven for 10 min. After cooling to room temperature the slides were washed in running water and rinsed in Tris-buffered saline (pH 7.6), and the immunostaining procedure was performed as per kit instructions. Peroxidase activity was demonstrated using diaminobenzidine (DAB), and the sections were counterstained using Harris' or Gill's hematoxylin.

Newly cut paraffin sections of ovarian tissues fixed in BoonFix were dewaxed at 37°C for 5 min in ultraclear (Klinipath, Duiven, Holland), then rehydrated by dipping 10× in alcohol 100% to alcohol 50% to demiwater, and finally heated in 10 mM citrate buffer, (pH 6.5) for 10 min in a 98°C microwave processor (RMS, Milestone, Sorisole, Italy) (Kok and Boon, 2003). The slides were cooled down to room temperature during 30 min and rinsed in phosphate buffer saline (PBS) (pH 7.4). Before staining, the slides were incubated for 20 min in a tray and covered with PBS and H_2O_2 (1.5% solution) to block endogenous peroxidase. The Fas staining was subsequently carried out in sequenza racks with 10 coverplates (Thermo Electron B.V., Breda, The Netherlands).

The slides were attached to the coverplates with PBS and 100 μL (1:100) of a dilution of the primary polyclonal antibody in 1% PBS/bovine serum albumin (BSA) (Organon Teknika B.V, Boxel, Holland) was added to each slide. The slides were incubated for 40 min in the covered sequenza rack, before washing for 5 min in PBS. For the second antibody, a similar solution of goat-anti-polyvalent/biotin (100 μL) was added and incubated for 10 min. The slides were rinsed with PBS for 5 min and 100 μL streptavidin–peroxidase was applied. The slides were rinsed in Tris-HCl buffer (pH 7.4) for 5 min.

The peroxidase-labeled complex was developed with 100 μL/slide DAB using the DAB kit (KPL, Gaithersburg, MD) for 8 min, after which the slides were rinsed in Tris-HCl buffer for 5 min, followed by 2 min in running tap water and 1 min in demineralized water. The sections were counterstained with Gill's hematoxylin, rinsed in water as explained earlier, dehydrated to xylene, and mounted with coverslip in a machine (Coveraid, Bayer, Mijdrecht, The Netherlands).

Grading of Lesions and Analysis of Antigen Expression

The tumors were classified according to the proportion of positive cells in the epithelium of the lesions as follows: ++++ = >75% of cells stain; +++ = 50–75% cells stain; ++ = cells stain 25–50%; + = <25% stain; ± staining of some cells < 10%; – no cells stain (van Haaften-Day *et al.,* 1996, 2003). With blinding to histopathologic classification and original diagnosis and after repeated randomization, all specimens were graded three times by two independent investigators. Results were recorded for analysis of intra- and interobserver reproducibility of classification of lesions into each of the six classes used.

Statistical Analysis

For all statistical comparisons of two groups an unpaired, two-tailed Student's t test (assuming equal variances) was used. A p-value of <0.05 was considered significant.

RESULTS AND DISCUSSION

Immunohistochemistry

Expression of Fas in normal ovarian epithelial cells and serous ovarian tumors is detailed in Table 39 (van Haaften-Day *et al.,* 2003). Intraobserver and interobserver reproducibility for classification of lesions based on fraction of positive epithelial cells was >95%. No cases were found with disagreement (intraobserver or interobserver) greater than 1 class. Where differences occurred, a case was classified according to the highest class chosen. No differences were noted between lesions fixed in classic buffered formaldehyde or FAA.

Table 39. Expression of Fas in Normal, Benign, Borderline, and Malignant Ovarian Tumors

	Fas					
Tissue/Tumor (Patient Number)	–	±	+	++	+++	++++
Normal (4)		2		1	1	
Benign (30)		1	10	14	5	
Borderline (22)			3	9	7	3
• *Low grade (18)*			2	8	5	3
• *High grade (4)*			1	1	2	
Malignant (34)		1	18	11	4	

++++: More than 75% stain; +++: 50–75% cells stain; ++ cells stain 25–50%; + less than 25% stain; ± staining of some cells (<10%); – no cells stain.
Fas expression in tissue from patients with borderline tumors was significantly different from both benign tumors (students t-test, p = 0.005, t = –2.94) and malignant tumors (p = 0.0001, t = 4.15).
(Data on lesions obtained from Australia.)

The fraction of epithelial cells positive for each of the markers differed significantly between individual tumors. All benign tissues expressed Fas, varying between cases from + to +++. The study originally included 4 cases of borderline lesions with a higher degree of abnormality. As is evident from Table 39, this group is too small for separate interpretation of our findings, and as such results were pooled for all lesions of borderline type. The epithelium in all 22 tumors of borderline malignancy expressed Fas as did the epithelium of all 34 malignant tumors and of all normal ovaries.

Overall, the epithelium of all 90 ovaries studied expressed Fas, in 34% of cases the epithelium stained positive in less than 25% of the cells (+), in 38% of cases 25–50% of the cells stained positive (++), and in 17% of cases 50–75% of the cells stained (+++). Only 3 of the borderline ovarian tumors had Fas expression in more than 75% of the epithelial cells (++++).

Although in the vast majority of cases Fas was located as expected on the cell membrane, in a few cases (Figures 74 and 75) localization in the cell cytoplasm could not only not be excluded but in fact seemed evident. In retrospect this also was a not uncommon finding in the original case set. No cases were found in which location of Fas was limited to the cytoplasm only. The interpretation of this find is as yet unclarified; however, the difference found is most likely an expression of a mutational defect possibly affecting either assembly, transport, or final incorporation into the cell membrane.

Statistical Analysis

Analysis of differences in distribution of Fas expression between groups was performed using unpaired, two-tailed student t-tests (assuming equal variances). There was no evident or statistically significant difference between the results of grading lesions fixed in classic formaldehyde (prior to 1985) and fixed in FAA (after 1985). Significantly increased Fas expression was found in borderline tumors compared to normal or benign epithelial disease as well as to malignant tumors (see Table 39).

The results of Fas expression of tissues embedded in formaldehyde-free "BoonFix" (Figures 76 and 77) compared with simultaneously embedded tissue fixed

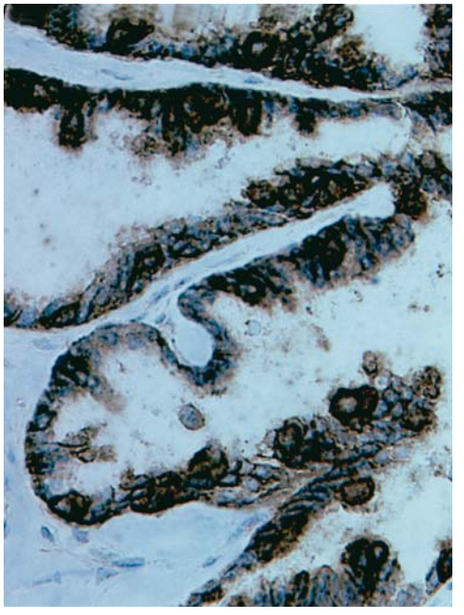

Figure 74. Photomicrograph of serous adenocarcinoma, stained for Fas antigen. Note the variable expression along epithelial surfaces of budding crypts. Areas with antigen expression limited to cell membranes alternate with areas of frank cytoplasmic antigen presence and areas of limited antigen density. Four-µm thick paraffin section, Boonfix fixation, Envision enhanced, DAB stain, Hematoxylin counterstain, microscopical magnification 200X.

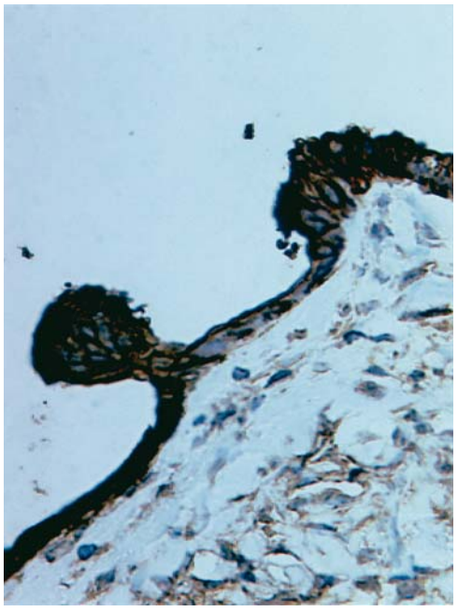

Figure 75. Photomicrograph of micropapillary structures of serous adenocarcinoma. Note almost exlusively cytoplasmic expression of Fas antigen in addition to membrane presence. Four-µm thick paraffin section, Boonfix fixation, Envision enhanced, DAB stain, Hematoxylin counterstain, microscopical magnification 400X.

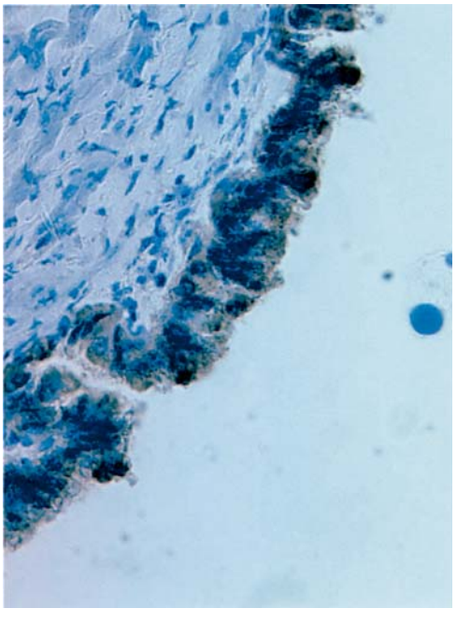

Figure 76. Photomicrograph of serous adenocarcinoma, stained for Fas antigen. Note more restricted expression of antigen in this image of immunocytochemistry without use of amplification. However, both cytoplasmic and cell membrane (surface) expression is evident. Four-µm thick paraffin section, Boonfix fixation, DAB stain, Hematoxylin counterstain, microscopical magnification 400X.

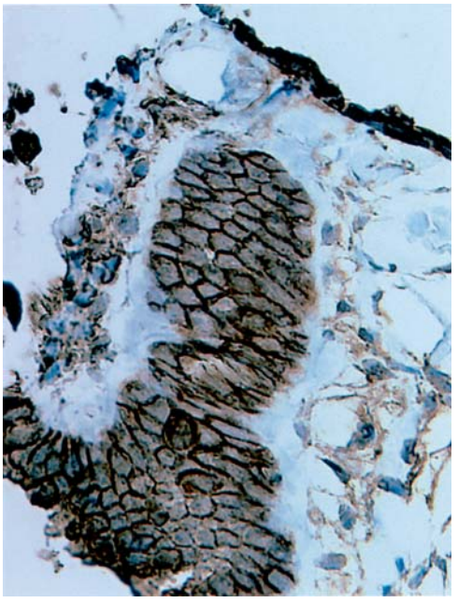

Figure 77. Photomicrograph of serous adenocarcinoma, stained for Fas antigen. Note localization of antigen as detected on cell membranes, inclusive of membrane surfaces positioned in between individual tumor cells rather than facing extracellular lumen space. Four-µm thick paraffin section, Boonfix fixation, Envision enhanced, DAB stain, Hematoxylin counterstain, microscopical magnification 400X.

in formaldehyde are given in Table 40. Although there are insufficient data for statistical analysis, it is evident that considerable differences in the degree to which Fas antigens are demonstrated occur related to primary fixation. It is obvious that formaldehyde fixation results in a considerable reduction of the number of detected epitopes and a reduction of microscopically detectable positive cells. The subsequent application of an amplification system, as was used in all of the Australian cases, to some degree masks this effect. However, for the purpose of scientific study the best possible antigen preservation should be preferred over secondary amplification strategies.

Apoptosis, caused by physiologic and pathologic stimuli, can be induced by receptor mechanisms. The so-called "death" receptors that initiate apoptosis are the TNF receptor system and the Fas receptor (Kam and Ferch, 2000; Rudin and Thompson, 1997).

Fas antigen expression is considered to reflect receptor activation. This was investigated in a spectrum of ovarian tissue from normal epithelium, through non-neoplastic precursor lesions to high-grade malignant ovarian tumors. Consistent with the view that apoptosis occurs naturally in most tissues, expression of Fas was found in all grades of tumor tissue, as well as normal

Table 40. Expression of Fas in Tissue Fixed in BoonFix or Formaldehyde

	Fas					
Tissue/Tumor	–	±	+	++	+++	++++
Borderline (2)						
BoonFix					X	X
Formalin	X	X				
Malignant (4)						
BoonFix				X	XX	X
Formalin	XX	XX				

++++: More than 75% stain; +++: 50–75% cells stain; ++ cells stain 25–50%; + less than 25% stain; ± staining of some cells (<10%); – no cells stain. (Data concerns lesions obtained in the Netherlands.)

ovarian surface epithelium. Expression of Fas in borderline serous tumors in our study was significantly greater than in either benign or malignant serous tumors. As yet no physiologic explanation is readily formulated to explain such differences, and thus again, mutation-associated dysfunction of the associated genes warrants being studied further.

An earlier study by Leithauser *et al.* (1993) reported staining of APO-1/Fas in the thecal cells of follicles of the ovary, whereas studies on follicular atresia provided strong evidence of the role of Fas in programmed cell death (Kondo *et al.,* 1996; Quirk *et al.,* 1995). Ben-Hur *et al.* (1999) and Zusman *et al.* (2001) report that they did not find Fas activity in the normal ovary; however, we did find such activity in all of the four normal ovaries studied. In the light of reports of apoptotic activity under explicit nonmalignant conditions in organs and structures as diverse as the eye (Griffith *et al.,* 1995) and Sertoli cells (Bellgrau *et al.,* 1995), and the limited number of cases studied, this apparent discrepancy warrants further study in a larger material. However, as a result of our findings, a role for antigen detectability against differences in thresholds resulting from differences in fixation can at this stage not be ruled out.

Expression of Fas in benign ovarian tumors at high levels was also found by Zusman *et al.* (2001), whereas Munakata *et al.* (2000) also found Fas expression in 74% of their study group. They also report expression of Fas not only on the cell surface but, also, in a number of cases intra-cytoplasmically. They found no significant difference in the frequency of Fas expression between histologic types. At this stage we have limited our analysis to the epithelial fraction of the lesions. Obviously apoptosis occurs in the stroma of these lesions. Future studies on this aspect and on its relation (if any) with apoptotic activity of the epithelium are foreseen. Similarly we have not at this stage included an assessment of the relationship between apoptotic activity in the epithelium and the presence or absence of stromal (T-) lymphoid cells.

It has been shown that many tumors down-regulate Fas expression, thereby impairing cellular recognition by cytotoxic T lymphocytes (CTLs) and natural killer (NK) cells. In addition, new evidence has been found that tumors can up-regulate expression of FasL, which binds to Fas present on CTLs, triggering apoptosis, the so-called "Fas counterattack" (Abrahams *et al.,* 2003; O'Connell *et al.,* 1999).

It is appreciated that there must be a correlation between the fraction of cells undergoing apoptosis and the number of final end-stage apoptotic cells (apoptotic bodies). With potential variability of the duration of apoptotic involution and the possibility of apoptotic arrest (in analogy to mitotic arrest) this relationship may be complex, but a study will nevertheless be informative. In conclusion, changes in Fas expression in ovarian tumors have been demonstrated by the presented approach, which may have relevance to tumor behavior or response to treatment. These features may additionally modulate immune surveillance and tumor recognition by the cellular immune responses.

Acknowledgments

I thank Dr. R. Veldhuizen and Dr. C. Burger for providing ovarian tissues and Dr. D. van Velzen for his support and critical review of the manuscript.

References

Abrahams, V.M., Kamsteeg, M., and Mor, G. 2003. The Fas/Fas Ligand system and cancer: immune privilege and apoptosis. Review. *Mol. Biotech. 25*:19–30.

Bellgrau, D., Gold, D., Selawry, H., Moore, J., Franzusoff, A., and Duke, R. 1995. A role for CD95 ligand in preventing graft rejection. *Nature 377*:630–632.

Ben-Hur, H., Gurevich, P., Huszar, M., Ben-Arie, A., Berman, V., Tendler, Y., Tchanishev, R., Zinder, O., Mor, G., Zaltsman, Y.,

Kohen, F., and Zusman, L. 1999. Apoptosis and apoptosis-related proteins in the epithelium of human ovarian tumors: immunohistochemical and morphometric studies. *Eur. J. Gynaecol. Oncol. 20*:249–253.

Foghi, A., Ravandi, A., Teerds, K.J., van der Donk, H., and Dorrington, J. 1998. Fas-induced apoptosis in rat thecal/interstitial cells signals through sphingomyelin-ceramide pathway. *Endocrinology 139*:2041–2047.

Griffith, T.S., Brunner, T., Fletscher, S.M., Green, D.R., and Ferguson, T.A. 1995. Fas ligand-induced apoptosis as a mechanism of immune privilege. *Science 270*:1189–1192.

Itoh, N., Yonehara, S., Ishii, A., Yonehara, M., Mizushima, S-I., Sameshima, M., Hase, A., Seto, Y., and Nagata, S. 1991. The polypeptide encoded by cDNA for human cell surface antigen Fas can mediate apoptosis. *Cell 66*:233–243.

Kam, P.C.A., and Ferch, N.I. 2000. Apoptosis: mechanisms and clinical implications. *Rev. Article Anaesthesia 55*:1081–1093.

Kok, L.P., and Boon, M.E. 2003. Microwave stimulation of coagulant formalin-free fixatives. In: Kok, L.P., and Boon, M.E. *Microwaves for the Art of Microscopy*, Leiden, The Netherlands, Coulomb Press Leyden:139–150.

Kondo, H., Maruo, T., Peng, X., and Mochizuki, M. 1996. Immunological evidence for the expression of the Fas antigen in the infant and adult human ovary during follicular regression and atresia. *J. Clin. Endocrin. Metab. 81*:2702–2710.

Leithauser, F., Dhein, J., Mechtersheimer, G., Koretz, K., Bruderlein, S., Henne, C., Schmidt, A., Debatin, K.M., Krammer, P.H., and Moller, P. 1993. Constitutive and induced expression of APO-1 a new member of the nerve growth factor/tumour necrosis factor receptor superfamily, in normal and neoplastic cells. *Lab. Invest. 69*:415–429.

Munakata, S., Enomoto, T., Tsujimoto, M., Otsuki, Y., Miwa, H., Kanno, H., and Aozasa, K. 2000. Expressions of Fas ligand and other apoptosis-related genes and their prognostic significance in epithelial ovarian neoplasms. *Br. J. Cancer 82*:1446–1452.

Nagata, S. 1997. Apoptosis by death factor. *Cell 88*:355–365.

Nagata, S., and Golstein, P. 1995. The Fas death factor. *Science 267*:1449–1456.

O'Connell, J., Bennett, M.W., O'Sullivan, G.C., Collins, J.K., and Shanahan, F. 1999. The Fas counterattack: cancer as a site of immune privilege. *Immunol. Today 20*:46–52.

Quirk, S.M., Cowan, R.G., and Huber, S.H. 1997. Fas antigen-mediated apoptosis of ovarian surface epithelial cells. *Endocrinology 138*:4558–4566.

Quirk, S.M., Cowan, R.G., Joshi, S., and Henrikson, K.P. 1995. Fas antigen-mediated apoptosis in human granulosa/luteal cells. *Biol. Reprod. 52*:279–287.

Rudin, C.M., and Thompson, C.B. 1997. Apoptosis and disease: regulation and clinical relevance of programmed cell death. *Ann. Rev. Med. 48*:267–281.

Russell, P., and Farnsworth, A. 1997. *Surgical Pathology of the Ovaries*, 2nd ed. New York: Churchill Livingstone.

Scully, R.E., Young, R.H., and Clement, P.B. 1998. Tumours of the ovary, maldeveloped gonads, fallopian tube, and broad ligament. In: Mclean, I.A., Burnier, M.A., Zimmerman, L.E., and Jacobiec, F.A. (eds). *Atlas of Tumor Pathology*, Third Series, Washington, DC: Armed Forces Institute of Pathology.

Suda, T., Takahashi, S., Golstein, P., and Nagata, S. 1993. Molecular cloning and expression of the Fas ligand, a novel member of the tumor necrosis factor family. *Cell 75*:1169–1178.

van Haaften-Day, C., Russell, P., Boyer, C.M., Kerns, B-J., Wiener, J.R., Jensen, D.N., Bast, R.C., and Hacker, N.F. 1996. Expression of cell regulatory proteins in ovarian borderline tumors. *Cancer 77*:2092–2098.

van Haaften-Day, C., Russell, P., Davies, S., King, N.J.C., and Tattersall, M.H.N. 2003. Expression of Fas and FasL in human serous ovarian epithelial tumors. *Hum. Pathol. 34*:74–79.

Zusman, I., Gurevich, P., Gurevich, E., and Ben-Hur, H. 2001. The immune system, apoptosis and apoptosis-related proteins in human ovarian tumors (a review). *Int. J. Oncol. 18*:965–972.

This Page Intentionally Left Blank

19

Role of Immunohistochemical Expression of Lewis Y Antigen in Ovarian Carcinoma

David C. Chhieng, Cristina Rodriguez-Burford, and William E. Grizzle

Introduction

Ovarian epithelial cancers are the leading cause of deaths from gynecologic cancers, and their incidence is reported to be on the rise in North America (American Cancer Society, 2002). Most ovarian cancers are of epithelial origin, accounting for 80–90% of cases (Perez *et al.,*1991).

Unfortunately, ovarian carcinoma (OC) often is diagnosed late in the course of the disease, when spread of this type of cancer has already metastasized to the peritoneal cavity. Although the current platinum-based chemotherapy for the treatment of advanced ovarian cancer can result in a response rate of 70–80%, long-term survival remains poor, with a median disease-free survival of 16–22 months and a 5-year survival rate of only 20–30% (Kaye, 2001). The majority of patients die of recurrent, drug-resistant disease. Therefore, improved therapies are needed and should be directed to the peritoneal cavity where most relapses occur.

Among the novel therapies being investigated are those that use immunologic or gene-therapy approaches. One method is immunotherapy, which was first developed in the 1980s. One type of immunotherapy consists of delivering therapeutic agents conjugated to monoclonal antibodies that bind to the surface of the cancer cells (Alvarez *et al.,* 1997; Bombardieri *et al.,* 1997; Epenetos *et al.,* 1987; Meredith *et al.,* 1996; Murray, 2000; Press and Rasey, 2000; Stewart *et al.,* 1988; Verhaar-Langereis *et al.,* 2000). The therapeutic agents used include radioisotopes, toxins, chemotherapeutic agents, cytokines, or immunologic cells (Dillman, 2001). Early trials using radioisotopes conjugated to the monoclonal antibodies such as Carcinoembryonic antigen (CEA) and Tag 72, delivered intraperitoneally, have shown promising beneficial effects (Alvarez *et al.,* 1997; Epenetos *et al.,* 1987; Meredith *et al.,* 1996). In addition, studies using imaging and dosimetry have demonstrated selective tumor localization and slow absorption into the bloodstream (Chatal *et al.,* 1989; Colcher *et al.,* 1987; Ward *et al.,* 1987). Another immunologic approach is the use of vaccines, which stimulates the host to mount an immune response directed against antigen expressed on cancer cells (Livingston and Ragupathi, 1997). A phase I clinical trial showed that two-thirds of the patients produced antibodies to Lewis Y antigen after being immunized with a Lewis Y pentasaccharide conjugated to a carrier protein and an immunologic adjuvant; in addition, a proportion of these patients had strong anti-tumor cell reactivity (Sabbatini *et al.,* 2000).

One factor that contributes to the success of immunotherapy is the discovery of epitopes that are overexpressed in ovarian cancer cells; this has opened

Handbook of Immunohistochemistry and *in situ* Hybridization of Human Carcinomas, Volume 4: Molecular Genetics, Gastrointestinal Carcinoma, and Ovarian Carcinoma

up the possibility of using these structures as potential targets for immunotherapy. Among the possible candidates, Lewis Y antigen has received a particular attention because of its high expression in a number of tumor types, including ovarian. Lewis Y antigen is expressed in 75% of ovarian cancers by using immunohistochemistry (IHC), irrespective of patients' secretor status (Yin *et al.,* 1996). In the majority of the cases, the expression ranges from moderate to high. Furthermore, anti-Lewis Y antigen monoclonal antibodies show a high degree of specificity for Lewis Y structures and minimal cross-reactivity with other blood-group determinants.

However, many questions regarding immunotherapy have yet to be answered. One major question is the extent to which antigen expression varies between the primary tumor and metastatic sites. An ideal antigen for immunotherapy should be strongly and uniformly expressed on the external membrane of all cancer cells. Many solid neoplasms, including ovarian cancer, often demonstrate regional variation in the phenotypic expression of antigens. These regional differences in the immunophenotypic profile within the same tumor have been referred to as intratumoral heterogeneity. This issue of intratumoral heterogeneity has several significant implications with regard to immunotherapy. The first implication is the choice of monoclonal antibodies that are used for targeting the cancer. The second implication is the source of tissue, primary versus metastatic, that should be obtained to determine the antigenic profile of the tumor of a particular patient.

Our hypothesis was that there is no difference between primary and metastatic ovarian cancers in the expression of Lewis Y antigen that has been used as specific targets for immunotherapy. To test our hypothesis, tumor samples of both primary and metastatic lesions (including cases with matched primary and metastatic lesions) were obtained from patients with OC. We then evaluated immunohistochemically for the expression of Lewis Y antigen.

MATERIALS

Solvents, Media, and Solutions

1. Xylene (histologic grade).
2. 70%, 95%, and 100% Ethanol.
3. Deionized water (dH_2O).
4. Tris buffer: 0.05 M Trizma base, 0.15 M NaCl, 0.01% Triton X-100, and dH_2O (pH 7.6). To make 4 L, add 24.23 g Trizma base, 35.06 g NaCl, 16 drops Triton X-100, and dH_2O (up to 4.0 L), then adjust pH to 7.6. Record date of preparation and store at room temperature. Use within 3 months.
5. Phosphate buffer saline: 137 mM NaCl, 2.7 mM KCl, 8.1 mM anhydrous Na_2HPO_4, 1.5 mM anhydrous KH_2PO_4, and dH_2O (pH 7.44). To make 1 L, add 8 g NaCl, 0.2 g KCl, 1.15 g anhydrous Na_2HPO_4, 0.2 g anhydrous KH_2PO_4, and dH_2O (up to 1 L), then adjust pH to 7.44. Record date of preparation and store at 4°C. Use within 3 months.
6. 3% Hydrogen peroxide (H_2O_2): Dilute commercial 30% H_2O_2 solution to 3% H_2O_2 in dH_2O (10-fold dilution). To make 100 ml 3% H_2O_2, add 10 ml 30% H_2O_2 to 90 ml dH_2O. Record preparation date and store at 4°C. Limit the use of 3% H_2O_2 to 1 week after preparation.
7. 1.0% Bovine serum albumin (BSA), 1.0 mM ethylenediamine tetraacetic acid (EDTA), 1.5 mM NaN_3, and PBS (pH 7.6) to make PBE buffer. To make 100 ml PBE, add 1.0g BSA, 0.0202g EDTA, 0.00975 g NaN_3, and PBS (up to 100 ml), then adjust pH to 7.6. Record date of preparation and store at 4°C. Use within 3 months. For better results, sprinkle the BSA around the beaker, add the other reagents, and leave at room temperature for ~1 hr. Add the stir bar after the BSA is completely dissolved. Mixing the reagents in this manner reduces the chance for the BSA to aggregate.
8. 1% Goat serum: Add 200 µl goat serum (Sigma-Aldrich Co., St. Louis, MO) to 20 ml PBE and filter through a 0.2 µ filter. Record date of preparation and store at 4°C. Use within 1 month.
9. Mayer's hematoxylin (Sigma-Aldrich Co.) filtered using Whatman paper. Record date of preparation and store at room temperature. Use within 3 months.
10. Permount (Fisher Scientific, Hampton, NH) mounting medium. Store at room temperature.

Antibodies and Detection Systems

11. Mouse monoclonal, anti-Lewis Y (BR-96 clone): This antibody was provided by M.B. Khazaeli, University of Alabama, Birmingham, AL. Store at 4°C. Commercial antibodies of the BR-96 clone are readily available.
12. Link and Labeling Secondary Detection Reagents: A multi-species (mouse/rabbit) detection system obtained from Signet Laboratories.
13. Diaminobenzidine (DAB) tetrachloride substrate: Prepared according to the manufacturer's instructions using a Liquid DAB concentrated substrate pack (Biogenex Co., Sam Ramon, CA). This solution should be prepared fresh for each use. Caution: DAB is a suspected carcinogen, so the use of gloves is recommended.

Other Materials and Equipment

14. Histoprep Marker (Fisher Scientific, Pittsburgh, PA).
15. Superfrost Plus slides (Fisher Scientific).
16. Glass staining dishes with slide insert and handle (Fisher Scientific).
17. PAP pen (hydrophobic slide marker) (Biogenex).
18. Staining racks (Fisher Scientific) and corresponding plastic containers.
19. Glass coverslip (the size of the coverslip should be large enough to cover entire tissue section on slide).
20. Humidity chamber.
21. Oven heated to 58°C.
22. Plastic hemostats for handling slides out of xylene prior to attaching coverslips to slides.
23. Microtome.
24. Light microscope equipped with brightfield optics (40X and 100X).

METHODS

Formalin-fixed and paraffin-embedded tissues of patients who underwent surgery for primary or recurrent OC were retrieved from hospitals throughout the southeastern region of the United States during 1993 to 2000 as part of a therapeutic trial for recurrent ovarian cancer at the University of Alabama at Birmingham. A total of 81 specimens, including 41 primary OCs and 408 metastatic lesions, were available for immunohistochemical evaluation. Among these cases, 48 (24 pairs) were matched primary and metastatic lesions from the same patients. The metastatic sites from which tissues were obtained included the omentum; serosa of the uterus, bowel, and urinary bladder; and peritoneum of the pelvic cavity. A multi-tissue paraffin block containing cases known to be positive for Lewis Y was used as a positive control.

Sectioning of Tissues and Slide Preparation

1. Label Superfrost Plus slides with solvent-resistant Histoprep marker.
2. Cut 5 µ thick tissue sections from paraffin blocks using a microtome.
3. Heat slides at 58°C for 1 hr to better adhere tissue sections to the slides.
4. Deparaffinize tissue sections by immersing slides in 3 changes of xylene for 5 min each.
5. Rehydrate tissue sections by immersing slides in 100%, 95%, and 70% ethanol, each for 5 min.
6. Place slides in a Tris buffer bath for 5 min.

Delineating Tissue Sections

1. After draining excess buffer off the slide, delineate the tissue section using a PAP pen (hydrophobic slide marker), but do not touch the specimen with the PAP pen.
2. Immediately after delineating the tissue, each slide should be placed on a slide rack and the entire tissue section should be covered with Tris buffer.
3. Repeat the procedure for delineating tissue sections with all slides.

Note: It is important that the tissue specimens are covered with Tris buffer so that the tissue section does not dry during this step.

Inactivation of Endogenous Peroxidase

1. Drain slides by gently tapping off excess liquid and carefully blotting around the tissue section.
2. Cover each tissue section with 3% H_2O_2 and incubate at room temperature for 5 min.
3. Wash the tissue sections with dH_2O.
4. Place slides in a Tris buffer bath. Wash the tissue sections in 2 changes of Tris buffer for 5 min each at room temperature.

Blocking Step: Reducing Nonspecific Staining

1. Drain slides by gently tapping off excess liquid and carefully blotting around the tissue section.
2. Place slides in humidified chambers (magnetic immunostaining trays).
3. Cover each tissue section with 1% goat serum and incubate at room temperature for 1 hr.

Primary Antibody Step

1. Prepare the primary antibody: mouse monoclonal, anti-Lewis Y (clone BR96) at a concentration of 20 µg/ml diluted in PBE buffer. This concentration (20 µg/ml) is very sensitive, and higher concentrations result in nonspecific staining. This solution should be made fresh.
2. Drain goat serum from slides by gently tapping off excess liquid and carefully blotting around the tissue section.
3. Place slides in humidified chambers (magnetic immunostaining trays).
4. Cover each tissue section with the primary antibody, anti-Lewis Y (clone BR-96), and incubate at room temperature for 1 hr.

Note: Negative controls remain in 1% goat serum and are also incubated for 1 hr at room temperature in a humidified chamber.

5. Wash the tissue sections with Tris buffer.

6. Place slides in a Tris buffer bath. Wash the tissue sections in 2 changes of Tris buffer for 5 min each at room temperature.

Link and Label Step

1. Drain slides by gently tapping off excess liquid and carefully blotting around the tissue section.
2. Place slides on slide rack.

Note: It is very important that the slide racks and humidity chambers are level on a flat surface.

3. Cover each tissue section with the linking reagent (anti-mouse/rabbit secondary antibody) and incubate for 10 min at room temperature.
4. Wash the tissue sections with Tris buffer.
5. Place slides in a Tris buffer bath. Wash the tissue sections in 2 changes of Tris buffer for 5 min each at room temperature.
6. Drain slides by gently tapping off excess liquid and carefully blotting around the tissue section.
7. Place slides on slide rack.
8. Cover each tissue section with the labeling reagent (avidin-horseradish peroxidase conjugate) and incubate for 5 min at room temperature.
9. Wash the tissue sections with Tris buffer.
10. Place slides in a Tris buffer bath. Wash the tissue sections in 2 changes of Tris buffer for 5 min each at room temperature.

Develop Color in Peroxidase Substrate

1. Drain slides by gently tapping off excess liquid and carefully blotting around the tissue section.
2. Place slides on slide rack.
3. Cover each tissue section with liquid DAB and incubate for 7 min at room temperature.

Note: The liquid DAB allows for the visualization of the antibody–antigen complex.

4. Wash the tissue sections with distilled water.
5. Place slides in a distilled water bath. Wash the tissue sections in 2 changes of d H_2O for 5 min each at room temperature.

Counterstaining

1. Immerse slides in hematoxylin for ~30 sec.

Note: The amount of time that tissue sections are exposed to hematoxylin varies depending on freshness of the hematoxylin.

2. Immediately place slides in a tap-water bath and rinse under running tap water for 4 min.

Note: The ions in the tap water allow for the stain to become a blue hue.

Mounting the Tissue Specimens

1. Dehydrate tissue sections by immersing slides in 70%, 95%, and 100% ethanol, each for 5 min.
2. Immerse slides in 3 changes of xylene for 5 min each.
3. Using a plastic hemostat, remove one slide at a time and drain excess xylene.

Note: Avoid allowing the tissue specimen to dry.

4. Attach a glass coverslip to each slide using Permount.

Note: Prepared slides can be stored at room temperature.

The slides were evaluated using a light microscope equipped with brightfield optics. Each slide was examined independently by at least two investigators to minimize bias. Both the intensity and extent of immunostaining were estimated. Staining present on the membrane and in the cytoplasm of the tissue specimen was evaluated. Positive staining was defined as the presence of staining at any intensity in 10% or more of the tumor cells. A semi-quantitative score was also calculated, as previously described (Manne *et al.*, 1997). Briefly, the proportion of immunostained cells at each intensity level was multiplied by the corresponding intensity (0–4). The products were then added to obtain an immunoscore. The resulting score ranged from 0 (no staining) to 4.

Statistical analyses were conducted on the matched cases. All significance tests were two-sided with $\alpha = 0.05$. The Wilcoxon Signed-Rank test was used to examine if there was a difference in the cytoplasmic and membranous immunoscores for Lewis Y antigen (BR-96) between the primary lesions and the metastatic lesions in the matched cases. Spearman correlation was used to determine if any associations existed among the immunoscores of the Lewis Y antigen (BR-96) in the matched cases. Similar statistical analyses were also conducted with all samples, primary and metastatic lesions of matched and unmatched cases.

RESULTS

These 41 primary OCs and 40 metastatic lesions were from 57 patients, including 24 patients with pairs of primary and matched metastatic lesions. The ages of the entire study population ranged from 32 to 88 years with a mean and median of 57 and 56.5, respectively. All except two patients were Caucasian, the remaining two patients were African American. Thirty-five patients were postmenopausal, and 10 were premenopausal; information on the menopausal status was not available for 12 patients. At the time of diagnosis 19 patients were receiving hormone replacement therapy.

Thirty-four (59%) tumors were International Federation of Gynecology and Obstetrics (FIGO) grade 3, 19 (33%) were FIGO grade 2, and 5 (8%) were FIGO grade 1. Of the cancer 60% were of serous subtype, followed by adenocarcinoma, not otherwise specified (20%), and endometrioid (10%). Mucinous and clear cell subtypes accounted for the remaining 10%. The majority (89%) of the patients had stage III/IV disease at the time of diagnosis.

The Spearman's Rank test was used to assess interobserver correlation between biomarker scores for Lewis Y antigen (BR-96) in both the cytoplasm and membrane. The results indicated that agreement was significantly strong for Lewis Y antigen (BR-96) cytoplasmic staining (correlation coefficient = 0.929, $p < 0.001$) and was also significantly strong for Lewis Y antigen (BR-96) membrane staining (correlation coefficient = 0.855, $p < 0.001$). As a result of the strong correlations, observer scores were subsequently averaged. All primary lesions demonstrated both positive cytoplasmic and membranous expression with Lewis Y antigen (BR-96), whereas cytoplasmic and membranous staining with Lewis Y antigen (BR-96) was absent in one and two of the metastatic lesions, respectively. No statistically significant differences were noted between primary and metastatic lesions for both cytoplasmic and membranous scores of Lewis Y antigen (BR-96). There was no statistically significant difference in the scores of Lewis Y antigen (BR-96) between matched primary and metastatic tumors. No discordant staining pattern between primary and matched metastatic disease was observed for expression of Lewis Y antigen (BR-96) (Figure 78).

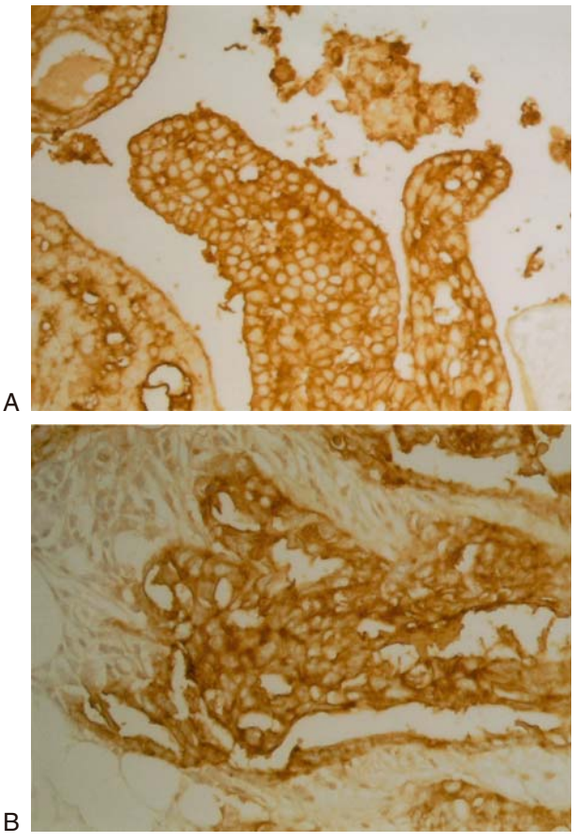

Figure 78. Strong membranous staining of Lewis-Y antigen (BR-96) in primary **(A)** and matched metastatic **(B)** ovarian carcinoma (100X).

DISCUSSION

The development of monoclonal antibodies that are selectively directed against antigens present on tumor cells has made targeted therapy possible. One approach consists of selective delivery of a therapeutic agent to tumor cells with minimum damage to normal tissue; another approach consists of stimulating host-immune response directed against the targeted antigen. Patients with advanced OC are ideal candidates for immunotherapy because the tumor is often confined to the peritoneal cavity and can be treated by the intraperitoneal route. In addition, the cells of the epithelial ovarian cancers express antigenic structures such as Lewis Y antigen that are often not shared by normal tissues. Clinical trials using both approaches have shown promising beneficial effects (Alvarez *et al.,* 1997; Epenetos *et al.,* 1987; Meredith *et al.,* 1996; Sabbatini *et al.,* 2000).

For the therapeutic agent to exert its anti-tumor activity in patients with cancer who are receiving immunotherapy, the monoclonal antibodies used for targeting must be able to selectively recognize and bind to the carcinoma cells. It should be noted that if a large proportion of cells express surface antigen and are distributed uniformly throughout a specific lesion, cells not expressing the surface antigen may be damaged by a bystander effect. Nevertheless, an important component for the overall success of immunotherapy is the extent of expression of the antigen within cells of an individual tumor. An ideal antigen for immunotherapy shows that the antigen is expressed uniformly and preferentially on the external surface of all cancer cells. Heterogeneity in the expression of an antigen within an individual tumor, and particularly between primary and metastatic lesions, may result in the failure of recognition and binding of the monoclonal antibodies to antigen-negative tumor cells; hence, the delivery of the therapeutic agents or host immunologic response will be inefficient for a proportion of tumor cells and the therapy will be less effective.

In the present study, none demonstrated discordant expression of Lewis Y antigen (BR-96) between paired

primary and metastatic lesions. We demonstrated that the expression of Lewis Y antigen was highly conserved between primary and metastatic lesions for the group with primary and matched metastatic lesions as well as for a larger population of unpaired primary and metastatic tumors. Our data indicated that there was little clonal divergence between primary and metastatic ovarian cancers for Lewis Y antigen.

Our findings are largely in accordance with the literature. In one study, no significant variation was noted from primary and various metastatic sites in the same patient in the immnuophenotypic expression of 19 monoclonal antibodies that reacted with cell-surface glycoproteins and carbohydrate antigens including Lewis Y antigens in 31 specimens from 12 patients with advanced OC (Rubin *et al.,* 1991). These authors also reported that intratumoral antigenic heterogeneity was seen, but this heterogeneity was much less consistent within the specimens from the same individual patient.

Studies using different biomarkers such as DNA (deoxyribonucleic acid) content, p53, $p185^{erbB-2}$, EGFR (epidermal growth factor receptor), and Ki67 have demonstrated conflicting findings. Using the same cohort of patients from the current study, we did not observe any significant difference in the expression of p53, $pl85^{erbB-2}$, CEA, and Tag 72 between primary and matched metastatic lesions (Chhieng *et al.,* 2003; Rodriguez-Burford *et al.,* 2004). Several investigators also reported no or minimal difference in the DNA content and the expression of multi-drug resistance-1 gene product (MDR1), p53, $pl85^{erbB-2}$, Ki67, CD44, and EGFR between primary and metastatic OCs (Goff *et al.,* 1998; Kaern *et al.,* 1994; Kimball *et al.,* 1997; Sakai *et al.,* 1999; Tewari *et al.,* 2000). However, some investigators have reported significant discrepancies in some of the same markers such as the DNA content, EGFR, microvessel density in terms of CD31, and Ki67 between primary and metastatic lesions (Goff *et al.,* 1998; Sakai *et al.,* 1999; Zangwill *et al.,* 1993).

Our study did not demonstrate any significant differences in the expression of Lewis Y antigen (BR-96) between primary and metastatic lesions. One possible reason is that Lewis Y antigen is not linked to the development of the metastasis of OCs. Another possible explanation is that the mutational events involving this marker in epithelial OCs occur early in the carcinogenesis of ovarian cancer, prior to the development of metastases. Therefore, studying the expression of Lewis Y antigen in early-stage tumors may be warranted. We did not correlate the expression of this marker with patient outcome because the majority of the patients (89.4%) had stage III or IV disease and all patients had failed conventional chemotherapy and therefore had dismal outcomes. We also did not correlate the results with pathologic parameters such as histologic grade and subtypes because the majority of our cases were skewed toward tumors of FIGO grade 3 and serous subtype.

Although IHC has been widely accepted as an ancillary technique in conjunction with routine histologic evaluation to offer additional diagnostic and prognostic information, immunohistochemical analysis of antigen expression is never truly quantitative, even when performed by the same laboratories, because IHC is a multistep procedure, many factors such as tissue fixation and processing, through antigen retrieval, to the selection of monoclonal antibodies and detection systems, to the final steps of evaluation and scoring, may play a part in influencing the results of IHC. To limit the impact of these variables, we have standardized our protocol to ensure the results are highly reproducible. However, if different protocols are used, different results could be seen.

In conclusion, our observations confirmed our hypothesis that the phenotypic expression of Lewis Y antigen (BR-96) is conserved between primary and metastatic lesions in both unpaired and paired populations. This finding supports the continued investigations of immunotherapies directed against Lewis Y antigen in the context of OC. Additionally, in instances when this antigen is selected as a target for immunotherapy, the status of expression of a particular tumor can be obtained by analyzing a sample from a primary lesion or one from a metastatic lesion. Similar experimental designs are warranted to determine if there is any divergence between primary and metastatic lesions in the expression of other biomarkers chosen to be the target for immunotherapy.

References

Alvarez, R.D., Partridge, E.E., Khazaeli, M.B., Plott, G., Austin, M., Kilgore, L., Russell, C.D., Liu, T., Grizzle, W.E., Schlom, J., LoBuglio, A.F., and Meredith, R.F. 1997. Intraperitoneal radioimmunotherapy of ovarian cancer with 177Lu-CC49: A phase I/II study. *Gynecol. Oncol. 65*:94–101.

American Cancer Society. 2002. *Cancer Facts and Figures: 2002*. Atlanta, GA: Americn Cancer Society.

Bombardieri, E., Ferrari, L., Spinelli, A., Maffioli, L., Seregni, E., and Buraggi, G. 1997. Radioimmunotherapy of ovarian cancer with radiolabelled monoclonal antibodies: biological basis, present status and future perspectives. *Anticancer Res. 17*:1719–1729.

Chatal, J.F., Saccavini, J.C., Gestin, J.F., Thedrez, P., Curtet, C., Kremer, M., Guerreau, D., Nolibe, D., Fumoleau, P., and Guillard, Y. 1989. Biodistribution of indium-111-labeled OC 125 monoclonal antibody intraperitoneally injected into patients operated on for ovarian carcinomas. *Cancer Res. 49*:3087–3094.

Chhieng, D.C., Rodriguez-Burford, C., Talley, L.I., Sviglin, H., Stockard, C.R., Kleinberg, M.J., Barnes, M.N., Partridge, E.E., Khazaeli, M.B., and Grizzle, W.E. 2003. Expression of CEA,

Tag-72, and Lewis-Y antigen in primary and metastatic lesions of ovarian carcinoma. *Hum. Pathol. 34*:1016–1021.

Colcher, D., Esteban, J., Carrasquillo, J.A., Sugarbaker, P., Reynolds, J.C., Bryant, G., Larson, S.M., and Schlom, J. 1987. Complementation of intracavitary and intravenous administration of a monoclonal antibody (B72.3) in patients with carcinoma. *Cancer Res. 47*:4218–4224.

Dillman, R.O. 2001. Monoclonal antibodies in the treatment of malignancy: basic concepts and recent developments. *Cancer Invest. 19*:833–841.

Epenetos, A.A., Courtenay-Luck, N., Dhokia, B., Snook, D., Hooker, G., Lavender, J.P., Hemmingway, A., Carr, D., Paraharalambous, M., and Bosslet, K. 1987. Antibody-guided irradiation of hepatic metastases using intrahepatically administered radiolabelled anti-CEA antibodies with simultaneous and reversible hepatic blood flow stasis using biodegradable starch microspheres. *Nucl. Med. Commun. 8*:1047–1058.

Goff, B.A., Ries, J.A., Els, L.P., Coltrera, M.D., and Gown, A.M. 1998. Immunophenotype of ovarian cancer as predictor of clinical outcome: evaluation at primary surgery and second-look procedure. *Gynecol. Oncol. 70*:378–385.

Kaern, J., Trope, C.G., Kristensen, G.B., and Pettersen, E.O. 1994. Flow cytometric DNA ploidy and S-phase heterogeneity in advanced ovarian carcinoma. *Cancer 73*:1870–1877.

Kaye, S.B. 2001. Future directions for the management of ovarian cancer. *Eur. J. Cancer 37*:S19–23.

Kimball, R.E., Schlaerth, J.B., Kute, T.E., Schlaerth, A.C., Santoso, J., Ballon, S.C., and Spirtos, N.M. 1997. Flow cytometric analysis of lymph node metastases in advanced ovarian cancer: clinical and biologic significance. *Am. J. Obstet. Gynecol. 176*:1319–1326; discussion 1326–1327.

Livingston, P.O., and Ragupathi, G. 1997. Carbohydrate vaccines that induce antibodies against cancer. II. Previous experience and future plans. *Cancer Immunol. Immunoth. 45*:10–19.

Manne, U., Myers, R.B., Moron, C., Poczatek, R.B., Dillard, S., Weiss, H., Brown, D., Srivastava, S., and Grizzle, W.E. 1997. Prognostic significance of Bcl-2 expression and p53 nuclear accumulation in colorectal adenocarcinoma. *Int. J. Cancer 74*:346–358.

Meredith, R.F., Khazaeli, M.B., Plott, W.E., Grizzle, W.E., Liu, T., Schlom, J., Russell, C.D., Wheeler, R.H., and LoBuglio, A.F. 1996. Phase II study of dual 131 I-labeled monoclonal antibody therapy with interferon in patients with metastatic colorectal cancer. *Clin. Cancer Res. 2*:1811–1818.

Murray, J.L. 2000. Monoclonal antibody treatment of solid tumors: a coming of age. *Semin. Oncol. 27*:64–70; discussion 92–100.

Perez, R.P., Godwin, A.K., Hamilton, T.C., and Ozols, R.F. 1991. Ovarian cancer biology. *Semin. Oncol. 18*:186–204.

Press, O.W., and Rasey, J. 2000. Principles of radioimmunotherapy for hematologists and oncologists. *Semin. Oncol. 27*:62–73.

Rodriguez-Burford, C., Chhieng, D.C., Stockard, C.R., Kleinberg, M.J., Barnes, M.N., Partridge, E.E., Weiss, H.L., and Grizzle, W.E. 2004. p53 and erb-2 are not associated in matched cases of primary and metastatic ovarian carcinomas. *Dis. Markers 19*:11–17.

Rubin, S.C., Finstad, C.L., Hoskins, W.J., Provencher, D., Federici, M.G., Lloyd, K.O., and Lewis, J.L. Jr. 1991. Analysis of antigen expression at multiple tumor sites in epithelial ovarian cancer. *Am. J. Obstet. Gynecol. 164*:558–563.

Sabbatini, P.J., Kudryashov, V., Ragupathi, G., Danishefsky, S.J., Livingston, P.O., Bornmann, W., Spassova, M., Zatorski, A., Spriggs, D., Aghajanian, C., Soignet, S., Peyton, M., O'Flaherty, C., Curtin, J., and Lloyd, K.O. 2000. Immunization of ovarian cancer patients with a synthetic Lewis(y)-protein conjugate vaccine: a phase 1 trial. *Int. J. Cancer 87*:79–85.

Sakai, K., Kaku, T., Kamura, T., Kinukawa, N., Amada, S., Shigematsu, T., Hirakawa, T., Kobayashi, H., Ariyoshi, K., and Nakano, H. 1999. Comparison of p53, Ki-67, and CD44v6 expression between primary and matched metastatic lesions in ovarian cancer. *Gynecol. Oncol. 72*:360–366.

Stewart, J.S., Hird, V., Snook, D., Sullivan, M., Myers, M.J., and Epenetos, A.A. 1988. Intraperitoneal 131 I- and 90Y-labelled monoclonal antibodies for ovarian cancer: pharmacokinetics and normal tissue dosimetry. *Int. J. Cancer Suppl. 3*:71–76.

Tewari, K.S., Kyshtoobayeva, A.S., Mehta, R.S., Yu, I.R., Burger, R.A., DiSaia, P.J., and Fruehauf, J.P. 2000. Biomarker conservation in primary and metastatic epithelial ovarian cancer. *Gynecol. Oncol. 78*:130–136.

Verhaar-Langereis, M.J., Zonnenberg, B.A., de Klerk, J.M., and Blijham, G.H. 2000. Radioimmunodiagnosis and therapy. *Cancer Treat. Rev. 26*:3–10.

Ward, B.G., Mather, S.J., Hawkins, L.R., Crowther, M.E., Shepherd, J.H., Granowska, M., Britton, K.E., and Slevin, M.L. 1987. Localization of radioiodine conjugated to the monoclonal antibody HMFG2 in human ovarian carcinoma: assessment of intravenous and intraperitoneal routes of administration. *Cancer Res. 47*:4719–4723.

Yin, B.V., Finstad, C.L., Kitamura, K., Federici, M.G., Welshinger, M., Kudryashov, V., Hoskins, W.J., Welt, S., and Lloyd, K.O. 1996. Serological and immunochemical analysis of Lewis Y (Ley) blood group antigen expression in epithelial ovarian cancer. *Int. J. Cancer 65*:406–412.

Zangwill, B.C., Balsara, G., Dunton, C., Varello, M., Rebane, B.A., Hernandez, E., and Atkinson, B.F. 1993. Ovarian carcinoma heterogeneity as demonstrated by DNA ploidy. *Cancer 71*:2261–2267.

This Page Intentionally Left Blank

20

Role of Immunohistochemical Expression of ETS-1 Factor in Ovarian Carcinoma

Jiro Fujimoto, Syed Mahfuzul Alam, Israt Jahan, Wenshu Sun, Hideki Sakaguchi, Hiroshi Toyoki, Eriko Sato, and Teruhiko Tamaya

Introduction

Angiogenesis is essential for development, growth, and advancement of solid tumors. The angiogenic factors vascular endothelial growth factor (VEGF) (Fujimoto *et al.,* 1998c,d, 1999c, 2001), basic fibroblast growth factor (bFGF) (Fujimoto *et al.,* 1997a,b), platelet-derived endothelial cell growth factor (PD-ECGF) identified with thymidine phosphorylase (TP) (Fujimoto *et al.,* 1998a,b, 1999a,b, 2000b), and interleukin (IL)-8 (Fujimoto *et al.,* 2000a, 2002a) are involved in angiogenesis, in ovarian cancers, and other gynecologic cancers. The factor bFGF is expressed in both cancer and interstitial cells of ovarian cancers, and its levels correlate with clinical stage but not with patient prognosis (Fujimoto *et al.,* 1997b). The factor PD-ECGF is dominantly expressed in interstitial cells of ovarian cancers, and its remarkably high level correlates with poor patient prognosis (Fujimoto *et al.,* 1998a). The factor VEGF, particularly $VEGF_{165}$ isomer, is dominantly expressed in cancer cells of primary ovarian cancers, and its levels correlate with patient prognosis, regardless of histopathologic findings (Fujimoto *et al.,* 1998d, 2001). Furthermore, the cases with higher VEGF levels in peritoneal disseminated lesions than in the primary tumors had poor prognosis (Fujimoto *et al.,* 2001).

During angiogenesis, ETS-1 is strongly expressed in vascular endothelial cells and in the adjacent interstitial cells (Wernert *et al.,* 1992). Once angiogenesis has ended, ETS-1 expression is down-regulated distinctly (Maroulakou *et al.,* 1994). The representative angiogenic factors VEGF and bFGF immediately induce ETS-1 expression in the early stage of angiogenesis, while the inhibition of ETS-1 expression leads to suppression of angiogenesis (Iwasaka *et al.,* 1996; Tanaka *et al.,* 1999). The proteases urokinase type plasminogen activator (uPA), matrix metalloprotease (MMP)-1, MMP-3, and MMP-9 conserve an ETS-binding motif. Transcription factor ETS-1 converts vascular endothelial cells to angiogenic phenotypes by inducing proteases uPA, MMP-1, MMP-3, and MMP-9 and integrin $\beta 3$ gene expression (Oda *et al.,* 1999).

The proto-oncogene ETS-1 expressed in various cancer cells of gastric, pancreatic, esophageal, and hepatocellular and cholangiocellular carcinomas, thyroid and astrocytic tumors, and ovarian and uterine cancers works on tumor progression as a proto-oncogene (Davidson *et al.,* 2001; Ito *et al.,* 1998, 2000a,b; Kitange *et al.,*

Handbook of Immunohistochemistry and *in situ* Hybridization of Human Carcinomas, Volume 4: Molecular Genetics, Gastrointestinal Carcinoma, and Ovarian Carcinoma

1999a; Nakayama *et al.,* 1996, 1999; Saeki *et al.,* 2000). The proto-oncogene ETS-1 is up-regulated and involved in the overexpression of MMP-7 in hepatocellular carcinoma cells (Ozaki *et al.,* 2000) and positively regulates the expression of uPA in breast cancer, glioma, astrocytoma, and meningioma cells related to invasive potential and phenotypes (Kitange *et al.,* 1999a,b, 2000; Nakada *et al.,* 1999; Watanabe *et al.,* 1998). Expression of ETS-1 is induced by bFGF in glioma cells related to invasive potential (Kitange *et al.,* 1999b) and by VEGF in astrocytomas related to angiogenesis (Valter *et al.,* 1999). Furthermore, overexpressed ETS-1 is recognized as an angiogenic mediator in gastric, oral squamous cell, and uterine carcinomas (Fujimoto *et al.,* 2002b,c; Pande *et al.,* 1999; Tsutsumi *et al.,* 2000). This status prompted us to investigate the clinical significance of ETS-1 expression in the primary tumor and peritoneal disseminated lesions of ovarian cancers.

MATERIALS

1. Xylene.
2. 100%, 90%, and 70% Ethanol.
3. Phosphate buffer saline (PBS).
4. 10 mM Citrate buffer.
5. H_2O_2 Solution: Make 3% H_2O_2 in PBS before use.
6. Skim-milk solution: 0.8% (12 g) skim milk in 150 ml PBS.
7. First antibody: Rabbit anti-human ETS-1 (C-20, Santa Cruz Biotechnology, Santa Cruz, CA).
8. Anibody dilution solution: 0.1% bovine serum albumin in PBS.
9. Second antibody: Biotin-labeled affinity-isolated goat anti-rabbit immunoglobulin in PBS (Dako, Dako, Carpinteria, CA).
10. Streptavidin solution: Streptavidin-conjugated to horseradish peroxidase in PBS (Dako).
11. Diaminobenzidine (DAB) solution: 45 mg 3, 3′-DAB in 150 ml 50 mM Tris-HCl with 50 μ 1 H_2O_2.
12. 0.2% Methyl green.
13. Glycerol.

METHODS

Immunohistochemical Staining for ETS-1

1. Cut 3-µm sections of formalin-fixed and paraffin-embedded tissues of primary tumor and peritoneal disseminated lesion of ovarian cancers with a microtome and dry the sections overnight at 37°C on a silanized slide.

2. To deparaffinize, soak in 100% xylene for 15 min at room temperature 2×.

3. To rehydrate, soak in 100% ethanol for 10 min, 90% ethanol for 10 min, 70% ethanol for 10 min, and PBS for 5 min at room temperature.

4. To emphasize recognition for ETS-1 antigen, soak in citrate buffer (10 mM), microwave at 100°C for 10 min, and cool for a few minutes.

5. To block endogenous peroxidase, soak in H_2O_2 solution for 20 min at room temperature.

6. To block nonspecific staining, rinse with PBS for 10 min, soak in skim-milk solution for a few seconds, and rinse with PBS for a few seconds at room temperature.

7. To react with the first antibody, prepare rabbit anti-human ETS-1 at dilutions of 1:2000 with antibody dilution solution, and incubate with the diluted antibody overnight at 4°C.

8. Rinse with PBS for 10 min, soak in skim-milk solution for a few sec, and rinse with PBS for a few sec at room temperature.

9. To react with the second antibody, biotin-labeled affinity-isolated goat anti-rabbit immunoglobulin, after tapping off the excess fluid, wipe carefully, and incubate with several drops of the second antibody for 10 min at room temperature.

10. Rinse with PBS for 10 min, soak in skim-milk solution for a few seconds, and rinse with PBS for a few seconds at room temperature.

11. To react with streptavidin, after tapping off the excess fluid, wipe carefully, and incubate with several drops of the streptavidin solution for 10 min at room temperature.

12. Rinse with PBS for 10 min, soak in skim-milk solution for a few sec, and rinse with PBS for a few sec at room temperature.

13. To get brown color, soak in DAB solution. After the brown color comes up sufficiently (up to 20 min), withdraw from DAB solution and rinse with PBS for few seconds at room temperature.

14. To stain background, soak in 0.2% methyl green for 15 min, and rinse with running water at room temperature.

15. To dehydrate, soak in 70% ethanol for a few seconds 2×, 90% ethanol for few seconds 2×, 100% ethanol for few seconds 2×, xylene for 5 min 2×, and xylene for 10 min at room temperature.

16. To prepare the slide to see under a microscope, add a few drops of glycerol over the slide, and cover it with micro coverglass.

17. To evaluate immunohistochemical staining for ETS-1 antigen, histoscore, a histochemical score, (histoscore), is calculated by the formula: Σ (i + 1) X Pi, in which i = cellular staining intensity (range 1–4,

0 indicates no staining) and Pi = percentage of stained cells (McCarty *et al.,* 1985).

RESULTS AND DISCUSSION

The proto-oncogene ETS-1 was distributed in cytoplasm of the cancer cells and in nucleus of vascular endothelial cells (Khatun *et al.,* 2003) as shown in Figure 79. Histoscores of ETS-1 in the endothelial cells correlated with microvessel counts, regardless of histopathologic type (Fujimoto *et al.,* 2004; Khatun *et al.,* 2003). In primary tumor, ETS-1 histoscores increased with advancing disease stage of ovarian cancers, regardless of histopathologic type. In the patients who underwent curative resection, which produced macroscopically disease-free status, the 24-month survival rate of the 30 patients with high ETS-1 was 30%, whereas that of the other 30 patients with low ETS-1 was 70% (Khatun *et al.,* 2003). The proto-oncogene ETS-1 was expressed in stromal cells and tumor cells of ovarian cancers, and ETS-1 is thus a novel prognostic marker in advanced-stage ovarian cancers. In detail, ETS-1 expression in both tumor and stroma correlated with poor survival (Davidson *et al.,* 2001). However, they did not track down the reason. Higher ETS-1 expression in stromal cells than in tumor cells can contribute to greater advancement of ovarian cancer and can be recognized as a prognostic marker. Generally, distinct ETS-1 expression in vascular endothelial cells has been associated with accelerated angiogenesis (Maroulakou *et al.,* 1994; Wernert *et al.,* 1992). The proto-oncogene ETS-1 is considered to be activated as a direct angiogenic mediator for the initiation and maintenance stages of angiogenesis and an excellent indicator of poor patient prognosis in ovarian cancers. Therefore, ETS-1 expressed in stromal cells, especially the vascular endothelial cells, might contribute to advancement of ovarian cancers as an angiogenic mediator and lead to poor patient prognosis. Any ETS-1 expressed in cancer cells is likely to be indirectly associated with angiogenesis as a proto-oncogene.

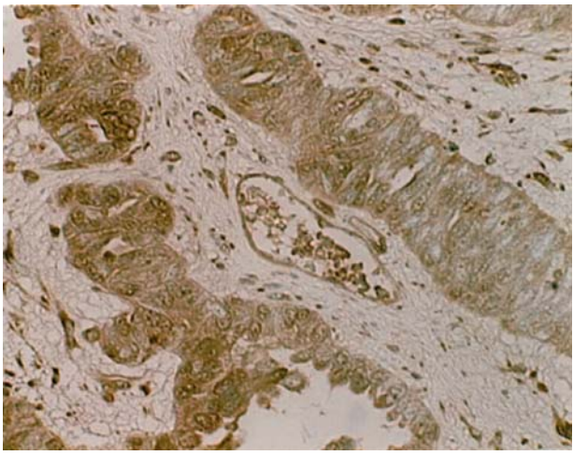

Figure 79. Immunohistochemical staining for ETS-1 in ovarian carcinoma.

Furthermore, no cases revealed decreased ETS-1 histoscores in cancer cells and vascular endothelial cells from the primary tumor to the peritoneal metastatic lesion. Increased ETS-1 histoscores in the vascular endothelial cells from the primary tumor to the metastatic lesion was found in 20 of the 30 cases. Increased ETS-1 histoscores in the cancer cells from the primary tumor to the peritoneal disseminated lesion was found in only 4 of the 30 cases. The survival rate of patients with increased ETS-1 histoscores in the vascular endothelial cell was poorer than that of patients with no change in those from the primary tumor to the peritoneal disseminated lesions (Fujimoto *et al.,* 2004). The proto-oncogene ETS-1 might be associated with peritoneal disseminated metastasis as the most important pathway of ovarian cancer metastasis; as an angiogenic mediator, a more reliable indicator for patient prognosis; and as an oncogene product to activate tumor invasion.

Histoscores of ETS-1 correlated with VEGF levels, regardless of histopathologic type (Khatun *et al.,* 2003). The factor VEGF has been shown to induce ETS-1 expression in vascular endothelial cell lines (Iwasaka *et al.,* 1996). It is produced from cancer cells and moves to the stromal cells, especially to the VEGF receptor sites on the vascular endothelial cells in ovarian cancers (Fujimoto *et al.,* 2001). In the cancer cells, VEGF might induce ETS-1 expression and acts as an oncogene. However, its function is not clear yet. In the vascular endothelial cells, VEGF from the cancer cells might induce ETS-1 expression, and ETS-1 acts as an angiogenic mediator in ovarian cancers. This indicates that ETS-1 is an angiogenic mediator linked to VEGF and preserves angiogenic switching in the linkage to angiogenic factors to maintain advancement.

Inhibition of specifically expressed angiogenic factors is a novel strategy for suppression of development, growth, and especially advancement of solid tumors. Even if the main angiogenic factors can be suppressed by some agents, angiogenesis might be suppressed only transiently, which could lead to temporary suppression of tumor growth and secondary spreading. In such a scenario, other angiogenic factors would be induced, and would link to ETS-1 in the recruitment for alternate angiogenic activation, as a type of tolerance to angiogenic inhibitors. Therefore, suppression of the major angiogenic factors along with suppression of ETS-1

recruitment might be more effective as an anti-angiogenic therapy than mere suppression of major angiogenic factors. A specific inhibitor for ETS-1, transdominant mutant ETS-1, has already been shown to act as a dominant negative molecule and can be used as an efficient tool for angiogenic inhibition (Nakano *et al.,* 2000).

In conclusion, ETS-1, a proto-oncogene and a transcription factor for angiogenesis, is an angiogenic mediator linked to VEGF and preserves angiogenic switching in the linkage to angiogenic factors to maintain advancement, especially peritoneal disseminated metastasis, and a prognostic factor for advanced ovarian carcinomas.

References

Davidson, B., Reich, R., Goldberg, I., Gotlieb, W.H., Kopolovic, J., Berner, A., Ben-Baruch, G., Bryne, M., and Nesland, J.M. 2001. ETS-1 messenger RNA expression is a novel marker of poor survival in ovarian carcinoma. *Clin. Cancer Res. 7*:551–557.

Fujimoto, J., Ichigo, S., Hori, M., Hirose, R., Sakaguchi, H., and Tamaya, T. 1997a. Expression of basic fibroblast growth factor and its mRNA in advanced uterine cervical cancers. *Cancer Lett. 111*:21–26.

Fujimoto, J., Ichigo, S., Hori, M., Hirose, R., Sakaguchi, H., and Tamaya, T. 1997b. Expression of basic fibroblast growth factor and its mRNA in advanced ovarian cancers. *Eur. J. Gynaecol. Oncol. 18*:349–352.

Fujimoto, J., Ichigo, S., Sakaguchi, H., Hirose, R., and Tamaya, T. 1998a. Expression of platelet-derived endothelial cell growth factor (PD-ECGF) and its mRNA in ovarian cancers. *Cancer Lett. 126*:83–88.

Fujimoto, J., Ichigo, S., Sakaguchi, H., Hirose, R., and Tamaya, T. 1998b. Expression of platelet-derived endothelial cell growth factor (PD-ECGF) and its mRNA in uterine endometrial cancers. *Cancer Lett. 130*:115–120.

Fujimoto, J., Ichigo, S., Hirose, R., Sakaguchi, H., and Tamaya, T. 1998c. Expressions of vascular endothelial growth factor (VEGF) and its mRNA in uterine endometrial cancers. *Cancer Lett. 134*:15–22.

Fujimoto, J., Sakaguchi, H., Hirose, R., Ichigo, S., and Tamaya, T. 1998d. Biologic implications of the expression of vascular endothelial growth factor subtypes in ovarian carcinoma. *Cancer 83*:2528–2533.

Fujimoto, J., Sakaguchi, H., Hirose, R., Wen, H., and Tamaya, T. 1999a. Clinical implication of expression of platelet-derived endothelial cell growth factor (PD-ECGF) in metastatic lesions of uterine cervical cancers. *Cancer Res. 59*:3041–3044.

Fujimoto, J., Sakaguchi, H., Hiose, R., Ichigo, S., and Tamaya, T. 1999b. Expression of platelet-derived endothelial cell growth factor (PD-ECGF) in uterine cervical cancers. *Br. J. Cancer 79*:1249–1254.

Fujimoto, J., Sakaguchi, H., Hirose, R., Ichigo, S., and Tamaya, T. 1999c. Expression of vascular endothelial growth factor (VEGF) and its mRNA in uterine cervical cancers. *Br. J. Cancer 80*:827–833.

Fujimoto, J., Sakaguchi, H., Aoki, I., and Tamaya, T. 2000a. Clinical implications of expression of interleukin 8 related to angiogenesis in uterine cervical cancers. *Cancer Res. 60*: 2632–2635.

Fujimoto, J., Sakaguchi, H., Aoki, I., and Tamaya, T. 2000b. The value of platelet-derived endothelial cell growth factor as a novel predictor of advancement of uterine cervical cancers. *Cancer Res. 60*:3662–3665.

Fujimoto, J., Sakaguchi, H., Aoki, I., Khatun, S., and Tamaya, T. 2001. Clinical implications of expression of vascular endothelial growth factor in metastatic lesions of ovarian cancers. *Br. J. Cancer 85*:313–316.

Fujimoto, J., Aoki, I., Khatun, S., Toyoki, H., and Tamaya, T. 2002a. Clinical implications of expression of interleukin-8 related to myometrial invasion with angiogenesis in uterine endometrial cancers. *Ann. Oncol. 13*:430–434.

Fujimoto, J., Aoki, L., Toyoki, H., Khatun, S., and Tamaya, T. 2002b. Clinical implications of expression of ETS-1 related to angiogenesis in uterine endometrial cancers. *Ann. Oncol. 13*: 1598–1604.

Fujimoto, J., Aoki, I., Toyoki, H., Khatun, S., and Tamaya, T. 2002c. Clinical implications of expression of ETS-1 related to angiogenesis in uterine cervical cancers. *Ann. Oncol. 13*: 1605–1611.

Fujimoto, J., Aoki, I., Toyoki, H., Khatun, S., Sato, E., Sakaguchi, H., and Tamaya, T. 2004. Clinical implications of expression of ETS-1 related to angiogenesis in metastatic lesions of ovarian cancers. *Oncology 66*:420–428.

Ito, T., Nakayama, T., Ito, M., Naito, S., Kanematsu, T., and Sekine, I. 1998. Expression of the ETS-1 proto-oncogene in human pancreatic carcinoma. *Mod. Pathol. 11*:209–215.

Ito, Y., Miyoshi, E., Takeda, T., Sakon, M., Noda, K., Tsujimoto, M., Monden, M., Taniguchi, N., and Matsuura, N. 2000a. Expression and possible role of ETS-1 in hepatocellular carcinoma. *Am. J. Clin. Pathol. 114*:719–725.

Ito, Y., Miyoshi, E., Takeda, T., Sakon, M., Tsujimoto, M., Yokosaki, Y., Monden, M., and Matsuura, N. 2000b. ETS-1 expression in extrahepatic bile duct carcinoma and cholangiocelluar carcinoma. *Oncology 58*:248–252.

Iwasaka, C., Tanaka, K., Abe, M., and Sato, Y. 1996. ETS-1 regulates angiogenesis by inducing the expression of urokinase-type plasminogen activator and matrix metalloproteinase-1 and the migration of vascular endothelial cells. *J. Cell Physiol. 169*: 522–531.

Khatun, S., Fujimoto, J., Toyoki, H., and Tamaya, T. 2003. Clinical implications of expression of ETS-1 in relation to angiogenesis in ovarian cancers. *Cancer Sci. 94*:769–773.

Kitange, G., Kishikawa, M., Nakayama, T., Naito, S., Iseki, M., and Shibata, S. 1999a. Expression of the ETS-1 pro-oncogene correlates with malignant potential in human astrocytic tumors. *Mod. Pathol. 12*:618–626.

Kitange, G., Shibata, S., Tokunaga, Y., Yagi, N., Yasunaga, A., Kishikawa, M., and Naito, S. 1999b. ETS-1 transcription factor-mediated urokinase-type plasminogen activator expression and invasion in glioma cells stimulated by serum and basic fibroblast growth factors. *Lab. Invest. 79*:407–416.

Kitange, G., Tsunoda, K., Anda, T., Nakamura, S., Yasunaga, A., Naito, S., and Shibata, S. 2000. Immunohistochemical expression of ETS-1 transcription factor and the urokinase-type plasminogen activator is correlated with the malignant and invasive potential in meningiomas. *Cancer 89*:2292–2300.

Maroulakou, I.G., Papas, T.S., and Green, J.E. 1994. Differential expression of ETS-1 and ETS-2 proto-oncogenes during murine embryogenesis. *Oncogene 9*:1551–1565.

McCarty, K.S. Jr., Miller, L.S., Cox, E.B., Konrath, J., and McCarty, K.S. Sr. 1985. Estrogen receptor analyses. Correlation of biochemical and immunohistochemical methods using monoclonal antireceptor antibodies. *Arch. Pathol. Lab. Med. 109*: 716–721.

Nakada, M., Yamashita, J., Okada, Y., and Sato, H. 1999. ETS-1 positively regulates expression of urokinase-type plasminogen activator (uPA) and invasiveness of astrocytic tumors. *J. Neuropathol. Exp. Neurol. 58*:329–334.

Nakano, T., Abe, M., Tanaka, K., Shineha, R., Satomi, S., and Sato, T. 2000. Angiogenesis inhibition by transdominant mutant ETS-1. *J. Cell Physiol. 184*:255–262.

Nakayama, T., Ito, M., Ohtsuru, A., Naito, S., Nakashima, M., Fagin, J.A., Yamashita, S., and Sekine, I. 1996. Expression of the ETS-1 proto-oncogene in human gastric carcinoma: correlation with tumor invasion. *Am. J. Pathol. 149*:1931–1939.

Nakayama, T., Ito, M., Ohtsuru, A., Naito, S., Nakashima, M., and Sekine, I. 1999. Expression of the ETS-1 proto-oncogene in human thyroid tumor. *Mod. Pathol. 12*:61–68.

Oda, N., Abe, M., and Sato, Y. 1999. ETS-1 converts endothelial cells to the angiogenic phenotype by inducing the expression of matrix metalloproteinases and integrin β3. *J. Cell Physiol. 178*:121–132.

Ozaki, I., Mizuta, T., Zhao, G., Yotsumoto, H., Ham, T., Kajihara, S., Hisatomi, A., Sakai, T., and Yamamoto, K. 2000. Involvement of the ETS-1 gene in overexpression of matrilysin in human hepatocellular carcinoma. *Cancer Res. 60*:6519–6525.

Pande, P., Mathur, M., Shukla, N.K., and Ralhan, R. 1999. ETS-1: a plausible marker of invasive potential and lymph node metastasis in human oral squamous cell carcinomas. *J. Pathol. 189*: 40–45.

Saeki, H., Kuwano, H., Kawaguchi, H., Ohno, S., and Sugimachi, K. 2000. Expression of ETS-1 transcription factor is correlated with penetrating tumor progression in patients with squamous cell carcinoma of the esophagus. *Cancer 89*:1670–1676.

Tanaka, K., Abe, M., and Sato, Y. 1999. Roles of extracellular signal-regulated kinase 1/2 and p38 mitogen-activated protein kinase in the signal transduction of basic fibroblast growth factor in endothelial cells during angiogenesis. *Jpn. J. Cancer Res. 90*:647–654.

Tsutsumi, S., Kuwano, H., Asao, T., Nagashima, K., Shimura, T., and Mochiki, E. 2000. Expression of ETS-1 angiogenesis-related protein in gastric cancer. *Cancer Lett. 160*:45–50.

Valter, M.M., Hugel, A., Huang, H.J., Cavenee, W.K., Wiestler, O.D., Pietsch, T., and Wernert, N. 1999. Expression of the ETS-1 transcription factor in human astrocytomas is associated with FMS-like tyrosine kinase-1 (FLT-1)/vascular endothelial growth factor receptor-1 synthesis and neoangiogenesis. *Cancer Res. 59*:5608–5614.

Watanabe, T., Yoshida, K., Shindoh, M., Kaya, M., Fujikawa, K., Sato, H., Seiki, M., Ishii, S., and Fujinaga, K. 1998. The ETS-1 and ETS-2 transcription factors activate the promoters for invasion-associated urokinase and collagenase genes in response to epidermal growth factor. *Int. J. Cancer 77*: 128–137.

Wernert, N., Raes, M.B., Lassalle, P., Dehouck, M.P., Gosselin, B., Vandenbunder, B., and Stehelin, D. 1992. c-ets1 proto-oncogene is a transcription factor expressed in endothelial cells during tumor vascularization and other forms of angiogenesis in humans. *Am. J. Pathol. 140*: 119–127.

This Page Intentionally Left Blank

21

Role of MCL-1 in Ovarian Carcinoma

Kazushi Shigemasa

Introduction

In recent years, many of the genes involved in apoptosis have been identified and cloned (Korsmeyer, 1999; Kroemer, 1997). Some of the most important regulators of apoptosis are BCL-2 and its related proteins, MCL-1, BCL-XL, and BAX. BCL-2, MCL-1, and BCL-XL all function as inhibitors of cell death, whereas BAX functions as a cell-death promoter. BCL-2 family members appear to regulate apoptosis by forming either homodimers or heterodimers with each other. In light of its anti-apoptotic function, high BCL-2 expression levels in cancer cells might be expected to prolong cell survival, allowing the development and progression of tumor cells and ultimately resulting in poor patient survival rates. In fact, BCL-2 expression is reported to be a poor prognostic marker in certain tumor types, including prostate cancer, leukemia, and high-grade lymphoma (Campos *et al.,* 1993; McDonnell *et al.,* 1992; Yunis *et al.,* 1989).

However, several earlier studies have shown that high BCL-2 expression levels actually correlate with improved survival in patients with lung, breast, or ovarian cancer, suggesting that other death checkpoint regulators, such as BAX, MCL-1, and BCL-XL, may interfere with BCL-2 functioning in certain tumor types (Henriksen *et al.,* 1995; Herod *et al.,* 1996; Leek *et al.,* 1994; Pezzella *et al.,* 1993). Regulation of apoptosis in tumor cells therefore appears to be a highly complicated process involving a cascade of events requiring both pro-apoptotic and anti-apoptotic factors. Several earlier studies revealed a striking association between increased MCL-1 expression levels and a poor prognosis in cancers. Lomo *et al.* (1996) observed a correlation between cell survival and MCL-1 expression in peripheral blood B cells. BCL-2 expression levels were unaltered in this system, suggesting the possible involvement of MCL-1 rather than BCL-2 in the regulation of apoptosis in these cells. Rieger *et al.* (1998) reported that MCL-1 protein expression was associated with early tumor recurrence and shorter survival in patients with malignant glioma, whereas there was no prominent association with the expression of p53, RB (retinoblastoma), BCL-2, BCL-X, or BAX.

Because ovarian cancer is often asymptomatic in its early stages, the majority of patients with ovarian cancer are diagnosed at an advanced clinical stage. Despite recent advances in surgical treatment and chemotherapy, the 5-year survival rate for patients with ovarian cancer has remained at less than 50% for the past 30 years (Parker *et al.,* 1996). It is therefore important to elucidate the mechanisms involved in the development and progression of ovarian cancer. Although the majority of genetic alterations involved

Handbook of Immunohistochemistry and *in situ* Hybridization of Human Carcinomas, Volume 4: Molecular Genetics, Gastrointestinal Carcinoma, and Ovarian Carcinoma

in ovarian carcinomas (OCs) remain largely unknown, decreased cell death is believed to be a major contributor to pathologic cell accumulation in ovarian neoplasm.

The aim of this study was to examine the potential role of MCL-1 and other BCL-2 family members in the development and progression of ovarian cancer. The expression of MCL-1 protein in ovarian tumors was investigated immunohistochemically. Messenger ribonucleic acid (mRNA) expression levels of the proapoptotic factor BAX and anti-apoptotic factors, BCL-2, MCL-1, and BCL-XL, were compared in ovarian tumors and normal ovaries using semi-quantitative polymerase chain reaction (PCR) experiments. The results were analyzed in terms of tumor type, clinical stage, histologic grade, and histologic type, and the prognostic significance of the expression levels of each factor in patients with ovarian cancer was assessed.

MATERIALS

Materials for Immunohistochemistry

1. Samples of epithelial ovarian tumor tissue were collected from 93 patients (21 low malignant potential [LMP] tumors and 72 adenocarcinomas). All patients were surgically treated between 1989 and 1997, histologically diagnosed, and received follow-up care in the Department of Obstetrics and Gynecology at Hiroshima University Hospital. Clinical staging was determined in accordance with the criteria of the International Federation of Gynecology and Obstetrics (FIGO) staging system. Most of the patients with stage Ic, stage II, stage III, or stage IV ovarian cancer had received cisplatin-containing chemotherapy after surgery. The mean follow-up time was 48 months (range 21–140 months).

2. 0.1 *M* Citric acid monohydrate: 21.01 g citric acid monohydrate; bring up to 1 L with distilled water.

3. 0.1 *M* Trisodium citrate dihydrate: 29.41 g trisodium citrate dihydrate; bring up to 1 L with distilled water.

4. 0.01 *M* Sodium citrate buffer (pH 6.0): 18 ml of 0.1 *M* citric acid monohydrate and 82 ml of 0.1 *M* trisodium citrate dihydrate; bring up to 1 L with distilled water; adjust the pH to 6.0 with HCl.

5. 0.1 *M* Phosphate buffer (pH 7.4): 28.7 g disodium hydrogen phosphate•12H_2O and 3.3 g sodium dihydrogenphosphate•2H_2O; bring up to 1 L with distilled water; adjust pH to 7.4 with HCl.

6. 0.01 *M* Phosphate buffer saline (PBS) (pH 7.2): 100 ml of 0.1 *M* phosphate buffer and 8.5 g NaCl; bring up to 1 L with distilled water, adjust pH to 7.2 with HCl.

7. Vectastain Elite ABC kit (rabbit immunoglobulin [I_g]G) (PK-6101, Vector Laboratories, Burlingame, CA).

8. Anti-MCL-1 (S-19) rabbit polyclonal antibody (sc-819, Santa Cruz Biotechnology, Santa Cruz, CA).

9. AEC (3-amino-9-ethylcarbozole) Substrate Kit (K0697, Dako Corp., Carpinteria, CA).

Place 2 ml of acetate buffer into a clean glass test tube (2 ml of solution is sufficient to stain 10 slides). Add 1 drop of AEC to the test tube and mix well. Add 1 drop of H_2O_2 to the test tube and mix well.

10. Gel Tol AqueoMounting Medium (Code No. 484950, IMMUNON Thermo Shandon, Osaka, Japan).

Materials for Semi-Quantitative Polymerase Chain Reaction

1. Fresh surgical specimens of 36 ovarian tumors (6 adenomas and 30 carcinomas) were collected. The specimens were obtained immediately following the surgical procedure and were cut in half. One half was processed for histologic examination to determine the percentage of tumor cells in the samples, which was never lower than 80%. The other half was used for mRNA preparation. In addition, 8 normal ovaries were obtained from patients before undergoing surgery for benign gynecologic disease. Tissues were frozen in liquid nitrogen and stored at −80°C prior to mRNA isolation. All patients with cancer were surgically treated, histologically diagnosed, and received follow-up care in the Department of Obstetrics and Gynecology at Hiroshima University Hospital. Clinical staging was determined in accordance with the criteria of the FIGO. The mean follow-up time was 36 months (range 15–60 months); 82% of the patients were followed for more than 2 years.

2. RiboSep mRNA isolation kit (Becton Dickinson Labware, Bedlord, MA).

3. Advantage RT-for-PCR kit (Catalog No. K1402-2, Clontech, Palo Alto, CA).

4. Oligonucleotide primer sequences used for PCR.
   - BAX sense primer, 5′-AGCTGAGCGAGTGTCTCAAG-3′
   - BAX antisense primer, 5′-TCTTCCAGATGGTGAGCGAG-3′
   - BCL-2 sense primer, 5′-TGCCACCTGTGGTCCACCTG-3′
   - BCL-2 antisense primer 5′-TGTGGCCTCAGCCCAGACTCAC-3′
   - MCL-1 sense primer, 5′-TCTCTCGGTACCTTCGGG-3′
   - MCL-1 antisense primer, 5′-GCACTTACAGTAAGGCTATC-3′

BCL-XL sense primer, 5′-CATTCAGTGAC-CTGACATCC-3′
BCL-XL antisense primer, 5′-TTCTCCTG-GATCCAAGGCTC-3′
β-tubulin sense primer, 5′-TGCATTGA-CAACGAGGC-3′
β-tubulin antisense primer was 5′-CTGTCTTGACATTGTTG-3′

5. Ampli Taq DNA (deoxyribonucleic acid) polymerase (Perkin Elmer, Foster City, CA).

6. 100 bp DNA Ladder (Code No. DNA-030, TOYOBO Corp., Osaka, Japan).

7. Agarose (Catalog No. 50070, Bio Whittaker Molecular Applications, Rochland, ME).

8. Tris-acetate buffer (TAE): 0.04 M tris-acetate and 0.001 M ethylene diamine tetraacetic acid (EDTA).

9. Ethidium bromide tablets (Catalog No. 161-0430, Bio-Rad Laboratories, Hercules, CA).

10. Printgraph-Densitograph system (ATTO Corp., Tokyo, Japan).

METHOD

Immunohistochemistry

1. Formalin-fixed and paraffin-embedded sections (4 μm thick) were cut and mounted on aminopropyl triethoxysilane-treated slides.

2. The slides were routinely deparaffinized with xylene and rehydrated with a series of ethanol washes.

3. Nonenzymatic antigen retrieval was performed using a 500 W microwave heat treatment in 0.01 *M* sodium citrate buffer (pH 6.0) for 3 min 7×.

4. Rinse for 5 min in distilled water.

5. Immunohistochemical staining was performed by using the avidin-biotin peroxidase complex technique (Vectastain Elite ABC kit [rabbit IgG], Vector Laboratories) according to a previously described method (Shigemasa *et al.,* 2002).

6. Endogenous peroxidase and nonspecific background staining were blocked by incubating slides with methanol containing 0.3% H_2O_2 for 30 min.

7. Slides were rinsed with PBS for 15 min.

8. Normal serum blocking was performed with incubating slides with normal goat serum for 30 min.

9. After blotting excess normal goat serum from sections using a Kimwipes paper (Kimberly-Clark Corp.), slides were incubated with Anti-MCL-1 (S-19) rabbit polyclonal antibody (Santa Cruz Biotechnology) for 3 hr at room temperature. The working dilution of the primary antibody was 1:50.

10. Rinse as in **Step 7.**

11. Slides were incubated with biotinylated anti-rabbit IgG for 30 min.

12. Rinse as in **Step 7.**

13. Slides were incubated with ABC reagent for 30 min.

14. Rinse as in **Step 7.**

15. The final products were visualized by using the AEC substrate system (Dako Corp.).

16. Sections were counterstained with Mayer hematoxylin for 20 sec.

17. Slides were washed with distilled water for 30 min.

18. Positive and negative controls were used for each section. As the positive control, we included normal endometrium tissues. Normal rabbit serum IgG (Vector Laboratories) in place of the primary antibody was used as a negative control. Slides were incubated with normal rabbit serum for 3 hr at room temperature. The working dilution of normal rabbit serum IgG was 1:25.

19. The percentage of positive tumor cells was scored as follows. When no positive tumor cell stain could be identified or when there were less than 5% focally distributed positive tumor cells, the staining was considered negative. When 5–50% of the tumor cells showed positive staining, staining was considered partial positive. When more than 50% of the tumor cells showed positive staining, staining was considered diffuse positive.

20. Increased MCL-1 protein expression was defined as a diffuse positive staining of MCL-1. A Kaplan-Meier survival curve of patients with ovarian cancer was categorized according to the negative, partial-positive, or diffuse-positive expression of MCL-1.

Messenger Ribonucleic Acid Extraction

1. mRNA was isolated using a RiboSep mRNA isolation kit (Becton Dickinson Labware).

2. 0.5–1.0 g of tissue samples were grounded in a mortar and pestle under liquid nitrogen.

3. 10 ml of lysis buffer and 2 mg of proteinase-K were added, and the slurry was homogenized for 30 sec.

4. The tissue lysate was incubated for 2 hr at 45°C.

5. 600 μl of 5 *M* NaCl was added to adjust the NaCl concentration.

6. 10 ml of tissue lysate was added to an oligo (dT9) cellulose tube containing 1 ml of binding buffer, and this tube was incubated for 1 hr.

7. Oligo (dT) cellulose was pelleted by centrifugation and washed with 5 ml of binding buffer several times.

8. Washed oligo (dT) cellulose was transferred to a column, and mRNA was eluted with elution buffer.

9. The amount of mRNA recovered was measured by ultraviolet spectrophotometry.

Complementary Deoxyribonucleic Acid Synthesis

1. Complementary DNA (cDNA) was synthesized by random hexamer priming using Advantage RT-for-PCR kit (Clontech).
2. The cDNA synthesis reaction was performed with 2 µg of mRNA and 20 pmol of random hexamer primer in 20 µl of a solution containing 50 m*M* Tris-HCl (pH 8.3), 75 m*M* HCl, 3 m*M* $MgCl_2$, 500 µ*M* each dNTP, one unit of RNase inhibitor, and 200 units of Molony-Murine Leukemia Virus reverse transcriptase.
3. After 4 hr of incubation at 42°C, the reaction was heated at 94°C for 5 min to stop cDNA synthesis.
4. cDNA was diluted to a final volume of 100 µl.
5. The efficiency of cDNA synthesis was estimated using glyceraldehydes-3-phosphate dehydrogenase (G3PDH) amplimers (Clontech) as a positive control.

Semi-Quantitative Polymerase Chain Reaction

1. mRNA expression levels of BAX, BCL-2, MCL-1, and BCL-XL were determined by semi-quantitative PCR amplification technique.
2. β-tubulin cDNA amplification was used as the internal PCR control.
3. The predicted sizes of the amplified genes were 396 bp for BAX, 330 bp for BCL-2, 504 bp for MCL-1, 204 bp for BCL-XL, and 454 bp for β-tubulin.
4. The PCR reaction mixture consisted of cDNA derived from 50 ng of mRNA, 5 pmol of sense and antisense primers, 200 µmol of dNTPs, and 0.625 U of Ampli Taq DNA polymerase with reaction buffer (Perkin Elmer) in a final volume of 25 µl.
5. Each PCR cycle involved 30 sec of denaturation at 94°C, 60 sec of primer annealing at 55°C for MCL-1 and BCL-XL, 60 sec at 60°C for BAX, or 60 sec at 62°C for BCL-2 and β-tubulin, and 30 sec of extension at 72°C.
6. 28 cycles of PCR were carried out in a Thermal Cycler (Perkin Elmer).
7. Tubes containing all ingredients except templates were included in all runs as a negative control.
8. The PCR products were separated on 2.0% agarose gels and identified by ethidium bromide staining. The density of each PCR product was determined using a Printgraph-Densitograph system (ATTO Corporation). Expression ratio (target gene: β-tubulin) as measured by densitometry was used to evaluate gene expression. The results are expressed as the mean ± standard deviation (SD).
9. The differences in the mean value of the expression ratio of target genes between groups were assessed with respect to tumor type, clinical stage, histologic grade, and histologic type.
10. In addition, the ovarian cancer cases were classified into the following two groups according to the expression ratio of each of the target genes: low-expression cases, <median value and high-expression cases, >median value.
11. A Kaplan-Meier survival curve of patients with ovarian cancer was categorized according to the high or low expression of BAX, BCL-2, MCL-1, and BCL-XL.

Statistical Methods

1. The χ^2 test of significance and Fisher's exact probability were used to analyze the distribution of diffuse-positive MCL-1 expression cases according to clinicopathologic characteristics.
2. Statistical significance of differences in survival rates was tested by log-rank.
3. An unpaired t test was used to assess the differences in the mean value of the target gene: β-tubulin mRNA expression ratios between groups.
4. Significance was defined as $p < 0.05$. The Statview software package (Abacus Concepts, Berkeley, CA) was used for the statistical tests.

RESULTS AND DISCUSSION

To investigate the presence of MCL-1 protein in ovarian tumor cells, we performed immunohistochemical staining of 21 low malignant potential (LMP) tumors and 72 adenocarcinomas. As shown in Figure 80, MCL-1 was immunolocalized in the cytoplasm of cancer cells but not in the underlying stromal cells. The total amount of positive MCL-1 protein expression, including both partial-positive and diffuse-positive cases, was 90% (19/21) for ovarian LMP tumors and 86% (62/72) for carcinomas. Table 41 shows the percentage of diffuse-positive MCL-1–expressing tissues as determined by immunohistochemical analysis. Of ovarian LMP tumors 57% (12/21) and 72% (52/72) of carcinomas were diffuse positive for MCL-1 expression. The percentage of diffuse-positive MCL-1–expressing mucinous carcinomas was significantly higher than that of mucinous LMP tumors ($p = 0.032$). In terms of histologic types, there was a significantly higher percentage of diffuse-positive MCL-1–expressing serous and mucinous carcinomas compared to clear cell carcinomas (serous versus clear cell, $p = 0.009$; mucinous versus clear cell, $p = 0.013$). The percentage of diffuse positive MCL-1–expressing tissues significantly correlates with advanced clinical stage and high histologic grade (stage I/II versus stage III/IV: $p = 0.0004$; grade 1 versus grade 2/3: $p = 0.009$).

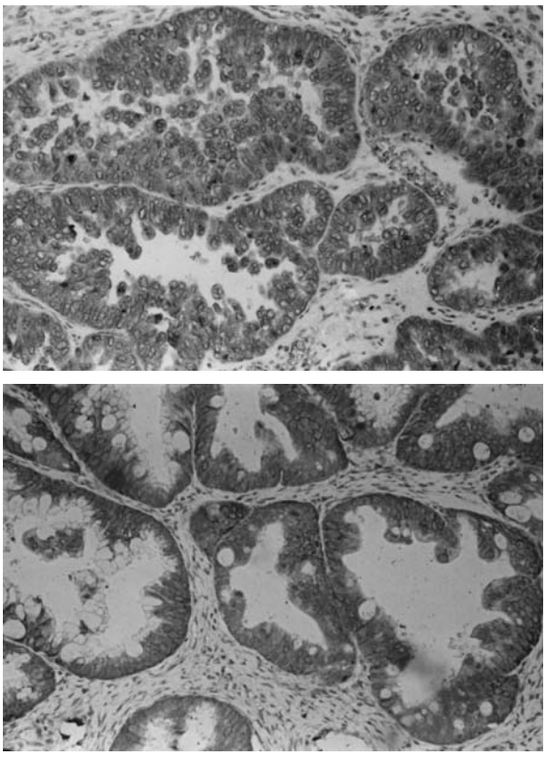

Figure 80. Immunohistochemistry. Cytoplasmic expression of MCL-1 protein was observed in ovarian adenocarcinoma cells. **A:** Serous adenocarcinoma, 50X. **B:** Mucinous adenocarcinoma, 50X.

Table 41. Immunohistochemical Expression of MCL-1 in Ovarian Tumors

Tumor Type	N	Diffuse-Positive Expression of MCL-1[a] (%)
Ovarian LMP tumor	21	12 (57)
Histologic Type		
Serous	7	5 (71)
Mucinous	14	7 (50)[b]
Ovarian carcinoma	72	52 (72)
Histologic Type		
Serous	26	22 (85)[c]
Mucinous	16	14 (88)[b,d]
Endometrioid	16	10 (63)
Clear cell	14	6 (43)[c,d]
Clinical Stage		
Stage I/II	41	23 (56)[e]
Stage III/IV	31	29 (94)[e]
Histologic Grade		
Grade 1	48	30 (63)[f]
Grade 2/3	24	22 (92)[f]

[a]Diffuse positive = more than 50% positive tumor cells.
[b]Mucinous LMP tumor versus mucinous carcinoma; $p = 0.032$, Fisher's exact test.
[c]Serous carcinoma versus clear cell carcinoma; $p = 0.009$, Fisher's exact test.
[d]Mucinous carcinoma versus clear cell carcinoma; $p = 0.013$, Fisher's exact test.
[e]Stage I/II versus stage III/IV; $p = 0.0004$, χ^2 test.
[f]Grade 1 versus grade 2/3; $p = 0.009$, χ^2 test.
LMP, Low malignant potential.

The Kaplan-Meier survival curve of 52 patients with ovarian cancer was categorized according to the immunohistochemical expression levels of MCL-1. Log-rank testing revealed that increased MCL-1 protein expression was significantly correlated with poor survival in OCs ($p = 0.0097$).

To evaluate the mRNA expression of BAX, BCL-2, MCL-1, and BCL-XL in ovarian tumors and normal ovaries, we performed semi-quantitative PCR. The mean and SD of the BAX, BCL-2, MCL-1, and BCL-XL expression ratios determined for the various tumor subtypes are shown in Table 42. The mean value of the relative BAX expression ratio was significantly higher in both ovarian cancer samples ($p = 0.005$) and adenoma samples ($p = 0.005$) than in normal ovary samples. The mean relative BCL-2 expression ratio was significantly lower in ovarian cancers than in either ovarian adenomas ($p = 0.010$) or normal ovaries ($p = 0.0003$). MCL-1 expression was significantly higher in both ovarian cancer ($p = 0.028$) and adenoma samples ($p = 0.007$) than in normal ovary samples. There was no significant difference in BCL-XL expression levels in ovarian cancer versus normal ovaries. Finally, there was no statistical difference between the BAX, BCL-2, MCL-1, and BCL-XL mRNA expression levels in terms of clinical stage, histologic grade, or histologic type in ovarian cancer samples.

The Kaplan-Meier survival curves for 30 patients with ovarian cancer were compared with the tumor-tissue expression levels of BAX, BCL-2, MCL-1, and BCL-XL. Analysis of all four target genes failed to reveal an association between expression levels and survival prognosis in all cases studied. However, when the analysis was restricted to 18 patients with FIGO stage III disease, log-rank testing revealed that high BAX mRNA expression was significantly correlated with better survival in stage III OCs ($p = 0.0498$). The most significant association was found between high MCL-1 mRNA expression levels and poor prognosis in stage III ovarian cancers ($p = 0.0187$). No significant correlations were found between BCL-2 or BCL-XL mRNA expression levels and survival in stage III carcinomas.

Molecular mechanisms underlying high MCL-1 expression levels should be elucidated to clarify the

Table 42. Relative Expression Levels of BAX, BCL-2, MCL-1, and BCL-XL mRNA in Normal Ovaries and Ovarian Tumors

	TN	BAX Mean ± SD	BCL-2 Mean ± SD	MCL-1 Mean ± SD	BCL-XL Mean ± SD
Normal ovary	8	0.72 ± 0.29	0.81 ± 0.12	1.57 ± 0.05	2.26 ± 0.68
Ovarian adenoma	6	1.20 ± 0.19[a]	0.72 ± 0.20	1.79 ± 0.11[d]	2.18 ± 0.29
Ovarian adenocarcinoma	30	1.12 ± 0.32[b]	0.34 ± 0.33[c]	1.72 ± 0.17[e]	2.22 ± 0.59
Clinical Stage					
Stage I	11	1.17 ± 0.40	0.35 ± 0.35	1.74 ± 0.20	2.21 ± 0.40
Stage II/III	19	1.10 ± 0.29	0.33 ± 0.32	1.71 ± 0.15	2.23 ± 0.68
Histologic Grade					
Grade 1	15	1.16 ± 0.35	0.35 ± 0.35	1.73 ± 0.19	2.21 ± 0.39
Grade 2/3	15	1.08 ± 0.31	0.33 ± 0.31	1.71 ± 0.15	2.23 ± 0.69
Histologic Type					
Serous	14	1.13 ± 0.37	0.38 ± 0.38	1.73 ± 0.16	2.20 ± 0.38
Mucinous	7	1.17 ± 0.34	0.25 ± 0.25	1.69 ± 0.14	2.43 ± 0.98
Endometrioid	6	1.06 ± 0.10	0.30 ± 0.21	1.70 ± 0.24	1.95 ± 0.45
Clear cell	3	1.10 ± 0.53	0.42 ± 0.41	1.77 ± 0.20	2.38 ± 0.24

[a]Adenoma versus normal; $p = 0.005$, unpaired t test.
[b]Adenocarcinoma versus normal; $p = 0.005$, unpaired t test.
[c]Adenocarcinoma versus normal; $p = 0.0003$, adenocarcinoma versus adenoma; $p = 0.010$, unpaired t test.
[d]Adenoma versus normal; $p = 0.007$, unpaired t test.
[e]Adenocarcinoma versus normal; $p = 0.028$, unpaired t test.

cause of resistance to chemotherapeutic agents. It has been reported that MCL-1 is induced after stimulation by various growth factors or cytokines (Leu *et al.,* 2000; Puthier *et al.,* 1999). Wei *et al.* (2001) reported that interleukin (IL)-6 regulated the MCL-1 expression through the PI3K/Akt–dependent pathway in human cervical cancer, which might facilitate the oncogenesis of cervical cancer by modulating the apoptotic threshold. It has also been reported that vascular endothelial growth factor (VEGF) induces MCL-1 expression and inhibits apoptotic death in hematopoietic cells (Katoh *et al.,* 1998). Therefore, we examined the expression levels of both IL-6 and VEGF mRNA in our ovarian cancer samples. However, neither IL-6 nor VEGF expression levels correlated with those of MCL-1 (data not shown), indicating that signal-transduction pathways stimulated by other growth factors or cytokines may be involved in transcriptional regulation of the MCL-1 gene in ovarian cancers.

BCL-2 family members form homodimers or heterodimers with each other, and these complex protein–protein associations direct cells either toward survival or death, although the precise mechanisms of these processes are unclear (Kroemer, 1997; Korsmeyer, 1999). Marone *et al.* (1998) reported that BCL-2, BAX, and BCL-XL were present to a variable degree in both normal and neoplastic ovarian tissues and that their mRNA and protein levels were directly correlated. Several earlier studies have suggested that BCL-2 mRNA or protein expression levels were higher in normal ovaries than in OCs, whereas both BAX and BCL-XL expression was higher in carcinomas (Marone *et al.,* 1998; Witty *et al.,* 1998). In the present study, we observed decreased BCL-2 and increased BAX and MCL-1 mRNA expression levels in ovarian cancers compared with those in normal ovaries, although we did not find any statistical difference between the level of BCL-XL mRNA expression in normal ovaries versus ovarian cancer samples. Increased BAX expression and decreased BCL-2 expression in ovarian cancer cells seem to be paradoxical, given the proposed pro-apoptotic function of BAX and anti-apoptotic function of BCL-2. It is likely that increased BAX and decreased BCL-2 expression in ovarian cancer cells may be counteracted by other anti-apoptotic proteins that bind to BAX or BCL-2. The present study suggests the possibility that significantly elevated MCL-1 expression might replace the functioning of BAX and BCL-2 in ovarian cancer cells.

Several earlier studies have shown that immunohistochemical expression of BCL-2 is associated with improved survival in patients with ovarian cancer (Henriksen *et al.,* 1995; Herod *et al.,* 1996). However, in the present study using semi-quantitative PCR, low BCL-2 expression was not associated with a survival advantage. Diebold *et al.* (1996) have reported that

BCL-2 expression failed to reveal a correlation with the prognosis in the total study population of patients with ovarian carcinoma. Therefore, the relationship between BCL-2 expression and prognosis in patients with ovarian cancer is still controversial. However, decreased BCL-2 expression in ovarian cancer cells compared to that in ovarian adenomas and normal ovaries suggests that BCL-2 regulation may play an important role in the development of ovarian cancer.

In the present study, we found that high BAX mRNA expression was significantly correlated with a better survival in stage III ovarian carcinomas. It has been reported that immunohistochemical expression of BAX is also significantly associated with improved prognosis of patients with ovarian cancer (Baekeland *et al.,* 2000; Schuyer *et al.,* 2001). The protein p53 is known to be a direct transcriptional activator of the BAX gene (Miyashita and Reed, 1995), and p53 accumulation in tumor cells, which presumably is correlated with the presence of p53 missense mutations, is associated with a poor prognosis in ovarian cancer (Bosari *et al.,* 1993; Shigemasa *et al.,* 2003). It has been reported that a cisplatin-resistant ovarian cancer cell line was found to have reduced BAX mRNA levels, which is consistent with the loss of the ability of p53 to transactivate BAX as a consequence of p53 mutation (Perego *et al.,* 1996). Tai *et al.* (1998) have demonstrated that reduced expression of BAX was related to lower response rates in patients with ovarian cancer treated with chemotherapy. Therefore, ovarian cancer tissues expressing low levels of BAX mRNA may be partly related to the loss of p53-dependent transcription in at least some patients and may be expected to be associated with poorer survival rates.

In this study, we used semi-quantitative polymerase chain reaction (PCR) to show that high MCL-1 mRNA expression significantly correlates with poor survival for patients with stage III OCs. Furthermore, we used immunohistochemistry to demonstrate that increased MCL-1 protein expression significantly correlates with advanced clinical stage, high histologic grade, and poor survival for patients with ovarian cancer. Baekeland *et al.* (2000) also reported that immunohistochemical expression of MCL-1 was significantly associated with poorer prognosis for patients with stage III ovarian cancer. These results suggest that MCL-1 may be involved in the regulation of apoptosis in ovarian cancer cells and that it may play an important role in taking over the functions of BAX and BCL-2. MCL-1 expression levels have the potential to become a useful prognostic marker in patients with ovarian cancer.

Although these preliminary observations will have to be confirmed with larger samples of patients with ovarian cancer, determination of a selected apoptosis-related protein such as MCL-1 would be a useful prognostic molecular marker for OCs. An expansion of these findings would argue for the use of apoptosis-related proteins as a therapeutic agent in the treatment and prevention of ovarian cancers.

Acknowledgments

The author would like to thank Dr. Osamu Katoh (Department of Environment and Mutation, Research Institute for Radiation Biology and Medicine, Hiroshima University) for his support and helpful discussion.

References

Baekeland, M., Holm, R., Nesland, J.M., Trope, C.G., and Kristensen, G.B. 2000. Expression of apoptosis-related proteins is an independent determinant of patient prognosis in advanced ovarian cancer. *J. Clin. Oncol. 18*:3775–3781.

Bosari, S., Viale, G., Radaelli, U., Bossi, P., Bonolidi, E., and Coggi, G. 1993. p53 accumulation in ovarian carcinomas and its prognostic implications. *Human Pathol. 24*:1175–1179.

Campos, L., Rouault, J-P., Sabido, O., Oriol, P., Roubi, N., Vasselon, C., Archimbaud, E., Magaud, J-P., and Guyotat, D. 1993. High expression of BcL-2 protein in acute myeloid leukemia cells is associated with poor response to chemotherapy. *Blood 81*:3091–3096.

Diebold, J., Baretton, G., Felchner, M., Meier, W., Dopfer, K., Schmidt, M., and Lohrs, U. 1996. BcL-2 expression, p53 accumulation, and apoptosis in ovarian carcinomas. *Anatomic Pathol. 105*:341–349.

Henriksen, R., Wilander, E., and Oberg, K. 1995. Expression and prognostic significance of BCL-2 in ovarian tumours. *Br. J. Cancer 72*:1324–1329.

Herod, J.J.O., Eliopoulos, A.G., Warwick, J., Niedobitek, G., Young, L.S., and Kerr, D.J. 1996. The prognostic significance of BCL-2 and p53 expression in ovarian carcinoma. *Cancer Res. 56*:2178–2184.

Katoh, O., Takahashi, T., Oguri, T., Kuramoto, K., Mihara, K., Kobayashi, M., Hirata, S., and Watanabe, H. 1998. Vascular endothelial growth factor inhibits apoptotic death in hematopoietic cells after exposure to chemotherapeutic drugs by inducing MCL-1 acting as an antiapoptotic factor. *Cancer Res. 58*: 5565–5569.

Korsmeyer, S.J. 1999. BcL-2 gene family and the regulation of programmed cell death. *Cancer Res. Suppl. 59*: 1693s–1700s.

Kroemer, G. 1997. The proto-oncogene BCL-2 and its role in regulating apoptosis. *Nature Med. 3*:614–620.

Leek, R.D., Kaklamanis, L., Pezzella, F., Gatter, K.C., and Harris, A.L. 1994. BcL-2 in normal human breast and carcinoma, association with oestrogen receptor-positive, epidermal growth factor receptor-negative tumours and *in situ* cancer. *Br. J. Cancer 69*:135–139.

Leu, C.M., Chang, C., and Hu, C. 2000. Epidermal growth factor (EGF) suppresses staurosporine-induced apoptosis by inducing MCL-1 via the mitogen-activated protein kinase pathway. *Oncogene 19*:1665–1675.

Lomo, J., Smeland, E.B., Krajewski, S., Reed, J.C., and Blomhoff, K. 1996. Expression of the Bcl-2 homologue MCL-1 correlates with survival of peripheral blood B lymphocytes. *Cancer Res. 56*:40–43.

Marone, M., Scambia, G., Mozzetti, S., Ferrandina, G., Iacovella, S., Pasqua, A.D., Benedetti-Panici, P., and Mancuso, S. 1998. BcL-2, BAX, BcL-Xl, and Bcl-Xs expression in normal and neoplastic ovarian tissues. *Clin. Cancer Res. 4*:517–524.

McDonnell, T.J., Troncoso, P., Brisbay, S.M., Logothetis, C., Chung, L.W.K., Hsieh, J-T., Tu, S-M., and Campbell, M.L. 1992. Expression of the protooncogene BcL-2 in the prostate and its association with emergence of androgen-independent prostate cancer. *Cancer Res. 52*:6940–6944.

Miyashita, T., and Reed, J.C. 1995. Tumor suppressor p53 is a direct transcriptional activator of the human BAX gene. *Cell 80*:293–299.

Parker, S.L., Tong, T., Bolden, S., and Wingo, P.A. 1996. Cancer statistics. *CA Cancer J. Clin. 46*:5–27.

Perego, P., Giarola, M., Righetti, S.C., Supino, R., Caserini, C., Delia, D., Pierotti, M.A., Miyashita, T., Reed, J.C., and Zunino, F. 1996. Association between cisplatin resistance and mutation of p53 gene and reduced BAX expression in ovarian carcinoma cell systems. *Cancer Res. 56*:556–562.

Pezzella, F., Turley, H., Kuzu, I., Tungekar, M.F., Dunnill, M.S., Pierce, C.B., Harris, A., Gatter, K.C., and Mason, D.Y. 1993. Bcl-2 protein in non-small-cell lung carcinoma. *N. Eng. J. Med. 329*:690–694.

Puthier, D., Bataille, R., and Amiot, M. 1999. IL-6 up-regulates MCL-1 in human myeloma cells through JAK/STAT rather than ras/MAP kinase pathway. *Eur. J. Immunol. 29*:3945–3950.

Rieger, L., Weller, M., Bornemann, A., Schabet, M., Dichgans, J., and Meyermann, R. 1998. BcL-2 family protein expression in human malignant glioma: a clinical-pathological correlative study. *J. Neu. Sci. 155*:68–75.

Schuyer, M., van der Burg, M.E.L., Henzen-Logmans, S.C., Fieret, J.H., Klijn, J.G.M., Look, M.P., Foekens, J.A., Stoter, G., and Berns, E.M.J.J. 2001. Reduced expression of BAX is associated with poor prognosis in patients with epithelial ovarian cancer: a multifactorial analysis of TP53, p21, BAX and BcL-2. *Br. J. Cancer 85*:1359–1367.

Shigemasa, K., Katoh, O., Shiroyama, Y., Mihara, S., Mukai, K., Nagai, N., Ohama, K. 2002. Increased MCL-1 expression is associated with poor prognosis in ovarian carcinomas. *Jpn. J. Cancer Res. 93*:542–550.

Shigemasa, K., Tian, X., Gu, L., Shiroyama, Y., Nagai, N., and Ohama, K. 2003. Expression of cyclooxygenase-2 and its relationship to p53 accumulation in ovarian adenocarcinomas. *Int. J. Oncol. 22*:99–105.

Tai, Y.T., Lee, S., Niloff, E., Weisman, C., Strobel, T., and Cannistra, S.A. 1998. BAX protein expression and clinical outcome in epithelial ovarian cancer. *J. Clin. Oncol. 16*: 2583–2590.

Wei, L.H., Kuo, M.L., Chen, C.A., Chou, C.H., Cheng, W.F., Chang, M.C., Su, J.L., and Hsieh, C.Y. 2001. The anti-apoptotic role of interleukin-6 in human cervical cancer is mediated by up-regulation of MCL-1 through a PI3K/Akt pathway. *Oncogene 20*:5799–5809.

Witty, J.P., Jensen, R.A., and Johnson, A.L. 1998. Expression and localization of BcL-2 related proteins in human ovarian cancers. *Anticancer Res. 18*:1223–1230.

Yunis, J.J., Mayer, M.G., Arnesen, M.A., Aeppli, D.P., Oken, M.M., and Frizzera, G. 1989. BcL-2 and other genomic alterations in the prognosis of large-cell lymphoma. *N. Eng. J. Med. 320*:1047–1054.

22

Role of Elf-1 in Epithelial Ovarian Carcinoma: Immunohistochemistry

Noriyuki Takai and Isao Miyakawa

Introduction

Elf-1 is an Ets-related transcription factor that was originally cloned from a human T-cell library by hybridization with a probe encoding the deoxyribonucleic acid (DNA) binding domain (Ets domain) of the human Ets-1 complementary DNA (cDNA) (Thompson *et al.,* 1991). Elf-1 is involved in developmental processes (Janknecht *et al.,* 1989), mitogenic activation of cells (Janknecht *et al.,* 1995), oncogenesis (Moreau-Gachelin *et al.,* 1988), and viral gene activation (Wasylyk *et al.,* 1990). Because many of the Ets family members are proto-oncogenes (Wasylyk *et al.,* 1993), Elf-1 may also function as a proto-oncogene. Elf-1 contains a LXCXE retinoblastoma protein (Rb)-binding motif near its amino terminus. The activity of Elf-1 is regulated by interactions with the Rb protein, and these interactions are in turn regulated in a cell cycle–dependent fashion. Thus, it has been suggested that Elf-1 may serve as an important regulator of cell cycle–specific gene expression (Bredemeier-Ernst *et al.,* 1997). Elf-1 has been evaluated for its expression in human breast tumors and its ability to bind and transactivate the HER-2/neu promoter (Scott *et al.,* 2000). Given these findings, it will be important to correlate the overexpression of Elf-1 with the proliferative states of ovarian carcinoma (OC) cells. Moreover, Elf-1 plays significant roles in tumor invasion and vascular development by regulating the respective gene expressions of the urokinase type plasminogen activator *(uPA)* (Schmitt *et al.,* 1997) and *Tie2* (Dube *et al.,* 2001) genes.

The Ets family proteins control the expression of the *uPA* gene by binding to an inducible enhancer region. The gene *uPA* activates numerous matrix metalloproteinases and concomitantly promotes the proteolysis of the extracellular matrix, tumor-cell migration, and intravasation and extravasation and the activation of mitogens, effectors of angiogenesis, and effectors of the osteoblastic reaction important for bone metastases (Schmitt *et al.,* 1997). Tumor-cell invasiveness and metastatic capacity are highly correlated with the expression of uPA and its receptor (uPAR) and are blocked by their inhibitors. The respective expression profiles of uPA and uPAR are prognostic indicators for the clinical outcome of many cancers (Schmitt *et al.,* 1997), including ovarian adenocarcinoma (Tecimer *et al.,* 2000).

To date, enhanced expression of Elf-1 has been reported in high-grade prostate cancer (Gavrilov *et al.,* 2001), breast cancer (Scott *et al.,* 2000), osteosarcoma (Bassuk *et al.,* 1998), and HeLa cells (Bassuk *et al.,* 1998). Furthermore, we have previously demonstrated that the overexpression of c-Ets 1 in both endometrial and epithelial OC was associated significantly with the malignant potential of these tumors (Takai *et al.,*

2000, 2002a). On the basis of these observations, we examined the localization of Elf-1 protein in OCs and analyzed the relationship between Elf-1 protein expression and the malignant potential (histologic classification, clinical stage, histologic grade, clinical outcome, and survival rate) of this carcinoma.

MATERIALS AND METHODS

Tissue Sources and Patient Characteristics

Tissue samples were obtained from a total of 36 patients, including 26 patients with epithelial OC and 10 patients with benign cystadenomas of the ovary. All samples were obtained between October 1997 and December 2000 at the Department of Obstetrics and Gynecology, Oita University Hospital. Informed consent was obtained from all patients. The histology of each sample was examined by three gynecologic pathologists to confirm the presence of ovarian tissue.

We collected data on the following characteristics of patients with OC: histologic classification, clinical stage, histologic grade, clinical outcome, and survival rate as of February 2003. Histologic classification and grade were examined by reviewing all of the formalin-fixed and paraffin-embedded sections obtained for routine clinical diagnosis. The malignant and benign ovarian tissues were fixed in 3% paraformaldehyde, blocked in Optimal Cutting Temperature (OCT; Sakura Finetechnical, Tokyo, Japan) compound, and sectioned for immunohistochemical and hematoxylin and eosin (H&E) staining for histologic confirmation.

Antibodies

Antibodies were obtained from the following sources: Rabbit anti-human Elf-1 polyclonal antibody (known to detect normal Elf-1 protein) was from Santa Cruz Biotechnology (Santa Cruz, CA), mouse anti-human cytokeratin monoclonal antibody and mouse anti-human proliferating cell nuclear antigen (PCNA) monoclonal antibody from Dako (Copenhagen, Denmark), and fluorescein (FITC)-labeled donkey anti-rabbit immunoglobulin G (IgG) and rhodamine (Rd)-labeled donkey anti-mouse IgG antibodies from Jackson Immunoresearch Laboratories (West Grove, PA).

Immunohistochemistry

The H&E-stained sections were used to select the most cellularized portion of the tumor and the area with the lowest architectural differentiation in the case of heterogeneity. The ovarian tissues were processed for double indirect immunolocalization, as described previously (Takai *et al.,* 2000). Tssues were fixed in 3% paraformaldehyde for 30 min, washed 3× in phosphate buffer saline (PBS), infiltrated with 5–15% sucrose followed by OCT (Sakura Finetechnical), and frozen in liquid nitrogen. Sections (6-μm thick) were prepared using a cryostat (Slee International, Tiverton, RI) and collected on silanized microscope slides (Dako). Fixed sections were permeabilized in cold methanol for 5 min, washed 3× in PBS for 5 min, and incubated for 30 min with 1% bovine serum albumin (BSA) (Sigma, St. Louis, MO) in PBS. Sections were then incubated for 1 hr with two primary antibodies—a rabbit anti-Elf-1 antibody and a mouse anti-cytokeratin or PCNA antibody—followed by rinsing 3× in PBS for 5 min each.

The sections were then incubated for 30 min with secondary antibodies conjugated to FITC or Rd, washed 3× in PBS for 5 min, and mounted with Vectorshield (Vector Laboratories, Burlingame, CA). All incubations and washes were performed at room temperature. Samples were examined with a Zeiss Axiophot Epifluorescence microscope (Carl Zeiss, Oberkochen, Germany) equipped with filters to selectively view the FITC and Rd images. Preabsorption of the primary antibody with excess positive-control proteins (purchased as blocking peptide from Santa Cruz Biotechnology, Santa Cruz, CA) at room temperature for 1 hr was used as a negative control. Prostate carcinoma tissue served as the positive control for Elf-1 immunostaining (Gavrilov *et al.,* 2001). The intensities, percentages, and patterns of immunohistochemical staining were recorded separately for each sample slide. The percentage of nuclear-stained cells was calculated by counting at least 1000 tumor cells at high magnification (400X).

Statistical Analysis

Data are presented as the mean ± standard deviation (SD) for each group. Statistical analysis was performed using analysis of variance (ANOVA) and Mann-Whitney nonparametric test and Kruskal-Wallis test followed by Dunn's posttest. The statistical significance of intergroup differences was evaluated by Fisher's test. Kaplan-Meier curves were compared by means of a homogeneity test and the log-rank test. P values <0.05 were considered statistically significant.

RESULTS

Patient Characteristics

A total of 26 epithelial OC tumor samples were included in this study (8 serous cystadenocarcinomas, 7 mucinous cystadenocarcinomas, 9 endometrioid

Table 43. Correlation between Patient's Clinical Characteristics and Immunohistochemical Expression of Elf-1

Patient	Histologic Classification	Clinical Stage (FIGO, 1988)	Histologic Grade	Outcome	Elf-1–Stained Cells (%)	PCNA–LI (%)
1	serous	IA	grade 1	DOD	23.6	46.4
2	serous	IA	grade 1	NED	4.9	30.1
3	serous	IC	grade 2	NED	3.9	21.6
4	serous	IIIB	grade 2	DOD	19.9	61.6
5	serous	IIIC	grade 1	NED	9.3	60.8
6	serous	IIIC	grade 2	DOD	31.2	40.5
7	serous	IIIC	grade 3	DOD	44.0	77.4
8	serous	IV	grade 2	DOD	60.3	39.4
9	mucinous	IA	grade 1	NED	1.1	32.2
10	mucinous	IA	grade 1	NED	3.9	17.1
11	mucinous	IA	grade 1	NED	2.8	37.5
12	mucinous	IC	grade 1	AWD	11.7	20.8
13	mucinous	IIA	grade 3	NED	2.7	12.2
14	mucinous	IIIA	grade 2	NED	30.8	43.1
15	mucinous	IIIC	grade 3	DOD	49.9	59.9
16	endometrioid	IB	grade 1	NED	3.6	19.2
17	endometrioid	IC	grade 1	NED	1.9	39.1
18	endomethoid	IC	grade 1	AWD	20.2	60.7
19	endometrioid	IC	grade 1	NED	4.7	70.2
20	endometrioid	IIC	grade 1	AWD	28.9	17.3
21	endometrioid	IIIA	grade 3	DOD	77.9	50.9
22	endometrioid	IIIC	grade 2	NED	49.6	50.8
23	endometrioid	IIIC	grade 3	AWD	81.0	65.8
24	endometrioid	IIIC	grade 3	DOD	86.2	43.3
25	clear cell	IC	grade 2	AWD	37.5	67.7
26	clear cell	IIIA	grade 2	NED	28.1	53.2

AWD: Alive with disease, DOD: died of disease, NED: no evidence of disease, PCNA–LI: PCNA–labeling index.

adenocarcinomas, and 2 clear cell adenocarcinomas) (Table 43). Each sample was graded according to the International Federation of Gynecology and Obstetrics (FIGO) classification by three gynecologic pathologists without knowledge of the samples' Elf-1 expression. Other characteristics (clinical stage and clinical outcome as of February 2003) are shown in Table 43. As controls, 10 benign ovarian cystadenoma samples were also examined in this study.

Localization of Elf-1 Protein in Benign Ovarian Cystadenoma and Ovarian Carcinoma Samples

To examine the location of Elf-1 expression within the benign ovarian cystadenoma, we carried out immunohistochemical staining with anti-Elf-1 antibody. Elf-1 was weakly detected in 0–5.5% of the nuclei of benign cystadenoma of the ovary. To explore the possibility that Elf-1 is expressed in other cell types beyond epithelial cancer cells, we carried out double staining using antibodies against Elf-1 and cytokeratin, which is a specific marker for epithelial cells. Elf-1 was positively stained in all carcinoma cases (see Table 43). Elf-1 was primarily detected in the nucleus of OC cells, although some cytoplasmic staining was evident (Figure 81). We quantified the nuclear staining only because the majority of Elf-1 proteins were seen in the nucleus and Elf-1 was reported to be a transcription factor.

Correlation between the Percentages of Elf-1–Positive Tumor Cells and Proliferating Cell Nuclear Antigen–Labeling Index

The antigen PCNA is known to be present at all stages of the cell cycle except G0, and production of antibodies against PCNA serves as a marker of proliferating cells. To compare Elf-1 staining with this proliferative marker, we carried out Elf-1 staining along with PCNA staining. Some PCNA-positive cells were positive for Elf-1, and we found that Elf-1 expression was highly correlated with the proliferation index in OC tissues as calculated by the PCNA-labeling nuclei ratio (PCNA – LI = $20.858 + 0.144 \times$ Elf-1; $r^2 = 0.268$; $p = 0.04$).

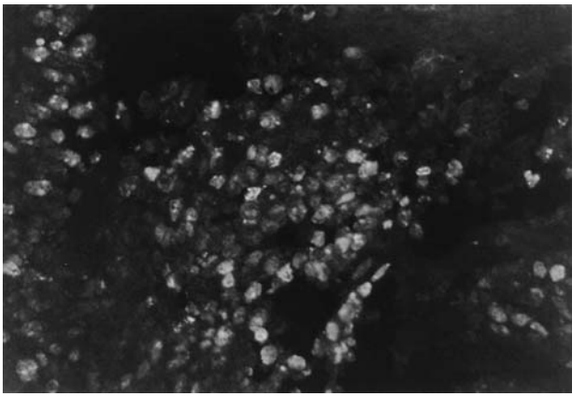

Figure 81. Photomicrographs of an ovarian carcinoma specimen from a patient with a grade 3 tumor. The nuclei of many cancer cells invading the stroma are positive for Elf-1. Original magnification, 200X.

Relationship between the Percentages of Elf-1–Positive Tumor Cells and Malignant Potential of Ovarian Carcinomas

In tumor-tissue samples from patients with OC, the percentage of Elf-l–stained cells was 10.8 ± 11.8% for stage I and II and 47.6 ± 24.9% for stage III and IV tissues (see Table 43, Figure 82). The number of Elf-1–positive cells was significantly higher for stage III and IV than for stage I and II ($p < 0.01$).

In tumor-tissue samples from ovarian carcinoma, the percentage of Elf-1–stained cells was 9.7 ± 9.4% for grade 1, 32.7 ± 17.3% for grade 2, and 57.0 ± 31.7% for grade 3 tissues (see Table 43, Figure 83). The number of Elf-1–positive cells was significantly higher in ovarian carcinomas designated as grade 3 than in carcinomas designated as grade 1 ($p < 0.01$) and significantly higher in grade 2 than in grade 1 carcinomas ($p < 0.01$).

In a comparison of patient outcomes, the percentage of Elf-l–stained cells was 11.3 ± 15.1% in patients with no evidence of disease, 35.9 ± 27.0% in those still alive but with disease, and 49.1 ± 24.4% in those dead as a result of disease (see Table 43, Figure 84). The number of Elf-1–positive cells was significantly higher in those dead from disease than in those with no evidence of disease ($p < 0.01$).

In a follow-up study of the 26 cases after surgical resection of the primary tumor (range: 24–60 months), four patients had died of disease. When the patients were divided into two groups according to the level of Elf-1 expression, we found that the prognosis of the two groups differed significantly ($p < 0.01$). The prognosis of patients with high levels of Elf-1 expression

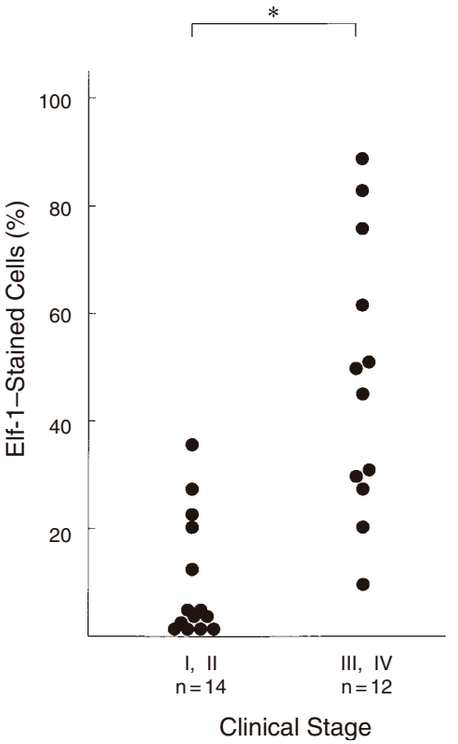

Figure 82. Percentage of Elf-1–stained cells at each clinical stage. Elf-1 expression was significantly higher in stages III and IV than in stage I or II (*: $p < 0.01$).

(>25%, n = 12) was significantly worse than that of those with low Elf-1 expression (≤25%, n = 14). The mean percentage of Elf-1 expression was about 25%, so this cutoff was used to divide the cases into the high and low groups. Comparing among histologic classifications, the percentage of Elf-1–stained cells was 24.6 ± 19.9% in serous cystadenocarcinoma, 14.7 ± 18.9% in mucinous cystadenocarcinoma, 39.3 ± 35.1% in endometrioid adenocarcinoma, and 32.8 ± 6.6% in clear cell adenocarcinoma (see Table 43). The Elf-1 positive rate was not statistically significant across histologic classifications.

DISCUSSION

We have been studying the molecular mechanisms underlying the carcinogenesis of endometrial and OC (Takai *et al.,* 2000, 2001 a–d, 2002a–d). In the current study, we examined the expression levels of Elf-1 in OC to elucidate the possible pathologic function of Elf-1 in OC. In OC, expression of Elf-1 was found to be significantly associated with clinical stage, histologic grade, and patient outcome. However, we cannot conclude that evaluation of Elf-1 staining is a better

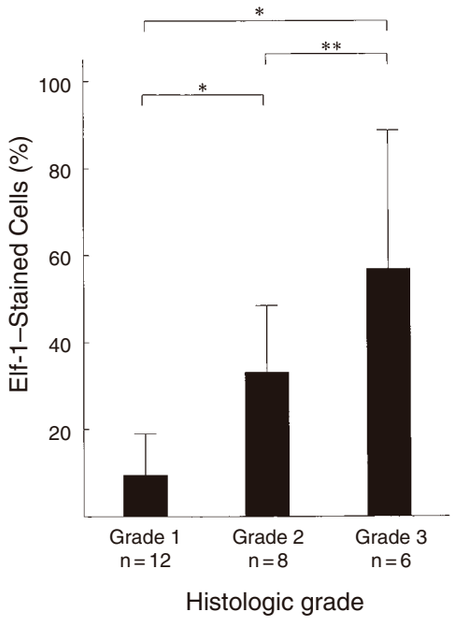

Figure 83. Percentage of Elf-1–stained cells for each histologic grade. Each bar represents the mean ± SD. Elf-1 expression was higher in ovarian carcinomas designated as grade 3 than in those designated as grade 1 (*: $p < 0.01$) or 2 (**: $p = 0.08$), and higher in ovarian carcinomas designated as grade 2 than in those designated as grade 1 (*: $p < 0.01$).

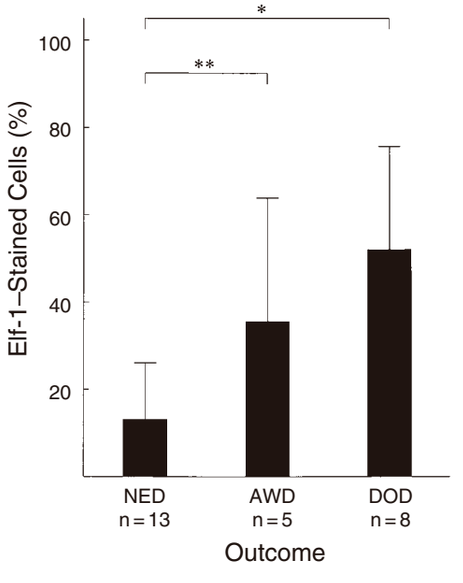

Figure 84. Percentage of Elf-1–stained cells for each patient outcome. Each bar represents the mean ± SD. Elf-1 expression was significantly higher for those dead as a result of disease than in those alive with no evidence of disease (*: $p < 0.01$) and higher in those still alive but with disease than in those alive with no evidence of disease (**: $p = 0.02$). AWD: Alive with disease, DOD: died of disease, NED: no evidence of disease.

predictor than staining for other tumor markers, because we did not compare Elf-1 expression with the expression of other markers. This study only suggests that Elf-1 expression parallels the presence of known histopathologic markers of the aggressiveness of ovarian carcinoma. In the future, a multivariate analysis should be performed to independently compare Elf-1 expression with outcome.

Immunohistochemical analysis confirmed the presence of Elf-1 primarily in the nucleus and partially in the cytoplasm of ovarian carcinoma cells, whereas benign ovarian cystadenoma cells were found to show rare and weak Elf-l immunoreactivity. In OC cells, as has been seen in prostate (Gavrilov *et al.,* 2001) and breast (Scott *et al.,* 2000) cancer cells, immunofluorescence staining of Elf-1 clearly showed that Elf-1 was expressed mainly in the nucleus, with comparatively weaker cytoplasmic staining. Given that Elf-1, with a molecular weight of 68 kDa, is too large for passive transport through the nuclear pores, active transport is assumed to be involved in the nuclear localization of Elf-1 (Bredemeier-Ernst *et al.,* 1997).

In OC, the most significant factors determining patient prognosis are histologic classification, clinical stage, and histologic grade. Statistical analysis showed that the frequency of Elf-1 expression within OC cells was significantly associated with clinical stage ($p < 0.01$) and was significantly higher in grade 3 than in grade 1 ($p < 0.01$) carcinomas, although the number of grade 3 cancers was small. Taken together, these results suggest that the presence of Elf-1 could be used as a prognostic marker to discriminate subpopulations of aggressive tumors.

In our study, double staining with Elf-1 and PCNA revealed that a proportion of OC cells co-expressed Elf-1 and PCNA. Furthermore, Elf-1 expression was highly correlated with the PCNA-labeling nuclei ratio. We therefore speculate that Elf-1 may play a role in cell proliferation in OC cells. We showed that patients with low Elf-1 expression had significantly longer survival rates than patients with high Elf-1 expression. These results should be considered with reservation because of the short follow-up period and small number of patients. We hope to confirm the present results in a larger number of patients and with a longer follow-up period. Analysis of Elf-1 expression could prove to be both a useful diagnostic marker and an important source of prognostic information in OC.

References

Bassuk, A.G., Barton, K.P., Anandappa, R.T., Lu, M.M., and Leiden, J.M. 1998. Expression pattern of the Ets-related transcription factor Elf-1. *Mol. Med. 4*:392–401.

Bredemeier-Ernst, I., Nordheim, A., and Janknecht, R. 1997. Transcriptional activity and constitutive nuclear localization of the Ets protein Elf-1. *FEBS Lett. 408*:47–51.

Dube, A., Thai, S., Gaspar, J., Rudders, S., Libermann, T.A., Iruela-Arispe, L., and Oettgen, P. 2001. Elf-1 is a transcriptional regulator of the Tie2 gene during vascular development. *Circ. Res. 88*:237–244.

Gavrilov, D., Kenzior, O., Evans, M., Calaluce, R., and Folk, W.R. 2001. Expression of urokinase plasminogen activator and receptor in conjunction with the ets family and AP-1 complex transcription factors in high grade prostate cancers. *Eur. J. Cancer. 37*:1033–1040.

Janknecht, R., Cahill, M.A., and Nordheim, A. 1995. Signal integration at the c-fos promoter. *Carcinogenesis 16*:443–450.

Janknecht, R., Taube, W., Lüdecke, H.J., and Pongs, O. 1989. Characterization of a putative transcription factor gene expressed in the 20-OH-ecdysone inducible puff 74EF in *Drosophila melanogaster. Nucleic Acids Res. 17*:4455–4464.

Moreau-Gachelin, F., Tavitian, A., and Tambourin, P. 1988. Spi-1 is a putative oncogene in virally induced murine erythroleukaemias. *Nature 331*:277–280.

Schmitt, M., Harbeck, N., Thomssen, C., Wilhelm, O., Magdolen, V., Reuning, U., Ulm, K., Hofler, H., Janicke, F., and Graeff, H. 1997. Clinical impact of the plasminogen activation system in tumor invasion and metastasis: prognostic relevance and target for therapy. *Thromb. Haemost. 78*:285–296.

Scott, G.K., Chang, C.H., Erny, K.M., Xu, F., Fredericks, W.J., Rauseher, F.J. III, Thor, A.D., and Benz, C.C. 2000. Ets regulation of the erbB2 promoter. *Oncogene 19*:6490–6502.

Takai, N., Miyazaki, T., Fujisawa, K., Nasu, K., and Miyakawa, I. 2000. Expression of c-Ets1 is associated with malignant potential in endometrial carcinoma. *Cancer 89*:2059–2067.

Takai, N., Miyazaki, T., Fujisawa, K., Nasu, K., Hamanaka, R., and Miyakawa, I. 2001a. Expression of Polo-like kinase (PLK) in ovarian cancer is associated with histological grade and clinical stage. *Cancer Lett. 164*:41–49.

Takai, N., Miyazaki, T., Fujisawa, K., Nasu, K., and Miyakawa, I. 2001b. Id1 expression is associated with histological grade and invasive behavior in endometrial carcinoma. *Cancer Lett. 165*: 185–193.

Takai, N., Miyazaki, T., Fujisawa, K., Nasu, K., Hamanaka, R., and Miyakawa, I. 2001c. Polo-like kinase (PLK) expression in endometrial carcinoma. *Cancer Lett. 169*:41–49.

Takai, N., Miyazaki, T., Fujisawa, K., Nasu, K., and Miyakawa, I. 2001d. Expression of receptor tyrosine kinase EphB4 and its ligand ephrin-B2 is associated with malignant potential in endometrial cancer. *Oncol. Rep. 8*:567–573.

Takai, N., Miyazaki, T., Nishida, M., Nasu, K., and Miyakawa, I. 2002a. c-Ets1 is a promising marker in epithelial ovarian cancer. *Int. J. Mol. Med. 9*:287–292.

Takai, N., Miyazaki, T., Nishida, M., Nasu, K., and Miyakawa, I. 2002b. Expression of survivin is associated with malignant potential in epithelial ovarian carcinoma. *Int. J. Mol. Med. 10*: 21l–216.

Takai, N., Miyazaki, T., Nishida, M., Nasu, K., and Miyakawa, I. 2002c. Survivin expression correlates with clinical stage, histological grade, invasive behavior and survival rate in endometrial carcinoma. *Cancer Lett. 184*: l05–116.

Takai, N., Miyazaki, T., Nishida, M., Nasu, K., and Miyakawa, I. 2002d. Ca^{2+}/calmodulin-dependent protein kinase IV expression in epithelial ovarian cancer. *Cancer Lett. 183*:185–193.

Tecimer, C., Doering, D.L., Goldsmith, L.J., Meyer, J.S., Abdulhay, G., and Wittliff, J.L. 2000. Clinical relevance of urokinase-type plasminogen activator, its receptor, and its inhibitor type 1 in ovarian cancer. *Int. J. Gynecol. Cancer 10*: 372–381.

Thompson, C.C., Brown, T.A., and McKnight, S.L. 1991. Convergence of Ets- and notch-related structural motifs in a heteromeric DNA binding complex. *Science 253*:762–768.

Wasylyk, B., Hahn, S., and Giovanne, A. 1993. The Ets family of transcription factors. *Eur. J. Biochem. 211*:7–18.

Wasylyk, B., Wasylyk, C., Flores, P., Begue, A., Leprince, D., and Stehelin, D. 1990. The c-ets proto-oncogenes encode transcription factors that cooperate with c-Fos and c-Jun for transcriptional activation. *Nature 346*:l91–l93.

23

Role of Immunohistochemical Expression of OCT4 in Ovarian Dysgerminoma

Antoinette Thomas and Liang Cheng

Introduction

OCT4 (OTF3, POU5Fl), is a POU-domain, octamer-binding transcription factor expressed in both mouse and human embryonic stem and germ cells (Hansis *et al.,* 2000, 2001). This protein is found in pluripotent cells of the embryo, primordial germ cells, and oocytes (Hansis *et al.,* 2000, 2001; Pesce *et al.,* 1998). The *oct4 (pouf1)* gene maps to the human chromosome 6p21.3 (Guillaudeaux *et al.,* 1993), and is down-regulated during differentiation to endoderm and mesoderm. After the ninth day of gestation, OCT4 expression is virtually undetectable in somatic cells. In adults, OCT4 messenger ribonucleic acid (mRNA) expression is found in the primordial germ cells of the ovary and testis and maturing oocytes but not in resting oocytes, brain, heart, liver, spleen, skeletal muscle, lung, kidney, or pancreas (Hansis *et al.,* 2000, 2001; Pesce *et al.,*1998).

OCT4 is a protein involved in normal development, which functions by regulating numerous downstream target genes. Abnormal OCT4 expression in mice may be associated with abnormal expression of critical developmental genes, and the absence of these proteins has been linked to early lethality (Looijenga *et al.,* 2003*).* Similar findings in human embryos support the conclusion that OCT4 is involved in the regulation of the differentiation of cells with pluripotent potential in humans (Hansis *et al.,* 2000, 2001). In malignant transformation, reactivation of OCT4 expression and translation do not commonly occur, although the protein is normally found in human embryonic germ cells and in the undifferentiated tumors that arise from them (Looijenga *et al.,* 2003).

Dysgerminoma of the ovary is an uncommon tumor, which can cause diagnostic difficulty. The prognosis and treatment options for dysgerminoma are vastly different from other tumor types (Williams, 1998; Zaghloul and Khattab, 1992) and an accurate diagnosis is critical for patient management. In this chapter we will describe how we used OCT4 immunohistochemistry (IHC) to aid in the diagnosis of dysgerminoma and exclusion of tumors that may mimic its appearance but have different biologic and therapeutic implications.

MATERIALS

Cases

Specimens from oophorectomies were obtained from the surgical pathology files. The tissues had been previously fixed in a 10% neutral buffered solution.

Handbook of Immunohistochemistry and *in situ* Hybridization of Human Carcinomas, Volume 4: Molecular Genetics, Gastrointestinal Carcinoma, and Ovarian Carcinoma

Paraffin-embedded tissue blocks were cut in 4 µm sections and were subsequently transferred to glass slides.

Materials for Immunohistochemical Staining

1. Affinity-purified polyclonal goat anti-OCT4 antibody (C20, sc 8629; Santa Cruz Biotechnology, Santa Cruz, CA; 1:500 dilution).
2. 1 mmol/L ethylenediamine tetraacetic acid (EDTA), pH 8.0.
3. 95°C waterbath.
4. 3% H_2O_2.
5. Protein Block (Dako, Carpinteria, CA).

METHODS

1. Prepare 95°C waterbath.
2. Place formalin-fixed and paraffin-embedded tissue sections cut at 4–5 µm thick sections on slides, and dry for 10 min at 65–70°C. Cool at room temperature, and check to see that all water has dried from the slides.
3. Deparaffinize, clear, and rehydrate. Once slides have begun deparaffinization, the tissue sections should not be allowed to dry until the immunostaining is complete.
4. Treat slides for 30 min at room temperature with an affinity-purified polyclonal goat anti-OCT4 antibody (C20, sc 8629; Santa Cruz Biotechnology, 1:500 dilution).
5. Incubate slides at 95°C for 30 min in 1 mmol/L EDTA (pH 8.0) for antigen retrieval.
6. Treat slides for 15 min in 3% H_2O_2 for inhibition of endogenous peroxidase activity.
7. Treat slides for 20 min in Protein Block (Dako) to block nonspecific binding sites.
8. Dehydrate and place a coverslip.

RESULTS AND DISCUSSION

Thirty-three cases of dysgerminoma from 33 patients, including 3 metastatic dysgerminomas, stained positively for OCT4. The tumor showed a universal nuclear staining pattern (greater than 90%) with little or no background staining (Figure 85). Rare, focal cytoplasmic staining was observed; however, because OCT4 is

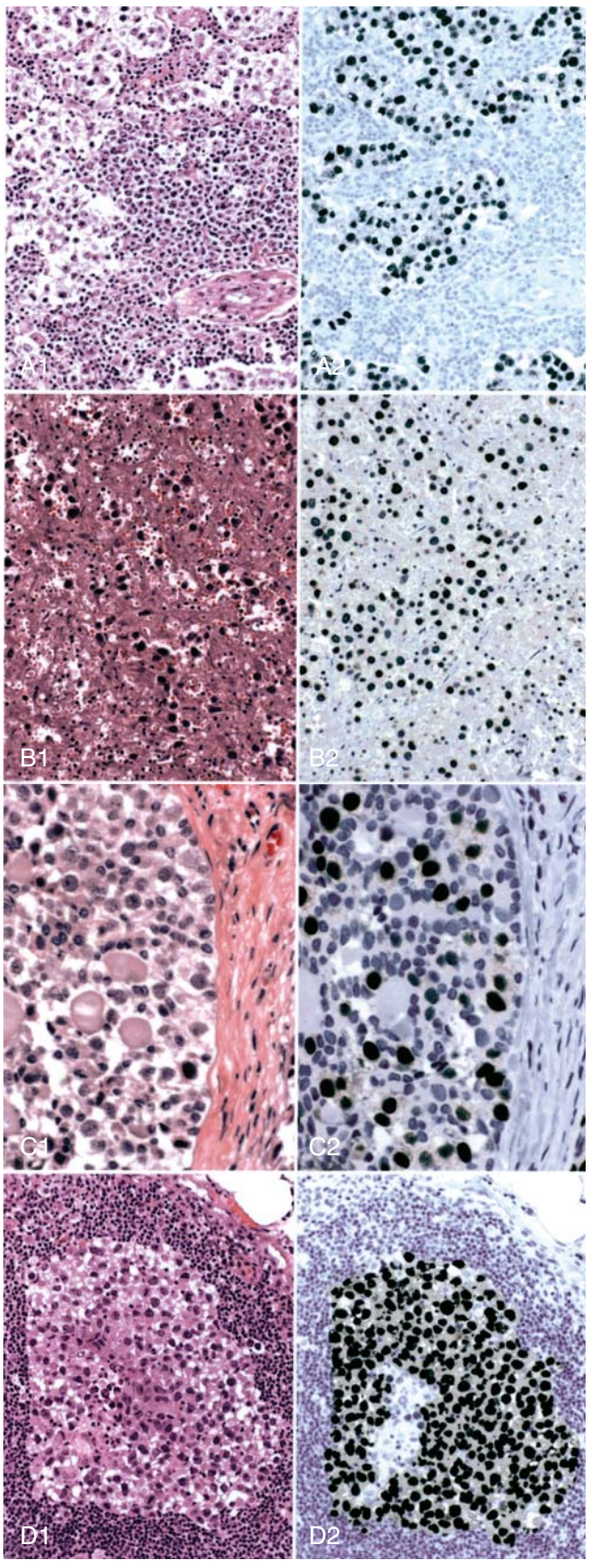

Figure 85. OCT4 immunostaining highlights dysgerminoma cells. **A:** Classic dysgerminoma. **B:** Dysgerminoma with necrosis. **C:** Germ cell components of gonadoblastoma are positive for OCT4. **D:** Metastatic dysgerminoma. **A1–D1:** Hematoxylin and eosin staining. **A2–D2:** Corresponding OCT4 immunostaining.

a nuclear transcription factor, only nuclear staining is considered a positive result. In cases of dysgerminoma with tumor necrosis, all cases showed universal nuclear positivity in areas of viable tumor; even nonviable tumor cells also appeared to be staining positively for OCT4 (see Figure 85B).

In addition, the following nondysgerminomatous tumors (111 cases) from the ovary were included in the study: mature teratoma, 14 cases; yolk-sac tumor, 4; Leydig cell tumor, 1; Sertoli cell tumor, 1; Sertoli-Leydig cell tumor, 13; granulosa cell tumor, 22; Brenner tumor, 3; carcinoid tumor, 4; struma ovarii, 2; fibroma, 5; thecoma, 1; clear cell adenocarcinoma, 14; serous adenocarcinoma, 5; endometrioid adenocarcinoma, 4; small cell carcinoma (hypercalcemic type), 6; stromal sarcoma, 1; malignant lymphoma, 6; metastic malignant melanoma, 1; metastatic carcinoid, 2; metastatic small cell carcinoma, 1; and metastatic lobular carcinoma of the breast, 1 (Table 44). All tumors were classified according to accepted criteria (Scully *et al.,* 1998). The International Federation of Gynecology and Obstetrics (FIGO) staging system for ovarian neoplasms was used (Greene *et al.,* 2002).

OCT4 immunostaining also highlights the germ-cell component of gonadoblastoma (see Figure 85C). Sex-cord cells of gonadoblastoma and syncytiotrophoblastic giant cells associated with dysgerminoma were immunohistochemically negative for OCT4. The oocytes of primordial follicles were negative for OCT4. None of the other tumor types, including mature teratoma, yolk-sac tumor, Sertoli-Leydig cell tumor, granulosa cell tumor, Brenner tumor, carcinoid tumor, struma ovarii, fibroma, thecoma, serous adenocarcinoma, endometrioid adenocarcinoma, diffuse large B-cell lymphoma, small cleaved B-cell lymphoma, Burkitt's lymphoma, metastatic malignant melanoma, metastatic carcinoid, metastatic small cell carcinoma, and metastatic lobular carcinoma of the breast showed OCT4 nuclear immunoreactivity, except for clear cell adenocarcinoma of the ovary. The staining of OCT4 in clear cell adenocarcinoma is usually focal (<10%) (Figure 86).

Dysgerminoma is a rare neoplasm, representing only 1–2% of all ovarian malignancies (Koonings *et al.,* 1989). Approximately 80% of cases are found in patients younger than 25 years of age, and thus it is of great importance to preserve fertility (Robboy *et al.,* 2002).

Table 44. Results of OCT4 Immunostaining in Various Histologic Types of Ovarian Tumors

Tumor Type	Number of Cases	OCT4 Immunostaining Results
Dysgerminomas	32	Positive in all cases, strong and diffuse
Gonadoblastoma	2	Positive in germ cell component
Metastatic dysgerminomas	3	Positive in all cases, strong and diffuse
Mature teratoma	14	Negative
Yolk-sac tumor	4	Negative
Leydig cell tumor	1	Negative
Sertoli cell tumor	1	Negative
Sertoli-Leydig cell tumor	13	Negative
Granulosa cell tumor		
Adult type	13	Negative
Juvenile type	9	Negative
Brenner tumor	3	Negative
Carcinoid tumor	4	Negative
Struma ovarii	2	Negative
Fibroma	5	Negative
Thecoma	1	Negative
Clear cell adenocarcinoma	14	Focal (<10%) positivity in 4 cases
Serous adenocarcinoma	5	Negative
Endometrioid adenocarcinoma	4	Negative
Small cell carcinoma, hypercalcemic type	6	Negative
Stromal sarcoma	1	Negative
Malignant lymphoma		
Diffuse B-cell type	2	Negative
Burkitt's lymphoma	3	Negative
Small cleaved B-cell type	1	Negative
Metastic malignant melanoma	1	Negative
Metastatic carcinoid	2	Negative
Metastatic small cell carcinoma	1	Negative
Metastatic lobular carcinoma of the breast	1	Negative

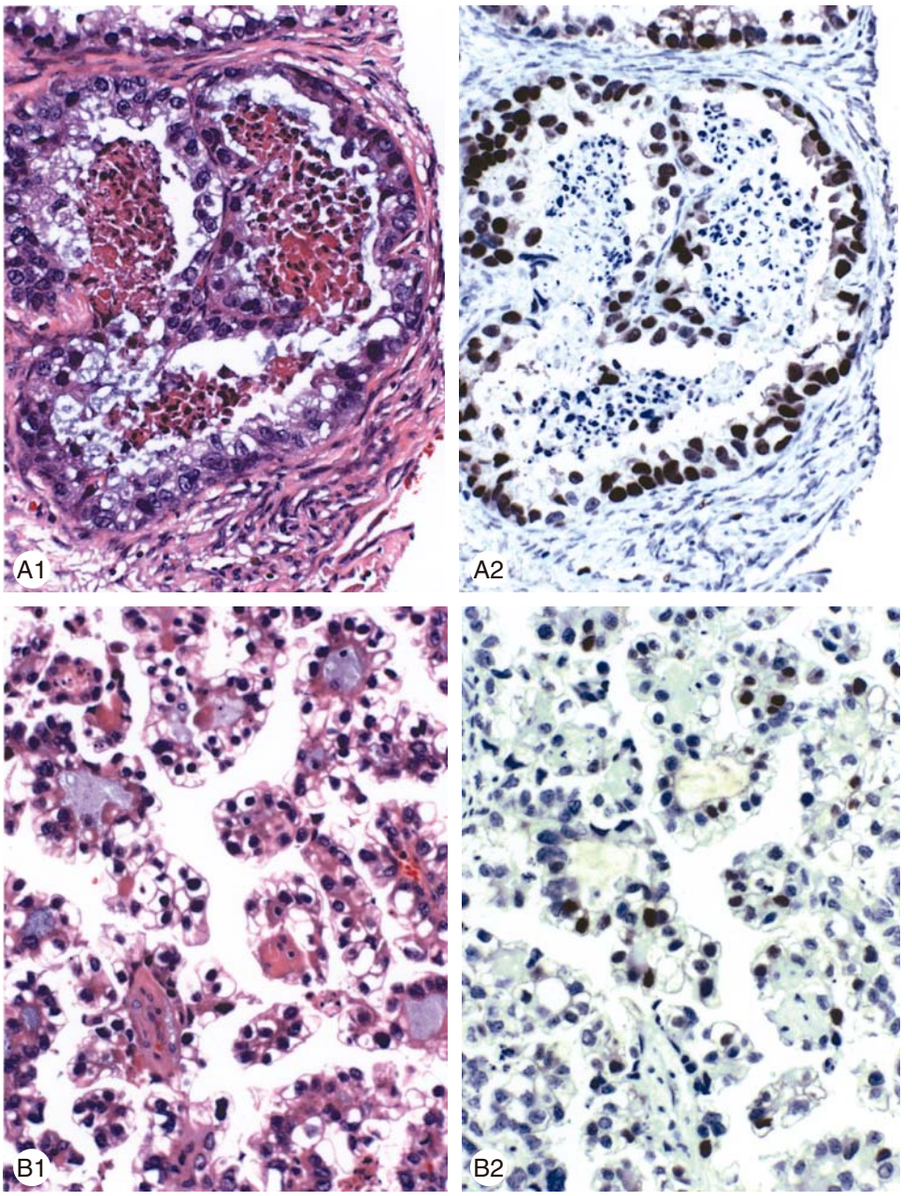

Figure 86. OCT4 immunostaining in clear cell adenocarcinoma of the ovary (**A** and **B**). Focal nuclear immunoreactivity for OCT4 is often noted. **A1** and **B1:** Hematoxylin and eosin staining. **A2** and **B2:** Corresponding OCT4 immunostaining.

Although dysgerminomas are rapidly growing tumors, they are confined to one ovary (FIGO stage 1A) in two-thirds of cases and to bilateral ovaries (stage 1B) in an additional 10% of instances. Metastatic spread occurs through the lymphatic system, first to the common iliac and inferior paraaortic lymph nodes and subsequently to mediastinal and supraclavicular nodes. Hematogenous spread to distal organs occurs late in the clinical course and most commonly deposits in the liver, lungs, kidneys, and bones (Robboy *et al.,* 2002).

Dysgerminomas have 5-year survival rates of 75–90% even with metastatic disease because it is radiosensitive and responds to cisplatin-based chemotherapy regimens (Williams, 1998; Zaghloul and Khattab, 1992). Grossly, dysgerminomas are usually firm, solid tumors with a smooth gray–white appearance with prominent

vessels and a smooth fibrous capsule. The size can vary from a few centimeters to masses that can extend up to 50 cm in greatest dimension. Histologically, the tumor is comprised of aggregates of cords of uniform, polyhedral cells (15–25 micrometers) with well-defined cell borders that are morphologically similar to primordial germ cells. The cells have an abundant amount of pale, slightly granular eosinophilic or clear cytoplasm. The round, centrally located nucleus contains a granular chromatin pattern, with usually one or occasionally two nucleoli. The cells are separated by connective tissue septae often containing lymphocytes. Ovarian dysgerminomas may co-exist with other malignant germ cell tumor types, and the prognosis of mixed germ cell tumors is dependent on the most aggressive germ cell element. Adequate sampling of the neoplasm is important to distinguish dysgerminoma from other germ cell tumors, especially yolk-sac tumor, because identifying the different malignant germ cell elements is of significant prognostic importance (Kurman *et al.,* 2002). In addition to yolk-sac tumor, the differential diagnosis for dysgerminoma includes undifferentiated carcinoma, clear cell adenocarcinoma, lymphoma, melanoma, granulosa cell tumor, and metastatic breast carcinoma, all of which have a significantly worse prognosis than dysgerminoma. The use of immunohistochemical panels facilitates a correct diagnosis. We should emphasize that cytokeratins can be focally positive in dysgerminoma (Lifschitz-Mercer *et al.,* 1995). Placental-like alkaline phosphatase (PLAP) reactivity can be seen in both dysgerminoma and other types of germ cell tumors, as well as in nonneoplastic germ cells (Burke and Mostofi, 1988). Juvenile granulosa cell tumor should also be considered in the differential diagnosis in the young age group, although histologically these tumors generally contain poorly formed follicular structures not seen in dysgerminomas (Kurman *et al.,* 2002). The combination of inhibin and OCT4 inimunostaining is useful in making the correct diagnosis. The cytoplasm of the dysgerminoma cells contains glycogen, which can be detected by periodic acid-Schiff (PAS) reaction. This reaction, however, varies from strong to very weak because the amount of glycogen is variable and prolonged fixation in formalin removes glycogen from the cells (Kurman *et al.,* 2002). The presence of a granulomatous response may obscure the underlying dysgerminoma cells. The presence of tumor necrosis often compromises the interpretation of immunohistochemical results as a result of high staining background. In our experience, OCT4 reliably identified dysgerminoma cells in the presence of necrosis (see Figure 85). Thus, it may be useful in the detection of small foci of metastatic dysgerminoma in extraovarian sites. We also found that focal OCT4 staining is common in clear cell adenocarcinoma of the ovary. Dysgerminomas occur most often in adolescent and young-adult women, whereas most clear cell adenocarcinomas occur in postmenopausal women. The difference in age-related incidence of dysgerminoma and clear cell adenocarcinoma of the ovary and the presence of papillary and tubulocystic patterns, as well as strong immunostaining for cytokeratin and negative staining for PLAP in the latter, aids in the differential diagnosis of these neoplasms.

OCT4 is involved in maintaining pluripotentiality and has been shown to be necessary for developmental functions of early embryogenesis and cell-type specific terminal differentiation events (Hansis *et al.,* 2000, 2001). The presence of OCT4 protein is related to pluripotency of human germ cell tumors and identifies tumor cells of primordial or embryonic germ cell origin, such as testicular seminoma and embryonal carcinoma (Looijenga *et al.,* 2003). No expression is demonstrated in more differentiated germ cell tumors, including yolk-sac tumor, immature and mature teratoma, and choriocarcinoma (Looijenga *et al.,* 2003). Our study is in agreement with that of Looijenga and co-workers who also found positive OCT4 immunoreactivity in 2 dysgerminoma cases (Looijenga *et al.,* 2003). In this large series of 33 dysgerminomas, we found nearly 100% staining of dysgerminoma cells in all cases. There was little or no background staining. The germ cell component of gonadoblastoma was also positive for OCT4. In contrast, none of the other tumor types showed OCT4 nuclear immunoreactivity with the exception of clear cell adenocarcinoma. Unlike its testicular counterpart, embryonal carcinoma is rarely seen in the ovary, and the distinction of embryonal carcinoma from dysgerminoma may be difficult. We had no cases of embryonal carcinomas, but presumably such a case would be positive for OCT4 because testicular embryonal carcinoma shows strong OCT4 nuclear immunoreactivity (Cheng *et al.,* 2004; Jones *et al.,* 2004; Looijenga *et al.,* 2003). Additional biomarkers, such as CD30 and c-kit, may be useful to distinguish embryonal carcinoma from dysgerminoma. Further investigation is warranted.

The histogenesis of dysgerminoma has been debated. Dysgerminoma may originate from the primordial germ cells that migrate to the ovary from the wall of the yolk sac during early embryogenesis (Witschi, 1948). Although Teilum believed that dysgerminoma is a primitive germ cell tumor that has not acquired the potential for further differentiation (Teilum, 1965), evidence has emerged that dysgerminoma cells have the potential for further differentiation (Lifschitz-Mercer *et al.,* 1995; Van Nierkerk *et al.,* 1993). Parkash and Carcangiu suggested that dysgerminoma may represent the stage of

earliest germ cell tumor differentiation that may give rise to other germ cell tumor types (1995). The strong and diffuse OCT4 immunostaining in dysgerminoma is indicative of the pluripotential nature of these tumor cells. Our data also support the viewpoint that gonadoblastoma is a biphasic tumor composed of germ cells and sex-cord cells. OCT4 immunostaining highlights the germ cell element. The ability of OCT4 to identify a small number of germ cells in gonadoblastoma would make it a useful marker for the distinction of gonadoblastoma from a similar tumor without germ cells, such as the sex-cord tumor with annular tubules.

In conclusion, OCT4 IHC is a useful diagnostic adjunct for the identification of primary ovarian dysgerminoma and gonadoblastoma. OCT4 may aid in the detection of small foci of metastatic dysgerminoma in extraovarian sites and may also help distinguish dysgerminoma from other primary and metastatic tumors in the ovary. Although clear cell adenocarcinoma may also show focal OCT4 positivity, clinical and histologic features are distinct from those seen in dysgerminomas.

References

Burke, A.P., and Mostofi, F.K. 1988. Placental alkaline phosphatase immunohistochemistry of intratubular malignant germ cells and associated testicular germ cell tumors. *Hum. Pathol. 19*:663–670.

Cheng, L. 2004. Establishing germ cell origin for metastatic tumors using OCT4 immunohisotochemitsry. *Cancer 101*:2006–2010.

Greene, F.L., Page, D.L., Flemming, I.D., Fritz, A.G., Balch, C.M., Haller, D.G., and Morrow, M. 2002. *American Joint Committee on Cancer Staging Manual,* 6th ed. New York: Springer-Verlag.

Guillaudeux, T., Mattei, M.G., Depetris, D., Le Bouteiller, P., and Pontarotti, P. 1993. *In situ* hybridization localizes the human OTF3 to chromosome 6p21.3→p22 and OTF3L to 12p13. *Cytogenet. Cell Genet. 63*:212–214.

Hansis, C., Grifo, J.A., and Krey, L.C. 2000. Oct-4 expression in inner cell mass and trophectoderm of human blastocysts. *Mol. Hum. Reprod. 6*:999–1004.

Hansis, C., Tang, Y.X., Grifo, J.A., and Krey, L.C. 2001. Analysis of Oct-4 expression and ploidy in individual human blastomeres. *Mol. Hum. Reprod. 7*:155–161.

Jones, T.D., Ulbright, T.M., Eble, J.N., Baldridge, L.A., and Cheng, L. 2004. OCT4 is a sensitive and specific marker for testicular seminoma and embryonal carcinoma. *Am. J. Surg. Pathol. 7*:935–940.

Koonings, P.P., Campbell, K., Mishell, D.R.J., and Grimes, D.A. 1989. Relative frequency of primary ovarian neoplasms: a 10-year review. *Obstet. Gynecol. 74*:921–926.

Kurman, R.J. (ed). 2002. *Blaustein's Pathology of the Female Genital Tract,* 5th ed. New York: Springer, 969–977.

Lifschitz-Mercer, B., Walt, H., Kushnir, I., Jacob, N., Diener, P.A., Moll, R., and Czernobilsky, B. 1995. Differentiation potential of ovarian dysgerminoma: an immunohistochemical study of 15 cases. *Hum. Pathol. 26*:62–66.

Looijenga, L.H., Stoop, H., de Leeuw, H.P., de Gouveia Brazao, C.A., Gillis, A.J., van Roozendaal, K.E., van Zoelen, E.J., Weber, R.F., Wolffenbuttel, K.P., van Dekken, H., Honecker, F., Bokemeyer, C., Perlman, E.J., Schneider, D.T., Kononen, J., Sauter, G., and Oosterhuis, J.W. 2003. POU5F1 (OCT3/4) identifies cells with pluripotent potential in human germ cell tumors. *Cancer Res. 63*:2244–2250.

Parkash, V., and Carcangiu, M.L. 1995. Transformation of ovarian dysgerminoma to yolk sac tumor: evidence for a histogenetic continuum. *Mod. Pathol. 8*:881–887.

Pesce, M., Wang, X., Wolgemuth, D.J., and Scholer, H. 1998. Differential expression of the Oct-4 transcription factor during mouse germ cell differentiation. *Mech. Dev. 71*:89–98.

Robboy, S.J., Anderson, M., Russell, P. (eds). 2002. *Pathology of the Female Reproductive Tract.* London: Churchill Livingstone, 641–646.

Scully, R.E., Young, R.H., and Clement, P.B. *Tumors of the Ovary, Maldeveloped Gonads, Fallopian Tube, and Broad Ligament.* Washington, DC: Armed Forces Institute of Pathology.

Teilum, G. 1965. Classification of endodermal sinus tumor (mesoblastoma vitellinum) and so-called "embryonal carcinoma" of the ovary. *Acta. Pathol. Microbiol. Scan 64*:407–429.

Van Niekerk, C.C., Ramaekers, F.C., Hanselaar, A.G., Aldeweireldt, J., and Poels, L.G. 1993. Changes in expression of differentiation markers between normal ovarian cells and derived tumors. *Am. J. Pathol. 142*:157–177.

Williams, S.D. 1998. Ovarian germ cell tumors: an update. *Semin. Oncol. 25*:407–413.

Witschi, E. 1948. Migration of the germ cells of human embryos from the yolk sac to the primitive gonadal folds. *Contrib. Emryol. 32*:69–80.

Zaghloul, M.S., and Khattab, T.Y. 1992. Dysgerminoma of the ovary: good prognosis even in advanced stages. *Int. J. Radiat. Oncol. Biol. Phys. 24*:161–165.

24

Immunohistochemical Validation of B7-H4 (DD-O110) as a Biomarker of Ovarian Cancer: Correlation with CA-125

Takashi Miyatake and Kenneth R. Shroyer

Introduction

Gene-chip microarray and proteomic methods have led to the detection of a wide range of potential diagnostic biomarkers. Biomarker validation using whole-tissue lysates or even microdissected cellular specimens, however, can provide only limited data about the specific association of the putative targets with lesional cell populations. Thus, many markers that have shown initial promise at the messenger ribonucleic acid (mRNA) or protein expression level have subsequently been discovered to reflect contamination by nonmalignant cellular tissue components, including stromal, endothelial, or inflammatory cells, rather than representing tumor cell-specific gene expression. Thus, in the era of gene-chip microarray and proteomic analyses, immunohistochemical analyses have reemerged as essential tools for cancer biomarker validation.

In this chapter we describe the application of conventional avidin-biotin complex (ABC)-based immunohistochemical methods for the validation of a novel biomarker of ovarian cancer, the B7-H4 (DD-O110) protein.

Despite aggressive surgery and chemotherapy, the prognosis for the women with ovarian cancer is poor, with a 1-year survival rate of 79% and a 5-year survival rate of 53% for all stages (American Cancer Society, 2003). Although ovarian cancer has a 5-year survival rate of 95% if diagnosed at an early stage, most cases are no longer confined to the ovary and have disseminated to other pelvic tissues, peritoneal surfaces, or lymph nodes at the time of initial diagnosis (American Cancer Society, 2003). Only 25% of all ovarian cancers are detected at an early stage. Thus, significant improvement in the survival of patients with ovarian cancer could depend on the development of novel screening tests to increase the detection of early-stage disease.

The gold-standard molecular marker for ovarian cancer is CA-125. The CA-125 antigen is a mucin-type glycoprotein with a protein moiety that is rich in serine, threonine, and proline (Lloyd *et al.,* 1997). Immunohistochemical investigations have shown that CA-125 is expressed in 61% of all ovarian surface epithelial carcinomas, including 92% of serous adenocarcinomas and 67% of endometrioid adenocarcinomas but in only

Handbook of Immunohistochemistry and *in situ* Hybridization of Human Carcinomas, Volume 4: Molecular Genetics, Gastrointestinal Carcinoma, and Ovarian Carcinoma

13% of mucinous adenocarcinomas (Jacobs and Bast, 1989). CA-125 has not been useful as a serologic marker for ovarian cancer because of low sensitivity for the detection of early-stage disease and frequent elevation in various benign disorders, including diverticulitis, uterine fibroids, endometriosis, benign ovarian cysts, tubo-ovarian abscesses, ectopic pregnancy, pregnancy, and menstruation (Jacobs *et al.,* 1999; Sjovall *et al.,* 2002). Thus, CA-125 has shown generally limited utility as a diagnostic marker for early-stage ovarian cancer.

Quantitative polymerase chain reaction (PCR) of more than 200 human tissue samples indicated that B7-H4 is highly expressed in human breast and ovarian cancers, but there is little or no B7-H4 expression in most normal tissues. B7-H4 (B7x, B7S1, or DD-O110) is a member of the B7 family that is known to be involved in the down-regulation of antigen-specific immune responses (Carreno and Collins, 2003). B7-H4 binding to receptors on activated T or B lymphocytes results in inhibition of T-cell activation, interleukin-2 (IL-2) production, and the development of cytotoxicity (Choi *et al.,* 2003; Prasad *et al.,* 2003; Sica *et al.,* 2003). Immunohistochemical studies have confirmed that B7-H4 is highly expressed in most breast and ovarian cancers and in a minority of non–small-cell lung cancers (Choi *et al.,* 2003; Tringler *et al.,* 2005). On the basis of these observations, it has been hypothesized that the expression of B7-H4 could help to cloak tumor cells from cell-mediated immune surveillance (Choi *et al.,* 2003; Tringler *et al.,* 2005).

In this chapter we will describe how we applied conventional immunohistochemical methods to validate the expression of B7-H4 as a biomarker of serous and endometrioid cancers of the ovary. In addition, we will describe our approach to compare the expression of B7-H4 and CA-125 in histologic sections to determine if B7-H4 could potentially complement CA-125 as a marker of early-stage disease.

MATERIALS

Immunohistochemical Staining

1. Formalin-fixed and paraffin-embedded tissue blocks of ovarian cancers (archival collections of the Department of Pathology, University of Colorado Health Sciences Center), including 12 serous adenocarcinomas and 12 endometrioid adenocarcinomas, were used.

2. B7-H4 (A57.1) mouse monoclonal antibody, immunoglobulin G_1 (IgG_1) (obtained through collaboration with diaDexus Inc., South San Francisco, CA), 0.4 µg/ml final concentration: Add 10 µl of 4 mg/ml B7-H4 stock antibody solution to 990 µl of antibody diluent (Antibody Diluent with Background Reducing Components, DakoCytomation, Carpinteria, CA). Add 80 µl of 1:99 B7-H4 stock solutions to 7920 µl of antibody diluent.

3. CA-125 mouse monoclonal antibody, IgG_1 (Clone Ov185: 1, Labvision, Westinghouse, CA), 1:10 final dilution: Add 800 µl of CA-125 antibody to 7200 µl of antibody diluent.

4. B7-H4 negative control immunoglobulin, IgG_1 (BD PharMingen, San Diego, CA), 0.4 µg/ml final concentration: Add 12.8 µl of IgG_1 κ (250 µg/ml stock concentration) to 7987 µl of antibody diluent.

5. CA-125 negative control immunoglobulin: IgG_1 (BD Pharmingen), 1.0 µg/ml final concentration: Add 32 µl of IgG_1 κ (250 µg/ml stock concentration) to 7968 µl of antibody diluent.

6. Full-length recombinant B7-H4 protein for B7-H4 blocking study (obtained through collaboration with diaDexus Inc.), 0.78 µg/ml final concentration.

7. Charged glass slides (Superfrost Plus, Fisher Scientific, Pittsburgh, PA).

8. Xylene.

9. 95% and 100% Ethanols.

10. 3.0% Hydrogen peroxide: Add 30 ml of 30% hydrogen peroxide to 270 ml of deionized water.

11. 20 mmol/L Sodium citrate buffer (pH 6.0) 20× stock solution: Add 94.4 g of sodium citrate and 16.8 g of citrate acid monohydrate to 1000 ml of deionised water. Adjust pH to 6.0 with 6N HCl. Store at 4°C. Dilute 1:19 for heat antigen-retrieval buffer. Readjust pH after dilution, as needed.

12. TBS-T buffer (Tris buffered saline/TWEEN-20; 10 mM Tris-HCl, 150 mM NaCl, 0.05% TWEEN-20, pH 7.6): Add 13.9 g of Tris crystallized free base, 60.6 g of Tris hydroxymethyl, and 87.66 g of sodium chloride to 750 ml of deionised water. Adjust pH to 7.6 with 6N HCl. Add 5 ml of TWEEN-20 and dilute to 1000 ml with deionized water. Store at 4°C. For working solution, dilute 1:9 with deionized water (2000 ml final).

13. Decloaking Chamber (Biocare Medical, Walnut Creek, CA).

14. DakoCytomation Autostainer Universal Staining System (DakoCytomation).

15. R.T.U. Vectastain Elite ABC Kit (R.T.U. Biotinylated Universal Antibody and anti-rabbit/mouse IgG, R.T.U Elite ABC Reagent Vector Labs, Burlingame, CA).

16. DakoCytomation Automation Hematoxylin (DakoCytomation).

17. DakoCytomation Liquid DAB (diaminobenzidine) (DakoCytomation).

18. Microscope slide coverslips (Fisher Finest Premium Cover Glass, Fisher Scientific, Pittsburgh, PA).

19. Toluene-based mounting medium (Richard-Allan Scientific, Kalamazoo, MI).

20. Tabletop refrigerated microcentrifuge (IEC Micromax/Micromax RF, Thermo Electron Corp., Waltham, MA).
21. Conventional light microscope (e.g., Olympus BX4 4–40× objectives).

METHODS

Immunohistochemical Staining

1. Cut and mount 5 µm thick sections of formalin-fixed and paraffin-embedded tissue blocks of ovarian tumors on charged glass slides.
2. Bake slides at 60°C overnight in slide drying oven.
3. Deparaffinize sections in 3 changes of xylene for 5 min each.
4. Soak sections in 3 changes of 100% ethanol for 5 min each, followed by 2 changes of 95% ethanol for 5 min each.
5. Bake slides at 60°C for 10 min in slide drying oven.
6. Soak the slides by 15 dips in 95% ethanol and rehydrate in 3 changes of deionized water for 5 min each.
7. Block endogenous peroxidase activity by incubating sections in 3% hydrogen peroxidase for 15 min.
8. Wash the slides in 3 changes of deionized water for 5 min each.
9. Perform antigen retrieval by heating sections in 20-mmol/L citrate buffer (pH 6.0) for 10 min at 25 psi in decloaking chamber.
10. Allow sections in citrate buffer to return to room temperature (20 min).
11. Wash sections in deionized water for 5 min.

Steps 12 to **24** are executed using the DakoCytomation Autostainer Universal Staining System:

12. Rinse the tissue sections with TBS-T.
13. Incubate each section with 300 µl of corresponding primary antibodies at room temperature (1 hr for B7-H4 and IgG_1 negative control and 30 min for CA-125 and IgG_1 negative control).
14. Rinse the slides with TBS-T.
15. Apply 300 µl R.T.U. Biotinylated Universal Antibody, anti-rabbit/mouse IgG and incubate for 30 min at room temperature.
16. Rinse the slides with TBS-T.
17. Apply 300 µl R.T.U. Elite ABC Reagent and incubate for 30 min at room temperature.
18. Rinse the slides with TBS-T.
19. Apply 300 µl DakoCytomation Liquid DAB and incubate for 3 minutes.
20. Rinse the slides with deionized water to stop reaction.
21. Apply 300 µl DakoCytomation Automation Hematoxylin and incubate for 3 min.
22. Rinse the slides with deionized water.
23. Rinse the slides with TBS-T.
24. Rinse the slides with deionized water.
25. Dehydrate sections in 95% ethanol (15 dips) followed by 100% ethanol (15 dips).
26. Soak slides in xylene (15 dips) and coverslip using mounting medium.

B7-H4 Immunohistochemical Blocking Study

Preincubate B7-H4 antibody with full-length recombinant B7-H4 protein (final concentration 0.25 µg/ml) for 1 hr at room temperature. Centrifuge at 2l,000xg (IEC Micromax/Micromax RF, Thermo Electron Corp.) for 10 min. Substitute supernatant for unblocked B7-H4 antibody solution and complete immunohistochemical staining procedures as described earlier.

Evaluation of B7-H4 Staining

The slides were observed by conventional light microscopy, with review of the entire histologic section from each case to evaluate for possible tumor microheterogeneity in antigen distribution. The proportion of B7-H4 and CA-125–positive tumor cells was estimated based on review of the entire tumor area of histologic sections, and the cells were scored on a scale from 0% to 100%. The cellular patterns of staining of B7-H4 and CA-125 were scored as (1+): predominantly apical membranous staining or (2+): circumferential membranous with dense cytoplasmic staining.

Statistical Analysis

The relationship between the proportion of B7-H4–positive cells and CA-125–positive cells was estimated by Spearman's rank correlation test. The Fisher's exact test was used for the assessment of the relationship between the patterns of staining and pathologic features. P-values ≤ 0.05 were considered to be statistically significant. Statistical analyses were done using SAS v9.1 (SAS Institute, Cary, NC).

RESULTS AND DISCUSSION

The validation of potential cancer biomarkers depends on the specific localization of the intended target antigen to malignant cellular components of tissues. Thus, the evaluation of immunohistochemical staining should include assessment of specificity and the association of signal with malignant tumor cells versus stromal cells;

inflammatory specificity of CA-125 staining was evaluated primarily by the utilization of matched nonimmune IgG negative-control sections and by evaluation of staining patterns in the context of histomorphology.

Both B7-H4 and CA-125 were detected in all cases, including 12 of 12 (100%) endometrioid adenocarcinomas and 12 of 12 (100%) serous adenocarcinomas. Both markers showed intense tumor cell membranous staining with variable levels of cytoplasmic staining and no nuclear reactivity. B7-H4 was detected in a higher proportion of tumor cells and showed greater signal at the level of individual cells than was seen for CA-125. Specifically, the proportion of tumor cells that expressed B7-H4 ranged from 40% to 100% (median 100%) in endometrioid carcinomas and from 20% to 100% (median 100%) in serous carcinomas. At the cellular level, B7-H4 showed intense circumferential membranous and cytoplasmic staining (pattern 2+) in 11 of 12 endometrioid tumors and in 11 of 12 serous tumors (Figure 87A and C). The proportion of tumor cells that stained for CA-125 staining ranged from 20% to 100% (median 65%) in endometrioid carcinomas and from 5% to 95% (median 55%) in serous carcinomas. In contrast to the pattern seen for B7-H4, a high proportion of cases showed a predominantly apical membranous pattern of CA-125 staining (pattern 1+) (see Figure 87B and D).

The proportion of B7-H4 and C-125-positive cells and the cellular patterns of staining did not show statistically significant correlations with histologic type, grade, or stage. Of note, however, B7-H4 was detected in a median of 100% of both stages I and II and advanced-stage cancer cells, but CA-125 was only detected in a median of 75% of stages I–II and 65% of stages III–IV cancer cells. Furthermore, there was a significant correlation between the proportion of B7-H4 and CA-125 positive cells in endometrioid adenocarcinomas ($p = 0.007$) but not in serous carcinomas ($p = 0.885$).

Current observations regarding the cellular localization of B7-H4 staining are consistent with a previous report by Choi *et al*. (2003). The previous report, however, summarized staining results in 26 ovarian cancer cases but did not subclassify results with regard to tumor histologic type, grade or stage. The previous study was also limited to the evaluation of frozen sections because the antibody used was apparently nonreactive with formalin-fixed archival histologic sections. Our observations are also consistent with previous studies

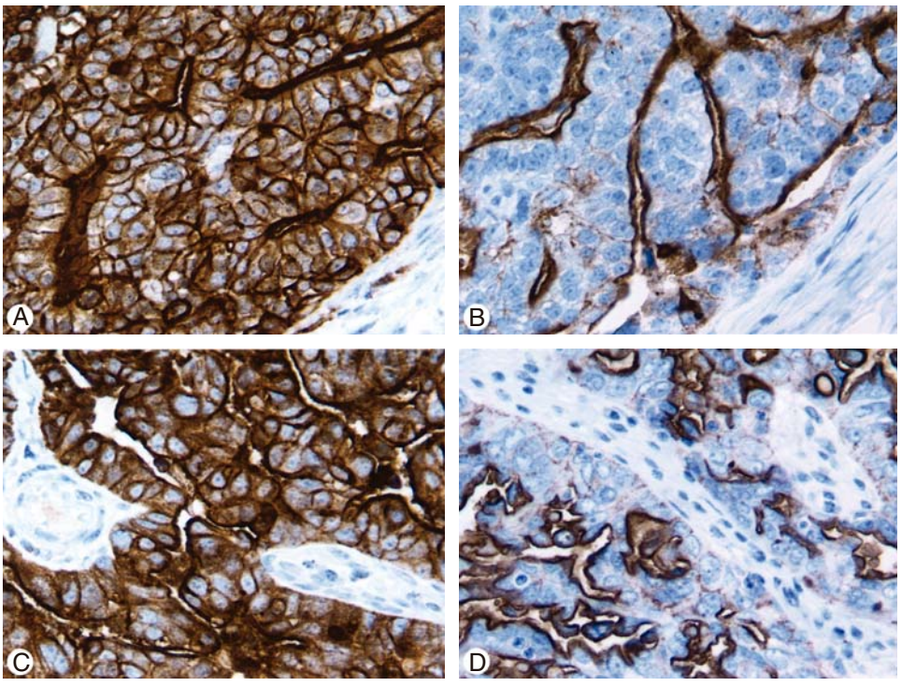

Figure 87. Immunohistochemical localization of B7-H4 and CA-125 proteins in ovarian tumors. **A:** B7-H4, endometrioid carcinoma; **B:** CA-125, endometrioid carcinoma; **C:** B7-H4, serous carcinoma; **D:** CA-125, serous carcinoma. Note 2+ circumferential membranous and cytoplasmic staining for B7-H4 **(Panels A, C),** and 1+ apical membranous with faint cytoplasmic staining for CA-125 **(Panels B, D)** (400X).

that have reported a predominantly apical membranous pattern of CA-125 detection in ovarian adenocarcinomas (Lagendijk *et al.,* 1999; Multhaupt *et al.,* 1999).

The current study was designed to specifically validate B7-H4 as a biomarker of ovarian serous and endometrioid adenocarcinomas. These tumors represent the two most common histologic types of ovarian surface epithelial–derived cancers. The third most common type, mucinous adenocarcinoma, was deliberately excluded from the study because most of these tumors are negative for both B7-H4 and CA-125 (Jacobs and Bast, 1989; Shroyer, unpublished observation). Although both B7-H4 and CA-125 were detected in essentially all serous and endometrioid tumors, B7-H4 appeared to detect a higher proportion of tumor cells and to show increased staining at the cellular level.

The current study was fundamentally observational in nature and did not address the functional role of B7-H4 (or CA-125) in ovarian cancer. Previous studies, however, suggest that both of these biomarkers may contribute to the suppression of immune surveillance (Carreno and Collins, 2003; Choi *et al.,* 2003; Kui Wong *et al.,* 2003; Sica *et al.,* 2003; Prasad *et al.,* 2003). Whereas B7-H4 may bind to a receptor on T cells to induce cell cycle arrest and inhibition of cytokine secretion, CA-125 may use its carbohydrate sequences as functional groups to induce specific immunomodulatory effects and to promote tumor progression (Kui Wong *et al.,* 2003). Thus, both B7-H4 and CA-125 expression may shield tumor cells from cell-mediated immune surveillance.

In conclusion, immunohistochemical studies validate B7-H4 as a biomarker of serous and endometrioid ovarian cancer. Data regarding the proportion of positive tumor cells and the cellular pattern of staining indicate that B7-H4 has the potential to complement CA-125 as a biomarker of early-stage disease and should be further investigated as a potential diagnostic or therapeutic target in patients with advanced-stage ovarian cancer.

Acknowledgments

This study was supported by a grant from diaDexus, Inc. The B7-H4 monoclonal antibody was developed and initially characterized at diaDexus, Inc. The authors appreciate the review of this manuscript by Drs. J. Papkoff, N. Kim, and Iris Simon. The authors also appreciate the expert statistical support provided by Dr. Kathleen Torkko, Department of Pathology, University of Colorado at Fitzsimons.

References

American Cancer Society: *American Cancer Society Facts and Figures 2003*. Washington, DC: American Cancer Society, 1–52.

Carreno, B.M., and Collins, M. 2003. BTLA: a new inhibitory receptor with a B7-like ligand. *Trends. Immunol. 24*: 524–527.

Choi, I.H., Zhu, G., Sica, G.L., Strome, S.E., Cheville, J.C., Lau, J.S., Zhu, Y., Flies, D.B., Tamada. K., and Chen, L. 2003. Genomic organization and expression analysis of B7-H4, an immune inhibitory molecule of the B7 family. *J. Immunol. 171*: 4650–4654.

Jacobs, I., and Bast, R.C. Jr. 1989, The CA-125 tumour-associated antigen: a review of the literature. *Hum. Reprod. 4*:1–12.

Jacobs, I.J., Skates, S.J., MacDonald, N., Menon, U., Rosenthal, A.N., Davies, A.P., Woolas, R., Jeyarajah, A.R., Sibley, K., Lowe, D.G., and Oram, D.H. 1999. Screening for ovarian cancer: a pilot randomised control trial *Lancet 353*:1207–1210.

Kui Wong, N., Easton, R.L., Panico, M., Sutton-Smith, M., Morrison, J.C., Lattanzio, F.A., Morris, H.R., Clark, G.F., Dell, A., and Patankar, M.S. 2003. Characterization of the oligosaccharides associated with the human ovarian tumor marker CA125. *J. Biol. Chem. 278*:28619–28634.

Lagendijk, J.H., Mullink, H., van Diest, P.J., Meijer, G.A., and Meijer, C.J. 1999. Immunohistochemical differentiation between primary adenocarcinomas of the ovary and ovarian metastases of colonic and breast origin: comparison between a statistical and an intuitive approach. *J. Clin. Pathol. 52*: 283–290.

Lloyd, K.O., Yin, B.W., and Kudryashov, V. 1997. Isolation and characterization of ovarian cancer antigen CA 125 using a new monoclonal antibody (VK-8): identification as a mucin-type molecule. *Int. J. Cancer. 71*:842–850.

Multhaupt, H.A., Arenas-Elliott, C.P., and Warhol, M.J. 1999. Comparison of glycoprotein expression between ovarian and colon adenocarcinomas. *Arch. Pathol. Lab. Med. 123*: 909–916.

Prasad, D.V., Richards, S., Mai, X.M., and Dong, C. 2003. B7S1, a novel B7 family member that negatively regulates T cell activation. *Immunity 18*:863–873.

Sica, G.L., Choi, I.H., Zhu, G., Tamada, K., Wang, S.D., Tamura, H., Chapoval, A.I., Flies, D.B., Bajorath, J., and Chen, L. 2003. B7-H4, a molecule of the B7 family, negatively regulates T cell immunity. *Immunity 18*:*849–861*.

Sjovall, K., Nilsson, B., and Einhorn, N. 2002. The significance of serum CA 125 elevation in malignant and nonmalignant diseases. *Gynecol. Oncol. 85*:175–178.

Tringler, B., Zhou, S., Pilkington, G., Torkko, K.C., Singh, M., Lucia, M.S., Heinz, D.E., Papkoff, J., and Shroyer, K.R. 2005. B7-H4 is highly expressed in ductal and lobular breast cancer. *Clin. Cancer Res. 11*:1842–1848.

This Page Intentionally Left Blank

25

Role of Immunohistochemical Expression of Alpha Glutathione S-Transferase in Ovarian Carcinoma

Andrew J. Tiltman

Introduction

The glutathione S-transferases (GST) are a group of dimeric isoenzymes, which have a wide distribution within the body and many different functions. In general they conjugate with hydrophobic molecules to allow further metabolism including the detoxification of foreign and endogenous toxins and intracellular transport (Mannervik, 1985; Meister and Anderson 1983). They are classified into three groups: basic, near neutral, and acidic, respectively known as alpha, mu, and pi GST. Previously known as ligandin, α-GST has intracelluar transport functions in hepatocytes and is found within the proximal convoluted tubules of the kidney, where its function is uncertain. It has also been shown to act as $\delta^{4\text{-}5}$ isomerase, an isoenzyme required for steroidogenesis (Benson *et al.,* 1977; Pettersson and Mannervik, 2001), and δ^5 androstene-3-17-dione has been shown, *in vitro,* to be one of its ligands. Immunohistochemistry (IHC) has demonstrated α-GST in steroid-producing cells in the ovary, testes, and adrenal cortex (Campbell *et al.,* 1980; Tiltman, 1984; Tiltman and Haffajee, 1999b). It has also been shown to be present in both benign and malignant ovarian neoplasms (Green *et al.,* 1993; Tiltman and Ali, 2001).

MATERIALS

1. Phosphate buffer saline (PBS) (pH 76).
2. Trypsin.
3. Citrate buffer: Citric acid, pH 6.0/Tris base, pH 10.0/Tris urea, pH 9.5/Tris ADTA pH 9.
4. Quenching solution: 3 ml Hydrogen peroxide + 97 ml methanol/3 ml hydrogen peroxide + 97 ml distilled water.
5. Primary antibody: Polyclonal antibody to alpha glutathione S-transferase (α-GST) (Novocastra Laboratories, Newcastle upon Tyne, UK).
6. Secondary antibody: Universal biotinylated horse anti-rabbit/mouse immunoglobulin G (IgG); 1:200 dilution in PBS.
7. Avidin-biotin complex immunodetection kit.

8. Diaminobenzidine (DAB).
9. Mayer's hematoxylin.

METHODS

Controls

1. Positive control use normal ovarian corpus luteum.
2. Negative controls—omit primary antibody.

Antigen Retrieval

Only required when tissue has been fixed in formalin for longer than 48 hr.

1. Incubate sections in 1% trypsin in PBS for 15 min at 37°C.
2. Rinse in running tap water.
3. Immerse slides in citrate buffer (pH 6.0) for 10 min, 700-W microwave at medium power.
4. Rinse in PBS (pH 7.6).

Immunohistochemistry

1. Dewax and hydrate sections.
2. Treat for antigen retrieval if required.
3. Incubate slides in quenching solution for 30 min.
4. Rinse well in PBS.
5. Incubate with primary antibody, dilution 1/100, overnight at 4°C.
6. Rinse in PBS.
7. Apply secondary antibody for 30 min.
8. Rinse in PBS.
9. Apply avidin-biotin complex immunodetection system.
10. Rinse in PBS.
11. Stain with DAB for 5 min.
12. Rinse in tap water.
13. Counterstain with Mayer's hematoxylin.
14. Dehydrate and mount.

RESULTS

Positive staining may be intracytoplasmic or intranuclear, and the distribution needs to be distinguished. With strong intracytoplasmic staining there may be overlayering of the nucleus.

Sex-Cord Stromal Tumors

Sex-cord stromal tumors show strong positive intracytoplasmic staining in steroid hormone–producing cells.

1. In most adult granulosa cell tumors the tumor cells show weak intranuclear staining and negative or equivocal intracytoplasmic staining. Most show strong intracytoplasmic staining of stromal cells lying between tumor cells. Juvenile granulosa cell tumors frequently show strong intracytoplasmic staining of tumor cells. Luteinized granulosa cell tumors may also show strong positive intracytoplasmic staining of tumor cells. Unilocular granulosa cell tumors frequently show intracytoplasmic staining.
2. Theca cell tumors are generally weakly positive unless they show luteinization when the intracytoplasmic staining is strong. Fibromas and fibrosarcomas are generally negative.
3. Luteinized cells of sclerosing stromal tumors are strongly intracytoplasmic positive.
4. The Leydig cells of Sertoli–Leydig cell tumors are strongly intracytoplasmic positive. Sertoli cells are variable, with most showing some weak intranuclear staining but negative in the cytoplasm.
5. Steroid cell tumors show positive intracytoplasmic staining, but this might be weak in those examples showing marked cytoplasmic clearing.

Epithelial/Stromal Tumors

With the exception of mucinous carcinomas the tumor cells of epithelial tumors of the ovary are generally negative. The stromal cells, however, often show positive intracytoplasmic staining (Figure 88).

1. Benign serous tumors and serous carcinomas are negative. Occasional tumors show some stromal intracytoplasmic positivity.

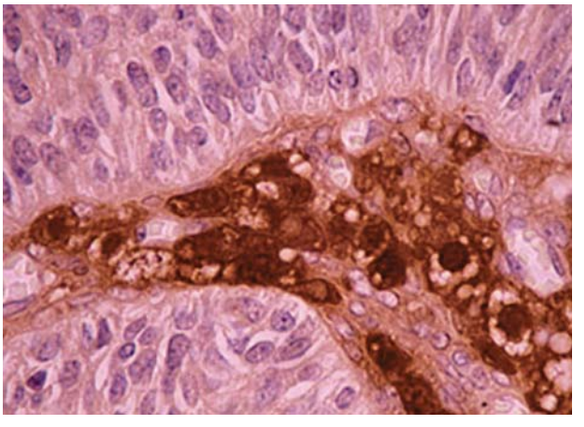

Figure 88. Malignant Brenner tumor with functioning stroma. Patient had raised serum testosterone. Tumor cells are negative. Stromal cells show positive staining for alpha-glutathione S-transferase (α-GST).

2. Mucinous carcinomas usually show some focal intracytoplasmic staining in tumor cells. Approximately half of the borderline tumors show focal staining, but it is generally negative within benign mucinous cystadenomas. Some intracytoplasmic staining of stromal cells is almost always present.

3. Endometrioid carcinomas show negative staining for tumor cells, but stromal cell may show focal or diffuse intracytoplasmic staining.

4. Brenner tumors and transitional cell carcinomas are generally negative, but all show positive intracytoplasmic staining of the stromal cells.

Germ Cell Tumors

1. Dysgerminomas are totally negative.

2. Yolk-sac tumors may show positive intranuclear and intracytoplasmic staining in focal areas. If intestinal differentiation is present, this may show intracytoplasmic staining. Yolk-sac tumors may show positively stained luteinized cells in the nonneoplastic stroma. Hepatoid cells in a Yolk-sac tumor have not been tested but are expected to be positive.

3. Immature teratomas are generally negative. There is no record of the status of mature teratomas, but this would depend on the adult-type tissues present.

DISCUSSION

The transferase α-GST, particularly isoenzyme A1-1, has been shown to act as δ^{4-5} isomerase, which is active in the conversion of dehydroepiandrosterone to androstenedione and pregnenolone to progesterone (Benson *et al.,* 1977; Pettersson and Mannervik, 2001). Previous immunohistochemical studies of the normal ovary have demonstrated a distribution of α-GST consistent with that function (Tiltman 1984; Tiltman and Haffajee, 1999b). It has also been demonstrated in the steroid-producing cells of the adrenal cortex and testis (Campbell, 1980). However, significant amounts of α-GST are also present in the liver and kidney, where their functions are various but include the intracytoplasmic transport of hydrophobic substances. Among others, the ligands include steroid hormones. Thus, the interpretation of the significance of immunohistochemical localization of α-GST by the polyclonal antibody commercially available is complicated by this multiplicity of function. In the correct setting, intracytoplasmic localization of α-GST is thought to represent a steroidogenic function and the intranuclear localization represents an intracellular transport function. The function of intracytoplasmic α-GST in cells not normally steroidogenic is unknown.

In the normal ovary, theca cells are responsible for androstenedione and testosterone production and the granulosa cells convert these to estrone or estradiol respectively by aromatization using the enzyme P450-arom. Normal granulosa cells lack 17α-hydroxylase (P450c17), which is required for androstenedione production. Progesterone production by the granulosa cells of the corpus luteum does require δ^{4-5} isomerase as a co-enzyme with 3 β-hydroxysteroid dehydrogenase in the conversion of pregnenalone to progesterone.

Some adult-type granulosa cell tumors are estrogenic. Clearly malignant granulosa cells might manifest functions not found in normal cells, but the positive staining for δ^{4-5} isomerase in the stromal cells and not tumor cells suggests that the estrogenic activity of granulosa cell tumors is the result of functionally active stromal cells. Some luteinized granulosa cell tumors produce progesterone (Young *et al.,* 1994). Because this requires the δ^{4-5} isomerase activity, the granulosa cells are, as expected, positive. Occasional granulosa cell tumors are androgenic, and a disproportionate number of these are unilocular granulosa cell tumors (Nakashima *et al.,* 1984). Unilocular granulosa cell tumors usually show positive intracytoplasmic staining in keeping with this finding.

Normal and neoplastic Leydig cells are androgen producing. 3 β-hydroxysteroid dehydrogenase, which co-acts with δ^{4-5} isomerase in steroidogenesis, has been immunohistochemically demonstrated in the Leydig but not the Sertoli cells in Sertoli–Leydig cell tumors (Costa *et al.,* 1994). Thus, Leydig cells show strong positive intracytoplasmic staining for α-GST. This strong staining of the Leydig cells may help to confirm the diagnosis of poorly differentiated Sertoli–Leydig cell tumors. Sertoli cells show only weak staining in both the cytoplasm and nucleus. This might indicate an intracellular transport function.

Some epithelial tumors, including metastatic carcinomas, have a hormonally functioning stroma (Scully *et al.,* 1998). Stromal cells, particularly in mucinous and endometrioid tumors, have been shown to contain enzymes related to steroidogenesis (Janovski and Paramanandhan, 1973). It seems probable, therefore, that the positive staining for α-GST in the stromal cells of epithelial tumors reflects the capability of these cells for steroidogenesis.

The frequent positive staining in the stroma of mucinous and the uncommon staining in serous tumors reflects the observation that the former are more frequently estrogenic than the latter. Estrogen production requires aromatization of androstenedione or testosterone. Although aromatase activity has been demonstrated by ovarian carcinoma cells *in vitro* (Thompson *et al.,* 1988), a peripheral conversion in adipose tissue appears more likely. 17β-hydroxysteroid dehydrogenase has been demonstrated in the epithelial cells of

both mucinous and serous carcinomas (Sasano *et al.*, 1996). 17β-hydroxysteroid dehydrogenase acts to convert estrone to estradiol. If both aromatase and 17β-hydroxysteroid dehydrogenase activity is present in ovarian carcinoma cells, the focal positive staining for α-GST in epithelial cells might be demonstrating δ^{4-5} isomerase. Other GSTs, particularly π-GST, are involved with detoxification of endogenous and exogenous toxins. Because intracytoplasmic positive staining is seen more frequently in malignant rather than benign mucinous tumors, it is possible that a detoxification function of α-GST is up-regulated in these cells.

Yolk-sac tumors show both intracytoplasmic and intranuclear staining, suggesting some intracellular transport function. Embryologically, the yolk sac is in close association with the hepatobiliary anlagen. This may be the reason for hepatoid differentiation in some yolk-sac tumors, and the staining for α-GST in the tumor cells may be a recapitulation of the staining of hepatocytes. It seems unlikely that it indicates any steroidogenic activity.

In conclusion, IHC for α-GST in ovarian cancer is best used as a marker for steroidogenesis. This may be to confirm hormone production or, with association with a panel of other antibodies, to confirm a diagnosis of, for example, poorly differentiated Sertoli–Leydig cell tumors. The increased frequency of positive staining of the tumor cells in mucinous carcinomas as opposed to the usual negative staining in benign mucinous tumors is probably of limited value in diagnosis.

References

Benson, A.M., Talalay, P., Keen, J.H., and Jakoby, W.B. 1977. Relationship between the soluble glutathione dependent delta 5′3-ketosteroid isomerase and the glutathione S-transferases of the liver. *Proc. Natl. Acad. Sci. USA 74*:158–162.

Campbell, J.A.H., Bass, N.M., and Kirsch, R.E. 1980. Immunohistochemical localization of ligandin in human tissues. *Cancer 45*:503–510.

Costa, M.J., Morris, R., and Sasano, H. 1994. Sex steroid biosynthesis enzymes in ovarian sex-cord stromal tumors. *Int. J. Gynecol. Pathol. 13*:109–119.

Green, J.A., Robertson, L.J., and Clarke, A.H. 1993. Glutathione S-transferase expression in benign and malignant ovarian tumors. *Brit. J. Cancer 68*:235–239.

Janovski, N.A., and Paramanandhan, T.L. 1973. *Ovarian Tumors: Tumors and Tumor Like Conditions of the Ovaries, Fallopian Tubes and Ligaments of the Uterus.* Philadelphia: Saunders, 120.

Mannervik, B. 1985. The isoenzymes of glutathione transferase. *Adv. Enzymol. and Related Areas 57*:357–417.

Meister, A., and Anderson, M.E. 1983. Glutathione. *Ann. Rev. Biochem. 52*:711–760.

Nakashima, N., Young, R.H., and Scully, R.E. 1984. Androgenic granulosa cell tumors of the ovary. *Arch. Pathol. Lab. Med. 108*:786–791.

Pettersson, P.L., and Mannervik, B. 2001. The role of glutathione in the isomerization of δ^5 androstene-3-17-dione catalyzed by human glutathione transferase A1-1. *J. Biol. Chem. 276*: 11698–11704.

Sasano, H., Suzuki, T., Niikura, H., Kaga, K., Sato, S., Yajima, A., Rainey, W.E., and Nagura, H. 1996. 17β-Hydroxysteroid dehydrogenase in common epithelial ovarian tumors. *Mod. Pathol. 9*:386–391.

Scully, R.E., Young, R.H., and Clement, P.B. 1998. Ovarian tumors with functioning stroma. In: Tumors of the ovary, maldeveloped gonads, fallopian tube and broad ligament. *Atlas of Tumor Pathology: Third Series.* Washington, DC: AFIP, pp. 373–378.

Thompson, M.A., Adelson, M.D., Kaufaran, L.M., Marshall, L.D., and Cable, D.A. 1988. Aromatization of testosterone by epithelial tumor cells cultured from patients with ovarian cancer. *Cancer Res. 48*:6491–6497.

Tiltman, A.J. 1984. Ligandin in the human ovary. *J. Pathol. 142*: 61–66.

Tiltman, A.J., and Ali, H. 2001. Distribution of alpha glutathione S-transferase in ovarian neoplasms: an immunohistochemical study. *Histopathology 39*:266–272.

Tiltman, A.J., and Haffajee, Z. 1999a. Sclerosing stromal tumors, thecomas and fibromas of the ovary: an immunohistochemical profile. *Int. J. Gynecol. Pathol. 18*:254–258.

Tiltman, A.J., and Haffajee, Z. 1999b. The distribution of glutathione S-transferases in the human ovary: an immunohistochemical study. *Gynecol. Obstet. Invest. 47*:247–250.

Young, R.H., Oliva, E., and Scully, R.E. 1994. Luteinized adult granulosa cell tumors of the ovary: a report of four cases. *Int. J. Gynecol. Pathol. 13*:302–310.

26

Role of Immunohistochemical Expression of Aminopeptidases in Ovarian Carcinoma

Fumitaka Kikkawa, Kazuhiko Ino, Hiroaki Kajiyama, Kiyosumi Shibata, Seiji Nomura, and Shigehiko Mizutani

Introduction

Cell-surface aminopeptidases, such as neutral endopeptidase (NEP/CD10), insulin-regulated aminopeptidase (IRAP/P-LAP), and dipeptidyl peptidase IV (DPPIV/CD10), degrade a variety of peptide factors and hormones and influence many cellular functions. Studies have shown that these aminopeptidases play key roles in regulating growth, differentiation, and signal transduction of many cellular systems by modulating the activity of peptide factors. Thus, abnormalities in the expression pattern or enzymatic function of these aminopeptidases should result in altered peptide activation or inactivation. These alterations may lead to disruption of normal cellular homeostasis and may contribute to neoplastic transformation or tumor progression.

We demonstrated in 2001 that neutral endopeptidase (NEP)/CD10 is highly expressed in stromal cells of the normal endometrium and grade 1 endometrial endometrioid adenocarcinoma, but its expression is decreased or lost with advancing tumor grade (Suzuki *et al.*, 2001). In contrast to NEP expression in endometrial stroma, DPPIV is known to be expressed in endometrial glandular cells. We also demonstrated that DPPIV was expressed and localized in normal endometrium and endometrial endometrioid adenocarcinoma and that DPPIV expression decreased with the advancing tumor grade (Khin *et al.*, 2003). We also found that P-LAP (placental leucine aminopeptidase) was expressed in endometrial adenocarcinoma and that the expression increased with advancing grade (Suzuki *et al.*, 2003).

Ovarian carcinoma (OC) is a major cause of death from gynecologic malignancy. However, the regulatory mechanisms responsible for malignant transformation and progression in this tumor remain to be clarified. Studies have demonstrated that certain peptide growth factors and peptide hormones are involved in the progression of epithelial OCs. Expression and function of cell-surface aminopeptidases in OC have not yet been studied. This chapter focuses on expression and localization of these aminopeptidases in ovarian tumor by immunohistochemical analysis, and on expression patterns related to neoplastic transformation, differentiation, and histologic type.

Handbook of Immunohistochemistry and *in situ* Hybridization of Human Carcinomas, Volume 4: Molecular Genetics, Gastrointestinal Carcinoma, and Ovarian Carcinoma

MATERIALS AND METHODS

Tissues

Formalin-fixed and paraffin-embedded tissues were surgically obtained from patients with myoma uteri or ovarian tumor who underwent surgery at Nagoya University Hospital. Tumor histology and grade were determined according to the criteria of the World Health Organization (grade 1, well-differentiated; grade 2, moderately differentiated; grade 3, poorly differentiated). Clinical staging was determined according to the Federation of International Gynecology and Obstetrics (FIGO).

Immunohistochemistry

Immunohistochemical staining was performed using the avidin-biotin immunoperoxidase technique (Histofine SAB-PO kit, Nichirei, Tokyo, Japan). Sections were cut at a thickness of 4 μm, then deparaffinized and rehydrated. For heat-induced epitope retrieval, deparaffinized sections in 10 mM citrate buffer were treated 3× for 5 min at 90°C and 750 W in a microwave oven. Endogenous peroxidase activity was blocked by incubation with 3% H_2O_2 in methanol for 15 min, and nonspecific immunoglobulin binding was blocked by incubation with 10% normal rabbit or goat serum in phosphate buffer saline (PBS) for 10 min. The primary antibody for aminopeptidases was added to the tissue sections and incubated overnight in a moist chamber at 4°C. Mouse monoclonal antibody (mAb) to human NEP/CD10 (NCL-CD10-270) was purchased from Novocastra Laboratories (Newcastle, UK) and used at dilution of 1:50. Mouse mAb to human DPPIV (TS-145) was generously donated by Dr. Ryuzo Ueda, Nagoya City University. Rabbit polyclonal antibody was generously donated by Dr. Masafumi Tsujimoto and used at a dilution of 1:200. After washing with PBS, secondary biotinylated antibody (Nichirei, Tokyo, Japan) was applied for 10 min at room temperature. After washing with PBS, horseradish streptavidin-peroxidase conjugate was applied for 30 min, then the sections were incubated with the peroxidase substrate, 3-amino-9-ethylcarbazole (AEC, Nichirei) as a chromogen in PBS containing 0.01% H_2O_2 for 10–15 min to develop a red reaction product. Finally, slides were counterstained with Mayer's hematoxylin. For the negative control, mouse immunoglobulin G (IgG) was replaced with primary antibody. Sections from placenta, normal endometrium of secretary phase, and normal kidney proximal tubules were used as a positive control for P-LAP, NEP, and DPPIV staining, respectively. Staining intensity was scored semi-quantitatively on a 3-tiered scale (negative: –; weakly positive: +; strongly positive staining; ++) relative to known positive and negative controls. Each specimen was scored 2×, independently by 2 investigators.

Statistics

The nonparametric Kruskal-Wallis test was performed to compare the staining scores among all groups. In addition, the staining score was compared among histologic types using the Mann-Whitney test with Bonferroni correction. $P < 0.05$ was considered significant.

RESULTS AND DISCUSSION

Neutral Endopeptidase Expression

Introduction

Neutral endopeptidase is a 90-100 kDa cell-surface metalloprotease that efficiently degrades a number of bioactive peptides and cytokines, including endothelin-1 (ET-1), enkephalins, atrial natriuretic peptide, gonadotropin-releasing hormone (GnRH), and bombesin-like peptides. Human NEP has been cloned and is identical to CD10, the common acute lymphoblastic leukemia antigen, which is a differentiation antigen for early B-lymphoid progenitors in the B-cell differentiation pathway. Human NEP has been shown to be widely distributed in various tissues and cell types and to control the biological activities of many peptide substrates by reducing the local concentrations available for receptor binding and signal transduction. Previous studies showed that NEP is expressed in bronchial epithelium, renal proximal tubules, epithelial cells of the small intestine and prostate, placental trophoblasts, and endometrial stromal cells. Moreover, NEP plays important roles in the maintenance of homeostasis of these normal tissues (Head *et al.,* 1993, Ino *et al.,* 2000). Human NEP has been reported to be involved in neoplastic transformation and tumor progression in certain human malignancies including lung, breast, and prostate carcinomas by degrading ET-1 and bombesin, which function as autocrine growth factors in these tumors (Burns *et al.,* 1999, Cohen *et al.,* 1996, Papandreou *et al.,* 1998; Shipp *et al.,* 1991). Chu and Arber (2000) reported the expression of NEP in 505 nonhematopoietic neoplasms and found that only 3 of 27 (11%) ovarian adenocarcinomas expressed NEP in the carcinoma cells. However, they did not document NEP expression in stromal cells of OC. We have also demonstrated that expression of NEP in the stromal cells of endometrial endometrioid adenocarcinoma decreased with advances in tumor grade, whereas

stroma1 ET-1 increased. These findings suggested a potential role for stromal NEP in the regulation of differentiation and progression of endometrial adenocarcinoma via degradation of ET-l (Suzuki *et al.,* 2001). Based on these findings, in this section we focused the expression and localization of NEP in benign, borderline-malignant and malignant ovarian tumor tissues with different histologic types using the immunohistochemical technique. We also discuss the possible role of this enzyme in neoplastic transformation and progression of OC.

Neutral Endopeptidase Expression in Ovarian Tumors

First, NEP expression was examined in 10 normal ovarian tissue specimens by immunohistochemical staining. Immunoreactivity of NEP was not detected in any stromal cells or surface epithelial cells in normal ovaries. Similarly, there was no NEP immunoreactivity in benign ovarian tumors including 5 serous and 4 mucinous cystadenomas. In contrast, NEP was strongly stained in the stromal cells of 6 of 7 (86%) serous borderline tumors but not in 4 mucinous borderline tumors. In OCs, NEP was also mainly localized in stromal cells surrounding or adjacent to carcinoma cells, but carcinoma cells showed slight NEP expression in some cases (Figure 89A). Human NEP was expressed in 13 of 20 (65%) serous, 8 of 10 (80%) endometrioid, and 7 of 10 (70%) clear cell adenocarcinomas as shown in Table 45. However, in most mucinous adenocarcinomas, there was no NEP immunoreactivity observed, and NEP was weakly detected in only 1 of 9 (12%) mucinous adenocarcinomas. There was a difference in the frequency of stromal NEP expression among 4 different histologic types. The staining intensity of stromal NEP expression in all serous tumors (n = 32) is shown in Figure 90. Benign serous adenomas were not stained, whereas serous borderline tumor and grade 1 carcinoma highly expressed NEP and the intensity of NEP immunoreactivity decreased as the tumor grade of the serous adenocarcinomas advanced. However, the stromal NEP expression level did not directly relate to the FIGO clinical stage of any patients with OC (data not shown).

The findings of alterations in the expression pattern of NEP during neoplastic transformation and progression suggest that stromal NEP expression is specifically up-regulated with transformation of tumor-cell behavior from the benign to borderline phenotype, which has proliferative and angiogenic properties but still no invasive potential. Abnormalities in expression pattern or catalytic function of the peptidases result in altered peptide activation, which disrupts normal cellular homeostasis and may contribute to neoplastic transformation or tumor progression.

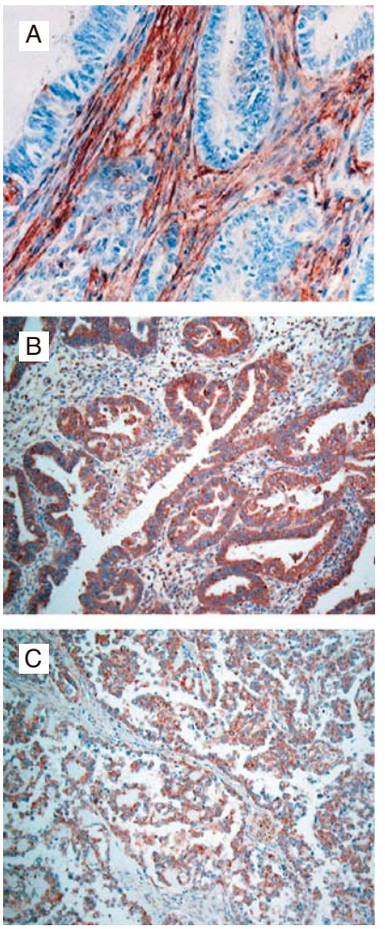

Figure 89. Immunohistochemical expression in ovarian epithelial tumors. **A:** NEP (neutral endopeptidase; magnification 200X) in endometrioid adenocarcinoma (Grade 1), **B:** P-LAP (magnification 200X) in serous adenocarcinoma (Grade 1), **C:** DPPIV (dipeptidyl peptidase IV; magnification 200X) in clear cell adenocarcinoma (Grade 2).

In contrast to the high expression of NEP in serous borderline tumors and G1 adenocarcinomas, stromal NEP expression decreased as the tumor grade of serous adenocarcinomas advanced, suggesting the involvement of NEP in regulating differentiation of OC. These results are consistent with our previous report showing the decrease or loss of NEP expression in the stromal cells in poorly differentiated uterine endometrial endometrioid adenocarcinoma (Suzuki *et al.,* 2001). Sato *et al*. (1996) also reported that NEP expression was decreased or lost in the poorly differentiated stomach and colon adenocarcinomas, although NEP was localized to carcinoma cells but not to stromal cells in these gastrointestinal tumors.

Table 45. Summary of Stromal Neutral Endopeptidase (NEP) Expression in Different Histologic Types

Histologic Type		Intensity of Staining			
		–	+	++	Total Number
Serous	Carcinoma	7	10	3	20
	Borderline	1	3	3	7
	Benign	5	0	0	5
Mucinous	Carcinoma	8	1	0	9
	Borderline	4	0	0	4
	Benign	4	0	0	4
Endometrioid	Carcinoma	2	4	4	10
Clear cell	Carcinoma	3	3	4	10

Functional significance of NEP expression in ovarian adenocarcinoma remains to be clarified. Previous studies reported that NEP plays a functional role in neoplastic transformation and tumor progression of the lung, breast, and prostate carcinomas by degrading specific peptide substrates such as ET-1 and bombesin, which are autocrine growth factors for these tumors (Burns *et al.,* 1999; Cohen *et al.,* 1996). Studies have shown that ET-1 is produced from ovarian adenocarcinoma cells and works through ET-A receptors as an autocrine growth factor *in vitro* and *in vivo* (Bagnato *et al.,* 1999). Endothelin-1 was also reported to promote tumor angiogenesis and tumor cell invasion in OC (Rosano *et al.,* 2001). The hormone GnRH is also one of the NEP substrate; GnRH and its receptor are expressed in OC cells and acts as an autocrine/paracrine regulator of OC cell proliferation (Ohno *et al.,* 1993). In the adjacent stroma of OC cells NEP could modulate growth, invasion, and angiogenesis through regulating receptor binding of these peptide growth factor because NEP is an enzyme responsible for degrading ET-1 and GnRH. Thus, the following mechanisms are conceivable: 1) absent NEP expression in benign cystadenomas suggests the absence of possible growth factors (ET-l or GnRH) autocrine system in benign ovarian tumors, 2) stromal NEP can act as a modulator of the growth factors autocrine/paracrine systems in borderline-malignant and malignant ovarian tumors, and 3) decrease or loss of stromal NEP in G3 serous carcinomas may contribute to growth factor-mediated progression of adenocarcinoma cells. Further studies are required to clarify the detailed mechanism of NEP involvement in peptide-dependent malignant formation and progression of ovarian tumors.

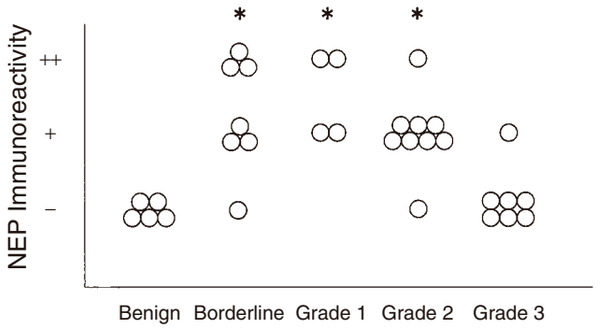

Figure 90. Immunoreactivity of NEP in serous ovarian tumors. Intensity of immunoreactivity was scored semiquantitatively on a three-tiered scale (negative: –; weakly positive: +; strongly positive staining: ++) relative to the known positive and negative controls. Each specimen was scored 2×, independently by two investigators.

The frequencies of positivity of stromal NEP expression differed between mucinous adenocarcinoma and the other three histologic types. The reason for the absence of NEP expression in the stroma of most mucinous adenocarcinomas and all mucinous borderline tumors remains unclear. An alternative mechanism may be involved in tumor progression of mucinous ovarian tumors rather than peptide-mediated malignant transformation and progression. More cases of mucinous tumors should be analyzed because 8 of the 9 cases of mucinous adenocarcinoma analyzed in the present series were FIGO stage Ia, and NEP expression was detected in only one of these tumors.

In conclusion, NEP was specifically expressed in the stroma of ovarian borderline and malignant tumors, and its expression seemed to be regulated by the histologic type or degree of differentiation. Our findings suggest that NEP plays a role in neoplastic transformation and progression of epithelial ovarian tumors possibly through the degradation and modulation of specific peptide factors.

Placental Leucine Aminopeptidase Expression

Introduction

Placental leucine aminopeptidase, which is identical to cystine aminopeptidase (CAP; EC 3.4.11.3), is the enzyme responsible for the complete inactivation of endocrine or paracrine oxytocin activity in placenta (Mizutani *et al.,* 1985). We found that serum P-LAP activity rises progressively with gestational age until near term and decreases in patients with spontaneous preterm delivery. These suggest that this enzyme is involved in fetal development and the regulation of the uterotonic effects of oxytocin (Yamahara *et al.,* 2000). Several groups have isolated a P-LAP complementary deoxyribonucleic acid (cDNA) clone from a human

placental cDNA library (Laustsen *et al.,* 1997; Rogi *et al.,* 1996). Structural analysis demonstrated that P-LAP is a type II membrane-bound protein belonging to the Ml family of zinc metallopeptidases, which also contains APN/CD 13, NEP/CD 10, and APA/BP-1. Contrary to the initial hypothesis that P-LAP is restricted to the placenta, Northern Blotting analysis and immunohistochemistry (IHC) demonstrated a widespread distribution of P-LAP in human tissues (Rogi *et al.,* 1996). It is interesting that an enzyme homologous to P-LAP, with 87% identity at the amino acid level, has been cloned from a rat adipocyte cDNA library and named insulin-regulated membrane aminopeptidase (IRAP) (Keller *et al.,* 1995). It was shown to be present in glucose transporter isotype GLUT4 vesicles of rat adipocytes and is co-translocated from the cytosol to the cell membrane with GLUT4 by insulin stimulation in adipocytes and skeletal muscle cells (Kandror *et al.,* 1994). Therefore, IRAP may be involved in glucose homeostasis via insulin-induced trafficking of GLUT4 vesicles and has now been extensively examined in adipose tissue and muscles.

The roles of P-LAP, especially in tissues other than the placenta, remain unclear. In 2003, we reported that P-LAP is present in human endometrial endometrioid adenocarcinoma tissues and that it works as a regulator of carcinoma cell growth (Suzuki *et al.,* 2003). Furthermore, we found that P-LAP expression is associated with the poor prognosis in endometrial adenocarcinoma patients (Shibata *et al.,* 2004). We presented here the immunohistochemical expression and localization of P-LAP in benign, borderline, and malignant ovarian-epithelial tumors of different histologic types.

Placental Leucine Aminopeptidase Expression in Ovarian Tumors

Expression of P-LAP was detected by IHC in ovarian adenocarcinoma cells but not in stromal cells (see Figure 89B). The staining intensity is summarized in Table 46. Immunoreactivity of P-LAP was detected in 1 of 6 (17%) serous cystadenomas and 1 of 5 (20%) mucinous cystoadenomas and these two cases were weakly positive (see Table 46). Four of 9 (44%) serous borderline tumors and 3 of 5 (60%) mucinous borderline tumors expressed P-LAP. One case of mucinous borderline tumor showed strong immunoreactivity, whereas the other cases were weakly stained. In OC, P-LAP was localized in both the cell membrane and the intracellular region of carcinoma cells. Sixty-nine of 80 (86%) cases were P-LAP positive in carcinoma cells. The positivity rate of P-LAP expression in invasive carcinoma was significantly increased compared to that in either benign or borderline tumor. There was a significant difference of P-LAP expression rates among 4 different histologic types. In 23 of 29 (79%) in serous adenocarcinoma, P-LAP was expressed, and 9 cases (31%) were strongly positive. In endometrioid adenocarcinoma, 15 of 17 (88%) were P-LAP positive, and 6 cases (35%) were strongly positive. In mucinous adenocarcinomas, 13 of 14 (93%) were P-LAP positive, and 10 cases (71%) were strongly positive. All cases of clear cell adenocarcinoma were P-LAP positive, and 15 of 20 cases (75%) were strongly positive. Significant difference was observed between serous adenocarcinoma and clear cell adenocarcinoma. In addition, P-LAP expression tended to increase with advancing grade in serous adenocarcinoma.

Table 46. Summary of Placental Leucine Aminopeptidase (P-LAP) Expression in Tumor Differentiation and Histology

Histologic Type		Intensity of Staining			Total Number
		–	+	++	
Serous	Carcinoma	6	14	9	29
	Borderline	5	4	0	9
	Benign	5	1	0	6
Mucinous	Carcinoma	1	3	10	14
	Borderline	2	3	0	5
	Benign	4	1	0	5
Endometrioid	Carcinoma	2	9	6	17
Clear cell	Carcinoma	0	5	15	20

The possible involvement of several cell-surface aminopeptidases, such as NEP, DPPIV, and aminopeptidase A (APA), were reported in several types of carcinomas. The expressions of these aminopeptidases commonly show the negative correlation with tumor grade (Fujimura *et al.,* 2000; Suzuki *et al.,* 2001). On the contrary, P-LAP expression was observed more frequently in OC than in normal or borderline tumor, although staining intensity has not yet been qualitated. In endometrial adenocarcinoma, we found a positive correlation between P-LAP and both surgical stage and tumor grade (Shibata *et al.,* 2004). To investigate functional roles of P-LAP, we transfected P-LAP cDNA into endometrial adenocarcinoma cells (AMEC) and ovarian carcinoma cells (SKOV). Both transfectants showed higher invasive potential than parental cells (data not shown). The enzyme P-LAP should degrade certain peptide factors on the cell surface before their binding to receptors. Oxytocin, a good P-LAP substrate, can inhibit carcinoma cell growth in several kinds of carcinoma cells (Cassoni *et al.,* 1997; Morita *et al.,* 2004; Suzuki *et al.,* 2003). Therefore, P-LAP should inactivate certain negative peptide factors such as

oxytocin, and promote carcinoma cell progression, such as invasion, migration, and growth. Although detailed molecular mechanisms still remain to be clarified, P-LAP should be one of the candidates for molecular therapy against carcinoma.

Dipeptidyl Peptidase IV Expression

Introduction

Dipeptidyl peptidase IV (DPPIV) is a cell-surface aminopeptidase that was originally characterized as a T-cell differentiation antigen (CD26) and has been reported to be present on epithelial cells of various tissues, including lung, liver, kidney, intestine, prostate, and placenta (ten Kate *et al.,* 1986). The aminopeptidase DPPIV has been reported to show a variety of functions—not only serine protease activity, which liberates N-terminal X-proline from peptide, but also various cellular processes such as regulation of immune response, signal transduction, and interaction with molecules of the extracellular matrix (Loster *et al.,* 1995; Nemoto *et al.,* 1999). Besides its expression in normal tissues, DPPIV expression and its roles in human tumors have been reported in hematologic malignancies and in certain solid tumors including melanoma, thyroid carcinoma, prostate carcinoma, and colon carcinoma (Bogenrieder *et al.,* 1997; Morrison *et al.,* 1993; Tanaka *et al.,* 1995; ten Kate *et al.,* 1986). Furthermore, a number of studies have provided evidence to indicate that DPPIV may play a role in tumor progression such as cell adhesion and invasion (Cheng *et al.,* 1998). In human endometrium, we have demonstrated that DPPIV is highly expressed in glandular cells of the normal endometrium and grade 1 endometrial adenocarcinoma cells, but its expression is decreased or lost with advancing tumor grade (Khin *et al.,* 2003).

In the following section, we show the DPPIV expression in various ovarian adenocarcinoma cell lines and tumors and its effect on the progression of OC.

Dipeptidyl Peptidase IV Expression in Ovarian Carcinoma

As shown in Figure 89C, we confirmed DPPIV expression in various OC tissues by immunohistochemical staining using DPPIV-specific mAb provided by Dr. Ueda (Nagoya City University, Japan), and the intensity of immunohistochemical staining varied from tissue to tissue. Thus, it would be beneficial to establish a DPPIV-overexpressing subline to clarify a role of DPPIV *in vitro* and *in vivo.* Therefore, DPPIV cDNA was transfected into OC cells (SKOV3), derived from serous cystadenocarcinoma (Kajiyama *et al.,* 2002; Kajiyama *et al.,* 2003). Whereas both parental SKOV3 cells and vector-transfected cells (SKpcDNA) showed a long-bipolar, spindle-shaped morphology like fibroblasts with a scattered and unorganized growth pattern, the shape of DPPIV-transfected cells (SKDPIV) was round with a cobblestone-like appearance. In the case of SKDPIV cells, cell–cell adhesion seemed to be tighter than that in SKOV3 or SKpcDNA cells. Although there were no significant differences in cell proliferation among SKOV3, SKpcDNA, and SKDPIV, the number of cells that had migrated on transwell cell-culture assay was significantly reduced in SKDPIV cells compared with that in either parental SKOV3 or SKpcDNA cells. Matrigel invasion assay was also reduced in SKDPIV cells compared with that in parental SKOV3 and SKpcDNA cells. In gelatin zymography, pro-MMP-2 activity was remarkably reduced in SKDPIV cells, whereas SKpcDNA cells showed the same level of pro-MMP-2 activity as parental SKOV3 cells. We further investigated whether DPPIV suppresses the formation of peritoneal metastasis in ovarian carcinoma using nude mice. Peritonitis carcinomatosa was observed approximately 4 weeks after the inoculation of SKOV3 or SKpcDNA cells into mice. A number of disseminated tumors were observed throughout the whole peritoneal cavity, especially on the omentum, mesentery, and liver surface with a large amount of bloody ascites 30 days after inoculation of SKpcDNA cells. A similar appearance was also observed in a mouse injected with parental SKOV3 cells. In contrast, a mouse injected with SKDPIV cells macroscopically had no disseminated tumor with a small amount of ascites at autopsy. In addition, the number of disseminated tumors at death in the group of mice injected with SKDPIV cells was obviously much less than the numbers in the other two groups. Only several disseminated tumors in this group of mice were observed even 60 days after the inoculation of SKDPIV cells. All mice finally died of peritonitis carcinomatosa. However, mice injected with SKDPIV cells survived significantly longer than those injected with SKOV3 cells or SKpcDNA cells (mean survival days: 64.9 ± 4.7 days [SKDPIV], 35.7 ± 2.8 days [SKOV3], 36.6 ± 1.8 days [SKpcDNA], respectively; $p < 0.0001$). Figure 91 summarizes these results by DPPIV transfection.

Because the addition of DPPIV inhibitors such as diisopropyl fluorophosphate (DFP) and diprotin A (DPA) could not restore the reduced invasion and migration potential, the enzyme activity of DPPIV might not be involved in either migration or invasion of SKDPIV cells. Pethiyagoda *et al.* also showed that DPPIV had an anti-invasive activity in melanoma cells, and this effect was not restored by the deletion mutant of the

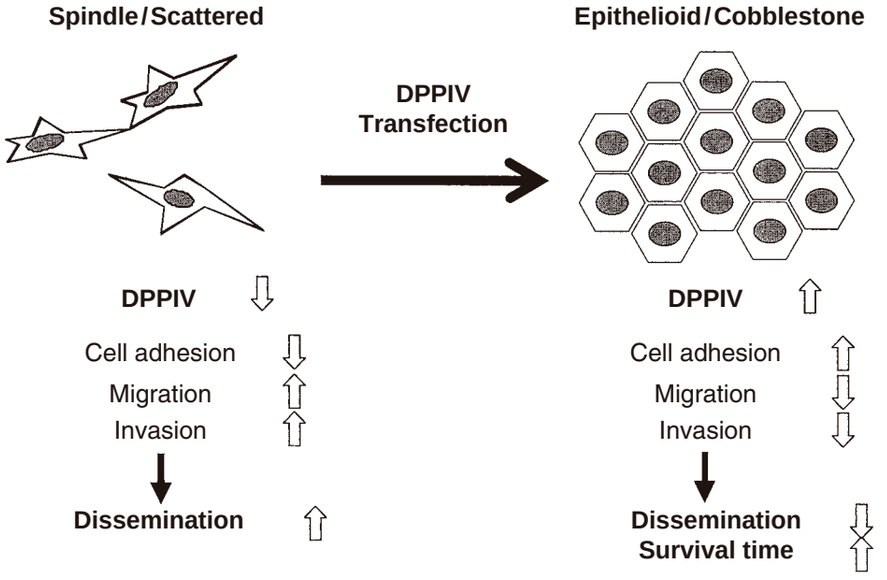

Figure 91. Scheme of functional mechanisms of dipeptidyl peptidase IV (DPPIV) transfection.

active site of enzyme activity of DPPIV (Pethiyagoda *et al.,* 2000). However, Wesley *et al.* (1999) reported that transfection of the enzyme activity lacking cDNA mutant into melanoma cells did not suppress tumorgenicity or anchorage-independent growth, nor did it reverse the blocking of differentiation. Additional studies are needed to determine whether the enzyme activity is related to anti-invasiveness. It is reasonable to speculate that the tight adhesion between carcinoma cells is contradictory to the invasiveness of carcinoma cells. The mechanisms of low migration potential and morphologic change in DPPIV-overexpressing cells are not clear. However, tight cell-cell adhesion caused by DPPIV may inhibit cell motility and invasiveness. Overexpression of DPPIV in OC cells results in the reduction of both intraperitoneal dissemination of carcinoma cells and prolongation of survival time *in vivo.* Similar findings were reported by Wesley *et al.,* who showed that the transfection of DPPIV into melanoma cells resulted in a loss of tumorigenicity and therefore a marked decrease in the tumor size of subcutaneously injected melanoma in nude mice (Wesley *et al.,* 1999). Taken together, DPPIV should act as a negative factor for carcinoma cell progression.

The mechanisms of tumor metastasis consist of various steps such as detachment from the primary tumor, adhesion, migration and invasion of carcinoma cells in metastasized organs. In lung endothelial cells DPPIV also functions as an adhesion molecule for the metastasis of breast carcinoma cell (Cheng *et al.,* 1998). Indeed, we found that the adhesion of SKOV3 cells to mesothelial monolayer cells is slightly increased by the transfection of DPPIV into SKOV3 cells (Kikkawa *et al.,* 2003). However, the results that much fewer disseminated tumors were observed 60 days after inoculation with DPPIV-overexpressing cells than those of parental- and vector-transfected cells suggest that most adherent cells could not grow or were eliminated as a result of loss of migration and invasive potential because of DPPIV overexpression.

There have been many reports that various bioactive substances in malignant ascites such as interleukin-1β, tumor necrosis factor, and various chemokines, all of which might be the candidates for substrate of DPPIV, were associated with both progression and survival of carcinoma (Wesley *et al.,* 1999). Therefore, this enzyme may have an effect on the progression of carcinoma *in vivo* in relation to these bioactive substances. In addition, pro-MMP-2 activity was remarkably reduced in DPPIV-transfected cells in gelatin zymography. Because matrix metalloproteinases (MMPs) are involved in carcinoma invasion, low invasive potential in DPPIV transfected cells might be partially the result of reduced MMP-2 activity.

In conclusion, *in vitro* and *in vivo* data indicated that DPPIV may be linked to decreased intraperitoneal dissemination of OC through reducing both the invasion and migration potential of OC cells. The potential of DPPIV for treating intraperitoneal metastatic carcinoma including gene therapy seems promising, although

extensive work is required before this enzyme can become available for clinical use.

CONCLUSION

The presence and function of cell-surface aminopeptidases in carcinoma cells has been investigated. The expression of NEP and DPPIV seemed negatively related to the degree of malignant potential of carcinoma cells (Khin *et al.,* 2003; Suzuki *et al.,* 2001). However, the high expression of P-LAP and APN were reported in highly malignant endometrial and pancreatic carcinoma (Ikeda *et al.,* 2003; Suzuki, *et al.,* 2003). Because these aminopeptidases degrade several peptide factors, their functions may vary in different types of carcinoma and tissue. Not all substrates of these enzymes have been identified, and this is likely impossible. However, investigations have shown the importance of small peptides in cellular functions, such as proliferation and mobility. Therefore, cell-surface aminopeptidases, which could modulate the signal transduction before the factors bind to their receptors, have received increasing attention. In fact, inhibitors of DPPIV have been extensively studied for clinical use in treating diabetes mellitus. We consider that inhibitors of cell-surface aminopeptidases could be newly developed for clinical use in treating carcinoma in the near future.

Intracellular mechanisms based on molecular biology have been highlighted in recent research. However, it is very important to know whether certain molecules are present or absent in target tissues and cells because the nature of carcinoma cell lines changes from that of their original tissues or cells during long-term culture. The IHC method is a convenient and important method of demonstrating the presence and localization of certain molecules. This method should be used first, and thereafter the functional roles of certain molecules should be extensively investigated.

References

Bagnato, A., Salani, D., Di Castro, V., Wu-Wong, J.R., Tecce, R., Nicotra, M.R., Venuti, A., and Natali, P.G. 1999. Expression of endothelin 1 and endothelin A receptor in ovarian carcinoma: evidence for an autocrine role in tumor growth. *Cancer Res. 59*:720–727.

Bogenrieder, T., Finstad, C.L., Freeman, R.H., Papandreou, C.N., Scher, H.I., Albino, A.P., Reuter, V.E., and Nanus, D.M. 1997. Expression and localization of aminopeptidase A, aminopeptidase N, and dipeptidyl peptidase IV in benign and malignant human prostate tissue. *Prostate 33*:225–232.

Burns, D.M., Walker, B., Gray, J., and Nelson, J. 1999. Breast cancer cell-associated endopeptidase EC 24.11 modulate's proliferative response to bombesin. *Br. J. Cancer 79*:214–220.

Cassoni, P., Sapino, A., Fortunati, N., Munaron, L., Chini, B., and Bussolati, G. 1997. Oxytocin inhibits the proliferation of MDA-MB231 human breast-cancer cells via cyclic adenosine monophosphate and protein kinase A. *Int. J. Cancer 72*: 340–344.

Cheng, H.C., Abdel-Ghany, M., Elble, R.C., and Pauli, B.U. 1998. Lung endothelial dipeptidyl peptidase IV promotes adhesion and metastasis of rat breast cancer cells via tumor cell surface-associated fibronectin. *J. Biol. Chem. 273*:24207–24215.

Chu, P., and Arber, D.A. 2000. Paraffin-section detection of CD10 in 505 nonhematopoietic neoplasms: frequent expression in renal cell carcinoma and endometrial stromal sarcoma. *Am. J. Clin. Pathol. 113*:374–382.

Cohen, A.J., Bunn, P.A., Franklin, W., Magill-Solc, C., Hartmann, C., Helfrich, B., Gilman, L., Folkvord, J., Helm, K., and Miller, Y.E. 1996. Neutral endopeptidase: variable expression in human lung, inactivation in lung cancer, and modulation of peptide-induced calcium flux. *Cancer Res. 56*:831–839.

Fujimura, H., Ino, K., Nagasaka, T., Nakashima, N., Nakazato, H., Kikkawa, F., and Mizutani, S. 2000. Aminopeptidase A expression in cervical neoplasia and its relationship to neoplastic transformation and progression. *Oncology 58*:342–352.

Head, J.R, MacDonald, P.C., and Casey, M.L. 1993. Cellular localization of membrane metalloendopeptidase (enkephalinase) in human endometrium during the ovarian cycle. *J. Clin. Endocrinol. Metab. 6*:769–776.

Ikeda, N., Nakajima, Y., Tokuhara, T., Hattori, N., Sho, M., Kanehiro, H., and Miyake, M. 2003. Clinical significance of aminopeptidase N/CD13 expression in human pancreatic carcinoma. *Clin. Cancer Res. 9*:1503–1508.

Ino, K., Suzuki, T., Uehara, C., Nagasaka, T., Okamoto, T., Kikkawa, F., and Mizutani, S. 2000. The expression and localization of neutral endopeptidase 24.11/CD10 in human gestational trophoblastic diseases. *Lab. Invest. 80*:1729–1738.

Kajiyama, H., Kikkawa, F., Khin, E., Shibata, K., Ino, K., and Mizutani, S. 2003. Dipeptidyl peptidase IV overexpression induces up-regulation of E-cadherin and tissue inhibitors of matrix metalloproteinases, resulting in decreased invasive potential in ovarian carcinoma cells. *Cancer Res. 63*:2278–2283.

Kajiyama, H., Kikkawa, F., Suzuki, T., Shibata, K., Ino, K., and Mizutani, S. 2002. Prolonged survival and decreased invasive activity attributable to dipeptidyl peptidase IV overexpression in ovarian carcinoma. *Cancer Res. 62*:2753–2757.

Kandror, K.V., Yu, L., and Pilch, P.F. 1994. The major protein of GLUT4-containing vesicles, gp160, has aminopeptidase activity. *J. Biol Chem. 269*:30777–30780.

Keller, S.R., Scott, H.M., Mastick, C.C., Aebersold, R., and Lienhard, G.E. 1995. Cloning and characterization of a novel insulin-regulated membrane aminopeptidase from Glut4 vesicles. *J. Biol. Chem. 270*:23612–23618.

Khin, E.E., Kikkawa, F., Ino, K., Kajiyama, H., Suzuki, T., Shibata, K., Tamakoshi, K., Nagasaka, T., and Mizutani, S. 2003. Dipeptidyl peptidase IV expression in endometrial endometrioid adenocarcinoma and its inverse correlation with tumor grade. *Am. J. Obstet. Gynecol. 188*:670–676.

Kikkawa, F., Kajiyama, H., Ino, K., Shibata, K., and Mizutani, S. 2003. Increased adhesion potency of ovarian carcinoma cells to mesothelial cells by overexpression of dipeptidyl peptidase IV. *Int. J. Cancer 105*:779–783.

Laustsen, P.G., Rasmussen, T.E., Petersen, K., Pedraza-Diaz, S., Moestrup, S.K., Gliemann, J., Sottrup-Jensen, L., and Kristensen, T. 1997. The complete amino acid sequence of human placental oxytocinase. *Biochem. Biophys. Acta. 1352*:1–7.

Loster, K., Zeilinger, K., Schuppan, D., and Reutter, W. 1995. The cysteine-rich region of dipeptidyl peptidase IV (CD 26) is the

collagen-binding site. *Biochem. Biophys. Res. Commun. 217*: 341–348.

Mizutani, S., Sumi, S., Oka, K., Yamada, R., Kurauchi, O., Taira, H., Narita, O., and Tomoda, Y. 1985. *In vitro* degradation of oxytocin by pregnancy serum, placental subcellular fractions and purified placental aminopeptidases. *Exp. Clin. Endocrinol. 86*:310–316.

Morita, T., Shibata, K., Kikkawa, F., Kajiyama, H., Ino, K., and Mizutani, S. 2004. Oxytocin inhibits the progression of human ovarian carcinoma cells *in vitro* and *in vivo*. *Int. J. Cancer 109*: 525–532.

Morrison, M.E., Vijayasaradhi, S., Engelstein, D., Albino, A.P., and Houghton, A.N. 1993. A marker for neoplastic progression of human melanocytes is a cell surface ectopeptidase. *J. Exp. Med. 177*:1135–1143.

Nemoto, E., Sugawara, S., Takada, H., Shoji, S., and Horiuch, H. 1999. Increase of CD26/dipeptidyl peptidase IV expression on human gingival fibroblasts upon stimulation with cytokines and bacterial components. *Infect. Immun. 67*:6225–6233.

Ohno, T., Imai, A., Furui, T., Takahashi, K., and Tamaya, T. 1993. Presence of gonadotropin-releasing hormone and its messenger ribonucleic acid in human ovarian epithelial carcinoma. *Am. J. Obstet. Gynecol. 169*:605–610.

Papandreou, C.N., Usmani, B., Geng, Y., Bogenrieder, T., Freeman, R., Wilk, S., Finstad, C.L., Reuter, V.E., Powell, C.T., Scheinberg, D., Magill, C., Scher, H.L., Albino, A.P., and Nanus, D.M. 1998. Neutral endopeptidase 24.11 loss in metastatic human prostate cancer contributes to androgen-independent progression. *Nat. Med. 4*:50–57.

Pethiyagoda, C.L., Welch, D.R., and Fleming, T.P. 2000. Dipeptidyl peptidase IV (DPPIV) inhibits cellular invasion of melanoma cells. *Clin. Exp. Metastasis 18*:391–400.

Rogi, T., Tsujimoto, M., Nakazato, H., Mizutani, S., and Tomoda, Y. 1996. Human placental leucine aminopeptidase/oxytocinase: a new member of type II membrane-spanning zinc metallopeptidase family. *J. Biol. Chem. 271*:56–61.

Rosano, L., Varmi, M., Salani, D., Di Castro, V., Spinella, F., Natali, P.G., and Bagnato, A. 2001. Endothelin-1 induces tumor proteinase activation and invasiveness of ovarian carcinoma cells. *Cancer Res. 61*:8340–8346.

Sato, Y., Itoh, F., Hinoda, Y., Ohe, Y., Nakagawa, N., Ueda, R., Yachi, A., and Imai, K. 1996. Expression of CD10/neutral endopeptidase in normal and malignant tissues of the human stomach and colon. *J. Gastroenterol. 31*:12–17.

Shibata, K., Kikkawa, F., Kondo, C., Mizokami, Y., Kajyama, H., Ino, K., Nomura, S., and Mizutani, S. 2004. Placental leucine aminopeptidase (P = LAP) expression is associated with chemosensitivity in human endometrial carcinoma. *Gynecol. Oncol. 95*:307–313.

Shipp, M.A., Tarr G.E., Chen, C.Y., Switzer, S.N., Hersh, L.B., Stein, H., Sunday, M.E., and Reinherz, E.L. 1991. CD10/neutral endopeptidase 24.11 hydrolyzes bombesin-like peptides and regulates the growth of small cell carcinomas of the lung. *Proc. Natl. Acad. Sci. USA 88*:10662–10666.

Suzuki, T., Kikkawa, F., Ino, K., Nagasaka, T., Tamakoshi, K., and Mizutani, S. 2001. Imbalance between neutral endopeptidase 24.11 and endothelin-1 expression in human endometrial carcinoma. *Oncology 60*:258–267.

Suzuki, Y., Shibata, K., Kikkawa, F., Kajiyama, H., Ino, K., Nomura, S., Tsujimoto, M., and Mizutani, S. 2003. Possible role of placental leucine aminopeptidase in the antiproliferative effect of oxytocin in human endometrial adenocarcinoma. *Clin. Cancer Res. 9*:1528–1534.

Tanaka, T., Umeki, K., Yamamoto, I., Sakamoto, F., Noguchi, S., and Ohtaki, S. 1995. CD26 (dipeptidyl peptidase IV/DPPIV) as a novel molecular marker for differentiated thyroid carcinoma. *Int. J. Cancer 64*:326–331.

ten Kate, J., van den Ingh, H.F., Khan, P.M., and Bosman, F.T. 1986. Adenosine deaminase complexing protein (ADCP) immunoreactivity in colorectal adenocarcinoma. *Int. J. Cancer 37*:479–485.

Wesley, U.V., Albino, A.P., Tiwari, S., and Houghton, A.N. 1999. A role for dipeptidyl peptidase IV in suppressing the malignant phenotype of melanocytic cells. *J. Exp. Med. 190*:311–322.

Yamahara, N., Nomura, S., Suzuki, T., Itakura, A., Ito, M., Okamoto, T., Tsujimoto, M., Nakazato, H., and Mizutani, S. 2000. Placental leucine aminopeptidase/oxytocinase in maternal serum and placenta during normal pregnancy. *Life Sci. 66*:1401–1410.

This Page Intentionally Left Blank

27

Expression of Angiopoietin-1, Angiopoietin-2, and Tie2 in Normal Ovary with Corpus Luteum and in Ovarian Carcinoma

Kohkichi Hata

Introduction

Angiogenesis, the process of new vessels sprouting from the existing vasculature, is a critical process during early development (Risau, 1991). However, angiogenesis rarely occurs in the adult, except in response to cyclic hormonal stimulation in the ovary and uterus, in response to injury, and in response to pathologic conditions such as tumorigenesis and diabetes mellitus (Folkman and Shing, 1992; Reynolds *et al.,* 1992). Tie2 is a novel endothelium-specific receptor tyrosine kinase, which has been demonstrated to be essential for the development of the embryonic vasculature (Dumont *et al.,* 1995; Iwama *et al.,* 1993). Moreover, Tie2 is known to play a role in tumor angiogenesis. Peters *et al*. (1998) demonstrated the up-regulation of Tie2 expression in the pathologic neovasculature of breast tumors by immunohistochemistry and suggested that targeting the Tie2 pathway might yield a useful anti-cancer therapy. Lin *et al*. (1998) reported the potential utility of gene therapy for systemic delivery of an anti-angiogenic agent targeting the endothelium-specific receptor, Tie2, using an adenoviral vector constructed to deliver a recombinant, soluble Tie2 receptor capable of blocking Tie2 activation.

It has been revealed that Tie2 is also broadly expressed in the endothelium of quiescent adult vasculature (Wong *et al.,* 1997). Moreover, Tie2 is tyrosine-phosphorylated in both angiogenic tissues and quiescent adult tissues. These findings suggest a dual function for Tie2 in adult tissues involving both angiogenesis and vascular maintenance. In the foregoing study, we evaluated Tie2 gene expression in corpus luteum (CL) by reverse transcription polymerase chain reaction (RT-PCR), comparing to Doppler ultrasound-derived peak systolic velocity as an indicator of intraovarian angiogenesis, and suggested that Tie2 gene might be one of the key genes that modulates angiogenesis in CL formation and regression (e.g., in physiologic angiogenesis) (Hata *et al.,* 2000). Therefore, enthusiasm for therapeutic strategies perturbing Tie2 should be tempered by the possible disruption of critical roles for Tie2 in vascular maintenance.

Angiopoietin-1 (Ang1) has been identified as the major ligand for the angiogenic tyrosine kinase receptor Tie2, and has been assigned the responsibility for recruiting and sustaining periendothelial support cells. Angiopoietin-2 (Ang2) was found to disrupt blood vessel formation in the developing embryo by antagonizing

Handbook of Immunohistochemistry and *in situ* Hybridization of Human Carcinomas, Volume 4: Molecular Genetics, Gastrointestinal Carcinoma, and Ovarian Carcinoma

the effect of Ang1 and Tie2 and was thus considered to represent a natural Ang1/Tie2 inhibitor (Asahara *et al.,* 1998).

Sample Collection

To investigate the expression of *Ang1, Ang2,* and *Tie2* genes, we collected ovarian tissues from 33 patients during operation. The 14 patients having normal ovaries with CL ranged in age from 21 to 50 years (median 43 years), and all subjects had regular menstrual cycles. The final diagnoses were myoma uteri (n = 9), cervical cancer stage Ib (n = 2), serous cystadenoma (n = 2), and hemorrhagic corpus luteum (n = 1). The 19 patients with ovarian cancer were aged from 19 to 76 years (median 56 years), and 8 of them were premenopausal. Their tumors were classified as serous cystadenocarcinoma (stage Ia) (n = 1), mucinous cystadenocarcinoma (stage Ia) (n = 1), endometrioid carcinoma (stage Ia) (n = 1), clear cell carcinoma (stage Ia) (n = 1), mucinous cystadenocarcinoma (stage Ic) (n = 3), endometrioid carcinoma (stage II) (n = 1), serous cystadenocarcinoma (stage III) (n = 7), endometrioid carcinoma (stage III) (n = 1), undifferentiated carcinoma (stage III) (n = 1), and serous cystadenocarcinoma (stage IV) (n = 2).

These women were electively admitted to our gynecology ward. Asymptomatic women with a positive result from an ovarian cancer screening program were excluded. If the ovaries were removed for diagnostic or therapeutic purposes, then a portion of the tissue was taken for the subsequent analysis of specific gene expression. The remainder of each tissue was used for routine histologic investigation. All research was conducted with informed consent.

Tissue Specimen and Ribonucleic Acid Preparation

Fresh surgical specimens from all patients were obtained, and the tissues to be used for investigation were prepared carefully under a dissecting microscope to dissect ovaries into healthy tissue around the CL and cancerous tissue. The tissue samples were stored at −80°C for subsequent analysis. Normal placental tissues were used as a positive control for *Ang1, Ang2,* and *Tie2* gene expression. Normal liver tissues were used as a negative control for *Ang1* gene expression, and the breast carcinoma cell line MCF-7, which was kindly provided by Dr. Akira Yamauchi, was used as a negative control for *Ang2* and *Tie2* gene expression.

Reverse Transcription Polymerase Chain Reaction

Total ribonucleic acid (RNA) was isolated from frozen tissues using a commercially available extraction method (Isogen; Nippon Gene Inc., Tokyo, Japan). Complementary deoxyribonucleic acid (cDNA) was prepared by random priming from 1000 ng of total RNA using a First-Strand cDNA Synthesis kit (Pharmacia-LKB, Uppsala, Sweden). The primers chosen for sense (3′-5′) and antisense (5′-3′), respectively, were as follows: For human *Ang1* gene (GenBank accession number U83508) AACATGAAGTCGGAGATGGC and CAGCAGCTGTATCTCAAGTCG (174 bp of PCR product); for human *Ang2* gene (GenBank accession number AF004327) GAAGAGCATGGACAGCATAGG and GAGTCATCGTATTCGAGCGG (159 bp); and for human *Tie2* gene (GenBank accession number L06139) AACTCTGTGTGCAACTGGTCC and AAGTCATCTTCCGAGCTTGG (181 bp). The PCR was carried out in a Thermal Cycler (Perkin-Elmer Cetus, Northwalk, CT) with a mixture consisting of cDNA derived from 5 ng of RNA, 10 pmol of upstream and downstream primers for each of the gene sequences, and 5 pmol of primers for the β_2-microglobulin (β_2-MG) gene (GenBank accession number V00567) is ACCCCCACTGAAAAAGATGAG (upstream) ATCTTCAAACCTCCATGATGC (downstrean) (120 bp), 200 μmol of deoxynucleotide triphosphate, 37 kBq of [α-32P] dCTP, and 0.1 unit of *Taq* DNA polymerase with reaction buffer (Life Technologies, Rockville, MD) in a final volume of 10 μl. The condition for PCR was denaturation at 94°C for 1 min, annealing at 58°C for 1 min, and extension at 72°C for 1 min. Thirty cycles of PCR were performed for each specimen, and the products were separated on 9% polyacrylamide gels. The radioactivity was then determined by BAS 2000 Bioimage Analyzer (Fujix, Tokyo, Japan). The Angl, Ang2, and Tie2 expression was presented by the relative yield of each gene to that of the β_2-*MG* gene, respectively.

Probe Synthesis

The pKS+ vectors containing a 570-bp SpeI-EcoRI fragment of human Ang1 cDNA and a 640-bp EcoRI-HindIII fragment of human Ang2 cDNA (kindly provided by Dr. George D. Yancopoulos, Regeneron Pharmaceuticals, Tarrytown, NY) were linealized, and antisense and sense digoxigenin (DIG)-labeled Ang1 and Ang2 riboprobes were generated with the T7/T3 polymerase by *in vitro* transcription (Stratmann *et al.,* 1998).

In situ Hybridization

The frozen tissues were cut at 10 μm. The sections were fixed 10% formalin solution for 10 min, treated by 0.3% Triton X-100 for 10 min, and incubated at 37°C in 2 μg/ml of proteinase K for 25 min. Post-fixation was performed in a 10% formalin solution, and the sections were treated with 2 N HCl. The tissue was acetylated with 0.025% acetic anhydride for 10 min and incubated at room temperature in a 5× saline-sodium citrate (SSC)/50% formamide solution for 30 min. The riboprobes for Ang1 and Ang2 were diluted with hybridization solution (5× SSC, 10% dextran sulfate, 1× Denhardt's solution, 50 μg/ml of yeast tRNA and 50% formamide) and applied to each slide, and the sections were incubated at 50°C overnight. After hybridization, slides were treated with 20 μg/ml RNase A at 37°C for 30 min and washed for 15 min 4× in 0.1× SSC at 50°C. We incubated the sections with 750× diluted alkaline phosphatase-labeled anti-digoxigenin antibody (Fab fragment, Boehringer) at 4°C overnight. Staining was performed with a freshly prepared substrate solution of Nitro Blue Tetrazolium and 5-bromo-4-chloro-3-indolyl phosphate.

Immunohistochemical Staining

Formalin-fixed and paraffin-embedded tissue sections (5 μm) were stained for Tie2 using the Dako Envision Polymer System, horseradish peroxidase (HRP) method (Dako A/S, Glostrup, Denmark). Tissue sections were dewaxed in xylene, rehydrated in graded alcohol down to water, washed in phosphate buffered saline (PBS) (pH 7.25) for 5 min, and quenched in peroxidase-blocking reagent for 5 min to remove endogenous peroxidase activity. Subsequently, slides were incubated with the rabbit anti-human Tie2 primary antibody (Santa Cruz Biotechnology, Inc., Santa Cruz, CA) for 30 min at room temperature. The secondary antibody conjugated with the HRP-labeled polymer was used for 30 min at room temperature following the primary antibody. Finally, bound antibody complexes were stained for 10 min with 0.05% diaminobenzidine and 0.01% hydrogen peroxide in 0.05 M Tris-HCl buffer (pH 7.6). The slides were washed between each step with PBS (10 min 3×). The sections were counterstained with Mayer's hematoxylin. A positive control and a negative control were included in every run, and the primary antibody was replaced with normal rabbit serum in the negative control slides.

Statistical Analysis

The Mann-Whitney U test was used as appropriate for the evaluation of significant differences between end points. Correlation between end points was assessed by regression analysis. A P value <0.05 was considered to be statistically significant.

Reverse Transcription Polymerase Chain Reaction and Ang1, Ang2, and Tie2 Gene Expression

To determine the number of PCR cycles appropriate for quantification, PCR was performed from 20 to 50 cycles at increments of 5 cycles. The expression ratios of Angl, Ang2, and Tie2 to β_2-MG were reasonably constant from 25 to 40 cycles, respectively (data not shown). Therefore, in the subsequent experiments the values at 30 PCR cycles were defined as the expression of the target genes. The values of gene expression represent the mean values from at least three independent RT-PCR experiments.

The expression of *Ang1* gene was significantly higher in the normal ovary with CL than in ovarian cancer (median 0.54, range 0.18–1.06 versus median 0.14, range 0.06–0.75, $P = 0.0004$, Mann-Whitney U test). There was no significant difference between normal ovary with CL and the ovary with ovarian cancer with regard to *Ang2* and *Tie2* gene expression. A significant difference was noted between normal ovary with CL and ovary with ovarian cancer with *Ang1/Ang2* gene expression ratio (median 0.60, range 0.09–2.01 versus median 0.14, range 0.06–0.89, $P = 0.0005$, Mann-Whitney U test).

The relationship between the expression of *Ang1* gene and *Tie2* gene in normal ovary with CL was significant. The correlation co-efficient r was 0.619 for normal ovary with CL ($P = 0.018$). Such significant correlation was not found in ovarian cancer. Moreover, *Ang2* gene expression and *Ang1/Ang2* gene expression ratio showed no significant correlation with *Tie2* gene expression either in normal ovary with CL or in ovary with ovarian cancer.

In situ Hybridization

Transcripts for Ang1 were observed in corpus luteal cells and endothelial cells around CL and in tumor cells and endothelial cells at the periphery of tumor invasion. Ang2 transcripts were expressed in the same patterns.

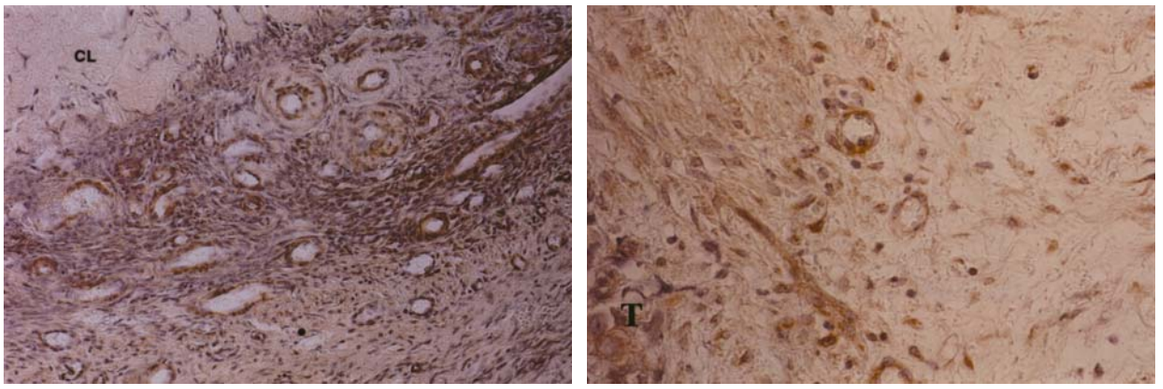

Figure 92. Immunohistochemical staining for Tie2 in a section of a corpus luteum *(CL)* **(A)** (original 50X) and of a ovarian cancer **(B)** (original 100X). Tie2 was localized primarily in the endothelial cells around CL and in those at the periphery of tumor *(T)* invasion. (Quoted from Hata *et al.,* 2002. *Oncology 62*:340–348).

Cellular Tie2 Expression

Tie2 was localized primarily in the endothelial cells around CL (Figure 92A) and in those at the periphery of tumor invasion (see Figure 92B). Weak Tie2 expression was occasionally observed in periendothelial cells (probably smooth-muscle cells and pericytes).

CONCLUSION

This study revealed that there was a significant difference in the *angiopoietin/Tie2* gene expression between physiologic and pathologic angiogenesis in the ovary. The anti-Tie2 therapy should be performed to inhibit only the pathologic angiogenesis; however, a therapeutic strategy perturbing Tie2 might suppress both physiologic and pathologic angiogenesis in the ovary. Further investigation into the specific signaling pathways of angiopoietin/Tie2 system used for vascular maintenance and angiogenesis might lead to more specific and effective strategies for both proangiogenic and anti-angiogenic therapy in ovarian cancer.

Acknowledgments

I thank Dr. George D. Yoancopoulos (Tarrytown, NY) for providing Ang1 and Ang2 cDNA clones.

References

Asahara, T., Chen, D., Takahashi, T., Fujikawa, K., Kearney, M., Magner, M., Yancopoulos, G.D., and Isner, J.M. 1998. Tie2 receptor ligands, angiopoietin-1 and angiopoietin-2, modulate VEGF-induced postnatal neovascularization. *Circ. Res. 83*:233–240.

Dumont, D.J., Fong, G.H., Puri, M.C., Gradwohl, G., Alitalo, K., and Breitman, M.L. 1995. Vascularization of the mouse embryo: a study of flt-1, tek, tie, and vascular endothelial growth factor expression during development. *Dev. Dyn. 203*:80–92.

Folkman, J., and Shing, Y. 1992. Angiogenesis. *J. Biol. Chem. 267*:10931–10934.

Hata, K., Fujiwaki, R., Nakayama, K., Fukumoto, M., and Miyazaki, K. 2000. Expression of *TP* and *TIE2* genes in normal ovary with corpus luteum and in ovarian cancer: correlation with ultrasound-derived peak systolic velocity. *Mol. Hum. Reprod. 6*:319–323.

Iwama, A., Hamaguchi, I., Hashiyama, M., Murayama, Y., Yasunaga, K., and Suda, T. 1993. Molecular cloning and characterization of mouse TIE and TEK receptor tyrosine kinase genes and their expression in hematopoietic stem cells. *Biochem. Biophys. Res. Commun. 195*:301–309.

Lin, P., Buxton, J.A., Acheson, A., Radziejewski, C., Maisonpierre, P.C., Yancopoulos, G.D., Channon, K.M., Hale, L.P., Dewhirst, M.K., George, S.E., and Peters, K.G. 1998. Antiangiogenic gene therapy targeting the endothelium-specific receptor tyrosine kinase Tie2. *Proc. Natl. Acad. Sci. USA 95*:8829–8834.

Peters, K.G., Coogan, A., Berry, D., Marks, J., Iglehart, J.D., Kontos, C.D., Rao, P., Sanker, S., and Trogan, E. 1998. Expression of Tie2/Tek in breast tumour vasculature provides a new marker for evaluation of tumour angiogenesis. *Br. J. Cancer 77*:51–56.

Reynolds, L.P., Killilea, S.D., and Redmer, D.A. 1992. Angiogenesis in female reproductive system. *FASEB 6*: 886–892.

Risau, W. 1991. Vasculogenesis, angiogenesis and endothelial cell differentiation during embryonic development. In: Feinberg F.N., Sherer G.K., Auerbach R. (eds.): *Development of the Vascular System*, Basel: Karger, 58–68.

Stratmann, A., Risau, W., and Plate, K.H. 1998. Cell type-specific expression of angiopoietin-1 and angiopoietin-2 suggesting a role in glioblastoma angiogenesis. *Am. J. Pathol. 153*: 1459–1466.

Wong, A.L., Haroon, Z.A., Werner, S., Dewhirst, M.W., Greenberg, C.S., and Peters, K.G. 1997. Tie2 expression and phosphorylation in angiogenic and quiescent adult tissues. *Circ. Res. 81*:567–574.

28

The Role of Immunohistochemical Expression of 1,25-Dihydroxyvitamin-D_3-Receptors in Ovarian Carcinoma

M. Friedrich, N. Fersis, D. Diesng, T. Cordes, S. von Otte, and K. Diedrich

Introduction

Ovarian carcinoma is a leading cause of death in gynecologic cancer. The first therapy of choice is R_0-R_1 cytoreduction followed by platin plus taxane chemotherapy. However, 5-year survival is only 15–20% because of the development of recurrent disease, which often displays features of multidrug resistance. Response to second-line therapy, at least in platin-resistant disease, is worse. New drugs are urgently required. Hormonal therapy of ovarian epithelial carcinomas has a long history of empiric use, but, although many of these malignancies express sex steroid hormone receptors, response rates to various forms of hormonal manipulation have been disappointing (Hunter *et al.,* 1992; Thigpen *et al.,* 1993; Williams *et al.,* 1992).

Epidemiologic studies have suggested the association of 1,25-dihydroxyvitamin D_3 ($1,25(OH)_2D_3$) deficiency with an increased risk of various malignancies including colon and breast cancers (Garland *et al.,* 1985). The molecular mechanisms involved in this phenomenon are still unknown. It has been shown that nuclear receptors for $1,25(OH)_2D_3$ (Vitamin D receptor, or VDR) are almost ubiquitously expressed in human tissues, including skin, intestine, kidney, parathyroid, uterine cervix, and breast (Friedrich *et al.,* 1998; Milde *et al.,* 1991; Reichrath *et al.,* 1998; Stumpf *et al.,* 1979). *In vitro* studies have demonstrated that $1,25(OH)_2D_3$ dose-dependently suppresses proliferation and induces differentiation in various cell types, including epithelial cells (Hosomi *et al.,* 1983; Smith *et al.,* 1986). The initial observation that calcitriol inhibits growth of cancer cells was made in melanoma cells (Colston K. *et al.,* 1981), but other cancer cell types such as colon, prostate, and breast cancer cells demonstrated response to 1,25-dihydroxyvitamin D_3 *in vitro* with an inhibition of cell growth (Colston K.W. *et al.,* 1989; Katakami *et al.,* 1988; Norman *et al.,* 1982; Welsh *et al.,* 1994). Such data indicated that calcitriol analogs may be effective in the treatment of certain malignancies. However, a major drawback of considering calcitriol as a therapeutic agent is its potent calcemic activity, leading to hypercalciuria and hypercalcemia at oral doses of more than a few micrograms per day. New vitamin D compounds

exerting less systemic side effects may be promising new tools for the treatment of gynecologic malignancies.

The aim of this study was to analyze immunohistochemical expression of VDR in normal and carcinomatous ovarian tissue to evaluate whether ovarian tissue may be a new potential target for biologically active vitamin D analogs. Additionally, VDR expression was compared immunohistochemically with the staining pattern of Ki-67 for analyzing whether VDR expression in ovarian tissue may be a function of proliferation. Furthermore, estrogen receptor (ER) and progesterone receptor (PR) were immunohistochemically analyzed to evaluate whether the expression of VDR correlates with the expression of these steroid hormone receptors.

MATERIALS AND METHODS

Ovarian Specimens

Freshly excised ovarian specimens (ovarian carcinomas [OCs]: n = 40, normal ovarian tissue: n = 14) were immediately embedded in OCT-Tissue-Tek II (Miles Laboratories, Naperville, IL), snap frozen in melting isopentane, precooled in liquid nitrogen, and stored at –80ºC. Almost all ovarian carcinomas were surface epithelial-stromal tumors (serous adenocarcinoma: n = 26; mucinous adenocarcinoma: n = 5; endometrioid adenocarcinoma: n = 4; clear cell adenocarcinoma: n = 3 transitional carcinoma: n = 1; müllerian mixed tumor: n = 1), and were obtained from patients who underwent surgery because of adnexal tumors. Usually, an exploratory laparotomy with bilateral salpingoophorectomy, omentectomy, abdominal hysterectomy, and appendectomy was performed. Intraoperatively, biopsies were taken from macroscopically visible tumor areas. All specimens of normal ovarian tissue as control were obtained from patients who underwent surgery for leiomyomas of the uterus and represent the surface epithelium of the ovary. Histologic examination by a certified pathologist confirmed diagnosis.

Primary Antibodies

The VDR was detected by monoclonal antibody (mAb) 9A7γ (Dianova, Hamburg, Germany) of which preparation and specificity was described previously (Pike *et al.,* 1982, 1983). This antibody (IgG2b) was raised against chicken intestinal VDR and cross-reacts with human, mouse, and rat VDRs but does not bind to glucocorticoid, PR, or ER. The epitope has been determined to reside between residues 90 and 104 of the human VDR, a location that is just C-terminal to the deoxyribonucleic acid (DNA)-binding fingers. This antibody perturbs, but does not inhibit, the receptor–DNA interaction. Proliferation was investigated applying mouse mAb Ki-67 directed against the Ki-67 antigen (clone Ki-67). The Ki-67 antigen is expressed during late G1 to G2 phases and is consistently absent in G0 phases of the cell cycle (Gerdes *et al.,* 1983, 1984). The receptors ER and PR were detected by Abbott ER-ICA Monoklonal kit and Abbott PgR-ICA Monoklonal kit, respectively.

Preparation of Sections and Fixation

Serial sections (5 µm) were cut on a cryostat, mounted on glass slides, and fixed in 3.7% paraformaldehyde in phosphate buffer saline (PBS; 10 min at room temperature), incubated in methanol (3 min at –20°C) and acetone (1 min at –20°C), and transferred into PBS.

In situ Detection of Primary Antibodies

The incubation steps were performed in a moist chamber at room temperature, covering the sections with 100 µl of the respective reagents. To reduce nonspecific staining, the slides were incubated with heat-inactivated normal rabbit serum (20 min at room temperature). The slides were then incubated (19 hours at 4°C) with the different primary antibodies (anti-VDR 1:1000; anti-Ki-67 1:100; anti-ER: 1:10,000; anti-PR: 1:10,000) or as control with polyclonal mouse immunoglobulin G1 (IgG1) at similar concentrations. After intermediate washing steps (Tris buffered saline [TBS] 2× 5 min), the sections stained for VDR were incubated with biotin-labeled rabbit anti-mouse IgG (Dakopatts, 1:400 for 30 min at room temperature) and incubated with streptavidin-peroxidase complexes (Dakopatts, 1:400 for 30 min at room temperature). After washing in PBS, the sections were incubated for 6 min with nickel-diaminobenzidine (DAB) (Sigma) to visualize the peroxidase reaction. The sections stained for Ki-67 were incubated with 3-amino-9-ethylcarbazole (AEC, Sigma A 5754) as a substrate for the peroxidase reaction. The detection of ER and PR was performed as recommended for the use of the immunocytochemical assaies ER-ICA and PgR-ICA. Sections were transferred into tap water, counterstained with eosin (0.5% for 1–2 sec), dehydrated, cleared in xylene, and mounted with Entelan.

Semi-Quantitative Analysis of Immunoreactivity

Microscopic analysis was performed by three independent observers (J.R., A.W.-H., and M.F.). The VDR-staining intensity (VDR-SI), percentage of

VDR-positive tumor cells (VDR-PP), and the resulting immunoreactivity VDR score (VDR-IRS) were assessed as described previously (Friedrich *et al.,* 1998; Reichrath *et al.,* 1998). In short, this immunoreactivity score (VDR negative: 0–1; weak VDR immunoreactivity: 2–3; moderate VDR immunoreactivity: 4–6; strong VDR immunoreactivity: 8–12) was determined by multiplication of the values for VDR-SI (VDR-SI: 0 = no staining; 1 = weak staining; 2 = moderate staining; 3 = strong staining) and the values for percentage of VDR-positive tumor cells (VDR-PP: 0 = 0%; 1 = 1–10%; 2 = 11–50%; 3 = 51–80%; 4 = 81–100%). Sections stained for Ki-67 were assessed by counting the number of Ki-67-positive and -negative cells in the strongest stained tumor area (magnification 400X, at least 200 tumor cells were counted). Sections stained for ER and PR were assessed as described previously by Remmele *et al*. (1986).

Statistical Analysis

Statistical analysis was performed by using Krukal-Wallis and Mann-Whitney U-Wilcoxon Rank Sum W Tests. Statistical significance was defined with $p < 0.05$.

RESULTS

Vitamin D Receptor Expression in Normal Ovarian Tissue

A total of 16.67% of the normal ovarian surface epithelium was VDR negative, whereas the remaining 83.33% revealed weak to moderate VDR immunoreactivity (mean VDR-SI: 1.0 SD: +/– 0.87; mean VDR-PP: 57.14 SD: +/– 43.10; mean VDR-IRS: 2.86 SD: +/– 2.48). In the ovarian specimens, the connective tissue always gave negative staining results. Fibroblasts, identified by their shape; endothelial cells of capillaries, arterioles, and venules; and pericytes or smooth-muscle cells in the microvascular wall revealed either negative or weak staining for VDR.

Vitamin D Receptor Expression in Ovarian Carcinomas

Nuclear immunoreactivity for VDR was detected in all 40 ovarian carcinomas analyzed. Results of VDR staining were heterogeneous, with visual differences between individual tumor cells (Figure 93). Intensity of VDR immunostaining and number of VDR-positive cells were consistently and markedly increased in OCs (mean VDR-SI: 2.31, SD: +/– 0.80; mean VDR-PP: 89.86%, SD: +/– 1.91%; mean VDR-IRS: 8.49, SD: +/– 3.80) as compared to normal ovarian tissue.

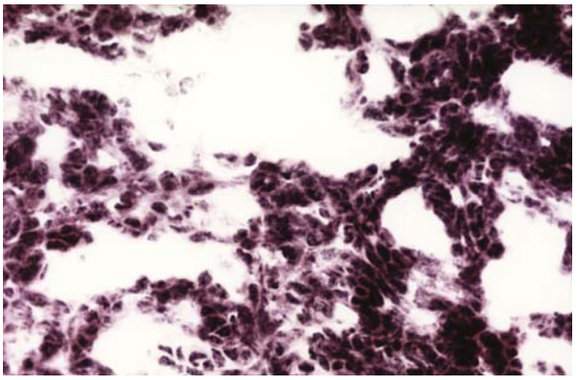

Figure 93. Expression of vitamin D receptor (VDR) in ovarian carcinoma. Notice strong immunoreactivity for VDR in ovarian carinoma. Original magnification: 160X.

This up-regulation was statistically significant (VDR-PP: $p < 0.001$; VDR-SI: $p < 0.001$; VDR-IRS: $p < 0.001$).

Comparing Vitamin D Receptor Expression in Ovarian Carcinomas with the Proliferation Marker Ki-67

Analyzing co-expression of VDR with Ki-67, no significant correlation was found (VDR-IRS: $p = 0.498$; VDR-SI: $p = 0.57$; VDR-PP: $p = 0.66$). Five out of 40 ovarian carcinomas revealed 0–9% of Ki-67-positive tumor cells, whereas 16 specimens showed 10–25%, and the remaining 19 specimens showed more than 25% Ki-67-immunoreactive cells (mean percentage of Ki-67-positive tumor cells: 29.44%, SD: +/– 21.00%).

Comparing Vitamin D Receptor Expression in Ovarian Carcinomas with the Expression of Estrogen Receptor and Progesterone Receptor

Nuclear immunoreactivity for ER and PR was detected in 40% and 32.5%, respectively, of all OCs analyzed. Staining of ER and PR was heterogeneous, with visual differences between individual tumor cells. Values of ER-IS or PR-IS as well as of ER-PP or PR-PP were markedly reduced as compared to VDR-IS and VDR-PP, respectively (mean ER-IS: 0.38, SD: +/– 0.65; mean ER-PP: 8.53%, SD: +/– 17.90%; mean ER-IRS: 0.68, SD: +/– 1.34; mean PR-IS: 0.35, SD: +/– 0.81; mean PR-PP: 6.76%, SD: +/– 18.54%; mean PR-IRS: 0.79, SD: +/– 2.23). Analyzing co-expression of VDR with ER (VDR-IRS: $p = 0.31$; VDR-SI: $p = 0.20$; VDR-PP: $p = 0.50$) and PR (VDR-IRS: $p = 0.71$; VDR-SI: $p = 0.40$; VDR-PP: $p = 0.63$), no statistically significant correlation was found.

Comparing Vitamin D Receptor Expression with Histopathologic Data of the Ovarian Carcinomas

No statistically significant correlation (VDR-IRS: $p = 0.39$; VDR-SI: $p = 0.35$; VDR-PP: $p = 0.40$) of VDR expression and different histologic types of OCs was observed. Comparing the expression of VDR with the histologic grading (VDR-IRS: $p = 0.29$; VDR-SI: $p = 0.08$; VDR-PP: $p = 0.27$) and the primary tumor stage (VDR-IRS: $p = 0.58$; VDR-SI: $p = 0.73$; VDR-PP: $p = 0.88$), no statistically significant correlation was found.

DISCUSSION

The mAb 9A7γ has been successfully used in the immunohistochemical investigation of VDR in various tissues such as chicken intestine, rat brain, disaggregated rat bone cells, rat osteosarcoma 17/2.8 cells (Clemens *et al.,* 1988), fibroblasts (Barsony *et al.,* 1990; Berger *et al.,* 1989), and normal and psoriatic human skin (Berger *et al.,* 1989; Milde *et al.,* 1991; Reichrath *et al.,* 1996, 1997) as well as in tissues from the human uterine cervix (Rafi *et al.,* 1997; Reichrath *et al.,* 1998) and from the human breast (Friedrich *et al.,*1997, 1998).

To our knowledge, this is the first report demonstrating VDR expression immunohistochemically in OCs. Measurement of VDR receptors in OCs using a radio-labeled ligand-binding assay was described previously (Saunders *et al.,* 1992). Although Saunders *et al.* (1992) demonstrated VDR expression in 50% of ovarian tumors analyzed, we found high percentage of VDR-stained cells and moderate to strong VDR staining intensity in almost all specimens of OCs analyzed. The receptor VDR-IRS in OCs was increased as compared to normal ovarian tissue, indicating up-regulation of VDR in OCs as described previously for cervical carcinomas (Rafi *et al.,* 1997; Reichrath *et al.,* 1998) and breast carcinomas (Friedrich *et al.,* 1997, 1998).

It has been shown that the steroid hormone responsiveness is directly proportional to the number of corresponding receptors (Costa and Feldman, 1987). Because VDR mediates the biologic effects of calcitriol and analogs on proliferation and differentiation in target cells (Haussler *et al.,* 1988; Norman *et al.,* 1982), strong VDR expression may indicate an increased sensitivity of ovarian tissue to endogeneous or therapeutically applied calcitriol. However, we cannot exclude the possibility that VDR function in ovarian carcinomas may be altered (i.e., by a functionally inactivating mutation in the VDR gene).

It is interesting that only in a small proportion of all analyzed tumors was the staining pattern of VDR concordant with the staining pattern of the Ki-67 antigen. This finding indicates that VDR expression is not exclusively a function of cellular proliferation in these tumor cells; instead, it may be determined by additional different and yet unknown mechanisms. We and others have shown that cytokines and other factors that stimulate transmembrane-signaling pathways alter VDR levels in keratinocytes and other cell types *in vitro* (Krishnan *et al.,* 1995; Reichrath *et al.,* 1991). Surrounding stroma of OCs often contains an increased number of inflammatory cells. Cytokines and inflammatory peptides excreted by these cell types may up-regu1ate VDR expression in adjacent tumor cells.

It has been shown that 1,25-dihydroxyvitamin-D_3 potentiates tumor necrosis factor (TNF)–induced cytotoxity on human cancer cells (Demirpence *et al.,* 1994; Rocker *et al.,* 1994). This effect is most likely the result of a VDR-mediated action that may be potentiated in OCs by the increased VDR expression. Apoptosis is an asynchronous cellular process with cytoplasmic and nuclear condensation, disruption of the cytoskeleton, and condensation of intermediate filaments around the nucleus (Tenniswood *et al.,* 1992; Wyllie, 1987). It has been shown that calcitriol induces apoptosis in various tumor cells (Naveilham *et al.,* 1994; Welsh *et al.,* 1994). Apoptotic cells have been described in OCs (Ghahremani *et al.,* 1998; Spriggs and Makhija, 1998; Wehrli *et al.,* 1998); VDR-mediated mechanisms may be involved in the induction of apoptosis in OCs.

Androgen and corticosteroid receptor proteins, ER, and PR have been observed in a high percentage of women suffering from epithelial ovarian cancer. Using immunohistochemical techniques, a positivity for ER and PR of ~35–82% is described (Kommoss *et al.,* 1991; Nardelli *et al.,* 1987). Results of our investigation are comparable with these studies. Our findings do not demonstrate a correlation comparing IRS for VDR with IRS for ER and PR, indicating that expression of these steroid hormone receptors is independently regulated in OCs. The activity of various single-agent hormonal therapies in refractory epithelial ovarian cancer is quite low. Thus, in refractory epithelial ovarian cancer, response rates of 0–32% are described for progestin therapy (Geisler *et al.,* 1985; Slayton *et al.,* 1981; Trope *et al.,* 1982), 0–17.1% for tamoxifen therapy (Hatch *et al.,* 1991; Slevin *et al.,* 1986), and 15.4–60.0% (only 5 patients) for gonadotropin-releasing hormone analogs (GnRH) (Bruckner and Motwani, 1989; Parmar *et al.,* 1988). These agents are usually used in refractory settings for palliation, and there is limited experience in the primary setting. Mostly, complete and partial responses were observed only in women whose tumors were ER positive or both ER and PR positive.

Determinations of ER level may be of value in the treatment of women with endometrioid OC to determine hormonal sensitvity. It is highly likely that receptor-positive tumors are limited to women with well-differentiated endometrioid carcinomas. Progestins are suggested to have moderate to high activity in first-line therapy for the management of well-differentiated endometrioid OCs. Thus, Rendina *et al.* (1982) described a response rate of 55% with medroxyprogesterone acetate therapy in 31 previously untreated patients with well-differentiated endometrioid OCs. In case of refractory disease, it is possible that patients most likely to respond to tamoxifen are ER positive because their tumors may be biologically less virulent than receptor-negative tumors. A Gynecologic Oncology Group study revealed a 17% objective response rate in a group of 105 women with refractory ovarian cancer treated with 20 mg tamoxifen 2× day (Hatch *et al.,* 1991).

Although Cross *et al.* (1996) described increasing VDR protein levels during the development of human colon cancer from a precancerous state up to stage pT3 with dramatically declining VDR density at later stages, in OCs we could not demonstrate a relationship between primary tumor stage and histologic grading on the one hand and VDR expression on the other hand. Thus, expression of VDR protein does not seem to be influenced by primary tumor stage or histologic grading, but by different, so far unknown, mechanisms.

Our study adds to the body of evidence that new vitamin D analogs exerting less calcemic side effects may be promising new drugs in the treatment of OCs. It can be speculated whether combination therapy of these new vitamin D analogs with other steroid hormones such as progesterone, tamoxifen, or even GnRH analogs may exert synergistic anti-tumor effects on growth of OCs.

In conclusion, immunohistochemical expression of VDR in OC was found (n = 40). Immunoreactivity of VDR (mAb 9A7γ) was compared with the staining pattern of the proliferation marker Ki-67, ERS, and PRs. The percentage of positive tumor cells, the intensity of staining, and a resulting immunoreactivity score were determined for the semi-quantitative evaluation of VDR, ER, and PR expressions. A total of 16.7% of the normal surface ovarian epithelium was VDR negative, whereas the remaining 83.3% revealed weak to moderate VDR immunoreactivity (mean VDR-SI: 1.0 SD: +/– 0.87; mean VDR-PP: 57.14 SD: +/– 43.10; mean VDR-IRS: 2.86 SD: +/– 2.48). Moderate to strong nuclear immunoreactivity for VDR was detected in almost all ovarian carcinomas analyzed (mean VDR-IRS: 8.49, SD: +/– 3.80; mean VDR-SI: 2.31, SD: +/– 0.80; mean VDR-PP: 89.86%, SD: +/– 1.91%). Both the intensity of VDR immunostaining and the number of VDR-positive cells were statistically significantly increased in OCs as compared to normal ovarian tissue. By analyzing co-expression of VDR with the proliferation marker Ki-67 or with the estrogen and progesterone receptors no statistically significant correlation was found. Our findings indicate the following: 1) VDR expression is statistically, significantly increased in OCs as compared to normal ovarian tissue; 2) up-regulation of VDR in OCs is not exclusively induced by increase in proliferation, but by different unknown mechanisms; 3) expression of VDR in ovarian carcinomas is independently regulated from that of the expression of ER and PR; and 4) ovarian tissue may be a new target organ for therapeutically applied vitamin D analogs exerting less calcemic side effects. New vitamin D analogs may be promising drugs for the treatment of advanced OCs.

References

Barsony, J., Pike, J.W., DeLuca, H.F., and Marx, S.J. 1990. Immunocytology with microwave-fixed fibroblasts shows 1α,25-dihydroxyvitamin D_3-dependent rapid and estrogen-dependent slow reorganization of vitamin D receptors. *J. Cell Biol. 111*:2385–2388.

Berger, U., Wilson, P., McClelland, R.A., Colston, K., Haussler, M.R., Pike, J.W., and Coombes, R.C. 1989. Immunocytochemical detection of 1,25-dihydroxyvitamin D_3 receptors in normal human tissues. *J. Clin. Endo. Metab. 67*:607–613.

Bruckner, H.W., and Motwani, B.T. 1989. Treatment of advanced refractory ovarian carcinoma with a gonadotropin-releasing hormone analogue. *Am. J. Obstet. Gynecol. 161*:1216–1218.

Clemens, T.L., Garrett, K.P., Zhou, X.Y., Pike, J.W., Haussler, M.R., and Dempster, D.W. 1988. Immunocytochemical localization of the 1,25-dihydroxyvitamin D_3 receptor in target cells. *Endocrinology 122(4)*:1224–1227.

Colston, K., Colston, M.J., and Feldman, D. 1981. 1,25-dihydroxyvitamin D_3 and malignant melanoma: the presence of receptors and inhibition of cell growth in culture. *Endocrinology 108*:1083–1086.

Colston, K.W., Berger, U., and Coombes, R.C. 1989. Possible role for vitamin D in controlling breast cancer cell proliferation. *Lancet 1(8631)*:188–191.

Costa, E.M., and Feldman, D. 1987. Measurement of 1,25-dihydroxyvitamin D_3 receptor turnover by dense amino acid labelling: changes during receptor upregulation by vitamin D metabolites. *Endocrinology 120*:1173–1178.

Cross, H.S., Bajna, E., Bises, G., Genser, D., Kallay, E., Potzi, R., Wenzl, E., Wrba, F., Poka, R., and Peterlik, M. 1996. Vitamin D receptor and cytokeratin expression may be progression indicators in human colon cancer. *Anticancer Res. 16*:2333–2338.

Demirpence, E., Balaguer, P., Trousse, F., Nicolas, J.C., Pons, M., and Gagne, D. 1994. Antiestrogenic effects of all-trans-retinoic acid and 1,25-dihydroxyvitamin D_3 in breast cancer cells occur at the estrogen response element level but through different molecular mechanisms. *Cancer Res. 54(6)*:1458–1464.

Friedrich, M., Rafi, L., Schmidt, W., Tilgen, W., and Reichrath, J. 1997. Immunohistochemical analysis of 1,25-dihydroxyvitamin D_3 receptor (VDR) and retinoid-X-receptor α (RXRα) in breast carcinoma. In: Norman, A.W., Bouillon, R., and Thomasset, M.,

eds. *Vitamin D: Chemistry, Biology and Clinical Applications of the Steroid Hormone.* Proceedings of the Tenth Workshop on Vitamin D, Straßburg, France, May 24–29, 1997. Riverside: University of California, 475–476.

Friedrich, M., Rafi, L., Schmidt, W., Tilgen, W., and Reichrath, J. 1998. Expression of 1,25-Dihydroxyvitamin D_3 receptor in breast carcinoma. *J. Histochem. Cytochem. 46(11)*: 1335–1337.

Garland, C., Shekelle, R.B., Barrett-Connor, E., Criqui, M.H., and Rossof, A.H. 1985. Dietary vitamin D and calcium and risk of colorectal cancer: a 19-year prospective study in men. *Lancet 1*:307–309.

Geisler, H.E. 1985. The use of high-dose megestrol acetate in the treatment of ovarian adenocarcmoma. *Semin. Oncol. 12*: 20–22.

Gerdes, J., Lemke, H., Baisch, H., Wacker, H.H., Schwab, U., and Stein, H. 1984. Cell cycle analysis of a cell proliferation-associated human nuclear antigen defined by the monoclonal antibody Ki-67. *J. Immunol. 133*:1710–1715.

Gerdes, J., Schwab, U., Lemke, H., and Stein, H. 1983. Production of mouse monoclonal antibody reactive with a human nuclear antigen associated with cell proliferation. *Int. J. Cancer 31*: 13–20.

Ghahremani, M., Foghi, A., and Dorrington, J.H. 1998. Activation of Fas ligand/receptor system kills ovarian cancer cell lines by an apoptotic mechanism. *Gynecol. Oncol. 70(2)*:275–281.

Hatch, K.D., Beechem, J.B., Blessing, J.A., and Creasman, W.T. 1991. Responsiveness of patients with advanced ovarian carcinoma to tamoxifen: a gynecologic oncology group study of second line therapy in 105 patients. *Cancer 68*:269–271.

Haussler, M.R., Mangelsdorf D.J., Komm, B.S., Terpening, C.M., Yamaoka, K., Allegretto, E.A., Baker, A.R., Shine, J., McDonnell, D.P., and Hughes, M. 1988. Molecular biology of the vitamin D hormone. *Recent Prog. Horm. Res. 44*:263–305.

Hosomi, J., Abe, E., Suda, T., and Kuroki, T. 1983. Regulation of terminal differentiation of cultured mouse epidermal cells by 1α-25-dihydroxyvitamin D_3. *Endocrinology 113*:1950–1957.

Hunter, R.W., Alexander, N.D., and Soutter, W.P. 1992. Meta-analysis of surgery in advanced ovarian carcinoma: is maximum cytoreduction surgery an independent determinant of prognosis? *Amer. J. Obstet. Gynecol. 166*:504–511.

Katakami, Y., Nakao, Y., Katakami, N., Koizumi, T., Ogawa, R., Yamada, H., Takai, Y., and Fujita, T. 1988. Cooperative effects of tumor necrosis factor-alpha and 1,25-dihydroxyvitamin D_3 on growth inhibition, differentiation, and c-myc reduction in human promyelocytic leukemia cell line HL-60. *Biochem. Biophys. Res. Commun. 152*:1151–1157.

Kommoss, F., Pfisterer, J., Geyer, H., Thome, M., Sauerbrei, W., and Pfleiderer, A. 1991. Estrogen and progesterone receptors in ovarian neoplasms: discrepant results of immunohistochemical and biochemical methods. *Int. J. Gynecol. Cancer 1*:147–149.

Krishnan, A.V., Cramer, S.D., Bringhurst, F.R., and Feldman, D. 1995. Regulation of 1,25-dihydroxyvitamin D_3 receptors by parathyroid hormone in osteoblastic cells: role of second messenger pathways. *Endocrinology 136*:705–712.

Milde, P., Hauser, U., Simon, T., Mall, G., Ernst, V., Haussler, M.R., Frosch, P., and Rauterberg, E.W. 1991. Expression of 1,25-dihydroxyvitamin D_3 receptors in normal and psoriatic skin. *J. Invest. Dermatol. 97*:230–239.

Nardelli, G.B., Lamaina, V., DaiPozzo, M., and Onnis, G.L. 1987. Determination of ER in ovarian cancer using monoclonal antibody technology. *Clin. Exp. Obstet. Gynecol. 3*:185–187.

Naveilhan, P., Baudet, C., Berger, F., Benabid, A.L., Brachet, P., and Wion, D. 1994. Induction of glioma cell death by 1,25-dihydroxyvitamin D_3. In: Norman, A.W., Bouillon, R., and Thomasset, M., eds. *Vitamin D: A Pluripotent Steroid Hormone: Structural Studies, Molecular Endocrinology and Clinical Applications*. New York: Walter de Gruyter, 644–645.

Norman, A.W., Roth, J., and Orci, L. 1982. The vitamin D endocrine system: steroid metabolism, hormone receptors and biological response (calcium binding proteins). *Endo. Rev. 3*:331–335.

Parmar, H., Rustin, G., Lightman, S.L., Philips, R.H., Hanham, I.W., and Schally, A.V. 1988. Response to D-Trp-6-luteinizing hormone releasing hormone (Decapeptyl) microcapsules in advanced ovarian cancer. *Br. Med. J. 296*:1229.

Pike, J.W., Donaldson, C.A., Marion, S.L., and Haussler, M.R. 1982. Development of hybridomas secreting monoclonal antibodies to the chicken intestinal 1α-25-dihydroxyvitamin D_3 receptor. *Proc. Natl. Acad. Sci. USA 79*:7719–7723.

Pike, J.W., Marion, S.L., Donaldson, C.A., and Haussler, M.R. 1983. Serum and monoclonal antibodies against the chick intestinal receptor for 1,25-dihydroxyvitamin D_3. *J. Biol. Chem. 258*: 1289–1292.

Rafi, L., Reichrath, J., Müller, S.M., Tilgen, W., Schmidt, W., and Friedrich, M. 1997. Expression of 1,25-dihydroxyvitamin D_3 receptors (VDR) in cervix carcinomas. In: Norman, A.W., Bouillon, R., and Thomasset, M., eds. *Vitamin D: Chemistry, Biology and Clinical Applications of the Steroid Hormone*. Proceedings of the Tenth Workshop on Vitamin D, Straßburg, France, May 24–29, 1997. Riverside: University of California, 477–478.

Reichrath, J., Collins, E.D., Epple, S., Kerber, A., Norman, A.W., and Bahmer, F.A. 1996. Immunohistochemical detection of 1,25-dihydroxyvitamin D_3 (VDR) receptors in human skin. *Path. Res. Pract. 192*:281–289.

Reichrath, J., Hügel, U., Klaus, G., Fusenig, N.E., and Rauterberg, E.W. 1991. Modulation of 1,25-dihydroxyvitamin D_3 receptor expression in HaCaT keratinocytes. In: Norman, A.W., Bouillon, R., and Thomasset, M., eds. *Vitamin D: Gene Regulation, Structure Function Analysis and Clinical Application*. New York: Walter de Gruyter, 445–446.

Reichrath, J., Müller, S.M., Kerber, A., Baum, H.P., and Bahmer, F.A. 1997. Biological effects of topical calcipotriol (MC 903) treatment in psoriatic skin. *J. Am. Acad. Dermatol. 36*:19–28.

Reichrath, J., Rafi, L., Müller, S.M., Mink, D., Reitnauer, K., Tilgen, W., Schmidt, W., and Friedrich, M. 1998. Immunohistochemical analysis of 1,25-dihydroxyvitamin D_3 receptor in cervical carcinoma. *Histochem. J. 30*:561–567.

Remmele, W., Hildebrand, U., Hienz, H.A., Klein, P.J., Vierbuchen, M., Bebhnken, L.J., Heicke, B., and Scheidt, E. 1986. Comparative histological, histochemical, immunohistochemical and biochemical studies on estrogen receptors, lectin receptors, and barr bodies in human breast cancer. *Arch. Virchows 93*:1292–1297.

Rendina, G.M., Donadio, C., and Giovannini, M. 1982. Steroid receptors and progestinic therapy in ovarian endometrioid carcinoma. *Eur. J. Gyneacol. Oncol. 3*:241–246.

Rocker, D., Ravid, A., Liberman, U.A., Garach-Jehoshua, O., and Karen, R. 1994. 1,25-Dihydroxyvitamin D_3 potentiates the cytotoxic effect of TNF on human breast cancer cells. *Mol. Cell Endocrinol. 106(1-2)*:157–162.

Saunders, D.E., Christensen, C., Lawrence, W.D., Malviya, V.K., Malone, J.M., Williams, J.R., and Deppe, G. 1992. Receptors for 1,25-dihydroxyvitamin D_3 in gynecologic neoplasms. *Gynecol. Oncol. 44(2)*:131–136.

Slayton, R.E., Pagnano, M., and Creech, R.H. 1981. Progestin therapy for advanced ovarian cancer: a phase II Eastern Cooperative Group Trial. *Cancer Treat. Rep. 65*:895–896.

Slevin, M.L., Harvey, V.J., Osborne, R.J., Shepard, H.J., Williams, C.J., and Mead, G.M. 1986. A phase II study of tamoxifen in ovarian cancer. *Eur. J. Cancer Clin. Oncol. 22*:309–312.

Smith, E.L., Walworth, N.C., and Holick, M.F. 1986. Effect of 1α-25-dihydroxyvitamin D_3 on the morphological and biochemical differentiation on cultured human epidermal keratinocytes grown in serum-free conditions. *J. Invest. Dermatol. 86*:709–714.

Spriggs, D.R., and Makhija, S. 1998. Ovarian cancer staging: time for a closer look? *J. Clin. Oncol. 16(8)*:2577–2578.

Stumpf, W.E., Sar, M., Reid, F.A., Tanaka, Y., and DeLuca, H.F. 1979. Target cells for 1,25-dihydroxyvitamin D_3 in intestinal tract stomach, kidney, skin, pituitary and parathyroid. *Science 206*: 1189–1190.

Tenniswood, M.P., Guenette, S., Lakins, J., Mooibroek, M., Wong, P., and Welsh, J. 1992. Active cell death in hormone dependent tissues. *Cancer Metastasis Rev. 11*:197–220.

Thigpen, J.T., Bertelsen, K., Eisenhauer, E.A., Hacker, N.F., Lund, B., and Sessa, C. 1993. Longterm follow-up of patients with advanced ovarian carcinoma treated with chemotherapy. *Ann. Oncol. 4*:35–40.

Trope, C., Johnson, J.E., Sigurdsson, K., and Simonson, E. 1982. High-dose medroxyprogesterone acetate for the treatment of advanced ovarian carcinoma. *Cancer Treat. Rep. 66*:1441–1443.

Wehrli, B.M., Krajewski, S., Gascoyne, R.D., Reed, J.C., and Gilks, C.B. 1998. Immunohistochemical analysis of bcl-2, bax, mcl-1, and bcl-X expression in ovarian surface epithelial tumors. *Int. J. Gynecol. Pathol. 17(3)*:255–260.

Welsh, J., Simboli-Campbell, M., and Tenniswood, M. 1994. Induction of apoptotic cell death by 1,25-dihydroxyvitamin D_3 in MCF-7 breast cancer cells. In: Norman, A.W., Bouillon, R., and Thomasset, M., eds. *Vitamin D: A Pluripotent Steroid Hormone: Structural Studies, Molecular Endocrinology and Clinical Applications*. New York: Walter de Gruyter, 526–527.

Williams, C.J., Stewart, L., Parmar, M., and Guthrie, D. 1992. Meta-analysis of the role of platinum compounds in advanced ovarian carcinoma. The Advanced Ovarian Trialists Group. *Semin. Oncol. 199*:120–128.

Wyllie, A.H. 1987. Apoptosis: cell death in tissue regulation. *J. Pathol. 153(3)*:313–316.

This Page Intentionally Left Blank

29

Role of Immunohistochemical Expression of Antigens in Neuroendocrine Carcinoma of the Ovary and Its Differential Diagnostic Considerations

Stephen L. Strobel

Introduction

Ovarian neuroendocrine carcinomas (NEC) are uncommon neoplasms, comprising less than 1% of primary ovarian cancers (Eichhorn and Young, 2001). Because of the frequent association with conventional ovarian surface carcinomas, particularly mucinous and endometrioid types, NEC are generally regarded as a dedifferentiated form of surface neoplasia with neuroendocrine expression. Small-cell (pulmonary type) and non–small-cell variants exist (Fukunaga *et al.,* 1997; Strobel and Graham, 2003). Both variants are highly malignant, with extremely poor prognosis and therapeutic response. Most patients with these tumors die within 2 years of diagnosis.

A variety of other neoplasms, both primary and metastatic to the ovary, can resemble NEC. Thorough sampling of the surgical pathology specimens for routine histologic examination is perhaps the single most important factor for proper identification of these tumors. However, in that NEC and their differential diagnostic considerations often have discernible histochemical profiles, immunohistochemical analysis of tissue sections represents a valuable diagnostic adjunct. As a result, the use of immunohistochemistry (IHC) is now generally regarded as a standard tool for the diagnosis of these tumors.

METHODS AND MATERIALS

For the standard evaluation of NEC, tissue sections are fixed in 10% buffered formalin, processed for microscopic examination, embedded in pariffin, cut at 4 μm thickness, and stained with hemotoxylin and eosin. For all immunohistochemical stains, paraffin sections are cut at 4 μm thickness and placed on ++ charged slides.

The following antibodies and clones are routinely used for neuroendocrine neoplasia: chromogranin A (Dako Corporation, Carpinteria, CA), neurospecific enolase

Handbook of Immunohistochemistry and *in situ* Hybridization of Human Carcinomas, Volume 4: Molecular Genetics, Gastrointestinal Carcinoma, and Ovarian Carcinoma

(NSE, Dako), and synaptophysin (Dako). For synaptophysin only, a heat-induced epitope retrieval procedure is performed using Dako Target Retrieval Solution.

Role of Immunohistochemistry

Immunohistochemical evaluation of neoplasia is best accomplished with panels of selected markers (antibodies), which permit the identification of the tumor in question and the exclusion of other histologic "mimics." Selected immunohistochemical panels (Gown, 1999) are excellent for the evaluation of a wide range of neoplasia.

Neuroendocrine neoplasms, regardless of site, classically express markers of neuroendocrine differentiation: chromogranin A, synaptophysin, and neuron-specific enolase. Low molecular weight cytokeratin (identified by antibody 35 BetaH11 or CAM5.2) represents a nonspecific epithelial marker also frequently identified in neuroendocrine neoplasms. In contrast, high molecular weight cytokeratin (identified by antibody 34 BetaEl2) is not expressed. Residual surface epithelial cancer cells may also express other cytokeratin markers, particularly cytokeratin 7, which may serve to distinguish high-grade epithelial elements from neuroendocrine elements in a tumor.

Specific (singular) immunohistochemical markers are of considerable utility in the identification of the primary site for NEC and for distinguishing other neoplasms commonly included in the differential diagnosis for neuroendocrine tumors. These markers should never be used in isolation; they should serve as supplemental diagnostic tools to be studied in conjunction with other standard clinical and pathologic features of ovarian neoplasia. Their application, when appropriate, is discussed in the corresponding sections that follow.

Variations of Ovarian Neuroendocrine Neoplasia

Primary ovarian carcinoids represent a subset of neuroendocrine neoplasms, which typically follow a benign clinical course (Davis *et al.,* 2001). These may be divided into insular, trabecular, stromal, and mucinous variants based on their histomorphology. Co-existent other forms of primary ovarian neoplasia, particularly teratomas, are frequent. Because of their well-differentiated histologic features, ovarian carcinoids are seldom confused with primary ovarian NEC.

Metastatic carcinoid tumors in the ovary demonstrate a more aggressive clinical behavior, intermediate between that of primary ovarian carcinoid tumors and neuroendocrine carcinomas. Common primary sites include lung, gastrointestinal tract, and mediastinum. Appropriate treatment is based on identification of the primary site.

Metastatic high-grade NEC in the ovaries closely resembles primary ovarian NEC. Pulmonary origin represents the most common primary site, although NEC has been described in essentially every organ system (Eichhorn *et al.,* 1993). Bilateral ovarian involvement, absence of association with other primary ovarian neoplasms, and histologic evidence of blood vessel or angiolymphatic invasion are features that favor a metastatic origin.

All of these neoplasms express classic neuroendocrine markers (chromogranin A, synaptophysin, and neuron-specific enolase) (Figure 94), although the degree of antigen expression may vary, depending on the histologic grade of the tumor. Specific (singular) immunohistochemical markers that may aid in the identification of a nonvarian primary site include: thyroid transcription factor-1, lung primary (Lau *et al.,* 2002); gross cystic disease fluid protein–15, breast primary (Sapino *et al.,* 2001); cytokeratin 20 expression with lack of thyroid transcription factor 1 expression, Merkel cell (neuroendocrine) carcinoma of the skin (Leech *et al.,* 2001); and gastrin-releasing peptide or gastrin-releasing peptide receptor, gastrointestinal (carcinoid) primary (Scott *et al.,* 2004).

The IHC method is also being used with increasing frequency as a prognostic indicator for NEC, particularly when the lung is the primary site. CD117 (c-kit protein) expression represents a negative prognostic factor for large cell NEC (Casali *et al.,* 2004). Beta III immunoreactivity is a poor prognostic indicator associated with both small and large cell NEC (Katsetos *et al.,* 2000). Analysis for drug-resistant proteins may aid in the prediction of appropriate therapeutic protocols (Okada *et al.,* 2003). Further studies are necessary to indicate whether these markers have similar prognostic and therapeutic significance in primary ovarian NEC.

Ovarian Sex-Cord Stromal Tumors

Granulosa cell tumors are generally well-differentiated neoplasms with characteristic histologic features (nuclear grooves, Call-Exner bodies), readily appreciated on routine histologic examination (Uygun *et al.,* 2003). However, occasional tumors may demonstrate relatively diffuse, high-grade nuclear atypia, creating the potential for confusion with NEC. Poorly differentiated Sertoli-Leydig cell tumors, although less common, may also enter into this differential diagnostic consideration (Oliva *et al.,* 2001).

Sex-cord stromal tumors have a characteristic immunohistochemical profile (Riopel *et al.,* 1998): expression of alpha inhibin and vimentin and absence

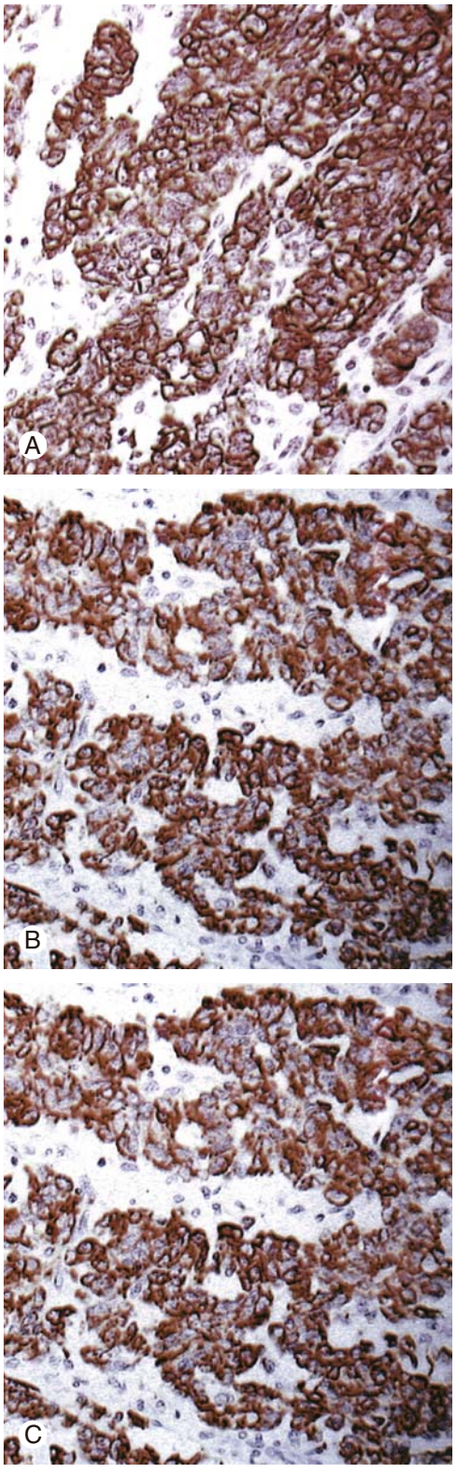

Figure 94. A: tumor, adult histotype (OGCTA): Most of neoplastic cells show immunostaining for estrogen receptor beta (ERβ). 400X. **B:** Ovarian granulosa cell tumor, adult histotype (OGCTA): Only a minority of neoplastic cells show immunostaining for proliferating cells nuclear antigen (PCNA) 400X. **C:** Ovarian granulosa cell tumor, adult histotype (OGCTA): Absent immunopositivity of neoplastic cells for p53 protein. 400X.

of expression of epithelial membrane antigen, cytokeratin 7, and neuroendocrine markers. Calretinin may be included as an additional positive marker, although its expression appears to be less specific than inhibin (Shah *et al.,* 2003).

Alpha inhibin, and a similar polypeptide hormone, activin B, can be measured in the blood and have been suggested as markers for the post-operative follow-up of patients with granulosa cell tumors (Vihko *et al.,* 2003). In selected cases, analysis of chromosomal aberrations in tumors, particularly trisomy 12 and 14 and monosomy 22, can add supportive evidence for a diagnosis of granulosa cell tumor (Mayr *et al.,* 2002).

Metastatic Gastric and Mammary Carcinoma in the Ovary

High-grade (diffuse/signet-ring cell) adenocarcinoma of the stomach metastasizes to the ovary with relative frequency. Immunohistochemical evidence of expression of epithelial membrane antigen and pancytokeratin and absence of expression of alpha inhibin and neuroendocrine markers distinguish a metastatic adenocarcinoma from primary ovarian sex-cord or neuroendocrine tumors, respectively. Confirmation of the gastric primary is made on clinical grounds. Expression of other immunohistochemical markers such as p53 (Bataille *et al.,* 2003), E-cadherin (Chen *et al.,* 2003), seprase (Okada *et al.,* 2003), and heat-shock protein 90α (Zuo *et al.,* 2003) may have significant prognostic implications for these tumors.

Metastatic lobular carcinoma of the breast may also exhibit a diffuse infiltrative pattern, which can mimic small cell carcinoma, lymphoma, or signet-ring cell adenocarcinoma. Lobular carcinoma classically expresses high molecular weight cytokeratin (CK34); low molecular weight cytokeratin (CK35); and the specific singular marker, gross cystic disease fluid protein-15. Estrogen and progesterone receptor expression is variable.

Lymphomas

Lymphomas may be primary or secondary in the ovary and are generally included in the differential considerations of small and large "blue cell" tumors

(Vang *et al.,* 2001). From a practical standpoint, positive expression of leukocyte common antigen (CD45), and the absence of expression of cytokeratins, synaptophysin, chromogranin A, and alpha inhibin, permits accurate identification of lymphoma. Subclassification of lymphomas or leukemias is possible with extended immunohistochemical panels (Gown, 1999). This accurate subclassification is necessary for the initiation of appropriate therapy. Specific cytogenetic and molecular markers also exist for many forms of lymphoid neoplasia (Jaffe *et al.,* 1998).

Sarcomas

Ovarian involvement by a sarcoma is uncommon. Endometrial stromal sarcoma represents the histologic variant most likely to be confused with NEC or primary ovarian sex-cord stromal tumor (Young *et al.,* 1984). Endometrial stromal sarcomas express CD10 and are negative for neuroendocrine markers and alpha inhibin.

Because neuroendocrine carcinomas frequently coexist with (arise from) a high-grade ovarian surface carcinoma, distinction from an ovarian carcinosarcoma may also occasionally be considered (Harris *et al.,* 2003). Ovarian carcinosarcomas demonstrate a biphasic expression of epithelial markers (cytokeratins and epithelial membrane antigen) and mesoenchymal markers (such as vimentin and muscle actins), but they fail to express lymphoid, neuroendocrine, or sex-cord stromal tumor markers.

Small Blue Round-Cell Tumors

Although these neoplasms are generally regarded as tumors of childhood, small blue round-cell occasionally enter into the differential diagnostic considerations for neuroendocrine carcinoma. In addition to carcinomas and lymphomas (previously discussed), neuroblastoma, primitive neuroectodermal tumor, Ewing's sarcoma, rhabdomyosarcoma, and desmoplastic small round-cell tumor are included in this category. With the exclusion of neuroendocrine markers, the following immunohistochemical panel usually is applied to these tumors: cytokeratins (carcinoma), CD45 and lymphoma subset markers (lymphoma), neurofilaments (neuroblastoma), CD99 (PNET/Ewing's sarcoma) (Kawauchi *et al.,* 1998), myogenin (rhabdomyosarcoma), and cytokeratin and Wilm's tumor-I/Wilms tumor gene product (desmoplastic small round-cell tumor) (Ordonez, 1998). Wilms tumor-I protein overexpression is a consequence of the t(11:22)(p13:q12) translocation unique to desmoplastic small round-cell tumors.

Small-cell carcinoma of the ovary, hypercalcemic type (Young *et al.,* 1994) is generally also included in this category. This represents a distinct form of ovarian neoplasia that usually involves young women (average age approximately 24 years) and is frequently associated with hypercalcemia (in approximately 60% of cases). A large cell ovariant of this tumor also exists. The associated hypercalcemia represents a paraendocrine phenomenon associated with human parathyroid hormone–related protein production (Matias-Guiu *et al.,* 1994). The neoplastic cells in these tumors are generally small and round, with hyperchromatic nuclei and brisk mitotic activity. Immunohistochemical studies demonstrate epithelial markers (cytokeratins and epithelial membrane antigen) and occasional mesenchymal markers (such as vimentin) to varying degrees, in contrast to the neuroendocrine markers identified in the ovarian small cell carcinomas in older women.

Malignant Melanoma

Malignant melanoma has been regarded as the "great mimic" of virtually all other malignant neoplasms and should always be considered in the differential diagnosis of a high-grade ovarian neoplasm when other immunohistochemical studies are inconclusive. A variety of markers, including HMB-45, Melan-A/MART-1 (melanoma antigen), and tyrosinase can be used to confirm a diagnosis of malignant melanoma (Young and Scully, 1991). Many institutions use a cocktail of these antibodies to improve the sensitivity.

Adjunct Studies

In selected cases, additional ancillary studies may be used to support routine histologic and immunohistochemical findings. CD56 (neural cell–adhesion molecule) detection with flow cytometric analysis can aid in the diagnosis of primary or recurrent NEC when samples of only limited cellularity (such as fine-needle aspiration biopsies or cytologic washings) are available for analysis (Cornfield *et al.,* 2003). Electron microscopy can identify certain cellular organelles, such as neurosecretory granules or premelanosomes, if IHC is equivocal (Dickersin and Scully, 1993). The value of detecting specific cytogenetic abnormalities has been discussed previously.

In conclusion, NECs, small- and non–small-cell variants, represent uncommon but highly malignant forms of primary ovarian cancer. Distinction from other forms of ovarian neoplasia, both primary and metastatic, is imperative to ensure appropriate therapy and to

predict prognosis. A valuable and often essential component for the accurate histologic characterization of these tumors is IHC. Awareness of neoplastic "mimics" and use of appropriate immunohistochemical panels, in conjunction with pertinent clinical features, permits consistent classification in the vast majority of cases. The IHC method may also serve a role in the prediction of therapeutic response and prognosis for many tumors. In rare instances when immunohistochemical results are equivocal, adjunct special studies such as electron microscopy, flow cytometric immunophenotyping, and cytogenetic analysis may assist with proper classification.

References

Bataille, F., Rummele, P., Dietmaier, W., Gaag, D., Klebl, F., Reichle, A., Wild, P., Hofstadter, F., and Hartmann, A. 2003. Alterations in p53 predict response to preoperative high dose chemotherapy in patients with gastric cancer. *Mol. Pathol. 56*:286–292.

Casali, C., Stefani, A., Rossi, G., Migaldi, M., Bettelli, S., Parise, A., and Morandi, U. 2004. The prognostic role of c-kit protein expression in resected large cell neuroendocrine carcinoma of the lung. *Ann. Thorac. Surg. 77*:247–252, discussion 252–253.

Chen, H.C., Chu, R.Y., Hsu, P.N., Hsu, P.I., Lu, J.Y., Lai, K.H., Tseng, H.H., Chou, N.H., Huang, M.S., Tseng, C.J., and Hsiao, M. 2003. Loss of E-cadherin expression correlates with poor differentiation and invasion into adjacent organs in gastric adenocarcinomas. *Cancer Lett. 201*:97–106.

Cornfield, D., Liu, Z., Gorczyca, W., and Weisberger, J. 2003. The potential role of flow cytometry in the diagnosis of small cell carcinoma. *Arch. Pathol. Lab. Med. 127*:461–464.

Davis, K.P., Hartmann, L.K., Keeney, G.L., and Shapiro, H. 2001. Primary ovarian carcinoid tumors. *Gynecol. Oncol. 61*: 259–265.

Dickersin, G.R., and Scully, R.E. 1993. An update on the electron microscopy of small cell carcinoma of the ovary with hypercalcemia. *Ultrastruct. Pathol. 17*:411–422.

Eichhorn, J.H., and Young, R.H. 2001. Neuroendocrine tumors of the genital tract. *Am. J. Clin. Pathol. 115* Suppl:S94–S112.

Eichhorn, J.H., Young, R.H., and Scully, R.E. 1993. Nonpulmonary small cell carcinomas of extragenital origin metastatic to the ovary. *Cancer 71*:177–186.

Fukunaga, M., Endo, Y., Miyazawa, Y., and Ushigome, S. 1997. Small cell neuroendocrine carcinoma of the ovary. *Virchows Arch. 430*:343–348.

Gown, A.M. 1999. Immunohistochemical determination of primary sites of carcinoma. *J. Histotechnol. 22*:209–215.

Harris, M.A., Delap, L.M., Sengupta, P.S., Wilkinson, P.M., Welch, R.S., Swindel, R., Shanks, J.H., Wilson, G., Slade, R.J., Reynolds, K., Jayson, G.C. 2003. Carcinosarcoma of the ovary. *Br. J. Cancer 88*:654–657.

Jaffe, E.S., Harris, N.L., Diebold, J., and Muller-Hermelink, H.K. 1998. World Health Organization Classification of lymphomas: a work in progress. *Ann. Oncol.* Suppl *5*:S25–S30.

Katsetos, C.D., Kontogeorgos, G., Geddes, J.F., Herman, M.M., Tsimara-Papastamatiou, H., Yu, Y., Sakkas, L.I., Tsokos, M., Patchefsky, A.S., Ehya, H., Cooper, H.S., Provencio, J., Spano, A.J., and Frankfurter, A. 2000. Differential distribution of the neuron-associated class III beta-tubulin in neuroendocrine lung tumors. *Arch. Pathol. Lab. Med. 124*:535–544.

Kawauchi, S., Fukuda, T., Miyamoto, S., Yoshioka, J., Shirahama, S., Saito, T., and Tsukamoto, N. 1998. Peripheral primitive neuroectodermal tumor of the ovary confirmed by CD99 immunostaining, karyotypic analysis, and RT-PCR for EWS/FLI-1 chimeric mRNA. *Am. J. Surg. Pathol. 22*:1417–1422.

Lau, S.K., Luthringer, D.J., and Eisen, R.N. 2002. Thyroid transcription factor-1: a review. *Appl. Immunohistochem. Mol. Morphol. 10*:97–102.

Leech, S.N., Kolar, A.J., Barrett, P.D., Sinclair, S.A., and Leonard, N. 2001. Merkel cell carcinoma can be distinguished from metastatic small cell carcinoma using antibodies to cytokeratin 20 and thyroid transcription factor 1. *J. Clin. Pathol. 54*:727–729.

Matias-Guiu, X., Prat, J., Young, R.H., Capen, C.C., Rosol, T.J., Delellis, R.A., and Scully R.E. 1994. Human parathyroid hormone-related protein in ovarian small cell carcinoma: an immunohistochemical study. *Cancer 73*:1871–1881.

Mayr, D., Kaltz-Wittmer, C., Arbogast, S., Amann, G., Aust, D.E., and Diebold, J. 2002. Characteristic pattern of genetic aberrations in ovarian granulosa cell tumors. *Mod. Pathol. 15*:951–957.

Okada, D., Kawamoto, M., Koizumi, K., Tanaka, S., and Fukuda, Y. 2003. Immunohistochemical study of the expression of drug-resistant proteins in large cell neuroendocrine carcinoma of the lung. *Jpn. J. Thorac. Cardiovasc. Surg. 51*:272–276.

Okada, K., Chen, W.T., Iwasa, S., Jin, X., Yamane, T., Ooi, A., and Mitsumata, M. 2003. Seprase, a membrane-type serine protease, has different expression patterns in intestinal- and diffuse-type gastric cancer. *Oncology 65*:363–370.

Oliva, E., Young, R.H., and Scully, R.E. 2001. Ovarian Sertoli cell tumors: a clinicopathologic study of 56 cases emphasizing their immunohistochemical profile. *Virchows Arch. 439*:337.

Ordonez, N.G. 1998. Desmoplastic small round cell tumor. II. An ultrastructural and immunohistochemical study with emphasis on new immunohistochemical markers. *Am. J. Surg. Pathol. 22*:1314–1327.

Riopel, M.A., Perlman, E.J., Seidman, J.D., Kurman, R.J., and Sherman, M.E. 1998. Inhibin and epithelial membrane antigen immunohistochemistry assist in the diagnosis of sex cord-stromal tumors and provide clues to the histogenesis of hypercalcemic small cell carcinomas. *Int. J. Gynecol. Pathol. 17*:46–53.

Sapino, A., Papotti, M., Righi, L., Cassoni, P., Chiusa, L., and Bussolati, G. 2001. Clinical significance of neuroendocrine carcinoma of the breast. *Ann. Oncol.* 12 Suppl *2*:S115–S117.

Scott, N., Millward, E., Cartwright, E.J., Preston, S.R., and Coletta, P.L. 2004. Gastrin releasing peptide and gastrin releasing peptide receptor expression in gastrointestinal carcinoid tumors. *J. Clin. Pathol. 57*:189–192.

Shah, V.I., Freites, O.N., Maxwell, P., and McCluggage, W.G. 2003. Inhibin is more specific than caretinin as an immunohistochemical marker for differentiating sarcomatoid granulosa cell tumor of the ovary from other spindle cell neoplasms. *J. Clin. Pathol. 56*:221–224.

Strobel, S.L., and Graham, R. 2003. Primary non-small cell neuroendocrine carcinoma of the ovary. *J. Histotechnol. 26*:73–76.

Uygun, K., Aydiner, A., Saip, P., Basaran, M., Tas, F., Kocak, Z., Dincer, M., and Topuz, E. 2003. Granulosa cell tumor of the ovary: retrospective analysis of 45 cases. *Am. J. Clin. Oncol. 26*:517–521.

Vang, R., Medeiros, L.J., Warnke, R.A., Higgins, J.P., and Deavers, M.T. 2001. Ovarian non-Hodgkin's lymphoma: a clinicopathologic study of eight primary cases. *Mol. Pathol. 14*:1093–1099.

Vihko, K.K., Blauer, M., Puistola, U., and Tuohimaa, P. 2003. Activin B in patients with granulosa cell tumors: serum levels in comparison to inhibin. *Acta. Obstet. Gynecol. Scand. 82*: 570–574.

Young, R.H., Oliva, E., and Scully, R.E. 1994. Small cell carcinoma of the ovary, hypercalcemic type: a clinicopathologic analysis of 150 cases. *Am. J. Surg. Pathol. 18*:1102–1116.

Young, R.H., Prat, J., and Scully, R.E. 1984. Endometrioid stromal sarcomas of the ovary. *Cancer 53*:1143–1155.

Young, R.H., and Scully, R.E. 1991. Malignant melanoma metastatic to the ovary: a clinicopathologic analysis of 20 cases. *Am. J. Surg. Pathol*. *15*:849–860.

Zuo, D.S., Dail, J., Bo, A.H., Fan, J., and Xiao, X.Y. 2003. Significance of expression of heat shock protein90alpha in human gastric cancer. *World J. Gastroenterol. 9*:2616–2618.

30

Role of Immunohistochemistry in Elucidating Lung Cancer Metastatic to the Ovary from Primary Ovarian Carcinoma

Bernice Robinson-Bennett and Aaron Han

Introduction

Virtually any cancer can establish a metastatic process in the ovary. The rich blood supply to the ovary, especially in the perimenopausal female, makes it a fertile haven for the growth of metastatic tumor cells. The ostium created from follicular rupture at the time of ovulation may act as a portal of entry for malignant cells that are circulating in the peritoneal cavity. Metastatic cancer in the ovary is responsible for approximately 10–30% of all reported ovarian cancers (Parker and Curie, 1992). The primary sites are frequently the gastrointestinal (GI) tract, the uterus, and the breast. There is usually a significant time lapse between the initial primary diagnosis and the tumor metastasizing to the ovaries. An average of up to a 47-month interval has been cited in some studies (Webb *et al.,* 1975).

In general, the metastatic process usually occurs by six different routes, including direct extension from neighboring structures, dissemination and seeding through peritoneal fluid, metastasis through the fallopian tube lumen, lymphatic spread, hematogenous spread; and iatrogenic metastasis.

Carcinoma of the lung metastasizes to the ovary very rarely (Young and Scully, 1985; Mazur *et al.,* 1984). Similar to primary ovarian carcinoma (OC), when metastatic lesions to the ovary occur they are not preceded by clinical symptoms. Ovarian cancer in the setting of a previously diagnosed pulmonary malignancy can present a diagnostic dilemma. Microscopic evaluation and definitive diagnosis of metastatic cancers can be challenging because there can be wide variations in histologic patterns. The tissue distortion that may occur in biopsy specimens and the stromal reaction that may be produced by a small area of metastasis may add to the difficulty of the pathologic interpretation. In this chapter we will review the case of a woman with a 5-year history of progressive papillary adenocarcinoma of the lung presenting with new bilateral ovarian masses and how organ or tissue site-specific markers using immunohistochemistry (IHC) were used to differentiate a metastatic process from a primary OC (Householder *et al.,* 2002).

Immunohistochemistry Basics

Immunohistochemistry involves the use of specific antibodies to localize and bind corresponding antigens in cells and tissues (Colvin *et al.,* 1995; Dabbs, 2002).

Handbook of Immunohistochemistry and *in situ* Hybridization of Human Carcinomas, Volume 4: Molecular Genetics, Gastrointestinal Carcinoma, and Ovarian Carcinoma

Combined with microscopy, it has major significance in identifying the functions and localization of cellular proteins. A compound that absorbs or emits light is used in labeling the binding reaction. There are different protocols used in IHC. Most require that tissues be fixed, dehydrated, and embedded in resins before sectioning and immunolabeling. The most widely used method is enzyme–antibody-labeled IHC. Detection is based on stable color changes that occur when enzyme–antibody complexes are bound to specific antigens. The two most commonly used enzymes are alkaline phosphatase and peroxidase.

The peroxidase enzyme used in the method described later is isolated from the root of the horseradish plant. As described by Eissa, there are several reasons for the widespread use of the peroxidase enzyme. These include availability in its pure form, possession of inherent antigenic properties, the ability to block endogenous peroxidase activity before staining, and availability of a wide variety of chromagens to localize reactions (Eissa, 1998). The technique can be applied to paraffin-embedded and formalin-fixed tissues. The major limitation of the technique is the survival of the specific antigen and maintenance of acceptable tissue and cellular structures after fixation, dehydration, and embedding processes. If an antigen is extremely sensitive to fixation, unfixed frozen specimens can also be used successfully.

The two-step indirect method is used in the method described here. This method is thought to be more sensitive than the direct method because of the increase in the available number of epitopes to be identified in the antigen–antibody reaction, thus enhancing amplification of the signal. This method uses the binding of an unconjugated primary antibody to its antigen, followed by the application of the enzyme horseradish peroxidase (HRP)–labeled secondary antibody to its corresponding primary antigen. The chromagen is subsequently added to complete the color reaction.

Proper sectioning technique should be used because thick, folded sections can lead to false-positive results. A section thicknesses of 4 μm is believed to be optimal. Paraffin sections that are stored for long periods may also result in loss of certain tissue antigens (Hayat, 2000).

Staining should be performed at room temperature. At temperatures greater than 37°C there may be evaporation and drying of tissues accompanied with loss of antigen–antibody binding capacity. The incubation period may be reduced if temperatures are elevated above 37°C in a waterbath or hot tub (Eissa, 1998). Sodium-azide buffers should be avoided because their use in excess may hinder the binding of the peroxidase enzyme to its substrate.

A potential problem of immunohistochemical technique is undesirable background staining, which is probably the result of nonspecific binding of primary antibodies to collagen and connective tissue in the specimen. The chromagen 3,3-diaminobenzidine (DAB) tetrahydrochloride produces a dark-brown coloration at the site of the antigen–antibody reaction as a result of an oxidation reaction, which is catalyzed by peroxidase antibody. Positive staining of necrotic or crushed cells should be disregarded. True positive reaction is characterized by heterogeneity in distribution in single cells or among groups of cells or throughout the tumor. The intensity in staining as well as localization of staining to the appropriate cell compartment (nucleus versus cytoplasm versus cell membrane) is important in the appropriate evaluation of staining. The Ventana ES Automated System (Ventana BioTek Systems, Tuscon, AZ) was used for the immunohistochemical studies.

MATERIALS

1. Tissue fixed in 10% neutral buffer formalin.
2. Sections embedded and cut at 3–4 μm for IHC. We usually use Fisher Scientifics (Pittsburgh, PA) brand Superfrost slides.
3. Xylene and graded alcohols for clearing.
4. 10x Citra antigen-retrieval fluid; steamer or microwave for antigen retrieval.
5. Proteases for pretreatment.
6. Inhibitor for blocking endogenous peroxides activity.
7. Primary antibodies. Biotinylated immunoglobins.
8. Wash solution (phosphate buffer saline, or PBS) for rinses between steps.
9. Developing reagents, including avidin-HRPO, DAB, hydrogen peroxide.
10. Coverslips.

METHODS

1. 3–4 μm section are cut from paraffin blocks of tissues and placed on slides. Appropriate positive and negative controls are cut.
2. Slides are placed on a metal plate and heated or dried in the oven at 60°C for at least 30 min.
3. Staining is performed on the automated machine by Ventana Systems (Nexxus). In our protocol, the machine is turned on at this step in the procedure. Slides are removed from the oven and placed in slide holders for the deparaffinization step.
4. Slides are placed in xylene 2× for 10 min each time.
5. Slides are hydrated through graded alcohols 100% then 95%.
6. Slides are hydrated in distilled water.
7. Slides are placed with distilled water in steamer for antigen-retrieval step.

8. 1× Citra buffer is added to the steamer. Certain antibodies that do not require antigen retrieval skip to **Step 15.**
9. After water reaches a vigorous boil in a steamer, the chamber and the slides are placed on the base of a steamer.
10. Steam antigen retrieval for 30 min.
11. Appropriate primary and secondary antibodies are placed on the Nexxus instrument.
12. Caps and fluids are checked on the machine.
13. After antigen-retrieval step is complete, remove the cap, and allow the buffer to cool prior to removing the slides.
14. Remove the slides and attach the appropriate label for the primary antibody. The order and barcode are determined and printed out by the Nexxus stainer.
15. Cover slides with appropriate wash solutions.
16. Once the automated stainer is loaded, press "Run" and follow the appropriate instruction from the computer screen.
17. The automated steps include the following (18–26) starting with tissue incubation with primary antibody (Colvin *et al.,* 1995; Dabbs, 2002).
18. Rinse the slides with wash solution or buffered saline 3×.
19. Incubate the biotinylated secondary antibody.
20. Rinse slide with wash solution or buffered saline 3×.
21. Incubate with avidin-biotin peroxidase complex.
22. Rinse slide with wash solution or buffered saline 3×.
23. Incubate slide with DAB.
24. Rinse slide with wash solution or buffered saline 3×.
25. Counterstain with hematoxylin.
26. When staining is finished, slides can be removed and placed in a rack.
27. Rinse slides in warm running water with dish detergent until the water runs clear. This removes the liquid coverslip used in the Ventana system.
28. Dehydrate the slides through graded alcohols (95% then 100%) and cleared in xylene.
29. Coverslips are applied. This can be manually performed or by an automated system.

RESULTS AND DISCUSSION

Case Presentation

This patient is a 42-year-old Gravida 4 Para 2022 (G4P2022) female who initially presented to her internist with symptoms of bronchitis and pleuritic chest pain. Her history is significant for a 12 pack per year history of tobacco use. A chest radiograph was obtained at that time, which revealed a 5-cm nodule in the right lower lobe of the lung and a 1-cm nodule in the right upper lobe. The patient subsequently underwent bronchoscopy with biopsy, which revealed the presence of papillary adenocarcinoma with pleural involvement. The diagnosis of a primary thyroid carcinoma was ruled out based on clinical presentation and by a lack of immunohistochemical staining of the tumor for thyroglobulin. The patient underwent an extensive evaluation for distant metastasis, which failed to show any evidence of distant spread. The patient had a second opinion from a tertiary cancer center, which concurred with the diagnosis of a primary lung cancer.

The patient's gynecologic evaluation at the time of her initial presentation was unremarkable. This included a negative Papanicolau test, pelvic examination, pelvic ultrasound, computed tomography (CT) scan, and endometrial biopsy. Multiple chemotherapeutic agents were used to treat the patient's lung cancer, including etoposide, cisplatin, paclitaxel, gemcitabine, and docetaxel. Annual surveillance was done in the form of CT scans, which showed evidence of disease progression; however, the patient remained relatively asymptomatic.

Five years after the initial diagnosis, the patient had a CT scan that showed a moderate amount of free fluid in the pelvis. A pelvic ultrasound was obtained, which revealed a normal uterus but an enlarged right ovary with simple cysts measuring 5.8 cm in the greatest dimension. The left ovary measured 3.1 cm in the greatest dimension. A follow-up ultrasound was performed 3 months later, and there was progressive enlargement of the ovaries with septations. By this time, the ovarian enlargement was appreciated on bimanual examination.

A diagnostic laparoscopy was performed with bilateral tubal ligation. At the time of surgery there were diffuse tumor nodules studding the right hemidiaphragm. The ovaries were grossly enlarged, the right was described as measuring 7–8 cm × 6 cm, and the left measured approximately 5 cm × 6 cm. The ovarian surfaces had tumor implant, the largest measuring approximately 3 cm on the right ovary. Ovarian biopsies were obtained as well as aspirate of the cul-de-sac fluid. Frozen section of the ovarian biopsy showed papillary adenocarcinoma that was morphologically similar to the lung lesion. One such similarity was the broad fibroblastic stalks in the tumor papillae. A laparotomy was deferred on the basis of diffuse tumor involvement in a relatively asymptomatic patient. The patient was subsequently started on taxotere.

Two months later a CT scan was obtained showing bilateral adnexal masses, each measuring approximately 11 cm in the greatest dimension. The patient had

developed a new symptom of pelvic pressure, and a total abdominal hysterectomy with bilateral salpingo-oophorectomy was performed.

Immunohistochemistry was used to confirm metastatic disease to the ovary and to exclude a new ovarian primary cancer. Two years after the diagnosis of metastatic pulmonary carcinoma to the ovaries, the patient presented to the emergency department with progressive shortness of breath and later died of irreversible respiratory failure.

Immunohistochemical Findings

The staining pattern of pulmonary papillary adenocarcinoma shows a tumor that was positive for carcinoembryonic antigen (CEA) thyroid transcription factor-1 (TTF-1) (Figure 95), E- cadherin, cytokeratin (CK) 7, and surfactant, but negative for cancer antigen-125 (CA-125), CK20, vimentin, and N-cadherin. This constellation of staining was consistent with a primary lung tumor and inconsistent with an ovarian primary tumor.

Diagnosis of Ovarian Tumors

Two common problems exist in the recognition and diagnosis of ovarian cancer. First, one has to distinguish cancer from benign and borderline lesions with an assessment of the degree of malignancy as well as the histomorphology. Second, one must distinguish between primary ovarian cancer and a metastatic process. Microscopic and immunohistochemical studies may be complementary in facing these diagnostic challenges. However, currently prostate-specific antigen and thyroglobulin remain the only immunohistochemical markers that are entirely site or organ specific. It is of utmost importance that the primary tumor site be unequivocally identified because the selection of treatment modalities and chemotherapeutic agents used is contingent on this diagnosis. Given the few unique individual markers that are site or organ specific, the use of a panel of markers in the identification of primary tumor sites will continue to prove beneficial.

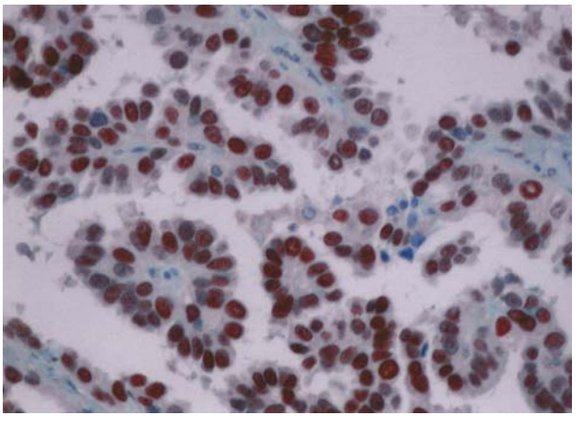

Figure 95. Papillary forming tumor cells showing nuclear positivity for TTF-1 immunostain consistent with lung primary (400X magnification).

In the case presented here, the patient's history of smoking and presentation with an initial lung lesion and a negative metastatic workup and clinically benign ovaries are consistent with a lung primary. The 5-year length of survival of this patient also favors primary lung carcinoma. The 5-year survival rate for the papillary adenocarcinoma of the lung is ~24% compared with a 10% 5-year survival rate for stage IV primary ovarian cancer (Travis *et al.,* 1995). Additionally, the immunohistochemical staining profile of the tumor is consistent with a primary lung cancer. The usefulness of the specific antigens will be further discussed later in this chapter.

Cadherins

Cadherins are calcium-dependent integral membrane glycoproteins that are located on cell-surface membranes and play key roles in intercellular adhesions (Takeichi, 1991). They are a part of a larger superfamily of adhesion molecules, which include integrins, selectins, and immunoglobulins. Three cadherins were described initially, form the classical cadherins, and are characterized by their distinct tissue distributions: E-cadherin in simple epithelia, N-cadherin in neuronal and mesenchymal tissue, and P-cadherin originally described in placental tissue but also found to be present in basal epithelia.

Cancer cells commonly exhibit decreased intercellular adhesiveness when compared to normal epithelial cells. Cadherins are known tumor-suppressor genes (Hedrick *et al.,* 1993; Zarka *et al.,* 2003), and their decreased expression has been shown to correlate with increased aggressive tumor behavior (Hirohashi, 1998; Takeichi, 1993).

Because of the relative tissue-restricted expression of cadherins, antibodies specific to cadherins have been used in the past to differentiate mesotheliomas from lung adenocarcinomas. E-cadherin is positive whereas N-cadherin is negative in lung adenocarcinoma, and N-cadherin is positive whereas E-cadherin is negative in mesothelioma (Han *et al.,* 1997; Peralta Soler *et al.,* 1995).

E-cadherin interacts with intracytoplasmic anchor molecules called catenins, and this binding establishes cell adhesion (Takeichi, 1991). The intensity of

expression in different tissue areas may directly correlate with the level of differentiation (Kalogeraki *et al.,* 2003). Poorly differentiated areas express E-cadherin weakly when compared to better differentiated areas in certain adenocarcinomas (Davidson *et al.,* 2000; Imai *et al.,* 2004). E-cadherin acts as an invasion suppressor molecule (Frixen *et al.,* 1991; Hedrick *et al.,* 1993). The first step in invasion and metastasis is the detachment of the cancer cells from the primary tumor. This presumably occurs when cell–cell adhesion is weakened either by reduced or abnormal expression of E-cadherin–catenin complex (Takeichi, 1993). The tumor cells become motile, invade through the basement membranes into surrounding tissues, enter circulation and extravasate into tissue and organs, and proliferate into a metastatic focus with subsequent enlarging volume. Depletion or lack of expression in catenin is thought to be responsible for metastasis when seen in tumors that are E-cadherin positive (Bremnes *et al.,* 2002). Decreased E-cadherin expression has been shown to be associated with a higher degree of invasiveness, increased malignant potential, and decreased survival in certain tumors (Charpin *et al.,* 1998; Williams *et al.,* 1993).

In lung cancer, aggressive and infiltrating carcinoma cells show impaired expression of the E-cadherin–catenin complex (Williams *et al.,* 1993). In the case presented the tissue stained positive for E-cadherin. Hence, it may have been an abnormality in the catenin molecules that contributed to the late metastasis to the ovaries. However, most cases of lung cancers do have an appreciable level of E-cadherin expression, and the presence of this antigen favors a lung primary; it is also known that a down-regulation of E-cadherin may be transient and can be reactivated in the metastatic foci (Bukholm *et al.,* 2000; Graff *et al.,* 2000).

In contrast to the expression of E-cadherin in primary lung cancers, most OCs, except mucinous types, fail to express E-cadherin and more typically express N-cadherin (Davies *et al.,* 1998; Peralta-Soler *et al.,* 1997). In the case presented, the ovarian tumor was described as poorly differentiated yet stained positive for E-cadherin and negative for N-cadherin. N-cadherin is absent in more than 95% of pulmonary adenocarcinomas and positive in more than 95% of serous OCs (Peralta-Soler *et al.,* 1997). Together, these cadherin findings favor a metastatic lung tumor rather than a primary ovarian tumor.

Cancer Antigen-125

The antigen CA-125 is an antigenic determinant of a high molecular weight glycoprotein that is present in 80% of nonmucinous OCs and 68.2% of serous carcinomas of the ovary (Tamakoshi *et al.,* 1996). It can be detected by paraffin IHC using the monoclonal antibody OC 125 that was generated by immunizing laboratory mice with a cell line that was established from human OC. The CA-125 antigen often circulates in the serum of patients with ovarian cancer and as such has been successfully used in disease monitoring during treatment as well as a marker for recurrent disease.

The antigen CA-125 may be elevated in a variety of benign, physiologic states and reactive disorders, including pregnancy, menstruation, endometriosis, adenomyosis, and leiomyomas. This may be partially explained by the distribution of CA-125 in the adult and fetus. The use of IHC using biotin-avidin immunoperoxidase technique may identify CA-125 among fetal tissues in the müllerian duct and in the coelomic epithelia. It is observed in the adult derivatives of the müllerian duct: fallopian tubes, endometrium, and endocervix. It is also found in the derivatives of the coelom; including the pleura, peritoneum, and pericardium.

The antigen CA-125 may be detected in 32% of lung cancers (Niloff, 1992). However, in the normal adult ovarian tissue there is no expression of CA-125. The highest levels of CA-125 are found in patients with ovarian cancer, and the blood level may be reflective of a patient's tumor burden. In patients who are premenopausal the sensitivity of the serum CA-125 is 50% compared to 84% in patients who are post-menopausal (Finkler *et al.,* 1988).

Carcinoembryonic Antigen

The antigen CEA was first identified in different stages of embryonic development and was subsequently found in human neoplasm (Colvin *et al.,* 1995). It is a 180 kD macromolecular glycoprotein containing ~50% carbohydrate and is encoded by 29 genes that are located on the long arm of chromosome 19 in tandem arrangement. There is significant heterogeneity of the CEA molecule based on the carbohydrate moiety and the amino-acid content. The N-acetylglucosamine asparagines peptide is important in the antigenicity of the molecule. In tissue, CEA is produced in the columnar epithelial cells and subsequently concentrated along the luminal border of the cell membrane.

Many CEA antibodies are available for detecting various CEA epitopes. Initially CEA was thought to be specific to the fetal intestinal mucosa and intestinal carcinomas. However, it is now well accepted that CEA is also present in tumors other than those arising in the colon. The antigen has a wide distribution and is found in the bronchus, biliary tract, small and large intestine, pancreatic duct, endocervix, and certain thyroid cells. Usually CEA does not stain adenocarcinoma of the ovary, particularly serous, clear cell or

endometrioid types (Wick and Siegal, 1988). However, carcinomas metastatic to the ovary exhibit diffuse immunostaining (Fleuren and Nap, 1988).

Cytokeratin Subtypes

The CKs are intermediate filament proteins that are associated with epithelial differentiation and are characteristically found in all epithelial cells and epithelial tumors. There are at least 20 different types of polypeptides, which are divided into acidic and basic groups based on molecular weight and isoelectric point (Colvin *et al.,* 1995; Moll *et al.,* 1982, 1992). Use of IHC with labeled antibodies may be of significant importance in analyzing metastatic tumors to the ovary (McCluggage, 2002). Subtyping of CK becomes particularly useful in cases in which a definitive diagnosis may be difficult to achieve based on histology alone. This diagnostic dilemma is usually encountered in poorly differentiated carcinomas with minimal glandular formation, when there is invasion and disruption of the architecture of neighboring structures, and when there is an unknown primary tumor.

The normal adult ovarian surface epithelium usually expresses CK7, CK8, CK18, and CK19 (Marjoniemi, 2004). Of special interest in immunohistochemical analysis of unknown primary tumors are CK7 and CK20. A basic, type II keratin, ~54kD, CK7 is found in the glandular epithelium of various organs including breast, endometrium, lung, and ovary; CK20 is a 46kD acidic, type I polypeptide with unique and relatively confined range of tumor expression in gastrointestinal adenocarcinomas (Wang *et al.,* 1995). Whereas GI adenocarcinomas are frequently CK20 positive, adenocarcinomas of the lung and female genital tract are almost always CK20 negative (Moll *et al.,* 1992). CK20 is expressed primarily in tumors arising from the GI tract, urothelium, and Merkel's cells (Moll *et al.,* 1982, 1992).

In an immunohistochemical study, OCs exhibited positive staining for CK7 and CA-125 and negative staining for CEA and CK20 (Langendik *et al.,* 1988). Pulmonary adenocarcinomas and mesotheliomas demonstrate CK7+/CK20–immunophenotype (Chhieng *et al.,* 2001; Wang *et al.,* 1995). On rare occasions, pulmonary adenocarcinomas express both CK7 and CK20 (Ritter *et al.,* 1998). The CK staining pattern observed in the case presented was compatible with a lung primary, but the CK7 and CK20 pattern was not a distinguishing marker for lung versus ovarian primary adenocarcinoma.

Surfactant

Pulmonary surfactant apoproteins are located mainly in type II pneumocytes and have demonstrated expression in bronchioalveolar carcinomas and adenocarcinomas of the lung. Monoclonal antibody, PE-10, is used for immunohistochemical study of surfactant apoprotein-A (SP-A) (Nicholson *et al.,* 1995). PE-10 immunoexpression is unique to type II pulmonary macrophages and the walls and perivascular tissue of small- to medium-sized blood vessels in the lung (Goldman *et al.,* 2001; Sheppard, 2000). Mesotheliomas do not exhibit positive staining with PE-10 antibody and therefore can be differentiated from pulmonary adenocarcinoma. PE-10 is suitable for use with paraffin sections, frozen sections, and cell smears. Surfactant expression, although having an overall sensitivity of 45%, is very specific for tumors arising from the lung (Kaufmann *et al.,* 2000). In the case presented, positive surfactant staining of the ovarian tumor favors a primary lung carcinoma metastatic to the ovary.

Thyroid Transcription Factor-1

A 38–40 kD transcription factor, TTF-1 (also known as thyroid-specific enhancing protein or NKx2) is expressed almost exclusively in thyroid and lung neoplasms (Gomez-Fernandez *et al.,* 2002; Sheppard, 2000). Transcription factors are nuclear proteins that have essential roles in gene expression and in determining and maintaining cellular phenotype and morphogenesis (Roh and Hong, 2002). Lung epithelial morphogenesis is under regulation from TTF-1 (Yatabe *et al.,* 2002). The TTF-1 also controls the expression for SP-A (Whitsett and Glasser, 1998).

One of the most useful roles of TTF-1 is the recognition and diagnosis pulmonary carcinoma in cases where histologic assessment may be insufficient for an unequivocal diagnosis to be made. Up to 96% of pulmonary adenocarcinomas express TTF-1 (Nakamura *et al.,* 2002). As early as 11 weeks in embryonic development, TTF-1 is expressed in all pulmonary epithelial cells (Sheppard, 2000). During the course of development, it is down-regulated in the tracheal and bronchial epithelium but retains predominant expression in Clara cells and type II pneumocytes. It is found in all types of lung carcinomas. It is found in up to 70% of adenocarcinoma, up to 38% in squamous cell carcinoma, and in 40% of large cell carcinoma (Fabbro *et al.,* 1996; Gomez-Fernandez *et al.,* 2002; Roh and Hong, 2002). In immunohistochemical studies using antibodies against TTF-1 positive staining was observed in thyroid and lung cancer but not in cancers arising from the breast, colon, kidney, ovary, or prostate (Gomez-Fernandez *et al.,* 2002).

Staining for thyroglobulin can easily differentiate between thyroid and lung cancer, as was done in the case presented. In cases of pulmonary adenocarcinoma,

antibodies to TTF-1 have demonstrated a sensitivity of up to 76% and specificity of 100% (Abutaily *et al.,* 2002; Gomez-Fernandez *et al.,* 2002). The factor TTF-1 is negative in 25–40% of lung adenocarcinoma (Gomez-Fernandez *et al.,* 2002; Yatabe *et al.,* 2002). Only nuclear staining to TTF-1 represents "true" reactivity; any cytoplasmic staining should be disregarded. Tumors that exhibit a higher immunoreactivity tend to exhibit a worse prognosis. Thus, the TTF-1 expression in our case also supports a lung origin in the ovarian tumor (see Figure 95).

Vimentin

Vimentin, also known as fibroblast intermediate filament, is the major intermediate filament found in nonmuscle cells (Colvin *et al.,* 1995). These cell types include fibroblast, endothelial cells, macrophages, melanocytes, Schwann cells, and lymphocytes. This is in contrast to keratin, which is the intermediate filament found in epithelial cells. Vimentin is composed of a single subunit and has a molecular weight of approximately 57 kD. *In vivo,* vimentin is not usually present in normal epithelial cells; however, it has been cultured *in vitro* in epithelial cells and may also show expression in tumor cells of epithelial origin, usually in paraffin tissue following antigen retrieval. Mesenchymal and endothelial cells usually stain vimentin positive and thus act as a measure of internal quality control in immunoreactivity. Absence of immunostaining in these areas often indicates that there is significant damage to tissue antigens and loss of structural architecture.

The benign normal ovarian surface epithelium is a single layer of epithelial cells that is of specialized mesodermal origin lining the ovary. It is very complex and appears to exhibit characteristics typical of mesenchymal cells both *in vivo* and when grown in culture. These cells often express vimentin, and up to 40% of ovarian cancer cases are vimentin positive. However, there is no clinical correlation between vimentin staining and the degree of tumor differentiation or presence of nodal disease. Use of vimentin is significantly limited by its lack of specificity, which is a result of its wide distribution in a variety of cell types in early embryonic life before they are replaced by more specific intermediate filaments later in development.

Using immunologic methods, vimentin can be readily demonstrated in frozen sections as well as paraffin sections. However, in formalin-fixed tissue, there may be reduced vimentin staining, and results could be inconsistent. Some of this inconsistent expression can be reduced using antigen-retrieval methods. In general, primary OCs are more frequently vimentin positive compared to primary pulmonary adenocarcinoma. Therefore, lack of vimentin staining in this case would tend to favor a lung primary over an ovary primary carcinoma.

Conclusion

Metastases of adenocarcinomas from varying numbers of primary sites, including breast, salivary gland, lung, pancreas, colon, stomach, endometrium, and the genitourinary tract cannot be reliably distinguished by histopathology alone. Identifying the specific site of origin is critical because it carries important therapeutic and prognostic implications. Because determining the primary site of adenocarcinoma based on cytomorphology can be difficult, IHC using tissue-specific markers has become an attractive technique in elucidating the site of the primary tumor. Until unique and individual markers are available that are site specific, the use of a panel of markers to identify the primary tumor site will prove beneficial. Furthermore, using panels of genes and proteins in characterizing patient tumors is a direction in which clinical oncology is headed (Callagy *et al.,* 2003).

In this chapter, we have used a panel of markers to differentiate lung cancer from ovarian cancer in a patient who presented with tumors in the ovaries following an initial presentation of lung cancer. The panel of antibodies directed against CA-125, CEA, E-cadherin, N-cadherin, CK7, CK20, TTF-1, surfactant, and vimentin was useful in this setting. Thus the ability to use organ-specific markers by the immunohistochemical technique is a powerful diagnostic tool in the workup of patients with cancer.

References

Abutaily, A.S., Addis, B.J., and Roche, W.R. 2002. Immunohistochemistry in the distinction between malignant mesothelioma and pulmonary adenocarcinoma: a critical evaluation of new antibodies. *J. Clin. Pathol. 55*:662–668.

Bremnes, R.M., Veve, R., Hirsch, F.R., and Franklin, W.A. 2002. The E-cadherin (Cell-cell adhesion complex and lung cancer invasion, metastasis and prognosis. *Lung Cancer 36*:115–124.

Bukholm, I.K., Nesland, J.M., and Borrensen-Dale, A.L. 2000. Re-expression of E-cadherin, alpha-catenin and beta-catenin, but not of gamma-catenin, in metastatic tissue from breast cancer patients. *J. Pathol. 190*:15–19.

Callagy, G., Cattaneo, E., Daigo, Y., Happerfield, L., Bobrow, L.G., Pharoah, P.D., and Caldas, C. 2003. Molecular classification of breast carcinomas using tissue microarrays. *Diag. Mol. Pathol. 12*:27–34.

Charpin, C., Garcia, S., Bonnier, P., Martini, F., Andrac, L., Choux, R., Lavaut, M., and Allasia, C. 1998. Reduced E-cadherin immunohistochemical expression in node negative breast carcinomas correlates with 10 year survival. *Am. J. Clin. Pathol. 109*:431–438.

Chhieng, D.C., Cangianella, J.F., Zakowski, M.F., Goswami, S., Cohen, J.M., and Yee, H.T. 2001. Use of thyroid transcription

factor0l, PE-10, and cytokeratin7 and 20 in discriminating between primary lung carcinoma and metastatic lesions in fine needle aspiration biopsy specimen. *Cancer 93*:330–336.

Colvin, R.B., Bhan, A.K., and McCluskey, R.T. 1995. *Diagnostic Immunopathology.* New York: Raven Press.

Dabbs, D.J. 2002. *Diagnostic Immunohistochemistry*. Philadelphia: Churchill Livingstone.

Davidson, B., Berner, A., Nesland, J.M., Risberg, B., Berner, H.S., Trope, C.G., Kristensen, G.B., Bryne, M., and Flores, V.A. 2000. E-cadherin and alpha-beta and gamma-catenin protein expression is up-regulated in ovarian carcinoma cells in serous effusions. *J. Pathol. 192*:460–469.

Davies, B.R., Worsley, S.D., and Ponder, B.A. 1998. Expression of E-cadherin, alpha-catenin and beta-catenin in normal ovarian surface epithelium and epithelial ovarian cancers. *Histopathology 32*:69–80.

Eissa, S. 1998. *Tumor Marker*. New York: Chapman and Hall.

Fabbro, D., DiLoreto, C., Stamerra, O., Beltrami, C.A., Lonigro, R., and Damante, G. 1996. TTF-1 gene expression in human lung tumors. *Eur. J. Cancer 32A*:512–517.

Finkler, N.J., Bebacerraf, B., Lavin, P.T., Wojciehowski, C., and Knapp, R.C. 1998. Comparison of serum CA-125, clinical impression, and ultrasound in the preoperative evaluation of ovarian masses. *Obstet. Gynecol. 72*:659–664.

Fleuren, G.J., and Nap, M. 1988. Carcinoembryonic antigen in primary and metastatic ovarian tumors. *Gynecol. Oncol. 30*: 407–415.

Frixen, U., Behrens, J., Sachs, M., Eberle, G., Voss, B., and Warda, A. 1991. E-cadherin mediated cell-cell adhesion prevents invasiveness of human carcinoma cell line. *J. Cell Biol. 113*:173–185.

Goldmann, T., Galle, J., Weidorn, K.H., Deutschbein, M.E., Neuhaus, M., Brancheid, D., and Vollmer, E. 2001. Diagnostic value of immunohistochemically detected surfactant–apoprotein-A in malignant tumors located in the lungs: report of two cases. *Ann. Diagn. Pathol. 5*:84–90.

Gomez-Fernandez, C., Jorda, M., Delgado, P.I., and Ganjei-Azar, P. 2002. Thyroid transcription factor-1: a marker for lung adenocarcinoma in body cavity fluids. *Cancer 96*:289–293.

Graff, J.R., Gabrielson, E., Fujii, H., Baylkin, S.B., and Herman, J.G. 2000. Methylation patterns of the E-cadherin 5′CpG island are unstable and reflect dynamic, heterogenous loss of E-cadherin expression during metastatic progression. *J. Biol. Chem. 28*: 2727–2732.

Han, A.C., Peralta-Soler, A., Knudsen, K.A., Wheelock, M.J., Johnson, K.R., and Salazar, H. 1997. Differential expression of N-cadherin in pleural mesotheliomas and E-cadherin in lung adenocarcinomas in formalin-fixed paraffin-embedded tissue. *Hum. Pathol. 28*:641–645.

Hayat, M.A. 2000. *Principles and Techniques of Electron Microscopy: Biological Applications,* 4th ed. Cambridge: Cambridge University Press.

Hedrick, L., Cho, K.R., and Vogelstein, B. 1993. Cell adhesion molecules as tumor suppressor. *Trends Cell Biol. 3*:36–39.

Hirohashi, S. 1998. Inactivation of E-cadherin mediated cell adhesion system in human cancers. *Am. J. Pathol. 153*:333–339.

Householder, J., Han, A., Edelson, M.I., Eager, J.M., and Rosenblum, N.G. 2002. Immunohistochemical confirmation of pulmonary papillary adenocarcinoma metastatic to ovaries. *Arch. Pathol. Lab. Med. 126*:1101–1103.

Imai, T., Horiuchi, A., Shiozawa, T., Osada, R., Kikuchi, N., Ohira, S., Oka, K., and Konisha, I. 2004. Elevated expression of E-cadherin and alpha-, beta-, and gamma-catenins in metastatic lesion compared with primary epithelial ovarian carcinoma. *Hum. Pathol. 35*:1469–1476.

Kalogeraki, A., Bouros, D., Zoras, O., Karabekios, S., Chalkiadakis, G., Stalhopoulos, E., Siafakas, N., and Delides, G.S. 2003. E-cadherin expression of fine needle aspiration biopsies in primary lung adenocarcinomas is related to tumor differentiation and invasion. *Anticancer Res. 23*:3367–3371.

Kaufmann, O., and Dietel, M. 2000. Thyroid transcription factor-1 is the superior immunohistochemical marker for pulmonary adenocarcinomas and large cell carcinomas compared to surfactant proteins A and B. *Histopathology 36*:8–16.

Lagendik, J.H., Mullinki, H., Van Diest, P.J., Meijer, G.A., and Meijer, C.J.1988. Tracing the origin of ovarian adenocarcinomas with unknown primary using immunohistochemistry: differential diagnosis between colonic and ovarian carcinomas as primary sites. *Hum. Pathol. 29*:491–497.

Marjoniemi, V.M. 2004. Immunohistochemistry in gynaecologic pathology: a review. *Pathology 36*:109–111.

Mazur, M.T., Hsueh, S., and Gersell, D.J. 1984. Metastasis to the female genital tract: analysis of 325 cases. *Cancer 53*: 1978–1984.

McCluggage, W.G. 2002. Recent advances in immunohistochemistry in gynaecological pathology. *Histopathology 40*:309–326.

McCluggage, W.G. 2000. Recent advances in immunohistochemistry in the diagnosis of ovarian neoplasms. *J. Clin. Pathol. 53*:327–334.

Moll, R., Lowe, A., Laufer, J., and France, W.W. 1992: Cytokeratin 20 in human carcinomas. A new histodiagnostic marker detected by monoclonal antibodies. *Am. J. Pathol. 140*:427–447.

Moll, R., Werner, W., Schiller, F.D. 1982. The catalog of human cytokeratins: patterns of expression in normal epithelia, tumors and cultured cells. *Cell 31*:11–24.

Nakamura, N., Miyagi, E., Murata, S., Kawaoi, A., Katoh, R. 2002. Expression of thyroid transcription factor-1 in normal and neoplastic lung. *Mod. Pathol. 10*:1058–1067.

Nicholson, A.G., McCormick, C.J., Shimosato, J., Butcher, D.N., and Sheppard, M.N. 1995. The value of PE-10, a monoclonal antibody against pulmonary primary and metastatic lung tumors. *Histopathology 27*:57–60.

Niloff, J.M. 1992. Tumor markers. In: Hoskins, W.J., Perez, C.A., and Young R.C. (eds). *Principles and Practice of Gynecologic Oncology*. Philadelphia: Lippincott.

Parker, R.T., and Curie, J.L. 1992. Metastatic tumors of the ovary. In: Coppleson. M. (ed). *Gynecologic Oncology: Fundamental Principles and Clinical Practice*. New York: Churchill Livingstone.

Peralta-Soler, A., Knudsen, K.A., Jaurand, M.C., Johnson, K.R., Wheelock, M.J., Klein-Szanto, A.J.P., and Salazar, H. 1995. The differential expression of N-cadherin and E-cadherin distinguishes pleural mesotheliomas from lung adenocarcinomas. *Hum. Pathol. 26*:1363–l369.

Peralta-Soler, A., Knudsen, K.A., Tescon-Miguel, A., NcBrearty, F.X., Han, A.C., and Salazar, H. 1997. Expression of N-cadherin and N-cadherin in surface epithelial-stromal tumors of the ovary distinguishes mucinous from serous and endometrioid tumors. *Hum. Pathol. 28*:734–739.

Ritter, J.H., Boucher, L.D., and Wick, M.R. 1998. Peripheral pulmonary adenocarcinomas with bronchioalveolar features: immunophenotypes correlate with histologie patterns. *Mod. Pathol. 11*:566–572.

Roh, M.S., and Hong, S.H. 2002. Utility of thyroid transcription factor-1 and cytokeratin 20 in identifying the origin of metastatic carcinomas of cervical lymph nodes. *J. Kor. Med. Sci. 17*: 512–517.

Sheppard, M.N. 2000. Specific markers for pulmonary tumors. *Histopathology 36*:273–276.

Takeichi, M. 1991. Cadherin cell adhesion receptors as morphogenetic regulators. *Science 251*:1451–1455.

Takeichi, M. 1993. Cadherins in cancer: implications for invasion and metastasis. *Curr. Opin. Cell Biol. 5*:806–811.

Tamakoshi, K., Kikkawa, F., Shibata, K., Tomoda, K., Obata, N.H., Wakahara, F., Tokuhashi, Y., Ishikawa, H., Kawai, M., and Tomoda, Y. 1996. Clinical value of CA-125, Cal9-9, CEA, CA72-4, and TPA in borderline ovarian tumor. *Gynecol. Oncol. 62*:67–72.

Travis, W.D., Travis, L.B., and Devesa, S.S. 1995. Lung cancer. *Cancer 75*:191–202.

Wang, N.P., Zee, S., Zarbo, R.J., Bacchi, CE., and Gown, A.M. 1995. Coordinate expression of cytokeratins 7 and 20 defines unique subsets of carcinomas. *App. Immunohistochem. 3*:99–107.

Webb, M.J., Decker, D.G., and Mussey, E. 1975. Cancer metastatic to the ovary. *Obstet. Gynecol. 45*:391–396.

Wick, M.R., and Siegal, G.P. 1988. Monoclonal antibodies to carcinoembryonic antigen in diagnostic immunohistochemistry. In: Wick, M.R., and Siegal, E.P. (eds). *Monoclonal Antibodies in Diagnostic Immunohistochemistry*. New York: Marcel Dekker.

Whitsett, J.A., and Glasser, S.W. 1998. Regulation of surfactant protein gene transcription. *Biochim. Biophys. Acta.* 1408: 303–311.

Williams, CL., Hayes, V.Y., Hummels, A.M., Tarara, J.E., and Halsey, T.J. 1993. Regulation of E-cadherin mediated adhesion by muscarinic acetylcholine receptor in small cell lung carcinoma. *J. Cell Biol. 121*:643–654.

Yatabe, Y., Mitsudomi, T., and Takahashi, T. 2002. TTF-1 expression in pulmonary adenocarcinomas. *Am. J. Surg. Pathol. 26*: 767–773.

Young, R.H., and Scully, R.E. 1985. Ovarian metastases from cancer of the lung: Problems in interpretation—A report of seven cases. *Gynecol. Oncol. 21*:337–350.

Zarka, T.A., Han, A.C., Edelson, M.I., and Rosenblum, N.G. 2003. Expression of cadherins, p53 and Bcl2 in small cell carcinomas of the cervix: potential tumor suppressor role for N-cadherin. *Int. J. Gynecol. Cancer 13*:240–243.

This Page Intentionally Left Blank

Index

Note: Italic page numbers refer to illustrations.

B

C

D

E

F

G

H

I

J

K

L

M

N

O

P

Q

R

S

T